american society for mass spectrometry

28th

ANNUAL CONFERENCE ON MASS SPECTROMETRY AND ALLIED TOPICS

May 25–30, 1980
Waldorf Astoria Hotel
New York City

JEFFREY R. WYATT

THE TWENTY-EIGHTH ANNUAL CONFERENCE ON MASS SPECTROMETRY AND ALLIED TOPICS

MAY 26-30, 1980

NEW YORK, NEW YORK

TABLE OF CONTENTS

1. Introduction I
2. Acknowledgements II
3. Proceedings of the 28th Annual Conference. V
4. Author Index 722
5. Minutes of Annual Business Meeting 733
6. ASMS Committees. 735
7. Committee, Subcommittee and Workshop Reports 736
8. ASTM Committee E-14 and ASMS Officers. 763
9. Constitution and By-Laws of ASMS 764
10. Valdimir Cermak, 1920-1980 773
11. List of Participants, 28th Annual Conference 774

PRINTED IN U.S.A.

INTRODUCTION

In this volume are collected the short or extended abstracts of papers presented at the Twenty-Eighth Annual Conference on Mass Spectrometry and Allied Topics held in New York City, May 25-30, 1980. It is intended that this volume be distributed only to members of ASMS and non-member registrants at the Conference and, therefore, it should not be considered a publication. It is requested that any future references to individual reports be cited in the form: Author(s), presented at 28th Annual Conference on Mass Spectrometry and Allied Topics, New York, N.Y., May 25-30, 1980.

I would like to express my thanks to the contributors for their co-operation in meeting the various deadlines. Special thanks are due to Burnaby Munson, Vice-President, Programs, and Henry Fales, Secretary, for supplying their various contributions in such excellent form for immediate use. To Mrs. Linda Suska of Extranuclear Laboratories goes a special expression of gratitude, for it was she who performed the many varied tasks required to convert countless separate sheets of paper into book form and did them so rapidly, cheerfully and efficiently. Finally, the appreciation of ASMS is extended to ASTM and Mr. Robert Meltzer who, for the first time this year, printed and distributed the volume.

Wade L. Fite, Editor

The American Society for Mass Spectrometry

President:	James A. McCloskey, Department of Medicinal Chemistry, University of Utah, Salt Lake City, Utah 84112
Vice President (Programs):	Burnaby Munson, Department of Chemistry, University of Delaware, Newark, Delaware 19711
Vice President (Arrangements):	W. Alan Wolstenholme, Kearns Group, 300 Broad Street, Stamford, Connecticut 06902
Secretary:	Henry M. Fales, National Institutes of Health, Building 10, Room 7N322, Bethesda, Maryland 20014
Treasurer:	Margaret A. Frisch, IBM, Thomas J. Watson Research Center, Box 218, Yorktown Heights, New York 10598
Past President:	Jean H. Futrell, Department of Chemistry, University of Utah, Salt Lake City, Utah 84112
Members-at-Large:	Wade L. Fite, Extranuclear Laboratories, Inc., Box 11512, Pittsburgh, PA 15238
	Catherine C. Fenselau, Department of Pharmacology and Experimental Therapeutics, Johns Hopkins University School of Medicine, 725 N. Wolfe Street, Baltimore, Maryland 21205
Chairman, ASTME-14:	Mynard Hamming, Continental Oil Company, Research and Development Department, Box 1267, Ponca City, Oklahoma 74601

The American Society for Mass Spectrometry is grateful for support of the 1980 Conference from the following sponsors and corporate members.

Company	Representatives
BALZERS HIGH VACUUM 8 Sagamore Park Road Hudson, New Hampshire 03051	Dr. Philip Irving
BELL ASSOCIATES 2211 South 19th Avenue Phoenix, Arizona 85005	Mr. Daniel Adams
COMMERCIAL TESTING/ENGINEERING 490 Orchard Street Golden, Colorado 80401	Mr. M. L. Jacobs
CORNELL UNIVERSITY G-24 Uris Hall Ithaca, New York 14853	Mr. Dan Bartholomew
CVC INC. 525 Lee Road, P.O. Box 1886 Rochester, New York 14603	Mr. Larry Gilbert
E. I. DUPONT DE NEMOURS & CO. 1500 S. Shamrock Avenue Monrovia, California 91016	Dr. Ed Chait
EXTRANUCLEAR LABORATORIES, INC. 250 Alpha Drive, P.O. Box 11512 Pittsburgh, Pennsylvania 15238	Mr. Michael McKeown
FINNEGAN CORPORATION 845 W. Maude Avenue Sunnyvale, California 94086	Mr. Michael Story
FINNEGAN INSTITURE 11 Triangle Park Drive Cincinnati, Ohio 45246	Dr. Don DeJongh
GALILEO ELECTRO-OPTICS Galileo Park Sturbridge, Massachusetts 01518	Mr. P. W. Graves
HEWLETT PACKARD 1601 California Avenue Palo Alto, California 94304	Dr. James Serum
HEYDEN & SON, INC. 247 South 41st Street Philadelphia, Pennsylvania 19104	Mr. Joel Packman
INFICON LH INC. 6500 Fly Road East Syracuse, New York 13057	Mr. Russ Carr
ION INSTRUMENTS INC. 1875 North 105 Street & East Avenue P.O. Box 51373 Tulsa, Oklahoma 74116	Mr. B. A. Hopper

KEARNS GROUP 58 Buckingham Drive Stamford, Connecticut 06902	Mr. G. L. Kearns
KEITHLEY INSTRUMENTS 28775 Aurora Road Cleveland, Ohio 44139	Mr. R. J. Erdman
KOR ISOTOPES INC. Division of Eco-Control Inc. 56 Rogers Street Cambridge, Massachusetts 01241	Mr. Joel C. Bradley
KRATOS-AEI SCIENTIFIC INSTRUMENTS 3344 North Torrey Pines La Jolla, California 92037	Mr. R. P. Fedchenko
LKB INSTRUMENTS Biodynamics P.O. 50100 Indianapolis, Indiana 46250	Mr. R. Martens
MASSPEC, INC. P.O. Box 9314 College Station, Texas 77840	Dr. Ron D. Grigsby
MERCK & CO. ISOTOPES P.O. Box 2000 Rahway, New Jersey 07065	Dr. S. P. Manrao
NIH/EPA CHEMICAL INFORMATION SYSTEMS 2519 Farringdon Road Baltimore, Maryland 21209	Dr. Al Fein
NUCLIDE CORPORATION 642 East College Avenue State College, Pennsylvania 16801	Mr. L. F. Herzog
PERNICKA CORPORATION 1026 West Maude Street, Suite 301 Sunnyvale, California 94086	Mr. J. C. Pernicka
R. D. S., INC. 1020 Corporation Way Palo Alto, California 94304	Mr. David Sparkman
SCIEX INC. 55 Glencameron Road, Suite 202 Thornhill, Ontario CANADA L3T 1P2	Dr. A. Lovett
SCIENTIFIC GLASS ENGINEERING 2007 Kramer Lane Austin, Texas 78758	Mr. K. O. Mahler
SHRADER ANALYTICAL LABORATORY 3450 Lovett Avenue Detroit, Michigan 48210	Dr. S. R. Shrader
STOHLER ISOTOPE INC. 49 Jones Road Waltham, Massachusetts 02154	Mr. Jack Turgel

TEKNIVENT CORPORATION 10774 Trenton Avenue St. Louis, Missouri 63132	Mr. P. F. Berger
UTHE TECHNOLOGY INC. 325 North Mathilda Avenue Sunnyvale, California 94086	Mr. J. D. Burden
VACUMETRICS INC. 2261 Palma Drive Ventura, California 93003	Mr. R. Ducet
VARIAN MAT, USA 25 Hanover Road Florham Park, New Jersey 07932	Mr. H. Radduth

PROCEEDINGS OF THE TWENTY-EIGHTH ANNUAL CONFERENCE

Paper No.		Page No.
*PL-1	CURRENT CONCEPTS OF MOLECULAR MECHANISMS OF CHEMICAL CARCINOGENESIS I. Bernard Weinstein	1
*PL-2	CHEMICAL IONIZATION: NEGATIVE ASPECTS F. H. Field	2

FOSSIL/SYNTHETIC FUELS

MAMOA1	MASS SPECTROMETRIC GROUP TYPE ANALYSIS OF POLAR NITROGEN CONCENTRATES John T. Swansiger, H. T. Best, and D. A. Danner	14
MAMOA2	COAL LIQUID CHARACTERIZATION BY MS BIOMARKERS IN WYODAK COAL & HYDRO. LIQUID R. J. Pancirov, T. R. Ashe and Z. Baset	16
MAMOA3	ANALYSIS OF COAL LIQUEFACTION PRODUCTS USING MIKES AND QQ MASS SPECTROMETERS D. Zakett and R. G. Cooks	18
MAMOA5	MASS SPECTROMETRIC METHODS FOR THE QUANTITATIVE ANALYSIS OF TRACE ORGANIC CONSTITUENTS IN ALTERNATE FUELS L.R. Hilpert, J.M. Brown, R.G. Christensen, H.S. Hertz, W.E. May, K.L. Richie, and E. White	20
MAMOA6	GCMS ANALYSIS OF COAL LIQUID AND ITS CATALYTICALLY HYDROGENATED PRODUCTS D. M. Schoengold, B. W. Wilson, M. R. Petersen, and R. A. Pelroy	22
MAMOA7	MASS SPECTRAL ANALYSES OF SULFUR COMPOUNDS IN A LUBE OIL BASESTOCK EXTRACT C. S. Hsu and J. M. Kelliher	23
MAMOA8	RELATIVE FIELD IONIZATION EFFICIENCIES OF HYDROCARBON COMPOUNDS S. E., Jr. Buttrill and G. A. St. John	24
MAMOA9	ALKYLBENZENES DERIVED FROM CAROTENES IN COALS BY GC-MS-C E. J. Gallegos	26
MAMOA10	DIRECT ANALYSIS OF CARBOXYLIC ACIDS IN OIL SAMPLES BY CAPILLARY GC/MS Jacob Shen	28

INSTRUMENT TECHNIQUES, ISOTOPE RATIO

MAMOB1	APPLICATION OF THE MS80 AND A NEW HIGH RESOLUTION SELECTED ION MONITORING ROUTINE TO THE DETERMINATION OF TRACE LEVELS OF TCDD K.R. Compson, J.R. Chapman, G.A. Warburton, P.A. Ryan, A. Carrick	30

*Plenary Lecture

Paper No. Page No.

MAMOB2 DEVELOPMENT AND APPLICATION OF AN ALL GLASS CAPILLARY GC-HIGH RESOLUTION MS INTERFACE AND SCAN CIRCUIT FOR ISOMER DETERMINATIONS OF CHLORODIOXINS IN BIOLOGICAL TISSUES, COMBUSTION STACK GASSES, AND OTHER ENVIRONMENTAL AND INDUSTRIAL SAMPLES
J. G. Solch, G. F. Vanness, C. D. Miller, H. R. Dufour, M. L. Taylor, and T. O. Tiernan. 32

MAMOB3 AUTOMATED MULTIPLE MODE MASS SPECTROMETRY (AMMS): I. EVALUATION OF THE PERFORMANCE OF SEVERAL AMMS DESIGNS BASED ON THEIR EFFICIENCY FACTORS
C. Chang. 34

MAMOB4 SCANNING MICROPIPETTE MOLECULE MICROSCOPY
J. A. Jarrell and J. G. King. 36

MAMOB5 DETERMINATION OF THE DIFFUSION COEFFICIENT OF WATER IN POLYMERIC MATERIALS BY PRECISION ABRASION MASS SPECTROMETRY
Michael A. Grayson and Clarence J. Wolf. 38

MAMOB7 A FULLY AUTOMATIC SYSTEM CALIBRATION FOR URANIUM
K. Habfast and D. Tuttas. 40

MAMOB8 PRECISE SULFUR ISOTOPE RATIO MEASUREMENTS ON SO2 AND SF6
H. Nielsen and C. Brunnee. 41

MAMOB9 AN ISOTOPE DILUTION MASS SPECTROMETRIC METHOD FOR THE ACCURATE DETERMINATION OF UREA IN HUMAN SERUM
Michael J. Welch, E. White, L. Sniegoski , R. Schaffer, H. S. Hertz, and A. Cohen. 42

MAMOB10 MEASUREMENT OF VERY LOW ABUNDANCE ISOTOPES USING A REVERSE GEOMETRY DOUBLE FOCUSSING THERMAL IONIZATION MASS SPECTROMETER
P. J. Turner, T. O. Merren, and E. F. Hall. 44

MAMOB11 THE USE OF INTERMEDIATE RANGE MASS SPECTROMETRY IN THE MEASUREMENT OF HEAVY METHANES AS ATMOSPHERIC TRACERS
D. J. Frank. 46

MAMOB12 SYSTEMATIC ERRORS IN ISOTOPE RATIO MEASUREMENTS USING THERMAL IONIZATION AND PULSE-COUNTING DETECTION
J. D. Fassett. 47

PYROLYSIS, FD, ION MOLECULE REACTIONS

MAMOC1 ADVANCES IN PYROLYSIS-MASS SPECTROMETRY
J. Haverkamp, W. Windig, D. Valerio, and P. G. Kistemaker. 49

MAMOC2 THE FROG EMBRYO AS A MODEL FOR CELL AND TISSUE CHARACTERIZATION BY PYROLYSIS MASS SPECTROMETRY
Henk L. C. Meuzelaar, Marcus Jacobsen, Johan Haverkamp , and David L. Pope. 51

MAMOC3 THE GC/MS ANALYSIS OF THE PYROLYSIS PRODUCTS FROM A SPECIFICALLY LABELLED DEUTERATED URETHANE
Kent J. Voorhees and Robert P. Lattimer. 52

Paper No. Page No.

MAMOC4 THERMAL DEGRADATION PRODUCTS FROM PVC, PLASTICIZER, AND ANTIMONY TRIOXIDE
J. A. Nikora and G. F. Smith. 54

MAMOC5 MECHANISMS OF OZONATION OF N,N'-DI-(1-METHYLHEPTYL)-P-PHENYLENEDIAMINE
Robert P. Lattimer, E. Ray Hooser, Hugh E. Diem, Robert W. Layer, and C. K. Rhee. 57

MAMOC6 ACID-ENHANCED FIELD DESORPTION OF ZWITTERIONS
T. Keough and A. J. Destefano. 59

MAMOC7 THE ROLE OF COLLISION COMPLEXES IN THE REACTION OF SiH_3^+ WITH C_2H_4
R. N. Abernathy and F. W. Lampe. 61

MAMOC8 GeH_5^+ AND THE PROTON AFFINITY OF GERMANE
S. N. Senzer and F. W. Lampe and R.N. Abernathy. 63

MAMOC9 COMPLEX FORMATION BY THE METHYL MERCURY CATION FROM CIMS STUDIES OF DIMETHYL MERCURY
J. A. Stone, R. Camicioli, M.C. Baird and D. Splinter. 65

MAMOC10 THERMOCHEMICAL STUDIES OF ION CLUSTERS: BOND ENERGIES AND RELATIONSHIP TO SOLVATION
A. W., Jr. Castleman, P. M. Holland, T. D. Mark, K. I. Peterson, N. Lee, and R. G. Keesee. 68

MAMOC11 NEUTRAL PRODUCTS OF NUCLEOPHILIC SUBSTITUTION IN THE GAS PHASE
Thomas Hellman Morton, David G. Hall, and Chakra Gupta. 70

GC, IONIZATION PROCESSES, CI, ORGANIC MECHANISMS

MAMP1 APPLICATIONS OF HIGH PERFORMANCE GC2/MS
Uwe Rapp and G. Dielmann. 73

MAMP2 PHOSPHATE DETERMINATION EMPLOYING AN ^{18}O LABELED CARRIER
Thomas P. Krick, G. Graff, and N. D. Goldberg. 74

MAMP3 A PHOTODISSOCIATION STUDY OF THE OZONE IONS
Marvin L. Vestal and J. F. Hiller. 76

MAMP4 ELIMINATION OF THE CENTRAL CARBON IN THE FRAGMENTATION OF THE PROPANE ION
J. P. Gilman, Ta-Cheng Hsieh, and G. G. Meisels. 78

MAMP5 LASER INDUCED PHOTODISSOCIATION OF BROMOETHANE MOLECULAR IONS
Fred W. Brill and John R. Eyler. 80

MAMP6 ION FLUORESCENCE FOLLOWING HeIa IONIZATION
Robert C. Dunbar and D. W. Turner. 81

MAMP7 IR PHOTODISSOCIATION OF GAS-PHASE IONS BY CO_2 LASER INTERACTION WITH A FAST ION BEAM
Robert C. Dunbar, G. Coggiola, P. C. Cosby, and J. R. Peterson. 82

Paper No.		Page No.
MAMP8	PHOTOION AND PHOTOELECTRON SPECTROSCOPY IN H20 EXCITED BY SYNCHROTRON RADIATION IN THE RANGE OF 12 TO 35 eV O. Dutuit, T. Govers, K. Ito, A. Tabche-Fouhaile, P. Morin, I. Nenner, T. Baer, and P.M. Guyon.	83
MAMP9	AN EXACT MEASUREMENT OF THE FRAGMENTATION RATE CONSTANTS FOR THE LOWER 2-KETONES Lloyd J. Hendricks.	85
MAMP10	REACTIVE COLLISION OF HIGH RYDBERG(HR) ARGON ATOMS WITH HALOGENATED MOLECULES I. Dimicoli and R. Botter.	87
MAMP11	CHARGE-TRANSFER AND COLLISIONAL EXCITATION IN Kr+ AND Xe COLLISIONS E. Grant Jones.	89
MAMP12	WITHDRAWN	
MAMP13	SENSITIVITY AND LINEAR RANGE COMPARISONS OF ATMOSPHERIC PRESSURE IONIZATION (API) AND CHEMICAL IONIZATION (CI, 1 TORR) MASS SPECTROMETRY SYSTEMS D. I. Carroll, J. Nowlin, R. N. Stillwell, and E. Horning.	91
MAMP14	HIGH RESOLUTION NEGATIVE ION CHEMICAL IONIZATION MASS SPECTROMETRY Ismet Dzidic, F. Montgomery, D. I. Carroll, and E. Horning.	92
MAMP15	SELECTIVITY OF REAGENT GASES AS USED IN THE ANALYSIS OF FLAVOR MIXTURES W. A. Wolstenholme, M. Hohn, and Uwe Rapp.	94
MAMP16	DEHYDRATION OF M+BUTYL COMPLEX IONS OF BENZYL ALCOHOL IN ISOBUTANE CIMS Joachim G. Liehr, Gareth A. Brenton, J. H. Beynon, James A. Mccloskey, and Wilhelm J. Richter.	95
MAMP17	CALIBRATION SUBSTANCES FOR NEGATIVE CHEMICAL IONIZATION MASS SPECTROMETRY Andries P. Bruins.	96
MAMP18	ON THE MECHANISM OF THE RETRO DIELS-ALDER REACTION M.-J. Bobenrieth, J. R. Hass, L. A. Levy, and L. Pruitt	98
MAMP19	THE EI INDUCED FRAGMENTATION OF THE VINYLIDENE CARBONATES R. T. Aplin, G. P. Cottam, and M. C. Grossel.	100
MAMP20	ESTIMATION OF FACTORS FOR CORRECTING ION GAUGE PRESSURE TO TRUE PRESSURE John E. Bartmess, R. Georgiadia and G. Caldwell.	102

Paper No. Page No.

INSTRUMENT DESIGN

MPMOA1 A TANDEM MASS SPECTROMETER FOR CID WITH SIMULTANEOUS DETECTION AND VARIABLE DISPERSION
A. J. H. Boerboom, G. J. Louter, and J. Haverkamp. 103

MPMOA2 QUADRUPOLE AND ELECTROSTATIC COLLISION CELLS FOR QUADRUPOLE MS/MS INSTRUMENTATION
Charles A. Boitnott, Urs Steiner, and Michael S. Story. 105

MPMOA3 DESIGN AND APPLICATIONS OF A NEW TRIPLE ANALYZER MASS SPECTROMETER
M. L. Gross, P. A. Lyon, F. W. Crow, and S. Evans. 107

MPMOA4 IS THERE A BETTER GEOMETRY THAN THE QUADRUPOLE?
M. H. Friedman, Leonid Kelner, A. L. Yergey, and J.E. Campana. 109

MPMOA5 EFFECT OF CONTINUOUSLY VARYING ro IN A QUADRUPOLE MASS SPECTROMETER
Juliette W. Ioup, George M., Jr. Wood, and Mostofa Mosharrafa. 111

MPMOA6 THE ION OPTICS OF A SPLIT-POLE MASS SPECTROMETER
C. R. Lagergren. 113

MPMOA7 QUANTITATION OF MASS SPECTRAL DATA FROM AN ELECTRO-OPTICAL ION DETECTOR
C. E. Giffin, R.A. Britten and R.A. Johansen. 115

MPMOA8 ELEMENTAL ANALYSIS BY A NOVEL MICROWAVE PLASMA/MASS SPECTROMETER SYSTEM
D. J. Douglas and J. B. French. 117

MPMOA9 A MULTIPLE SELECTED ION MONITORING SYSTEM FOR HIGH SPEED, HIGH DYNAMIC RANGE AND HIGH PRECISION CYCLING
L. F. Herzog and T. J. Eskew. 119

GC/MS

MPMOB1 FURTHER DEVELOPMENTS IN QUANTITY OPTIMIZED TWO DIMENSIONAL GAS CHROMATOGRAPHY FOR MASS SPECTROMETRY
Ralph J. May and Woodfin V., Jr. Ligon. 121

MPMOB2 WITHDRAWN

MPMOB3 THE ULTIMATE IN CAPILLARY GC/MS COUPLING
P. A. Leclercq, G. J. Scherpenzeel, and C. A. Cramers. 123

MPMOB4 IDENTIFICATION OF MASS SPECTRA FROM GC-MS DATA. THEORETICAL LIMITATIONS ON GC/MS ANALYSIS.
David Rosenthal and William F. Hargrove. 125

MPMOB5 APPLICATIONS OF A NEW DATA ACQUISITION INTERFACE IN QUALITATIVE AND QUANTITATIVE GC-MS
A. Carrick, C. D. Park, M. J. Hoyle, P. A. Ryan, C. J. Wakefield, and K. R. Compson. 127

Paper No. Page No.

MPMOB6 REAL-TIME QUALITATIVE AND QUANTITATIVE ANALYSIS OF GC/MS DATA OF COMPLEX MIXTURES FOR ENVIRONMENTAL POLLUTANT ANALYSIS
Glenn I. Ouchi. 129

MPMOB7 DETERMINATION OF ETHYLDICHLOROSILANE IN METHYLCHLOROSILANES BY CAPILLARY GC-FID AND GC-MS
Gerald F. Dudding and Gerald T. Sorensen. 130

MPMOB8 A FUNDAMENTAL APPROACH TO MEASUREMENT PARAMETER SELECTION FOR QUANTITATIVE ISOTOPE DILUTION GC/MS DETERMINATIONS
B. N. Colby and A. R. Rosecrance and M.E. Colby. 132

MPMOB9 GAS CHROMATOGRAPHY-MASS SPECTROMETRY WITH METASTABLE PEAK MONITORING APPLIED TO THE ANALYSIS OF STEROID HORMONES
Simon J. Gaskell, Elizabeth M. H. Finlay, and Adrian W. Pike. 133

MPMOB10 A METHOD FOR THE DETERMINATION OF ORGANOTIN PVC STABILIZER IN SERUM
Marcia Marconi, M. Gara, D. Nelson, and R. Dawe. 135

MPMOB11 AN IMPROVED THERMAL DESORPTION GC-MS METHOD FOR TRACE ORGANICS SAMPLED ONTO TENAX RESIN FROM AMBIENT AIR
C. Herndon, Jr. Williams, Larry D. Ogle, and D. Scott Lewis. 136

MPMOB12 NEW DEVELOPMENTS IN CAPILLARY COLUMN GC/MS ANALYSIS USING DOUBLE FOCUSSING SPECTROMETERS
D. S. Millington, V. Parr, B. N. Green, and K. Hall. 139

ION MOLECULE REACTIONS

MPMOC1 TANDEM MASS SPECTROMETRIC STUDIES OF THE REACTIONS OF N+ AND O2
L. N. Morgenthaler and J. F. Paulson. 140

MPMOC2 STUDIES OF MODEL ION-MOLECULE REACTIONS BY TRIPLE QUADRUPOLE MASS SPECTROMETRY.
J. Chakel, H. Gregg and C. Enke. 142

MPMOC3 BEAM STUDIES OF THE REACTION OF H3O+ AND OH- WITH H2O AT ENERGIES OF 0.3-1.0 eV
Michael J. Henchman and J. F. Paulson. 144

MPMOC4 WITHDRAWN

MPMOC5 FORMATION AND THERMODYNAMIC PROPERTIES OF HYDRATED NO_3^- IONS
Richard L. C. Wu and T. O. Tiernan. 145

MPMOC6 ENERGETICS OF THE CHARGE-STRIPPING PROCESS FROM NEGATIVE IONS OCCURRING IN A DOUBLE-FOCUSING MASS SPECTROMETER
J. H. Beynon, J. E. Szulejko, I. Howe, and J. H. Bowie. 147

MPMOC7 IS THE INTERMOLECULAR ENTROPY CORRECTION TERM IN GAS PHASE IONIC EQUILIBRIA VALID?
G. G. Meisels. 148

Paper No. Page No.

MPMOC8 ON THE QUESTION OF INTERMOLECULAR ENTROPY EFFECTS IN LOW PRESSURE ION-MOLECULE EQUILIBRIA: AN ANALYSIS BASED ON THE LANGEVIN MODEL
M. T. Bowers, Walter J. Chesnavich, and Horia Metiu. 150

MPMOC9 THERMONEUTRAL ISOTOPE EXCHANGE REACTIONS OF CATIONS IN THE GAS PHASE
Sharon G. Lias and Pierre Ausloos. 151

MPMOC10 NEAR THERMAL CHARGE TRANSFER REACTIONS IN Kr/CO and Xe/O2 MIXTURES
James B. Laudenslager. 152

MPMOC11 INFRARED CHEMILUMINESCENCE STUDIES OF ION-MOLECULE REACTIONS
T.W. Zwier, M. Maricq, C. Simon, V. Bierbaum, G. Ellison, and S. Leone. 153

MPMOC12 ELECTRON AFFINITY MEASUREMENTS USING EQUILIBRIUM ELECTRON TRANSFER REACTIONS
Elaine K. Fukuda and Robert T., Jr. Mciver. 155

MPMOC13 COMPARATIVE ION-MOLECULE CHEMISTRY OF A CARBENE ANION RADICAL AND THE CORRESPONDING CARBANION
Richard N. Mcdonald, A. K. Chowdhury, and D. W. Setser. 156

ENVIRONMENTAL/COMPUTER APPLICATIONS

MPMP1 CONTINUOUS ON-LINE MONITORING OF HOT COMBUSTION GASES BY APCI/MS
B. A. Thomson, T. Sakuma, J. Fulford, J. B. French, and N. M. Reid. 158

MPMP2 GC/MS INVESTIGATIONS OF HETEROCYCLIC PARTICULATE ORGANIC MATTER (POM) FOUND IN THE ENVIRONMENT
R. C. Lao, R. S. Thomas, and S. W. Lee. 160

MPMP3 WITHDRAWN

MPMP4 FUNCTIONAL ASSESSMENT OF ADEQUATE GC/MS INSTRUMENTAL OPERATION IN THE MASTER ANALYTICAL SCHEME
J. F. Ryan, L. Rando, D. Perry, J. Gebhart, J. Bursey, K. Tomer, and E. Pellizzari. 162

MPMP5 ESTIMATION OF RELATIVE RESPONSE FACTORS FOR ANALYSIS OF ORGANICS IN WATER
J. Bursey, K. Tomer, E. Pellizzari, J. F. Ryan, L. Rando, and D. Perry. 165

MPMP6 FACTORS AFFECTING THE PRECISION OF M.S. RESPONSE DATA OBTAINED IN THE MASTER ANALYTICAL SCHEME FOR ANALYSIS OF ORGANICS IN WATER
K. Tomer, J. Bursey, E. Pellizzari, J. F. Ryan, L. Rando, and D. Perry. 167

MPMP7 QUANTITATIVE ASPECTS OF GC/MS ANALYSIS
A. D. Sauter, D. Betowski, M. Hiatt, and E. P. Meier. 169

Paper No. Page No.

MPMP8 WITHDRAWN

MPMP9 SEMI-AUTOMATIC ANALYSIS OF VOLTATILE ORGANICS IN AIR TO 1 PPB
Samuel Insalaco and Paul P. Dymerski 170

MPMP10 WITHDRAWN

MPMP11 QUANTITATIVE ANALYSIS BY GC-MS OF VOLATILE ORGANIC COMPOUNDS
Hans Grade and Woodfin V., Jr. Ligon 172

MPMP12 CHEMICAL KINETICS OF FREE RADICAL REACTIONS RELEVANT TO PHOTOCHEMICAL SMOG FORMATION
K.R. Ryan, I.D. Plumb, J.R. Steven and M.F.R. Mulcahy 173

MPMP13 METHANE ENHANCED NEGATIVE-IONIZATION MASS SPECTRA OF SELECTED S-TRIAXINE HERBICIDES
J.A. Nystrom, Y. Tondeur, J.R. Hass and M. Bursey 175

MPMP14 MIKES ANALYSIS FOR SULFAMETHAZINE
M. K. Hofffman, D. J. Harvan, and J. R. Hass. 177

MPMP15 THE ANALYSIS OF SULFAMETHAZINE RESIDUES IN CATTLE TISSUE USING GAS CHROMATOGRAPHY-CHEMICAL IONIZATION MASS SPECTROMETRY
M. O. Poeppel, Steven J. Stout, A. J. Manuel, and W. A. Steller. 179

MPMP16 CONFIRMATION OF SULFONAMIDE RESIDUES IN ANIMAL TISSUES BY GAS CHROMATOGRAPHY/ELECTRON IMPACT POSITIVE AND NEGATIVE ION CHEMICAL IONIZATION MASS SPECTROMETRY
Tung Sun. 181

MPMP17 DECONVOLUTING MASS SPECTRA OF MIXTURES USING A MINICOMPUTER
Mark Weiss, Steve Sokolow. 183

MPMP18 AN IN-HOUSE LIBRARY SEARCH SYSTEM DESIGNED FOR TRACE ANALYSES
D. Thomas Terwilliger and Walter C. Davidson. 184

MPMP19 COMPUTER IDENTIFICATION OF UNKNOWN MASS SPECTRA WITH NEW GENERATION SYSTEMS
I. K. Mun, B. L. Atwater, K. S. Haraki, R. Venkataraghavan, and Fred W. Mclafferty. 186

MPMP20 A LIBRARY SEARCH ROUTINE FOR THE IDENTIFICATION AND QUANTITATIVE DETERMINATION OF PRIORITY POLLUTANTS
A. Carrick, J. R. Chapman, F. J. Street, G. A. Warburton, C. J. Wakefield, K. R. Compson, and D. Hazelby. 188

MPMP21 THE STATUS OF THE NIH/EPA MSSS
D. P. Martinsen, R. S. Heller, G. W. A. Milne, William L. Budde, and S. R. Heller. 190

MPMP22 "HARDWARE" BACKGROUND/FOREGROUND DATA SYSTEM: AN ESSENTIAL DEVELOPMENT IN SUPPORT OF METABOLIC PROFILING ON MAGNETIC SECTOR MASS SPECTROMETERS
F. Martin, S. Johnson, M. Mcpherson, and Jack F. Holland. 192

Paper No. Page No.

MPMP23 A NEW APPROACH TO COMPUTER CONTROLLED METASTABLE SCANNING IN ORGANIC MASS SPECTROMETRY
P. Powers, J. C. Bill, R. Reinsch, A. J. Gilbert, and M. J. Wallington. 193

INORGANIC/SOLIDS

TAMOA1 ON THE REAL-TIME MEASUREMENT OF PARTICLES IN AIR BY DIRECT-INLET SURFACE IONIZATION MASS SPECTROMETRY
J. J. Stoffels and C. R. Lagergren 195

TAMOA2 COMPUTER CONTROLLED SCANNING LASER MASS SPECTROMETRY
R. J. Conzemius, J. Capellen, and H. J. Svec 196

TAMOA3 POSITIVE AND NEGATIVE ION PRODUCTION IN SPARKED SF6
L. C. Frees, L. G. Christophorou, H. W. Ellis, and I. Sauers 197

TAMOA4 THERMODYNAMIC STABILITY OF RARE EARTHPLATINUM METAL DIATOMICS
K. A. Gingerich, S. K. Gupta, R. Haque, B. M. Nappi, and M. Pelino. 199

TAMOA5 A PRECISE METHOD FOR THE MASS SPECTROMETRIC ANALYSIS OF SILVER
L. P. Dunstan, K. A. Brletic, and E. L. Garner. 201

TAMOA6 ABSOLUTE Li ISOTOPE RATIO MEASUREMENTS
E. L. Callis, A. E. Essling, G. Reedy, and R. J. Meyer. 202

TAMOA7 WITHDRAWN

TAMOA8 SECONDARY ION MASS SPECTROMETRIC ANALYSIS OF COBALT HARDENED GOLD ELECTROPLATE SURFACES
Rudolf Schubert. 203

TAMOA9 ANALYSIS OF AEROSOL PARTICLES BY MASS SPECTROMETRY
M.P.Sinha, C.E. Giffin, D.D. Norris and S.K. Friedlander. 204

TAMOA10 FURTHER DEVELOPMENT OF PARTICULATE IMPACT MASS SPECTROMETRY
Frank T. Greene. 206

SYMPOSIUM ON STRUCTURE ELUCIDATION OF NATURAL PRODUCTS

TAMOB1 BIOACTIVE COMPOUNDS FROM MARINE AND MICROBIAL SOURCES
Kenneth L., Jr. Rinehart. 207

TAMOB2 STRUCTURE DETERMINATION OF SLOW REACTING SUBSTANCE : A POSSIBLE CHEMICAL MEDIATOR OF HUMAN ASTHMA
R. C. Murphy. 208

TAMOB3 ANTIBIOTICS DERIVED FROM HIGHER PLANTS
L. A. Mitscher, D. L. Flynn, J. K. Swayze, T. Veysoglu, T.Z. Wu and Y.H. Park. 209

TAMOB4 BETTER SURVIVAL THROUGH NATURAL PRODUCTS
M. S. Blum. 213

Paper No. Page No.

ORGANIC MECHANISMS

TAMOC1 MULTIPLE CONCERTED REARRANGEMENTS IN ETHYLENE LOSS FROM 4,4-DIMETHYL-1-PENTENE
Arnold M. Falick, P. Tecon, and T. Gaumann. 215

TAMOC2 MECHANISM OF FRAGMENTATION OF SOME C5 OLEFINIC ALCOHOLS
A. G. Harrison, J. Hegedus-Vajda, N. E. Middlemiss, J. J. Zwinselman, and N. M. M. Nibbering. 217

TAMOC3 THE "EVEN-ELECTRON RULE"
Asher Mandelbaum and Miriam Karni. 219

TAMOC4 RETRO DIELS ALDER FRAGMENTATION ACCOMPANIED BY HYDROGEN MIGRATIONS IN SOME ADDUCTS OF BICYCLOALKENYLS
Asher Mandelbaum and Ana Fraiman. 221

TAMOC5 MASS SPECTRAL BREAKDOWN OF METAL DITHIOCARBAMATE CHELATES
J. R. Dias, S. Gomiscek, and M. Zigon. 223

TAMOC6 REARRANGEMENT IONS - AN AID OR AN INTERFERENCE IN IDENTIFICATION OF SULFUR COMPOUNDS
Norman G. Foster. 225

TAMOC7 MASS SPECTROMETRY OF ORTHO-SUBSTITUTED BIARYLS: PHENYLNAPHTHLPHENYL SYSTEMS
Jayanti R. Patel and Joseph H. Boyer. 227

TAMOC8 SUBSTITUENT EFFECTS IN THE MASS SPECTRA OF ALKYL-SUBSTITUTED SULFAMIDES UNDER DIFFERENT IONIZATION CONDITIONS
Erwin Baumgartner and A. Popitsoh. 229

TAMOC9 PREPARATION AND MASS SPECTRAL CHARACTERIZATION OF METHYLTHIO DERIVATIVES OF NAPTHALENE
Wanda G. Stillwell, M. G. Horning, W.-S. Tsang, and G. W. Griffin. 231

ION MOLECULE REACTIONS/ENVIRONMENTAL

TAMP1 WITHDRAWN

TAMP2 STUDIES OF LOW VOLATILITY COMPOUNDS BY ION CYCLOTRON RESONANCE MASS SPECTROMETRY
M. J. Locke, R. L. Hunter, P. Cruz, P. N. Borer, and Robert T., Jr. Mciver. 232

TAMP3 THERMOCHEMISTRY OF INTRAMOLECULAR SOLVATION IN PROTONATED AND RADICAL IONS: DIAMINES, TRIAMINES, AMINO ALCOHOLS, DIPHENYL ALKANES AND NORMAL ALKANES.
M. Mautner, E. Hunter, P. Hamlet, F. Field, P. Ausloos and L. Sieck. 233

TAMP4 TEMPERATURE DEPENDENCE OF THE EQUILIBRIUM $CO_2^{+\cdot} + 2CO_2 = (CO_2)_2^{+\cdot} + CO_2$
K. R. Jennings, J. V. Headley, and R. S. Mason. 235

TAMP5 ION CHEMISTRY AND LIGAND BINDING ENERGIES OF Cu^+ AND RELATED METAL CATIONS
Roger W. Jones and Ralph H. Staley. 237

Paper No.		Page No.
TAMP6	GAS PHASE ION CHEMISTRY AND RELATIVE LIGAND BINDING ENERGIES OF Al+, Mn+, Cr+, Ti+, AND RELATED CATIONS Manfred M. Kappes, Jack S. Uppal, and Ralph H. Staley.	239
TAMP7	SELECTIVE CHEMICAL IONIZATION REAGENT GASES FOR POLYNUCLEAR AROMATICS AND AROMATIC NITROGEN COMPOUNDS D. M. Schoengold.	241
TAMP8	FRACTIONATION OF ENVIRONMENTAL ORGANIC EXTRACTS WITH DIMETHYLSULFOXIDE. APPLICATIONS TO DIESEL EXHAUST PARTICULATES Thomas R. Henderson, Charles R. Clark, Ray L. Hanson, and Robert E. Royer.	243
TAMP9	ANALYSIS OF POLYHALOGENATED AROMATIC HYDROCARBONS BY CAPILLARY COLUMN GC-NEGATIVE ION CIMS F. W. Crow and Alf Bjorseth.	245
TAMP10	IDENTIFICATION OF PCB'S OF NATURAL ORIGIN BY GC/MS Bori Shushan and Robert K. Boyd.	246
TAMP11	QUANTITATIVE DETERMINATION OF HALOCARBONS IN THE TROPOSPHERE BY SELECTED ION MONITORNG F. Bruner, G. Crescentini, P. Ciccioli, and E. Brancaleoni.	247
TAMP12	FORMATION OF CHLOROFORM FROM THE REACTIONS OF HYPOCHLORITE AND E. COLI Donald L. Dugger.	249
TAMP13	SINGLE IONIZATION OF AMMONIA CLUSTERS AND DOUBLE IONIZATION OF HETERONUCLEAR RARE GAS DIMERS T. D. Mark, K. I. Peterson, A. W., Jr. Castleman, H. Helm, and K. Stephan.	251
TAMP14	CROSSED BEAM STUDIES OF THE REACTIONS OF CO+ WITH O2 AND NO K. R. Jennings, M. F. Jarrold, and D. M. Hirst.	253
TAMP15	SOLVATION OF K+ BY BENZENE. A NEW HIGH PRESSURE FLOW ION SOURCE J. Sunner, K. Nishizawa, and P. Kebarle.	255
TAMP16	ALKALI METAL ION REACTIONS OF ATMOSPHERIC INTEREST B. Rowe, A. A. Viggiano, D. L. Albritton, and F. C. Fehsenfeld.	256
TAMP17	PHOTOIONIZATION MASS SPECTROMETRY OF ALLENE AND PROPYNE Y. Gleitman and Chava Lifshitz.	257
TAMP18	GAS PHASE STUDY OF NO+ COMPLEXES William D. Reents and Ben S. Freiser.	258
TAMP19	SUNLIGHT PHOTODEGRADATION OF PURIFIED POLYBROMINATED BIPHENYL(PBB) CONGENERS STUDIED BY GCMS D. G. Patterson, L. W. Yert, D. L. Orti, and J. S. Holler.	260
TAMP20	QUANTITATION OF HALOGENATED ORGANIC COMPOUNDS C. E. Parker and P. W. Albro , T. Cochran and J. Robinson.	262
TAMP21	THE DETERMINATION OF HEXACHLOROPENTADIENE AT THE ng/L LEVEL IN DRINKING WATER BY GC/MS Frank M. Benoit and David T. Williams.	263

Paper No. Page No.

TAMP22 WITHDRAWN

SYMPOSIUM ON STRUCTURES & ENERGETICS OF GASEOUS IONS

TPMOA1 TOWARDS A GENERAL METHOD FOR ESTIMATING THE HEATS FORMATION OF ORGANIC IONS IN THE GAS PHASE
John L. Holmes, M. Fingas, and F. P. Lossing. 264

TPMOA2 WITHDRAWN

TPMOA3 ANGLE RESOLVED MASS SPECTROMETRY: A NEW APPROACH TO ION STRUCTURE AND ENERGETICS
R. G. Cooks, P. H. Hemberger, J. L. Laramee, and A. Hubik. 265

TPMOA4 MOLECULAR SPECTROSCOPY OF GAS PHASE MOLECULAR IONS.
R. Claude Woods. 269

TPMOA5 STEREOCHEMICAL STRUCTURES OF MOLECULAR IONS DETERMINED THROUGH "COULOMB EXPLOSION" TECHNIQUES WITH FAST (MeV) MOLECULAR-ION BEAMS
D. S. Gemmell. 270

TPMOA6 SPECTROSCOPIC STUDIES OF OPEN-SHELL ORGANIC CATIONS IN THE GASEOUS PHASE
John P. Maier. 274

BIOLOGICAL/PHARMACOLOGY

TPMOB1 QUANTITATIVE ANALYSIS OF DISATURATED LECITHINS BY NH3-CIMS WITH A SOLIDS PROBE
A. L. Yergey, M. H. Kody, and N. L. Gershfeld. 275

TPMOB2 QUANTIFICATION OF ARABINITOL IN SERUM BY SELECTED ION MONITORING AS DIAGNOSTIC TECHNIQUE IN INVASIVE CANDIDIASIS
John Roboz, Robert Suzuki, Gail Schulman, and James Holland. 277

TPMOB3 GC/MS MEASUREMENT OF (15N2) UREA ENRICHMENT IN PLASMA AS 2-HYDROXYPYRIMIDINE TFA DERIVATIVE-APPLICATION IN QUANTITATIVE ESTIMATION OF UREA PRODUCTION IN HUMANS
Kou-Yi Tserng, Satish Kalhan, and Peter Adam. 278

TPMOB4 GC/MS ANALYSIS OF ORGANIC ACID IN RAT HEART MUSCLE
Shin-Ichi Haraguchi, H. Toshima, T. Kuhara, T. Shinka, and I. Matsumoto. 279

TPMOB5 QUANTITATION OF 6-HYDROXYMELATONIN BY GC-NEGATIVE CIMS
M. Tetsuo and S. P. Markey. 282

TPMOB6 QUANTITATION OF PHENOLS AND PHENOLIC ACIDS IN UREMIC SERUM USING GAS CHROMATOGRAPHY-MASS SPECTROMETRY
T. Niwa, T. Ohki, K. Maeda, A. Saito, and K. Kobayashi. 284

Paper No. Page No.

TPMOB7 PROFILING OF UREMIC ULTRAFILTRATE BY HIGH RESOLUTION GAS CHROMATOGRAPHY-MASS SPECTROMETRY
T. Niwa, K. Maeda, T. Ohki, A. Saito, and K. Kobayashi. 286

TPMOB8 GAS CHROMATOGRAPHY/MASS SPECTROMETRIC ANALYSIS OF ORGANIC ACIDS IN AMNIOTIC FLUID AND A COMPARISON WITH THOSE OF UMBILICAL CORD BLOOD AND THE FIRST NEONATAL URINE
K. Mitsutake, T. Shinka, T. Kuhara, I. Matsumoto, K. Kabashima, H. Abe, and T. Kato. 288

TPMOB9 OPTIMIZATION OF URINARY MASS PROFILING PROCEDURES TO OBTAIN GREATER RESOLUTION OF DONOR ATTRIBUTES
W. Aberth, J. C. Engels, A. Sheets, and B.E. Blaisdell. 290

TPMOB10 SELECTED-ION-MONITORING DETECTION OF ACETYLCHOLINE AND CHOLINE CONCENTRATION ALTERATIONS IN CAUDATE NUCLEUS ISOLATED IN SITU
Pat Haug, Manabu Suzuki, Jutta Moritz, Cordula Nitsch, Alan Wagner, R. Hassler and W. Wunn. 292

TPMOB11 STUDIES ON THE MECHANISM OF THE ENZYMATIC FORMATION OF GABA AND 2-PYRROLIDINONE FROM DELTA-1 PYRROLINE
P. S. Callery, L. A. Geelhaar, M. Stogniew, and M.S.B. Nayar. 294

TPMOB12 DISCRETE BRAIN AREA ACETYLCHOLINE CONCENTRATION UNALTERED BY EXPERIMENTALLY INDUCED EPILEPSY
Pat Haug, Wolfgang Wunn, Manabu Suzuki, Cordula Nitsch, B. Schmude, and Rolf Hassler. 295

TPMOB13 IDENTIFICATION AND QUANTITATION OF METHOTREXATE (MTX) METABOLITES IN ANIMALS AND PATIENTS RECEIVING HIGH-DOSE MTX BY HIGH-PRESSURE LIQUID CHROMATOGRAPHY AND FIELD DESORPTION MASS SPECTROMETRY
M. Przybylski, J. Preiss, and J. Fischer. 297

SOLIDS, LC/MS

TPMOC1 SIMS USING A CEC-110 ANALYZER
J.R.Wyatt, R.J. Colton, J.J. Decorpo, J. Campana and T. Barlak. 298

TPMOC2 ANALYTICAL APPLICATIONS OF MOLECULAR SIMS
S. E. Unger, R. J. Day, T. M. Ryan, L. Liu, and R. G. Cooks and K. Busch. 299

TPMOC3 STATIC SIMS WITH KINETIC ENERGY ANALYSIS
M. J. Vasile. 301

TPMOC4 ION MICROPROBE AND ION MICROSCOPE ANALYSIS OF PARTICULATES
D. S. Simons and D. E. Newbury. 303

TPMOC5 A SSMS NEAR SURFACE ANALYSIS OF B IN IRRADIATED ZIRCALOY-2: ION IMPLANTATION STANDARDS AS A CALIBRATION TECHNIQUE
W. H. Christie, J. A. Carter, R. E. Eby, L. Landau, and W. R. Musick. 305

TPMOC6. RAPID ANALYSIS OF INJECTED SOLUTION SAMPLES BY GLOW DISCHARGE MASS SPECTROMETRY
W. W. Harrison, P. J. Savickas, R. W. Marquis, and T. J. Loving. 306

Paper No. Page No.

TPMOC7 NEGATIVE IONS OF SPUTTERED COMPONENTS IN A GLOW DISCHARGE
W. W. Harrison and B. L. Bentz. 308

TPMOC8 AN LC-MS USING ION IMPACT
Richard D. Smith and James E. Burger. 310

TPMOC9 COMBINED LIQUID CHROMATOGRAPH-MASS SPECTROMETER FOR INVOLATILE BIOLOGICAL SAMPLES
Marvin L. Vestal, C. R. Blakley, and J. C. Carmody. 312

TPMOC10 ION PAIR REVERSED PHASE LIQUID CHROMATOGRAPHY MASS SPECTROMETRY
D. P. Kirby, B. L. Karger, Paul Vouros, B. Petersen, and B. Hidy. 314

TPMOC11 STUDIES OF PESTICIDES BY COMBINED LC/MS
David E. Games, Nakandalage C. A. Weerasinghe, and Steven A. Westwood. 316

TPMOC12 COMBINED LC/MS IN STUDIES OF NATURAL PRODUCTS
David E. Games, Christine Eckers, Wilhelm Kuhnz, and Emyr Lewis and M.L. Games. 318

TPMOC13 A NEW SOFT IONIZATION TECHNIQUE FOR MASS SPECTROMETRY OF COMPLEX MOLECULES
Marvin L. Vestal, C.R. Blakley, and J.C. Carmody 320

INSTRUMENTAL TECHNIQUES, CID/CA

TPMP1 CONSECUTIVE REACTIONS IN A REVERSED GEOMETRY MASS SPECTROMETER
J. H. Beynon, C. J. Proctor, B. Kralj, and J. Marsel. 322

TPMP2 HIGH-RESOLUTION MS/MS VIA MULTI-SECTOR MASS SPECTROMETERS
D. H. Russell, E. H. Mcbay, and T. R. Mueller. 323

TPMP3 TLC/CIMS: A THIN-LAYER CHROMATOGRAM SCANNER DIRECTLY COUPLED FOR CHEMICAL IONIZATION MASS SPECTROMETRY
Louis Ramaley, W. D. Jamieson, and R. G. Ackman. 324

TPMP4 THE ELECTRO-OPTICAL ION DETECTOR (EOID) - A COMPUTER-AGE DETECTOR FOR MASS SPECTROMETRY
R. A. Britten and R. Johansen and C. Griffin 326

TPMP5 A SIMPLE DFTPP INLET FOR ABUNDANCE TUNING A GC/MS
A. R. Rosecrance, M. E. Zinnecker, and B. N. Colby. 328

TPMP6 A REFERENCE COMPOUND FOR THE DETERMINATION OF RESOLVING POWER
Leonid Kelner and David Rosenthal. 329

TPMP7 A POWERFUL MULTISPECTROMETER DATA SYSTEM FOR LABORATORY APPLICATIONS
P. Powers, J. C. Bill, P. H. D'Arcy, and M. J. Wallington, J. Hopkinson. 331

TPMP8 ACCURACY OF MASS AND RELATIVE ABUNDANCE MEASUREMENT USING KRATOS MS-25S COUPLED TO THE BERKELEY LOGOS-II COMPUTER
F. C. Walls, R. Mcpherron, A. L. Burlingame, and J. D'Angona. 333

Paper No.		Page No.
TPMP9	A SENSITIVE FIELD IONIZATION QUADRUPOLE MASS SPECTROMETER Steve Young and S. E., Jr. Buttrill.	334
TPMP10	NEW INSTRUMENTATION FOR MS/MS G. L. Glish, D. Zakett, P. H. Hemberger, and R. G. Cooks.	335
TPMP11	A MICROCOMPUTER BASED FOURIER TRANSFORM MASS SPECTROMETER T. J. Buckley, R. J., Jr. Doyle, and John R. Eyler.	337
TPMP12	INFLUENCE OF ALIGNMENT ON THE PERFORMANCE OF ROUND ROD QUADRUPOLE MASS FILTERS Donald M. Mintz.	338
TPMP13	SOME OBSERVATIONS ON THE DETECTION AND AMPLIFICATIONS OF ION CURRENT SIGNALS William J. Fies.	340
TPMP14	MODIFICATION OF CEC 21-110 TO ALLOW FOR RAPID SCANNING G. J. Greenwood, J. F. Stewart, and D.D. M. Cantor.	341
TPMP15	THE INVERTED PENDULUM AS A MODEL OF THE QUADRUPOLE MASS FILTER A. L. Yergey, E. H. Seeliger, Leonid Kelner, J. E. Campana, and M. H. Friedman.	343
TPMP16	THE PERFORMANCE OF A FULLY LAMINATED MAGNET FOR AN INTEGRATED GC/MS/DS COMBINATION D. S. Millington, P. Burns, and B. N. Green.	345
TPMP17	A SIDE-ENTRY FIELD DESORPTION PROBE SYSTEM FOR A 21-110 MASS SPECTROGRAPH T. J. Eskew, L. F. Herzog, Douglas F. Barofsky, and William R., Jr. Anderson.	347
TPMP18	ADVANTAGES OF "MULTI-RADIUS" MAGNETIC MASS SPECTROMETERS FOR RAPID SCANNING APPLICATIONS D. J. Marshall and L. F. Herzog.	349
TPMP19	RECENT APPLICATIONS OF A TANDEM DOUBLE-FOCUSING MASS SPECTROMETER M. P. Barbalas, P.J. Todd, F. P. Pagano, R. F. Pegues, and Fred W. Mclafferty.	351
TPMP20	METASTABLE SPECTRA OF COMPLEX MIXTURES: LINKED SCAN TECHNIQUES APPLIED TO PHARMACEUTICAL FINAL PRODUCT IDENTIFICATION TESTING Wayne K. Duholke and Lloyd E. Fox.	353
TPMP21	APPLICATIONS OF MIKES AND MIKES-CID ON SMALL SYSTEMS Andreas J. Illies, Shuying Liu, and M. T. Bowers.	355
TPMP22	STRUCTURAL STUDIES OF $C_2H_3O^+$ AND $C_3H_5O^+$ IONS BY COLLISION-INDUCED DISSOCIATION Thomas A. Lehman, J. R. Hass, and Maurice M. Bursey.	356
TPMP23	MASS ANALYZED ION KINETIC ENERGY SPECTROSCOPY AS A TOOL FOR THE DETERMINATION OF THE STEREOCHEMISTRY OF RING JUNCTIONS IN STEROID STEREOISOMERS Ze'Ev V. I. Zaretskii, Edmund A. Larka, I. Howe, and J. H. Beynon.	358

Paper No. Page No.

ENVIRONMENTAL

WAMOA1 UTILITY OF GC/MS SYSTEMS IN SEVERAL CONFIRMATORY PROCEDURES OF FORENSIC TOXICOLOGY
Thomas V. Briggle, Ana Barquet, Carmen Morgade, and Carl D. Pfaffenberger. 360

WAMOA2 MASS SPECTRAL IDENTIFICATION OF IMPURITIES IN PHENAZOPYRIDINE HYDROCHLORIDE
David L. Heikes and Donald L. Myers. 362

WAMOA3 ANALYSIS OF N-NITROSODIETHANOLAMINE (NDELA) IN COSMETICS, SHAMPOOS, AND RAW MATERIALS BY GAS CHROMATOGRAPHY-MASS FRAGMENTOGRAPHY
Birendra N. Pramanik and Aaron D. Cooper. 364

WAMOA4 USE OF GC/MS AND DEUTERIUM OXIDE TO DIFFERENTIATE BETWEEN CHLOROFORM AND DERIVED CHLOROFORM IN HUMAN BLOOD SERUM
Carl D. Pfaffenberger, Anita J. Peoples, and Thomas V. Briggle. 366

WAMOA5 MASS SPECTROMETRIC ANALYSIS OF HIGH MOLECULAR WEIGHT ORGANIC POLLUTANTS
Lorne M. Isabelle, James F. Pankow, and Douglas Barofsky 368

WAMOA6 EVOLVED GAS ANALYSIS OF COAL FLY ASH BY MASS SPECTROMETRY
M. R. Schure, P. W. Ryan, M. R. Sine, and D. F. S. Natusch. 370

WAMOA7 GC/MS ANALYSIS OF AEROSOLS FORMED FROM DIESEL EXHAUST
John G., Jr. Windsor, Sandy P. Parks, and Michael L. Barnes. 372

WAMOA8 MIKE SPECTRA OF ORGANOPHOSPHINES INSECTICIDES DESORBED FROM SOIL
A. Vincze, P. Bel, and L. Gefen. 374

WAMOA9 A COMPARISON OF NEGATIVE IONIZATION- AND ELECTRON IMPACT-MS FOR ANALYSIS OF TOXAPHENE-LIKE RESIDUES IN THE ENVIRONMENT
G. R. Dubay, D. L. Stalling, M. A. Ribick, J. D. Petty, and C. Rappe 376

WAMOA10 USE OF GC/MS WITH POSITIVE/NEGATIVE ION C.I. AND LOW RESOLUTION ACCURATE MASS ASSIGNMENT TO IDENTIFY IMPURITIES IN A PERHALOGENATED FIRE RETARDANT
W. D. Jamieson, C. G. Flinn, and V. Zitko. 378

WAMOA11 APPLICATIONS OF THE ELECTRO-OPTICAL ION DETECTOR MASS SPECTROMETER
Heinz Boettger 380

WAMOA12 DETECTION OF PCP'S AND CHLORO-PESTICIDES IN HUMAN FAT BY GC/MS
Uwe Rapp, G. Dielmann, and E. Schulte 381

WAMOA13 DEVELOPMENT OF A MASTER SCHEME FOR THE ANALSIS OF ORGANIC COMPOUNDS IN WATER
E. Pellizzari, K. Tomer, J. Bursey, L. S. Sheldon, L. C. Michael, S. L. Yung, R. W. Wiseman, J. F. Ryan, J. Gebhart, L. Rando, and A. W. Garrison 382

Paper No. Page No.

BIOCHEMISTRY

WAMOB1 HIGH RESOLUTION MASS SPECTROMETRY OF tRNA HYDROLYSATES
H. Pang and James A. Mccloskey. 384

WAMOB2 QUANTITATION OF CYTOKININS BY GC-MS-SIM
Brenda Basile, James A. Mccloskey, and Takeshi Hashizume. 386

WAMOB3 FIELD DESORPTION MASS SPECTROMETRY OF OLIGOPEPTIDES
Douglas F. Barofsky, Terry D. Lee, Elisabeth Barofsky, William R., Jr. Anderson, and G. Doyle, Jr. Daves. 388

WAMOB4 POLYPEPTIDE SEQUENCING USING NICI AND MS/MS
Mary Sisak, Donald F. Hunt, John M. Ballard, Alexander M. Buko, Anne B. Giordani, and Jeffrey Shabanowitz. 390

WAMOB5 GAS CHROMATOGRAPHY/MASS SPECTROMETRY CHARACTERIZATION OF MANNANS DERIVED FROM MEDICALLY SIGNIFICANT YEASTS
L. W. Yert, E. Reiss, D. G. Patterson, B. K. Ibrahim, and J. S. Holler. 392

WAMOB6 STRUCTURE ELUCIDATION OF SLOW REACTING SUBSTANCE AND SLOW REACTING SUBSTANCE OF ANAPHYLAXIS
H.R. Morris, C.W. Taylor, P.J. Piper, J.R. Tippins and M.N. Samhoun. 394

WAMOB7 USE OF CARBOXYL 18O-LABELLED SPECIES IN EICOSANOID RESEARCH
R. C. Murphy, R. Mathews, and W. C. Pickett. 396

WAMOB8 CHEMICAL IONIZATION SELECTED-ION-MONITORING MASS SPECTROMETRIC ANALYSIS OF DEUTERIUM TRIPLE-LABELED BLOOL LIPIDS
William K. Rohwedder. 397

WAMOB9 THE FIRST DEMONSTRATION OF AVENASTEROL IN HUMAN PLASMA
D. M. Desiderio, J. Z. Sabbatini, J. Ragland, and G. Whittington. 398

WAMOB10 RAPID SIMULTANEOUS ASSAY OF SERUM ESTRONE (E1), ESTRADIOL (E2), AND ESTRIOL (E3) USING METHYL ETHER ACETATE (MEA) DERIVATIVES ON CAPILLARY GC-EI-MS
Kou-Yi Tserng, Robert K. Danish, and Juliana S. Bendt. 400

WAMOB11 COMPUTERIZED GAS CHROMATOGRAPHY MASS FRAGMENTOGRAPHIC ANALYSIS OF LITHOCHOLIC ACID IN LIVER TISSUE
Izumi Maruyama, R. Kumashiro, K. Tanikawa, T. Shinka, T. Kuhara, and I. Matsumoto. 401

WAMOB12 GC-MS IDENTIFICATION OF THE FECAL BILE ACIDS OF ALLIGATOR MISSISSIPPIENSIS, AN ANIMAL MODEL FOR HUMAN BILE ACID BIOSYNTHESIS
G. S. Tint, B. Dayal, A. K. Batta, S. Shefer, and G. Salen. 403

WAMOB13 CHEMICAL IONIZATION MASS SPECTROSCOPIC APPROACH TO STRUCTURE DETERMINATION OF METABOLITES
A. K. Bose and B. Pramanik. 405

WAMOB14 MASS SPECTRAL FRAGMENTATION OF STEROIDAL TRIENES GENERATED IN SITU
J. R. Dias. 407

Paper No. Page No.

STRUCTURES & ENERGETICS OF IONS

WAMOC1 THE GAS-PHASE HEATS OF FORMATION OF KETO AND ENOL IONS OF CARBONYL COMPOUNDS
F. P. Lossing and John L. Holmes. 409

WAMOC2 THE STRUCTURE OF THE GAS PHASE ION C6H5+
Chava Lifshitz, D. Gibson, and K. Levsen. 410

WAMOC3 STRUCTURES OF SMALL POSITIVE IONS: C3H5+ AND C2H4N+
M. T. Bowers, Shuying Liu, P. A. M. Kemper, Andreas J. Illies, H. Webb, D. H. Aue, R. Stradling, K. R. Jennings, and J. R. Gilbert. 411

WAMOC4 ION STRUCTURES, REARRANGEMENTS AND ENERGY PARTITIONING IN [ALKANE]+. FRAGMENTATIONS
John L. Holmes, Y. Mollah, J. K. Terlouw, and P. C. Burgers. 412

WAMOC5 REACTIONS OF TRANSITION METAL CONTAINING IONS WITH ALKANES
Douglas P. Ridge. 413

WAMOC6 THE THERMOCHEMISTRY AND DISSOCIATION DYNAMICS OF STATE SELECTED THIOPHENE IONS
James J. Butler and T. Baer. 415

WAMOC7 INTERCONVERSION OF IONIC STRUCTURES: NITROMETHANE AND METHYLNITRITE IONS
G. G. Meisels, Ta-Cheng Hsieh, Morris J. Weiss, and J. P. Gilman. 418

WAMOC8 THE STRUCTURE AND STABILITY OF ALKALI HALIDE MOLECULES AND IONS
Joseph Berkowitz, G. L. Goodman, and C. H. Batson. 420

WAMOC9 *LASER INDUCED DISSOCIATION OF POSITIVE AROMATIC IONS*
J. H. Beynon, E. S. Mukhtar, I. W. Griffiths, and F. M. Harris. 422

WAMOC10 REARRANGEMENTS OF DIENE RADICAL CATIONS USING PHOTODISSOCIATION SPECTROSCOPY
Robert C. Dunbar and G. B. Fitzgerald. 423

WAMOC11 CHLORIDE AFFINITIES & HEATS OF FORMATION OF SUBSTITUTED BENZYL CATIONS OBTAINED FROM MEASUREMENTS OF CHLORIDE TRANSFER EQUILIBRIA
P. Kebarle, D. K. Sen Sharma, and K. Hiraoka. 424

WAMOC12 THEORY FOR PREDICTING STRUCTURES OF INTERMEDIATE COMPLEXES OF IONIC CYCLOADDITIONS
J. O. Lay and M. L. Gross. 425

WAMOC13 PROTON-TRANSFER REACTIONS, HYDRO-EXCHANGE REACTIONS AND PROTON-TRANSFER/HYDROGEN-EXCHANGE REACTIONS
MIchael J. Henchman, D. Smith and N. G. Adams 427

WAMOC14 PREDICTION OF PROTON AFFINITIES OF AROMATIC MOLECULES
D. A. Herold, T. A. Elwood, J. O. Johnson, and J. H. Futtrell. 428

Paper No. Page No.

SOLIDS, FOSSIL FUELS, BIOMEDICAL

WAMP1 WITHDRAWN

WAMP2 STUDIES OF ALKALI HALIDES BY THERMAL IONIZATION AND CHARGE-TRANSFER NEGATIVE IONIZATION IN A CHEMICAL IONIZATION SOURCE
J. R. Lloyd and F. H. Field. 430

WAMP3 KINETICS OF THERMAL DESORPTION AND PHASE TRANSFORMATION OF AMORPHOUS CARBON FILMS
Margaret A. Frisch and Joyce A. Thompson. 431

WAMP4 NEW SOFTWARE STRATEGIES FOR HIGH PRECISION SOLID SAMPLE ISOTOPE ANALYSIS. THE MAT 261
K. Habfast and H. Ravens. 432

WAMP5 THE DETERMINATION OF BERYLLIUM IN AMBIENT AIR PARTICULATE BY SPARK SOURCE MASS SPECTROMETRY
E. Hunter Daughtrey, Jr. & J. Kent Bostick, Jr. 433

WAMP6 SIMS SPECTRA OBTAINED FROM NBS 660 STEEL BOMBARDED BY CAESIUM+ IONS
Marcel Baril. 435

WAMP7 CHLOROETHYLNITROSOUREA QUANTITATION WITH GAS CHROMATOGRAPHY MASS SPECTROMETRY
R. J. Weinkam and T. Y. Liu. 437

WAMP8 SELECTED ION MONITORING CAPILLARY COLUMN GLC-MS ASSAY FOR TIMOLOL AND 13C3-TIMOLOL IN HUMAN PLASMA
Josephine R. Carlin, R.W. Walker, R.O. Davies, R.F. Ferguson, and W.J.A. Vandenheuvel 438

WAMP9 GC-MS QUANTITATION OF IMPURITIES IN IMIPRAMINE AND DISIPRAMINE STANDARDS AND PHARMACEUTICAL FORMULATIONS
J. Saady, N. Narasimhachari and R.O. Friedel 439

WAMP10 WITHDRAWN

WAMP11 POTENTIAL GABA PRECURSORS: SYNTHESIS OF DEUTERIUM LABELED L-GLUTAMINE AND 4-AMINOBUTANAMIDE
M. Stogniew, L. A. Geelhaar, and P. S. Callery. 441

WAMP12 SIMULTANEOUS QUANTITATION OF PHENYTOIN, ITS PARA-HYDROXYLATED METABOLITE, AND THEIR STABLE ISOTOPE LABELLED ANALOGS BY GC-MS: DEVELOPMENT AND APPLICATIONS OF THE METHOD
Agnes Van Langenhove, C. E. Costello, J. E. Biller, K. Biemann, and T. R. Brown. 442

WAMP13 REDUCTIVE METABOLISM OF FURAZOLIDONE IN THE RAT
J. Cohen, R. Abraham, B. Dixit, J. Knapp, L. Wong & J. Alvin 444

WAMP14 SELECTED-ION-MONITORING EVIDENCE THAT ACETYLCHOLINE IS NOT A CORTICOSTRIATAL NEUROTRANSMITTER
P. Haug, N. Schroder, J. Kim, and R. Hassler 446

Paper No. Page No.

WAMP15 PLASMA DESORPTION MASS SPECTROMETRY OF UNDERIVATIZED METABOLITES OF CARBAMAZEPINE AND IMINOSTILBENE
M. G. Horning, K. Lertratanangkoon, and J. Nowlin. 448

WAMP16 IDENTIFICATION AND MASS SPECTRAL CHARACTERIZATION OF A DEETHYLATED PROCAINAMIDE METABOLITE
T. I. Ruo and J. P. Thenot. 449

WAMP17 MASS SPECTROMETRIC STUDIES ON IMPORTANT NEUROPEPTIDES
H. R. Morris, A. Dell, and M. Judkins. 450

WAMP18 GAS CHROMATOGRAPHIC MASS SPECTROMETRIC SEQUENCING OF PEPTIDES AND PROTEINS CONTAINING Y-CARBOXYGLUTAMIC ACID
S. A. Carr and K. Biemann. 452

WAMP19 PYROLYSIS OF POLYESTERS
F. Messier and D. C. DeJongh 454

WAMP20 PREPARATION OF DEUTERATED 4-HYDROXY-3-METHOXYMANDELIC ACID
Kym F. Faull and Jack D. Barchas. 455

WAMP21 GC-MS QUANTITATION OF SEVERAL NITROGEN HETEROCYCLES IN SOLVENT REFINED COAL
K. L. Richie, L. R. Hilpert, J. M. Brown, F. R. Guenther, and H. S. Hertz. 456

WAMP22 AN INVESTIGATION OF THE PYROLYSIS OF A COMPOSITE GREEN RIVER OIL SHALE BY TGA-MS AND FAST-SCANNING PY-MS
L. H. Wojcik, David L. Pope, L. R. Frank, C. Greenwalt, Henk L. C. Meuzelaar, and J. H. Futtrell. 458

WAMP23 RAPID CHARACTERIZATION OF COAL SAMPLES BY PYROLYSIS MASS SPECTROMETRY
Henk L. C. Meuzelaar, Ralph E. Wood, J. H. Futtrell, and L. H. Wojcik. 460

CID/CA

RAMOA1 GAS PHASE ION STRUCTURES BY IN-SOURCE TRAPPING/COLLISIONAL ACTIVATION MASS SPECTROMETRY
M. A. Rudat and C. N. Mcewen. 462

RAMOA2 ISOMERIZATION REACTIONS IN METASTABLE C4H6O7+ IONS
P. C. Burgers, John L. Holmes, and J. K. Terlouw. 464

RAMOA3 IDENTIFICATION OF THE STRUCTURAL ELEMENTS OF ORGANIC IONS BY TRIPLE QUADRUPOLE MASS SPECTROMETRY
R. K. Latven, B. Newcome, and Chris Enke. 465

RAMOA4 FIELD DESORPTION/COLLISION-INDUCED DISSOCIATION (FD/CID) MASS SPECTROMETRY OF DINUCLEOSIDE PHOSPHATES
A. L. Burlingame and M. Linscheid. 467

RAMOA5 APPLICATION OF MS/MS TECHNIQUES TO THE IDENTIFICATION OF POLYCYCLIC AROMATIC HYDROCARBON METABOLITES
Gary Mcclusky, Shing-Kwan Huang, and James K. Selkirk. 469

RAMOA6 DETERMINATION OF PYRROLIZIDINE ALKALOIDS IN RANGE PLANTS BY LINKED FIELD B2/E SCANS
William F. Haddon and Russel J. Molyneux. 472

Paper No. Page No.

RAMOA7 DISTINGUISHING ISOMERIC FRAGMENT IONS FROM PENICILLINS BY COLLISIONAL ACTIVATION
J. L. Occolowitz, M. P. Barbalas, and Fred W. Mclafferty. 474

RAMOA8 ANALYTICAL APPLICATIONS OF TRIPLE STAGE QUADRUPOLE MASS SPECTROMETRY
Anne B. Giordani, Donald F. Hunt, and Jeffrey Shabanowitz. 476

RAMOA9 SIMPLIFIED "TRIPLE QUADRUPOLE" FOR MS-MS
M. W. Siegel. 478

RAMOA10 A TANDEM DOUBLE-FOCUSING MASS SPECTROMETER FOR GAS-PHASE ION STUDIES
P. J. Todd, D. C. Mcgilvery, M. A. Baldwin, and Fred W. Mclafferty. 481

HIGH MASSES

RAMOB1 MASS SPECTRAL STUDY OF RAPIDLY HEATED POLYSTYRENE
H. R. Udseth and L. Friedman. 483

RAMOB2 PHOSPHAZENE MIXTURES: REFERENCE COMPOUNDS FOR CHEMICAL IONIZATION AS WELL AS FIELD DESORPTION MASS SPECTROMETRY
Charles R., Jr. Snelling, Richard M. Milberg, J. Carter, Jr. Cook, and Kenneth L., Jr. Rinehart. 484

RAMOB3 CHARACTERIZATION OF ANILINE-ACETONE CONDENSATION PRODUCTS BY LIQUID CHROMATOGRAPHY AND MASS SPECTROSCOPY
Robert P. Lattimer, E. Ray Hooser, and Paul M. Zakriski. 486

RAMOB4 POLYMER CHARACTERIZATION BY ELECTROHYDRODYNAMIC IONIZATION MASS SPECTROMETRY
Kelsey D. Cook, S.-T. F. Lai, and K. W. Chan. 488

RAMOB5 A GENERAL METHOD FOR ACQUISITION OF LOW INTENSITY MASS SPECTRA AT VERY HIGH MASS
Woodfin V., Jr. Ligon. 490

RAMOB6 HIGH MASS FIELD DESORPTION STUDIES OF BIOLOGICALLY IMPORTANT MOLECULES
A. Dell, R. A. Mcdowell, and H. R. Morris. 493

RAMOB7 FIELD DISORPTION (FD) & FIELD DESORPTION/COLLISION-INDUCED DISSOCIATION (FD/CID) MS OF MICROBACTERIAL POLYSACCHARIDES
J. D'Angona, M. Linscheid, A. L. Burlingam, H. Yamada, C. E. Ballou and A. Dell 495

RAMOB8 FORMATION OF COMPLEXES WITH MULTIVALENT IONS AS A MEANS OF EXTENDING THE MASS SCALE IN FDMS
Gordon W. Wood and Wing Fung Sun. 497

Paper No. Page No.

IONIZATION PROCESSES

RAMOC1 KINETIC ENERGY RELEASE IN DISSOCIATIVE ELECTRON CAPTURE PROCESSES OF SULFURYL HALIDES
J. L. Franklin and Jia-Shen Wang. 499

RAMOC2 TIME RESOLVED APPEARANCE POTENTIALS AND BREAKDOWN CURVES BY TRAPPED ION MASS SPECTROMETRY
Chava Lifshitz. 500

RAMOC3 SELF-SCAVENGING OF ELECTRONS IN METHYL IODIDE
Cornelius S. Klots and R. N. Compton. 502

RAMOC4 PHOTOELECTRON-PHOTOION COINCIDENCE STUDY OF THE BROMOBENZENE ION
Roger Stockbauer, Henry Rosenstock, and Albert C. Parr. 504

RAMOC5 TRIPLY DIFFERENTIAL PHOTOIONIZATION STUDIES OF SMALL MOLECULES
Albert C. Parr, Roger Stockbauer, J. L. Dehmer, B. E. Cole, D. L. Ederer, and John B. West. 505

RAMOC6 RECENT PHOTOELECTRON-PHOTOION COINCIDENCE STUDIES ON BENZONITRILE AND PYRIDINE FRAGMENTATION
Henry Rosenstock, Roger Stockbauer, and Albert C. Parr. 506

RAMOC7 TWO-LASER MULTIPHOTON DISSOCIATION OF IODOBENZENE CATION
J. D. Hays, J. P. Honovich, N. B. Lev, and Robert C. Dunbar. 507

RAMOC8 TRANSMISSION CHARACTERISTICS OF COLLIMATED HOLE THRESHOLD PHOTOELECTRON DETECTORS
Peter M. Hierl, Ta-Cheng Hsieh, J. P. Gilman, Morris J. Weiss, and G. G. Meisels. 508

RAMOC9 MULTIPLE TRANSITION STATES IN ION-MOLECULE REACTIONS; A UNIFIED STATISTICAL THEORY APPROACH
M. T. Bowers, Walter J. Chesnavich, and Lewis Bass. 510

RAMOC10 THE COINCIDENCE SPECTRUM FOR LOSS OF ACETIC ACID FROM 2-BUTYL ACETATE AND THE INLET TEMPERATURE DEPENDENCE OF THE STEREOSELECTIVITY FOR THAT LOSS
Mark Green, Richard McCluskey, Loyd Bumm, and Jurgen Vogt. 511

RAMOC11 FLUORESCENCE EXCITATION SPECTRA OF IONS AND NEUTRAL FRAGMENTS OF MOLECULES BY PHOTON IMPACT
I. Nenner, A. Tabche-Fouhaile, K. Ito, H. Frolish, P. Morin, and P. M. Guyon. 512

Paper No. Page No.

SYMPOSIUM ON SYNTHESIS OF STABLE ISOTOPE LABELLED COMPOUNDS FOR MASS SPECTROMETRY

RAMP1 SYNTHESIS OF HIGH ISOTOPIC PURITY 2H3-LABELED STANDARDS FOR THE MASS SPECTRAL QUANTITATION OF ESTRADIOL AND ESTRONE
Ian J. Massey and L. Tokes. . . . . .

RAMP2 SYNTHESIS OF DEUTERATED OCTADECENOIC ACID POSITIONAL AND GEOMETRIC ISOMERS
William K. Rohwedder, E. A. Emken, R. O. Adlof, W. J. Dejarlais, and H. Rakoff. 516

RAMP3 SYNTHESIS OF PUTATIVE PRECURSORS OF SECONDARY PRODUCTS LABELED WITH STABLE ISOTOPES (CARBON-13 AND NITROGEN-15)
Edward Leete, Jim Mcdonell, Joe Porwoll, and Ming-Li Yu. 517

RAMP4 SYNTHESIS OF STABLE ISOTOPE ANALOGS OF BIOGENIC AMINES
S. P. Markey, W.J.W. Mayer, and J. Oliver. 519

RAMP5 BIOSYNTHESIS WITH FULLY DEUTERATED MICROORGANISMS
Henry L. Crespi. 521

RAMP6 ORGANIC SYNTHESIS WITH STABLE ISOTOPES: AMINO ACIDS
T. W. Whaley. 523

RAMP7 BIOSYNTHESIS WITH STABLE ISOTOPES: ALGAL SYSTEMS
Victor H. Kollman. 524

RAMP8 REGIOSPECIFIC SYNTHESIS OF THE PYRIMIDINE RING
Richard H. Griffey, John L. Roberts, and C. Dale Poulter. 526

RAMP9 SURVEY OF STABLE ISOTOPE LABELED MATERIALS AVAILABLE FOR USE IN CONNECTION WITH MASS SPECTROMETRY
J. C. Bradley, A.M. Ajami, and S.S. Yuan. 528

RAMP10 ISOTOPICALLY-ENRICHED CARBOHYDRATES: SYNTHESIS AND USE IN CHEMICAL AND BIOCHEMICAL STUDIES
A.S. Serianni, H.A. Nunez, J. Pierce, P.R. Rosevear, E.L. Clark, and R. Barker. 529

RAMP11 THE PREPARATION OF SOME C-DEUTERATED CARBOHYDRATES BY CATALYTIC EXCHANGE
H.J. Koch. 530

SYMPOSIUM ON FORENSIC APPLICATIONS OF MASS SPECTROMETRY

RPMOA1 MASS SPECTROMETRY IN FORENSIC TOXICOLOGY AND DRUG ANALYSIS
Michael J. Whitehouse and L. V. Jones. 531

RPMOA2 GAS CHROMATOGRAPHY-MASS SPECTROMETRY, AN ESSENTIAL TECHNIQUE IN MEDICO-LEGAL INVESTIGATION
Bryan S. Finkle. 535

RPMOA3 APPLICATION OF GAS CHROMATOGRAPHY/MASS SPECTROMETRY TO PROBLEMS IN FORENSIC DRUG ANALYSIS
George F. Yamnitzky and Jeffrey M. Weber. 536

RPMOA4 DISCRIMINATING BETWEEN METHAMPHETAMINE AND PHENTERMINE BY CHEMICAL IONIZATION-MASS SPECTROMETRY
Steven K. Lorch and John D. Snyder. 537

Paper No. Page No.

RPMOA5 MASS SPECTRAL COMPARISON OF DIPHENETHYLAMINES OF FORENSIC INTEREST
T. C. Kram. 538

RPMOA6 PYROLYSIS MASS SPECTROMETRY IN FORENSIC SCIENCE
Ian Jane 540

RPMOA7 GUNPOWDER ANALYSIS BY MASS SPECTROMETRY
D. R. Hardy. 544

RPMOA8 THE TOXICOLOGICAL ANALYSIS OF DRUGS IN RACEHORSE URINE USING TLC-GC/MS
Jack D. Henion and G. A. Maylin. 546

RPMOA9 GC/MS OF ALKYLATED ACIDS IN TOXICOLOGY
D. E. Gallis, J. A. Rudy, and C. B. Woodward. 550

RPMOA10 THE DEVELOPMENT OF AN ANALYSIS FOR 9-THC IN BLOOD
Michael P. Mcgee, C. Valentour, and Randall P. Edwards. 552

PHARMACOLOGY

RPMOB1 STEROID PROFILES OF HEALTHY INDIVIDUALS
Gerhard Spiteller, Peter Pfeifer, and Josef Reiner. 554

RPMOB2 STERIOD PROFILES IN CHRONIC DISEASES
G. Spiteller, P. Pfeifer, J. Reiner, & H.-J. Egger 556

RPMOB3 PLASMA LEVELS OF FENTANYL IN DOGS BY GAS CHROMATOGRAPHY-MASS SPECTROMETRY
Shen-Nan Lin, Tseng-Pu F. Wang, Richard M. Caprioli, and Benjamin P. O. Mo. 558

RPMOB4 FORMYLATION OF SECONDARY AMINES WITH DIMETHYLFORMAMIDE DIMETHYLACETAL
J. P. Thenot, T. I. Ruo, and O. J. Bouwsma. 559

RPMOB5 ANALYSIS OF THE ANTICANCER DRUG METHYL-G BY GAS CHROMATOGRAPHY AND MASS SPECTROMETRY
Carl Johann Nielsen, Sylvia K. Daley, and Jon N. Peace. 560

RPMOB6 GC-MS STUDIES OF PHENELZINE AND ITS ACYL DERIVATIVES
N. Narasimhachari and R. O. Friedel. 562

RPMOB7 A SELECTED ION RECORDING GCMS-TECHNIQUE USED IN BIOAVAILABILITY STUDIES OF ETILEFRINE
H.-J. Forster and K. L. Rominger. 564

RPMOB8 AN IMPROVED GC-MS METHOD TO MEASURE TELEMETHYLHISTAMINE IN RAT BRAIN
J. K. Khandelwal, Lindsay B. Hough, and Jack Peter Green. 566

RPMOB9 DEVELOPMENT OF PRECISE QUANTITATIVE METHODS FOR USE IN CLINICAL CHEMISTRY
J. S. Holler, D. G. Patterson, and L. W. Yert. 567

Paper No. Page No.

RPMOB10 NEGATIVE ION CHEMICAL IONIZATION MASS SPECTROMETRY AS A STRUCTURAL TOOL IN THE DETERMINATION OF THE MAJOR METABOLITES OF PROBUCOL IN THE MONKEY
John Coutant, Ester Madrid Bargar, and Robert Barbuch. 568

RPMOB11 MASS SPECTROMETRY AND CHEMISTRY OF REDUCED PYRIMIDINE NUCLEOSIDES AND RELATED ANALOGUES
J. A. Kelley, V. E. Marquez, P. S. Liu, and J. S. Driscoll. 569

RPMOB12 A RAPID METHOD FOR DETECTION OF VITAMIN B_{12} AND FOLIC ACID DEFICIENCY BY GCMS
E.J. Norman, H.K. Berry, O.J. Martello & M.D. Denton 570

RPMOB13 THE STUDY OF THEOPHYLLINE METABOLISM IN PREMATURE INFANTS USING GC/MS
Kou-Yi Tserng, K. C. King, F. N. Takieddine, and Peter Adam. 571

ION MOLECULE REACTIONS

RPMOC1 REACTIONS OF ORGANIC ANIONS WITH ORGANOMETALLIC COMPOUNDS
S. A. Sullivan and C. H. Depuy. 572

RPMOC2 ON THE FORMATION OF ANIONIC CLUSTER IONS FROM DIETHYL ETHER AND ETHYL VINYL ETHER UNDER ICR CONDITIONS
K. R. Jennings and R. Van Doorn. 574

RPMOC3 BIMOLECULAR CLUSTERING OF ALCOHOLS WITH ALKOXIDES
John E. Bartmess and G. Caldwell. 576

RPMOC4 REACTIONS OF ANIONS WITH ALKYL NITRITES IN THE GAS PHASE
Gary K. King, M. Matti Maricq, and C. H. Depuy. 577

RPMOC5 EXCESS ENERGY AND FRAGMENTATION IN 1,3-DITHIANES AND 1-3, DITHIOLANES
J.E. Bartmess, R.L. Hays and S.R. Wilson 579

RPMOC6 REACTIONS OF Fe(CO)5 NEGATIVE IONS WITH ACTIVATED OLEFINS
Gary H. Weddle and Douglas P. Ridge. 580

RPMOC7 A LOW PRESSURE STUDY OF THE REACTION CH3+ + HCN = CH3.HCN+; A CASE FOR RADIATIVE ASSOCIATION
V. G. Anicich, W. T. Huntress, M. J. Mcewan, P. R. Kemper, and M. T. Bowers. 582

RPMOC8 EFFECTS OF SOLVATION ON INTRAMOLECULAR HYDROGEN BONDING
M. Mautner, E. P. Hunter, P. Hamlet, and F. H. Field. 583

RPMOC9 ION CHEMISTRY OF METHYLFLUOROPHOSPHINES AND PHOSPHORANES
J. Radtke, K.-P. Wanczek, and H. Hartmann. 584

RPMOC10 STUDIES IN NEUTRALIZED ION BEAM SPECTROSCOPY (ENERGETICS OF HIGHLY UNSTABLE NEUTRALS)
Brian Wesley Williams, Paul M. Curtis, and Richard F. Porter. 586

RPMOC11 ION-MOLECULE REACTIONS OF THIIRANE AND ITS MIXTURE WITH AMMONIA. ION STRUCTUR DETERMINATION WITH ICR.
K.-P. Wanczek, G. Baykut, and H. Hartmann. 587

Paper No. Page No.

RPMOC12 THE REACTIONS OF ELECTRONICALLY EXCITED O+ IONS
B. Rowe, D. W. Fahey, F. C. Fehsenfeld, and D. L. Albritton. 589

RPMOC13 KINEMATICS OF AR+ + H2O COLLISIONS: CHARGE TRANSFER (H2O+) AND CHEMICAL REACTION (ARH+)
Z. Herman and J. Glosik. 590

DESORPTION, TCDD, LC/MS

RPMP1 MASS SPECTROMETRY CONFIRMATION AND QUANTIFICATION OF 2,3,7,8-TETRACHLORODIBENZO-P-DIOXIN (TCDD) RESIDUES IN FRESH WATER FISH
R. L. Harless and R. G. Lewis. 592

RPMP2 EVALUATION OF COMMERCIALLY AVAILABLE CAPILLARY COLUMNS AND CHROMATOGRAPHIC CONDITIONS FOR THE ANALYSIS OF SPECIFIC TETRACHLORODIBENZO-P-DIOXIN ISOMERS
B. Mason Hughes, J. R. Troost, J. F. Ryan, and Aubry E. Dupuy. 594

RPMP3 ANALYSIS OF TCDD USING METASTABLE AND COLLISIONAL ACTIVATION METHODS
E. K. Chess, F. W. Crow, P. A. Lyon, and M. L. Gross. 596

RPMP4 DEVELOPMENT OF METHODOLOGY AND INSTRUMENTATION FOR THE DETERMINATION OF CHLORODIOXINS IN ENVIRONMENTAL SAMPLES BY CAPILLARY-LOW RESOLUTION MASS SPECTROMETRY
G. F. Vanness, J. G. Solch, M. L. Taylor, and T. O. Tiernan. 598

RPMP5 IMPROVED SIGNAL AVERAGING SYSTEM FOR HIGH RESOLUTION SELECTED ION MONITORING DETECTION OF TETRACHLORODIBENZO-P-DIOXINE (TCDD'S)
F. L. Deroos and L. E. Slivon. 600

RPMP6 QUANTITATION OF TCDD'S IN ENVIRONMENTAL SAMPLES USING HIGH RESOLUTION MULTIPLE ION DETECTION
Mark Weiss, D. J. Harvan, and J. R. Hass. 602

RPMP7 TG-MS STUDY OF THE VACUUM THERMAL DEGRADATION OF THE PBT AND PBO RIGID ROD POLYMER SYSTEMS
E. Grant Jones, James M. Pickard, Donald L. Pedrick, and Ivan J. Goldfarb. 603

RPMP9 PYROLYSIS MASS SPECTROMETRY OF MACROMOLECULAR BIOMATERIALS
J. Haverkamp, W. Eshuis, and P. M. M. Van Haard. 604

RPMP10 DETERMINATION OF VOLATILE CONSTITUENTS OF INSTALLED POWER CABLE BY GC/MS
M. S. Miller, R. W. Morrow, E. T. Creech, T. R. Oldham, and C. C. Wright. 606

RPMP11 APPLICATIONS OF THE BALDWIN-MCLAFFERTYLC/MS INTERFACE TO THE ANALYSIS OF MOLECULES OF BIOCHEMICAL IMPORTANCE
Christine N. Kenyon. 608

RPMP12 SIMPLE INTERFACE PROBE FOR LC/MS
P.C. Price, R.A. McDonie and S.L. Wellons 610

Paper No. Page No.

RPMP13 CHEMICAL DERIVATIZATION FOR COMBINED HIGH PERFORMANCE LIQUID CHROMATOGRAPHY-MASS SPECTROMETRY
M. A. Quilliam and E. Y. Osei-Twum 612

RPMP14 LC/MS APPLICATION TO TANNERY EFFLUENT ANALYSIS
Alfred D., Jr. Thruston and John M. Mcguire. 614

RPMP15 APPLICATION OF COMBINED LC/MS TO THE ANALYSIS OF SELECTED CEPHALOSPORINS AND PENCILLINS
T. A. Roy, F. L. Deroos, B. Hidy, and C. C. Howard. 615

RPMP16 LASER DESORPTION MASS SPECTROMETRY OF INVOLATILE SAMPLES
Marvin L. Vestal and E. D. Hardin. 616

RPMP17 LASER DESORPTION CHEMICAL IONIZATION
Robert J. Cotter and Catherine Fenselau. 18

RPMP18 LASER DESORPTION CI MASS SPECTROMETRY
William Bone, Jeffrey Shabanowitz, and Donald F. Hunt. 620

RPMP19 FLASH DESORPTION-ELECTRON IMPACT MASS SPECTROSCOPY: A NEW DEVICE TO CONTROL SAMPLE PROBE HEATING AND BEAM SWITCHINGS
Terry D. Lee, William R., Jr. Anderson, and G. Doyle, Jr. Daves. 621

RPMP20 APPLICATIONS OF A NEW DIRECT INTRODUCTION PROBE FOR DESCRIPTION CHEMICAL IONIZATION
J.R. Chapman, S. Evans, C.J. Wakefield, K.R. Compson, and D. Hazelby 622

RPMP21 THE FIRST VIABLE EI/CI LC/MS INTERFACE
Paul P. Dymerski. 624

CHEMICAL IONIZATION

FAMOA1 EFFECT OF REACTION EXOTHERMICITY ON PROTON TRANSFER CI MASS SPECTRA
J. A. Herman and A. G. Harrison. 625

FAMOA2 TEMPERATURE DEPENDENT IONIC FRAGMENTATION IN THE CHEMICAL IONIZATION MASS SPECTRA OF SEMICARBAZONES
D. A. Herold, T. A. Elwood, and J. H. Futtrell. 627

FAMOA3 T JUMP TYPE EXPERIMENTS WITH A CI SOURCE
T. F. Magnera, J. Sunner, and P. Kebarle. 629

FAMOA4 AN INVESTIGATION OF STANDARD COMPOUNDS FOR EVALUATING INSTRUMENT PERFORMANCE IN POSITIVE ION AND NEGATIVE ION CHEMICAL IONIZATION MASS SPECTROMETRY
Steven J. Stout, M. O. Poeppel, S. J. Cardaciotto, and W. G. Millen. 630

FAMOA5 REAL-TIME TRACE ANALYSIS BY ATMOSPHERIC PRESSURE CHEMICAL IONIZATION: TRACE COMPOUND IDENTIFICATION BY HIGHLY SELECTIVE CHEMICAL IONIZATION
W. R. Davidson and S. Nacson. 632

FAMOA6 THE LOCATIONS OF OLEFINIC BONDS IN MONO- AND DI-UNSATURATED COMPOUNDS
K. R. Jennings and R. J. Greathead. 634

Paper No. Page No.

FAMOA7 SIMPLIFIED TECHNIQUE FOR POSITIVE AND NEGATIVE ION ADDUCT CHEMICAL IONIZATION MASS SPECTRA OF MULTIFUNCTIONAL COMPOUNDS OF LOW VOLATILITY
A. K. Bose, B. Pramanik, K. Tabei, and A. D. Bates. 636

FAMOA8 NEW CHEMICAL IONIZATION REAGENT IONS: REACTIONS OF CU+ WITH ESTERS AND KETONES IN THE GAS PHASE
R. C. Burnier, G. D. Byrd, and Ben S. Freiser. 638

FAMOA9 ACETAL FORMATION IN POLYOLS AND DETECTION BY MASS SPECTROMETRY
R. A. Sanders and R. P. D'Alonzo. 639

FAMOA10 DETECTION OF NEUTRAL PRODUCTS FROM CHEMICAL IONIZATION REACTIONS
Charles R. Hauer, Jeffrey M. Mcguire, and Burnaby Munson. 641

IONIZATION OF THERMOLABILE COMPOUNDS

FAMOB1 FIELD-INDUCED ION EVAPORATION MASS SPECTROSCOPY
B.A. Thomson, J.V. Iribarne and P. Dziedzic 642

FAMOB2 IONIZATION OF INVOLATILE COMPOUNDS BY SOLUTION DROPLET VAPORIZATION
E. R. Lory and Fred W. Mclafferty. 644

FAMOB3 ELECTRON IONIZATION-FLASH DESORPTION MASS SPECTROMETRY OF TETRA-ALKYL AMMONIUM HALIDE SALTS
G. Doyle, Jr. Daves, Terry D. Lee, and William R., Jr. Anderson. 646

FAMOB4 DIRECT EXPOSURE CHEMICAL IONIZATION MASS SPECTRA OF EXPLOSIVES
Jehuda Yinon. 647

FAMOB5 MASS SPECTRA OF LESS VOLATILE COMPOUND BY LIQUID SURFACE IONIZATION AT ATMOSPHERIC PRESSURE
M. Tsuchiya, K. Seita, and T. Taira. 649

FAMOB6 FIELD ASSISTED CHARGE TRANSFER MECHANISMS IN THERMALLY GENERATED REACTION ZONES ON FIELD EMITTERS
R. Olinger, J. Dye, and Jack F. Holland. 651

FAMOB7 LASER DESORPTION MASS SPECTROMETRY OF ORGANIC MOLECULES
P. G. Kistemaker, G. J. Q. Van Der Peyl, A. J. H. Boerboom, and J. Haverkamp. 652

FAMOB8 MASS SPECTROMETRY OF INORGANIC AND ORGANIC SUBSTANCES USING LASER INDUCED DESORPTION AND IONIZATION
L. V. Phillips, H. J. Heinen, S. Meier, M. Henning, H. Vogt, and R. Wechsung. 654

FAMOB9 REPETITIVE PULSING - A VERSATILE, SCANNING-INSTRUMENT-COMPATIBLE TECHNIQUE FOR LASER DESORPTION MASS SPECTROMETRY OF NONVOLATILE ORGANIC COMPOUNDS
F. Heresch, E. R. Schmid, and J. F. K. Huber. 655

FAMOB10 POSITIVE AND NEGATIVE FISSION FRAGMENT (^{252}Cf) MASS SPECTRA OF EIGHT COMPOUNDS
B.T. Chait, F.H. Field and W.C. Agosta 657

Paper No. Page No.

FAMOB11 CHLOROPHYLL: A PROBE INTO THE MECHANISMS OF 252Cf-PDMS
J. E. Hunt and R. D. Macfarlane. 659

FAMOB12 A DIRECT EXPERIMENTAL COMPARISON OF MASS SPECTRA OBTAINED WITH LOW ENERGY ION AND HIGH ENERGY 252 Cf FISSION FRAGMENT BOMBARDMENT
K. G. Standing, W. Ens, B. T. Chait, and F. H. Field. 661

IR/COMPUTER APPLICATIONS

FAMOC1 FOURIER TRANSFORM GC/MS
Edward B., Jr. Ledford, Robert L. White, Sahba Ghaderi, C. L. Wilkins, and M. L. Gross. 662

FAMOC2 A SECOND-GENERATION RAPID SCAN ION CYCLOTRON RESONANCE MASS SPECTROMETER
R. L. Hunter and Robert T., Jr. Mciver. 664

FAMOC3 ICR SPECTROSCOPY: THREE BASIC EXPERIMENTS
G. Parisod and T. Gaumann. 665

FAMOC4 RESOLUTION AND SIGNAL-TO-NOISE RATIO IN FOURIER TRANSFORM MASS SPECTROMETRY
Edward B., Jr. Ledford, Sahba Ghaderi, Robert L. White, M. L. Gross, and C. L. Wilkins. 667

FAMOC5 PHASE CORRECTION IN FOURIER TRANSFORM MASS SPECTROSCOPY
ROBERT B. Spencer and William J. Horsley. 669

FAMOC6 ELECTRON IMPACT IONIZATION OF ISOTOPICALLY-ENRICHED OXYGEN AND NITROGEN
George M. Woods 671

FAMOC7 TOWNSEND DISCHARGE IONIZATION PROBE FOR A FINNIGAN 4000 MASS SPECTROMETER
K. V. Wood, R. C. Scheibel, and O. P. Tanner. 673

FAMOC8 COMPUTER MODELLING FOR ION SOURCE DESIGN
R. N. Stillwell and D. I. Carroll. 674

FAMOC9 A TOTALLY AUTOMATED DATA ACQUISITION/REDUCTION SYSTEM FOR ROUTINE TREATMENT OF MASS SPECTROSCOPIC DATA BY FACTOR ANALYSIS
Patricia C. Tway, L. J. Cline-Love, and Hugh B. Woodruff. 675

FAMOC10 AN INTERFACE AND DATA ACQUISITION SYSTEM FOR TWO SPECTROMETERS
T. R. Mueller, H. S. Mckown, R. J. Warmack, and D. H. Smith. 677

FAMOC11 DECONVOLUTION OF PEAK SEQUENCES BASED ON ISOTOPE DISTRIBUTION
J. Van Katwijk. 680

FAMOC12 DECONVOLUTION OF MASS SPECTROMETER DATA
Juliette W. Ioup, George M., Jr. Wood, Billy T. Upchurch, George E. Ioup, and Grayson H., Jr. Rayborn. 682

Paper No. Page No.

BIOCHEMISTRY, FD/FI

FAMP1 MEASUREMENT OF OXYGEN ISOTOPE EXCHANGE IN VIVO AS AN INDEX OF BIOLOGICAL ACTIVITY
K. L. Clay and R. C. Murphy. 684

FAMP2 DEUTERIUM ISOTOPE EFFECTS IN THE DEAMINATION OF PUTRESCINE WITH DIAMINE OXIDASE
E. M. Jakubowski and P. S. Callery. 685

FAMP3 LOCATION OF DEUTERIUM LABEL IN BIOSYNTHESIZED BIOTINE: I. USE OF LINKED SCAN AND MIKES TECHNIQUES TO STUDY THE ORIGIN AND STRUCTURE OF THE ION m/z 166
D. Fraisse, F. Frappier, M. Jouany, A. Marquet, and J. C. Tabet. 686

FAMP4 MASS SPECTRAL APPROACHES TO GLYCOCONJUGATE ANALYSIS
V. N. Reinhold. 687

FAMP5 NEGATIVE CHEMICAL IONIZATION SPECTRA OF SOME GLUCURONIDES, INTRODUCED BY THERMAL DESORPTION FROM A PLATINUM WIRE INSIDE THE CI SOURCE
Andries P. Bruins. 688

FAMP6 OPENING OF THE BAY-REGION DIOL-EPOXIDE IN POLYCYCLIC AROMATIC HYDROCARBONS
Lan K. Wong and Jinn Wu. 690

FAMP7 THE MASS SPECTRAL CHARACTERIZATION OF DITHIASUCCINOYL (DTS) AMINES AND AMINO ACIDS
George Barany, D. V. Bowen, R. B. Merrifield, and F. H. Field. 692

FAMP8 CHARACTERIZATION OF COMPLEX FATTY ACIDS BY POSITIVE/NEGATIVE ION AMMONIA CHEMICAL IONIZATION
Roger A. Upham, Gary R. Gray, M.Y.H. Wong, and S. J. Danielson. 694

FAMP9 STRUCTURAL DETERMINATION OF ALKENES AND ESTERS OF MONO-SATURATED FATTY ACIDS BY GCMS
D. A. Kidwell and K. Biemann. 696

FAMP10 THE MECHANISM OF THE MAIN FRAGMENTATION REACTION IN VITAMIN D3
Ze'Ev V. I. Zaretskii. 698

FAMP11 ANALYSIS OF LEUCINE METABOLITES IN THE URINE OF A PATIENT ACCOMPANYING A DEFECT OF TYROSINE METABOLISM USING GC/MS/COM SCREENING SYSTEM
T. Shinka, T. Kuhara, I. Matsumoto, and M. Kawamura. 700

FAMP12 KETONE BODY FORMATION IN STARVATION AND IN DIABETES MELLITUS
I. Matsumoto, T. Kuhara, Izumi Maruyama, R. Kumashiro, and K. Tanikawa. 702

FAMP13 COMPARISON OF THE QUANTITATION OF MURAMIC ACID SELECTED ION MONITORING AND SINGLE REACTION MONITORING
T.W. Cochran, A. Fox, J.H. Schwab, D.J. Harvan, C.E. Parker and J.R. Hass 704

Paper No. Page No.

FAMP14 ROUTINE HIGH RESOLUTION GAS CHROMATOGRAPHY/MASS SPECTROMETRY OF COMPLEX BILE ACID MIXTURES FROM BIOLOGICAL SAMPLES
Joanne O. Whitney, E. Roitman, M. M. Thaler, and A. L. Burlingame. 705

FAMP15 EVALUATION OF FLUOROMETRIC ASSAY METHODS FOR SEROTIN IN PLATELETS, PLASMA AND WHOLE BLOOD SAMPLES BY GCMS
M. Mumtaz, N. Narasimhachari, and R. O. Friedel. 707

FAMP16 COMPARISON OF PATTERN RECOGNITION METHODS FOR THE ANALYSIS OF METABOLIC PROFILES
L. Verkh, R. Abbott, M. Anbar, James H. Mcreynolds, and M. Scanlon. 709

FAMP17 DIAGNOSIS OF VIRAL INFECTIONS BY MULTICOMPONENT MASS SPECTROMETRIC ANALYSIS
James H. Mcreynolds, R. Abbott, M. Anbar, H. Fadden, W. Rieth, M. Scanlon, L. Verkh, and B. Wolff. 710

FAMP18 SELECTED ION MONITORING VALIDATION OF CHROMATOGRAPHIC, SPECTROPHOTOMETRIC AND BINDING METHODS OF QUANTITATION OF COMPOUNDS IN BIOLOGICAL FLUIDS
Susan E. Hattox and FRANK Hatch. 712

FAMP19 EFFECT OF LARGE INGESTIONS OF VITAMIN C ON URINARY METABOLIC PROBILES
B.E. Blaisdell. J.C. Engels. C.S. Tsao. A. Sheets & W. Aberth . . . 714

FAMP20 ANALYSIS OF FOOD, DRUG AND COSMETIC DYES BY FIELD DESORPTION AND DESORPTION CHEMICAL IONIZATION MASS SPECTROMETRY
Peter A. Dreifuss, John A. G. Roach, Sandra J. Bell, Denis Andrzejewski, William C. Brumley, James A. Poppiti, and James A. Sphon. 716

FAMP21 FIELD DESORPTION CONSTANT TEMPERATURE POWER SUPPLY
David F. Fraley, W. Stephen Woodward, and Maurice M. Bursey. 717

FAMP22 FURTHER SURFACE MODIFICATION STUDIES ON FIELD DESORPTION EMITTERS
Maurice M. Bursey, Tim L. Youngless, and Neil B. H. Henis. 719

FAMP23 THE VOLCANO FIELD IONIZATION SOURCE
C. A. Spindt. 720

PL1 CURRENT CONCEPTS OF MOLECULAR MECHANISMS OF CHEMICAL CARCINOGENESIS. I. BERNARD WEINSTEIN. Division of Environmental Sciences and Cancer Center/Institute of Cancer Research, Columbia Univ., New York, N.Y. 10032

Epidemiologic studies suggest that most human cancers result from exposure to environmental factors. Rational approaches to identifying specific human carcinogens require knowledge of their cellular and molecular mechanisms of action. At least two categories of causative agents can be identified in the carcinogenic process, initiating carcinogens and tumor promoters. A unifying principle in the action of initiating carcinogens is that they generate electrophiles that bind covalently to DNA and other cellular macromolecules. The molecular details of nucleic acid binding will be illustrated with two carcinogens, N-2-acetylaminofluorence (AAF) and benzo(a)pyrene (BP). Activated derivatives of AAF form covalent adducts predominantly on the C-8 position of guanine. This causes a conformational change in the DNA helix termed "base displacement". The major metabolite of BP responsible for covalent binding to DNA, mutagenesis and carcinogenesis is BP 7,8-dihydrodiol-9,10-oxide (BPDE), which forms an adduct with the N-2 position of guanine. Stereochemical aspects of this adduct and evidence that the bound BP residue resides in the minor groove of the DNA helix will be reviewed. BPDE also forms a minor adduct with the N-6 position of adenine. The binding of the bulky AAF and BP residues to nucleic acids interferes with DNA replication and transcription. In contrast to initiating carcinogens, the tumor promoter 12-O-tetradecanoyl-phorbol-13-acetate (TPA) does not bind covalently to nucleic acids and is not mutagenic. TPA exerts several effects including induction of phenotypic changes that mimic those seen in tumor cells, modulation of differentiation, and alterations in membrane structure and function. The genetic effects of initiating carcinogens and the epigenetic effects of tumor promoters can be explained in terms of a multistep model of carcinogenesis.

CHEMICAL IONIZATION: NEGATIVE ASPECTS

By

F.H. FIELD

The Rockefeller University

New York, N.Y. 10021

It is a historical fact that low pressure negative ion mass spectrometry has never been used as much as its positive ion counterpart. The reason for this is that the production of negative ions occurs predominantly by electron capture under resonance conditions, that is, capture occurs only of electrons having energy within a limited range which is appropriate to the substance effecting the capture. The production of large numbers of electrons with such restricted energies at low pressures has been enough of an experimental task to limit the use of low pressure negative ion mass spectrometry. One hastens to recognize the efforts and contributions of a significant body of workers who have made many investigations of low pressure negative ion mass spectrometry, for their efforts have resulted in the development of a meaningful body of knowledge about the chemistry of gaseous anions. However, the utilization of this body of knowledge has been impeded by experimental difficulties.

The use of high pressure in the mass spectrometer ion source as in chemical ionization changes and improves the situation markedly. One can calculate that a beam of electrons with an energy of several hundred volts has only a limited degree of penetration through a gas at a pressure of approximately 1 torr, and, indeed, such a beam of electrons is either completely or largely stopped by 1 torr of gas in most mass spectrometer ionization chambers. In passing through the gas the electrons effect ionization of the gas molecules, and the secondary electrons produced in this ionization are also stopped by subsequent collisions. Thus, there results in the gas a body of electrons having a distribution of energy. The mean value of the distribution is generally not well-defined, but it will be relatively low. Thus electrons are available for capture by many substances in the mass spectrometer without the exercise of particular care or effort on the part of the operator, and the abundant production of negative ions becomes a practical possibility.

The first use of negative chemical ionization (NCI) was probably made by Dougherty and co-workers in 1972[1] Scattered papers appeared in he literature in the next few years, and since approximately 1976 an increasing interest in the subject has been manifested.

We first consider the matter of reagent substances to be used in NCI. An important property of chemical ionization in general is its capability of using different reactant substances to achieve different analytical goals. One expects (and this expectation is confirmed in practice) that the properties of negative ions and of electrons will be markedly different from those of positive ions. Thus one expects that positive and negative mass spectrometry will yield different analytical information. I give in Table 1 various ions which have been used as reactant ions in NCI.

TABLE 1

NCI REACTANT IONS

ION	ΔH_f (KCAL/MOLE)	$D(H^+-A^-)$ (KCAL/MOLE)
e^-	-	-
Cl^-	-56.6	332
O_2^-	-10.1	350
F^-	-60.0	370
CH_3O^-	-36.0	377
O^-	+25.2	381
OH^-	-32.8	390
NH_2^-	+24	400

I include the electron (e^-) in Table 1 as an organization ploy. The ΔH_f values for the ions may be looked upon as measures of their general reactivity in the sense that ions with high values of ΔH_f will react readily and extensively, and conversely. $D(H^+-A^-)$ is the heterolytic bond dissociation energy of the molecule HA, and these values constitute measures

of the relative reactivity of A^- as a base. Examining several of the individual ions listed in Table 1, we note that NH_2^- has a large ΔH_f value and a large $D(H^+-A^-)$ value, and thus it may be expected to be very reactive in general and a very strong base. $O^{-\cdot}$ will also be very reactive in general and be quite strong as a base, but OH^- with a large $D(H^+-A^-)$ and a much smaller ΔH_f value will be a strong base, but less reactive generally. At the other end of the scale, Cl^- will be relatively unreactive both in general and as a base.

Let us now consider the free electron (e^-) as a reactant. The capture of low energy electrons at high pressures has come to be referred to as electron capture NCI, and this is to be contrasted with NCI using a reactant ion such as OH^-, which has come to be referred to as reactant ion NCI. We may represent these two processes by the equations

Electron capture NCI

$$AB + M + e^- \longrightarrow AB^- + M \qquad (1)$$
$$\hookrightarrow A + B^- \qquad (1a)$$

Reactant ion NCI

$$R^- + ABH \longrightarrow AB^- + RH \qquad (2)$$
$$\hookrightarrow A + B^- \qquad (2a)$$

$R^- = OH^-, CH_3O^-$, etc.

Here we have also represented the possibility that dissociative ionization may occur.

It has been reported, especially by D.F. Hunt and co-workers, that the sensitivity for quantitation is much higher by electron capture NCI than by positive chemical ionization (PCI), and the enhancement of sensitivity may be by as much as a factor of 1000. This finding has generated much interest, and this interest has been maintained until the present. The experimental conditions are simple, and the method is thus quite practical. A moderating gas the only function of which is to slow down and stop the ionizing electrons is introduced into the ionization chamber of the mass spectrometer at a pressure of approximately 1 torr. CH_4, N_2, i-C_4H_{10}, and CF_4 are several of the substances which have been used for this purpose. I give in Table 2 the relative sensitivities for electron capture NCI and for PCI found by Hunt and co-workers.[2]

TABLE 2

POSITIVE AND NEGATIVE ION CURRENT RATIOS

COMPOUND	MW	N/P
2,4,6-Trinitrotoluene	227	1042
O,O-Diethyl-O-p-Nitrophenyl Thiophosphate	291	102
Pentafluorobenzonitrile	193	953
Pentafluorobenzanilide	287	443
N-(Pentafluorobenzylidene) Aniline	271	1021
Phenyl Pentafluorobenzoate	288	682
Benzil	210	495
Phthalic Anhydride	148	124
9,10-Anthraquinone	208	166

N/P is the ratio of the response obtained in negative and positive chemical ionization for the introduction of equal amounts of the several materials listed in the table. One observes that N/P values range from approximately 100 to approximately 1000, which demonstrates quantitatively the much higher sensitivity by electron capture NCI for these compounds. However, one should keep in mind that these compounds are strongly electronegative and as such their sensitivity for PCI may be relatively low. However, Table 3 contains some results by Hunt and

TABLE 3

LIMITS OF DETECTION

CMPD	DERIV. CMPD	AMT. INJ.	S/N
Dopamine	$(TMSO)_2C_6H_3(CH_2)_2N{=}CHC_6F_5$	25 fg.	4

(TABLE 3 con't.)

TH Cannabinol	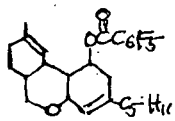	10 fg.	1
Amphetamine	$C_6F_5CNHCHCH_2C_6H_5$ (O, CH_3)	10 fg.	4
Amphetamine	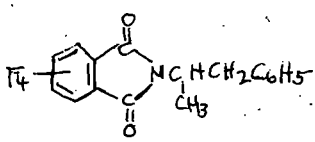	10 fg.	12

Crow[3] which show that absolute sensitivities by electron capture NCI can be very high, namely, on the order of 10 femtograms. Table 3 also illustrates a derivatization technique which is of importance in electron capture NCI; that is, the material used as a derivatizing agent is chosen so as to enhance not only the volatility of the material to be investigated, but also to provide a material with a high probability of capturing electrons. Thus the derivatizing agent used for dopamine (Table 3) is pentafluorobenzaldehyde (C_6F_5CHO). Tetrahydrocannabinol was derivatized with pentafluorobenzoyl chloride (C_6F_5COCl), and amphetamine was derivatized both with perfluorobenzoyl chloride and with tetrafluorophthalic anhydride ($C_6F_4(CO)_2O$).

Other workers have also found that the sensitivity of electron capture NCI is higher than that of PCI, and I give in the following several arbitrarily selected illustrative examples. Lewy and Markey[4] have devised an assay for melatonin using electron capture NCI. They utilized the technique of employing a derivatizing agent that enhances the electron capture probability, namely, perfluoropropionic anhydride. This derivatization reaction is given in equation (3)

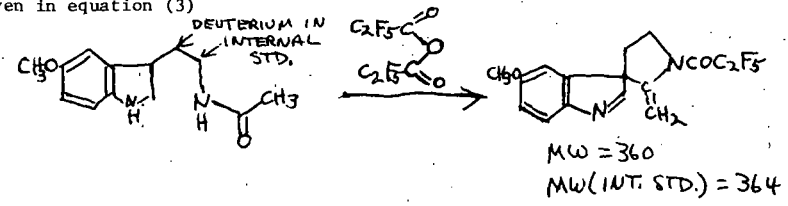

(3)

The base peak in the PCI spectrum of derivatized melatonin is the $(M+1)^+$ ion at m/z 361, and that in the electron capture NCI spectrum is the peak formed by dissociative electron capture at m/z 320. Lewy and Markey find that the sensitivity in electron capture NCI at m/z 320 is 150 times greater than that in PCI at m/z 361. Furthermore, Lewy and Markey state that they can routinely determine the concentration of melatonin in plasma at concentrations as low as 1 pg./ml.

Garland and Min[5] have made assays of clonazepam by electron capture NCI and by PCI.

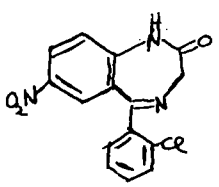

CLONAZEPAM
MW 315

The NCI spectrum consists of the $(M-1)^-$ ion at m/z 314 as the base peak, the $M^{\cdot -}$ peak at m/z 315 with a relative intensity of 75% of the base, and an $(M-36)^-$ peak at m/z 279 with an

intensity 30% of the base. Quantitation was made at the $(M-1)^-$ ion in NCI and at the $(M+1)^+$ ion in PCI, and it is found that the sensitivity in electron capture NCI is 20 times larger than that in PCI. Garland and Min point out that the sensitivity of the assay and the behavior of the mass spectrometer in NCI is particularly dependent upon the cleanliness of the ion source of the mass spectrometer.

Prescott, Campana, and Risby[6] have published an illuminating study of the quantitative analysis of chromium complexes by PCI and by electron capture NCI. These workers have determined the minimum amount of chromium that is detectable using various chelating agents in electron capture NCI and PCI. The quantitation in NCI is made at the $M^-\cdot$ ion and in PCI at the $(M+1)^+$ ion. The results are given in Table 4. The chelating agents used are acetyl

TABLE 4

MINIMUM DETECTABLE AMT. CR (Grams)

CR CHELATE	POSITIVE $(M+1)^+$	NEGATIVE $M^-\cdot$	R_1	R_2
CR $(HFA)_3$	1.3×10^{-9}	2.4×10^{-13}	CF_3	CF_3
CR $(TFA)_3$	1.2×10^{-11}	2.9×10^{-13}	CF_3	CH_3
CR $(FOD)_3$	1.9×10^{-12}	1.9×10^{-13}	t-Bu	C_3F_7
CR $(THD)_3$	8.6×10^{-12}	8.6×10^{-11}	t-Bu	t-Bu
CR $(ACAC)_3$	8.6×10^{-13}	8.6×10^{-12}	CH_3	CH_3

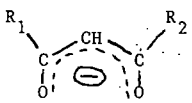

acetonates with varying degrees of fluorination. The chelates are listed in Table 4 in order of decreasing degree of fluorination as one proceeds from the top to the bottom of the table. Alternatively one can think that the electron withdrawing tendency of the chelate decreases as one proceeds from top to the bottom in the table. One makes the interesting observation that as the electron withdrawing tendency decreases (electron releasing tendency increases) the sensitivity for PCI exhibits a monotonic increase, but the sensitivity for electron capture NCI remains about the same for all the chelates containing fluorine, but decreases sharply for the non-fluorinated chelates. If one compares the sensitivity for PCI and NCI for the same complexes, the NCI sensititivity is higher for the fluorinated complexes but lower for the protonated complexes. This is another manifestation of a point made earlier that sensitivity in chemical ionization depends on the chemical nature of materials being investigated. A straightforward comparison of positive and negative sensitivities for CR $(HFA)_3$ gives the result that the negative method is approximately four orders of magnitude more sensitive than the positive method. On the other hand, however, a comparison of CR $(AcAc)_3$ indicates that the positive method is a factor of ten more sensitive than the negative method. For purposes of evaluating intrinsic sensitivity of the positive method and negative method, neither of these comparisons is valid, for the most significant comparison is that of the sensitivity of the best compound for the negative method with that of the best compound for the positive method, and when one does this with the data given in Table 4, one comes to the conclusion that electron capture NCI for the assay of chromium is approximately four times more sensitive than the positive method.

Let us enquire if theory offers any insight as to whether electron capture NCI should exhibit higher sensitivity than PCI. Following Siegal and Fite[7] we write

FOR SAMPLE POSITIVE ION FORMATION

$$\frac{d(M^+)}{dt} = k_+(R^+)(M) - \frac{F}{V}(M^+) - \frac{D\pm}{r_o^2}(M^+) - R_e(M^+)(e) - R_i(M^+)(M^-) \quad (4)$$

FOR SAMPLE NEGATIVE ION FORMATION

$$\frac{d(M^-)}{dt} = k_-(e)(M) - \frac{F}{V}(M^-) - \frac{D\pm}{r_o^2}(M^-) - R_i(M^-)(R^+) - R_i(M^-)(M^+) \quad (5)$$

k_+ and k_- = Ion Formation Rate Constants
$F/V\ (M^+)$ and $F/V\ (M^-)$ = Ion Flow Out of Source
R_e and R_i = Recombination Rate Constants

SIMPLIFYING AND REARRANGING $\left(\frac{d(M^+)}{dt} = 0\right)$

$$\frac{I^-}{I^+} \alpha \frac{(M^-)}{(M^+)} = \frac{k_-}{k_+} \times \frac{R_i + C}{R_i + C} \cong \frac{k_-}{k_+} \qquad (6)$$

One observes that as a good approximation the end result is that the ratio of the negative ion current to the positive ion current under equivalent conditions is equal to the ratio of the rate constant for electron capture by sample molecules to the rate constant for the reaction of sample molecules with reactant ion in the positive case.. For positive ions it is well known that the maximum values for the reaction of reactant ions with sample molecules (k_+) is 3-4 x 10^{-9} cc/mol. sec. For negative ions formed by electron attachment, the rate constant (k_-) may well be larger than k_+ because of the high mobility of electrons in the chemical ionization plasma.

Rather than just guess at attachment rates, it is desirable to find experimental values, and a suitable set may be found in Massey's book "Negative Ions."[8] The attachment rate constants for thermal electrons taken from this work are given in Table 5.

TABLE 5

ATTACHMENT RATE COEFFICIENTS (THERMAL ELECTRONS)
(10^{-8} CM^3SEC^{-1})

CH_3Cl	CH_2Cl_2	$CHCl_3$	CCl_4	C_2HCl_3	1,1,1-$C_2H_3Cl_3$	1,1,2-$C_2H_3Cl_3$
5.4 x 10^{-3}	1.4 x 10^{-3}	0.34	24	0.17	1.4	0.013
CF_3Cl	CF_2Cl_2	$CFCl_3$	$C_2F_3Cl_3$	CHF_2Cl	$CHFCl_2$	CHF_3
0.040	-	9.8	3	5.4 x 10^{-3}	0.11	0.10
CF_4	CH_3Br	CH_2Br_2	$C_2H_2Br_4$	CF_3Br	CF_2Br_2	CH_3I
7 x 10^{-5}	0.29	2.8	1.5	1.1	23	2.2
C_2H_5I	$Fe(C_2H_5)_4$	$Fe(CO)_5$	$(CH_3C_5H_4)Mn(CO)_3$			
0.42	9 x 10^{-3}	0.1	0.04			

These are mostly halogenated compounds, and one observes very wide variations in the values of the rate constants. For example, in proceeding from CH_3Cl to CCl_4 the rate constant increases from the value of 5.4 x 10^{-11} cc/mol. sec. to a value 2.4 x 10^{-7} cc./mol. sec., an increase of a factor of approximately 5000. The value for CH_3Cl is appreciably smaller than maximum rate constants for reactions of positive ions; whereas that for CCl_4 is appreciably greater. Rather startling differences in the rate constants occur as a function of molecular structure. Thus the rate constant for CH_3CCl_3 is approximately 100 times greater than that for the isomeric $CHCl_2CH_2Cl$. A very striking difference is to be observed between the values for CCl_4 and CF_4. The value of 2.4 x 10^{-7} cc/mol. sec. shows that CCl_4 captures electrons very strongly, whereas the very small value of 7 x 10^{-13} cc/mol. sec. for CF_4 shows that for practical purposes CF_4 does not capture electrons at all. This table illustrates the fact that one can expect wide and oftentimes unpredictable variations in the sensitivity for electron capture NCI. However, for some substances the sensitivity by NCI is greater (and sometimes very much greater) than the sensitivity for PCI.

One should also keep in mind the fact that the selective aspects of ionization by electron capture NCI serve to enhance the sensitivity of the method. Thus impurities which could contribute an interfering background oftentimes will not be ionized because their structures are not appropriate, and thus the signal to noise ratio for the compound of interest (which will be ionized) will be relatively high.

It is useful at this point to consider the factors which determine the electron affinity of molecules, that is, the factors which will affect the sensitivity of substances for assay by electron capture NCI. I shall not give a rigorous treatment, but it would be nice to examine some qualitative ideas which will rationalize observations and perhaps have some predictive value. We start by stating the truism that for electron capture to occur an incom-

pletely occupied molecular orbital of sufficiently low energy must be available in the substance of interest. If one has atomic or molecular entities with incomplete shells the matter is simple in that the unfilled orbital can accept another electron to form the negative ion. For example, $OH^{\cdot}$ can produce OH^- ($EA(OH^{\cdot})$ = 42 kcal/mole); $C_6H_5CH_2^{\cdot}$ can produce $C_6H_5CH_2^-$ (EA(benzyl) = 20 kcal/mole); $Cl^{\cdot}$ can produce Cl^- ($EA(Cl^{\cdot})$ = 83 kcal/mole.).

However, in negative CI one is primarily concerned with closed shell (even electron) molecules, and how does one deal with them? For large unsaturated conjugated systems resonance and delocalization will lower the energy of unoccupied orbitals so that an electron affinity can result. Thus the electron affinity of benzene is negative (benzene does not form a stable $C_6H_6^-$ ion), but in pentacene the orbitals are sufficiently larger and delocalization is sufficiently greater that the electron affinity of pentacene is approximately 30 kcal/mole. The presence of electronegative groups on the conjugated molecule will lower the energy of unoccupied orbitals so that a positive electron affinity can result. As was mentioned above, the electron affinity of benzene is negative, but by contrast that of hexafluorobenzene (C_6F_6) is greater than 42 kcal/mole. However, it has been shown that a theoretical treatment of this phenomenon is not simple.[9]

It is reasonable to think that the electron affinities of molecules are affected by the same structural and resonance factors that affect the wavelength of light absorption in organic molecules. Light absorption has long been understood, and this understanding has become a fundamental part of the body of knowledge of organic chemists. Thus it is a useful guide for most mass spectrometrists to realize that molecular electron affinities seem in general to be increased by the same structural factors which increase the wavelength of light absorption in molecules. The reason for this is straightfoward; namely, light absorption in molecules oftentimes involves the promotion of an electron from an occupied to an unoccupied orbital as in $N \rightarrow \pi^*$ and $\pi \rightarrow \pi^*$ transitions. In electron capture the electron goes into the lowest unoccupied orbital, which one expects to be the orbital into which the electron is promoted in light absorption. Obviously the absolute energies involved in these two cases are not at all the same, but one expects that the trends in these energies with structural factors will be similar.

The molecules considered above are unsaturated in a chemical sense, but saturated molecules such as SF_6 and CCl_4 also capture electrons (sometimes with the occurrence of dissociation), and how does one account for this? For such molecules the lowest lying unoccupied molecular orbital is oftentimes the anti-bonding orbital associated with one of the bonds. The energy change produced by capturing an electron into this orbital can be thought of as consisting of two parts: (1) The repulsive energy involved in putting an electron in this high energy orbital (an anti-bonding electron), and (2) the attractive energy resulting from the interaction of the electron with one or more electronegative atoms in the molecule. The first factor produces a weakening of the molecular bond, and the amount of the weakening is a measure of the repulsiveness of the orbital. In general, the stronger the bond in the unionized molecule the more repulsive (the higher in energy) will be the anti-bonding orbital. This matter may be represented in several ways, and a particularly simple method is given by Massey[8]. Thus for the capture of a thermal electron

$$AB + e + M \longrightarrow AB^- + M \qquad (7)$$

$$\hookrightarrow A + B^- \qquad (7a)$$

the following relation obtains

$$EA(AB) = D(AB^-) - D(AB) + EA(B) \qquad (8)$$

where
$EA(AB)$ = electron affinity of AB
$D(AB^-)$ = bond dissociation energy in AB^-
$D(AB)$ = bond dissociation energy in AB
$EA(B)$ = electron affinity of B (assumed to be the electronegative atom in the molecule)

This relationship can be easily derived from a thermochemical cycle. Since the captured electron goes into an anti-bonding orbital, the bond dissociation energy of the ion AB^- ($D(AB^-)$) will be less than the bond dissociation energy of the neutral molecule ($D(AB)$), and the difference in the bond dissociation energies of the ion and the neutral molecule will be a measure of the energy of the anti-bonding orbital. As was mentioned above, in general one can expect the anti-bonding orbital to be higher in energy the stronger the bond in the neutral molecule. One sees from equation (8) (and one can understand intuitively) that when $-(D(AB^-)-D(AB))$ becomes greater than $EA(B)$ the electron affinity of the molecule AB ($EA(AB)$) becomes negative; that is, the energy of the anti-bonding orbital can become so high that the repulsive energy of the electron in it would exceed the attractive interaction between the electron

and the electronegative atom B. Electron capture cannot then occur. Capture does occur when these energy relationships are reversed.

Let us illustrate this concept with two examples. First, consider the difference in behavior of O_2 and N_2. O_2 has an electron affinity of 10 kcal/mole, and the stable $O_2^{-\cdot}$ ion is easily formed by electron capture. By contrast N_2 has a negative electron affinity, and N_2^- does not exist in stable form. For O_2 and N_2 one knows the energies of the lowest excited states which involve electron promotion, and they are

$$O_2 \quad {}^3\Sigma_u^+ \quad 103 \text{ kcal./mole}$$

$$N_2 \quad {}^3\Sigma_u^+ \quad 144 \text{ kcal./mole}$$

These will not be the energies of a captured electron in negative ions produced from O_2 and N_2 but we may assume as approximation that the values will represent the relative energies of such captured electrons. We may conclude that

$$-(D(N_2^-) - D(N_2)) > -(D(O_2^-) - D(O_2)) \qquad (9)$$

Perhaps more important than this, however, is the fact that EA(O) = 34 kcal./mole whereas EA(N) = 0, and thus from equation (8) one concludes that the electron affinity of N_2 must be negative, but one can understand that $EA(O_2)$ can be finite.

Perhaps even more interesting is to attempt an explanation for the fact pointed out previously that CCl_4 has a finite electron affinity and captures electrons at a high rate, whereas CF_4 does not capture at all. This is initially puzzling because the electron affinities of Cl and F are both large and approximately equal: EA(Cl) = 83 kcal./mole; EA(F) = 78 kcal./mole. The explanation for the difference in electron capture behavior must then be looked for in the different values of the bond dissociation energies of the two molecules. From known heats of formation one calculates that for

$$CF_3\text{-}F \longrightarrow CF_3 + F \qquad (10)$$

$$D(CF_3\text{-}F) = 130 \text{ kcal./mole}$$

$$CCl_3\text{-}Cl \longrightarrow CCl_3 + Cl \qquad (11)$$

$$D(CCl_3\text{-}Cl) = 71 \text{ kcal./mole}$$

That is, the C-F bond in CF_4 is very strong, but the C-Cl bond in CCl_4 is 59 kcal./mole weaker. One makes the hypothesis that the C-F bond strength in CF_4 is so large that

$$-(D(CF_3\text{-}F^-) - D(CF_3\text{-}F)) > EA(F) \qquad (12)$$

which produces a negative electron affinity in CF_4. The weaker bond dissociation energy in CCl_4 can result in the converse of the situation in CCl_4.

We turn now to another matter of importance in electron capture NCI, namely the effect of ion source pressure. We recall that non-dissociative electron capture must be a three-body process; that is, the exothermicity of the electron attachment process must be removed from the molecule or else the electron will ultimately detach itself. Thus the sensitivity in electron capture NCI can be dependent upon source pressure, and one can expect that this dependence will be greater than that involved in PCI. The natural lifetimes of the excited negative ions produced by electron attachment vary widely from one compound to another, and one can show that for lifetimes on the order of 1-10 μsec the source pressure should be on the order of 1 torr or sensitivity loss will occur because of electron auto-detachment.

It is of interest to examine the values of experimentally determined negative ion lifetimes to get a feel for the magnitudes involved. Values taken from the compilation by Christophorou[10] are given in Table 6. One sees that a wide range of lifetimes occurs, and

TABLE 6

NEGATIVE MOLECULAR ION LIFETIMES

CMPD	ION	LIFETIME (μsec.)
$C_6H_5NO_2$	$(\phi NO_2)^{-*}$	35
$C_6H_4(NO_2)_2$	$(C_6H_4(NO_2)_2)^{-*}$	470
Glyoxal	$((CHO)_2)^{-*}$	2.5
Benzil	$(\phi COCO\phi)^{-*}$	~ 90

TABLE 6 (con't.)

Benzoin	$(\phi CHOHCO\phi)^{-*}$	10
Perfluoro-n-Hexane	$(n\text{-}C_6F_{14})^{-*}$	44
Perfluorocyclohexane	$(Cy\text{-}C_6F_{12})^{-*}$	340

One sees that a wide range of lifetimes occurs, and one recognizes that the longer the lifetime the easier it is to form negative ions by electron capture and the lower the pressure needed in the mass spectrometer. Indeed, some lifetimes are so long that electron capture ions can be observed in low pressure mass spectrometry. It is of interest to note the factor of nine difference in the lifetimes given in Table 6 for benzil and benzoin. One can think that the reduction of the ketone group which converts benzil to benzoin affects the amount of resonance in benzoin and lowers its electron affinity compared with that of benzil, and one knows from arguments presented by Christophorou[10] that this in turn lowers the lifetime of the excited negative ion. The very large difference in the lifetimes of perfluoro-n-hexane and perfluorocyclohexane is not understandable in terms of any of the concepts offered here and constitutes an interesting manifestation of the vagaries of behavior which can be observed in electron capture NCI.

A summarizing statement concerning electron capture NCI is that it serves very well for the quantitative analyses of appropriate compounds, but because of the variability of behavior from one compound to the next (whether this be understood or not understood) it is not a suitable method for the qualitative analyses of unkown materials.

I turn now to reactant ion NCI, starting with Cl^- as the reactant for reasons of historical interest. I pointed out earlier that Cl^- is a weak base and a low energy ion, and as a consequence it reacts by attachment to the substances of interest. It is rather selective in its reactions. Cl^- attachment behavior given by Dougherty and co-workers[11] is summarized in Table 7.

TABLE 7

Cl^- Attachment Spectra at 200°C

Formation reactions:

$$CH_2Cl_2 + e \longrightarrow Cl^- + CH_2Cl \ (?) \qquad (13)$$

$$Cl^- + CH_2Cl_2 \longrightarrow CH_2Cl_3^- \qquad (14)$$

Reactions:

Strong attachment: RI for $(M+Cl)^-$ = 100

Carboxylic acids, amides, amino acids, aromatic amines, phenols

Moderate attachment: RI for $(M+Cl)^-$ = 1-20

Aliphatic alcohols and amines, carbonyl compounds, ethers, nitroaromatics, chlorinated hydrocarbons

No Attachment

Aliphatic and aromatic hydrocarbons, tertiary amines, nitriles.

The spectra produced are strongly dependent upon experimental conditions in the mass spectrometer and especially on the temperature of the ion source.

Relatively recently A.K. Bose and co-workers[12] have used Cl^- attachment to obtain interesting spectra of two tetrasaccharides, and thus the method is of continuing use. However, because of its sensitivity to experimental conditions and to the structures of the substances being investigated it is likely that its use will be limited to appropriate specific cases.

$O_2^{-\cdot}$ has been used as a reactant ion, and it has been particularly investigated in connection with its use in atmospheric pressure ionization mass spectrometers. The ion is easily formed by the three-body capture of a low energy electrons by O_2, and its reactions have been elucidated by Horning and co-workers[13]. The ion is a relatively weak base, but it will abstract protons from relatively acidic substances such as acetic acid. The electron affinity of O_2 is relatively low (10 kcal/mole) so it will ionize materials with higher proton affinities by electron transfer. Thus,

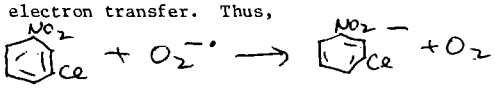

(15)

However, $O_2^{-\cdot}$ also has nucleophilic properties, and it undergoes a nucleophilic attack on ortho and para nitrochlorobenzene:

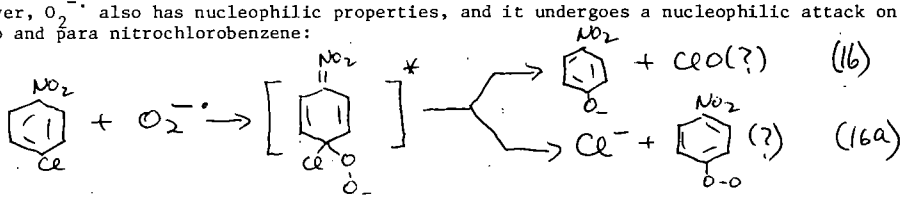

Here I use the para isomer as an example for the sake of simplicity. One observes that the reaction can take two paths to produce a substituted phenoxide ion and/or Cl^-. The ratio of phenoxide to chloride ion depends upon the strength of the electron withdrawing groups on the molecule involved, with phenoxide ion production being favored for molecules with extensive electronegative substitution. Thus, in hexachlorobenzene the ratio of phenoxide to chloride is 58, but it is zero for dichlorobenzene. This behavior can be rationalized by concepts presented previously, for the presence of many electronegative groups on the benzene ring will lower the energy of the aromatic molecular orbitals into which the charge from the phenoxide group can be delocalized by resonance. Thus the energy of the phenoxide ion will be lowered and its production favored.

$O^{\cdot -}$ is a strong base, a very high energy ion, and it has an odd electron. All of these factors may be expected to produce a highly reactive ion, and this is found in actuality. The reactions of this ion were first investigated by Jennings and co-workers[14] and Bohme and Young[15] and are given in Table 8. The number of spectra available for the evaluation of the

TABLE 8

REACTIONS OF $O^{-\cdot}$

Formation: $N_2O + e \longrightarrow N_2 + O^{-\cdot}$ (17)

Reactions:

1. H· abstraction

$O^{-\cdot} + CH_3CN \longrightarrow OH^- + CH_2CN$ (18)

2. H^+ abstraction

$C_6H_5CH_3 + O^{-\cdot} \longrightarrow C_6H_5CH_2^- + OH$ (19)

3. H_2^+ abstraction

$CH_2 = CH_2 + O^{-\cdot} \longrightarrow CH_2 = C^{-\cdot} + H_2O$ (20)

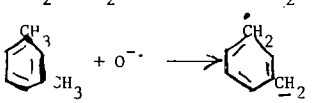

(21)

4. H· displacement

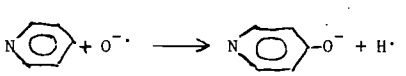

(22)

5. R· displacement

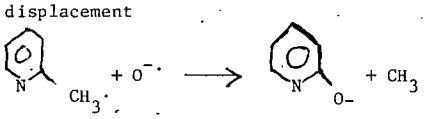

(23)

6. Miscellaneous

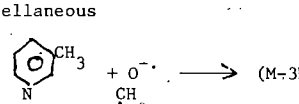

(24)

$C_3H_7\text{-}\underset{OH}{\overset{CH_3}{C}}\text{-}CH_3 + O^{-\cdot} \longrightarrow (M-17)^- = CH_3CH_2CH = \underset{O^-}{C}\text{-}CH_3 + OH + CH_4$ (25)

reactions of $O^{\cdot -}$ is not large, but the kinds of reactions listed in Table 8 lead one to expect that $O^{\cdot -}$ will produce relatively complex spectra with extensive fragmentation. The practical utility of the ion as an analytical reactant cannot be reliably evaluated, but one guesses that it will be limited to specialized cases.

The final reactant to be discussed here is OH^-, and the reactions of this ion have been relatively extensively investigated in that the OH^- spectra of about 90 compounds have been measured and published in the last three years.[16] OH^- is a strong base, but a relatively low energy ion, and consequently it reacts primarily by abstracting protons. However, it does undergo some nucleophilic reactions. It is a strong enough base that it will abstract protons from a wide range of compounds, and of the organic compounds investigated so far it has failed to react only with paraffin and cycloparaffin hydrocarbons and benzene.

Even though OH^- is a strong base and proton abstraction is strongly exothermic for many substances, the amount of fragmentation found in OH^- NCI seems to be lower than one might predict on the basis of the energetics. The reason for this is probably that in the proton abstraction reaction the new bond formed is in the H_2O product, and one intuitively expects that a disproportionately large fraction of the exothermicity of the reaction will result in excitation of this H_2O, rather than contributing to dissociation of the product anion which is of interest. This is the converse of the situation which obtains in positive ion chemical ionization. Thus, for example, in proton transfer from CH_5^+ to a sample molecule the bond formed is in the product cation, and a disproportionate amount of the exothermicity of the reaction will be available to produce fragmentation of the ion.

OH^- can be easily formed in a mass spectrometer using a mixture of approximately equal amounts of N_2O and H_2 or CH_4. A total pressure in the ionization chamber of 1-2 torr is suitable. The reactions which occur are

$$N_2O + e \longrightarrow N_2 + O^{-\cdot} \qquad (26)$$

$$O^{-\cdot} + \begin{cases} H_2 \\ CH_4 \end{cases} \longrightarrow OH^- + \begin{cases} H \\ CH_3 \end{cases} \qquad (27)$$

It is necessary that the temperature in the ionization chamber be higher than approximately 200°C, for if it is lower the production of OH^- declines. The reason for this is probably that the hydrogen atom transfer producing OH^- in reaction (27) has a small activation energy which slows down the reaction at lower temperatures.

I give in Table 9 the OH^- spectra of relatively acidic substances, namely, carboxylic acids, alcohols, ketones, and amino acids. One sees that the ions produced are limited to

TABLE 9

		% Total Ion.	
		M-1	M-3
Carboxylic acids:	stearic acid	100	-
	eicosanic acid	100	-
Alcohols:	1-pentanol	66	34
	3-decanol	66	34
	2-methyl-2-pentanol	97	-
	3-ethyl-3-pentanol	100	-
Ketones:	3-pentanone	97	3
	cycloheptanone	90	8
	2,4-pentanedione	100	-
Amino acids:	leucine	79	10
	phenylalanine	78	10

$(M-1)^-$ and $(M-3)^-$. The $(M-1)^-$ ions are the result of simple proton abstraction, and $(M-3)^-$ ions are presumably produced by proton abstraction followed by the loss of the elements of H_2. This reaction is particularly predominant in alcohols, in which case the ion formed is probably the resonance stabilized enolate ion. The formation of $(M-3)^-$ ions is fairly commonplace in OH^- NCI. One observes from Table 9 that high intensity $(M-1)^-$ ions are produced even from tertiary alcohols, and this behavior is markedly different from the behavior of such compounds in PCI. In the positive case the energy of the tertiary carbonium ion is so low that fragmentation invariably occurs to produce the carbonium ions, and virtually all evidence for the presence of the hydroxyl funtionality is lost. In OH^- NCI the converse is the case, and this difference provides a nice illustration of different results obtained using the two

modes of ionization.

The OH^- NCI spectra of several esters are given in Table 10, and one observes that the

TABLE 10

OH^- CI SPECTRA OF ESTERS

	Rel. Int. (% Total Ion.)		
	$(M-1)^-$	m/z 59	Other
methylacetate	92	8	-
ethylacetate	60	40	-
n-propylacetate	42	58	-
methyloctanoate	67	-	CH_3O^- (23) $C_7H_{15}COO^-$ (7)
TMS-eicosanoate	10	-	$C_{19}H_{38}COO^-$ (89)

major reactions are those that produce $(M-1)^-$, the acid anion, and the alkoxyl ion. The formation of the alkoxyl ion, which is the one expected to predominate on the basis of condensed phase chemistry, in fact occurs with a relatively low probability, and the dominant reaction seems to be proton abstraction. This is an illustration of the differing chemistry that obtains in condensed phase and in gas phase. Table 11 gives the spectra of three cholesteryl

TABLE 11

OH^- SPECTRA OF ESTERS

CHOLESTERYL ESTERS (RCOOX)

	Rel. Int. (% Total Ion.)		
	M-1	$RCOO^-$	$(XO-H_2O)$
CHOLESTERYL ACETATE	53	37	10
CHOLESTERYL STEARATE	53	42	5
CHOLESTERYL BENZOATE	0	100	

esters. Of interest in these compounds is the large $(M-1)^-$ ion observed in cholesteryl acetate and cholesteryl stearate, for this gives information about the identity and molecular weight of these compounds, which tends to be lost because of fragmentation in PCI mass spectrometry, as, for example, with i-butane as reactant. The absence of the $(M-1)^-$ ion in cholesteryl benzoate may be attributed to the absence of an extractable proton on the group alpha to the carbonyl of the ester function in this compound.

Finally, I give in Table 12 some relative sensitivities of methadone and several of its

TABLE 12

COMPARISON OF SENSITIVITY IN OH^- NCI AND CH_4 PCI

Compound	Sensitivity Ratio $\Sigma I_s(NCI)/\Sigma I_s(PCI)$[a]
methadone	5
1-α-methadol	15
Pyrrolidone	4.5
Pyrrolidine	2.3
Pyrroline	4.2

[a]Ratio of sample ion currents in NCI and PCI.

metabolites by OH^- NCI and CH_4 PCI. One has no reason to expect a priori that a very large difference in sensitivity will be found between reactant ion NCI and reactant ion PCI. Table 12 shows that in fact this is the case. However, one sees that there is a small difference in sensitivity in favor of the reactant ion NCI, and in one other investigation a similar small difference in favor of NCI was observed. I know of no obvious reason for this kind of behavior, although the enhanced sensitivity for 1-alpha-methadol exhibited in Table 12 is large enough possibly to be analytically of interest.

REFERENCES

1. R.C. Dougherty, J. Dalton, and F.H. Biros, Org. Mass Spectrom. 6, 1171 (1972).
2. D.F. Hunt, G.C. Stafford,Jr., F.W. Crow, and J.W. Russell, Anal. Chem. 48, 2098 (1976).
3. D.F. Hunt, and F.W. Crow, Anal. Chem. 50, 1781 (1978).
4. A.J. Lewy and S.P. Markey, Science 201, 743 (1978).
5. W.A. Garland, and B.H. Min, J. Chromatog. 172, 279 (1979).
6. S.R. Prescott, J.E. Campana, and T.H. Risby, Anal. Chem. 49, 1501 (1977).
7. M.W. Siegel and W.L. Fite, J. Phys. Chem. 80, 2871 (1976).
8. H. Massey, "Negative Ions" Cambridge Univ.Press, Cambridge (1976).
9. J.R. Frazier, L.G. Christophorou, J.G. Carter, and H.C. Schweinler, J. Chem. Phys. 69, 3807 (1978).
10. L.G. Christophorou, "The Lifetimes of Metastable Negative Ions," in Advances in Electronic and Electron Physics, 46, 55 (1978).
11. H.P. Tannenbaum, J.D. Roberts, and R.C. Dougherty, Anal. Chem. 47, 49 (1975).
12. A.K. Ganguly, N.F. Cappuccino, H. Fujiwara, and A.K. Bose, J.C.S. Chem. Comm. 148, (1979)
13. I. Dzidic, D.I. Carroll, R.N. Stillwell, and E.C. Horning, Anal. Chem. 47, 1308 (1975).
14. A.P. Bruins, A.J. Ferrer-Correia, A.G. Harrison, K.R. Jennings, and R.K. Mitchum, Adv. in Mass Spectrom. 7, 355 (1978). J.H.J. Dawson and K.R. Jennings, J. Chem. Soc. Faraday Trans. II, 72, 700 (1976).
15. D.K Bohme and L.B. Young, J. Am. Chem. Soc. 92, 3301 (1970).
16. A.L.C. Smit and F.H Field, J. Am. Chem. Soc. 99, 6471 (1977); A.L.C. Smit and F.H. Field, Biomed. Mass Spectrom. 5, 572 (1978); T.A. Roy, F.H. Field, Y.Y. Lin, and L.L. Smith, Anal. Chem. 51, 272 (1979); A.P. Bruins, Anal. Chem. 51, 967 (1979).

MASS SPECTROMETRIC GROUP TYPE ANALYSIS OF POLAR NITROGEN CONCENTRATES

H. T. BEST, D. A. DANNER, AND J. T. SWANSIGER
GULF RESEARCH & DEVELOPMENT COMPANY
P. O. DRAWER 2038, PITTSBURGH, PA 15230

INTRODUCTION

The development of shale oil and coal liquefaction processes has created a need for an analytical procedure to characterize the various nitrogen containing species. Characterization of the nitrogen types is important in terms of process development, especially for hydrodenitrogenation, where the aromaticity and location of nitrogen in the molecule affect the rate of reaction. Nitrogen can act as a catalyst poison in post-processing of synfuels. There is also the possibility of extracting nitrogen components for their chemical value.

A low ionizing voltage analysis was developed for polar nitrogen concentrates from shale oil and coal liquids. The data are reported by carbon number for ten nitrogen types with a maximum alkyl substitution of ten carbons. Ten aromatic types, dibenzothiophenes, and phenols are included since they often are contaminates in the polar concentrates - depending on the separation scheme used.

EXPERIMENTAL

The following parameters were used for data acquisition:

Spectrometer:	CEC 21-103C
Resolution:	1:600
Inlet:	All Glass @ 350°C
Source:	250°C
Ionizing Potential:	10 ev
Scan:	m/e 60 ⟶ 600

RESULTS AND DISCUSSIONS

The low voltage calibration was obtained for the unsubstituted polar nitrogen types and standardized to an existing aromatic calibration using ethyl benzene as an internal standard. The calibration components were selected as representative of species found in shale oils and coal liquids, however, obvious redundancies exist, e.g., pyridines and anilines. After standardization, the nitrogen type calibrations were extrapolated through the C_{25} range, except where overlapping occurred. In this case, the calibration for the higher molecular weight compound was inserted. Figure 1 shows the calibration curves for the 10 nitrogen types.

Several separation techniques were used to obtain nitrogen concentrates including HPLC, Sep-Pak silica cartridges, and acid-base extraction. The HPLC separations appear to be the most reliable. Note that the high concentration of phenolics in SRC-II products do not appear to be a serious interference. Table I shows a comparison of the three separation techniques applied to a Paraho gas oil.

The group type analysis has been applied to SRC-II products and shale oil distillates as shown in Table II. These data are reported on a hydrocarbon free basis, however, the polar fractions usually contain residual hydrocarbons which require that the spectrum be de-isotoped to correct for the ^{13}C contribution to the nitrogen type molecular ion.

The alkyl chain length is of interest since it can affect the separation and accuracy of the mass spectral analysis. The SRC-II products and Paraho mid-distillates both have relatively short alkyl side chains while the Paraho gas oil has long alkyl chains which may cause errors due to ion series overlaps.

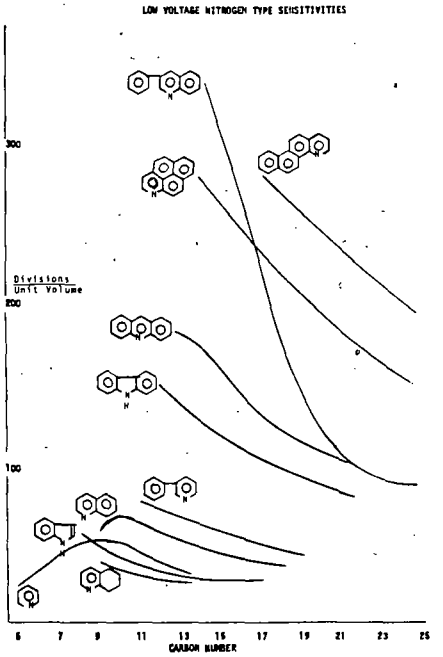

TABLE I
COMPARISON OF SEPARATION TECHNIQUES
PARAHO GAS OIL - LRMS DATA

	HPLC	SEP-PAK[R]	ACID/BASE
Pyridines: Vol.%	8	6	0
Indoles	7	6	2
Tetrahydroquinolines	5	4	0
Quinolines	22	26	40
Carbazoles	16	18	14
Pyridylbenzenes	19	19	21
Phenylquinolines	8	7	6
Acridines	6	7	11
Pyridophenanthrenes	4	3	2
Pyridobenzonaphthalenes	5	4	4
	100	100	100

TABLE II
LRMS NITROGEN GROUP TYPE ANALYSIS
(HPLC POLAR CUTS)

	SRC-II	PARAHO MID-DIST.	PARAHO GAS OIL
Pyridines: Vol.%	4	22	8
Indoles	13	25	7
Tetrahydroquinolines	18	18	5
Quinolines	22	19	22
Carbazoles	9	2	16
Pyridylbenzenes	19	8	19
Phenylquinolines	2	2	8
Acridines	8	1	6
Pyridophenanthrenes	1	1	4
Pyridobenzonaphthalenes	4	2	5
	100	100	100
Wt.% Polars in Sample	12.1	13.9	26.2

COAL LIQUID CHARACTERIZATION BY MASS SPECTROMETRY
BIOMARKERS IN WYODAK COAL AND WYODAK HYDROPYROLYSIS LIQUID

R. J. Pancirov, T. R. Ashe and Z. Baset
Exxon Research and Engineering Company
Linden, New Jersey 07036

It is well known that fossil fuel sources contain the organic remains of biological precursors prevailing at the time of their formation. Those materials that have the stability to retain their structural integrity through geologic time are known as "biological markers." These biomarkers have been observed in many types of materials, including oil shale, kerogen, petroleum, and coal. Over the past decade increasing interest in source rock/oil correlations and kerogen composition has led to a number of publications covering the biomarker content of these materials. Only recently has this technology been applied to coal.

This paper deals with some results we have obtained on a Wyodak coal extract and a Wyodak hydropyrolysis liquid. In particular, the report outlines the data that we have obtained on some of the "biomarkers" present in these liquids. These materials are generally present in low concentrations and only through the use of complex separation schemes and GC/MS/DS can they be identified and characterized.

n-Paraffins: In both the extract and the pyrolyzate the n-paraffin distribution ranged from C_{16}-C_{33}. There were no detectable amounts of branched isoprenoid paraffins. The major differences between the two samples is that in the coal extract there is a predominance of the odd over even carbon numbers (odd/even >2) compared with a slight odd preference observed in the pyrolyzate. In addition, the pyrolysis liquid contained substantially more paraffins than the extract (2.4 wt. % vs. 0.4 wt. %, respectively). Decarboxylation of the fatty acids alone could not explain the high concentration of these materials. Also, extensive extraction of the coal with pyridine did not reveal a significant increase in n-paraffins. It is inferred therefore that these long chains were cleaved from the basic coal structure during pyrolysis.

Pristene: A substantial amount of the olefins present in the coal pyrolyzate were contained in two GC peaks corresponding to prist-1-ene and prist-2-ene. It is important to note that the coal extract did not contain any detectable amounts of pristane or phytane. It is reasonable then to assume that pristane was chemically bound into the coal structure by labile linkages such as ethers or esters, and during pyrolysis these

bonds were cleaved to produce pristene.

Pentacyclic Triterpanes: There are some important basic differences between the pentacyclics observed in the extract and those in the pyrolyzate. First, those detected in the extract are predominantly unsaturated, while in the pyrolyzate they are saturated; and second, the major isomer present in the extract is the 17βH, the kinetically favored isomer, while in the pyrolyzate the 17αH isomer (thermodynamically stable) is also present. This would imply that the coal probably did not experience temperatures much above 70°C during catagenesis.

Long Chain Alkyl Benzenes: A series of long chain alkyl benzenes was detected in the pyrolyzate. There were at least four major benzene compound types observed at each carbon number, the predominant species being the n-alkyl benzene covering the carbon number range from C_{14}-C_{34}. The coal extracts did not contain any detectable amount of these compounds. This suggests that the phenyl alkanes were chemically bound into the coal structure and were cleaved during pyrolysis.

ANALYSIS OF COAL LIQUEFACTION

D. ZAKETT AND R. G. COOKS
CHEMISTRY DEPARTMENT, PURDUE UNIVERSITY W. LAFAYETTE, IN 47907

Mass spectrometry/mass spectrometry (ms/ms)[1] provides a rapid method for the identification of individual constituents[2] of solvent refined coal. For example, the presence of 3-methylindole is confirmed by a comparison (Figure 1) of the ms/ms spectrum of m/z 132 in SRC II (isobutane chemical ionization) with that of the authentic compound. Isomeric compounds can often be distinguished (Figure 2). When more than one constituent occurs at the same mass, simple chemical derivatizations of the coal liquid facilitate identification of the individual constituents.

Molecular weight profiles for specified classes of constituents can be obtained by means of scans which are selective for a particular reaction type.[3] This determination can be done in conjunction with derivatization, e.g. acetylation of the mixture. Figure 3 compares the chemical ionization mass spectrum of acetylated SRC II, with a scan taken for all constituents which undergo the reaction $m_1^+ \rightarrow (m_1 - 42)^+ + 42$. This reaction is due, in part, to ketene loss from acetyl groups. The two prominent homologous series of ions 165, 179, 193, 207 and 177, 191, 205 correspond to phenolic compounds which have been acetylated. Independent ms/ms spectra on these suspected phenols at m/z 123 (165 - 42) and at 135 (177 - 42) confirm that these compounds are a C_2-phenol and an indanol, respectively. Adduct ions generated in the chemical ionization source for particular classes of compound provide another route to distinguishing functional classes and furans are identified in coal liquids by their tendency to form adducts with the butyl cation. Dissociation of the adducts, for example by butene loss, provides the means of recognizing them and profiling their molecular weights. Figure 4 shows the ms/ms spectrum of one such butyl ion adduct which shows butene loss and butyl ion formation. This spectrum is similar but not identical to that of dibenzofuran and is indicative of an isomer.

Constituents of coal liquids have been examined using ms/ms instrumentation of both the sector type (the MIKE spectrometer) and the quadrupole type.[4] The spectra obtained for kilovolt energy collisions (MIKES) and electron volt collisions (double quadrupole,[5] QQ) can be quite different. Figure 5 illustrates this feature for protonated dimethylnaphthalene. It is shown elsewhere that the ms/ms spectra change continuously from low to high kinetic energy.[6] Both conditions give useful spectra but direct comparisons between sector and quadrupole based ms/ms data are not always possible, at least for chemical ionization.

1. R. W. Kondrat and R. G. Cooks, Anal. Chem., 50, 81A (1978).
2. D. Zakett, V. M. Shaddock and R. G. Cooks, Anal. Chem., 51, 1849 (1979).
3. D. Zakett, A. E. Schoen, R. W. Kondrat and R. G. Cooks, J. Amer. Chem. Soc., 101, 501 (1979).
4. R. A. Yost and C. G. Enke, Anal. Chem., 51, 1251A (1979).
5. D. Zakett, R. G. Cooks and W. J. Fies, Anal. Chim. Acta., in press.
6. G. L. Glish, D. Zakett, P. H. Hemberger and R. G. Cooks, ASMS, 1980, TPMP11.

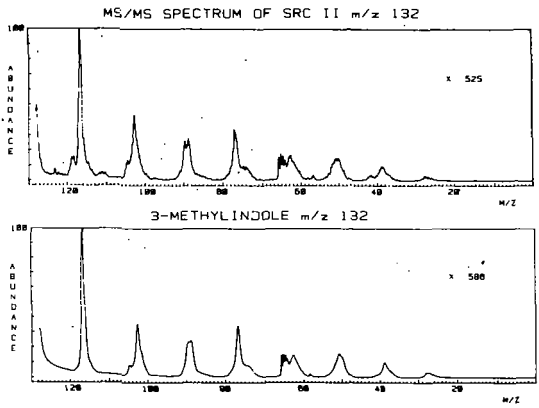

FIGURE 1. Identification of 3-Methylindole in a Coal Liquid Sample by ms/ms.

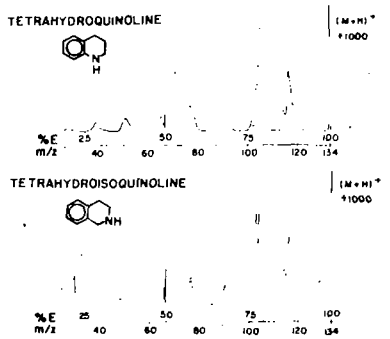

FIGURE 2. Isomer Distinction From ms/ms Spectra of Protonated Molecules.

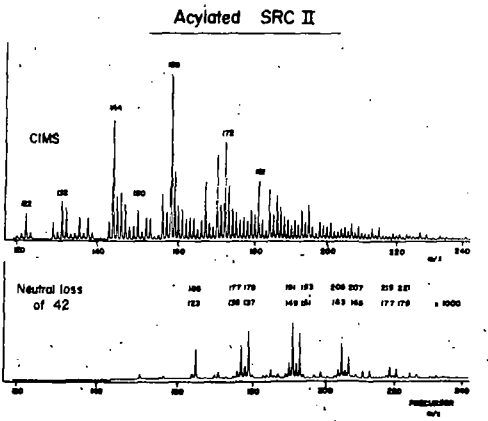

FIGURE 3. Mass Spectrum of Acylated Coal Liquid Compared to a Mass Scan for Specific Functionalities Taken by Fixing the Mass of the Neutral Fragment in a Collision-Induced Dissociation.

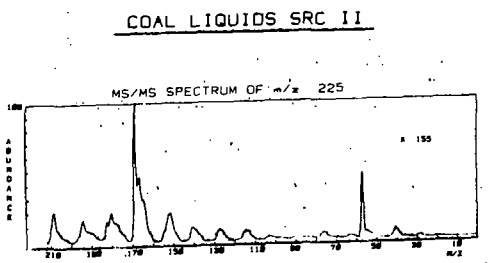

FIGURE 4. Ms/ms Spectrum of Butyl Ion Adduct of a Furan.

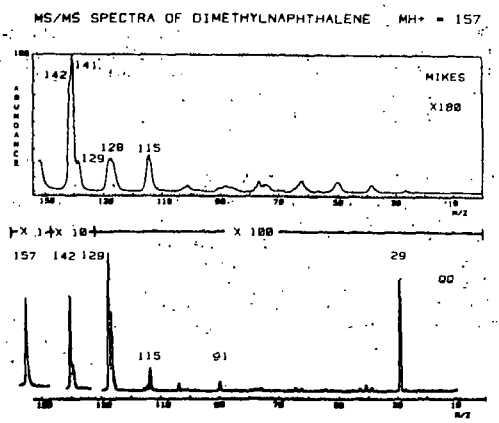

FIGURE 5. Differences Between ms/ms Spectra of Protonated Dimethylnaphthalene Using Sector (MIKES) and Quadrupole (QQ) Instruments.

MASS SPECTROMETRIC METHODS FOR THE QUANTITATIVE ANALYSIS OF TRACE ORGANIC CONSTITUENTS IN ALTERNATE FUELS

L. R. Hilpert, J. M. Brown, R. G. Christensen, H. S. Hertz, W. E. May, K. L. Richie, and E. White V

Organic Analytical Research Division
Center for Analytical Chemistry
National Bureau of Standards
Washington, DC 20234

Introduction

With the increasing number of analyses being performed on alternate fuels to assess their content of toxic/carcinogenic compounds, it is vital that the analyses be accurate and comparable among laboratories. Two ways of assuring accuracy in trace organic analysis are the use of adequate analytical methodology and the use of suitable quality assurance standards or Standard Reference Materials (SRMs). The National Bureau of Standards has recently released an SRM Shale Oil which has been certified for the concentrations of phenol, o-cresol, fluoranthene, pyrene, benzo(e)pyrene, and benzo(a)pyrene. This material is the first SRM for organics in an alternate fuel matrix and is intended for use in evaluating the reliability of analytical methods for the determination of trace level organic compounds in complex matrices such as petroleum, synthetic fuels, and environmental extracts. Gas chromatography, high performance liquid chromatography, and gas chromatography-mass spectrometry were used in performing the certification analyses. The phenolic compounds were also determined on the NBS liquid chromatograph-mass spectrometer system.

Experimental

A summary of the analytical methods used for the shale oil SRM 1580 certification are shown in Table I. The GC/MS determinations were performed using selected ion monitoring (SIM) and a standard addition technique for quantitation. The polynuclear aromatic hydrocarbons (PAH) were determined on a 30 m SE-54 wall coated open tubular (WCOT) column interfaced to a quadrupole mass spectrometer through a 25 cm length of Pt/Ir tubing (0.15 mm ID). 1-2 µL aliquots of the diluted (1:10) shale oil sample were analyzed directly without any prior sample clean-up. The molecular ion of the analyte was monitored in 0.1 amu increments to insure that the voltage was sampled at the top of the mass peak; a dwell time of 100 ms was used to give at least 20 data points across the chromatographic peak. To compensate for variable injection volumes onto the GC column and the possibility of non-reproducible split ratios, a second compound natively present in the shale oil and in the same compound class as the analyte was also monitored as an internal standard. Area ratios of the analyte peak to IS peak were plotted vs. the amount of analyte added to the shale oil, and the concentration of the analyte was determined from the curve's intercept with the abcissa, using a linear least squares analysis.

The phenols were determined by GC/MS with SIM on HPLC-generated shale oil fractions. Approximately 15 mg of the shale oil were chromatographed on a preparative scale aminosilane column, and sample fractions were collected to include the analytes and an internal standard. Details of the use of HPLC for cleaning up complex samples have recently been published (1). Fraction volumes were then reduced under a stream of dry N_2, and suitable aliquots chromatographed on a 20 m Pluronic L-64 WCOT column. A standard addition technique was used for quantitation.

Phenol and o-cresol concentrations were also determined on the NBS LC/MS system. An LC/MS interface has been designed which allows essentially all of the sample in the effluent of a conventional liquid chromatograph to be introduced into a differentially pumped quadrupole mass spectrometer (2). 1.5 µL of the shale oil were chromatographed on a polar amino/cyano column using 2 percent isopropanol/hexane as the mobile phase at a flow rate of 1 mL/min. The LC/MS system was operated in the EI mode at a source pressure of 7×10^{-5} torr. The molecular ions for phenol and o-cresol were monitored in real time and the concentrations in the shale oil determined by comparison of peak heights with a series of external standards.

Results and Discussion

The results of independent determinations of the five certified organic compounds in the shale oil SRM are shown in Table I. As can be seen, the agreement among values obtained by independent techniques of sample fractionation and quantitation is excellent. The ability to determine individual compounds in complex matrices such as the shale oil by direct injection of the oil without any prior sample clean-up is particularly noteworthy. The combination of the high resolving power of the wall coated open tubular capillary columns and the specificity of selected ion monitoring detection allows determination of many PAH free from non-analyte interferences. The SE-30, SE-54, and Pluronic L-64 WCOT columns have also proven to be extremely durable with lifetimes of several months of daily use without any significant loss of resolution.

The LC/MS determination of phenol and o-cresol in the shale oil illustrates the use of a novel LC/MS interface for the analysis of complex mixtures. The LC effluent is concentrated by allowing it to flow down an electrically heated wire with the current to the wire controlled by a feedback loop from a volume sensing photocell. The concentrated effluent flows through a small needle valve which regulates the flow into the mass spectrometer and is constructed such that liquid is sprayed into the ion source. Five determinations of phenol and o-cresol concentrations in the shale oil SRM were made over a two month period. The results of these determinations (also shown in Table I) compare well with the certified values of 407 ± 50 μg/g for phenol and 385 ± 50 μg/g for o-cresol.

Table I

SRM 1580 Shale Oil

Summary of Analytical Methods

Compound	Concentration μg/g	Sample Preparation Technique	Analytical Technique
Fluoranthene	55 ± 5*	Direct Injection	GC/MS
	53 ± 2	HPLC	HPLC
Benzo(a)pyrene	20 ± 1	Direct Injection	GC/MS
	23 ± 1	HPLC	HPLC
Benzo(e)pyrene	17 ± 1	Direct Injection	GC/MS
	20 ± 3	HPLC	HPLC
Phenol	412 ± 35	HPLC	GC/MS
	402 ± 4	Acid/Base Extraction	GC
	419 ± 33	Direct Injection	LC/MS
o-cresol	386 ± 42	HPLC	GC/MS
	384 ± 9	Acid/Base Extraction	GC
	440 ± 90	Direct Injection	LC/MS

*Uncertainty is one standard deviation from the mean.

References

(1) Hertz, H. S., Brown, J. M., Chesler, S. N., Guenther, F. R., Hilpert, L. R., May, W. E., Parris, R. M., and Wise, S. A., Methods for the Quantitative Determination of Individual Organic Compounds in Shale Oil, Anal. Chem., in press.

(2) Christensen, R. G., Hertz, H. S., Meiselman, S., and White V, E., A Liquid Chromatograph/Mass Spectrometer Interface Incorporating Continuous Sample Preconcentration, in preparation.

MAMOA6 GCMS ANALYSIS OF COAL LIQUID AND ITS CATALYTICALLY HYDROGENATED PRODUCTS, B. W. WILSON, D. M. SCHOENGOLD, M. R. PETERSEN, and R. A. PELROY, Physical Sciences Dept. and Biology Dept., Battelle, Pacific Northwest Laboratory, Richland, WA 99352.

Coal liquid has been compared to its hydrogenated products by GCMS and Ames *Salmonella* assay. The upgraded materials were found to consist principally of hydroaromatic species with substantial reduction in the concentrations of nitrogen, sulfur and oxygen containing compounds. Of particular interest was the drastic decrease in primary aromatic amine content which appeared to correlate with the reduction in mutagenic activity in the hydrotreated products. These analyses have been of particular value in understanding the formation and fate of primary aromatic amines during coal liquefaction and hydrogenation and have been used to guide further biological testing of upgraded coal liquids.

MASS SPECTRAL ANALYSES OF SULFUR COMPOUNDS IN A LUBE OIL BASESTOCK EXTRACT

C. S. Hsu and J. M. Kelliher
Exxon Research and Engineering Company
Linden, New Jersey 07036

A "polar" extract of lube oil basestock from a florisil column separation was further separated on silicic acid. Most of the eluted material was found to be in the aromatic fraction from the silicic acid column. Approximately 40% of the compounds in this fraction were sulfur-containing.

Gas chromatographic analysis of the complex aromatic fraction resulted in poor resolution between components. The use of a combined gas chromatography - mass spectrometry system interfaced with a data system (GC/MS/DS) was found to be a powerful tool for analyzing such a complex mixture. Furthermore, the application of selected ion chromatograms (SIC) for data reduction enhances the capabilities of GC/MS/DS for handling compound types unresolved by GC analysis.

ASTM D 3239 is designed for gas oils with sulfur contents of not more than one percent. A method of combining ASTM D 3239, high resolution mass spectrometry, and selected ion chromatography, is suggested for compound type analysis of high boiling aromatic fractions with high sulfur contents.

By ASTM D 3239 alone, the sulfur contribution from the thiophenic compounds was calculated to be 2.9%, while the Dietert sulfur for this cut was 5.46%. From high resolution mass spectral data and selected ion chromatograms, it was found that in addition to the sulfur compounds included in the ASTM calculations, acenaphthenothiophenes (-18S) and acenaphthalenothiophenes (-20S) were also present in significant amounts. After adjustments for the contributions from the -18S and -20S series, the calculated sulfur content was 4.8%.

RELATIVE FIELD IONIZATION EFFICIENCIES OF HYDROCARBON COMPOUNDS

S. E. Buttrill, Jr. and G. A. St. John
Mass Spectrometry Development Program
SRI International
Menlo Park, CA 94025

The eventual use of field ionization (FI) mass spectrometry for routine quantitative analysis of complex mixtures will require a knowledge of the relative FI efficiencies of a wide variety of chemical compounds. As one part of a project to develop methods for the analysis of middle distillate fuels obtained from non-petroleum sources, we have determined the relative FI sensitivities of over 80 pure hydrocarbon compounds.

The general method was similar to that used by Scheppele, et al (Ref 1) in their pioneering study. Mixtures were prepared using weighed quantities of pure hydrocarbons. Samples of each mixture were introduced into the mass spectrometer via an all-glass, batch inlet system. We used the SRI volcano style FI source (Ref 2) on a 10 inch radius 90^{0} magnetic sector mass spectrometer operating at a mass resolution of 500 and an overall sensitivity of 2-4 x 10^{-6} ions/molecule. Toluene was included in all mixtures as an internal standard. All field ionization sensitivities are given on a relative scale where 1.00 is the relative sensitivity of toluene.

Table 1 compares the results of this work with those obtained by Scheppele, et al. The agreement is considered good in view of the great differences in FI sources used (razor blade versus volcano style).

Table 1. Relative FI Sensitivities (per mole)

Compound	Ref. 1	This Work
Benzene	0.88	0.88
Toluene	1.00	1.00
Ethylbenzene	0.98	1.04
Mesitylene	1.12	1.22
Propylbenzene	1.00	1.18
Naphthalene	1.23	1.42
Tetralin	1.12	1.34
Fluorene	1.42	1.11

Table 2. Relative Field Ionization Sensitivities (Toluene = 1.00)

Compound	Rel. Sens.	Compound	Rel. Sens.	Compound	Rel. Sens.
xylenes	1.13	naphthalene	1.42	fluorene	1.11
ethylbenzene	1.04	2-methylnaphth.	1.48	perhydrofluorene	0.62
o-ethyltoluene	1.29	2-ethylnaphth.	1.42	n-heptane	0.43
p-ethyltoluene	1.25	2,3,5-trimethyl-		n-octane	0.46
n-propylbenzene	1.18	naphthalene	1.22	n-nonane	0.41
i-propylbenzene	1.24	1,2-dihydro-		n-decane	0.39
i-butylbenzene	1.17	naphthalene	1.44	n-undecane	0.46
phenylhexane	1.18	tetralin	1.34	n-dodecane	0.46
phenylocatane	0.86	decalin	0.78	n-tridecane	0.44
phenylnonane	0.77	biphenyl	1.32	n-tetradecane	0.44
phenyldecane	0.61	cyclohexylbenzene	1.12	n-pentadecane	0.47
phenyldodecane	0.56	dicyclohexyl	0.74	n-hexadecane	0.32
phenyltridecane	0.44	indan	1.25	c-octane	0.53
		hexalydroindan	0.54	ethyl-c-hexane	0.56

Additional results are summarized in Table 2. Several interesting trends are evident. First, the FI sensitivity for saturated compounds is significantly lower than for aromatics, generally by a factor of 2 to 4. The highest efficiency measured in this study was that of 2-methylnaphthalene at 1.48 times that of toluene. The lowest was for n-hexadecane at 0.32 or a factor of 4.6 less. It is important not to place too much importance on this number since it represents a ratio of the two extreme values, both of which are therefore suspect.

The elementary theory of field ionization predicts an exponential dependence of field ionization rate on the ionization potential of the molecule. Because the relative sensitivities of the compounds listed in Table 2 are so nearly equal, we can conclude that field ionization is not the rate limiting step in the conversion of neutral molecules to ions in the field ionization source. Other factors, such as the rate sample molecules reach the field emission sites, must control the rate of ion formation.

The relative FI efficiencies of the alkanes showed more variability than those of the aromatics. They tend to be lower at higher field ionization voltages. In order to obtain maximum accuracy in the analysis of fuels, it will be necessary to run standard mixtures at the same time to calibrate the relative FI sensitivities of the various compound classes. In this way, we expect to achieve accuracies of $\pm 5\%$ in the determination of the absolute concentrations of individual fuel components.

ALKYLBENZENES DERIVED FROM CAROTENES IN COALS BY GC-MS-C

By E. J. Gallegos

Seven homologous series of alkylbenzenes ranging in carbon number from about C_{10} to C_{35} have been tentatively identified in United States Tertiary, Cretaceous, and Carboniferous coals using GC-MS-C. Figure 1 shows a typical profile MAP of the homologous alkylbenzenes observed in Wyodak coal C_{15} to about C_{30}. Figure 2 gives the alkylbenzene multiplet at C_{28} including structure assignments.

The assigned alkylbenzene structures were deduced in light of selective microbial and geothermal modification of carotenoids.

Gama Carotene, $C_{40}H_{56}$, and chlorobactene, $C_{40}H_{52}$, were used as typical carotenoids which through diagenetic chain methyl removal and aromatization and degradation during maturation can produce the seven homologous series of alkylbenzenes observed by GC-MS-C.

Sequential loss of the various methyl groups from the aromatic rings in all possible combinations will yield alkylbenzenes whose electron impact spectra will have base peaks at m/e 92, 106, 120, and 134. See Table I. A total of seven n-alkylbenzene isomers having zero to three methyl substituents on the aromatic ring can thus be derived from the two proposed perecursor carotenoids.

After the chain methyl groups are removed assume that maturation preference is to remove all methyl substituents from the aromatic ring. Next preference is to leave one methyl substitution, etc., to the three methyl substitutions. Then the relative concentrations of the various isomers of alkylbenzenes of a given carbon number would line up as shown in Table I.

Gama Carotenes appear to be more common in nature according to the literature. This possibility and the fact that an alkylbenzene which will give a base peak at m/e 92 can be arrived at from both Gama Carotene and chlorobactene suggesting that this m/e 92 base peak molecule isomer will be present in the highest concentration. This is the case, see Figure 2. This sort of argument is used to justify concentration and structure of the remaining isomers.

The structure of the m/e 92 base peak isomer homologs is also supported by the similar mass spectra given in the literature for n-dodecyl, tetradecyl, and hexadecyl benzenes all of which show a base peak at m/e 92, etc., which are consistent with the mass spectrum of Isomer I, Figure 3, and its homologs.

Table II gives the relative concentrations of the alkylbenzene in the total column effluent for the three coals of different rank studied.

Table II

Alkylbenzene Concentration in Three U.S. Coals

Wyodak, Tertiary	1.50
Navajo, Cretaceous	0.90
River King, Carboniferous	0.06

Support for the arguments presented would be greatly enhanced if some class of microbes were discovered which likes to clip methyl groups preferentially from a carbon chain.

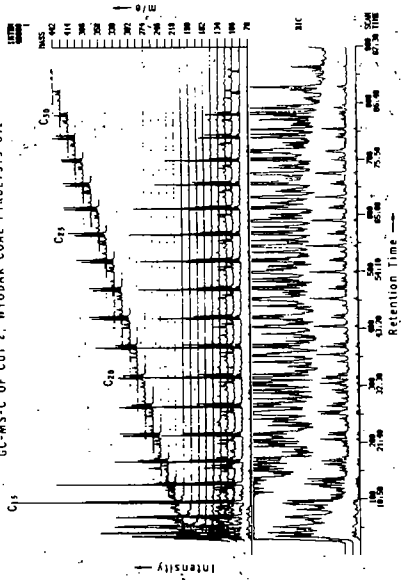

FIGURE 1
ALKYLBENZENE MAP C_nH_{2n-6}, WHERE n = 10 TO 32
GC-MS-C OF CUT 2, WYODAK COAL PYROLYSIS OIL

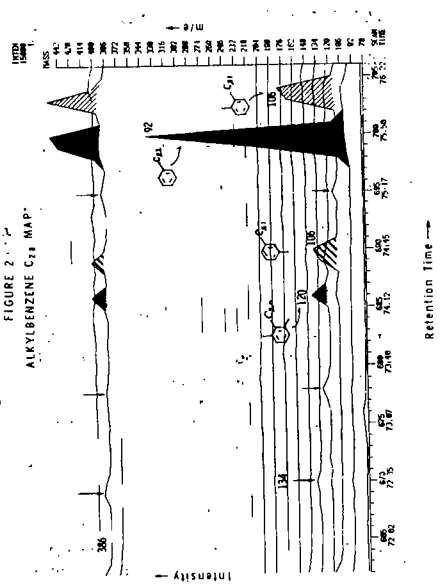

FIGURE 2
ALKYLBENZENE C_{23} MAP

TABLE I

ALKYL BENZONE ISOMERS
POSSIBLE FROM GAMMA
CAROTENE (A) OR CHLOROBACTENE (B)

From Type A	From Type B	Isomer
Cn 92	Cn 92	1
Cn 106	Cn 106	2
	Cn 106	3
Cn 120	Cn 120	4
	Cn 120	5
	Cn 120	6
	Cn 134	7

FIGURE 3
MASS SPECTRA OF C_{23} ALKYLBENZENE ISOMERS
FOUND IN COAL

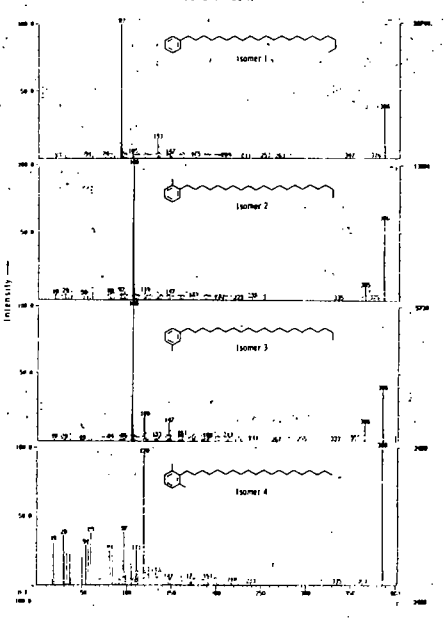

DIRECT ANALYSIS OF CARBOXYLIC ACIDS IN OIL SAMPLES BY CAPILLARY GC/MS

Jacob Shen, The Standrd Oil Company (Ohio), 4440 Warrensville Center Road, Cleveland, Ohio 44128

The characterization of organic acids in heavy end petroleum products necessitates solvent extraction and group separation steps prior to more detailed compositional analysis by MS or GC/MS. These extraction and separation procedures are usually tedious and time consuming. We report a rapid one step GC/MS method for analysis of carboxylic acids in petroleum products. The method requires no prior extraction or separation and involves only a minimum amount of sample preparation work.

Experimental

Typically about 0.2 ml (approximately 200 mg) petroleum product were weighed into a graduated test tube (15 X 120 mm). n-Butyl acetate (0.8 ml) was added to dissolve the sample. Methanolic tetramethyl ammonium hydroxide 24% (1 ml) and methanol (1 ml) were added and the mixture was shaken. n-Butyl acetate (4 ml) was then added and the solution became clear. The solution was warmed in a hot water bath for five minutes. Methyl iodide (1 ml) was added afterwards. Tetramethyl ammonium iodide precipitated on standing. The supernatant solution (1 μl) was directly injected into the GC/MS system.

Results and Discussion

That alkyl esters can be quantitatively prepared from their corresponding acids by this method has been reported previously (1,2). Our modified procedures have not altered the quantitative nature of the method. Recovery efficiency of acids from heavy end petroleum products is excellent. Table I shows that various amounts of oleic acid spiked into the dewaxed petroleum oil can all be recovered as methyl oleate quantitatively by using the esterification procedures described. Quantitative GC/MS analysis was carried out by MID via the monitoring of the m/e = 296 ion. Furthermore, rapid quantitative analysis of a whole batch of samples by MID can be accomplished by injecting the samples in immediate succession without having to wait for the completion of the first GC run. For example, a total of fifteen sample injections can be easily made in 30 minutes and that the entire GC/MS analysis can be completed in less than an hour.

When badly degraded petroleum samples that have high acid numbers are to be analyzed, they can generally be dissolved directly in methanolic tetramethyl ammonium hydroxide solutions. It is therefore not necessary to first dissolve the sample in n-butyl acetate prior to the addition of methanolic tetramethyl ammonium hydroxide solution. Figure 1 shows the acids identified in a used petroleum oil sample. Clearly a series of n-carboxylic acids from C_7 to C_{20} are the major acid components present in this used oil sample.

References

1. R. H. Greeley, J. Chromatogr., 88, 229 (1974)
2. J. C. West, Anal. Chem., 47, 1708 (1975)

Table I.

Analysis of Olefic Acid in Dewaxed Petroleum Oil[a]

Amount of Pet. Oil	Amount of Oleic Acid Spiked	Relative Amount of Oleic Acid	Relative Integrated Area of m/e=296 Ion[b]
--	13.59	1.0	1.0
167.69	12.07	0.9	0.9
161.68	7.61	0.5	0.5

[a] 1 ml sample injected each time at a split ratio of 75:1. A 30 m glass WCOT SP-1000 column was used and the column temperature was kept at 210°C isothermally.

[b] An average of five runs.

Figure 1

GC/MS identification of carboxylic acids in badly degraded petroleum oil that can be directly dissolved in methanoleic tetramethyl ammonium hydroxide solutions.

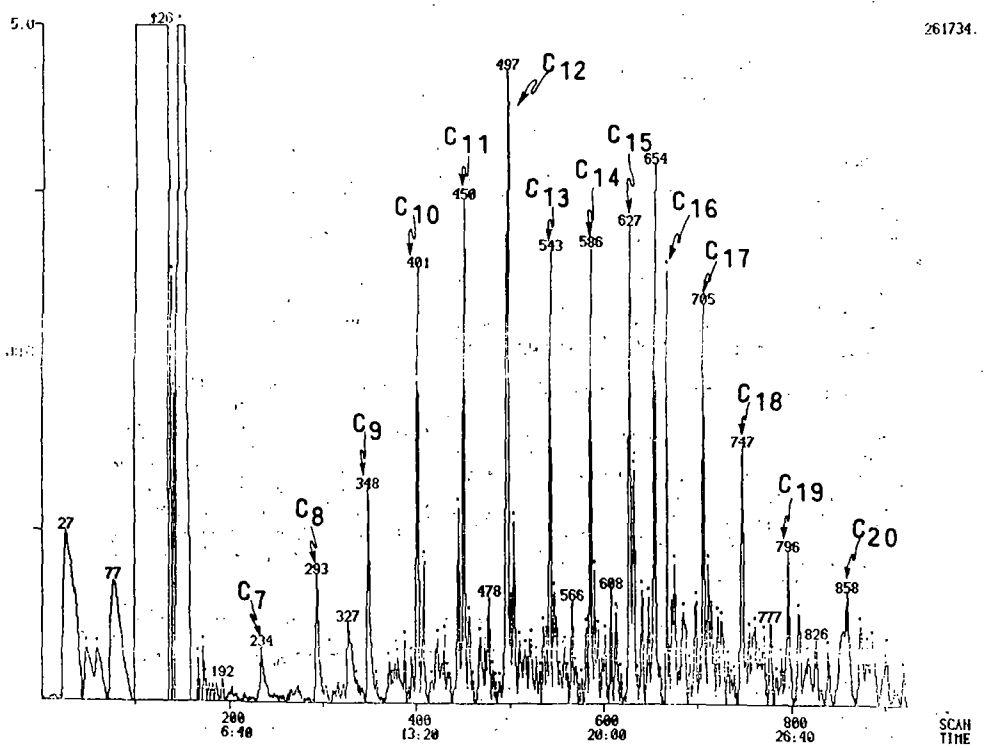

MAMOB1 Application of the MS80 and a New High Resolution Selected Ion Monitoring Routine to the Determination of Trace Levels of TCDD

K.R. Compson, J.R. Chapman, G.A. Warburton, P.A. Ryan, A. Carrick

The MS80 is a new high performance, medium resolution mass spectrometer in which the principal design criteria were the gc performance and sensitivity, particularly at high resolution. This feature is exemplified by the sensitivity of 5×10^{-10} coulombs per microgramme at 7,500 resolution, a characteristic that is particularly important in mass measurement, where accuracy is a function of both resolution and sensitivity, and selected ion monitoring in which detection limits are often not restricted by the sensitivity of the mass spectrometer but by background contributions yielding ions at the masses being monitored. This problem can be overcome by using a resolution that is sufficient to separate the ions of interest from the background.

The highly toxic environmental pollutant tetrachlorodibenzodioxin (TCDD) provides an excellent example of this problem. This is because of the likelihood of its occurrence in association with polychlorinated biphenyls (PCB) and the pesticide residue DDE. The table below shows the resolutions required for separation of the major TCDD ion from abundant ions in PCB and DDE.

	COMPOSITION	MASS	RESOLUTION NEEDED
TCDD	$C_{12}H_4O_2{}^{35}Cl_3{}^{37}Cl$	321.8936	
DDE	$C_{14}{}^{35}Cl{}^{37}CL_3$	321.9292	9,045
PCB	$C_{12}H_3{}^{35}Cl$	321.8677	12,442

Quantitative determination, of course, is assisted by high resolution chromatography but this is not always sufficient and there is also a requirement for a fast screening technique that would be suitable for use with a direct insertion probe.

A new DS55 program has been developed to assist with this type of problem. This uses the precisely calibrated display facility of the MS50 or MS80 and MS25, when fitted with the peak matching system, to sweep over the peak. The width of the sweep is set by the mass spectrometer. Data is acquired during each sweep and DS55 is then able to perform smoothing, averaging and background subtraction. It is possible to sweep sequentially over up to four masses.

The technique has been demonstrated using a sample containing 50pg of TCDD and 500 pg of DDE, the mass spectrometer was an MS80 at a resolution of 7,500. Data was acquired during the gc run and then displayed as the total ion current chromatogram (t.i.c) and mass chromatograms of each of the ions monitored. This is illustrated in figure 1. The data system monitored m/z 321.8936, the largest peak in the molecular ion group of TCDD with a sweep of 1000 parts per million. In figure 2 the scans acquired during elution of the TCDD peak have been summed and the peak profile displayed. After this the peak area can be calculated and normalized to an internal standard, the area considered being delineated by means of the cursor of the VDU.

Figure 3 shows the result of summing during elution of both the 50 pg TCDD and 500 pg DDE peaks. This is equivalent to the output of evaporation from a direct insertion probe. The peaks are, from lowest mass, TCDD, DDE and two impurities, the first probably PFK, the second unknown.

The area under each peak may be calculated by dropping perpendiculars as shown or by skimming.

Finally figure 4 illustrates the sensitivity of the MS80/DS55 system showing the t.i.c. response at 7,500 resolution of an injection of 2 picogrammes of TCDD.

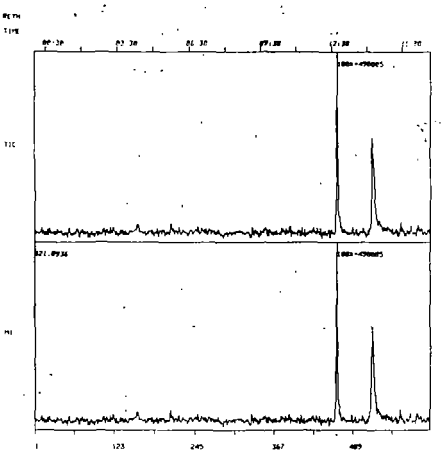

Fig.1 MS80 HRMPM: Run summary 500pg DDE + 50pg TCDD

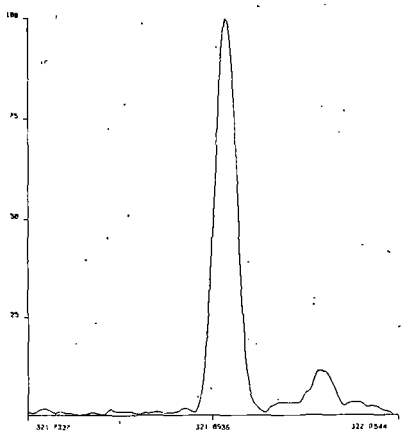

Fig.2. MS80 HRMPM: Summed mass profile 50pg TCDD

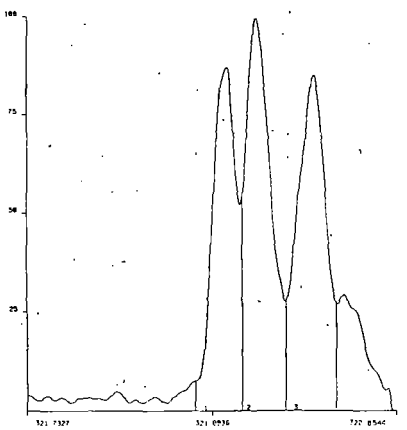

Fig.3. MS80 HRMPM: Summed mass profile 500pg DDE + 50pg TCDD

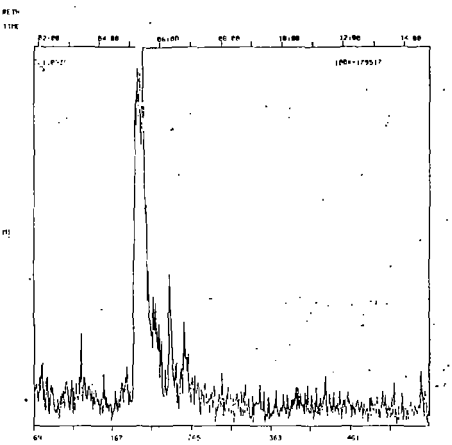

Fig.4. MS80 HRMPM: Mass chromatogram. 2pg TCDD

Development and Application of an all Glass Capillary GC-High Resolution MS Interface and Scan Circuit for Isomer Determinations of Chlorodioxins in Biological Tissues, Combustion Stack Gases, and other Environmental and Industrial Samples.

J.G. Solch, G.F. VanNess, C.D. Miller, H.R. DuFour, M.L. Taylor, and T.O. Tiernan, The Brehm Laboratory and Departments of Chemistry and Pharmacology/Toxicology, Wright State University 45435

Of the 75 possible chlorinated dibenzo-p-dioxins (CDDs); mono thru octachlorinated dibenzo-p-dioxins are known and amongst these the following numbers of isomers are possible: monochlorinated, 2; dichlorinated, 10; trichlorinated, 14; tetrachlorinated, 22; pentachlorinated, 14; hexachlorinated, 10; heptachlorinated, 2; octachlorinated, 1. The relative toxicity and the probable origin of a particular CDD can be ascertained (in some instances) if the CDD isomer in question is correctly identified and quantitated. Consequently in order to thoroughly characterize the CDDs entering the environment via combustion processes, applications of pesticides, and waste chemical effluents, this laboratory has proceeded to develop high resolution gas chromatographic-high resolution mass spectrometric (HRGC-HRMS) methodology for quantitating CDD isomers in various specimens. The extraction methodology developed in our laboratory for various types of samples has been described in detail elsewhere (1-3). The HRGC-HRMS instrumental technique developed for quantitating the CDD isomers in the prepared sample extracts is detailed below.

The instrumentation employed to accomplish the HRGC-HRMS analysis of TCDD isomers comprises a Varian 3740 Gas Chromatograph coupled with an AEI MS-30 Mass Spectrometer. Both the gas chromatograph and the mass spectrometer have been modified as follows. The gas chromatograph is equipped with a glass capillary WCOT column which in turn is coupled to the mass spectrometer via a heated, all-glass transfer line (0.5 mm ID). The column is coupled to the transfer line via a zero dead volume fitting which accommodates the end of the curved glass column (no straightening required). The transfer line is coupled to the mass spectrometer source housing via an AEI glass reintrant. The AEI MS-30 mass spectrometer has been modified to include a newly engineered step-scan circuit which is shown diagramatically in Figure 1. This new circuit is incorporated into the ESA circuitry of the mass spectrometer. A Nicolet 1074 Signal Averaging Computer drives the scan circuit which at the start of scanning switches the ESA voltage to a preset value corresponding to a point on the mass scale slightly less (~ 0.01 amu) than m/z 319.8966 which is the molecular ion for TCDD. The ESA, following a preset delay, scans across the mass peak (scan time = 25 milliseconds) and the signal is acquired both on an integrating capacitor and by the Nicolet. Following completion of the scan, the integral of the signal is shunted to a sample-and-hold capacitor and finally this signal is routed thru a RC filter to one channel of a 4 channel recorder. Subsequently the ESA voltage is switched to the next voltage corresponding to the TCDD molecular ion with one ^{37}Cl (321.8936) and the scan/integration process is repeated. In all, intensities for 4 masses are acquired during a 0.1 second interval. The speed of the new step-scan circuit permits the AEI MS-30 to be capable of performing high resolution mass spectral (~ 1:10,000) multiple peak monitoring of isomers separated by capillary gas chromatography. The parameters for the HRGC-HRMS system described above are asfollows: 1) Gas Chromatograph: column, 60M OV101 WCOT glass capillary column; carrier gas,hydrogen 30 cm/sec; temperatures, injector 230°, column 190° then programmed to 230° at 1°/min, transfer line 250°; injection mode, splitless (tridecane solvent); mass spectrometer: ionizing voltage 70 eV; source temperature 250°.

Analyses of several highly pertainent samples have been performed using the HRGC-HRMS system. The results obtained are shown graphically in Figures 2-4. In addition to the HRGC-HRMS result for 11 TCDD isomers shown in Figure 2, the results for a sample of chemical waste containing apparently only the 2, 3, 7, 8 isomer are shown in Figure 4 and finally TCDDS plus other unidentified components of an incinerator stack sample are shown in Figure 3. Work is continuing in our laboratory to implement this highly sophisticated technique in performing TCDD isomer-specific analyses of environmental and biological samples.

References

1. G.F. VanNess, J.G. Solch, M.L. Taylor, and T.O. Tiernan, Presented at the 28th Annual Conference on Mass Spectrometry and Allied Topics, New York, New York, 1980.

2. G.F. VanNess, J.G. Solch, M.L. Taylor, and T.O. Tiernan, Submitted to Chemosphere.

3. T.O. Tiernan, J.G. Solch, G.F. VanNess, and M.L. Taylor, Submitted to Science.

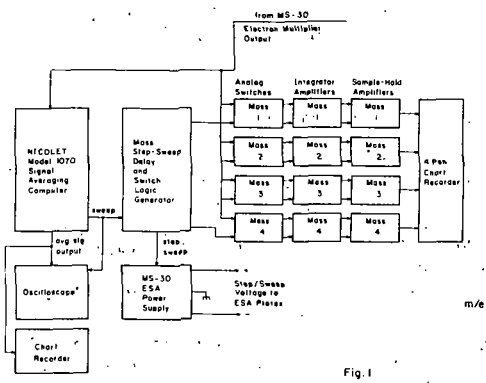

Fig. 1

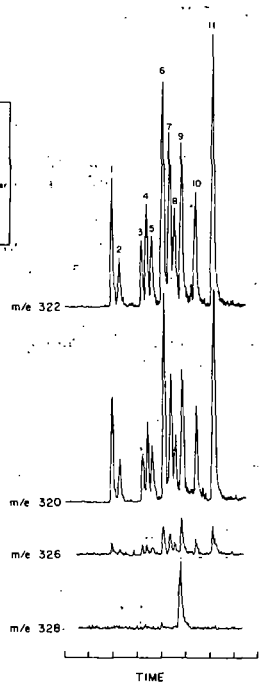

Fig. 2
Capillary HRMS Chromatogram for 2.0μl TCDD Isomer Mix
(Contains 2.0ng $^{37}Cl_4$-TCDD)

TCDD ISOMERS
1) 1,3,6,8
2) 1,3,7,9
3) 1,4,6,9
4) 1,3,7,8
5) 1,2,6,8
6) 1,2,7,9
7) 1,2,6,9
8) 1,2,3,4
9) 2,3,7,8
10) 1,2,6,7
11) 1,2,8,9

50mV Full Scale for all Ions

Effective Resolution ≈ 9200

Fig. 3
49% MRI-1
(Refuse incinerator)

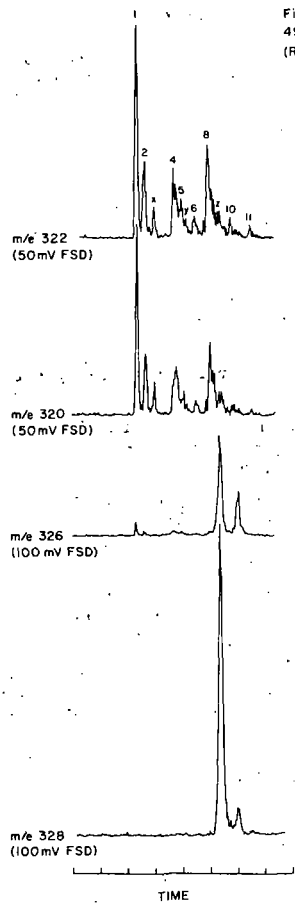

Fig. 4
90% KC COMP-2
(Chemical Sludge)

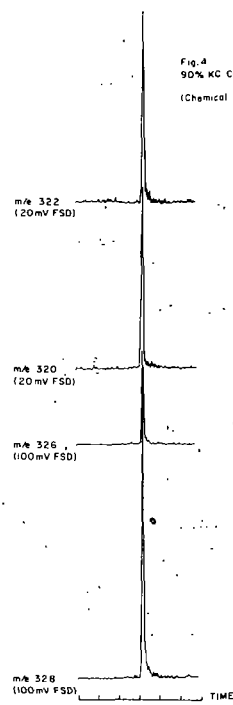

2

AUTOMATED MULTI-MODE MASS SPECTROMETRY (AMMS): I. EVALUATION OF THE PERFORMANCE OF SEVERAL AMMS DESIGNS BASED ON THEIR EFFICIENCY FACTORS

C. CHANG

Brehm Laboratory and Dept. of Chem., Wright State Univ., Dayton, Ohio 45435

In a GC-MS system in order to facilitate the chemical analysis it is desirable that each GC sample peak be analyzed under various mass spectrometric operating modes including variations of the ionization modes (EI,CI, etc.), ion charge polarities (positive and negative ions), and CI reagent gases. The advantage of this multiple mode operation is obvious in view of the sheer large numbers of the available different spectra for sample analysis. More importantly, the newly created synergetic advantage resulting from the use of proper combinations of two or more spectra in reaching unequivocal results for sample analysis can not be overestimated.

From the view point of multiple mode operation the history of the development of the mass spectrometers for analytical application can be largely divided into three generations. The first generation mass spectrometer is a mass spectrometer designed exclusively for operation under one operating mode. Most mass spectrometers currently in operation are still of this type. The second generation mass spectrometer is defined as a mass spectrometer capable of multiple mode operation but requiring manual operation (and consequently some down time) in switching from the first operating mode to the second. Finally, the third generation mass spectrometer is one capable of performing multiple mode operation in an automatic fashion. Automated multi-mode mass spectrometry (AMMS) can thus be defined as the technique in which two or more different operating modes are conducted simultaneously or sequentially in rapid succession with the cycle for each period short compared to the sample residence time.

To properly evaluate the performance of the AMMS designs a term "Efficiency Factor" is employed which is defined as follows:

$$\text{Efficiency Factor} = n\Sigma\, T_i \cdot S_i$$

The term n is the total number of different operating modes conducted in each cycle. The term, T_i, is defined as the time efficiency factor for the ith operating mode and can be expressed mathematically as follows:

$$T_i = \frac{\text{ith operating mode analysis time}}{\text{cycle period}}$$

Similarly the term, S_i, is defined as the sample efficiency factor for the ith operating mode and can be expressed as follows:

$$S_i = \frac{\text{amount of sample delivered to the ionization region for the ith operation}}{\text{amount of sample available during ith operation}}$$

The calculation of the efficiency factor is based on the following two assumptions: 1. All operating modes within each cycle are assumed to be of equal importance for the sample analysis: 2. The duration of each cycle is limited to 4 sec or less in order to meet the requirements of current capillary GC interfaces.

The present formula has a built-in factor (n) which favors a higher number of operating modes during each cycle. This factor represents the synergetic effect of the multiple mode operation and is the main driving force for the current instrumental development trend.

Several contemporary AMMS designs evaluated here include CI/EI double beam (AEI), Tandem CI/EI (Extranuclear), Alternate CI/EI (Kratos), and PPINICI (Finnigan). The calculation of the efficiency factors for these designs are listed in Table I. Also included in this table are the cycle formats of these designs. The solid line between arrows is the mass scan time for each CI or EI operation and is assumed to be one second for simplicity. The dashed line indicates the case where significant switching time (for magnet resetting, gaseous flow and ion focusing readjustments, etc.) is required. The duration of the switching time is again assumed to be one second.

Table 1. THE EFFICIENCY FACTORS OF SEVERAL CONTEMPORARY AMMS DESIGNS

MS Designs	Cycle Formats	Periods (sec.)	n	Efficiency Factors
CI/EI double beam source (AEI-30)	CI / EI	2	2	$2\,(\frac{1}{2} \times \frac{1}{2} + \frac{1}{2} \times \frac{1}{2}) = 1$
Tandem CI/EI (Extranuclear)	CI EI	2	2	$2\,(\frac{1}{2} \times 1 + \frac{1}{2} \times a) = 1 + a$
Alternate CI/EI (Kratos MS-25)	CI EI	4	2	$2\,(\frac{1}{4} \times 1 + \frac{1}{4} \times 1) = 1$
PPINICI (Finnigan)	+CI -CI	2	2	$2\,(\frac{1}{2} \times 1 + \frac{1}{2} \times 1) = 2$

The calculations of the efficiency factors for all these designs are straightforward except for the sample efficiency factor for the Tandem CI/EI source during the EI operating mode. This is due to the following complications. In this design, the sample is indirectly introduced into the EI source region via the CI source. After entering the CI source the sample gas will leak out through not only the ion exit slit but also through any other openings such as the electron entrance slit and will then be pumped away. Even for gas molecules which do leak out from the ion exit slit a substantial portion may still not reach the EI ionization region before being pumped away. One other cause to the potential reduction of the EI sensitivity is the depletion of the sample due to chemical ionization within the CI source. A 10% sample depletion was estimated in the manufacturers report. However, it should be pointed out that a much higher depletion rate is likely for samples which undergo reactions such as thermal electron capture, with rate constants as high as 1×10^{-7} cc/sec-molec. In view of these complications, the actual value of the sample efficiency factor during the EI operation cannot be specified but instead is designated as "a" which ranges from 0 to 1 depending on the experimental conditions.

Clearly from the above table the development of AMMS is currently in its early stage and further technical improvement still lies ahead. Listed in the following are several problem areas which deserve further attention for future instrumental improvement.

1. Ion source. The design of the ion source should be further improved such that each operating mode is possible with little or no compromise in both spectral quality and detection sensitivity. For the single-ionization region AMMS design, an efficient switching mechanism is desirable for providing the desired ion source conductance during each operating mode and for eliminating ion source memory effects.

2. CI reagent gas inlet system. Largely due to the inefficiency in the conventional CI reagent gas inlet system design, automated CI/EI or CI/CI operation has not been practical for the single-ionization region AMMS. The typical mode switching time is at least several seconds which is 1-2 orders of magnitude longer than that required (0.1 sec or less) for present day capillary GC-MS operation.

3. Positive ion and negative ion analysis. It is generally recognized that both positive ions and negative ions useful for the sample analysis are formed simultaneously within the source under typical CI operating conditions. However, they are only known to be extracted alternately (for analysis) one at a time during which time the ions of opposite polarity are lost. The best remedy is therefore simply to extract these ions out of the ion source and subsequently analyze them simultaneously. This approach should assure the best sample efficiency and time efficiency and provide better correlation between the obtained positive and negative ion spectra.

For the purpose of solving these problems a new AMMS instrument was proposed (patent applied for) which is designed to achieve several goals, among them, that of automated multiple mode operation consisting of a cycle format of [± CI (reagent A) / ± EI / ± CI (reagent B) / ± EI]. A total of eight mass spectra can be obtained within 4 sec. with a minimum of 0.9 sec per mass scan. Further work is still currently underway.

SCANNING MICROPIPETTE MOLECULE MICROSCOPY

J. A. Jarrell and J.G. King

Research Laboratory of Electronics and Department of Physics
M.I.T., Cambridge, MA 02139

The in vitro localization of the pathways of water transport is a problem of general interest in epithelial physiology. We have developed an instrument, a scanning micropipette molecule microscope, which provides a real-time measure of water transport, with a spatial resolution of 2-5 μm, across a living epithelium.

A simplified diagram is shown in Figure 1. There is a perfusion chamber that will allow simultaneous observation of a sample and the tip, 1-10 μm in diameter, of a quartz micropipette. The tip of the micropipette is sealed with a small plug of a permeable material such as dimethyl siloxane-polycarbonate copolymer or cellulose acetate. The shank of the micropipette is connected via a flexible vacuum coupling to the inlet of a quadrupole mass spectrometer and is hence under vacuum. The micropipette is inserted in solution and scanned over (or placed at various points on) the surface of the sample, much as in the microelectrode experiments of Fromter and Diamond[1]. Molecules which permeate the plug in sufficient amount can be detected by the quadrupole mass spectrometer. Thus spatial variations in the concentrations of the permeating molecules can be mapped out and correlated with the in vitro morphology as observed with the light microscope.

The instrument was first used to detect spatial variations in fluxes of dissolved helium. Figure 2 is a trace of the mass spectrometer output current as the micropipette tip (3 μm od) was scanned over a 5 μm diameter hole in polycarbonate film. The lower half-chamber was perfused with helium-saturated water. The upper half chamber was perfused with normal water.

The instrument was subsequently adapted for the detection of deuterated water fluxes by the addition of a liquid nitrogen cold trap and an in-line uranium reduction furnace based on that of Nief and Botter[2]. The hot uranium reduces HDO to HD and UO_2 and H_2O to H_2 and UO_2 with an efficiency close to unity. This conversion step results in improved time response and sensitivity. Figure 3 is a trace of the mass spectrometer output current as the micropipette tip (2.5 μm od) was scanned over a 3 μm diameter hole in polycarbonate film. The upper half-chamber was perfused with normal Ringer's, the lower half-chamber with 32% HDO Ringer's. Figure 4 is a trace of the mass spectrometer output current as the micropipette tip was scanned over the opening of an unstimulated mucus-secreting duct in the abdominal skin of the frog. All experimental conditions were the same as were used in figure 3. The maximum signal over the duct is nearly three times as large as that over the epithelium, thus indicating that the flux density of HDO emerging from the gland-duct opening is significantly higher than that through the adjacent epithelial cell layers.

Figure 5 demonstrates the time response of the instrument using a 7.5 μm od tip and a 4.5μm thick cellulose acetate plug. The micropipette tip was immersed in a well-stirred 9ml saline bath. The vertical arrows indicate successive injections of 5 μl of D_2O into the bath resulting in concentration increments of HDO of about 0.11%.

These results represent a few of the possible applications of scanning micropipette molecule microscopy to problems in biology and medecine. Even in a non-scanning mode, the rapid time response and small volume sampled could be used to great advantage in studies of preparations such as isolated tubules or capillaries. Furthermore, for many applications, a high-grade mass spectrometer is not necessary, since the conversion of HDO to HD reduces the necessary resolving power of the mass spectrometer substantially. A modified leak detector might suffice for many applications.

The authors wish to acknowledge the contributions of Dr. John W. Mills at MGH. This work was supported by the Johnson & Johnson Associated Industries Fund, the Whitaker Health Science Fund, the Francis L. Friedman Chair and NIH Grant #HL-06664.

1) E. Fromter and J. Diamond, Nature(New Biology) 235, 9 (1972)
2) G. Nief and R. Botter, Advances in Mass Spectrometry, (Pergamon Press, Oxford 1959), pp 515-525.

Fig. 1

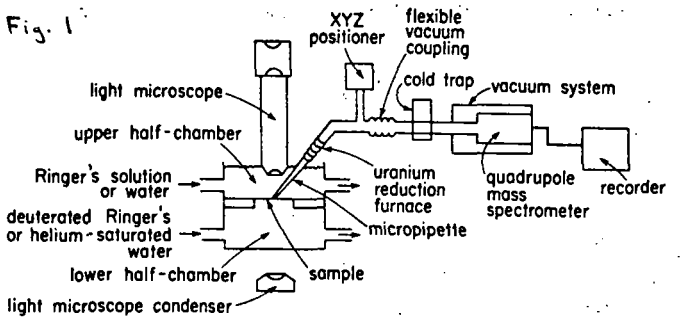

Fig. 2

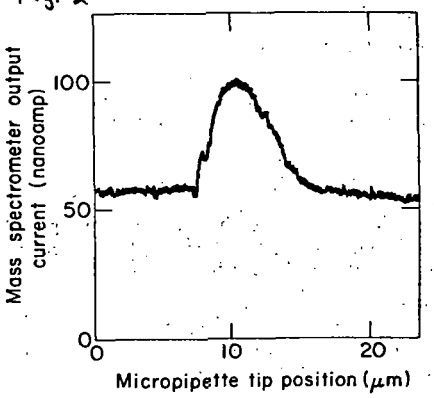

Fig. 3

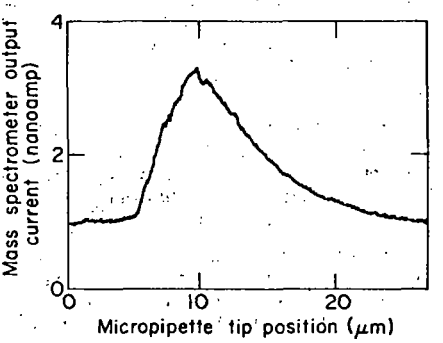

Fig. 4

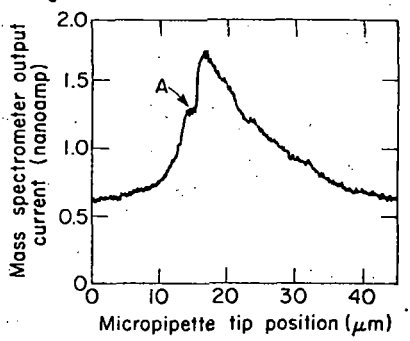

Fig. 5

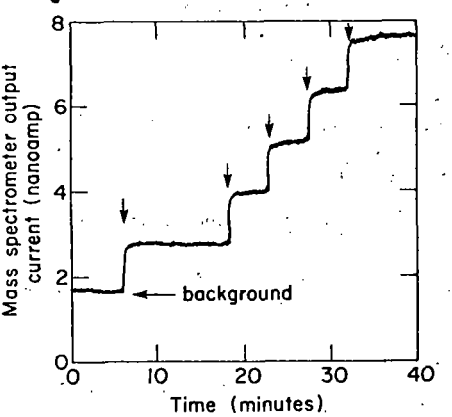

DETERMINATION OF THE DIFFUSION COEFFICIENT OF WATER IN POLYMERIC MATERIALS BY PRECISION ABRASION MASS SPECTROMETRY*

Michael A. Grayson and Clarence J. Wolf
McDonnell Douglas Research Laboratories
St. Louis, MO 63166

INTRODUCTION

A technique for measuring diffusion coefficients by precision abrasion mass spectrometry (PAMS)[1] has been developed at McDonnell Douglas Research Laboratories (MDRL). In this method, the evolution of water from the sample is continuously monitored during the abrasion of a precise volume of the sample, inside the ion-source housing of a time-of-flight mass spectrometer. Data from this experiment are used to determine the distribution profile of volatile compounds trapped within the polymer (or composite) matrix. The total amount of material and the diffusion coefficient are readily calculated from the data.

APPARATUS AND PROCEDURE

A block diagram of the apparatus used to perform PAMS experiments is shown in Fig. 1. The sample stage is attached to the shaft of the three-axis micropositioner (Perkin Elmer-Ultek) which is integral with the bottom ion-source housing flange of the TOFMS. Each axis of the micropositioner is controlled by a stepping motor and controller. This arrangement permits precise control of the position and movement of the sample in each of the three principal axes.

A cutting tool, whose axis of rotation is along one of the three principal axes, is used to abrade the sample. A motor generator and controller (Electro-Craft) provides rotary power to the tool chuck. The output of the motor generator is connected to the shaft of a rotary high-vacuum feedthrough (Ferrofluidics) by a flexible coupling. A precision chuck (Albrecht) is press-fit to a taper on the vacuum-side of the rotary feedthrough shaft. The entire assembly is mounted to a vacuum flange which attaches to a side arm in the ion-source housing of the TOFMS.

The procedure for measuring diffusion coefficients is to expose a series of well-characterized samples to a carefully controlled environment of temperature and humidity. At different time intervals, a sample is removed from the environmental chamber and a PAMS experiment is performed to measure the quantitative distribution profile of the diffusant in the sample. A series of measurements is made and averaged for each exposure time.

DATA ANALYSIS

The behavior of the diffusant in the sample is assumed to obey Ficks law:

$$\frac{\partial c}{\partial t} = D \frac{\partial^2 c}{\partial x^2}, \tag{1}$$

where c is the concentration of the diffusant in the sample,
t is the time of exposure to the diffusant,
x is the position in the sample, and
D is the diffusion coefficient.

Crank[2] develops a series solution for this partial differential equation:

$$c(x,t) = c_o \left\{ 1 - \frac{4}{\pi} \sum_{n=0}^{\infty} \frac{(-1)^n}{2n+1} \cos\left[\frac{(2n+1)\pi x}{2\ell}\right] \exp\left[-D\left\{\frac{(2n+1)\pi}{2\ell}\right\}^2 t\right] \right\}, \tag{2}$$

where ℓ is the thickness of the sample. For the case when $(Dt/\ell^2) < 1.0$, the series converges in less than 10 terms. Since PAMS measurements provide an experimental determination of c(x, t), the truncated series solution of Eq. (2) is used to curve fit the average moisture concentration profile to determine a best fit value of the diffusion coefficient.

EXPERIMENTAL

The diffusion coefficient for desorption of water from a graphite epoxy composite sample was determined. The sample, 2.5 x 2.5 x 0.6 mm, was exposed to a constant humidity environment for more than 6 months to saturate

*This research was conducted under the McDonnell Douglas Independent Research and Development Program.

the composite. The sample was partially dried, and the moisture concentration profile was measured by PAMS. The sample was abraded at a rotary tool speed of 300 rpm with a tungsten carbide, four-fluted, 1.6 mm diameter end mill. The sample was fed to the cutting tool at a rate of 3.2×10^{-2} mm/s while the ion current at m/e 18 was recorded during abrasion. The surface of the sample facing the tool was covered with a sheet of aluminum foil and a thin scrap (~ 1 mm) of the graphite epoxy composite. This precaution was taken to prevent the moisture distribution profile from being altered during exposure of the sample to the vacuum of the mass spectrometer.

The concentration of water as a function of position in the sample was expressed in terms of weight percent using the following equation:

$$W_{H_2O}\,\% = \frac{I_{H_2O} \cdot S_{H_2O}}{\pi \rho r^2 v} \times 100, \qquad (3)$$

where I_{H_2O} is the ion current at an ion characteristic of water (μA),
S_{H_2O} is the sensitivity of the mass spectrometer to water at the characteristic ion (g/s · μA),
ρ is the bulk density of the composite (g/cm^3),
r is the radius of the cutting tool (cm), and
v is the stage velocity (cm/s).

The averaged data from three separate holes abraded in a sample are shown by the dots in Fig. 2. A value for the diffusion coefficient of 4.2×10^{-13} m^2/s was calculated from this data by an appropriate curve-fitting routine. The solid line represents the calculated concentration profile for water in the sample using a diffusion coefficient of 4.2×10^{-13} m^2/s.

These experiments indicate that PAMS can be successfully used to measure the concentration of a diffusant in a polymeric material and that the data can be used to determine the diffusion coefficient. It is important to note that PAMS is not limited to measurements involving water but can also be used to determine the diffusion coefficients and/or concentration gradient for any diffusant that is volatile at room temperature and whose exposure to the sample can be controlled. Thus, in principle, PAMS can be used to measure the diffusion coefficient of oxygen, nitrogen, or other gases as well as acetone, benzene, or other plasticizers in the polymeric medium. It is also possible to apply this technique to measure diffusion coefficients in anistropic materials, for example either parallel to or perpendicular to the fiber plane in composites.

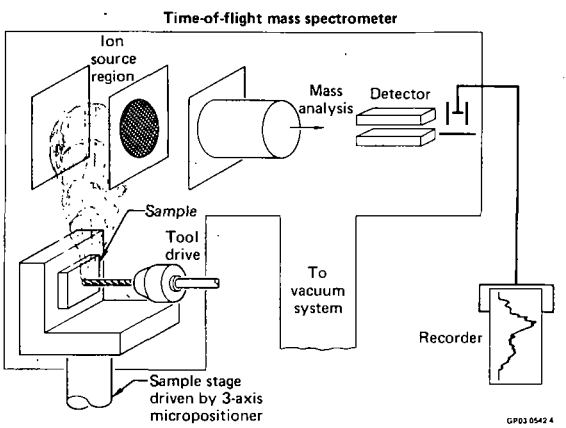

Fig. 1 Precision abrasion mass spectrometer apparatus

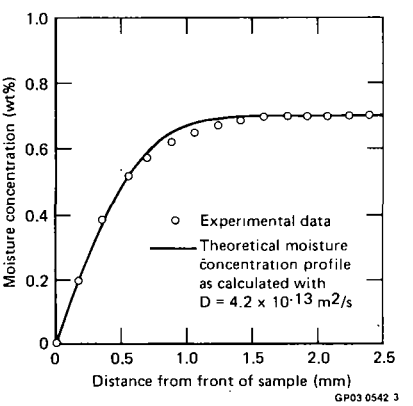

Fig. 2 Moisture concentration profile in a Graphite/Epoxy composite

REFERENCES

(1) *C.J. Wolf and M.A. Grayson, Pittsburgh Conference on Analytical Chemistry and Applied Spectroscopy, March 1980, Atlantic City, NJ, p. 548.*

(2) *J. Crank, The Mathematics of Diffusion (Clarendon Press, Oxford, 1975) p. 22.*

MAMOB7 A FULLY AUTOMATIC SYSTEM CALIBRATION FOR URANIUM, K. HABFAST and D. TUTTAS, Varian MAT GmbH, Bremen/West Germany

Using the MAT 260 automatic MFTIS mass spectrometer, a System Calibration has been performed. Standard Reference Material (SRM) of Uranium with ^{235}U content between 0.5% and 97.5% has been used. The whole experiment runs completely automatically, controlled by a desk top computer.
The goal was to get high precision, high accuracy, low sample consumption, and high sample throughput simultaneously.
External precision is better than 0.02% (1σ), Accuracy is better than 0.05% (95% confidence level).
Sample amount for one measurement is 1 µg.
Total measuring time for one sample is less than one hour.
The measuring procedure and remaining sources of error will be discussed together with a procedure for measuring the minor isotopes of uranium.

MAMOB8 PRECISE SULFUR ISOTOPE RATIO MEASUREMENTS ON SO_2 and SF_6. H. NIELSEN, Geochemical Institute, Univ. Göttingen, and C. BRUNNÉE, Varian MAT GmbH, Bremen, Germany.

Since the $\delta^{34}S$ scale is defined exclusively by its "zero standard", δ values far from zero may be subject to systematic errors. C.E. REES from McMaster Univ., Hamilton/Ont., proposes the establishment of additional reference marks on the δ scale, in order to eliminate these uncertainties. Our paper discusses the determination of the "best δ values" of the new McMaster substandards.

SO_2 has been discredited as a sample gas for high precision measurements due to its strong memory. Some researchers therefore prefer SF_6, which yields results which are numerically a few percent higher than the data from SO_2 measurements previously published. The preparation of SF_6 samples, however, involves hazards inherent when handling highly toxic gases; also the mass range of the SF_5^+ ions is not easily accessible to instruments having a small deflection radius. Therefore, it was considered worthwhile to study the possibilities of reducing the memory inherent in SO_2.

We applied a modern, commerically manufactured stable isotope gas mass spectrometer which was modified by slightly "opening" the ion source in order to reduce the memory correction. Our $\delta^{34}S$ values, obtained on SO_2 samples prepared from REES' new substandards, agree with his SF_6 measurements and thus show SO_2 to be a quite suitable gas for high precision work.

Finally, the simultaneous determination of $\delta^{33}S$ and $\delta^{34}S$ using a triple collector system which was fitted with our instrument provided us with a very sensitive means of checking for impurities which may have been superimposed on the mass number 64 to 66 ion beams.

AN ISOTOPE DILUTION MASS SPECTROMETRIC METHOD FOR THE ACCURATE DETERMINATION OF UREA IN HUMAN SERUM

M. Welch, E. White V, L. Sniegoski, R. Schaffer, H. S. Hertz, and A. Cohen

Organic Analytical Research Division
Center for Analytical Chemistry
National Bureau of Standards
Washington, DC 20234

INTRODUCTION The measurement of urea levels in serum is an important and commonly used test for kidney function. A need exists for a highly accurate method for serum urea to provide a basis for comparison of the routine methods used in the clinical laboratory. Isotope dilution mass spectrometry (IDMS) has proven to be a highly accurate and precise technique for determining cholesterol (1), glucose and uric acid (2) in human serum. IDMS has now been applied to the determination of urea levels in serum. In this procedure, urea is converted to a derivative, 6-methyluracil di-TMS, which has excellent stability for gas chromatographic introduction to the mass spectrometer.

METHODS. Calibration Standards. Two sets of five calibration standards each were prepared by mixing known amounts of Standard Reference Material Urea and urea-$^{13}C,^{15}N_2$ such that the labeled/unlabeled ratios of the standards covered the range of 4 to 5 in approximately equal increments. The standards within each set were prepared by mixing weighed aliquots of carefully prepared aqueous solutions of each of the two materials. Each calibration standard was derivatized as described below.

Isolation of Urea from Serum. For each sample prepared, a known weight of serum was added to an aqueous solution containing a known weight of urea-$^{13}C,^{15}N_2$. The amount of each added was such that the unlabeled/labeled ratio would fall within the range of the calibration standards. After thorough equilibration, the mixture was freeze-dried. The urea was extracted from the residue and sublimed. The sublimed product was dissolved in water and treated with chloroform extractions to remove impurities. The urea was then isolated by freeze-drying.

Derivatization. The purified urea was converted to 6-methyluracil, using a reaction described by Kondrat'eva, et. al. (3). To the urea in a small vial was added diketene and acetic acid. The vials were capped and heated at 115-125 °C for 90 minutes to convert urea to 6-methyluracil. The excess reagents were then evaporated under a stream of nitrogen. N,O-bis(trimethylsilyl)acetamide (BSA) was then added to each vial to convert the derivative to the di-TMS form. The derivative was left in the excess BSA for the GC-IDMS measurements.

Sample Measurements. Introduction of samples into the mass spectrometer was via a gas chromatograph equipped with a 15 meter, support-coated, open tubular column coated with a nonpolar silicone phase. The column was operated isothermally at 110 °C, giving a retention time for 6-methyluracil di-TMS of approximately 20 minutes. The gas chromatograph was interfaced to the mass spectrometer via a Biemann-Watson type single stage separator, to which a make-up gas flow was added at the end of the GC column.

The mass spectrometer was a magnetic sector instrument with modifications and additions (1), operated in the electron impact mode at 70 eV. Magnetic switching was employed to sequentially monitor m/z 255 and 258, the $(M-15)^+$ ions for the unlabeled and labeled urea derivative, respectively. The magnetic field was set to dwell for one second alternately at each selected mass. A triangular waveform of 43 Hz, was applied to a pair of beam deflection plates to sweep the ion beam back and forth across the detector slit. This signal was displayed on an oscilloscope to provide continuous visual monitoring of peak shapes and positions. The signal from the multiplier fed to a scaler-timer where the signal was converted into digital counts. The counts were fed to a programmable calculator which accumulated the counts for the two ions separately. The accumulated counts for each ion across the chromatographic peak were corrected for background and then ratioed.

To measure the samples prepared from serum with the highest possible precision, we bracket the samples with calibration standards. The following bracketing scheme was employed. A preliminary measurement of the ratio of the sample was made. The calibration standards which were closest in ratio, above and below, to the sample were chosen. One of these standards was injected, followed 5.5 minutes later by the sample, and 5.5 minutes after that by the other standard. The ratios were then measured for each of the peaks. The amount of unlabeled urea in the sample was found by linear interpolation of the sample ratio between the standard ratios. The order of injection was reversed on a second day, with the mean of the two days' runs taken as the reported result. However, if the two values disagreed by more than 0.5 percent, a third measurement was made, with the three values averaged for the reported result. No measurable interferences were found when the appropriate regions around sample and standard peaks were checked for responses at m/z 255 and 258.

RESULTS Before the calibration standards were used for bracketing samples, the consistency of the two sets of standards was demonstrated by bracketing each standard with the closest standards from the other set. The results, given in Table I, are the means of the two days' runs and show that no systematic bias is seen between the two sets.

Table I. Crosscheck of Two Standard Sets

$$\text{ratios} = \frac{\text{wt of SRM urea}}{\text{wt of urea-}^{13}C,^{15}N_2}$$

Set 1				Set 2			
Standard	Measured wt. ratio	Weighed ratio	% Diff.	Standard	Measured wt. ratio	Weighed ratio	% Diff.
A	*	.23944		F	.23243	.23294	-.22
B	.22666	.22734	-.30	G	.21642	.21625	+.08
C	.22126	.22084	+.19	H	.21162	.21165	-.01
D	.20559	.20558	.00	K	.20375	.20370	+.02
E	.19952	.19974	-.11	J	*	.19606	

*Standard fell out of the bracketing range of the other set.

The within-day precision of the method for serum samples was determined by analyzing eight aliquots of one serum pool. The results of the measurements of these samples are shown in Table II. The agreement between day 1 and day 2 was good, with only one out of eight disagreeing by more than 0.5 percent. The mean values cover a range of 0.52 percent with a coefficient of variation of 0.17 percent. Thus the results demonstrated excellent precision. Although this technique should be highly specific, and no evidence of bias has been found, more measurements, particularly at different masses and under CI conditions need to be made to ensure that no significant biases exist.

Table II. Within-Day Study of Eight Aliquots from One Serum Pool

mg urea/g serum

	1	2	3	4	5	6	7	8
Day 1	.33370	.33248	.33315	.33352	.33242	.33221	.33309	.33404
Day 2	.33214	.33234	.33327	.33427	.33380	.33253	.33184	.33011
Day 3								.33237
Mean	.33292	.33241	.33321	.33390	.33311	.33237	.33247	.33217

Overall Mean = .33282

REFERENCES

(1) A. Cohen, H. S. Hertz, J. Mandel, R. C. Paule, R. Schaffer, L. T. Sniegoski, T. Sun, M. J. Welch, and E. White V, Clinical Chemistry, in press.

(2) A. Cohen, H. S. Hertz, R. Schaffer, L. T. Sniegoski, M. J. Welch, and E. White V, presented at the 27th Ann. Conf. of Mass Spectrometry and Allied Topics, Seattle, WA, June 3-8, 1979.

(3) G. V. Kondrat'eva, V. D. Gunar, G. A. Kogan, and S. S. Zav'yalov, Izvestiya Akademii Nauk SSSR, Seriya Khimicheskaya, 7, 1219-1223 (1966).

MEASUREMENT OF VERY LOW ABUNDANCE ISOTOPES USING A REVERSE GEOMETRY DOUBLE FOCUSING THERMAL IONISATION MASS SPECTROMETER

P.J. TURNER, T.O. MERREN, E.F. HALL.

VG-MICROMASS LTD., ION PATH, ROAD THREE, WINSFORD, CHESHIRE.

INTRODUCTION.

REQUIREMENTS.

Accurate measurement of low abundance isotopes requires the use of a mass spectrometer with good abundance sensitivity characteristics. This is defined as the contribution of a given peak to the height of a peak at unit mass separation.

In a good single focusing instrument a value of 2 parts in 10^6 may be expected at unit mass separation from the ^{238}U peak working with an analyser pressure in the low 10^{-9} torr region.

Vacuum in this part of the instrument is usually limited by the degree of differential pumping which may be achieved across the source slit. This will be of the order of 40 for typical pump speeds and slit dimensions.

SOURCE OF SCATTERED IONS OR TAILS.

Some of the mechanisms which may cause poor abundance sensitivity are: (a) Ions will collide with residual atmosphere in the analyser and a certain proportion of the ions will arrive at the collector with a reduced energy and hence appear at a mass lower than their true value. (b) Ions may be generated in the mass spectrometer at energies other than that corresponding to the nominal accelerating voltage. These ions may appear on either side of the peak. (c) Ions may collide with residual ions in the source. All of these mechanisms for tailing of peaks may be compensated if a large radius electrostatic analyser is used beyond the magnetic analyser in a double focusing configuration.

ELIMINATION OF TAILS.

By definition, ions of slightly incorrect energy originating in the source will be focused back to their correct position in the mass spectrum, whilst the ions of incorrect energy generated elsewhere in the system will be eliminated from the mass spectrum if their energy lies outside the band pass of the electrostatic analyser.

In the Micromass 54-38, a 38cm radius filter has been fitted after the magnetic analyser in such a way that z focusing of the ion beam and conventional double focusing are simultaneously obtained. Compared with the standard 54E geometry a reduced image distance is used so that analyser drift length is minimised and a higher energy resolving power can be obtained by using a narrow intermediate resolving slit. The general layout of the instrument is shown in fig. 1, and in normal operation, an energy resolving power of 340 is used.

Beam align plates are provided at the intermediate focal point and also just before the final collector slit.

ABUNDANCE SENSITIVITY ON URANIUM SAMPLES.

The abundance sensitivity characteristics of the 54-38 were measured using NBS U005 standard samples. The ^{234}U and ^{236}U isotopes are present at levels of 22 ppm and 47 ppm respectively and provide a convenient calibration means for measuring the tails of the ^{238}U peak. The height of these tails was measured at the 237 amu point as a function of the ion source housing pressure. Fig. 2 shows the results of these measurements, and in particular it can be seen that the abundance sensitivity drops below 0.1 ppm for source pressures below 5×10^{-8} torr. Fig. 3 is a spectrum taken under these conditions, and in addition to demonstrating the excellent abundance sensitivity, the spectrum shows that at the level of the order of 0.1 ppm there are a number of other peaks present.

On the light mass side of each of the uranium peaks, a small peak may be seen. This may be separated by closing down the collector slit and its presence as a genuine peak as opposed to a reflection, may be established by turning off the side filaments.

Mass measurement of this peak yields a value of 235.77, which is in close agreement with a calculated value of 235.78 for a $^{41}K\ ^{39}K_5^+$ ion. However, the calculated intensity of the ratio for the 236/234 interfering peaks is .827, whereas the observed value is nearly twice this figure. It might then be postulated that ^{40}Ca is also involved in the interfering species, but the resolving power required to check this (30,000) is not avilable on the 54-38.

CONCLUSIONS.

An important corollary of the improved abundance sensitivity of the instrument is its capability of measuring minor isotopes with a high degree of accuracy in samples which may be sufficiently badly contaminated to produce a high background pressure in the mass spectrometer source housing. The two stage mass spectrometer represents not merely an improved performance machine but a machine very suitable as a work-horse for routine samples requiring precision results. Operational procedure and software for the machine are identical to that for the single focusing version.

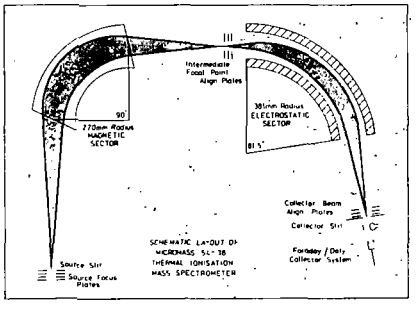

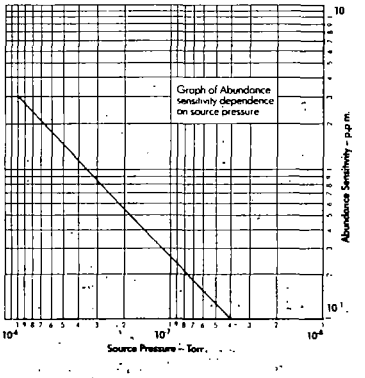

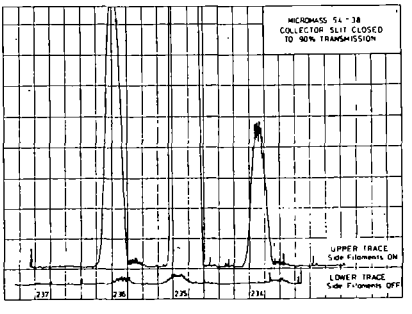

MAMOB11 THE USE OF INTERMEDIATE RANGE MASS SPECTROMETRY IN THE MEASUREMENT OF HEAVY METHANES AS ATMOSPHERIC TRACERS, D. J. FRANK, Los Alamos Scientific Laboratory, P. O. Box 1663, MS-514, Los Alamos, New Mexico, 87545

Methane-21 ($^{13}CD_4$) and methane-20 ($^{12}CD_4$) are of potential use as nonradioactive long-range atmospheric tracers. The natural backgrounds of these heavy methanes in the atmosphere are virtually nonexistant and therefore are detectable to a few parts in 10^{16}. The capability necessary to collect and purify methane from the atmosphere and then to measure its isotopic composition relative to normal atmospheric methane have been developed here at LASL. The preparation and purification system consists of a modified chromatographic process capable of handling up to 50 ℓ of whole air and producing 0.5- to 2-cc methane samples of greater than 99% purity. The isotopic ratio of methane-21 and methane-20 relative to normal methane-16 is measured in a National Bureau of Standards type mass spectrometer modified to make isotopic abundance measurements of the order of 10^{12}.

SYSTEMATIC ERRORS IN ISOTOPE RATIO MEASUREMENTS USING THERMAL IONIZATION AND PULSE-COUNTING DETECTION

J. D. Fassett
National Bureau of Standards
National Measurement Laboratory
Center for Analytical Chemistry
Washington, DC 20234

Pulse-counting detection provides the ultimate sensitivity for measuring mass spectrometric ion beam currents and is the method of choice when ion beam currents available are limited by design or by nature. For radioactive samples, the desirability of making measurements on minimum size samples is obvious to minimize safety risks to the analysts and contamination of the mass spectrometer. For these reasons, a pulse-counting, electron multiplier detector has been installed at NBS to allow isotopic analysis of nanogram amounts of uranium and plutonium. This detection system replaces the Faraday cup and vibrating reed electrometer detector more commonly used in thermal ionization mass spectrometry.

The primary sources of error in a mass spectrometric analysis are isobaric interferences, uncontrollable contamination (blank), baseline determination, measurement system calibration, and control of isotopic fractionation. These potential errors are common to both Faraday cup and electron multiplier detection. The lower noise level ($< 1x10^{-19}$ amps) of pulse-counting detection relative to Faraday cup detection ($> 1x10^{-16}$ amps) results in increased sensitivity to isobaric interferences and blank contributions and thus, the control of these errors becomes more critical in pulse counting detection. By the same token, pulse-counting detection can be used to more effectively evaluate these sources of error for high accuracy mass spectrometric procedures using the Faraday cup. This evaluation has been done for strontium with the identification of a persistent hydrocarbon peak at mass 86 of typically $.5\text{-}5x10^{-16}$ amps under the conditions of strontium measurement (1600°C).

The usual sources of background and interferences are the filament material, reagents, and sample. In general, highly pure reagents and chemically separated samples are used to eliminate interferences from the reagents and sample. In the case of strontium, zone-refined rhenium filaments are rigorously degassed (> 2000°C, 2 hours) to clean the filaments. No detectable ($< 10^{-15}$ A) contributions to the ion currents are observed from the filament under the strontium operating conditions (1). This rigorous degessing procedure was instituted because interferences were detected under less rigorous procedures. With the pulse-counting mass spectrometer, filaments that had been subjected to differing degas procedures have been evaluated. It was observed that at 1600°C both ^{88}Sr and ^{85}backgrounds were less than 10^{-17} amps for the rigorously degassed filaments. With less rigorously degassed filaments, ^{88}Sr remained less than $5x10^{-17}$ amps; ^{85}Rb had increased to greater than $1x10^{-16}$ amps. In all the filaments examined, there was the 86 peak present with the mass shift of a hydrocarbon. Similarly, a hydrocarbon was consistently observed at the 84 mass position of 10-20% the 86 intensity. The background for a number of different filaments is tabulated in the accompanying table.

The origin of the 86 peak was deduced to be from the source itself and not from the filament. The overall extent of the hydrocarbon interference problem was evaluated for the source by scanning the mass region from 140-40 with the liquid nitrogen cold trap both warm and cold. The most intense hydrocarbon peaks were observed at mass positions 44, 58, 72, 86, and 100 with 44 and 86 the most intense of the series. When the background is scanned with the source warm intensities increased by as much as 200 times.

It is hypothesized that the most intense hydrocarbon interferences are due to amine ions originating from proteinaceous material (dirt) built up in the source. This material would be expected to have low volatility and thus be extremely persistent, but thermally degradable to amine molecules which, relative to other organic molecules, have a low ionization potential and thus higher thermal ionization efficiency. Pertinent to this hypothesis, Davis has observed a 20% thermal ionization efficiency for nicotine and has presented spectra of normal laboratory air and laboratory air with cigarette smoke (2).

The conclusions are: (1) A pulse-counting mass spectrometer can be used effectively to evaluate background and interferences in Faraday cup measurements. (2) Hydrocarbons must be considered in Faraday cup measurements. (3) Continual source cleanliness and general clean conditions should always be stressed.

(1) L. J. Moore, J. R. Moody, I. L. Barnes, J. W. Gramlich, T. J. Murphy, P. J. Paulsen and W. R. Shields, Anal. Chem., 45, 2386 (1973).

(2) W. D. Davis, Environ. Sci. Technol., 11, 593 (1977).

Table I

Blank Filament Background

(1600°C, 20 minutes)

Filament Type-Re	Preheat	Intensities at Mass * 88	87	86	85	84
Zone refined	3 hrs., 5 amps	15	30	480	55	135
Zone refined	30 min., 4 amps	5	10	245	20	60
Regular	3 hrs., 5 amps	5	35	500	30	90
Regular	30 min., 4 amps	35	40	1250	105	200
Regular	None	240	820	390	2600	75

*Counts per second: 1 CPS = 1.6×10^{-19} Amps

ADVANCES IN PYROLYSIS MASS SPECTROMETRY

J. Haverkamp, W. Windig, D. Valerio and P.G. Kistemaker

FOM Institute for Atomic and Molecular Physics, Kruislaan 407, Amsterdam, The Netherlands

During the last decade fast heating pyrolysis mass spectrometry has become a powerful analytical tool for studying complex and high molecular weight organic materials. An important impetus hereto was the work of Meuzelaar et al. at the FOM Institute in Amsterdam, who developed a fully automated Curie point pyrolysis-quadrupole MS system capable of quick batchwise analysis of large series of samples. This system shows a high degree of reproducibility as was demonstrated in some recent papers [1-3]. Apparently, the most important factors influencing the spectrum concern the pyrolyzate transfer from pyrolysis reactor to the ion source, and mass spectrometric conditions, rather than pyrolysis conditions (e.g. sample size, temp. rise time, equilibrium temp., total heating time) provided the latter factors are properly chosen.

The pyrolyzate transfer line is built up of the glass pyrolysis reactor tube wherein the Curie point wire is mounted and a gold-coated expansion chamber (heated on 150°C) between the reactor and the ion source. In our normal set-up the glass reaction tube is at ambient temperature. It is the coldest part of the transfer line and forms a trap for less volatile pyrolyzate components. However, by mounting a thin metal foil at the inner side of the glass tube the reactor wall can be heated simultaneously with the Curie point wire. Using a 25 μm stainless steel foil, a wall temperature of 220° can be reached in 0.8 s, whereas the wire reaches its equilibrium temperature (510°C) within 0.2 s. The use of this simple modification e.g. in the analysis of nucleic acids (Fig. 1) gives a significant increase in the characteristicity of the Py-MS spectrum as typical fragments representing the nucleobases are much more pronounced.

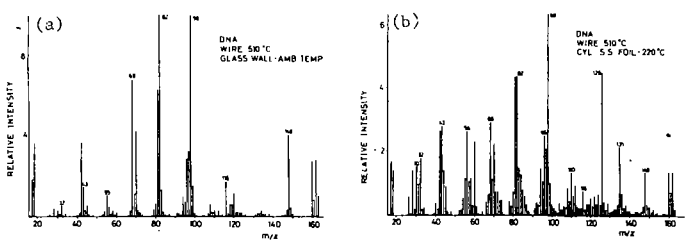

Fig. 1 - Pyrolysis mass spectrum of herring sperm DNA (a) with cold glass reactor and (b) with a S.S. foil reactor at 220°C. Curie point of the wire: 510°C.

Note the increase in intensities of e.g. m/z 126 and 135, probably representing the intact bases thymine and adenine.

Other points of development in Curie point pyrolysis-MS concern the analysis of the pyrolyzate in terms of chemical components. As the fragments analyzed are rather small (m/z 15-200) the spectra of biomaterials like bacteria, cell-fractions etc. are very complex; at almost each of the mass values various pyrolytic fragments can contribute. To get insight into the identity of the components and their (macro)molecular origin two new approaches have to be mentioned:

1) The structure elucidation of pyrolysis fragments using on-line Curie point pyrolysis-MS-CID-MS. For this purpose a new instrument was developed in our institute [4]. E.I.-Ionized pyrolyzate components of particular m/z value are sorted out in the first magnetic sector MS, they are subjected to collisional induced dissociation and, subsequently, the fragment spectrum is analyzed in the second magnetic sector MS, equipped with simultaneous ion detection. This instrument and some applications will be discussed separately [A.J.H. Boerboom et al., paper MPMOA 1].

2) The second approach is a numerical one; the use of factor analysis in the interpretation of Py-mass spectra of (chemically) related complex samples [3]. A valuable indication for the origin of a peak is the correlation of its intensity variation over the various spectra with

the variation of other mass peaks, thus yielding a series of correlated peaks that then can be interpreted chemically. On factor analysis, which is a reliable and comprehensive way for finding correlations in peak intensities, the spectra (= sets of partly correlated mass peak intensities) are transformed into new uncorrelated sets of variables (factors). A factor is a linear combination of correlated mass peak intensities and, therefore, factor analysis has data-reduction capability. Applied to Py-mass spectra of complex organic mixtures, a factor can reflect the presence of a particular chemical component in that mixture. An example of this new approach in pyrolysis mass spectrometry is the detection of ppm contaminations of the toxic compound DEAE-Dextran in polio-virus vaccine. On introduction in the series of virus preparations some standard preparations with different concentrations of DEAE-Dextran, the main factor describes this component, whereas the "factor scores" can be used as a quantitative measure.

References

[1] H.L.C. Meuzelaar, Proc. 26th ASMS Conference, St. Louis, USA (1978) p.29
[2] W. Windig et al., J. Anal. Appl. Pyrol. 1 (1979) 39
[3] W. Windig et al, ibid. 2 (1980), in press;
W. Windig et al., manuscript in preparation
[4] G.J. Louter et al., Int. J. Mass Spectrom. Ion Phys. 33 (1980),335
[5] J. Haverkamp et al., Anal. Biochem. 104 (1980), in press

MAMOC2 THE FROG EMBRYO AS A MODEL FOR CELL AND TISSUE CHARACTERIZATION BY PYROLYSIS MASS SPECTROMETRY, HENK L. C. MEUZELAAR, MARCUS JACOBSEN, JOHAN HAVERKAMP and DAVID L. POPE, Biomaterials Profiling Center, University of Utah, Salt Lake City, UT 84108.

Several studies have established the feasibility of direct characterization of cell and tissue samples by pyrolysis mass spectrometry without prior fractionation or derivatization. A major problem in the evaluation of Py-MS profiles of such samples are the potentially high levels of intra- and inter-individual variability. This places heavy demands on the selection of representative samples as well as on the minimum number of samples which have to be analyzed in order to obtain statistically meaningful results. An elegant way to limit nonrelevant intersample variability in complex biological samples is to select samples that are genetically as well as physiologically closely related and differ only in a limited number of detectable properties. Obviously, the level of inter sample variability could be strongly reduced if cells or cell groups from a single developing organism could be characterized. Frog embryo cells and tissues are particularly suited for such experiments. The cells are large enough to permit direct Py-MS analysis of individual cells up to the 64 or 128 cell stage. Moreover, the embryos are readily available, can be produced under genetically controlled conditions and can be grown in simple well defined media. Finally, frog embryos are among the best studied vertebrate embryos and techniques for isolation of selected individual cells, cell transplantation, cytoplasmic aspiration and intracellular injection are well established. In addition to serving as a model system for comparing and optimizing Py-MS techniques, the frog embryo model may provide insight in early cell differentiation mechanisms and possibly provide a new tool for *in-vitro* toxicity studies in higher organisms.

THE GC/MS ANALYSIS OF THE PYROLYSIS PRODUCTS FROM A SPECIFICALLY LABELLED DEUTERATED URETHANE

Kent J. Voorhees
Department of Chemistry/Geochemistry
Colorado School of Mines
Golden, Colorado 80401

Robert P. Lattimer
B.F. Goodrich Research and Development Center
Brecksville, Ohio 44141

A previous study of the pyrolysis products of a urethane system formulated from PAPI and propoxylated trimethyol propane (TMP) led to the postulation of a mechanism to explain the thermal degradation reactions in urethanes(1). The proposed mechanism is illustrated in Figure 1. The reactions shown in this scheme can be summarized as a series of low energy concerted reactions---urethane degradation(2), allyl ether rearrangement(3), ketoether rearrangement and the methyl vinyl ether rearrangement(4). This proposed sequence of reactions can be used to successfully explain the formation of a majority of the pyrolysis products; however, a small number of species can not be explained using these reactions and suggest that additional mechanistic routes might be occurring. To clarify the general decomposition scheme for urethanes, a specifically labelled deuterated urethane polymer(5) has been prepared and pyrolyzed.

The general product distribution produced from a 550°C pyrolysis of the deuterated foam separated on a Chromosorb 101 column were similar to those previously reported(1). The calculated values from the deuterium distribution in these compounds from separate electron impact and field ionization GC/MS results are summarized in Table 1. The pyrolysis and analysis conditions (i.e., source temperature, separator temperature, etc.,) have been varied without significant changes in the deuterium distributions. In addition, a control experiment using a mixture of acetone and acetone-d_6, flashed from the pyrolysis device followed by analysis using similar conditions as those for the pyrolysis GC/MS experiments, showed no scrambling.

The deuterium distribution for the polyol fragments have also been determined from isobutane chemical ionization GC/MS data. Table II summarizes these results for selected species. The deuterium distribution can be explained in most of the polyol species using the proposed mechanism; however, the compounds assigned as ketoethers compounds are isotopically pure, but deficient in deuterium content. In general, more isotopic scrambling was observed in many of the low molecular weight species (methane, ethanol, propene) suggesting that formation of these species resulted from free radical type reaction. The higher alkenes and aromatic species arising from degradation of the isocyanate protion of the polymer are fairly isotopically pure.

The results from this study suggest the degradation of urethanes proceed by a series of concerted reactions plus a smaller percentage of free radical reactions. Distribution of deuterium in compounds like ethanal suggest formation by free radical reactions, however, mechanistically they are very difficult to explain. Model compounds investigation will be necessary to fully understand the urethane thermal degradation scheme.

REFERENCES

1. K.J. Voorhees, F.D. Hileman, I.N. Einhorn and J.H. Futrell, J. Polym. Sci. Poly. Chem. Ed., 16, 213(1978).

2. E. Dyer, G.C. Newborn, and G.C. Wright, J. Amer. Chem. Soc., 81, 2138(1959).

3. G.G. Smith and F. Kelly, Progress in Physical Organic Chemistry, Vol. 8, A. Streitwieser and R.W. Taft, Eds., Interscience, New York, 1971.

4. M.J. Molera, J.M. Gamboa, J.H. Garcia Dominque and A. Conto, J. Gas Chromatogr., 6, 594 (1968).

5. K.J. Voorhees, W.H. McClennen and N.A. Mumford, J. Labelled Cmpds. and Radiopharm., in press.

TABLE I

Deuterium percentages of selected compounds produced during pyrolysis

Compound	Deuterium Percentage	Compound	Deuterium Percentage
methane	53	pentene	96
methane-d_1	15	pentene-d_1	3
methane-d_2	12	pentene-d_2	1
methane-d_3	21		
propene	6	phenylisocyanate	98
propene-d_1	3	phenylisocyanate-d_1	2
propene-d_2	55		
propene-d_3	36		
ethanal	51	benzonitrile	93
ethanal-d_1	11	benzonitrile-d_1	5
ethanal-d_2	11	benzonitrile-d_2	2
ethanal-d_3	26		
butene	88	aniline	93
butene-d_1	4	aniline-d_1	6
butene-d_2	7	aniline-d_2	1
butene-d_3	1		
		propanal-d_3	90
acetone-d_3	100	propanal-d_4	10

TABLE II

Summary of deuterium distribution for polyol fragments

Compound	Deuterium Distribution
propoxy-TMP-d_3	∿ 100%
diproxy-TMP-d_6	∿ 100%
tripropoxy-TMP-d_9	∿ 100%
propoxypropene-TMP-d_6	∿ 100%
propoxypropene-TMP-d_5	∿ 100%
dipropoxypropene-TMP-d_9	∿ 100%
dipropoxypropene-TMP-d_8	∿ 100%
methyloxypentanone-TMP-d_2	∿ 100%
dipropenyl-TMP-d_4	∿ 100%
dipropenyl-TMP-d_6	∿ 100%

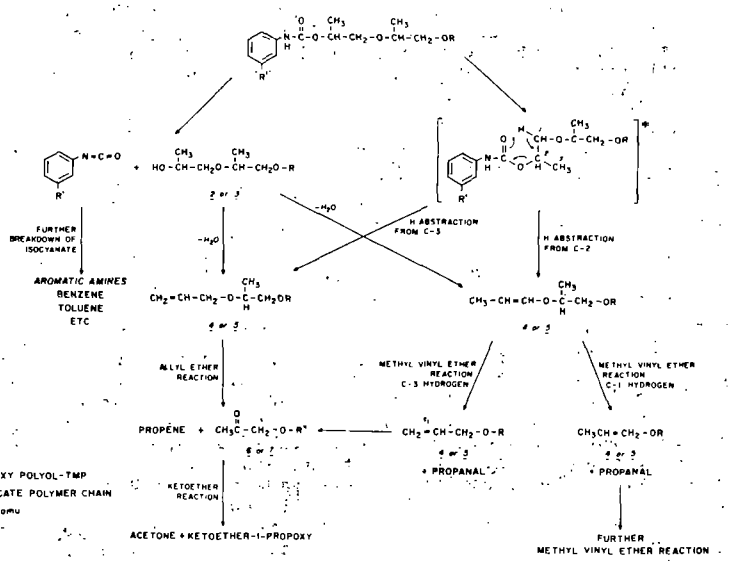

Figure 1. The reaction scheme of the thermal breakdown of urethanes

THERMAL DEGRADATION PRODUCTS FROM PVC, PLASTICIZER, AND ANTIMONY OXIDE

John A. Nikora and Gregory F. Smith, The BFGoodrich Chemical Group, Avon Lake Technical Center, Avon Lake, Ohio 44012.

Antimony trioxide, when reacted with a chlorinated or brominated synergist, produces an effective flame retardant system. Previous studies have shown that antimony trioxide is ineffective as a flame retardant without a source of halide[1,2]. Antimony trioxide reacts with hydrogen chloride or bromide to produce the corresponding antimony oxyhalides which, through a series of reactions, release volatile antimony trihalide. The effectiveness of Sb_2O_3 as a flame retardant depends upon its products escaping into the flame[3]. Antimony trioxide is widely used in PVC, ABS polymers, polyurethanes, and other systems. The non-halide polymers require the addition of a halide.

A concern expressed about the products generated from Sb_2O_3 and a source of chloride, as well as the potential for Sb_2O_3 to alter the degradation mechanism of PVC, resulted in a study of PVC formulated with plasticizer and Sb_2O_3. Similar studies with molybdenum trioxide have shown changes in the precombustion products obtained from PVC[4-6]. In the case of MoO_3, the oxide catalyzed the dehydrochlorination of PVC while reducing the level of benzene formation and the flame spread in low enthalpy inputs. In high enthalpy tests, MoO_3 was not an effective flame retardant[6].

In this paper, the effects of Sb_2O_3 on the thermal degradation of PVC and two different plasticizers were investigated by the combined techniques of pyrolysis-GC/MS, TGA, and the NBS smoke chamber. The chamber was used to provide measurements of time-integrated concentrations for aromatic and aliphatic hydrocarbons, CO, and CO_2. The GC/MS was used to identify the thermal degradation products and to look for new products which would support a change in the degradation mechanism. While the formation of $SbCl_3$ reported with laser pyrolysis experiments[3] could not be confirmed by our experiments, it was confirmed by degradation experiments in the mass spectrometer's source. PVC samples containing no plasticizer, bis-2-ethylhexylphthalate, diphenyl-p-tert-butylphenylphosphate, and Sb_2O_3 were prepared on a heated mill at 170°C.

PVC Formulations	1	2	3	4	5	6
PVC Resin	100*	100	100	100	100	100
Antimony Trioxide		8			6	6
Phthalate			40		40	
Phosphate				24		24
Percent PVC	100	93	71	81	69	77

*Parts per hundred of resin by weight.

TGA data was obtained on each sample with a Cahn RG balance in 20% O_2 at 10C° min^{-1} from 25° to 800°C. The PVC formulations were degraded at 600°C with a Chemical Data System's Pyro-probe. The probe's platinum heating coil was calibrated to a temperature of 600°C with a Doric Trendicator thermometer. The formulations were degraded in open-ended Pyrex tubes fitted into the spiral at the end of the probe using the fastest temperature rise time. The separations were made on stainless steel columns packed with either Porapak QS or Dexsil 300 on WAW. A switching system enabled the pyrolyses to be carried out in air and the separations in helium. A DuPont 21-490 mass spectrometer and data system was used for product identifications. Samples were combusted in the NBS chamber with a 2.5W/cm^2 radiant heater. A sample from the chamber was analyzed for CO, CO_2, aromatics, and aliphatics by non-dispersive infrared. A continuous reading, as a function of time, was obtained for each of these. During the course of each experiment, samples were taken by syringe for HCl analysis.

The rate of release of degradation products from PVC and color formation are important considerations when processing PVC. Similar concerns may also be expressed for animal testing since animals respond to the degradation products and the timing of release. TGA investigations of the effect of Sb_2O_3 on the described PVC have shown, in two cases, that the degradation products were released at a lower temperature with antimony. A 10° drop (versus 60° for MoO_3[6]) in the temperature at which hydrogen chloride was evolved was observed. The TGA measurements obtained on the plasticized-PVC's were less clear in the initial stages because of the plasticizer's volatility.

The yield of thermal degradation products was determined in the smoke chamber. Results from the yields of these were expressed in terms of the integrated concentration-time values at 20 minutes. These values were used because the differences appeared to be maximized at 20 minutes.

Concentration-Time Values (ppm-min x 10^{-3})

	Formulation	HCl	CO	Aromatics	Aliphatics
1.	PVC	129	6.4	6.4	4.2
2.	PVC-Sb	113	6.9	4.7	3.6
3.	PVC-Phthalate	84	4.3	5.6	2.6
5.	PVC-Phthalate-Sb	74	4.3	4.4	3.1
4.	PVC-Phosphate	101	4.7	6.2	3.8
6.	PVC-Phosphate-Sb	92	2.9	4.0	2.6

The levels of HCl and aromatics were reduced with Sb_2O_3. When adjusted for PVC content, the reduced levels were still evident.

Adjusted Values Ratioed to Pure PVC

	Formulation	HCl	CO	Aromatics	Aliphatics
1.	PVC	1.0	1.0	1.0	1.0
2.	PVC-Sb	0.9	1.2	0.8	0.9
3.	PVC-Phthalate	0.9	1.0	1.2	0.9
5.	PVC-Phalate-Sb	0.8	1.0	1.0	1.1
4.	PVC-Phosphate	1.0	0.9	1.2	1.1
6.	PVC-Phosphate-Sb	0.9	0.6	0.8	0.8

Additional effects of Sb_2O_3 on the degradation of PVC and the products formed were investigated with the Pyro-probe-GC/MS system. The samples were degraded in air at 600°C. Major differences in products were related to plasticizer (see table at end of report).

Antimony trioxide changes the PVC degradation mechanism as reflected by the catalyzed evoluation of HCl and the reduced aromatic hydrocarbons.

REFERENCES

(1) J. J. Pitts, P. H. Scott, and D. G. Powell, Cellular Plastics, 35, January/February, 1970.

(2) A. Ballistreri, S. Forti, G. Montaudo, S. Pappalardo, and E. Scamporrino, Polymer, 20, 783 (1979).

(3) R. M. Lum, J. Polym. Sci., Polym. Chem. Ed., 15, 489 (1977).

(4) W. H. Starns, Jr. and D. Edelson, Macromolecules, 12, 797 (1979).

(5) D. Edelson, V. J. Kuck, R. M. Lu,, E. Scalco, W. H. Starnes, Jr., and S. Kaufman, "Anomalous Behavior of Molybdenum Oxide as a Fire Retardant for Polyvinyl Chloride", Spring Technical Meeting of the Combustion Institute, Canadian Section, Kingston, Ontario, May, 1979.

(6) R. M. Lum, J. Appl. Sci., 23, 1247 (1979).

GC/MS Identifications

Component(s)	1	2	3	4	5	6
C_2-C_5 Aliphatics	X	X	X	X	X	X
C_6 - Aliphatics		X		X	X	X
C_7 - Aliphatics		X	X		X	X
C_8 - Aliphatics			X		X	
Hydrogen Chloride	X	X	X	X	X	X
Mono-/Dichloromethane	X	X	X	X	X	X
Chloroform	X	X				X
Chloroethane	X	X	X	X	X	X
VCM	X	X	X	X	X	X
Chloropropane		X		X	X	
Benzene/Toluene	X	X	X	X	X	X
C_2-C_5 Benzenes	X	X	X	X	X	X
Chlorobenzene	X	X	X	X	X	X
C_7H_7Cl	X	X		X		X
Indane/Indene	X	X	X	X	X	X
Phenol				X		X
Naphthalene	X	X	X	X	X	X
Methyl Indene	X	X	X	X	X	X
C_1 & C_2 - Naphthalenes	X	X	X	X	X	X
Chloronaphthalene	X	X	X	X	X	X
Biphenyl	X	X	X	X	X	X
$C_{13}H_{12}$	X	X	X	X	X	X
Diphenylacetylene	X	X	X	X	X	X
Diphenyl - C_2's& C_3's	X	X	X	X	X	X
Octanol/Octanal			X		X	
Benzaldehyde			X		X	
Phthalate			X		X	
Triphenylphosphate				X		X
Phosphate				X		X

Mechanisms of Ozonation of N,N'-di-(1-methylheptyl)-p-phenylenediamine

by

Robert P. Lattimer, E. Ray Hooser, Hugh E. Diem, Robert W. Layer, C. K. Rhee

The BFGoodrich Research and Development Center
9921 Brecksville Road
Brecksville, Ohio 44141

The ozonation products of a common rubber antiozonant-N,N'-di(1-methylheptyl)-p-phenylenediamine (DOPPD)- have been separated by liquid and/or gas chromatography (see Figures 1 and 2). Molecular weights of about thirty LC-separated components have been measured by field desorption mass spectroscopy. Elemental formulas have been determined by atomic composition mass spectroscopy. Other structural details have been elucidated by electron impact mass spectroscopy and attenuated total reflectance infrared spectroscopy. Structures for some of the key components are given below.

Two principal mechanisms appear to govern the ozonation of DOPPD. Amine oxide formation leads to observed nitrosoaryl and nitroaryl products. The second major mechanistic pathway is side-chain oxidation. This leads to a number of low molecular weight components, including some that contain an amide moiety. A third (minor) mechanistic pathway involves a nitroxide radical intermediate and leads to the formation of a stable dinitrone species.

The "surface film" formed on ozonation of a black-loaded natural rubber sheet containing DOPPD has also been examined. The film contains appreciable quantities of unreacted DOPPD and many of the same low molecular weight components as observed in the ozonized liquid antiozonant. It is clear that DOPPD blooms to the rubber surface and acts as a "scavenger" for ozone. The results are consistent with a combined "scavenger/protective film" mechanism for antiozonant protection.

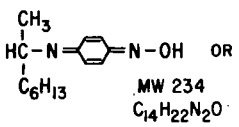

MW 234
$C_{14}H_{22}N_2O$

OR

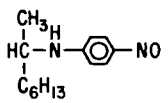

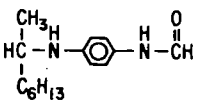

MW 248
$C_{15}H_{24}N_2O$

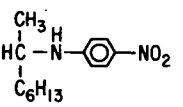

MW 250
$C_{14}H_{22}N_2O_2$

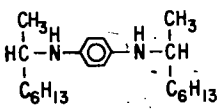

MW 332 (DOPPD)
$C_{22}H_{40}N_2$

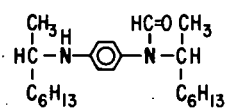

MW 360
$C_{23}H_{40}N_2O$

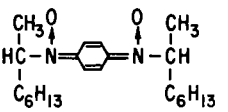

MW 362
$C_{22}H_{38}N_2O_2$

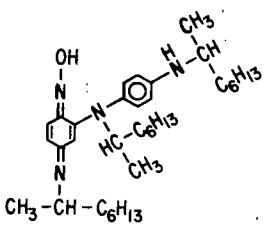

MW 564
$C_{36}H_{60}N_4O$

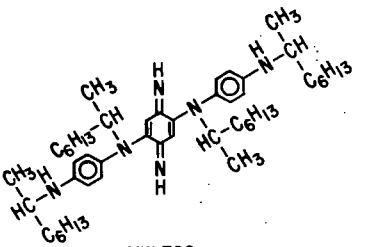

MW 766
$C_{50}H_{82}N_6$

Figure 1. Liquid Chromatogram of DOPPD (after Ozonation)

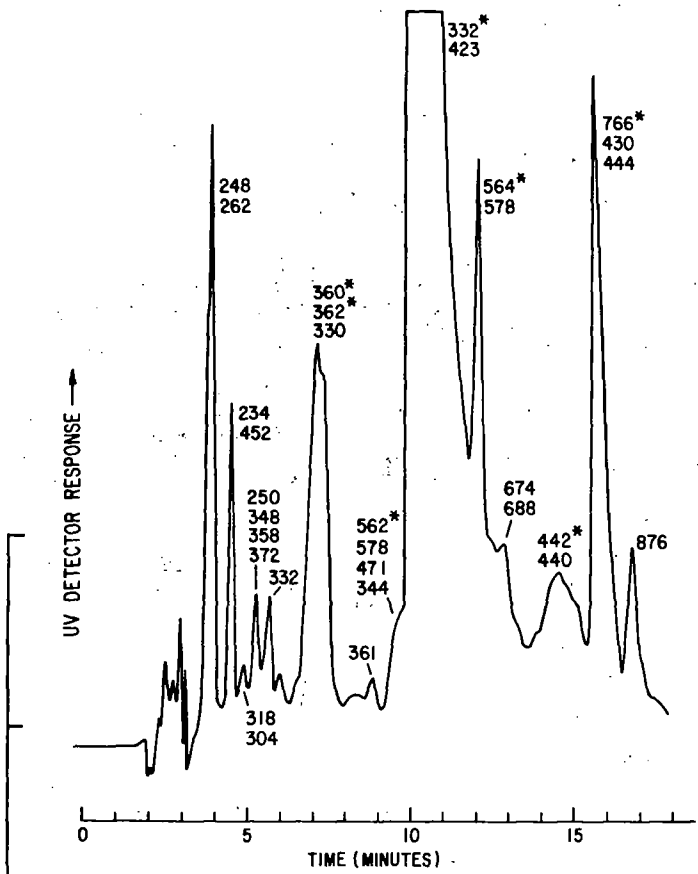

Figure 2. Reconstructed Ion Chromatogram (GC-MS) for Ozonized DOPPD.

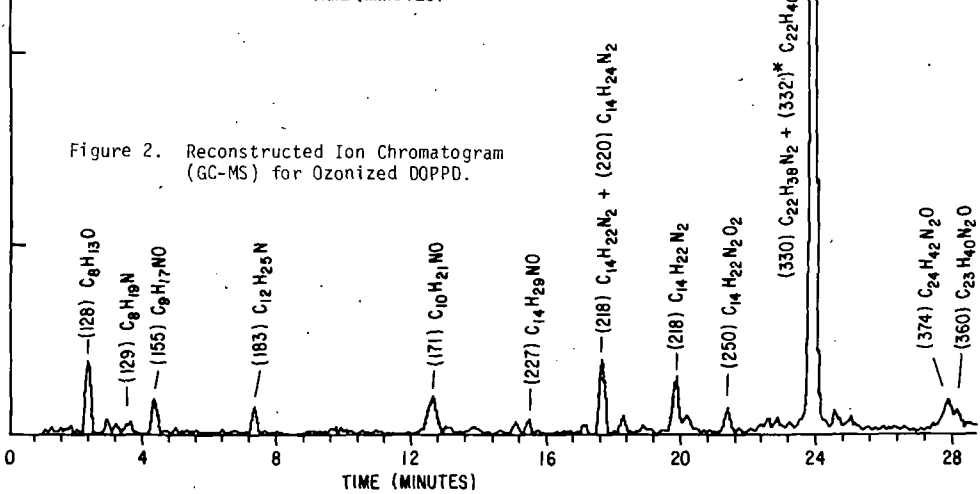

Acid-Enhanced Field Desorption of Zwitterions, T. Keough and A. J. DeStefano, The Procter & Gamble Co., Miami Valley Laboratories, P.O. Box 39175, Cincinnati, OH 45247

The highly temperature dependent FD spectra of zwitterionic compounds often contain only a weak, if detectable, protonated molecular ion. The spectra are dominated by fragment ions and adduct ions formed by thermally initiated intermolecular processes.

We have found that addition of a strong, relatively non-volatile acid (p-toluenesulfonic) to solutions of zwitterions prior to FD analysis yields several beneficial results: (1) a dramatic increase in sensitivity for the protonated molecular ions of most zwitterions studied, (2) a sharp decrease in the emitter current required to achieve desorption, and (3) elimination of fragmentation.

The first figure shows oscillographic output obtained in the molecular ion region of the indicated quaternary ammoniosulfonate. The spectrum on the left is typical of "normal" FD results while that on the right is typical of results obtained after simply adding a few drops of a 1M solution of p-toluenesulfonic acid to the solution of the zwitterion. Both scans were recorded with an identical detector sensitivity. The spectrum recorded in the presence of acid exhibits a protonated molecular ion and isotope peaks that are at least two orders of magnitude more intense than observed in the absence of acid.

This technique has been successfully applied to a wide range of zwitterions including amino acids, ammoniocarboxylates, -phosphonates, -phosphates, -sulfonates and -sulfates. Therefore, sensitivity enhancement and minimization of fragmentation have been observed for zwitterions with weakly basic anionic groups (ammoniosulfonates and -sulfates) as well as for zwitterions with anionic groups that are very basic (amino acids, ammoniocarboxylates). A more volatile strong acid, HCl, does not exhibit a similar sensitivity enhancement for zwitterions with weakly basic anionic groups. This is illustrated by the analysis of an ammoniosulfonate, Figure 2. The spectrum recorded in the presence of HCl (middle scan) is very similar to that obtained without addition of an acid (upper scan). Both spectra exhibit weak protonated molecular ions and are dominated by fragments such as $(M+H-SO_3)^+$ and a series of ions formed by cleavage at the ether linkages. The spectrum recorded in the presence of p-toluenesulfonic acid (bottom scan), on the other hand, exhibits only MH^+ at high sensitivity. Since the sulfonate group is less basic than the solvent (water) used for these analyses, both acids initially protonate the solvent and not the sulfonate group directly. Upon introduction of the acidified solution into vacuum, a volatile acid such as HCl is evaporated along with the solvent and the compound is not converted to the quaternary ammonium salt. A less volatile acid such as p-toluenesulfonic is not simply pumped away with solvent. Therefore, p-toluenesulfonic acid enhances FD sensitivity while HCl does not.

Table 1 summarizes our findings to date. Addition of a strong, relatively non-volatile acid to a solution of a zwitterion prior to FD analysis results in high sensitivity for protonated molecular ions. Fragmentation and intermolecular processes are suppressed because the sample desorbs at substantially reduced emitter heating currents. A relatively non-volatile strong acid is required for analysis of zwitterions with weakly basic anionic groups. This technique is superior to alkali ion attachment for the analysis of zwitterions since the latter approach exhibits much poorer sensitivity and requires a high thermal activation (resulting in fragmentation). Finally, the choice of solvent is important. The potential for acid-catalyzed solvolysis exists and a solvent must be selected that minimizes this problem.

Acknowledgments

We gratefully acknowledge the contributions that our colleagues have made to this work. J. D. Pryne recorded many of the FD spectra. E. P. Gosselink and C. R. Degenhardt synthesized and purified many of the compounds examined in this study. R. A. Sanders, R. G. Laughlin and R. P. Oertel made valuable suggestions throughout the course of this work.

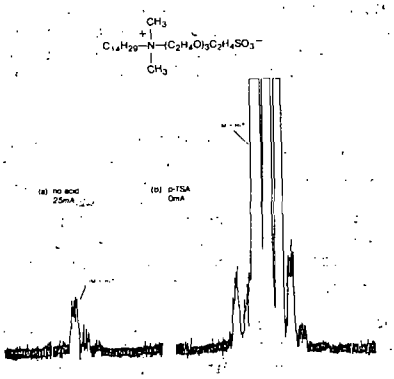

Figure 1: Comparison of FD intensities for the protonated molecular ion of the indicated quaternary ammoniosulfonate. Spectrum (a) was recorded without acid and (b) after addition of acid.

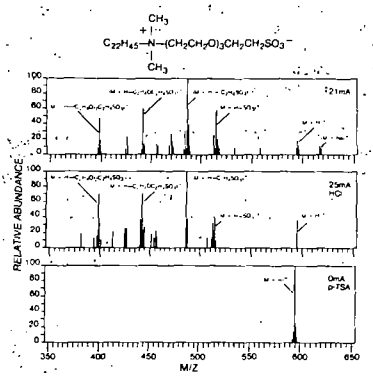

Figure 2: FD spectrum of an ammoniosulfonate without addition of acid (upper), after addition of HCl (middle), and after addition of p-toluenesulfonic acid (lower).

Table 1: Summary of Results on Acid-Enhanced Field Desorption

1. High sensitivity for $(M+H)^+$ with a variety of zwitterionic compounds.
2. Fragmentation and intermolecular processes are suppressed.
3. Non-volatile strong acid is required for analysis of zwitterions with weakly basic anionic groups.
4. Superior to alkali ion attachment which requires high temperature.
5. Choice of solvent is important:
   A. affects relative concentration of sample and acid
   B. potential for acid-catalyzed solvolysis

THE ROLE OF COLLISION COMPLEXES IN THE REACTION OF SiH_3^+ WITH C_2H_4,

R. N. ABERNATHY AND F. W. LAMPE, Dept. of Chemistry, The Pennsylvania State University, University Park, Pa. 16802

The ionic products of the reaction of silyl ion with ethylene were investigated using a 180 degree tandem mass spectrometer. The instrument employed a dc discharge and a Wien velocity filter to produce the primary ion beam which after deceleration entered a collision cell. The product ions were detected using an on-line quadrupole mass filter and an electron multiplier which was mounted off-axis.

The reaction of silyl ion with ethylene had previously been investigated by Allen and Lampe (1). A collisionally unstabilized collision complex, $SiC_2H_7^{+*}$, was directly detected. The dependence of the relative amount of complex upon pressure of ethylene was related to a mechanism which involved collisional stabilization. Due to the large energy spread of the primary ion beam (FWHM = 1 eV) and the rather large values for the rate constant for collisional stabilization of the complex ($k_s = 3x10^{-9}cm^3/sec$), a reinvestigation was warranted.

The current investigation centers on the reaction of SiH_3^+ at a laboratory energy of 2.6 eV with C_2H_4, and its dependence upon pressure of ethylene in the collision cell. If collisional stabilization is used to explain the pressure dependence of the relative amount of $SiC_2H_7^+$ detected, then extremely large values of k_s ($9x10^{-8}cm^3/sec$) are required. Through examination of the ionic products of the reaction of SiH_3^+ with C_2D_4, it was observed at the lowest pressures used that the ratio of intensities of m/q 32 to m/q 33 was the same as the ratio of intensities of m/q 64 to m/q 65. This occurrence could not be explained by a mechanism of collisional stabilization assuming scrambling of H and D. A mechanism which better explains the observed products would be as follows:

$$(SiH_3^+)_o + C_2H_4 \xrightarrow{\sigma_C} (SiC_2H_7^{+*})_o \qquad (1)$$

$$(SiH_3^+)_o + C_2H_4 \xrightarrow{\sigma_D} SiCH_3^+ + CH_4 \qquad (2)$$

$$(SiC_2H_7^{+*})_o \xrightarrow{k_{bo}} (SiH_3^+)_1 + C_2H_4 \qquad (3)$$

$$(SiC_2H_7^{+*})_o \xrightarrow{k_{fo}} SiC_2H_5^+ + H_2 \qquad (4)$$

$$(SiH_3^+)_1 + C_2H_4 \xrightarrow{k_{1C}} (SiC_2H_7^+)_1 \qquad (5)$$

$$(SiH_3^+)_1 + C_2H_4 \xrightarrow{k_{1D}} SiCH_3^+ + CH_4 \qquad (6)$$

Step (5) explains the relationship between the intensities of m/q 32 and 33 and the intensities of 64 and 65. As can be seen from the above mechanism, the pressure dependence of the intensity of $(SiC_2H_7^+)_1$ is the same as would be expected for a collisionally stabilized complex. At the energy and pressures currently under consideration, the initial complex is so short-lived ($3x10^{-8}$sec) that it undergoes unimolecular decomposition long before it could be collisionally stabilized. A value of $7.5x10^{-10}cm^3/sec$ was obtained for the value of k_1 in the current study ($k_1 = k_{1C} + k_{1D}$). The results are consistent with RRKM calculations, and the mechanism fits the experimental data.

In conclusion at the pressures used in this work (0.25 to 5 mtorr), there is apparently a transition from a mechanism which involves collisional stabilization at very low energies ($\tau \geq 10^{-6}$sec) to a mechanism where collisional stabilization plays no observable role at higher energies ($\tau \leq 10^{-8}$ sec). The energy and pressure domain currently investigated is in the latter category. Therefore reaction of moderated primary is the mechanism of formation of long lived complexes at 2.64 eV lab.

(1) W. N. Allen and F. W. Lampe; JACS 99 6816 (1977).

GeH_5^+ AND THE PROTON AFFINITY OF GERMANE, R. N. ABERNATHY, S. N. SENZER, AND F. W. LAMPE, Department of Chemistry, The Pennsylvania State University, University Park, Pa. 16802

The reactions of GeH_4 with various deuterated ions have been studied in a tandem mass spectrometer. Relative cross sections of the reactions have been determined at 1 micron pressure in the range 2-10 eV (Lab) by the relationship

$$\sigma_{rel} = j_{product}/(j^+_{reactant} P)$$

where the j's are currents and P is the pressure. The form of the dependence of the relative cross section on the kinetic energy of the reactant ion was used to classify experimentally the reactions as exothermic or endothermic.

A typical scan of the ionic products of the collision of 2.50 eV $C_2D_3^+$ ions from deuterated ethane with GeH_4 is shown in Fig. 1.

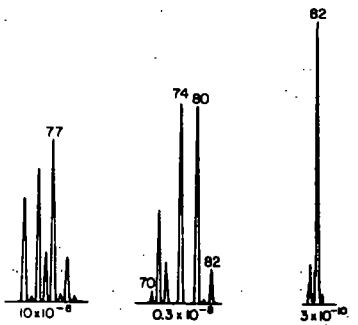

As may be seen from this figure, the principal reaction is the formation of GeH_3^+ but the product ion at m/e = 82 can only be GeH_4D^+, which unambiguously indicates the formation of protonated germane, and thus it must be concluded that the reaction

$$C_2D_3^+ + GeH_4 \rightarrow GeH_4D^+ + C_2D_2 \qquad (1)$$

is occuring. Product ions at m/e = 78 and 80 give further evidence to this result. The non-statistical, in fact, almost neglible appearance of the GeH_2D^+ product suggests that the formation of GeH_3^+ does not proceed via breakdown of GeH_4D^+ but rather is the result of a direct hydride ion removal from GeH_4.

The existence of GeH_5^+ had been predicted on purely theoretical grounds,[1] but to our knowledge, the experimental observation of this ion has not been reported previously. The formation of GeH_4D^+ has also been observed in collisions of GeH_4 with $C_2D_2^+$ from C_2D_4, $C_2D_5^+$ and $C_3D_7^+$ from C_3D_8, and D_3S^+

from D_2S, with some typical dependencies of the reaction cross sections on reactant ion kinetic energy being shown in Figs. 2A and 2B.

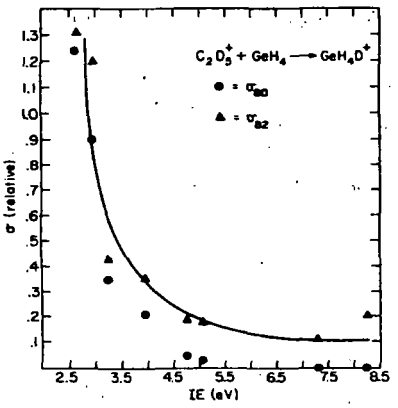

Figure 2A

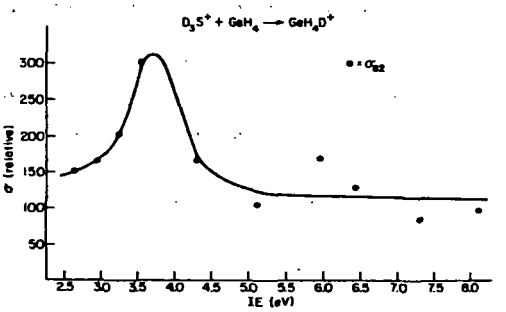

Figure 2B

The decrease in cross section with increasing kinetic energy over the entire range indicates that formation of GeH_4D^+ by proton transfer from $C_2D_2^+$, $C_2D_3^+$ and $C_2D_5^+$ are exothermic reactions. On the other hand, in Fig. 2B, the reaction cross section for GeH_4D^+ formation from D_3S^+ increases with increasing reactant ion energy, from a threshold near zero to a maximum, indicating that the reaction is endothermic. Using tabulated thermochemical data for all species except GeH_5^+ in the pertinent proton transfer reaction enables us to assign upper and lower limits of 164 kcal/mole and 162 kcal/mole to the proton affinity of germane, roughly 1 eV greater than the value of 6.04 eV determined from the difference in energies calculated for GeH_5^+ and GeH_4.[3] Using the above values, the upper and lower limits to the standard enthalpy of formation of GeH_5^+ are calculated to be 224 kcal/mole and 222 kcal/mole respectively.

1. H. Hartmann, L. Papula, and W. Strehl, Theoret. Chim Acta (Berl) 19 (1970) 160.

2. J. L. Franklin, J. G. Dillard, H. M. Rosenstock, J. T. Herron, K. Draxl, and F. H. Field, Natl. Stand. Ref. Data Serv., Natl. Bur. Stand. (U.S.), 26 (June 1969).

3. H. Hartmann, L. Papula, and W. Strehl, Theoret. Chim Acta (Berl) 19 (1970) 164.

Complex Formation by the Methylmercury Cation from CIMS Studies of Dimethylmercury

J.A. Stone, R. Camicioli, M.C. Baird, and D. Splinter, Department of Chemistry, Queen's University, Kingston, Ontario, Canada K7L 3N6.

The methane chemical ionization mass spectrum of dimethylmercury ($(CH_3)_2Hg$) has been studied in a field free, high pressure source at total pressures from 0.2 to 4 torr and temperatures from 298K to 600K. Both CH_5^+ and $C_2H_5^+$ react with $(CH_3)_2Hg$ and at all temperatures, in the absence of additives, the major product ion is $(CH_3)_3Hg_2^+$. Minor ions at low temperature are CH_3Hg^+ and $(CH_3)_2HgH^+$ in roughly equal proportions while at high temperature only CH_3Hg^+ is observed. The following reaction scheme is consistent with these observations and with time resolved studies.

$$CH_5^+ + (CH_3)_2Hg \longrightarrow CH_4 + (CH_3)_2HgH^{+*}$$

$$(CH_3)_2HgH^{+*} \longrightarrow CH_3Hg^+ + CH_4$$

$$\xrightarrow{M} (CH_3)_2HgH^+$$

$$CH_3Hg^+ + (CH_3)_2Hg \xrightarrow{M} (CH_3)_3Hg_2^+$$

$$(CH_3)_2HgH^+ + (CH_3)_2Hg \longrightarrow (CH_3)_3Hg_2^+ + CH_4$$

$(CH_3)_2HgH^+$ is protonated dimethylmercury while $(CH_3)_3Hg_2^+$ is the analogous compound with the proton replaced by the methylmercury cation. It is suggested that both species contain a three centre, two electron bond. The behaviour of CH_3Hg^+ in the condensed phase does have analogies with that of the proton. For example both form salts with strong acids e.g. $HClO_4$ and CH_3HgClO_4. The series of gas phase proton basicities might be expected to have its counterpart in a series of methylmercury cation affinities for the same bases. We have commenced the study of such a series using pulsed high mass spectrometry.

When a base such as benzene is also present then two extra products are formed, the relative yields of which are dependent on the total pressure. Both methyl cation and methylmercury cation addition occurs, the latter increasing at the expense of the former with increasing pressure.

$$CH_3Hg^+ + C_6H_6 \longrightarrow C_6H_6 \cdot HgCH_3^{+*}$$
$$C_6H_6 \cdot HgCH_3^{+*} \longrightarrow C_6H_6 \cdot CH_3^+ + Hg$$
$$\xrightarrow{M} C_6H_6 \cdot HgCH_3^+$$

When two bases are present their methylmercury cation adducts are in equilibrium with each other and with the neutral bases. Provided the methylmercury cation affinities are not too far apart (<12kJ mol^{-1}), $\Delta G°$ values may be obtained. Some values are listed below and are compared with those for the proton for the same base pairs. The gap between 2-chloropyridine and mesitylene is too large for measurement.

Gas Phase Bacisity Differences

($\Delta G°$, kJ mol^{-1})

	Methylmercury Cation	Proton[1]	Temp. (K)
tri-n-propylamine ——— triethylamine	3.0	9.2	573
triethylamine ——— diethylamine	7.1	28.9	573
diethylamine ——— pyridine	3.6	16.3	573
pyridine ——— propylsulfide	1.8	65.3	573
propylsulfide ——— 2-chloropyridine	6.6	-41.8	573
⋮			
mesitylene ——— m-xylene	9.6	29.3	413
m-xylene ——— o-xylene	1.2	3.3	413
o-xylene ——— p-xylene	0.1	2.5	413
p-xylene ——— n-butylbenzene	0.44	1.25	413
n-butylbenzene ——— cumene	1.8	0	413
cumene ——— ethylbenzene	3.2	5.02	413
ethylbenzene ——— toluene	4.1	3.8	413
toluene ——— benzene	10.9	23.8	413
ethylbenzene ——— methylacetate	0.8	5.9	573
methylacetate ——— nitrobenzene	2.4	12.6	573
nitrobenzene ——— toluene	0.5	2.5	573

In only one case, that of n-propylsulfide, is there a deviation from a strict correlation of the ordering of basicities for both cations at the temperatures employed. If the qualitative Hard-Soft acid base concept is employed then the anomalously large relative affinity between the soft sulfide base and the soft methylmercury cation is not unexpected.

Reference

1. K.N. Hartman, S. Lias, P. Ausloos, H.M. Rosenstock, S.S. Schroyer, C. Schmidt, D. Martinsen and G.W.A. Milne. A Compendium of Gas Phase Basicity and Proton Affinity Measurements. NBSIR 79-1777; (1979).

THERMOCHEMICAL STUDIES OF ION CLUSTERS: BOND ENERGIES AND RELATIONSHIP TO SOLVATION

A. W. Castleman, Jr., P. M. Holland, T. D. Märk, K. I. Peterson, R. G. Keesee, N. Lee, Department of Chemistry and Chemical Physics Lab., CIRES, University of Colorado, Boulder, Colorado 80309, USA

For a number of years we have been employing high pressure mass spectrometric techniques to investigate the formation and properties of clusters formed by the attachment of molecules to ions. The results, in conjunction with theoretical models, find application in elucidating the nature of bonding, structure, and the dynamics of ion cluster formation. Research in this area is also particularly valuable in the field of interface physics which is concerned with the molecular details of the collective effects responsible for phase transitions, nucleation phenomena, the development of surfaces, and ultimately ion solvation and formation of the condensed state. In addition to this fundamental importance, such findings also often have a bearing on problems in the atmospheric sciences, radiation chemistry, and combustion processes. The experimental technique is designed to provide a direct measurement of the equilibrium constants for desired reactions. Bond energies and entropies for the successive requisite clustering steps are determined from conventional thermodynamic relationships.

In order to compare the solvating properties of ammonia to that of water, investigations of the thermochemical properties of lithium, sodium, potassium and rubidium clustered to ammonia were made.[1] A comparison of the bond energies of the monoligand clusters shows that the ammonia molecule bonds more strongly than H_2O to all alkali metal ions. This is consistent with a simple molecular orbital model which is based on the difference in ionization potentials of the metal and ligand, and with predictions based on the extended Hückel method. A significant feature of the data is seen in comparing the lithium and sodium results to those obtained for potassium and rubidium. In the case of the first two, a significant decrease in bond energy for the attachment of the fifth ammonia molecule to a cluster containing 4 ligands was observed, while in the case of potassium and rubidium, no such well defined solvation shell was observable. These findings, which are in agreement with solution phase measurements, suggest the existence of a solvation shell of 4 ligands in the case of both lithium and sodium, the smallest two alkali metal ions.

Thermionic emission sources have also been employed in investigations of the bonding of water and ammonia to the transition metal ions Cu^+ and Ag^+. An interesting finding is that the first two clusters of NH_3 are bound much more strongly to Ag^+ and Cu^+ than even to Li^+, but that there is a significant drop for the attachment of the third ammonia molecule. Nevertheless, the results establish that additional ammonia ligands beyond the $Cu^+(NH_3)_2$ complex still have significant bond energies (12-15 kcal/mol up to the fifth cluster), although less than those of the corresponding water ligands in the analogous complex. This suggests that the $Cu^+(NH_3)_2$ observed in aqueous solution is due to preferred bonding to solvent molecules rather than an intrinsic inability to bind additional ammonia ligands. A further interesting feature of the data is that water bonds slightly more strongly to Cu^+ than to Ag^+.

Experiments have also been made[2-4] for the clustering of water, sulfur dioxide, and carbon dioxide to various negative ions including HCO_3^-, NO_2^-, Cl^-, NO_3^-, CO_3^-, SO_3^-, and I^-. Interestingly, the relative pattern of bond energies for the association of one neutral molecule to a negative ion was found to be the same for water (a protic polar molecule), sulfur dioxide (an aprotic polar molecule), or carbon dioxide (a non-polar molecule). A comparison of data shows that the order of the magnitude of the enthalpy changes on the association of the first neutral for a series of negative ions parallel the gas-phase basicity of those anions. For any given ion, the relative order of the addition enthalpies among the neutrals is dependent on the polarizabilities of the neutrals and on the covalency in the ion-neutral bond.

The results of the studies of water and ammonia clustering to both the positive and negative ions have led to a new correlation[5] relating bond energy in the gas phase to solvation in the condensed phase. Referring to Figures 1a and 1b, it can be seen that the ratio of ΔH°_{solv} (standard heat of solvation) to the summed gas phase enthalpies, $\Delta H^{\circ}_{0,n}$, approaches a value which is independent of the nature of the ion at very small cluster sizes. The correlation is related to the Born equation which expresses the energy necessary to place a charge in the cavity of a dielectric medium.

In addition to the above, experiments with alkali metal ions have revealed previously unreported clusters involving Na_2^+ bound to H_2O and CO_2 and NaOH to Na^+.[7] While water was found to bond to Na_2^+, its reaction with Li_2^+ led directly to the species $Li^+ \cdot LiOH$. In the case of the sodium system, a second water addition was required before the formation of the NaOH bonded to Na^+ along with the water. These measurements have led to a value for the binding energy of NaOH to Na^+ of approximately 2eV. These findings are important in confirming the stability of complexes proposed by Ferguson[7] to account for certain non-proton hydrates detected by rocket-borne mass spectrometers in the upper atmosphere.

References:

(1) A.W. Castleman, Jr., P.M. Holland, D.M. Lindsay, and K.I. Peterson, J. Am. Chem. Soc., 100, 6039 (1978)

(2) R.G. Keesee, N. Lee, and A.W. Castleman, Jr., J. Am. Chem. Soc., 101, (10) 2599 (1979)

(3) N. Lee, R.G. Keesee, and A.W. Castleman, Jr., J. Chem. Phys., 72(2), 1089 (1980)

(4) R.G. Keesee, N. Lee, and A.W. Castleman, Jr., "Properties of Clusters in the Gas Phase V. Complexes of Neutral Molecules onto Negative Ions," J. Chem. Phys. (in press)

(5) N. Lee, R.G. Keesee, and A.W. Castleman, Jr., "On the Correlation of Total and Partial Enthalpies of Ion Solvation and the Relationship to the Energy Barrier to Nucleation," J. Colloid & Interface Sci. (in press)

(6) T.D. Märk, K.I. Peterson, and A.W. Castleman, Jr., "New Gas Phase Inorganic Ion Cluster Species and Their Atmospheric Implications," Nature (in press)

(7) E.E. Ferguson, Geophys. Res. Lett., 5, 1035 (1978)

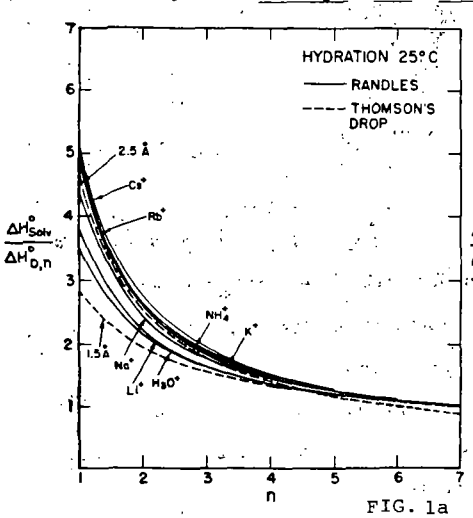

FIG. 1a

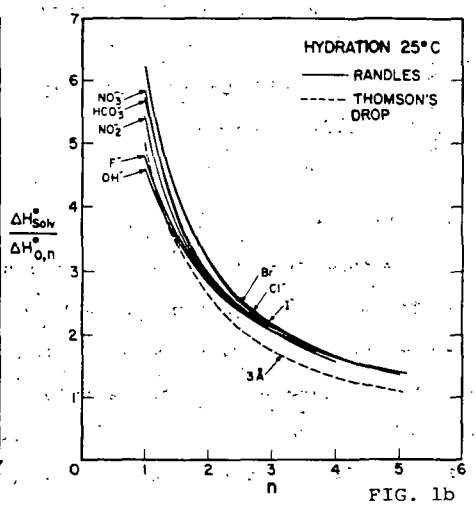

FIG. 1b

NEUTRAL PRODUCTS OF NUCLEOPHILIC SUBSTITUTION IN THE GAS PHASE.

Thomas Hellman Morton, David G. Hall, & Chakra Gupta

Department of Chemistry, Brown University

Providence, Rhode Island 02912

Over the past few years, we have been engaged in a study of gas-phase ion chemistry through examination of neutral products from cation reactions at pressures below 10^{-3} Torr. We generate ions by electron impact in a specially constructed Electron Flow Bombardment (EBFlow) reactor and collect all products in a liquid nitrogen-cooled trap. Subsequent gas chromatographic analysis enables us to differentiate isomeric products, and we have reported studies of molecular ion decompositions[1,2], ion-molecule reactions[3], and cation rearrangements[4]. In the present investigation, we have probed the stereochemistry of the gas phase nucleophilic displacement represented below for the reaction of an alcohol with its protonated parent ion:

$$ROH + ROH_2^+ \xrightarrow{-H_2O} R_2OH^+ \qquad (1)$$

ELECTRON BOMBARDMENT FLOW REACTOR

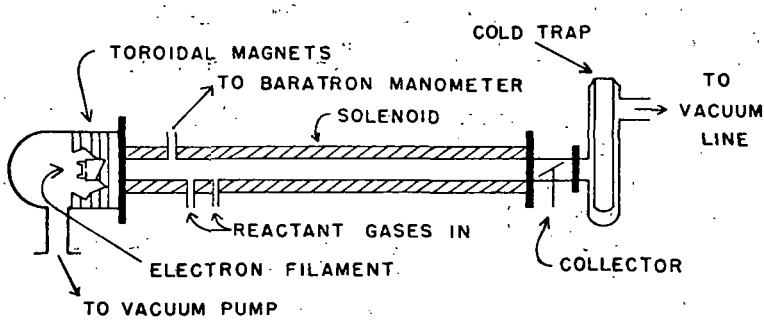

Our procedure for examining neutral products is to run the reaction in the presence of a base, which serves to deprotonate the reaction product and yield a neutral ether, which can be characterized by subsequent chromatographic analysis. Speranza and Angelini[5] have performed comparable studies using H_2O displacement of HCl from various protonated methylchlorocyclohexanes at atmospheric pressure (ions generated by γ-radiolysis). Their analyses of recovered cyclohexanols indicates that inversion of stereochemistry occurs approximately twice as often as retention, a result they interpret as supporting a backside attack mechanism.

ICR studies of reaction 1 have been reported by Beauchamp and Caserio[6] using 2-butanol. If

backside attack is the preferred pathway, then optically active 2-butanol should produce the meso (achiral) isomer of di-sec-butyl ether, as shown in the scheme below. Beauchamp, Caserio , and McMahon report[7], however, that tert-butanol undergoes the same reaction. This result is hard to reconcile with a backside displacement mechanism and has led to the hypothesis of a frontside displacement mechanism. In this pathway, as shown below, a vibrationally excited proton-bound dimer is formed that undergoes rearrangment to expel water. If optically active 2-butanol reacts with its protonated parent ion via this pathway, then the chiral isomer of di-sec-butyl ether results. A third possibility, which can be used to reconcile all of the experimental data, is that an ion-molecule complex is produced by collision of the alcohol with its protonated parent. This pathway resembles the S_N1 reaction in solution, with the exothermicity of complex formation leading to cleavage of the $C-OH_2^+$ bond of the protonated parent ion in the ion-molecule complex. This solvolytic displacement mechanism for the gas phase, as illustrated below, should lead to a mixture of meso and d,l di-sec-butyl ethers.

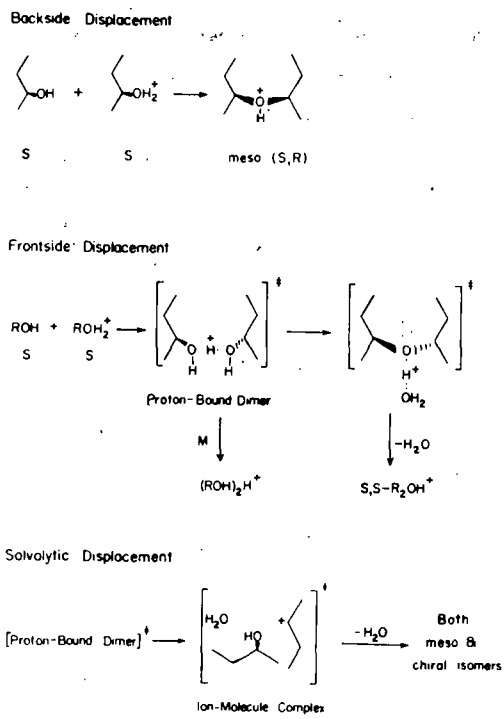

We find that 70 eV electron bombardment of optically active 2-butanol (5×10^{-4} Torr) in the presence of amine base (2×10^{-4} Torr) produces di-sec-butyl ether. Because there may be other processes besides reaction 1 that yield the ether in the EBFlow reactor, our interpretation of the data depends upon several control experiments that we have run. First of all, the products we observe do not come from filament pyrolysis, since lowering the electron energy below ionization threshold causes our product yield to disappear. Secondly, we rule out the reaction

$$R^+ + ROH \rightarrow R_2OH^+ \qquad (2)$$

on the basis of the following experiment: 70 eV electron bombardment of 5×10^{-4} Torr isopropanol plus 2×10^{-4} Torr NH_3 plus 2×10^{-4} Torr 2-bromobutane (an excellent source of C_4H_9 cations[8]) yields diisopropyl ether, but only a relatively small quantity of isopropyl sec-butyl ether. The ratio i-Pr_2O/sec-BuO-i-Pr > 5, and the isopropyl sec-butyl ether that is seen can be largely attributed to a reaction that occurs among the reactants simply upon standing.

The most important set of experiments are the relative yields of d,l and meso isomers of di-sec-butyl ether as a function of the base used. A relatively weak base, such as NH_3 (whose proton affinity is about the same as that of dibutyl ether), will deprotonate R_2OH^+ or proton-bound dimers $(ROH)_2H^+$ inefficiently. Therefore ions, such as the proton-bound dimers, can cluster further with 2-butanol, making solvolytic pathways more likely. However, a strong base, e.g. trialkylamines, should deprotonate R_2OH^+ and $(ROH)_2H^+$ with virtually unit efficiency. Large clusters of $(ROH)_nH^+$ are interecepted, and we expect the product distribution to reflect a greater contribution from reaction 1. Our experimental results confirm this expectation: radiolysis of pure (+) or of pure (-) 2-butanol with NH_3 affords a meso/d,l ratio of 1.2, while radiolysis in the presence of tripropylamine gives these isomers in a ratio ≥ 3. Thus, our results appear to confirm a backside displacement mechanism as the predominant pathway.

1. Burns, F.B.; Morton, T.H. JACS 1976, 98, 7308-7313.
2. Morton, T.H. JACS 1980, 102, 1596-1602.
3. Marinelli, W.J.; Morton, T.H. JACS 1978, 100, 3536-3539; 1979, 101, 1908.
4. Hall, D.G.; Morton, T.H. JACS, in press.
5. Speranza, M.; Angelini, G. JACS 1980, 102, 3115-3120.
6. Beauchamp, J.L.; Caserio, M.C. JACS 1972, 94, 2638-2646.
7. Beauchamp, J.L.; Caserio, M.C.; McMahon, T.B. JACS 1974, 96, 6243-6251.
8. McLafferty, F.W. Anal. Chem. 1962, 34, 2-15.

MAMP1 APPLICATIONS OF HIGH PERFORMANCE GC^2/MS.

U.RAPP and G.DIELMANN, Varian GmbH, Bremen, F.R. Germany

The separation and thereby possible characterization of naturally occurring complex mixtures such as wax esters, triglycerides and hydrocarbon fractions is of great importance especially with regard to industrial technical revenue.

Two different fields of interest will be presented with examples:

1. High performance glass capillary separation power.
By means of artificial and technical hydrocarbon mixtures the utmost separation power of commercially available capillary columns will be shown. The excellent separation power is maintained when passing the interface to the mass spectrometer, which is used as the ideal detector in the scanning mode.

2. High temperature glass capillary performance.
Packed columns have been used until recently for the analysis of high boiling substances. Now capillary columns were made available for the high temperature range needed. Natural wax ester mixtures and triglycerides were analysed up to the C_{60} carbon number range.

On the mass spectrometric side electron impact ionization as well as chemical ionization were used. Ammonia as reagent gas was found to be an advantageous choice, because in the case of the esters unambiguous attributions of the molecular weights were achievable.

As GC/MS interface a standard open split coupling was used demonstrating the versatility needed for the different GC requirements mentioned above.

PHOSPHATE DETERMINATION EMPLOYING AN ^{18}O LABELED CARRIER

G. GRAFF[2], T.P. KRICK[1] and N.D. GOLDBERG[2]
DEPTS. of BIOCHEMISTRY[1] and PHARMACOLOGY[2]
U. of MINNESOTA, ST. PAUL, MN 55108

Objective: Develop a method to accurately determine both the amount of phosphate present in a sample and the distribution of ^{18}O incorporated in the phosphate while analyzing small quantities of material.

Rationale: The necessity of using a labeled carrier arises from the fact that small amounts of phosphate chromatograph poorly. The trimethylsilyl (TMS) derivative of phosphate was chosen for its ease of derivatization and the simplicity of its spectrum (fig. 1).

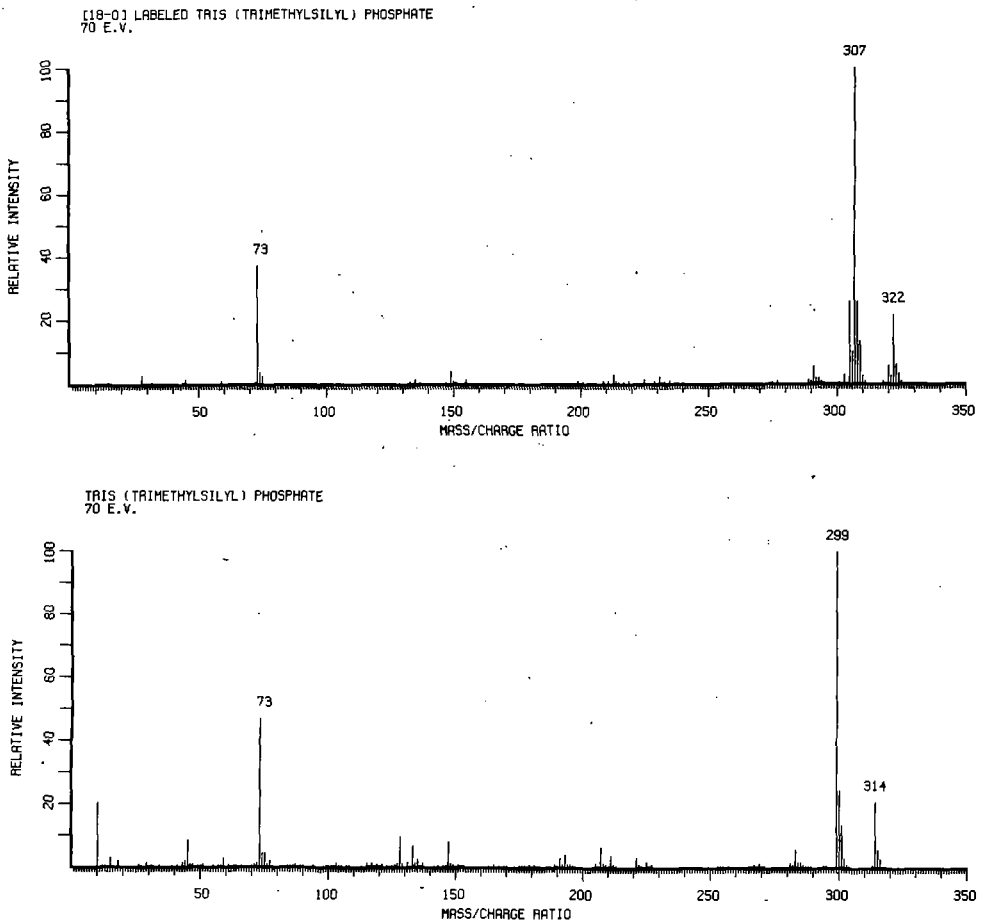

Figure 1. Mass Spectra of $^{18}O_4$ labeled and unlabeled TMS Phosphate.

The GLC detection of tris (trimethylsilyl) phosphate was found to be non-linear with > 90% loss in the range of 1 ng when analyzed on a 3% OV-17 column. This loss was determined by measuring the phosphate vs. naththalene ratio response over a concentration of 3 logs (Fig. 2A, 2B). By measuring the change in the ratio of m/e 299 (M-15 of $^{16}O_4$ TMS phosphate) vs. m/e 305 (M-15 of $^{16}O^{18}O_3$ TMS phosphate) ions after repeated injections, the loss was determined to be due in column absorption. Several polar and non-polar columns showed similar absorption characteristics. To circumvent this problem, a $^{18}O_4$ labeled phosphate carrier was added to the sample. The addition of carrier permitted accurate determination of phosphate at levels of > 5 ng by computing the ratio of labeled to unlabeled ions (Fig. 2c).

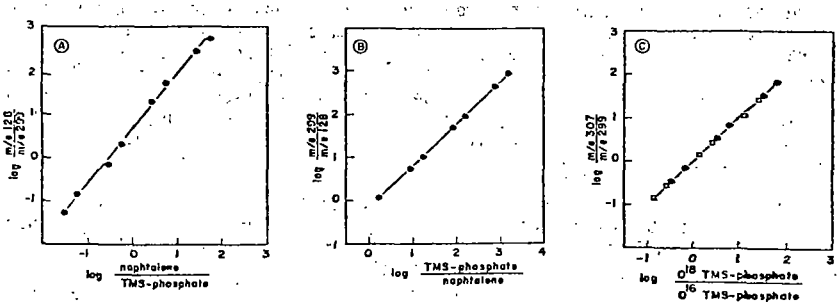

Figure 2 A. TMS Phosphate vs. Naphthalene, Naphthalene = 238 ng
B. Naphthalene vs. TMS Phosphate, TMS Phosphate = 2.58 ug.
C. $^{18}O_4$ TMS Phosphate vs. $^{16}O_4$ TMS Phosphate, $^{18}O_4$ TMS Phosphate = 1.82 ug.

Method: After isolation and addition of the carrier, the phosphoric acid was converted to its TMS derivative by first changing it to its ammonium salt then, after lyophilization, silylating by adding BSTFA/Pyridine in a sealed tube and heating 15 min. at 120 degrees. The sample was than injected onto a 3% OV-17 column at 95 degrees several times while recording the intensity of the ions at m/e 299, 301, 305, 307, 309, 314 (M+), 316, 318, 320, and 322. The ^{18}O enrichment as their individual molecular species was determined by correcting for the contribution of the carrier, correcting for natural isotopic abundances and finally computing the isotope ratios. An example of these results can be seen in Table I from the hydrolysis of cGMP in ^{18}O water.

Table 1 Hydrolysis of cGMP in [^{18}O] Water

% [^{18}O] enrichment of water	$^{16}O_4$	$^{18}O_1{}^{16}O_3$	$^{18}O_2{}^{16}O_2$	$^{18}O_3{}^{16}O_1$
20.5	79.5 ± 0.7	19.7 ± 1.0	0.2 ± 0.4	0.6 ± 0.6
39.1	57.6 ± 1.5	41.5 ± 1.1	0.1 ± 0.1	0.8 ± 0.5
50.7	49.4 ± 1.1	49.6 ± 1.4	0.2 ± 0.5	0.9 ± 0.7
65.7	34.4 ± 0.6	64.8 ± 0.8	0.4 ± 0.3	0.4 ± 0.5

Conclusion: This method of using TMS derivatives of phosphate with ^{18}O labeled carrier should be useful in the analysis of small quantities of phosphate deriving from a variety of phosphate containing cellular constituents that occur in limited quantities or are obtained from small tissue samples.

A PHOTODISSOCIATION STUDY OF THE OZONE IONS

J. F. Hiller and M. L. Vestal

Department of Chemistry
University of Houston
Houston, TX 77004

The tandem quadrupole instrument described by Vestal and Futrell (1) consists of three in-line quadrupoles and a pulsed nitrogen pumped dye laser. Ions generated in a CI source are focussed via retarding lenses into a primary mass analyzer. The selected primary ions pass into a transmission quadrupole (rf only) where they are intersected by the laser beam and photodissociated. Fragment ions are mass selected in the final quadrupole and synchronously counted with the laser flash. The laser beam may intersect the ion beam perpendicularly, as in the original design, to give good absolute cross-sections, or collinear with the ion beam, after the manner of McGilvery and Morrison (2), to give good relative cross-sections with approximately two orders of magnitude higher sensitivity.

Ozone and its ions are of interest in the study of the D-region of the ionosphere. The negative ion of ozone, O_3^-, has been of particular interest to investigators because of its rapid photodissociation in the visible region. The photodestruction of the solid state alkali ozonides was observed by Spiker and Anderson (3) in 1973. The free O_3^- ion was first examined by photodestruction spectroscopy in 1978 by Cosby, Moseley, Peterson and Ling (4) between 2.2 and 2.45 eV. Cosby et al. verified the primary destruction channel as (i) in this region. They were also able to make two possible assignments of the vibronic transitions involved (see Table). The photodissociation was examined by Vestal and Mauclaire (5) who found two possible channels for the process:

$$O_3^- + h\nu \rightarrow O^- + O_2 \qquad \text{(i)}$$

$$O_3^- + h\nu \rightarrow O_2^- + O: \qquad \text{(ii)}$$

which had approximately equal probabilities in the energy range 2.85-3.05 eV, with (i) predominating below 2.8 eV. Due to the low resolution of the Hg vapor light source, Vestal and Mauclaire were unable to make spectroscopic assignments. Novick, Engelking, Jones, Futrell, and Lineberger (6) have examined O_3^- by photoelectron, photodetachment and photodestruction spectroscopy. The study by Lineberger and coworkers gave a set of vibrational ground state frequencies which were considerably different from those of Cosby et al. (see Table 1).

We have examined the photodissociation of O_3^- between 1.9 and 3.3 eV photon energies with high resolution in both channels. Several features are immediately apparent from a cursory examination of Fig. 1. First, it appears that both O^- and O_2^- are produced from the same transition, though some features are more prominent in one curve than the other. The more complicated structure at photon energies greater than 2.65 eV suggest the appearance of a second excited state. The vibrational origin (T_{00}) for the first excited state is clearly at or near 2.15 eV. A close examination of an expanded view of this region shows a great deal of structure to the transition in this region. Because photoelectron and photodetachment measurements may be expected to give good values for the ground state vibrations, the values obtained by Lineberger et al. (6) were used to provide the fundamental ground state frequencies. Since the photodestruction process in this region is mostly through channel (i), the values obtained by photodissociation are very close to those of Cosby et al. for the excited state fundamental frequencies. Using this set of frequencies (Table 1), we can account for all the major structure below 2.3 eV assuming only one quanta or less of ground state vibrational excitation.

Acknowledgement

This work was supported by the Robert A. Welch Foundation.

References

1. M. L. Vestal and J. H. Futrell, Chem. Phys. Letters 4, 559, (1974).
2. D. C. McGilvery and J. D. Morrison, Int. J. of Mass. Spectrosc. and Ion Phys.
3. R. C. Spiker and L. Andrews, J. Chem. Phys. 59 (4), 1851, (1973).
4. P. C. Cosby, J. T. Moseley, J. R. Peterson and J. H. Ling, J. Chem. Phys. 69 (6), 2771, (1978).
5. M. L. Vestal and G. H. Mauclaire, J. Chem. Phys. 67 (8), 3767, (1977).
6. S. E. Novick, P. C. Engelking, P. L. Jones, J. H. Futrell and W. C. Lineberger, J. Chem. Phys. 70 (6), 2652, (1979).
7. G. P. Smith and L. C. Lee, J. Chem. Phys. 71 (5), 2323, (1979).
8. J. F. Hiller and M. L. Vestal, this work.

TABLE 1

FREQUENCIES AND BAND ORIGINS OF O_3^-

Technique	T_{00}(eV)	GROUND STATE ν_1(cm^{-1})	GROUND STATE ν_2(cm^{-1})	EXCITED STATE ν_1(cm^{-1})	EXCITED STATE ν_2(cm^{-1})
Photodestruction[4]	2.146	790(50)	419(20)	855(20)	290(20)
OR[4]	2.163	928(50)	403(20)	794(20)	282(20)
Photodestruction[7]	2.16	928	403	787	282
Photoelectron[6]		1040(60)			
Photodetachment[6]		982(30)			
Photodestruction[6]			550(50)		
Photodissociation[8]	2.147	976	548	823	282

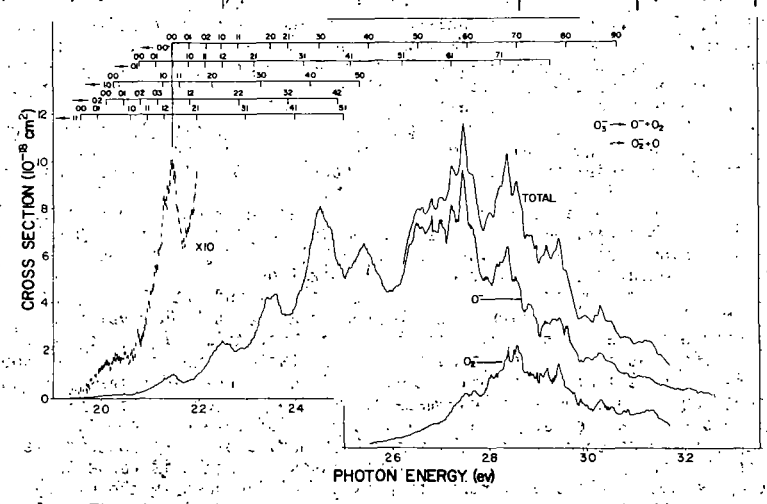

Fig. 1 The absolute photodissociation cross-section of O_3^- as a function of photon energy. The lower curve is the O_2^- product channel, the middle curve is the O^- channel, and the upper curve is the sum.

ELIMINATION OF THE CENTRAL CARBON IN THE FRAGMENTATION OF THE PROPANE ION

Jerome P. Gilman, TaCheng Hsieh and G. G. Meisels
Department of Chemistry, University of Nebraska

The dissociation of the propane molecular ion has been investigated by a wide variety of methods including charge-exchange collisions with positive ions (1), labelling techniques (2-5), metastable process analysis (2-4), photoionization (6) and threshold photoelectron coincident photoion mass spectrometry (5,7). Applications of the quasiequilibrium theory of mass spectra (QET) have been successful in explaining many of the features of the propane mass spectrum (8,9). However, no single scheme has adequately explained all observed facts.

This investigation deals with the elimination of the central carbon in the fragmentation leading to the loss of methane from propane ion. Theoretical calculations neglect this decomposition pathway (8,9) and experimental evidence is inconclusive (5). We have examined the relative extent of center carbon involvement in the formation of ethylene ion and methane from propane ion using propane-2-^{13}C by the processes

$$CH_3{}^{13}CH_2CH_3^+ \longrightarrow CH_2{}^{13}CH_2^+ + CH_4 \qquad (1)$$

$$CH_3{}^{13}CH_2CH_3^+ \longrightarrow CH_2CH_2^+ + {}^{13}CH_4 \qquad (2)$$

in a threshold photoelectron-coincident photoion mass spectrometer (TPE-CPIMS) and a double focussing electron impact mass spectrometer.

The TPE-CPI apparatus has been described previously (10); ions and photoelectrons produced by monochromatic light are drawn out of the photoionization region where each is separately detected by channeltron electron multipliers. Electrons first pass through a channel hole structure which rejects energetic electrons. Mass analysis is achieved by time-of-flight or quadrupole mass spectrometry. Only ions formed in coincidence with near-zero energy electrons are detected. The energy resolution at a photon energy of 14eV is 21 meV while the transmission of 55 meV electrons is 13% and that of 0.5eV electrons is 1.7%. Unlabelled propane was Matheson research grade (99.99% min. purity). Propane-2-^{13}C was purchased from Merck, Sharp and Dohme and contained approximately 10% unlabelled propane. Electron impact mass spectra and metastable transitions leading to methane loss were investigated on a Kratos AEI-MS50 high resolution double focussing mass spectrometer.

Breakdown graphs of propane and propane-2-^{13}C (figures 1 and 2) were corrected for non-zero kinetic energy electrons transmitted through the threshold photoelectron detector. Additional correction for the presence of unlabelled propane leads to relative abundances (as % of total ion count) of methane loss from the center and end carbons, respectively (figure 3). Process (2) may be preceded by randomization, reactions 1 and 2 may be competitive single step cleavages, or the observations may be a result of some combination of both. However, the competition is essentially independent of internal energy from 11.80 to 13.00eV, with $k_2/(k_1 + k_2) = 0.11 \pm 0.03$ (figure 4). Approximately 11% of the ethylene ions formed in this energy range result from elimination of the central carbon. If randomization precedes dissociation, the carbon skeletons of 33% of the parent ions have randomized before fragmentation.

Metastable ion intensities arising from the loss of methane from the end carbons and the center carbon lead to relative intensities, analogous to $k_2/(k_1 + k_2)$, of 0.02; electron impact studies under high resolution indicate $k_2/(k_1 + k_2) = 0.09$ in the range 12.0 to 18.0 eV (figure 5), in good agreement with the photoionization results.

Metastable data differ from the results obtained using EI and TPE-CPI MS (0.02 compared with about 0.10). This may result from two phenomena. First, observations on metastable ions sample ions which have dissociation rate constants on the order of 5×10^5 to 5×10^6 sec^{-1}. The ions are thus selected by rate constant. However, TPE-CPI experiments involve ions having selected internal energies. Second, observed relative intensities of metastable ions depend on a number of parameters. The most important of these are the shape and position of the rate constant curve as a function of internal energy. Curves which cross steeply the rate constant range within which metastables are observed lead to lower intensities than those where the rate constant passes through this range only gradually. The matter is complicated further by possible differences in the energy deposition function in the energy ranges where the rate constant is in the metastable range.

Experimental results can be interpreted using hypothetical rate constant curves shown in figure 6. The curves are structured from those calculated by Vestal (8). Curve c represents the rate constant for methane loss involving the center carbon and curve b that for the terminal carbons; curve c is postulated to rise sharply with internal energy. The

coincidence and EI data (figures 4 and 5) indicate that the ratio of methane loss from the central carbon to loss involving the end carbon is essentially constant such that curve c parallels curve b (separated by log 0.11). Since the observed ion intensity of process (2) is approximately 50 times less than the intensity observed in process (1) in the metastable experiment, curve c should rise more sharply in the metastable window than curve b.

We believe that our results suggest that randomization of the molecular ion does not precede fragmentation leading to methane loss, but that center carbon loss occurs in a concerted step-wise cleavage involving a transition state tighter than that for methane loss involving the terminal carbons.

We acknowledge gratefully the support of the Department of Energy and the University of Nebraska Foundation.

1. E. Patterson and E. Lindholm, Ark Fys. 24, 49 (1962). 2.a. C. Lifshitz and M. Shapiro, J. Chem. Phys. 45, 4242 (1966). b. C. Lifshitz and M. Shapiro, J. Chem. Phys. 46, 4912(1967). 3. C. Ottinger, J. Chem. Phys. 47, 1452 (1967). 4. P. Wolkoff and J. Holmes, J. Am. Chem. Soc. 100, 7346 (1978). 5. R. Stockbauer and M. Inghram, J. Chem Phys. 65, 4081 (1976). 6. W. Chupka and J. Berkowitz, J. Chem. Phys. 47, 2921 (1967). 7. B. Brehin, J. Eland, R. Frey and H. Schulte, Int. J. of M.S. and Ion Phys. 21, 373 (1976). 8. M. Vestal "Fundamental Processes in Radiation Chemistry", Interscience, New York (1968). 9. M. Vestal and J. Futrell, J. Chem. Phys. 52, 978 (1970). 10. C. Batten, J. Taylor and G. Meisels, J. Chem. Phys. 65, 3316 (1976).

BREAKDOWN GRAPH OF PROPANE (DECONVOLUTED)

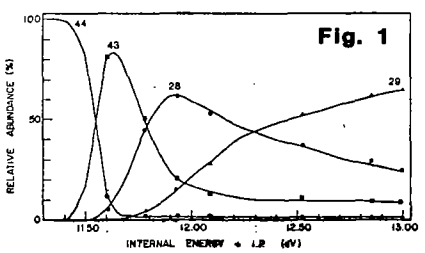

BREAKDOWN GRAPH OF PROPANE-2-^{13}C (DECONVOLUTED)

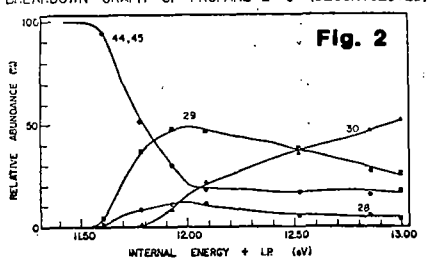

RELATIVE ABUNDANCE OF METHANE LOSS IN PROPANE-2-^{13}C

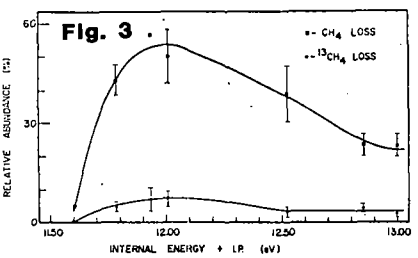

RANDOMIZATION OF $^{13}CH_4$ LOSS IN PROPANE-2-^{13}C

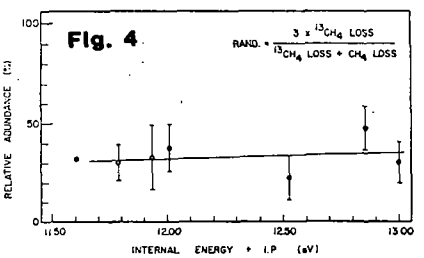

RANDOMIZATION OF $^{13}CH_4$ LOSS (ELECTRON IMPACT)

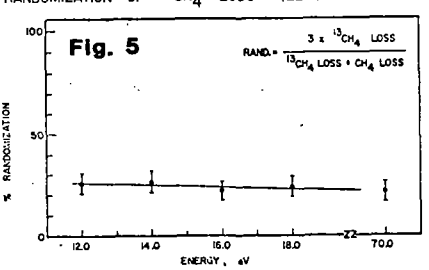

HYPOTHETICAL RATE CONSTANT CURVES

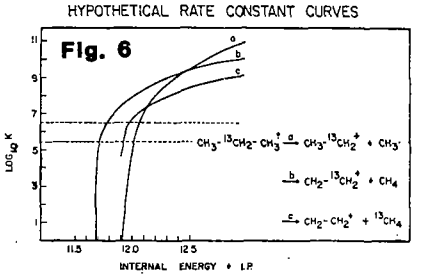

MAMP5 LASER INDUCED PHOTODISSOCIATION OF BROMOETHANE MOLECULAR IONS, FRED W. BRILL and JOHN R. EYLER, Dept. of Chem., Univ. of Fla., Gainesville, FL 32611

We have continued our studies of the laser-induced photodissociation of alkyl halide ions by investigating the various photofragmentation pathways of $C_2H_5Br^+$ ions using a flashlamp-pumped dye laser coupled with a pulsed ion cyclotron resonance (icr) mass spectrometer. Our work with $C_2H_5Cl^+$ ions[1] has shown that photofragmentation of this ion appears to occur directly from excited electronic states of the ion and does not involve internal conversion to highly vibrationally excited ground state ions followed by decomposition which might be predicted statistically by the methods of quasi-equilibrium theory (QET). Thus we were particularly interested in studying the processes $C_2H_5Br^+ \rightarrow C_2H_4^+ + HBr$ and $C_2H_5Br^+ \rightarrow C_2H_5^+ + Br$, since these two have approximately the same endoergicities and require only 15-25 kcal/mol to promote dissociation, well within the photon energy range of our dye laser.

Studies to date on $C_2H_5Br^+$ have shown that like $C_2H_5Cl^+$ this ion apparently fragments directly from excited electronic states, two of which are accessible with the energies of our dye laser. In contrast to our earlier studies, we see virtually no $C_2H_4^+$ ions produced at a number of wavelengths in the 450-650 nm region. This is similar to electron impact fragmentation data reported by Collin.[2]

We will report spectra of the photodisappearence of $C_2H_5Br^+$ and the photofragmentation branching ratio for $C_2H_4^+/C_2H_5^+$ in the 450-650 nm region, and discuss reasons for the behavior seen in this system as compared to that found with $C_2H_5Cl^+$.

[1] L. N. Morgenthaler and J. R. Eyler, J. Chem. Phys. 71, 1486 (1979).
[2] J. Collin, Bull. Soc. Roy. Sci. Liege 25, 426 (1956).

MAMP6 ION FLUORESCENCE FOLLOWING HeIα IONIZATION, R. C. DUNBAR, Department of Chemistry, Case Western Reserve University, Cleveland OH 44106, and D. W. TURNER, Phys. Chem. Lab., Oxford Univ.

A spectrometer is described for detecting visible and near-UV fluorescence following photoionization. Wavelength resolution is of the order of 2nm, and there are capabilities for observing wavelength-resolved fluorescence decay times in coincidence with mass-analyzed ions, and for determining wavelength-resolved fluorescence lifetimes by an ion-drift method. Photoionization of pentafluorocyanobenzene yields a parent-ion fluorescence spectrum reminiscent of polyfluorobenzene ion spectra, while other nitriles yield either no fluorescence, or CN neutral emission through a non-ionizing process. Wavelength resolved fluorescence lifetime spectra of CO_2^+ and CS_2^+ $\tilde{A}\rightarrow\tilde{X}$ emissions were obtained. CO_2^+ shows no wavelength dependence of the fluorescence lifetimes; the CS_2^+ spectrum, while perhaps non-uniform, does not show wavelength variation which can be readily attributed to different excited state lifetimes. It is concluded that neither of these ions has dramatic variation in excited state lifetimes, although the data precision for CS_2^+ is still modest. An average lifetime of CO_2^+ $\tilde{A}^2\pi_u$ of 123 nsec was found, and an average of 3.8 μsec for CS_2^+ $\tilde{A}^2\pi_u$.

MAMP7 IR PHOTODISSOCIATION OF GAS-PHASE IONS BY CO_2 LASER INTERACTION WITH A FAST ION BEAM, M. G. COGGIOLA, P.C. COSBY, R.C. DUNBAR AND J. R. PETERSON, Molecular Physics Center, SRI, Menlo Park, CA 94025 and Department of Chemistry, Case Western Reserve University, Cleveland, Ohio 44106

Irradiation of the SRI fast ion beam with a CW CO_2 laser results in a small fraction of ion photodissociation. Ions studied include CF_3I^+, $C_2F_5^+$, $C_2F_5Br^+$, $C_2F_5I^+$, $C_3F_7I^+$, $C_3F_6^+$ and $C_6F_6^+$. A mechanism is proposed in which a single IR photon effects dissociation of ions which emerge from the ion source with internal excitation nearly sufficient to cause spontaneous dissociation. The photodissociation products were in all cases the most stable products. Kinetic energy releases were measured, ranging from 4 to 14 meV, and in cases where light-free metastable fragmentation ions was also observed, the photodissociation energy release was larger than the metastable energy release. For all cases except CF_3I^+, an RRKM model gives reasonable quantitative agreement with these observations.

The dependence of photodissociation on CO_2 laser wavelenth shows well defined peaks in several cases, and is evidently constrained by the infrared absorption properties related to C-F stretching modes in the ion.

PHOTOION AND PHOTOELECTRON SPECTROSCOPY IN H_2O EXCITED BY SYNCHROTRON RADIATION IN THE RANGE OF 12 TO 35 eV.

O. DUTUIT[a], K. ITO[b], A. TABCHE-FOUHAILLE[b], T. GOVERS[a], T. BAER[c], P.M. GUYON[d], P. MORIN[b], I. NENNER[b]

LURE*, Bât. 209C, Centre Universitaire d'Orsay, 91405 ORSAY (France)

(a) L.R.E.I. Bât 350, Centre Univ. d'Orsay, 91405 Orsay (France)

(b) CEN Saclay, DPC/SPP/SP, BP2, 91190 Gif Sur Yvette (France)

(c) Dept. of Chemistry, Univ. of North Carolina, Chapel Hill, North Carolina 27514 (USA)

(d) L.C.A.M. Bât 351, Centre Univ. d'Orsay, 91405 ORSAY (France)

Pulsed Synchrotron Radiation (1 ns FWHM at 13.5 MHz frequency) from the Orsay Storage Ring (ACO) was used to investigate the photo-ionization and photo-dissociation of H_2O and D_2O. We present here two kinds of experimental results : time of flight photoelectron spectra at selected excitation energies in H_2O and threshold photoelectron-photoion coincidences in D_2O, D_2O beeing chosen for better mass resolution.

Incident light dispersed by a normal incidence monochromator is refocused at the center of the photo-ionization chamber, where it crosses a jet of gas, effusing from a fine hypodermic needle. The incident light (0.5-2 Å FWHM) is continuously monitored by a visible photomultiplier mounted behind a sodium salicylate coated window. Electrons and ions are extracted in opposite directions at right angles from the photon and gas beams. The methods for the electron-ion coincidences experiment as well as for the analysis of the photoelectron time of flight spectra have been previously described in detail [1,2].

Photoelectron time of flight spectra in H_2O were recorded at selected excitation energies between 12.6 and 35 eV. From these spectra, we derive the partial photo-ionization cross sections for the $\tilde{X}(^2B_1)$, $\tilde{A}(^2A_1)$ and $\tilde{B}(^2B_2)$ states of H_2O^+. In the case of the $H_2O^+(\tilde{X})$ state, one observes a large structure centered at 19 eV, which is not predicted by the calculations of HILTON et al [3] or WILLIAMS and LANGHOFF [4]. We attribute it to autoionization of Rydberg series converging to the $\tilde{B}(^2B_2)$ state.

In addition, the kinetic energy distribution of the low energy electrons is peaked around 0 eV, when one encompasses the first dissociation limit of H_2O^+ into $H + OH^+(X)$. This is in agreement with STOCKBAUER'S[5], observation of a strong enhancement of the threshold ($<$ 20 meV) electron yield at 18.1 eV.

No threshold peaks were detected in the electron time of flight spectra obtained at photon energies between 21 and 35 eV. In particular, no such

peak was observed in the 30-35 eV region, where one expects excitation of the $2a_1$ state [6], despite the large value of the analyser transmission of zero energy electrons. This behaviour might possibly reflect a small value of the partial cross section at threshold electron energy, when one excites this repulsive state.

Additional information concerning the dissociation of energy selected states of D_2O^+ was obtained, using the threshold electron-ion coincidence technique, up to 21 eV , i.e. slightly above the third dissociation limit into $D + OD^+(a)$ at 20.4 eV. The results confirm ELAND'S [7] finding that D^+ production competes with the formation of $OD^+(X)$ from the D^+ threshold upwards. In addition, we find that this dissociation channel, which is attributed to predissociation of the $\tilde{B}(^2B_2)$ state by $\tilde{A}(^2A_1)$, remains important up to 21 eV, where "direct" dissociation into $D + OD^+(a)$ is energetically accessible.

(1) T. BAER, P.M. GUYON, I. NENNER, A. TABCHE-FOUHAILE, R. BOTTER, L.F.A. FERREIRA, T. GOVERS, J. Chem. Phys. 70, 1585 (1979)

(2) P. MORIN, I. NENNER, P.M. GUYON, O. DUTUIT, K. ITO, submitted to J. Chimie Phys.

(3) P.R. HILTON, S. NORDHOLM and N.S. HUSH, Chem. Phys. Lett. 64, 515 (1979)

(4) G.R. WILLIAMS and P.W. LANGHOFF , Chem. Phys. Lett. 60, 201 (1979)

(5) R. STOCKBAUER, to be published

(6) K.H. TAN, C.E. BRION, Ph. E. VAN DER LEEUW and M.J. VAN DER WIEL, Chem. Phys. 29, 299 (1978)

(7) J.H.D. ELAND, Chem. Phys. 11, 41 (1975)

---

* Laboratoire propre du CNRS conventionné à l'Université Paris-Sud.

MAMP-9 AN EXACT MEASUREMENT OF THE FRAGMENTATION RATE CONSTANTS FOR THE LOWER 2-KETONES, Lloyd J. Hendricks, Colorado School of Mines, Golden, Colo. 80401

I. PROBLEM: The measurement of the fragmentation rate constants involved in mass spectrometry from mass spectral data.

II. SOLUTION: Exact equations were developed for each ion fragment intensity as a function of time at a single energy for the fragmentation model: (Ref 1,2)

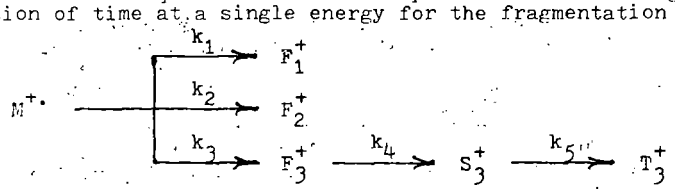

These equations were then modified to the conditions of observation in the mass spectrometer. For example, the molecular ion intensity of interest is the value observed at the detector, whereas that observed for the single secondary ion is its intensity at the source exit decreased by the exponential decay from the secondary to the tertiary ion occurring over the time of flight from the source exit to the detector. After forming ion abundance ratios to eliminate the unknown initial intensity of the molecular ion, the following set of equations result:

1) $k_0 = k_1 + k_2 + k_3$

2) $$R_{1M} = \frac{F_1}{M} = \frac{k_1}{k_0} \frac{(1 - \exp(-k_0 t_s))}{\exp(-k_0 t_d)}$$

3) $$R_{2M} = \frac{F_2}{M} = \frac{k_2}{k_0} \frac{(1 - \exp(-k_0 t_s))}{\exp(-k_0 t_d)}$$

4) $$R_{3M} = \frac{F_3}{M} = \frac{k_3}{k_0 - k_4} \exp(+(k_0 - k_4) t_d)\,(1 - \exp(-(k_0 - k_4) t_s))$$

5) $$R_{SM} = \frac{S_3}{M} = \frac{k_3 k_4}{k_0 - k_4} \exp(+(k_0 - k_5) t_d) \left[\frac{\exp(-(k_0 - k_5) t_s) - 1}{k_0 - k_5} - \frac{\exp(-(k_4 - k_5) t_s) - 1}{k_4 - k_5} \right]$$

6) $$R_{TM} = \frac{T_3}{M} = \frac{k_3 k_4}{k_0 - k_4} \exp(+k_0 t_d) \left[\frac{k_0 \exp(-k_5 t_s) - k_5 \exp(-k_0 t_s)}{k_0 (k_0 - k_5)} - \frac{k_4 \exp(-k_5 t_s) - k_5 \exp(-k_4 t_s)}{k_4 (k_4 - k_5)} + \frac{1}{k_4} - \frac{1}{k_0} \right]$$

The parameters t_d and t_s are respectively, the time the ion in question is detected and the time the ion leaves the source, both relative to t = 0 at the molecular ion formation. This set of 6 equations in 6 unknowns was solved on the computer by the International Mathematical and Statistical Library routine ZXSSQ, which is a modified Levenberg-Marquardt algorithm for solving simultaneous non-linear equations. Input data are ion abundance ratios obtained from charge-exchange ionization mass spectra to approximate the monoenergetic excitation needed for the equations. The data was taken by J. Turk (Ref. 3) The process was repeated for various energies obtainable by charge exchange to find the rate constants at as many energies as possible.

These equations normally have steep-walled minima in the curve-fitting process for the solutions. When M(obs.) = 0.0, however, an alternate set of equations must be used that are not always so well-behaved, frequently having broad,

shallow minima. Trial-and-error recalculations starting from the output data are then used to refine the fit and get still better output data. The largest remaining uncertainties are in the values of t_d and t_s, which are calculated from the instrumental dimensions and voltages. Experimental values for the parameters, if available, would be better.

III. RESULTS Tables of rate constants at eleven energies for the three compounds studied——2-butanone, 2-pentanone and 2-hexanone——were prepared. Using this data, the mass spectra can be recalculated as a check on the overall accuracy of the data. These were found to have an average error of less than 0.02% from the experimental mass spectra. Plots of ion intensities as a function of time elapsed since molecular ion formation were prepared, as were plots of rate constants as functions of energy. From the latter, some work was done on fitting the data to simple Arrhenius plots. Interestingly, the case of the secondary ion, 71^+, going to the tertiary ion, 29^+, from 2-pentanone, may be fitted to an Arrhenius plot over a range of nearly 4 eV (7 data points) with a coefficient of determination of 0.987. This must imply that the secondary ions are relaxing rapidly upon formation to a single state from which they then subsequently fragment to the tertiary fragment ion.

Rate Constants for 2-hexanone

eV	k_1	k_2	k_3	k_4
10.5	6.08E04	8.75E04	1.95E04	---
10.75	7.55E04	1.34E05	2.80E04	---
11.4	1.54E05	1.86E05	8.35E04	1.28E05
12.4	2.18E05	1.38E05	6.53E04	9.70E04
12.7	5.01E05	1.74E05	7.80E04	2.69E05
13.8	1.10E06	1.43E05	2.48E05	3.08E05
14.0	4.12E05	7.90E04	1.01E05	6.17E05
15.3	1.54E05	2.03E04	1.58E05	4.79E05
15.85	2.38E05	3.34E04	1.60E05	4.45E05
21.6	9.26E05	2.28E05	5.44E05	3.08E05
24.6	2.24E05	6.33E04	1.44E05	2.17E05

where k_1 is rate constant for the 100^+ (molecular ion) going to 43^+; k_2 is 100^+ going to 58^+; and k_3 is 100^+ going to 85^+. k_4 is 85^+ going to 29^+. These values are for t_s = 3.5 microseconds and t_d = 10.0 microseconds.

(With these values for t_d and t_s, the smallest rate constant observed was 6.7E03 for 2-pentanone (58^+ from the molecular ion 86^+) and the largest was 1.92E06 for 2-pentanone (71^+ going to 29^+). Both were observed at 15.3 eV.)

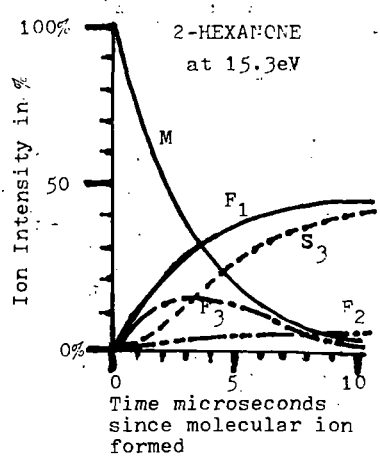

The above figure shows a typical plot of the ion intensities as functions of time at a single energy. From such plots, the amount of ion intensity in the mass spectrum background may be calculated also.

IV. CONCLUSIONS If the fragmentation pathway is known, rate equations which correctly describe the fragmentation can be developed and solved for the rate constants. The resultant data can be analyzed further for correlations.

REFERENCES:
1) L.P. Hills, J.H. Futrell and A.L. Wahrhaftig, J. Chem. Phys., 51, 5255(1969)
2) Wendell Forst, Theory of Unimolecular Reactions, Academic, New York, 1973, especially Chapter 10, pp. 258-343.
3) J. Turk and R.H. Shapiro, Org. Mass Spec., 5, 1373 (1971)
ACKNOWLEDGMENTS:
Hills, Futrell and Wahrhaftig (Ref. 1) for the mathematical inspiration. The Colorado School of Mines and Betty L. Hendricks for the funding. Garon Smith for help with the computer programs and Michael J. Pavelich for discussions of the statistics involved. Gerald R. DePoorter for checking the equations.

REACTIVE COLLISIONS OF HIGH RYDBERG ARGON ATOMS WITH HALOGENATED MOLECULES.

I. DIMICOLI, I. NENNER and R. BOTTER,
CEN/Saclay, D.P.C., B.P. N° 2, 91190 Gif-sur-Yvette (France).

A high Rydberg state (HR) of an atom is characterized by a large value of the principal quantum number n and a longue radiative life time which increases with increasing n and principal angular quantum number l. Collisions of rare gas atoms (A) in HR states at thermal energy with various molecules (XY) have been investigated in a number of laboratories (1). Depending on the nature of the molecule different ionizing processes have been observed : ionization of the HR atom (XY = H_2O, SO_2, NH_3...), associative (C_6F_6, SF_6) and dissociative (CCl_4, CCl_3F, CH_3I) electron attachment, Penning ionization (H_2, CCl_4, CF_4 , CCl_3F) etc...

In the present study, the electron transfer processes in the collision of HR argon atoms with a number of molecules (SF_6, C_6F_6, CCl_4, CCl_3F, CH_3I) have been investigated. The variation of the absolute cross sections as a function of the principal quantum number n and the HR argon velocity in the range 500-2100 m/s have been measured.

A schematic diagram of the apparatus is shown in Fig. 1. A beam of ground state argon atoms obtained with a supersonic molecular beam generator is excited by a magnetically confined electron beam. Only electrically neutral, long-lived excited specied (metastables and HR) are allowed to reach the interaction zone where the beam intersects at right angle an effusive jet of target molecules. This latter zone is situated in the first accelerating region of a coincidence time-of-flight mass spectrometer. The main advantage of our mass spectrometer besides high efficiency, reduced discriminatory effects and good resolution, is the possitility of measuring simultaneously all ionizing channels of the collision and of identifying the two charged collision products of every process. Depending on the polarity of the extracting fields either the positive or the negative collision products are accelerated into the 20 cm long field free region, while the negative or positive species formed in coincidence with them are drawn in the opposite direction and start a time-to-amplitude converter. Every peak of the coincidence mass spectrum corresponds to a different output channel of the collision. When the positive charged products are mass analysed, the starts are given by the respective negative species. Electrons will have a flight time of a few ns between the point of formation and the detector, while the negative ions will reach the detector within $\sim$ 1 µs. Therefore, a positive ion (Ar^+ for example) will appear about 1 µs earlier in the TOF mass spectrum than the same ion produced in coincidence with an e^-. Depending on the life time of the negative ions against autodetachment an electron can be ejected in flight to the detector and additional counts will appear in the region between the two peaks. If an exponential law is assumed for the process of autodetachment, the life times are easely determined from the shape of the curves. A field ionization technique is used to determine the n-dependence of the observed processes. The absolute values of the relative cross sections are obtained by normalization based on absolute cross sections measured by us in a collision chamber experiment.

The principal output channel of the Ar(HR) - XY collision is the associative (C_6F_6, SF_6) and dissociative (CCl_4, CCl_3F, CH_3I) electron attachment. The variation of the cross section as a function of the velocity of Ar(HR) for different n-ranges is given in figures 2 and 3 in the case of SF_6 and CCl_4. Theoretical models view the collisional ionization of the HR atoms as being dominated by the interaction between the essentially free Rydberg electron and the target molecule and the treatment made in terms of the inelastic scattering of free low electrons by these molecules. The velocity dependence of the cross section for dissociative attachment for CCl_4 with $n < 26$ (Fig. 3), typical for reactions with an energy threshold, and the long life time of the SF_6^- ion against autodetachment can not be explained by the simple theoretical model of MATSUZAWA (2). These results indicate that the ion core Ar^+ would play a role in the outcome of the collision and that the interaction between the high Rydberg rare gas core and the target molecule can not be neglected. A model has been proposed by the present authors (3) based on the assumption that the reaction proceeds via the "orbiting controlled" ionic-covalent curve crossing mechanism. At the crossing point between the ionic (A^+, XY^-) and covalent (A, XY) potential surfaces an electron is transferred from A to XY (harpooning) and the new collision partners A^+ and XY^- form, under the influence of the Coulombic force, the complex (A^+ - XY^-). The dissociation of XY^- (case of dissociative attachment) and the autodetachment process (case of SF_6 and C_6F_6) are explained

in terms of the overlapping of the potential surfaces of the molecule XY and its parent negative ion.

REFERENCES.

(1) G.F. HILDEBRANDT, F.G. KELLERT, F.B. DUNNING, K.A. SMITH, and R.F. STEBBINGS, J. Chem. Phys. 68, 1349 (1978) and references therein.

(2) M. MATSUZAWA,
J. Chem. Phys. 55, 2685 (1971)
J. Phys. Soc. Jpn. 32, 1088 (1972)
J. Phys. Soc. Jpn. 33, 1108 (1972)
J. Electron. Spectrosc. Relat. Phenom. 4, 1 (1974)

(3) I. DIMICOLI and R. BOTTER
J. Chim. Phys. (1980) in press.

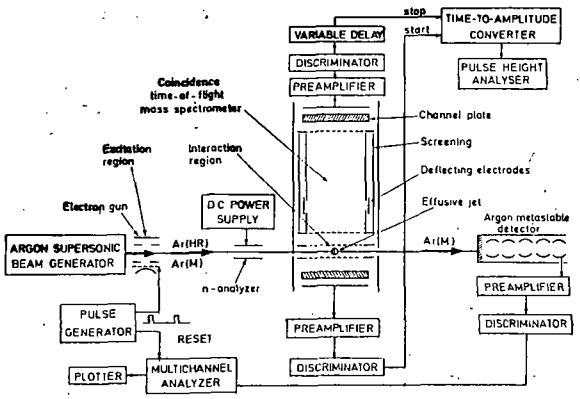

Fig. 1 - Schematic diagram of the apparatus.

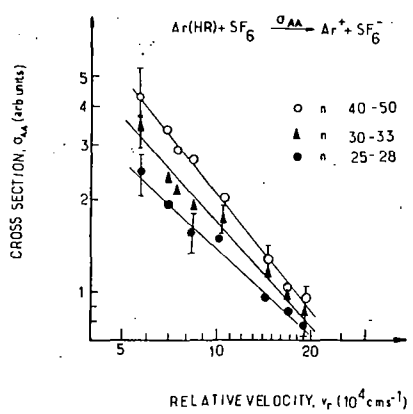

Fig. 2 - Relative cross section for the ion pair formation in the collision of HR argon atoms in the SF_6 as a function of the relative velocity v_r for different n-ranges.

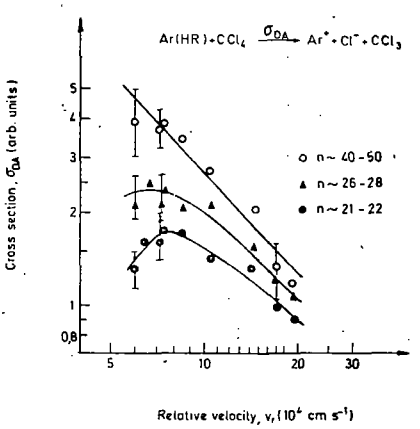

Fig. 3 - Relative cross section for the ion pair formation in the collision of HR argon atoms in the CCl_4 as a function of the relative velocity v_r for different n-ranges.

Charge-Transfer and Collisional Excitation in Kr^+ + Xe Collisions[1]

E. Grant Jones
Department of Chemistry and The Brehm Laboratory
Wright State University, Dayton, Ohio 45435

Recently it has been shown that symmetric ion-atom reactions in the rare gases, Rg, can be very efficient in exciting RgI resonance radiation.[2,3] In Xe, for example, the symmetric reactions excite the 147.0- and 129.6-nm XeI resonance lines and in Kr, the symmetric reactions excite the 123.6- and 116.5-nm KrI resonance lines. Similar excitation has been reported for a few asymmetric collisions in the heavy rare-gases.[4] The instrumentation required for these studies includes a mass spectrometer to prepare the incident ion beam and a 1-m vuv monochromator to monitor the radiation produced during reaction in a collision cell. From 100 eV(lab) collisions of Kr^+ with Xe the emission spectrum shown in Fig. 1 includes both KrI and XeI resonance lines. In this experiment the impacting Kr^+ beam is formed by 25V electron impact and consists of a mixture of ions in the $^2P^0_{3/2}$ and $^2P^0_{1/2}$ states. The pertinent reactions occurring during bimolecular collisions are

$$Kr^+(^2P^0_{3/2,1/2}) + Xe(^1S_0) \rightarrow Kr^* + Xe^+ \qquad (1), \text{ and}$$

$$\rightarrow Kr^+ + Xe^* \qquad (2).$$

Each reaction is endothermic and is driven by the conversion of translational energy of the collision into internal energy. The kinetic energy dependency of the four major lines in Fig. 1 is shown in Fig. 2. Note that each emission process is characterized by a kinetic energy threshold above which, the cross section increases monotonically to 50 eV(c.m.). The cross sections for the processes requiring the least energy conversion, namely those populating the lowest resonance level in Kr, ie $5s[3/2]^0_1$, and Xe, ie $6s[3/2]^0_1$, have the largest magnitude. This finding was also reported for the symmetric reactions and is consistent with that expected for endothermic collision processes. The cross sections shown in Fig. 2 are apparent because of the mixed state of the reacting beam. Since reaction (1) is a charge-transfer process and reaction (2) is collisional excitation, this system can serve as a model to compare possible competition between the two channels. The relative importance of these two channels at different collision energies is shown in Fig. 3. Further experiments have shown significant effects of the J-state preparation of the reactant $Kr^+(^2P_J)$ beam. This study will be published in The Physical Review.

1. Research supported in part by the Air Force Aeropropulsion Laboratory, Air Force Systems Command, Wright-Patterson Air Force Base under Contract No. F33615-77-3141.

2. E. G. Jones, "Excitation of XeI Resonance Lines in Xe^+/Xe Collisions," Phys. Rev. A: in press.

3. E. G. Jones, "Electronic Excitation in Symmetric Ion-Atom Collisions," Proceedings of the Twenty-Seventh Annual Conference on Mass Spectrometry and Allied Topics, Seattle, Washington, June 3-8, 1979.

4. E. G. Jones "Optical Emission From Ion-Atom and Ion-Molecule Interactions," AFAPL-TR-78-99 (AFAPL, Wright-Patterson AFB, December, 1978).

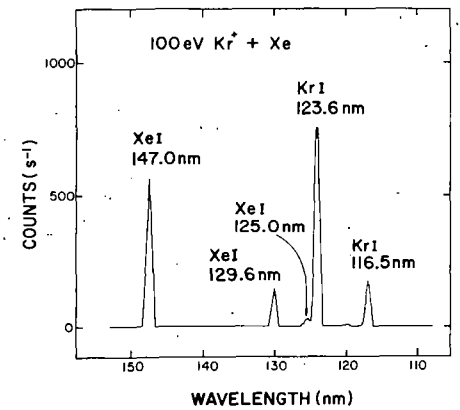

Fig. 1

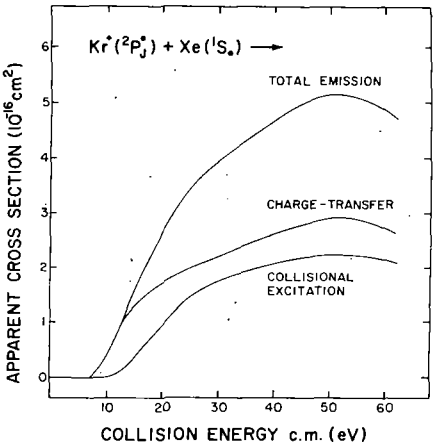

Fig. 3

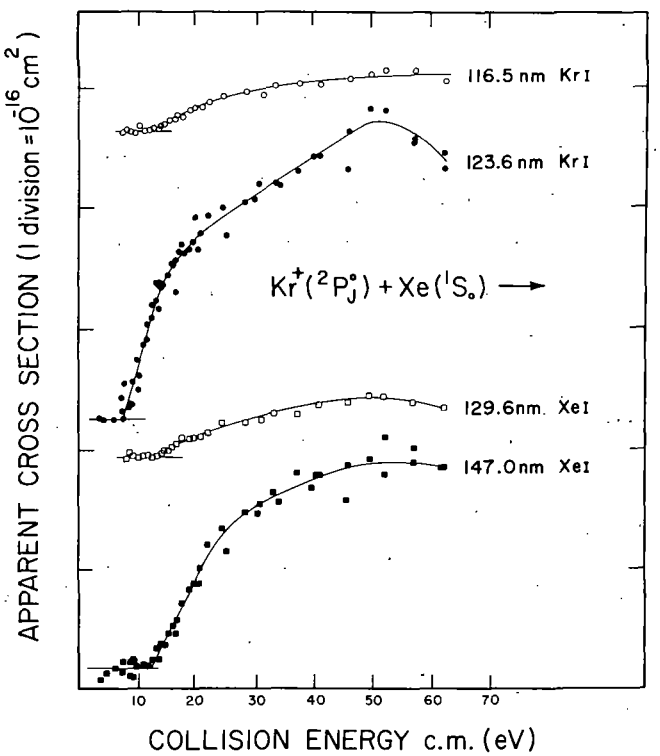

Fig. 2

MAMP13 SENSITIVITY AND LINEAR RANGE COMPARISONS OF ATMOSPHERIC PRESSURE IONIZATION (API) AND CHEMICAL IONIZATION (CI, 1 TORR) MASS SPECTROMETRY SYSTEMS,

D. I. CARROLL, J. G. NOWLIN, R. N. STILLWELL, AND E. C. HORNING, INST. FOR LIPID RESEARCH, BAYLOR COLLEGE OF MEDICINE, HOUSTON, TEXAS 77030.

Ion source equations developed in this laboratory, and by M. W. Siegel of Extranuclear Laboratories, indicate that ionization source pressure should not, within certain limits, be a factor in determining the ionization efficiency of the source. If this is true, the sensitivities of both API and CI systems should be essentially the same.

Measurements of the limiting sensitivity of detection and linear range have been made for a number of compounds using both the API system and a Finnigan 1015 CI system modified for negative ion operation. These data indicate that the limiting sensitivities of detection of the two systems are indeed very similar. The linear range of the API source, using a ^{63}Ni ionization foil, is limited to three or four orders of magnitude. The linear range of a corona discharge API source, however, is similar to that of a CI source.

The ion source equations and experimental data will be presented.

HIGH RESOLUTION NEGATIVE ION CHEMICAL IONIZATION MASS SPECTROMETRY

I. Dzidic, F. Montgomery, D. I. Carroll and E. C. Horning

Institute for Lipid Research, Baylor College of Medicine, Texas Medical Center
Houston, Texas 77030

EXPERIMENTAL

Mass spectra were determined with a CEC 21-110B double focusing instrument, modified for high pressure operation (1)
For the negative ion operation the following modifications have been made:

1. Wires on magnet terminals were reversed.
2. Electric sector cables were exchanged.
3. Hall probe was turned over.
4. John Fluke Mod. 410B power supply replaced acc. voltage.

High resolution mass spectra were recorded on Ilford Q2 silver bromide plates. Marker (sulphur) and sample compounds were introduced simultaneously by direct introduction probe. Methane, SF_6 and N_2O were used as reagent gases.

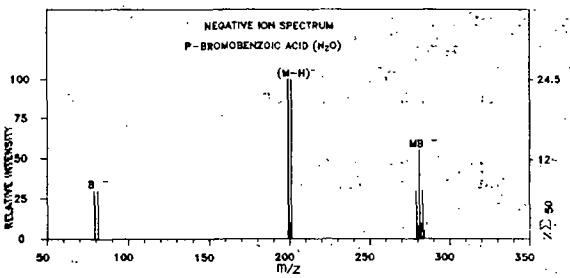

Figure 3

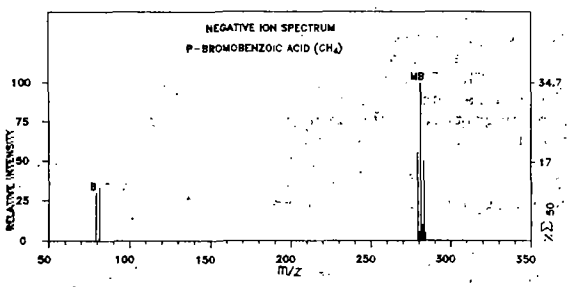

Figure 2

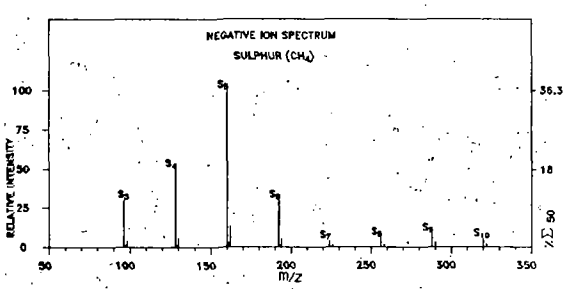

Figure 1

RESULTS

MASS REFERENCE COMPOUNDS

As previously reported (2), sulphur ions are suitable S_n^- (n = 1-10) reference ions at lower masses. Figure 1 shows the sulphur spectrum obtained from direct probe introduction at 180°C, using methane reagent gas.

TABLE 1

HIGH RESOLUTION NEGATIVE ION SPECTRUM OF MIXTURE OF AZULENE, ACENAPHTHYLENE AND FLUORENE

INTENSITY	FOUND MASS	CALCULATED MASS	ERROR mmu	ELEMENTAL COMP.	ION IDENT.
*****	128.0676	128.0626	5	$C_{10}H_8$	M^- (AZULENE)
*****	152.0663	152.0626	4	$C_{12}H_8$	M^- (ACENAPHTHYLENE)
**	165.0773	165.0704	7	$C_{13}H_9$	$(M-H)^-$ Fluorene
****	166.0734	166.0782	5	$C_{13}H_{10}$	M^- Fluorene

METHANE REAGENT, ION SOURCE PRESSUE = 0.5 Torr
REFERENCE STANDARD SULPHUR (S_4^-, S_5^-, S_6^-, S_7^-)

TABLE 2

HIGH RESOLUTION NEGATIVE ION SPECTRUM OF PESTICIDE EPN

INTENSITY	FOUND MASS	CALCULATED MASS	ERROR mmu	ELEMENTAL COMP.
*****	138.0193	138.0191	0.2	$C_6H_4NO_3$
**	153.9845	153.9963	11	$C_6H_4NO_2S$
****	201.0057	201.0139	8	$C_8H_{10}O_2PS$
****	294.0091	293.9990	10	$C_{12}H_9NO_4PS$
***	323.0357	323.0381	2	$C_{14}H_{14}NO_4PS$

METHANE REAGENT, ION SOURCE PRESSURE (0.5 Torr)
REFERENCE STANDARD SULPHUR (S_4^-, S_5^-, S_6^-, S_7^-, S_8^-)

LOW RESOLTUION MASS SPECTRA

Figures 2 and 3 show the low resolution negative ion mass spectra of p-bromobenzoic acid. When methane was used as a reagent gas the Br^- ions are formed by dissociative electron attachment and subsequently the MBr^- are formed through hydrogen bonding to the negative Br^- ions. When N_2O was used as reagent the ion source contained in addition to thermal electrons the negative reagent ions O^-. The proton transfer from p-bromobenzoic acid to O^- ion occurs as illustrated by an appearance of $(M-H)^-$, see Figure 3. The $(M-H)^-$ were absent in the methane reagent as shown in Figure 2.

HIGH RESOLUTION MASS SPECTRA

High resolution negative ion spectra of several compounds are illustrated in Tables 1 and 2. The exact mass measurements have been determined and the accuracy of 0.1-10 mmn was obtained whenever the sample mass was interpolated between reference standards or the ragent ions. When SF_6 and N_2O were used as reagent gases the ionization of sample was accomplished by F^- and O^- ions. The sensitivity and accuracy of the negative high resolution chemical ionization mass determination is similar to that obtained for the positive ion electron impact technique.

1. I. Dzidic et al, Anal. Chem. 43, 1877 (1971)
2. Y. Hirata et al, Org. Mass Spectrom. 9, 913 (1974)

MAMP15 SELECTIVITY OF REAGENT GASES AS USED IN THE ANALYSIS OF FLAVOR MIXTURES. W. A. WOLSTENHOLME, Varian MAT Mass Spectrometry, Florham Park, N.J., USA, and M. HÖHN and U. RAPP, Varian GmbH, Bremen, F.R. Germany

The complexity of natural flavor mixtures is well known. Therefore high performance capillary columns are used predominantly for the separation and identification of the individual components, as well as for the fingerprinting of technical or natural aromas. Besides the Electron Impact Ionization the Chemical Ionization has shown its usefulness as a supplementary soft ionization mode for confirming molecular ion information.

Additionally, with the choice of reagent gases a compound class specific response can be obtained, since different substance classes show distinct responses depending on the gas chosen. This means that switching of reagent gases yields different GC traces, if the substances measured have different response factors. The selectivity of gases is obtained because the proton affinities of the substrates as well as of the reagent gases are different.

To demonstrate the selectivity we used ammonia and isobutane and compared their reconstructed gas chromatogram to the EI generated gas chromatogram. Results will be shown of different flavor mixtures such as arrack and Williams Christ pear samples.

MAMP16 DEHYDRATION OF M+BUTYL COMPLEX IONS OF BENZYL ALCOHOL IN ISOBUTANE CIMS, JOACHIM G. LIEHR, University of Texas Medical School at Houston, Texas, GARETH A. BRENTON, JOHN H. BEYNON, University College of Swansea, U.K., JAMES A. MCCLOSKEY, University of Utah, Salt Lake City, Utah, and WILHELM J. RICHTER, Ciba-Geigy, Basel, Switzerland.

In isobutane CIMS of benzyl alcohol, $(M+57-18)^+$ ions were observed which arise by dehydration of the $(M+C_4H_9)^+$ complex ions. Two possible mechanistic pathways are discussed:

I. Electrophilic aromatic substitution by t-butyl at the ortho-position of the aromatic ring and subsequent elimination of the replaced hydrogen together with the OH group as water.

II. Fast proton transfers are postulated within the cage-like $(M+57)^+$ complex ion resulting in an eventual condensation of the butyl and benzyl species with concomitant loss of water. In this way, substitution at the benzylic carbon would result in formation of a 2-methyl-4-phenyl-2-butyl ion.

Evidence in favor of the latter of the two mechanisms was derived from the isobutane CI spectrum of pentadeuterio-benzyl alcohol which shows the aromatic ring positions remaining unsubstituted. Collision-induced MIKE spectrometry was used to further support the second mechanistic concept. Collision induced MIKE spectra of ion $(M+C_4H_9-H_2O)^+$, m/z 147, generated from benzyl alcohol and of an ion of the same suspected 2-methyl-4-phenyl-2-butyl structure formed by elimination of H_2O from protonated 2-methyl-4-phenyl-butan-2-ol, were nearly identical and thus indicated identical ion structure.

CALIBRATION SUBSTANCES FOR NEGATIVE CHEMICAL IONIZATION MASS SPECTROMETRY, ANDRIES P. BRUINS, Dept. of Pharmacy, State University, A. Deusinglaan 2, 9713 AW Groningen, The Netherlands.

When our Finnigan 3300 quadrupole mass spectrometer is switched to negative chemical ionization operation, the voltages on the source and lens are generally not exactly the inverted values of the voltages that offer good positive ion operation. Furthermore, it may be necessary to reverse the polarity of the DC voltages on the quadrupole rods, in order to improve the peak shape. Finally, the reactant gas mixtures used for positive and negative CI may have a different composition and pressure.

As a result, there exists a difference in mass calibration and mass resolution so that the computer system (Finnigan 6110) has to be recalibrated, and the ratio of the RF and DC voltages on the quadrupole rods has to be readjusted, to restore unit mass resolutio n.

The development of desorption-chemical ionization, which allows spectra to be taken of underivatized nonvolatile materials of high molecular weight (e.g. purpureaglycoside A, MW 926, a glycoside from digitalis[1]) has made the evaluation of the high mass performance in the negative mode mandatory.

A suitable calibration compound:

a. can be introduced at a constant rate over an extended period of time
b. produces at least 10 negative ions of reasonable intensity, evenly spaced throughout the entire mass range (m/z 10 to 999).

The well known calibration compounds for electron impact mass spectrometry: perfluorotributyl amine (FC 43), high boiling PFK and tris(perfluoroheptyl)-s-triazine did not meet both requirements. FC 43 (MW 671) did not show ions above m/z 633 and showed only weak ions below m/z 414. No ions were observed above m/z 800 in the negative CI spectrum of PFK under normal operating conditions. The triazine spectrum was empty between m/z 436 and 641. The negative CI spectrum of PFK was qualitatively similar to the negative ion spectrum (probably taken with an EI source) reported in the literature[2]. A notable difference is the low relative abundance in our instrument of the F^- ion, which is the base peak in the literature spectrum.

Polyperfluoropropylene oxide has been demonstrated to be an excellent reference substance for electron impact mass spectrometry[3]. It appeared that this polyether is equally useful for negative CI. Samples of Fomblin Hivac 25 and Hivac 25/9 vacuum pump oils can be introduced from a solid probe at 120° or 150° C respectively over long periods, and produce negative ions at regular intervals between m/z 85 and 981.

The Finnigan 6110 data system enables the user to create his own special calibration table, containing a maximum of 10 ions. Using either Fomblin oil, this table starts at the Cl^- background ion and terminates with m/z 915. The ions between these extremes are chosen from the most important ions that are presented in the scheme on the next page, together with their composition and structure.

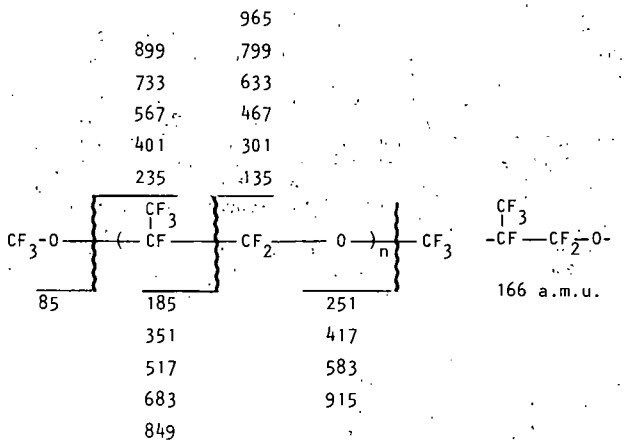

Acknowledgement:

Samples of Fomblin Hivac 25 and Hivac 25/9 were a generous gift from Dr. S.P. Markey.

1. A.P. Bruins, Anal. Chem. 1980, 52, 605-607.
2. R.S. Gohlke and L.H. Thompson, Anal. Chem. 1968, 40, 1004-1005.
3. W.V. Ligon, Anal. Chem. 1978, 50, 1228-1229.

ON THE MECHANISM OF THE RETRO DIELS-ALDER REACTION.

M.-J Bobenrieth, J.R. Hass, L.A. Levy and L. Pruitt,
NIEHS, P.O. Box 12233, Research Triangle Park, NC 27709

Cycloalkenes have been widely reported to undergo an electron impact (EI) induced cycloreversion reaction which usually has been interpreted as a retro Diels-Alder (RDA) process(1). Recent field ionization kinetics (FIK) results for tetralin(2) indicate that the major product ions formed at short times (10^{-10}-10^{-11}s) in the source result from a high energy process in which the proper atoms are lost for a RDA mechanism; in addition, lower energy specific and non-specific losses of C_2H_4 are observed. In a study of labelled 2-cyclohexen-1-ols(3), a 1,3 allylic rearrangement was found to compete with the RDA reaction. In the course of characterizing a series of 5,6,6a,7,12,12a-hexahydrobenz[a]-anthracene derivatives, we observed in addition to the expected RDA products, ions at one dalton less. The kinetic energy release (T) associated with a gas phase fragmentation reaction has been found useful for the characterization of the associated mechanisms. Assuming the (RDA - 1) ions are formed by an initial ring-opening reaction followed by H transfer then final cleavage, comparison of T for this reaction with T for the RDA reaction should allow us to distinguish between a stepwise and a concerted mechanism for the RDA process. In this paper we report the high resolution 70 eV mass spectra of compounds I-V, T for the formation of the RDA and (RDA-1) ions, and the CID-MIKE spectra of the RDA product ions.

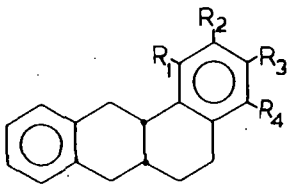

$R_1=R_2=R_3=R_4=H$ (I)
$R_1=R_3=R_4=H$ $R_2=-OCH_3$ (II)
$R_1=R_2=R_4=H$ $R_3=-OCH_3$ (III)
$R_1=R_2=R_3=H$ $R_4=-OCH_3$ (IV)
$R_2=R_3=H$ $R_1=-CH_3$ $R_4=-OCH_3$ (V)

Partial 70 eV mass spectra are shown in Table I.

TABLE I = PARTIAL MASS SPECTRA OF COMPOUNDS I TO V AT 70 eV

Selected Ions m/z	Elemental Composition	% RA[a] In Each Compound				
		I	II	III	IV	V
278 ($M^{+\cdot}$)[b]	$C_{20}H_{22}O$	-	-	-	-	15.92
264 ($M^{+\cdot}$)	$C_{19}H_{20}O$	-	17.10	14.41	13.41	-
234 ($M^{+\cdot}$)	$C_{18}H_{18}$	11.84	-	-	-	-
174 ($B^{+\cdot}$)	$C_{12}H_{14}O$	-	-	-	-	11.53
173 ($[B-H]^+$)	$C_{12}H_{13}O$	-	-	-	-	10.42
160 ($B^{+\cdot}$)	$C_{11}H_{12}O$	-	13.02	3.70	3.76	-
159 ($[B-H]^+$)	$C_{11}H_{11}O$	-	8.03	9.68	9.57	-
130 ($B^{+\cdot}$)	$C_{10}H_{10}$	2.67	-	-	-	-
129 ($[B-H]^+$)	$C_{10}H_9$	9.52	-	-	-	-
104 ($A^{+\cdot}$)	C_8H_8	28.02	8.57	17.75	18.24	6.97
103 ($[A-H]^+$)	C_8H_7	2.04	1.18	1.43	1.45	0.97

[a]The abundance of each ion is relative to the sum of all the ions and has been corrected for ^{13}C contribution.

[b]$M^{+\cdot}$ = Molecular Ion; $A^{+\cdot}$ and $B^{+\cdot}$ = Ions formed by the retro Diels-Alder Reaction.

The major fragments are the RDA ions at m/z 104 ($C_8H_8^{+\cdot}=A^{+\cdot}$), the complementary RDA ion ($=B^{+\cdot}$) and the $[B-1]^+$ ion.

Kinetic energy release measurements for the $M^{+\cdot}\rightarrow A^{+\cdot}+B$ and $M^{+\cdot}\rightarrow[B-H]^+ + [A,H]^\cdot$ (Table II) are all in the range 25-60 meV with no significant difference between the two fragmentations.

TABLE II = KINETIC ENERGY RELEASE (T) MEASUREMENTS

$T_2^{a,b}$ 10^{-3} eV	Reaction Studied $M^{+\cdot}\rightarrow[B-H]^+ + [A,H]^\cdot$ (2)	Compounds	Reaction Studied $M^{+\cdot}\rightarrow A^{+\cdot}+B$ (1)	$T_1^{a,b}$ 10^{-3} eV
37.1 ± 1.1	234 → 129	I	234 → 104	28.0 ± 7.3
44.4 ± 4.6	264 → 159	II	264 → 104	40.1 ± 6.8
37.2 ± 3.3	264 → 159	III	264 → 104	41.3 ± 3.8
34.7 ± 3.8	264 → 159	IV	264 → 104	36.5 ± 5.9
38.3 ± 4.2	278 → 173	V	278 → 104	59.2 ± 1.7

[a]Average of 4 determinations.

[b]Widths measured at 50% peak height and corrected for main beam width.

Thus these measurements indicate the RDA reaction to be stepwise. The CID-MIKE spectra of compounds I-V could not be distinguished from one another or the styrene molecular ion (reported to have the same structure as cyclo-octatetraene molecular ion(4)). However, the C_8H_8 ion generated from 1,3-dihydrobenz[c]thiophene-S-oxide gave an m/z 51 ion of 42% intensity relative to the most intense purely collision-induced ion at m/z 102 compared to the range of 18-25% for the others and an m/z 62 ion of 12% compared to the range of 5-7% for the others. Several other ions from the thiophene derivative were outside the range of intensities of I-V. Therefore, the C_8H_8 ions are unlikely to have the structure predicted by a concerted RDA reaction.

In conclusion, the retro Diels-Alder reaction for these compounds is not a concerted process. Rather, it seems likely that initial ring opening at an aliphatic ring junction is followed by carbon skeletal rearrangements and their cleavage at the second ring junction to give the observed C_8H_8 ions.

REFERENCES

1. F. Turecek and V. Hanus, Org. Mass Spectrom., 1, 4 (1980).
2. K. Levsen and F. Borchers, R. Stolze and H. Budzikiewicz, Org. Mass Spectrom., 9, 510 (1978).
3. D. Braem, F.O. Gulaçar, U. Burger and A. Buchs, Org. Mass Spectrom., 11, 609 (1979).
4. D. Smith, T. Baer, G.D. Willett and R.C. Ormerod, Int. J. Mass Spectrom. Ion Phys., 30, 155 (1979).

The Electron Impact Induced Fragmentation of Vinylidene Carbonates.

R.T. Aplin, G.P. Cottam, Dyson Perrins Laboratory, Oxford University, M.C. Grossel, Dept., of Chemistry, Bedford College, Univ., of London, U.K.

The principle mode of fragmentation of the molecular-ion of the vinylidene carbonates (I-III) derived from the corresponding benzoins is a "one step" loss of the elements of CO_2 plus CO, as is demonstrated by the presence of a broad metastable peak for the loss of 72 daltons in their normal electron impact mass spectra.

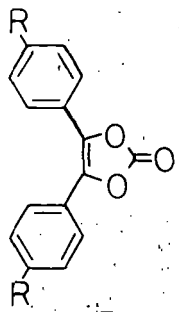

I R = H; II R=Me; III R=OMe

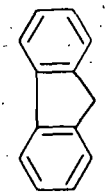

IV

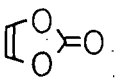

V

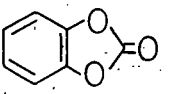

VI

Linked B/E scans[1] confirm that this fragmentation represents the major mode of breakdown of the molecular-ion. A second, very minor process was the loss of CO. This M-CO $^{+\bullet}$ ion is not apparent in the normal plotted spectrum (< 1%) but is the precursor of the relatively abundant Ar CO^+ ions.

The M - 72 $^{+\bullet}$ ion $C_{13}H_{10}$ for (I) has essentially one mode of fragmentation, the loss of $H^\bullet$, a process reminiscent of the behaviour of the molecular-ion of fluorene (IV, $C_{13}H_{10}$). Examination of the fragmentation of these two $C_{13}H_{10}$ $]^{+\bullet}$ species (B/E scans)[1] and the energy release (MIKES)[1] accompanying the loss of $H^\bullet$ showed identical behaviour for both (I and IV) indicating that the M-72 species derived from (I) has the same structure as the molecular-ion of fluorene. The loss of (CO_2 + CO) and the loss of $H^\bullet$ from [M-(CO_2 + CO)] varies linearly with the Hammett σ^+ value for the substituent. Neither vinylidene carbonate (V) nor cataechol carbonate (VI) exhibit the one step loss of (CO_2 + CO).

A facile pathway for the rearrangement of the vinylidene carbonates (I-III) to a fluorene structure is the conrotatory cyclisation to a dihydrophenanthrene (a), the process involved in the photo synthesis of phenanthrenes from (I-III).[2,3] Isomerisation to a 9, 10-dihydrophenanthrene would then allow the observed loss of $CO + CO_2$ (Scheme a - e). This initial rearrangements is comparable to the behaviour of hexahelicene[4] and cis and trans stilbine[5] on electron impact and provides further illustration of the similarities between electron impact and photo induced excited states.

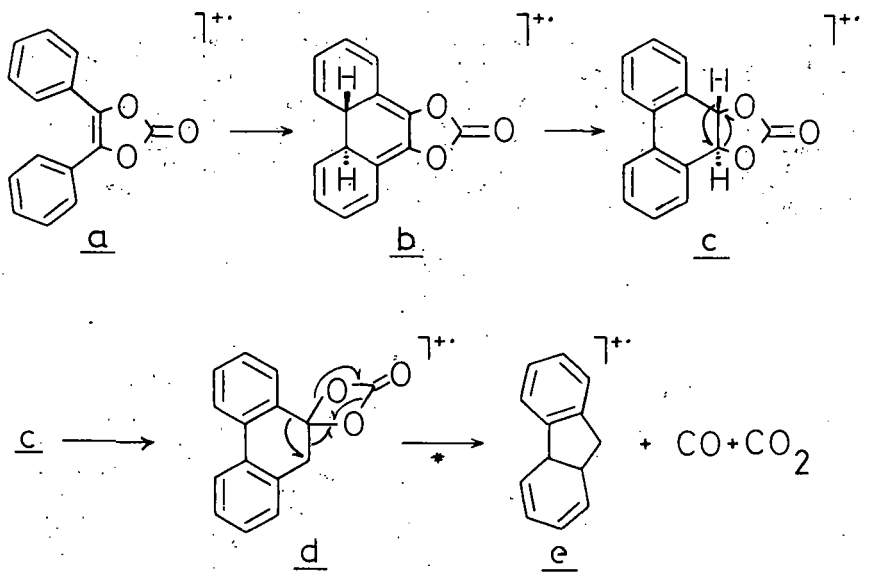

References

1. B/E and MIKES studies were carried out on a V. G. Micromass ZAB-IF.
2. I. Santos, Tet.Lett., 1978, 2716.
3. G.P. Cottam, Pt. II Thesis, Oxford 1980.
4. R. C. Dougherty, J.Amer.Chem.Soc., 1968, 90, 5788.
5. P.F. Donaghue, P.Y. White, J.H. Bowie, B.D. Roney and H. J. Rodd. Org. Mass. Spectrom., 1966, 2, 1061.

ESTIMATION OF FACTORS FOR CORRECTING ION GAUGE PRESSURE TO TRUE PRESSURE.

J.E. Bartmess, R. Georgiadis, and G.W. Caldwell, Dept. of Chemistry, Indiana University, Bloomington IN 47405

Ionization gauges do not read true pressure, but rather a effective pressure based on an average ionization cross section σ for a given compound over the energy range used (typically 150V). We have measured values of σ, as in Eqn. (1)

$$P_{true} = \frac{P_{IG}}{\sigma} \qquad (1)$$

for a variety of compounds using a Bayard-Alpert gauge (Huntington Mechanical Labs) with a Granville-Phillips controller vs. an MKS Baratron Type 146 capacitance manometer as the true pressure measuring device. For the 48 compounds studied σ is fairly well correlated ($r = .983$) with α, the polarizability in $Å^3$ and I_e, the emission current of the ion gauge in mA (typically 10 mA) as given in Eqn. (2). The worst case deviation is 30%.

$$\sigma = 0.029\ I_e(\alpha + 1) \qquad (2)$$

This correlation with polarizability (as in J.A. Beran and L. Kevan, J. Phys. Chem. (1969) 73, 3866) provides a better fit to the data than does that of J.W. Otvos and D.P. Stevenson (J. Am. Chem. Soc. (1956) 78, 546) based on number and radius of electrons. There is functional group dependent within Eqn. (2), however, with aromatics and ethers high, and nitroalkanes low. Chlorocarbons, ketones, alcohols, and thiols fit the equation to better than 5% deviation. Further studies of more functional groups and homologous series are in progress to refine the correlation.

A TANDEM MASS SPECTROMETER FOR COLLISION-INDUCED DISSOCIATION WITH SIMULTANEOUS DETECTION AND VARIABLE DISPERSION,

A.J.H. Boerboom, G.J. Louter and J. Haverkamp,

FOM-Institute for Atomic and Molecular Physics, Amsterdam, The Netherlands

Structural analysis of organic ions by means of collision-induced dissociation (CID) is a new technique in mass spectrometry. Experiments have been set up with a double-focusing mass spectrometer usually provided with a collision gas cell, as well as with a triple quadrupole mass spectrometer. Both instruments are double-discriminating instruments, i.e. from the ions emerging from the source only ions of one single mass are selected and in a subsequent stage the CID-spectrum of these ions is scanned. This does not only imply a considerable loss of ions, but also investiations on very fast processes in the ion source, like flash-pyrolysis or laser induced desorption, are impossible.

We designed a novel type of tandem mass spectrometer. Its main features are: 1. simultaneous detection of the mass spectrum, 2. post-acceleration of the fragment ions and 3. variable dispersion.

The first stage is a conventional magnetic sector type mass spectrometer ($R = 150$ mm, 50°). At the site of the detector slit a collision gas cell is situated. The fragment ions, leaving the exit slit of the collision cell, are post-accelerated up to 30 kV in order to reduce the relative energy spread, due to the dissociation energy. In this way both the resolution and the transmission are increased. The fragment spectrum is analysed by a second magnet (main radius = 750 mm, 15°). This makes possible the simultaneous detection of a large part of the spectrum. Quadrupole lenses are incorporated in the second stage in order to vary the dispersion, but also for rotation of the focal plane and improvement of the transmission. The ions are detected with a CEMA (Channeltron Electron Multiplier Array) and the signal is transported by light-optical means to a photo-diode array for further computer processing.

The ratio of the highest and lowest masses in a simultaneously detected spectrum may vary from 4 : 1 to 1.06 : 1. The resolution can be up to 600, the transmission from the collision cell to the CEMA ranges from 60-100%, the detection sensitivity can be as high as 1 ion per 10 seconds. As an application of this instrument the structure of the $m/z = 59$ compound in the pyrolysis products of Mycobacterium cell will be discussed.

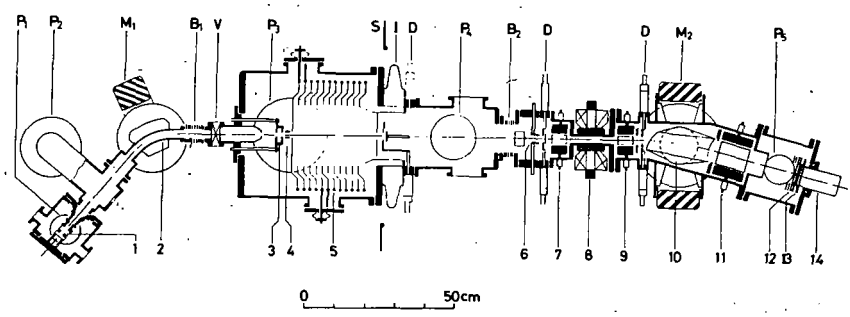

Fig. 1 - Top view of the apparatus. 1 - ion source, 2 - selection magnet, 3 - collision cell, 5 - post-acceleration section, 7,9,11 - electrical quadrupole lenses, 8 - magnetic quadrupole lens, 10 - analysing magnet, 12 - CEMA, 13 - phosphor screen, 14 - fiber optics.

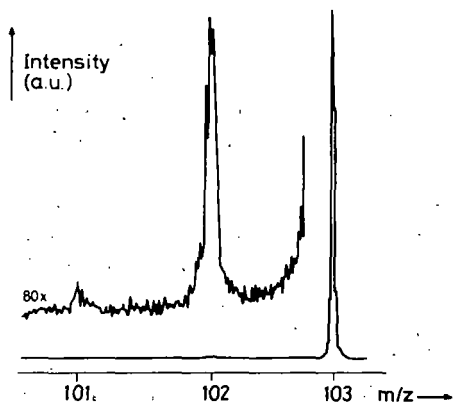

Fig. 2 - Ion optical close-up of precursor M = 103 and fragments M - 1 and M - 2 of benzonitril. Total measuring time 12 sec. Peak m/z = 101 has been formed by about 2 ions per second. The CID resolution for peak 103 is better than 1000.

QUADRUPOLE AND ELECTROSTATIC COLLISION CELLS FOR QUADRUPOLE MS/MS INSTRUMENTATION

Charles A. Boitnott, Urs Steiner
and
Michael S. Story

Finnigan Corporation
845 W. Maude Ave.
Sunnyvale, CA 94086

A quadrupole operated only with radio frequency voltage in a collision cell has been shown to have higher efficiencies than those reported for electrostatic collision cells. The purpose of this work is to show a direct comparison of the two cells in conjunction with the same quadrupole mass analyzers. Identical experiments were performed on a system configured in the triple quadrupole mode and then in the double quadrupole mode. A comparison is made of the processes of dissociation and scattering in the two modes of operation.

Interactions within the collision cell can be described utilizing a Lambert Beer expression for each interaction occurring. Each collisional process has a unique cross section for the hardware configuration of the instrument. An integration of the equations of all of the pertinent reactions with the appropriate cross sections can predict the pressure dependent fragmentation spectra of the considered ion. Similarly, cross sections for reactions can be determined from experimental data.

The collision cell pressure dependency on daughter ion intensity depends on dissociation of the principal ion and upon scattering of the principal and daughter ions. Two collision generation and further dissociation of daughter ions is also observed. For the single step dissociation, the low pressure dependency is dominated by scattering. An intermediate maximum is observed, the magnitude determined by the relative dependency of the two processes. The two step process is different in that the initial slope of the pressure dependency is zero and the maximum intensity occurs at higher pressure where scattering is a more dominate process.

Experiments were performed to compare a collision cell containing an rf only quadrupole and an electrostatic collision cell. Cell lengths were 14 cm and 0.635 cm. The compounds observed were xenon, cyclohexanone, FC43 and cyclohexane. Cross sections were determined for dissociation and scattering for the two cells and their relative magnitude considered as a measure of the relative performance. The quadrupole collision cell gave better performance in all cases than the electrostatic cell.

This improvement is primarily due to the focusing effect of the quadrupole. For scattering the improvement ratio is 2.2 for xenon, 8.7 for cyclohexanone, 8.9 for cyclohexane and 35 for FC43. Daughter ion generation were also stronger by a factor of 5 to 15 with the quadrupole chamber. As the maximum daughter signal depends on both of these processes, larger improvements were observed here with ratios of 19 to 25 being measured.

DESIGN AND APPLICATIONS OF A NEW TRIPLE ANALYZER MASS SPECTROMETER

M. L. Gross, P. A. Lyon, and F. W. Crow
Department of Chemistry
University of Nebraska
Lincoln, Nebraska 68588

and

S. Evans
Kratos, Ltd., Barton Dock Road
Urmston, Manchester
M31 2LD
United Kingdom

As part of the National Science Foundation Regional Instrumentation Facility for Mass Spectrometry at the University of Nebraska, a triple analyzer mass spectrometer has been designed, constructed and installed at the University of Nebraska. The principal analytical chemistry purpose of this instrument is for high performance mass spectrometry/mass spectrometry development and applications. A schematic drawing of the spectrometer is shown on the following figure.

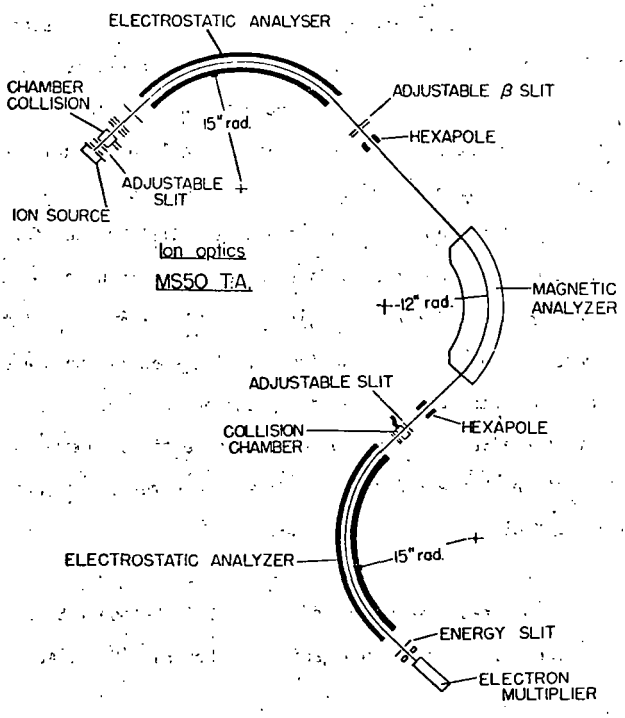

Using the spectrometer, unimolecular or collisionally activated decompositions can be studied in both the first and third field-free regions of the instrument. Investigations in the first field-free region will make use of linked B/E or $V^{1/2}/E$ scans or accelerating voltage scans. However, the unique feature of the spectrometer is the capability to select ion beams at high resolution and observe their decompositions in the third field-free region. Both unimolecular or collisionally activated processes have been investigated. The ultimate resolution of ESA I and the magnet is greater than 100,000 (static mode, 10% Valley definition), and collisional spectra have been taken at a main beam mass resolution of 25,000 (10% Valley) without the aid of signal averaging.

To evaluate the sensitivity of the instrument in an MS/MS mode, the m/z 322 ion of tetrachlorodibenzo-p-dioxin (TCDD) was selected at a resolution of about 2000. A full CA spectrum could be observed for 500 picograms of the TCDD. Based on this result, we project that low picogram quantities of materials can be quantitated in the MS/MS mode using selected fragmentation monitoring techniques. Accordingly, the technique may be an alternative to HPLC/MS.

In addition to the third analyzer and two collision cells, the spectrometer is equipped with the following ionization sources: electron impact, low voltage EI, chemical ionization and field ionization/field desorption. The magnet is an extended range magnet (up to 1750 amu at 8kV of acceleration) capable of scanning at rates of 0.7 sec/decade. All fields can be reversed for studies of negative ions.

In addition to analytical applications, the system will be used for fundamental studies of the structures and properties of gas-phase ions. We have demonstrated that "pure" CA spectra can be obtained for $[C_8H_8O_2]^{+\cdot}$ and $[C_9H_{12}O]^{+\cdot}$ at a resolution just sufficient to separate (10% Valley) the two isobaric ion signals (both are at m/z 136). No scattering of one beam into the focused beam could be detected.

The instrument is available for use within the scientific community of the United States. The authors at the Midwest Center for Mass Spectrometry, University of Nebraska, should be contacted.

Acknowledgement: This work has been supported by the U.S. National Science Foundation, Regional Instrumentation Facilities Program (Grant No. CHE78-18572).

Is There a Better Geometry Than the Quadrupole? M. H. Friedman[1], J. E. Campana[2], A. L. Yergey[3], and L. Kelner[3]. 1) US Army, MERADCOM Fort Belvoir, VA 22060. 2) US Naval Research Laboratory, Washington, DC 20375. 3) National Institutes of Health, Bethesda, MD 20205.

Introduction. Although research impetus on mass filters has been confined primarily to the quadrupole, the monopole, the three-dimensional quadrupole and approximations to these three, it is possible that other geometries would result in mass filters with improved resolution-transmission characteristics. The motive for this work is to find a mass filter geometry with better resolution-transmission characteristics or to show that other such geometries are not useful.

Results. Define functions $U_n(x,y)$ and $V_n(x,y)$ by:

$$z^n = (x + iy)^n = U_n(x,y) + iV_n(x,y). \tag{1}$$

Since z^n is an analytic function, it is known that the function $U_n(x,y)$ so defined satisfies Laplace's equation:

$$\nabla^2 U_n(x,y) = 0. \tag{2}$$

For any given value of ϕ_o the equations

$$U_n(x,y) = \phi_o/2 \tag{3a}$$

$$U_n(x,y) = -\phi_o/2 \tag{3b}$$

define a locus of points in the (x,y) plane. Electrodes, infinitely long in the z direction, are shaped to coincide with the locus defined by equations (3a) and (3b) and the separation between opposite electrodes is chosen to be $2r_o$. The geometries so defined for n = 1, ..., 5 are termed dipole, quadrupole, hexapole, octupole, and decapole geometries. For n = 2 the geometry so defined corresponds with the usual quadrupole geometry. In typical mass filter operation the potential ϕ_o has both AC and DC components:

$$\phi_o = \phi_{DC} - \phi_{AC} \cos \omega t . \tag{4}$$

The potential $\phi(x,y)$ in the region enclosed by the electrodes satisfy Laplace's equation (2) and the boundary conditions (3a) and (3b). With the electrodes so configured $\phi(x,y)$ is given by,

$$\phi(x,y) = K_n U_n(x,y), \tag{5}$$

where the constant K_n is easily found from the requirement that ϕ (x,y) match the voltages at the electrode surfaces. Knowing ϕ (x,y), the differential equation for the ion motion is found from Newton's Law:

$$F = m \frac{d^2 r}{dt^2} = -e \nabla \phi(x,y) \quad . \tag{6}$$

Since the electrodes are assumed to be infinitely long in the z direction the differential equation describing ion motion in the z direction is for all n:

$$m \frac{d^2 z}{dt^2} = 0 \quad . \tag{7}$$

Using equations (3) (4) and (5) equation (6), which describes the differential equation for ion motion, becomes for the quadrupole geometry (n = 2):

$$m \frac{d^2 x}{dt^2} + \frac{e}{r_o^2} (\phi_{DC} - \phi_{AC} \cos \omega t) x = 0 \tag{8a}$$

$$m \frac{d^2 y}{dt^2} - \frac{e}{r_o^2} (\phi_{DC} - \phi_{AC} \cos \omega t) y = 0. \tag{8b}$$

Equations (8a) and (8b) agree with well known results. In this paper the differential equations are found for n=1,2,3,4 and 5 which are generalizations of the quadrupole geometry. The differential equation of ion motion for the hexapole geometry (n = 3) is:

$$m \frac{d^2 x}{dt^2} + \frac{3}{2} \frac{e}{r_o^3} (\phi_{DC} - \phi_{AC} \omega t) (x^2 - y^2) = 0 \tag{9a}$$

$$m \frac{d^2 y}{dt^2} - \frac{3e}{3 r_o} (\phi_{DC} - \phi_{AC} \cos \omega t) (xy) = 0 \quad . \tag{9b}$$

Space limitations do not allow the results for n=1, 4 and 5 to be presented here. They will be given in a more complete subsequent publication.

Conclusion. Now that the differential equations of motion are known for the geometries associated with n = 1, 2, 3, 4 and 5 the transmission-resolution characteristics associated with these different geometries can be investigated by computer-simulation and compared with the widely used quadrupole (n=2) geometry.

EFFECT OF CONTINUOUSLY VARYING r_o IN A QUADRUPOLE MASS SPECTROMETER,

JULIETTE W. IOUP,* Physics/Pre-Engineering Department, Xavier University, New Orleans, LA, 70125, GEORGE M. WOOD, JR., NASA Langley Research Center, Hampton, VA, 23665, and MOSTOFA MOSHARRAFA, Cardiac Pacemakers, Inc., Minneapolis, MS, 55420

The differential equations of motion in cylindrical coordinates for an ion passing through a quadrupole were solved numerically using a fourth-order Runge-Kutta method based on Fehlberg's formulas. The computer code determines the position and velocity at the exit or the point of impact with the quadrupole rods for each ion. The position, velocity, and phase of the incident ions were varied to simulate an ion beam entering the quadrupole, and transmission curves calculated. A proposed configuration to minimize the effect of the fringing fields at the entrance was examined using the program. In this model, boundary conditions corresponding to different pole separations at the entrance and exit were specified so that the pole pieces would be aligned in a conical geometry with the entrance larger than the exit. Transmission peaks were calculated for ions entering in an annular ring with the ring axis parallel to the quadrupole axis, a 20 pi trajectory, and quadrupole resolutions of 100, 250, and 500. The ratio of quadrupole entrance/exit radius was varied between 1.00 (no tilting of the pole pieces) and 1.10 (separation of the pole pieces 10% larger at the entrance than at the exit). In general, the transmission peaks were shifted toward larger q values for the larger ratios.

A representative group of transmission peaks is shown in the figure. The incident r/r_o for entering ions was specified to be between 0.4 and 0.6, and the resolution was chosen to be 100. A peak was calculated for quadrupole entrance/exit radius ratios of 1.00, 1.01, 1.02, 1.05, and 1.10. The transmission peaks are shifted toward the larger q value and the peak heights increase slightly for the larger entrance/exit ratio. The full width at half maximum remains roughly constant or increases slightly for the larger entrance/exit ratio. A similar description can be given for the transmission peaks calculated for resolutions.

*Supported in part by NASA Research Grants NSG-1361 and NAG 1-16.

20 π TRAJECTORY
RESOLUTION = 100
$0.4 \leq r/r_o \leq 0.6$

CURVE	ENTRANCE/EXIT RADIUS
A	1.00
B	1.01
C	1.02
D	1.05
E	1.10

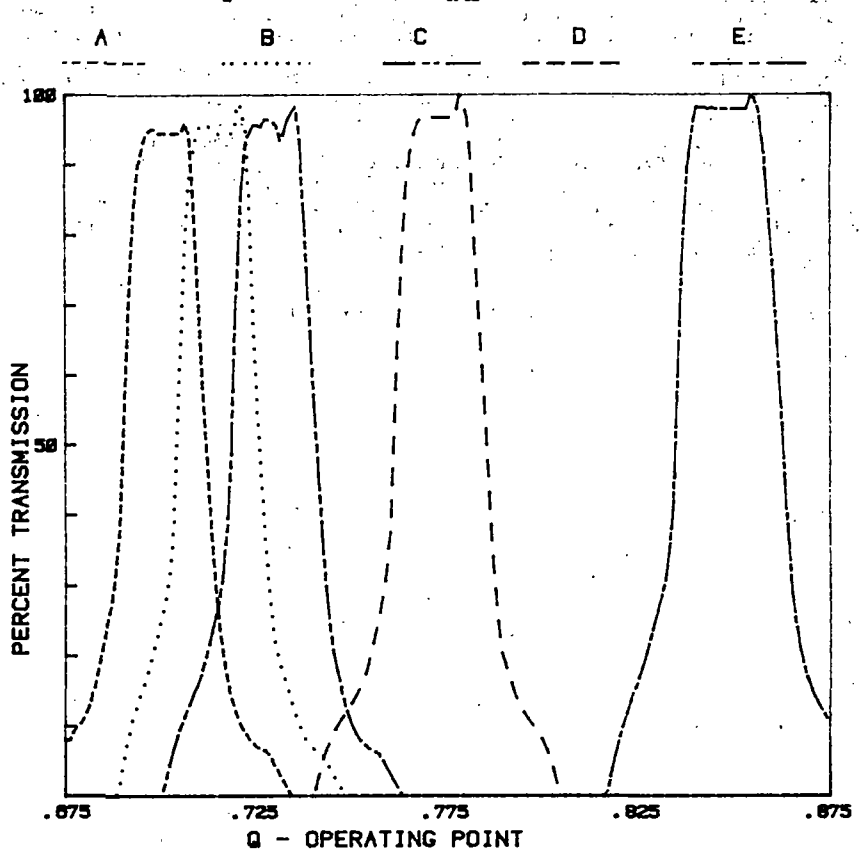

THE ION OPTICS OF A SPLIT-POLE MASS SPECTROMETER*

C. R. Lagergren
Pacific Northwest Laboratory**, Richland, WA 99352

A need arose in our laboratory for a mass spectrometer capable of measuring ion currents corresponding to a broad range of masses simultaneously and in real time. An instrument having its ion image surface located in relatively field-free space and reasonably well removed from magnet pole pieces was required in order to minimize the constraints on the development of a multi-channel ion detection system. Since the ion-optical features of the split-pole magnetic spectrograph introduced by Spencer and Enge[1] for precision nuclear spectroscopy would meet our needs, we decided to design and construct a mass spectrometer with a split-pole magnet.

The split-pole magnet was designed from ion optical calculations based on a first order transfer matrix method. In these calculations the magnetic field was assumed to be constant and equal within pole boundaries, zero in regions of the ion source and the image plane and equal to some small fraction of the pole field in the space between the split poles. The mass spectrometer layout as well as the magnet dimensions are shown in the first figure. Ions approach the first sector at a 45° angle and emerge from the second sector at approximately -25° for a total deflection angle (Φ) nearly a constant 110° for all masses.

After construction of the magnet the actual magnetic field in the mid-plane was mapped and emperical field functions were fitted to the measurement data. The functions were then used in calculating ion trajectories on a large digital computer by a Runge-Kutta method for the solution of the differential equations of motion. The final design and ion optical characteristics of the mass spectrometer were determined from these calculations. The remaining figures show the mass dispersion (D), the radial magnification (M_r) and the second-order abberation coefficient (C_2) for a particular case of magnet adjustment in which the entrance angle is 43.4°. For an ion source width (W_o) of 0.03 cm and a maximum initial divergence angle of $\pm 1^{\circ}$ the image line width (W_i) and corresponding resolving power (R) are also shown.

---

* This paper is based on work sponsored by the Division of Chemical Sciences and performed under U.S. Department of Energy Contract EY-76-C-06-1830.

** Operated by Battelle Memorial Institute for the Department of Energy.

1 J. E. Spencer and H. A. Enge, Nucl. Instr. and Meth. 49 (1967) 181.

MASS SPECTROMETER LAYOUT

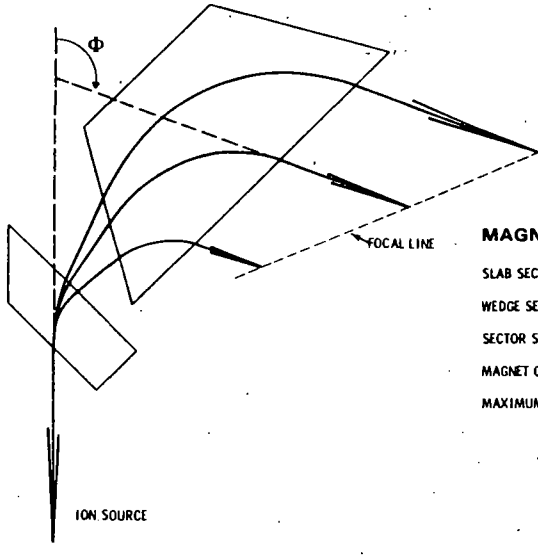

MAGNET DIMENSIONS

SLAB SECTOR THICKNESS	3.876 cm
WEDGE SECTOR ANGLE	59.57°
SECTOR SEPARATION	1.819 cm
MAGNET GAP	0.953 cm
MAXIMUM RADIUS OF CURVATURE	15.240 cm

DEFINITION OF ION OPTICAL TERMS

- DISPLACEMENT OF A MONOENERGETIC POINT SOURCE (Δd_i)

$$\Delta d_i = M_R \Delta X_o + D \frac{\Delta M}{M} + C_2 \alpha_o^2$$

- LINE WIDTH (W_i) ALONG FOCAL PLANE

$$W_i = \left|M_R W_o\right| + \left|C_2 \alpha_o^2\right|$$

- MASS RESOLVING POWER (R)

$$R = \frac{M}{\Delta M} = \frac{D}{W_i}$$

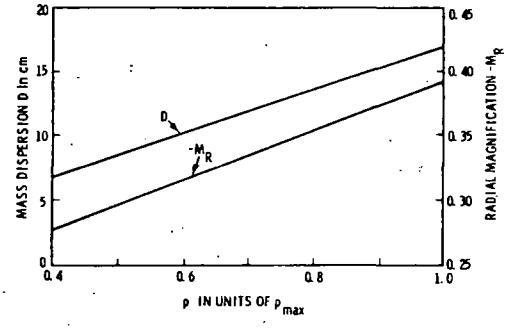

SECOND-ORDER ABBERATION COEFFICIENT

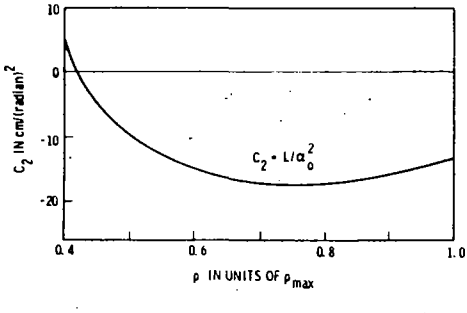

LINE WIDTH W_i AND RESOLVING POWER R FOR W_o = 0.03 cm AND $\alpha_o = \pm 1°$

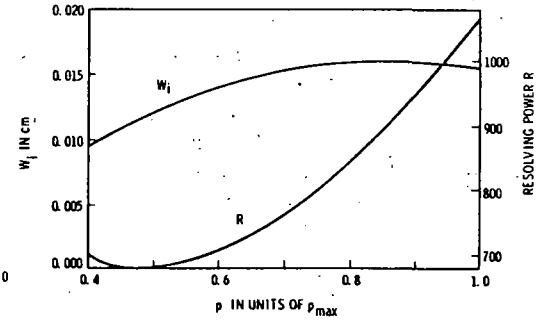

QUANTITATION OF MASS SPECTRAL DATA FROM AN ELECTRO-OPTICAL ION DETECTOR

C.E. GIFFIN, R.A. BRITTEN, AND R.A. JOHANSEN
Caltech Jet Propulsion Laboratory, Pasadena, Ca. 91003

For several years a mass spectrograph system has been under development at JPL that uses a unique electro-optical ion detector (EOID).[1,2] The basic MS is a CEC 21-110B mass spectrograph with a 356 mm focal plane. The EOID replaces the usual photoplate and comprises a string of fourteen two dimensional microchannel electron multiplier arrays (MCAs), a phosphor coated fiber optic vacuum window, fourteen fiber optic spectral image rotators, and fourteen 1024 element photodiode arrays (PDAs). Ultra high sensitivity ($\sim 1 \times 10^{-15}$ g) is achieved through the conversion of ions to electrons to photons such that a single ion arriving at the focal plane can be detected with a signal-to-noise ratio of 5. In addition, spectral integration times of 143 ms to 32 s are routinely used.

Because the EOID is made up of discrete elements (14 MCAs, 14 fiber optic rotators comprised of 42 multifiber bundles each, and 14,336 individual photodiode detectors) there exists a strong requirement for precise calibration of the EOID if quantitative data is to be extracted from the mass spectrograph system. This requirement is forced by the inability to achieve uniform MCA gain, uniform fiber optic light transmission, and uniform photodiode characteristics (responsivity, dark current, fixed pattern noise, offset) over the entire focal plane.

A microprocessor based system has been constructed which will perform a realtime end-to-end decalibration of the MS/EOID output on a diode-by-diode basis as each integrated spectrum is read out to the computer. The readout cycle time is approximately 10 μs per diode (143 ms for the entire focal plane) thus requiring a number of computations to be performed in significantly less than this time. A block diagram of the system is shown in Figure 1.

The basic equation that needs to be solved is:

$$R_x = \underbrace{\alpha_x S_x t_s}_{\text{Signal Contribution}} + \underbrace{\beta_x t_d}_{\text{Dark Current Contribution}} + \underbrace{b_x}_{\text{Offset}} \qquad (1)$$

where

x	= Diode number (x = 1 to 14,336)	t_s	= Signal integration time
R_x	= PDA output signal	β_x	= Rate of dark current buildup
α_x	= Responsivity to signal for diode x	t_d	= Dark current integration time
S_x	= Signal strength	b_x	= Fixed pattern offset

Equation (1) can be rewritten:

$$S_x = (R_x - b_x - \beta_x t_d)(\alpha_x t_s)^{-1} \qquad (2)$$

assuming linear dark current buildup per unit time and linear response of photodiodes to input signal strength.

In the above equations, b_x and β_x are determined by taking two background scans at two different dark current integrations t_d. The extrapolation of the data to $t = 0$ yields b_x and the slope of $R_x(t)$ defines β_x. α_x is determined by "sliding" mass peaks along the focal plane (by varying the analyzer magnetic field) and noting the peak height variation. The α_x value is scaled arbitrarily to translate the system output to the desired full-scale level.

A number of different operating modes of the MS/EOID are possible depending on the characteristics of the experiment being performed as well as the desired format of the data. These various modes allow for feedback control of ion beam shuttering, variations in integration time (by powers of 2), time-centering of spectral data, normalizing of spectral data, etc. Depending on the desired mode, Equation (2) will assume different forms. It is this mode-dependent form of Equation (2) which determines what coefficients need to be loaded into arrays A1-A3 to effect the required decalibration of the spectral data. Each array can hold 14,336 coefficients. Figures 2-5 are examples of different operation modes.

This research is sponsored under a grant from the National Institute of General Medical Sciences, NIH (Grant GM 20850).

References: 1. Giffin, et. al, ASMS Transaction (1979) p. 714; 2. Boettger, Giffin, et. al, Monograph on Multichannel Image Detectors, Y. Talmi, Ed. (1979) p. 291.

DATA FLOW & CONTROL SCHEMATIC FOR EOID DATA PROCESSOR

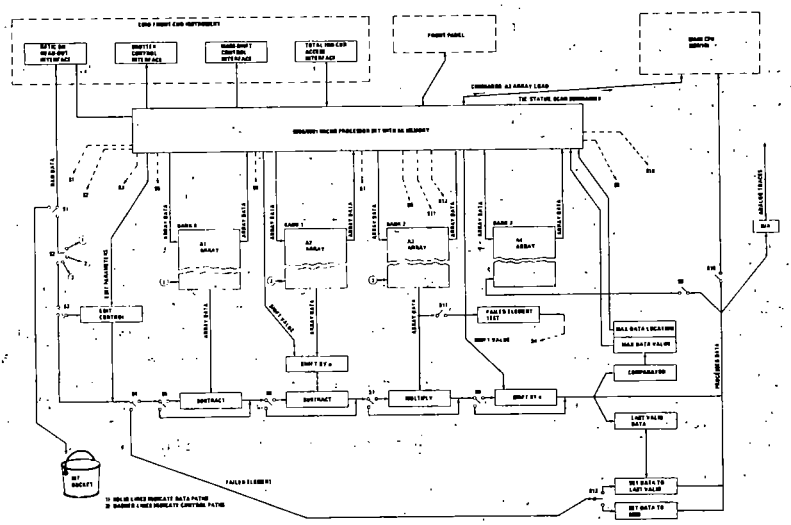

Figure 1

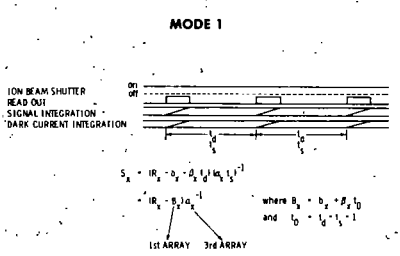

Figure 2

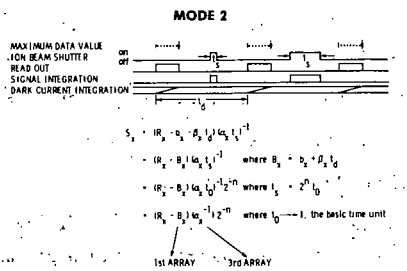

Figure 3

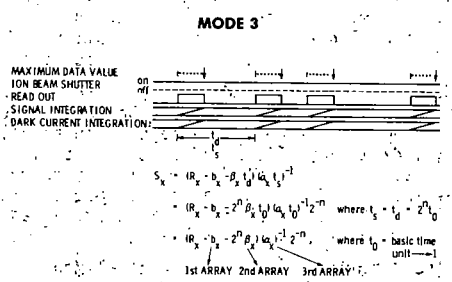

Figure 4

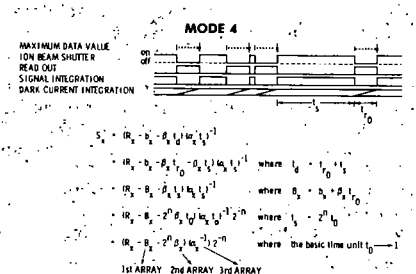

Figure 5

ELEMENTAL ANALYSIS BY A NOVEL MICROWAVE PLASMA/MASS SPECTROMETER SYSTEM. D.J. DOUGLAS, SCIEX INC. 55 Glencameron Road, Thornhill, Ontario and J.B. FRENCH, University of Toronto, Institute for Aerospace Studies, 4925 Dufferin Street, Downsview, Ontario, Canada.

In this report we describe developmental work on the coupling of a microwave induced plasma at atmospheric pressure to a quadrupole mass spectrometer. This technique, as a method for the elemental analysis of solutions, was pioneered by A.L. Gray (1) who successfully extracted ions from a DC arc plasma into a quadrupole mass filter. In later work the use of a higher power, radio frequency induced plasma (ICP) was reported (2). Our work, in accord with these earlier attempts, demonstrates that the technique promises elemental analysis with rapid sample throughput, broad dynamic range and high sensitivity, and furthermore is capable of providing isotope abundance data. The plasma system and vacuum interface reported here, overcome some of the problems of the earlier work.

The plasma used in this work was formed by a discharge through argon in a resonant microwave cavity (similar to a Beenaker cavity (3)). A spectroscopic study of the discharge indicates an electronic excitation temperature of 5500°K and an electron density of 10^{14} cm^{-3} (4). This electron density is orders of magnitude greater than that of argon in thermal equilibrium at 5500°K and indicates suprathermal excitation and ionization in the plasma. It is interesting to note that the power density in the discharge is $1x10^4$ watt cm^{-3}, considerably higher than an ICP. The microwave induced plasma system is compact with relatively low power consumption and minimal heat dissipation problems. Nevertheless the temperature of the plasma is comparable to that of other commonly used discharges and arcs.

Aqueous solutions were nebulized by an ultrasonic transducer (Plasmatherm Inc.) desolvated and carried into the plasma where the sample microparticulates are vapourized, dissociated and ionized. All sample handling is at atmospheric pressure and sample throughput time is a few seconds. Clearout time between samples is governed by the nebulizer, unless the quartz discharge tube is exposed to heavy loadings.

Ions are extracted from the tail flame of the plasma, through a differentialy pumped interface designed using gasdynamic molecular beam techniques. The ions then pass into the cryopumped vacuum chamber of a TAGA™ quadrupole mass spectrometer system. Previous workers using this technique have been plagued by clogging of the small orifice between the plasma and vacuum system. By contrast, the higher pumping speed of our system allows the use of substantially greater orifice diameters. No orifice plugging has occured despite lengthy runs with high salt content solutions. Furthermore, the plasma is inhaled directly into the vacuum system without formation of a cooler high pressure boundary layer (2). This reduces the possibility of ion molecule reactions which could complicate the mass spectra. Indeed, the background spectrum from this system is clean with few potential interferences.

The sensitivity of the system can be judged from Table 1 which reports detection limits for some metals of environmental interest, and compares these limits with those of current optical methods. The detection limits are defined as the concentration givng a signal 3 times the standard deviation of the background for a 10 second counting period.

In general the detection limits for the plasma/mass spectrometer method are in the parts-per-billion range or better, and exceed those of optical emission methods. (The less abundant nickel isotope Ni^{62} (3.59% abundance) was measured rather than Ni^{58} (68.3% abundance) owing to a background peak at mass 58 corresponding to 50 ppb Ni. This resulted in the somewhat higher detection limit for Ni.) To date, little attempt has been made to suppress the background noise. With background noise suppression and improved sample input it is likely that the already high sensitivity can be further improved.

For elements with an ionization potential above 9 eV there is a sharp drop in sensitivity. It is believed that this arises from charge transfer from the elemental ions to nitric oxide (NO) in the discharge (IP 9.25 eV). This nitric oxide is formed from trace N_2 and O_2 in the discharge or entrainment of air in the plasma tail flame. Work is

in progress to determine the source and importance of this compound. Once the basic mechanisms are better understood, there is good reason to believe that the effect can be mitigated. The rapid drop in sensitivity for elements of high ionization potential would, at first sight, seem to preclude the measurement of halogens in solution. However, an attractive feature of the TAGA™ system is the ability to detect both positive and negative ions. Halogens are readily detected as negative ions with the plasma source. No attempt has been made to optimize the ion extraction system for negative ions, but its seems likely that the detection limits for halogens can be extended to the parts-per-billion level.

For the elements indicated in Table 1 the ion count rate varied linearly with solution concentration for concentrations ranging over 4 orders of magnitude (i.e. from the detection limit up to 1-10 ppm). Reduction of the detection limits is likely to increase the dynamic range. A separate experiment was performed to observe the effect of an element of low ionization potential (Na 5.13 eV) on the signal from an element of high ionization potential (Cd 8.99 eV). Solutions containing 200 ppb Cd and a range of Na concentrations were run on the instrument. The cadmium count rate remained constant (within 20%) for sodium concentrations up to 100 ppm.

The MIP/TAGA™ system holds promise of minimal matrix effects over the 4-5 orders of magnitude operating range, as well as excellent sensitivities and detection limits for simultaneous multi-element determinations. It would seem from these initial results that the advantage of the ICP source over the MIP source for optical systems do not necessarily carry over to mass spectrometer based systems.

Table 1

DETECTION LIMITS ug/L (ppb)

Element	MIP/TAGA	ICP/AES	FLAME AA
Cd^{114}	2	1	1
Cr^{52}	0.1	2	2
Pb^{208}	1.0	15	10
Tl^{205}	1.0	112	20
Ag^{107}	0.1	6	1
Cu^{63}	0.1	2	4
Ni^{62}	8	5	5

References:

(1) A.L. Gray in Dynamic Mass Spectrometry, D. Price and J.F.J. Todd eds., 4, Chapter 10 (1975).

(2) R.S. Houk, V.A. Fassel, G.D. Flesch, H.J. Svec, A.L. Gray and C.E.Taylor, submitted to Anal. Chem., 1980.

(3) C.I.M. Beenaker, Spectrochimica Acta, 31B, 483, (1976).

(4) S. Wong, University of Toronto, Institute for Aerospace Studies, Technical Note number 225, (1980).

Acknowledgement: This work was carried out under the National Research Council of Canada, IRAP Contract No. TEA 501.

A MULTIPLE SELECTED-ION-MONITORING SYSTEM FOR HIGH SPEED, HIGH DYNAMIC RANGE AND HIGH PRECISION CYCLING. L. F. HERZOG, II AND T. J. ESKEW, JR., NUCLIDE CORP., 642 E. COLLEGE AVE., STATE COLLEGE, PA. 16801

With a properly designed high voltage supply, a magnetic MS can step from one peak to another as fast as a quadrupole MS, by stepping the ion accelerating voltage. (See, e.g., papers given at this conference by R. P. Stein in 1978 and T. J. Eskew in 1975.)

Magnetic mass spectrometers have an advantage over quadrupoles of equivalent cost in that they can produce peak tops that are rigorously flat-topped to higher resolutions. With a magnetic analyzer MS, an accurate measurement of ion current can be made merely by stepping to the center of the peak's flat top, while with a quadrupole, except at low resolutions, a scan over the peak is often made to insure measurement of maximum intensity.

With respect to maximum stepping speed, a photograph of a scope screen of Nuclide's MEC-4 connected to a 500 pF load capacitance shows that the circuit is able to slew through one kilovolt in about 60 microseconds; once the slew is completed it takes the circuit an additional 100 microseconds to settle to within 1% of its final value. When this MEC-4 is used to control a Nuclide 3-60-Sectorr, to switch between mass 28 and mass 17 (by switching the ion accelerating potential between approx. 2.5 and 3.5 kV) takes about 6 ms, to settle onto a peak top to within 0.5% of the final value. The difference in "settling time" between cases 1 and 2 is mostly accounted for by the electrometer amplifier. Indeed, to achieve fast peak stepping and high precision in intensity measurement one must shorten the amplifier's time response also.

The "inherent" time constant of Nuclide's EAH-300 electrometer amplifier with a 10^{11} ohm feedback resistor, but no capacitor other than the stray capacitance, is of the order of 20 milliseconds; but with a 10^{7} ohm resistor, this reduces to approx. 50 microseconds.

If one wants to measure two species of about <u>equal</u> intensity to, say ±1%, by peak-stepping, one can commence to take data as soon as either signal has decayed to below 0.5%; however, if one of them is only about 1% as intense as the other, one should wait until the larger signal has decayed to 0.005% of its initial value.

For RC=1 millisecond, it will take 10 milliseconds for a given signal to decay to 1%, while for RC=50 microseconds, this should occur in half a microsecond. To get to the 0.1% level adds 50% to these times; to the part in 10^4 level doubles them, and the part per million level triples them.

Unfortunately however, in practice signals do not fall to the levels calculated from the R and C values involved. Characteristically, there is an initial decrease which does follow the RC curve, but then the slope flattens out increasingly rapidly. This is referred to as "polarization", and it's magnitude depends on the properties of the capacitors, resistors, and insulators used. As an example, when the RC of a certain MEC-4 EAH-300 was set by a 10^{11} ohm resistor and a 1 picofarad capacitor made of glass, the calculated RC was 100 milliseconds, but it took 25 seconds for the signal to decrease to 0.01% of it's initial value, instead of the calculated 2 seconds; however, when this capacitor was replaced by one fabricated of polyethylene, with nothing else being changed, the same 20 volt signal fell to 2 mV in less than 3 seconds — approaching the expected performance.

Although such polarization can be reduced, it cannot be entirely eliminated — except by allowing the affected circuit element to "rest" for a long enough period for the voltage to dissipate to the desired degree. In view of this, can one in fact devise a S.I.M. system that can step say 10-100 times per second which will have a reasonably high "duty cycle" when it has to obtain accurate analyses of samples in which species of interest cover a wide dynamic range, say 10^4 - 10^6?

We believe this can best be done via a multi-detector array in which different ion detectors are assigned to different ion current domains. In such a system the polarization problem is avoided, since the resistors and capacitors which see the small currents do not ever see very much larger currents; hence, they cannot polarize them.

A magnetic mass spectrometer has a major advantage for high-dynamic-range SIM because it can focus ions at more than one point, along a focal line, simultaneously. Hence, as discussed in paper "TPMP19" at this meeting, one can arrange an array of ion detectors at various radii along the focal line to cover both a wide dynamic range and a wide mass range. The significant advantages of a multiradius, multiple detector MS for scanning applications are listed in the Abstract of that paper. For multiple selected ion monitoring, advantages 1 (increased dynamic range), 2 (obtaining high and low resolutions simultaneously), 3 (increased sensitivity), and 4 (a permanent magnet can sometimes be used) apply, but the reasons for the sensitivity increase are slightly different. It occurs because (a) required delays for settling are reduced because field-steps are

smaller, hence quicker, and because (b) ordinarily only one slit need be set for high resolution; the others, being wider, will be more efficient in detecting available ions.

In addition, accuracy is increased when the MS steps from one detector, as well as one mass, to another, simultaneously — since each detector always sees a current of a given intensity (or small range of intensities).

One application of a multi-beam SIM system with detectors covering a broad mass range we have investigated is studies of respiration in man, and even moreso, in small animals, which breathe more rapidly. In some such applications it is desired to monitor 4 or more species and obtain 5 or more data points per second for each — hence, to obtain 20 or more steppings and integrations per second with such a system, by stepping accelerating voltage, one can start collecting accurate data within 5-10 ms after initiating a step. If 10 millisec is allowed for settling after any step, and there are 20 steps/second, 800 millisec remains for data taking — an 80% efficiency level. In a program for sampling 6 species, 2 of which are trace-level, every 100 millisec, to improve precision, the trace species are sampled 5X as long as the others, and the overall data-taking efficiency is 70%.

Hence, in such systems it is, today, often the time-constant of the sample-inlet system rather than that of the mass spectrometer which sets a limit on the fastest useful scan rate.

Of course, precision is also limited by ion statistics, and from this standpoint also the multi-radius array technique offers significant advantages, since not only do all detectors not need be set at the highest resolution, but also, properly designed magnetic mass spectrometers deliver much higher proportions of entering molecules to the detector as ions than is true for other types, especially at low and high mass numbers.

The double-focusing Mattauch Herzog mass spectrograph is, of course, one very appropriate configuration for multi-radius detection since ions are simultaneously in excellent focus over a mass range as broad as, say, M to 50M. Since such spectrographs often have focal planes as long as, say, 40 cm, there is plenty of room for installing many detectors such as F-cups and "channel" electron multipliers. However, this can also be done with a direction-focusing only instrument: our 6-60-WR for example can detect *masses over the range M to 6M simultaneously. Undoubtedly a spectrograph with an EOID is* optimal; however, a spectrometer or spectrograph with several conventional F-cup and/or EM detectors can provide many of the same advantages at a considerably lower cost.

(Complete text and figures are available from the authors.)

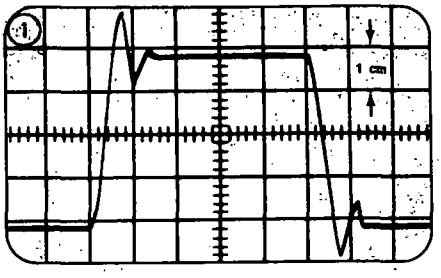

MEC-4 HV Stepping 1KV

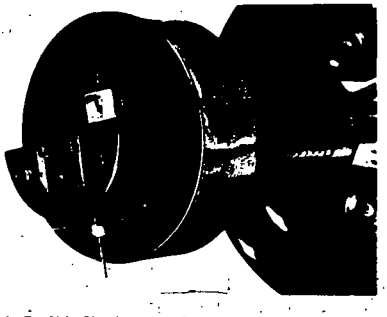

Side-By-Side Simultaneous Detectors (EM and F Cup)

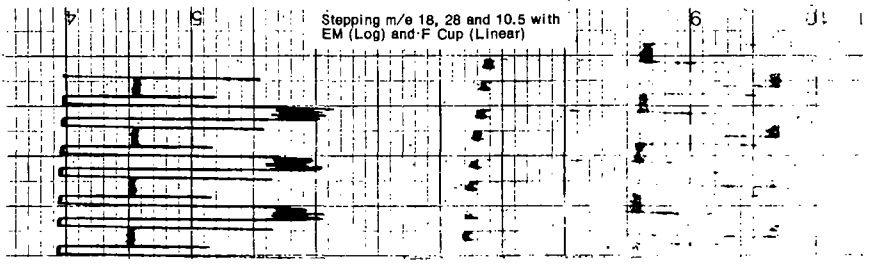

FURTHER DEVELOPMENTS IN QUANTITY OPTIMIZED TWO DIMENSIONAL GAS CHROMATOGRAPHY FOR MASS SPECTROMETRY, Ralph J. May and Woodfin V. Ligon, Jr., General Electric Company, Corporate Research and Development, Schenectady, New York 12301

We have previously described a design and prototype for a quantity optimized two dimensional gas chromatography system for mass spectrometry (ASMS, Seattle, June 1979, Paper RPMP-12). This system allows routine GC/MS analysis without concern for excessive sample quantities either injected or thermally desorbed from adsorbents.

In addition to this important fundamental advantage the GC-GC-MS affords a number of other important advantages. In particular, this system provides an effective dynamic range at the secondary chromatograph (all peaks on scale) of from 100% to 0.01% of the composition of any compound amenable to GC analysis. The lower limit can be easily extended by multiple injections and by use of a more sensitive mass spectrometer. (Present single injection lower detection limit is about 100ng for full mass spectra). This capability allows the use of the primary chromatograph to "clean up" impure samples with the elimination of time consuming preconcentration steps. In Figure 1 we show the analysis of impurities in diethylhexyl phthalate. In Figure 2 we show the direct analysis of 20ppm anthracene in naphthalene.

A second important advantage is the ability to exploit the full benefits of two dimensional gas chromatography. Particular regions of interest in the primary chromatograph can be rechromatographed on a different phase to yield different and potentially much improved separations not otherwise possible. In Figure 3 we show an enhanced separation where a small portion of the primary effluent has been manually selected and rechromatographed with much higher resolution on a second liquid phase.

Other features of this system include the production of both a normal primary chromatogram unperturbed by the interface operation and a quantity optimized chromatogram. The system operates either manually, for selection of particular components or areas of interest, or automatically to control the quantity of large peaks while transferring small components in their entirety. The system is amenable to analysis of any material which can be analyzed by conventional gas chromatography.

Other means of controlling the vacuum induced transfer such as digitally controlled pulsed valves are under investigation. Further, more general detectors are being studied for this application.

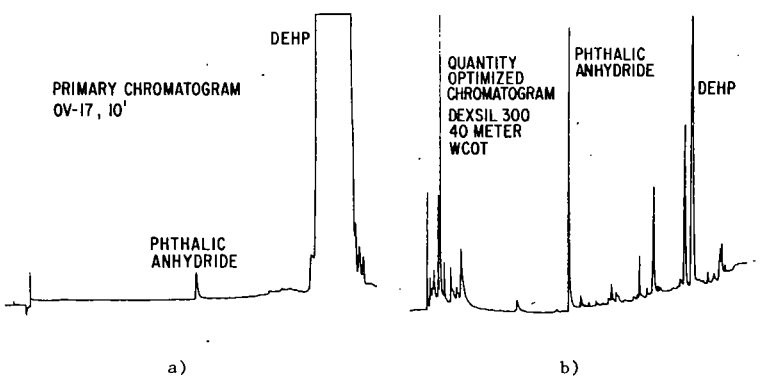

Figure 1. a) Normal chromatogram from neat injection of Di-2-ethylhexyl phthalate, b) quantity optimized chromatogram of the same sample.

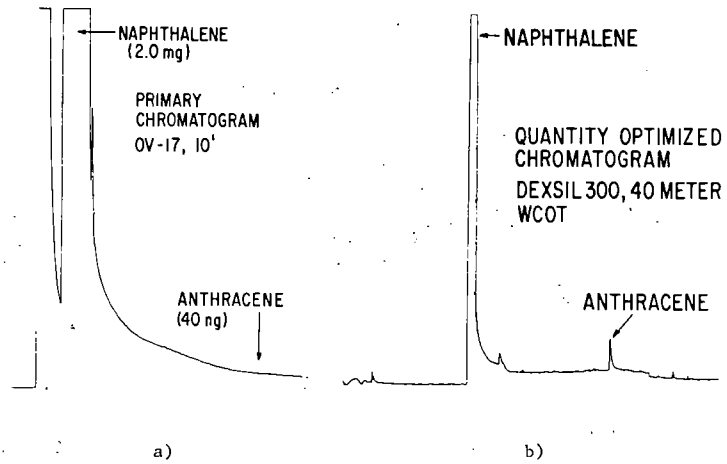

Figure 2. a) Normal chromatogram obtained from injection of a 20ppm solution of anthracene in naphthalene, b) quantity optimized chromatogram of the same sample after summation of three injections of a total of 15mg of the mixture.

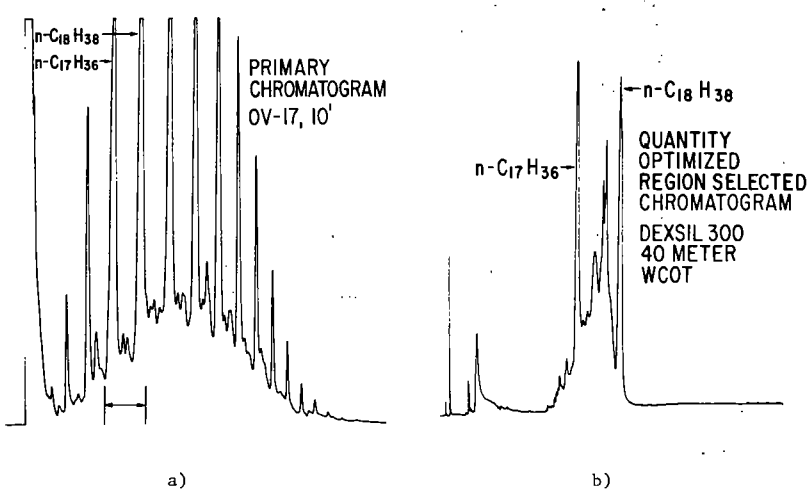

Figure 3. a) Normal chromatogram obtained from injection of a crude oil fraction BP=110-160° (0.8mm), b) quantity optimized chromatogram of a selected region indicated by the bars in 3a.

THE ULTIMATE IN CAPILLARY GC/MS COUPLING

P.A. Leclercq, G.J. Scherpenzeel and C.A. Cramers
Laboratory of Instrumental Analysis
Eindhoven University of Technology
Eindhoven, The Netherlands

In a directly coupled capillary GC/MS combination, the outlet of the column can be at more or less reduced pressure, dependent upon the method of coupling. Often it is claimed that a decreased outlet pressure has a deleterious effect on column efficiency. In practice up to 30% loss in efficiency has been reported. On the other hand, the optimum gas velocity can be shifted to higher values.
In this paper it will be shown that operation of capillary columns at very low outlet pressure ("vacuum GC") has many advantages over atmospheric outlet GC.

The flow through capillary columns is described by the Poiseuille equation. Band broadening in capillary columns is described by the Golay equation, extended to situations of appreciable pressure drop by Giddings [1-3]. Combining these equations, it can be shown that, neglecting the resistance to mass transfer in the liquid phase, the following optimum gas chromatographic conditions are valid [4-6]. Using the same column with the same carrier gas, the optimum inlet pressure P_i with vacuum outlet (P_o = 0) and atmospheric outlet ($P_o = P_1$), respectively, relate as

$$P_{i,opt,vac}^2 = P_{i,opt,atm}^2 - P_1^2$$

P_1 denotes atmospheric pressure.

The gain in optimum average carrier gas velocity using vacuum outlet, compared to its atmospheric outlet pressure analogon, is calculated to be

$$\frac{\bar{v}_{opt,vac}}{\bar{v}_{opt,atm}} = \frac{(P_{i,opt,atm}^3 - P_1^3)}{(P_{i,opt,atm}^2 - P_1^2)^{3/2}} = \frac{(P_{i,opt,vac}^2 + P_1^2)^{3/2} - P_1^3}{P_{i,opt,vac}^3}$$

This ratio, indicating the gain in the speed of analysis, increases strongly for lower inlet pressures ($P_{i,opt,vac} \ll P_1$), approaching $3P_1/(2P_{i,opt,vac})$. Lower inlet pressures means in practical terms the use of wide-bore and/or shorter columns. Despite the increased carrier gas velocity at low outlet pressures, the pumping capacity does not have to be increased, since the carrier gas flow (reduced to atmospheric pressure) remains constant at optimum gas chromatographic conditions.

The accompanying loss in efficiency is given by the minimum plate height relation

$$H_{min,vac} = \frac{9}{8} \frac{1}{f_{1,opt,atm}} H_{min,atm}$$

f_1 is the pressure gradient correction term derived by Giddings [2] and has a value between 1 ($P_i = P_o$) and 9/8 ($P_i \gg P_o$). Hence the loss in efficiency is 12.5% at most. The loss in efficiency can easily be compensated by using longer columns, while still having a gain in analysis time.

Experimental results indicate the validity of this theory (Table I), although the existence of the f_1 term could not be verified. While the column efficiency is not affected, the optimum inlet pressures and average gas velocities are dependent on the nature of the carrier gas. Using the chemical ionization reagent gases methane, isobutane or ammonia as carrier gas, the gain in speed of analysis is even higher [6] than obtained with nitrogen. The best GC/MS coupling device thus appears to be no device at all: just insert the column end into the ion source of a mass spectrometer. In addition to the gain in speed of analysis and/or GC resolving power, the many problems caused by wall effects and dead volumes in GC/MS interface lines are avoided by this method. Moreover, the gas chromatographic peaks are narrower and thus higher, lowering detection limits.

Table I. Comparison of data for a glass capillary SE-30 column, operated at optimum separation conditions at vacuum and atmospheric outlet pressures, respectively[a].

outlet pressure		$P_o = 0$				$P_o = P_1$
column length		L = 60 m			L = 30 m	
carrier gas		H_2	He	N_2	N_2	N_2
P_i [bar]	calc.	1.22	1.60	0.85	0.60	1.16
	meas.	-	1.55	0.80	0.60	1.25
$\bar{v}$ [cm/s]	calc.	66	40	23	32	11.7
	meas.	-	37	20	28	9.8
t_R [s]	calc.	279	456	798	282	783
	meas.	-	495	879	327	933
N (x 10^3)	calc.	190	190	190	95	107
	meas.	-	170	182	96	98
gain in $\bar{v}$	calc.	1.6	1.4	2.1	2.7	
	meas.	-	-	-	2.8	

[a] Column diameter 0.39 mm i.d.; film thickness 0.4 μm.
All data for n-$C_{12}H_{26}$ at 400 K (capacity ratio k = 2).
t_R = retention time. Number of plates $N = L/H_{min}$.

The advantageous effects described above hold for WCOT columns whereby the resistance towards mass transfer in the liquid phase is negligible compared to that in the gas phase. This is valid for capillaries with uniformly distributed thin liquid films, but also for wide-bore columns with thick films. The latter have higher sample capacities, show less adsorption, and facilitate injection.

References

1. M. Golay, in "Gas Chromatography, 1958" (D.H. Desty ed.), Butterworth, London, 1959, p.36.
2. J.C. Giddings, S.L. Seager, L.R. Stucki and G.H. Stewart, Anal. Chem. 32, 867, 1960.
3. J.C. Giddings, Anal. Chem., 36, 741, 1964.
4. C.A. Cramers, F.A. Wijnheymer and J.A. Rijks, J. High Res. Chrom. & Chrom. Comm., 2, 329, 1979.
5. C.A.Cramers and P.A. Leclercq, 27th Annual Conference on Mass Spectrometry and Allied Topics, Seattle, Wa., June 1979, p. 110.
6. C.A. Cramers, G.J. Scherpenzeel and P.A. Leclercq, submitted to J. Chromatogr.

IDENTIFICATION OF MASS SPECTRA FROM GC-MS DATA
THEORETICAL LIMITATIONS ON GC-MS ANALYSIS

David Rosenthal and William F. Hargrove

Chemistry and Life Sciences Group
Research Triangle Institute
Research Triangle Park, North Carolina 27709

When mixtures of compounds are subjected to GC/MS analysis, certain assumptions are made in the qualitative identification of the spectral data. Foremost among these assumptions is that the spectra of emerging eluents are totally or partially resolved and, based on the further assumption that the overlapping spectra have one or more peaks distinct from one another, it is possible to deconvolute the partly resolved spectra into their individual components. This assumption is only partly true, and as the number of components in a g.c. run increase, there occurs an increasing degree of ambiguity owing to the greater likelihood of peaks overlapping one another.

With current technology, full mass spectral scans can be carried out at one second intervals, however in practice it has been found that because of problems with ion statistics for weak peaks, most instruments achieve more reliable results when operated at a 1.5-2 sec/scan rate. Under these conditions, it can be shown that even if one achieves full deconvolution of components whose peak maxima occur as little as one scan apart, substantial numbers of components will be even less well separated (i.e., have identical retention times). Assuming that g.c. retention times correlate with molecular weight distribution, a typical one hour GC/MS capillary run with two second scans will contain multiple spectra per scan according to the relationship shown in Figure 1.

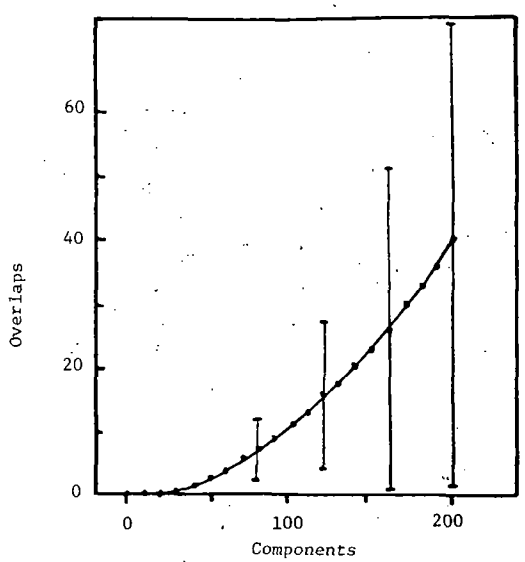

Figure 1. Probable number of coincident components and their standard deviations vs. number of compounds

This degree of overlapping may seem large, however the paradox is nevertheless true. Those readers familiar with the well-known common birthday paradox found in recreational mathematics will recognize the similarity of this situation to the present case.

The probabilities here are computed for exact overlaps. Near misses (components separated by one scan) can sometimes be resolved, however they present problems also, since one cannot always uniquely assign individual ions to each component. Thus it must be recognized that identification of multicomponent mixtures present theoretical limitations at a level not always heretofore realized.

As a practical example of this situation, a standard GC/MS run containing 35 known components was analyzed with particular attention to the presence of overlapping peaks. In this relatively simple case, one example of a precise overlap was found as well as one case in which two components differed by 1 scan (1.7 sec). In more complex mixtures, increasingly confounded data will surely be expected, as predicted in Figure 1.

This calculation was not made to justify improperly designed cleanup and search systems, however, it does explain the poor results often achieved using forward searches on complex mixtures, even with the use of well-designed software. The solution to this problem may well have to await more sophisticated data processing methods making use of additional parameters.

APPLICATIONS OF A NEW DATA ACQUISITION INTERFACE IN QUALITATIVE AND QUANTITATIVE GC-MS

A. Carrick, C.D. Park, M.J. Hoyle, P.A. Ryan, C.J. Wakefield, and K.R. Compson,
Kratos Ltd., Barton Dock Road, Urmston, Manchester M31 2LD, England.

Fast analogue data preprocessors have long been recognised as an essential part of high efficiency, high throughput mass spectrometer - computer systems.[1] The relatively recent commercial availability of fast arithmetic/logic integrated circuits which are uncommitted to any particular computational task - the so called "bit slices" - has now enabled proper exploitation of the principles of data preprocessing. In particular increases in speed of data acquisition and in dynamic range and precision of measurement have brought positive benefits to the mass spectrometer user beyond the straightforward returns of higher throughput.

The electronics of the Kratos preprocessor for DS55 series data systems is based on the "industry standard" AMD2901 bit slice chip. Design criteria for the preprocessor included three major aims - precision measurement capability over a 10^6:1 dynamic range of signal value, a digitisation rate of 200kHz (with the same dynamic range), and automatic zero signal level tracking and adjustment. These aims covered the measurement requirements of constantly improving gcms detection limits, the speed requirements of present and future fast scanning spectrometers, and the needs of users for a system simple to set up and operate. During project evaluation it became clear that a preprocessor capable of these tasks would also have enough computational power to cope with real time peak centroiding and this feature was also incorporated into the design. Finally compatibility with existing DS50 and DS50S systems hardware was assured so that present system users and not just new users could benefit.

THROUGHPUT TYPICAL SCANS

With P.P.	17525	44	1168	398
Without	19178	63	1279	304

OVERALL GAIN 30%

FIG 1. The DS55 system with and without the Preprocessor Interface. MS30, Single Beam, L.R. 1s/d, 15 scans at equilibrium

m/z	Theor Inten	SCAN NUMBER (single scans)								
		124	125	162	175	198	230	262	335	357
117	100	100	100	100	100	100	100	100	100	100
118	1.1	1.1	1.1	1.0	1.1	1.2	1.0	0.7	0.9	0.8
119	97.9	96.2	96.2	98.1	97.6	98.9	97.2	98.3	104.4	101.0
120	1.0	1.1	1.0	1.0	1.0	1.1	1.2	0.7	1.2	1.0
121	31.9	31.7	30.9	32.1	31.9	32.4	29.9	32.5	32.7	31.7
122	0.3	0.4	0.3	0.1	0.2	-	-	-	-	-
123	3.5	3.4	3.4	3.5	3.4	3.2	3.4	3.4	3.8	3.1
124	0.05	0.05	0.05	0.02	-	-	-	-	-	-

Largest Peak (not saturated) m/z 117 = 963520

Small Peak Range (m/z 118 = 64)

FIG 2. Repeat scans following a large injection of CCl_4, Unmodified MS25, 1 s/decade, 2m OV101

Our preprocessor has been available since late 1979, and in evaluating its performance close attention has been paid to its usefulness in general analysis *procedures and not merely specialised operations.*

From figures 1 and 2 the basic aims are clearly met in terms of speed, dynamic range and increase in throughput. Deriving from this, three important aspects of *system operation are improved. Detection limits in scanned operation with present* data system subtraction routines depend heavily on the accuracy and precision of intensity measured at low ion abundances. Figure 3 shows a decafluorotriphenylphosphine spectrum obtained from a "saturation recovery" style experiment[2]. A dilution series was used to test the ability of the system to measure low levels of material in the presence of "impurity". Excellent spectra from chromatographic peaks covering a concentration range in excess of 2500 to 1 were readily obtained. Detection limits in "static" operation modes (multiple peak monitoring) are particularly important and the ability of the preprocessor to record low level signals faithfully is a crucial part of high resolution techniques for ultra trace detection. Better recording techniques with digital smoothing mean less noise, fewer scans required in scan averaging procedures and faster (or more sensitive) experimentation (see paper MAMOB1).

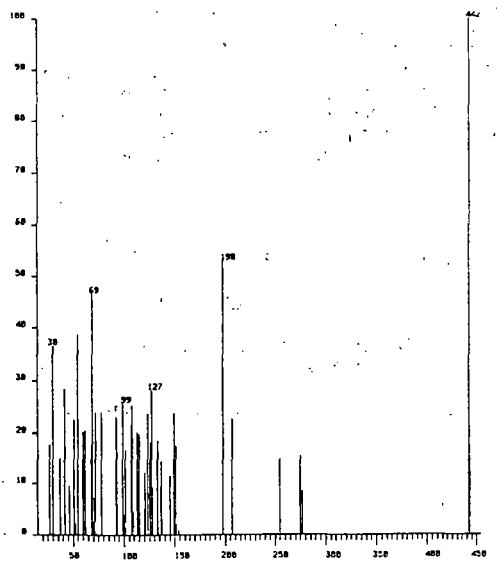

Fig.3 DFTPP subtracted spectum

Accurate mass measurements benefit from the preprocessors fast acquisition and smoothing, giving in the example (figure 3) measurable increase in accuracy at the particular sample flow rate chosen over methods based on classical acquisition techniques.

References

1. Chemical Society Specialist Periodical Reports - Mass Spectrometry Vol. 1. p.273 (1971)

2. Performance tests for evaluation of computerised gc-ms equipment and laboratories. W.C. Budde and J.W. Fichelberger. EPA report, Nov.1979

MPMOB6 **REAL-TIME QUALITATIVE AND QUANTITATIVE ANALYSIS OF GC/MS DATA OF COMPLEX MIXTURES FOR ENVIRONMENTAL POLLUTANT ANALYSIS,** GLENN I. OUCHI, Engineering Department, Finnigan Corporation, 575 N. Pastoria Avenue, Sunnyvale, CA 94086

A real-time minicomputer-based method has been developed for the qualitative and quantitative analysis of the GC/MS data acquired from complex organic mixtures. The method utilizes reverse library search using spectra of expected target compounds from a "user" library. The user library is built from spectra of standard compounds. Unknown compound spectra from GC/MS profiles can also be built into the user library for quantitative profile comparisons.

Target compound identification is based on relative retention data and mass spectral pattern matching. Quantitation is achieved by performing the appropriate calculations on the peak areas of a selected characteristic ion for each component and a selected ion of an internal standard. Multiple internal standards can also be used.

Since the method runs in real-time, data analysis is complete when the GC/MS acquisition is complete. Errors in sample preparation, such as no internal standard present, are detected during the acquisition.

This method has been extensively used for rapid and accurate environmental pollutant analysis.

#MPM0B7

DETERMINATION OF ETHYLDICHLOROSILANE IN METHYLCHLOROSILANES BY CAPILLARY GC-FID AND GC-MS

Gerald F. Dudding, G. T. Sorensen

Analytical Services Operation
GENERAL ELECTRIC COMPANY
Silicone Products Division
Mail Drop 12-07
Waterford, NY 12188

INTRODUCTION

Polysiloxanes make up the unique class of polymers which are known for their durability and heat and weather resistivity. Alkylchlorosilanes are the intermediates from which polysiloxanes are manufactured. Capillary gas chromatography coupled with FID or MS detection has found general use to control the quality of alkylchlorosilane intermediates. Use of FID and MS detectors for analysis of alkylchlorosilanes was reviewed by Smith. (1)

EXPERIMENTAL

Preparation of samples. Analytical standards, used to calibrate the response of the GC/FID, were prepared by mixing weighed amounts (mettler HIOT) of ethyldichlorosilane (Silar) and dimethyldichlorosilane (Silar) in 10 ml serum vials equipped with teflon lined septa (Supelco). Analytical standards for calibration of the GC/MS were prepared in the same manner, only weighed amounts of perdeuterochlorobenzene (Stohler) were also added as an internal standard.

Instrumentation. The GC/FID instrument was a Hewlett Packard model 5840 equipped with a glass lined injector/splitter and a J and W Scientific glass capillary column (OV-101, 55 m; 0.25 $\pm$ 0.01 mm I.D.).

The gas chromatograph/mass spectrometer/data system was a Finnigan model 9610 GC interfaced to a Finnigan model 4000 MS with dual chemical/electron ionization (CI/EI) source. An Incos data system, equipped with a Data General Nova 3 computer, acquired, stored and processed data from the quadrapole type mass spectrometer.

The MS operating conditions were: 70eV electron energy, 0.35 mA emission current, 10^{-8} A/V preamplifier sensitivity, 1600 eV electron multiplier, 250°C source temperature, 2 x 10^{-6} torr high vacuum. The masses chosen for selective ion detection were: (M/e), 52, 54, 82, 92, 99, 101, 117, 118, 119, 127, 129 and 131 with a 5.2 msec scan time per a m u.

The Incos data system enabled total ion current (RIC) and mass chromatograms (MC) to be constructed and the measurement of chromatographic peak areas for ethyldichlorosilane and perdeuterochlorobenzene respectively. These areas were used to quantitate the instrument's response to ethyldichlorosilane and perdeuterochlorobenzene in standard mixtures.

An HP 9845, equipped with software for polynomial regression analysis, was used to determine equations and correlation coefficients to fit curves to calibration data.

RESULTS AND DISCUSSION

Some of the difficulties encountered in the analysis of chlorosilanes by GC-FID are described by Smith. (1) He reported that the response of the FID to many chlorosilanes is relatively poor; the fewer the number of C atoms, the poorer the response.

Since chlorosilanes react with water, they must be handled under anhydrous conditions. Diluents for use in preparation of calibration mixtures also must be anhydrous. Therefore, the most appropriate diluent is another chlorosilane which has a different retention time than that for the species to be monitored. Teflon sealed vials were used for containers.

It was also necessary to routinely clean contaminated parts of the FID with dilute (<5%) aqueous HF, since combustion of organosilicon compounds in an oxygen-rich hydrogen flame produced considerable amounts of silica.

The instrument was conditioned with several injections of an ethyldichlorosilane mixture until the area of the ethyldichlorosilane peak approximated that for a previous analysis. Equal volumes (1.0 µl) of samples 55 - 5453 ppm ethyldichlorosilane in dimethyldichlorosilane were analyzed, and the areas of the peaks from ethyldichlorosilane were determined.

The second order polynomial regression analysis yielded a calibration curve (Figure 1) which had the highest correlation coefficient and the lowest standard deviation of scatter about the regression line.

Samples which could not be analyzed by GC-FID because they contained components whose gas chromatographic retention time were similar to that of ethyldichlorosilane were analyzed by GC-MS. The analysis utilized selective ion detection.

An internal standard method was chosen for calibrating the total ion current (area) to the concentration of ethyldichlorosilane. This allowed for change in the instrument's response presuming the change was equivalent for both ethyldichlorosilane and the internal standard.

Perdeuterochlorobenzene was chosen as the internal standard because its natural abundance was not detectable in samples to be tested and because its gas chromatographic retention time was different from ethyldichlorosilane. Four standards were prepared in dimethyldichlorosilane, for which the concentrations (ppm) of ethyldichlorosilane and perdeuterochlorobenzene are indicated: 31, 619; 80, 736; 113,699; 171, 723. Each standard was analyzed (4.0 µl) and the ratio obtained by dividing the total ion current (area) from ethyldichlorosilane by the calculated total ion current (area) from 700 ppm internal standard was determined. Since the ratio ought to be constant within the concentration range for which response to each species was linear, sample volume need not be accurately known.

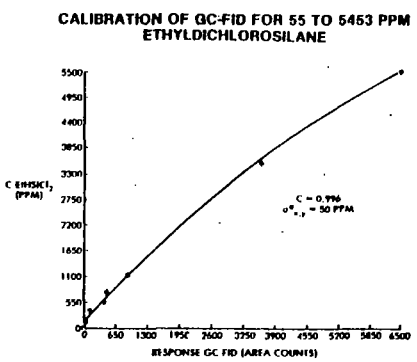

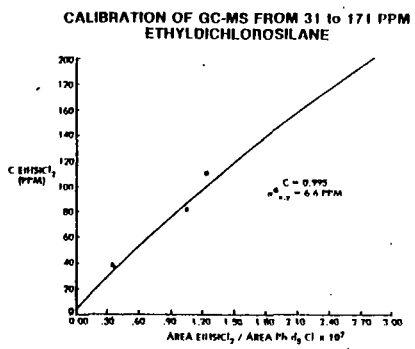

References

1. A. Lee Smith, ed., Analysis of Silicones, J. Wiley and Sons, NY 1974, pg. 217-246.
2. K. Eckschlager, Errors, Measurement and Results in Chemical Analysis, Von Nostrand Reinhold Co., New York, 1969, p. 143.

A FUNDAMENTAL APPROACH TO MEASUREMENT PARAMETER SELECTION FOR QUANTITATIVE ISOTOPE DILUTION GC/MS DETERMINATIONS, B. N. COLBY and A. E. ROSECRANCE, Systems, Science and Software, Box 1620, La Jolla, CA 92038 and M. E. COLBY, 2707 El Rastro, Carlsbad, CA 92008

The selection of measurement parameters, such as m/z's for isotope ratio determination and calculation method, has traditionally been carried out empirically, i.e., the methodology is based on what was found by trial and error to provide acceptable performance. This is not an unreasonable approach when one or even several compounds are to be quantitated. However, when a large number of compounds, say eight or more, are to be determined simultaneously, some standard set of decision criteria must be employed in order to minimize the time consumed for parameter selection. Because we are currently interested in the use of isotope dilution GC/MS for determinations of up to 47 compounds in a single GC/MS run, we developed such a set of decision criteria based on a mathematical model of isotope dilution. Using this model, it is possible to predict which two m/z's will lead to the best analytical results. In addition, it is possible to identify which calculation methods are applicable in specific situations, and to identify ideal spiking levels. This presentation will cover the development of parameter selection criteria based on the isotope dilution model and data will be presented to verify the appropriateness of these criteria.

GAS CHROMATOGRAPHY-MASS SPECTROMETRY WITH METASTABLE PEAK MONITORING APPLIED TO THE ANALYSIS OF STEROID HORMONES

Simon J. Gaskell, Elizabeth M.H. Finlay and Adrian W. Pike

Tenovus Institute for Cancer Research, Welsh National School of Medicine, Heath, Cardiff, CF4 4XX, U.K.

We have recently described gas chromatographic-mass spectrometric (GC-MS) analyses where a high specificity of detection is achieved by selective detection of metastable peaks attributable to fragmentations occurring in the first field-free region of a double-focusing mass spectrometer (1,2). Here we review applications of the new technique in three areas, viz. steroid profiling, identification of compounds at the picogramme level and quantitative analyses.

The profiling of androstanolones in blood plasma is complicated by the number of endogenous positional isomers and stereoisomers which are not fully separated by GC. During analyses of tert-butyldimethylsilyl (TBDMS) ethers by GC-high resolution (HR) MS with selected ion monitoring (SIM) of $|M-C_4H_9|^+$ ions, detection limits of ca. 20 pg are observed. Similar sensitivities of detection are achieved by metastable peak monitoring of the fragmentation, $|M-C_4H_9|^+ \rightarrow |M-C_4H_9-H(CH_3)_2SiOH|^+$. Relative responses with the two techniques differ, however, so that complementary evidence is obtained for characterisation of the androgen profile.

The identification of steroids in saliva is particularly difficult in view of the low concentrations. Following solvent extraction and simple gel chromatographic purification, testosterone and dehydroepiandrosterone (DHA) have been identified by GC-HRMS/SIM of the TBDMS ethers and the methyl oxime (MO), TBDMS ethers. Additional analysis of the latter derivative, with metastable peak monitoring of $M^{+\cdot} \rightarrow |M-C_4H_9|^+$, provides a more sensitive means of detection of testosterone but DHA is not observed in this instance, as expected on the basis of studies of the standard compound. Quantitative analyses indicate concentrations in the range 200-800 pmol/l for both steroids.

For quantitative determinations of steroids in blood plasma, the techniques of GC-HRMS/SIM and GC-MS with metastable peak monitoring are of complementary value. Both have been applied in the analysis of plasma pools used in the U.K. National Quality Control Scheme for testosterone. The GC-MS data provide "target values" by which the performance of routine methods (such as radioimmunoassays) may be assessed. Testosterone, after conversion to the oxime, is selectively isolated from plasma extracts by cation exchange chromatography on a derivatised Sephadex gel (3). The purified fraction is converted to the TBDMS oxime, TBDMS ether for GC-HRMS/

SIM ($|M-C_4H_9|^+$) or to the MO, TBDMS ether for GC-MS with metastable peak monitoring ($M^{+\cdot} \rightarrow |M-C_4H_9|^+$). For the former procedure, $|^2H_3|$-testosterone is the internal standard; 17-epitestosterone is used in the latter case. The two procedures give data in excellent agreement; linear regression gives the equation $y = 0.94x + 0.16$, where y ng/ml is the result of metastable peak monitoring and x ng/ml is the result of GC-HRMS/SIM. The correlation coefficient is 0.998.

1. Gaskell, S.J. and Millington, D.S. (1978), Biomed. Mass Spectrom. 5, 557.
2. Gaskell, S.J., Finney, R.W. and Harper, M.E. (1979), Biomed. Mass Spectrom. 6, 113.
3. Axelson, M. and Sjövall, J. (1976), J. Chromatogr. 126, 705.

A METHOD FOR THE DETERMINATION OF ORGANOTIN PVC STABILIZER IN SERUM

M. MARCONI, M. GARA, D. NELSON, AND R. DAWE, Travenol Laboratories, Inc., 6301 Lincoln Ave., Morton Grove, IL 60053

A procedure has been developed for the quantitation of parts-per-billion levels of an organotin in PVC stabilizer in organic solvents and serum. Dialkyltin compounds have been employed as stabilizers in PVC for several years, and their use in medical products is increasing. This paper describes a method that can be routinely used to measure di-n-octyltin-S,S'-bis-isoctylmercaptoacetate (OTM) at levels as low as 50 ppb in serum. The The procedure involves dilution of the serum sample and treatment with hydrobromic acid to obtain di-n-octyltindibromide, which is subsequently extracted from the serum into dichloromethane. Reaction with methylmagnesium bromide results in dimethyldi-n-octylstannane (OTMe). The stability and volatility of OTMe make it amenable to reproducible gas chromatographic analysis on a 6-foot, 3% OV-1 column. A coupled gas chromatograpic/mass spectrometric procedure with single- or multiple-ion monitoring is employed as a sensitive and selective means of quantitating OTM as its derivative. Masses 361 and 263 are monitored either singly or simultaneously. Concentrations of OTM between 50 and 100 ppb are normally analyzed producing routine recoveries of 55% to 65%, ± 8% relative standard deviation within this range.

Recently, the method has been modified to include the use of di-n-heptyltin-S,S'-bis-isoctylmercaptoacetate (HTM) as an internal standard. This compound is added to the serum before it is spiked with OTM. As with OTM, the internal standard is converted to the dialkyldimethylstannane derivative, specifically dimethyldi-n-heptylstannane (HTMe), during sample preparation. Samples are quantitatively analyzed for OTMe by combined gas chromatography/mass spectrometry. Multiple ion selection is used to monitor the M-CH_3 ions of both OTMe and HTMe which are m/e 361 and 333, respectively. The standard curve generated is then used to determine levels of OTM leached into serum during incubation in that serum of plastic parts produced from PVC stabilized with about 2% OTM. The OTM stabilizer can be detected in serum at the 50 ppb level with a standard deviation of 17%.

AN IMPROVED THERMAL DESORPTION GC-MS METHOD FOR TRACE ORGANICS SAMPLED ONTO TENAX® RESIN FROM AMBIENT AIR

C. Herndon Williams Jr., Larry D. Ogle, and D. Scott Lewis

Radian Corporation
P.O. Box 9948
Austin, Texas 78766

A thermal desorption method was developed and validated for the quantitative separation of a broad volatility range - from benzene to benzanthracene - of organic vapors sorbed on Tenax resin, prior to GC-MS analysis. The method was applied to the analysis of large ($\sim 6 m^3$) ambient air samples collected on Tenax at sites on the perimeter of a coal gasification facility. The samples were found to contain a complex mixture of potentially hazardous organic compounds. Aromatic hydrocarbon species from benzene to pyrene and other compounds containing the hetroatoms, O, S and N, were detected and identified at ambient levels in the range $\mu g/m^3$ - ng/m^3 (ppb-ppt).

The air samples were collected on a two-cartridge in-series Tenax vapor trap, downstream from a Hi Vol glass fiber filter. The Tenax resin in each cartridge ($\sim$2.5g) was removed from the trap and analyzed separately. Each Tenax sample was mixed to homogeneity and replicate aliquots were taken for screening by thermal desorption (ThD) GC-FID or analysis by ThD-GC-MS. The thermal desorption inlet consisted of a modified GC injection port and a pre-column cold trap, ahead of a metal GC column. The thermal desorption methodology was validated by QA studies which involved both real and simulated samples, dosing with deuterated standard compounds and parallel Soxhlet extraction of Tenax aliquots (see Fig. 1).

Thermal desorption for 10 minutes at 250°C under the He carrier gas flow of 30 mL/min was found to be required for complete separation of the vapors sorbed on the Tenax. Chromatography was carried out on a 10 ft x 1/8 inch OD nickel column packed with 10% OV-101, programmed from 50° to 250°C. The precision of analyses of duplicate Tenax aliquots by ThD-GC-FID was determined to be 10-15%. The mean recoveries by thermal desorption for five aromatics spiked on blank Tenax resin were all found to fall in the 90-110% range, as seen in Table 1. Thermal desorption of a 40 mg aliquot (1.7% of the initial 2.5g sample) was sufficient to detect vapor species down to $\sim$1 ppt in the $6 m^3$ air sample.

A thermal desorption GC-MS chromatogram of an unspiked Tenax aerosol sample is shown in Fig. 2. The upper trace shows peaks associated with the fragment ion at mass 85; most of these peaks were found to belong to a series of aliphatic hydrocarbons spanning from C_9 to C_{20}. The lower trace shows the total ion current, with indications of some of the major aromatic species that were found. Table 2 lists all the major compounds and isomer groups identified by GC-MS in the vapor samples associated with the coal gasification facility aerosol.

These results demonstrate the utility of the thermal desorption methodology reported here. The method has been validated for aromatics in the range from benzene (bp 80°C) to benzanthracene (bp 435°C) and has been found to quantitatively recover a number of classes of C-H-O-S-N compounds, with detection limits in the low ppt range for large air samples.

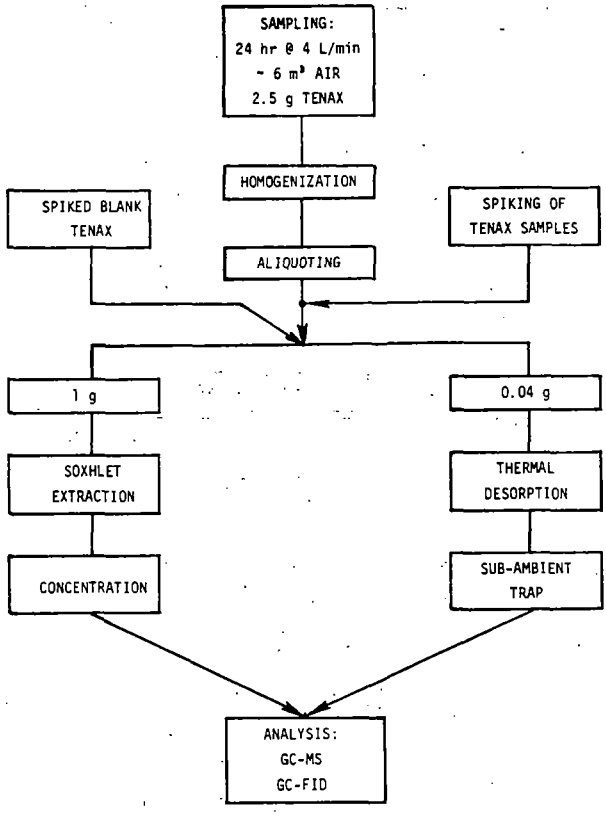

Figure 1. Separation and Analysis Scheme

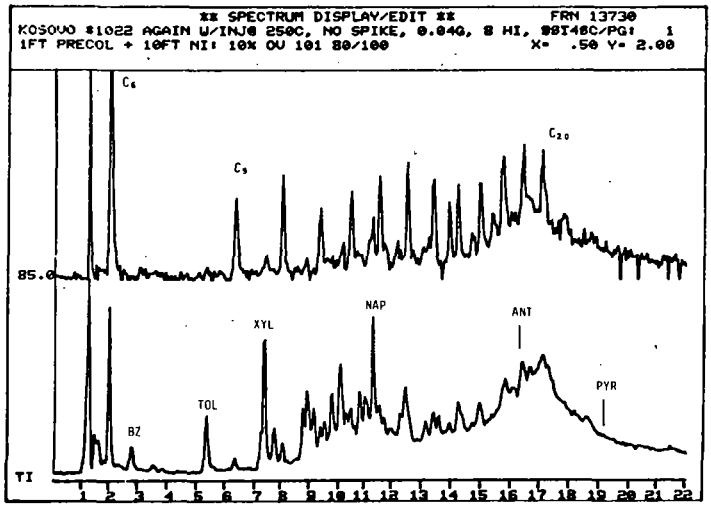

Fig. 2. Thermal Desorption GC-MS Chromatogram of unspiked Tenax Aerosol Sample

TABLE 1. MEAN RECOVERIES BY THERMAL DESORPTION FOR FIVE AROMATIC COMPOUNDS SPIKED ON BLANK TENAX RESIN

Compound Identification	Mean Recovery	Precision
1. d_6-Benzene	90%	± 10%
2. d_8-Toluene	91%	± 10%
3. d_8-Naphthalene	92%	± 10%
4. d_{10}-Anthracene	94%	± 10%
5. 1,2-Benzanthracene	113%	± 20%

TABLE 2. ORGANIC COMPOUNDS AND ISOMER GROUPS IDENTIFIED BY GC-MS IN THE TENAX AEROSOL SAMPLES

Compound or Isomer Group Identification	MW	Isomers Detected		MW	Isomers Detected
Aromatic Hydrocarbons			C-H-O Compounds		
Benzene	78	1	Phenol	94	1
Toluene	92	1	Methyl phenols	108	> 2
C_2-Alkyl benzenes	106	> 3	C_2-Alkyl phenols	122	> 5
C_3-Alkyl benzenes	120	> 6	Acetophenone	120	1
C_4-Alkyl benzenes	134	> 9	Dibenzofuran	168	1
Naphthalene	128	1	Diphenylquinone	260	1
Methyl naphthalenes	142	> 2	C-H-S Compounds		
Acenaphthene	154	1	Methyl thiophene	98	2
Fluorene	166	1	C_2-Alkyl thiophenes	112	> 4
Anthracene/Phenanthrene	178	> 1	C_3-Alkyl thiophenes	126	> 3
Methylanthracene	192	> 2	C-H-N Compounds		
Fluoranthene	202	1	Pyridine	79	1
Pyrene	202	1	Methyl pyridines	93	> 2
Aliphatic and Alicyclic Hydrocarbons			C_2-Alkyl pyridines	107	> 4
C_8-C_{28} Aliphatics	128-282	>12	C_3-Alkyl pyridines	121	> 5
Indane	118	1	Quinoline/Isoquinoline	129	2
Trimethylphenyl indane	236	1	Methyl quinolines	143	> 5
			C_2-Alkyl quinolines	157	>10

MPMOB12 NEW DEVELOPMENTS IN CAPILLARY COLUMN GC/MS ANALYSIS USING DOUBLE FOCUSSING SPECTROMETERS,

D.S.MILLINGTON, V.PARR, B.N.GREEN AND K.HALL, VG-Organic Ltd., Tudor Rd., Altrincham, Cheshire, England WA14 5RZ

The use of capillary columns in GC/MS has been increasing very rapidly and has provoked revolutionary changes in both the mass spectrometer and the dedicated data system. Remarkable improvements in the design of some commercial magnetic sector instruments have recently overcome the technical difficulties associated with scanning in less-than-1-second cycles, thus enabling the advantages of the sector MS to be fully realised in this rapidly expanding field. In particular, mass measurements to around 10ppm precision, obtained at low resolution with full sensitivity, and alternate CI/EI scanning are techniques not currently available with commercial quadrupole GC/MS/DS systems. However these techniques together provide unequivocal molecular formulae in addition to EI fragmentation patterns and the additional information is an extremely valuable interpretative aid when used with the library search in mixture analysis.

Fast computer-controlled selective ion monitoring at high resolution improves both the accuracy and detection limits achieved in quantitative analyses with capillary column GC/MS. In addition, owing to the development of a new fully laminated magnet, fast SIM with full sensitivity over the entire mass range is now practicable with the VG-MM7070 spectrometer.

MPMOCI TANDEM MASS SPECTROMETRIC STUDIES OF THE REACTIONS OF N^+ AND O_2.

Morgenthaler* L.N. and Paulson J.F. Air Force Geophysics Laboratory
Hanscom AFB MA 01731

The tandem mass spectrometer at AFGL[1] has been used to study reactions 1, 2, 3a and 3b over the range of collision energies (center of mass) from 0.35 to 25 eV.

$$N^+ + O_2 \rightarrow NO^+ + O + 6.7 \text{ eV} \qquad 1)$$

$$O_2^+ + N + 2.5 \text{ eV} \qquad 2)$$

$$O^+ + NO + 2.3 \text{ eV} \qquad 3a)$$

$$O^+ + N + O - 4.2 \text{ eV} \qquad 3b)$$

Reaction cross sections and the forward directed component of the product ion kinetic energy were measured for reactions 1, 2, and 3 (combination of 3a and 3b).

At very low (< 1 eV) collision energies, reactions 1 and 2 both contribute significantly to the overall reaction. However, the relative contribution of reaction 1 falls off with increasing collision energy. Above 7 eV reaction 1 decreases rapidly in importance (as E^{-3}), and reaction 3 increases in importance due to the contribution of reaction 3b. However, the combined contribution of reactions 3a and 3b never exceeds 15% of the total reaction cross section.

Reactions 1, 2, and 3a all proceed by direct stripping type mechanisms. That is, the momenta of NO^+ (reaction 1), N (reaction 2), and NO (reaction 3) are each equal to the momentum of the primary ion,. The distribution of forward directed kinetic energies of O^+ produced in reaction 3b is quite broad and is consistent with a direct mechanism. In this mechanism, NO^+ is first formed by a stripping type reaction; all the excess kinetic energy of the collision plus the exothermicity of the reaction are converted to internal excitation of the NO^+ product; and this excited state survives long enough to yield an isotropic distribution of O^+ ions. That the O^+ formed in reaction 3b does in fact come from dissociating NO^+ is supported by 1) the coincidence of the onset for the sharp decrease in cross section for reaction 1 and the increase in cross section for reaction 3, 2) the kinetic energy loss observed[2] in reaction 1, and 3) the kinetic energy spectrum of O^+. Another important implication of reaction 3b is that NO^+ is formed in either the $X^1\Sigma^+$ or $a^3\Sigma^+$ state in reaction 1.

Once dissociation is taken into account there is no energy left over for the formation of excited states of the O atom. It is still not clear which state of NO^+ is formed in reaction 1 at elevated collision energies, but in a recent study[3] at 300 K no evidence of the triplet state was observed.

Note a:
* NRC Research Associate 1979-80.

1. J.F. Paulson and P.J. Gale,"Advances in Mass Spectrometry" Vol.7A, 113, N.R. Daly ed. Heyden & Sons LTD.,London,1978.
2. J.C. Tully, Z. Herman and R. Wolfgang, J. Chem. Phys. 54, 1730 (1971).
3. D.L. Albritton et.al., J. Chem. Phys. 71, 3295 (1979).

STUDIES OF MODEL ION-MOLECULE REACTIONS BY TRIPLE QUADRUPOLE MASS SPECTROMETRY

MPM OC2

John Chakel, Hugh Gregg, John Allison, and Chris Enke
Department of Chemistry
Michigan State University, East Lansing, MI 48824

A triple quadrupole mass spectrometer of the original design of Yost and Enke[1] was used to study the mechanisms of the following reactions:

$$C_2H_5^+ + CH_4 \longrightarrow C_2H_3^+ + H_2 \quad (I)$$

$$CH_3^+ + CH_4 \longrightarrow \begin{cases} C_2H_5^+ + H_2 \\ C_2H_3^+ + 2H_2 \end{cases} \quad (II)$$

$$CH_3^+ + CH_3COCH_3 \longrightarrow \text{PRODUCTS} \quad (III)$$

The ion-molecule reaction was carried out in the quadrupole collision chamber which contained the reactant molecule. Quad 1 selected the reactant ion and quad 3 analyzed the reaction products. A plot of the parent ion intensity vs. the voltage on the quad collision chamber V_{Q2} (relative to the source) shows a sharp drop when V_{Q2} is positive enough to exclude a substantial fraction of the ions. The derivative of this curve indicates an energy spread of about 2-3 V for ions from the source. The value of V_{Q2} which excludes 50% of the parent ions is used as a reference point for ion axial energy. The reaction products were studied at various ion energies relative to this reference point.

Reaction (I) was studied as both $C_2H_5^+ + CD_4$ and $C_2D_5^+ + CH_4$. The loss was H_2 in the first case and D_2 in the second which confirms that the H_2 loss is from the $C_2H_5^+$ ion exclusively. At higher energies (10-20 V) a slight mixing (23%) of H and D is observed in the products.

Reaction (II) produces $C_2H_3^+$ even at low energies. Since this is not a product under thermal conditions, it results from the energy spread of ions entering the collision chamber. As the average ion energy is increased to 5 V the $C_2H_3^+$ product becomes dominant. Studies with deuterated ion and deuterated collision gas resulted in the following relative intensities of products at lower ion energy.

$$CH_3^+ + CH_4 \longrightarrow C_2H_5^+ > C_2H_3^+$$

$$CD_3^+ + CH_4 \longrightarrow \begin{cases} CH_3^+ > CHD_2^+ > CH_2D^+ \\ C_2H_3D_2^+ \geq C_2H_2D_3^+ > C_2H_4D^+ \\ C_2HD_2^+ > C_2H_2D^+ > C_2H_3^+ \end{cases}$$

$$CH_3^+ + CD_4 \longrightarrow \begin{cases} CHD_2^+ > CH_2D^+ > CD_3^+ \\ C_2H_2D_3^+ \geq C_2H_3D_2^+ > C_2HD_4^+ \\ C_2HD_2^+ > C_2H_2D^+ > C_2D_3^+ \end{cases}$$

These results are in good general agreement with those obtained by Huntress[2] using ICR, Abramson & Futrell[3] using tandem MS techniques and others. The energy spread of reactant ions prevents the detailed study of branching ratios at near-thermal energies.

Many products have been reported for reaction (III) 59^+ $(M+1)^+$, 58^+ (M^+), 55^+ $(C_4H_7^+)$, 57^+ $(C_3H_5O^+)$, 45^+ $(CH_3OCH_2^+)$, 43^+ (CH_3CO^+ and $C_3H_7^+$), 41^+ $(C_3H_5^+)$, 31^+ (CH_3O^+), and 29^+ $(C_2H_5^+)$ at thermal energies.[4] We have studied several of these as a function of ion axial energy in the triple quadrupole. The abundance of 58^+ agreed with Futrell's results at low energy and increased with increasing energy. The 59^+ product was large at low energy and decreased with increasing E. The use of CD_3^+ reactant showed that the selected ion was not the major source of H^+ in the formation of 59^+. Lowering the acetone pressure from 10^{-4} torr to 4×10^{-6} torr greatly decreased the 59^+ production to suggest the reaction $M^+ + M \rightarrow MH^+ + (M-H)$. Apparently this reaction occurs in Q_2 at "elevated" pressures because CH_3^+ transfers little kinetic energy in the charge transfer reaction. The result is a long residence time for the product in Q_2 where subsequent reaction can occur. All methane and all other acetone work reported here was done at the lower pressure.

Futrell reported 12% $C_3H_7^+$ and 28% $C_2H_3O^+$ for the 43^+ product. Observation of the reactions CD_3^+ with acetone and CD_3^+ with d-6 acetone failed to reveal any of the $C_3H_7^+$ product at any energy accessible in our system.

Products not observed at thermal energies (39^+, 42^+, and 28^+) were observed at increased axial energies. The $C_3H_3^+$ formation is exothermic, but apparently has a substantial activation energy.

References

1. Yost, R.A., and Enke, C.G., Anal. Chem., 51, 1251A (1979).

2. Huntress, W.T., J. Chem. Phys., 56, 5111 (1972).

3. Abramson, F.P. and Futrell, J.H., J. Chem. Phys., 45, 1925 (1966)

4. Smith, R.D., Elwood, T.A., Herold, D.A., and Futrell, J.H., Abstracts, 24th ASMS Conference, San Diego, CA, 1976.

MPMOC3 BEAM STUDIES OF THE REACTION OF H_3O^+ AND OH^- WITH H_2O AT ENERGIES OF 0.3 - 1.0 eV, M. J. HENCHMAN and J. F. PAULSON, AFGL, Bedford, MA 01730.

Isotopic exchange reactions have been studied for the systems $H_3O^+ + H_2O$ and $OH^- + H_2O$, using both deuterium and oxygen-18 labelling, to complement studies of the former reaction at 300 K, using the Selected Ion Flow Tube technique. At thermal energies the time for complete hydrogen exchange within the intermediate is found to be less than the lifetime of the intermediate. The following results were found at higher energies: (1). For both reactions the principal mechanism found at the highest energies ($\sim$ 1 eV) consists of the simple transfer of a proton, a result consistent with a lifetime too short for appreciable exchange. (2). For both reactions the relative contribution of exchange processes increases as the energy is decreased, a result consistent with a consequent increase in the lifetime of the intermediate. (3). For both reactions the data extrapolate to statistical distributions at thermal energies. (4). At the lowest energy ($\sim$ 0.3 eV) the distributions are far from statistical, a result consistent with simple estimates of the lifetime of the intermediate under these conditions. (5). For both systems a kinetic isotope effect is observed throughout the energy range studied, favoring H^+ transfer over D^+ transfer, both for the direct transfer and for the exchange observed within the intermediate.

Formation and Thermodynamic Properties of Hydrated NO_3^- Ions

Richard L. C. Wu and Thomas O. Tiernan
The Brehm Laboratory and Department of Chemistry
Wright State University, Dayton, Ohio 45435

Recently, cluster ions of NO_3^- with H_2O have been the subjects of extensive investigation because of their important role in the negative ion chemistry of the ionosphere.[1-3] The thermodynamic properties of such ions provide insights into the structure and stability of ionic clusters[4-5], and also are essential to the development of theoretical models of nucleation phenomena.[6-8] Thus far, most thermochemical data for cluster ions has been obtained from high pressure mass spectrometric measurements. In such experiments, equilibrium constants and their temperature dependence are measured, and Vant Hoff plots are constructed in order to determine the enthalpy and entropy of the clustering reactions. It is desirable, however, to have an independent measure of thermodynamic data for clustered ionic species, preferably derived from other types of experiments. Over the past few years, we have developed and applied ion-beam techniques to measure translational energy thresholds for collisional-induced dissociation (CID) reactions.[9-11] It has shown that reliable bond dissociation energies and ionic heats of formation can be obtained from such measurements. The purpose of this paper is to present additional experimental results obtained with such techniques, which bear on the formation and energetics of hydrated NO_3^- ions.

An in-line double mass spectrometer, previously described,[12] was used in the present study. The projectile ion $NO_3^-(H_2O)$ was produced by electron impact on mixtures of H_2O/N_2O, $NO/H_2O/NO_2$, H_2O/NO_2, $O_3/N_2O/H_2O$, $O_3/NO/H_2O$, and $NO/H_2O/NO_2/O_2$. The gas pressure in the ion source was on the order of 0.2 torr for these studies. It was found that the mixtures of H_2O/N_2O and $O_3/N_2O/H_2O$ produced the most intense beams of $NO_3^- \cdot H_2O$. The major product ions formed from the collisional induced dissociation of $NO_3^- \cdot H_2O$, upon impact with the inert gases, Xe and Ar, are NO_3^- and OH^-. The NO_3^- cross section, at maximum, is about three times that of the cross section for the OH^- product channel.

Typical excitation functions for the $NO_3^- \cdot H_2O/Ar$ collisional dissociation reaction are in Fig. 1. Corrections of the apparent translational energy thresholds were made to take account of the projectile ion energy spread and the Doppler motion of the neutral target. These correction procedures have been described previously.[10] The deconvoluted translational energy thresholds for the CID processes yield the bond dissociation energies of $D_0^0(NO_3^-\text{-}H_2O) = 0.4 \pm 0.1$ eV, and $D_0^0(OH^-\text{-}HNO_3) = 3.1 \pm 0.1$ eV. The error limits are estimated on the basis of the ranges of calculated threshold functions which gave a good fit to the experimental data. The Second Law enthalpy change for the clustering reaction, $NO_3^- + H_2O \rightleftarrows NO_3^- \cdot H_2O$, was studied recently by Lee et al[13] over the temperature range 380° to 500°K, and the value of $\Delta H_T^0 = 0.63 \pm 0.01$ eV was derived. The same technique was used previously by Kebarle et al[14], and a Second-Law value of $\Delta H_T^0 = 0.54$ eV was reported. These values are in good agreement with the results of the present study. However, it is interesting to note that there a second threshold is observed at 1.4 ± 0.2 eV for the CID excitation function measured in the present study. Presumably this is indicative of a different reaction channel, although further investigation is needed to fully interpret the present finding. The calculated bond dissociation energy of $D(OH^-\text{-}HNO_3)$ was reported by Kebarle et al,[15] based upon the thermodynamic cycle, $D(OH^-\text{-}HNO_3)\text{-}D(NO_3^-\text{-}H_2O) = D(OH^-\text{-}H^+)\text{-}D(NO_3^-\text{-}H^+)$, to be 3.5 eV, which is in fair agreement with the present direct measurement of (3.1 ± 0.1 eV).

A more detailed description of this study will be submitted for publication in the Journal of Chemical Physics.

Acknowledgement

This work was supported by the Air Force Office of Scientific Research under Contract F44620-76-C-0007 with Wright State University.

References

1. E. E. Ferguson, "Ion-Moleculre Reactions in the Atmosphere," chapter in "Kinetics of Ion-Molecule Reactions," (Ed. P. Ausloos) proceedings of the NATO Advanced Study Institute (Plenum Press, 1979, p. 377).

2. R. S. Narcisi, A. D. Bailey, L. Della Lucca, C. Sherman and D. M. Thomas, J. Atm. Terr. Phys. 33, 1147 (1971).

3. F. Arnold, J. Kissel, D. Krankowsky, H. Wieder, and J. Zahringer, J. Atm. Terr. Phys. 33, 1169 (1971).

4. C. L. Briant and J. J. Burton, J. Chem. Phys. 60, 2849 (1974).

5. A. W. Castleman, Jr. P. M. Holland, D. M. Lindsay, and K. I. Peterson; J. Am. Chem. Soc. 100, 6039 (1978).

6. A. W. Castleman, Jr., P. M. Holland, and R. G. Keesee, J. Chem. Phys. 68, 1760 (1978).

7. A. C. Zettlemoyer, Nucleation (Dekker, New York, 1969) Chapters 1-3.

8. A. W. Castleman, Jr., "Nucleation and Molecular Clustering About Ions," Advances in Colloid and Interface Science "Nucleation," Vol. 10, A. Zettlemoyer, (Elsevier, Amsterdam, (1979), pp 73-128.

9. T. O. Tiernan and R. L. C. Wu, Adv. Mass Spectrom. 7A, 136 (1978).

10. C. Lifshitz, R. L. C. Wu, T. O. Tiernan and D. T. Terwilliger, J. Chem. Phys. 68, 247 (1978).

11. R. L. C. Wu, T. O. Tiernan, and C. Lifshitz, Chem. Phys. Lett. 51, 211 (1977).

12. T. O. Tiernan, B. M. Hughes, and C. Lifshitz, J. Chem. Phys. 55, 5692 (1972).

13. N. Lee, R. G. Keesee and A. W. Castleman, Jr., J. Chem. Phys. 72, 1089 (1980).

14. J. D. Payzant, R. Yamdagni, and P. Kebarle, Can. J. Chem. 49, 3308 (1971).

15. R. Yamdagni and P. Kebarle, J. Am. Chem. Soc. 93, 7139 (1971).

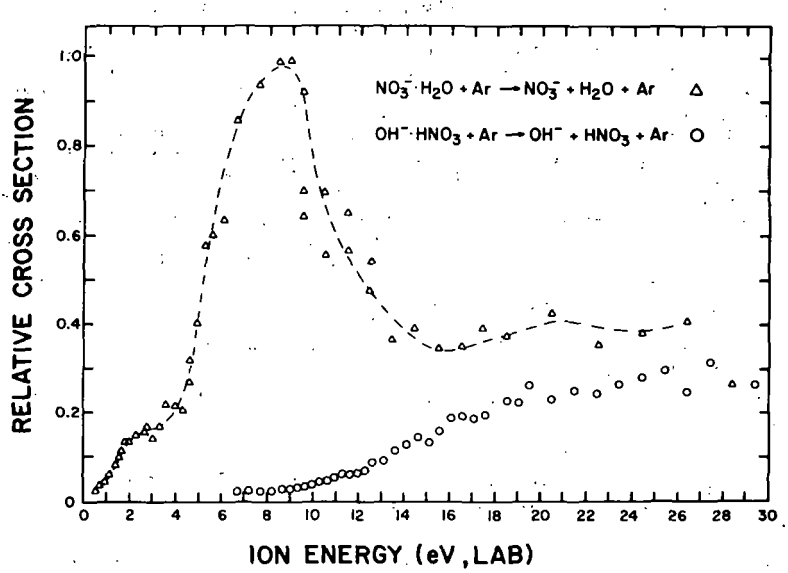

Fig. 1. Relative cross section for the collision-induced dissociation reaction $NO_3^- \cdot H_2O/Ar$ as a function of translational energy Δ- NO_3^- product ion; O- OH^- product ion.

ENERGETICS OF THE CHARGE-STRIPPING PROCESS FROM NEGATIVE IONS OCCURRING IN A DOUBLE-FOCUSING MASS SPECTROMETER, J.E. SZULEJKO, I. HOWE, J.H. BEYNON, Royal Society Research Unit, Univ. College, Swansea SA2 8PP, UK, and J.H. BOWIE, Department of Organic Chemistry, University of Adelaide, South Australia 5001.

A negative ion A^-, having high translational energy, may be converted into a non-decomposing ion A^+ after a glancing collision with a neutral molecule. If both A^- and A^+ are in the ground state and the collision gas acquires no excitation energy, the translational energy difference (ΔE_t) between A^- and A^+ is given by the equation ΔE_t = IE + EA, where IE, EA are the respective ionization energy and electron affinity of A. If IE is known, measurement of ΔE_t affords an estimation of EA.

Charge inversion, as described above, has been monitored in the second field-free region of a double-focusing, reversed geometry VG ZAB-2F mass spectrometer.[1,2] A variety of negative ions was studied, having translational energies up to 8000 eV. Different collision gases were employed. When helium was utilised as collision gas, a simple peak profile was observed for the product ion A^+. The translational energy loss, ΔE_t, as measured at the peak maximum, was used to estimate EA. For example, the electron affinities of Cl, S, S_2, CN, CS_2 and NO_2 were determined within an estimated accuracy of 0.4 eV.[1] Energetics of fragmentation reactions of certain A^+ ions have also been investigated.[2]

The translational energy loss, ΔE_t, has also been measured for a number of negative ionic species generated from electron impact on a CH_4/N_2O mixture at ~0.1 torr. Differences have been observed in the peak profiles for the product ion A^+, depending on the nature of the collision gas. The results employing helium and nitrogen as collision gas are shown in Table 1 for the six ionic species, O^-, OH^-, CN^-, NO^-, O_2^- and CNO^-.

TABLE 1. Energy Changes (eV) in the Reaction $A^- \rightarrow A^+$

A	IE(A)	EA(A)	ΔE min (IE + EA)	ΔE_t (obs) (He)	ΔE_t (obs) (N_2)		
O	13.6	1.5	15.1	14.8±0.5	15±1	22±4	
OH	13.2	1.8	15.0	16.0±0.5	16±1	22±3	
CN	14.0	3.8	17.8	17.5±0.5	17±1	23±3	
NO	9.3	0.1	9.4	17.5±0.5	10±1	17.5±1	26±3
O_2	12.1	0.5	12.6	15.5±0.5	13±2	23±3	
CNO	-	-	-	19.2±0.5	17±1	24±4	

Several features of the charge-inversion peaks are noteworthy. When nitrogen is employed as collision gas, electronic excitation of the collision gas occurs, which is reflected in fine structure observed in the A^+ peak profile. For the reaction $NO^- \rightarrow NO^+$ (with helium as collision gas), NO^+ is formed exclusively in an excited electronic state. However, with nitrogen as collision gas, formation of ground state NO^+ occurs. Analogous reactions appear to occur for O_2^- and CNO^-.

REFERENCES :

1. I. Howe, J.H. Bowie, J.E. Szulejko and J.H. Beynon, J.C.S. Chem. Commun., 983 (1979).

2. J.E. Szulejko, J.H. Bowie, I. Howe and J.H. Beynon, Int. J.Mass Spectrom. Ion Phys., (in press) 1980.

IS THE INTERMOLECULAR ENTROPY CORRECTION IN GAS PHASE IONIC EQUILIBRIA CORRECT?

G.G. Meisels, Department of Chemistry, University of Nebraska-Lincoln

Two years ago, Lias and Ausloos(1) first suggested that the entropy term associated with gaseous equilbria of ions and neutral species may require a term to account for the effect of the long-range (r^{-4}) interaction between the two species and, on the basis of a classical collision theory argument, proposed(1-4) that the correction term be of a form deriving from collision frequencies Z in the forward and reverse directions, that is:

$$K(eq) = (Z(f)/Z(r))(P(f)/P(r))\exp(-\Delta H/RT) = \exp(\Delta S/R - \Delta H/RT) \qquad \text{I}$$

$$\Delta S = R\ln(Z(f)/Z(r)) + R\ln(P(f)/P(r)) = \Delta S(int) + \Delta S(stat) \qquad \text{II}$$

where P designates the conventional "steric" factor. The first term of the right side of Equation II is interpreted as an intermolecular entropy term $\Delta S(int)$ and as a correction to the entropy $\Delta S(stat)$ calculated on the basis of statistical mechanics. Various arguments against this proposal based on microscopic reversibility, transition state theory(5) and statistical mechanics have been offered, and the views of the proposers on these have been discussed extensively.(6) We present here an analysis employing a simple model system which demonstrates that an intermolecular correction term violates an elementary probability theorem and conservation of angular momentum. Since such a term would have to apply to all systems it can not exist.

We choose for demonstration a charge transfer reaction

$$A^+ + B = A + B^+ \qquad (1)$$

between atomic species A and B of exactly equal ionization potentials and degeneracies but different polarizabilities $\alpha(A)$ and $\alpha(B)$. The elementary, fundamental principle that all quantum states of equal energy have equal a-priori probabilities underlies equipartition and all statistical mechanics; it requires without mathematical or further conceptual development that the equilibrium constant for reaction 1 is unity, K(stat) = 1, at all temperatures, as long as the densities are sufficiently low so that the intermolecular interactions can not affect the ionization potentials of A and B unequally.(7) The proposal of Ausloos and Lias,(1-4) however, leads to an equilibrium constant which must be corrected by the ratios of the forward and reverse collision frequencies. In the low temperature regime where all interactions except ion-induced dipole ones may be neglected, the collision frequencies are given by the polarization limit $Z(A^+) = 2\pi e\sqrt{\alpha(B)/\mu}$ is where e is the electronic charge and μ the reduced mass of the system and is equal in both directions.(8) Since there is an equal probability for the charge to be on either species when products separate, the equilibrium constant predicted by Ausloos and Lias is therefore not unity but $K(int) = \frac{1}{2} Z(A^+)/\frac{1}{2} Z(B^+) = \sqrt{\alpha(B)/\alpha(A)}$ and $\Delta S = \Delta S(int) = R\ln\sqrt{\alpha(B)/\alpha(A)}$. The principle of equal a-priori probabilities and the intermolecular correction are mutually exclusive.

The inclusion of an intermolecular correction in this case also violates conservation of angular momentum. The dynamic model for ion-molecule reactions is well established(8-10). It may be applied to a charge transfer reaction by restricting our demonstration system to one in which penetration of the centrifugal barrier (complex formation) is necessary for charge transfer. The description of an ion-molecule charge transfer collision may then be based on defining the maximum angular momentum L(max) (or the maximum impact parameter b(max)) at a given energy for which capture may occur. That is, only those encounters between A^+ and B for which the kinetic energy E exceeds the entrance rotational barrier $V(rot, \text{ in } A^+) = L(4)/(8\alpha(B)e^2\mu^2)$ may lead to capture and therefore collision. Conversely the kinetic energy determines the maximum angular momentum $L(m) = (8\alpha(B)e^2\mu^2E)^{1/4}$ or maximum impact parameter $b(max) = [(2e^2\alpha(B))/E]^{1/4}$ for which collision may occur. This, however, defines only the collision frequency but does not speak to the number of encounters which may lead to products $A + B^+$. In order for these to be formed, the products must be able to separate and this requires of course (11,12) that the (constant) energy exceed the rotation barrier in the exit direction $V(rot, \text{ exit } B^+)$. Since $\alpha(B)$ differs from $\alpha(A)$, $V(rot, \text{ exit } B^+) = V(rot, \text{in } A^+)\alpha(A)/\alpha(B)$. When $\alpha(A) \leq \alpha(B)$ this is no problem in the forward direction because then the exit barrier is always smaller than the entrance barrier, but that is then not the case for the reverse reaction. Now $V(rot, \text{ exit } A^+) = V(rot, \text{ in } A^+)$ and the rate constant (rather than collision frequency) for the reverse reaction is exactly equal to the rate constant or collision frequency for the slower forward reaction. This is illustrated in Figure 1 which shows the effective potential V(e) when m(A) = 40 a.u., m(B) = 20 a.u., and $\alpha(A)$ = 10 a.u., $\alpha(B)$ = 5 a.u. and E = 50 meV for impact parameters of $b(A^+)$ = 0.454 nm and $b(B^+)$ = 0.540 nm, respectively.

While impact parameters less than 0.454 nm permit charge exchange and complex formation in both directions, those between 0.454 and 0.540 a.u. allow the formation of the collision complex from A and B^+, but the complex cannot penetrate the rotational exit barrier to A^+ and B and the complex must redissociate to A and B^+. Therefore k(f)/k(r) = K = 1, and $\Delta S(int) = \Delta S = 0$, and not $R \ln \sqrt{\alpha(A)/\alpha(B)}$ as required by the correction hypothesis. This simple, well-established dynamic argument clearly demonstrates that intermolecular entropy effects are excluded on the basis of simple physical laws alone. It is an interesting conclusion that the effective collision rates of the forward and reverse reactions in equilibria must be the same.

If A and B represent molecular entities, the matter is more complicated because total angular momentum J is conserved and the rotational distributions of reactants and products must be considered also. The formalism is now more complex and requires assumptions(5,12) which make the argument less stringent.

It remains to be understood why some experimental measurements appear to require a collisional correction to yield entropy data consistent with other information. It is possible that the experiments in question may not have been performed under true equilibrium conditions and that a kinetic component remained, then ions are sampled within twenty collisions of their formation(13) the rate of formation in the reverse direction may become an influencing factor. Indeed, equilibrium measurements are also sensitive to relatively minor potential errors in the measurement of gas composition, mass dependent ion detector response, etc.(14).

The support of the Department of Energy under contract EY-2567 is acknowledged gratefully.

Literature Cited:

1. S. G. Lias and P. Ausloos, J. Am. Chem. Soc. 99, 4831 (1977). **2.** S. G. Lias, Chem. Phys. Letters 54, 147 (1978). **3.** P. Ausloos and S. G. Lias, J. Am. Chem. Soc. 100, 1953 (1978). **4.** S. G. Lias and P. Ausloos, J. Am. Chem. Soc. 100 6017 (1978). **5.** J. M. Jasinski, R. N. Rosenfeld, D. M. Golden and J. I. Brauman, J. Am. Chem. Soc. 101, 2259 (1979). **6.** S. G. Lias, in "Kinetics of Ion-Molecule Reactions", Proceedings of NATO Advanced Study Institute in Labaule, France, August, 1978; P. Ausloos, Editor; Plenum Press. **7.** At low density such stabilization would be independent of the nature of the ion but dependent on density and composition because it corresponds to the integral over attraction terms with all neutrals in the system. Those should become unequal for the two ions only at densities approaching those of the condensed phase. **8.** G. Gioumousis and D. P. Stevenson, J. Chem. Phys. 29, 294 (1958). **9.** E. W. McDaniel, "Collision Phenomena in Ionized Gases", J. Wiley, N.Y.(1964) p. 60 ff. **10.** M. Henchman, in "Ion-Molecule Reactions", V.1 , J. L. Franklin, Ed., Plenum Press, New York (1971), p. 101. **11.** This limitation was first pointed out by H. M. Rosenstock, US AEC report JLI-650-3-T, TID-4500 (1959); it is a precursor of phase space theory, [J. C. Light, J. Chem. Phys. 40, 3321 (1964)]. **12.** G. G. Meisels and G. M. L. Verboom, J. Am. Chem. Soc., in press. **13.** S.G. Lias, private commuinication. **14.** A. J. Illies and G. G. Meisels, J. Am. Chem. Soc., submitted.

Figure legend:

Figure 1. Effective potential for charge transfer reactions $A^+ + B \rightleftarrows A + B^+$ at impact parameters of 0.540 nm (upper curve) and 0.454 nm (lower curve) when μ = 13.33 a.u., $\alpha(A) = 2\alpha(B)$ = 10 a.u., and E = 50 meV.

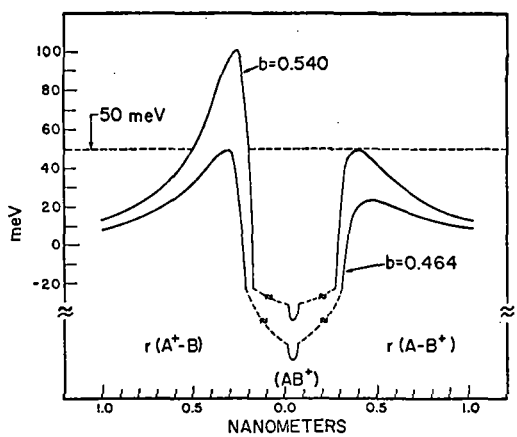

MPMOC8 ON THE QUESTION OF INTERMOLECULAR ENTROPY EFFECTS IN LOW PRESSURE ION-MOLECULE EQUILIBRIA: AN ANALYSIS BASED ON THE LANGEVIN MODEL, WALTER J. CHESNAVICH, HORIA METIU and MICHAEL T. BOWERS, Department of Chemistry, University of California, Santa Barbara, CA 93106

The question of whether or not intermolecular interactions can contribute to entropy changes in low pressure ion molecule equilibria is considered. A simple microcanonical model is developed which yields expressions for the forward rate constant $k_f(T)$ and the reverse rate constant $k_b(T)$ in the equilibria $A^+ + B \rightleftarrows C^+ + D$. The model conserves energy and angular momentum and is shown to obey the principle of microscopic reversibility (detailed balance). This model is shown to be consistent with $\Delta S^\circ_{id} = R\,\ell n\, Q_b/Q_f$ where Q_f and Q_b are the ideal partition functions of the reactants and products. These conclusions are in disagreement with recently published work which asserts that $\Delta S^\circ = \Delta S_{int} + \Delta S_{id}$, where $\Delta S_{int} = R\,\ell n(Z_f/Z_b)$ and Z_f and Z_b are the capture collision rate constants. It is shown this recently published expression violates microscopic reversibility. A new expression for capture rate constants for endoergic reactions is introduced and is used to show that that the origin of the disagreement mentioned above lies in the misuse and misinterpretations of the reaction probabilities for the forward and reverse reactions in generating the expression $\Delta S^\circ = \Delta S_{int} + \Delta S_{id}$.

MPMOC9 THERMONEUTRAL ISOTOPE EXCHANGE REACTIONS OF CATIONS IN THE GAS PHASE, P. AUSLOOS and S. G. LIAS, Chemical Thermodynamics Division, National Bureau of Standards, Washington, D. C. 20234

The rate constants of a number of isotope exchange reactions of the type ($RD^+ + MH \rightarrow RH^+ + MD$) have been measured. In all but two cases, the corresponding deuteron transfer reaction ($RD^+ + MH \rightarrow R + MHD^+$) is endothermic. As reported before (D. F. Hunt, et al, 26th Annual Conf., ASMS), the probability that a collision results in an isotope exchange shows a general decrease with increasing endothermicity of the corresponding deuteron transfer reaction from RD^+ to MH. This, and the fact that exchange is not observed when there is no H atom in the neutral molecule at the site of proton transfer (i.e. carbonyl compounds) identifies the transition state for isotope exchange with the transition state for proton (deuteron) transfer. An analysis of the results shows that when the formation of the ($R \cdot MHD^+$) complex is predicted to be highly exothermic for ($RD^+ + MH$) reactants, isotope exchange occurs with an efficiency close to unity, and when the formation of the ($R \cdot MHD^+$) complex is endothermic, exchange does not occur, or occurs with a very low rate constant. For reactants for which the proton transfer in the complex ($RD^+ \cdot MH \rightarrow R \cdot MHD^+$) is predicted to be neither highly exothermic nor endothermic, it is shown that the efficiency of reaction can be predicted by an expression: $P = \exp(-K/s)$ where s is the number of oscillators in the complex and K is a constant whose value depends approximately on the electronegativity of the atom in MH at which proton transfer occurs. When MH is a halogen-substituted benzene, factors involving the electron-donating and withdrawing effects of the halogen substituents on the ring predominate over the above-discussed factors in determining the probability of isotope exchange.

MPMOC10 NEAR THERMAL CHARGE TRANSFER REACTIONS IN Kr/CO and Xe/O_2 MIXTURES, JAMES B. LAUDENSLAGER, Jet Propulsion Laboratory, California Institute of Technology, Pasadena, CA 91103.

The near resonant asymmetric charge transfer reactions of Kr^+/CO, CO^+/Kr, Xe^+/O_2, and O_2^+/Xe have been studied using low pressure trapped ICR techniques. Reaction rate constants for all the reactions have been measured and equilibrium measurements have also been determined for the two reaction systems. The O_2^+/Xe rate constant exhibited a strong dependence on the internal energy of the O_2^+ ion. In order to measure the O_2^+/Xe rate constant for O_2^+ formed in the ground electronic state and the lowest vibronic level, it had to be generated by the Xe^+/O_2 reaction using a triple resonance ICR technique.

The ratio of measured rate constants for the forward and reverse reactions were compared to the experimental equilibrium constants determined using various ICR methods and these values were compared to equilibrium constants derived from statistical mechanics. For the case of Kr/CO all the experimental and calculated values for K_{eq} were in good agreement, but for the Xe/O_2 case there was a discrepancy between the measured and the calculated value for K_{eq}. It is possible for the Xe/O_2 case that only a steady state is obtained in the low pressure ICR experiments and a true thermodynamic equilibrium is not reached.

INFRARED CHEMILUMINESCENCE STUDIES OF ION-MOLECULE REACTIONS

Timothy S. Zwier, M. Matti Maricq,[a] C. J. S. M. Simon,[b]

Veronica M. Bierbaum, G. Barney Ellison[c] and Stephen R. Leone[d]

Department of Chemistry
University of Colorado
and
Joint Institute for Laboratory Astrophysics
National Bureau of Standards and University of Colorado
Boulder, Colorado 80309

Over the past several years, substantial progress has been made in understanding elementary exoergic neutral reactions by studying initial vibration and rotation product state distributions.[1-4]

Until recently, there has been very little work on the product state distributions of ion-molecule reactions. The most important reason for this delay is the difficulty in obtaining enough reactant ions under well-characterized conditions for detection of the excited product species. We report here the first quantitative results on vibrational product state distributions in thermal energy ion-molecule reactions.[5,6]

Our experimental method utilizes detection of the infrared chemiluminescence from the ion-molecule reaction products in a flowing afterglow (Figure 1). Chloride ion densities of about $10^8/cm^3$ are obtained in the reaction zone by electron bombardment of CCl_4. The ions are modulated by an ion shutter to distinguish the ion-molecule product emission from other interfering emissions that may be present. Neutral reactants are added immediately before the viewing region and the infrared chemiluminescence is detected with a large area 77K InSb detector.

Two thermal proton abstraction reactions have been studied in detail:

$$Cl^- + HBr \rightarrow HCl(v=0,1) + Br^- \qquad \Delta H = -9.8 \text{ kcal/mole}$$

$$Cl^- + HI \rightarrow HCl(v=0,1,2) + I^- \qquad \Delta H = -19.0 \text{ kcal/mole}$$

The initial relative HCl product vibrational distribution for the reaction $Cl^- + HI$ was determined to be $N_{v=1} = 1.00$, $N_{v=2} = 0.85 \pm 0.05$. The ratio of the total emission from $Cl^- + HBr$ to that from $Cl^- + HI$ was measured to be $39 \pm 2\%$. These results suggest substantial disposal of energy into product vibrations in these proton abstraction reactions. Work is presently under way on the analogous series of fluoride ion reactions with hydrogen halides which qualitatively confirms this conclusion.

Theoretical analyses of these results must take account of the deep attractive well in the potential energy surface produced by the ion-induced dipole and ion-permanent dipole forces. Little is known about the position, depth, or shape of this well, nor about its ultimate effects on the dynamics of ion-molecule reactions.

---

[a]Current address: Physical Chemistry Laboratory, Oxford University, Oxford OX1 3QZ, England.

[b]Permanent address: Physical Chemistry Laboratory, Oxford University, Oxford OX1 3QZ, England.

[c]Alfred P. Sloan Fellow.

[d]Staff Member, Quantum Physics Division, National Bureau of Standards, and Alfred P. Sloan Fellow.

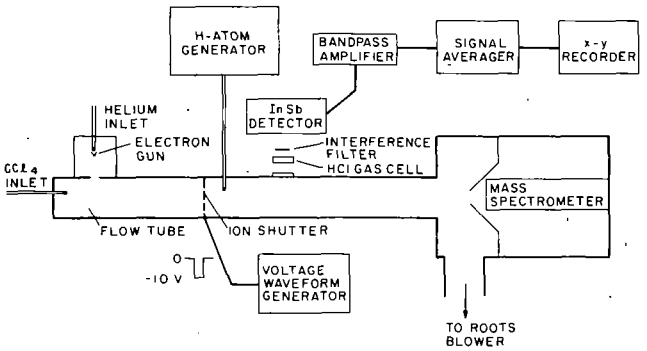

Figure 1. Schematic of flowing afterglow infrared chemiluminescence apparatus.

The initial vibrational product state distribution has also been obtained for the thermal associative detachment reaction:

$$C\ell^- + H \rightarrow HC\ell(v=0,1,2) + e^- \qquad \Delta H = -19.0 \text{ kcal/mole}$$

The ratio of HCℓ(v=2) to HCℓ(v=1) population formed in the reaction is $N_{v=2}/N_{v=1} = 0.60 \pm 0.03$. Allan and Wong[7] have shown a greater than tenfold increase in the cross section for the reverse process, dissociative attachment, with each increase in the initial vibrational level in HCℓ. This apparent contradiction is resolved as follows: Since the reduced mass drops by a factor of 2000 during the transformation from $C\ell^-$ + H to HCℓ + e^-, most of the angular momentum associated with the incoming particles, μvb, will remain as rotation in the product HCℓ, j_{rot}, i.e. $\mu vb = \mu' v' b' + j_{rot} \sim j_{rot}$. For a typical impact parameter of 4 Å associated with the near-Langevin rate constant of the reaction, the product HCℓ molecule possesses a J-value of 13. This corresponds to an average rotational energy of about 5 kcal/mole, while the HCℓ(v=2) energy level is only 3.5 kcal/mole below the average energy available to the products. Thus, energy conservation prohibits a high degree of rotational excitation from occurring simultaneously with HCℓ(v=2) formation. The net result is to restrict the range of impact parameters, and hence the cross section, for producing the v = 2 channel. In this way, HCℓ(v=2) formation occurs whenever possible, within the restrictions placed on it by angular momentum and energy conservation.

Bibliography

1. I. W. M. Smith, Adv. Chem. Phys. 28, 1 (1975).
2. J. M. Farrar and Y. T. Lee, Ann. Rev. Phys. Chem. 25, 357 (1974).
3. J. P. Toenies, in Physical Chemistry: An Advanced Treatise, edited by H. Eyring, D. Henderson and W. Jost (Academic, New York, 1974), Vol. VIA, Chap. 6.
4. J. C. Polanyi, Acc. Chem. Res. 5, 161 (1972).
5. T. S. Zwier, V. M. Bierbaum, G. B. Ellison and S. R. Leone, J. Chem. Phys., to be published.
6. T. S. Zwier, M. M. Maricq, C. J. S. M. Simpson, V. M. Bierbaum, G. B. Ellison and S. R. Leone, Phys. Rev. Lett. 44, 1050 (1980).
7. a) M. Allan and S. F. Wong, in Proceedings of the Gaseous Electronics Conference, 1979, Pittsburgh.
   b) S. F. Wong, in Symposium on Electron-Molecule Collisions, edited by I. Shimamura and M. Matsyawa (University of Tokyo, Tokyo, Japan 1979), p. 111.

MPMOC12 ELECTRON AFFINITY MEASUREMENTS USING EQUILIBRIUM ELECTRON TRANSFER REACTIONS, ELAINE K. FUKUDA and R.T. McIVER, JR., Dept. of Chem., Univ. of Cal., Irvine, CA 92717.

Electron affinities have historically been difficult quantities to measure accurately. With the advent of laser spectroscopic techniques atomic electron affinities are now known very accurately. However, molecular electron affinity determinations have intrinsic problems. These problems involve differences in structure between the ion and neutral and their Franck-Condon overlaps as well as the possible existence of hot bands.

To circumvent these problems, we determine relative electron affinities by studying equilibrium electron transfer reactions using a pulsed ion cyclotron resonance (ICR) spectrometer. Direct measurement of ion and neutral concentrations allow calculation of an equilibrium constant and therefore the free energy change. Multiple equilibrium overlaps have been used to verify all energy gaps. Double resonance experiments have been used to verify that electron transfer occurs in both directions.

In this paper we report a relative electron affinity scale which covers a 30 kcal/mol range with the benzophenone, nitrobenzene and benzoquinone families of compounds. To assign absolute electron affinities, various molecules with accurately known electron affinities are tied into the scale via direct equilibrium (for odd-electron species) or by double resonance (for even-electron species) bracketing techniques. After the relative scale is anchored to these accurate absolute known values, the scale can then be used as a check on other electron affinity values determined using different methods as well as being used to generate new electron affinity values.

COMPARATIVE ION-MOLECULE CHEMISTRY OF A CARBENE ANION RADICAL AND THE CORRESPONDING CARBANION. Richard N. McDonald,* A. K. Chowdhury, and D. W. Setser, Department of Chemistry, Kansas State University, Manhattan, Kansas 66506.

Cyclopentadienylidene anion radical (c-$C_5H_4^{\cdot-}$; m/z 64) was produced from diazocyclopentadiene by dissociative electron attachment in a flowing afterglow apparatus (298°K, v = 80 m s^{-1}, P_{He} = 0.5 torr). The reaction between c-$C_5H_4^{\cdot-}$ and CH_3OH proceeded exclusively by H· abstraction from the O-H group. However, the reactions of c-$C_5H_4^{\cdot-}$ with C_2H_5OH, $(CH_3)_2CHOH$, and $(CH_3)_3COH$ occurred by varying amounts of H· abstraction and protonation pathways depending on the ROH acidity. These bracketing results give PA(c-$C_5H_4^{\cdot-}$) = 377±2 kcal $mole^{-1}$ and ΔH_f°(c-$C_5H_4^{\cdot-}$) = 70.7±3.2 kcal $mole^{-1}$. The results of studies of H· abstraction by c-$C_5H_4^{\cdot-}$ yield a lower limit of HA(c-$C_5H_4^{\cdot-}$) from which ΔH_f°(c-$C_5H_4^{\cdot-}$) ≥ 67.7±3 kcal $mole^{-1}$ was calculated, in good agreement with the value given above. The IP(c-$C_5H_4^{\cdot-}$) = EA(c-C_5H_4) was determined to be 54.4±2 ≥ EA(c-C_5H_4) ≥ 41.5±7 kcal $mole^{-1}$ from the results of reactions of c-$C_5H_4^{\cdot-}$ with NO_2 and C_6F_6.

The cyclic structure of anion radical m/z 64 was confirmed by the fact that the same ion-molecule chemistry (rate constants and products) resulted from the anion product, c-$C_5H_5^-$, produced in the reactions (i)-(iii). The observed PA of c-$C_5H_4^{\cdot-}$ establishes the

$$\left.\begin{array}{ll}\text{(i)} & C_5H_4^{\cdot-} + CH_3OH \\ \text{(ii)} & \text{c-}C_5H_6 + O^{\cdot-} \\ \text{(iii)} & \text{c-}C_5H_6 + {}^-OCH_3\end{array}\right\} \longrightarrow \text{c-}C_5H_5^- \xrightarrow[\text{reactants}]{\text{neutral}} \text{products}$$

electronic configuration of this carbene anion radical as a σ-radical π-anion ($\sigma^1\pi^2$); the PA of the alternative $\sigma^2\pi^1$ species should be similar to that of phenyl anion (PA($C_6H_5^-$) = 398±7 kcal $mole^{-1}$).

c-$C_5H_4^{\cdot-}$ reacted with $H_2C{=}CHCN$ and $H_2C{=}CHCO_2CH_3$ yielding the (M-H) adducts. A slower reaction was measured between c-$C_5H_4^{\cdot-}$ and $H_2C{=}CHCl$, but no reaction was observed with $H_2C{=}CHF$ or $H_2C{=}CH_2$. The substituent effects of X in $H_2C{=}CHX$ on the rate constants for these reactions lead to the conclusion that these processes involve nucleophilic (not radical) additions by c-$C_5H_4^{\cdot-}$. The reactions of c-$C_5H_4^{\cdot-}$ with CH_3Br and CH_3Cl proceeded by both H· abstraction and nucleophilic displacement.

Similar ion-molecule reactions with c-$C_5H_5^-$ (from c-C_5H_6 + ${}^-OCH_3$) to those given above for c-$C_5H_4^{\cdot-}$ have been examined. Comparing these results and the known thermochemical data for c-$C_5H_5^-$, the following conclusions result:

(a) PA(c-$C_5H_4^{\cdot-}$) > PA(c-$C_5H_5^-$) by 21±4 kcal $mole^{-1}$, and

(b) $k_{\text{c-}C_5H_4^{\cdot-}} > k_{\text{c-}C_5H_5^-}$ by 60-100 in their nucleophilic reactions with $H_2C{=}CHX$ and CH_3Br.

The fast ion-molecule reaction of c-$C_5H_5^-$ with $(CF_3)_2CHOH$ proceeded exclusively by proton transfer ($\Delta H_{rxn} \leq -5$ kcal $mole^{-1}$). With less acidic alcohols, e.g. $(CH_3)_3COH$, C_2H_5OH, and CH_3OH, c-$C_5H_5^-$ formed the c-$C_5H_5^-$(HOR) clusters. The reaction of c-$C_5H_5^-$ with CF_3CH_2OH was observed to occur by the sequential production and decay of the cluster ions c-$C_5H_5^-$-($HOCH_2CF_3$) (1) and $CF_3CH_2O^-(HOCH_2CF_3)$ (2) followed by formation of the stable cluster $CF_3CH_2O^-(HOCH_2CF_3)_2$. The suggested mechanism for the reaction of c-$C_5H_5^-$ and CF_3CH_2OH is initial π-clustering to 1 followed by reaction of 1 with CF_3CH_2OH to yield cluster 2 and

the product of proton transfer, c-C_5H_6. This cluster-to-cluster anion switch mechanism must be driven by the increased stability of cluster 2 ($\geq 8\pm3$ kcal mole^{-1}) compared to that of cluster 1. We believe that these results are directly related to "contrathermodynamic" proton transfers which occur in solution, and to several gas-phase processes.

CONTINUOUS ON LINE MONITORING OF HOT COMBUSTION GASES BY APCI/MS, T. SAKUMA, J. FULFORD, J.B. FRENCH, N.M. REID AND B.A. THOMSON, SCIEX INC., 55 Glencameron Road, Unit 202, Thornhill, Ontario, Canada, L3T-1P2

There is an increasing desire to analyse the effluents of combustion processes, both to study the formation of products such as NO_x, SO_x, PAH, etc. which are of environmental concern, as well as to monitor the destruction efficiency of toxic substances. One instance of the latter which is receiving increased attention involves the search for a combustion source which is capable of destroying the large existing stockpiles of hazardous compounds (such as PCBs) and waste materials. The tests which are necessary to prove the safety of such a technique requires that the combustion gases be quantitatively analysed for traces of the compounds in order to ensure their complete destruction. In addition, certain industrial processes may be able to be studied and optimized by monitoring the waste or product gases of a burner for signature compounds indicative of proper or improper combustion conditions. In almost all of the above cases, the analysis would benefit from the ability to monitor the combustion gases continuously in real-time, in order to allow destruction efficiencies and residue levels to be measured continuously, or to allow real time process control.

This paper describes the use of an atmospheric pressure chemical ionization/mass spectrometer (APCI/MS) system (which has been previously used to analyse ambient air for the presence of trace compounds in real time[1,2]) for continuously monitoring the PCB levels in hot exhaust gases from a cement kiln, and for analysing the stack gas for a variety of other compounds, including PAHs. The latter work is preliminary, but has already revealed the potential of this technique in the area of process control.

EXPERIMENTAL - The TAGA™ 3000 is an APCI/MS system which has been connected to a cement kiln with a 25 m heated glass sampling line. The TAGA™ is located in a van at the foot of the stack, and the gases are drawn at 0.2 liters per second from a duct connecting the kiln to the stack. At the sampling position, the gas temperature is about 225°C and the water content is about 40%. The gas passes immediately through a sintered quartz filter in order to remove the larger particles, and then is diluted by adding 1.8 liters per second of heated ambient air. The gas passes through a 1" ID glass pipe which is kept at a temperature of about 150°C with heating tape and insulation. About 2 m upstream of the instrument, the gas temperature is lowered to 50°C by passing it through a thermostated heat exchanges. The dilution acts to lower the dewpoint of the gas to less than 50°C in order to prevent condensation in the ion source, as well as to reduce (to an acceptable level) the concentration of species in the gas which interfere in the chemical ionization process.

The analysis for PCBs is performed by using a specially designed adsorber[3] which traps the compounds from the gas for a period of two minutes, and then is heated to release them into a pure carrier which leads into the ion source. This allows repetitive measurements of the PCB levels to be obtained approximately every four minutes. Direct analysis of the stack gas for the presence of SO_x, PAH's, etc., has also been performed by drawing the diluted stack gas into the ionization chamber for continuous analysis.

RESULTS - The use of the adsorber or preconcentrator for the PCBs has allowed lower detection limits to be reached than could be achieved by direct analysis. Benzene charge transfer is used to ionize the PCBs, which are detected and measured as total monochlorobiphenyl, total dichlorobiphenyl, etc., rather than as individual isomers. The use of benzene as a charge transfer reagent makes the analysis only sensitive to those compounds which have lower ionization potentials than benzene, so that a continuous class separation of the species in the stack gas is effected. Nevertheless, some chemical interferents with the PCBs remain. The special software which controls the data acquisition, has therefore been designed to monitor two chlorine isotopes for each PCB species, and calculate isotope ratios and correlation coefficients. Identification of PCB in the stack gas is based on the molecular weight of the ion and the correct chlorine isotope ratio, as well as high correlation coefficients between the individual species. This technique has allowed the detection of PCBs (added to the stack gas in the sample line in a controlled amount) down to the level of 200 to 300 ng/m^3 for each of the six species (monochloro- to hexachlorobiphenyl). Detection limit is defined as a signal of 3 times the standard deviation of the background signal. Figure 1 shows the response curve for pentachlorobiphenyl in stack gas with the two largest isotopes.

The transfer efficiency of the sample line is an important concern, and has been measured by injecting PCBs into the sampling line immediately outside the duct (upstream of the filter), and into the sampling line just upstream of the instrument, and comparing

the responses. The transfer efficiency for all six chlorinated species is greater than 95%. Changes in concentration at the duct result in an almost immediate change at the instrument, so that within the limits of the 2 minute integration, the PCB levels can be monitored in real time. The technology to do continuous monitoring during a burn of fuel to which PCBs have been added is therefore in place; however, legal considerations have so far delayed the actual test burn.

PAHs have been injected into the stack gas in the sampling line in order to study the capability to monitor these species. The test was performed both by using the 2 minute adsorption system, and by drawing the diluted stack gas directly into the ionization chamber. Figure 2 shows a portion of the mass spectrum of the stack gas containing a mixture of PAHs, obtained by analysing the gas directly. Although detection limits have not been measured, preliminary indications with the adsorber suggest that they should be at least as low as the detection limits of PCB in the stack gas. Both PAHs and PCBs can also be measured in ambient air at levels down to the low ng/m^3 level.

Mass spectra of the stack were acquired while the oxygen content of the kiln was varied. Several of the prominent mass peaks which were tentatively identified suggest the presence of a variety of organic species, at the trace level, including ammmonia, alkyl and aryl amines, aldehydes, ketones, esters, polycyclic aromatic compounds, and heterocyclic compounds. The levels of these compounds appeared to be inversely correlated with the oxygen content of the kiln. In addition, mass peaks corresponding to Cl^-, HSO_4^- and $HSO_4^-(H_2SO_4)$ showed the presence of chlorinated species (which are added to the kiln to reduce the alkali content of the cement) and sulfuric acid. The presence of SO_3 was also indicated by a cluster containing this species.

CONCLUSION - The ability to sample hot moist stack gases for the analysis of trace organic and inorganic compounds in real time has been tested and proven by an on-line APCI/MS system at a coal fired cement kiln. PCBs and other compounds can be detected and identified in the gas at low levels on a continuous or semi-continuous basis. Being on-line in the combustion process appears to offer the possibility of real-time optimization of certain industrial processes by monitoring the gas stream for trace species.

1. D.A. Lane, B.A. Thomson, A.M. Lovett and N.M. Reid, Proc. 8th Int. Mass Spectrom. Conf., Oslo, Norway, August, 1979.
2. N.M. Reid, J.B. French, J.A. Buckley, D.A. Lane, A.M. Lovett and G. Rosenblatt. Proc. 4th Joint conference on Sensing of Environmental Pollutants, New Orleans, 1978.
3. B.A. Thomson, D.A. Lane, T. Sakuma, N.M. Reid, J.B. French, E.S.K. Quan and S. Nacson. Proc. 27th Annual Conf. on Mass Spectrom. and Allied Topics, Seattle, June, 1979.

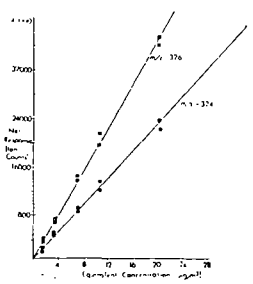

FIGURE 1. Instrument response vs. concentration of pentachlorobiphenyl (in μg/m^3) in the stack gas, measured at two different isotopes (m/z = 324 and m/z = 326)

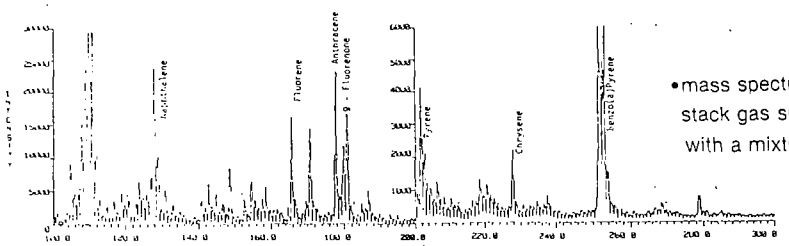

•mass spectrum of stack gas spiked with a mixture of PAH's

FIGURE 2.

GC/MS INVESTIGATIONS OF HETEROCYCLIC PARTICULATE ORGANIC MATTER FOUND IN THE ENVIRONMENT. R. C. Lao, R. S. Thomas and S. W. Lee. Chemistry Division, Air Pollution Control Directorate, Environment Canada, Ottawa, Canada, K1A 1C8

Increasing concern about analysis of the organic constituents of polluted environment has focussed attention on heterocyclic particulate organic matter (POM) because of the biological activity of many of these compounds. In terms of compositional complexity, heterocyclic POM cover the spectrum of simple to extremely complex. With increasing use of fossil fuels and the growing importance of coal and oil shale, the pyrolysis products of which are a rich blend of polycyclic and heterocylcic POM, raise many environmental and public health questions.

Environmental samples may contain POM from many of these sources. This implies that there is a need for separation and analytical techniques which will adequately resolve the numerous POM series. During the past two decades, this laboratory has maintained a major effort to elucidate the measurement of polycyclic POM in a variety of environmental samples. Recently we initiated a program to develop the analytical procedures for heterocyclic POM The instrument used is a Finnigan 4023 GC/MS with Incos data system. This is properly calibrated by FC-43 and DFTPP following the standard procedure. A 6 foot glass column (2 mm I.D.) packed with OV-17 was used to record the mass spectra of the POM compound. For the determination of relative retention times and response factors of these compounds a Perkin-Elmer Sigma-1 gas chromatograph equipped with high resolution glass capillary column was used in this study. The operational parameters are:

Flow pressure - helium	1.8 Kg/cm^2
Injection temperature:	300°C
FID temperature:	300°C
Initial temperature:	80°C held 2 minutes, program rate 6°C/min
Final temperature:	260°C

Column: Quartz capillary, 50 m, I.D. 0.2 mm, packed with liquid phase SP 2100, deactivated carbowax 20M

Injection system: Grob splitless

Ten of the aromatic nitrogen/oxygen compounds available from our POM stock were investigated. A small amount of standard compound was dissolved in spectro grade methylene chloride which has been distilled from glass. Of this sample solution 0.1-0.5 microliter was injected into the GC and GC/MS. The compounds investigated in this work were:

1. 7,8-benzoquinoline, $C_{13}H_9N$, M.W. = 179
2. Iminodibenzyl (10,11-dihydro-5H-dibenz(b.f.)-azepine), $C_{14}H_{13}N$, M.W. = 195
3. 2-nitrofluorene, $C_{13}H_9NO_2$, M. W. = 211
4. 9-anthracenecarbonitrile, $C_{14}H_9CN$, M. W. = 203
5. 9,10-dihydroacridine, $C_{13}H_{11}N$, M. W. = 181
6. 2,3-diaminonaphthalene, $C_{10}H_{10}N_2$, M. W. = 158
7. 4-amino-9-fluorenone, $C_{13}H_9NO$, M. W. = 195
8. 3-aminofluoranthene, $C_{16}H_9NH_2$, M. W. = 217
9. 1,2-benzanthraquinone, $C_{18}H_{10}O_2$, M. W. = 258

and 10. 6-aminochrysene, $C_{18}H_{13}N$, M. W. = 243

Each of the compounds is reported to be biologically active and each has been found to be present in the environment. The significance of the mass spectra of these compounds is the abundant parent ion peak and simple fragmentation patters which readily establish their identity and presence in any sample.

Mass spectra of these compounds are not included in any existing reference books. Spectral data will be provided to the workers who are investigating heterocyclic POM and to the EPA/NIH mass spectral data base.

Work will be underway to determine and identify the heterocyclic fractions of various environmental samples, such as airborne particulate, engine exhaust, incinerator emissions with added attention focussed on the heterocyclic POM which have not been reported previously.

FUNCTIONAL ASSESSMENT OF ADEQUATE GC/MS INSTRUMENTAL OPERATION IN THE MASTER ANALYTICAL SCHEME

by
D. PERRY, J. RYAN, L. RANDO and J. GEBHART
Department of Analytical Chemistry, Gulf South Research Institute
New Orleans, LA 70186
and
J. BURSEY, K. TOMER, AND E. PELLIZZARI
Research Triangle Institute,
Research Triangle Park, NC 27709

INTRODUCTION. As part of the development of EPA's Master Analytical Scheme (MAS), efforts have been made to provide the analyst using the MAS with a means of verifying correct operation of a GC/MS instrument from both chromatographic and mass spectrometric perspectives. For chromatographic evaluations, two multicomponent performance standard mixtures were developed, one for extractable compound analysis (semivolatiles) and a second for purgeable compound analysis (volatiles). Mass spectrometric performance (high/low mass balance) were assessed by using decafluorotriphenylphosphine (DFTPP) for extractable compounds and perfluorotoluene (PFT) for analysis of purgeable compounds.

TUNEUP MIXTURE FOR EXTRACTABLE COMPOUND ANALYSIS. To provide the analyst using the MAS with a means of verifying reproducibility and accuracy of data (acquisition and interpretation) it is necessary to monitor daily overall performance of the GC/MS system. Consequently, a specific compound mixture for a nonpolar capillary column was developed. Figure 1 illustrates the reconstructed gas chromatogram (RGC) of the test mixture for base/neutral extractable compounds. The RGC was obtained using a 25 m x 0.50 mm i.d. SCOT column with the flow rate of He at 3 ml/min. Backflush flow rate was 32 ml/min. A temperature program of 50°C (held for 5 min) to 200°C at 20°C/min was used. Sample size was 1 µl of performance standard (splitless injection) at a concentration of 40 ng/µl of each component. GC injection port and mass spectrometer transfer line temperatures were both 250°C.

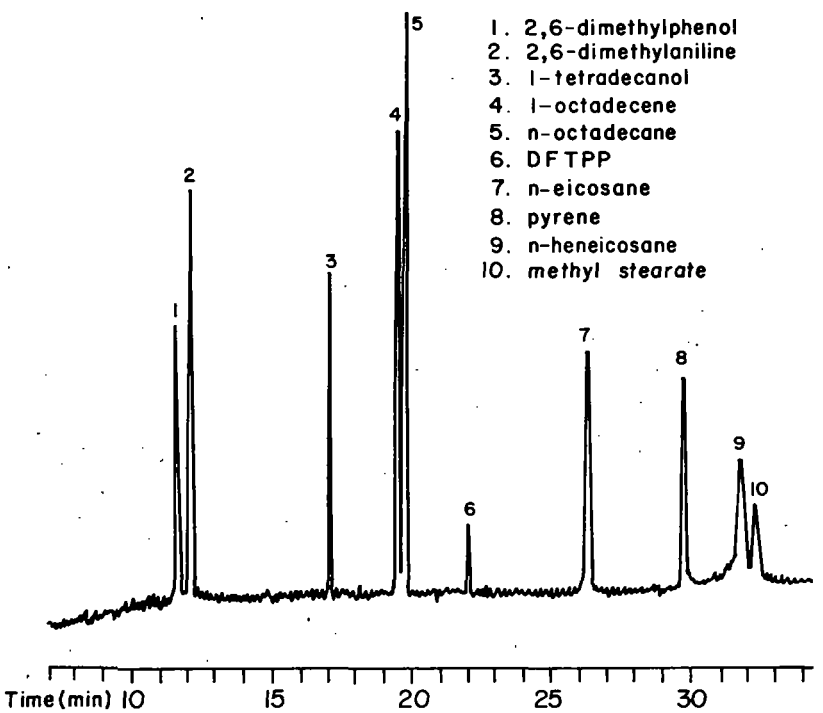

Figure 1. Reconstructed gas chromatogram of performance standard for extractable compound analysis.

The acidity/basicity of the column was measured as the ratio of peak areas of 2,6-DMA and 2,6-DMP. The ratio should be between 0.5 and 2.0 if the column's performance is to be satisfactory. The polarity of the column was measured by peak area of 1-tetradecanol, pyrene, or methyl stearate relative to that of n-eicosane. In each case, the ratio should be at least 0.2. The sensitivity of the system was measured by the signal-to-noise ratio obtained for pyrene. The ratio should be at least 40. The resolution of the column was assessed by the separation achieved between n-octadecane and 1-octadecene. There should be at least a 50 percent valley between the two peaks. The high/low mass spectral balance of the system was determined from the mass spectrum of DFTPP. The ratio of intensities between m/z 442 and 198 should be 0.4 to 0.7. The GC transfer line characteristics were evaluated by using methyl stearate. If the transfer line is inadequately heated, the methyl stearate will tail. A symmetrical peak for methyl stearate verifies that large, nonvolatile molecules can elute from the capillary column into the mass spectrometer.

TUNEUP MIXTURE FOR PURGEABLE COMPOUND ANALYSIS. Figure 2 shows the RGC of the performance standard for purge-and-trap analysis. Initially, 350 ng of each component was loaded onto a Tenax GC cartridge. The compounds were desorbed at 270°C for 8 min with a helium flow rate of 15 ml/min. The RGC was obtained by using a 25 m X 0.25 mm i.d. WCOT column with the flow rate of helium at 1.9 ml/min. A temperature program of 30°C (held for 2 min) to 250°C at 4°C/min was used. The mass spectrometer transfer line was 250°C.

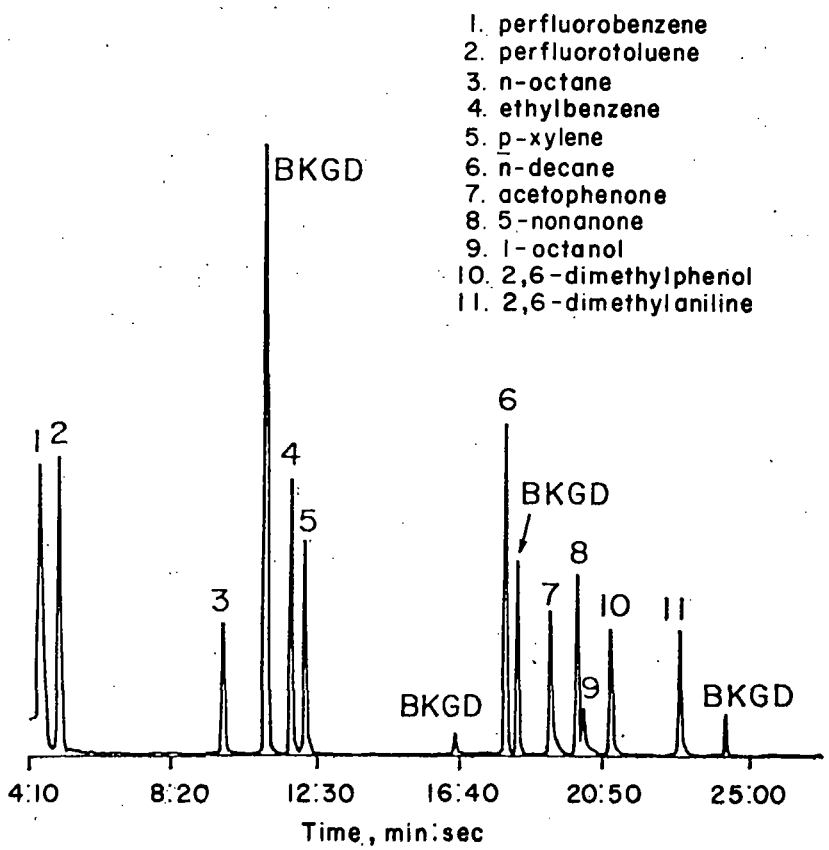

Figure 2. Reconstructed gas chromatogram of performance standard for purge-and-trap analysis.

The acidity/basicity of the column was measured as the ratio of peak areas of 2,6-DMA and 2,6-DMP to acetophenone. The ratio should be between 0.5 and 2.0. The absorptivity of the column was measured by the ratio of peak areas of 1-octanol to 5-nonanone. Because 1-octanol does not purge well, this value is subject to modest variation. Each analyst should establish baseline ratio values for his particular purge-and-trap systems. The resolution of the column was assessed by the separation achieved between ethylbenzene and p-xylene. There should be at least a 90 percent valley between the two peaks. Octane and decane were used to determine the HETP of the column. The mid/low mass spectral balance of the system was monitored by the mass spectrum of PFT. The ratio of m/z 217 and 69 should be between 0.2 and 0.4.

MASS SPECTROMETRIC PERFORMANCE CRITERIA. Tuning of a mass spectrometer is extremely important since the criteria used in tuning an instrument affects ion abundance measurements and, thus, quantitative data. Since the MAS will emphasize the use of capillary columns, the tuning standards were introduced not only by reservoir or direct probe, but also by GC column. A combination of FC-43 and DFTPP were chosen as tuning standards because of the ease of introduction and suitability for determination of high mass resolution and sensitivity for quadrupole mass spectrometers. FC-43 was used initially to tune the instruments; DFTPP and (PFT) were subsequently used to monitor the acceptability of tune for analyses resulting from extraction (semivolatiles) or purge-and-trap (volatiles) techniques, respectively.

Since GC/MS systems produced by different manufacturers will be used in the MAS, an acceptable tune was defined in terms of quality of spectrum achieved (i.e., a reasonable mass balance observed in a spectrum of DFTPP or PFT, rather than by defining the step-by-step means of achieving that tune). Eichelberger et al. (1) have selected DFTPP as a standard in previous work performed under their auspices. These criteria have primarily been set up to insure reasonably high mass intensity. In general, these criteria proved to be adequate to limit and define day-to-day variations in ion abundances obtained from DFTPP in the tuneup mixture. However, for any given instrument, a stable tune within the range of acceptable ion abundances must be defined and maintained. Minimal deviation (± 10 percent from that particular set of conditions) can be tolerated by the analyst.

ACKNOWLEDGMENT. This work is supported by the U.S. Environmental Protection Agency under Contract No. 68-03-2704.

Eicheberger et at., Anal. Chem., 47 7,995 (1975).

MPMP5 ESTIMATION OF RELATIVE RESPONSE FACTORS FOR ANALYSIS OF ORGANICS IN WATER

K. B. Tomer, J. T. Bursey, E. D. Pellizzari, Research Triangle Institute, P. O. Box 12194, Research Triangle Park, NC 27709 and J. Ryan, L. Rando and D. Perry, Gulf South Research Institute, P. O. Box 26518, New Orleans, LA 70186.

In the mass spectrometer, there are many variables which can affect the accuracy and precision utimately achieved in analytical determinations. The effect of several of these parameters, particularly the tuning of the ion source, can be widely variable from instrument to instrument, and prospective users of the Master Analytical Scheme will employ a wide variety of instrumentation. In the development of the Master Analytical Scheme, attempts have been made to minimize the differences in analytical results which might be anticipated from the use of several different instruments under different sets of conditions. Experiments have been performed: 1) to select suitable standards for instrument tuning (the choice was based on ease of introduction of the compound to the instrumental system and the presence of well-distributed ions over an appropriate mass range); 2) to determine an "optimum" standard spectrum for a given instrument to be reproduced easily within limits of deviation as narrow as possible; 3) to assess instrument stability (to determine how long the conditions which produce the "optimum" spectrum can be maintained within the acceptable limits of deviation); 4) to evaluate the effect of alteration of source tuning parameters on relative ion abundances in the standard spectrum (to detune the mass spectrometer from the set of conditions which produces the "optimum" spectrum and to assess the effect of these changes upon the system response to a set of compounds); and 5) to attempt to determine the relationship (if any) between system responses obtained from instrument to instrument and from laboratory to laboratory (to allow communal utilization of a central repository of system responses determined relative to a selected set of compounds).

The compound chosen as a standard for tuning the instrument for compounds in the volatile (purgeable) range is octafluorotoluene; in the semi-volatile range, the compound used for tuning is decafluorotriphenylphosphine (DFTPP). A multi-component solution (see Figure 1) was prepared and analyzed under varying conditions of tune, as evidenced by the differences observed in the DFTPP spectra obtained under the differing sets of conditions. The solution was analyzed in replicate using a Chrompack 25 m SE-30 50°C to 240°C at 12°C/min, with a 2 sec scan cycle. In the analysis of the data the response (as a Relative Molar Response) at one tune was plotted against the corresponding response at a second tune (see Figures 2 and 3). From these data it is possible to conclude that: 1) responses obtained on one instrument change in a consistent manner as the tune of the instrument changes; and 2) by performing a linear regression analysis of the responses at one tune versus the response at a second tune and determining the slope and intecept, one can calculate an RMR to use in quantitating unknowns if the corresponding response under the initial conditions is known. A set of data obtained under two different conditions of tune is shown in Table 1. By employing the types of correction described above, it can be seen that values for replicate samples are brought into relatively good agreement, in spite of the differing conditions of tune. This work was supported by EPA Contract No. 68-03-2704.

Reconstructed Gas Chromatogram of Standard S3.

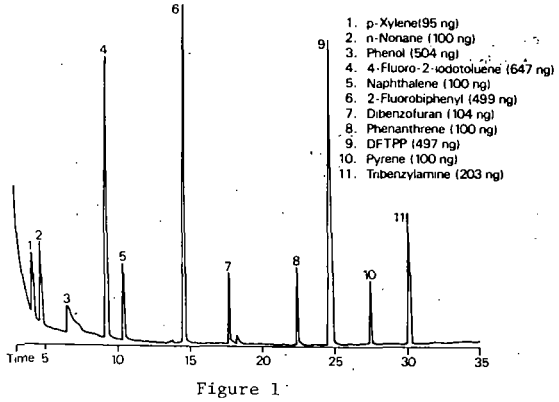

Figure 1

Plot of Molar Responses Relative to *m/z* 57 (Nonane).

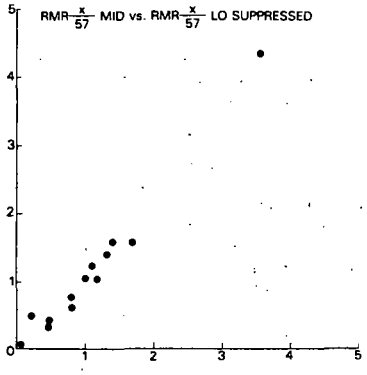

Figure 2.

Plot of Molar Responses Relative to *m/z* 106 (*p*-Xylene).

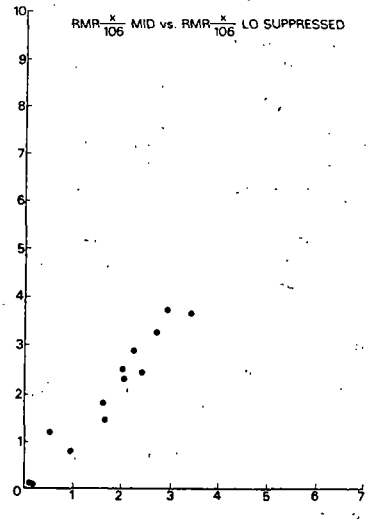

Figure 3

Table 1

Uncorrected[a] and Corrected[a] Concentrations of Purgeables from Duplicate Standard Samples in μg/Cartridge

	Standard							
	Perfluorotoluene				2,4,6-d_3-Anisole			
	Cartridge 1		Cartridge 2		Cartridge 1		Cartridge 2	
Compound	Uncorrected	Corrected	Uncorrected	Corrected	Uncorrected	Corrected	Uncorrected	Corrected
Naphthalene	11.2	19.6	8.24	18.24	13.8	11.0	13.8	10.96
Benzene	25.4	44.4	21.67	47.8	75.2	60.9	82.1	66.6
Toluene	12.8	24.0	8.58	19.0	29.2	34.7	44.3	19.0
Thiophene	.46	.82	.32	.79	1.17	.69	1.05	.89
Chlorobenzene	1.13	1.99	.67	1.57	2.74	1.96	2.09	1.43
Ethylbenzene	.51	.92	.20	.52	.62	.24	.74	.33
m,p-Xylene	2.99	5.24	1.60	3.81	8.92	6.99	6.10	4.70
o-Xylene	1.40	2.46	.70	1.63	3.21	2.34	2.07	1.41
Bromobenzene	1.52	2.68	.80	1.84	4.54	3.43	3.03	2.20
Trimethylbenzene	.55	1.09	.266	1.02	1.69	–[b]	.84	–[b]
Methylstyrene	.69	1.22	.39	.95	1.57	1.01	1.50	.95

[a]Both corrected and uncorrected used corrected response factors.
[b]Correction factor gave negative numbers for some isomers.

MPMP6 FACTORS AFFECTING THE PRECISION OF M.S. RESPONSE DATA OBTAINED IN THE MASTER ANALYTICAL SCHEME FOR ANALYSIS OF ORGANICS IN WATER, K. B. Tomer, J. T. Bursey, and E. D. Pellizzari, Research Triangle Institute, Research Triangle Park, NC 27709, J. Ryan, L. Rando, and D. Perry, Gulf South Research Institute, P. O. Box 26518, New Orleans, LA 70186.

In the development of a Master Analytical Scheme for the Analysis of Organics in Water, minimization of errors in quantitation is of critical importance. The origins of these errors as well as the means for reducing them must be recognized.

One major factor which may affect the precision of quantitative GC/MS data is the choice of internal standard. As part of our investigation of how the choice of standards can affect the precision of data a 41 component solution incorporating hydrocarbons, aromatics, phenolics, bases, halogenated and miscellaneous compounds was analyzed in both laboratories. We found that: 1) The precision of quantitative GC/MS data is unaffected by the chemical class of the internal standard used. Applying the F-Test (a test of statistical significance) at the 95% confidence level to the divergence of the standard deviations as a function of chemical class 70% were found to be not statistically significant; 2) The precision of quantitative GC/MS data is enhanced by using an internal standard which elutes close to the unknown. Applying the F-Test to the standard deviations as a function of retention time showed that 77% of the deviations diverged with statistical significance. These conclusions are illustrated by the data in Table 1. These data show that e.g. a hydrocarbon can be a better standard for a phenolic than another phenolic and that the CVs tend to minimize near the elution point of the unknown. Figure 1 is a plot of CVs as a function of retention time for octadecane as an unknown and shows graphically the increase in CV the further away from the unknown the internal standard elutes. To minimize the CVs associated with GC/MS quantitative data, then, standards should be chosen which cover the elution range. Figure 2 shows how the CVs for the solution can be minimized by choosing three standards covering the elution range. 3) The precision of quantitative GC/MS data is unaffected by the mass of the ions used in quantitation (Table 2).

In the analysis of many aqueous samples, overlap of components, even on capillary columns, prohibits the use of total ion current in quantitation. We examined the affect of using selected ion current instead of reconstructed ion current on the precision of quantitation by comparing the precision of the two in a solution where no overlap occurs. Our results, Table 3, shows the use of selected ion current is as precise for quantitation as is the use of reconstructed ion current. This work has been supported by EPA Contract No. 68-03-2704.

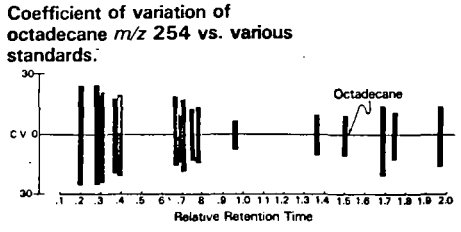

Figure 1

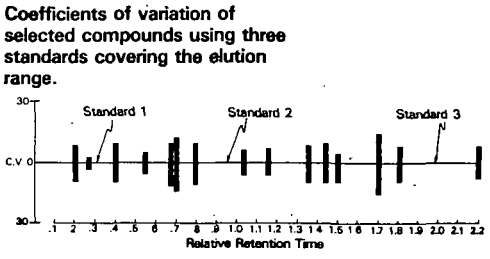

Figure 2

Table 1

Coefficients of Variation for RMRS of Phenolics

Compound								
Standard	Ion	RRT[a]	Phenol	Cresol	Dichloro-Phenol	Dimethyl-Phenol	t-Butyl-Phenol	p-Phenyl-Phenol
Octane	114	.198	7	9	12	11	8	22
	57		8	5	8	8	11	24
Xylene	91	.265	10	4	10	8	14	24
Methylene iodide	268	.297	10	5	11	14	13	22
Aniline	93	.387	8	8	15	7	9	17
Phenol	94	.4	–	8	9	11	10	20
Dichlorophenol	162	.685	10	8	–	12	14	23
Naphthalene	128	.71	12	17	17	16	16	11
Dibromobenzene	234	.713	15	14	15	12	15	11
3,4-Dimethyl-phenol	107	.718	12	15	16	–	11	18
Dodecane	57	.763	15	26	20	19	23	10
	170		18	18	24	18	16	8
Quinoline	129	.778	7	13	13	14	12	9
Butylbenzoate	105	.97	11	15	16	15	13	9
p-Phenylphenol	170	1.36	19	22	25	22	19	–
Carbazole	167	1.49	16	20	23	20	17	5
DFTPP	198	1.58	24	23	26	26	17	12
	442		21	21	22	26	19	14
Eicosane	57	1.691	22	26	16	24	23	8
	282		17	18	18	12	19	8
Pyrene	202	1.77	22	24	27	22	20	9
Tribenzylamine	91	1.98	27	26	25	22	27	9

[a]RRT = Relative Retention Time

Table 2

Mass Correlation vs. CV

Standard	m/z	RRT	Octane m/z 114	Octadecane m/z 254	Phenol m/z 94
Xylene[a]	91	.265[c]	9	26	
Methylene-iodide[a]	268	.293[c]	9	24	
Tribenzylamine[a]	91	1.98[c]			27
Eicosane[a]	282	1.69[c]			17
Pyrene[b]	202	0.67[d]			13
Tribenzylamine[b]	91	0.67[d]			17
Triphenylene[b]	228	1.03[d]			20

[a]Magnetic sector
[b]Quadrupole
[c]Retention time relative to midpoint of chromatogram
[d]Retention time relative to an external standard

Table 3

Precision of Total Ion Current Versus Selected Ion Plots

		Day 1	
Compound	m/z	% CV of RMR_{TIC}	% CV of RMR_{SIP}
p-xylene	91	17	13
n-nonane	57	13	12
phenol	94	12	8
4-fluoro-2-iodotoluene	236	7	7
naphthalene	128	7	8
2-fluorobiphenyl	172	5	5
dibenzofuran	168	3	5
phenanthrene	178	3	2
pyrene	202	7	6
tribenzylamine	91	8	7

RMR based on DFTPP as internal standard, m/z 442
Day 1 refers to Data Set V, Day 8 refers to Data Set VI, Day 17 refers to Data Set VIII.

QUANTITATIVE ASPECTS OF GC/MS ANALYSIS

A.D. SAUTER, L.D. BETOWSKI, M. HIATT AND E.P. MEIER, Environmental Monitoring Systems Laboratory, U.S. Environmental Protection Agency, Las Vegas, NV 89114.

The precision of response factor determination for three GC/MS analysis configurations was investigated for selected organic compounds (priority pollutants). Observations related to the source of precision errors inherent in the internal standard GC/MS quantitative analysis technique were discussed. The qualitative and quantitative advantages of quartz (fused silica) capillary columns were demonstrated. The potential of this new chromatographic technology and alternative ionization techniques for significantly reducing environmental GC/MS analysis acquisition time (50-70%) as compared to existing techniques (1) was delineated.

The long term response factor variation at multiple concentration levels was found to be generally acceptable (2) for "volatile" organic compounds that were injected via the purge and trap technique and analyzed (70 eV/EI) with the Organics in Water Analyzer.

The response factor precision for quartz capillary column (QCC) GC/MS analysis (70 eV/EI) of acidic and basic priority pollutants analyzed simultaneously at nanogram injected levels was generally excellent (i.e., relative standard deviation of response factors <10%).

For the same QCC chromatographic configuration, the pulsed positive ion/negative ion chemical ionization (methane @ 0.35 torr indicated) GC/MS analysis mode was employed to capitalize on the enhanced negative ion (N/P) sensitivity for nitrated, "large" polynuclear aromatic, and halogenated priority pollutants. Acceptable response factor precision was observed even at rapid scan rates (400 amu/0.3 sec).

---

1. Method 625, Federal Register, Dec. 3, 1979.

2. Budde, W.L. and Eichelberger, J.W., Performance Tests for the Evaluation of Computerized Gas Chromatography/Mass Spectrometry Equipment and Laboratories. EPA-600/4-80-025, U.S. Environmental Protection Agency, Cincinnati, Ohio, 1980.

SEMI-AUTOMATIC ANALYSIS OF VOLATILE ORGANICS IN AIR TO 1 PPB

Samuel E. Insalaco and Paul P. Dymerski
Division of Laboratories and Research,
New York State Department of Health, Albany, New York 12201

A semi-automatic desorption procedure is described for the analysis of volatiles in air as an alternative to solvent extraction of air sampling cartridges. Several popular adsorbent compositions were compared in performance by conventional thermal desorption and evacuated thermal desorption (V&T). With V&T, air cartridges are thermally desorbed under vacuum (<5 TORR). This allows the use of more tenacious adsorbents (e.g. Poropak N) with increased recoveries. This procedure combined with liquid nitrogen cooled trapping allows GC/MS analysis with minimum detectable limits of at least 1 ppb. The system was tested on a wide range of compounds from dichlorodifluoromethane (b.p.-29.4°C) to ethyl benzene (b.p.136.2°C). In addition, it was found that the trapping procedure resulted in higher recoveries of the lighter volatiles (e.g. purgable gases) on direct injection of standards. With the addition of the modified Finnigan 9610 capillary injection port [1] a rapid semi-quantitative means of air cartridge analysis by GC/MS was achieved.

Air cartridges were prepared from commercially available packings in several combinations. These included gel 15 (35/60 mesh), poropak N (80/100 mesh), and tenax (60/80 mesh). Silica gel/tenax cartridges were packed 1:2 and poropak N/tenax cartridges were packed 1:1. All cartridges contained ~0.5 g of packing (total) and measured 1/8" i.d. by 4" long.

Test cartridges were loaded under actual sampling conditions using a cartridge loading apparatus. This device designed by Dr. B. Bush[2] will load cartridges to produce a standard amount. The standard loading solution was prepared immediately before loading. All cartridges had been previously purged with helium at 200°C for 24 hours.

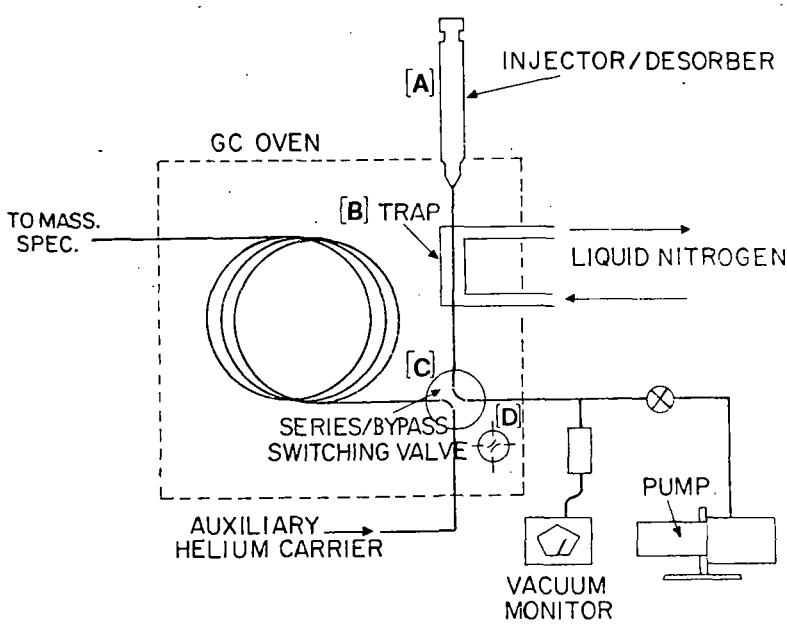

Cartridges were analyzed using normal thermal desorption and the V&T procedure. Normal conditions purged the cartridge contents onto a 60°C column for 4 minutes with carrier gas (30 ml/min). V&T conditions desorbed the cartridge under vacuum for 5 minutes with no carrier flow onto the cold trap. In all cases the injection port was 220°C (desorption temperature). Samples were analyzed on a 60/80 Carbopak B/1% SP-1000 column. The instrument used was a Finnigan 4021 GC/MS/DS. All conditions used were from the EPA Priority Pollutant protocol for volatiles in water (full scan, 35-350 a.m.u.).

A great deal of emphasis was placed on trapping and recovery of the highly volatile compounds such as dichlorodifluoromethane. It was found that with the cartridges used, breakthrough of these compounds was seen with 20 l sampling volumes in all packings except silica gel. The best sampling recoveries were seen using a 10 l sampling volume. V&T gave better recoveries than normal desorption for all compounds tested except carbon tetrachloride in which both processes appeared about equal. Evacuated recoveries were ~2-10 times greater than those for normally desorbed cartridges.

The overall best trapping and recovery for all compounds was seen using the poropak N/tenax cartridge; poropak N used alone was second. With the recoveries obtained for the poropak N/tenax cartridge using V&T, theoretical minimum detectable limits for the test compounds were calculated to be below 1 ppb. Because of the increased sensitivity obtained using V&T, this method is highly attractive for use with GC/MS.

In addition, it is interesting that trapping of directly injected standards gave higher responses than non-trapped direct injection on test compounds with boiling points below ~50-60°C. This will leave air sampling with cartridges and subsequent desorption analysis as a semi-quantitative technique until this anomoly can be resolved.

---

[1] Dymerski, P.P., R. Narang, and J. Knight. "A Finnigan 4000 MS Integrated Thermal Desorber for Air-Sampling Cartridges". The American Society for Mass Spectrometry, Seattle, Washington, June 1979, paper #WAMP-1.

[2] Dr. Brian Bush, Division of Laboratories and Research, New York State Dept. of Health, Albany, New York, 12201.

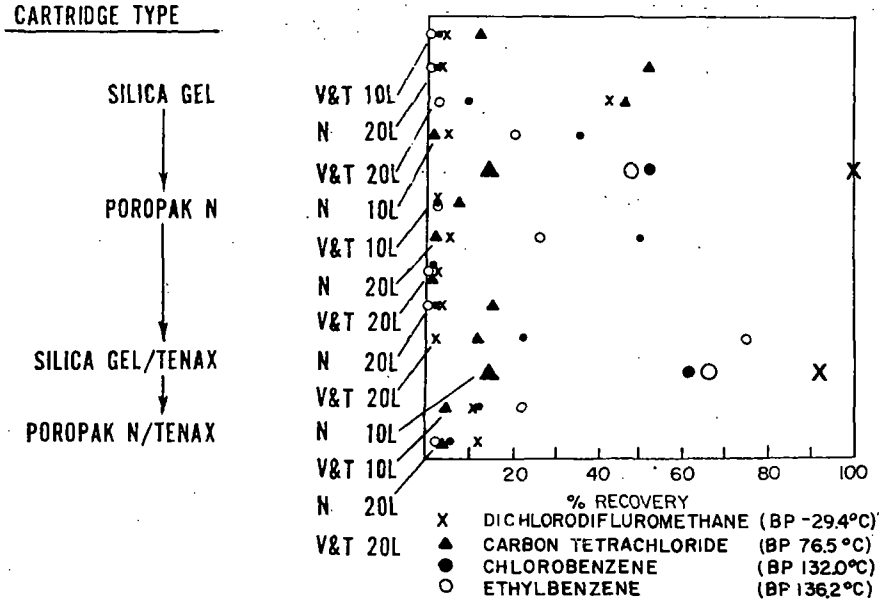

MPMP11 QUANTITATIVE ANALYSIS BY GC-MS OF VOLATILE ORGANIC COMPOUNDS IN WATER UTILIZING ISOTOPE DILUTION TECHNIQUES, HANS GRADE and WOODFIN V. LIGON, JR., General Electric Company, Corporate Research and Development, Schenectady, NY 12301

The purge and trap technique is a well established method for the quantitative analysis of volatile organics in water. This method is subject, however, to numerous efficiency factors which are unique to every compound studied. In this work the solvents, 1,1,1,-tri-chloroethane, methylene chloride, toluene and xylene were simultaneously analyzed by GC-MS using the purge and trap technique combined with isotopic dilution to largely eliminate efficiency considerations. The procedure used is outlined below. A standard consisting of the fully deuterated counterparts of the four solvents of interest was prepared in polyethylene glycol (average molecular weight 400). This non-purgeable, water miscible solvent allows the facile preparation by serial dilution of very dilute solutions of samples with very low water solubility. The use of this solvent eliminates the need to handle very small quantities without introducing a volatile organic diluent. Aliquots of the deuterated standards were added to the unknown samples and the solutions purged with nitrogen in the usual manner. The volatiles were trapped on various adsorbents, thermally desorbed and analyzed by GC/MS. Data was acquired by rapid repetitive scans of the mass range of interest. The quantitative measurements were made by a comparison of the areas observed for the respective deuterated and undeuterated components using computer generated selected ion chromatograms. Potential differences in purge and trap and mass spectrometric behavior between the labeled and unlabeled material were evaluated and corrected as appropriate. Using this procedure most errors due to instrumental variations and efficiency considerations are eliminated since the standards are carried through the entire analytical procedure. The limitations of this technique are largely confined to the availability of appropriate labeled standards.

CHEMICAL KINETICS OF FREE RADICAL REACTIONS RELEVANT TO PHOTOCHEMICAL SMOG FORMATION

K.R. Ryan and I.C. Plumb, CSIRO Division of Applied Physics, Sydney, Australia
J.R. Steven and M.F.R. Mulcahy, CSIRO Division of Process Technology, Sydney, Australia

In the polluted troposphere, organic peroxy radicals are thought to be important chain-carrying species for reactions in which hydrocarbons participate in the rapid photo-oxidation of nitric oxide. A consequence of this oxidation is the build-up of harmful levels of ozone. In extreme simplification these steps may be represented by the reactions

(1) $RCHO \xrightarrow{h\nu} R. + CHO$

(2) $R. + O_2 \xrightarrow{M} RO_2$

(3) $RO_2 + NO \rightarrow NO_2 + OR$

(4) $CHO + O_2 \rightarrow CO + HO_2$

(5) $HO_2 + NO \rightarrow NO_2 + OH$

(6) $OR + O_2 \rightarrow R'CHO + HO_2$

A measured rate coefficient of 8×10^{-12} cm^3 s^{-1} for Reaction (5)[1] establishes this as an important atmospheric process in both the stratosphere and the troposphere. Quite recently measurements from this laboratory and others[2] have shown that the rate coefficient for Reaction (3) when $R = CH_3$ is very similar to that found for Reaction (5). However, in order to assess properly the importance of peroxy radicals in the oxidation of NO, kinetic information on other organic peroxy radicals is required.

Using kinetic spectroscopy in systems at total gas concentrations up to 3×10^{18} cm^{-3}, Adachi and Basco[3] measured the rate of reaction of $C_2H_5O_2$ with NO and obtained a coefficient of 2.7×10^{-12} cm^3 s^{-1}, which is somewhat lower than the values obtained for HO_2 and CH_3O_2. In this study, we report a measurement at 295 K of the rate coefficient for the reaction of $C_2H_5O_2$ with NO, under conditions for which the total gas density was within the range (1.65 to 26.4) $\times 10^{16}$ cm^{-3}. Experiments were performed using a gas flow reactor sampled by a quadrupole mass spectrometer. A brief description of the apparatus has been given elsewhere[2]. $C_2H_5O_2$ was produced via the reactions

(7) $Cl + C_2H_6 \rightarrow C_2H_5 + HCl$

(8) $C_2H_5 + O_2 \xrightarrow{M} C_2H_5O_2$

(9) $C_2H_5 + O_2 \rightarrow C_2H_4 + HO_2$

As we are aware of no direct measurement of the rate coefficient for the reaction between C_2H_5 and O_2, this was measured over the gas density range of (2 to 20) $\times 10^{16}$ cm^{-3}. The results shown in Fig. 1 are clear evidence of a dependence of the rate coefficient on third body density and support the idea that the second-order limit is reached at modest gas densities. This observation is in agreement with early findings of Dingledy and Calvert[4].

Problems arise when attempting to measure the rate of reaction of $C_2H_5O_2$ with NO. Although, as shown in Fig. 1, O_2 reacts quite rapidly with C_2H_5, no parent ion corresponding to $C_2H_5O_2$ could be observed. Accordingly, for the reaction of $C_2H_5O_2$ with NO, attention was focussed on one of the products of the reaction, NO_2. Before this could be employed as a means of obtaining the required rate coefficient allowance had to be made for other possible sources of NO_2. In particular, it has been assumed[3] that for moderately high third body densities Reaction (8) proceeds to the exclusion of Reaction (9). However, for conditions appropriate to this study Reaction (9) has been detected but its overall contribution has not been specified.[5,6] In the present work, HO_2 was detected by photoionization using an argon rare-gas resonance lamp. Quantitative estimates of the importance of Reaction (9) as a function of total gas density were obtained by observing the C_2H_4 produced and relating this to the initial C_2H_5 concentration. In this way, it was possible to show that Reaction (9) accounts for ~ 16% of the total C_2H_5 reaction for a gas density of 3.3×10^{16} cm^{-3}, while for a density of 16.5×10^{16} cm^{-3} this value falls to ~ 8%.

It can be shown that for a fixed reaction length the NO_2 signal is given by

$$(NO_2+) = \frac{k_3 \, (NO_2+)_\infty \, [NO]}{k_w + k_3 \, [NO]} \left[1 - \exp - (k_w + k_3 \, [NO])t\right]$$

where $(NO_2+)_\infty$ represents the signal as $[NO]\to\infty$, k_w is the wall loss term for $C_2H_5O_2$ during the course of the reaction, and t is the reaction time. Fig. 2 shows a least squares fit to this equation for three different reaction lengths. The rate coefficients obtained are summarised on the diagram.

It can be seen from the results that acceptable agreement is obtained for k_3 for the three different reaction lengths. It can easily be shown that, for the value obtained for k_3, the fact that ~ 8% of $C_2H_5 + O_2$ reactions produce HO_2 will have less than a 2% effect on this value. With other likely sources of error taken into account, we conclude that the rate coefficient for Reaction (3) is $(7 \pm 2) \times 10^{-12}$ cm^3 s^{-1}.

References

1. C.J. Howard and K.M. Evenson, Geophys.Res.Lett. 4, 437, 1977.
2. I.C. Plumb, K.R. Ryan, J.R. Steven, M.F.R. Mulcahy, Chem.Phys.Lett. 63, 255, 1979.
   H. Adachi and N. Basco, Chem.Phys.Lett. 63, 490, 1979.
   R.A. Cox and G.S. Tyndall, Chem.Phys.Lett. 65, 357, 1979.
3. H. Adachi and N. Basco, Chem.Phys.Lett. 64, 431, 1979.
4. D.P. Dingledy and J.G. Calvert, J.A.C.S. 85, 856, 1963.
5. C.J. Howard, J.Chem.Phys. 67, 5258, 1977.
6. M. Leu, J.Chem.Phys. 70, 1662, 1979.

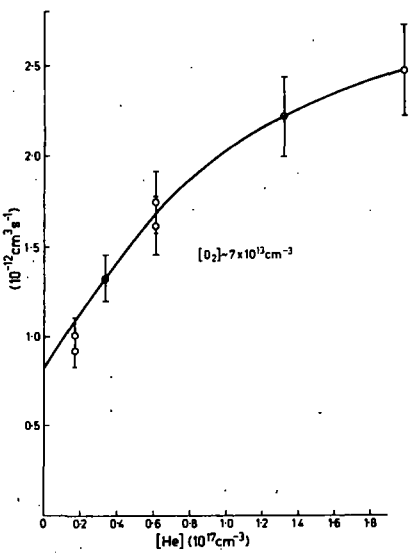

Figure I. Apparent two-body reaction rate coefficient as a function of helium concentration for the reaction of C_2H_5 with O_2.

$$[NO_2] = \frac{k_3 [NO] [NO_2]_\infty}{k_w + k_3 [NO]} \left[1 - \exp - (k_w + k_3 [NO]) t \right]$$

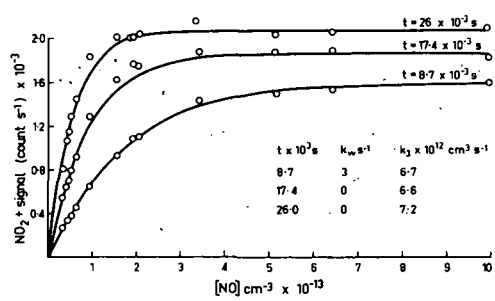

Figure 2. Experimental results for the production of NO_2 by reaction of $C_2H_5O_2$ with NO for three different reaction times. The smooth curves represent fits to the expression derived for $[NO_2]$. Total gas density is 16.5×10^{16} cm^{-3}.

METHANE ENHANCED NEGATIVE IONIZATION MASS SPECTRA OF SELECTED S-TRIAZINE HERBICIDES

J.A.NYSTROM*+, Y.TONDEUR*, J.R.HASS*, M.M.BURSEY+
* NIEHS,POB 12233,RTP,NC 27709
+ DEPT. OF CHEM., UNC, CHAPEL HILL, NC 27514

For years, a number of s-triazine compounds have been used extensively as a herbicide to destroy unwanted weeds. A prime example is Atrazine (V), a chlorinated herbicide used to control various problem weeds in tobacco farming. Recently high levels of Atrazine have been reported in runoff water in the Chesapeake Bay. Although the toxicity is relatively low for some test animals (ie. rats), toxicity to marine species, particularly phytoplankton, and the subsequent impact on the ecological system have not been fully characterized. Detection of these herbicides at various concentration levels will be necessary for a fuller understanding of their environmental impact.

In recent years, the application of negative ion mass spectrometry to compounds of environmental interest has greatly increased. For a number of these chemicals, the sensitivity has been shown to be greater for high negative ion mass spectrometry than for various positive ion mass spectrometric modes (EI, CI). This increased sensitivity is generally dependent upon the various electrophores (-F,-Cl,-Br,-I,-CN,etc.) present which can undergo electron capture processes. The s-triazine herbicides contain a central six membered aromatic ring with alternating carbons and nitrogens as well as one or more eletrophores on the sidechain (-Cl,I-IX; -Cl&-CN,VI&VIII). With these electrophores present on the sidechain and the central ring containing three nitrogens, one would expect these compounds to readily form negative ions under methane enhanced negative ionization(MENI) conditions. Characterization of the negative ions present in the s-triazine herbicides' mass spectra is necessary to determine the feasibility of using MENI for future sensitivity studies as applied to environmentally related problems.

S-Triazine Herbicides:

R	I	II	III	IV	V	VI	VII	VIII	IX
R_1	C_2H_5	$CH(CH_3)_2$	-	C_2H_5	$CH(CH_3)_2$	C_2H_5	o-Cl-	t-C_4H_9	-
R_2	C_2H_5	H	H	H	H	H	H	H	H
R_3	C_2H_5	$CH(CH_3)_2$	$CH(CH_3)_2$	C_2H_5	C_2H_5	$C(CN)(CH_3)_2$	Cl	C_2H_5	$C(CN)(CH_3)_2$

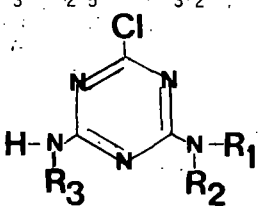

TABLE I. METHANE ENHANCED NEGATIVE IONIZATION MASS SPECTRA OF SELECTED S-TRIAZINE HERBICIDES

TABLE II. -/- CID/MIKES FOR $(M-H^+)^-$

I. 228		II. 228		III. 226		IV. 200	
FRAGMENT LOSS	%	FRAGMENT LOSS	%	FRAGMENT LOSS	%	FRAGMENT LOSS	%
66	8.5	77	2.2	44	14.2	43	1.9
65	7.1	43	21.5	43	2.6	37	3.3
64	7.1	37	1.8	18	21.4	30	19.5
45	8.1	17	100.0	17	51.4	29	18.6
44	3.1	2	14.6	16	52.0	15	28.4
32	70.3	1	52.6	2	55.8	3	11.8
31	50.6			1	100.0	2	35.0
30	52.2					1	100.0
28	59.1						
16	54.1						
2	47.2						
1	100.0						

I. TRIETAZINE		II. PROPAZINE		III. CYPRAZINE		IV. SIMAZINE		V. ATRAZINE		VI. CYANAZINE		VII. ANILAZINE		VIII. PROCYAZINE		IX. TERBUTYLAZINE	
M/Z	INT.	M/Z	INT.	M/Z	INT.	M/Z	INT.	M/Z	INT.	M/Z	INT.	M/Z	INT.	M/Z	INT.	M/Z	INT.
35	100.0	35	48.1	35	70.4	35	47.9	35	84.2	35	35.0	203	30.1	35	100.0	M/Z	INT.
37	33.4	37	16.3	37	24.0	37	20.8	37	29.5	37	13.6	204	4.5	37	32.9		
66	12.7	66	10.4	66	22.8	66	15.9	66	31.1	62	3.7	205	9.7	62	5.0	35	74.2
136	9.2	108	5.1	108	6.0	108	4.6	108	5.8	136	10.2	219	33.6	66	4.1	37	25.7
164	21.5	150	100.0	122	13.1	136	100.0	127	7.0	172	6.3	221	12.8	148	21.0	66	9.0
192	50.9	151	7.3	148	100.0	164	11.6	136	100.0	176	3.2	227	49.3	153	5.6	136	100.0
193	22.6	169	3.2	150	20.9	165	32.6	137	8.3	204	12.4	238	100.0	175	4.9	137	8.2
200	3.7	192	16.5	176	10.1	166	4.8	150	27.1	212	5.3	239	39.5	184	31.6	164	4.0
228	61.8	193	15.0	190	30.9	200	71.3	151	4.6	239	100.0	240	57.5	185	11.8	192	3.6
229	1.4	228	75.1	191	34.9	201	5.4	167	8.9	240	18.4	241	10.7	188	5.2	228	9.6
230	22.2	230	32.4	192	21.8	202	26.5	178	33.6	241	33.1	242	10.0	189	5.6	230	3.8
				226	63.8	203	3.0	179	36.0	242	7.8	220	5.4	190	4.3		
				227	2.9			180	13.1	245	25.4	222	4.1	216	54.8		
				228	20.9			214	68.1	277	12.1	223	35.8	217	5.8		
								216	27.2	279	3.2	224	1.0	224	2.5		
												225	35.1	225	3.2		
												226	2.0	248	19.9		
												227	11.7	251	61.7		
												228	1.2	252	39.8		
												229	1.2	253	18.6		
														254	13.9		
														287	14.1		
														289	10.7		
														291	1.4		

EXPRIMENTAL: Negative ion mass spectra were obtained with a Finnigan 3300 Quadrupole mass spectrometer equipped with a conversion dynode electron multiplier. A Finnigan/INCOS 2300 Data System was used to assimilate and process data.

Methane was used as a moderator gas at a pressure of 1 torr, as measured by a thermocouple gauge at the source. Analytical reference standards were obtained from the Environmental Protection Agency.

Negative ion MIKES and CID/MIKES spectra were obtained with a VG Micromass ZAB-2F equipped with a collision cell. A modified Finnigan/INCOS 2300 Data System was used to acquire and manipulate the data.

Methane was used as a moderator gas at a pressure of ca. .1 torr. Helium was used as the collision gas for the CID/MIKES experiments at a pressure ca, 10^{-4} torr (main beam attenuation of 50%). Source temperature was between 180 and 200°C. Resolution was set at 1,000 for M/Z=231. Accelerating voltage was set at 7kV.

Accurate mass measurements were made on M/Z=66 by peak matching with Cl_2^- at a resolution of 10,000 on a VG Micromass ZAB-2F mass spectrometer.

RESULTS: MENI spectra showed the following for compounds containing only Cl (I-V,VII,IX): 1. Cl^- ions (intensity > 40%). 2. $(M-H^\cdot)^-$ (intensity > 60% except VII(36%) and IX(10%)). 3. Loss of mass 36 and 37 ($M-H\cdot-Cl\cdot$ and $M-2H\cdot-Cl$) except IX (no mass loss of 36). 4. Loss of $Cl\cdot$ (II-V&VII). 5. Loss of alkyl group,only, not observed (intensity 4%0. 6. Loss of $H\cdot+Cl\cdot$ followed by loss of an alkyl group (except VII); this loss forms:a. II-V&IX was the base peak. b. R=isopropyl loss preferred 5 to 1 over the cyclopropyl loss (III). c. R=isopropyl preffered 4 to 1 over ethyl (V). 7. M/Z=66.0088, $C_2N_3^-$, present (except VII). MENI spectra for compounds containing Cl and CN (VI,VII) showed similar characteristics to the above results as well as the following: 1. An M^- observed ($(M-H\cdot)^- > M^-$). 2. No loss of $Cl^\cdot$. 3. Loss of alkyl group observed (VI,7%;VII,32%). 4. M/Z=66 observed in VIII (4.1%) but not in VI. 5. Formation of $(M+Cl)^-$.

MIKES analysis showed no unimolecular decompositions of the $(M-H^\cdot)^-$ for the four compounds studied (I-IV). -/- CID/MIKES for the $(M-H^\cdot)^-$ indicate the following: 1. Prominent losses involving $H^\cdot$ and $2H^\cdot$ (with the exception of II). 2. Loss of the alkyl group (III, loss of isopropyl preferred over cyclopropyl). 3. In all cases, one observes loss of $^\cdot CH_3$ and/or $^\cdot CH_3 + xH^\cdot$ (x=1-3). 4. In I,II, and IV, one observes loss of $Cl^\cdot$ or $2H^\cdot + Cl^\cdot$.

DISCUSSION: *The MIKES data for the $(M-H^\cdot)^-$ of compounds I-IV indicate no unimolecular decompositions* occurring in the second field-free region of the mass spectrometer. The unimolecular spectra showed only the main beam and its reflection peak (an artefact). Due to electron multiplier discrimination, any negative ions formed with an energy to charge ratio of less than approxiamentally one half the kinetic energy of the main beam will be lost. Collision induced dissociation MIKES data for the $(M-H^\cdot)^-$ ions indicate simple loss of hydrogens, sidechain alkanes, and a weak loss of $Cl^\cdot$ and combination thereof. This implies that rearrangement of the $(M-H^\cdot)^-$ ion has not occurred to any major extent. Due to the low intensity of the $Cl^\cdot$ loss in the CID/MIKES experiment, one is probably not dealing with a unimolecular fragmentation but most likely with an ion formed by dissociative electron capture. The source product ions are probably collisionally stabilized in the source and therefore would not be expected to undergo unimolecular decompositions. This can only be postulated until the negative ions have been studied over a range of source temperatures and pressures. Ion reaction pathways are inconclusive at this point. One might suggest the following processes are occurring: 1. Rapid decomposition is occurring in the source. 2. At various stages of decomposition ($(M-H^\cdot)^-$, $(M-H^\cdot-Cl^\cdot)^-$, $(M-H^\cdot-Cl^\cdot-R^\cdot)^-$, etc. for example), some ions have been collisionally stabilized before they can further decompose. 3. Observed product ions are most *likely collisionally stabilized before leaving the source (ie. no unimolecular decompositions* are observed).

CONCLUSIONS: 1. -/- CID/MIKES can be used to distinquish between different chlorinated s-triazine isomers (Example: I (R=Ethyl), large losses are at masses 29,30,31; II (R_x=Isopropyl), no 29,30,31 losses but a mass loss at 43). 2. The $(M-H^\cdot)^-$ does not appear to have undergone any major rearrangement. 3. At the source temperature (70°C) and pressure (1 torr) used, characteristic negative ions are $(M-H^\cdot)^-$, $(M-(H^\cdot+Cl^\cdot))^-$, $(M-(H^\cdot+Cl^\cdot+R^\cdot))^-$, and $C_2N_3^-$.
4. The dependence of negative ions on source temperature and pressure needs to be determined to further elaborate on the negative ion reaction pathways.

MIKES ANALYSIS OF SULFAMETHAZINE

D.J. Harvan, J.R. Hass, NIEHS, RTP, NC 27709, M.K. Hoffman, USDA-FSQS, Beltsville, MD 20705

Sulfa drugs have been used by hog producers since the early 1950's for the control of disease in swine. The drug must be withdrawn prior to slaughter in order that tissue levels be below the 0.1 ppm level, as specified by the Food and Drug Administration. In recent years the Department of Agricultures's Food and Quality Service has found unacceptably high levels of sulfa residues in 6-10% of the animals tested. The present method of analysis is selected ion monitoring GC/MS for the presence of N-methyl sulfamethazine, which is a time-consuming method.

In recent years, mass-analyzed ion kinetic energy spectrometry (MIKES), has been proposed as a rapid means of analysis without chromatography.[1-3] Within dynamic range limitations, the method has been quite useful for rapid screening.[4] By this method, the magnet of a double-focussing mass spectrometer is used to select an ion of interest. This "mass-selected" species is then collisionally excited, and the fragment ions analyzed in the electric sector of the instrument. We have investigated both positive and negative ion CID-MIKES as a rapid means of screening for the presence of N-methyl sulfamethazine (Scheme 1) in swine.

In the positive ion mode, the reaction $(M - SO_2H)^{+\cdot} \rightarrow (M - SO_2H - CH_3)^+$ was monitored.

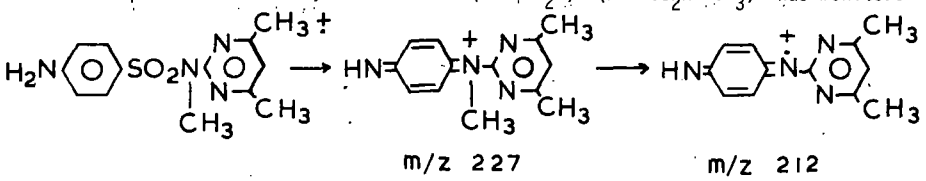

This gave S/N > 15:1 for 5 ng N-methylsulfamethazine by direct probe insertion. The percent standard deviation was 30% for 5 ng and 9% for 10 ng standard. The results for tissue samples are comparable to those obtained by selected ion monitoring GC/MS (Table 1).

In the negative ion mode, the reaction $(M - \text{aminodimethylpyrimidyl})^- \rightarrow (M - \text{aminodimethylpyrimidyl} - SO_2)^-$ of the trifluoroacetyl derivative was monitored (Scheme 2).

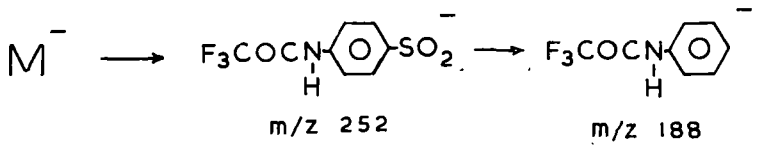

This gave a S/N > 50:1 for 1 ng and S/N > 5:1 for 100 pg standard. A percent standard deviation of 15% was observed for 1 ng standard. The results for several tissue samples are presented in Table 1.

The analysis was attempted using methane positive chemical ionization. The CID-MIKES spectrum of the protonated molecular ion of N-methylsulfamethazine-trifluoroacetyl derivative at m/z 389 gave intense signals for the loss of methyl and fluorine. However, the sensitivity was not sufficient to allow their use in this case.

The analysis was also attempted using EI CID-MIKES on the m/z 323 ion the trifluoroacetyl derivative. The sensitivity was comparable to EI sensitivity on the underivatized material. However, positive interferences were observed in the procedural blank, and thus ruled out this method.

The negative ion method was the most sensitive, giving approximately ten times lower detection limits. Although the extra step of derivatization is necessary, the procedure is still extremely simple. Both positive and negative ion MIKES analyses are very rapid. Approximately two minutes are required for each sample, with a standard being run in between each sample. The correlation between the two methods and the SIM GC/MS results are reasonable and sufficient for general screening.

A VG Micromass ZAB-2F mass spectrometer operated at a mass resolution of 1000 was used for the analyses. The majority of the data was acquired with a modified Finnigan/INCOS 2300 data system.[5]

TABLE 1

Sample	EI m/z 227→212	MNCI m/z 252→188	SIM GC/MS
1064A liver	20 ng	6 ng	37 ng
1167A liver	11	6	13
1169A muscle	18	Not Determined	20
1229A liver	4	6	15
1229A muscle	2	2	4
1311A muscle	9	13	8
1341A liver	9	4	6

REFERENCES

1. R.W. Kondrat and R.G. Cooks, Anal. Chem., 50, 81A 1978.
2. G.A. McClusky, R.W. Kondrat, and R.G. Cooks, JACS, 100, 6045, 1978.
3. R.W. Kondrat, G.A. McClusky, and R.G. Cooks, Anal. Chem. 50, 2017, 1978.
4. J.R. Hass, D.J. Harvan, and C.E. Parker: Am. Chem. Soc., 178th Natl. Meeting, Sept. 9-14, 1979.
5. M. Weiss, J. Karnofsky, J.R. Hass, D. Harvan: 27th Annual Conf. on Mass Spec., June 3-9, 1979, Seattle, Wash.

THE ANALYSIS OF SULFAMETHAZINE RESIDUES IN CATTLE TISSUE USING GAS CHROMATOGRAPHY-CHEMICAL IONIZATION MASS SPECTROMETRY

Manfred O. Poeppel, S. J. Stout, A. J. Manuel, W. A. Steller

American Cyanamid Company, Agricultural Research Division, P. O. Box 400, Princeton, New Jersey 08540

Introduction

There are currently about 10 different sulfonamides in common use as antibacterials for large food producing animals. The largest percentage of the sulfonamide market consists of sulfamethazine used in combination with antibiotics (e.g. AUREO S700 or AUREO SP 250 from American Cyanamid Company) to promote growth and prevent disease in cattle and swine. For many years the recognized official analytical procedure for the determination of sulfonamide residues in cattle tissues has been a Bratton-Marshall colorimetric method which unfortunately does not distinguish between individual sulfonamides or other aromatic amines. In 1977 residue methodology was significantly improved by A. J. Manuel and W. A. Steller who developed a GC-electron capture method which chromatographically resolved 7 of the most commonly used sulfonamides. Nevertheless, in the event of apparent violative sulfonamide residues (>0.1 ppm) in cattle tissues, further confirmation of the identity of the GC peak is required. The separation power of a gas chromatograph, when coupled with the structural information generated by a mass spectrometer permits the confirmation of an apparent drug residue with a very high degree of certainty. In addition, the ability to detect negative ions suggests the possibility of enhanced sensitivity for compounds that are routinely analyzed by GC-EC (e.g. sulfonamides).

Objective

Develop a GC-CIMS method to confirm the identity of apparent residues of sulfamethazine in cattle tissues at levels of 0.1 ppm or greater.

Experimental

Finely ground tissue is extracted with a 1:1 mixture of acetone:chloroform, the solids are filtered out, and 1N HCl is added. After evaporation of the organic solvent the extract is partitioned with hexane and the hexane phase is discarded. Then the aqueous phase is buffered to ph 6 so that the residue will partition into methylene chloride. Finally, the methylene chloride is evaporated and the sulfamethazine residue is methylated with diazomethane.

GC-CIMS analyses were carried out on a Finnigan Model 4000 equipped with an INCOS 2300 data system and with PI and NI detection capability. A 4' x 2 mm ID column packed with 3% OV-1 on 60/80 Gas Chrom Q was installed and CH_4 was used as the carrier-reagent gas. The positive ions monitored were at m/z 138^+ 166^+ and 293^+, while the negative ions monitored were at m/z 155^-, 156^- and 157^-.

Summary

As expected from its excellent response in electron capture, the response of methylated sulfamethazine in NICI (CH_4) is 100-fold greater than its response in PICI (CH_4) and response is linear from 5 pg to 10 ng. The ions at m/z 155^-, 156^- and 157^- are characteristic of the sulfonic acid portion of the molecule. However, the sulfonic acid moiety is common to many sulfonamides from which sulfamethazine is to be distinguished.

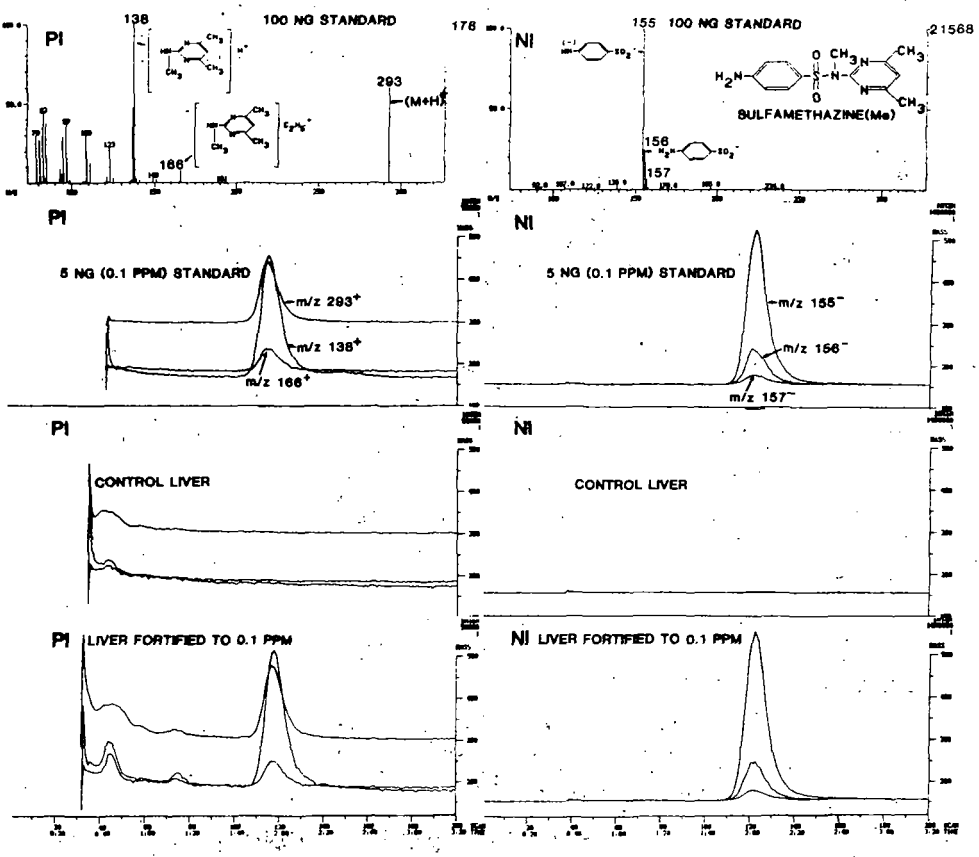

PICI (CH_4) generates an $(M+H)^+$ ion at m/z 293^+ and ions indicative of the amine portion of the sulfonamide at m/z 138^+ and 166^+. Response is linear from 2.5 ng to 25 ng. Although less sensitive than NICI (CH_4), PICI (CH_4) generates ions which differentiate sulfamethazine from other sulfonamides having the same sulfonic acid moiety.

While NICI (CH_4) alone cannot be used for confirmation of sulfamethazine, it does offer a means to check the quantitative data from PICI (CH_4) analyses and does provide additional confirmatory data. Also, on an instrument, equipped for pulsed positive ion negative ion operation, the high negative ion response allows the operator to set up an MID acquisition cycle with a very short interval for the negative ions and very long intervals for the less sensitive positive ions.

Conclusion

Analysis by GC-CIMS in both PI and NI modes provides adequate sensitivity, good linear range and sufficient structural information to confirm the identity of a violative residue of sulfamethazine in cattle tissues.

CONFIRMATION OF SULFONAMIDE RESIDUES IN ANIMAL TISSUES BY GAS CHROMATOGRAPHY/ELECTRON IMPACT, POSITIVE AND NEGATIVE ION CHEMICAL IONIZATION MASS SPECTROMETRY, TUNG SUN, USDA, FSQS, P.O. Box 6085, Athens, GA 30604

Seven sulfa drugs were methylated at N^1 position with diazomethane and studied by GC/MS with accurate mass measurements to assign the correct atomic compositions of the major ions in the EI and CI spectra except negative ion chemical ionization (NCI). They were sulfapyridine (S6), sulfamethazine (S9), sulfabromomethazine (S10), sulfachloropyrazine (S11), sulfadimethoxine (S16), sulfathiazole (S18), and sulfaquinoxaline (S21). They can be summarized in general as $A\text{-}SO_2\text{-}B$ where A is the same as p-aminophenyl and B is the various organic groups. In EI mass spectra, $(M\text{-}SO_2)^+$, $(M\text{-}SO_2\text{-}H)^+$, A^+, and B^+ are their characteristic ions with some surprising rearrangement ions $(A+O)^+$, $(A+NH)^+$, and $(A+CH_2)^+$. None have detectable molecular ions. Metastable peaks indicate that $(M\text{-}SO_2)^+$ is the precursor ion of $(M\text{-}SO_2\text{-}H)^+$, and A^+ is the parent peak of $(A\text{-}HCN)^+$ in all seven methyl derivatives. When selected ion monitoring (SIM) method was used for routine sample analyses, $(M\text{-}SO_2)^+$, $(M\text{-}SO_2\text{-}H)^+$, A^+, and B^+ were monitored and assigned the confirmation of sulfa drugs if all four peaks were found at about the right relative intensity and correct GC retention time. Thus far, the sulfa drug sulfamethazine has accounted for approximately 80% of the violations found in the kidney, liver, and muscle of swine, cattle, and poultry. Therefore, GC/SIM EIMS either in low or high resolution mass spectrometry was usually good enough to confirm the residue. When the result was questionable due to the interference of co-elution GC peaks, other ions such as $(A\text{-}HCN)^+$ and $(B\text{-}H_2CN)^+$ or rearrangement peaks like $(A+O)^+$, $(A+NH)^+$, $(A+CH_2)^+$, etc., were selected. Should doubt still exist, then GC with full EI spectrum and other methods, either PCI or NCI mass spectrum, were examined.

Isobutane was used as the reagent gas for positive ion chemical ionization (PCI). All seven N^1-methyl sulfa drugs have base peak (e.g. S6 and S11) or intense peaks as $(M+1)^+$ in their PCI spectra. Three rearrangement ions, BH_2^+, AH_2^+, and ASH_2^+, are very intense. A surprising peak $(BH_3\text{-}X)^+$ (where X = Br or Cl) of S10 and S11, which could occur by hydrogen-halogen exchange during chemical ionization followed by the similar process as BH_2^+, was formed. Other ions at $ASO_2H_2^+$, $ASOH_2^+$, ASH^+, and AS^+ are also detected at various

intensities.

In negative ion chemical ionization with 1:1 methane to nitrous oxide mixture or ammonia as reagent gas, the mass spectra were about the same. All seven N^1-methyl sulfa drugs show a weak $(M-H)^-$ ion without appreciable rearrangement fragment ions. The base peaks of S6 and S18 are at m/z 156^-, i.e. $(ASO_2)^-$, whereas the others are at m/z 155^-, i.e. $(ASO_2-H)^-$. This probably reflects the competition of the proton abstraction in the $(M-H)^-$ formation being on the side of B or A before the rupture of ASO_2-B bond. The other weak ions are $(A)^-$, $(B)^-$, and isotopic ion clusters of $(ASO_2)^-$ or $(ASO_2-H)^-$.

In SIM mode, most of the so far existing mass spectrometers, e.g. Finnigan 4010, Hewlett Packard 5992A, Varian MAT CH7A, etc., have limitation of monitoring one to eight ions only. If the sulfa drug containing sample is completely unknown, one has trouble to decide which ions need to be selected. Although AEI MS30 has the capability to monitor up to 24 masses, the sensitivity drops a lot if one trys to monitor so many ions or to run full mass spectrum. In NCI, the above seven derivatives all have the base peak either ASO_2^- or $(ASO_2-H)^-$. The problem can be solved by just selecting these two ions with GC retention time for the first screen sulfa drugs test. Confirmation can then be done by running second GC/SIM to cover more ions of these previous species detected.

Experimental. An AEI MS30 dual beam mass spectrometer was used for accurate mass measurements in both EI and PCI modes. Data acquisition was accomplished with DS-50S software and a NOVA 2 computer. The column was a 3-ft x 4-mm i.d. glass containing 3% OV-3 on 100/120 mesh supelcoport. Helium was used as carrier gas. Column was about 250°C.

A Finnigan 4010 GC/MS equipped with 6110 data system was used for NCI and for most of the routine GC/EIMS. All samples were introduced through a 6-ft x 2-mm i.d. 4% OV 210/1% OV 17 glass column. (For routine service 3% OV 7, 3% OV 225, and 3% OV 101 were usually used.) Helium was used as carrier gas.

Use of a company or product name by the Department does not imply approval or recommendation of the product to the exclusion of others which may also be suitable.

DECONVOLUTING MASS SPECTRA OF MIXTURES USING A MINICOMPUTER

Mark Weiss and Steve Sokolow, Finnigan Corporation, 545 Maude, Sunnyvale, Ca. 94086

When the mass spectra of pure compounds are accurately known, one mass spectrum of a mixture of these compounds can be deconvoluted using linear combinatorial analysis to determine the amount of each component. This deconvolution is the basis for many traditional analyses of complex mixtures (for example, PONA analysis).

The technique requires only that mass spectra with unchanging intensity ratios be routinely obtainable, and that there be at least as many masses in the spectra as there are components in the mixture.

We have used an INCOS minicomputer-based data system to both control scan and data acquisition from CEC-103 and CEC-104 mass spectrometers, and then perform the mixture deconvolution. Historically, a large computer was required to perform the needed matrix manipulations, and much time and effort was needed to transfer data and results from the (typically off-site) computer.

Using the same INCOS data system for both acquisition and arithmetic greatly speeds up the analysis time; an experiment need take no more than 10 minutes from sample injection to final report. The flexibility and availability of the dedicated data system also simplifies development of different analysis matrices with different combinations of compounds.

Experimental: The data system scans the electric sector of the CEC-103 over a narrow voltage range while keeping its magnet at a fixed position. The magnet is moved to 3 positions, and the resulting 3 scans combined into a single spectrum of extended mass range. The voltage scans are piecewise linear, but approach an exponential scan function, so that each mass is scanned for approximately the same time.

Mass peak data is collected in profile mode. Since the resolution of the CEC-103 is less than unit mass, intensity values based on mass peak area will be inaccurate due to interference from neighbor masses. Instead, the profile of the data is smoothed and its height used as the correct mass intensity value.

Data analysis: From a list of calibration compounds and a list of masses, the data system creates and stores a matrix in which each row is the mass intensities of a single calibration spectrum. A matrix of up to 40 compounds by 120 masses can be manipulated. This raw data matrix (R) need not be square; that is, the number of masses may be greater than the number of compounds. Using more masses increases analysis accuracy, and frees the user from having to select any special subset of masses.

Though the non-square matrix (R) cannot be inverted directly, it is possible to create another non-square matrix of weighting factors (W) which acts like the inverse of (R) in the sense that (W) * (R) yields the identity matrix. (W) is defined as:

$$W = (R*R^t)^{-1}*R^t$$

Since $(R*R^t)$ is square, it can be inverted, and used to make (W).

This final matrix (W) is now used to deconvolute a mixture: when the intensities of the mixture spectrum are multiplied by (W), the result is the un-normalized amount of each component in the mixture.

Results of the deconvolution are normallized, and output formatted in various ways as desired. The entire data collection and analysis can be automated, with a data acquisition occuring simultaneous with deconvoluting the just-acquired data.

AN IN-HOUSE LIBRARY SEARCH SYSTEM DESIGNED FOR TRACE ANALYSES, D. Thomas Terwilliger, Department of Chemistry, University of Pennsylvania, Philadelphia, PA, 19104, and Walter C. Davidson, Department of Chemistry, New York University, New York, NY, 10003.

The "STAR" program is a library search program specifically optimized to identify trace components in a mixture (1). It uses a combination of reverse searching, linear adjustment of spectra, and peak selection based only on abundance, all of which have been shown to be particularly applicable to trace analyses. This program has been extensively modified and improved from the original version reported previously (1) to operate on a laboratory mini-computer as part of the Varian MAT SS-100 GC/MS data system which is interfaced to a MAT-112 GC/MS. Full fortran programming capability was made available by adding the "VORTEX" operating system; "STAR" and all other programs added are run under "VORTEX". The library has been updated to include over 30,000 spectra which have been reformatted to be directly accessible by the data system. While only the 8 most abundant peaks from each reference spectrum are stored on the disk and used for the actual searching, complete spectra are available on tape; they can be listed out, plotted, or used for background subtraction by the system.

The search algorithm looks for the presence of the 8 most abundant peaks from each reference in the "N" most abundant peaks of the unknown. The operation of the algorithm can be varied from simulating a nearly ideal "reverse" search to a conventional "forward" search, depending on how contaminated the unknown spectrum is presumed to be. This is a simple operation which only involves specifying the number of peaks ("N") to consider for each unknown. If all peaks are considered, one gets a "reverse" search; if only 8 peaks are considered, one effectively gets a "forward" search, as the presence of any extra peaks in the unknown will necessarily insure the absence of one of the reference peaks in these 8 peaks.

Much care has been taken to insure that the algorithm runs at maximum speed. A pre-search, which requires only that the two most abundant peaks from the reference be present in the "N" most abundant peaks from the unknown, is first performed; typically only 5% of all reference spectra pass. A separate, compact "pre-search" file is used for this purpose; it contains only the two indicated mass values, thus minimizing I/O time. The complete 8 peak file is read only for references passing the pre-search. The library is sorted by molecular weight, and only references between a specified range are searched. This is useful when the operator has prior information on the expected identity of the unknown.

For maximum throughput, the program will operate either interactively or in a "batch" mode. In the interactive mode, the operator calls up one unknown at a time, and after examining the results, may elect to recall the complete spectrum of any reference, subtract it from the unknown, and then search the residual spectrum. Library spectra may also be plotted and/or printed for direct visual comparison. In the batch mode, any number of unknowns may be queued up and all run automatically with no intervention required. No residual searching is possible here, as only one tape drive is available, and all spectra are read from tape. A library of user collected spectra may also be added to the data base, and utilized in either mode. These spectra are searched first, and the main data base may be bypassed if a satisfactory match is found here, thus increasing the speed further.

Numerous other programs, listed below, have also been added to the system to enhance its performance.

DATA PROCESSING PROGRAMS

DISKAD	Adds spectra to the user library
ASRCH	Searches both libraries by title, formula, base peak, CAS #, or M.W.; and prints out all library information
ASCII	Converts "foreign" program tapes to VORTEX format
NBSRD	Prepares library files from "master" NBS library tape
NBSDIS	Converts "master" NBS library tape to SS/100 format
PBM	Converts spectra to "PBM/STIRS" format and transmits spectra directly to the above system via the modem
DISKOS	Bootstraps "DISKOS" system into core

"ASRCH" is very useful for determining if any given compounds exist in the library and for inventorying the user library. "PBM" is used for unknowns not identified satis-

factorily by "STAR". Since this is most likely due to lack of a suitable library entry, the "STIRS" program (2) may be used to obtain sufficient structural information to make the identification. Programs to enhance the GC resolution and improve the purity of the resultant unknown spectra are also being developed to be coupled with the above program.

To demonstrate the operation of "STAR", a mixture, obtained from Dr. D.I. Schuster of N.Y.U. and described only as the product of a photolysis reaction, was run, giving the T.I.C. trace shown in Fig. 1. From the known retention time of the starting material,

FIG. 1. ION CURRENT CHROMATOGRAM OF PHOTOLYSIS SAMPLE FOR "STAR" ANALYSIS

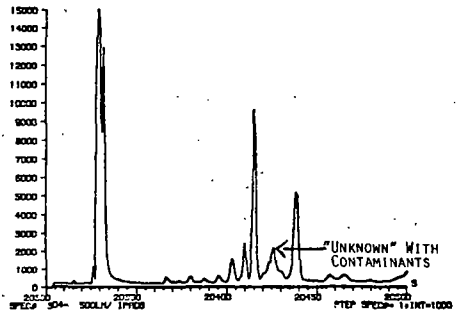

FIG. 2. PLOT OF SPECTRUM #20423

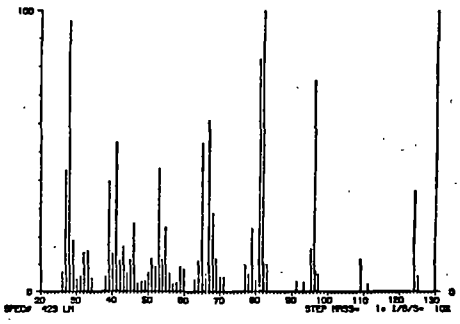

the indicated peak in Fig. 1. was selected and plotted as shown in Fig. 2. The T.I.C. trace indicates a high degree of contamination is likely. The results of running this spectrum are given below:

NO LIN ADJUST NO UNIQUE OPT		UNIQUE OPT ONLY		LIN ADJUST ONLY		WITH LIN ADJUST AND UNIQUE OPT	
SPEC #	SIM IND	SPEC #	SIM IND	SPEC #	SIM IND	SPEC #	SIM IND
1714	.69503	2849	.40842	873	.67880	4413	.42711
1688	.70831	6343	.42094	2858	.71023	6343	.43110
857	.71303	2855	.42865	1714	.72985	2858	.45583
2821	.75561	2858	.47105	857	.74958	2849	.47429
2858	.79764	2821	.54465	2821	.75658	2821	.54431

SPEC	857	2-HEPTYNE (8CI9CI)	96
SPEC	1688	CYCLOHEXANE, ETHENYL- (9CI)	110
SPEC	1714	3-OCTYNE (8CI9CI)	110
SPEC	2821	2-CYCLOHEXEN-1-ONE, 4,4-DIMETHYL- (8CI9CI)	124
SPEC	2858	1H-INDENE, OCTAHYDRO-, CIS- (9CI)	124

From the above table, spectrum # 2821 is the best overall match; and this did correspond to the starting material used in the reaction. To provide a comparison, the same spectrum was run through "PBM", and the correct result was only the 6th best match. The best 2 matches had incorrect molecular weights, even though there is a clear peak at m/e 124; and none of the other top 20 matches were isomers of the correct compound. Numerous other examples of the utility of this program have been given previously (1).

In conclusion, we have successfully modified the "STAR" program to operate "In-House" as part of our GC/MS data system. It is now run on a routine basis and provides library identifications comparable to, or better than commercially available systems.

(1) Anal. Lett. 10, 309 (1977).
(2) Adv. Mass Spectrom. 6, 999 (1974).

COMPUTER IDENTIFICATION OF UNKNOWN MASS SPECTRA.

VERSION 4 OF PBM/STIRS.

I.K. Mun, B.L. Atwater (Fell), K.S. Haraki,

R. Venkataraghavan, and F.W. McLafferty

Department of Chemistry, Cornell University, Ithaca, New York 14853

The Probability Based Matching (PBM) system[1] is designed for matching an unknown mass spectrum against a large reference collection of electron ionization spectra collected under a wide variety of experimental conditions. The superior performance demonstrated for earlier versions of PBM results from its statistical weighting of mass and abundance data and from rerunning the unknown spectrum after "skewing" the abundance data as a function of mass. Improved identification of multiple components in unknown mixture spectra is achieved by reverse-searching and automatic subtraction of the best-matching reference spectrum.[2] In Version 4 of PBM the values of the various matching criteria used previously have been converted into one reliability value reflecting the statistical probability that the observed degree of match will be a correct answer. These reliability values are based on statistics obtained by running 430 spectra selected at random from the reference file of unknowns; nearly the same results were obtained on a second, but different, random set of comparable size. Ranking the matched reference spectra according to this reliability value has also increased the performance of PBM. For example, at the 25% recall level the reliability has been increased from 68% to 76% for Class I matches, and from 92% to 95% for Class IV matches.

The Self-Training Interpretive and Retrieval System (STIRS)[1] is designed as an aide to the interpretation of unknown mass spectra, primarily those for which a suitably matching reference spectrum cannot be found by PBM. STIRS/Version 4 improvements include the prediction of molecular weight based on a statistical treatment of the primary neutral loss patterns of the best matching compounds to predict the neutral losses in the unknown. The unknown spectrum is tested for the presence of a molecular ion; if none is indicated the MW predictions use results from a new secondary-neutral-losses data class employing reference spectra without molecular ions. Confusion from isotopic peaks is minimized by prediction of the bromine and chlorine atom content of the unknown from isotopic abundances.[3] For unknown mass spectra selected at random, of which 15% have no molecular ion, there is a 91.3% probability that the highest confidence value

assignment is the correct molecular weight, and 94.7% for the first or second highest.

The substructure perception of STIRS has been improved by a new retrieval algorithm based on abundance weighting and, more importantly, by the inclusion of a new list of 600 substructures representing those giving the best performance out of 7,000 tested. For the best 192 of these the average recall was improved from 55% to 70% and false positives from 1.4% to 0.31%. A reliability value is determined for each substructure prediction (as described for PBM above), based on statistics determined using 900 spectra selected at random from the reference file. As an example, using the spectrum of CF_3-$CONHCH(CH_3)CH_2COO$-n-C_4H_9 as an unknown, STIRS predicted a molecular weight of 241 (correct, K = 23; MW 242, K = 0; MW 213, K = -8), with substructure predictions of methyl, 99%; C_2H_5, 99%; $-CF_3$, 99%; $-CO-CF_3$, 98%; -CO-O-, 97%; $CH_3-(CH_2)_3-$, 94%; $-NH-CO-CF_3$, 94%; $-O-(CH_2)_3CH_3$, 93%; $-CO-O-(CH_2)_3CH_3$, 92%; -O-CO-CH-NH, 88%; and -CO-NH-CH-CO-O-, 87%.

Version 4 of PBM/STIRS is now operational as a service over the TYMNET and TELENET computer networking systems from the Office of Computer Services, Uris Hall, Cornell University, Ithaca, New York.

---

[1] F.W. McLafferty and R. Venkataraghavan, J. Chromatogr. Sci., 17, 24 (1979).

[2] B.L. Atwater (Fell), R. Venkataraghavan, and F.W. McLafferty, Anal. Chem., 51, 1945-9 (1979).

[3] I.K. Mun, R. Venkataraghavan, and F.W. McLafferty, Anal. Chem., 49, 1723-6 (1977).

A LIBRARY SEARCH ROUTINE FOR THE IDENTIFICATION AND QUANTITATIVE DETERMINATION OF PRIORITY POLLUTANTS

J.R. Chapman, F.J. Street, G.A. Warburton, C.J. Wakefield, K.R. Compson
D. Hazelby, A. Carrick.
Kratos Ltd. Barton Dock Road, Urmston, Manchester M31 2LD, England.

The new Kratos DS55 library search comprises a number of search procedures which may be entered sequentially. The main search is based on the reverse search principle and, as such, is relatively immune to contributions from moderate levels of impurities in the unknown spectrum. The output from the main search comprises a matching score, a purity (or confidence) index and a comparison plot of library and unknown spectra. The purity index indicates the fraction of the unknown spectrum that is 'explained' by the library spectrum. Obviously this figure will fall when impurities are present so that the user is alerted to the fact that results cannot then be accepted with the highest confidence.

The pre-search is a rapid search which checks for the presence in the unknown spectrum of a limited number (4) of the major peaks from the library entry. Such a search on the main library considerably reduces the active list of spectra for consideration by the more detailed main search.

A number of other searches may be used to filter the EPA-NIH collection which forms the library data base. These are the molecular weight search, gc retention time search, formula search and the key search. The key search allows particular collections of spectra to be marked with a key so that unmarked library spectra are excluded from the comparison procedure if requested. All of these searches, together with the pre-search and main search, may be carried out sequentially and an active list of spectra examined at any stage in this process.

The separation by capillary gcms of a number of volatile standards from the EPA Priority Pollutants list is illustrated in Figure 1. The first gc peak is a doublet. The main search correctly indentifies the major component in the first two scans across this peak (scans 51-52) as 1,1-dichloroethane and the major component in the two succeeding scans (53-54) as 1,1,1-trichloroethane (figure 2). Mass chromatograms confirm these identifications. It will be noted that the pre-search has already reduced a library containing more than 30,000 spectra to a list of three possible candidates.

Quantitative data is also needed for components of interest. In Figure 3, a sophisticated quantitative package has been applied to the capillary gc analysis of a crude extract believed to contain polycyclic aromatics. The second trace shows the result of automatic baseline fitting and peak area delimiting by drop markers following a preliminary smoothing procedure. Peak heights and areas are automatically tabulated as shown following this process. The quantitative package may be applied to any mass chromatogram or to a chromatogram corresponding to a summed mass range over any number of scans. For example, the masses used in the pre-search for a particular component may be chosen. Figure 4 shows the output from the library search on a number of components carried out, in this case, on subtracted spectra.

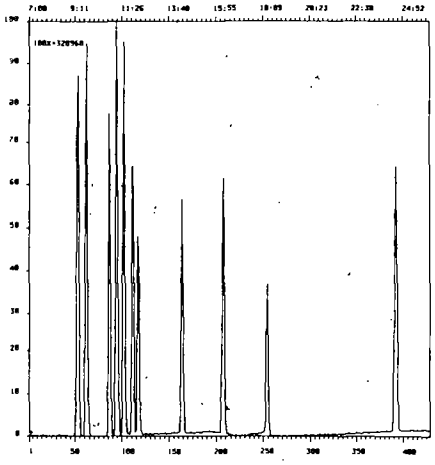

Fig.1. GC-MS separation of a Standard Mixture of EPA Priority Pollutants

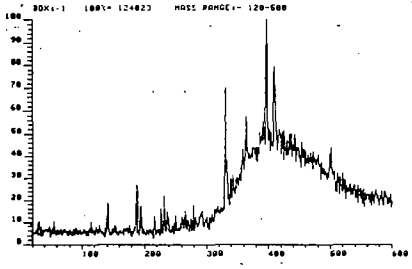

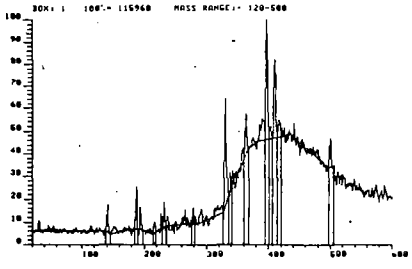

PAGE. 1

DS65 GC REPORT RUN: ICL3

PK. NO	MARKER TYPE	R.T. (SEC)	5% WDTH (SEC)	ST.	PEAK MAX	END	HEIGHT	AREA
1	BROP	364	15	138	141	145	0.20583E 5	0.39484E 6
2	BROP	483	11	185	187	190	0.29639E 5	0.62676E 6
3	BROP	499	12	190	193	198	0.19449E 5	0.31985E 6
4	BROP	561	10	214	217	219	0.11776E 5	0.14002E 6
5	BROP	608	9	229	232	236	0.22824E 5	0.31636E 6
6	BROP	728	8	276	278	281	0.19842E 5	0.18899E 6
7	BROP	865	19	327	330	336	0.74641E 5	0.19132E 6
8	BROP	879	9	336	339	341	0.36613E 5	0.15836E 6
9	BROP	944	-	360	364	368	0.66625E 5	0.49786E 6
10	BROP	1029	-	394	397	401	0.11592E 6	0.19236E 6
11	BROP	1063	-	406	410	414	0.96862E 5	0.13978E 6
12	BROP	1081	-	414	417	420	0.63713E 5	0.23936E 6
13	BROP	1296	-	498	500	505	0.64717E 5	0.43295E 6

Fig.3. Peak Area Calculation in a Chromatogram of an Extract Containing Polyaromatics

DS-55 LIBRARY SEARCH - MAIN SEARCH REPOR

RUNNAME:EPA11 SCAN: 51 DATE: 5/16/88 TI.

SCORE	FORMULA/NAME	MOL.WT.	MOL.ION.	R.T.	REL.PURITY	%	ENTRY
93	C2H4CL2 ETHANE, 1,1-DICHLORO-	98	0.5	0.0	1.0		836

DS-55 LIBRARY SEARCH - MAIN SEARCH REPORT

RUNNAME:EPA11 SCAN: 52 DATE: 5/16/88 TIME 1:35

SCORE	FORMULA/NAME	MOL.WT.	MOL.ION.	R.T.	REL.PURITY	KEYS	ENTRY
95	C2H4CL2 ETHANE, 1,1-DICHLORO-	98	0.5	0.0	1.0	0	836

DS-55 LIBRARY SEARCH - MAIN SEARCH REPORT

RUNNAME:EPA11 SCAN: 53 DATE: 5/16/88 TIME 1:36

SCORE	FORMULA/NAME	MOL.WT.	MOL.ION.	R.T.	REL.PURITY	KEYS	ENTRY
93	C2H3CL3 ETHANE, 1,1,1-TRICHLORO-	132	0.0	0.0	0.9	0	3698
79	C3H3CL3O PROPANOYL CHLORIDE, 2,2-DICHLORO-	160	0.0	0.0	0.7	0	7571
70	C2H3CL2NO2 ETHANE, 1,1-DICHLORO-1-NITRO-	143	0.0	0.0	0.7	0	5181

DS-55 LIBRARY SEARCH - MAIN SEARCH REPORT

RUNNAME:EPA11 SCAN. 54 DATE: 5/16/88 TIME 1:36

SCORE	FORMULA/NAME	MOL.WT.	MOL.ION	R.T.	REL.PURITY	KEYS	ENTRY
95	C2H3CL3 ETHANE, 1,1,1-TRICHLORO-	132	0.0	0.0	1.0	0	3698
82	C3H3CL3O PROPANOYL CHLORIDE, 2,2-DICHLORO-	160	0.0	0.0	0.9	0	7571
74	C2H3CL2NO2 ETHANE, 1,1-DICHLORO-1-NITRO-	143	0.0	0.0	0.9	0	5181

Fig.2. Library Search Outputs of Components of Unresolved GC Doublet

DS-55 LIBRARY SEARCH - MAIN SEARCH REPORT

RUNNAME:15ICL3 SCAN: 188 DATE: 5/16/88 TIME 1:18

SCORE	FORMULA/NAME	MOL.WT.	MOL.ION.	R.T.	REL.PURITY	KEYS	ENTRY
68	C11H10 NAPHTHALENE, 2-ME-	142	10.0	0.0	0.4	0	4900

DS-55 LIBRARY SEARCH - MAIN SEARCH REPORT

RUNNAME:15ICL3 SCAN: 193 DATE: 5/16/88 TIME 1:18

SCORE	FORMULA/NAME	MOL.WT.	MOL.ION.	R.T.	REL.PURITY	KEYS	ENTRY
64	C11H10 NAPHTHALENE, 1-ME-	142	10.0	0.0	0.4	0	4899

DS-55 LIBRARY SEARCH - MAIN SEARCH REPORT

RUNNAME:15ICL3 SCAN. 232 DATE: 5/16/88 TIME 1:19

SCORE	FORMULA/NAME	MOL.WT	MOL.ION.	R.T.	REL.PURITY	KEYS	ENTRY
77	C12H12 NAPHTHALENE, 1,7-DIME-	156	10.0	0.0	0.4	0	6986
73	C12H12 NAPHTHALENE, 1,4-DIME-	156	10.0	0.0	0.4	0	6983
72	C12H12 NAPHTHALENE, 1,5-DIME-	156	10.0	0.0	0.4	0	6984
72	C12H12 NAPHTHALENE, 1,2-DIME-	156	10.0	0.0	0.4	0	6985
72	C12H12 NAPHTHALENE, 1,3-DIME-	156	10.0	0.0	0.4	0	6987
72	C12H12 NAPHTHALENE, 2,3-DIME-	156	10.0	0.0	0.4	0	6989
70	C12H12 NAPHTHALENE, 1,6-DIME-	156	10.0	0.0	0.4	0	6988
70	C12H12 NAPHTHALENE, 2,6-DIME-	156	10.0	0.0	0.3	0	6990
69	C12H12 NAPHTHALENE, 2,7-DIME-	156	10.0	0.0	0.3	0	6991

DS-55 LIBRARY SEARCH - MAIN SEARCH REPORT

RUNNAME:35ICL3 SCAN: 270 DATE: 5/16/88 TIME 1:23

SCORE	FORMULA/NAME	MOL.WT.	MOL.ION.	R.T.	REL.PURITY	KEYS	ENTRY
74	C13H10 9H-FLUORENE	166	10.0	0.0	0.3	0	8446

DS-55 LIBRARY SEARCH - MAIN SEARCH REPORT

RUNNAME.35ICL3 SCAN: 397 DATE: 5/16/88 TIME 1:21

SCORE	FORMULA/NAME	MOL.WT	MOL.ION.	R.T.	REL.PURITY	KEYS	ENTRY
85	C16H10 FLUORANTHENE	202	10.0	0.0	0.5	0	13247
82	C16H10 PYRENE	202	10.0	0.0	0.5	0	13246

DS-55 LIBRARY SEARCH - MAIN SEARCH REPORT

RUNNAME 35ICL3 SCAN: 418 DATE: 5/16/88 TIME 1:21

SCORE	FORMULA/NAME	MOL.WT.	MOL.ION	R.T.	REL.PURITY	KEYS	ENTRY
75	C16H10 FLUORANTHENE	202	10.0	0.0	0.3	0	13247
74	C16H10 PYRENE	202	10.0	0.0	0.3	0	13246

Fig.4. Library Search Outputs of Extract Containing Polyaromatics

THE STATUS OF THE NIH/EPA MASS SPECTRAL SEARCH SYSTEM

D. P. Martinsen, Fein-Marquart Associates, Inc., Baltimore, MD 21212
R. S. Heller, University of Maryland, College Park, MD 20742
G. W. A. Milne, National Institutes of Health, Bethesda, MD 20205
W. L. Budde, U.S. Environmental Protection Agency, Cincinnati, OH 45268
S. R. Heller, U.S. Environmental Protection Agency, Washington, DC 20460

The Mass Spectral Search System (MSSS) is a set of programs which allow one to retrieve information from the NIH/EPA/MSDC Mass Spectral Data Base, the NBS file of proton affinities and gas-phase basicities, the Mass Spectrometry Bulletin and a file of CI mass spectra. The MSSS has been described before (1, 2). It is the purpose of this paper to present the new developments which have occurred during the past year.

A. The Data Base

The NIH/EPA/MSDC Mass Spectral Data Base has been updated and now contains 33,898 electron impact mass spectra. These spectra have been chosen from an archival file of over 60,000 mass spectra, retaining only one spectrum for each compound in the final data base. The data base may be searched online using MSSS. However, it may also be obtained on magnetic tape from the National Bureau of Standards (3), and in printed form from the Government Printing Office (GPO# 003-003-01987-9). The current 4-volume printed edition contains 25,560 spectra, but a supplement is in press, scheduled for release in August 1980, which will bring the total to 31,837 spectra. The chemical ionization data base has been enlarged to 1,295 spectra. In this data base, duplicates are retained and information is present for compounds using several different reagent gases and ion source conditions. The NBS file of gas-phase basicities and proton affinities contains approximately 650 measurements for 450 compounds. Citations to the literature describing each measurement or calculation are also provided.

B. The Search System

A number of significant developments have occurred in the MSSS during the past year. Results of data searches are now stored in temporary results files which are saved during the current MSSS session. These files contain a list of all compounds satisfying the criteria defined by the user using the various MSSS search options. Not only do these temporary results files provide greater flexibility in searching and displaying information within MSSS; they also increase the power of using MSSS in conjunction with other components of the NIH/EPA Chemical Information System (CIS). The CIS contains a wide variety of chemical data in addition to mass spectral data. Other components of the CIS contain such data as Carbon-13 NMR, powder diffraction, x-ray crystallographic data, single crystal parameters, toxicity data, and structure and nomenclature information. In using the temporary results files, results from MSSS may be displayed in other CIS components and results from various components may be combined in various ways. The options MERGE, INTER and NOT allow the creation of a new temporary results file containing, respectively, all references appearing in any of the input files, only those references common to all input files, or only those references appearing in one file but not in a second file. As an example of using these features, one may restrict a peak search in MSSS to those compounds containing a particular structural fragment defined by the Structure And Nomenclature Search System (SANSS) (using the INTER option). Alternatively, one could limit a peak search to those compounds not containing a particular structural fragment (using the NOT option). There are many such possibilities available.

Several other new options have been added to MSSS. The spectrum entry procedure has been modified so that it is necessary to enter the spectrum only once to do both Biemann (KB) and probability-based matching (PBM) searches, as well as a dissimilarity comparison. An option BATCH has been added which performs KB and PBM searches in a batch mode, storing results in a disk file for later examination. Thus, one may continue using other MSSS options, rather than letting the terminal sit idle while the sometimes lengthy searches are accomplished.

Of course, MSSS still contains the options for printing and plotting mass spectra, retrieving compounds according to molecular formula and weight, the Mass Spectrometry Bulletin searches, the proton affinity searches and the search of the chemical ionization data base.

References

1. D. P. Martinsen and R. S. Heller, presented at the 27th Annual Conference on Mass Spectrometry and Allied Topics, June 3-8, 1979.

2. S. R. Heller, G. W. A. Milne, and R. J. Feldmann, Science, 195, 253 (1977).

3. NIH/EPA/MSDC Mass Spectral Data Base, Office of Standard Reference Data, National Bureau of Standards, Washington, DC 20234.

MPMP22 "HARDWARE" BACKGROUND/FOREGROUND DATA SYSTEM: AN ESSENTIAL DEVELOPMENT IN SUPPORT OF METABOLIC PROFILING ON MAGNETIC SECTOR MASS SPECTROMETERS, F. Martin, S. Johnson, M. McPherson and J. Holland, Dept. of Biochem., Michigan State Univ., East Lansing, MI, 48824.

The processor time encumbered by on-line collection of magnetic sector, cyclic scanning data and the copious amounts of data generated in metabolic profiling have precluded the use of software background/foreground in the processing of such data. The length of time needed for data processing and outputting reduces the effective analysis time of a single processor system by more than half. Even with online access to a distributed computing network to enable the execution of library search routines on remote processors, operator interaction and data transfer still severely encumber sample analysis throughout. This problem has been resolved in a very economical manner by the addition of a second computer to the mass spectrometer data system. Software has been written to support downstream loading of the data acquisition programs into the added computer. The host processor executes a multitask, real-time executive program from a single terminal in a software background/foreground mode. The data collection routines are executed in the added computer as an extension of the software foreground program. Data interaction, processing, transfer and output routines can be simultaneously executed in the host processor. Data will be presented illustrating the operational advantages and increased sample throughput of this system.

A New Approach to Computer Controlled Metastable Scanning in Organic Mass Spectrometry.

J. C. Bill, A. J. Gilbert, R. F. Reinsch, M. J. Wallington and P. Powers.
VG Data Systems Limited, Tribune Avenue, Altrincham, Cheshire, England WA14 5TP.

Introduction

A study of the metastable transitions occurring in the first field free region of a double focusing sector mass spectrometer gives valuable information on the precursor/daughter relationships between ions in the mass spectrum.

Until now such studies have usually only been possible in an analogue manner by using specific interlinked power units. As a consequence, the technique has been difficult to use and has only received limited acceptance.

This paper discusses a new approach involving an extension to the computer controlled metastable scanning method first proposed by Haddon. (1)

A new microprocessor based digital scan unit has been developed which provides up to three separate channels for digital control of all analogue instrumental functions. Using this unit and a comprehensive software suite, the spectrometer magnet is scanned normally until the chosen precursor mass (B/E scan) or daughter mass (B^2/E scan) is reached. At this moment the scan departs from the $E/E_0 = 1$ axis along a precalculated curve chosen to give the appropriate linked scan. Subsequent scans may be of different linked scan precursors/daughters or, of course, of normally focused spectra.

The Scans

B/E	-	Select an ion and determine how it fragments. Used for mixture analysis, identification of small components and in stereo chemistry for separation of isomers or closely related compounds.
B^2/E	-	Select a daughter ion and determine its precursors. Gives complementary information to the B/E scan allowing proper identification of ambiguous precursor mass assignments in some B/E scans.
$\frac{B}{E}(1-E)^{\frac{1}{2}}$	-	Obtain a spectrum of all metastable peaks generated by reactions having the same mass loss. Useful in the analysis of isotopic constituents of labelled molecules. Allows unique identification of a molecule.

The Digital Scan Unit.

The Digital Scan Unit is a microprocessor controlled, programmable reference supply capable of controlling up to three voltage references and of scanning one or two of these simultaneously in one of a number of predetermined ways.

Input to the scan unit is via an ASCII serial link through which command strings are passed. Output from the unit is in the form of one, two or three voltage signals, each in the range 0-10v for input to programmable power supplies controlling Electrostatic Analyser Voltage, Magnet Current and Accelerating Voltage. These reference outputs can be stepped digitally in order to generate a specific ramp or they can be scanned exponentially up or down to any of a wide range of scan laws.

Performance

* B/E B^2/E and Constant Mass Loss linked scan spectra routinely available during GC/MS runs.
* Fast operation up to 3 sec/decade facilitates the determination of components of mixtures introduced via direct inlet probe.
* 10 linked scan precursor (B/E) or daughter (B^2/E) ions presettable before run.
* New real time feature permitting keyboard call for normal scan or different linked scan start mass during the run.
* Nominal mass assignment for B/E scans.
* Full spectrum profile for B^2/E scans.

(1) W. F. Haddon, Anal. Chem. 51 983-988 1979

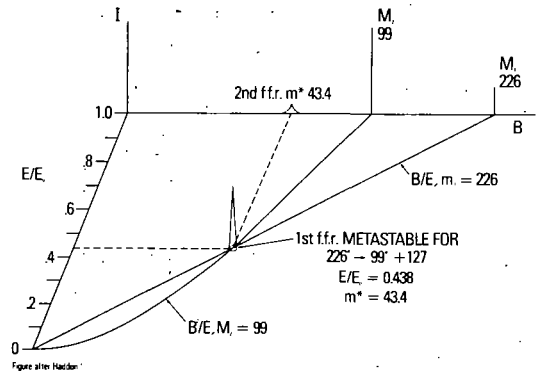

Figure after Haddon

SCHEMATIC DIAGRAM OF LINKED SCANS IN THE B-E PLANE

Figure 1.

Conventional mass scans take place at constant electrostatic sector voltage along the $E/E_0 = 1$ axis. Here, for simplicity, a simple two peak spectrum is assumed.

B/E scans are initiated once the required precursor mass (here $^m/e$ 226) has been reached and the scan then follows a straight line in the B-E plane.

B^2/E scans are initiated once the required daughter mass has been reached and the scan then follows a curve in the B-E plane.

All metastable peaks formed in the first field free region (f.f.r.) and having $^m/e$ 226 as a precursor lie on the B/E line. All those peaks for which $^m/e$ 99 is the common daughter lie on the B^2/E curve.

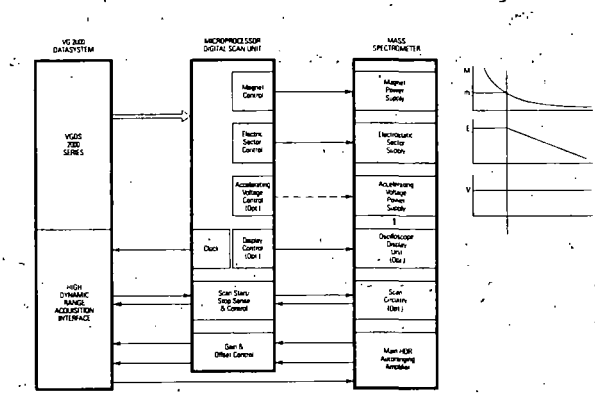

Figure 2.

SCHEMATIC DIAGRAM OF VG LINKED SCAN SYSTEM

The microprocessor based Digital Scan Unit accepts control character strings from the VGDS 2000 series datasystem and issues reference control signals to the main power units of the mass spectrometer.

At a predetermined mass in the magnet scan, a separate scan is made of the electrostatic sector voltage in such a way as to generate the appropriate linked scan.

The Digital Scan Unit issues its own synchronising clock pulses to ensure that scanning and signal digitisation are in step.

Independent control of amplifier gain and offset is provided within the Digital Scan Unit.

ON THE REAL-TIME MEASUREMENT OF PARTICLES IN AIR BY DIRECT-INLET SURFACE IONIZATION MASS SPECTROMETRY

J. J. Stoffels and C. R. Lagergren
Pacific Northwest Laboratory*, Richland, WA 99352

Abstract

A method for real-time analysis of particles in air was reported by W. D. Davis at the 1973 ASMS Conference. The method involves direct impaction of particles in the air onto the ionizing filament of a surface ionization mass spectrometer. We have developed direct-inlet surface ionization mass spectrometers using both dispersive magnetic analyzers and a non-dispersive quadrupole mass filter. We report here on investigations made with the instruments.

The instruments can be used for the measurement of mass concentration of a particulate substance in air or for the measurement of individual micrometer and sub-micrometer size particles. The former technique requires that the ionizing filament be operated at a relatively low temperature so that the ion currents from individual particles blend into a dc output signal. The latter technique requires that the filament be operated at a higher temperature so that the individual particles produce short bursts of ions which are resolved in time. The ion burst, then, is a measure of the amount and type of material in the particle.

Our work has focused on the latter technique with the objective of being able to measure, in real time, the size distribution of particulate substances in air. The temperature variation of the ion yield and of the decay time of the Cs^+ ion signal from cesium nitrate particles have been measured.

The distribution of integrated ion bursts has also been compared with the size distribution of cesium nitrate particles. The ion yield is not proportional to the mass or volume of the particles, but is approximately proportional to the surface area of the particles. In other words, the ion yield is inversely proportional to particle size.

Recent observations show that some particles may bounce on impact with the ionizing filament resulting in a significant loss of measurement sensitivity. The occurrence of particle bounce varies with particle material and size and with filament operating temperature. We have demonstrated that the particle bounce problem can be overcome by the use of a rhenium oven to trap and ionize the impacting particles.

---

*Operated by Battelle Memorial Institute for the Department of Energy.

TAMOA2 COMPUTER CONTROLLED SCANNING LASER MASS SPECTROMETER, R. J. CONZEMIUS, J. CAPELLEN, and H. J. SVEC, Ames Laboratory-USDOE and Dept. of Chem., Iowa State Univ., Ames, IA 50011

A scanning laser mass spectrometer[1] (SLMS) has been interfaced to a small computer allowing program control of the site of laser excitation as well as of the spectral information. Applications will be described of this automated system to metallurgical problems. A method will be shown for quantification of concentration profiles of trace levels of molybdenum in thorium in an electrotransport experiment. Measurement of important trace level variation of carbon in the microphases of super conducting alloys will also be shown.

Results of a recent worldwide review[2] indicates a great potential use for laser ionization in solids characterization. Most of the recent work has not been reported at ASMS conferences. Some very exciting advances will be described.

[1]R. J. Conzemius and H. J. Svec, Anal. Chem. 50, 1854 (1978).

[2]R. J. Conzemius and J. Capellen, to be published in Int. J. Mass Spectrom. Ion Phys.

POSITIVE AND NEGATIVE ION PRODUCTION IN SPARKED SF_6[#]

L. C. Frees, L. G. Christophorou[†], H. W. Ellis[*], and
I. Sauers, Atomic, Molecular and High Voltage Physics
Group, Oak Ridge National Laboratory, Oak Ridge, TN 37830

Sulfur hexafluoride has gained wide acceptance as an insulator for electrical power transmission systems. Its decomposition under electrical stress, however, is not fully understood. We have begun a study of ionization phenomena, resulting from high voltage discharges in high pressure ($p > 1.3$ kPa) gases. The apparatus consists of a spark source (Fig. 1) and quadrupole mass spectrometer (Extranuclear Laboratories SpectrEL System with ion-focusing lens assembly for atmospheric pressure ionization). The source, housing a pair of tungsten electrodes with a typical gap of 0.5 mm, permits positioning of the spark within 1.0 mm of the sampling orifice of the mass spectrometer. The data presented here were taken under the following spark conditions: -2.7 kV breakdown voltage, dropping to -50 V during the spark, 7A spark current, 2.7 μsec spark duration, and 27 Hz spark repetition frequency. Ions observed for negative high voltage breakdown in SF_6 at 5.3 kPa included F^-, F_2^-, SF_5^-, SF_6^-, SF_5^+, SF_4^+, SF_3^+, SF_2^+, SF^+, S^+, F^+, and traces of SOF^+.

In addition to mass spectra, we were able to examine the arrival time of mass-selected ions (Figs. 2 and 3) using a time-of-flight electronics module and multichannel analyzer. Preliminary work on negative ion arrival times indicates that for spark to aperture distances, d, in the range 1-2 mm, the arrival times of negative ions divide them into two groups, "fast" and "slow". The "fast" group exhibited energies as high as 100 eV, while the slow group contained 0-4 eV ions. These energies were confirmed by using the first element of the ion-focusing assembly in a retarding grid mode. At increasing d (2.0-2.5 mm) the intensities of the two groups diminished, but at still larger d (2.5-3.0 mm) a second peak sometimes appears in the SF_6^- and SF_5^- intensity vs. distance plots. The ions corresponding to this second peak were slow and they were possibly formed in the vicinity of the aperture by slow electrons. For all the positive ions detected, only slow ions were observed. All the ions (positive and negative) observed are associated with the onset of breakdown as variation in the spark pulse width was found to have no effect on the arrival time spectra. The effect of d (1.0-3.0 mm) and p (2.7-9.3 kPa) on ion intensities has been studied, and these data indicate that fast group ions will probably not be observed for pressures greater than ~13 kPa.

Arrival time spectra have been converted to ion kinetic energy spectra by an appropriate transformation. The fast group maxima in the intensity versus energy curves are at 34, 22, and 16 eV for F^-, SF_5^-, and SF_6^-, respectively. The slow group maxima are at 0 eV for SF_6^- and SF_5^- and at 3.3, 1.1, and 0 eV for F^-. The F^- data indicate that F^- ions may be produced with varied amounts of initial kinetic energy.

Further studies at pressures approaching 100 kPa are in progress. A complete understanding of the decomposition mechanisms in high pressure dielectric gases should aid the tailoring of dielectric gas mixtures for practical uses.

[#]Research sponsored by the Division of Electric Energy Systems, U.S. Department of Energy under contract W-7405-eng-26 with the Union Carbide Corporation.

[†]Also Department of Physics, University of Tennessee, Knoxville, Tennessee 37916

[*]Permanent address, Department of Natural Science, Eckerd College, St. Petersburg, Florida 33733

By acceptance of this article, the publisher or recipient acknowledges the U.S. Government's right to retain a nonexclusive, royalty-free license in and to any copyright covering the article.

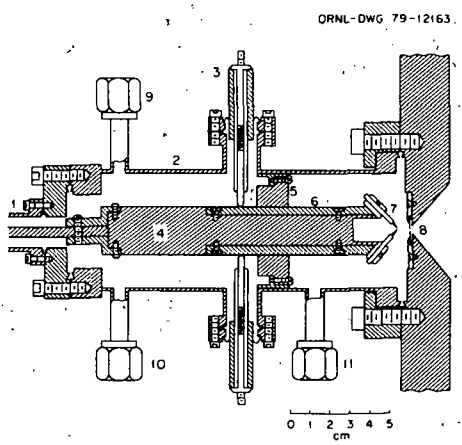

Figure 1 High pressure spark ion source 1) linear motion feedthrough, 2) vacuum wall, 3) high voltage feedthrough, 4) electrode insulator, 5) centering insulator, 6) electrode contact rails, 7) tungsten electrodes, 8) pinhole aperture, 9) vacuum line, 10) pressure gauge line, 11) gas inlet line

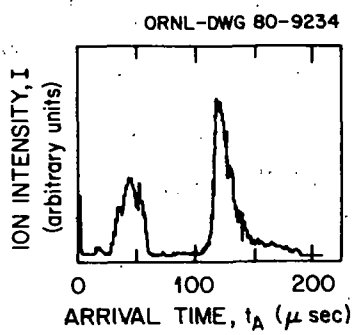

Figure 2 SF_6^- arrival time spectrum (d = 1.0 mm, p = 5.3 kPa

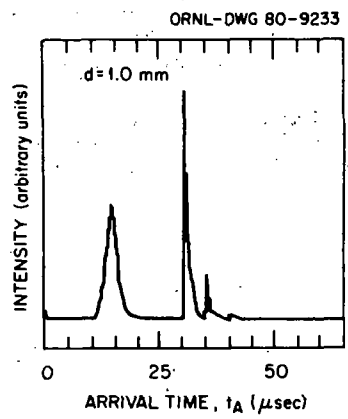

Figure 3 F^- arrival time spectrum (d = 1.0 mm, p = 5.3 kPa

THERMODYNAMIC STABILITY OF RARE EARTH-PLATINUM METAL DIATOMICS

K.A. Gingerich, S.K. Gupta, R. Haque, B.M. Nappi, and M. Pelino

Department of Chemistry, Texas A & M University, College Station, TX 77843

The diatomic rare earth-platinum metal intermetallic molecules are among the most stable ligand-free metal molecules known to date[1]. The measurement of their dissociation energies is of relevance to the study of alloy thermodynamics and metal clusters. In addition, the experimentally determined dissociation energies permit a test of the various empirical models of metal-metal bonding, such as the empirical valence bond model[1-3] and the atomic cell model.[4] The former has been found applicable to the diatomic intermetallic molecules containing a platinum metal and a lanthanide, actinide, group III, or group IV transition metal molecules except those of the lanthanides and actinides but including those of La and Th.[1,5]

In the present investigation we have used the Knudsen effusion mass spectrometric method to identify the molecules LaPt, IrY and PtY and to determine their dissociation energies. The results are compared with values predicted by the two empirical models.

The intermetallic molecules LaPt, IrY and PtY were observed in the equilibrium vapors above the corresponding alloy-graphite systems at high temperatures. Tantalum Knudsen cells with graphite inner liners and 0.040 in. diameter orifices were employed for each of the systems. In each case, the molar ratio of the platinum metal to the rare earth metal in the Knudsen cell charge was equal to three or greater. The energy of the ionizing electron beam was 19-22 eV. A small amount of pure gold was placed in the cells for the purpose of the determination of the absolute sensitivity of the instrument through the well known equilibrium reaction $Au_2(g)=2Au(g)$.[6] The details concerning the instrument and the experimental procedures have been described elsewhere [7].

The ionic species were identified by their m/z ratios and isotopic abundance measurements. The low appearance potentials measured for the molecular ions $LaPt^+$(5.4±0.8 eV), IrY^+(8.5±1.0 eV) and PtY^+(6.3±2.0 eV) assured their origin from the corresponding neutral molecules. The absolute partial pressures of the gaseous species observed were obtained from the ion currents by the relation $P_i=k_i I_i^+ T$, where the pressure calibration constants k_i were calculated fron that of gold, k_{Au}, and the relative ionization cross sections and electron multiplier gains.

The second and third-law analyses of the partial pressures measured as a function of temperature were carried out to determine the enthalpy changes for the following equilibrium reactions

$$LaPt(g) = La(g)+Pt(g),$$
$$IrY(g) = Ir(g)+ Y(g),$$
and
$$PtY(g) = Pt(g)+ Y(g).$$

The necessary thermodynamic functions for the diatomic species were calculated from the following estimated molecular constants (r_e in Å and ω_e in cm^{-1}): LaPt,2.62 and 280.6:IrY, 2.48 and 257.0; and PtY, 2.61 and 241.0. The electronic contributions to the thermodynamic functions were based on the estimated ground states of $^4\Sigma$, $^1\Sigma$, and $^2\Sigma$ for LaPt, IrY, and PtY, respectively. The experimental and derived thermochemical data for the diatomic molecules studied are presented in Table I.

Table I. Experimental reaction enthalpies and the derived thermochemical data for the gaseous molecules LaPt, IrY, and PtY (all values in $kJmol^{-1}$). [a)]

Reaction (temperature range)	ΔH_0^o (IInd-law)	ΔH_0^o (IIIrd-law)	$\Delta H_{f,298}^o$	D_0^o
LaPt(g)=La(g)+ Pt(g) (1959-2466K)	493.1 ± 13.4	498.1 ± 3.7	498 ± 14	496 ± 13
IrY(g)=Ir(g)+ Y(g) (2444-2787K)	458.6 ± 19.1	449.9 ± 2.7	638 ± 20	453 ± 16
PtY(g)=Pt(g)+ Y(g) (2456-2707)	475.1 ± 13.0	465.6 ± 4.1	516 ± 9	470 ± 8

a) The error limits cited with ΔH_0^o values are the standard deviations and those with $\Delta H_{f,298}^o$ and D_0^o values correspond to overall uncertainties.

The agreement between the second-law and third-law enthalpies is quite good for each of the three equilibria. The dissociation energies and the standard heats of formation are based on the mean of the two determinations.

Table II. Comparison of experimental dissociation energies with values calculated using valence bond and atomic cell models. (Values are in kJ mol^{-1}).

Molecule	D_0^o	D_0^o (calculated)	
	Experiment	Valence bond model	Atomic cell model
IrLa	573 ± 12 (ref. 8)	565	537
IrY	453 ± 16	451	522
LaPt	496 ± 13	423	484
LaRh	525 ± 17 (ref. 9)	540	470
PtY	470 ± 8	316	470
RhSc	440 ± 11 (ref.10)	387	467
RhY	442 ± 11 (ref.10)	424	452

In Table II, the experimental dissociation energies of LaPt, IrY, and PtY along with those of the other known[8-10] Group III-platinum metal diatomic molecules are compared with the values calculated by the empirical valence bond model and the atomic cell model. The values predicted by the atomic cell model agree well (withih 10 percent) with the experimental ones for all molecules except LaRh. In the case of the valence bond model, the calculated values compare very well with the experimental ones for all molecules except the platinum-containing molecules. As has been discussed previously,[1] the empirical valence bond model underestimates the dissociation energies for platinum-containing intermetallic molecules because of the non-availability of a suitable valence state for Pt atoms which can form more than two valence bonds. The overall trends in the dissociation energies of the platinum metal-rare earth diatomic molecules may be qualitatively interpreted in terms of the molecular orbital theory and the fact that the bonding efficiency of d-orbitals increases with the principle quantum number. Thus the molecule IrLa has the highest dissociation energy since both Ir and La are in the 5d series and the 12 valence electrons available occupy all of the six bonding MO's[11]. The molecules RhY and IrLa are isoelectronic with the Group VI transition metal dimers Mo_2 and W_2 respectively. On the basis of the dissociation energy of 404 ± 20 kJ mol^{-1} for Mo_2[12], one may predict the dissociation energy of W_2 to be 535 ± 40 kJ mol^{-1}.

Acknowledgment: The authors thank the National Science Foundation(Grant No. CHE-08711) for the support given this work.

References

1) K. A. Gingerich, Int. J.Quantum Chem. Symp. 12, 489 (1978).
2) K. A. Gingerich,Chem. Phys. Letters, 23 270 (1973).
3) K. A. Gingerich, J. C. S. Faraday II, 70, 471 (1974).
4) A. R. Miedema and K. A. Gingerich, J. Phys. B: Atom. Molec. Phys. 12, 2258 (1979).
5) A. R. Miedema, Faraday Symposium 14, paper 14/7 (1980), in print.
6) J. Kordis, K. A. Gingerich, and R. J. Seyse, J. Chem. Phys., 61, 5114 (1974).
7) K. A. Gingerich, in Proceedings of the 10th Materials Research Symposium on Characterization of High Temperature Vapors and Gases (Gaithesburg, Maryland: National Bureau of Standards, 1979), p. 289.
8) R. Haque, M. Pelino and K. A. Gingerich, J.Chem.Phys. 71. 2929 (1979).
9) D. L. Cocke, K. A. Gingerich and J. Kordis, High Temp. Sci. 5, 474 (1973).
10) R. Haque and K. A. Gingerich, J. Chem. Thermodynamics, in print.
11) J. G. Norman, Jr., H. J. Kolari, Inorg. Chem. 16, 987 (1977).
12) S. K. Gupta, R.H. Atkins and K. A. Gingerich, Inorg. Chem. 17, 3211 (1978).

TAMOA5 A PRECISE METHOD FOR THE MASS SPECTROMETRIC ANALYSIS OF SILVER, L. P. Dunstan, K. A. Brletic and E. L. Garner, National Bureau of Standards, National Measurement Laboratory, Center for Analytical Chemistry, Washington, DC 20234

A mass spectrometric method has been developed for the determination of precise isotopic abundance measurement of microgram quantities of silver. This procedure, which employs a platinum single silica gel approach, was developed for use in a redetermination of the atomic weight of silver. The atomic weight of silver was accurately determined by our laboratory in 1960[1] with an uncertainty of 1 part in 10^5. However, a high accuracy determination of the electrochemical equivalent of silver by Bower and Davis[2], has produced a situation where this value for the atomic weight is the largest known source of uncertainty in the Faraday constant.

The procedure requires five micrograms of silver as silver nitrate which is dried onto a layer of silica gel using electrical currents and a heat lamp. Finally, phosphoric acid is dried on top of the sample and the filament is transferred to a nitrogen atmosphere where a high temperature drying step is accomplished using a pyrometer. The mass spectrometric analysis is accomplished at a temperature of approximately 800°C. The key to the high precision of the method, nine parts in 10^5 (S.D.) for 23 degrees of freedom, is careful control of the sample drying and instrumental analysis parameters. The isotopic ratio data for the analysis of silver in a variety of high purity and geological samples will be presented.

[1]W. R. Shields, E. L. Garner, and V. H. Dibeler, J. Res. Nat. Bur. Stand. (U.S.), 66A (Phys. and Chem.), 1 (1962).

[2]V. E. Bower and R. S. Davis, to be published in J. Res. Nat. Bur. Stand. (U.S.), 85, No. 3, May/June 1980.

ABSOLUTE Li ISOTOPE RATIO MEASUREMENTS, E. L. Callis, A. E. Essling, G. Reedy, and R. J. Meyer, Chemical Engineering Division, Argonne National Laboratory, Argonne, IL 60439

Absolute Li isotope ratios were measured by triple-filament thermal ionization mass spectrometry using synthetic mixtures of ^7Li and ^6Li as standards. The separated Li isotopes, >99% enriched, were obtained from Oak Ridge National Laboratory as high purity metals. Spectrographic analyses were performed to verify the purity of the starting material. Master solutions of the ^6Li and ^7Li were prepared by dissolution of the metals in alcohol and dilute HCl, conversion of the Li to stoichiometric LiCl, and dissolution and dilution to a known weight of solution with high purity water. Weighed aliquots of the master solutions were then withdrawn for Li content measurements and preparation of calibration mixtures.

Two independent gravimetric methods were used to determine the LiCl content of the solutions: (1) Assay of Li by conversion of the LiCl to Li_2SO_4 and (2) Assay of Cl by precipitation as AgCl. Four determinations by each method for the ^6Li and ^7Li solutions were made. The results of the independent determinations agreed to within 0.1% for the ^7Li and within 0.3% for the ^6Li. The average of both results was taken as the best value of the Li concentration. Calibration mixtures having $^7Li/^6Li$ ratios of nominally 0.1, 1, and 10 were prepared from aliquots of the master solutions which had been diluted to an appropriate volume. The concentration of Li in the mixes was adjusted to 10 μgLi/mL in 0.5% HCl.

The mass spectrometer used in this work was a 30 cm radius, 90° instrument of National Bureau of Standards design. Approximately 0.05 μg of Li as LiCl was used for each analysis. The ionizing filament was operated at a temperature of 1550°C and ion intensity measurements were made on the Li^+ ion. Due to the large relative mass difference of the Li isotopes, strict control of ion-source parameters such as focusing, filament positioning, and ionizing filament temperature was necessary in order to make reproducible ratio measurements. The effect of ion-source focusing was reduced somewhat by the installation of magnetic shielding to reduce the stray field in the source region. Much of the run-to-run variability in measured isotopic ratio appears to be related to the condition of the ionizing filament. Although all filaments were degassed in a vacuum chamber at 1800°C, filaments from different batches, and often within a batch, showed systematic differences in the ratio measurements. Improved results were obtained when a single ionizing filament was used for a series of analyses, the calibration mixes and unknown samples being analyzed alternately. Several tests were made to assure that no memory effects were induced by this procedure. Using this technique, standards and samples can be intercompared with a precision of ±0.15%.

Several analyses were performed on two Li_2CO_3 reference materials distributed by the Department of Energy's Ames Laboratory,[1] and by the National Bureau of Standards. Only the Ames material has been standardized (by Flesch, *et al.*[1]) against synthetic standards. The results of these analyses are listed below:

Material	Corrected $^7Li/^6Li$ Ratio	Number of Determinations
NBS #9, Li_2CO_3	12.19 ± 0.06	8
AMES, Li_2CO_3	12.19 ± 0.06	9
AMES, published value[1]	12.02 ± 0.029	

The error limits listed for these measurements are the total estimated including uncertainty in the preparation of the calibration mixes and random errors associated with the mass spectrometric measurements. These results indicate that the two materials have the same $^7Li/^6Li$ ratio, within the precision of the measurement, ±0.15%. The reason for the discrepancy between the results of this work and the published values is not readily apparent. Further work is needed to resolve this question.

---

[1]Flesch, G. D., Anderson, A. R. and Svec, H. J., Int. J. Mass Spectrometry and Ion Physics, 12 (1973) 265-272.

SECONDARY ION MASS SPECTROMETRIC ANALYSIS
OF COBALT HARDENED GOLD ELECTROPLATE SURFACES

by

Rudolf Schubert
Bell Laboratories, Incorporated
6200 East Broad Street
Columbus, Ohio 43213

In Co hardened Au electroplate, the Co will diffuse to the surface with time, where it can form an insulating film. It is of interest to know the chemical form of this surface Co on electrical connectors. Secondary ion mass spectrometry is used to distinguish Co, CoO, Co_3O_4, and cobalt hydroxides in less than full monolayer quantities on impure surfaces. This distinction of compounds is made by comparing the positive and negative secondary ion spectra of Au electroplate with standard samples. Both Ar and O_2 are used for the primary beam. Spectra are compared from before and after UHV bakeout. It is shown that electroplated Au samples have different Co compounds on their surface depending upon the sample history. For Co hardened Au electroplate heat treated at 150°C in air, the surface Co is in the form of CoO and Co. When heat treated at 200°C in air, the surface Co appears to be in the form of a cobalt hydroxide. Numerous other surface species are also identified and discussed. This paper will appear in the Journal of the Electrochemical Society.

TABLE I

FRAGMENTATION PATTERNS OF PSI AND NSI
OF COBALT AND COBALT OXIDES

		Relative Intensities				
Sample	Pos./Neg.	^{59}Co	$^{59}Co^{16}O$	$^{59}Co^{16}O_2$	$^{59}Co_2$	$^{59}Co_2{}^{16}O$
Co Foil	P	100	0.5	-	6.9	0.4
	N	100	-	-		-
CoO Powder	P	100	1.1	-	1.2	1.0
	N	50	66	100	-	-
Co_3O_4 Powder	P	100	0.8	-	2.5	0.9
	N	7	40	100	-	-
Au a) No Heat Treatment	P	100		-		-
	N				-	-
Au b) 150°C, 2000 Hrs. in Air	P	100	0.5	-	1.0	0.2
	N	100	49	71	-	-
Au c) 200°C, 120 Hrs. in Air	P	100	0.4	-	0.7	0.1
	N	0.9	100	92	-	-

ANALYSIS OF AEROSOL PARTICLES BY MASS SPECTROMETRY

M.P. Sinha, C.E. Giffin, D.D. Norris
Jet Propulsion Laboratory, Pasadena, Ca. 91103 and
S.K. Friedlander, University of California, Los Angeles, Ca. 90024

Introduction: The chemical composition of aerosol particles are generally determined by bulk analysis methods after collection on a substrate. The analysis provides time average and size average composition mostly elemental in nature. The results can be applied to aerosols in their natural environment only with reservations. A continuous, real time analyzer of single aerosol particles is being developed in our laboratory using the mass spectrometric technique. This paper describes some of our preliminary results of Particle Analysis by Mass Spectrometry (PAMS).

Experimental: Figure 1 shows the experimental setup. It comprises a particle beam generator and a quadrupole mass spectrometer system. An air stream of monodisperse aerosol of known chemical composition is produced by a vibrating-orifice generator (TSI Model 3050) and is introduced into the plenum. An optical particle counter (Climet Instruments Model 208) is used to determine the number density and size of the particles in the plenum. The aerosol particle beam is finally generated after expansion through the capillary tube and the skimmer.[1] The particles then impinge one at a time on a hot rhenium filament placed within the ionizer of the spectrometer (UTI 100C). The resulting vapor is ionized by electron impaction producing a burst of ions from each particle. Each spike in Figure 2 is a record of such events from different particles (1 μm diameter) of dioctyl phthalate (DOP). The quadrupole is operated in the manual mode at different fragment mass peaks. The nonscanning mode is necessitated by the short pulse width (<100 μsec) of the ion bursts. The area under the pulse is the measure of the number of ions of the particular mass. The pulse height distribution of the signals is determined with a pulse height analyzer (ND-130) after suitably shaping them.

Results and Discussion: Figure 3 summarizes some of our results obtained with different aerosols. Ammonium sulfate is one of the most abundant components of urban aerosols. Adipic and glutaric acids are the secondary components believed to be formed by the oxidation of cyclohydrocarbons. The results show the inherent capability of this technique for the quantitative determination of the different compounds. Signals from different particles of diameter ranging from 0.8 μm to 2.1 μm show linear dependence with the volume of the particles. A typical pulse height distribution plotted on probability paper is shown in Figure 4. One standard deviation in the distribution is about 10% of the peak. Results from two component aerosols are shown in Figure 5. The relative intensities of the various mass fragments from the particles are somewhat different than those in the conventional EI mass spectra. The difference in the fragmentation pattern, we believe, results from the extremely transient nature of the heat transfer from the hot filament to the particle. From the measured ion current, it is found that the ratio of the number of molecules in a 1 μm particle to the number of ions at their characteristic peaks ranges between 10^{-4} to 10^{-5}. This accounts for the different losses, volatilization and ionization efficiences. The pulse shape of the ion bursts is dependent on the temperature of the Re-filament. Lower temperature, in general, increases the pulse width. The optimum temperature in the present studies was found to be about 450C.

Another system of practical importance studied in our laboratory is sulfate/sulfite analysis of aerosol particles. Impaction of $(NH_4)_2SO_4$ particles on hot Re-filament followed by electron bombardment results into fragment ions of SO^+, SO_2^+, and SO_3^+ from sulfate part of the salt. The relative intensities of these peaks are found to be 0.83:0.77:1.0. Similar studies with sodium sulfite aerosols give signals at SO^+ and SO_2^+ only. No signal of SO_3^+ could be detected at any temperature (350 - 1400 C). The absence of SO_3^+ ions from sulfite and its pronounced appearance from sulfate furnishes a simple method for the identification of sulfate and for the differentiation between sulfate and sulfite.

In conclusion, we have shown that the technique of PAMS holds the promise of a valuable tool for the chemical analysis of simple aerosols in real time. Work is also in progress towards the development of a rather soft method for the volatilization and ionization of aerosols. A Nd-Yag laser is being used for this purpose. A focal plane mass spectrometer with an electro-optical ion detector array[2] has been constructed. This will provide the entire mass spectrum (25-500 amu) from single particles. The work is supported by the National Science Foundation.

References:

1. G.W. Israel and S.K. Friedlander, J. Colloid Interface Sci. 24, 330 (1974).
2. C.E. Giffin, R. Britten, H. Boettger, J. Conley, and D. Norris, ASMS Transaction (1979).

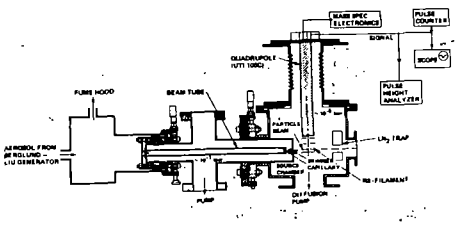

Figure 1: Experimental Setup

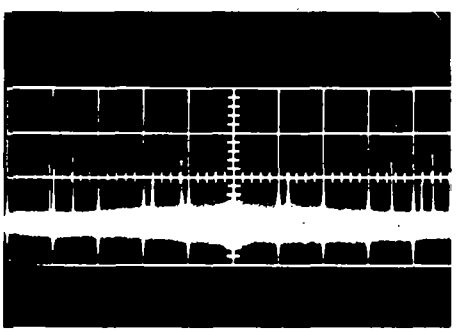

Figure 2: Pulses from Individual Particles

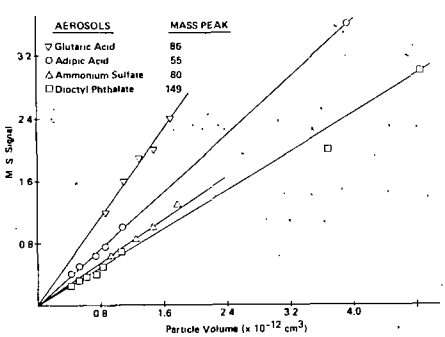

Figure 3: Signals from Different Aerosols Versus Particle Volume

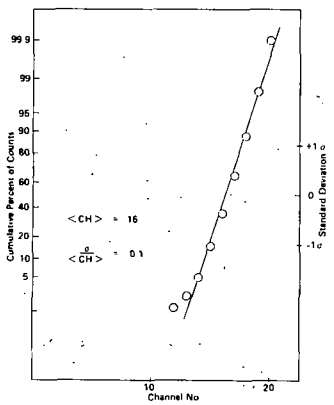

Figure 4: Pulse Height Distribution For DOP Particles

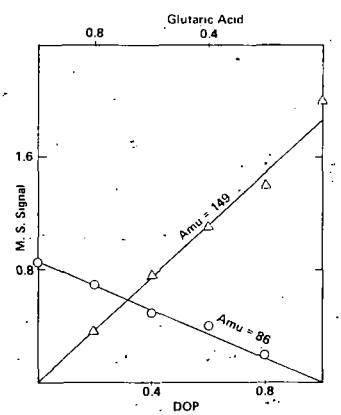

Figure 5: Signal Intensities of the Components Versus Their Mass Fractions

FURTHER DEVELOPMENT OF PARTICULATE IMPACT MASS SPECTROMETRY

Frank T. Greene
Midwest Research Institute
Kansas City, Missouri 64110

Particulate Impact Mass Spectrometry has been previously proposed and some preliminary results obtained.[1,2] In this technique droplets which contain the nonvolatile substance dissolved in a volatile solvent such as water are accelerated to approximately sonic velocities and impacted on a warm plate above the electron beam in the ion source of the mass spectrometer, where inelastic collisions occur. It is hypothesized that the nonvolatile compounds are carried into the vacuum of the ion source by the boiling solvent with no direct interaction with the impact plate. The volatilized material, which may be collimated into a molecular beam, is ionized by electron impact and mass analyzed.

A limited number of experiments intended to help characterize the volatilization process have been performed. It was found that, for droplets of aqueous solutions which had initial mean diameter of about 4 μm, both solvent and solute vaporize in mean times of approximately 100 μsec, and that, to within experimental error, solvent and solute vaporize simultaneously. Significant quantities of solvent clusters are produced during the vaporization of the droplet, indicating that a free-jet expansion is taking place. These data support the volatilization process suggested above. The presence of a large fraction of parent ions in the mass spectra of nonvolatile and thermally labile compounds, such as arginine and ascorbic acid, and the lack of dependence of the mass spectra on the impact plate temperature, indicate that the compounds are being volatilized without pyrolysis.

The technique has been tested using several volatile solvents, including water, methanol and heptane, and a number of nonvolatile and thermally labile compounds. With the present apparatus it is possible to detect less than 1 ng of most compounds. Major improvements in sensitivity appear possible. However, the present sensitivity should be adequate for many LCMS and other mass spectrometric applications.

This work was supported in part by the National Institute of General Medical Sciences, Grant No. 5-R01-GM24338-02.

---

1 Greene, F. T., "Particulate Impact Mass Spectrometry," Presented at the 23rd Annual Meeting of ASMS, Houston, TX, May 25-30, 1975.

2 Greene, F. T., "Mass Spectrometry of Nonvolatile Materials and Solutions by the Particulate Impact Technique," Presented at the 24th Annual Meeting of ASMS, San Diego, CA, May 9-13, 1976.

TAMOB1 BIOACTIVE COMPOUNDS FROM MARINE AND MICROBIAL SOURCES, Kenneth L. Rinehart, Jr., Roger Adams Laboratory, University of Illinois, Urbana, IL 61801

Our attention has focused in recent years on the identification of those compounds derived from marine sources (sponges, algae, etc.) which have antiviral, antifungal, antibacterial, or antitumor properties, employing preliminary assays in the field, followed by structural studies in Urbana. Where sample size allows, these studies have made extensive use of ^{13}C and ^{1}H NMR spectroscopy, as well as a variety of techniques of mass spectrometry (FDMS, GC/EIMS, GC/CIMS, GC/FIMS, at low and high resolution). Recent results of some of these structural studies of marine-derived bioactive compounds will be described. The important role of ^{13}C and ^{1}H NMR spectroscopy in assigning structures will also be illustrated by recent studies in our laboratory dealing with a bacterial cofactor and an antitumor agent from a microbial source.

TAMOB2 STRUCTURE DETERMINATION OF A SLOW REACTING SUBSTANCE: A POSSIBLE CHEMICAL MEDIATOR OF HUMAN ASTHMA, R. C. MURPHY, Dept. of Pharmacology, University of Colorado Medical School, Denver, CO 80262

Slow reacting substance of anaphylaxis (SRS-A) was initially described over 40 years ago as a myotropic agent released from sensitized lung tissue exposed to antigen. Subsequent biochemical and pharmacological studies have implicated SRS-A as an important mediator of the allergic bronchospasm in asthma. Previous studies with SRS-A had suggested that SRS-A is an acidic lipid which might be a metabolite of arachidonic acid. Spark source mass spectrometry first suggested that the molecule in addition contained sulfur. Recent advances in the production of a slow reacting substance from a neoplastic mast cell line by the calcium ionophore A23187 and purification by chromatographic techniques including reversed phase HPLC have enabled a few micrograms to be isolated for structural studies. The ultraviolet absorption spectrum of SRS indicated the presence of a conjugated triene with an adjacent auxochromic moiety. Radioactive arachidonic acid, cysteine, and glycine could be biochemically incorporated into SRS suggesting a peptide as well as lipid region in the structure. Raney nickel desulfurization led to the identification of 5-hydroxyeicosanoic acid by GC-MS. The position of the double bonds on this lipid backbone was assigned by ozonolysis products and UV absorption following incubation of SRS with lipoxygenase. The peptide portion of SRS was investigated by acid hydrolysis and the amino acids identified by GC-MS. Glycine and pyroglutamic acid were quantitated using the corresponding 0-18 labelled amino acids and GC-MS techniques. The possible biochemical pathway of SRS production will be discussed. Leukotriene has been suggested to name the members of this novel pathway of arachidonic metabolism with SRS now referred to leukotriene C.

Antibiotics Derived From Higher Plants

L. A. Mitscher, D. L. Flynn, Y. H. Park, J. K. Swayze, T. Veysoglu and T. S. Wu

Department of Medicinal Chemistry, University of Kansas

Lawrence, KS. 66045

In recent years, man has placed his primary reliance upon fermentation products derived from soil microorganisms in the struggle against communicable diseases caused by bacteria, fungi and yeasts. The intensity of the search coupled with the passage of time has resulted in progressively diminishing returns. Consequently, contemporary soil screening programs are highly sophisticated, labor intensive, and increasingly dependent upon rapid modern micromethods of structure determination in order to select for desirable compounds and to avoid reisolation of previously known agents. Another useful ploy is to search amongst the secondary metabolites of new or unusual genera for antibiotics with unusual structures with the expectation that such agents will possess different antimicrobial spectra and side effects than the agents in common medicinal use. Micromonospora, Microbispora, Streptosporangia, Nocardia and Fungi are examples of such less commonly studied genera of microorganisms. Marine organisms and higher plants are other examples of attempts to fish in less explored gene pools.

Investigation of higher plant extracts has many similarities to the contemporary search for antibiotics from more traditional sources. The latter work employs methods having facets of great interest to mass spectroscopists but is of great economic importance and involves closely guarded commercial secrets which cannot be discussed openly at this time.

Interestingly, plants are also susceptible to infection by microorganisms with deleterious consequences for the preparation and preservation of foodstuffs and the use of other economically valuable plants. Higher plants have no efficient circulatory system analogous to that of the animals and also have no corresponding immune system to counter infection. They are not, however, defenseless. Many plants contain regionally high concentrations of antimicrobial secondary metabolites which render them relatively immune from certain infections. In our laboratory, semi-random screening of domestic and foreign plants using a realistic collection of test microorganisms, identical to those used industrially, has shown that about 20% possess realistic concentrations of antimicrobial agents. In addition to preformed agents, many plants elaborate antimicrobial agents in response to infection by various plant pathogens. In a number of cases, inactive metabolites are converted to toxic substances by the enzymatic activity of the invasive organism itself. Substances toxic to the parasite which are elaborated in response to infection are known as phytoalexins and represent very interesting examples of host-parasite biology. They often possess narrow species specificity.

In many cases the antimicrobial agents found in higher plants are active against human pathogens. This is true even though in only a few cases are microorganisms simultaneously pathogenic to both plants and animals. Pseudomonas, Erwinia and, perhaps, Legionella are exceptionally eclectic organisms in this sense. While many of the agents responsible for the activity of plants are only moderately potent compared with established antibiotics,

this is not always so, and the potential for finding useful new therapeutic agents from such extracts is realistic, in our opinion. What is equally interesting scientifically is that the structures of these agents are dramatically different from those of clinically established antibiotics suggesting the likelihood of novel biochemical, antibacterial and toxicological properties.

As with all natural products fields, rapid modern separation techniques and means of structural analysis greatly facilitate this work. Mated hplc/ms techniques coupled with single ion focusing and other computerized methods show exceptional promise for impact on these studies when the present technical difficulties are overcome.

The plants selected may be chosen for study based upon folkloric reputation, by following through on the wealth of unexplored leads lying in the literature, or chosen at random based upon convenience, exoticness, known freedom of the plant from infection, etc. The frequency of confirmation or original discovery is roughly the same using either approach. Plants are chosen for further study based upon potency and the specific antimicrobial spectrum with special emphasis placed upon anti-Gram-negative, antitubercular, and antifungal activity. Extracts are fractionated into broad chemical classes (alkaloids, terpenes, etc.) based upon solvent distribution studies and the progress of the separation is followed by bioassay. Individual pure agents are isolated by various chromatographic means. When the plant has received prior chemical study, the kinds of metabolites previously known to be present helps measurably in early identification. In this respect, work with the higher plants is somewhat easier than with microbial systems because of the lesser genetic versatility of higher plants. Often only trace quantities of active substances are available and rapid progress depends upon obtention and correct structural interpretation of spectral data. Mass spectra, FT nmr, ir (including FT ir), uv and use of diagnostic color reactions are of particular help. When authentic samples are available, tlc, hplc, and, especially, hplc/ms are invaluable in identifying known agents preventing wasteful duplication of effort and expenditure of valuable resources. Even with fairly thoroughly previously investigated plants, such as *Ptelea trifoliata*, *Thalictrum rugosum* and *Glycyrrhiza glabra*, bioassay directed fractionation aided by intensive chromatography resulted in isolation and chemical and biological evaluation of novel antimicrobial agents.

When new agents are encountered, often in tiny amounts, mass spectrometry is an indispensible tool although success usually requires evidence from a constellation of microanalytical spectral methods. Antimicrobial agents from higher plants have, so far, belonged to classes of natural products studied previously by phytochemical methods. As a consequence, rapid progress can be made if the class of substance can be assigned. Characteristic ms fragmentation processes are indispensible here.

Glycyrrhiza glabra (licorice) from Spanish sources is an example of an economically valuable plant, used for its flavoring principles, which has received considerable chemical attention. Nevertheless, bioassay directed fractionation of the type described succeeded in the discovery of five substances active as antimicrobial agents and which were new to the literature. These are the isoflavans hispaglabridin A (1) and B (2), 3'-methoxyglabridin (3) and 4'-O-methylglabridin (4), and the flavanone 3-hydroxyglabrol (5). Their structures have been determined by chemical and spectroscopic means. The identification of glabridin

(6) and glabrol (7) as antimicrobial agents in the extracts represents the first time a potential pharmacological utility has been ascribed to these previously known materials.

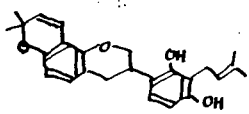

(1)

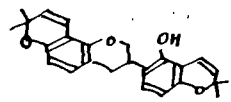

(2)

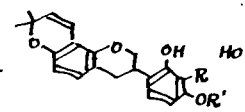

(3); R=OCH3, R'=H
(4); R=H, R'=CH3
(6); R=R'=H

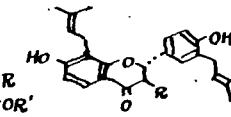

(5); R=OH
(7); R=H

Amorpha fruticosa (false indigo) is a common Kansas plant which also grows well in wet areas throughout the Midwest. Fractionation revealed the antimicrobial activity to be due to the presence of the rotenoid 11-hydroxytephrosin (8) and the bibenzyls amorfrutin A (9) and B (10). The amorfrutins belong to a small class of natural products just now being encountered with increasing frequency. Interestingly, similar materials present in this plant give a false positive color reaction for marihuana causing some difficulties in forensic circles.

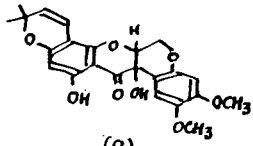

(8)

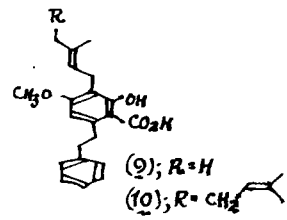

(9); R=H
(10); R=CH2

Peganum harmala of Iraqi origin was available to us only in small quantity so that the identification of the active constituents depended unusually heavily upon hplc/ms techniques and the availability of known standard constituents. This combination is being used increasingly heavily in such work and represents an extremely powerful new approach. Accordingly, the active β-carboline alkaloid harmine (11) and the quinazolines vascicine (12) and vascicinone (13) as well as the inactive β-carbolines harmaline (14) and harmalol (15) were identified in our extracts. Examination of analogous materials not found in P. harmala revealed that harmane (16) and harmol (17) were even more potent.

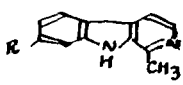

(11); R=CH3O
(16); R=H
(17); R=OH

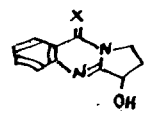

(12); X=H2
(13); X=O

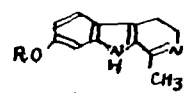

(14); R=CH3
(15); R=H

In summary, bioassay directed fractionation of a wide variety of higher plants is successful in uncovering a wide diversity of novel antimicrobial agents active in vitro against a broad spectrum of human pathogens. This work is dramatically dependent upon spectroscopic means of structure identification and mass spectrometry plays a central role.

BETTER SURVIVAL THROUGH NATURAL PRODUCTS, Murray S. Blum, Department of Entomology, University of Georgia, Athens, Georgia.

Many natural product chemists have six legs. These invertebrate chemists--the insects--synthesize an incredible variety of compounds that are utilized both for communication (pheromones) and defense (allomones). In the case of social insects, the same natural product may possess both functions, a development that emphasizes how these compounds have been parsimoniously exploited in the evolution of sociality. Our awareness of the versatility of insects and related arthropods as biosynthesizers of exocrine compounds has chiefly resulted from the utilization of mass spectrometry, especially in conjunction with gas chromatography (GC-MS), for the analysis of their glandular products. Indeed, GC-MS analytical results obtained in the last two decades have demonstrated that these animals are a virtual treasure-trove of often novel natural products. This conclusion is particularly applicable to the ants, a group of insects whose success as dominators of terrestrial ecosystems is probably correlated with their ability to produce and utilize a potpourri of compounds to thwart their omnipresent adversaries.

In addition to proteinaceous constituents, the venoms of myrmicine ants have proven to be an especially rich source of nitrogen heterocycles which possess pronounced activities as toxins and/or repellents. The venoms of fire ants, Solenopsis (Solenopsis) species, are dominated by 2,6-dialkylpiperidines which possess such distinctive mass spectra that they can be easily characterized.[1] Most species produce the cis- and trans-isomers of 2-methyl-6-n-undecylpiperidine, whereas compounds such as 2-methyl-6-n-pentadecylpiperidine and 2-methyl-6-(6-pentadecenyl)piperidine are restricted to the venoms of S. invicta and related fire ants.[2,3] The venom of S. xyloni is distinctive in containing 2-methyl-6-undecyl-$\Delta^{1,2}$-piperideine[2], a compound that may constitute a metabolic intermediate in the biosynthesis of the cis- and trans- isomers of 2-methyl-6-n-undecylpiperidine, the main constituents in the venom of this fire ant. However, whereas, the cis- and trans-isomers of seven unsymmetrical 2,6-di-n-alkylpiperidines have been identified as venomous constituents of fire ants[3], different nitrogen heterocycles are often synthesized by the more diminutive species in this genus, especially members of the subgenus Diplorhoptrum.

A large series of unsymmetrical trans-2,5-di-n-alkylpyrrolidines and their corresponding -pyrrolines are produced in the poison gland of S. punctaticeps[4], a common South African species. The characteristic mass spectra exhibited by pyrrolidines has made it possible to facilely identify them in extracts of a variety of ant species. On the other hand, thief ants in this genus are much more conservative heterocyclic chemists, each species producing only the trans-isomer of a single 2,5-di-n-alkylpyrrolidine. The venoms of S. molesta and S. texanas are dominated by 2-hexyl-5-pentylpyrrolidine, whereas that of S. fugax contains trans-2-butyl-5-heptylpyrrolidine[6], a compound previously identified in the venom of S. punctaticeps.[4] S. fugax, in common with other thief ants, utilizes its alkaloidal venom as the key element in a lifestyle characterized by stealing larvae from the nests of larger ants.[7] This plundering modus vivendi is made possible by the repellent action of trans-2-butyl-5-heptylpyrrolidine. When raiding workers of S. fugax are confronted by those of the host species, the former secrete their alkaloid-rich venom which acts as a mace for workers of the latter. Host ants flee from the venomous exudates of the aggressive thief ants, allowing these diminuitive raiders to plunder larvae that will eventually serve as a repast for the miniature warriors.[6] Thus, the evolution of alkaloidal venom maces has made it possible for thief ants to prey on their more formidable relatives with absolute impunity.

The virtuosity of Solenopsis species as synthesizers of nitrogen heterocycles is further demonstrated by the recent identification of 3-heptyl-5-methylpyrrolizidine as a venomous constituent of S. species near tennesseensis.[8] This novel alkaloid, which is substituted differently than the plant-derived pyrrolizidines, is a powerful repellent for a number of ant species. Therefore, it is obvious that a variety of venomous maces have been evolved by thief ants. However, that the biosynthesis of alkaloidal venoms is not limited to species in the genus Solenopsis is shown by the identification of distinctive nitrogen heterocycles as poison gland constituents of species of Monomorium, a closely related genus.

The venom of Pharaoh's ant, Monomorium pharaonis, consists of an indolizine in admixture with a series of unsymmetrical 2,5-dialkylpyrrolidines, some of which are terminally unsaturated.[9] Recently, a convenient synthesis of these pyrrolidines with side chain unsaturation was described, along with a presentation of their mass spectra.[10] In addition, 2-(1-hex-5-enyl)-5-nonylpyrrolidine was identified as a major component in the venoms of M. minimum and M. viridum. Subsequently, detailed analyses[11] of the venomous alkaloids produced by these two species and several related forms demonstrated that members of the genus Monomorium are versatile synthesizers of nitrogen heterocycles.

Mass spectra of methoxylated derivatives of the unsaturated side chains[12] confirmed the terminal positions of the double bonds. In addition to the previously identified 2-(1-hex-5-enyl)-5-nonylpyrrolidine[10], the venoms of several species were dominated by 2-(1-hex-5-enyl)-5-(1-non-8-enyl)pyrrolidine, a previously unidentified ant-derived alkaloid. *The venoms of both M. viridum and M. minimum also contain trace amounts of* the pyrrolidines with saturated side chains. In addition, the N-methyl derivatives of the pyrrolidines with either one or both side chains unsaturated, were produced as trace venomous constituents of several species of Monomorium. The poison gland products of most of these species also contained trace quantities of the $\Delta^{1,2}$-and $\Delta^{1,5}$-pyrrolines with a terminally unsaturated hexenyl side chain, as well as the pyrrolines with both side chains terminally unsaturated.[11] It will not prove surprising if the alkaloidal diversity that characterizes the venoms of these Monomorium species is characteristic of the poison gland secretions of other species in this large ant taxon. For ants in the genera Solenopsis and Monomorium, survival is an eight-letter word equalling alkaloid.

REFERENCES

1. J. G. MacConnell, M. S. Blum, and H. M. Fales, Tetrahedron, 27, 1129 (1971).
2. J. M. Brand, M. S. Blum, H. M. Fales, and J. G. MacConnell, Toxicon, 10, 259 (1972).
3. J. G. MacConnell, M. S. Blum, W. F. Buren, R. N. Williams, and H. M. Fales, Toxicon, 14, 69 (1976).
4. D. J. Pedder, H. M. Fales, T. Jaouni, M. Blum, J. MacConnell, and R. M. Crewe, Tetrahedron, 32, 2275 (1976).
5. T. H. Jones, M. S. Blum, and H. M. Fales, Tetrahedron Lett., 1979, 1031 (1979).
6. M. S. Blum, T. H. Jones, B. Holldobler, H. M. Fales and J. Jaouni, Naturwissenschaften, 67, 144 (1980).
7. B. Holldobler, Oecologia, 11, 371 (1973).
8. T. H. Jones, M. S. Blum, H. M. Fales, and C. R. Thompson, unpublished data.
9. F. G. Ritter and C. J. Persoons, Neth. J. Zool., 25, 261 (1975).
10. T. H. Jones, J. B. Franko, M. S. Blum, and H. M. Fales, Tetrahedron Lett., 1980, 798 (1980).
11. T. H. Jones, M. S. Blum, H. M. Fales, R. W. Howard, C. A. McDaniel, and M. B. DuBoise, J. Chem. Ecol., in press.
12. G. J. Blomquist, R. W. Howard, C. A. McDaniel, S. Remaley, L. A. Dwyer, and D. R. Nelson, J. Chem. Ecol. 6, 257 (1980).

Multiple Concerted Rearrangements in Ethylene Loss from 4,4-Dimethyl-1-pentene.

A.M. Falick*, Pierre Tecon+ and Tino Gaümann
Institute of Physical Chemistry, EPFL - Ecublens
CH-1015 Lausanne, Switzerland.

A number of recent studies of various alkene isomers have tended to show that in ionized alkene ions larger than C_5 or C_6 the extent of skeletal isomerization prior to decomposition is relatively small. In seeming contradiction to this conclusion are the data for C_2H_4 loss from labeled alkene ions, a reaction that appears to occur in conjunction with substantially more skeletal rearrangement than any other fragmentation. In the work described here, we have examined in detail the loss of ethylene from various ^{13}C-labeled analogs of 4,4-dimethyl-1-pentene, with a view to clarifying this apparent discrepancy.

Three main reactions were studied: loss of CH_3, C_2H_4 and C_3H_5 from the molecular ion. Normal 70 eV EI mass spectra and second field-free region (of a ZAB-2F) metastable spectra of the molecular ion were measured. Samples of 4,4-dimethyl-1-pentene sinfly labeled with ^{13}C in positions 1, 2,3,4, and 5, as well as several doubly labeled samples, were measured.

In Figure 1 are shown the results for loss of methyl from the molecular ion. In the source what occurs is mainly loss of one of the original methyl groups with minor loss of C-1. In the metastable region, loss of C-1 becomes more important and a small contribution from C-3 is present. Other than this minor amount, however, little or no skeletal rearrangement is seen in conjunction with CH_3 loss.

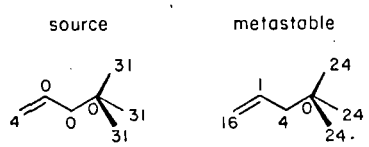

Figure 1. Percent participation of C-atoms in loss of methyl radical

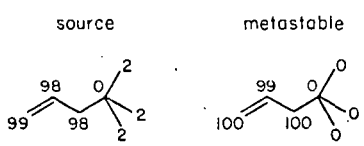

Figure 2. Percent participation of various C-atoms in loss of C_3H_5

In Figure 2 are presented the results for C_3H_5 loss. Again there is no evidence of significant skeletal rearrangement prior to or in conjunction with bond cleavage. Essentially the only reaction observed is the expected α-cleavage.

---

* Permanent address: Department of Chemistry, University of California, Berkeley, CA 94720

+ Present address: Department of Chemistry, Stanford University, Stanford, CA 94305

In striking contrast, however, are the results for ethylene loss (Fig. 3). From the data in Figure 3 and similar data obtained from doubly-labeled compounds, the relative participation of various pairs of C-atoms in the ethylene-loss reaction can be calculated. The results of these calculations are shown in Table 1.

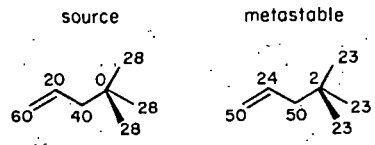

Figure 3. Percent participation of various C-atoms in loss of C_2H_4

The results can be accounted for on the basis of 3 or 4 main reactions plus contributions from several minor ones. Simultaneous loss of carbons 1+5, 3+5 or 1+2 are major processes both in the source and at longer lifetimes. Loss of carbons 2 and 3 together appears to become important only in the metastable region.

Loss of C-Atoms	source	metastable
1 + 5	46 ± 2%	33 ± 2%
3 + 5	36	33
1 + 2	14	11
2 + 3	1-7	12
1+3, 2+5, 5+5, 4+any		10-12

Table 1. Relative Participation of Different Pairs of C-Atoms in C_2H_4 Loss from 4,4-Dimethyl-1-pentene
Note: Loss of C-5 includes any of the three equivalent C-atoms.

The results for CH_3 and C_3H_5 loss, in agreement with published data on fragmentation of other alkenes, tend to show that the molecular ion does not undergo extensive rearrangement prior to decomposition. We therefore attribute the results for C_2H_4 loss to the operation of several essentially independent, parallel pathways for C_2H_4 loss, each of which is a concerted rearrangement/C_2H_4 loss reaction.

A full account of this work will be published in J. Am. Chem. Soc.

MECHANISM OF FRAGMENTATION OF SOME C_5 OLEFINIC ALCOHOLS

A. G. Harrison, J. Hegedus Vajda, N. E. Middlemiss, University of Toronto, Toronto, Canada

J. J. Zwinselman, N.M.M. Nibbering, University of Amsterdam, The Netherlands

The isomeric pentenols, 1, 2, and 3, show the base peak in their electron impact mass spectra at m/z 71 corresponding to $(M-CH_3)^+$, which logically would be expected to result from the loss of the allylic methyl group which also is α to the OH group.

$CH_3-CH=CH-CH(OH)CH_3$ (1) $CH_2=C(CH_3)CH(OH)CH_3$ (2) $CH_2=CH-C(OH)(CH_3)_2$ (3)

Examination of the mass spectrum of $CH_2=CHC(OH)(CD_3)_2$ shows that for fragmentation reactions occurring in the ion source CD_3 is lost almost exclusively; however, for fragmentation reactions observed as metastable ions some (10-20%) loss of CH_3 also is observed. The mass spectra of $CH_3-CH=CHCH(OH)CD_3$ and $CH_2=C(CH_3)CH(OH)CD_3$ show that both for fragmentation reactions occurring in the ion source and for fragmentation reactions occurring as metastable ions loss of CH_3 and loss of CD_3 are observed; the ratio for loss of CH_3 to loss of CD_3 is ∿1.5:1 for metastable ion fragmentations for both compounds. No significant loss of CHD_2 or CD_2H is observed for either ion source or metastable ion fragmentations.

The results of a field ionization kinetics study of $CH_2=C(CH_3)CH(OH)CD_3$ are shown in the Figure. Very similar results were obtained for $CH_3-CH=CHCH(OH)CD_3$. The results can be rationalized by a series of specific hydrogen migration reactions in competition with fragmentation as outlined in the Scheme for $CH_2=C(CD_3)CH(OH)CD_3$. Loss of CD_3 at very short reaction times leads to protonated methacrolein while following a 1,2 H migration loss of CH_3 leads to the more stable protonated methyl vinyl ketone. At even longer reaction times a 1,4 shift of the hydroxylic hydrogen leads to the ketonic molecular ion which fragments by loss of CD_3. A similar sequence of specific hydrogen shifts appears to occur for $CH_3-CH=CHCH(OH)CD_3$ leading eventually to the 2-pentanone molecular ion; the sequence is supported by the observation of a metastable ion for loss of C_2H_4, the expected McLafferty rearrangement fragmentation of the ketonic structure.

Metastable ion studies of the further fragmentation of the $(M-CH_3)^+$ and $(M-CD_3)^+$ ions show that the $(M-CH_3)^+$ ions which fragment as metastable ions have the structure $CH_2=CH-C(CH_3)=OH^+$ while the $(M-CD_3)^+$ ions which fragment as metastable ions have the $CH_3-CH=CHCH=OH^+$ or $CH_2=C(CH_3)CH=OH^+$ structure.

Full details of this work will be presented elsewhere.

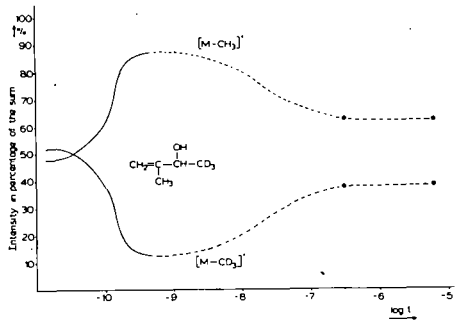
Intensity in percentage of the sum
100
90
80
70
60
50
40
30
20
10
[M-CH3]+
[M-CD3]+
-10
-9
-8
-7
-6
-5
log I

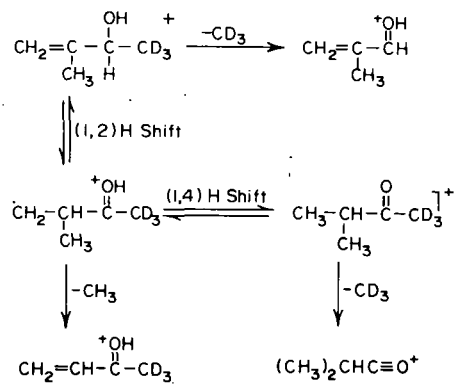
-CD3
(1,2) H Shift
(1,4) H Shift
-CH3
-CD3

The "Even Electron Rule"

Miriam Karni and Asher Mandelbaum
Department of Chemistry
Technion - Israel Institute of Technology, Haifa

Many (>200) exceptions to the "even-electron rule" (i.e. fragmentation processes $[\text{even}]^+ \rightarrow [\text{odd}]^{+\cdot}$ + radical·) have been found in the literature (unrecognized in most cases) and in the authors' laboratory.[1] The large number of violations suggests that although the generalization may be a useful guide for the interpretation and prediction of mass spectral behavior of many organic compounds, the term "rule" seems to be unjustified.

Some exceptions to the rule may be explained by aromatic stabilization of the resulting radical cations. Thus one could suggest that the relatively high stability of acenaphthylene radical cation is the driving force for the consecutive loss of two methyl radicals from the molecular ion of 1,2-dimethylacenaphthene 1 under electron impact.

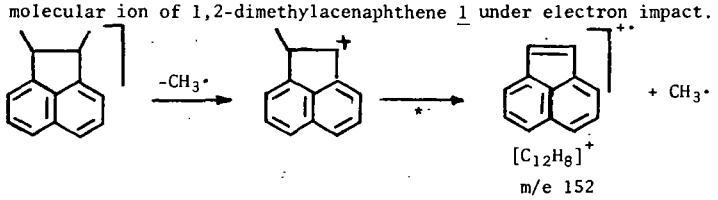

A similar loss of $CH_3\cdot$ has been observed in the even electron $[C_{13}H_{11}]^+$ ions formed from various diphenylmethyl derivatives and dimethyldiphenyls.

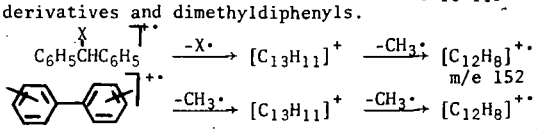

The appearance energies (A.E.) and enthalpies of formation of the $[C_{12}H_8]^{+\cdot}$ ions formed from 1,2-dimethylacenaphthene 1, 5,6-dimethylacenaphthene 2, 1,1-diphenylethane 3 and 2,2'-dimethyldiphenyl 4 are listed in the Table.

Table

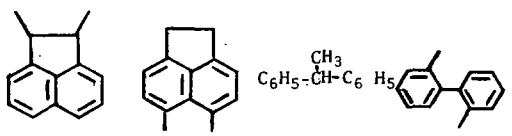

	1	2	3	4
A.E($[C_{12}H_8]^{+\cdot}$), eV[a]	14.9 13.6*	14.3*	14.2 13.1*	14.8 13.9*
ΔH_f°, kcal/mol	299 269*	28.4*	288 263*	302 281*

*Data obtained from measurements performed on metastable transitions (1st field free region).
[a]Estimated error ±0.3 eV.

Ionized biphenylene and acenaphthylene are two possible structures of the $[C_{12}H_8]^{+\cdot}$ radical cations. The enthalpies of formation of these ions are 290 and 247 kcal/mol respectively.[2] The thermochemical data (Table) as well as structural relationship (at least for 1 and 2) suggest that the $[C_{12}H_8]^{+\cdot}$ fragment ions have the acenaphthylene structure, and thus contain considerable amount of excess energy. The unusually high abundance of the $[C_{12}H_8]^{+\cdot}$ ions formed by the process $[C_{13}H_{11}]^+ \rightarrow [C_{12}H_8]^{+\cdot}$ in the first field-free region as well as deuterium labeling data show that this fragmentation is preceded by an extensive rearrangement. The high kinetic shifts (see Table) support this conclusion.

The high excess energy in the above processes indicates that they could be better explained by kinetic arguments than by aromatic stabilization. The low rate or absence of competing lower activation energy processes may be the reason for the relatively high abundances of ions formed by processes violating the "even-electron rule." This view finds support in the behavior of 1,2-diethylacenaphthene 5. The metastable analysis shows that the m/e 152 $[C_{12}H_8]^{+\cdot}$ ion is formed by a consecutive loss of two ethyl radicals only to a very small extent in the field-free region. Instead the $[M-C_2H_5]^+$ ion decomposes by the loss of C_2H_4 (resulting in the $[C_{12}H_3]^+$ ion) and $CH_3\cdot$ (resulting in the $[C_{13}H_{10}]^{+\cdot}$, again violating the rule).

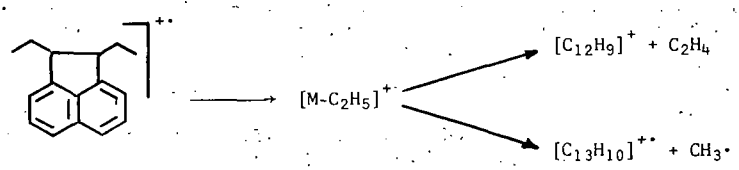

References

1. M. Karni and A. Mandelbaum, Org. Mass Spectrom., 15, 53 (1980), and references cited therein.

2. H.M. Rosenstock, K. Draxl, B.W. Steiner and J.T. Herron, J. Phys. Chem. Data, 6, Suppl. 1, I-185 (1977).

Retro Diels Alder Fragmentation Accompanied
by Hydrogen Migrations in some Adducts of Bicycloalkenyls.

Ana Fraiman and Asher Mandelbaum

Department of Chemistry
Technion - Israel Institute of Technology, Haifa

Retro Diels Alder (RDA) fragmentation accompanied by the migration of two hydrogen atoms from positions δ is the most important process occurring in adducts 1 under electron impact.[1] Models show that the migrating allylic H-atoms can be brought within a short distance from

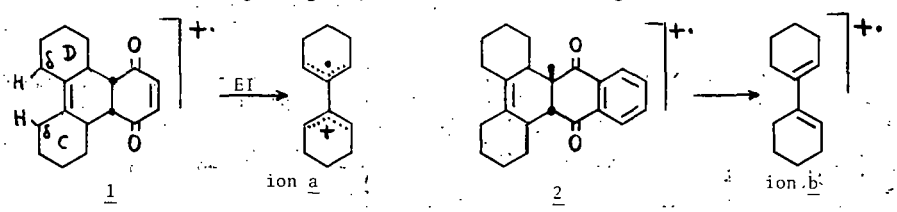

the carbonylic oxygens.[1] The relative abundance of the resulting fragment ions a is dependent on that distance, which can be changed by the variation of the size of rings C and D.[2] Adducts 2, containing an angular methyl group at the α-position, undergo a regular highly stereospecific RDA fragmentation under electron impact, yielding most abundant diene cation b.[3]

RDA fragmentation of adducts 2 under chemical ionization (CI) results in abundant protonated diene and quinone cations (ions c and d respectively).[4] Isotope effect observed in this process leads to the conclusion that the fragmenting $[M+H]^+$ ions are protonated at one of the carbonylic oxygen atoms, and the protonated diene (ion c) is formed by a RDA process

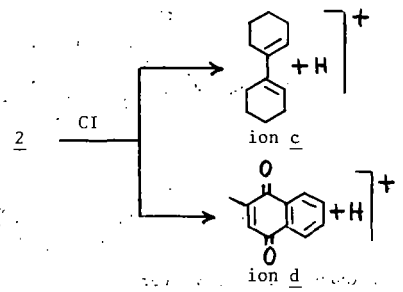

accompanied by the migration of that hydrogen towards the double bond region, while ion d is the result of a regular RDA fragmentation.[4]

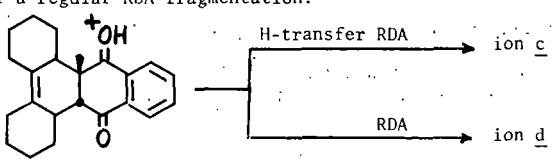

In order to obtain a direct evidence for the transfer of the hydrogen from a protonated carbonyl function in the course of RDA fragmentation, we prepared the hydroxyketones 3-6, which we expected to yield the protonated adduct e under electron impact by the loss of the alkyl group R. The hydroxyketones 3-5 (R=CH_3, C_2H_5, $(CH_3)_2CH$) do not exhibit an appreciable abundance of the m/e 335 ion e, and consequently do not yield ions c and d. The preferred route of fragmentation of these compounds is initiated by the ring cleavage:

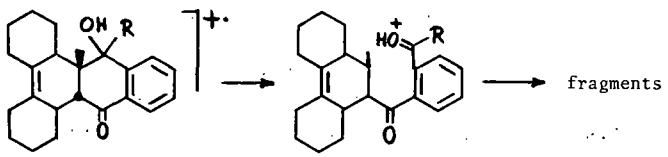

3. $R=CH_3$
4. $R=C_2H_5$
5. $R=(CH_3)_2CH$

The t-butyl substituted hydroxyketone 6 loses the substituent yielding the protonated adduct e, which, as expected, gives rise to both the protonated diene (ion c) and quinone (ion d), analogously to the CI process. Metastable transition were detected for both processes.

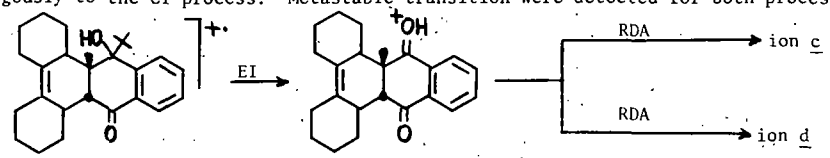

6 ion e

The disubstituted compounds 7 and 8 exhibit analogous RDA fragmentations accompanied by hydrogen migration from the oxygen function towards the double bond region:

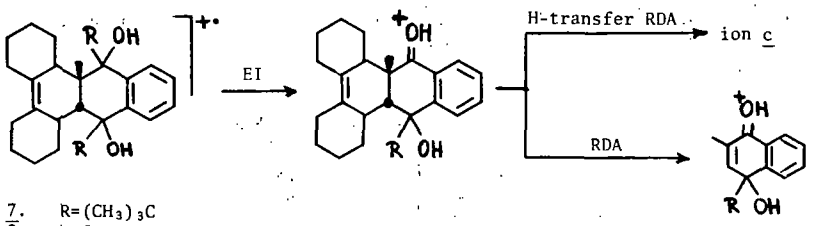

7. $R=(CH_3)_3C$
8. $R=C_6H_5CH_2$

Deuterium labelling shows that the migrating hydrogen atom originates at one of the hydroxyl functions in 8.

All the processes discussed above are highly stereospecific.

References

1. J. Deutsch and A. Mandelbaum, J. Am. Chem. Soc., 91, 4809 (1969).
2. J. Deutsch and A. Mandelbaum, J. Chem. Soc. B, 886 (1971).
3. A. Karpati, A. Rave, J. Deutsch and A. Mandelbaum, J. Am. Chem. Soc., 95, 4244 (1973).
4. S. Zitrin, J. Yinon and A. Mandelbaum, Tetrahedron, 34, 1199 (1978).

MASS SPECTRAL BREAKDOWN OF METAL DITHIOCARBAMATE CHELATES, J.R. Dias, Dept. of Chem., Univ. of MO, Kansas City, MO 64110 and M. Zigon & S. Gomiscek, Dept. of Chem., Univ. of Ljubljana, Ljubljana, Yugoslavia

The spectra of metal dithiocarbamate complex salts can be divided into ions derived from the ligand and ions containing metal. The following thiocarbonyl α-cleavage is more important for M containing metal than for M equal to hydrogen.

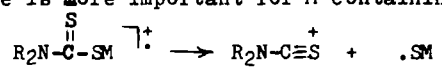

The thiocarbonyl α-cleavage ion (m/z 114) of tetramethylenedithiocarbamate (TMDTC) salts gives a characteristic ion at m/z 72 corresponding to the following fragmentation pathway.

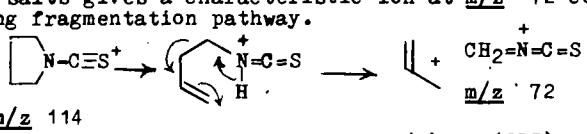

m/z 114 m/z 72

The presumed TMDTC complexes of Ag(I), As(III), Mn(IV), Mo(VI), Sn(IV), Te(II), Ti(IV), and V(V) proved to be samples comprised of mixtures of sulfur, bis(tetramethylene)thiourea, and (in the case of Ag and V) metal sulfides and/or oxides. TMDTC complexes of Cd(II), Co(III), Cr(III), Cu(II), Fe(III), Ni(II), and Zn(II) exhibited both $[M^{II}-L]^+$ and $[M^{II}-L+H]^{\cdot+}$ electron impact induced ions, whereas, the spectra of TMDTC complexes of Bi(III), Pb(II), and Sb(III) exhibited only the $[M^{II}-L]^+$ ion. The low ionization voltage (12eV) mass spectra suggests that the above pattern results from the greater stability of the following sp^2 hybridized $[M^{II}-L]^+$ ion (illustrated with Pb) possessing an inert gas electronic configuration which is produced only from the latter complexes.

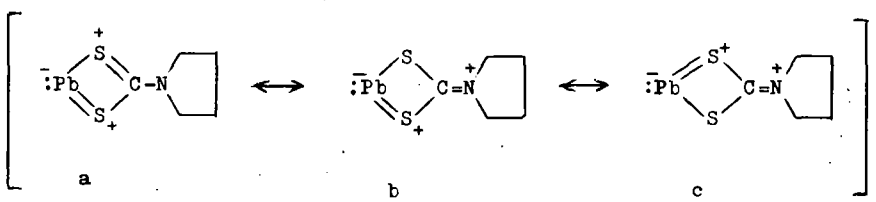

a b c

Table. Monoisotopic Mass Spectra (12eV) of Bis(dithiocarbamate) Salts.

Cpd	$[M]^{\cdot+}$	$[M-L+H]^{\cdot+}$	$[M-L]^+$	m/z 146	m/z 114
$Cu(TMDTC)_2$	355(100)	210(11)	209(3)	(27)	(84)
$Pb(TMDTC)_2$	500(22)		354(100)	(3)	(26)
$Zn(TMDTC)_2$	356(100)	211(2)	210(8)	(2)	(32)

Scheme I

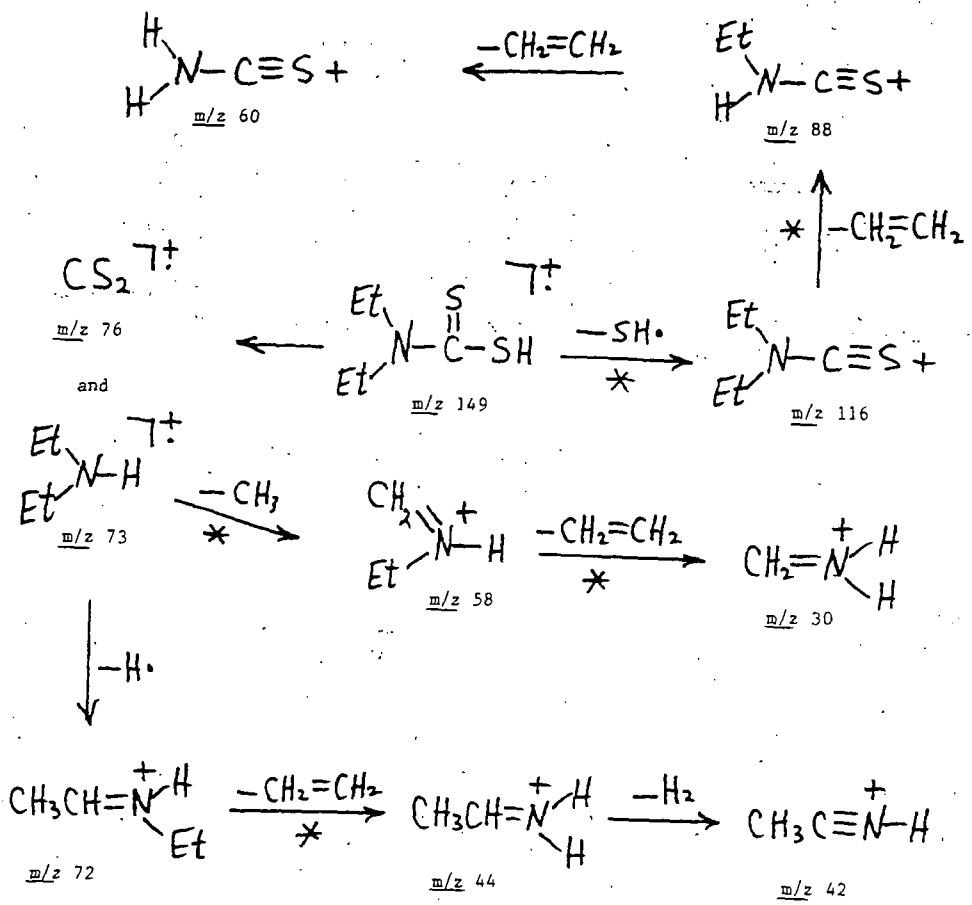
m/z 60
−CH2=CH2
m/z 88
−CH2=CH2
CS2 7+
m/z 76
and
m/z 149
−SH•
m/z 116
m/z 73
−CH3
m/z 58
−CH2=CH2
m/z 30
−H•
m/z 72
−CH2=CH2
m/z 44
−H2
m/z 42

REARRANGEMENT IONS-AN AID OR AN INTERFERENCE IN IDENTIFICATION OF SULFUR COMPOUNDS, NORMAN G. FOSTER, DEPT. OF CHEMISTRY, TEXAS WOMAN'S UNIVERSITY, DENTON, TEXAS 76204

The mass spectra of 20 classes of sulfur compounds have been investigated in the period 1952 to date by workers in two laboratories of the United States Bureau of Mines and the Texas Woman's University. This paper summarizes the main features exhibited by these classes and further groups the classes according to their general behavior. In aliphatic situations the sulfur atom is shown to have a propensity for forming rearrangement ions containing hydrogen atoms. Most of these ions are of odd m/z. In aromatic moieties similar rearrangements occur but ions of even m/z form. These ions are often the largest intensity, and persist in appearing at low ionization voltages. Ring expansion ions are commonly encountered, as are Retro-Diels-Alder rearrangement ions. Charge competition between fragments is observed for some species.

While the sulfur atom often acts as its own isotopic label, some carbon-13 and deuterium labeling is employed to establish mechanisms. The sulfur atom with available d-orbitals and hybridization in excited species may account for the observed behavior of the sulfur compounds.

These rearrangements, especially those which appear at low ionization voltages may lead to difficulties for the analyst in "characterization" problems or those attempting to use mass fragmentography when sulfur compounds are present. The accompaning table presents a synopsis of mass spectral behavior of these various classes of sulfur compounds.

References

1. Kinney, I.W. Jr., and Cook G.L. Anal. Chem. 24, #9, 1391 (1952)
2. Cook, G.L. and Foster, N.G., Proc. Amer. Petrol. Inst. 41 199 (1961)
3. Sample, S. and Djerassi, C.; J. Amer. Chem. Soc. 88, 1937 (1966)
4. Levy, E.J. and Stahl, W.A., Anal. Chem., 33, 707 (1961)
5. Cook, G. L. and Dineen, G.V. U. S. Bur. Mines Rep. Invest. #6698 (1965)
6. Dooley, J. E. Kendall, R.F. & Hirsch, D.E.
7. Foster, N.G., Hirsch, D.E., Kendall, R.F., and Eccleston, B.H. U.S. Bur. Mines Rep. INVEST #6433 (1964)
8. IBID #6671 (1965)
9. Foster, N.G. IBID #6741 (1966)
10. Foster, N.G. and Higgins R.W., Org. Mass Spectrom 1, 191 (1968)
11. Earnshaw, D.G., Cook, G.L. and Dinneen, G.U., J. Phys. Chem. 68 296 (1964)
12. Bowie, J. H., Lawesson, S.-O., Madsen, J.O., Nolde, C. Schroll, G., and Williams, D.H. J. Chem. Soc. B, 946 (1966)
13. Foster, N.G. Shiu, Diana W-K., and Higgins, R.W. Bio Med. Mass Spectrom 1, 297 (1974)
14. Foster, N. G. Chandrasurin, P. and Higgins, R.W. Biomed. Mass Spectrom 6 260 (1979)
15. Foster, N.G., Higgins, R.W. and Hamming, M.C. Japan Jour. of Mass Spectroscopy 27 #4, 275 (1979)
16. Gallegos, E.J. and Kiser, R.W. J. Phys. Chem 66 136 (1962)
17. McCollum, J.D. and Meyerson, S. J.Amer. Chem. Soc. 85 1739 (1963)
18. Bowie, J.H. Lawesson, S.-O., Madsen, Schroll, G, and Williams, D.H., J. Chem. Soc. B, 951 (1966)
19. Bowie J. H., Cooks, R.G., Lawesson, S.-O. and Nolde, C., J. Chem. Soc. B 616 (1967)
20. Meyerson, S. and Fields, E.K. Org. Mass Spectrom 1 263 (1968)
21. Cilento, G. Chem. Rev. 60, 147 (1960)

REARRANGEMENT IONS IN SOME SULFUR COMPOUNDS

CLASS	REARRANGEMENT IONS	PRINCIPLE SPECTRAL BEHAVIOR
Alkanethiols	M-34, M-33	Primary give alkene ions & fragments. Secondary give alkyl ions & fragments.
Cycloalkylthiols	M-34, M-33	Similar, Base Varies, Even with Cis, Trans.
Thiaalkanes	m/z 35,48,61(sec)	47 ($CH_2=SH^+$), 2-thiapropane shows 21% m/z 27.
Thiacycloalkanes	M-28	Simpler lose 28, some $M^+ \rightarrow R$ + base, some $\longrightarrow$ base by ring cleavage.
Thiacycloheptane	m/z 87, ring specie	Base peak by concerted rearrangement.
Dithiaalkanes	$RSSH^+$, $HSSH^+$ (var. int.)	Also RSSR', $\rightarrow$ R'SSH, RSSR, R'-SSR'
Arylthiaalkanes	m/z 110	Thiophenol ion. Methyl subs. $\rightarrow 124^+$ etc.
Naphthylthiaalkanes	m/z 160	Alpha and beta subs. almost indistinguishable.
Alkylthiophenes, n&iso	m/z 98,85,84	Beta cleavage prominent, hydrogen rearrangements.
neopentyl subs.	m/z 98,97,57	Charge competition between fragments.
isopropyl & t-Butyls	M-15	Still beta cleavage, fewer rearrangement ions.
di-t-butyls	M-30	Beta and beta prime cleavages.
Alkylbenzo(b)thiophenes	m/z 148,etc.	Alkyl chain cleves beta to ring.
Dibenzothiophenes	m/z 198	For benzodithiophenes gives m/z 204
Phenylthienylmethane	m/z 97 is 10 times 91	Beta Cleavage to give sulfur moiety largest.
Tetrahydrodibenzothiophene derivs.	RETRO DEALS-ALDER M-28	Where possible for two or more saturated rings gives M-56, etc.
Hexahydrodibenzothiophene	m/z 110 and small m/z 80	Two beta hydrogen shifts and two cleavages to give thiophenol and cyclohexadiene ions.
Thiatetralins	Undergo RDA	M-28 if sulfur in the 1-position M-46 if sulfur in the 2-position.
Thiaindans	M-1	An unusual case, see Ref. #2.
1-(2-Thienyl)-1-thiaalkanes	m/z 116 (base)	A ring expansion, m/z 71^+ is diagnostic.
1-(2-benzo(b)thienyl)-1-thiaalkanes	m/z 166 (base)	Ring expansion, m/z 129^+ is diagnostic.
1-(5-ethyl-2-thienyl)-1-thiaalkanes	m/z 144 (base)	m/z 99^+ is diagnostic, Ethyl group carried into rearrangement.
1-(2-thienyl)-3-thiaalkanes	m/z 110, var. base	No m/z 98 rearrangement ion. No RSH ions.
1-(2-thienyl)-4-thiaalkanes	m/z 124 (base)	98 now greater than 97, no RSH ions.
Thienothiophenes	none observed	only two compounds studied.

See Also: M.C. Hamming and N. G. Foster "Interpretation of Mass Spectra of Organic Compounds", Academic Press, New York (1972) pp 571-579

MASS SPECTROMETRY OF ORTHO-SUBSTITUTED BIARYLS: PHENYLNAPHTHYL AND NAPHTHYLPHENYL SYSTEMS

Jayanti R. Patel* and Joseph H. Boyer

Department of Chemistry, University of Illinois, Chicago Circle Campus, Chicago, IL 60680

INTRODUCTION

The mass spectral fragmentation patterns of several ortho-substituted biphenyls upon electron impact indicated that their fragmentation behavior strongly depended upon the position of their substitution[1,2]. The cyclization between two phenyl groups via the functional groups has been investigated[2]. The direct displacement of functional groups upon an electron impact also has been studied for ortho-substituted biphenyls[3,4]. Such exclusion of functional groups is explained in terms of a displacement of intramolecular mechanism[4] and ipso-substitution[3,5]. Investigation of the effect of ortho-substituents in phenylnaphthyl and naphthylphenyl systems has been discussed in this study.

EXPERIMENTAL

Mass spectral data were collected using a A. E. I. MS 30 double beam mass spectrometer. The following mono-substituted phenylnaphthyl and naphthylphenyl compounds and various heterocyclic intermediates were prepared as previously described[6,7].

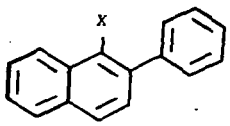

A

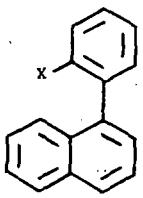

B

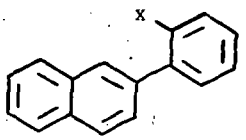

C

X	NC	CN	NHCHO	NH_2	NO_2
A	1	4	7	10	13
B	2	5	8	11	14
C	3	6	9	12	15

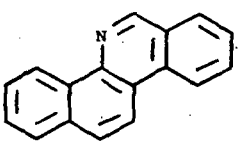

16

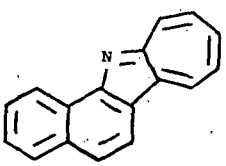

17

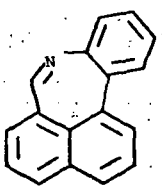

18

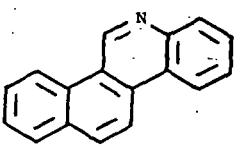

19

*Current Address: Sandoz, Inc., Crop Protection, Rt. 10, E. Hanover, NJ 07936

RESULTS AND DISCUSSION

In addition to the fragmentation patterns commonly observed for aromatic isocyanides upon electron impact[8], biaryl isocyanides 1 - 3 showed several mass spectral features which suggest the occurrence of structural rearrangement of these ortho-substituted biaryls to corresponding heterocyclic compounds 16 - 19. The mass spectral study of independently synthesized[6,7] heterocycles 16 - 19 confirmed this mechanism. The observed similarity in the mass spectral fragmentation patterns of these isocyanides and isomeric heterocycles suggests the formation of common intermediates. An isomerization of 1-isocyano-2-phenylnaphthalene (1) to benzo[g]cyclohept[b]indole, (17), and benzo[c]phenanthridine (16), 1-(2'-isocyanophenyl)naphthalene (2) to benzo[e]naphth[1,8-cd]-azepine (18), and 2-(2'-isocyanophenyl)-naphthalene (3) to benzo[i]phenanthridine (18) have been observed upon irradiation[7]. The thermal isomerization of isocyanides 1 and 2 to corresponding heterocycles and cyanides and isocyanide 2 to only corresponding cyanide also have been noted. The mass spectral fragmentation patterns obtained for isomeric biaryl cyanides 4 - 6 were also found identical to corresponding isocyanides. Thus, the photochemical and mass spectral rearrangements were proved to be parallel in the case of ortho-isocyano-biaryls 1 - 3.

The significant fragment ions which appear in the mass spectra of 1-formamido-2-phenylnaphthyl (7), 1-(2'-formamidophenyl)naphthalene (8) and 2-(2'-formamidophenyl) naphthalene (9), are accountable for the facile loss of CO, HCO, H_2 and H_2O from molecular ions. The validity of the fragmentation process of these formamides upon electron impact is supported by the mass spectra observed for independently prepared intermediates and reported mass spectra for the compounds identical to proposed intermediates[10]. The formation of benzocarbazole is also observed in mass spectral study of independently prepared corresponding biarylamines 10 - 12. The occurrence of doubly charged ions representing isomeric heterocyclic intermediates in the mass spectra of these formamides also support the proposed mechanism. The observed subsequent fragment ions which would be anticipated indeed for correctly assigned major intermediates are also conclusive.

The spectra of 1-nitro-2-phenylnaphthalene (13), 1-(2'-nitrophenyl)naphthalene (14) and 2(2'-nitrophenyl)naphthalene (15) are sufficiently different than normal nitro aromatic compounds to confirm their positional identity of ortho-nitro-biaryls[4]. A significant feature apparent in the mass spectra of these nitro compounds is the formation of heterocyclic intermediates identical to that of the ortho-substituted nitrobiphenyls[4]. The photolysis of 1-nitro-2-phenylnaphthalene[11], contrary to corresponding isocyanides, did not give structurally similar heterocyclic intermediates. Thus, the photochemical and mass spectral rearrangements are not parallel in case of ortho-substituted nitro-biaryls.

REFERENCES

1. J. L. Laseter, et. al., Org. Mass Spectrom. 4, 599, 1970.
2. C. F. Sheley and R. T. Patterson, Org. Mass Spectrom. 9, 731, 1974.
3. J. R. Patel, I. R. Politzer, G. W. Griffin and J. L. Laseter, Bio. Med. Mass Spectrom. 5, 664, 1978.
4. C. B. Thomas and J. S. Willson, J. Chem. Soc. Perkin II, 778, 1972.
5. J. G. Traynham, Chem. Rev. 79, 723, 1979.
6. J. H. Boyer and J. R. Patel, Synthesis 205, 1978.
7. J. H. Boyer and J. R. Patel, J. Chem. Soc. Parkin I, 1070, 1979.
8. B. Zeeh, Org. Mass Spectrom., 1, 315, 1968.
9. J. H. Boyer and J. R. Patel, J. Chem. Soc. Chem. Comm., 855, 1977.
10. a. S. Yamada, et. al., Org. Mass Spectrom., 15, 1, 1980.
    b. K. G. Das, et. al., J. Am. Chem. Soc., 86, 3729, 1964.
11. J. R. Patel and J. H. Boyer, Chemosphere, 99, 1980.

Since details of this and related work will be published elsewhere, only a brief discussion appears here.

Substituent Effects in the Mass Spectra of Alkyl-Substituted Sulphamides under Different Ionization Conditions

E. BAUMGARTNER and A. POPITSCH, Institute of Inorganic Chemistry, University of Graz, A-8010 G R A Z
AUSTRIA

The 70 eV electron impact and CH_4 chemical ionization spectra of a series of alkyl-substituted sulphamides have been obtained. The investigated compounds consisted of:

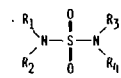

R_1	R_2	R_3	R_4	
H	H	H	H	SULPHAMIDE
CH_3	H	CH_3	H	DI (SYM) - METHYL
CH_3	CH_3	H	H	DI (ASYM) - METHYL
CH_3	CH_3	CH_3	H	TRI - METHYL
CH_3	CH_3	CH_3	CH_3	TETRA - METHYL
C_2H_5	H	C_2H_5	H	DI (SYM) - ETHYL
C_2H_5	C_2H_5	H	H	DI (ASYM) - ETHYL

The major fragmentation and rearrangement reactions of the compounds can be seen on Scheme 1.

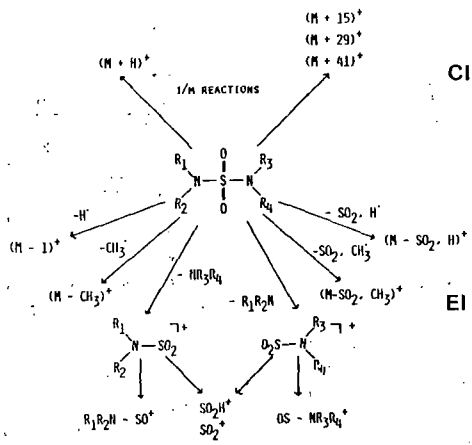

Scheme 1

As shown by the results of Table I hydrogen abstraction under EI conditions depends to a great extend on the substituents. In case of asymmetric compounds the process of hydrogen abstraction is favoured.

This can be reasoned by the possible interaction of an amide hydrogen with the lone pair electrons of nitrogen, which facilitates breaking of the N-H bond.

Loss of a methyl radical is a major process of the ethyl-substituted sulphamides, leading to the base peak in their EI-spectra.

Fragmentation data of S-N bond cleavage are summarized in Table II. The data show, that braking of the S-N bond not only depends on the substituents but also on the energy involved in the ionization process. Under CI conditions great stability of the $(CH_3)_2N\text{-}SO_2^+$ fragment ion was detected. S-N bond cleavage of symmetric compounds led to the base peak in the EI-spectra. Under CI conditions the same reaction was only a minor fragmentation process.

Expulsion of SO_2 was found to occur with a subsequent loss of hydrogen or a methyl radical, leading to the rearranged ions $(M\text{-}SO_2,H)^+$ and $(M\text{-}SO_2,CH_3)^+$, respectively (Table III). These processes, already known for a series of sulphonyl compounds, were found to be more intense under low energy ionization conditions (CI) and were again favoured in case of the asymmetric substituted compounds.

Table I: Hydrogen abstraction (EI)

Compound	$(M-1)^+/M^+$
Sulphamide	---
Dimethyl (sym)-	0,16
Dimethyl (asym)-	0,74
Trimethyl-	0,29
Tetramethyl-	0,08

Table II: S-N bond cleavage

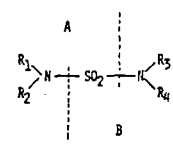

Asym. Compounds				Rel. Int. (%)			
				EI		CI	
R_1	R_2	R_3	R_4	A^+	B^+	A^+	B^+
CH_3	CH_3	H	H	28	40	99	2
CH_3	CH_3	CH_3	H	86	86	16	3
C_2H_5	C_2H_5	H	H	2	12	54	4
Sym. Compounds				A = B			
H	H	H	H	100			5
CH_3	H	CH_3	H	100			1
CH_3	CH_3	CH_3	CH_3	100			21
C_2H_5	H	C_2H_5	H	30			10

Table III: SO_2-Expulsion

Compound	Peak	Rel. Int. (%) EI	CI
Trimethyl - SA	$M - SO_2, H$	3	8
	$M - SO_2, CH_3$	--	3
Tetramethyl - SA	$M - SO_2, CH_3$	0.5	3
Diethyl (asym) - SA	$M - SO_2, H$	0.5	2
	$M - SO_2, CH_3$	2	8
Diethyl (sym) - SA	$M - SO_2, H$	0.2	1
	$M - SO_2, CH_3$	0.5	3

PREPARATION AND MASS SPECTRAL CHARACTERIZATION OF METHYLTHIO DERIVATIVES OF NAPHTHALENE. W. G. STILLWELL AND M. G. HORNING, Institute for Lipid Research, Baylor College of Medicine, Houston, TX 77030. W.-S. TSANG AND G. W. GRIFFIN, Department of Chemistry, University of New Orleans, New Orleans, LA.

Methylthio derivatives of naphthalene have been prepared by treating naphthalene-1,2-oxide, anti-1,2:3,4-naphthalene diepoxide, syn-1,2:3,4-naphthalene diepoxide, 1β,2α-dihydroxy-3α,4α-epoxy-1,2,3,4-tetrahydronaphthalene and 1β,2α-dihydroxy-3β,4β-epoxy-1,2,3,4-tetrahydronaphthalene with methanethiol. The products obtained from these reactions were converted to the O-trimethylsilyl derivatives and analyzed by gas chromatography and electron ionization mass spectrometry. Mass spectral fragmentation patterns and gas chromatographic properties for the synthetic compounds were determined. Mass spectra of the methylthio derivatives of naphthalene exhibited characteristic losses of SCH_3 or $HSCH_3$ from the molecular ions. Rearrangement ions at m/z 149 $(CH_3S{=}CH{-}OTMS)^+$ and m/z 191 $(TMSO{=}CH{-}OTMS)^+$ were prominent in the compounds containing a methylthiotrihydroxytetrahydronaphthalene or a di(methylthio)dihydroxytetrahydronaphthalene group; the molecular ions of these compounds were in very low abundance. Diagnostic fragment ions were present in the mass spectra of the substituted tetrahydronaphthalene derivatives indicating the loss of carbons 2 and 3 with their substituents via a retro Diels-Alder process. These observations were used to identify compounds obtained in metabolic studies in animals. This work was supported by Grants GM-24092 (Baylor College of Medicine) and CA-18346 (University of New Orleans).

TAMP2 STUDIES OF LOW VOLATILITY COMPOUNDS BY ION CYCLOTRON RESONANCE MASS SPECTROMETRY, M.J. LOCKE, R.L. HUNTER, P. CRUZ, P.N. BORER, and R.T. McIVER, JR., Dept. of Chem., Univ. of Cal., Irvine, CA 92717

Ion cyclotron resonance (ICR) mass spectrometry has proven to be an effective technique in recent years for the study of gaseous ion-molecule reactions. Generally, these studies have been limited to those compounds which exhibit sufficient vapor pressures for analysis, such as gases, most liquids, and a very few low melting solids. Recently we undertook studies of a series of low volatility compounds of biological interest. Included in this list are nucleic acid free bases, nucleosides, porphyrins, amino acids, peptides, and carbohydrates. Most of these compounds are generally regarded as troublesome, whether analysis is performed by ICR or conventional mass spectrometry.

Our studies have focused in two directions: 1) measurement of various physical-chemical parameters such as gas-phase acidity and basicity; and 2) development of analytical methods for these compounds. Toward these ends we have found it necessary to investigate several volatilization techniques not previously used with ICR spectrometers. Our results comparing these various volatilization techniques will be presented. Development of ICR analytical methods has focused on identification of rare chemically modified nucleic acid residues. Chemically modified residues may be important links in the cancer causing processes occuring *in vivo*. Analytical techniques which can identify the extremely small quantities of modified residues present in hydrolyzed DNA are necessary for the study of these *in vivo* processes. Our analysis results for the various common and modified residues will be presented.

THERMOCHEMISTRY OF INTRAMOLECULAR SOLVATION IN PROTONATED AND RADICAL IONS: DIAMINES, TRIAMINES, AMINO ALCOHOLS, DIPHENYL ALKANES AND NORMAL ALKANES.

M. MEOT-NER (MAUTNER), E. P. HUNTER, P. HAMLET, F. H. FIELD, The Rockefeller University, New York, NY 10021; P. AUSLOOS AND L. W. SIECK, National Bureau of Standards, Washington, D.C. 20234.

Proton transfer and charge transfer equilibria involving polyfunctional, flexible structures were measured by pulsed high pressure mass spectrometry. In the product ions intramolecular solvation of the charge can occur leading to non-covalently bonded cyclic structures. The increased proton affinities or decreased ionization energies of the polyfunctional compounds, as compared with appropriate references, is used to evaluate ΔH cyclization in the large, flexible ions. ΔS of the transfer reactions yields ΔS cyclization.

In polyfunctional ammonium ions $X(CH_2)_nNH_3^+$, X=OH or NH_2, intramolecular H bonding occurs, but it is weakened, compared with intermolecular H bonds, due to ring strain, constrained H bond geometry and polarization of the X function. These factors, denoted as ΔH strain, weaken internal H bonding in $NH_2(CH_2)_nNH_3^+$ by 17 kcal when n=2, 8 kcal when n=3 and 4 kcal when n=4. In parallel, with increasing ring size ΔS cyclization becomes more negative, from -8 e.u. for n=2 to -17 e.u. for n=4.

In $HO(CH_2)_nNH_3^+$ the magnitude of the strain factors and ΔS cyclization are similar to $NH_2(CH_2)_nNH_3^+$. In triamines $NH_2(CH_2)_nNH_2^+(CH_2)_nNH_2$ the ring strain and ΔS cyclization are also similar to $NH_2(CH_2)_nNH_3^+$, which indicates that even in the protonated triamines only one internal H bonded ring is formed.

The thermochemistry of charge transfer reactions from cyclic reference compounds to n-alkanes and to 1,4 diphenyl butane indicates that intramolecular solvation of the charge leads to constrained structures in the molecular ions of hydrocarbons. Thus, for charge transfer from 1,2 $(CH_3)_2C_6H_4^+$ to $C_6H_5(CH_2)_4C_6H_5$, ΔH= -5.6 kcal mol^{-1}, ΔS= -7.5 e.u. The results suggest that intramolecular bonding occurs between the phenyl groups in the product ion, leading to ΔS cyclization ≈ -7 e.u. Measurements on protonated diphenylbutane show that in this ion intramolecular interactions are similar to the radical ion. In contrast, no intramolecular bonding appears to occur in either the radical or protonated ion of diphenyl ethane.

Charge transfer equilibria between cyclic alkanes and normal alkanes were measured between 300 and 450°K using high pressure photionization mass spectrometry. ΔH ionization of n-alkanes decreases monotonically with increasing n, from 230.2 kcal mol^{-1} for n-C_4H_{10} to 215.2 kcal mol^{-1} for n-$C_{11}H_{24}$. The decrease of ΔH ionization between nC_6H_{14} and nC_7H_{16} is larger by ca. 1.5 kcal mol^{-1} than expected from the series up to nC_6H_{14}; also, ionization of nC_7H_{16} involves an entropy change of 6.6 e.u. For larger n-alkanes ΔS ionization becomes increasingly more negative, up to -15.6 e.u. for the ionization of n-$C_{11}H_{24}^+$. These results indicate that internal solvation of the charge, leading to constrained, probably folded structures, occurs in C_7 and larger n-alkane ions.

TABLE I

Themochemistry of Proton or Charge Transfer Reactions from Reference Compounds A^+ to Flexible Molecules B; Enthalpies and Entropies of Cyclization of the Flexible ions B^+ or BH^+; Strain Factors Weakening the Intramolecular Bond in B^+ or BH^+.

A	B	$-\Delta H°$ [a]	$-\Delta S°$ [b]	$-\Delta H°_{cyc}$ [a]	$-\Delta S°_{cyc}$ [b]	$\Delta H°_{strain}$ [a]
$Me_2NH_2^+$	$NH_2(CH_2)_2NH_2$	5.3	5.8	6.7	8.0	16.7
Me_3NH^+	$NH_2(CH_2)_3NH_2$	9.0	13.3	14.2	14.7	8.8
Pr_2NH^+	$NH_2(CH_2)_4NH_2$	10.1	14.3	17.9	17.1	5.1
$Me_2NH_2^+$	$NH_2(CH_2)_2OH$	0.2	0.3	--	--	--
Me_3NH^+	$NH_2(CH_2)_3OH$	3.5	11.9	8.8	11.9	8.2
Pyridine H^+	$NH_2(CH_2)_4OH$	12.9	16.1	13.7	16.9	3.3
i-$Pent_3NH^+$	$NH_2(CH_2)_2NH(CH_2)_2NH_2$	0.2	5.0	7.1	6.8	15.9
i-$Pent_3NH^+$	$NH_2(CH_2)_3NH(CH_2)_3NH_2$	10.2	13.4	17.1	14.8	5.9
1,2 $Me_2C_6H_4H^+$	$C_6H_5(CH_2)_2C_6H_5$	1.5	1.6	--	--	--
1,2 $Me_2C_6H_4H^+$	$C_6H_5(CH_2)_4C_6H_5$	5.9	11.8	3.4	11.8	5.1
1,2 $Me_2C_6H_4^+$	$C_6H_5(CH_2)_2C_6H_5$	0.8	0.2	--	--	--
1,2 $Me_2C_6H_4H^+$	$C_6H_5(CH_2)_4C_6H_5$	5.6	7.5	4.8	7.5	11.4
c $C_6H_{12}^+$	n C_5H_{12}	-6.4[c]	1.8[c]	--	--	--
c $C_6H_{12}^+$	n C_6H_{14}	-2.8[c]	2.5[c]	--	--	--
c $C_6H_{12}^+$	n C_7H_{16}	1.2	6.6	--	6.6	--
c $C_6H_{12}^+$	n C_8H_{18}	4.4	8.8	--	8.8	--
c $C_6H_{12}^+$	n C_9H_{20}	7.5[c]	10.6[c]	--	10.6	--
c $C_6H_{12}^+$	n $C_{10}H_{22}$	9.5[c]	13.2[c]	--	13.2	--
c $C_6H_{12}^+$	n $C_{11}H_{24}$	11.6[c]	15.6[c]	--	15.6	--

a. in kcal mol^{-1}
b. in e.u.
c. obtained from thermochemical ladder of change transfer reactions.

TEMPERATURE DEPENDENCE OF THE EQUILIBRIUM

$CO_2^{+\cdot} + 2CO_2 \rightleftharpoons (CO_2)_2^{+\cdot} + CO_2$

J. V. Headley, R. S. Mason and K. R. Jennings

Department of Chemistry and Molecular Sciences,
University of Warwick, Coventry, CV4 7AL, U.K.

A high pressure source with pulsed electron beam[1] was used with an MS50 mass spectrometer (Kratos Scientific Instruments Ltd.) to study reactions of $CO_2^{+\cdot}$ and $CO^{+\cdot}$ with their parent molecules under field free conditions. In the CO_2 work, charging up of the stainless steel ion exit plate prevented ions from leaving the source but this was largely overcome by gold plating on nickel giving satisfactory performance above 440 K. Ions were generated using a 10 μs electron pulse and abundances of ions were measured as a function of time.

The equilibrium

$$CO_2^{+\cdot} + 2CO_2 \overset{K}{\rightleftharpoons} (CO_2)_2^{+\cdot} + CO_2 \qquad (1)$$

was studied as a function of pressure and temperature by measuring abundances of $CO_2^{+\cdot}$ and $(CO_2)_2^{+\cdot}$ ions up to 2.5 ms after the electron pulse, equilibrium being attained after about 0.5 ms. The equilibrium constant

$$K = I_{(CO_2)_2^{+\cdot}} / I_{CO_2^{+\cdot}} \cdot [CO^2]$$

has been shown to be independent of pressure over the range 1-3 Torr and has been studied over the temperature range 460-560 K. A good linear van't Hoff plot of 25 measurements of K was obtained and a least squares analysis of the results leads to the data:

ΔH_1^o	ΔS_1^o	$(\Delta G_1^o)_{298}$	$(\Delta H_f^o)_{298}(CO_2)_2^+$
-66.1 ± 2.5 kJ mol^{-1}	-95.4 ± 4.6 JK^{-1}mol^{-1}	-92.0 ± 2.5 kJ mol^{-1}	$+475.3 \pm 2.5$ kJ mol^{-1}

The value of ΔH_1^o is in good agreement with the value -75.3 ± 11.7 kJ mol^{-1} obtained by Warneck using a fast flow method and a bracketing technique[2].

The accuracy of the method depends on the accuracy of the measurement of the ion current ratio ($I_{(CO_2)_2^{+\cdot}}/I_{CO_2^{+\cdot}}$) and taking into account mass discrimination by the detector, sampling errors at the ion exit slit, and errors arising from the diffusion of ions within the source, the observed ratio should be multiplied by 1.66 under the most unfavourable conditions. This does not affect the value of ΔH_1^o and the error introduced into the value of ΔS_1^o is less than that introduced by scatter in the data. Interference from competing reactions and collisional decomposition of ions after acceleration was neglected since K was independent of pressure.

An attempt was made to obtain similar data for the corresponding reaction between $CO^{+\cdot}$ and CO but equilibrium was not established under any experimental conditions which could be used. A study was therefore made of the reaction

$$CO^{+\cdot} + 2CO \overset{k_2}{\not\rightleftharpoons} (CO)_2^{+\cdot} + CO \qquad (2)$$

as a function of pressure and temperature. Over the pressure range 0.5-3.0 Torr, third order kinetics were observed at all temperatures between 324 K and 550 K. The results are consistent with a previous value in the literature[3] and the

temperature dependence of k_2 fits the relationships

(a) k_2 = constant × $T^{-3.1}$ (*cf.* $k_2' \propto T^{-3.2}$ for $O_2^{+\cdot}/(O_2)_2^{+\cdot}$ system)[4]

(b) $k_2 = 1.87 \times 10^{-30} \exp(-1365/T)$ cm^6 $molecule^{-1}s^{-1}$.

A full account of this work will be submitted for publication in the International Journal of Mass Spectrometry and Ion Physics.

References

1. D. K. Bohme, K. R. Jennings, R. S. Mason, J. A. Stone and R. S. Stradling (unpublished work)
2. A. B. Rakshit and P. Warneck, *Int. J. Mass Spec. Ion Phys.* (in press)
3. L. W. Sieck, *Int. Journal Chem. Kin.*, 10, 335 (1978)
4. J. D. Payzant, A. J. Cunningham and P. Kebarle, *J. Chem. Phys.*, 59, 516 (1978)

Ion Chemistry and Ligand Binding Energies of Cu^+ and Related Metal Cations.

Roger W. Jones and Ralph H. Staley, Department of Chemistry, Massachusetts Institute of Technology, Cambridge, MA 02139

A pulsed laser has been used to evaporate and ionize transition metals, as a source of metal ions for studies of their gas-phase ion chemistry by ion cyclotron resonance spectroscopy. The ion-molecule reactions of Cu^+ and Ag^+ with alkyl chlorides and alcohols have been examined. Alkyl chlorides are dehydrochlorinated by both metals, which bind either the alkene or HCl fragment, and eliminate the other fragment. Reaction sequences of the alkyl chlorides with the metal ions consist of dehydrochlorination and ligand displacement steps. This usually results in final products consisting of the metal ions with two ligands attached. Chloride transfer to both metal ions is also observed. Such transfers allow determination of the chloride affinities of the metal ions. Our results give $D(Cu^+\text{-}Cl^-)$ = 186 ±6 kcal/mole and $D(Ag^+\text{-}Cl^-)$ = 160 ±6 kcal/mole, in agreement with previous determinations. Both metals dehydrate and dehydrogenate the alcohols. Either dehydration fragment may be retained by the ion, but the dehydrogenated alcohols are always retained in preference to H_2. As with the alkyl chlorides, the final products are the dicoordinated metal ions.

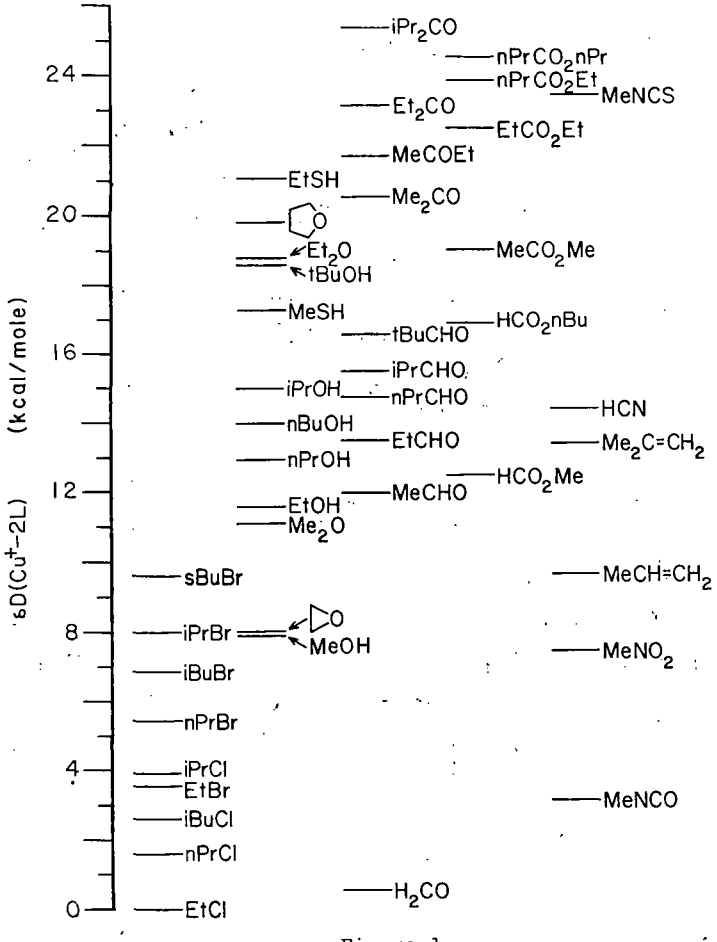

Figure 1

Ligand exchange reactions involving dicoordinated metal ions are readily observed. Exchange reactions 1 and 2 have been studied for M = Cu and Co.

$$M(L)_2^+ + L' \rightleftharpoons M(L)(L')^+ + L \qquad (1)$$

$$M(L)(L')^+ + L' \rightleftharpoons M(L')_2^+ + L \qquad (2)$$

The equilibrium constants and hence the free energy changes for these reactions have been measured for a large number of pairs of ligands, L and L'. By combining these energy changes, we have constructed relative ligand binding energy ladders for both Cu^+ and Co^+. Results involving isobutylene and nitromethane have been corrected for symmetry number changes.

Figure 1 shows the relative binding energies of 43 ligands to Cu^+. Results for Co^+ are similar as is evident from the comparison in Figure 2. Relative energies, $\delta D(M^+-2L)$, are used in the figures, with the zero on each of the binding energy scales arbitrarily chosen, EtCl for Cu^+ and MeOH for Co^+. In both scales the sulfur compounds are stronger ligands than the analogous oxygen compounds, although as Figure 2 shows, the effect is greater for Cu^+. This and similar features suggest that both metal ions are soft acids.

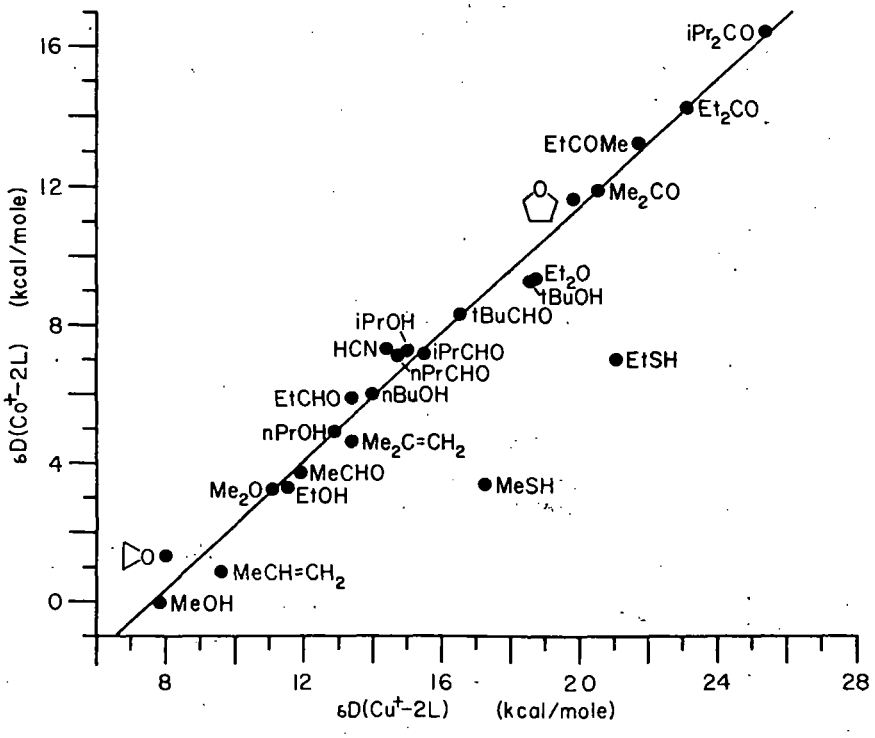

Figure 2

Gas Phase Ion Chemistry and Relative Ligand Binding Energies of Al^+, Mn^+, Cr^+, Ti^+ and Related Cations. Manfred M. Kappes, Jack S. Uppal and Ralph H. Staley, Dept. of Chem., Mass. Inst. of Tech., Cambridge, MA 02139

A pulsed Nd-YAG laser is used to generate metal cations in the gas phase for studies of their ion chemistry by ion cyclotron resonance spectroscopy. Direct results from these experiments include determination of thermochemical data such as chloride affinities, as well as, for some of the metals studied, relative ligand binding energies.

(1) Titanium - New chloride affinity values of $D(Ti^+-Cl^-)$ = 185 ±5 kcal/mol and $D(TiCl^+-Cl^-)$ = 202 ±6 kcal/mol are inferred. Homolytic Ti^+-halogen bond dissociation energies are also obtained: $D(Ti^+-F)$ = 118 ±9 kcal/mol, $D(Ti^+-Cl)$ > 86 kcal/mol, $D(Ti^+-Br)$ > 71 kcal/mol, and $D(Ti^+-I)$ > 57 kcal/mol. Observation of hydride transfer from CH_3F to TiF_2^+ implies a lower limit for the hydride affinity of TiF_2^+ of $D(TiF_2^+-H^-) \geq 288$ kcal/mol. Reactions with chloroethylenes include oxidation to give TiO_2^+. This charge transfers to several of the chloroethylene neutrals; an ionization potential for $TiCl_2$ of $IP(TiCl_2)$ = 9.76 ±0.11 eV is inferred.

(2) Aluminum - The ion chemistry of many of the metal cations studied includes elimination reactions which lead to species having a single ligand bound to the metal. For example Al^+ dehydrates EtOH to give $Al(H_2O)^+$. Subsequent displacement of water by EtOH leads to a product which can then be used as a starting point for competitive ligand exchange reactions. Through determination of ligand exchange equilibria, relative binding energies of Al^+ to 30

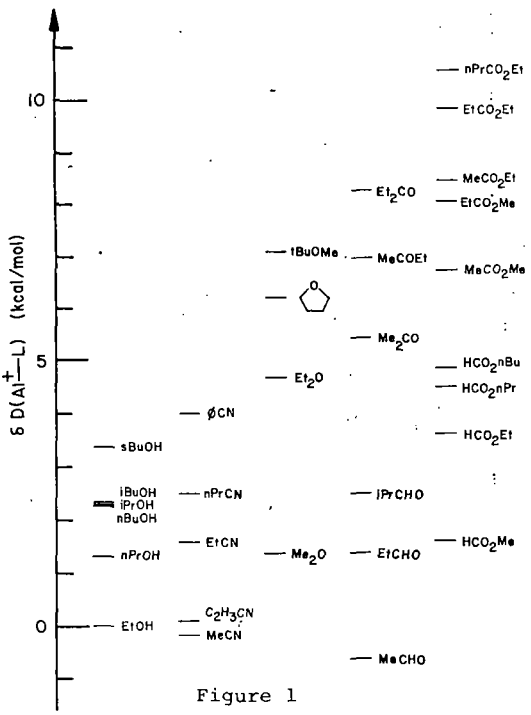

Figure 1

organic molecules are measured (figure 1). The results are compared to other ligand binding energy scales. A relatively good correlation of the Al^+ data with proton affinities is found.

(3) Manganese - Mn^+ reacts with n-PrCl to give $Mn(C_3H_6)^+$ by elimination. Displacement of propylene by n-PrCl results in $Mn(nPrCl)^+$. This species can be used as an initiator for a series of ligand exchange reactions, leading to the determination of relative gas phase ligand binding energies to Mn^+. The 33 ligands for which Mn^+ binding energies are obtained include alcohols, ethers, aldehydes, ketones, esters, nitriles, amines and sulphides (figure 2). Correlation of the Mn^+ data to similar data sets obtained for Cu^+ is informative when considered in terms of hard and soft acid-base theory. In general Mn^+ appears to behave as a harder acid than Cu^+.

(4) Other metals - Work done in the past on the ion chemistry of Cr^+ indicates that this species is particularly reactive towards many organic molecules, and therefore not suitable for ligand binding energy studies. Work underway on Cr^+ focuses on reaction mechanism elucidation. A determination of Ni^+ ligand binding energies to over 50 organic molecules has just recently been completed. Results correlate well with both Cu^+ and Co^+ data sets (see paper TAMP5).

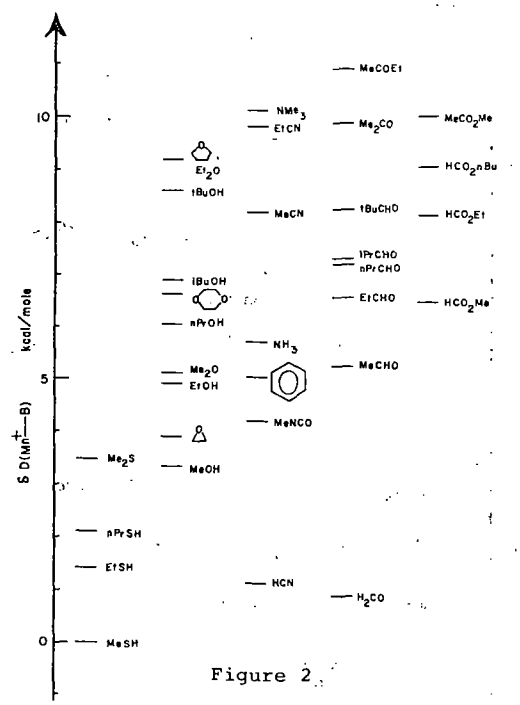

Figure 2

Selective Chemical Ionization Reagent gases for Polynuclear Aromatics and Aromatic Nitrogen Compounds

Donald M. Schoengold
Chemical Methods and Kinetics Section
Physical Sciences Department
Pacific Northwest Laboratory

Application of specific ionization techniques for quantitative analysis of trace level compounds in complex matrices can provide a major improvement in laboratory throughput and analytical precision by elimination of the cleanup steps necessary to ensure that the matrix does not interfere with the analysis. Techniques which are commonly used to enhance specificity include low ionizing voltage methods and high resolution. THe first approach often does not simplify the spectra enough and always involves a large loss of sensitivity which may be intolerable in trace-level analysis. The second approach requires expensive equipment which is not present in many laboratories.

Chemical ionization using selective reagent gases offers another approach to this problem which is much simpler and can be done with commonly available equipment. Since the polynuclear aromatic and aromatic nitrogen compounds which are of special interest because of their carcinogenic or mutagenic potential have higher proton affinities than many of the major interfering compounds in the matrix, chemical ionization specificity can be achieved by choosing a reagent gas which has a proton affinity higher than the interferences and lower than the compounds of interest.

Reagent gases of special interest are ammonia (proton affinity = 207kcal/mole) and methylamine (PA = 211 kcal/mole). These compounds give simple high pressure spectra and the proton affinities are in the range of the compounds we wish to determine. We have studied a series of polynuclear aromatic and aromatic nitrogen compounds as well as a set of compounds typical of the interfering matrix in liquid fuel samples using electron impact and methane, ammonia, monomethylamine and dimethylamine chemical ionization. The chemical ionization reagent gases are listed in order of increasing proton affinity and thus in order of increasing specificity.

The results (Table I) showed that both ammonia and monomethylamine are very useful reagent gases for the polynuclear aromatics and are also useful for aromatic nitrogen compounds. Methane gave good sensitivity for these compounds but almost no specificity. Dimethylamine gave so little response for any of the compounds that it was not useful and the results are not included in the table.

The monomethylamine sensitivities of the 3 molecular weight 252 polynuclear aromatics showed that the benzo(a)pyrene had a much higher sensitivity than either perylene or benzo(e)pyrene.

The very high sensitivity for dibenzothiophene by ammonia chemical ionization is also of potential interest since there is some evidence that polynuclear sulfur compounds may be carcinogenic and it may be that ammonia chemical ionization will give enhanced sensitivity for these compounds.

TABLE I

Normalized Molecular Weight of Quasi-Molecular Weight Sensitivities

	EI	methane	ammonia	methylamine
C19	0.1	3	--	--
n-Hexylbenzene	22	29	0.03	--
2,3,5-trimethylphenol	40	144	5	--
1,5-dimethylnaphthalene	87	161	2	
anthracene	100	100	100	100
pyrene	35	50	24	53
fluoranthene	98	75	1	93
chrysene	67	36	1	32
benzo(a)pyrene	43	14	34	111
perylene	22	8	18	2
benzo(e)pyrene	42	12	6	10
3,4-dimethylaniline	52	104	6	153
2,4,6-trimethylpyridine	73	43	38	2113
2-naphthol	13	10	3	--
2-methylindole	63	140	38	524
2,6-dimethylquinoline	54	90	16	--
carbazole	98	118	7	--
acridine	64	53	15	--
6-naphthylamine	113	233	30	44
1-aminoanthracene	105	6	0.8	--
1-aminopyrene	9	2	0.1	--
6-aminochrysene	1	--	0.02	--
1-aminofluorene	45	78	0.8	--
4-azafluorene	182	650	56	4615
dibenzothiophene	72	--	433	--

FRACTIONATION OF ENVIRONMENTAL ORGANIC EXTRACTS WITH DIMETHYLSULFOXIDE. APPLICATIONS TO DIESEL EXHAUST PARTICULATES

Thomas R. Henderson, Charles R. Clark, Ray L. Hanson and Robert E. Royer
Lovelace Inhalation Toxicology Research Institute
P. O. Box 5890
Albuquerque, New Mexico 87115

Environmental samples often require both fractionation and concentration to be suitable for GC/MS analysis and bioassay. Since often only mg amounts of material are available, it is important to develop methods of fractionation which are efficient for small samples and yet simple enough to allow bioassay and analysis of large numbers of samples.

One of the methods of fractionating organic samples is column chromatography on Sephadex LH-20 polymers. This method is particularly useful for large samples, but presents difficulties in separating large numbers of samples, since the procedures are tedious and difficult to automate.

Another method for fractionating complex organic samples has been solvent:solvent extraction with dimethylsulfoxide (Me_2SO). This approach has the advantage of being applicable to small samples and being directly bioassayable, since Me_2SO is the solvent commonly used in the Ames' bioassay procedure. Previous studies of Me_2SO extraction of aromatics have shown that the extraction can be quantitative (1) and that back extraction of aromatics into hexane may be achieved after dilution of Me_2SO extracts with H_2O (1,2).

Diesel exhaust samples often contain unburned fuel crankcase oil and miscellaneous oxidation products. Bioassay and analysis requires fractionation for detection and quantitation of mutagenic components.

METHODS

Diesel exhaust samples were collected from a light-duty diesel vehicle. The engine displacement was 1.5 liters and the engine was operated on the highway FET cycle. The samples were collected in a dilution tunnel at the Transportation Systems Center - Department of Transportation on Pallflex T60A20, 20" x 20" filters. CH_2Cl_2 extracts were prepared with sonication for 1 hour, and the solvent evaporated using a rotary evaporator with the final few ml removed with a stream of dry N_2. The non-volatile residue was weighed and dissolved in hexane for Me_2SO fractionation or tetrahydrofuran (THF) for Sephadex chromatography.

Sephadex LH-20 was swelled overnight in THF, and a 15 mm x 1 m column prepared. A 0.5 to 1 g sample of extract was applied and fractions collected after elution with (a) 70 ml THF; (b) 30 ml THF; (c) 15 ml THF; (d) 15 ml THF; (e) 15 ml THF; and a final fraction (f) eluted by 300 ml of methanol. These fractions were evaporated and dissolved in Me_2SO for Ames bioassay.

Me_2SO fractionation was carried out as follows on 0.5 to 1 g of extract:

Sample dissolved in hexane —— extracted 3X, Me_2SO ——> Hexane Layer ('Aliphatics')
——> Me_2SO Layer (lyophilize an aliquot)

Me_2SO Layer Aliquot —— dilute with 2 vol H_2O, extract with hexane ——> Hexane Layer ('Aromatics')
——> Me_2SO/H_2O Layer (lyophilize)

The hexane fractions were concentrated by rotary evaporation and weighed. The lyophilized residue was weighed. Aliquots were dissolved in Me_2SO for bioassay. Bioassay procedures were as described previously (3) with Salmonella TA-100.

GC^2/MS analyses were carried out on a Finnigan 4023 for EI spectra and solid probe CI analyses were carried out on a Finnigan 3200. The model 4023 was equipped with a Quadrex 20M WCOT OV-101 quartz capillary column inserted directly into the ionizer. Methane was used as the reagent gas for CI. Both instruments were interfaced to an

INCOS data system with 3.1C software.

RESULTS AND DISCUSSION

The direct mutagenic activity of these pooled diesel extracts were found to be concentrated in the aromatic fraction by Me_2SO extraction, and in Sephadex fractions (c) and (d). Sephadex fraction (d) and the Me_2SO aromatic fraction had nearly identical specific activities, ca 1500 revertants/mg. These fractions comprised 0.9% and 0.7% respectively of the starting extract by weight.

GC^2/MS analyses of the Me_2SO aromatic fraction showed that the major components detectable were polycyclic aromatic hydrocarbons, none of which are known to be direct mutagens in the Ames' bioassay, such as pyrene, benzopyrenes, benzofluoranthenes, etc. CI/solid probe analysis showed the Me_2SO aromatic fraction contained more high boiling components (which exhibited CI ions in the range 350 to 425 AMU) than the Me_2SO/H_2O Fraction. The aliphatic fraction was found by CI/solid probe to range in hydrocarbons from C_{15} to C_{40}.

Preliminary extraction with dilute HCl and NaOH was attempted, but the activity of the aromatic fractions obtained with Me_2SO were much lower. It is possible that losses in activity result from acid or basic extraction. Hence these steps were omitted. Small amounts of activity were found in lyophilized HCl extract, but no analyses were carried out because of small sample size.

These results show that fractionation with Me_2SO may greatly aid in concentrating the mutagenic activity in environmental samples, and by diluting with H_2O the activity can often be recovered by hexane extraction. These fractions may serve as a starting point for further fractionation and identification, if sample sizes permit, or may provide an indication of the chemical class of compounds which exhibit biological activity if insufficient quantities of sample are available.

REFERENCES

1. Haenni, E. O.; Howard, J. W. and Joe, F. L. (1962). J. Assoc. Off. Agr. Chemists 45: 67.
2. Natusch, E. F. S., and Tomkin, B. A. (1978). Anal. Chem. 50: 1429.
3. Ames, B. N., McCann, J., and Yamasaki, E. (1975). Mutat. Res. 31: 347.

ACKNOWLEDGEMENTS

Research performed under U. S. Department of Energy Contract Number DE-AC04-76EV01013.

TAMP9 ANALYSIS OF POLYHALOGENATED AROMATIC HYDROCARBONS BY CAPILLARY COLUMN GC-NEGATIVE ION CIMS. FRANK W. CROW[1] and ALF BJØRSETH[2], Battelle Columbus Laboratories, 505 King Avenue, Columbus, Ohio 43201.

Negative ion chemical ionization mass spectrometry (NICIMS) is evaluated as a method for qualitative and quantitative determination of polyhalogenated aromatic hydrocarbons. The major compounds of interest are chlorinated and brominated benzenes. Aroclor 1242, Aroclor 1268 and 1,2,3,4-tetrachlorodibenzo-p-dioxin are also studied. Each compound or mixture of compounds was analyzed by glass capillary column gas chromatography - CI mass spectrometry using different modes of ionization in the mass spectrometer. Sensitivity comparisons between the various modes are made. The ionization modes employed were methane positive ion CIMS, methane negative ion CIMS, methane/ CH_2Cl_2 negative ion CIMS and methane/oxygen negative ion CIMS.

TAMP10 IDENTIFICATION OF PCB's OF NATURAL ORIGIN BY GC/MS, BORI SHUSHAN and ROBERT K. BOYD, Chemistry Department, University of Guelph, Guelph, Ontario, Canada N1G 2W1

It was recently shown (Corke *et al.*, J. Agric. Food Chem. 27, 664 (1979)) that bacteria containing a nitrate reductase enzyme system convert 3,4-dichloroaniline, and herbicides prepared therefrom, into various products including 3,3',4,4'-tetrachlorobiphenyl. In addition other tetrachlorobiphenyl isomers are formed, as well as tri- and dichlorobiphenyls. The present work describes our partly successful attempts to identify which isomers are present. Methods used include GC retention times, EI mass spectra, and B/E linked scan studies of metastable molecular ions.

QUANTITATIVE DETERMINATION OF HALOCARBONS IN THE TROPOSPHERE BY SELECTED ION MONITORING.

F. Bruner and G. Crescentini.
Istituto di Scienze Chimiche -Università di Urbino-
P.za Rinascimento,6-61029 - Urbino Italy

P. Ciccioli - Istituto Inquinamento Atmosferico C.N.R. Area Ricerca di Roma
Via Salaria Km. 29.5 00016 Monterotondo Scalo

E. Brancaleoni - Servizio di Spettrometria di Massa. Area Ricerca di Roma
Via Salaria Km. 29.5 00016 Monterotondo Scalo

Monitoring of halocarbons in the troposhere is becoming more and more important to undestand their impact on ozone depletion in the stratosphere.In particular, the knowledge, with a high degree of accuracy, of the trend of the concentration with time and of the presence of unusual fluorochloro compounds is very important to establish wether there are tropspheric sinks for halocarbons or not.

The most used analytical technique involves GC with EC detection. However, the repetibility and reproducibility of the ECD are not as good as they should be according to the needs of quantitative analysis.

The non specifity of the ECD for trace compounds, especially in the presence of much higher concentration of other halocarbons in also known.

The method here described is a very specific one (1) and involves mass spectrometry in the selected ion monitoring mode (mass fragmentography) for qualitative and quantitative analysis of tropospheric samples of halocarbons.A VG micromass 70-70 F equipped with the multiple ion detector (MID), compled with a DANI mod 3900 gascromatograph equipped with an injection device for air samples, is used, with a very selective column, previously described (2).

A program for the MID had to be written in order to minimize the effect of acceleration voltage changes when focusing different ions. The program is summarized in table 1.

Resolution is kept sufficiently high to allow the separation of ions with the same nominal m/e value but different elemental composition. This is done mainly for quantitative purposes.

Permeation tubes are used as primary standards and a known amount of the halocarbons of interest is injected into the column prior and after the actual atmospheric sample. Calibration curves are also obtained in this way. Two of these for F 11 and F 21 are shown in figure 1.

The method ensures a reproducibility of data expressed as standard deviation, of 10%.

In figure 2 a typical chromatogram obtained with the MID is shown.

It is interesting to note that F 22 is well detected, which is in practice impossible with the ECD, due to the signal from air and water that is overlapping to this scarcely retained halocarbon.

LITERATURE CITED

1) G. CRESCENTINI AND F. BRUNER , NATURE , 279, 312, (1979)
2) F. BRUNER ,G. BERTONI AND G. CRESCENTINI, J. CHROMATOGR. , 167, 399, (1978)

TABLE I

Program 1				Program 2			
Reference mass: $C_3H_8O^+$ (m/e: 58.0417)				Reference mass: $C_7H_7^+$ (m/e: 91.0546)			
Compound	Ion	m/e	E/E_0	Compound	Ion	m/e	E/E_0
CHF_2Cl	$CHF^{35}Cl^+$	66.9751	86	$CFCl_3$	$CF^{35}Cl_2^+$	100.9361	90
	$CHF^{37}Cl^+$	68.9721	84		$CF^{35}Cl^{37}Cl^+$	102.9361	88
CF_2Cl	$CF_2^{35}Cl^+$	84.9647	68	$C_2F_3Cl_3$	$CF^{35}Cl_2^+$	100.9361	90
	$CF_2^{37}Cl^+$	86.9627	66		$CF^{35}Cl^{37}Cl^+$	102.9361	88
$CHFCl_2$	$CHF^{35}Cl^+$	66.9751	86	CH_3CCl_3	$CH_3C^{35}Cl^+$	96.9612	93
	$CHF^{37}Cl^+$	68.9721	84		$C^{35}Cl_3^+$	116.9065	77
CH_2Cl_2	$CH_2^{35}Cl^+$	83.9627	69	CCl_4	$C^{35}Cl_3^+$	116.9065	77
$C_2F_4Cl_2$	$CF_2^{35}Cl^+$	86.9627	66	C_2HCl_3	$C_2H^{35}Cl_2^+$	94.9455	95

Table 1 - MID Programs for mass fragmentography of halocarbons in air samples.

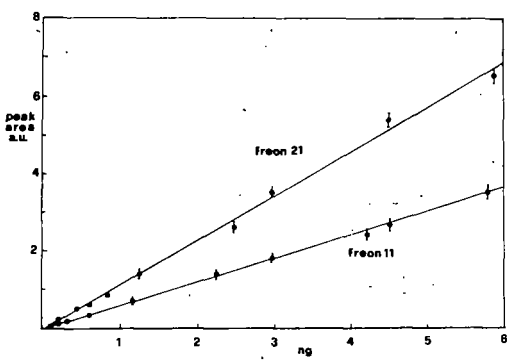

Figure 1 - Calibration curves for F11 and F 21.

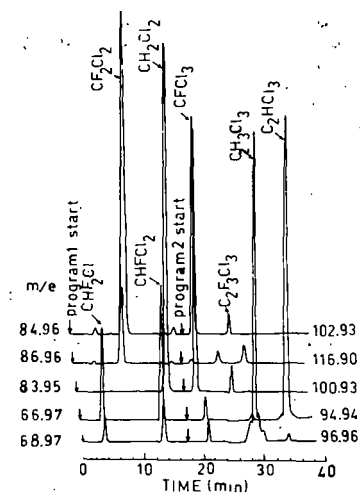

Figure 2 - Typical mass fragmentogram of a thirty liter air sample.

FORMATION OF CHLOROFORM FROM THE REACTION OF HYPOCHLORITE AND E. COLI

Donald L. Dugger

GTE Laboratories Incorporated
Waltham, MA 02154

The formation of trihalomethanes during the chlorination of drinking water is well established. There remains, however, some doubt regarding the precursors that undergo the classical haloform reaction. Simple methyl ketones react too slowly in the pH range of typical drinking water to account for the rapid formation and rather large quantitites of chloroform found in many water supplies. Rook[1] proposed that natural humic substances were the precursors for haloform formation. Indeed his studies with both natural and commercial humic acid have demonstrated that chloroform is produced by the chlorination of this material. This paper presents data which shows that another naturally occurring material, namely bacteria, can also produce chloroform when chlorinated with hypochlorite. The reason for chlorinating water in the first place is to "kill" the bacteria which is present in most natural water. The process by necessity implies a chemical reaction taking place between the bacteria and the hypochlorite. The product(s) of this reaction is the basis of this study.

Various concentrations of lyophilized cells of E. Coli in distilled water were reacted with hypochlorite solution over a pH range of 3 to 10 with and without the addition of bromide ions. The reactions, carried out at 3°C, were stopped at various time intervals by the addition of sodium thiosulfate solution. The samples were analyzed using the purge and trap technique and GC/MS.

The results illustrated in Figure 1 indicate that bacteria does react with hypochlorite to produce chloroform. In fact, within the detection limit of the method (~1 ppb), no other chlorinated compounds are produced. The reaction was found to be pH and temperature dependent, and approximately 75% complete by 10 hours at 3°C. The results suggest that E. Coli bacteria produces about 5 times more chloroform than an equivalent amount of humic acid at 25°C. Brominated haloforms are produced by the addition of bromide ions to the solution. This is illustrated in Figure 2. The relative concentrations of the brominated species appears to be dependent upon the bromide ion concentration.

[1] Rook, J. J., 1974 "Formation of Haloforms During Chlorination of Natural Waters". Water Treat. Exam. 23(2):234

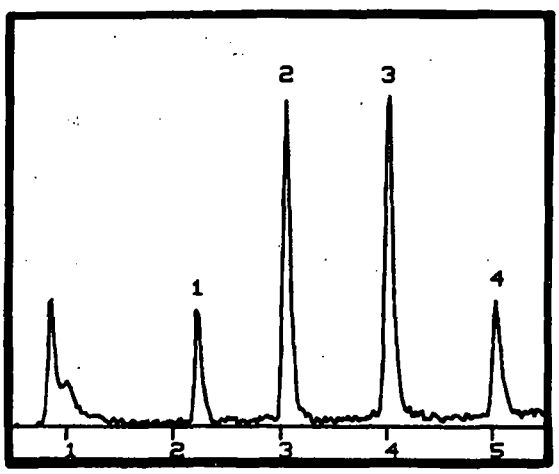

Figure 2. Chromatogram of haloforms produced when bromide ions are present in the solution. 1) Chloroform; 2) Bromodichloro methane; 3) Dibromochloro methane; 4) Bromoform.

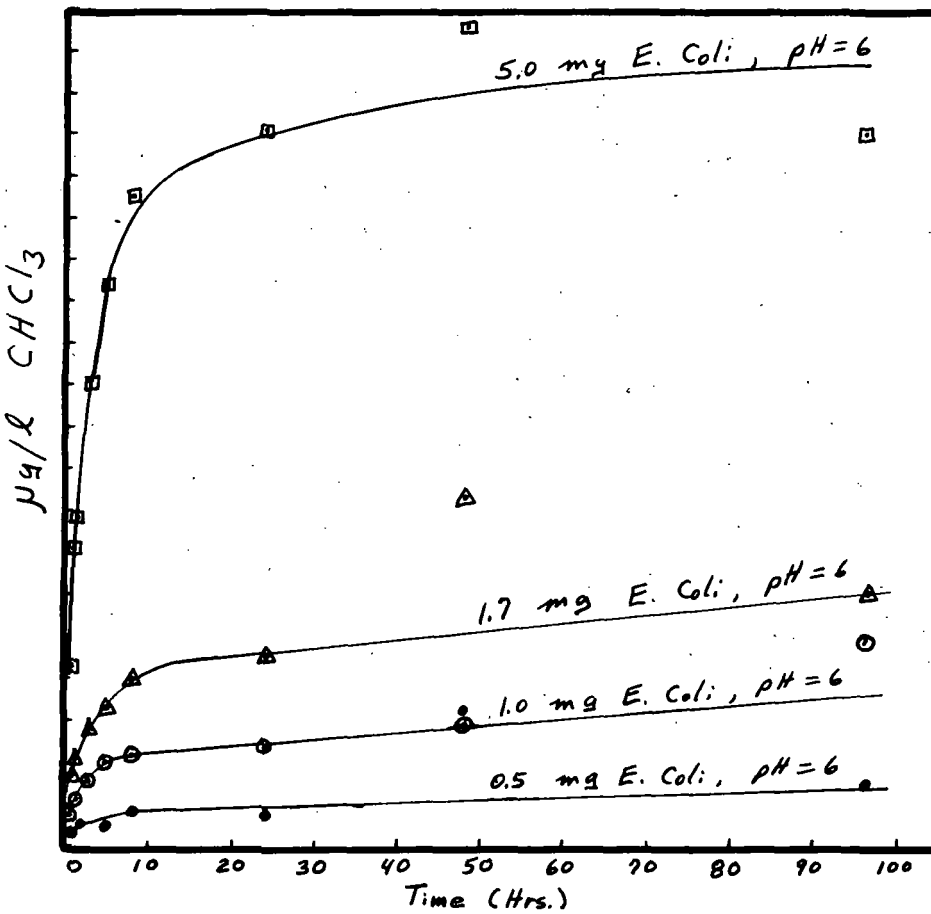

Figure 1. Chloroform production versus time for various concentrations of E. Coli bacteria reacted with sodium hypochlorite.

SINGLE IONIZATION OF AMMONIA CLUSTERS AND DOUBLE IONIZATION OF HETERONUCLEAR RARE GAS DIMERS

T.D. Märk*, K. I. Peterson, A.W. Castleman, Jr.

Dept. of Chemistry and Chemical Physics Laboratory, CIRES**
University of Colorado, Boulder, Colorado 80309

H. Helm*** and K. Stephan

A. f. Kernphysik u. Gaselektronik, Inst. f. Experimentalphysik
Leopold Franzens Universität, A-6020 Innsbruck, Austria

Studies of the formation and properties of atomic and molecular cluster systems (van der Waal's molecules) are requisite in providing a basic understanding of the forces responsible for cluster stability. Currently, our laboratories at CU and LFU are engaged in an extensive program concerned with the investigation of small gas-phase clusters by electron impact and photoionization mass spectrometer techniques. The overall objective of the work is to measure ionization cross section functions and to deduce the appearance potentials of clusters. The results serve to elucidate the structure of the clusters and contribute to an understanding of the dynamics of cluster formation. Experiments have recently been completed for the single electron impact ionization of NH_3, CO_2 and H_2O clusters and for the double electron impact ionization of (NeXe) and (ArXe).

The experimental apparatus employed in each case is comprised of a supersonic free jet expansion coupled with appropriate molecular beam mass spectrometric detection techniques. A new approach to mass spectrometric measurement and analysis was developed during the course of the studies made at LFU[1,2] involving extensive and detailed consistency checks on the extraction and collection efficiency of ions. The operating conditions of the apparatus at CU were chosen by comparison with those at LFU. Considerable attention was given to careful cross checks between the results obtained in the two laboratories, and it was found the data obtained in the two apparatuses were in excellent agreement; f.i., a value of 13.50 ± 0.10 eV was found for the process $Kr_2 + e \rightarrow Kr_2^+ + 2e$ compared to 13.45 ± 0.3 previously determined at LFU(1).

At the present time there is a paucity of information concerning appearance potentials of homomolecular clusters. In addition, the available data are deduced from photoionization studies. For purpose of comparison, we have conducted an extensive investigation of the electron impact ionization of $(NH_3)_x$ where x ranged up to 7. Related studies have been conducted with the H_2O and CO_2 dimer. Quite unexpectedly the electron impact appearance potentials obtained for these clusters are within the error bars equal to the appearance potentials of the respective monomer. This agrees with a qualitative finding by Leckenby and Robbins[3] for CO_2 dimer. However, our results are in contrast to the findings of photoionization studies 4-6 and to values deduced from thermochemical properties obtained with high pressure mass spectrometry techniques[7]. The present observations can be explained by a post collision interaction effect including dissociative recombination as proposed recently[8] in order to explain differences in observed appearance potentials of the rare gas dimers[1,9].

Related studies were made regarding the formation of doubly charged rare gas dimers. Doubly ionized molecules may exist in long lived states when chemical forces active at short internuclear distances are able to impose a sufficiently attractive well over the repulsive coulomb interaction of the ions ($R^+ + R^+$). Very little information is known so far about the interaction potentials of doubly charged rare gas dimers R_2^{++}. However, due to the strong polarization attraction and on the basis of recent calculations[10] for weakly bound states of the rare gas oxides (which have an outer shell that is isoelectronic with the doubly charged rare gas dimers) we expected some bound states to arise from the interaction $Xe^{++} + Ne$. Recently, we have been able to verify the existence of $(NeXe)^{++}$ produced via the process $NeXe + e \rightarrow NeXe^{++} + 3e$ and to determine an appearance potential which is similar to that of Xe^{++}. However, we have also discovered a long lived (>20 μs) state of $(ArXe)^{++}$ with an appearance potential slightly greater than Xe^{++} (see Fig. 1).

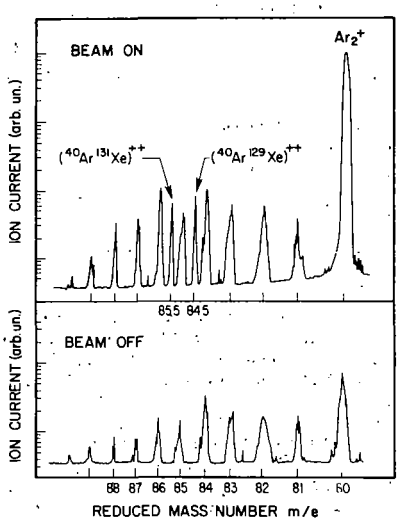

Fig. 1

References

(1) H. Helm, K. Stephan and T.D. Märk, Phys. Rev., A19 (1979) 2154.
(2) K. Stephan, H. Helm and T.D. Märk, Adv. Mass Spectrometry, 8 (1980).
(3) R.E. Leckenby and E.J. Robbins, Proc. Roy. Soc. London, A291 (1968) 389.
(4) C.Y. Ng, D.J. Trevor, P.W. Tiedemann, S.T. Ceyer, P.C. Kronebusch, B.H. Mahan and Y.T. Lee, J. Chem. Phys., 67 (1977) 4235.
(5) G.G. Jones and J.W. Taylor, J. Chem. Phys., 68 (1978) 1768.
(6) S.T. Ceyer, P.W. Tiedemann, B.H. Mahan and Y.T. Lee, J. Chem. Phys., 70 (1979) 14.
(7) I.N. Tang and A.W. Castleman, Jr., J. Chem. Phys., 62 (1975) 4576.
(8) T.D. Märk, A.W. Castleman, Jr. and H. Helm, Xth SPIG, Dubrovnik (1980).
(9) C.Y. Ng, D.J. Trevor, B.H. Mahan and Y.T. Lee, J. Chem. Phys., 65 (1976) 4327.
(10) T. H. Dunning and P.J. Hay, J. Chem. Phys., 66 (1977) 3767.

* On leave as a CIRES Visiting Fellow from the Inst. of Experimentalphysik, Leopold Franzens Universität, A-6020 Innsbruck, Austria.

** The Cooperative Institute for Research in Environmental Sciences is jointly sponsored by the University of Colorado and NOAA.

*** Present address: Molecular Physics, SRI International, Menlo Park, California 94025.

CROSSED BEAM STUDIES OF THE REACTIONS OF CO^+ WITH O_2 AND NO

M. F. Jarrold, D. M. Hirst and K. R. Jennings

Department of Chemistry and Molecular Sciences,
University of Warwick, Coventry, CV4 7AL, U.K.

At Warwick we have initiated a programme to study the dynamics of four centre reactions. These reactions have not been extensively studied and are much less well understood than the reactions of an atomic ion with a neutral molecule. A crossed beam apparatus is a useful tool for studying the dynamics of ion molecule reactions because it provides information on the velocity and angular distributions of the products. In addition some information on the total cross section can be derived from the data. By varying the translational energy of the ionic reactant it is possible to study the dynamics of an ion-molecule reaction as a function of translational energy. We have used the crossed beam apparatus recently developed at Warwick to study the reactions (1-3).

$$CO^+ + O_2 \rightarrow CO_2^+ + O \qquad \Delta H = -0.58 \text{ eV} \qquad (1)$$

$$CO^+ + NO \rightarrow CO_2^+ + N \qquad \Delta H = +0.81 \text{ eV} \qquad (2)$$

$$CO^+ + NO \rightarrow NCO^+ + O \qquad \Delta H = +2.70 \text{ eV} \qquad (3)$$

Ions are produced by EI, mass selected by a quadrupole mass filter and focussed using an electrostatic octopole lens (4). This beam source produces ion beams with intensities and angular distributions close to the fundamental space charge limit. The angular divergence of the ion beam is typically 2° (FWHM). Measured energy distributions of the ion beam are given by $\Delta E(FWHM) = 0.16 + 0.042.E$ eV, where E is the nominal ion energy. Good quality ion beams can be obtained at energies substantially below 1 eV. The neutral beam, which intersects the ion beam at 90°, is derived from a differentially pumped capillary array. The neutral beam maximum angular divergence is 16°. Energy and angular distributions of the products are measured using a detector which can be rotated in both planes about the crossing region. The detector consists of an RPD energy analyser and a quadrupole mass filter. Ions are detected at the end of the quadrupole using a channeltron electron multiplier and pulse counting, or a Faraday cup and electrometer. The RPD analyser consists of 3 electrodes covered with fine mesh grid, and is heated to 150^oC to avoid surface charging problems. Care has been taken to ensure that the energy analyser and detector have near ideal transmission functions. The energy resolution is approximately 0.04 E, and the angular resolution of the detector is approximately 3°. Product ion energy distributions are recorded in a multichannel analyser, and angular distributions are measured using an up-down counter. The neutral beam is chopped and background counts subtracted. Data from the multichannel analyser is output on an X-Y plotter or fed to a CBM "PET" microcomputer.

This work provided the first reported observations of reactions (1-3). Reaction (1) presumably possesses an activation barrier since no CO_2^+ product was detected in thermal energy SIFT experiments. This is unusual for simple exothermic ion-molecule reactions. In all the reactions the most probable product translational energy was found to be

significantly less than the predictions of the simple spectator stripping model, indicating that substantial coupling of the motion of all atoms is occurring in reactive collisions. Relative total cross sections have been derived from the data. In all three reactions the total cross section was found to rise to a maximum and then decline due to dynamic restrictions on product stability. At low initial translational energy only ground electronic state products are observed. However, at high energy where total cross sections are low there is evidence for the formation of electronically excited neutral in reactions (1) and (2) with substantially more electronically excited product being observed in reaction (2) than in reaction (1). It appears that virtually none of the products from reaction (3) are electronically excited. At high initial energy the observed product stability limits suggest that the majority of the CO_2^+ product formed in the upper vibrational levels of the $X^2\Pi_g$ ground state undergoes a spin forbidden predissociation to a repulsive $^4\Sigma$ state which correlates adiabatically with $O^+(^4S)$ + CO $(^1\Sigma)$, before reaching the detector. In reaction (2) we found that we can rationalise much of our data for back scattered CO_2^+ by a simple mechanism in which the ionic reactant CO^+ is considered to approach the NO with the collision axis collinear with the NO bond axis. As the reactants approach their relative kinetic energy is converted into potential energy as the C-O-N "bonds" are compressed. At the classical turning point the O atom is considered to be transferred to the CO^+. As the products recoil, the kinetic energy gained will be equal to the energy stored in the NO compression. We assume the initial kinetic energy to be partitioned equally between the NO and CO compressions, so the product would be expected to recoil with an energy equal to half of the initial energy. The NCO^+ appears as a minor product from CO^+-NO collisions at low energy but increases relative to CO_2^+ as the initial energy is raised and the cross section for CO_2^+ formation is low due to product stability restrictions. Reaction (3) is 2.70 eV endothermic and it appears that a significant fraction of the product is derived from the reaction of the small components of vibrationally and electronically excited CO^+ in the ion beam. The variation of product NCO^+ internal excitation with initial energy suggests that reaction occurs on a surface in which at least part of the reaction endoergicity appears as barriers as the reactants approach or products separate.

References

1. M. F. Jarrold, K. Birkinshaw and D. M. Hirst, *Mol. Phys.*, 1980, 39, 787
2. M. F. Jarrold and D. M. Hirst, *Mol. Phys.* in press
3. M. F. Jarrold and D. M. Hirst, submitted
4. K. Birkinshaw, D. M. Hirst and M. F. Jarrold, *J. Phys. E.*, 1978, 11, 1037

TAMP15 SOLVATION OF K^+ BY BENZENE. A NEW HIGH PRESSURE FLOW ION SOURCE. J. SUNNER, K. NISHIZAWA and P. KEBARLE, Dept. of Chemistry, University of Alberta, Edmonton, Canada, T6G 2G2.

The gas phase equilibria

$$K^+(C_6H_6)_{n-1} + C_6H_6 = K^+(C_6H_6)_n$$

were studied over a wide temperature range with a high pressure mass spectrometer. Clusters with up to 4 benzene molecules were observed. The enthalpy changes for the successive addition, $\Delta H^\circ_{n-1,n}$ were -19, -18, -14 and -12 kcal mol^{-1} respectively. STO-3G calculations on $Na^+(C_6H_6)$ showed that the favoured geometry had C_{6v} symmetry with the Na^+ being on the symmetry axis. A similar geometry is expected for $K^+(C_6H_6)$. For $K^+(C_6H_6)_4$, a tetrahedral complex, with all four benzene molecules facing the ion is likely. Addition of a fifth molecule leads to a very weak interaction. In order to compare the solvation of K^+ by water and benzene, and examine the thermodynamic consistency of the present data with earlier $K^+(OH_2)_n$ measurements the exchange equilibria: $K^+(C_6H_6)_x(H_2O)_y + C_6H_6 = K^+(C_6H_6)_{x+1}(H_2O)_{y-1} + H_2O$ were studied. These results showed that while benzene is favored over water in small clusters, the trend reverses as the size of the clusters increase. The mixed cluster equilibria provide data for the construction of thermodyanamic cycles which show that the equilibrium measurements are thermodynamically consistent. A new fast flow high pressure ion source, used in some of the above experiments, will be briefly described.

TAMP16 ALKALI METAL ION REACTIONS OF ATMOSPHERIC INTEREST, B. R. Rowe, A. A. Viggiano, D. L. Albritton and F. C. Fehsenfeld, Aeronomy Laboratory, NOAA/ERL, Boulder CO 80302

Several association and switching reactions involving clusters of Na^+ and K^+ ions with stratospheric neutral molecules have been examined at 420 K and below in a variable temperature flowing afterglow. From equilibrium constants determined, the bond dissociation energies of the clusters are deduced. For Na^+, in order of increasing stability, these clusters are $Na^+ \cdot N_2$, $Na^+ \cdot CO$, $Na^+ \cdot CO_2$, $Na^+ \cdot HCl$, $Na^+ \cdot SO_2$, $Na^+ \cdot HNO_3$ and $Na^+ \cdot H_2O$. These measurements indicate that sodium compounds, NaX, that react with the $H_3O^+ \cdot nH_2O$ ions in the stratosphere will convert these ioms into the clusters $Na^+ \cdot nH_2O$, thereby supporting the recent assignment[1] of these clusters as some of the ions observed during stratospheric rocket and balloon flights.[2] The results will be reported and the implication of these measurements for atmospheric ion chemistry will be discussed.

1. E. E. Ferguson, Geophys. Res. Lett. 5, 1035 (1978).
2. F. Arnold, H. Bohringer, and G. Henschen, Geophys. Res. Lett. 5, 6531 (1978).

Photoionization Mass Spectrometry of Allene and Propyne

Gleitman, Y. and Lifshitz, Chava

Department of Physical Chemistry, The Hebrew University of Jerusalem, Israel

Ion-molecule reactions were studied in allene and propyne by photoionization mass spectrometry (PIMS). The Hebrew University photoionization mass spectrometer was constructed in a manner similar to that described by Le Breton and coworkers[1]. It was tested by the reaction, $C_2H_4^+$ (C_2H_4,CH_3) $C_3H_5^+$ in ethylene, whose reaction cross section has previously been measured as a function of internal energy of the reactant ion[1].

The ethylene ion reaction, as well as the reaction $C_3H_4^+$ (C_3H_4,H) $C_6H_7^+$ in allene and propyne, proceed via long-lived collision complexes. All three reactions are exothermic. The cross section for the allene reaction decreases with increasing vibrational energy of the ion, in a manner reminiscent of the ethylene system. This seems to be the rule for exothermic reactions proceeding via long-lived collision complexes[2].

There are several ways in which highly excited vibrational levels of the electronic ground state of the ion can be populated. These include: (1) Radiationless transitions from excited electronic states of the ion; (2) Autoionization from Rydberg states, whose ionization limits, are excited electronic states of the ion. Both of these processes populate vibrationally excited states of the $C_2H_4^+$ ion, which lead to a reduced cross section of its ion-molecule reaction. The population of vibrationally excited states of the ethylene ion is demonstrated for photon energies $\geq$ 11.5 eV, in agreement with the increase of the threshold photoelectron cross section at that energy[3].

Direct ionization populates very few vibrational levels in propyne. In allene[4], on the other hand, the Jahn-Teller effect populates levels at photon energies from 9.68 eV to 10.74 eV. This leads to the reduced cross section for the ion-molecule reaction in allene, at increased wavelengths, observed in this study.

The rate coefficients for ions produced from allene and propyne by electron impact ionization are known[5] to be quite different: Propyne - 15.5×10^{-10} cc/molecule·sec; Allene - 5.9×10^{-10} cc/molecule·sec. We believe that this reflects the different degrees of vibrational excitation of the respective parent ions.

The detailed dependence of these ion-molecule reaction cross sections on vibrational, as well as, translational energy is being studied for comparison with theoretical calculations.

REFERENCES

[1]P.R. Le Breton, A.D. Williamson, J.L. Beauchamp and W.T. Huntress, J. Chem. Phys. 62 (1975) 1623.

[2]T.O. Tiernan and C. Lifshitz, The Role of Excited States in Ion-neutral Collisions. The Excited State in Chemical Physics, Vol. II, ed. J. Wm. McGowan, Advances in Chemical Physics, Eds. I. Prigogine and S. Rice, Wiley-Interscience, 1980 in press.

[3]R. Stockbauer and M.G. Inghram, J. Chem. Phys. 62 (1975) 4862.

[4]R.K. Thomas and H. Thompson, Proc. Roy. Soc. A339 (1974) 29.

[5]J.J. Myher and A.G. Harrison, J. Phys. Chem. 72 (1968) 1905.

The NO^+ affinities (NOA) of 28 bases were determined using ion cyclotron resonance (ICR) spectrometry (cf. Table). The NOAs are observed to correlate with the proton affinities (PA) and the first ionization potentials (IP) of the bases for a specific class of compounds. The linearity with IP suggests that bonding to NO^+ is through the highest filled orbital. Exceptions to the correlation with IP ($C_6H_5CF_3$, C_6H_5F and C_6H_5Cl with the alkylbenzenes) are found to correlate better with their second IP suggesting that in these cases the second highest filled orbital is involved with bonding to NO^+.

The photodissociation spectra of the NO^+ complexes were obtained as well. The NO^+ complexes of benzene, toluene and mesitylene have λmax at 327 nm and onsets for dissociation at 580 nm. The NO^+ complex of diethyl ether has a λmax at 300 nm and an onset for dissociation at 450 nm. The NO^+ complex of ethanol has a λmax at ≤240 nm and an onset for dissociation at 440 nm. The NO^+ complexes of ethyl acetate, acetone and 3-pentanone have λmax at ~265 nm and an onset for dissociation at 580 nm. The NO^+ complex of diisopropyl ketone has a λmax at 350 nm and an onset for dissociation at 580 nm. All these spectra exhibit a broad absorption band which is characteristic of charge-transfer complexes. It is evident that the spectra are identical within a class of compounds (the ester and ketones may be similar because NO^+ is bound to the carbonyl in both classes). However, when the site of charge changes from NO (as with 3-pentanone) to the base (as with diisopropyl ketone), the spectrum is altered considerably. Thus the site of charge in the complex may be determined by the photodissociation technique.

Table

NO^+ Affinities, Ionization Potentials and Proton Affinities

BASE	NOA[a]	IP[b]	PA[c]
NO	13.6[d]	9.26	124.9[l]
H_2O	18.5[e]	12.60	176.4
MeOH	36.2[f]	10.84	188.3
EtOH	40.4[f]	10.47	192.5
$C_6H_5CF_3$	~40.4[g]	9.68	178.2[j]
Me CHO	41.14	10.22	191.1
t-BuOH	41.2[f]	~10.1[g]	197.5[k]
i-PrOH	42.6[f]	10.15	195.5[k]
C_6H_5F	43.01	9.20	184.9[e]
EtCHO	43.33	9.96	194.1
C_6H_5Cl	43.74	9.06	185.1[e]
n-PrCHO	44.37	9.80	195.8
$C_6H_5NO_2$	44.53	9.9	197.2[e]
MeOAc	45.02	10.27	201.5
Me_2CO	46.21	9.70	200.0
C_6H_6	46.29	9.24	186.2[e]
C_6H_5CN	46.3	9.70	199.7[e]
Et_2O	46.46	9.51	203.5
EtOAc	46.72	10.10	204.2
n-PrOAc	47.19	10.04	204.7[e]
MeEtCO	47.41	9.51	203.1[l]
Et_2CO	48.12	9.32	204.6[l]
C_6H_5CHO	48.36	9.4[h]	203.7[e]
C_6H_5Me	49.36	8.82	194.8
C_6H_5Et	49.66	8.76	195.7
$(i\text{-}Pr)_2CO$	49.82	8.96	208[m]
i-C_6H_5Pr	50.26	8.59	196.9[n]
n-C_6H_5Pr	50.34	8.72	196.5

References

a) in kcal/mole: data are from this work unless noted otherwise. Relative values are ±0.20 kcal/mole for this work. Absolute values (except for NO, H_2O, MeOH, i-PrOH and t-BuOH) are relative to NOA (EtOH) from ref. f below.

b) in eV: ref. unless noted otherwise: Rosenstock, H. M.; Draki, K.; Steiner, B. W.; Herron, J. T.; J. Phys. Chem. Ref. Data, Suppl. 1, 1977, 6.

c) in kcal/mole based upon $PA(NH_3)$ = 208.4 kcal/mole; ref. unless noted otherwise: Wolf, J. F.; Staley, R. H.; Koppel, I.; Taagepera, M.; McIver, R. T., Jr.; Beauchamp, J. L.; Taft, R. W.; J. Am. Chem. Soc. 1977, 99, 5417-5429.

d) Ng, C.Y.; Tiedemann, P. W.; Mahan, B. H.; Lee, Y. T.; J. Chem. Phys. 1977, 66, 3985-3987.

e) Kebarle, P.; Ann. Rev. Phys. Chem. 1977, 28, 445-476.

f) Corrected for $PA(NH_3)$ = 208.4 kcal/mole : Farid, R.; McMahon, T. B.; Int. J. Mass Spectrom. Ion Phys. 1978, 27, 163-183.

g) Average of two values: 9.97eV and 10.23eV; ref. a above.

h) Rebalais, J. W.; Colton, R. J.; J. Electron Spectrosc. 1972/73, 1, 83-99.

i) Calculated from ΔH_f's (ref. a above) and IP ($DNO^{\cdot}$) = 10.29eV: Kohout, F. C.; Lampe, F. W.; J. Chem. Phys. 1966, 45, 1074-1075.

j) From STO - 3G calculation; corrected for $PA(NH_3)$ = 208.4 kcal/mole: McKelvey, J. M.; Alexandratos, S.; Streitweiser, A., Jr.; Abboud, J.-L. M.; Hehre, W. J.; J. Am. Chem. Soc. 1976, 98, 244-246.

k) Adjusted to agree with PA(EtOH) = 192.5 kcal/mole: Hiraoka, K.; Kebarle, P.; J. Am. Chem. Soc. 1977, 99, 360-366.

l) Beauchamp, J. L.; private communications.

m) This work, estimated from equilibrium measurement with $(i\text{-}Pr)_2O$; $PA((i\text{-}Pr)_2O)$ = 209.1 kcal/mole: Beauchamp, J. L.; private communications.

n) Corrected for $PA(NH_3)$ = 208.4 kcal/mole: Hehre, W. T.; McIver, R. T., Jr.; Pople, J. A.; v. Schleyer, P. R.; J. Am. Chem. Soc. 1974, 96, 7162-7163.

o) Estimated by observation of equilibrium with EtOH through double resonance examination. Interfering reactions prevented exact determination.

SUNLIGHT PHOTODEGRADATION OF PURIFIED POLYBROMINATED BIPHENYL (PBB) CONGENERS STUDIED BY GCMS

D.G. Patterson, L.W. Yert, D.L. Orti, and J.S. Holler
Toxicology Branch, Clinical Chemistry Division, Bureau of Laboratories, Center for Disease Control, Public Health Service, Department of Health and Human Services, Atlanta, Georgia 30333

In 1973 and 1974, a segment of Michigan's population was exposed to grain, meat, dairy, and poultry products that had been contaminated with Firemaster FF-1, a polybrominated biphenyl (PBB) mixture consisting primarily of hexabrominated biphenyl. PBBs have low acute toxicity, but are fat-soluble, biologically persistent, and capable of causing chronic injury to the liver, kidneys, skin, and lymphatic tissue. In addition, PBBs have been found in chronic rat-feeding studies to induce neoplastic liver nodules (1).

PURPOSE

Degradation of PBBs in the environment can occur by metabolic as well as photochemical pathways. We have undertaken the study of PBB photochemistry in order to assess the environmental significance of this nonbiological degradation pathway.

PHOTOLYSIS OF 2,2',3,3',4,4',5,5'-OCTABROMOBIPHENYL (12)

Hexabrominated PBBs Formed in the Photochemical Degradation of PBB-12. PBB-6 (See Figures 4 and 5) appears after approximately 3 hours and persists throughout the experiment. The identification of this PBB is based upon an identical retention time and mass spectrum with PBB-6 in Firemaster. The major hexa PBB at 6.9 min. (See Fig. 5; this peak actually contains two minor and one major hexa PBB) does not correspond to the major hexa PBB-4 in Firemaster (See Fig. 4) as verified by simultaneous injection of authentic PBB-4.

Heptabrominated PBBs Formed in the Photochemical Degradation of PBB-12. The four possible hepta PBBs which could be formed from PBB-12 (barring bromine rearrangement) are depicted in Fig. 1. Figure 5 clearly shows no PBB-9 and preliminary information indicates that the two hepta PBBs at approximately 18 minutes may be 8 and a which would indicate the loss of meta and para bromines in preference to the ortho bromine (firm conclusions must await confirmation).

PHOTOLYSIS OF 2,2',3,4,4',5,5'-HEPTABROMOBIPHENYL (8)

The photodegradation of PBB-8 (390 min. aliquot) is shown in Figure 7 and the results for losses of bromine from various positions in PBB-8 are depicted in Figure 2. The major hexa PBB which is formed, PBB-4, results from loss of a meta bromine in the more highly substituted biphenyl ring.

PHOTOLYSIS OF 2,2',3,3',4,4',5-HEPTABROMOBIPHENYL (9)

The photodegradation of PBB-9 (240 min. aliquot) is shown in Figure 6 and the results for losses of bromine from various positions in PBB-9 are depicted in Figure 3. The formation of PBB-5 indicates that the rate for meta bromine loss is greater than for ortho loss in PBB-9.

CONCLUSIONS

In previous studies of the photolysis of PCBs containing ortho and meta chlorines, the ortho chlorine has been shown to be preferentially lost, while the meta chlorine is preferentially lost in PCBs containing meta and para chlorines. This same order of reactivity ortho > meta > para has been supported by several previous photolysis studies using the Firemaster PBB mixture.

The present photolysis study was conducted with purified hepta and octa PBBs isolated from Firemaster and the results indicate that the order of reactivity does not depend solely on the position of substitution of the halogen on the biphenyl ring, but that other factors (probably both steric and electronic) must be considered in the more highly substituted PBBs.

Previous studies indicate that the toxicity of PBB congeners is related to their ability to produce a 3-methylcholanthrene-type (MC) induction of hepatic microsomal enzymes. A significant result of the present study is the formation of the only known PBB component in Firemaster which has MC-like (2) effects (PBB-6) during the photolysis of both PBB-8 and 12. These two PBBs represent 22% and 1%, respectively, of the Firemaster FF-1 which was involved in the Michigan PBB incident.

(1) Landrigan, P.J., et. al. Annals New York Academy of Sciences 1979, 284-294.
(2) Dannan, G.C., et. al. Biochem. Biophys. Res. Comm., 1978, 85, 450-458.
See also Molecular Basis of Environmental Toxicity, Bhatnagar, R.S., Editor, Ann Arbor Science Publishers, Inc., Ann Arbor, Michigan, 1980, 173-212.

Figure 1. PHOTOLYSIS OF 2,2',3,3',4,4',5,5'-OCTABROMOBIPHENYL (12)

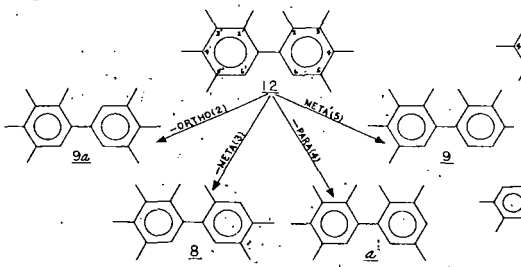

Figure 2. PHOTOLYSIS OF 2,2',3,4,4',5,5'-HEPTABROMOBIPHENYL (8)

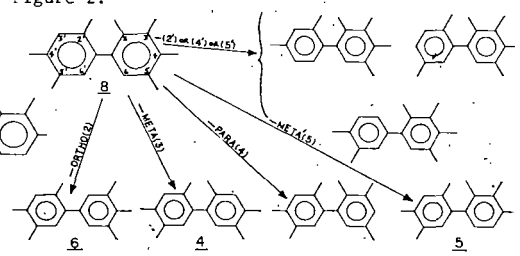

Figure 3. PHOTOLYSIS OF 2,2',3,3',4,4',5-HEPTABROMOBIPHENYL (9)

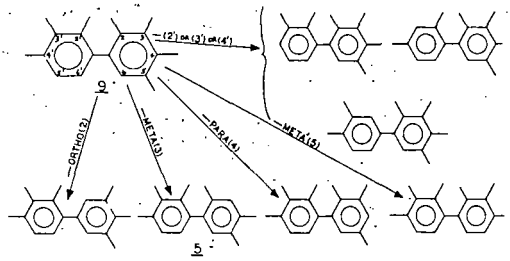

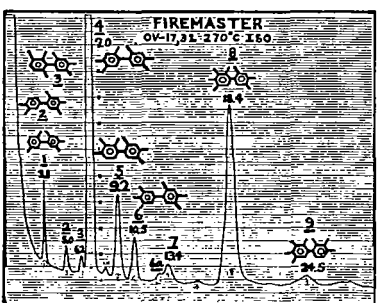

Figure 4. Firemaster FF-1 (for structural determinations, see ref. 2).

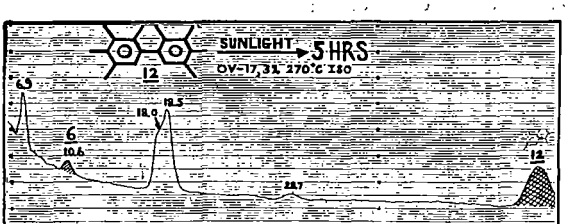

Figure 5. Photolysis of 2,2',3,3',4,4',5,5'-Octabromobiphenyl (12).

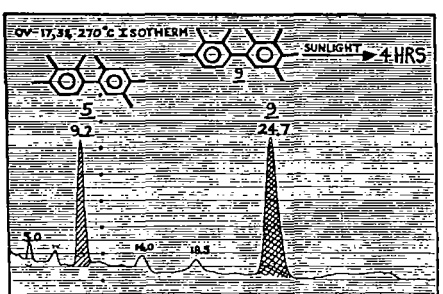

Figure 6. Photolysis of 2,2',3,3',4,4',5-Heptabromobiphenyl (9).

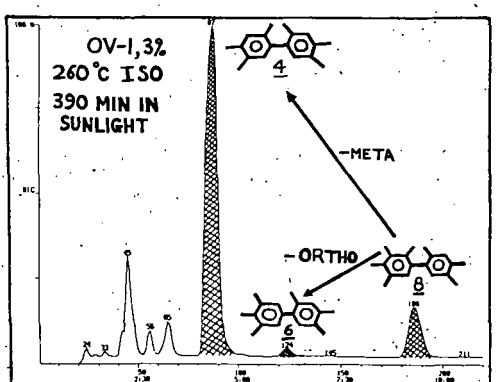

Figure 7. Photolysis of 2,2',3,4,4',5,5'-Heptabromobiphenyl (8).

QUANTITATION OF HALOGENATED ORGANIC COMPOUNDS

C.E. Parker[1], P.W.Albro[1], T.W.Cochran[1], and J.D.Robinson[2]

The analytical chemist is often asked to quantitate many isomers of a given compound class with standards for only a few of these isomers. This paper addresses the question of how accurate such a quantitation is likely to be, and which ions should be monitored to avoid potential interferences. Compounds representing the following classes were studied: polychlorinated biphenyls (PCBs), polychlorinated diphenyl ethers (PCDPEs), and polychlorinated naphthalenes (PCNs). These compounds were selected since they coelute from alumina columns in commonly used fractionation schemes for environmental samples.

Results from quantitation by Gas Chromatography/Electron Impact Mass Spectrometry based on Total Ion Current (TIC) peak areas and Reconstructed Gas Chromatogram peak areas for selected ions were compared with results from Gas Chromatography using a Hydrogen Flame Ionization Detector (HFID).[3] Mixtures of individual standards, synthetic mixtures, and transformer fluids were studied.

The worst interference problems occurred for the quantition of PCNs in the presence of PCBs. For a PCB with four chlorines, the all 37-Cl isotope has the same nominal mass as the all 35-Cl M^+ ion of pentachloronaphthalene. For a pentachlorobiphenyl, the two highest peaks in the molecular ion cluster overlap the two lowest peaks in the molecular ion cluster of a hexachloronaphthalene, and so on. This potential interference is often overlooked. Some of this interference problem can be avoided by the selection of appropriate retention-time "windows", and by the monitoring of higher isotope peaks for the quantitation of PCNs. For the mixtures studied here, quantitation on the $(M+2)^+$ ions for PCNs was sufficient to avoid interference from PCBs, and thus was more accurate than quantitation on the M^+ ions. Retention-time windows were also needed to avoid interference in PCDPE analysis, where intense $(M-2Cl)^+$ peaks from more highly chlorinated PCDPEs interfere with the quantitation of less chlorinated PCDPEs.

Quantitation based on the TIC and $(M+2)^+$ ion peak areas was compared with HFID results for PCBs and PCDPEs. Fairly good agreement among these three methods was obtained. Least squares correlations are shown below:

For PCBs: (TIC) = 1.0515 (HFID) - 0.4886 ; r = 0.9995
(TIC) = 0.8413 (M+2) + 2.1508 ; r = 0.9899
(M+2) = 0.58 (HFID) + 0.45 ; r = 0.9888

The Relative Molar Responses (RMRs) for PCBs, based on 2,4,5,2'5'=1.000, were
(RMR) = 0.132 (# of chlorines) + 0.202 ; r = 0.9956

For the quantitation of PCDPEs:
(TIC) = 0.4952(RMR-corrected HFID) + 11.6565 ; r = 0.7702
(M+2) = 0.6835(RMR-corrected HFID) + 7.3157 ; r = 0.6829

Quantitation was not attempted for PCNs due to lack of pure standards.

Correlations between the TIC, (M+2), and HFID peak areas for a variety of PCB and PCDPE isomers must mean that the portion of the Total Ion Current carried by the molecular ion cluster must be fairly constant within a certain class of compounds. To examine this, a set of 18 PCB standards with from three to eight chlorines was studied. The average Percent of the TIC carried by the molecular ion cluster was 38.2 ± 5.4 %. Similarly, for a set of 8 PCDPEs containing from six to nine chlorines, the Percent of the TIC in the molecular ion cluster was 30.8 ± 7.1 %. For a mixture of PCNs, 9 components containing from four to six chlorines gave a Percent TIC in the molecular ion cluster of 48.0 ± 6.8 %.

TIC peak areas have generally been thought to be the best approximation to HFID peak areas (and to true relative concentrations), since they are expected to show less variation between isomers than would be obtained by monitoring any specific ion. Unfortunately, it is impossible to use TIC peak areas for quantitation in most environmental analyses due to overlapping GC peaks, so quantitation is usually done by monitoring one or more ions in the molecular ion cluster. These results seem to indicate that, since the %TIC in the molecular ion cluster is quite constant, errors introduced by doing quantitation this way and by using one isomer as a standard for another are less than might be expected.

Two methods of perchlorination ($SbCl_5$) and the B M C reagent) were tried on these three classes of compounds, and the results were compared with summing the (M+2) peak areas. The approximate molar percentages of each class could be estimated from the (M+2) peak areas as follows:

PCDPEs x 3.4 ; PCNs x 0.8 ; and PCBs x 1.14

Perchlorination was more accurate for determining the relative molar percentages of PCBs and PCDPEs than was the (M+2) area method, but perchlorination was unsuccessful for PCNs.

---

[1]NIEHS, P.O. Box 12233, Research Triangle Park, NC 27709

[2]VG Data Systems, Tribune Ave., Altrincham, England

The Determination of Hexachlorocyclopentadiene at the ng/L level in Drinking Water by GC/MS.

Frank M. Benoit and David J. Williams, Health and Welfare Canada, Ottawa, Canada, K1A 0L2.

Hexachlorocyclopentadiene (HCCP), a precursor for a number of widely used pesticides, attracted considerable attention when relatively high levels (ppb) were detected in a Louisville Ky sewage treatment plant following the (illegal) dumping of a large quantity of HCCP into the sewage system[1]. This incident lead to the inclusion of HCCP as a priority pollutant in the EPA Consent Decree. However, HCCP has rarely been reported[2] in waters not subjected to point source contamination, as was the case in Louisville. In the course of our studies on the use of XAD-2 macroreticular resin for the extraction of organic contaminants from water, we detected HCCP in numerous drinking water samples but experienced difficulties in estimating the quantities detected. We noted an apparent decrease in the concentration of HCCP in our extracts over the period of a few days. In order to test the stability of HCCP in dilute (ca. 100 ng/L) solutions, aliquots of a HCCP solution in hexane left exposed on the laboratory bench were compared over a period of nine days to aliquots of the same solution that were stored in the dark. The concentration of HCCP in the exposed sample was observed to decrease with time. A plot of ln (HCCP) vs time was found to be linear, indicating a unimolecular decay of HCCP; a half-life of 2.2 days for the decay was calculated. Similar results were obtained when aqueous solutions of HCCP were studied. The decay of HCCP in solution was even more rapid when outside light (99% decay in ca. 8 hours on a cloudy day) or a uv lamp (100% decay in ca. 4 hours) was used as the source of light. No decay of HCCP was observed in solutions stored in the dark, in amber, or in red (low actinic ware)coloured glassware. In all subsequent experiments HCCP solutions were kept in red coloured glassware and exposure of samples to light during the extraction, drying and concentration was minimized.

To measure the efficiency of XAD-2 resin for the extraction of HCCP from water, laboratory tap-water was passed through two XAD-2 cartridges connected in series such that the effluent from cartridge 1 was passed through cartridge 2. It was found that not all the HCCP present in tap-water was retained on cartridge 1 but that from 9 to 27% of the HCCP breaks through to cartridge 2, depending upon the number of times (from 0 to 7) the XAD-2 resin had been used previously. The loss of efficiency with usage of XAD-2 resin was not observed for other non-polar organics studied previously. In an additional experiment, where an XAD-2 cartridge was artifically loaded with HCCP (ca. 80 ng/L) we were able to recover only 58% of the loaded material.

Improved results were obtained by extraction of water samples with an organic solvent. Two solvents were used with similar success, hexane and methylene chloride. Samples of drinking water, which had been previously irradiated with a uv lamp to destroy the HCCP that was present, were loaded with ca 100 ng/L HCCP. We were able to recover from 79 to 88% of the loaded material. When a Florisil column was used to remove extraneous materials from the extracts, there was little effect on the overall recovery.

Samples of Ottawa drinking and raw waters were collected directly from the water treatment plant at various times during the year. This was done to eliminate the possibility that contamination of the water with HCCP could occur in the distribution system. HCCP levels were found in the range 57 to 110 ng/L in the treated waters but were non-detectable in the raw waters. This indicates that the HCCP is introduced during the water treatment process. The HCCP levels were fairly constant over the time period tested.

References

1. D.L. Morse, J.R. Kominsky, C.L. Wisseman and P.J. Landrigan, J. Am. Med. Assoc., 241, 2177 (1979).

2. A.D. Thruston, J. Chromatogr. Sci., 16, 245 (1978).

3. P.W. Albro and C.E. Parker, "General Approach to the Fractionation and Class Determination of Complex Mixtures of Chlorinated Aromatic Compounds", J.Chromatog., in press.

TOWARDS A GENERAL METHOD FOR ESTIMATING THE HEATS FORMATION OF ORGANIC IONS IN THE GAS PHASE, J.L. HOLMES, M. FINGAS and F.P. LOSSING, (University of Ottawa, Ottawa, Ontario, Canada K1N 9B4).

An additivity scheme for calculating the gas phase heats of formation, ΔH_f, of a wide range of organic compounds was published in 1969[1]. A survey of ΔH_f data to the end of 1971[2] for organic ions in the gas phase, shows that ionic heats of formation cannot be reproduced by a simple additivity system using atom and group equivalents. ΔH_f values for ions in an homologous series decrease with increasing ion size, but not monotonically. Since the Data Supplement[2] ca 8000 ionisation energy values have been published, many involving reliable methods such as photoelectron spectra, photoionisation spectra and energy selected electron impact studies. In this presentation it will be demonstrated that ΔH_f for homologous series of odd electron organic ions can be represented to $\pm$ 1 kcal mol^{-1}, by a simple linear equation of the form $\Delta H_f[M]^{+\cdot} = \alpha - \beta \log n$, where α and β are constants and n is the number of atoms in the ion. Such equations hold up to C_8-C_{10} members. The addition of third term, $\Delta H_f[M]^{+\cdot} = \alpha' - \gamma n - \beta' \log n$ permits the extension of the equation to beyond C_{25}. The empirical relationships are consistent with current ideas on ion stabilities, but no theoretical rationale has been developed. The two-term equations have been developed for over thirty homologous series and the effects of chain branching and a variety of substituent effects have been evaluated. These correction terms are in general not the same as those appropriate for the neutral species. Among items which will be illustrated are charge delocalization effects, ring strain energies and the use of graphical cross-relationships to predict the effects of substitution by hetero-atom containing groups.

Even electron ion series obey similar equations although less data are available for such species.

1. S.W. Benson, F.R. Cruickshank, D.M. Golden, G.R. Haugen, H.E. O'Neal, A.S. Rodgers, R. Shaw and R. Walsh, Chem. Rev. 69, 279 (1969).
2. H.M. Rosenstock, K. Draxl, B.W. Steiner and J.T. Herron, J. Phys. Chem. Ref. Data, Suppl. 1, 6 (1977).

ANGLE RESOLVED MASS SPECTROMETRY: A NEW APPROACH TO ION STRUCTURE AND ENERGETICS

R. G. COOKS, P. H. HEMBERGER, J. L. LARAMEE AND A. R. HUBIK
CHEMISTRY DEPARTMENT, PURDUE UNIVERSITY W. LAFAYETTE, IN 47907

When a polyatomic ion (m_1^+) of kilovolt translational energy collides with a target species (N) the ion may be excited internally; if so, it will experience a loss in translational energy and it will be deflected through some angle θ. If there exists a relationship between the scattering angle and the internal energy (Δε) deposited in the projectile, then selection of this angle could be used as a means of selecting ion internal energy. This paper confirms the connection between scattering angle and energy deposition, provides the form of this relationship, and gives examples of applications of angle resolved mass spectrometry.

The experiments were performed on two instruments, a conventional geometry double focusing mass spectrometer (Hitachi RMH-2) modified[1] for collisional and angular selection in the inter-sector region and a reverse geometry (MIKES) instrument in which collisions occur after mass-selection and in which scattering is monitored in a plane orthogonal to that of analysis.[2] The experimental arrangement employed in the MIKES is illustrated in Figure 1 and a comparison is made between the performance of the two instruments in Figure 2. This test employs the Ar^+/Ar collision at 0.4° (lab) with elastic and energy loss peaks being monitored. Product ions generated by collision-induced dissociation (CID) are observed in the momentum spectrum in the RMH-2 and in the kinetic energy spectrum in the MIKES. The latter arrangement provides MIKE spectra which are differential in angle and these are free of the interferences which can occur when collision-induced dissociations are observed in a conventional mass spectrum.

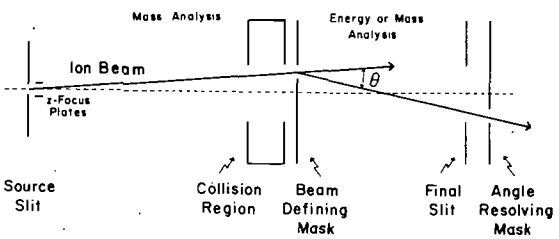

FIGURE 1. Angular Selection in the Non-Focusing Z-Direction Using a Reverse Geometry Mass Spectrometer.

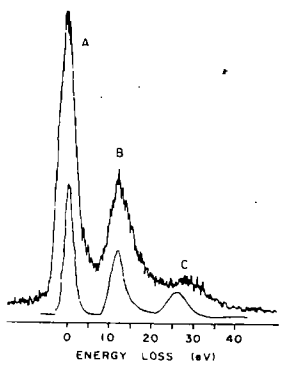

FIGURE 2

FIGURE 2. Ar^+/Ar Energy Loss Spectra Taken With a Conventional (lower) and a Reverse Geometry Mass Spectrometer at 0-4° Scattering Angle.

The correlation between ion internal energy after CID and the scattering angle through which the products are collected is seen when breakdown curves (ion abundances vs. internal energy) are compared[3] to plots of ion abundances vs. scattering angle. Figure 3 shows a typical result. It is convenient to express the internal energy of a dissociating ion in terms of the abundance ratio of two fragment ions. For methanol molecular ion, the ratio of the abundances of the fragments 29^+ and 31^+ increases almost linearly with internal energy from ca. 3·5 to 5·5eV (as deduced from charge exchange data[4]). The form of correlation between $\overline{\Delta\varepsilon}$ and θ can therefore be tested by measuring the abundance ratio $29^+/31^+$ as a function of scattering angle. The result (Figure 4) shows a quadratic dependence of Δε upon θ. The effect of the target gas is simply related to its mass (Figure 5) with light targets being more effective at collisional excitation, in part because of the kinematics in this case.

For coulomb scattering where the interaction potential takes the form $V(r) \propto 1/r$, the energy transfer is proportional[5] to the square of the inverse of the impact parameter, b, i.e. $\Delta\varepsilon \propto 1/b^2$. Then remembering[6] that the impact parameter (b) is related to the scattering angle (θ) and the projectile energy (E) by $b \propto \frac{1}{E\theta}$, we have that $\Delta\varepsilon \propto E^2\theta^2$. The data of Figure 4 show this form of θ dependence. Other results[7] show that the energy deposition

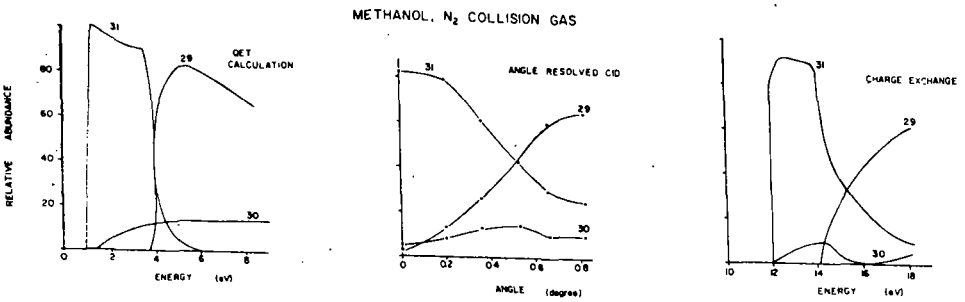

FIGURE 3. Breakdown Curves Obtained Theoretically .. 'by Charge Exchange (ref 4) Compared with Data From Angle Resolution.

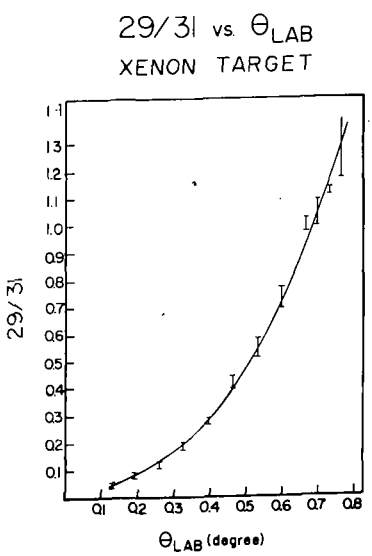

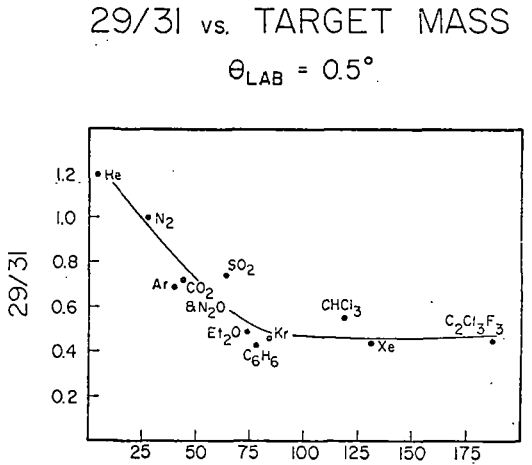

FIGURE 5. Greater Effectiveness of Lower Mass Targets in Exciting Methanol Molecular Ions

FIGURE 4. Fragment Ion Ratio Expressing Energy Deposition in Methanol Molecular Ion as a Function of Scattering Angle.

depends upon the impact parameter and hence upon the projectile energy in the fashion just suggested. Figure 6 shows that a constant energy is deposited in nitromethane when the impact parameter ($1/E\theta$) is maintained constant.

Some applications of angle resolved mass spectrometry can be cited. Figure 7 shows that cyclopropane and propene give only slightly different $C_3H_6^{+\cdot}$ collision-induced dissociations when monitored at 0.7° scattering angle (RMH-2 data). At higher angles differences become more pronounced; Figure 8 shows data for tetrahydrofuran which is believed to give a cyclic ion compared with propene which gives a linear ion.[8] This system was chosen because these ions are indistinguishable[9] in conventional collisional activation (CA) spectra. Processes which are dependent upon internal energy such as hydrogen/deuterium scrambling in ionized diphenylpropane, have also been examined as a function of scattering angle.[10] Dramatic changes in the degree of label incorporation in particular fragment ions are observed. In addition, direct comparisons with field ionization kinetics (FIK)[11] show that angle resolved experiments provide internal energy selection which correspond to life-times approaching 10^{-11}s and up. Data for $CH_3CH{=}CH{-}CH(OH){-}CD_3$ are given in Figure 9.

In summary, this paper has shown some of the factors underlying the relationship between

scattering angle and ionic excitation. The accessibility of high energy ion chemistry by angle resolved measurements has been demonstrated and examples of its application given for ion structural problems which are not amenable to study by conventional forms of collision-induced dissociation.

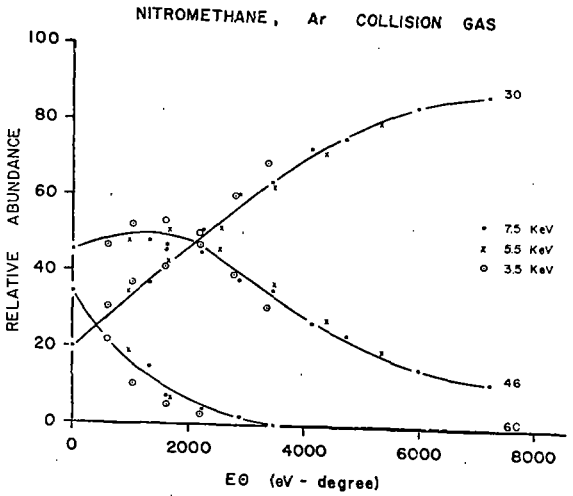

FIGURE 6. Dependence of Energy Deposition Upon Impact Parameter, viz. EΘ.

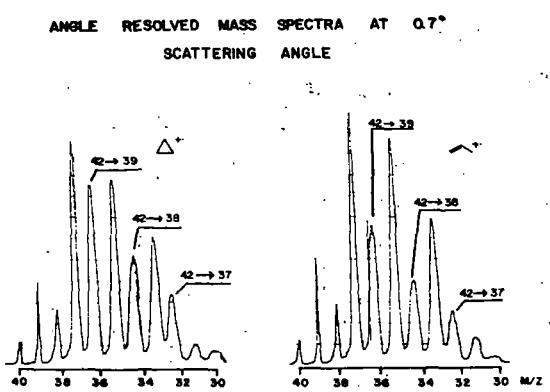

FIGURE 7. Collision-Induced Dissociations Observed at 0.7° in the Mass Spectra of Cyclopropane and Propene.

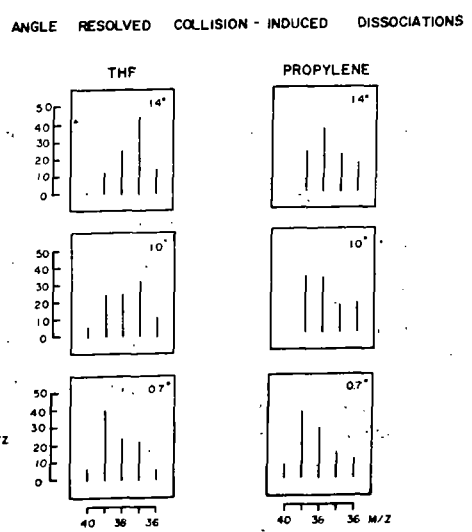

FIGURE 8. Striking Differences in Collision-Induced Dissociations for Isomeric $C_3H_6^{+\cdot}$ Ions at Higher Angles.

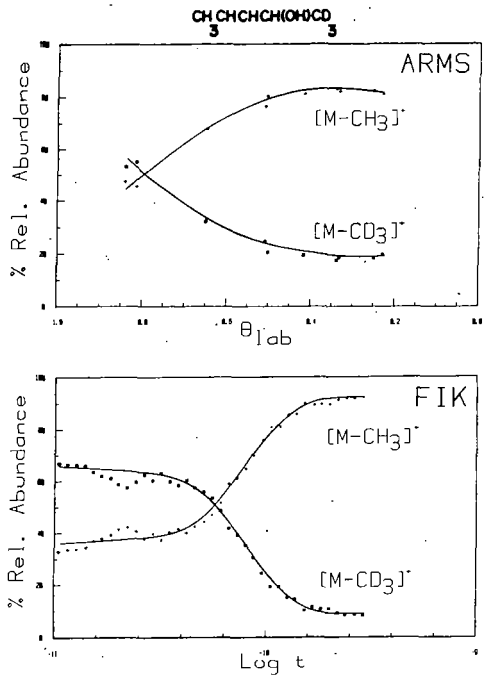

FIGURE 9. Comparison of Dissociations in CH_3-CH=CH-CH(OH)CD_3 Examined by Angle Resolved Mass Spectrometry and Field-Ionization Kinetics.

1. J. A. Laramee, J. J. Carmody and R. G. Cooks, Int. J. Mass Spectrom. Ion Phys., 31, 333 (1979).
2. D. M. Fedor and R. G. Cooks, Anal. Chem., 52, 679 (1980).
3. J. A. Laramee, P. H. Hemberger and R. G. Cooks, J. Amer. Chem. Soc., 101, 6460 (1979). J. A. Laramee, P. H. Hemberger and R. G. Cooks, Int. J. Mass Spectrom. Ion Phys., 33, 231 (1980).
4. P. Wilmenius and E. Lindholm, Ark. Fys., 21, 97 (1962).
5. J. D. Jackson, Classical Electrodynamics (J. Wiley, New York, 1972, p. 619).
6. F. T. Smith, R. P. March, W. Aberth, D. C. Lorents and O. Heinz, Phys. Rev., 161, 31 (1967).
7. A. R. Hubik, P. H. Hemberger, J. A. Laramee, and R. G. Cooks, J. Amer. Chem. Soc., 102, 000 (1980).
8. J. L. Holmes, J. K. Terlouw, P. C. Burgers and R. T. B. Rye, Org. Mass Spectrom., 15, 149 (1980).
9. F. W. McLafferty, T. J. Todd, D. C. McGilvery and M. A. Baldwin, J. Amer. Chem. Soc., 102, 3360 (1980).
10. Unpublished results in collaboration with Professor H.-F. Grutzmacher.
11. Unpublished results in collaboration with Professor N.M.M. Nibbering.

MOLECULAR SPECTROSCOPY OF GAS PHASE MOLECULAR IONS, R. CLAUDE WOODS, Department of Chemistry, University of Wisconsin, Madison, Wisconsin 53706

In the past several years we have been able to develop a technique that for the first time has permitted observation of microwave spectra of free molecular ions. The ions are formed and studied in the plasma of a low pressure DC glow discharge. Three different discharge tubes are available with diameters 4", 6", and 18" and lengths 23', 12', and 14' respectively. Radiation is generated in various parts of the region from 8 to 200 GHz and is typically made monochromatic and stable to one part in 10^8. The source frequency is digitally programmable in increments as fine as 1 kHz by a minicomputer. The microwaves are passed through the discharge tube which serves as the cell for a straightforward absorption spectroscopy experiment. Molecules (including molecular ions) absorb microwave photons and undergo transitions from one rotational state to another at characteristic frequencies that can be measured to eight significant figures. Using quantum mechanics and non-linear statistics these frequencies can lead to very accurate values of molecular structure (angles and distances) and other parameters found in the appropriate model Hamiltonian, e.g., quadrupole coupling constants, electron spin densities at a nucleus, or vibrational perturbations. The resolution of the experiment is intrinsically very high, and the sensitivity has been adequate to see several ions and other transient species. So far we have detected HCO^+, CO^+, and HN_2^+ and also several interesting neutral molecules, including CN, HNC, SiO, and the $a^3\Pi$ metastable state of CO, that are also produced in discharge plasmas. For CO^+ we have improved the precision of the rotational constant by several orders of magnitude relative to the previous optical results. For both HCO^+ and HN_2^+ we have measured six different isotopic forms and determined very good values for the two bond distances. These are the most accurately known molecular structures for any polyatomic ions. Our laboratory observations have confirmed these ions as the carriers of the radioastronomical lines tentatively attributed to them and have made possible astronomical detection of the deuterium forms and other rare isotopes. Studies of microwave relative intensities can reveal rotational and vibrational temperatures in the discharge, and studies of linewidths can lead to velocity distributions or collision cross sections of ions with other gas molecules.

Current research is mainly aimed at extending these microwave measurements to other molecular ions. This is being achieved partly by increasing the total ion density in the discharge, partly by improving the sensitivity of the microwave spectrometer, and partly by the addition of additional diagnostic instrumentation, including a high resolution UV-visible emission spectrometer that monitors photons leaving the discharge tube and a quadrupole mass spectrometer that samples neutral molecules or positive or negative ions leaving the discharge through a pinhole in the wall. The quadrupole mass spectrometer system is operational now and has been interfaced to a laboratory minicomputer. The presence of the mass spectrometer makes it possible now for us to optimize the concentration of a particular desired ion by varying flow rate, gas mixture, pressure discharge current, etc. We can also combine the mass spectral relative ion concentrations with total ion densities (plasma densities) measured by microwave interferometry to obtain approximate absolute ion densities. These can tell us in advance whether or not microwave experiments are practical in a given case. Using these new facilities we hope to be able to obtain microwave spectra of several interesting new ions, including perhaps some negative ions, for which there is presently extremely little spectroscopic or structural data.

STEREOCHEMICAL STRUCTURES OF MOLECULAR IONS DETERMINED THROUGH "COULOMB EXPLOSION" TECHNIQUES WITH FAST (MeV) MOLECULAR-ION BEAMS

Donald S. Gemmell

Physics Division, Argonne National Laboratory, Argonne, IL 60439

In most experimental techniques used to derive the stereochemical structures of molecular ions, the difficulty in obtaining a sufficient column density of the ions to be studied presents a severe limitation. Thus, for example, photon emission or absorption techniques usually involve searching for extremely weak and narrow lines in the presence of background radiation. Where such methods have been successfully applied, they result in very precise structure determinations. However, it has only proved possible to measure a handful of molecular-ion structures with these "standard" techniques (excluding diatomics, only about a dozen molecular ions have so far had their geometrical structures experimentally determined—and these are all triatomic). This situation contrasts strongly with that for neutral molecules for which the experimental problems are much less severe and for which thousands of structures have been determined.

Recent studies on the dissociation of fast (MeV) molecular-ion beams in thin foils suggest a novel alternative approach to the determination of molecular-ion structures. At these high beam velocities (typically a few percent of the speed of light) each dissociating molecular-ion projectile rapidly loses many (sometimes all) of its electrons in sudden violent collisions with electrons in the foil target. The projectile then undergoes a so-called "Coulomb explosion" as the now highly charged and monatomic fragments repel one another apart via their mutual Coulomb forces. These fragments emerge downstream from the foil with their velocities shifted both in magnitude and direction from the beam velocity. Typically the Coulomb explosion results in energy shifts of a few keV and angular shifts of a few mrad for the dissociation fragments. In this paper we describe high-resolution measurements of the joint energy and angle distributions for these fragments. Such measurements (especially when two or more fragments are detected in coincidence) offer promising possibilities for deducing the stereochemical structures of the molecular ions constituting the incident beam.

Figure 1 shows schematically the apparatus used for measurements at Argonne's 4-MV Dynamitron accelerator.[1,2]

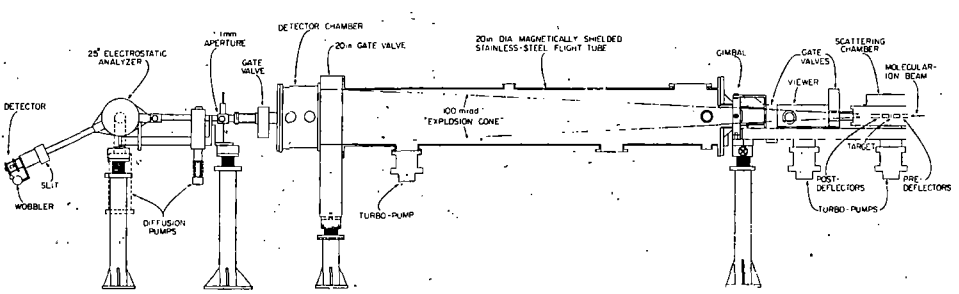

Fig. 1

A typical measurement on a single fragment species from a diatomic projectile (protons from 2-MeV HeH^+ dissociating in an 85-Å carbon foil) is shown in Fig. 2(a) together with [Fig. 2(b)] a computer simulation.[3,4] The peaks in these ring patterns are due to polarization "wake" effects.

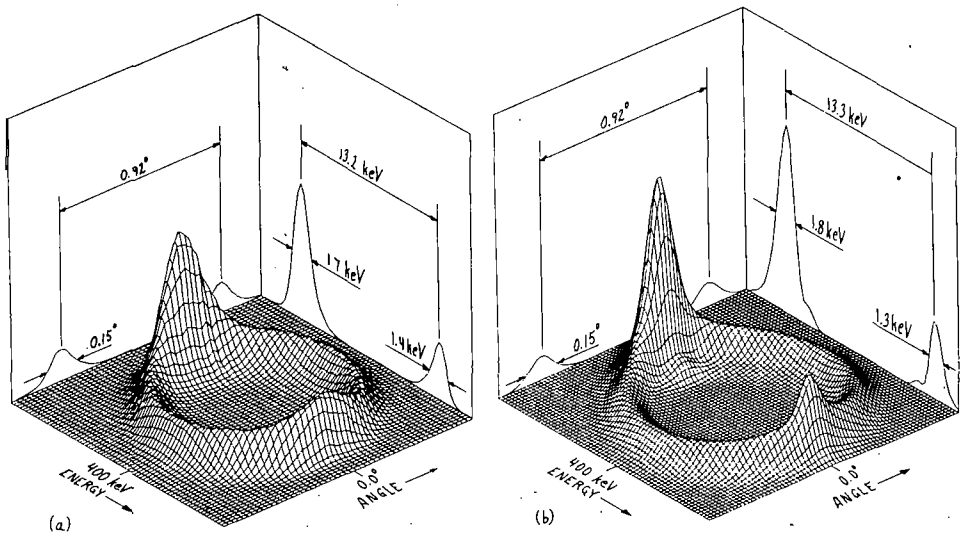

Fig. 2

Measurements of the diameters of such rings and the shapes of the rims have yielded the bond lengths (to about 0.01 Å) and the distribution of internuclear separations for several diatomic molecular-ion projectiles.

For polyatomic projectiles [e.g. H_3^+, CO_2^+, N_2O^+, $C_3H_3^+$, and CH_n^+ (n = 1–4)] measurements on single fragment species reveal the gross structures of the incident molecular ions.[5–8] Figure 3 shows some results for CO_2^+ and N_2O^+ (both linear).

Measurements in which two or more fragments from a given projectile are detected in coincidence offer possibilities for more accurate structure determinations for polyatomic projectiles than do measurements on single fragments. Coincidence measurements have been commenced recently at Argonne[1,8] and Fig. 4 shows some data for 3.6-MeV OH_2^+ dissociating in a 80-Å thick carbon foil. Figure 4 is a plot of the coincidence counting rate in two detectors measuring the protons from OH_2^+ as a function of the angular separation of the detectors.[8]

A preliminary analysis of data of this type yields a bond length of 1.0 ± 0.04 Å and a H-O-H angle of 110 ± 2° for the OH_2^+ ions. This agrees well with the results of optical experiments.[9] Refinements now being implemented in both the experimental and analysis techniques should lead to substantially improved accuracy in this method which is applicable to a wide variety of molecular-ion species.

Alternative but related approaches using imaging techniques are being developed at Brookhaven[10] and at the Weizmann Institute.[11]

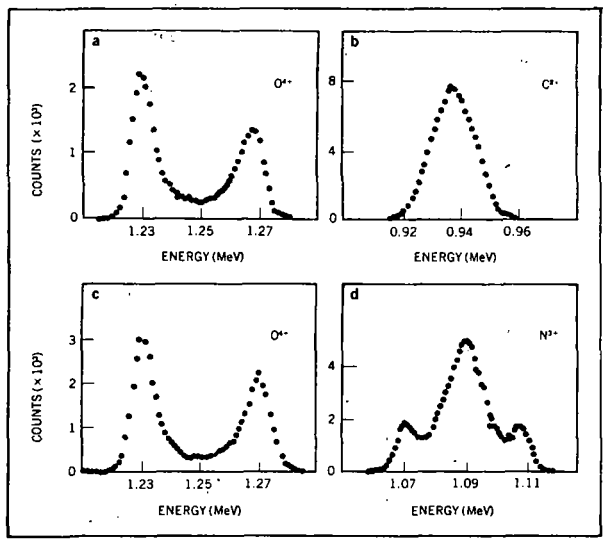

Energy spectra for (top left) O^{4+} and (top right) C^{2+} arising from 3.5-MeV CO_2^+ incident on a 133-Å carbon foil and for (bottom left) O^{4+} and (bottom right) N^{3+} arising from 3.5-MeV N_2O^+ incident on a 160-Å carbon foil. Particles detected are those emerging parallel to incident beam. The left-hand spectra indicate all the O atoms in both CO_2^+ and N_2O^+ are on the "outside" and that the two O atoms in CO_2^+ occupy equivalent positions. Right-bottom spectrum show two non-equivalent positions for the N atoms in N_2O^+, one on the "outside" and one roughly in the center. Right-top spectrum indicates C atom is roughly in the center of CO_2^+. (From reference 6)

Fig. 3

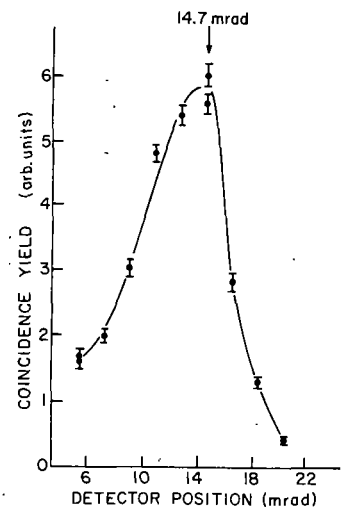

Fig. 4

The work described here has been performed for the most part in collaboration with P. J. Cooney, E. P. Kanter, W. J. Pietsch, I. Plesser and Z. Vager.

This research was conducted under the auspices of the U. S. Department of Energy, Division of Basic Energy Sciences.

References

[1] D. S. Gemmell, Chemical Reviews (to be published).

[2] D. S. Gemmell, Nucl. Instrum. Methods 170, 41 (1980).

[3] Z. Vager and D. S. Gemmell, Phys. Rev. Lett. 37, 1352 (1976).

[4] E. P. Kanter, P. J. Cooney, D. S. Gemmell, K.-O. Groeneveld, W. J. Pietsch, A. J. Ratkowski, Z. Vager and B. J. Zabransky, Phys. Rev. A20, 834 (1979).

[5] J. J. Gaillard, D. S. Gemmell, G. Goldring, I. Levine, W. J. Pietsch, J.-C. Poizat, A. J. Ratkowski, J. Remillieux, Z. Vager and B. J. Zabransky, Phys. Rev. A 17, 1797 (1978).

[6] D. S. Gemmell, E. P. Kanter and W. J. Pietsch, Chem. Phys. Lett. 55, 331 (1978).

[7] D. S. Gemmell, E. P. Kanter and W. J. Pietsch, J. Chem. Phys. 72, 1402 (1980).

[8] D. S. Gemmell, P. J. Cooney, and E. P. Kanter, Nucl. Instrum. Methods 170, 81 (1980).

[9] H. Lew, Can. J. Phys. 54, 2028 (1976).

[10] G. Goldring, Y. Eisen, P. Thieberger and H. E. Wegner, in Proceedings of the Workshop on "Physics with Fast Molecular-Ion Beams", ANL/PHY-79-3, Argonne National Laboratory, 20-21 August 1979, ed. D. S. Gemmell, p. 27.

[11] Z. Vager (private communication).

Spectroscopic Studies of Open-Shell Organic Cations in the Gaseous Phase

John P. MAIER
Physikalisch-chemisches Institut der Universität Basel,
Klingelbergstrasse 80, CH-4056 Basel, Switzerland

The radiative decay of about hundred open-shell organic cations in the lowest excited electronic states has by now been detected. The emission spectra yield vibrational frequencies of several of the totally symmetric fundamentals for the cationic ground states and provide a means of measuring the lifetimes of such cations in the excited state. In the case of a dozen cations an exceptional decay is manifested as the radiative as well as pathways leading to fragment ions are in competition. Both the channels can then be used to probe the relaxation mechanisms.

In order to investigate these open-shell cations in greater depth, three complementary spectroscopic techniques are now being used. High resolution emission spectra can be recorded to obtain rotational structure for the smaller cations using a crossed electron-sample beam apparatus. Vibrational frequencies of the cations in the excited state are being inferred from laser induced excitation spectra. The third approach relies on the detection of coincidences between energy analysed photoelectrons and the emitted photons. This yields the emission quantum yields of the cations, in selected vibrational levels, as well as their cascade free lifetimes. Examples of such studies illustrate how a detailed insight into the structure and decay behaviour of open-shell cations under isolated conditions is achieved.

TPMOB1

QUANTITATIVE ANALYSIS OF DISATURATED LECITHINS IN HUMAN SERUM BY NH_3-CIMS USING A SOLIDS PROBE

A.L. Yergey, M.H. Kody and N.L. Gershfeld

Office of the Scientific Director
National Institute of Child Health and Human Development

and

Laboratory of Physical Biology
National Institute of Arthritis, Metabolism and Digestive Diseases

National Institutes of Health
Bethesda, MD 20205

A quantitative mass spectrometric analysis for lipids has not been published; the existing mass spectrometric methods tend to be qualitative or semi-quantitative.[1,2] Since previous work has shown that disaturated lecithins may be implicated as an independent risk factor in atherosclerosis[3], the need for a quantitative mass spectrometric analysis for these materials, to serve both as a corroborative method for and, ultimately, to expand the present analytical scheme[3], is greatly increased.

The naturally occurring disaturated phosphatidyl cholines (lecithins) of interest contain the 16/16, 16/18, and 18/18 saturated fatty acid residues. Both synthetic and naturally occurring mixtures of these compounds were examined. In addition, the synthetic lecithins 16/17 (used as an internal standard) and 16/15 were used in studies of the mass spectrometric behavior of these materials.

The lecithins were analyzed as their diglyceride acetate derivatives. Triglycerides have been shown to yield $(m + NH_4)^+$ ions under NH_3 chemical ionization conditions.[1] The instrument conditions employed in our analysis of the diglyceride acetated were 1 torr NH_3 and a source temperature of 290°C. Samples were introduced to the mass spectrometer on the solids probe. Ten μl aliquots of the diglyceride acetates in ethyl acetate solution were taken up into a capillary tube that is open at both ends; the open-ended tube prevents bumping of the solvent during evaporation. Solvent was removed at room temperature and a pressure of 50 torr. The capillary tube in the probe tip is heated by conduction. The NIH Isotope Ratio Calculator was used to scan a three amu window of each of the $(m + NH_4)^+$ ions. Ion intensities were converted to digital signals, and intensities accumulated until evolution of the sample was completed. Intensity ratios between a single channel were then calculated and printed.

Standard curves were determined as functions of the concentration relative to the 16/17 internal standard. Each standard curve includes the range of values expected in plasma samples and covers a ten-fold change in the concentration of the specific compound. The standard curves are the family of regression lines of differing slopes that are shown in Table I.

Table I

	15/16	16/16	16/17	16/18	18/18
m	1.74	1.14	1.00	.678	.196
b	.15	.21	--	.02	.02

The slopes are response factors. These response factors, though differing from unity, are independent of concentration, since the standard curves are linear with respect to fixed amounts of the 16/17 internal standard. The wide range of response factors may be due to differences in vapor pressure of the acetates at the source temperature, coupled with differences in concentration gradients between the probe tip and the effective ionizing region of the source. Concomitantly, ions of the slower evolving, higher molecular weight materials would thereby tend to be lost in the instrumental background. The intercepts are appreciably different from zero for the 16/16, 16/18, and 18/18 curves. The most likely

source of this difference for the first two compounds is possible contamination of the internal standard with 16/16 and 17/17 (indistinguishable in mass from 16/18) compounds. Any contamination would be a constant and thus would not affect determination of actual samples. The 18/18 intercept is probably a consequence of low signal intensity due to a low response factor.

Analysis of serum samples is complicated by the fact that the disaturated lecithins represent only 1-3% of total serum lecithins. Large amounts of triglycerides and cholesterol are also present. Extensive clean-up of serum samples as described in reference 3 was necessary prior to analysis. An aliquot of the 16/17 synthetic phosphatidyl choline was added to 200 μl of serum prior to starting the clean-up.

Results from the analysis of two serum samples are given in Table II.

Table II

	16/16 (ng/μl)	16/18 (ng/μl)	18/18 (ng/μl)
C	11.5	5.9	0.74
H	6.5	1.1	0.0

Sample C is from a subject with a history of atherosclerosis, and sample N is from a healthy normal volunteer. Note that the amounts of each disaturated lecithin are greater in sample C than in sample H. The actual amounts of material determined are in accord with GC analyses of these samples.

A quantitative mass spectrometric method for analysis of disaturated lecithins in human serum has been developed. The general approach of this method is most likely applicable to the general problem of quantitation of lipids by mass spectrometry.

References

1. T. Murata and S. Takahashi, Anal. Chem. 49, 728 (1977).
2. N. Nicolaides and J.M.B. Apon, Biomed. Mass. Spectrom. 4, 337 (1977).
3. N.L. Gershfeld, Science 204, 506 (1979).

QUANTIFICATION OF ARABINITOL IN SERUM BY SELECTED ION MONITORING AS DIAGNOSTIC TECHNIQUE IN INVASIVE CANDIDIASIS.

John Roboz, Robert Suzuki, Gail Schulman and James Holland
Dept. Neoplastic Diseases, The Mount Sinai School of Medicine of The City University of New York, New York City, N.Y. 10029

In immunosuppressed patients fungemia is usually not transient. Probably as many as 90% of all invasive Candida infections are not diagnosed early enough to permit effective treatment because there is a lack of rapid and reliable diagnostic tests. D-arabinitol was identified by mass spectrometry as a metabolite of Candida albicans and Candida tropicalis. For quantification serum was deproteinized with acetone, the supernatant was evaporated to dryness, the silyl derivative was formed and an aliquot was injected into a combined gas chromatograph-mass spectrometer system. Erythritol or 2-deoxy-galactitol was the internal standard. The protonated molecular ions, obtained in chemical ionization with isobutane, were monitored. For 39 normal subjects the mean endogenous arabinitol was 0.52 μg/ml (S.D. = ± 0.34). An increment of 0.2 μg/ml arabinitol could be quantified. Of 11 cases with diagnosed invasive candidiasis 9 had arabinitol levels ≫1.2 μg/ml (8 μM) in the range 1.2 - 25.0 μg/ml; the remaining 2 were in the normal range. Six cases of colonized candidiasis gave normal arabinitol levels. The arabinitol levels of one patient with acute myelocytic leukemia have been monitored for 9 months. Arabinitol levels increased from normal to 2.5 μg/ml. Maximum levels coincided with the diagnosis of candidiasis based on liver biopsy cultures. After antifugal therapy arabinitol levels remained relatively high for several weeks followed by a slow decrease to normal. The technique is sufficiently sensitive and specific to justify serial sampling in patients at high risk.

This work was partially supported by Grant No. CA-15936 from the National Cancer Institute, NIH, and the T.J. Martell Memorial Foundation for Leukemia Research.

TPMOB3 GC/MS MEASUREMENT OF ($^{15}N_2$)UREA ENRICHMENT IN PLASMA AS 2-HYDROXYPYRIMIDINE TFA DERIVATIVE-APPLICATION IN QUANTITATIVE ESTIMATION OF UREA PRODUCTION IN HUMANS.

KOU-YI TSERNG, SATISH KALHAN, and PETER ADAM. Dept. of Pediatrics, Case Western Reserve University at Cleveland Metropolitan General Hospital, Cleveland, OH.

Quantification of urea turnover in humans has usually been done by tracer dilution techniques using ($^{15}N_2$)-urea. The plasma or urine ^{15}N-enrichment is then measured with a ratio mass spectrometer after converting urea to nitrogen. Such methods are not only time consuming, but also require large sample size, which may not be feasible for pediatric population.

The use of an organic mass spectrometer to determine the ^{15}N-enrichment of intact urea molecules reduces the sample size requirement. A micro method which utilizes GC/MS and uses only 100 µl of plasma (20 µg urea) has been developed. Urea, after being eluted from ion exchange resins, is reacted with malonaldehyde under acid condition which converts it to 2-hydroxypyrimidine (2-HP). The trifluoroacetate derivative of 2-HP is then prepared and the $^{15}N_2$-enrichment is determined with selected ion monitoring ($^{m}/e$ 125 vs. 123). The low (M + 2) background of $^{m}/e$ 123 ion (0.4%) makes it possible to measure the $^{15}N_2$-enrichment as low as 0.1%. The 2-HP TFA derivative of urea is superior to other described derivatives, such as di-TFA, di-TMS, or barbiturate, in terms of chromatographic and mass spectrometric properties.

Rates of urea turnover have been estimated in pregnant mothers and newborn infants. Data show that urea production rate is attenuated during pregnancy. In addition, newborn infants of diabetic mothers have similar rates of urea production as normal infants.

GAS CHROMATOGTAPHY-MASS SPECTROMETRIC ANALYSIS OF ORGANIC ACIDS IN RAT HEART MUSCLE

Shin-Ichi Haraguchi, Hironori Toshima, °Tomiko Kuhara,
°Toshihiro Shinka and °Isamu Matsumoto

The 3rd Department of Internal Medicine and °Research Institute of
Medical Mass Spectrometry, Kurume University School of Medicine,
Kurume, Fukuoka 830, Japan

Biochemical studies on the heart had been focused on the metabolism of limited compounds. The capability of gas chromatography-mass spectrometry which analyzes many compounds simultaneously, ideally matches to the wide-range survey of the metabolism in the heart. For this purpose, we made a profile of organic acids from the rat heart muscle.

Hearts of 200-250 g rats were excised immediately after decapitation, and successively frozen in dry ice-acetone. The tissues were rinsed with a saline solution to remove the blood in the heart, and then minced with scissors. After 20 ug of heptadecanoic acid per mg protein was added as an internal standard, they were homogenized and deproteinized with cold ethanol. The protein concentration was determined by a Bio-Rad Protein Assay method. Organic acids were extracted from the supernatant with a mixture of diethyl ether and ethyl acetate. After trimethylsilylation, the samples were analyzed by GCMS with a 3% OV-17 column on Gas Chrom Q (80-100 mesh). Oven temperature was programmed at a rate of 6°C/min from 80°C up to 290°C. The temperature of a molecular separator was kept at 290°C and the electron energy was 75 eV. The data were processed with a Chromatopac 4B and a JMA-2000 data acquisition and processing system.

Over 30 peaks were detected on the TIM chromatogram as shown in Fig. 1, and most of them were identified by comparison of their retention time and mass spectra. The quantitative data were statistically treated to obtain the mean value and the standard deviation of each compound. Thus, a standardized profile of organic acids of the healthy rat heart muscle was established.

The detection of palmitate and stearate in large amounts substantiates the concept that fatty acids largely contribute to the great requisition of energy for the pump function. Also, TCA cycle intermediates should increase for the energy supply. However, succinate and malate were detected as relatively small peaks. This can be assumed to have resulted from the lower recovery of these compounds by the extraction method used.

Polyhydroxy acids of 3-deoxypentonate and 3-deoxy-2-C-(hydroxymethyl)pentonate were detected as relatively large peaks. This finding of the existence of polyhydroxy acids in the rat heart muscle is the first report, though a series of straight and branched chain polyhydroxy carboxylic acids had been previously found in the rat and human serum by Kuhara et al. (1), and in the rat brain tissues by Yamada et al. (2).

In order to practically apply the analytical method to the diagnosis of heart diseases, what conditions should be satisfied is the next thing to be examined. It is at least inevitable for the method to be able to detect such an extremely trace amount of samples as are obtainable by biopsy. To examine this point, a gas chromatogram obtained with 5 mg rat heart muscle was compared with that with 100 mg one. The relative peak areas of not all but most of the compounds were the same, but those of polyhydroxy acids were not. The profiles of organic acids in heart muscle 6 min and 30 sec after decapitation were compared in order to investigate the variation with the time course. The both total and individual amount of organic acids remarkably decreased except a few specific compounds. However, under the conditions where the amount of samples and the time after decapitation were kept constant, reproducible profiles could be obtained even with a trace amount of samples. This result indicates that the analytical method is sufficiently applicable to the diagnosis of heart disease. Further studies on the conditions will be continued.

(1) Kuhara, T., Matsumoto, I., Oomura, Y., Sakata., T., Fukushima, M., Tsutsui, K. and Hashimoto, K., Recent Developments in Mass Spectrometry in Biochemistry and Medicine, 6 (1980).
(2) Yamada, S., Kuhara, T., Matsumoto, I. and Inanaga, K., Proc. Jap. Soc. Med. Mass Spectrom., 4, 293 (1979).

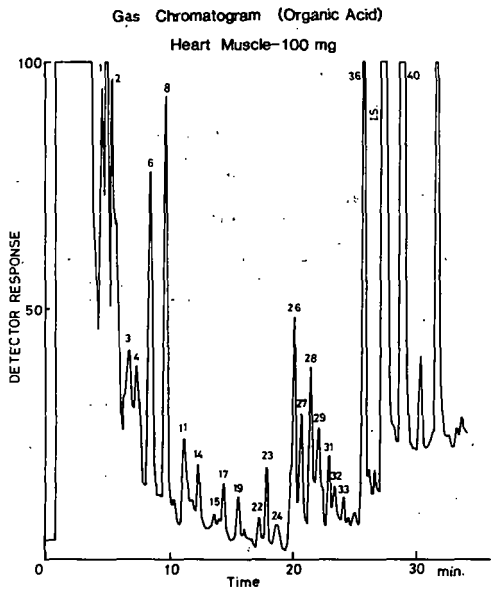

The peaks were identified as follows : 1) LACTIC ACID, 2) GLYCOLIC ACID, 4) 3-HYDROXYPROPIONIC ACID, 11) PHOSPHORIC ACID, 14) FUMARIC ACID + SUCCINIC ACID, 15) 2-DEOXYTETRONIC ACID, 17) 3-DEOXY-2-C-(HYDROXYMETHYL)TETRONO-1,4-LACTONE, 19) MALIC ACID + DIDEOXYPENTONIC ACID, 22) 3-DEOXY-2-C-(HYDROXYMETHYL)TETRONIC ACID, 23) 3-DEOXYPENTONO-1,4-LACTONE, 24) 3-DEOXYPENTONIC ACID, 26) 3-DEOXY-2-C-(HYDROXYMETHYL)PENTONO-1,4-LACTONE, 28) 3-DEOXY-2-C-(HYDROXYMETHYL)-PENTONIC ACID, 36) PALMITIC ACID, 40) STEARIC ACID.

Fig.1

QUANTIFICATION OF 6-HYDROXYMELATONIN BY GC-NEGATIVE CIMS

M. Tetsuo and S. P. Markey

Laboratory of Clinical Science, NIMH
Bethesda, Maryland 20205

The role of the mammalian pineal gland and its hormone, melatonin are not well understood. Extensive studies have been done by measuring the unchanged hormone using bioassay, radioimmunoassay or mass spectrometry. However, rapid metabolism of the free hormone and facile clearance of its metabolite result in low levels (pg/ml) of circulating or urinary melatonin. The instability of melatonin and its low concentrations in biological fluids account for difficulties in obtaining high accuracy and precision in sample collection and assay procedures. Studies on the metabolic fate of melatonin indicate that the hormone is predominantly metabolized by hydroxylation at the 6 position, followed by sulfate and glucuronide conjugation (1). Measurement of urinary conjugated 6-hydroxymelatonin which should be present in 100-1000-fold greater concentration than the free hormone would facilitate analytical assay as well as provide information regarding the integrated production rate of melatonin.

Since the occurrence of endogenous 6-hydroxymelatonin conjugate in human urine by GC-MS was demonstrated in this laboratory (2), this study was initiated to develop a quantitative assay to estimate the rate of melatonin production and changes in this rate during different intervals of the day. Negative CIMS was chosen after testing EI and positive CI and noting a 30-50-fold sensitivity enhancement using electron capture negative CI. The higher nighttime excretion of urinary 6-hydroxymelatonin could be assayed by EI, but low daytime levels require the sensitivity and specificity of negative CIMS in which less interfering chemical background is observed.

The assay utilizes tetradeuterated 6-hydroxymelatonin sulfate as an internal standard added to a 3 ml urine aliquot containing 0.5% ascorbic acid and 0.13% EDTA. Urinary phosphates were precipitated with barium hydroxide and then enzymatic hydrolysis (glusulase) was performed in 0.1 M acetate buffer (pH 4.5) at 37°C for 3 hours. The reaction mixture was washed with hexane and the liberated compounds were extracted with dichloromethane. A stable t-butyldimethylsilyl-pentafluoropropionyl derivative was formed according to the modified procedure of Sisak et al. (2) for assay by negative ion electron capture chemical ionization GC-MS. GC-MS was performed with a Finnigan 1015 chemical ionization analyzer modified for negative ion detection with Extranuclear SpectrEL electronics. GC was performed on a glass column (0.2 cm x 2 m) packed with 3% OV-17 on 100-120 mesh Gas Chrom Q with methane as carrier gas. Column temperature was 230°C, injection 250°C, GC-MS interface 250°C, negative CI ion source 180°C. Selected ion monitoring was performed under computer control with SIRS system (3). Ions at m/z 470 (M-HF) and 450 (M-2HF) for non deuterated and at m/z 473 (M-DF) and 453 (M-HDF_2) for tetradeuterated internal standards were monitored. Standard curves were drawn by plotting the ratio of m/z 450/453 against known amount of 6-hydroxymelatonin and linearity was shown in the working range (0-200 ng/3 ml of water).

In order to assess the method, urine was collected from 7 normal drug free adult male volunteers of average age 35 years (range 21-52). Samples were obtained during 12 sequential six-hour intervals (3 days) under normal conditions of work, activity, diet and sleep. The mean daily urinary conjugated 6-hydroxymelatonin was 15.5 μg (range 6.5 - 22.8 μg). Urine samples at 6 hour intervals clearly demonstrated a 10-fold diurnal variation from 0.8 μg/6 hr during the day to 8.6 μg/6 hr at night. Intraassay variation over 18 hours was 53.8 ng/3 ml urine $\pm$ 2.94 (S.D.) and interassay variation over a two week period was 51.8 ng/3 ml urine $\pm$ 1.08 (S.D.).

This method has been applied to animal urines (monkey, rat, hamster). However, the assay precision for animal urines is sometimes lower because of lower metabolite levels and the different character of interfering compounds. In order to improve the resolution and sensitivity of the method, capillary GC was attempted.

The flexibility and strength of fused silica WCOT columns affords the opportunity to insert the capillary column directly into the ion source, avoiding column inter connections, transfer lines, and dead volumes. The fused silica column is threaded through heated 1/16 in. o.d. stainless transfer lines and a 1/16 in. Swagelok tee connector which is used for CI reactant gas make-up. While simplifying the capillary-ms interface, such a system requires either low volume (high split) or solid injection in order to avoid exposing the ion source to

organic solvents. An all glass solid injector system was tested to permit normal sample volumes (1-5 μl) to be injected with good mass transfer to the capillary and maintenance of high chromatographic resolution. Isothermal and programming modes were tested with the objective of maximizing repetitive sample analysis without sacrificing resolution. Isothermal analyses with retention times of 5 minutes were compared for capillary and packed columns. Although the peak width at half height is 0.1 min on capillary and 0.31 min on packed column, the quantitative results were quite similar for both modes. The promise of higher sensitivity, lower background, and faster analysis with capillary GC has yet to be realized in our system.

References

1. Kopin, I.J., Pare, C.M.B., Axelrod, J., and Weissbach, H. (1961) J. Biol. Chem. 236, 3072-3075.
2. Sisak, M.E., Markey, S.P., Colburn, R.W., Zavadil, A.P., and Kopin, I.J. (1979) Life Sci. 25, 803-806.
3. Barden, L.K., Tate, R.L., Schultz, A.R., and Markey, S.P. (1979) Proceedings of the 27th Annual Meeting on Mass Spectrometry and Allied Topics, Seattle, 233-254.

QUANTITATION OF PHENOLS AND PHENOLIC ACIDS IN UREMIC SERUM USING GAS CHROMATOGRAPHY-MASS SPECTROMETRY

Niwa, T., Ohki, T., Maeda, K., Saito, A. and Kobayashi, K.

Department of Internal Medicine, Nagoya University Branch Hospital, 1-1-4, Daiko-cho, Higashi-ku, Nagoya, Japan.

Summary

A mass fragmentographic method for the determination of phenol, p-cresol, catechol, hydroquinone and 9 phenolic acids in uremic serum was described. Concentrations of phenolic compounds in uremic serum were higher than in normal serum.

Introduction

Many compounds are increased in uremic serum such as urea, creatinine, uric acid, guanidines, aromatic and aliphatic amines, phenols, phenolic acids and indoles. Retention of phenols in uremic serum has been considered to be the cause of uremic symptoms, anemia and impaired coagulation. The authors investigated abnormal metabolites which were accumulated in uremic blood by GC-MS [1,2].

Methods

Blood samples. Serum or plasma samples were obtained from 7 uremic non-hemodialyzed patients, 10 uremic hemodialyzed patients and 10 healthy subjects.

Sample preparation. Serum or plasma was ultrafiltrated using CF 25 Amicon filter. After addition of 10μg of p-ethylphenol and 2μg of 4-chlororesorcinol as internal standards in 100μl of distilled water, 1ml of the ultrafiltrate was acidified to PH 1, saturated with NaCl, and extracted three times with 3ml of ethyl acetate. The extract was dehydrated over anhydrous Na_2SO_4, reduced to 100μl using N_2 stream, and trimethylsilylated with 80μl of BSA and 20μl of TMCS at room temperature for 2 h. Three μl of the sample was subjected to GC-MS. For quantitation of phenolic acids, 1.15μg of p-n-amylbenzoic acid was used as an internal standard. The extract was evaporated and trimethylsilylated at 70°C for 1 h.

GC-MS. The instrument used for combined GC-MS consisted of a gas chromatograph, JGC-20K (JEOL Ltd., Tokyo, Japan), and a mass spectrometer, JMS D-300 (JEOL). For quantitation of phenol (m/z 166) and p-cresol (m/z 165), 5% TXP column (1m x 2mm) was used. The column temperature was programmed from 80°C to 140°C at 4°C/min. For quantitation of catechol (m/z 254) and hydroquinone (m/z 254), 1% OV 101 column (2m x 2mm) was used, and the column temperature was programmed from 150°C to 200°C at 4°C/min. For quantitation of phenolic acids, the column temperature was programmed from 115°C to 170°C at 4°C/min with 1% OV 101 column. Ionizing energy was 22eV. Ionization current was 300μA. Mass fragmentography was carried out with multiple ion detection unit.

Results

Concentrations of 4 phenols and 9 phenolic acids in uremic serum using mass fragmentography are listed in Table 1. It is interesting to note that the concentration of phenol in uremic serum correlated significantly with those of serum creatinine and urea. Three patients with the highest value of phenol in uremic serum had the similar uremic symptoms, the cerebral disorder (coma or lethargy) and the bleeding tendency. Phenol appeared to be responsible for these symptoms. Phenol was confirmed to be present in normal serum at a concentration of 0.86±0.63 μ mole/l by monitoring two ions 166, M^+, and 151, $(M-15)^+$. o-

Table 1. Concentrations of phenolic compounds in uremic serum

	Uremia (μ mole/l) (mean±SD, n=17)	Normal (μ mole/l)
phenol	30 ±38	0.86± 0.63 (mean±SD, n=10)
p-cresol	20 ±33	ND (not detected)
catechol	0.43± 0.72	ND
hydroquinone	0.46± 0.77	ND
m-hydroxybenzoic acid	0.29± 0.31	≦0.14
p-hydroxybenzoic acid	13 ±16	≦0.2
o-hydroxyphenylacetic acid	0.76± 0.60	≦0.072
m-hydroxyphenylacetic acid	0.47± 0.28	≦0.14
p-hydroxyphenylacetic acid	16 ±15	≦0.39
vanillic acid	1.3 ± 1.2	≦0.071
p-hydroxymandelic acid	1.1 ± 0.77	≦0.20
homovanillic acid	1.6 ± 1.1	≦0.14
vanilmandelic acid	2.2 ± 1.9	≦0.16

Cresol and m-cresol were not detected in uremic and normal serum. Concentration of p-cresol in uremic serum did not correlate with those of serum creatinine and urea. The uremic patients with coma showed very low levels of p-cresol in their sera. Concentration of hydroquinone in uremic serum correlated significantly with those of serum creatinine and urea. It seems that the production of phenol and hydroquinone by the intestinal bacterial flora is increased in the uremic patients with coma.

Concentrations of 9 phenolic acids did not significantly correlate with serum creatinine. In some patients concentrations of m-hydroxybenzoic acid, p-hydroxybenzoic acid, and m-hydroxyphenylacetic acid were in the normal range, but concentrations of the other acids were always higher than in normal controls.

References

1. Niwa, T., Ohki, T., Maeda, K., Saito, A., Ohta, K. and Kobayashi, K. (1979) Clin. Chim. Acta 96, 247-254.
2. Niwa, T., Ohki, T., Maeda, K., Saito, A. and Kobayashi, K. (1979) Clin. Chim. Acta 99, 71-83.

PROFILING OF UREMIC ULTRAFILTRATE BY HIGH RESOLUTION GAS CHROMATOGRAPHY-MASS SPECTROMETRY

Niwa, T., Maeda, K., Ohki, T., Saito, A. and Kobayashi, K.

Department of Internal Medicine, Nagoya University Branch Hospital,
1-1-4, Daiko-cho, Higashi-ku, Nagoya, Japan.

Summary

Uremic ultrafiltrate was analyzed by glass capillary column GC-MS. Sample preparation consisted of acidification, extraction, evaporation and trimethylsilylation. Some thirty compounds were identified by EI, CI and high resolution mass spectrometry. Some of these were previously unidentified compounds in the uremic ultrafiltrate.

Introduction

High resolution gas chromatography-mass spectrometry is gaining importance in the clinical chemistry laboratory to separate and identify several hundred components from physiological fluids. In patients with endstage renal failure, many metabolites are retained in the blood, causing various uremic symptoms. The clinical state of the uremic patients can be improved by dialysis of blood to remove toxic metabolites that would be normally excreted by the kidneys. Recently GC-MS has been used to identify such abnormal metabolites [1,2].

Methods

Ultrafiltrate samples. Blood ultrafiltrate (1.5 l) was obtained from 4 uremic patients and 2 patients with psoriasis vulgaris during the hemodialysis treatment using the extracorporeal ultrafiltration method. Although the psoriatic patients had normal renal function, the psoriatic lesion was treated by hemodialysis. Since it was difficult to obtain a large volume of ultrafiltrate from a healthy subject, the psoriatic ultrafiltrate was used as a control to compare with the uremic ultrafiltrate. The hemodialyzer used was polyacrylonitrile, RP-6.

Sample preparation. Two hundred ml of the ultrafiltrate was acidified to PH 1 by addition of HCl, saturated with NaCl, and mixed with 600ml of ethyl acetate. The mixture was shaken for 1 h. As an internal standard 40μg of p-n-amylbenzoic acid was added to the extract. The extract was dried over anhydrous Na_2SO_4, and trimethylsilylated with N,O-bis(trimethylsilyl) acetamide and trimethylchlorosilane. Two μl of the sample was subjected to high resolution gas chromatography-mass spectrometry.

GC-MS. The instrument used for combined GC-MS consisted of a gas chromatograph, JGC-20K (JEOL, Ltd., Tokyo, Japan), a double focussing mass spectrometer, JMS D-300 (JEOL) and a computer system JMA 2000 (JEOL). The gas chromatograph was fitted with OV1 open tubular glass capillary column (30m x 0.25mm). The carrier gas was helium with a flow rate of 0.2ml/min. The split ratio was 30 to 1. The column temperature was programmed from 135°C to 154°C at 1°C/min, from 154°C to 165°C at 2°C/min, and from 165°C to 270°C at 3°C/min. EI mass spectra were recorded under the following conditions: ionizing energy 22eV, ionization current 300μA, separator temperature 270°C, ion source temperature 210°C and accelerating voltage 3KV.

Results

Peak identification in uremic ultrafiltrate. Each component of the profile was identified by EI and CI mass spectra, and high resolution data in conjunction with its gas chromatographic relative retention time (with respect to p-n-amylbenzoic acid). The mass spectra of the

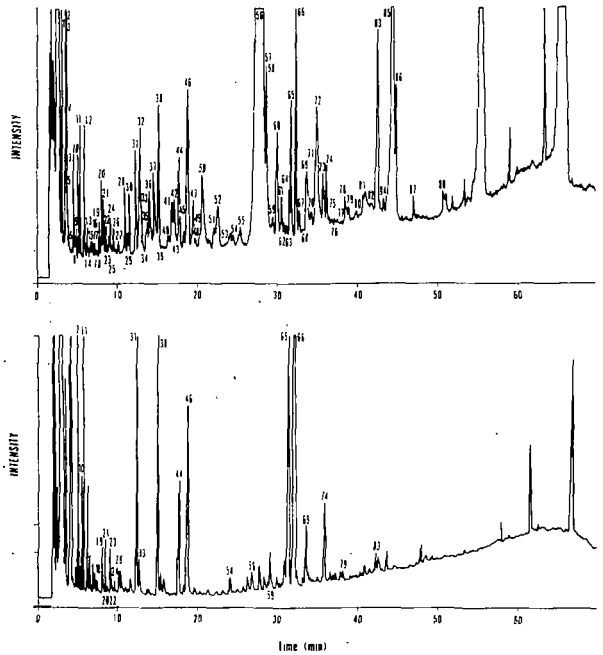

Gas chromatogram of the trimethylsilylated ethyl acetate extract from uremic ultrafiltrate (upper chromatogram) and from psoriatic ultrafiltrate (lower chromatogram)

unknown compounds were compared with published mass spectra and the mass spectra obtained in our laboratory. The peaks are: 7. α-hydroxybutyric acid, 10. β-hydroxybutyric acid, 11. α-hydroxyisovaleric acid, 13. β-hydroxyisovaleric acid, 15. 2-ethylhydracrylic acid, 20. phosphoric acid, 21. glycerol, 23. succinic acid, 26. catechol, 28. 4-deoxyerythronic acid, 29. 4-deoxythreonic acid, 30. resorcinol, 31. xyloisosaccharinolactone, 33. hydroquinone, 37. 3-methylglutaconic acid, 37'. 2-methoxyresorcinol, 38. 2-deoxytetronic acid, 41. 3-methylglutaconic acid, 42. 3-methoxycatechol, 49. 2,4-dimethyladipic acid, 50. 3-methyladipic acid, 50'. methoxyhydroquinone, 52. o-hydroxyphenylacetic acid, 54. threonic acid, 55. m-hydroxyphenylacetic acid, 55'. pimelic acid, 56. p-hydroxyphenylacetic acid, 58. lauric acid, 65. α-isosaccharinolactone, 66. β-isosaccharinolactone, 69. p-n-amylbenzoic acid, 71. vanillic acid, 72. homovanillic acid, 76. azelaic acid, 78. 3,4-dihydroxyphenylacetic acid, 81. dihydroxymethoxybenzoic acid, 81'. vanilmandelic acid. Many previously unidentified compounds in uremic ultrafiltrate were detected in our profile: catechol, resorcinol, hydroquinone, 2-methoxyresorcinol, 3-methoxycatechol, methoxyhydroquinone, 2-ethylhydracrylic acid, 4-deoxyerythronic acid, 4-deoxythreonic acid, 3-methylglutaconic acid, xyloisosaccharinolactone, isosaccharinolactone and 3,4-dihydroxyphenylacetic acid.

References

1. Niwa, T., Ohki, T., Maeda, K., Saito, A., Ohta, K. and Kobayashi, K. (1979) Clin. Chim. Acta 96, 247-254.
2. Niwa, T., Ohki, T., Maeda, K., Saito, A. and Kobayashi, K. (1979) Clin. Chim. Acta 99, 71-83.

GAS CHROMATOGRAPHY/MASS SPECTROMETRIC ANALYSIS OF ORGANIC ACIDS IN AMNIOTIC FLUID AND A COMPARISON WITH THOSE OF UMBILICAL CORD BLOOD AND NEONATAL URINE

K. Mitsutake, T. Shinka, T. Kuhara, I. Matsumoto, °K. Kabashima, °H. Abe, and °T. Kato, Res. Inst. of Medical Mass Spectrom. and °Dept. of Obstet. and Gynec. Kurume Univ. Sch. of Med., Kurume, Fukuoka, 830, Japan

In order to make it possible to diagnose inherited metabolic diseases in the early stage of pregnancy, it is necessary to know how the metabolism of the fetus reflects metabolic profiles of amniotic fluid as a first step. Therefore, we have studied the profiles of organic acids in amniotic fluid for three years. In this report, we compared and investigated the organic acid profiles of amniotic fluid, cord blood, maternal blood, fetal urine and neonatal urine.

Fourteen specimens of amniotic fluid, 5 specimens of maternal blood and 7 specimens of cord blood were obtained at delivery or Ceasarean section at term. Twelve specimens of fetal urine were obtained at first urination after birth and 30 specimens of neonatal urine at 4 days after birth. Sample preparation was performed as follows. Amniotic fluid, cord blood and maternal blood were deproteinized with cold ethanol. Organic acids were extracted with a mixture of diethyl ether and ethyl acetate three times under acidic conditions. The combined extracts were evaporated to dryness under a nitrogen stream and the residue was derivertized with trimethyl-trifluoroacetamide (BSTFA). For the GC/MS analysis, JEOL JMS-D 100 combined with a JMA-2000 data acquisition and processing system was used. A 2 m glass column packed with 3% OV-17 was used for the separation of organic acids. Column temperature was kept at 80°C for 2 min and then programmed from 80°C to 290°C at 6°C/min.

Figure 1 shows a gas chromatogram of organic acids in amniotic fluid. Of more than 46 peaks detected, 25 peaks were identified by comparison of their mass spectra and methylane unit values with reference data. Lactate, glycolate, 2-hydroxybutyrate, phosphate, lactate dimer and palmitate were detected in relatively large peaks. Figure 2 shows a gas chromatogram of organic acids in fetal urine. Compared with that of amniotic fluid, 3 obvious differences were observed. First of all, lactate was less abundant in the fetal urine. Secondly, peak No. 9 on the gas chromatogram of the fetal urine consisted mainly of urea, while that of amniotic fluid was phosphate. Thirdly, peak No. 4 of the fetal urine was found to contain 3-hydroxypropionate, whereas that of the amniotic fluid was found to contain 3-hydroxybutyrate as a major component and 3-hydroxypropionate as a minor one.

Figures 3-5 indicate the percentages of typical compounds as calculated by each peak area to total peak area on gas chromatograms of amniotic fluid, cord blood, maternal blood, fetal urine and neonatal urine. In Figure 3, lactate concentrations in the body fluids were shown. A strikingly high percentage (31.9%) was noted in amniotic fluid and this high concentration indicates that the origin of lactate could not be traced to the fetal urine. On the other hand, lactate concentration in the cord blood was twice as high as that in the maternal blood. These observations are consistent with the finding that the fetal metabolism is under anerobic condition (1). As shown in Figure 4, palmitate concentrations mutually differ. Particularly, it is worthy to note that palmitate concentration in the cord blood was about half of the maternal blood. This indicates that fatty acids in maternal blood are difficult to pass through the placental membrane and that fetus has an independent lipid metabolism (2). Figure 5 shows the concentration of 3-hydroxybutyrate. This compound was detected in amniotic fluid, cord blood and maternal blood, but neither in fetal nor neonatal urine. This indicates that 3-hydroxybutyrate in amniotic fluid did not originate from the fetal urine. Both of the amounts of the amniotic fluid and fetal urine formation per day were estimated at approximately 500 ml (3), but this does not mean that all of the organic acids in the amniotic fluid originated from the fetal urine, since the whole amniotic fluid was completely replaced in every 2.9 hrs.

Quantitatively, the profiles of palmitate, stearate, citrate and glycolate from amniotic fluid were similar to that of fetal urine, whereas those of lactate, 3-hydroxybutyrate and phosphate were similar to that of cord blood. 3,4-Dihydroxybutyrate existed in amniotic fluid, fetal urine and cord blood, but not in maternal blood. A comparison of the metabolic profile of organic acids in amniotic fluid with those of maternal blood, cord blood and fetal urine did not result in finding any close similarities. However, as stated above, it was found that many components had considerable similarities with those of fetal urine and cord blood. Therefore it could be assumed that the organic acid composition of amniotic fluid is related to the fetal metabolism.

(1) Villee, C. A., Pediatrics, 22, 935 (1958).
(2) Nishimura, T., Shusanki-Igaku, 61, 899 (1976).
(3) Abramovich, D. R., Obstet. Gynecol., 54, 15 (1979).

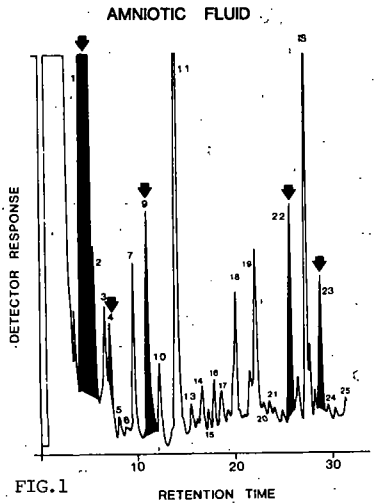

FIG.1

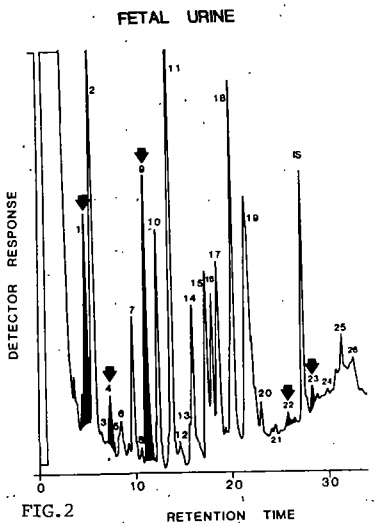

FIG.2

Metabolic profiles of organic acids in amniotic fluid and fetal urine

Fig.1; 1: lactate 4: 3-hydroxybutyrate, 3-hydroxypropionate 9: phosphate, urea 11: 3,4-dihydroxybutyrate, lactate dimer

Fig.2; 1: lactate 4: 3-hydroxypropionate 9: urea 11: 3,4-dihydroxybutyrate

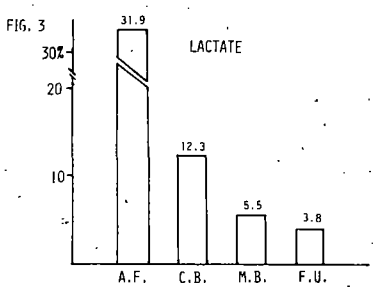

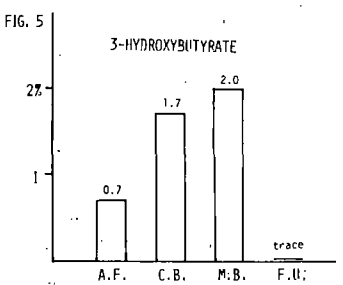

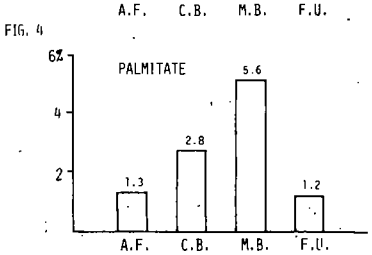

A.F.; amniotic fluid (n=14)
C.B.; cord blood (n=7)
M.B.; maternal blood (n=5)
F.U.; fetal urine (n=12)

Fig.3-5; The quantities of lactate, 3-hydroxybutyrate and palmitate in the body fluids as indicated by percentages of each peak area to total peak area.

OPTIMIZATION OF URINARY MASS PROFILING PROCEDURES TO OBTAIN GREATER RESOLUTION OF DONOR ATTRIBUTES

TPM0B9

W. Aberth, J. Engels, A. Sheets, and E. Blaisdell
Linus Pauling Institute of Science and Medicine, Menlo Park, CA 94025

Techniques for mass profile analysis of urine are being developed in this laboratory with the object of obtaining biomedical information about the sample donors. The profiles are produced by summing a series of repetitive mass scans (1) from a volcano field ion (2) mass spectrometer (3). We have begun work on establishing protocols for sample collection, storage, and analysis to reduce sample deterioration and provide the conditions necessary for optimum information retrieval from the urine profiles.

An experiment on human urine was designed to determine: 1) the degree of time deterioration at room temperature; 2) the effect of pretreating the samples by centrifugation. A fresh urine sample was divided into two halves, one of which was centrifuged 15 minutes at 2400 rpm. Mass profiles were obtained at half-hour intervals from both halves over a period of six hours. Fig. 1 is a cumulative histogram of the probabilities that the slopes of the least squares estimate straight lines of intensities as a function of time are not zero. It shows that a significant change in the mass profile of urine begins to occur very shortly (probably within one hour) after the sample is obtained. Samples that are not immediately stored at a low temperature may lose some informational quality. Fig. 1 also shows that the effect of centrifugation is small.

A second experiment was performed to determine if the cells contained in urine or the organic salt precipitates (which occur after freezing and thawing) contributed substantially to the mass profiles. A single urine specimen was divided into five parts. One part was millipore filtered (0.45 μpore) prior to freezing, one part was millipore filtered after freezing and thawing, one part was millipore filtered both before and after freezing and thawing, one part received no filtration, and one part was passed through the millipore filter syringe without the filter in place. Profiles for each part were obtained in quadruplicate and an analysis of variance of their differences was performed. No significant difference was found between the parts, indicating that the presence of cells and precipitate in urine does not contribute to the mass profile.

Since each mass position in a urine profile is occupied, each peak likely represents more than one compound. Multiple compounds at mass position will tend to reduce the informational quality of the peak amplitude. An additional separation of compounds by volatility can be accomplished by programming the sample probe in temperature steps and obtaining a mass profile for each step. This will increase the number of peaks available for analysis and reduce the number of major compounds comprising each peak. Fig. 2 shows beam intensity as a function of probe temperature and demonstrates the degree that compounds can be separated by volatility. Fig. 3 shows how the amplitude of several mass peaks varies with probe temperature. The peak amplitude is obtained from a spectrum that was summed for 15 minutes while the probe temperature was adjusted to the value shown on the plot. The shape of these curves suggests the presence of two or more compounds.

A further separation of compounds may be achieved by altering the pH of the sample to enhance the volatization of basic, acidic or neutral sample components. Fig. 4 is a plot of several mass peaks as a function of sample pH. The values were adjusted to pH 13 by titration with NaOH and to a lower pH by back titration with H_3PO_4. The profiles were obtained over a 15 minute period as the probe temperature was increased from 100°C to 140°C. The curves in Fig. 4 demonstrate that the volatility of some compounds is strongly a function of the sample pH value.

It thus appears that by obtaining several mass profiles at selected pH and temperature cuts, over 1,000 high quality mass peaks can be produced for pattern recognition purposes. Our future efforts will be directed to utilize these techniques to increase the diagnostic power of our profile analysis.

References

1. Scolnick, M. E., Aberth, W., and Anbar, M., Int. J. Mass Spectrom. Ion Phys. 17, 139 (1975)
2. Aberth, W. and Spindt, C. A., Int. J. Mass Spectrom. Ion Phys. 25, 183 (1977)
3. Aberth, W., 27th Ann. Conf. on Mass Spectrom. Allied Topics, June 3-8, 1979, p. 458

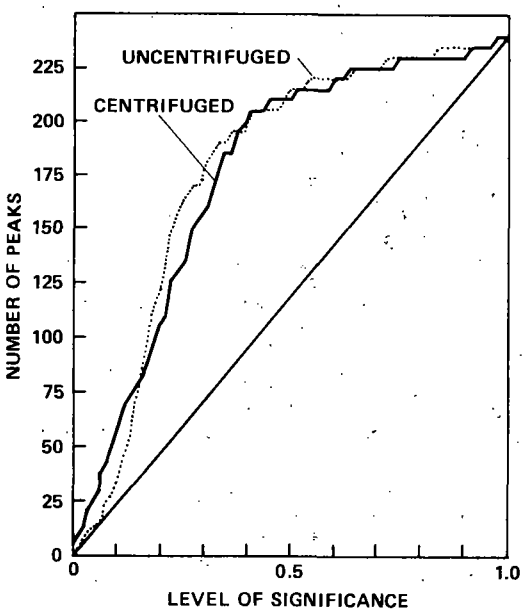

Fig.1. Cumulative histogram indicating a significant change in urine sample over a 6-hour period at room temperature.

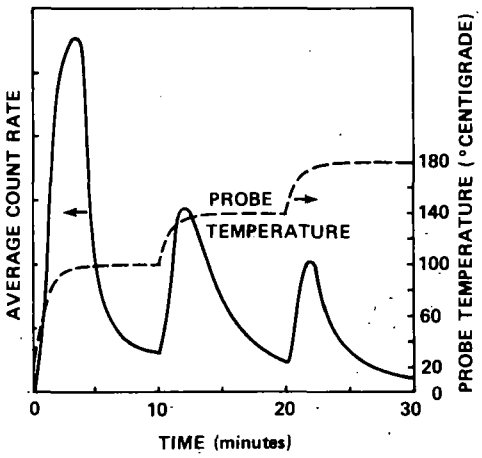

Fig.2. Average ion intensity vs. time with corresponding probe temperature. Sample is .5 µl urine.

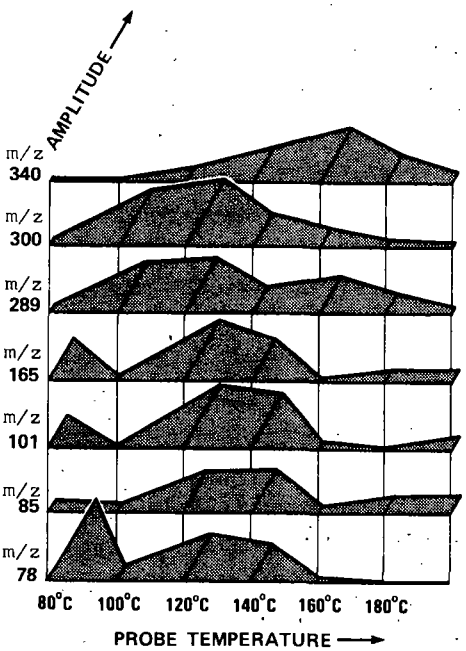

Fig.3. Integrated amplitude of various mass peaks as function of probe temperature. Sample is 1 µl urine.

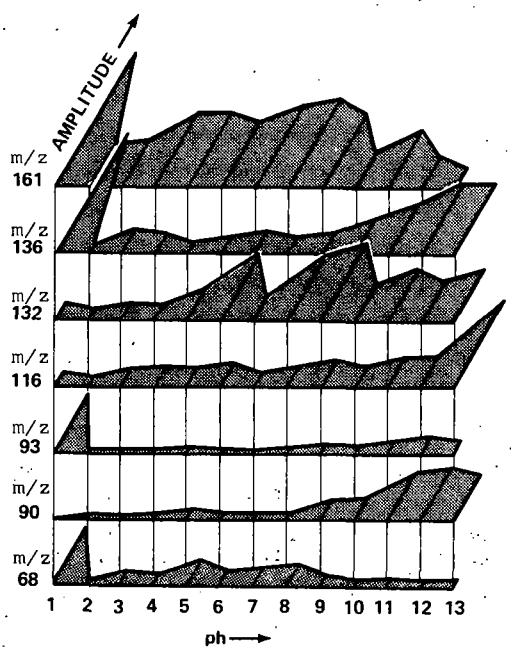

Fig.4. Integrated amplitude of various mass peaks as a function of sample pH. Sample is .5 µl urine.

SELECTED-ION-MONITORING DETECTION OF ACETYLCHOLINE AND CHOLINE CONCENTRATION ALTERATIONS IN CAUDATE NUCLEUS ISOLATED IN SITU

PAT HAUG, MANABU SUZUKI, WOLFGANG WUNN, JUTTA MORITZ, CORDULA NITSCH, ALEKSANDER WAGNER, and ROLF HASSLER Neurobiologische Abteilung, Max-Planck-Institut für Hirnforschung, Deutschordenstraße 46, D6 Frankfurt/M. West Germany

The caudatum is a higher order integrative center. Kittens from which the caudate nucleus has been removed persist in following moving objects, are hyperreactive to auditory stimuli, exhibit learning deficits and an inability to perform two motor acts concurrently (1). It has proven possible to isolate a cylinder of caudate tissue from all afferent and efferent connections while almost preserving the vascular supply to the cylinder from the base of the brain. In the isolated caudate cylinder, only two out of nine types of boutons remain intact (2): type V boutons (interpreted as intrastriatal collaterals of GABA-ergic strio-nigral neurons) and type IX boutons (interpreted as cholinergic terminals of intrinsic neurons). Decreases in the levels of dopamine, 5-hydroxytryptamine, gamma - aminobutyric acid glutamic acid, and aspartic acid in such an isolated cylinder have been taken as additional evidence for the transmitter role of these substances (3). Therefore, an attempt was made to gain further evidence for the intrinsic and extrinsic transmitter role of acetylcholine in the caudatum by using this isolation technique.

Under pentobarbital anesthesia, the parietal cortex was unilaterally removed from adult cats by suction and a cylindrical tube 5 mm in diameter pushed vertically through the caudate nucleus down to the bone. Two and four weeks later the animals were decapitated and the cylinder was removed together with a similar control cylinder taken postmortally from the contralateral side. The cylinders were divided into their dorsal, intermediate and ventral portions, weighed and immediately frozen in liquid nitrogen. Decapitation rather than microwave irradiation was used because no commercial microwave apparatus is available for uniform irradiation of cat or rabbit brain, non-uniformity of radiation has been observed with rats (4), the stress before sacrifice is greater and longer owing to the necessity of positioning the head accurately, discrete brain areas are more easily removed from fresh tissue, an 11% weight loss has been noted (5), and ultrastructural evidence for membrane disruption has been reported (6) as well as spattering of dopamine (5) and GABA (4).

Acetylcholine and choline were extracted using ion pair formation with dipicrylamine and converted to ß-dimethylaminoethyl acetate and propionate (7,8). A Carlo Erba Gas Chromatograph was connected via a single stage jet separator to a Vacuum Generators Micromass 12F mass spectrometer with a Multiple-Ion-Monitor under the control of a Vacuum Generators Data System 2000 including a VT 55 display and two floppy disks. A 200 millisecond/channel dwell time was used to successively monitor the dimethylmethylenimmonium ions at m/z 58, 64, and 60. The 2 m x 2 mm 5% Poly A 135 and 5% OV 101 on Chromosorb WHP 100-120 mesh column was kept at a temperature of 137°C, the injector at 165°C and the helium flow at 15 ml/min. A source temperature of 200°C was used with 70 ev ionizing energy and an emission current of 100 mA.

As can be seen in Figure 1, a significant decrease was found in the concentration of the upper isolated side as compared with the upper non-isolated side two, but not four weeks after operation. This portion would correspond to the head of the striatum where Simke and Saelens (9) found a dramatic decrease in ChAc activity two to four weeks after lesion of the parafascicular nucleus of the thalamus. However, this portion would be expected to have a more severe degree of ischemia than the other two portions owing to interruption of the arteria chorioidea anterior (the choline concentration was reduced in all three isolated portions). Reduction of choline (10), pyruvate or glucose (11,12) has been shown to result in reduced acetylcholine synthesis. Thus, the reduction in the acetylcholine concentration of the upper portion of the isolated caudate cylinder may be due to the decreased availability of its precursors.

The ventral portion of the cylinder shows a significant increase in comparison to the non-isolated side (the intermediate portion was not significant). This may reflect either an accumulation of acetylcholine, which is not used as a transmitter in the inactive intrinsic neurons, or sprouting of cholinergic intrinsic terminals toward sites denervated from their extrinsic connections as occurs in the hippocampus (13).

Preliminary experiments suggest that administration of morphine increases the concentration of acetylcholine in all three portions of the isolated caudate. Morphine increases the overall mouse brain concentration (14), reduces acetylcholine turnover in the cortex, nucleus accumbens, septum and hippocampus, but not in the caudate (15), and blocks the release of acetylcholine which normally follows local electrical stimulation (16).

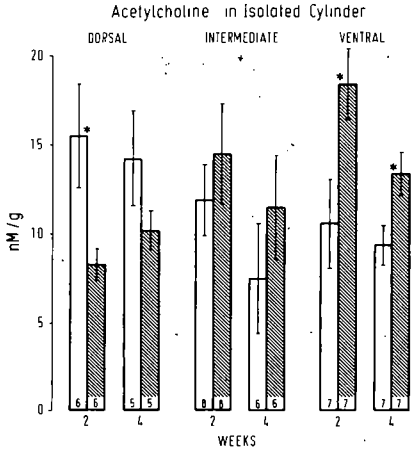

Figure 1:
Acetylcholine in isolated caudate cylinder

non-isolated

isolated

Bars at top of column indicate ± SEM, numbers at bottom of column indicate number of animals, * indicates significance of p ($p < 0.05$)

1. J.R. Villablanca and Ch. E. Olmsted, Apl. Neurophysiol. 43, 88 (1979)
2. R. Hassler, Adv. Neurol. 24, 93 (1979)
3. K. Taniyama, C. Nitsch, A. Wagner, and R. Hassler, Exp. Brain Res. (submitted)
4. C. Nitsch, F. Nitsch, B. Schmude, Y. Okada, unpublished
5. Y. Maruyama and M. Kusaka, Life Sciences, 23, 1603 (1978)
6. N.S. Sharpless and L.L. Brown, Brain Res. 140, 171 (1978)
7. B. Karlèn, G. Lundgren, I. Nordgren, and B. Holmstedt, Choline and Acetylcholine, I. Hanin, ed., Raven Press, New York, 163 (1974)
8. P. Haug, W. Wunn, M. Suzuki, C. Nitsch, and B. Schmude, Proc. ASMS Meeting Abstract 300. New York 1980
9. H.P. Simke and J,K. Saelens, Brain Res. 126, 487 (1979)
10. E.L. Cohen and R.J. Wurtman, Life Sciences, 1095 (1975)
11. P. Lefresne, P. Guyenet and J. Glowinski, J. Neurochem. 20, 1083 (1973)
12. R.S. Jope, M.H. Weiler and D.J. Jenden, J. Neurochem 30, 949 (1978)
13. C. Nitsch, J.K. Kim and C. Shimada, Prog. Brain Res. 51, 193 (1979)
14. K. Hawa, H. Kameto, T. Kakunaga and N. Moriboyashi, Biochemical Pharmacol. 441 (1964)
15. G. Zsilla, G. Racagni, D. L. Cheney and E. Costa, J. Neurochem. 16, 25 (1977)
16. T.L. Yakash and H.I. Yamamura, Brain Res. 83, 520 (1975)

TPMOB11 STUDIES ON THE MECHANISM OF THE ENZYMATIC FORMATION OF GABA AND 2-PYRROLIDINONE FROM DELTA-1 PYRROLINE,

P.S. Callery, L.A. Geelhaar, M. Stogniew and M.S.B. Nayar, Dept. of Medicinal Chem./Pharmacognosy, Univ. of Maryland, Baltimore, MD. 21201

Putrescine is known to be converted to 4-aminobutanoic acid (GABA) and the corresponding lactam, 2-pyrrolidinone, in mammalian liver preparations. The oxidative deamination of product of putrescine formed by reaction with diamine oxidase is Δ^1-pyrroline. As part of a program to study alternate pathways for GABA production, the relationship between the putrescine metabolites Δ^1-pyrroline, GABA, and 2-pyrrolidinone was examined. Δ^1-Pyrroline was incubated at 37°C with 10,000 g supernatant fractions of liver from adult male Dutch rabbits. The two major metabolites were GABA and 2-pyrrolidinone as determined by mass spectrometric assays. Incubations were terminated with trichloroacetic acid and theGABA and 2-pyrrolidinone were separated by cation exchange chromatography. GABA was derivatized with dimethylformamide dimethyl acetal and analyzed by GC-MS using single ion monitoring with the GABA isomer, 3-aminobutanoic acid, as internal standard. 2-Pyrrolidinone was hydrolyzed to GABA and measured as above. Incubation of GABA and 2-Pyrrolidinone showed that the matabolites did not interconvert. Product formation was found to be linear for incubation times up to 25 minutes. The ratio of GABA to 2-pyrrolidinone formed was found to be constant (0.65 ± 0.03) over a wide range of substrate concentations. Appartent K_m values for theproducts were found to be similar which suggests that either GABA and 2-pyrrolidinone are formed from separate enzymes with the same K_m or the more likely possibility that the two products arise from a common intermediate. Acetaldehyde and cyanide inhibited the formation of both products to the same extent. The results of these studies are consistent with the existence of a single soluble enzyme, perhaps xanthine oxidase or aldehyde oxidase, which catalyzes the formation of GABA and 2-pyrrolidinone from Δ^1-pyrroline through a common intermedate, such as a thiohemiacetal.

DISCRETE BRAIN AREA ACETYLCHOLINE CONCENTRATION UNALTERED BY EXPERIMENTALLY INDUCED EPILEPSY

PAT HAUG, WOLFGANG WUNN, MANABU SUZUKI, CORDULA NITSCH, BERND SCHMUDE, and ROLF HASSLER Max-Planck-Institut für Hirnforschung, D6 Frankfurt, W-Germany

Seizures have been induced in rabbits 22-28 minutes after injection of the potent convulsant methoxypyridoxine. As in vitamin B_6 deficiency, glutamate decarboxylase is inhibited so that the concentration of the inhibitory neurotransmitter substance gamma-aminobutyric acid decreases (1). This decrease is significant before the onset of generalized seizures. The intriguing question of whether or not this fall is accompanied by a corresponding fall or compensating increase in acetylcholine has never been answered.

Adult rabbits weighing 2.5 - 3.5 kg were anesthetized with ether. To avoid possible alteration resulting from hypoxidosis, rabbits were artificially ventilated and immobilized. Platinum electrodes were implanted for EEG monitoring. After the animals had recovered, they were intravenously injected with 100 mg/kg methoxypyridoxine. Fourty minutes later (after the second to third generalized seizure) the animals were decapitated together with controls, and tissue samples removed from the caudate, septum, hippocampus, cerebellar cortex, and frontal cortex.

The tissue samples were first extracted with 1 ml 4% perchloric acid containing 1 nM acetylcholine D_9 perchlorate and 5 nM choline D_2 iodide as internal standards. Duplicate 350 ul aliquots were further extracted by adding 1.5 ml of 0.5 M Na_2HPO_4 buffer and 1 ml 2.4 mM dipicrylamine in dichloromethane (2). The water phase was discarded and 1 ml pH 9 carbonate buffer was added. Aliquots of 700 ul (lower organic phase) were then evaporated and free choline propionylated with redistilled propionyl chloride in washed chloroform. After evaporation with N_2, the samples were reacted with sodium benzenethiolate reagent (3) under dry N_2 at 80°C for 45 min. The reagents were removed by washing three times with pentane after adding 10 ul 0.5 M citric acid. The derivatives were forced into the organic phase with 10 ul chloroform and 10 ul ammonium citrate buffer.

Computerized selected-ion-monitoring was carried out on the ß-dimethylaminoethyl acetate and propionate derivatives after their separation by gas chromatography. The Vacuum Generators multiple ion monitor could be run with either magnetic or voltage alternation. Magnetic alternation has the advantage that peak areas are directly proportional to the ion abundance. The purity of the D_6 standard was 95.1% by field desorption (4), 92.9 % by 100 ms magnetic alternation and 92.7% by magnetic scan; the purity of the D_2 standard was 95.3% by field desorption (4), 94.3% by 100 ms magnetic alternation and 92.6% by magnetic scan. The accuracy could be further increased by broadening the chromatographic peak by decreasing the column temperature, lowering the electron energy, and monitoring the molecular ion. Voltage alternation, although the higher mass peaks are defocused and require an external standard for calibration, is more sensitive since no time is lost for magnet stabilization. Some gain in sensitivity was obtained by attention to detail in preparation of GC column (5). The 2 m x 2 mm 5% Poly A 135 and 5% OV 101 on Chromosorb WHP 100-120 mesh column was kept at a temperature of 137°C and a flow rate of 15 ml/min helium. The dimethylmethylenimmonium ions at m/z 58, 64, and 60 were successively monitored using voltage alternation with a dwell time of 200 milliseconds.

From Figure 1, it can be seen that there was no significant difference in the concentration of acetylcholine in the caudate, septum, hippocampus, cerebellar cortex or cerebral cortex. Choline was not altered in any of the regions except for the septum where it increased to 119% ($p < 0.02$). The fact that acetylcholine did not change was surprising since in a preliminary study with freely moving rabbits, an increase was observed 10 min after injection of methoxypridoxine -- unfortunately the effect of the drug on frog rectus muscle was not controlled (6). The GABA receptor antagonist picrotoxin induces an increase in striatal acetylcholine concentration (7,8). Also the

concentration of acetylcholine in the ep mouse, which is particularly sensitive to convulsions, is higher than normal and falls after convulsions are induced (9). More recently, infusion of GABA or GABA-minetic drugs into the striatum has been reported to lead to an increase in acetylcholine concentration (10). To establish the validity of the implication of our results, i.e. that the regulation of acetylcholine content is independent of the GABA system, turnover studies with deuterated acetylcholine were begun. Preliminary results indicate that subsequent to methoxypyridoxine, there is a large increase in the acetylcholine turnover rate in the cortex and a moderate increase in the caudate, septum, hippocampus, and cerebellum.

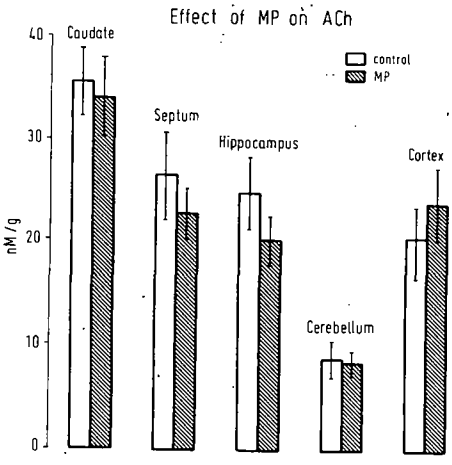

Figure 1: Effect of methoxypyridoxine (MP) on acetylcholine concentration. Bars at top of column indicate SEM; eight animals were used for each determination.

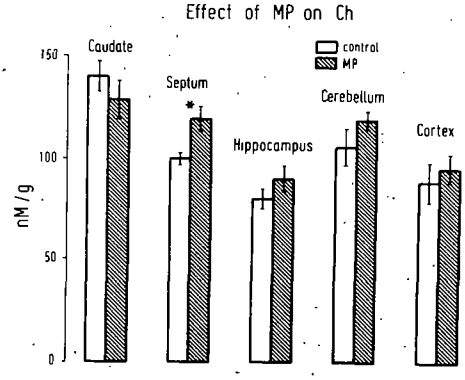

Figure 2: Effect of methoxypyridoxine (MP) on choline concentration. Bars at top of column indicate SEM. Asterisk indicates significance of $p < 0.02$ using the Student's T-test for unpaired variables. Eight animals were used for each determination.

1. C. Nitsch and Y. Okada, Brain Res. 105, 173 (1976)
2. B. Karlén, B. Lundgren, I. Nordgren and B. Holmstedt, Choline and Acetylcholine: Handbook of Chemical Assay Methods, ed. by I. Hanin, p. 163, Raven Press, New York (1974)
3. D.J. Jenden and I. Hanin, Choline and Acetylcholine: Handbook of Chemical Assay Methods, ed by I. Hanin, p. 135, Raven Press, New York (1974)
4. W.D. Lehman, H.R. Schulten, and N. Schröder, Biomed. Mass Spectr. 5, 10, 591 (1978)
5. M. Suzuki, Y. Yamato, and T. Watanabe, J. Agric. Chem. Soc. Jpn. 47, 1 (1973)
6. C. Nitsch, Doctoral Dissertation, Frankfurt (1975)
7. G. Sveneby and E. Roberts, J. Neurochem. 23, 275 (1974)
8. F. Javoy, C. Euvrard, A. Herbet, and J. Glowniski, Brain Res. 126, 383 (1977)
9. M. Kurokawa, H. Naruse, and M. Kato, Prog. in Brain Res. 21A, Correlative Neurosciences Fundamental Mechanisms, ed. by T. Tokizane and J.P. Schadé, pp 112, Elsevier Pub. Co., Amsterdam (1966)
10. B. Scatton and G. Bartholini, Eur. J. Pharmacol. 56, 181 (1979)

Acknowledgements: Thanks are given to Jutta Moritz for the tedious and careful extraction, Merck for the methoxypyridoxine, and the Alexander von Humboldt Stiftung for a stipend (P.H.)

TPMOB13 IDENTIFICATION AND QUANTITATION OF METHOTREXATE (MTX) AND MTX METABOLITES IN ANIMALS AND PATIENTS RECEIVING HIGH-DOSE MTX BY HIGH-PRESSURE LIQUID CHROMATOGRAPHY AND FIELD DESORPTION MASS SPECTROMETRY.

M. PRZYBYLSKI, J. PREISS and J. FISCHER, Institut für Org. Chemie and I. Medizin. Klinik und Poliklinik, Universität Mainz, D-6500 Mainz, West Germany.

Specific and sensitive methods for the identification and quantitation of the anticancer drug MTX and its metabolites have been worked out, using high-pressure liquid chromatography (HPLC) and field desorption mass spectrometry (FD-MS). MTX and the MTX metabolites, 7-hydroxy-MTX, 4-amino-4-deoxy-N(10)methylpteroic acid and 2,4-diamino-6-carboxypteridine were isolated from plasma and urine of rat and monkey at various MTX doses by reverse-phase, ion-paired HPLC on a C18 bondapak column, and rechromatography in a volatile buffer system. Structure identification was obtained by the abundant molecular ions and partially by characteristic fragments in their FD mass spectra. Both the HPLC assay and FD-MS were used to determine concomitantly MTX and 7-hydroxy-MTX levels in plasma and urine of patients receiving high-dose MTX therapy. Preparation of plasma samples for HPLC was carried out by diafiltration, while only little purification with a short C18-cartridge was required for FD-selected ion monitoring of molecular ions, using MTX-monoalkyl esters as internal standards. First pharmacokinetic data obtained from three patients with osteosarcoma receiving high-dose MTX/leucovorin rescue showed prolonged 7-hydroxy-MTX plasma levels compared to MTX, and indicate the utility of specifically monitoring MTX and MTX metabolite levels.

SIMS USING A CEC-110 ANALYZER

R. J. Colton, J. E. Campana, T. M. Barlak,
J. J. DeCorpo and J. R. Wyatt

Code 6110
Chemistry Division
Naval Research Laboratory
Washington, D. C. 20375

Secondary ion mass spectrometry (SIMS) currently finds broad application in fundamental and applied surface science with unrealized research potential in chemistry, physics and the biological sciences. Experimental and theoretical studies of ion-surface interaction and secondary-ion emission mechanisms are the subject of current and much needed future research. The validity of such experimental studies depends on mass analysis of secondary ions without energy and mass discrimination or a method to correct for such instrumental artifacts.

Molecular SIMS instrumentation most frequently employs the quadrupole mass filter (QMF) for mass analysis. The QMF is chosen for this application because of its compactness; its rapid mass-scan rate capability; and its ability to operate at or near ground potential, permitting the secondary ion source to be operated at low potentials.

The disadvantages of the QMF are severe energy and mass discrimination; furthermore, these problems are exacerbated in SIMS because the kinetic energy distribution of the secondary ions formed in the SIMS methodology is inherently wide compared to the energy bandwidth of the QMF. Therefore, quadrupole SIMS instruments employ an energy prefilter which decreases the overall ion transmission. Our experience with such quadrupole instrumentation is that the ion transmission and mass resolution of the QMF as a function of mass is extremely dependent on the applied voltages of the energy prefilter and the ion optics between the prefilter and the QMF.

Standard reference compounds for ion abundance calibration do not currently exist in SIMS as they do in organic mass spectrometry, making relative ion abundance measurements virtually impossible. Previous work with quadrupole SIMS instrumentation in our laboratory characterized organic species deposited on silver. The $[Ag]^+$, $[MH]^+$, and $[AgM]^+$ species (M is an intact organic species) were found to vary significantly in relative intensity as a function of the QMF electronics control settings and applied voltages of the pre-quadrupole optics. This exemplifies the severity of mass discrimination in the QMF and the need for suitable reference compounds in quadrupole SIMS.

A new SIMS instrument has been constructed using a double-focusing mass analyzer in order to overcome the aforementioned limitations of quadrupole SIMS instrumentation. This new instrument has been characterized by studying a variety of samples in both the static and dynamic SIMS modes. The instrument has been found to have high transmission and excellent high-mass performance. A paper discussing this work has been submitted to the Review of Scientific Instruments.

ANALYTICAL APPLICATIONS OF MOLECULAR SIMS

S. E. UNGER, R. J. DAY, T. M. RYAN, L. LIU, K. L. BUSCH, AND R. G. COOKS
CHEMISTRY DEPARTMENT, PURDUE UNIVERSITY W. LAFAYETTE, IN 47907

Molecular secondary ion mass spectrometry (SIMS) provides the surface sensitivity of Auger electron spectrometry or ion scattering spectrometry with the ionization capabilities of field or plasma desorption mass spectrometry.[1] Micromonolayer molecular sensitivity has been demonstrated for certain organic salts where detection limits of 10 pg/cm^2 have been obtained.[2] SIMS spectra of nonvolatile, thermally-labile compounds such as choline esters show large intensities of the intact cations and characteristic fragment ions.[3] These quaternary ammonium salts may be separated chromatographically and ionized from paper or directly from plant tissue. Other organic salts such as arsonium, sulfonium, and stable carbonium salts yield intact cations. For example, Figure 1 shows the positive ion SIMS spectrum of tropylium chloride. Some diquaternaries provide intact dications in this method of ionization (Figure 2).

The ionization of nonvolatile compounds by SIMS is greatly extended by the use of ammonium chloride mixed into the sample matrix. The positive SIMS spectrum of the pure quaternary salt carnitine HCl shows extensive intermolecular methylation, yielding the methyl ester ion at m/z 174 (Figure 3a). Mitigation of methylation of the salt by the addition of ammonium chloride to the matrix is seen in Figure 3b. Several nucleosides and the disaccharide sucrose, as well as many inorganic complexes have previously not shown molecular or pseudo-molecular ions in SIMS. Addition of ammonium chloride diluent to the Mo dimer complex shown in Figure 4 resulted in an intact molecular ion. Similarly, sucrose exhibits a large cationized species , $(Ag+M)^+$, under ion bombardment when mixed with ammonium chloride (Figure 5). The spectrum also shows fragment ions which are characteristic of the sucrose structure.

In the positive ion SIMS spectrum, molecular information is present from $M^{+\cdot}$, $(M+H)^+$, and $(C+M)^+$ species.[4] Formation of metal and organic adduct ions, $(C+M)^+$, is general for both the organic and the metal[5], however, specific organic compounds such as Cu-selective 2,9-dimethylphenanthroline introduce selectivity into the process.[6] The cationization process is also observed in SIMS spectra of metals exposed to organic vapors. Figure 6 shows the formation of $(Pt+M)^+$ ions in SIMS for Pt foil exposed to thiophene, M. Such adduct ions may be of fundamental importance in the study of active surfaces such as catalysts.

The complexity of the positive SIMS spectra versus the relative simplicity of the negative SIMS spectra is related to the relative efficiency of cationization, $(C+M)^+$, in the positive ion spectra to the analogous process anionization, $(A+M)^-$, in the negative ion spectra. Negative SIMS spectra are, therefore, generally simplier than their positive ion counterpart, exhibiting large intensities of $(M-H)^-$ for organic acids and $M^{-\cdot}$ for less acidic compounds such as phenols. The negative SIMS spectra of various substituted benzoic acids are similar to MIKE spectra of selected $(M-H)^-$ ions generated by N_2O/CH_4 negative chemical ionization.

1. A. Benninghoven, W. Sichtermann, Org. Mass Spectrom., 12, 595 (1977).
2. S. E. Unger, T. M. Ryan, and R. G. Cooks, Anal. Chim. Acta., in press.
3. R. J. Day, S. E. Unger, and R. G. Cooks, J. Amer. Chem. Soc., 101, 501 (1979).
4. R. J. Day, S. E. Unger, and R. G. Cooks, Anal. Chem., 52, 557A (1980).
5. R. J. Day, S. E. Unger, and R. G. Cooks, Anal. Chem., 52, 353 (1980).
6. R. J. Day, S. E. Unger, and R. G. Cooks, J. Amer. Chem. Soc., 101, 499 (1979).

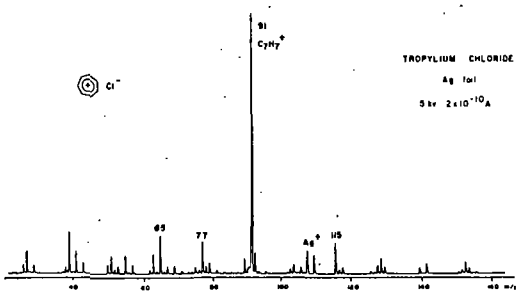

FIGURE 1

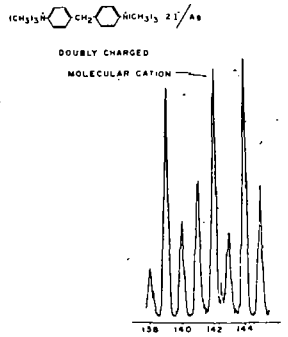

FIGURE 2

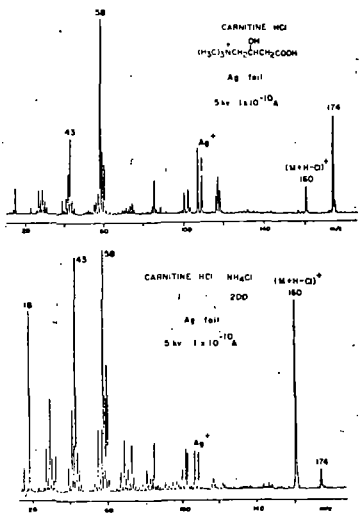

FIGURE 3

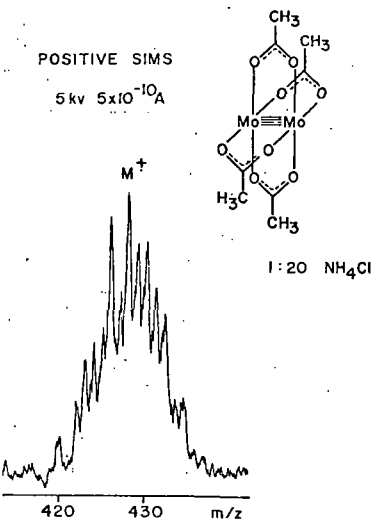

FIGURE 4

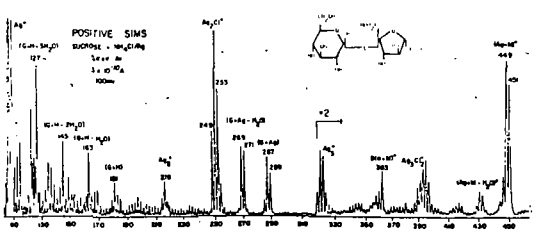

FIGURE 5

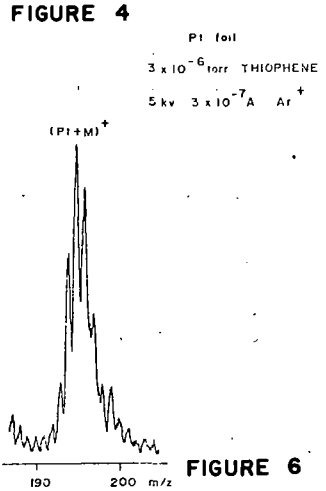

FIGURE 6

STATIC SIMS WITH KINETIC ENERGY ANALYSIS

M. J. Vasile
Bell Laboratories
Murray Hill, New Jersey 07974

Secondary ions ejected from copper surfaces have been energy and mass analyzed with a unique instrument employing a resistive disk energy filter and a quadrupole mass filter. The primary ion beam was generated in a differentially pumped chamber by electron impact ionization of argon, and the kinetic energy and current densities employed (o.5 kV to 3kV; $1x10^{-9}$ A/cm^2 - $1x10^{-8}$ A/cm^2) are in the static SIMS range. Results typical of this instrument are as follows: Secondary ion signals of the order of $3x10^4$ cps on the $^{63}Cu^+$ ion were obtained at the maximum in the kinetic energy distributions which occurred between 10 and 12 eV (primary ion current density = $8x10^{-9}$ A/cm^2). The halfwidths of the Cu^+ kinetic energy distributions were of the order of 14eV and the signals persisted to kinetic energies in excess of 70 eV. The kinetic energy distribution maxima and halfwidths showed very little dependence upon primary ion kinetic energy from 0.5 kV to 3kV. The high energy segment of these distributions exhibited a $1/E^n$dependence, with n=4 for 0.5 kV, n=3 for 1 kV and 1.5 kV, and n=2.5 for 2, 2.5 and 3 kV.

A variety of surface treatments produced molecular ions, some of which were quite unexpected. Plasma oxidation of an hydrocarbon film on the Cu foil surface yeilded a very intense $CuOH^+$ secondary ion, as well as Cu_2^+, Cu_2H^+, Cu_2O^+, Cu_2OH^+, and Cu_3^+ at much lower signal levels. Thermal desorption of acetic acid from a single crystal copper surface also yielded a $CuOH^+$ secondary ion, with intensity comparable to the Cu^+ ion. The kinetic energy distribution of the Cu_2^+ ion was found to be 2eV narrower than that of Cu^+, and its maximum was shifted to lower energies. The $CuOH^+$ kinetic energy distribution lacked a high energy tail and had a 6 eV halfwidth, typical of most molcular ions.

Exposure of the single crystal copper surface to 10^6 L oxygen at 250^oC produced an intensification of the Cu^+, ion, and the molecular species Cu_2^+, Cu_2O^+, $Cu_2O_2^+$, Cu_3^+, Cu_3O^+ and $Cu_3O_2^+$. The oxide species CuO^+ was lacking in the positive ion spectrum. The surface oxide film formed under these conditions is believed to be Cu_2O, and the kinetic energy distributions of the Cu^+ and Cu_2^+ were almost indistinguishable, which suggests that the Cu^+ ion is originating from a restructured surface.

ION MICROPROBE AND ION MICROSCOPE ANALYSIS OF PARTICULATES

D.S. Simons and D.E. Newbury
Center for Analytical Chemistry
National Bureau of Standards
Washington, D.C. 20234

An ion microprobe can be used to obtain trace elemental and isotopic information from individual particles with dimensions greater than about one micrometer. Conventionally this type of analysis has been restricted to instruments with primary beam diameters of less than ten micrometers. An ion microscope instrument with a primary beam diameter of hundreds of micrometers also has the capability of analyzing individual particles by using an aperture at an image plane to restrict the analysis area. We have compared these two types of instruments in three different types of particle analyses-ion imaging of a particle field, elemental analysis, and isotopic analysis. The two instruments used in this study were the ARL Ion Microprobe Mass Analyzer located at NBS and the CAMECA IMS-3F Ion Microanalyzer located at Charles Evans and Associates, San Mateo, CA.* Samples used were microchips and microspheres in a size range of 1 to 20 micrometers made from homogeneous research glasses. Glass K227 is a lead silicate and K378 is a 5 component glass containing sodium, silicon, zinc, barium, and uranium. The uranium concentration in K378 is 0.2 atom percent, and it has a natural isotopic composition.

Ion images of a field of K378 particles were taken with each instrument. All of the elements could be detected in the image where a particle was present using either instrument. The image acquisition time of the ion microscope was about 30 times faster than that of the ion microprobe for the same field size. This is expected because the ion microscope collects the entire image simultaneously while the primary beam of the ion microprobe must be scanned, resulting in a much lower average current density. The spatial resolution and image quality of the ion microscope was also noticeably better.

The intensities of the Pb and Si ion signals from individual microspheres of K227 glass were measured to assess the inter-particle precision of the Pb/Si ion ratio. The data are summarized in Table I. The precision of the ion microscope is somewhat better. A plausible explanation is the computer-controlled mass tuning of the CAMECA, compared with the manual operation of peak selection on the ARL instrument at NBS.

Isotope ratios were measured for lead in K227 and uranium in K378 particles. These results are summarized in Tables II and III. For the lead measurements the ion microprobe has a better inter-particle precision and a smaller mass bias. For the uranium both instruments do surprisingly well, considering that the 235 isotope has a concentration of only 14 ppm atomic in the glass. The ARL IMMA has an inherent advantage in isotope ratio measurements because it has the capability of rapid electrostatic switching between isotopes, while the CAMECA employs slower magnetic switching.

In summary, both the ion microprobe and the ion microscope have demonstrated that they are capable of performing ion imaging and precise elemental and isotopic analyses of individual particles with micrometer dimensions.

*Certain commercial instruments are identified in this paper in order to adequately specify the experimental procedure. In no case does such identification imply recommendation or endorsement by the National Bureau of Standards, nor does it imply that the equipment identified is necessarily the best available for the purpose.

K227 MICROSPHERES
PB/SI RELATIVE SENSITIVITY

	Ion Microprobe	Ion Microscope
No. of Particles	10	5
S_{PB}/S_{SI}	2.13	3.44
R.S.D. (%)	16	7

TABLE I

K227 MICROSPHERES
PB ISOTOPE RATIOS

	Ion Microprobe	Ion Microscope	Natural Lead
No. of Particles	10	6	
206/208	0.461	0.511	0.461
R.S.D. (%)	0.6	3.4	
207/208	0.412	0.451	0.422
R.S.D. (%)	0.2	3.7	

TABLE II

K378 MICROCHIPS
URANIUM ISOTOPE RATIOS

	Ion Microprobe	Ion Microscope	Natural Uranium
No. of Particles	10	2	
235/238	0.00731	0.00734	0.00725
R.S.D. (%)	2.4	0.4	

TABLE III

TPMOC5 A SSMS NEAR SURFACE ANALYSIS OF B IN IRRADIATED ZIRCALOY-2: ION IMPLANTATION STANDARDS AS A CALIBRATION TECHNIQUE,* W. H. CHRISTIE, J. A. CARTER, R. E. EBY, L. LANDAU and W. R. MUSICK, Analytical Chemistry Division, Oak Ridge National Laboratory, Oak Ridge, TN 37830.

Standards prepared by ion implantation of ^{11}B into Zircaloy-2 were used to calibrate a spark source mass spectrometer (SSMS) near surface analysis method. The analytical method was predicated on the idea that both standards and samples could be sparked in a SSMS under essentially identical and reproducible conditions. Calibration runs gave linear log-log results for plots of $^{11}B^+/^{122}Sn^+$ versus B concentration in the standards. Calibration plots were determined on the basis of 5 to 6 replicate determinations for 3 different implant standard concentration levels. A series of irradiated Zircaloy-2 cladding samples were analyzed in a SSMS that had been modified to handle radioactive samples. Based on the ion implantation standards, these irradiated Zircaloy-2 samples were shown to contain not more than 0.06 μg cm^{-2} total B in the near surface region.

The ion implantation standards were prepared by ion implanting $^{11}B^+$ at 100 keV into Zircaloy-2, under high vacuum conditions, at doses in the 3×10^{15} to 3×10^{16} B atoms cm^{-2} range. Accuracy of the relative implant dose levels and lateral homogeneity was verified by secondary ion mass spectrometry.

*Research sponsored by the U. S. Department of Energy, Division of Basic Energy Sciences, under Contract W-7405-eng-26 with the Union Carbide Corporation.

RAPID ANALYSIS OF INJECTED SOLUTION SAMPLES
BY GLOW DISCHARGE MASS SPECTROMETRY

P.J. Savickas, R.W. Marquis, T.J. Loving, and W.W. Harrison
Department of Chemistry, University of Virginia, Charlottesville, VA. 22901

Glow discharge mass spectrometry has previously been applied in our laboratory to the analysis of solutions. (1,2) Samples have been applied to metal and/or graphite cathodes, dried to a residue film, and the cathodes inserted into the source for analysis. The turn-around-time for such an approach is long, and acceptable precision requires considerable care in electrode positioning and the selection of duplicate electrodes. We have now designed and constructed a glow discharge ion source which allows the rapid in-place application of microliter sample solutions onto a small pyrolytic graphite cathode. The same source can also be used for atomic absorption studies of the plasma to follow atom density profiles in the source chambers.

Experimental

The source is a coaxial cathode type (2) coupled to a quadrupole mass filter (3). Figure 1 shows a somewhat simplified sketch. The discharge is

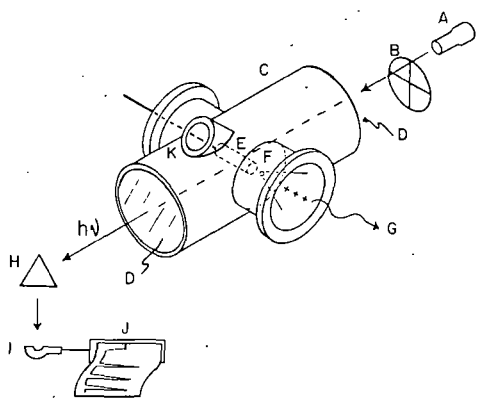

Figure 1. Coaxial cathode ion source with atomic absorption capabilities.

struck between the cathode [E] and anode [F], which is a plate with a 0.5 mm ion exit orifice. The extracted ion beam [G] is directed to the quadrupole for analysis. A sample injection port [K] allows rapid application of microliter aliquots of a solution directly onto the cathode, where it is dried to a residue film. Two quartz windows [D] seal the sidearms of the source through which the hollow cathode [A] beam passes. A chopper [B], tuned amplifier [H], and photomultiplier [I] form a modulated system to discriminate against emission from the discharge. Cathode materials used have been copper and graphite.

Results and Discussion

Figure 2 shows atomic profiles for a copper cathode in an argon discharge. In Figure 2a, the decrease in copper atom density with distance from the cathode is shown. It is interesting to note that the copper atoms extend rather far into the discharge. Figure 2b shows results from the sampling area in front of the ion exit orifice. The population remains essentially constant across the face of the cathode (in the cathode-anode interspace around the ion exit) and then drops off at the same rate as the beam moves away from the cathode surface.

We have used terbium as an example of a rare earth element which presents analytical difficulty for many trace element techniques. Figure 3 shows the mass spectrometric response from some of our initial (nonoptimized) efforts to analyze terbium solutions.

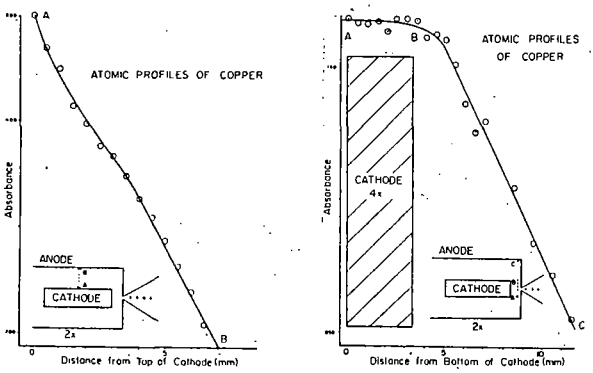

2a 2b

Figure 2. Atomic density profiles for copper in an argon discharge using a copper cathode. Coaxial cathode ion source.

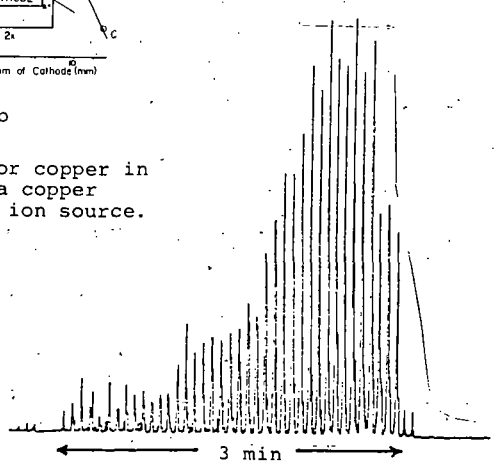

Figure 3. Time dependent response for a 30μl, 10ppm Tb solution on a pyrolytic graphite cathode. Repetitive scans of $^{159}Tb^{+}$.

References

1. E.H. Daughtrey and W.W. Harrison, Anal. Chem. 47, 1029 (1975).

2. W.A. Mattson, B.L. Bentz, and W.W. Harrison, Anal. Chem. 48, 489 (1976).

3. B.L. Bentz, C.G. Bruhn, and W.W. Harrison, Int. J. Mass. Spec. Ion Phys. 28, 409 (1978).

NEGATIVE IONS OF SPUTTERED COMPONENTS IN A GLOW DISCHARGE

B.L. Bentz and W.W. Harrison
Department of Chemistry, University of Virginia,
Charlottesville, Virginia 22901

To date most analytical and discharge diagnostic studies in glow discharge mass spectrometry have dealt with positive ions arising from the discharge gas, and of recent prime interest, the sputtered population (1,2). Sampling the negative ion composition of the plasma discharge has not enjoyed the attention directed toward the positive ion analog. Relatively few literature reports concern studies of negative ion species in glow-type discharges (3). Still fewer reports describe negative ion formation involving the sputtered species in a dc glow discharge (4,5). This report concerns sampling a coaxial cathode ion source (CCIS) in the negative ion mode.

Experimental

The coaxial cathode ion source is a stable dc diode abnormal glow discharge localized between concentric cylindrical electrodes. Strips of medium purity metal foils (Ag, Pt, Mo) and turnings of metal wire (Au) were supported on a graphite coaxial cathode suitably aligned in the CCIS. Copper and stainless steel(SS) 304 bulk materials were machined into the coaxial cathode geometry and analyzed directly. Argon and oxygen served as discharge gases. The coaxial cathode source typically operated at 133-400 Pa source pressure with discharge currents up to 30mA, and voltages of 600-800 V. This sputter-ionization source was interfaced to the quadrupole solids mass spectrometer described previously (2).

Results and Discussion

Our aim was to study the potential of the glow discharge to generate negative ions and evaluate qualitatively the types of negative ions so produced. The determination of negative ions associated with the sputtered species could prove interesting from both fundamental and analytical viewpoints. The relative concentration of low energy electrons (6) in the negative glow plasma of a glow discharge can make it conducive to electron attachment reactions.

Our prime interest was studying negative ions related to the sputtered species. Au (Figure 1) and Ag, having high positive electron affinities of 2.31 eV and 1.30 eV, respectively, gave relatively intense M^- ions. $^{197}Au^-$ was also observed in an argon discharge, although the ion signal intensity was reduced by ~20 fold. When sputtering a silver sample, no AgO_x^- analogs were seen. In contrast to the strong M^- ion signals observed with Ag and Au, Pt and Cu samples yielded MO_2^- forms. These observations are similar to those of a recent SIMS study, where abundant MO_2^- secondary ions were detected from pure metal targets subjected to O_2^+ ion beam bombardment (7).

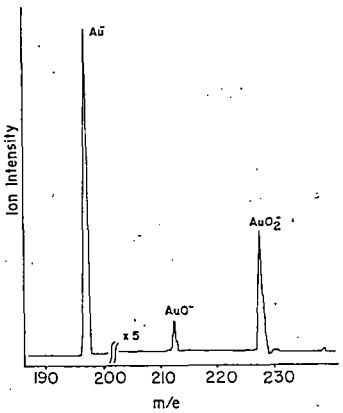

Figure 1. Mass spectrum obtained from a sputtered gold sample in an oxygen glow discharge.

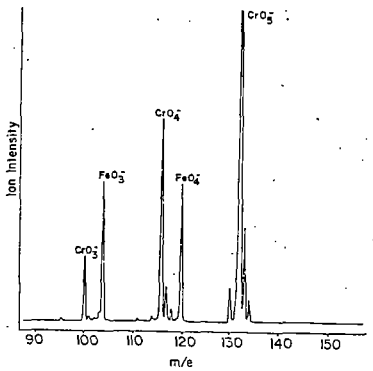

Figure 2. Mass spectral segment obtained when sputtering a SS 304 coaxial cathode in an O_2 discharge.

Benninghoven (8), has reported ion yields of oxygen-containing secondary ions MO_n^- for a number of oxidized elements. The secondary ion sputter yields of CrO_3^- and MoO_3^- are the largest among the oxide forms for these two elements. In the CCIS glow discharge, Cr and Mo also yield strong MO_3^- ions, although the MO_5^- species is the most intense. The iron component of a SS 304 coaxial cathode yielded FeO_3^- and FeO_4^- ions (Figure 2), where Cr species are present also. Simons et al. observed FeO_2^- as the dominant iron negative ion species when examining low alloy steels in a SIMS study (7).

References

1. J. W. Coburn and E. Kay, Appl. Phys. Lett., 18 (1971) 435.
2. B. L. Bentz, C. G. Bruhn, and W. W. Harrison, Int. J. Mass Spectrom. Ion Phys., 28 (1978) 409.
3. I. Kuen, F. Howorka, and R. Varney, Int. J. Mass Spectrum. Ion Phys., 28 (1978) 101.
4. H. Hotop and W. C. Lineberger, J. Chem. Phys., 58 (1973) 2379.
5. H. Hotop, R. A. Bennett, and W. C. Lineberger, J. Chem. Phys., 58 (1973) 2373.
6. C. S. Willet, "Introduction to Gas Lasers: Population Inversion Mechanisms", Pergamon Press, Oxford, 1979, Chap. 3.
7. D. S. Simons, J. C. Sheffield, and J. R. Hanrahan, 26th Annual Conference on Mass Spectrometry and Allied Topics, St. Louis, Mo., May 28-June 2, 1978, paper RB-12.
8. A. Benninghoven, Surf. Sci., 53 (1975) 596.

AN LC-MS USING ION IMPACT

Richard D. Smith* and James E. Burger
Chemical Methods and Kinetics Section
Physical Sciences Department
Battelle, Pacific Northwest Laboratory
Richland, Washington 99352

The need for a liquid chromatograph-mass spectrometer interface which can efficiently handle nonvolatile and thermally unstable molecules is well recognized. Field desorption (FD) mass spectrometry is effective for the analysis of many such compounds but a direct interface between the chromatograph and the mass spectrometer has not been constructed due to the high voltages and precise mechanical alignment required. Existing commercial LC-MS interfaces use either: (a) a direct introduction of a small flow of the LC effluent directly into a heated chemical ionization (CI) source; or (b) deposition of the effluent on a moving ribbon with evaporation of the volatile mobile phase and progression through a series of vacuum locks, and volatilization or pyrolysis of the material in or adjacent to a conventional CI or electron impact (EI) ion source. These and related interfaces have been demonstrated to be effective for a wide range of compounds, but their application for the analysis of nonvolatile and thermally labile compounds is limited. Recently, it has been recognized that a variety of alternate ionization methods produce mass spectra which are remarkably similar to those obtained by FD. These techniques include "in-beam" chemical ionization on Teflon probes or special surfaces, secondary ion mass spectrometry (SIMS), Californium-252 plasma desorption, and laser desorption (LD).

We have recently constructed a moving ribbon LC-MS interface for operation with either SIMS or LD ionization methods and have begun to explore the ion impact approach. Figure 1 is a schematic illustration of the LC-MS interface and its integration into an analysis scheme which will use either SIMS or LD. The LC effluent is deposited on a slowly moving (5-30 cm/min) continuous ribbon (0.63 cm wide, 0.008 cm thick, 320 cm long). Ribbons of high purity (>99.999%) nickel, molybdenum, and platinum have acceptable mechanical properties and are readily spot welded to form the continuous ribbon. A unique feature of the interface is the inclusion of a 100-cm long evaporation region for the LC mobile phase before the first vacuum slit. This also allows the semipermanent storage of material. Evaporation is assisted by gentle heating (with the temperature of the ribbon maintained below the boiling point of the liquid) from strip heaters located just above and below the ribbon, a continuous flow of preheated argon, preheating of the liquid effluent, and the relatively slow speed of the ribbon. Preliminary tests show that one can readily evaporate to dryness a variety of liquids (hexane, water, etc.) deposited at 2 cm^3/min and at a ribbon speed of 20 cm/min prior to the first vacuum chamber. At the slowest speeds, some loss of chromatographic resolution appears unavoidable for less volatile solvents due to the finite period required for evaporation of the mobile phase and flow of the liquid on the ribbon surface. Three regions of differential pumping are employed prior to the high vacuum surface. The first two regions are pumped by Leybold-Heraeus S30A "hot pumps" (at 10 liter/sec) to limit the effects of condensable vapors during long-term pump operation, and the third by a 1500 liter/sec turbomolecular pump. The main drive wheel is also used to adjust ribbon tension and is motor driver through three universal joints; at no point does the sample surface of the ribbon contact another surface. Typical working pressures are approximately 20 torr, 0.5 torr, and 10^{-5} torr in the three differentially pumped regions. The pressure in high vacuum chamber ranges from 10^{-7} to 10^{-6} torr depending upon the required gas flow for the ion gun and mass spectrometer collision chamber.

Ions formed at the surface pass through a Bessel Box energy filter and are analyzed using either a single or a new double quadrupole mass spectrometer (Extranuclear Laboratories, Inc., Pittsburgh, PA) which incorporates a chamber for collision-induced dissociation (CID) fabricated of leaky dielectric material (approximating the middle quadrupole of triple quadrupole analyzers). The use of CID in conjunction with the LC-MS interface should greatly increase chemical specificity and the deconvolution of complex chromatograms. (The CID complements SIMS or LD ionization modes since these processes often produce spectra with intense molecular or quasi-molecular ion peaks and limited fragmentation.) The major difficulty of the SIMS ionization mode results from the high sensitivity for surface contaminants. This difficulty arises from the high sensitivity of the technique for surface species. We have demonstrated detection limits of <0.01 ngrams for an easily ionized material (arginine) while scanning (Figure 2). The large "background" is clearly associated with material on the ribbon; improved ribbon clearing techniques suggest the possibility of greatly enhanced detection limits.

The moving ribbon interface has several potential advantages when used with SIMS or LD ionization modes, and CID in a double or triple quadrupole analyzer. First, the long evaporation region at atmospheric pressure easily allows complete evaporation of the LC mobile phase prior to the first vacuum slit. This reduces sample loss and degradation of chromatographic resolution with splashing and atomization of liquid. Second, the SIMS or LD ionization modes are highly localized processes; this allows the use of slower ribbon speeds than by "flash" heating for volatilization without loss of chromatographic resolution and removes ribbon temperature as an important variable in determining sensitivity. Third, the ribbon length and slow ribbon speed allow temporary storage of the separated materials for LC runs of 10-60 minutes, depending upon ribbon speed and required resolution, when the "cleanup" heaters and solvent clearer are "off." This is an important advantage since the SIMS or LD technique will consume only a minute amount of sample during the normal analysis. Figure 2 illustrates this behavior for arginine samples ranging from 1.0 ng/cm^2 to 500 mg/cm^2. The behavior for successive ribbon rotations (25 min/rotation) shows evidence of surface damage for larger samples. (The "noise" is periodic in nature and representative of contamination.) Thus, temporary storage allows selected portions of the separated materials stored on the ribbon to be reanalyzed after completion of the separation and initial analysis. Selected ribbon locations can be analyzed for extended periods to increase the signal/noise ratio and detection limits. More important, however, the subsequent analysis allows one to completely utilize the CID capability of a double quadrupole mass spectrometer, which can only be applied during the initial separation to a limited extent due to mass spectrometer scan speed limitations. Thus, the SIMS ionization mode uniquely complements the storage capability of the interface; we are continuing to explore these analytical techniques using both the SIMS and LD ionization modes.

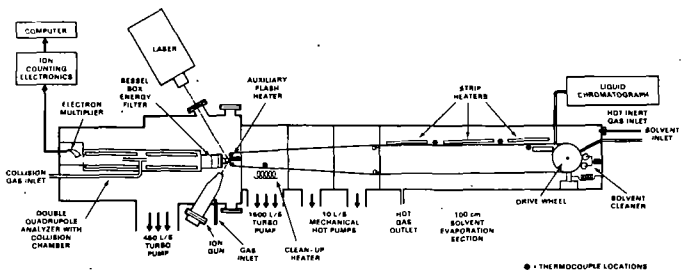

FIG. 1. Schematic illustration of the LC-MS using a moving ribbon interface, ionization by SIMS or LD, and analysis using a double quadrupole mass spectrometer.

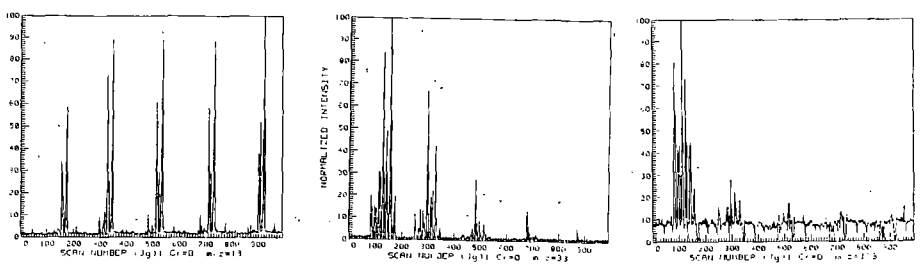

FIG. 2. Normalized intensities for ions at m/z 173, 33, and 18 for high current Ar^+ ion bombardment of seven samples of arginine in water deposited for one minute intervals alternated with blanks. Concentrations range from the equivalent of 1.0 nanogram/cm^2 to 1.0 milligram/cm^2 in decade intervals. Note the suppression of ionization indicated for m/z 173 for the most concentrated sample and the evidence of surface damage leading to a decrease of the m/z 173 and 33 ion counts and an increase in m/z 18 counts.

COMBINED LIQUID CHROMATOGRAPH-MASS SPECTROMETER FOR INVOLATILE BIOLOGICAL SAMPLES

C. R. Blakley, J. J. Carmody, and M. L. Vestal

Department of Chemistry
University of Houston
Houston, TX 77004

A new liquid chromatograph-mass spectrometer (LC-MS) has been developed in our laboratory for application to analyses of biological molecules of extremely low volatility. This new "simplified" LC-MS system uses oxy-hydrogen flames to rapidly vaporize the total LC effluent and molecular and particle beam techniques to efficiently transfer the sample to the ionization source of the mass spectrometer. This new instrument is comparable in cost and complexity to a combined gas chromatograph-mass spectrometer (GC-MS), but extends the capabilities of combined chromatograph-mass spectrometry to a broad range of biologically important compounds not previously accessible.

A simplified schematic diagram of the apparatus is shown in Figure 1; a more detailed description of the LC-MS system and its performance is given elsewhere (1). Briefly, the effluent from the LC enters the vaporizer through a stainless steel capillary tube which is heated near the end to ca. 1000 C by four small oxy-hydrogen flames. As a result of rapid heating, a jet of vapor and aerosol is produced near the exit from the stainless steel tube. The jet then undergoes an adiabatic expansion, and a portion passes through the skimmer to the ion source where the beam impinges on a nickel plated copper probe which is electrically heated to ca. 250 C. The ion source is equipped with an electron gun for producing ions for normal CI operation. Under typical operating conditions, about 95% of the liquid is vaporized and the remainder is in the form of a highly collimated particle beam which is accelerated by the rapid expansion of the vapor. In our present geometry these particles typically have a mass of about 10^{-7} g and carry a charge of ca. $5x10^{-12}$ coulombs each. Involatile samples appear to be carried preferentially by the particles, and our preliminary results indicate that 50-80% of an involatile solute, e.g. adenosine, is transmitted to the ion source with about 5% of the solvent.

During the course of the development of the LC-MS system, spectra have been obtained on several hundred biologically important molecules; however, particular attention has been given to amino acids, peptides, nucleosides, and nucleotides. A few examples of recent results are presented in Figures 2 through 4, where both positive and negative CI mass spectra are presented for a few representative examples. The amino acid, arginine, is considered a difficult compound for conventional EI or CI mass spectrometry and ions characteristic of the intact molecule are often not observed. In the present work intense ions indicative of the molecular weight ($M+H^+$ or $M-H^-$) are observed along with a few structurally significant fragments. These results are typical of the 20 amino acids which have been investigated.

Several dipeptides have been studied; they appear similar to the amino acids in that they also generally yield intense ions characteristic of the molecular weight; however, the fragmentation patterns are considerably more complex. Insufficient data are presently available to determine the utility of the spectra for determination of the structure of the dipeptides.

In most of our earlier work we used the elements of nucleic acids--bases, nucleosides, and nucleotides--as test compounds which provided a convenient series of biologically important molecules of increasing difficulty. The purine and pyrimidine bases present no particular problem; we have generally obtained spectra in which the protonated molecular ion is the base peak in the positive ion CI spectrum. The nucleosides are substantially more difficult. While the intensities of the fragment ions are relatively stable and easily reproduced, the intensity of the MH^+ ion in positive CI is very sensitive to the operating conditions. A spectrum corresponding to perhaps the "best" positive CI result on adenosine is given in Figure 3. For all of the nucleosides studied the $(b+2H)^+$ and b^- ions are always observed as very intense fragments in the positive and negative ion CI, respectively, and

are usually the base peaks in the spectra. In positive ion CI the MH^+ ion is nearly always observed, but its relative intensity varies from being the base peak as shown in Figure 3 down to a few percent of the base peak depending on the nucleoside, the size of the sample, and details of the operating conditions which are not yet fully understood.

The nucleotides represent the most difficult molecules which we have studied. The positive CI spectrum for 5'-AMP is shown in Figure 4. The intensity of the MH^+ ion is very sensitive to the operating conditions. Spectra showing pseudo-molecular ion intensities comparable to or greater than those shown in Figure 4 have been obtained frequently for several nucleotides; on the other hand, under superficially similar operating conditions, the pseudo-molecular ions are sometimes not observed. Some further improvements in our techniques for operating the instrument and particularly in controlling and monitoring the vaporizer will probably be required before application of the combined LC-MS to molecules as involatile and thermally labile as the nucleotides can be considered routine. Nevertheless, the present results do show that vaporization and ionization of intact nucleotide molecules is feasible.

Acknowledgement

This work was supported by the Institute of General Medical Sciences (NIH) under Grant GM24031. The authors wish to thank Ms. L. M. Marks for preparing the figures for publication, and Professor J. A. McCloskey for providing samples of nucleosides and nucleotides.

Reference

1. C. R. Blakley, J. J. Carmody, and M. L. Vestal, accepted by Anal. Chem., May (1980).

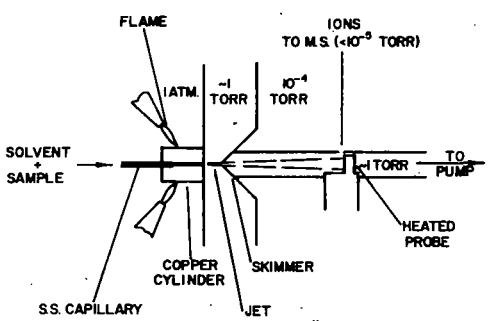

Figure 1. Simplified schematic diagram of the experimental apparatus.

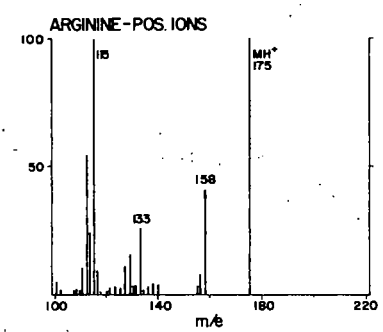

Figure 2. Chemical ionization mass spectrum of Arginine above mass 100.

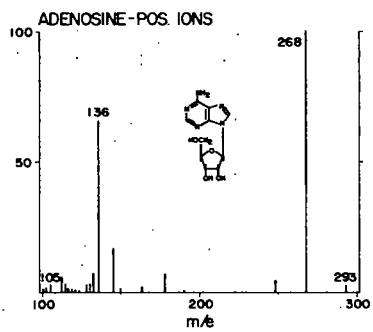

Figure 3. Chemical ionization mass spectrum of Adenosine above mass 100.

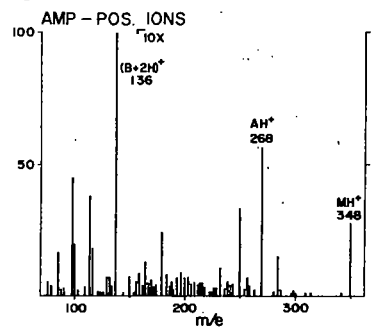

Figure 4. Chemical Ionization mass spectrum of 5'-adenosine monophosphate.

ION PAIR REVERSED PHASE LIQUID CHROMATOGRAPHY-MASS SPECTROMETRY

D.P. Kirby, B.L. Karger, and Paul Vouros
Institute of Chemical Analysis
Northeastern University
Boston, Massachusetts 02115

B. Petersen and B. Hidy
Battelle Columbus Labs
Columbus, Ohio 43201

The on-line combination of Reversed Phase LC and MS has recently been demonstrated (1). A segmented flow continuous extraction interface was used to transfer solutes from an aqueous, buffered mobile phase into an immiscible, volatile organic phase, which was then admitted to the MS via a moving belt. The complexity of the original interface has been greatly reduced (Figure 1). The use of solvent rather than air segmentation to control dispersion through the system and the use of vacuum to "pump" the phase separator together obviate the need of a peristaltic pump. Moreover, the use of a simple air displacement system to deliver organic solvent eliminates the need of an additional mechanical pump. Combined liquid flows of 2 ml/min are easily accommodated, and phase separation efficiencies of 80% are routinely achieved. Band broadening is comparable to that obtained with the original configuration.

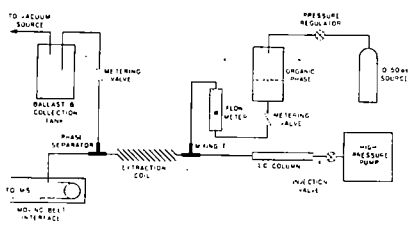

Figure 1. Diagram of LCMS system showing continuous extraction interface and peripheral equipment.

Ion pairing, which currently finds wide application in LC for the analysis of ionic compounds, offers a means of increasing extraction efficiency in the interface by variation of the hydrophobicity of the counter ion. It also, as will be shown, provides a means of derivatizing certain types of ionic compounds for MS analysis.

In anticipation of combining the on-line LCMS system with ion pairing, we investigated the compatibility with MS analysis of a series of model ion pairs consisting of n-alkyl sulfate or sulfonate counter ions and amine solutes (2). Neat sodium alkyl sulfate salts produced characteristic alkene spectra (loss of $NaHSO_4$) by DIP (EI or CI). The corresponding sulfonate salts yielded no spectra. Introduction into the MS of ion pairs formed with either type of counter ion resulted in nearly identical EI spectra which contained all the major ions associated with both the counter ions and solutes, and with essentially the same relative intensities as were observed with the neat materials (Figure 2).

Under CI (isobutane) conditions both sulfate and sulfonate ion pairs yielded the same solute spectra but different counter ion spectra. Sulfate ion pairs produced alkene fragment ions, as expected, whereas the sulfonates produced a single ion corresponding to the protonated sulfonic acid. In no case was a higher mass ion indicative of an intact ion pair observed. Mechanistically, it seems most likely at this point that a thermally activated proton transfer within the ion pair yields neutral species which subsequently (or concurrently) vaporize in a manner analogous to that observed by Kralj et al (3). Hence, ion pairing can be used to convert certain ionic compounds to a volatile form but without the mass increment usually encountered with other types of derivatization.

In view of the above results we evaluated the on-line LCMS combination. The continuous extraction interface was used with a Finnigan 4000 quadruple equipped with an Incos computer and a moving belt inlet. Mobile phases were typically 0.1 M NaH_2PO_4, 25-50% MeOH, and 5-20 mM counter ion. Results obtained from the injection of a series of basic drugs are shown in Figure 3.

Although the combined system was not optimized for sensitivity, both EI and CI spectra were readily obtained with on-column injections of 100 ng of solutes, whereas, under SIM conditions, many compounds could be detected with 10-50 ng injections.

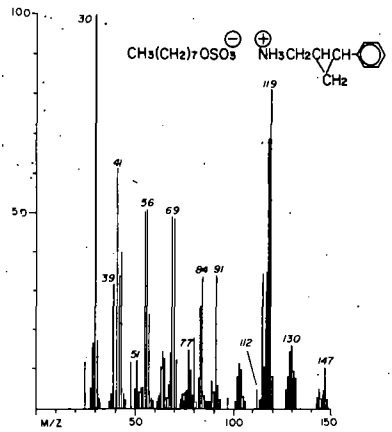

Figure 2. EI (70 eV) spectrum obtained from a model ion pair. The ion pair was extracted from an acidic phosphate buffer with CH_2Cl_2 and was admitted to the MS via DIP. Bold lines are solute related ions.

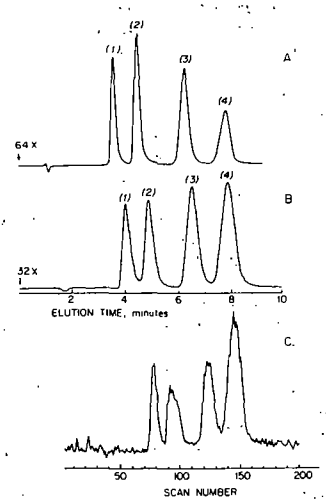

Figure 3. Chromatograms resulting from on-column injection of (1) Procainamide (2) N-acetyl procainamide (3) N-propionyl procainamide and (4) Lidocaine. A: UV detection of LC column effluent. B: UV detection of organic phase after continuous extraction interface. C: MS (CI) detection of organic phase after continuous extraction interface (total ion chromatogram).

REFERENCES

(1) B.L. Karger et al, Anal. Chem. 51, 2324 (1979).
(2) A more detailed account of this work has been accepted for publication in Science.
(3) B. Kralj et al, Biomedical Mass Spectrom. 2, 215 (1975).

STUDIES OF PESTICIDES BY COMBINED LC/MS

DAVID E. GAMES, NAKANDALAGE C.A. WEERASINGHE and STEVEN A. WESTWOOD

Department of Chemistry, University College, P.O. Box 78, Cardiff CF1 1XL, Wales.

Many classes of pesticide and their metabolic products are not amenable to GC/MS study because of their low volatility or thermal lability. LC/MS is the method of choice when compounds of this type are encountered and we describe here some of the areas where we have found the technique to be of assistance.

The potential of LC/MS for the identification and quantification of natural pesticides of the rotenone type has been shown.[1] We have applied the technique in the examination of carbon tetrachloride extracts of Timbo dust. The extract consists predominantly of four main components (see table 1) two of which have been identified as rotenone and rotenelone the other two components are isomers of rotenone and rotenelone respectively and remain to be fully characterized.

Care has to be taken when examining compounds with free acid groups e.g. phenoxyacid herbicides or the metabolic products of synthetic pyrethrin pesticides, since esterification can readily occur either in extraction procedures or during LC examination LC/MS is useful in detecting this phenomenon. Nievely when developing LC methods for a mixture of 2,4-D, 2,4,5-T, silivex and trichlorophon we made up our solution in methanol prior to LC study. LC/MS examination showed that the first three of these compounds are rapidly methylated under these conditions whereas trichlorophon remains in the free acid form.

Identification of the nature of the poison which has killed animals in the wild is often difficult particularly if rotenticides are involved. We have recently commenced a study of the applicability of LC/MS to the identification of coumain rodenticides and α-chloralose and their metabolites in tissue extracts. These studies are in an early stage but we have found LC/MS is capable of identifying warfarin, brodifacoum, difenacoum and α-chloralose in the low ng range. Negative chemical ionization appears to have application in this area giving complementary structural information to that obtained in the positive mode for the coumarins and providing a characteristic spectrum for α-chloralose (see table 1).

Chlorine attachment negative CI[2] is a convenient technique for confirming MW assignments. LC/MS studies of β-endosulphan indicate that it is not always necessary to have a freon or methylene chloride as reagent gas. Three experiments were conducted using methane as the reagent gas in the negative CI mode. The first consisted of dissolving the sample in chloroform and using a mixture of ethylacetate and hexane as eluant this gave the chlorine attachment ion as the base peak in the spectrum. Dissolving the sample in ethanol showed no sign of the attachment ion whereas use of a mixture of chloroform and hexane as the eluant with the sample dissolved in ethanol gave a spectrum which was a mixed spectrum (see table 1).

Metabolic studies of the carbamate pesticide CIPC have been considerably assisted by the availability of LC/MS. In earlier studies crude extracts of hydrolyzed and non-hydrolyzed rat urine were studied and a wide range of metabolites were shown to be present.[3] Partial structural assignments were made on the basis of the mass spectral data and were subsequently confirmed by comparison with synthetic standards. A major portion of the metabolites are present in conjugated form and we have recently isolated extracts containing a number of them. Combined LC/MS of the synthetic glucuromide 2-aminophenyl-β-D-glucuronide using ammonia CI showed that the technique can be used to characterize glucuronides. Encouraged by this we examined the conjugated metabolites of CIPC. Although excellent TIC traces were obtained we only obtained spectra characteristic of the aglycones. Although spotting solutions of the crude mixtures onto the interface gave spectra containing weak $(M+1)^+$ ions at the expected mass for glucuronides. We are presently investigating alternative reagent gases in an attempt to overcome this problem. Negative CI with methylene chloride as reagent gas shows some promise in this context since the model glucuronide gave an excellent spectrum by LC/MS under these conditions.

Table 1. Mass spectra obtained during LC/MS of Pesticides

Compound		m/z (% relative intensity)
Peak 1 Timbo dust (rotenelone)	A	411(23), 410(16), 393(100), 323(10), 208(13)
Peak 2 Timbo dust	A	411(30), 410(19), 393(100), 208(15)
Peak 3 Timbo dust (rotenone)	A	395(100), 192(10)
Peak 4 Timbo dust	A	395(100), 192(8)
brodifacoum	A	525(76),523(79),179(11), 163(100), 129(46)
	B	524(25),522(29),442(100),290(44), 161(3)
α-chloralose	B	347(13),345(25),343(19), 308(9), 310(9), 295(12),293(37),291(37), 277(16),275(16), 273(98),160(92),159(67), 118(100)
β-endosulphan	C	446(19),444(56),442(98), 440(100), 438(54), 406(14),404(22),402(10)
	D	409(10),407(35),405(42), 403(23), 371(34), 369(45),368(28),277(17), 275(25), 273(25), 271(22),269(42),267(31), 241(25), 240(19), 239(11),237(15),236(17), 234(44), 231(100)
	E	444(7), 442(16),440(17), 409(16), 407(41), 405(52),403(28),371(31), 369(51), 367(32), 277(29),275(49),273(39), 271(35), 269(70), 267(57),243(15),241(43), 240(32), 239(13), 237(20),236(28),235(18), 234(72), 231(75)

A. Methane CI
B. Methane CI negative
C. Chloroform solvent, ethyl acetate/hexane eluant
D. Ethanol solvent, ethylacetate/hexane eluant
E. Ethanol solvent, chloroform/hexane eluant

References

1. M.J. McAdams and M.L. Vestal, J. Chromatogr. Sci. 18, 110 (1980).

2. H.P. Tannenbaum, J.D. Roberts and R.C. Dougherty, Anal. Chem., 47, 49 (1975).

3. D.E. Games, C. Eckers, E. Lewis, K.R.N. Rao, M. Rossiter and N.C.A. Weerasinghe in "Advances in Mass Spectrometry" Vol.8, ed. A. Quayle, Heyden, London, 1980, in press.

COMBINED LC/MS IN STUDIES OF NATURAL PRODUCTS

DAVID E. GAMES, MARGUERITE L. GAMES, CHRISTINE ECKERS, WILHELM KUHNZ AND EMYR LEWIS

Department of Chemistry, University College, P.O. Box 78, Cardiff CF1 1XL, Wales.

Combined LC/MS can now be utilized in the laboratory in a relatively routine way similar to GC/MS. We describe here some of the areas where we have found an LC/MS system of the moving belt type (Finnigan)[1] to have been of considerable assistance.

Our methodology consists of taking a crude plant extract and initially examining it by field desorption mass spectrometry. This provides us with a molecular weight profile for the mixture and serves as a check for decomposition or loss of compound during subsequent chromatographic study. After optimization of LC conditions LC/MS is performed. Since we do not have a gradient former, we find that runs using reversed phase columns and adsorption columns are useful, in ensuring that polar compounds are eluted and in that separations are often effected with one type of phase which do not occur with the other. The choice of mass spectral ionization method depends on the class of compound being investigated. EI has proved most useful in our studies of ergot alkaloids of non-peptide type. A combination of EI and CI has been most effective in our studies of phenolic components of Dalbergia species.[2] In contrast CI only has proved the most effective technique for studies of the coumarins occurring in members of the Umbelliferae family.

Direct examination of the crude plant extract serves mainly to assist in identification of the major components present. If the plant has been studied previously these are usually known compounds. Hence the crude extract is next partially resolved either by column chromatography or preparative LC and the fractions obtained studied in a similar way to locate new compounds. This has resulted in the location of a number of novel structural types. Although mass spectrometry is of considerable assistance in structural assignment we have found it necessary to isolate components of interest by preparative LC and carry out chemical and spectroscopic studies to provide complete characterization.

At the present time LC/MS systems are not capable of handling the full range of compounds studied by LC. In order to ascertain some of the limitations of our system we have carried out a study of nucleosides, saccharides and glycosides. A mixture of uridine, cytidine and adenosine gave an excellent reconstructed TIC trace with methane CI, however although the bases present could be readily identified the spectra failed to provide MW information. Ammonia CI was more effective in this context and the on-line spectra obtained are given in table 1. We noted however that there was a significant increase in the intensity of ions in the MW region when samples were spotted onto the interface when compared with the on-line spectra (table 1). Use of methylene chloride in the negative CI mode gave improved MW information in the on-line situation abundant $[M+Cl]^-$ ions being obtained (table 1). In the case of glycosides we obtained excellent on-line data from a mixture of 6-bromo-2-naphthyl-β-D-glycopyranoside, 4-nitrophenyl-α-D-galactopyranoside, salicin and aesculin, see table 1. A mixture of xylose, fructose, glucose and sucrose also behaved well (table 1). However so far we have failed to obtain MW data from trisaccharides using either ammonia in positive CI or methylene chloride in negative CI. This appears to represent a limit for current LC/MS systems of the moving belt type.

References

1. W.H. McFadden, H.L. Schwartz and S. Evans, J. Chromatogr, 122, 389 (1976).
2. T. O'Criodain, D.M.X. Donnelly, D.E. Games and W. Kuhnz, unpublished work.

Table 1. Chemical Ionization Mass Spectra.

Compound		m/z (% rel. intensity)
Xylose	A	168(45), 150(100), 132(51), 115(30), 114(25), 108(34)
	B	168(100),150(89), 132(16), 108(39)
Fructose	A	198(61), 180(100), 162(11), 127(11), 120(11), 108(23)
	B	198(74), 180(100), 162(10), 138(11), 120(7), 108(17)
Glucose	A	198(58), 180(100), 162(23), 138(27), 120(29), 108(10)
	B	198(96), 180(100), 162(17), 138(58), 120(48), 108(37)
Sucrose	A	360(0.5),342(1), 198(9), 180(100),162(28), 144(24)
		360(13), 342(3), 198(35), 180(100),162(15), 144(6)
Uridine	A	262(13), 245(100), 150(15), 130(48), 113(80)
	B	262(33), 245(100), 150(24), 130(79), 113(57)
	C	281(33), 279(100), 243(14), 111(97)
Adenosine	A	268(20), 150(5), 136(100),106(17)
	B	268(12), 150(5), 136(100)
	C	304(26), 302(78), 172(8), 170(24), 134(100)
Cytidine	A	244(10), 150(11), 112(100)
	B	244(14), 150(5), 112(100)
	C	280(33), 278(100), 110(15)
6-bromo-2-naphthyl-β-D-glucopyranoside	A	404(23), 402(25), 224(16), 222(16), 180(100)
p-nitrophenyl-α-D-galactopyranoside	A	319(2), 180(17), 110(100)
salicin	A	304(6), 286(7), 180(36), 124(100)
aesculin	A	341(10), 196(25), 180(35), 179(100)

A. on-line LC-MS NH_4CI

B. spotting NH_4CI

C. on-line LC-MS CH_2Cl_2 negative CI

A NEW SOFT IONIZATION TECHNIQUE FOR MASS SPECTROMETRY OF COMPLEX MOLECULES

C. R. Blakley, J. J. Carmody, and M. L. Vestal

Department of Chemistry
University of Houston
Houston, TX 77004

In the course of developing a new combined LC-MS system we have discovered a new ionization technique which appears widely applicable to mass spectrometry of involatile molecules. The purpose of this communication is to present the first results from this new ionization technique. The apparatus is described separately in this conference (1) and in more detail elsewhere (2). Ions are produced by a combination of partial vaporization by very rapid heating of a liquid solution containing the sample and final vaporization by impact of an aerosol containing the sample on a heated metal plate. No ionizing source such as an electron beam or strong electric field is required. Mass spectra obtained on some test compounds including an underivatized pentapeptide and two dinucleotides are very similar to those obtained by field desorption (FD). The new technique is compatible with on-line chromatography, and it is fast, sensitive, and relatively simple and inexpensive.

Both positively and negatively charged particles are produced, and both the magnitude of the charge and the relative numbers of positive and negative particles depend on the properties of the solvent and on the vaporization conditions. The best conditions for the new ionization technique in our preliminary studies using 0.2 M formic acid as the solvent at input flow rates in the range of 0.5 to 1 ml/min. Under these conditions the current measured to an electrically isolated probe inside the ion source and at source potential is typically $+10^{-8}$ amp average; the current is modulated at a frequency of about 2000 hz which apparently corresponds to the arrival rate of individual particles.

When the charged particle undergoes a high energy impact with the heated probe, it is wholly or partially vaporized and some of the resulting molecules are ionized. The ions observed using a quadrupole mass filter are primarily the protonated or cationized species produced by chemical ionization; however, it appears that much less energy is transferred to the ions in the present technique as compared to more conventional CI. For example, the spectrum of adenosine 5'-monophosphate (AMP) obtained by the new technique is shown in Figure 1. The protonated molecular ion is not observed by conventional chemical ionization but spectra very similar to that shown in Figure 1 are obtained by field desorption (3). The spectrum shown in Figure 1 was obtained in a single scan from 10 to 600 amu in 4 seconds; the peaks below mass 100 are background ions due to the solvent. When one considers that the concentration of the sample was about 10 ppm relative to the solvent, the ratio of sample ions to background ions is amazingly high. The behavior of AMP by this new ionization technique is fairly typical of all of the nucleosides and nucleotides investigated to date. In all cases, intense MH^+ ions are observed together with a few structurally significant fragments.

Spectra obtained on two dinucleotides are shown in Figures 2 and 3. These spectra are very similar to those obtained by Schulten using field desorption (4). As shown in the FD work, these spectra are sufficient to uniquely determine the structure of the dinucleotide. In particular, the protonated cyclophosphates (mass 306 for CpG and mass 330 for ApU) are observed for the nucleoside in position 1, but the corresponding cyclophosphate containing the other nucleoside (mass 346 for CpG and mass 307 for ApU) is not detected.

The new ionization technique has been applied to a number of other interesting classes of compounds. All of the common amino acids have been investigated as well as several di- and tripeptides and one pentapeptide. Preliminary studies have been conducted on a number of other interesting systems including antibiotics, saccharides, and vitamins. In general, protonated and/or cationized molecular ions are observed as major peaks in the spectra.

At present the overall ionization and detection efficiency for the new ionization technique is between one and two orders of magnitude lower than for conventional chemical ionization in our apparatus; however, the background ionization of the solvent is lower by 4 or 5 orders of magnitude in the new technique. This latter fact coupled with the reduced

amount of fragmentation that is generally observed leads to the surprising result that the detection limit for the protonated molecular ion of most of the involatile substances investigated is substantially lower with the electron beam turned off! Typically, sample input rates in the range of from 1 to 10 ng/sec are sufficient to obtain reproducible, "clean" spectra when scanning at rates on the order of 100 amu/sec over the full spectral range. Higher sensitivities are obtained using single ion monitoring or scanning over a limited mass range. Some results obtained for adenosine by scanning over a 5 amu range centered on the MH^+ ion at mass 268 are shown in Figure 4. In these experiments 200 picograms injected gave an integrated response about 5 times the noise level.

Clearly, a large amount of additional work will be required before the full valve of the new ionization technique can be determined. Some of the details of the ionization process are not yet fully understood, and it is unlikely that our present techniques and apparatus are optimum.

Acknowledgement

This work was supported by the Institute of General Medical Sciences (NIH) under Grant GM24031. The authors wish to thank Ms. L. M. Marks for preparing the figures for publication, and Professor J. A. McCloskey for providing samples of nucleosides and nucleotides.

References

1. C. R. Blakley, J. J. Carmody, and M. L. Vestal, paper TPMOC9.
2. C. R. Blakley, J. J. Carmody, and M. L. Vestal, accepted by Anal. Chem., May (1980).
3. K. L. Olson and K. L. Rinehart, Jr., Methods in Carbohydrate Chemistry, Vol. 9, in press.
4. H. R. Schulten and H. M. Scheibel, Nucleic Acid Res. 3, 2027 (1976).

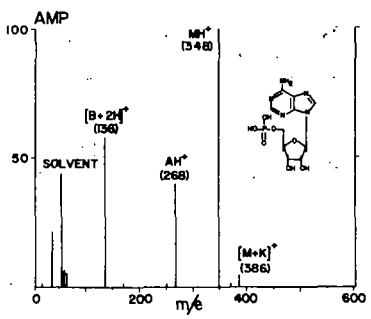

Figure 1. Positive ion mass spectrum of AMP obtained by the new technique.

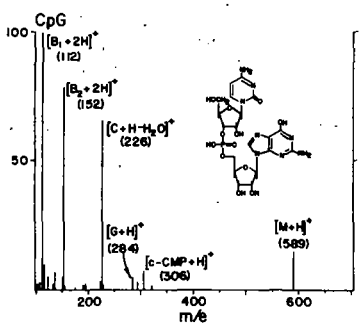

Figure 2. Positive ion mass spectrum of CpG obtained by the new technique.

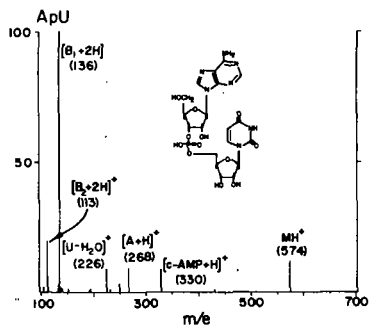

Figure 3. Positive ion mass spectrum of ApU obtained by the new technique.

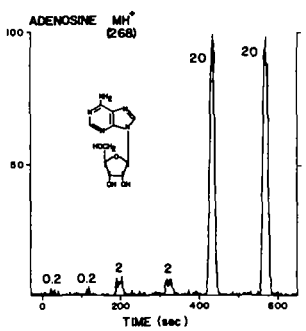

Figure 4. Response of the MS to a series of injections of Adenosine.

CONSECUTIVE REACTIONS IN A REVERSED GEOMETRY MASS SPECTROMETER, C.J. Proctor and J.H.Beynon, Royal Society Research Unit, University College of Swansea, Swansea, SA2 8PP, UK, and B.Kralj and J. Marsel, Institut Jožef Stefan, University of Ljubljana, Ljubljana, Yugoslavia.

A consecutive reaction is one which occurs in two distinct steps. For example, an ion may fragment according to the sequence $m_1^+ \rightarrow m_2^+ \rightarrow m_3^+$. The first step of the reaction may be studied using metastable m_1^+ ions extracted from the source that fragment in a field-free region. The pattern of energy release T_1 can be measured. The second step of the reaction may be examined in two ways. Metastable m_2^+ ions formed in fast reactions within the source may be studied. Alternatively, metastable m_2^+ ions formed as products of reaction of metastable m_1^+ ions in the first field-free region may be studied in the second field-free region. The fragmentation pattern (MIKE spectrum) and the patterns of energy release T_2 and T_2^c for the m_2^+ ions formed in the above two ways are characteristic of their structures which may thus be compared. Cases have been found of identical fragmentation behaviour of the m_2^+ ions formed in the two ways; in other cases their behaviour is different, indicating a difference in structure.

Consecutive reactions of organic ions have been found to occur for a wide range of compound types. This has several consequences. Firstly, if the peak shape for the reaction $m_1^+ \rightarrow m_2^+$ is used for obtaining the distribution of kinetic energy release T_1, the calculated distribution obtained will be in error due to the further fragmentation of some of the metastable (and unstable) ions m_2^+ formed before the product ions are collected and measured. The presence of such an error can be confirmed if an overall reaction of metastable m_1^+ ions to give m_3^+ ions can be observed as taking place in a single field-free region. This shows that some intermediate products m_2^+ are unstable and fragment again within the same field-free region.

If, and only if, the beam of m_1^+ ions is precollimated before entering the first field-free region, the product m_2^+ ion beam is collimated and the product m_3^+ ion beam is collimated (all collimation being in both the y- and z-directions), the metastable peaks can be used to select ions with a narrow range of internal energies. The metastable peak for the reaction $m_1^+ \rightarrow m_2^+$ occurring in the first field-free region can then be scanned in stages across the intermediate slit, thus allowing ions of different internal energy into the second field-free region. The unimolecular and collision-induced behaviour of such ions can then be investigated. This has been done and cases found where both the reactivity and collisional activation behaviour vary with internal energy.

TPMP2 HIGH-RESOLUTION MS/MS VIA MULTI-SECTOR MASS SPECTROMETERS.*

D. H. RUSSELL, E. H. MCBAY AND T. R. MUELLER, Analytical Chemistry Division, Oak Ridge National Laboratory, Oak Ridge, TN 37830.

The reversed-geometry or mass-analyzed ion kinetic energy (MIKE) spectrometer was originally introduced for the study of gas-phase ion chemistry. However, the application of this instrument design to the direct analysis of complex mixtures has evolved rather rapidly. In addition, the problem solving capabilities of the MIKE or mass spectrometry/mass spectrometry (MS/MS) instrument has spawned the introduction of new instrument designs and instrument types, e.g., the multi-sector high-resolution MS/MS and the multiple quadrupole instruments. To achieve high resolution MS/MS capabilities, a number of instrument configurations may be employed. The instrument employed for this study is a conventional geometry double focusing instrument to which was added a second electric sector, i.e., an electric sector/magnet/electric sector (EBE) configuration. To date, high resolution MS/MS experiments have been performed at resolving powers of 15,000 - 20,000 with detection levels of ca. 20×10^{-9} g. An alternative method for performing high-resolution analysis requires the simultaneous use of two metastable ion scan methods. The high-resolution MS/MS experiment and the use of multiple metastable scan methods for performing high resolution MS/MS analysis will be discussed.

TLC/CIMS: A THIN-LAYER CHROMATOGRAM SCANNER DIRECTLY COUPLED FOR CHEMICAL IONIZATION MASS SPECTROMETRY*

L. Ramaley, Dept. of Chemistry, Dalhousie Univ., Halifax, N.S., Canada
W. D. Jamieson, Atlantic Regional Laboratory, National Research Council of Canada, 1411 Oxford Street, Halifax, N.S., Canada
R. G. Ackman, Nova Scotia Technical College, Halifax, N.S., Canada

A TLC scanner has been developed which directly couples to an unmodified Finnigan 4000 quadrupole mass spectrometer. The scanner consists of a rectangular plate chamber which connects directly to the ion source through about 30 cm of heated nickel tubing. A bellows isolation valve is inserted in this line to allow opening of the TLC chamber without venting the spectrometer. The plate holder which carries 1 x 10 cm plates is moved within the chamber by a rack and pinion gear connected to a stepper motor through a rotary motion feedthrough (Varian #954-5151). Normal scan speeds are 50 and 100 s/cm. Desorption energy is supplied from a 150 W, 24 V projector lamp (#FCS) focused on the plate by an ellipsoidal mirror (Melles Griot #02REM013) through an infrasil window in the chamber. Surface temperatures of 300°C can be achieved in this manner. CI reagent gas sweeps over the plate beneath the window and carries desorbed samples directly into the ion source. An inlet for vacuum and venting to the atmosphere is provided to allow rapid changes in pressure in the chamber for speed and ease of operation.

The TLC scanner has been tested to date mainly by scanning plates on which varying amounts of representative compounds have been spotted at different locations to simulate chromatograms. The plates chosen for these studies (Applied Science Laboratory, Permakote) have a sintered silica gel layer and are reusable. These were chosen for the robust nature of the adsorbent. The background is mainly due to the CI reagent gas itself, usually methane, plus peaks at m/z 249 and 251 probably due to ReO_4^+ oxidized from the filament by water vapor desorbed from the plate and chamber. Peaks at m/z 93 and 170 are due to material in the TLC chamber itself. Very little background is evident with a thoroughly activated plate.

Sensitivity is markedly dependent on both the thermal stability of the sample and its mass spectral behavior. A stable compound such as phenanthrene which gives a CI spectrum with a strong peak at the mass of the molecular ion plus one can be detected in a full sweep scan at levels of 10 ng and at levels of 100 pg with an MID scan. A compound such as cholesterol which appears to decompose on desorption and produces many small fragment peaks at low m/z can be detected to only about 100 ng with a full sweep scan or 10 ng with an MID scan. Methyl stearate could not be detected at all. Response is non-linear, the ion counts increasing more rapidly than sample amount. Reproducibility for spots of the same amount is about 20%. There is some evidence that two compounds adsorbed at the same location interact. Thus the method at present should be considered semiquantitative.

On a relative basis, the peaks on the mass chromatograms appear twice as wide as the spots on the plate, resulting in a loss of spatial resolution by about a factor of two. This is partly caused by heat remaining in the plate in regions that have passed the heating area and by a small memory effect in the chamber itself. The R_f values obtained show good reproducibility. For stable, relatively non-volatile compounds such as many aromatic hydrocarbons the method is "non-destructive" in that much of the sample remains on the plate and can be detected by rescanning the plate or any other appropriate means. Each scan results in a decrease in sensitivity and spatial resolution.

In general the method is fast and simple and provides both qualitative and quantitative imformation about the sample that has been chromatographed. It is best suited to materials of medium to low volatility which do not markedly decompose on desorption from the plate.

*NRCC No. 18243

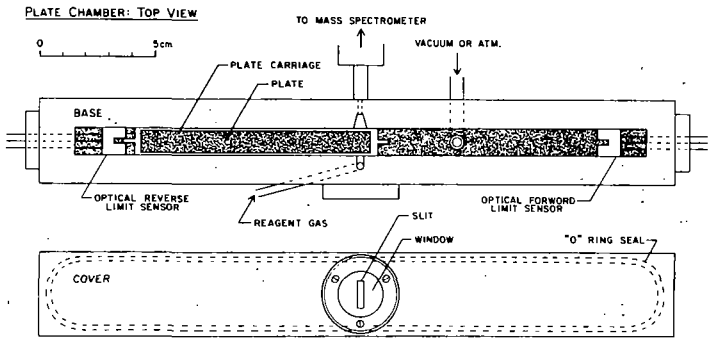
PLATE CHAMBER: TOP VIEW
0
5cm
TO MASS SPECTROMETER
VACUUM OR ATM.
PLATE CARRIAGE
PLATE
BASE
OPTICAL REVERSE LIMIT SENSOR
REAGENT GAS
OPTICAL FORWORD LIMIT SENSOR
SLIT
WINDOW
"O" RING SEAL
COVER

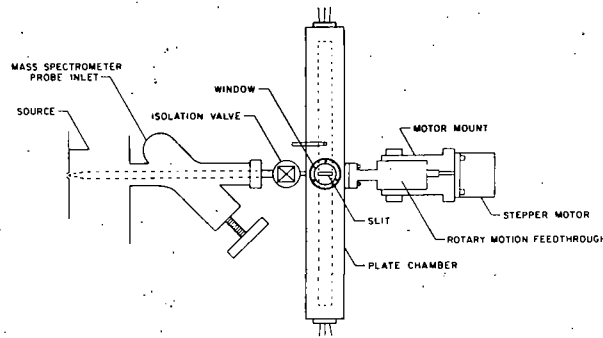
MASS SPECTROMETER PROBE INLET
SOURCE
ISOLATION VALVE
WINDOW
MOTOR MOUNT
SLIT
STEPPER MOTOR
ROTARY MOTION FEEDTHROUGH
PLATE CHAMBER

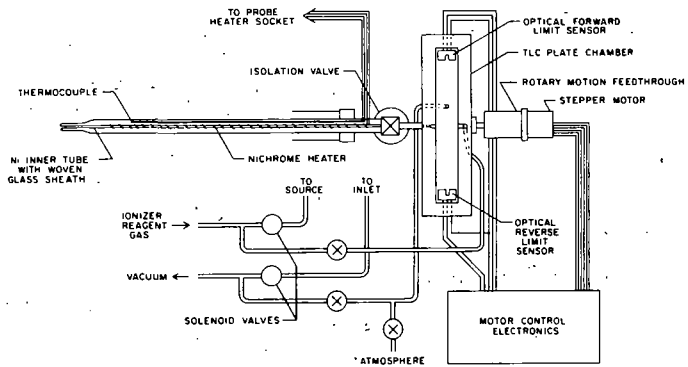
TO PROBE HEATER SOCKET
OPTICAL FORWARD LIMIT SENSOR
TLC PLATE CHAMBER
ISOLATION VALVE
ROTARY MOTION FEEDTHROUGH
STEPPER MOTOR
THERMOCOUPLE
Ni INNER TUBE WITH WOVEN GLASS SHEATH
NICHROME HEATER
TO SOURCE
TO INLET
IONIZER REAGENT GAS
OPTICAL REVERSE LIMIT SENSOR
VACUUM
SOLENOID VALVES
ATMOSPHERE
MOTOR CONTROL ELECTRONICS

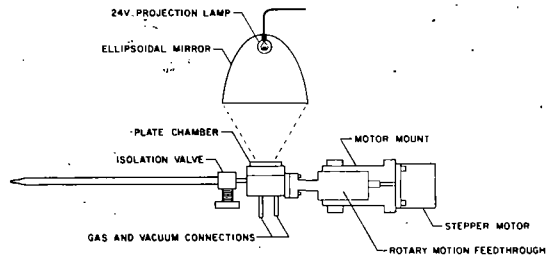
24V. PROJECTION LAMP
ELLIPSOIDAL MIRROR
PLATE CHAMBER
ISOLATION VALVE
MOTOR MOUNT
STEPPER MOTOR
GAS AND VACUUM CONNECTIONS
ROTARY MOTION FEEDTHROUGH

THE ELECTRO-OPTICAL ION DETECTOR ("Electronic Photoplate"), A COMPUTER-AGE DETECTOR FOR MASS SPECTROMETRY by R.A. Britten, C.E. Giffin, and R.A. Johansen; Jet Propulsion Laboratory, Pasadena, California 91103

At last year's ASMS conference, C.E. Giffin and H.G. Boettger reported that an electro-optical ion detector (EOID), mounted on a CEC 21/110B Mattauch-Herzog mass spectrometer, gave a strong signal output for a 4,4'-dibromo-biphenyl sample of only 8×10^{-15} grams.[1] Now that the ultra-high sensitivity which had been projected for EOID's has become a demonstrated reality, it is appropriate to consider some data analysis aspects of EOID operation. EOID data reflects at a number of points the unique construction of the EOID itself. The less desirable features of this data can usually be corrected by computerized data analysis, often in real time.

Basic features of EOID construction and operation have been described elsewhere.[1,2] An ion from a mass spectrometer strikes a microchannel electron multiplier array (MCA) where successive generations of secondary electron emission produce a gain of about 10^4. The secondary electrons are electrically drawn across a small gap to a phosphor coating on a fiber optics plate where they produce optical line images which are then transmitted through the vacuum wall. The MCA and phosphor are tilted with respect to the magnetic field to avoid having secondary electrons lost by being trapped on fringe field lines. The tilted line images which result are brought back into alignment by special fiber optic rotator devices[1] outside the vacuum wall. Photodiode arrays (PDA's) accept light from the rotators and produce the final electrical output signal. Each PDA is an inch wide, has 1024 sensing elements, and is read out under computer control.

The rotators leave their imprint on the data. Figure 1 shows the detector output which results when flat light illuminates a rotator. The sharp points on the large scallops show the location of fiber optic bundle junctions. Figure 2a shows the distorted output peak shape which results when a mass spectral peak stradles a bundle junction. Rather surprisingly, corrections based on flat light data provide only partial compensation. Better compensation (figure 2b) comes from an "end-to-end" calibration procedure which involves using a slow magnetic scan to sweep mass spectral peaks over ranges of adjacent PDA elements (figure 3). This procedure gives aggregate relative sensitivity figures for the MCA-phosphor-window-rotator-PDA as it exists for each PDA element (pixel). Only a limited magnetic scan is allowed to avoid having the somewhat cycloidal electron trajectories in the MCA-phosphor gap flip to a new cycle. Data from PDA elements swept at different times by two or more peaks provide the key to linking these limited scans and obtaining a relative sensitivity calibration for the entire detector.

To avoid possible light loss due to misalignment at the rotator-PDA junction, rotators are deliberately made a little narrower than the sensitive areas of PDA's. Data from a few "overhang" elements at each end of the PDA is ignored in the data analysis (Figure 1), and an appropriate element number to detector position conversion is done prior to doing mass calculations.

Mass scale calibration for an EOID is somewhat more complicated than for other detectors because the EOID is a segmented device in which adjacent MCA's feed adjacent PDA's. In an ideal Mattauch-Herzog instrument, observed mass is a quadratic function of position along the focal plane. With EOID data, observed masses show an approximate quadratic dependence (Figure 4), but there are discontinuities at points corresponding to some MCA plate junctions. The discontinuities seen in Figure 4 probably reflect either damaged plates or imperfect junctions. The changes in slope (i.e., changes in mass dispersion) probably reflect a lack of complete parallelism between the MCA plates and the phosphor. A computer routine which recognizes index peaks in a PFK spectrum and which avoids extrapolating across MCA plate boundaries provides mass values which are more than adequate to make the unambiguous integer (an half integer) mass assignments required in ordinary chemical work. (Figure 5).

The EOID is an integrating detector, and anything that interferes with the complete uniformity of sample integration times can yield results that superficially resemble noise. If computer peripheral output devices are operated in parallel with data acquisition or if computations are done in the background, subtle time and sequencing errors may result. A useful tool for recognizing the existence of such errors is a log-log plot of r.m.s. fluctuations versus average output value for a number of different diode elements. Timing errors manifest themselves as an observed power dependence (slope) that is greater than one half.

The EOID is sometimes referred to as an "electronic photoplate" because it combines some of the best features of electron multiplier detectors and photoplate detectors. This nickname obscures the fact that much of the data analysis for EOID is concerned with artifacts that have no real counterpart in electron multiplier or photoplate technologies (bundle junctions, overhang elements, MCA plate boundaries, etc.). Nonetheless the term electronic photoplate will probably continue to be used because the EOID is the product of a computer age and because most of its artifacts can be corrected through computerized data analysis in a manner that is nearly transparent to the casual user. Paper MPMOA9 at this conference describes a microprocessor-based device which will control EOID data acquisition operations and make several types of corrections in real time.

This research is sponsored under a grant from the National Institute of General Medical Sciences, NIH (Grant GM 20850).

References: 1. Giffin, et. al, ASMS Transaction (1979) p. 714; 2. Boettger, Giffin, et. al, Monograph on Multichannel Image Detectors, Y. Talmi, Ed. (1979) p. 291.

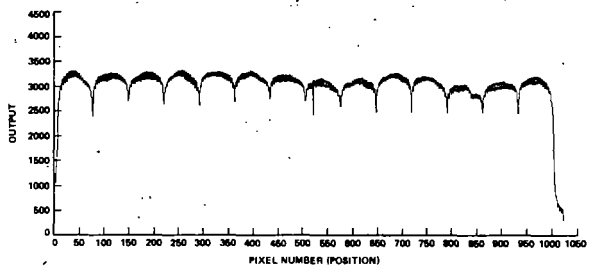

Figure 1

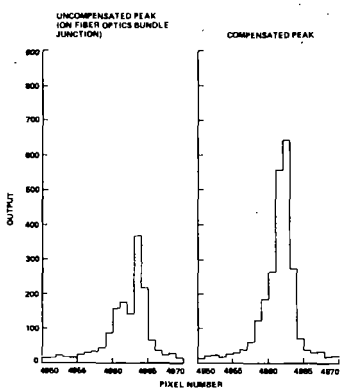

Figures 2a, 2b

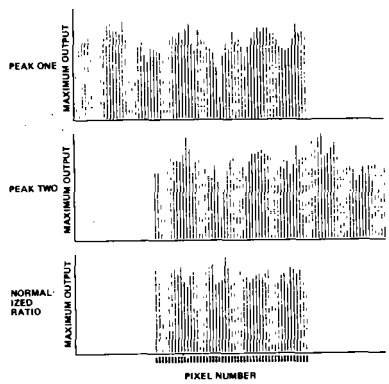

Figure 3

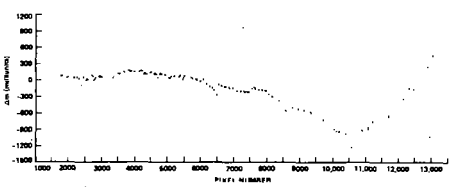

Figure 4

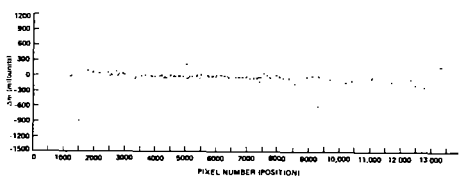

Figure 5

A SIMPLE DFTPP INLET FOR ABUNDANCE TUNING A GC/MS, A. E. ROSECRANCE, M. E. ZINNECKER and B. N. COLBY, Systems, Science and Software, Box 1620, La Jolla, CA 92008

Decafluorotriphenylphosphene (DFTPP) has been identified by the U. S. Environmental Protection Agency as a suitable reference material for the demonstration of acceptable GC/MS/DS abundance patterns (1). Abundance pattern verification is performed by injecting 50 ng of DFTPP into a GC/MS/DS followed by comparison of the acquired data with acceptable abundance windows for specific m/z's. A consequence of using a GC inlet is the extremely short residence time of the DFTPP in the ion source, far too short to allow instrument tuning required to correct for noncompliant abundance values. Abundance tuning with another compound, such as perfluorotributylamine (FC43), has proven cumbersome. Consequently, an alternative inlet for DFTPP was developed. This inlet, located inside the GC column oven, consists of a sample reservoir and a 10-port high-temperature valve. A constant flow of DFTPP is achieved by diverting the normal carrier gas flow through the sample reservoir, past the GC column and into the MS through the jet separator. Abundance tuning is accomplished easily with this inlet and the patterns produced are equivalent to those subsequently generated from GC/MS analyses. This paper provides details of the construction and performance of this inlet system.

(1) Federal Register, Vol. 44, Number 233, Part III, pp. 69542, (Monday, December 3, 1979).

REFERENCE COMPOUNDS FOR THE DETERMINATION OF RESOLVING POWER

Leonid Kelner, Biomedical Engineering and Instrumentation Branch, DRS, National Institutes of Health, Bethesda, MD 20205, and David Rosenthal, Chemistry and Life Sciences Group, Research Triangle Institute, Research Triangle Park, NC 27709.

Our previous experience with the analysis of polychlorinated and polybrominated biphenyls in environmental samples (1) has suggested that these compounds may be useful as reference compounds for the evaluation of mass spectrometer performance, specifically mass spectrometer resolution.

The procedure which might be conceived of for the determination of resolving power based on the usual definition for resolution can not be readily adapted in practice because the definition requires the presence of mass spectral peaks of equal intensity at adjacent masses, a situation which nearly never obtains with real compounds. However, decachlorobiphenyl (DCB) and decabromobiphenyl (DBB) show in their spectra easily recognized clusters of known intensity ratios separated by 35 or 79 mass units, respectively, which cover the entire effective range of low resolution mass spectrometer operation (m/z 100 - 1000).

Fig. 1 shows the molecular ion clusters at resolving powers of 250 and 500 for DCB and 500 and 900 for DBB. These curves were obtained by the summation of weighted theoretical curves of normal distribution adjusted to conform to the appropriate relationship between resolution and peak width. Analogous curves were drawn in the range of resolution 100-500 for DCB, and 100-900 for DBB. These curves show a strong dependence between resolution and the ratio of the minima on either side of the base ion to the base intensity. Because the curves are somewhat unsymmetrical, the average value for the two minima on either side of the base ion was chosen for measurement. The function MIN (R) is thus defined as:

$$\mathrm{MIN}\ (R) = \frac{(\mathrm{MIN}_1 + \mathrm{MIN}_2)/2}{I},$$

where MIN_1 - intensity of minima on the left side of base peak

MIN_2 - intensity of minima on the right side of base peak

I - intensity of base peak

R - resolving power

Figure 2 shows a plot of MIN (R) vs. resolution calculated for the DCB and DBB molecular ion cluster (5% non-contributory valley definition).

These theoretical results were then compared with actual data obtained on an LKB-2091 magnetic sector instrument and a Finnigan 4000 quadrupole mass spectrometer. The data were determined using the direct insertion probe and the electron impact ionization (EI) ion source. Close agreement was found for DCB for M/z 498 in the range RES = 150-500, and for DBB at m/z 944 in the range RES = 300-900.

This experiment suggests a procedure to determine the resolving power of any low resolution mass spectrometer. The method can be used at the two masses tested (m/z 498 and m/z 944), as well as other masses by utilizing the range of clusters present in the spectra of DCB and DBB. The method is applicable not only for EI, but also for CI (chemical ionization) instruments, since the molecular ion clusters for DCB and DBB are present and strong in both positive and negative chemical ionization mode.

It is felt that this procedure can be standardized to become the basis of a routine test for the resolving power of low resolution mass spectrometers (magnetic sector as well as quadrupoles).

Acknowledgements: We wish to express our appreciation to Drs. H. Fales, A. Yergey, and S. Markey of NIH for valuable discussions and instrument support.

1. M.D. Erickson, J.T. Bursey, L. Kelner, R.A. Zweidinger, D. Rosenthal, and E.D. Pellizzari, Biomedical Mass Spectrometry, v.7, in press (1980).

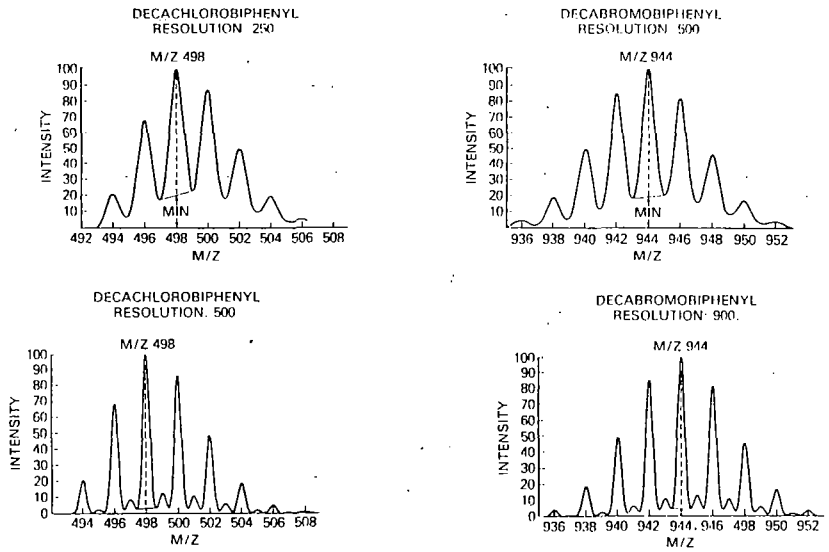

FIGURE 1 CALCULATED MOLECULAR CLUSTERS FOR DCB AND DBB

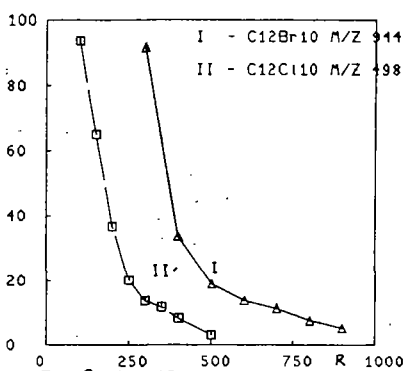

Fig.2 MIN=f(R) calculated from the theor.mol. clusters

A Powerful Multispectrometer Data System for Laboratory Applications.

J.C. Bill, P.H. D'Arcy, M.J. Wallington, J.A.V. Hopkinson, P. Powers
VG Data Systems Limited, Tribune Avenue, Altrincham WA14 5TP, England.

Introduction

Many laboratories are finding an increasing need to employ more than one mass spectrometer in order to handle their day-to-day analytical requirements.

The spectrometers are often of different makes and types and it is usually uneconomic to purchase separate data systems for each one. Furthermore, it makes sense to have a common data storage and retrieval system with common access to major peripherals.

The unique MULTISPEC concept utilises processing distributed between computers of comparable power to handle properly the problems of simultaneous operation of several mass spectrometers.

MULTISPEC-11 employs the powerful DEC PDP11/34 as a host processor to support the main system peripherals and bulk storage. Satellite PDP8A processors handle acquisition, mass measurement and local data interpretation. MULTISPEC-11 is provided as standard with a Printronix printer plotter and the new DEC VS11 colour visual display. A powerful interpretive software suite written in PASCAL makes the fullest use of DEC's RSX-11M Multitasking Operating System to give background interpretation faciities for up to 4 users in addition to the local facilities for data manipulation provided at each spectrometer.

MULTISPEC-11 Features include:-

* Powerful PDP11/34 Host Processor.
* Fast profile acquisition interfacing with standard or optional high dynamic range operation.
* Operation with any mix of fast or slow scanning, quadrupole or sector spectrometers using either their own scan law or under direct control by data system.
* Local interpretive terminals can be used during scan acquisition for background data manipulation or to display any of a wide selection of Interscan reports.
* Support for additional peripherals and bulk storage even on satellite processors.
* Optional Link to other systems for Laboratory Data Management or Chromatographic Data Analysis.

MULTICHROM - The New Chromatography Data System

The MULTICHROM series of datasystems makes use of the latest advances in computer hardware technology and software techniques to provide the analyst with the most competent and flexible data system currently available for both gas and liquid chromatography.

The basic design concepts of MULTICHROM ensure a flexible and easily expandable system offering considerably more power and capability than is offered by "intelligent" dedicated controllers and integrators, yet with significant savings in cost for medium and large scale chromatography laboratories.

The MULTICHROM concepts of flexibility and expandability start at the chromatograph. The task of data acquisition and optionally of control are delegated to a dedicated microprocessor based unit (MICROCHROM) equipped with a high dynamic range integrating ADC. The basic task of the module is to sample chromatograph data at a rate defined by parameters loaded from the host system, to hold successive samples in its own memory until they can be transmitted to the host system and to measure retention time. The basic module additionally responds to local "start" and "stop" commands. Communication with the host system is via a high speed asynchronous serial digital line using 20mA current loop for high noise immunity. Where cost per chromatograph is of prime importance, and sample rates are not excessive, up to four adjacent chromatographs can be interfaced to a single MICROCHROM.

Appropriately configured systems can combine the chromatography function with that of Laboratory Data Management and can incorporate links to MULTISPEC or other VG Mass Spectrometry systems.

MULTICHROM features include:-

* Choice of PDP11/23 or 11/34 computer architectures according to required cost and performance.
* Distributed processing techniques using Microchrom intelligent microprocessor based control and acquisition units.
* Operation with a wide choice of configurations to suit the speed and usage of different laboratories.
* Full colour high resolution VS11 interactive graphics terminal.
* PASCAL coded interpretation and manipulative software operating under RSX11M.
* Ability to store and manipulate raw data.
* Quality Control on routine samples giving an alert for analyses whose components fall outside preset limits.

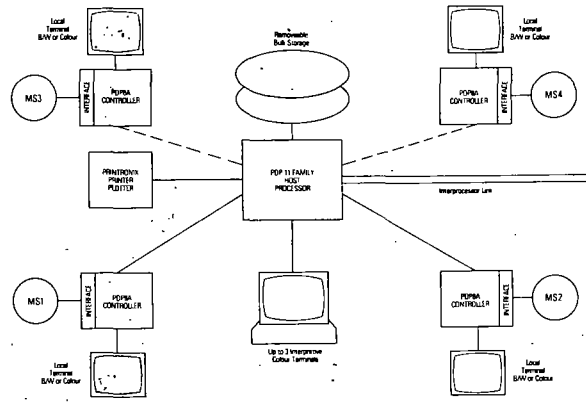

MULTISPEC-11 MASS SPECTROMETER DATA SYSTEM

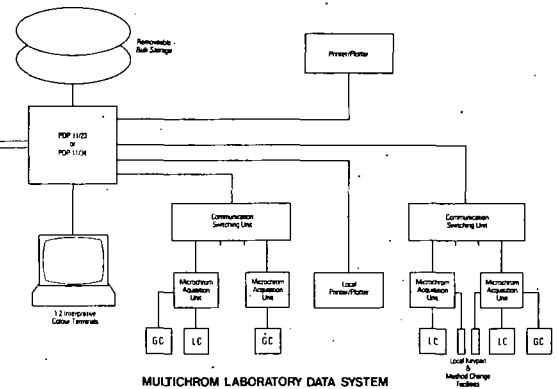

MULTICHROM LABORATORY DATA SYSTEM

Figure 1.

Printronix printer/plotter provides fast high quality output of both text and graphical nature on plain paper without the smudging often associated with electrostatic processes.

Large bulk storage provides for extensive sample and library records with two or more easy to use removable disc transports.

New VS11 Colour Vector Graphic Display provides high speed high quality spectral displays.

Optional Data Highway to Laboratory Data Management system and/or Laboratory Chromatographic system allows inter-relation of analytical data from different techniques.

Figure 2.

Choice of host processor to suit required price and performance.

Chromatography Communications Switching Unit permits the connection of up to four Microchrom Acquisition Units dependent on required data rates.

Microchrom Acquisition Unit permitting a maximum of four chromatographs to be interfaced.

Optional Local Keypad incorporates method change facilities for use locally at selected chromatographs.

TPMP8 ACCURACY OF MASS AND RELATIVE ABUNDANCE MEASUREMENT USING KRATOS MS-25S COUPLED TO THE BERKELEY LOGOS-II COMPUTER, A.L. BURLINGAME*+, J. D'ANGONA*, R. McPHERRON+ AND F.C. WALLS+, *Dept. of Pharmaceutical Chemistry, Univ. of Calif., San Francisco 94143 and +Biomedical Mass Spectrometry Resource, Space Sciences Lab., Univ. of Calif., Berkeley 94720

In line with our long-standing concern regarding the factors involved in routine performance of double focussing mass spectrometers, we have investigated the accuracy of mass and relative ion abundance measurement for the Kratos MS-25S coupled to our LOGOS-II/Xerox Sigma 7 computer system.

Since the MS-25S is a smaller geometry Nier-Johnson type instrument with electric hexapole lens before and after the magnetic sector, it was of interest to ascertain this information as a function of sample flow rate, scan rate and dynamic resolution for comparison with our earlier studies on performance of our MS-9 with hexapoles at resolving powers below 10,000 (1).

Evaluation of these parameters viz a viz various modes of instrument operation will be presented.

This work was supported by NIH DRR Grant RR00719.

1. A.L. Burlingame, J.J. Chang and P.T. Holland, 20th Annual Conf. on Mass Spectrometry and Allied Topics, Dallas, Texas, 1972, p. 287.

A SENSITIVE FIELD IONIZATION QUADRUPOLE MASS SPECTROMETER

Steven E. Young and S. E. Buttrill, Jr.
SRI International, Menlo Park, CA 94025

A commercially available volcano style field ionization source (Micronics) was interfaced with an Extranuclear Laboratories model 324-9 (3/4" rods) quadrupole mass filter. The source was fitted with a re-entrant focus lense and an entrance lense. The entrance lense consists of either a tube of nickel mesh perpendicular to a flat plate and extending into the quadrupole rod assembly or a similar arrangement with the Extranuclear ELFS ferrite tube. The detector uses a modified Galileo model 4770 continuous dynode electron multiplier. The ion entrance (hole in the front plate) to the multiplier has a diameter slightly larger than $2r_0$, is covered with 98% transmission mesh and is electrically isolated from other elements of the multiplier. The standard ion beam deflector was removed and replaced with one large enough for the new ion entrance hole. The bottom of the deflector consists of metal mesh to allow energetic neutrals to pass through.

Thymine (M.W. 126) was used for tuning up the instrument. Fifty ng samples of perylene (M.W. 252) were used for evaluation of the sensitivity of the instrument with the detector in the pulse counting mode. While monitoring m/z 252 the total number of ion pulses for the perylene sample were counted. This number divided by the number of molecules in the sample (1.19×10^{14}) gave an overall efficiency of 4×10^{-6}, with several measurements as high as 8×10^{-6}.

Typical voltages used are as follows: volcano +17 V, counterelectrode -1.82 kV, focus -75V, adaptor plate and ELFS -60V, front plate of multiplier -250V, ion beam deflector +150V, electron multiplier dynode -2900V.

The use of the ELFS biased at the optimum potential for a particular source lense configuration improves sensitivity by a factor of two compared with a tubular screen lense of similar geometry. If the ELFS is operated at ground potential, sensitivity is equivalent to that obtained with a biased tubular lense.

The major difficulty encountered was the necessity of maintaining precise alignment of the volcano ion source, counter electrode, and focus lense. Misalignment causes the ion beam to be focused off-axis and drastically reduces overall instrument sensitivity.

The present field ionization quadrupole mass spectrometer system is several orders of magnitude more sensitive than previous quadrupole systems. The sensitivity of 4×10^{-6} corresponds to 100 counts per 10 femtograms, an easily detectable signal. Of course, the major difficulty with samples of this size is introducing them into the mass spectrometer without significant contamination or loss. The well known advantages of quadrupole mass spectrometers (rapid scanning, multiple ion monitoring) will be of great value in future applications such as GC/FIMS.

NEW INSTRUMENTATION FOR MS/MS

G. L. GLISH, D. ZAKETT, P. H. HEMBERGER AND R. G. COOKS
CHEMISTRY DEPARTMENT, PURDUE UNIVERSITY W. LAFAYETTE, IN 47907

Mass spectrometry/mass spectrometry (MS/MS) is a rapidly growing technique.[1] The instrumental mainstay of the technique has been the reversed geometry instrument (BE or MIKES). We present here two recently constructed instruments whose performance will be compared to that of the BE instruments. The first instrument consists of a magnet (B) for one stage of analysis and a quadrupole (Q) for the other stage of analysis. The configuration that will be discussed here will be BQ, however, operation in the QB set-up is possible and will be discussed at a later date. The second instrument to be considered here is composed of two quadrupoles (QQ).[2] Schematics of the BQ, QQ and BE instruments are shown in Figure 1.

The major difference between the two new instruments and the BE is the energy of the ions when they undergo collision-induced dissociation (CID) between the two analyzers. The ion energy in the BE instruments is typically 3-7 kilovolts, while in the QQ it varies from 1-120 volts; in the BQ low energies are accessible and the upper limit is yet to be fixed. A comparison of the MS/MS spectra (collision-induced) of 5-indanol taken with the three instruments is shown in Figure 2. As can be seen, the BQ energy range effectively spans the gap between the QQ and BE as far as fragmentations are concerned.

A very exciting prospect for using low energy mass-selected ions is that not only do dissociations occur in the collision cell but also association reactions between the selected ion and target gas can occur.[3] Thus reactions similar to those observed in ion cyclotron resonance spectrometry are accessible and can be used for structure differentiation. An example of this on the QQ is the differentiation of the enol and keto forms of $C_3H_6O^+$. This is accomplished by the reactions shown in Scheme 1. With the BQ ion-molecule reactions can also be studied at energies greater than those available in icr, as is shown by the example of $Ar^+ + N_2 \rightarrow ArN^+ + N$ (and $N_2^+ + Ar \rightarrow ArN^+ + N$) from 30 to 100 ev. It is particularly noteworthy that the effects of relative kinetic energy on this type of reaction can be followed.

The usefulness of MS/MS for direct mixture analysis has been adequately demonstrated on BE instruments. Besides taking a normal MS/MS spectrum for confirmation of a species present in a mixture, one can also screen a mixture for certain type compounds by alternative scanning methods.[4] One such procedure is to scan the two analyzing sectors together at a fixed mass difference, thus detecting only ions that lose a certain neutral mass between the two analyzers. This is readily done on the QQ, an example being a neutral loss scan for the loss of 46 amu (NO_2) from a mixture containing both nitro compounds and others (Figure 3). Only the nitro compounds respond in the linked scan.

1. R. W. Kondrat and R. G. Cooks, Anal. Chem., 50, 81A (1978).
2. a) D. Zakett, W. J. Fies and R. G. Cooks, Anal. Chim. Acta., in press.
   b) M. W. Siegel, Anal. Chem., in press.
3. G. L. Glish, P. H. Hemberger and R. G. Cooks, Anal. Chim. Acta., in press.
4. a) D. Zakett, A. E. Schoen, R. W. Kondrat and R. G. Cooks, J. Amer. Chem. Soc., 101, 6781 (1978).
   b) W. F. Haddon, Org. Mass Spectrom., in press.

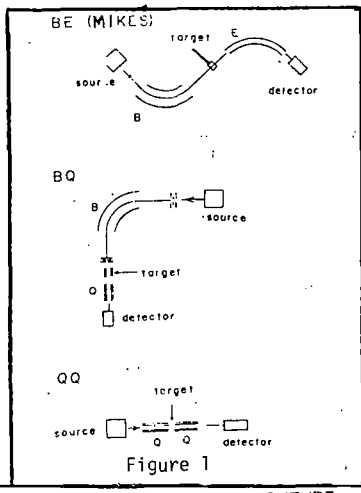

Figure 1

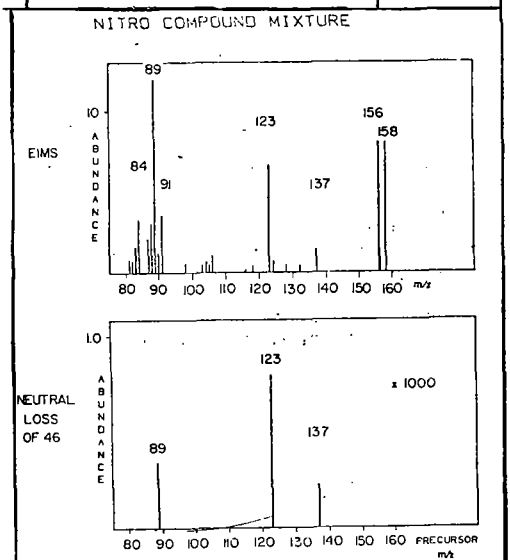

Figure 3

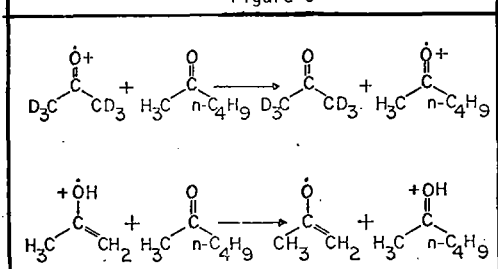

Scheme 1

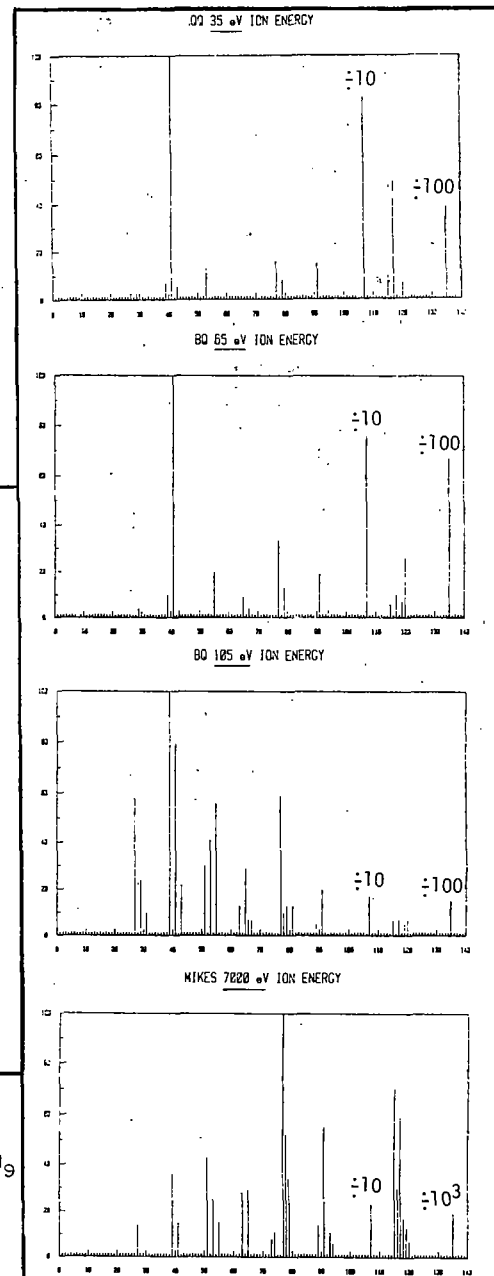

Figure 2

TPMP11 A MICROCOMPUTER BASED FOURIER TRANSFORM MASS SPECTROMETER, T. J. BUCKLEY, R. J. DOYLE, JR., and J. R. EYLER, Dept. of Chem., Univ. of Fla., Gainesville, FL 32611

In the past several years we have undertaken development of a Fourier transform ion cyclotron resonance (fticr) mass spectrometric detection system in our laboratories. Reports of our early progress have been given at the past two ASMS meetings.[1] As opposed to other fticr systems which utilize relatively expensive minicomputers for fourier transformation, our particular system is composed of two 6502 microprocessor-based computers in a master-slave configuration. The master microcomputer is an APPLE II and is primarily involved in program development, graphics, data analysis, and control of the slave. A KIM 1 microcomputer performs the routine tasks of the slave such as data acquisition, instrument control and production of pulses for the fticr electronics. Communication with our campus computer is also available by the use of an acoustic phone coupler.

Our fticr mass spectrometer is now working on a routine basis and is capable of signal averaging up to 4K of data points. By use of a differential amplifier, mixer, various filters and signal generators, all under computer control, we have obtained mass spectra with higher resolution and mass range than are capable from our conventional marginal oscillator detection system.

We will present system block diagrams and spectra of the limited (8-15 amu) regions which our system as currently configured can obtain. These will include spectra of certain bromine and chlorine ions (e.g. $(C_2H_5)_2Br^+$) chosen to test our ability to obtain accurate isotope ratios. We are currently expanding our system by adding a fast transient digitizer and frequency synthesizer, and interfacing it to a gas chromatograph. Any results obtained from these modifications will also be presented.

[1] 26th ASMS Conference, paper RD-6; 27th ASMS Conference, paper WAMP-14.

INFLUENCE OF ALIGNMENT ON THE PERFORMANCE OF ROUND ROD QUADRUPOLE MASS FILTERS

Donald M. Mintz

Finnigan Corporation
845 W. Maude Ave.
Sunnyvale, CA 94086

We are conducting theoretical investigations into the performance of round rod quadrupole mass filters. We seek to understand the variation of instrumental performance with degree of alignment of the round rods. The present study examines only those field distortions produced by symmetric displacements of the rods (e.g., change r/r_o).

Previous studies of mass filter performance have studied either only hyperbolic rod mass filters or simple perturbations from purely hyperbolic mass filters. Phase space methods[1] have principally been used under those circumstances, though peak simulation has been employed in one case[2], a comparison of optimized round rod and hyperbolic rod mass filters. Phase space methods become exceptionally cumbersome and lack rigor (x and y motions are no longer separable) when extensive perturbations of a purely hyperbolic field are present. Such is the case with a set of systematically perturbed round rods. Here the method of choice is peak shape simulation involving large numbers of ions.

The procedure for calculating peak shapes for a round rod mass filter is simple in principle. First, the electrostatic field is obtained inside the mass filter. Second, an ensemble of ions is propagated through that electrostatic field, which is temporally modulated. The variation of transmission percentage from that ensemble yields a mass spectral peak shape.

In practice, this procedure was modified in a compromise of accuracy and minimum run-time. As a start, only axially uniform mass filters were considered. The potential was calculated on a rectangular potential grid by the technique of successive overrelaxation using principally an 8-point solution to Laplace's equation. The irregular boundaries imposed by the curved boundaries required careful explicit compensation. Potential arrays were finally fitted to a two-dimensional multipole expansion:

$$\Phi(R,\theta) = \sum_{n=1} A_{2n} \left(\frac{R}{R_o}\right)^{2n} \cos(2n\,\theta)$$

by an accurate multi-linear least squares approach. Adequate convergence to a multipole expansion is obtained with an expansion extending only to 28-pole. Next, several types of rod misalignments were characterized in terms of the associated higher order multipoles (field faults) in the above expansion. This is facilitated by the near-linearity in the variation of field distortion multipoles with the corresponding physical distortions, for distortions generally 1% or less of r_o.

Particles were propagated in the analytic field determined by the multipole field, rather than in the gridwise-specified field originally calculated. This offered advantages principally in accuracy, but also in speed for particles near curved electrode surfaces. Initially, ions were taken uniformly distributed spatially on a 2.54 mm disk (r_o = 2.75 mm), with zero component of transverse velocity, and with a uniform distribution of initial RF phases. A variety of axial kinetic energies, ion masses, and RF frequencies was studied, as well as the extent of misalignment. Accurate integrations over many RF cycles were obtained using small time steps (1/600 of RF cycle) and a Taylor series integrator[3].

The following gross rod misalignments were studied:

1. changing r/r_o from 1.144 (optimum) to 1.15 and 1.16 (0.5% and 1.4% changes, respectively)
2. leave r/r_o = 1.144 for one pair of oppositely located rods and increase the r_o of the other opposite pair by 0.0127 mm (0.5%)

At low mass (m/e 40), those field perturbations produce very small effects on peak shape. Initial ion energy has a much stronger role in determining peak shape. At moderate mass (m/e 400), peak shapes are a strong function of both ion energy and extent of r/r_o distortion. As an example, at 5 eV, for spectra at equivalent operating (a,q) points, the peak for r/r_o = 1.144 was a bit more triangular in shape than the peak for r/r_o = 1.15. At the lowest energy studied, 1.3 eV, r/r_o = 1.16 produced pronounced double peaking, which is probably due to one of the resonant effects discussed by Dawson[4]. In addition, the variation of peak shifts and peak broadening predicted for optimized round rod filters as compared to hyperbolic rod filters confirms Pocek's earlier findings[2].

References

1. P.H. Dawson, M. Meunier, Int. J. Mass Spectrom. Ion Phys. 29, 269 (1979)
2. K.L. Pocek, PhD. Thesis, Stanford University, 1979.
3. C. Weber, Philips Tech. Rev. 24, 130 (1962).
4. P.H. Dawson Quadrupole Mass Spectrometry and its Applications (Elsevier, Amsterdam, 1976) Chap. 5

TPMP13 SOME OBSERVATIONS ON THE DETECTION AND AMPLIFICATIONS OF ION CURRENT SIGNALS, WILLIAM J. FIES,

Research Department, Finnigan Corporation, 845 W. Maude Avenue, Sunnyvale, CA 94086

This report attempts to set down some practical guidelines for the design of the electrometer and subsequent signal processing system for use with a quadrupole mass spectrometer. It combines theoretical treatment with measurements on a real system. It treats the range of signal amplitudes and bandwidths that are applicable to GC/LC-MS and to solid probe MS analysis (greater than 10 ions/sec and greater than 1 Hz bandwidth). Therefore, no treatment of counting systems is included. It will be shown that Johnson noise is not a factor and can be ignored, that amplifier noise can be overcome by use of an electron multiplier with reasonable gain, and that that the theoretical limit set by the quantum noise of the ion beam (shot noise) is generally the detection limit. Under these conditions the detection limit and the bandwidth (and, hence, the scan rate) are inversely related in a fundamental way that does not depend on the quality of the detection system.

MODIFICATION OF A CEC-21-110 TO ALLOW FOR RAPID SCANNING

G. J. Greenwood, J. F. Stewart and D. M. Cantor
Phillips Petroleum Company, Bartlesville, Oklahoma 74004

Replacement of the magnet and electric sector power supplies on the CEC 21-110 high resolution mass spectrometer with programmable solid state supplies has allowed rapid reproducible scanning under either computer or manual control. This new equipment allows increased system flexibility and simplified operation and maintenance. Our experience with the new system shows extremely high reliability.

The new electric sector power supply shown in Figure 1 allows the operator greater flexibility, stability, and tuning control than was originally available on the 21-110 mass spectrometer. The new control unit and power supplies allow:

1. Repetitive scanning at selectable sweep times of 0.1 s to 6 s.
2. Continuously variable sweep width.
3. Variable +10 Volt offset to each of the ESA plates with respect to chassis common.
4. Manual scanning control over the accelerating potential.
5. Programming of the ESA supplies for metastable studies.

The power supplies for the electric sector plates are two Fluke 4156 high voltage supplies. The supplies were modified to allow the voltages to be referenced with respect to the ESA control unit in Figure 1. The supplies provide a 100, 200, 300, or 400 V reference to the ion accelerator and allow acceleration potentials of 8, 6, 4, and 2 kV. Voltages are selected through panel switches on the Fluke power supplies. The scan speeds are varied by a 50 KΩ 10 turn potentiometer. Scan width is adjusted by varying a 10 KΩ potentiometer that controls the amplitude of the sawtooth. Since the positive ESA power supply is the reference for the ion accelerator, the accelerating potential can be scanned manually over a 10 mass unit range by varying the potential of the positive power supply (Mass Offset). The ESA is kept in focus with respect to the accelerating potential by varying the voltages on both the positive and negative power supplies. Balance and focusing of the ESA plates is accomplished by using an additional power supply to float the scanning circuit with respect to ground. Voltages on both ESA plates can be varied plus or minus with respect to ground by varying the output from the floating (scan) common. Balancing of the ESA plate potentials can also be accomplished by varying the front panel switches of the Fluke power supplies. Short term stability (<20 min.) of the circuit is <10 ppm.

The new magnet supply shown in Figure 2 is similar in configuration to that provided with the instrument. However, the new unit allows the analyst much greater flexibility. The new control unit and power supply allow:

1. Digital control of scan speeds via a front panel thumbwheel switch.
2. Rapid changeover from uncalibrated to calibrated settings.
3. Continuously adjustable scan speeds between 10 dec to 2000 dec.
4. Manual and computer control of scan start and stop.
5. Manual course and fine control settings.

The Hewlett-Packard 6274B power supply is run in the voltage programming mode and maximum output voltage to the magnet is limited by zener diodes. Scan speeds used for computer acquisition of mass spectral data are set digitally by fixed resisters, a 10 μf polycarbonate capacitor and an 8-channel analog multiplexer (Analog Devices, AD7503). Using the configuration shown in the schematic scan speeds of 10, 15, 30, 60, 120 and 240 seconds/decade can be achieved. A continuously variable scan speed is also available, using a 5 MΩ potentiometer. Longer scan speeds are obtained by switching a 2000 μf capacitor into parallel with the 10 μf capacitor. The unit was found to have a short term stability (10 minutes) of <10 ppm. The time required to reset the magnet from 1.5 kilogauss to 8.5 kilogauss is 15 seconds. This figure could be lowered further by using 40 volt zener diodes in the Hewlett Packard power supply. For our applications, a 15 second reset is adequate. Therefore, a total scan and reset of the magnet could be taken from m/e 800-m/e 28 (at an 8 KV in ion acellerating potential) every 30 seconds. In our laboratory, mass calibrations have been holding for 2-4 weeks. This is taken to be indicative of the magnet supply's stability.

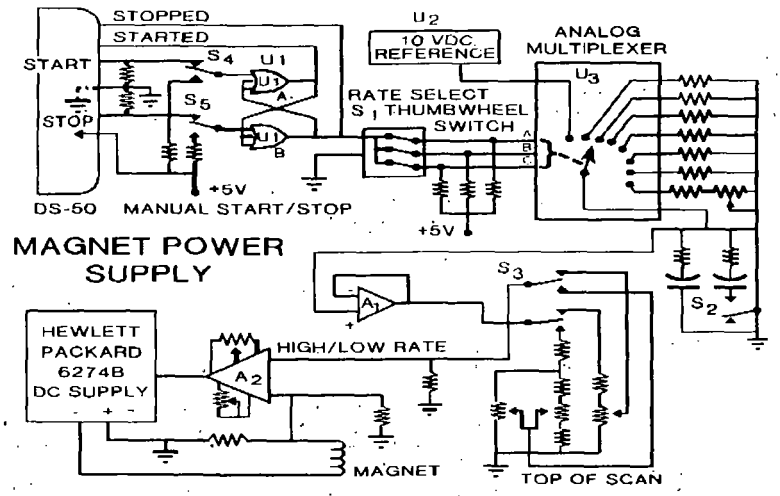
STOPPED
STARTED
START
STOP
S4
U1
S5
U1
A
U1
B
+5V
DS-50
MANUAL START/STOP
U2
10 VDC
REFERENCE
ANALOG
MULTIPLEXER
U3
RATE SELECT
S1 THUMBWHEEL
SWITCH
A
B
C
+5V
MAGNET POWER
SUPPLY
S3
A1
S2
HEWLETT
PACKARD
6274B
DC SUPPLY
HIGH/LOW RATE
A2
MAGNET
TOP OF SCAN

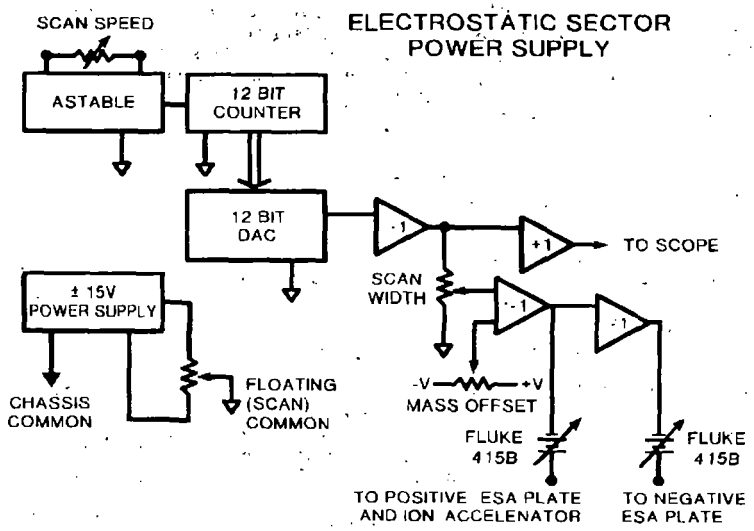
SCAN SPEED
ELECTROSTATIC SECTOR
POWER SUPPLY
ASTABLE
12 BIT
COUNTER
12 BIT
DAC
-1
+1
TO SCOPE
SCAN
WIDTH
± 15V
POWER SUPPLY
-1
-1
CHASSIS
COMMON
FLOATING
(SCAN)
COMMON
-V
+V
MASS OFFSET
FLUKE
415B
FLUKE
415B
TO POSITIVE ESA PLATE
AND ION ACCELENATOR
TO NEGATIVE
ESA PLATE

TPMP16 THE INVERTED PENDULUM AS A MODEL OF THE QUADRUPOLE MASS FILTER

A.L. Yergey[1], M.H. Friedman[2], J.E. Campana[3], L. Kelner[4] and E.H. Seeliger[1]

[1]NICHD and [4]BEIB, NIH, Bethesda, MD20205
[2]MERADCOM, U.S. Army, Ft. Belvoir, VA 22060
[3]Department of Pharmacology and Experimental Therapeutics
Johns Hopkins Medical School, Baltimore, MD 21205

A pendulum can in theory be made to undergo stable oscillations above, rather than below, its point of support, by providing an oscillating vertical drive force to the support point. The equation of motion describing these stable oscillations can be expressed in the canonical form of the Mathieu equation, and thus the inverted pendulum can serve as a mechanical analog of an ion undergoing stable oscillations in the normally unstable yz plane of a quadrupole mass filter. We have made an inverted pendulum apparatus for both pedagogical purposes and for experimentally verifying expressions for the calculation of the characteristic exponent, β. The equation of motion for the pendulum results directly from application of the Lagange equation to expressions for the kinetic and potential energy of a thin solid rod pendulum:

$$T = (1/2)\,\dot{\theta}^2 I + (1/2)\,m\dot{Z}^2 - \dot{\theta}\dot{Z}\,(ml/2) \qquad (1)$$
$$V = (mgl/2)\cos\theta \qquad (2)$$

where T and V are the kinetic and potential energy respectively, θ is the angle the pendulum makes with the vertical, $\dot{Z}$ is the motion of the support point in the vertical axis, m and l are the mass and length of the pendulum, I is the moment of inertia of the pendulum, and g is the acceleration due to gravity. The geometry of the inverted pendulum system is shown in Fig. 1.

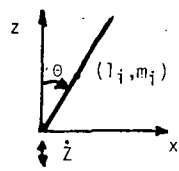

Figure 1

In putting the equation of motion into the canonical form of the Mathieu equation, (3) is obtained:

$$\ddot{\theta} - (3/2\ l)\,(g + b\omega^2 \cos wt)\,\theta = 0 \qquad (3)$$

where b and ω are the amplitude and frequency of the driving oscillation and t is time. The unitless parameters, a, q, u and ξ are defined in equation (4) as:

$$u = \theta, \quad a = -6g/l\omega^2, \quad \xi = \omega t/2, \quad q = 3b/l \qquad (4)$$

and the Mathieu equation can then be written in canonical form. The equation of motion of an ion in the yz plane of the quadrupole mass filter is:

$$\ddot{y} - \frac{2e}{r_o^2 m}\,(U + V\cos\omega t)\,y = 0 \qquad (6)$$

Comparison of equations (3), (4) and (6) shows that the angle the pendulum makes with the vertical, θ, is analogous to the displacement from the quadrupole axis, y, that the analog of (e/m) in the quadrupole is l^{-1} in the pendulum, that the potential terms g and U for the pendulum and quadrupole are analogs and that the terms for the amplitude of the oscillation, b and V, are analogous.

Demonstration of these analogies is made by observing the functioning inverted pendulum apparatus. The device consists of a rotating wheel that connects by a drive rod to a shaft upon which the pendulum support point is located. The shaft is supported by a linear bearing. The pendulum support shaft is driven at frequency ω by rotating the drive wheel. The value of ω is set by the speed of the DC motor rotating the wheel. The amplitude of

the support point oscillation is set by the amount of eccentricity in the drive rod mounting. Typical operating values for a rigid rod pendulum of 15 cm length are an amplitude of 3 cm, with the wheel operating at 550 RPM (appox. 8.2 Hz). Operation of the inverted pendulum in upright oscillation at a variety of conditions was photographed using a high speed motion picture camera[2]. Calibration of the film speed by photographing a watch sweep second hand permitted the calculation of precise drive frequency and fundamental oscillation frequency values. These two quantities were used to calculate the characteristic exponent, β, from the expression given by Dawson[3]:

$$\omega_o = \beta\omega/2 \qquad (7)$$

where ω_o and ω are the fundamental and drive frequencies respectively. These experimentally determined quantities were compared to values of β calculated from expressions given by Langmuir[4] and McLachlan[5].

In general the observed values of β are about 16% higher than those obtained from calculation, but are within an acceptable range of experimental error. The differences probably arise from use of less than ideal bearings in mounting the pendulum to the support point, and from use of a non-sinusoidal drive.

References

1. P.H. Dawsan (ed.), Quadrupole Mass Spectrometry and Its Applications, Elsevier, Amsterdam, 1976, p. 13.

2. Copies of the film or a video-tape made from it may be obtained from ALY.

3. Dawson, ibid, pg. 19.

4. R.F. Wuerker, H. Shelton and R.V. Langmuir, J. Appl. Phys. 30, 343 (1969).

5. N.W. McLachlan, Theory and Application of Matheiu Functions, Oxford University Press, New York, 1947.

THE PERFORMANCE OF A FULLY LAMINATED MAGNET FOR AN INTEGRATED GC/MS/DS COMBINATION, P. BURNS, B.N. GREEN AND D.S. MILLINGTON, VG-Organic Ltd., Tudor Road, Altrincham, Cheshire, England WA14 5RZ.

INTRODUCTION

Previously, magnetic sector instruments have compared unfavourably with quadrupoles in two main areas, namely, speed of changing mass over a wide range and ease of mass control. Most of these limitations can be ascribed to the electromagnet design and its method of control. Several commercial instruments already have partially laminated magnets which give improved speed, while the use of Hall probes for field control has helped to improve control of mass. Nevertheless, eddy currents in the magnetic material seriously limit the performance of sector instruments at the speed required for the analysis of capillary column eluents.

A major breakthrough has been achieved with the production of a fully laminated magnet for the VG-Micromass 70-70, in which eddy currents have been drastically reduced. With this magnet plus an appropriate power supply, scan rates down to 0.1 second per decade and cycle times of less than 0.3 second per decade in mass are obtained. Moreover, the defocusing effects which occur at fast scan rates with conventional magnets are greatly reduced. More significantly, by the virtual elimination of eddy current effects and lower hysteresis, wide range magnetic selected ion monitoring has become practicable, with ultimate cycle times for 4 masses in the range 50-500, for example, reduced to below 0.3 second.

SCAN PERFORMANCE

Assuming the power supply has sufficient capacity to change the current in the inductance of the magnet, it is the build up of eddy currents in the core and poles which sets a practical limit to the scan rate achievable. With the 5 inch radius magnet of conventional design, eddy current limitations become significant at about 500 ms/decade. Moreover, even at slower rates, eddy currents in the pole tips cause a change in the focus of the ion beam, necessitating refocusing the instrument for different scan rates.

With the laminated magnet, the scan rate limit set by the core itself is less than 30ms/decade. In addition, changes in the focus with scan rate have been reduced. For example, at 5000 resolution with the focus optimised statically, there was no significant reduction in the resolution down to 1.5 seconds/decade.

The ultimate scan rate with full mass range coils (800 at 4kV ion energy) driven by a 50 amp power supply is about 150ms/decade. Figure 1 is a UV recording of a complete scan cycle over the mass range 614-25 with field control using a Hall probe. A mixture of perfluorotributylamine and air was used as a sample. The scan rate was 190ms/decade and scan was started with the mass spectrometer tuned to the 614 peak at about 700 resolution. Note that at the end of the reset time of 170ms, the instrument was tuned to the 614 peak again ready for the next scan, indicating the excellent reproducibility of the scan cycle, ideal for data system control. The cycle time was 440ms.

By using smaller coils which give a reduced mass range of 600 at 4kV, even shorter cycle times can be achieved. This is illustrated in Figure 2 where the scan rate was 110ms/decade and the cycle time 255ms. Again note that the mass spectrometer was tuned to the same peak at the beginning and end of the scan cycle, in this case the 502 peak.

SELECTED ION MONITORING (SIM) PERFORMANCE

As with scanning, magnetic SIM with solid core magnets is speed limited by eddy currents. Also, until the eddy currents die down, they give rise to an error between the field measured by the Hall probe and the field experienced by the ion beam. With the laminated magnet these effects are insignificant and low resolution magnetic SIM has become feasible.

As an illustration, Figure 3 is a UV recording of the mass spectrometer output made whilst the magnet was being switched to select 4 peaks at masses 50, 119, 414 and 502. These masses were tuned in statically and within the limits of the flat top on the peaks (about 500 ppm) were at the same settings dynamically. In this example, the smaller coils were used. The cycle time was 670ms out of which 100ms was spent on each peak measuring the intensity giving a total settling time per cycle of 270ms.

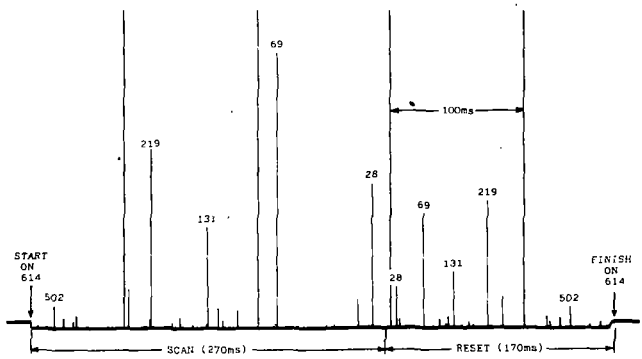

Figure 1. 190ms/decade field controlled scan cycle taken with the laminated magnet on the MM7070HS. Cycle time 440ms.

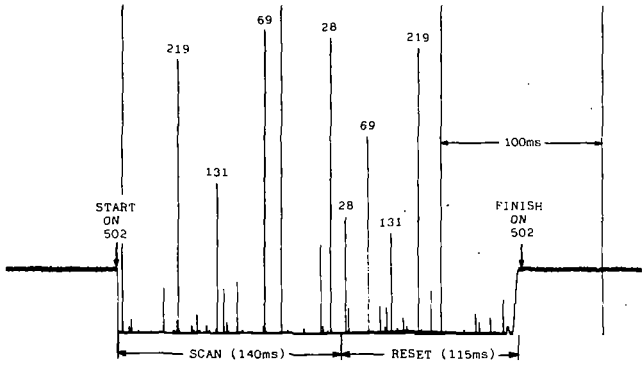

Figure 2. 110ms/decade field controlled scan cycle taken with the laminated magnet on the MM7070HS. Cycle time 255ms.

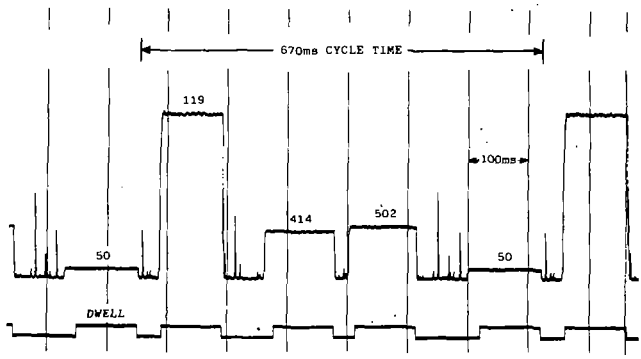

Figure 3. Wide mass range selected ion monitoring with the laminated magnet on the MM7070HS. Settling time per cycle 270ms.

A SIDE-ENTRY FIELD DESORPTION PROBE SYSTEM FOR A 21-110 MASS SPECTROGRAPH, D. F. BAROFSKY & W. R. ANDERSON, JR., DEPT. CHEM. & BIOCHEM. SCI., OREGON GRADUATE CENTER, BEAVERTON, OR 07005; AND T. J. ESKEW AND L. F. HERZOG, NUCLIDE CORP., STATE COLLEGE, PA. 16801

We have designed and tested a combined FI/FD ionizer to retrofit conveniently to 21-110 mass spectrographs with electron bombardment (EI) sources. This ionizer-probe is unusual in that it inserts from the side, using an existing port. This leaves the large end-port of the 21-110 open for the addition of a very high speed pumping system, suitable for CI work, etc.

It is also similar in design to the newest FI/FD probe Nuclide offers for it's 12-90-G spectrometer and GRAF-III spectrograph.

Switchover between FI and FD operation and EI ionization is instantaneous; EI-mode operation is unimpaired.

The new ionizer has been extensively tested in continuing FD-mode investigations of peptides at the Oregon Graduate Center. The 21-110 it modifies has also been equipped with a very high-speed source pump attached via a "tee" housing; this provides a large window for viewing the source region.

Sensitivity in the FD operating mode is sufficient to provide intense photoplate spectra from 10 nanogram to microgram sized peptide samples.

Once it has been properly positioned, the probe can be removed and reinserted dependably without tedious readjustment, and exhibits good positional stability when in use.

A routine run requires approx. 15 minutes from the beginning of probe insertion through the completion of probe removal and loading of the next sample.

It is anticipated that this design can be adapted to many mass spectrometers of other makes and models.

Probe Design Considerations

We elected to have the probe enter the ionization chamber from the side, parallel to the source lens plates, because the relative position of emitter and slit (optical axis) is the adjustment that affects intensity most significantly.

A fine-threaded micrometer mechanism was therefore included in the design, for adjusting the emitter's position in the plane parallel to the cathode while the MS is in operation.

Another mechanism was provided for setting the emitter-to-cathode spacing of the probe. This was made "bench" adjustable, because once this distance is set correctly, readjustment is required only rarely.

Electrical connections are made inside the vacuum via a "docking" mechanism, to avoid the need to carry high voltages out through the probe, which would entail substantial complications.

The probe is supported by two bearings, 200 mm apart, to minimize position-drift and consequent deterioration of performance during operation.

Optimizing Operating Conditions

Optimal operating conditions were determined by generating a set of transmission-curves for various emitter positions and source potential values.

Example of Operation: Peptide Studies

Initial use of the new probe has been in studies of peptides. Some results of these investigations will be presented at this conference as paper WAMOB3, "Field Desorption Mass Spectrometry of Oligopeptides" by D. F. Barofsky et al.

In these studies, until now photoplate recording of FD spectra has been used exclusively. The amount of peptide sample required to obtain a spectrum ranges from a few nanograms to about 0.5 microgram, depending on the behavior of the particular compound on the probe.

After the probe is inserted, the emitter's position is optimized by maximizing the field ionization (FI) signal of bromobenzene (which is leaked into the source continuously), using the electron multiplier detector. Magnetic field is then adjusted to focus the mass range of interest onto the photoplate, and emitter heating is commenced, using the total ion monitor plate to monitor the heterogeneous ion current. Ordinarily, complete sample evaporation requires about a minute. Afterwards, the emitter is flashed to 1000°C to clean it. Emitters are sometimes used more than 50 times.

After taking an FD spectrum, the photoplate is racked and an EI spectrum of perfluorokerosene is recorded just below it to provide "chemical mass marker" lines from which to measure the masses of lines of the unknown.

Emitter Conditioning

A new FI/FD emitter-conditioning system with special features for side-entry emitters has also been designed and tested at Oregon Graduate Center.

One objective was to keep this system as inexpensive as was consistent with good practice. Consistent with this, the vacuum chamber consists of a glass cylinder, removable to facilitate cleaning, with a metal cap-plate. It is mounted on a lucite base through which the electrical leads are brought.

Since benzonitrile, used to activate emitters, deteriorates some greases, silicone is used for vacuum seals. However, Santovac was found to be an acceptable pumping fluid. Benzonitrile flows-through continuously at approx. 10^{-2} torr; activation is less successful with a "static" atmosphere of benzonitrile.

Up to six emitters can be conditioned at once. Each has its own power supply for heating, and electrometer for measuring current. Each emitter is in it's own. pie-slice shaped wire-mesh chamber; these have an arc of a common cylindrical (mesh) outer cylinder as one wall. A glass liner surrounds the mesh cylinder. Six phototransistors disposed at 60° around the outside of the glass vacuum chamber measure the temperatures of individual emitters. A common HV supply is used; it can be set at 5, 7.5 or 10 kV.

Currents are 10^{-9} to 10^{-7} amperes; activation typically requires eight hours or more.

Emitters are 8 micron tungsten, nickel-welded to tungsten posts, then cleaned electrolytically in H_2SO_4, using a technique described more fully in IJMSIP (Vol. 14, PP 3-14 (1974)).

The complete text and figures for this paper will be furnished on request to Publications Dept., Nuclide Corporation.

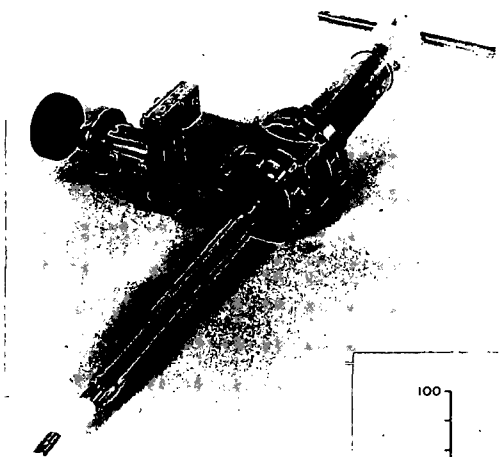

Side-Entry FI/FD Probe

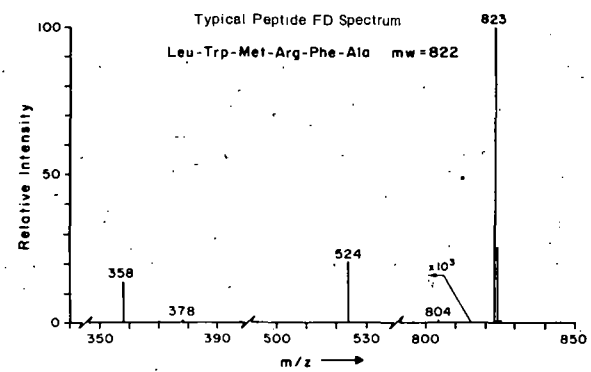

ADVANTAGES OF "MULTI-RADIUS" MAGNETIC MASS SPECTROMETERS FOR RAPID SCANNING APPLICATIONS,

L. F. HERZOG, NUCLIDE CORP., 642 E. COLLEGE AVE., STATE COLLEGE, PA. 16801 AND D. J. MARSHALL, AGV-NUCLIDE, P. O. BOX 135, ACTON, MA 01720

Multiradius mass spectrometers are magnetic-analyzer instruments with two or more ion detectors disposed at various radii.

Such instruments have been used for a long time with magnetic and electric fields fixed; well-known examples are:

(A) Multi-isotope simultaneous-detection arrays - e.g., for m/e 44-5-6 of CO_2, or the 5 isotopes of Nd, etc., and

(B) Mass spectrographs, detecting all masses between, e.g., M and 36 M on a photographic plate, simultaneously.

However, instruments with many ion detectors covering a wide mass range also offer, we believe, numerous advantages in applications requiring spectrum scanning and selected ion monitoring. The scanning mode is discussed in this paper. Some of the advantages we believe "MRMS" offers for obtaining spectra are the following:

1. Increased dynamic range can be achieved by using, simultaneously, both Faraday cups and electron multipliers, having as wide a range of gains and detection limits as fits the application.

2. High resolution and low resolution spectra can be obtained simultaneously - by setting the collector (image) slits of different detectors at different widths.

3. Increased sensitivity results:

(A) Since "N" collectors are operating simultaneously, for wide-mass-range scans, ion detection efficiency will increase N-fold if all have identical sensitivity

(B) However, the efficiency increase will usually be much greater than N-fold, since ordinarily only one detector need be set for whatever the highest resolution required may be. The rest can all have wider slits and hence higher sensitivities.

4. "Effective" scan rates can be faster, for a given scan rate, since no single collector need scan the full mass range of interest. This is especially helpful as regards magnetic scanning, for which fast scans rates (e.g., 1 sec/decade) introduce serious complications. For example, if an instrument with one detector has a maximum scan rate of 3 sec per mass-decade it can scan more than one decade in 1 sec if a second detector is added at a radius such that it detects M/4 when the first detector detects M.

5. Actual scan rates (relative to a single detector) can be much greater - since electric-field (e.g. H.V.) scanning alone can often cover the entire desired mass range, when it is divided into overlapping segments scannable by varying ion acceleration by, say a factor of 3 to 8. (Rates approaching T-O-F MS scan rates can in fact be used.)

6. Often, the ion analyzer can be a permanent magnet, since, if there are detectors at high, medium, and low radii, ion acceleration voltages so low they are inefficient with respect to ion transmission need not be used in order to focus high masses onto a detector.

7. Exact mass determination is facilitated - since "known" peaks in a spectrum, recorded at radii R_1, R_2, R_3, etc. can be used as reference masses from which the masses of species recorded at R_N can be calculated.

Useful configurations:

Most magnetic analyzer configurations are amenable to multiradius detection, including designs which only provide excellent focus at one point; these can be used, e.g., in cases when it is permissible for resolution (measured in terms of $\Delta M/M$) to decrease as mass decreases - as it does, for example, in quadrupoles which have so-called "unit" resolution.

We first applied this technique to a 6"60° sector analyzer, in a so-called "wide range" multiple Faraday cup detector instrument we first offered in 1958. It appears retrospectively that the idea was premature then, the range of applications being limited, largely, by limitations in data processing which existed before computers.

More recently, it was applied to our 3-60-Sectorr, an inexpensive MS often used for "surveys" of gas samples, in which constituents of interest may cover a concentration range as high as 10^7. This range was provided by placing an electron multiplier and a Faraday cup behind slits placed side-by-side near the symmetrical focus. Indeed, such a tandem detector can cover the entire range from 100% to one part per billion, as exhibits presented in this paper illustrate.

Another (two-pen) recorder trace presented herewith shows how, by using slits of different widths, one can also scan simultaneously at two resolutions. Indeed, by making one or both of these slits externally variable, one can also vary the resolution at will.

In order to be able to reduce scan speed significantly to cover a given mass range, or eliminate the need to use an electromagnet, however, one must place the detectors at radii which are quite different. In the 6-60-WR (mentioned above) the ratio of masses simultaneously detected by the highest and lowest mass detectors was six. In a version of the 12-90-G we now offer, it is 8. If one then scans the ion acceleration over a factor of five, say from 1000 to 5000 volts, the mass range covered in a single scan is M to 40M - for example, mass 25 to mass 1000.

In a double-focusing Mattauch-Herzog mass spectrograph such as our GRAF-III, the mass range available in excellent double focus at a single setting may range from M to 50 M - i.e. mass 12 to mass 600. The focal plane is some 40 cm long, hence many discrete detectors can be mounted behind slits along it. These can include multipliers and F-cups. With such an ion detection array, one need only scan over a very short range of ion accelerating voltages to obtain a comprehensive mass spectrum of say, the mass range 12-1200 amu.

As regards efficiency, as well as resolution capabilities, there is no doubt that that spectrograph design is best with which one can manage to pack along the photoplate enough detectors to sample all m/e simultaneously - for example, using an array of tiny electron multipliers. Hence we, and others, have such systems under development currently.

The complete text of this paper, with the slides, is available from the authors on request. (Paper MPMOA1F discusses the utility of multi-radius detector arrays for selected ion monitoring.)

Graf III Spectrograph - Typical Locations for Multi-Radius Simultaneous Ion Detection

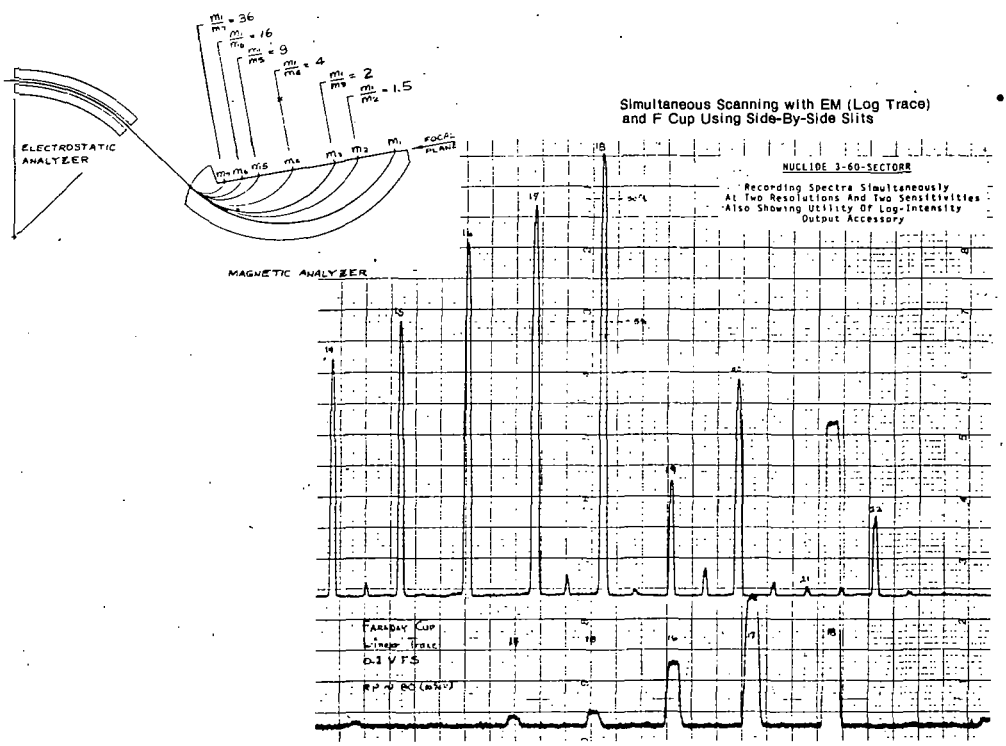

RECENT APPLICATIONS OF A TANDEM DOUBLE-FOCUSING MASS SPECTROMETER

M.P. Barbalas, P.J. Todd, P.F. Pagano, R.F. Pegues,

and F.W. McLafferty

Department of Chemistry, Cornell University, Ithaca, New York 14853

A tandem double-focusing mass spectrometer of increased resolution and sensitivity has been described separately at this meeting.[1] This paper outlines a variety of ion structure and mixture analysis problems to which it has been applied.

Isomeric $C_3H_6^{+\cdot}$ ions of cyclopropane and propene structures can be distinguished by the very small abundance difference (0.08% vs. 0.14% of base peak) in the doubly charged ions in their collisional activation (CA) spectra.[2] CHN^+ and CH_2N^+ isomers have been studied; after high-resolution separation of interfering $C_2H_3^+$ ions, CA spectra show that HNC^+ and HCN^+ ions have different structures. HNC^+ is more stable, being formed from nitriles, isonitriles, N-methyl-substituted formamides, and pyridine. $HC{\equiv}NH^+$ is the only CH_2N^+ isomer formed from a variety of precursors, including CH loss from CH_3CN; measurement of these spectra necessitated separation of the CH_2N^+ precursor ions from interfering C_2H_4, CO, N_2, and ^{13}CHN ions. In confirmation, $HCND^+$ and $DCNH^+$ ions give different CA spectra.[3] Contrary to a previous study, the CA spectra of benzoyl ions are independent of ion internal energy; only one isomer is formed from a variety of precursors.[4] A data base (printed or magnetic tape) containing reference CA spectra of over 500 different ions may be obtained from the authors.[5]

Studies have been made on the determination of tetrachlorodibenzodioxin (TCDD) at trace levels without the need for extensive cleanup or the use of gas chromatography. Following favored techniques for ppt TCDD determination by high-resolution MS, the *m/z* 322 peak of TCDD is separated at high (11,000) resolution. The CA spectrum of this shows a unique peak for the loss of COCl not found in the spectra of possible interfering ions from common contaminants such as PBCs and DDE; separation of the CA peaks by high resolution in MS-II greatly reduces the interference from the $(M - Cl_2)^+$ ions of the contaminants. A CA peak for benzo loss provides a valuable indication of the distribution of chlorine atoms between the aromatic rings of isomeric dioxins. Several other analytical determinations of specific larger molecules in highly complex mixtures are being investigated, for which the high resolution MS-I in effect serves as an efficient cleanup procedure,

with specific identification by multiple ion monitoring in the high-resolution MS-II.

---

[1]F.W. McLafferty, P.J. Todd, D.C. McGilvery, and M.A. Baldwin, J. Am. Chem. Soc., 102, 3360-3 (1980).

[2]R.D. Bowen, M.P. Barbalas, F.P. Pagano, P.J. Todd, and F.W. McLafferty, Org. Mass Spectrom., 15, 51 (1980).

[3]F.W. McLafferty and D.C. McGilvery, J. Am. Chem. Soc., accepted.

[4]F.W. McLafferty, A. Hirota, M.P. Barbalas, and R.F. Pegues, Int. J. Mass Spectrom. Ion Phys., accepted.

[5]F.W. McLafferty, A. Hirota and M.P. Barbalas, Org. Mass Spectrom., accepted.

METASTABLE SPECTRA OF COMPLEX MIXTURES: LINKED SCAN TECHNIQUES APPLIED TO PHARMACEUTICAL FINAL PRODUCT IDENTIFICATION TESTING

Wayne K. Duholke and Lloyd E. Fox
The Upjohn Company, Kalamazoo, Michigan 49001

The potential of linked scanning mass spectrometry as a highly specific method for the identification of small quantities of drug in complex pharmaceutical mixtures was investigated. While the early studies of metastable ions (1-3) were primarily dedicated to structural elucidation and the determination of fragmentation pathways in pure compounds, they also suggested that metastable studies and, in particular, linked scanning could be very valuable in mixture analysis (4).

To determine the value of linked scan metastable studies on a conventional geometry double-focusing instrument such as the VG-7070, the direct non-separative identification of prostaglandins in suppository and tablet bases and steroids in topical creams and ointments was investigated. For these product classifications, the present final product identification method is TLC separation and UV readout. These products cannot be identified by infrared spectroscopy without time-consuming separative chemistry.

In the chemical ionization spectrum of the prostaglandin dinoprostone (PGE_2), using ammonia reagent gas, two major fragment ions and a large molecular ion are seen (Figure 1). However, the corresponding spectra of the suppository base and the actual product clearly show that identification without prior separation of drug from excipient would not be possible by employing only chemical ionization mass spectrometric techniques.

In contrast, the B/E linked scan spectra of the same entities are shown in Figure 2. The molecular precursor ion at m/z 352 for the prostaglandin and the characteristic daughter ions at m/z 335 and m/z 317 corresponding to $(M-OH)^+$ and $[M-(H_2O+OH)]^+$, respectively, are easily seen in the clean spectrum of the suppository product. The excipient provides little contribution to the precursor ion intensity and no detectable contributions at the masses of the daughter ions. The B/E linked scan analysis shown in Figure 3 of the tablet product and excipient of the same prostaglandin also showed high specificity. The excipient exhibits some ion intensity at the mass of the drug precursor but no significant ion population at the masses of the daughter ions.

Since dinoprostone and the other prostaglandins are fairly labile compounds, a relatively cool source temperature of 150°C was maintained. Ample daughter ions were measurable without collision gas for all of the prostaglandins tested. The steroids, being more stable, were analyzed at a higher source temperature of 250°C and required a collision gas in the first field-free region to induce dissociation of the protonated molecular ions. In the example shown in Figure 4, the excipient of a topical cream product does exhibit ions in the region of the product/bulk drug protonated molecular ion but nothing detectable in the region of the daughter ions. Figure 5 shows an example where the excipient contribution to the product's linked scan spectrum is considerable, but there is no interference at the mass of the major daughter ion, m/z 357. This particular product contains only 0.025% active drug.

The previous examples used only the B/E linked scan spectra of the dissociation of the metastable molecular ion for identification. However, the linked scan technique can often be applied to the dissociation of a characteristic fragment ion with little loss of specificity. For example, consider 15(R)-15 methyl PGE_2, molecular weight 366 and fragments at m/z 348 and m/z 330. The linked scan spectra of these two fragments as shown in Figure 6 are still highly distinctive. Therefore, if there is no molecular ion or an unacceptable amount of interference from the excipient in the region of the drug's molecular ion, a daughter ion spectrum of a characteristic ion precursor in a cleaner region of the spectrum could be used.

The representative list of steroids and prostaglandins in Table I was subjected to B/E linked scan analysis. Characteristic daughter ion spectra were obtained in all, though a few of the steroids such as prednisone, prednisolone and hydrocortisone provided only weak daughter ion spectra due to their very stable pseudo-molecular ions.

The B/E linked scanning technique was shown to have potential for qualitative mixture analysis in pharmaceutical preparations. The specificity of the method was maintained for both prostaglandin and steroid product categories with little interference from excipients such as suppository or ointment bases. Non-separative final product identification tests can be performed with rapid, direct measurements.

References:

1. R. G. Cooks, J. H. Beynon, R. M. Caprioli and G. R. Lester, "Metastable Ions," Chap. 5, Elsevier, Amsterdam, The Netherlands, 1973.
2. F. W. McLafferty, et al, J. Amer. Chem. Soc., 97, 2298 (1975).
3. R. W. Kondrat and R. G. Cooks, Anal. Chem., 50, 85 (1978).
4. G. L. Glish, V. M. Shaddock, K. Harmon and R. G. Cooks, Anal. Chem., 52, 165 (1980).

FIGURE 1

NH_3 CI MASS SPECTRA

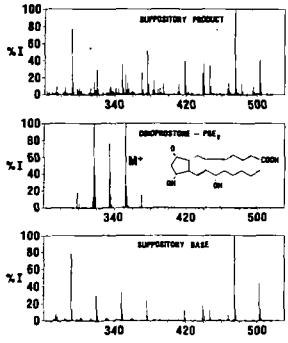

FIGURE 2

NH_3 CI B/E SCAN FOR DAUGHTER IONS OF M^+

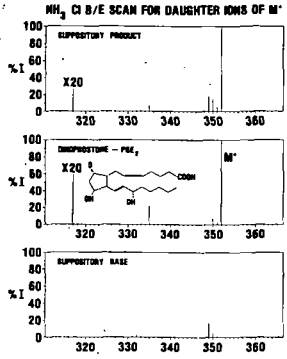

FIGURE 3

NH_3 CI B/E SCAN FOR DAUGHTER IONS OF M^+

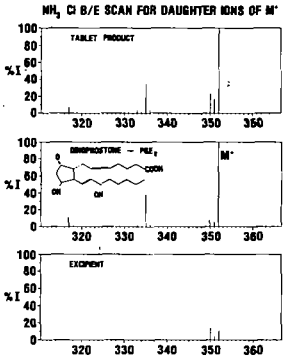

FIGURE 4

NH_3 CI B/E SCAN FOR DAUGHTER IONS OF MH^+

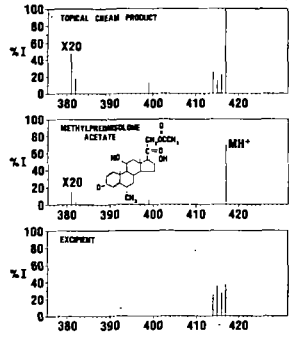

FIGURE 5

NH_3 CI B/E SCAN FOR DAUGHTER IONS OF MH^+

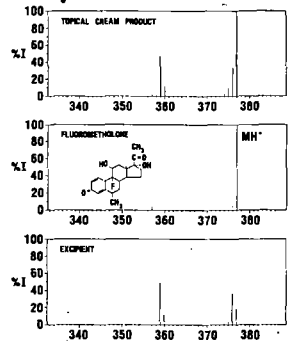

FIGURE 6

NH_3 CI B/E SCANS FOR DAUGHTER IONS OF Me-PGE_2 FRAGMENTS

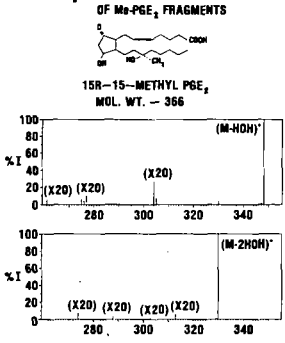

TABLE I

DEGREE OF DISSOCIATION IN FIRST FIELD FREE REGION OBSERVED BY B/E SCANS

PROSTAGLANDINS	
PGE_2	HIGH
15R-15M-PGE_2	HIGH
$PGF_{2\alpha}$	HIGH
STEROIDS	
CORTISONE ACETATE	MODERATE*
DIFLORASONE DIACETATE	MODERATE*
FLUOROMETHOLONE	MODERATE*
HYDROCORTISONE	LOW*
HYDROCORTISONE ACETATE	MODERATE*
METHYLPREDNISOLONE	MODERATE*
METHYLPREDNISOLONE ACETATE	MODERATE*
PREDNISONE	LOW*
PREDNISOLONE	LOW*
PREDNISOLONE ACETATE	MODERATE*

*WITH COLLISION GAS IN FFFR

TPMP21 APPLICATIONS OF MIKES AND MIKES - CID ON SMALL SYSTEMS, Michael T. Bowers, Andreas J. Illies and Liu Shuying, Dept. of Chem., Univ. of Calif., Santa Barbara, Ca. 93106

Mass analysed ion kinetic energy spectroscopy (MIKES) and collision induced dissociation (CID) are often used to investigate the structure of ions formed in the ion source. In this work both methods are used in the study of $C_2H_3N^+$ (m/e=41) produced both by electron impact on a number of different precursors and by ion-molecule reactions. In cases involving ion-molecule reactions, ion cyclotron spectroscopy (ICR) is used to help identify the reaction leading to the ion of interest.

Other applications of MIKES and MIKES-CID will be presented. Specifically we are investigating reactions of simple ions in order to determine reaction mechanisms. Examples will be given for metastables generated via curve crossing and tunnelling through centrifugal barriers.

A temperature variable ion source designed specifically for use with the VG Micromass ZAB-2F will be presented. Examples of the temperature dependence of MIKES spectra will be included.

STRUCTURAL STUDIES OF $C_2H_3O^+$ AND $C_3H_5O^+$ IONS BY COLLISION-INDUCED DISSOCIATION.

THOMAS A. LEHMAN, MAURICE M. BURSEY AND J. RONALD HASS. National Institute of Environmental Health Sciences, Research Triangle Park, NC 27709, and Department of Chemistry, Univ. of North Carolina, Chapel Hill, NC 27514

Title ions were generated from cyclic and acyclic molecules by electron impact and subjected to collision-induced dissociation (CID) in a VG Micromass ZAB-2F reversed geometry instrument. The assumption that identical CID spectra imply ions alike in structure and (at least very nearly) in internal energy was made in inferring ionic structures. With minor exceptions, the same product ions result from the dissociations of all the ions of m/z 43, so that in this case structural information must be inferred from fragment ion intensity differences. A deuterium label confirmed the loss of the functional hydrogen to form the m/z 43 ion from acetaldehyde.

$C_3H_5O^+$ spectra were obtained from 3-pentanone, 1,2-epoxypropane, 2,3-epoxybutane and acetone. Charge reversal (-/+) CID spectra of m/z 43 from acetaldehyde and m/z 57 from acetone are sufficiently different from the conventional +/+ spectra that it is clearly not the same positive-ion structures that dissociate unimolecularly in the two cases after interaction with the collision gas.

CID-MIKES SPECTRA OF M/Z 43 IONS

	12	13	14	15	24	25	26	27	28	29	40	41*	42
Acetone	2.1	7.4	13	28	0.9	2.1	1.8	0.4	5	4	2	9	24
Acetaldehyde	1.5	5.1	7.8	47	0.7	1.5	1.3	0.3	4	3	1.4	8	19
CH_3CDO	1.8	6.3	11	46	0.8	1.8	1.8	0.6	5	4	1.3	5.3	14
Propanal	1.8	6.7	10	37	0.8	2.0	2.0	0.5	4	5	1.5	6	24
1,2-epoxypropane	2.5	6.5	11	26	1.0	2.3	2.0	0.5	5	4	1.6	10	28

*Includes a contribution from the reflected main beam

CID-MIKES SPECTRA OF M/Z 57 IONS

	12	13	14	15	24	25	26	27	28	29	30	31
Acetone (charge reversed)			8.0	6.0			5.2	11.7		7.4		
Acetone			tr	tr		0.6	3.6	8.8	1.7	53	1.1	6.6
1,2-epoxy-2-methylpropane						0.9	4.6	10.1	2.2	51	1.0	4.6
2,3-epoxybutane			tr	tr		1.0	5.0	10.6	3.8	52	0.8	6.5
3-pentanone	0.1	0.4	0.9	0.7	0.2	0.8	2.8	6.0	4.2	76		0.2

M/Z 57 SPECTRA (concluded)

	36	37	38	39	40	41	42	43	52	(52.8)	53	54	55	56
			2.0	13		5.2	24	18						
		1.7	2.5	3.6			1.6			1.0			7.7	6.4
		1.7	2.2	2.9		1.2	6.7	1.7		0.9			5.9	2.3
		1.6	2.2	3.3			1.7			1.0			6.6	3.8
	0.1	0.5	0.5	0.6	0.2	0.9	2.2	0.1	0.1		0.4	0.1	0.6	1.9

Experiments were done at 70 eV electron energy and from 6 to 8 keV accelerating energy. Source temperature was approx. 200 deg C.

In order to make objective comparisons between quite similar spectra, particularly in the case of the m/z 43 ions, we calculated the coefficient of correlation based on the relative intensities of signals of the same m/z in pairs of spectra. The results for m/z 43 are shown in the table.

CORRELATION COEFFICIENTS FOR CID-MIKES SPECTRA OF THE M/Z 43 IONS
(All pairs of signals are included in the calculation)

	A	B	C	D
A. Acetone				
B. Acetaldehyde	.92			
C. CH_3CDO	.89	.99		
D. Propanal	.97	.98	.96	
E. 1,2-Epoxypropane	.99	.88	.83	.95

The correlation between m/z 43 of acetone and acetaldehyde was not as good as expected, whereas that between acetone and 1,2-epoxypropane was surprisingly good. In the m/z 57 series, the correlation coefficients between acetone and the epoxy compounds were again quite good, so that the fragmentations of acetone and these epoxy conpounds appear to occur from common isomers at these masses. McLafferty et al (JACS 95, 3886) report that protonated ethylene oxide falls apart to give an ion of structure $CH_3CH{=}\overset{+}{O}H$.

When CID-MIKES spectra are used to infer ion structures, the analysis is frequently based solely on the signals that remain after all the metastable ion (MI) signals are removed. Having noticed that weak signals were present for most of our ions at the low pressures where one expects to see only true metastable processes, we studied a well-characterized MI system, m/z 45 from ethanol and 2-propanol. The results for ethanol are shown in the figure. The lowest pressure is 5.5×10^{-9} torr gauge reading, which is considerably lower than the pressure in the collision cell. It is, in any case, the pressure at which MI studies are done. The clear pressure dependence of all but the m/z 19 and 29 ions shows that these are the only ions that are formed by unimolecular processes at the lowest pressures, and hence are true metastable ions. The data at each pressure are derived from a computer-controlled experiment in which the results of 100 scans are averaged.

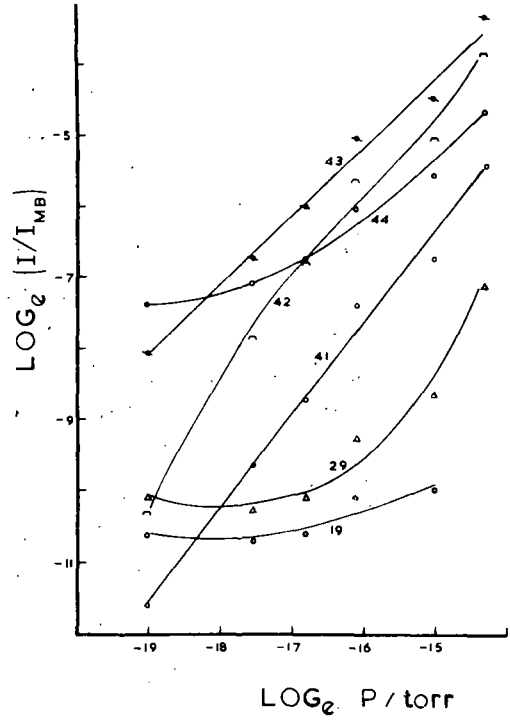

MASS ANALYZED ION KINETIC ENERGY SPECTROSCOPY AS A TOOL FOR THE DETERMINATION OF THE STEREOCHEMISTRY OF RING JUNCTIONS IN STEROID STEREOISOMERS,

ZE'EV V.I. ZARETSKII, Isotope Dept., The Weizmann Inst. of Sci., Rehovot, Israel, and EDMUND A. LARKA, IAN HOWE AND JOHN H. BEYNON, Royal Soc. Research Unit, Univ. College of Swansea, SA2 8PP, United Kingdom.

It is well known that mass analyzed ion kinetic energy (MIKE) spectroscopy provides a sensitive method for distinguishing small differences in ion structures. The MIKE spectra of cis-A/B and trans-A/B stereoisomeric steroids, hydrocarbons (1-6) and ketones (7-20) recorded on a VG-Micromass ZAB-2F reverse geometry mass spectrometer[1], are distinctly different.

In steroid hydrocarbons those peaks corresponding to the loss of the ring A from the molecular ion[2] are more abundant in the more strained cis-A/B(5β)-steroids as compared to their trans-A/B(5α)-isomers. Note that when the mode of C/D rings junction is changed, the MIKE spectra are sharply different. On the other hand the differences in MIKES are less pronounced in those stereoisomeric pairs where the mode of A/B rings junction is changed, leaving the configuration at C-14 (C/D junction) unchanged. In steroid ketones those peaks attributed to the loss of CH_3, H_2O and the A ring[2] from the molecular ion are more intense in the case of the more strained cis-A/B(5β)-ketones as compared to their trans-A/B (5α)-isomers. The striking differences between the MIKE spectra of the steroidal ketones studied suggests that the MIKE technique may be used for determinating the stereochemistry of not only the A/B, but also the B/C and C/D ring junctions in steroidal ketones, even if the second isomer is unavailable. This fortunate situation, rarely observed in the conventional mass spectrometry of stereoisomeric steroids, demonstrates a unique strength of MIKE spectroscopy.

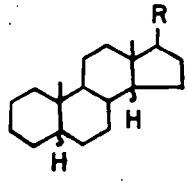

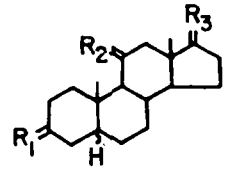

1 R=H	5α 14α	7 R_1=O, R_2=R_3=H_2	5α
2 R=H	5β 14α	8 R_1=O, R_2=R_3=H_2	5β
3 R=H	5α 14β	9 R_1=R_2=H_2, R_3=O	5α
4 R=H	5β 14β	10 R_1=R_2=H_2, R_3=O	5β
5 R=C_2H_5	5α,14α	11 R_1=R_3=O, R_2=H_2	5α
6 R=C_2H_5	5β,14α	12 R_1=R_3=O, R_2=H_2	5β
		13 R_1=R_2=R_3=O	5α
		14 R_1=R_2=R_3=O	5β

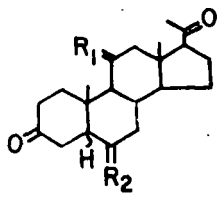

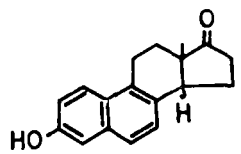

15 R_1=O, R_2=H_2 5α

16 R_1=O, R_2=H_2 5β

17 R_1=H_2, R_2=O 5α

18 R_1=H_2, R_2=O 5β

19 14α

20 14β

References

[1]R.P. Morgan, J.H. Beynon, R.H. Bateman and B.N. Green, Int. J. Mass Spectrom. Ion Phys. 28, 171 (1978).

[2]Z.V.I. Zaretskii, Mass Spectrometry of Steroids, John Wiley and Sons, N.Y.; Israel Universities Press, Jerusalem (1976).

UTILITY OF GC/MS SYSTEMS IN SEVERAL CONFIRMATORY PROCEDURES OF FORENSIC TOXICOLOGY

Thomas V. Briggle, Ana Barquet, Carmen Morgade and Carl D. Pfaffenberger

University of Miami School of Medicine
Chemical Epidemiology Division
15655 S.W. 127 Ave., Miami, Florida 33177

Mass Spectrometry has recently become a powerful tool in the field of forensic medicine. The following two case histories emphasize its utility by showing the integral relationship GC/MS played in the detection and confirmation of toxic components in a suspected suicide and the poisoning of a 2-month old child.

On the 24th of September, 1979 the mother of the child noticed an acute rash on the arms, legs, and body of the infant. The child was taken to a county clinic for treatment. The nurse practitioner who first saw the child was unsure of the diagnosis and asked the mother to return that afternoon to consult a pediatrician. The mother returned and scabies was diagnosed. The mother was given a prescription for a topically applied medicine. The label on the bottle read as follows:

Jeff M.
9/24/79
"Quell" Lotion
External Use Only
Apply as Directed
B.C. Primary Health Care Pharmacy

The nurse instructed the parent to apply the lotion once every four hours, then wash it off before the next application. The child received four applications and was then brought back to the clinic. His condition had worsened, and other family members were being afflicted. The same nurse then instructed the mother to bathe the child in warm water, apply the lotion from the neck down, and to leave the medication on for 24 hours. The mother did as instructed and upon awakening the following day, found the child face down and no longer breathing.

Our laboratory received cardiac blood, urine and brain tissue from the deceased infant after an autopsy had been performed. The brain tissue received analysis different from the blood and urine samples and following a rigorous clean-up procedure. The sample was initially analyzed by GC using an electron capture detector. A single peak was detected with a relative retention time equal to that of the organochlorine pesticide, Lindane. Lindane is the active ingredient (1% concentration) in "Quell" lotion. Further clean-up was required, and the component then was analyzed and confirmed via solid probe analysis. Quantification and confirmation in the various samples were as follows:

TOXIN	SAMPLE	CONC. (ppb)
Lindane	Urine	2
Lindane	Blood	33
Lindane	Brain Tissue	110

It should be mentioned that this is only the second time in the history of pesticide residue analysis that a pesticide has been known to cross the blood brain barrier. However, the child was born two months premature. Because of the possible lack of development of the Glial cells, which form the blood brain barrier, only a partial closing of brain capillary openings may have existed at the time of exposure, i.e., the blood brain barrier may have been incomplete.

Sam W, a suspected suicide case, was found unconscious at his place of work. He was noticed by an unidentified individual who, alert to his condition, called an ambulance. Containers labelled "Paraquat" and "Malathion" were found next to the victim's body. The man was rushed to the hospital and admitted at 1:59 P.M., July 19, 1979. He was still unconscious and his breath smelled strongly of insecticide. Because of the odor of his breath and the insecticide containers found near him, he was given an immediate lavage containing activated charcoal. Our laboratory received samples of the victim's blood, urine and stomach lavage. A lavage analysis, done in hopes of making a quick detection of the potential toxins, was performed. When the analytical sample was injected into a GC, a component eluted (flame photometric detection) which did not have the relative retention time of either suspected poisons, Malathion or Paraquat. The value was identical to that of a common weed killer, Dimethoate. This potent herbicide can be separated, using the proper GC parameters and chromatographic packing material, to yield three subcomponents in urine or blood. However extraction and separation procedures are lengthy procedures. The victim was treated according to the initial G.I. analysis, viz., large doses of atropine were administered. The patient responded well to treatment and by 10:00 P.M., 7/19/79 was responding to

commands and showing more normal vital signs. At 11:15 P.M., however, the victim underwent a seizure and arrested. All attempts to revive the patient were futile, and he was pronounced dead at 12:30 A.M., July 20, 1979.

1:50 P.M. Vital Signs		10:00 P.M. Vital Signs	
B.P.	136/88	B.P.	124/04
RESP.	22	RESP.	19
PULSE	120	PULSE	71

In order to confirm the lavage analysis and confirm that the atropine therapy was appropriate, the blood sample was analyzed by GC and GC/MS after two separate clean-up procedures were performed. The final solution was dried and confirmed by solid probe analysis. The following are the concentrations of Dimethoate metabolites found in the premortem blood of the deceased.

SAMPLE	TOXIN	CONC. (ppb)
Blood	DMP*	722
Blood	DMTP*	112
Blood	DMDTP*	23

*DMP - Dimethylphosphate
*DMTP - Dimethylthiophosphate
*DMDTP - Dimethyldithiophosphate

This investigation was supported through Cooperative Agreement No. CR 807051-01-1 with the Epidemiologic Studies Program, Health Effects Branch, Hazard Evaluation Division of the Environmental Protection Agency, Washington, D. C. 20460.

MASS SPECTRAL IDENTIFICATION OF IMPURITIES IN PHENAZOPYRIDINE HYDROCHLORIDE

David L. Heikes and Donald L. Myers, U. S. Food and Drug Administration
1009 Cherry Street
Kansas City, Missouri 64106

The Compendial Monographs Evaluation and Development Program of the Food and Drug Administration is a comprehensive study of the suitability and adequacy of compendial methods. Selection of drugs for inclusion in this program is based upon their wide usage and therapeutic significance. Results of the program will be used by the Compendial Operations Staff to seek revisions and additions to the United States Pharmacopeia.

Under the auspices of this program phenazopyridine hydrochloride (2,6-diamino-3-phenylazopyridine monohydrochloride) has undergone extensive study in the Kansas City District Laboratory of the Food and Drug Administration. This report, however, will include only the portion of this study directed toward identification of impurities in phenazopyridine hydrochloride bulk and dosage forms.

Initial detection of several impurities was accomplished with thin-layer chromatography using 250μ silica gel GF plates, multiply developed with 25% acetone in benzene and visualized with sequential exposure to nitrous acid and N-(1-naphthyl)-ethylenediamine dihydrochloride (Marshall's Reagent). Through the use of gel permeation chromatography nearly all the phenazopyridine was removed from its impurities. For this purpose a ORPVA 2000 column 20mm x 20cm was eluted with 10% methanol in benzene and the phenazopyridine band was visually detected and separated. The resulting impurity-enriched thin layer-chromatogram indicated the presence of 10 distinct spots.

A gas-liquid chromatogram was obtained which provided adequate separation of most of the impurities. Correlation was made with each of the thin-layer spots and gas-liquid chromatographic peaks by scraping the spot from the plate, dissolving in chloroform and injecting on a 1.8m x 2mm glass column of 3% OV-7 at 210° using electron capture (^{63}Ni) detection.

GC/MS analysis using a DuPont 21-491B Mass Spectrometer and the above described column has shown the identity of three of the spots to be p-phenylazoaniline, p-phenylazophenol and β,β'-bis(phenylazo)-α,α'-diaminopyridine. Their mass spectra are represented as Figure 1 through 3, respectively. Work is continuing on this project.

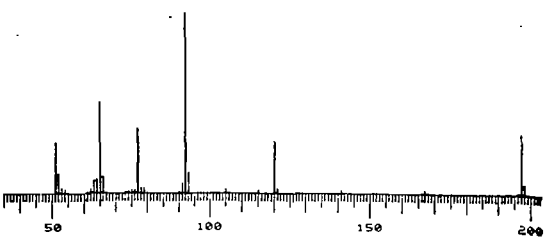

Figure 1

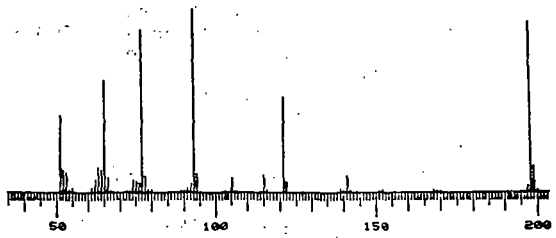

Figure 2

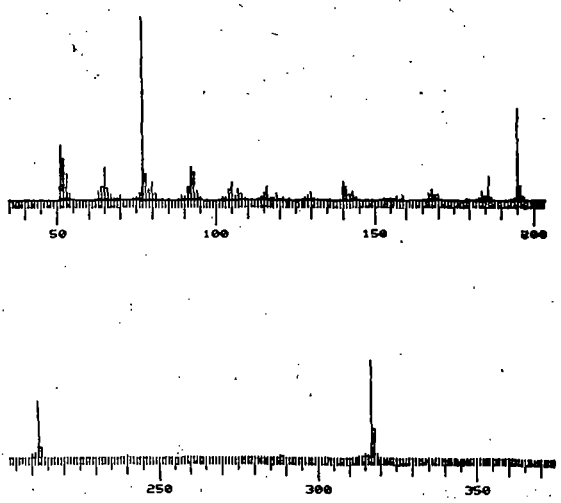

Figure 3

"Analysis of N-Nitrosodiethanolamine (NDELA) in Cosmetics, Shampoos, and Raw Materials by Gas Chromatography - Mass Fragmentography"

BIRENDRA N. PRAMANIK and AARON D. COOPER,
Vick Divisions Research & Development,
Richardson-Merrell Inc.
One Bradford Road
Mt. Vernon, NY 10553

N-Nitrosodiethanolamine (NDELA) in cosmetic products, shampoos, and raw materials can be extracted efficiently with ethyl acetate. However, the co-extraction of a number of other components such as triethanolamine, diethanolamine, fragrance materials, etc. presents severe problems in separation of NDELA pure enough for quantitation. The commonly employed column chromatographic separation is time consuming. We have found that in Step 4 of sample preparation procedure, NDELA of sufficient purity can be isolated in about 5 minutes using SEP-PAK cartridges (Waters Associates, Inc.) and carefully chosen solvents for elution. For less complex mixtures the use of SEP-PAK C_{18} with hexane as the eluant removes the impurities first; then, NDELA can be eluted with ethyl acetate. When the mixture is more complex, SEP-PAK silica gel can be used and methylene chloride is the solvent of choice for removing many of the impurities. Subsequent elution with ethyl acetate provides an extract of satisfactory purity. The ethyl acetate solutions are taken to dryness and silylated with BSTFA to provide samples for mass spectral determination.

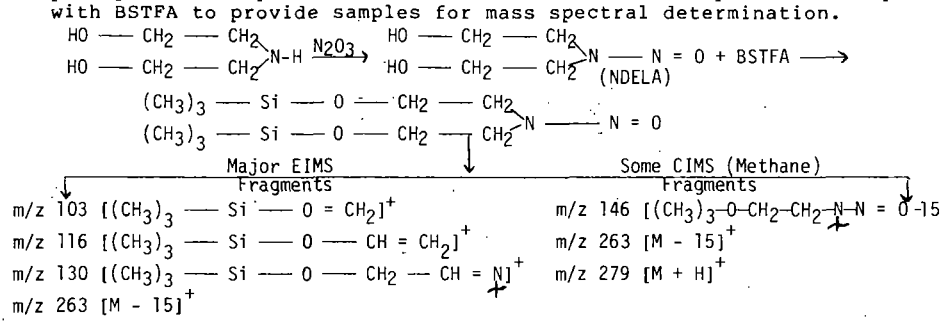

GC-MS using Selective ion monitoring, is a method of high selectivity and sensitivity. Although fragmentography, using peaks at the m/z 116 or 130 in the EIMS, is often satisfactory for quantification, in some cases interferences from impurities are observed. CIMS (methane) provides a superior method for quantitation. An intense fragment ion which appears at m/z 146 (base peak) can be conveniently used for quantitation of NDELA in the CIMS mode.

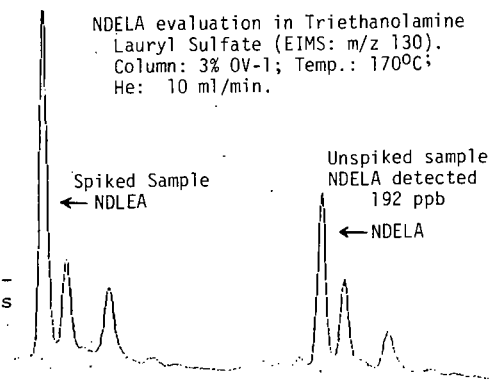

The detection limit varies from 5 ppb to 30 ppb, depending on the complexity of the mixture. The identity of NDELA is determined on the basis of GC retention time and UV decomposition studies. The full mass spectrum can be obtained when the concentration present exceeds 200 parts per billion.

SAMPLE PREPARATION PROCEDURE

SCHEME I

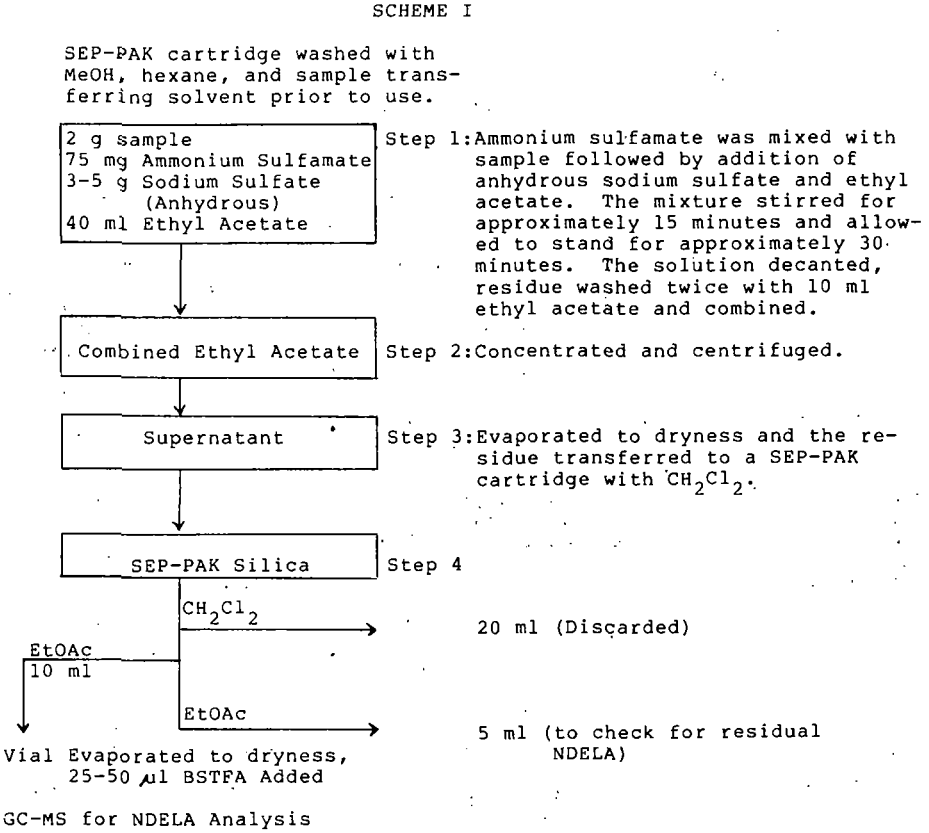

Scheme-2 could be followed for sample preparation if the residue from Step-3 (Scheme-1; evaporation of supernatant) is soluble in hexane.

SCHEME 2
From Step 3

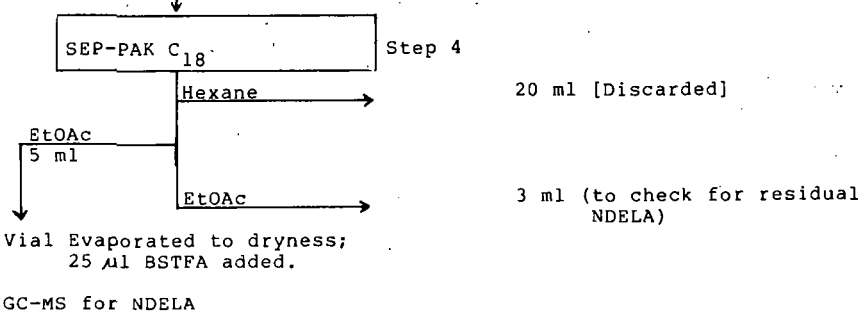

USE OF GC/MS AND DEUTERIUM OXIDE TO DIFFERENTIATE BETWEEN CHLOROFORM AND DERIVED CHLOROFORM IN HUMAN BLOOD SERUM

Carl D. Pfaffenberger, Anita J. Peoples and Thomas V. Briggle

University of Miami School of Medicine
Chemical Epidemiology Division
15655 S.W. 127 Ave., Miami, Florida 33177

Over the past two years our laboratories have been trying to determine if a correlation exists between the average serum chloroform levels of several human populations and the level of chloroform present in the drinking water that these people use. We chose to study four populations in southern Florida which had been drinking, for at least the previous five years, mainly water containing the average trihalomethane levels indicated in Table 1.

TABLE 1

WATER SOURCE	THM (ppb)	AVE. SERUM $CHCl_3$ (ppb)
Well Water	<1	11
Preston Plant	141	24
Cooper City	307	42
Florida City	<20	~12

Well water from privately owned wells located in southern Dade County typically contains less than 1 ppb total trihalomethanes (THMs). Finished water from the Preston Water Works located in Hialeah, Florida, contains an avg. of 141 ppb THMs, and Cooper City municipal water typically contains over 300 ppb THMs. The municipal water of Florida City is very slightly chlorinated well water and usually has less than 20 ppb THMs. One hundred females between 20 and 70 years of age were chosen from each area; the participants were screened to eliminate any who were exposed to chloroform or dry-cleaning solvents. The last column in Table 1 indicates the average serum chloroform levels found for these groups.

On one occasion a dry-cleaning establishment asked us to analyze the blood serum of four workers for the possible presence of dry-cleaning solvents, particularly tetrachloroethylene or perchloroethylene (PERC or PCE). Not only PCE but also chloroform was detected in the workers' blood, and in levels much higher than those observed during our drinking water study as indicated in Table 2. In fact, in each case more chloroform than PERC was detected.

TABLE 2

WORKER WAS:	$CHCl_3$ (ppb)	PCE (ppb)
In the dip room	6000	2300
In & out dip room	3000	800
Occas. in dip room	350	100
A spot cleaner	300	150

PERC is metabolically converted to trichloroacetic acid in mammalian liver. Hepatic $P_{450/448}$ oxidases convert perchloroethylene into perchloroethylene oxide which rearranges to trichloroacetyl chloride which, in turn, is hydrolyzed to trichloroacetic acid (TCA). Under our analytical conditions, blood serum is heated in a Tekmar purging device and volatile compounds are thereby transferred to an adsorbent trap composed of Tenax GC and silica gel. While the serum is being heated, TCA decomposes into CO_2 and trichloromethylcarbanion which, in turn, abstracts a proton from water to yield chloroform. The decomposition of TCA into CO_2 and $CHCl_3$ occurs in the purging device, not on the analytical column or within the mass spectrometer.

Chloroform is conveniently identified by its relative retention time (GC) and its base peak at m/z = 83 which is actually part of a triplet for the $CHCl_2^{\oplus}$ ion. The cluster appears at m/z 83, 85 & 87 with respective realtive intensity ratios of 7:5:1. That conversion of TCA to $CHCl_3$ does occur under our conditions of analysis was demonstrated several times by first exhaustively pre-purging a serum/antifoam mixture to remove any TCA and/or chloroform present, then adding a known quantity of TCA and re-purging the analytical sample. Throughout this series of investigations, one ml of blood serum was purged after adding it to 1.5 ml of a pre-purged aqueous emulsion containing 1% Dow Corning Antifoam B. TCA is quantitatively converted to chloroform and carbon dioxide under our analytical conditions (Path A):

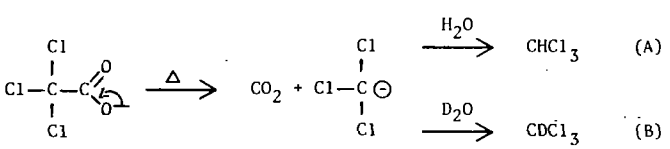

According to the proposed mechanism, if the analysis were to be run in deuterium oxide instead

of water, d-chloroform would form, and the expected triplet would be shifted to m/z = 84, 86 and 88 in the same ratio, 7 to 5 to 1. This is observed if TCA is added to exhaustively pre-purged and lyophilized serum which has been reconstituted with D_2O; that is, the one amu shift is essentially complete. However if one fortifies exhaustively pre-purged but unlyophilized serum with known amounts of TCA, the shift is incomplete because serum is an aqueous mixture. In our lab, one ml of pre-purged serum in 1.5 ml pre-purged antifoam in D_2O gives a 60% shift, which is consistent with an H_2O to D_2O ratio of 2 to 3. For unpurged, unfortified samples the situation is even more complex.

First it was demonstrated that chloroform in the presence of D_2O and no water does not lead to d-chloroform under our analytical conditions. However, unpurged, unfortified (actual) samples contain both chloroform and chloroform precursors such as trichloroacetic acid and its salts. Therefore chloroform will appear as the 83-85-87-amu cluster whereas TCA-derived chloroform will appear about 40% in the aforementioned cluster and 60% in the 84-86-88-amu cluster. This was demonstrated for two of the serum samples from dry cleaners.

In the first dry cleaner the normal and shifted peaks were essentially equal as shown in Figure 1. The observed ratios were 42 to 29 to 5 which represent normalized values of 55 to 38 to 7. These values correspond closely with the theoretical ratios, 54 to 38 to 8.

Figure 1

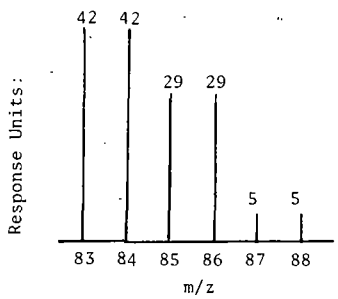

If it is assumed that the shifted values at m/z = 84, 86 and 88 are completely attributable to TCA and represent 60% of the TCA present in the sample, then 40% of 42 or 16.8 units are attributable to chloroform derived from TCA and 42 + 16.8 or 58.8 of the total 84 units are derived from TCA. This represents 70% of the chloroform quantified or 4200 ppb TCA-derived chloroform, leaving 30% or 1800 ppb chloroform not derived from TCA.

For the second dry cleaner, the normal peaks were in the ratio of 46 to 31 to 5.5 and the shifted peaks were in the ratio of 44 to 28.5 to 4.5. When normalized, the ratios of 58 to 36 to 6 for $CHCl_2^{\oplus}$ and 57 to 37 to 6 for $CDCl_2^{\oplus}$ approached theoretical values. In this case, if 44 units represent 60% of the TCA present in the sample, then 17.6 units of the 46 appearing at m/z = 83 are attributable to chloroform derived from TCA, and 44 + 17.6 or 61.6 of the total 90 units are derived from TCA. This represents 68% of the chloroform quantified or 2040 ppb TCA-derived chloroform, leaving 32% or 960 ppb of chloroform not derived from TCA.

The findings from the dry-cleaning study must be taken into consideration when interpreting the drinking water results, and several questions must be answered. Our next step will be to apply this methodology to some of the participants in the drinking water study and determine if any d-chloroform results. It should be mentioned that no tetrachloroethylene was detected in any of the drinking water sources included in our study, but the possibility of inhalation of PERC vapors has not been ruled out. Air sampling studies are about to be initiated to determine the ambient air levels of PERC in the four areas under study.

We gratefully acknowledge the financial and technical assistance of the United States Environmental Protection Agency, especially the support under EPA Grant No. R804611-03.

MASS SPECTROMETRIC ANALYSIS OF HIGH MOLECULAR WEIGHT ORGANIC POLLUTANTS*

Lorne M. Isabelle, James F. Pankow, and Douglas F. Barofsky

Department of Environmental Science
Oregon Graduate Center
Beaverton, Oregon 97006

In this study, FDMS was applied in a preliminary, qualitative determination of chlorophenoxyphenols, in soil and water samples. The lighter chlorophenoxhphenols are manufactured for use as bactericides and fungicides (e.g., 5-chloro-2-(2,4-dichlorophenoxy)-phenol), while those of longer chain length are known to form as by-products during the manufacture of these bactericides[1] as well as during the production of other pesticides such as 2,4-dichlorophenoxyacetic acid ("2,4-D") and polychlorophenols[2-4].

The biological activity of the chlorophenoxyphenols is not limited to bactericidal and fungicidal properties. Indeed, the mutagenicities of 5-chloro-2-(2,4-dichlorophenoxy)-phenol and 2,3,4-trichloro-6-(2,4-dichlorophenoxy)-phenol have been found to be similar to those of acridine orange and dimethylnitrosamine, respectively[5]. While higher chlorophenoxyphenols have not been studied, it is not unreasonable to suspect them of possessing similar toxicity.

This study was instigated by the presence of large amounts of chlorophenoxyphenols in chemical dump sites such as the one at Alkali Lake in southern Oregon where 25,000 55 gallon drums of 2,4-D and 4-chloro-2-methylphenoxy acetic acid (MCPA®) manufacturing wastes have been disposed and by the continued production of chlorophenoxyphenols as products and by-products of pesticide manufacturing processes.

Mass spectra were obtained with a Hitachi-Perkin Elmer RMU-6E, single focusing mass spectrometer modified with a field ionization/field desorption ion source. Emitter temperatures were controlled manually by varying the amount of heating current passing through the emitter. For each sample run, FD mass spectra were obtained at a number of different heating currents. The spectra presented here were obtained by summing the peak intensities from each of these spectra.

Distillation residues from the commercial production of 2,4-dichlorophenol by Cl_2 chlorination of phenol were obtained from a commercial firm. A stock solution of 23.8 μg/μL of these tarry residues was prepared in methanol. Samples of natural ground water which have become contaminated with chlorophenoxyphenol wastes were obtained on 10/09/79 from a well 35 m from the boundary of the chemical disposal site at Alkali Lake, Oregon. Contaminated soil samples were obtained simultaneously from the Alkali Lake disposal site. Extracts of the natural ground water and soil samples, the chlorophenol residue stock solution, and spiked water samples were loaded on emitters with a microsyringe. In each case, approximately 0.5 μL of sample was applied. FDMS immediately followed the emitter loading.

Table I presents a tabulation of the various possible chlorophenoxyphenols of n = 1-5. Each isotopic grouping or cluster is represented in Table I by its lowest molecular weight member; members within a cluster differ by two mass units. Many of these compounds are evidenced in the FD mass spectrum (Spectrum 1) of the 2,4-dichlorophenol distillation residue. The m/z values representing the isotopic clusters evident in Spectrum 1 have been placed in boxes in Table I. The combination of the mass, proper chlorine isotopic cluster proportions, and the presence of the other series members is a strong indication that the peaks in Spectrum 1 may be interpreted in terms of Table I.

The FDMS spectrum of the extract of the Alkali Lake chemical disposal site soil sample is shown in Spectrum 2. The considerable intensity of some of the peaks required that the log of the intensities be plotted. The presence of chlorophenoxyphenols of MW up to 540 is clearly indicated, and the relative proportions of the chlorine isotope clusters are in close agreement with the values expected based on the number of chlorines assigned to these peaks in Table I.

The isotope clusters of the peaks at MW values of 186, 196, 200, 220, and 234 indicate the presence of one, three, one, two, and two chlorines, respectively. These data, together with the fact that chlorinated herbicides and chlorinated herbicide manufacturing residues are known to have been disposed of at the Alkali Lake site, support the assignments of chlorophenoxyacetic acid, trichlorophenol, methylchlorophenoxyacetic acid (MCPA®), 2,4-dichlorophenoxyacetic acid (2,4-D), and 2,4-dichlorophenoxypropanoic acid (2,4-DP) for these peaks. Analysis by gas chromatography/mass spectrometry confirmed these assignments.

The spectrum of the extract of the well water obtained near the Alkali Lake site is shown in Spectrum 3. The (n=2) MW series 254, 288, 322, and 356 is clearly visible.

All of the assignments made in Spectra 1-3 have in common the presence of a metha-

---

* An extended version of this paper has been submitted to Analytical Chemistry (1980).

latable hydrogen (either carboxylic or phenolic). When each of the three extracts was treated with excess diazomethane, all of the peaks were shifted up by 14 amu, further confirming the above assignments.

The spectrum of the extract of the tap water sample which had been spiked at the 2.4 mg/L level with the 2,4-dichlorophenol distillation residue is presented in Figure 4. Since the distillation residue (total chlorophenoxyphenols) was added at the mg/L level, the individual chlorophenoxyphenols were present at the μg/L level. Thus, the intensities of the peaks of Spectrum 3 imply that the Alkali Lake well water is contaminated at the μg/L level or lower with the n=2 chlorophenoxyphenols.

In conjunction with solvent extraction as a preconcentration step, FDMS has been shown to be sensitive at the μg-level for individual chlorophenoxyphenols. This method has been used to analyze contaminated soil and ground water samples obtained near the Alkali Lake, Oregon, chemical disposal site. The fact that naturally-occurring organics such as the fulvic and humic acids did not pose a spectral interpretation problem in these analyses indicates that the semi-quantitative analysis of compounds such as the chlorophenoxyphenols may be carried out by FDMS with little or no sample clean-up.

ACKNOWLEDGEMENTS

The authors would like to thank Elisabeth Barofsky for her very skillful preparation of the field desorption emitters used in this study. We also thank Geo. Ward and Assoc., Inc., Portland, Oregon, for supplying the Alkali Lake samples.

REFERENCES

1. Hites, R.A.; Lopez-Avila, V.; Anal. Chem. 1979, 51, 1452A-1456A.
2. Nilsson, C.-A.; Renburg, L.; J. Chromatog. 1974, 89, 325-333.
3. Dienzer, M.; Lamberton, J.; Griffin, D.; Miller, T.; Biomed.Mass Spectrom. 1978, 5, 566-571.
4. Dienzer, M.; Griffin, D.; Miller, T.; Skinner, R.; Biomed.Mass Spectrom. 1979, 6, 301-304.
5. Fahrig, R.; Nilsson, C.-A.; Rappe, C.; in Pentachlorophenol, Rao, K.R., ed., Plenum: New York, 1977.

n = 1		n = 2		n = 3		n = 4		n = 5	
Cl_x	MW	Cl_x	MW	Cl_x	MW	Cl_x	MW	Cl_x	MW
1	128								
2	162								
3	196								
4	230								
5	264								
		1	220						
		2	254						
		3	288						
		4	322						
		5	356						
		6	390						
		7	424						
				1	312				
				2	346				
				3	380				
				4	414				
				5	448				
				6	482				
				7	516				
				8	550				
						1	404		
						2	438		
						3	472		
						4	506		
						5	540		
						6	574		
						7	608		
						8	642		
						9	676		
						10	710		
								1	496
								2	530
								3	564
								4	598
								5	632
								6	666
								7	700
								8	734
								9	768

TABLE I.

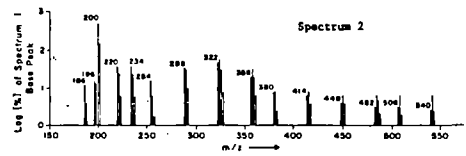

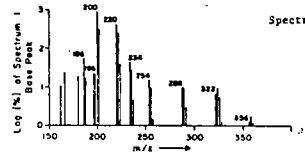

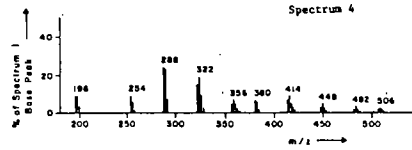

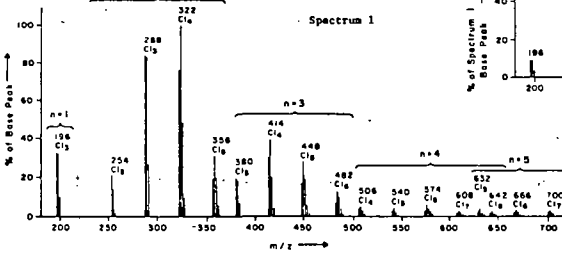

EVOLVED GAS ANALYSIS OF COAL FLY ASH BY MASS SPECTROMETRY

Schure, M.R.; Ryan, P.W.; Sine, M.R.; Natusch, D.F.S.N.
Department of Chemistry, Colorado State University, Fort Collins, Colorado 80523

The characterization of complex materials such as fly ash from coal fired power plants requires the application of several analytical techniques in order to acquire sufficient information. The work described here makes use of conventional GC/MS instrumentation to obtain information about fly ash samples which is complementary to that obtained by the more conventional techniques of ESCA, X-ray powder diffraction, thermogravimetric analysis and differential scanning calorimetry. The mass spectrometer is used to monitor gasses evolved as the fly ash is heated in an atmosphere of controlled composition.

A glass reactor was constructed with a porous frit so that carrier gas flows through the frit and percolates through a bed of fly ash. The reactor is placed inside the oven of a gas chromatograph, connected in place of the GC column. Gasses flowing out of the reactor are directed through the jet separator GCMS interface for mass spectral analysis. Before entering the chromatograph, helium carrier gas is diverted through a mixing manifold where it can be doped with small amounts of additives. The GC oven is heated at a controlled rate and the gasses evolved from the sample are monitored as a function of temperature by repetitively scanning the mass spectrometer as in a normal GCMS run.

The basic experiment is to place a few milligrams of sample in the reactor with pure helium carrier flow. The system is held at 150°C until all signal due to desorbed water, etc. is gone, then program the GC oven at 5 deg/min to its maximum temperature of 445°C. A sample of fly ash from the Corrette Power Plant (Montana) heated in this way showed evolution of H_2O which peaked at 410°C and evolution of lesser amounts of CO_2 which peaked at about 390°C. Differential scanning calorimetry had been unable to resolve two events, and only the EGA experiment showed that 2 separate events occurred in this temperature range. Repeating the experiment with 5 ppm of CO_2 in the carrier gas confirmed the conclusion that 2 independent events are involved because the CO_2 evolution peak was suppressed while the H_2O evolution peak was not affected. We interpret the H_2O evolution as coming from decomposition of a hydrated hematite mineral, and X-ray powder diffraction experiments support this interpretation. The CO_2 evolution we believe comes from an iron magnesium carbonate complex which is often found associated with hematite

When a few percent NO_2 is added to the carrier, the H_2O evolution is shifted down

to 370°C. One possible explanation is that NO_2 reacts with hematite to form an iron nitrate, forcing the H_2O evolution to occur. Supporting evidence for this is an ESCA study which shows that exposure of this fly ash to NO_2 does lead to formation of metal nitrates.

Preliminary experiments with Cl_2 as an additive have shown a rather complex set of evolved products. Several metal chlorides are volatile at the temperatures employed here, including $AlCl_3$ and $FeCl_3$. $SOCl_2$ is also a possible component of the gas evolved under Cl_2 atmosphere.

GC/MS ANALYSIS OF AEROSOLS FORMED FROM DIESEL EXHAUST

John G. Windsor, Jr., Sandy P. Parks, and H. Michael Barnes*

Northrop Services, Inc., Research Triangle Park, N.C. 27709
*U.S. Environmental Protection Agency, Research Triangle Park, N.C. 27711

Aerosol particles resulting from the combustion of fossil fuels (especially in the human respirable size range) are of great concern to environmental scientists. With the annual consumption of diesel fuel in the U. S. now over three million barrels a day and automobile manufacturers increasing their production of diesel-engine vehicles, the EPA at Research Triangle Park, N. C., began a series of smog chamber studies to examine the potential effects on the environment of the increase in aerosols formed by diesel fuel combustion. The experiments included taking twelve samples to identify organic compounds associated with these aerosols.

The large Calspan Environmental Simulation Facility at Buffalo, N.Y., was filled with diesel exhaust and subjected to varying environmental conditions: light or dark and varying concentrations of NO_x, SO_2, and O_3. Commercially available automobiles, whose operation and exhaust were previously characterized, were used to generate the diesel exhaust. (Diesel fuel, previously characterized and sufficient to conduct all of the experiments, was transported to Calspan.) After retention times of 6 to 24 h, the generated aerosols were collected on quartz filters with a modified Hi-Vol sampling apparatus. For several experiments, organic vapors were collected downstream of the filter with cartridges packed with Tenax-GC. Filters were solvent-extracted, and the crude extract was separated into fractions based on a solvent elution scheme from silica gel.

As the chamber samples were initially used to characterize our HP 5985 GC/MS system, each crude extract was analyzed for PAH (polycyclic aromatic hydrocarbons) on a packed Dexsil column using selected ion monitoring, and each PAH fraction was then analyzed on the Dexsil packed column and a fused silica capillary column using the total ion current signal. For the PAH species quantitated (see table), each method gave the same results. The PAH were the most concentrated species present; concentrations of the quantitated species are shown in the table. Each pair of columns represents "before-after" results: e.g., 3M was in the dark, 4M was irradiated.

CALSPAN - PAH DISTRIBUTION (μg/sample)

	SAMPLE DESIGNATION									
PAH SPECIES	32-1	32-2	44-1	44-2	3M	4M	16	18	22	29
Anthracene/phenanthrene	19	2.9	8.7	3.3	42	16	31	0.41	0.38	0.20
Methyl anthracene/phenanthrene	18	2.7	6.2	2.8	71	20	6.5	0.39	0.42	N.D.
Dimethyl anthracene/phenanthrene	24	3.3	5.1	3.9	70	17	2.5	0.12	0.42	1.3
Fluoranthene	23	5.2	9.2	7.1	75	13	27	0.65	0.70	0.32
Pyrene	19	4.1	8.4	4.0	40	7.5	17	0.21	0.22	0.16
Methyl fluoranthenes/pyrenes	5	0.3	2.0	0.5	8.6	1.8	5.3	0.06	0.24	0.16
Benzanthracene, Chrysene, Triphenylene	6	1.3	2.0	1.3	9.2	1.5	6.1	0.33	0.14	N.D.
Benzofluoranthenes	4	1.2	1.9	0.6	2.7	NA	4.2	0.89	0.40	N.D.
Benzopyrenes	3	0.9	1.6	0.5	—	—	—	—	—	—
TOTAL PAH	120	22	45	24	320	77	104	3.0	3.0	2.0

These interesting results require much more explanation than time permits here. The most important point from this data is the relative distribution of parent and alkylated PAH. The figure shows that the chamber PAH more closely resemble the PAH in petroleum products than in an urban-air sample we have analyzed. With more weathering, we expect the aerosol formed from diesel exhaust to develop an alkyl homolog distribution closer to that of the urban aerosol. The difference seen may be related to sampling technique; however, the same Hi-Vol sampler was used to collect the diesel exhaust and urban aerosol samples. Thus, the difference is most likely related to weathering of the aerosol.

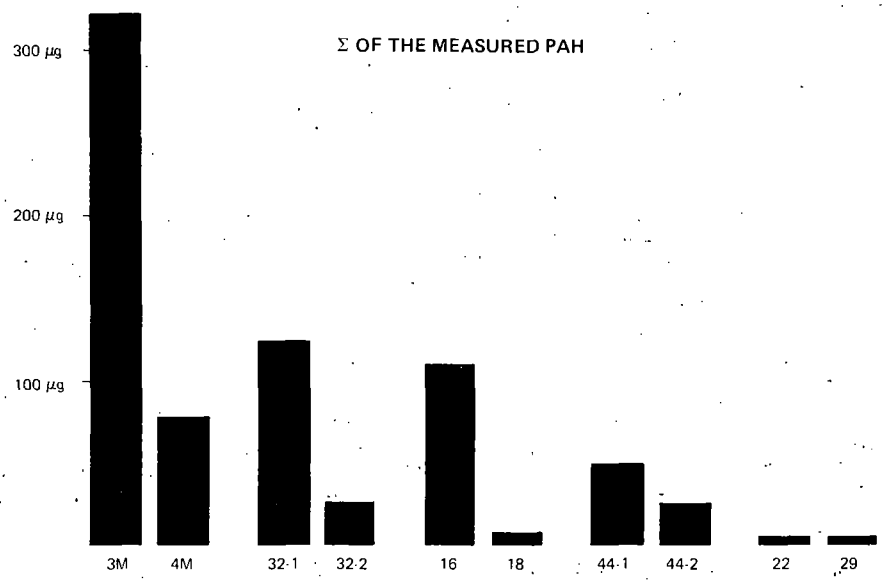

Other compounds identified in the aerosol but not quantitated were normal and branched chain alkanes and alkenes, benzo(ghi)fluoranthene, benzo(c)cinnoline, dibenzothiophene, methyl dibenzothiophene, dimethyl dibenzothiophenes, anthraquinone, benzanthrone, anthrone, dimethyl naphthothiophene, and alkylated biphenyl isomers. In the vapor phase, toluene, xylenes, ethyl benzene, propyl benzenes, butyl benzenes, naphthalenes, alkylated naphthalenes, acenaphthylene, and biphenyls were present.

We are continuing with the analysis of oxygenated fractions and will report on them in the future.

MIKE Spectra of Organophosphorus Insecticides Desorbed From Soil

A. Vincze, P. Bel and L. Gefen.
Israel Institute for Biological Research, Ness-Ziona, Israel.

A novel approach to tackle the problem of environmental monitoring is introduced. The data presented demonstrate that MIKES applied directly to soil samples can in certain cases be an acceptable alternative to GC/MS.

Environmental contamination by pesticides is a grave problem that needs no introduction. Residues on crops and in soil are most often determined by GC/MS after solvent extraction. While this technique is almost universal and allows for separation and quantitation(1) it has its drawbacks. Most important of which are sample loss during various stages of work-up and the time involved(2). It occurred to us that some of the disadvantages mentioned could be overcome if monitoring would be attempted on the solid sample as it is. MS/MS seemed to be the obvious solution. This technique, whether performed with double focussing magnetic mass spectrameters (3,4) or triple quadrupole ones (5,6), was successfully applied to mixture analysis (2,5-7). Thus, it seemed logical to assume that focussing the mass spectrometer on a relevant precursor ion of the particular analyte investigated in a crude soil sample and recording its metastable fragmentation series or C.I.D spectrum would give rise to a recognizable pattern. This spectrum would then be matched against standard spectra in a file. With dedicated instrumentation this could be done reasonably fast; 3 seconds per decade are claimed for a computerized B/E scanning (8). This is certainly much shorter than extraction, concentration and a capillary GC/MS run when starting with the same given soil-sample. Quantitation by single or multiple reaction monitoring (2,5) should also be feasible. One would tend to belittle the method on account of the small amount of such sort of sample that can be introduced via a direct probe. When the inability to concentrate a soil sample is borne in mind, crucible size could be a handicap indeed. We have overcome this shortcoming by designing and building several inlet systems which take between several grams and ~100 g of a soil sample, thus, up to about 10^4 average crucible loads. These fit into the GC oven. It is also important to note that since output signal is essentially an SID recording it is much more tolerant of electronic noise than under normal scanning conditions; this allows for higher additional amplification of the SEM output than in usual work with the same mass spectrometer.

The MIKES technique was employed for this study using a modest Varian MAT 112 CI/EI. Surprisingly, the literature is very poor in examples of MIKES of organophosphorus agents which prompted us to initiate a study of these for their own sake. This work is still under way, but for ascertaining presence of suspected agent in a sample by MIKES matching the spectrum obtained from it with a standard one should suffice. MIKES of neat agents and of soil samples spiked with them, has been determined for the following commercial insecticides: Parathion, Methylparathion, Malathion, Diazinon, Phorate, Folimat, Paraoxon, Metasystox R, S & i., Pirimiphos Me & Et. The pairs of MIKES for Diazinon and Malathion are reproduced in the figures appended and show a close fit. This was the case also with the other mentioned compounds. While the object of this study was to demonstrate feasibility of the idea proposed, it should be pointed out that sensitivity should be very good with dedicated MIKE spectrometers or triple quadrupole analysers. We believe that this application of MS/MS offers the environmental mass spectrometrist yet another tool in his arsenal and a welcome addition to GC/MS and LC/MS in those cases when samples are monitored or analysed for specific compounds.

Acknowledgments: The authors wish to express their gratitude to Messrs. N. Graziani, J. Green, D. Teicholtz, G. Shavit and M. Klein of this Institute's workshop and to Mr. A. Zeitak of I.S.I. Scientific.

References

1) B.J. Millard, "Quantitative mass spectrometry", Heyden & Sons, London (1978).
2) G.L. Glish, V.M. Shaddock, K. Harmon, and R.G. Cooks, Anal. Chem. 52 (1980).
3) J.H. Beynon, R.G. Cooks, J.W. Amy, W.E. Baitinger and T.Y. Ridley, Anal. Chem. 45, 1023A, (1973).
4) R.K. Boyd and J.H. Beynon, Org. Mass Spec. 12, 3 163 (1977).
5) R.A. Yost and C.G. Enke, Anal. Chem., 51, 1251A (1979).
6) D.F. Hunt, J. Shabanowitz and A.B. Giordani, Anal. Chem. 52 386,(1980).
7) F.A. McLafferty and F.M. Bockhoff, Anal. Chem., 50, 69-76 (1978).
8) W.F. Haddon, Anal. Chem., 51:7 983 (1979).
9) F.J. Biros and J.F. Ryan, III in 'Mass spec and NMR in pesticide chemistry' R.Haque & F.J. Biros Eds. Plenum N.Y. (1974).

MIKES of MALATHION

CI - i C_4H_{10}

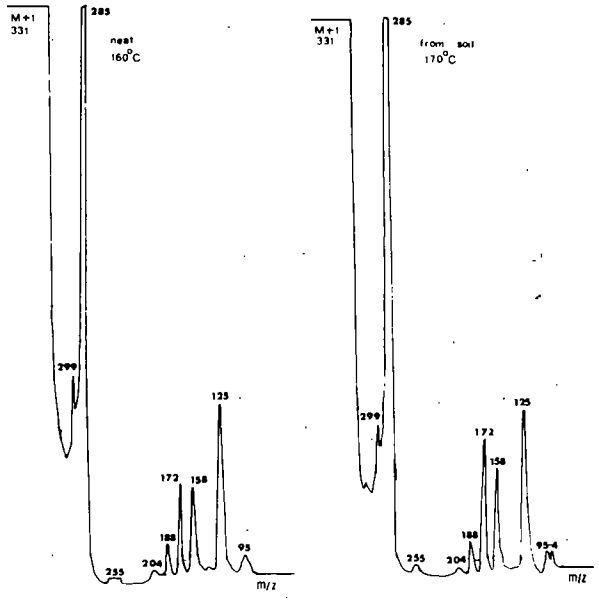

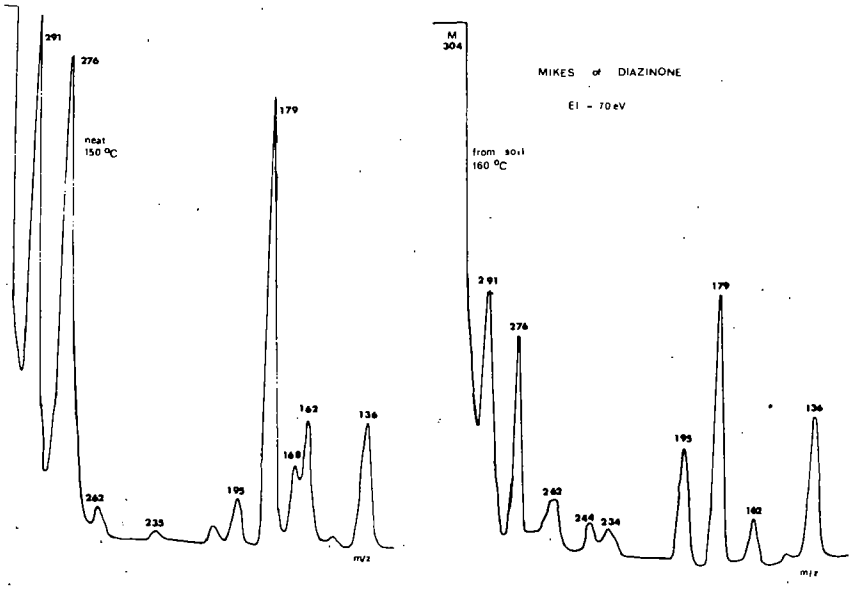

A Comparison of Negative Ionization- and Electron Impact-MS For Analysis of Toxaphene and Toxaphene-Like Residues in the Environment, G.R. Dubay, M.A. Ribick, D.L. Stalling, J.D. Petty, Col. Nat'l. Fisheries Res. Lab., RR-1 USDI-FWS, Columbia, MO 65201, C. Rappe', Univ. of Umea, Umea, Sweden.

The most widely used insecticide in the USA in 1976 was toxaphene[1] which is a complex mixture of more than 177 chlorinated terpenes.[2] Though toxaphene has very low mammalian toxicity, it was shown to be acutely toxic to fish at 0.5ppm in water and have chronic toxicity effects at 72ppb in water.[3] A threat may exist to remote fishery resources in light of the data that Bidleman et. al. published showing toxaphene can be transported over 800 miles in air and it falls out in rain water.[4] In addition, Swedish researches identified polychlorinated terpenes (PCTerps) very similar to toxaphene in fish from lakes in Sweden where toxaphene has never been used.[5]

Analysis of toxaphene from environmental matrices such as fish tissue requires a complex separation scheme to remove other contaminants which are ubiquitous in the environment. Despite use of a very lengthy and complete separation sequence, interferences exist from the chlordane complex and other compounds not sensitive to electron capture detection (ECD).[6] Treatment of the extracts with H_2SO_4/HNO_3 removes all interferences except chlordane.

Comparison of GLC chromatograms of a toxaphene standard and a lake trout extract from Lake Michigan shows them to be almost identical despite the fact that little or no toxaphene is used in this watershed. Using WCOT capillary columns for separation, differences are evident in the chromatograms of the toxaphene-like contaminants found in lake trout and toxaphene. Typically, packed column GC results in toxaphene being resolved into 10 to 15 peaks which represents the over 100 components of toxaphene. Capillary column analysis separates the mixture into 50 or more components depending on the efficiency of the column. Thus, analysis by WCOT capillary column is required for toxaphene and toxaphene-like residues if they are to be differentiated.

Mass spectrometry is capable of providing further information about PCTerps that comprise toxaphene and toxaphene-like residues. Use of EIMS with capillary columns for PCTerp analysis allows the identification of the molecular weight of a few components. However, PCTerps undergo extensive fragmentation resulting in extremely complex mass spectra with few components actually giving a molecular ion. The **response** factors of PCTerps are so low that it is very difficult to use EIMS for typical 1ppm or lower environmental residues. Selected ion detection can increase the sensitivity of EIMS by choosing peaks which are only common to PCTerps as was done by Budde and Eichelberger.[7] Unfortunately, this technique is not capable of distinguishing between some components of lake trout extracts and components of the toxaphene standard which did not have the same mass spectra.

We have found that negative ionization (NI) MS has much greater sensitivity for the analysis of PCTerps because the NI response factors are approximately two orders of magnitude greater than for EIMS. In addition to greater sensitivity, we found that CH_4-NIMS results in little fragmentation and the primary ion cluster formed represents loss of a single Cl from the molecule. Figure 1 shows the difference between NIMS and EIMS for toxicant B, a heptachloroterpene, identified by Casida et. al. to be one of the components of toxaphene having insecticidal qualities.[8] It is clear from Figure 1 that NI spectra of PCTerps are much simpler than EI spectra. Not only was an increase in sensitivity seen for PCTerps but it was found that the response of chlordane and other pesticides is not increased as greatly as for PCTerps.

Analysis of environmental mixtures is much easier using NIMS because it has greater sensitivity and much simpler spectra allowing determination of molecular weight. We have established a very close similarity in environmental residues containing PCTerps from several different areas including lake trout from Lake Michigan, gizzard shad from the Arroyo Colorado in Texas and seal fat from Baltic seals caught in Sweden . Using WCOT capillary column GC-NIMS it was found that 75% or more of the 20 most prominent components in toxaphene are found in both of the two fish extracts. Toxaphene is used in the Arroyo Colorado watershed and this residue corresponds most closely to toxaphene, but extracts from lake trout are not greatly different. The fat of Baltic seals exhibits a very close similarity to extracts of the fish for the higher molecular weight components of the mixture. Some of the differences present may be do to soil, sediment, or metabolic degradation since mammals metabolize toxaphene at differing rates[9] and sediment degradation may be dependent on the reductive potential present.[10] Thus, we suggest that capillary column GC-NIMS be used to characterize

the PCTerps found in the environment.

BIBLIOGRAPHY

1. Eicher, T.R., Andrilenas, P.A., & Anderson, T.W. , U.S. Dept. Agr., Agr. Econ. Rept. No. 418, 1978
2. Holmstead, R.L., Khalifa,S., & Casida, J.E., J. Agr. Food Chem., 22(6), 939 (1974)
3. Mayer, F.L.Jr., Mehrle, P.M.Jr., & Dwyer, W.F., U.S. Environ. Prot. Agency, EPA-600/3-77-069 June 1977
4. Bidleman, T.F., Matthews, J.R., Olney, C.E., Rice, C.P., J.A.O.A.C., 61(4), 820 (1978)
5. Jansson, B., Vaz, R., Blomkvist, G., Jenson, S., Sundstrom, G., & Olsson, M., Chemospere, 1979, 8(4), 181
6. Ribick, M.A., Smith, L.M., Dubay, G.R., & Stalling, D.L., ASTM Committee E35 on Aquatic Toxicology, Special Publications, October 1979, Chicago, IL
7. Budde, W., & Eichelberger, J.W., J. Chromatog., 134(1977), 147
8. Palmer, K.J., Wong, R.Y., Lundin, R.E., Khalifa, S., &Casida, J.E., JACS, 97(2), 181 (1975)
9. Saleh, M.A., Skinner, R.F., & Casida, J.E., J. Agr. Food Chem., 27(4), 731 (1979)
10. Williams, R.R., & Bidleman, T.F., J.Agr. Food Chem., 26(1), 280 (1978)

FIGURE 1

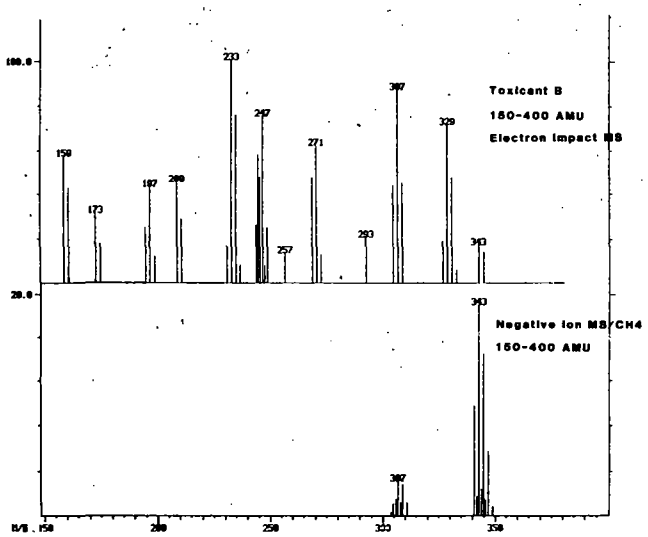

USE OF GC/MS WITH POSITIVE/NEGATIVE ION C.I. AND LOW RESOLUTION ACCURATE MASS ASSIGNMENT TO IDENTIFY IMPURITIES IN A PERHALOGENATED FIRE RETARDANT*

W. D. JAMIESON and C. G. FLINN,
Atlantic Regional Laboratory, National Research Council of Canada,
1411 Oxford Street, Halifax, N.S., Canada, B3H 3Z1;
V. ZITKO, Biological Station, Environment Canada, St. Andrew's, N.B.,
Canada, E0G 2X0

In a study of the uptake and excretion of Mirex and Dechloranes by juvenile Atlantic salmon, an impurity present in a formulation of the fire retardant "Dechlorane 604"[1] ($C_{13}H_4Cl_6Br_4$) accumulated more than the main compound. In that study, electron-impact GC/MS data were insufficient to identify this impurity[2]. We have used electron-impact and chemical ionization GC/MS to identify this bioaccumulated impurity and characterize seven other impurities in the "Dechlorane 604" used in the earlier study.

A Finnigan/INCOS 4023 GC/MS system fitted for electron-impact as well as positive or negative ion chemical ionization experiments (PPINICI) was used. Positive and negative chemical ionization mass spectral data were obtained using methane, isobutane and dichloro-difluoromethane as reagent gases. Gas chromatography conditions: 1000 x 4 mm borosilicate glass column; 3% OV-1 on 100/120 Chrom Q at 260°; He at 35 ml/min; injector, 250°; separator, 300°.

Mass spectrometry conditions: ionization, 70 ev; source, 250° (CCl_2F_2 C.I., 150°); "Finnigan-indicated" source pressures (C.I.), methane (0.30 Torr), isobutane (0.13 Torr), dichloro-difluoromethane (0.05 Torr); peak width 1000 mmu (500 mmu to evaluate m/z assignment accuracy); general m/z calibration by PFK (CH_4 negative C.I.), scan-corrected by OV-1 bleed peaks or added PFK (E.I.), ReO_3, ReO_4 peaks (negative C.I.). Software-controlled multiple ion detection techniques were used for some experiments.

A hexane extract of the juvenile salmon tissue was cleaned up by column chromatography on "Florisil" with hexane and 6% diethyl-ether/hexane eluants.

The most useful data were yielded by electron-impact and negative ion chemical ionization experiments. Retro-Diels-Alder fragmentation or production of [halogenated phenyl = CHCl]$^+$ ions informatively dominated the E.I. spectra of the main compound and those impurities not containing oxygen (from $C_{13}H_5Cl_6Br_3$, 338u and 359u). [M-COCl]$^+$ ions were prominent in the E.I. spectra of oxygen-containing impurities. Positive ion C.I. spectra were not useful. Negative ion C.I. spectra with CCl_2F_2 confirmed molecular ions by chlorine adduct ions. Negative ion C.I. spectra with isobutane had more abundant high m/z ions than with methane; major ions were produced by successive halogen losses (Br, BrCl, Cl, Cl_2) from [M]$^-$ or [M-H]$^-$.

Tuning for a peak width of 500 mmu rather than 1000 mmu did not produce m/z assignments that were significantly more accurate. An INCOS procedure developed aided correction of calibration by locking this to m/z standard peaks in each scan and improved m/z accuracy. INCOS 'PROFILE' and 'COMP' programs were amended.

The bioaccumulated impurity previously noted was identified as $C_{13}H_5Cl_6Br_3$. The data suggest selective accumulation of an isomer or isomers. A second, less abundant impurity was detected as having been bioaccumulated. These and other results are summarized in the Figure.

---

*NRCC No. 18242
[1]Hooker Chemicals and Plastics Corporation
[2]V. Zitko. Chemosphere 9, 73-78 (1980).

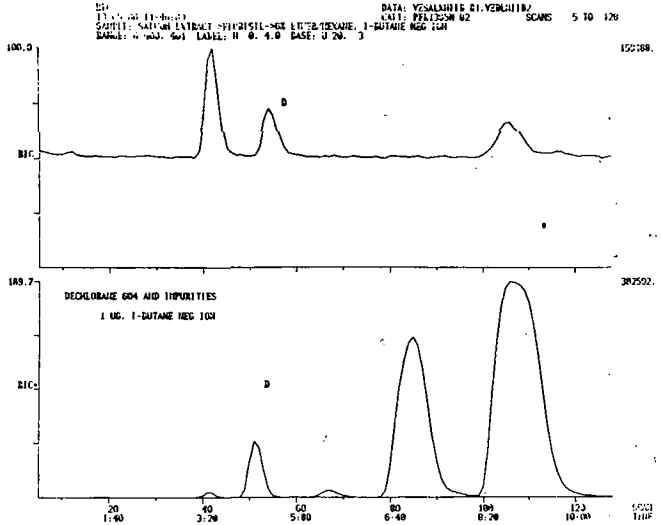

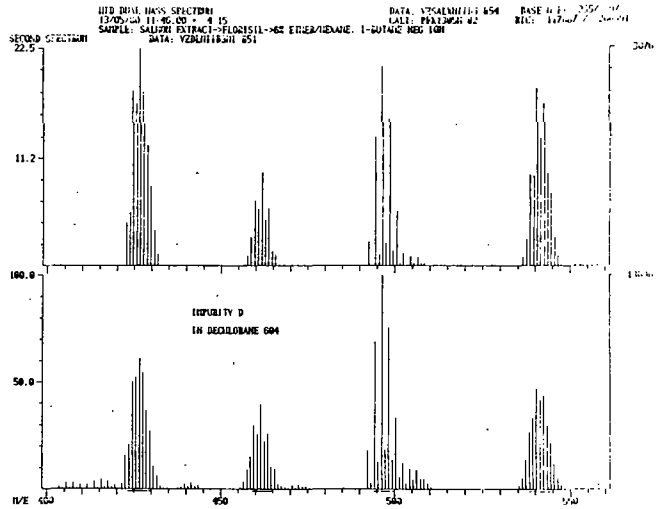

'Dechlorane 604' and Impurities

Compound	RRT	MW(u)	Characteristic Ions(u)
*($C_{10}Cl_{12}$)	0.24	(540)	400, 435*
*($C_{10}H_8BrCl_4O$)	0.29	(466)	362, 390*
$C_{10}H_8Br_2Cl_2$	0.39	564	294, 315
$C_{10}H_8Br_2Cl_4$	0.47	608	338, 359
$C_{10}H_8Br_2Cl_6$	0.63	598	328, 349
$C_{10}H_8Br_2Cl_4O$	0.67	544	481
$C_{10}H_8Br_2Cl_7$	0.80	642	372, 393
$C_{10}H_8Br_2Cl_6O$	0.86	588	525
$C_{10}H_8Br_2Cl_8$	1.00	686	416, 437

* - Isobutane, Neg. Ion C.I.; others E.I.

Accumulated by juvenile Atlantic salmon

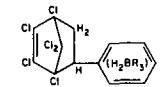

$C_{10}H_8Br_2Cl_6$
Isomer (s)

M.W. 608

Also accumulated. ($C_{10}Cl_{12}$, Mirex*)

APPLICATIONS OF THE ELECTRO-OPTICAL ION DETECTOR MASS SPECTROMETER (EOIDMS)

Heinz G. Boettger
Jet Propulsion Laboratory, California Institute of Technology

Amino acids, amino acid derivatives, and problems in vacuum pyrolysis have been studied using the EOIDMS in conjunction with low voltage electron impact ionization in order to:

1) Demonstrate further the utility of the EOIDMS as a tool for the detection and assay of subnanogram substances in complex mixtures.

2) Correlate vacuum pyrolysis spectra of tissue samples with the type of tissue or tissue fraction as a means of tumor detection and classification.

Samples were introduced into the ion source via a modified CEL probe at temperatures from 125-325°C and ionized by electron impact at voltages as low as 7 eV. Spectra were recorded on the EOID while integrating over the entire sample with detector read-out at intervals ranging from 150 millisecond to 32 seconds for all resolved ion currents from $^{m}/e = 30$ to $^{m}/e = 850$. Pyrolysis experiments were carried out via the technique of oven pyrolysis inside the ion source at temperatures of 250°C to 325°C and ionizing voltages from 7 - 12 eV.

Results will be presented from samples of:

1) All naturally occurring amino acid in form of their PTH-derivatives.

2) L-3', 3', 5-triiodothyronine and L-thyroxine

3) Normal and tumorous brain tissue samples in form of lyophilized whole and homogenized tissue as well as nuclear, mitochondrial, and microsomal fractions.

DETECTION OF PCB'S AND CHLORO-PESTICIDES IN HUMAN FAT BY GC/MS.

E.Schulte, Institut fur Lebensmittel-chemie der Universitat Munster and
U. Rapp, G. Dielmann, Varian MAT GmbH, Bremen, F.R. Germany

Since the legal regulations on admissible maximum levels of the various pesticides, fungicides and herbicides are becoming more and more severe, sophisticated analytical techniques have to be applied especially when working at low concentration levels. Extensive work has been performed on the detection and quantitative determination of those compounds whereby food and ecologically related samples were of most interest. Besides this it is very important to receive an overview on the pesticides' levels in humans.

A GC/MS system was used for the determination of p,p'-DDT, o,p'-DDT and DDD as well as the hexa-, hepta- and octa-chlorobiphenyls. Furthermore ß-hexachlorocyclohexane (HCH) and hexachlorobenzene (HCB) were detected. The analyses were performed by using capillary columns to yield as good separation as possible, e.g. to separate HCH and HCB.

The goal of the measurement was the quantitative determination of chlorinated hydrocarbons in human fat samples. The levels of the pollutants may result in an estimation of the load in human beings.

Problems arising during quantification by overlapping peaks will be discussed, e.g. if packed columns are used.

WAMOA 13 DEVELOPMENT OF A MASTER SCHEME FOR THE ANALYSIS OF ORGANIC COMPOUNDS IN WATER, E. D. Pellizzari, K. B. Tomer, J. T. Bursey, L. S. Sheldon, L. C. Michael, S. L. Yung, R. W. Wiseman, Research Triangle Institute, Research Triangle Park, NC 27709, J. Ryan, J. Gebhart and L. Rando, Gulf South Research Institute, P. O. Box 26518, New Orleans, LA 70186 and A. W. Garrison, Environmental Research Laboratory, U.S.E.P.A., Athens, GA 30605.

The goal of this research program has been to develop and/or validate methodologies which can be combined as a "Master Analytical Scheme" for the qualitative and quantitative analysis of volatile organic chemicals in water using GC/MS/COMP as the major analytical tool.

The first generation Master Analytical Scheme is intended to direct the user in the preferred way to perform the analysis of volatile organics in water. For the purpose of this program, volatile organics mean those which will elute from a gc column at 300° in 1 hour or less or which may be derivatized to meet these criteria. Volatile organics include: (1) intractables, defined as polar water soluble non-purgeable compounds; (2) purgeables, defined as highly volatile compounds, and (3) extractables, defined as intermediate to low volatility substances which are non-purgeable. Ten different chemical groups have been defined for consideration as well as five water types. Drinking and surface waters, municipal, industrial and energy waste effluents.

Table 1 presents a brief outline of the major areas that were investigated in the area of mass spectrometry. Simultaneously a computer program has been written which will provide a mean of calculating the amounts of each component present. Figure 1 presents a flow diagram of the sampling and analytical events that have been incorporated into the Master Analytical Scheme. The upper portion of the figure depicts the major steps for a sample carried through from sampling to quantification of individual components. Briefly, these steps are as follows:

(1) After sampling, the water is to be characterized by conducting a series of water quality measurements. This information will be important for selecting the analytical operations to be subsequently applied and for determining the levels of deuterated internal standards to be added. These measurements are to be made immediately upon obtaining the water sample and prior to embarking on a preservation and storage regime. For a specific water type a minimum of three samples will be needed for the characterization of the "purgeable", "extractable" and "intractable" organics.

(2) After adding internal standards, the procedure(s) will specify how to preserve and store each of the samples.

(3) For separation of organics from a matrix the samples will then be processed according to the selected procedures which have been defined by the water quality measurements.

(4) After the organic components have been separated from the aqueous matrix further processing will yield a series of fractions (approximately 6) to be presented for GC/MS/COMP analysis.

(5) With one exception glass capillaries will be used for resolving the components in each extract. Packed columns are to be used for the analysis of nonionic intractables (direct aqueous injection).

(6) Upon acquisition of information utilizing a full-scan mode qualitative analysis is to be performed either by computer searches or manual interpretation. For those compounds which have been unequivocally identified or identified as belonging to a particular chemical class then quantitative analysis is to be performed.

(7) A software program will provide for calculating the quantity of each component in each of the sample extracts using relative molar response factors (ratioed to the internal deuterated standards). Also it will correct for the recovery of each organic compound from the water matrix based on the recovery data which was generated under this program or by the user. Finally, it will calculate the concentration of each organic in the original water sample.

As an example, the analysis of the purgeables from an energy effluent is presented (Table 2).

This work has been supported by EPA Contract No. 68-03-2704.

Table 1 GENERAL OUTLINE OF MASS SPECTROMETRY EXPERIMENTS

- Instrument Standardization
  - Select a standard or standards for instrument tuning
  - Determine "Optimum" standard spectrum
  - Determine the effect of tuning parameters on relative ion abundances
  - Determine instrument stability
  - Determine the effect of filament/source change on tune and relative ion abundances
  - Quality control check for GC/MS transfer line
  - Determine dependence of RVR on instrument
- Quantitative Aspects
  - Determine the number of data points per chromatographic peak required for reproducibility (SCOT, WCOT, PACKED)
  - Determine whether to use peak heights or areas for quantitation
  - Determine utility of TIC vs SIP for quantitation in different aqueous media
  - Determine the relationship of SIP to SIC
  - Determine the relationship of concentration and RVR
  - Determine LOD's for purgeables, extractables, intractables in various matrices
  - Determine RVRs
  - Determine the nature of the relationship between RVRs determined on different instruments
  - Assess various methods of estimating RVRs
  - Assess time stability of RVRs
  - Determine key compounds for interlaboratory cross-correlation of RVRs
  - Assess utility of other ionization techniques (CI,NCI)
- Qualitative Aspects

Table 2. QUANTITATION OF PURGEABLES FROM ENERGY SAMPLES

Compound	Concentration (ppM) PFT	d_3-anisole	Avg ± S.D.
naphthalene	9.5	5.5	7.5 ± 2.3
benzene	23.1	31.4	27.4 ± 5.3
toluene	11.2	13.5	12.1 ± 3.7
thiophene	0.4	0.3	0.4 ± 0.05
chlorobenzene	0.9	0.8	[a]0.9 ± 0.1
ethylbenzene	0.4	0.1	0.3 ± 0.2
m,p-xylene	2.2	3.0	2.6 ± 0.7
o-xylene	1.0	0.9	1.0 ± 0.03
bromobenzene	1.3	1.6	[a]1.4 ± 0.2
trimethylbenzene	0.2	0.1	0.1 ± 0.06
methylstyrene	1.6	1.8	1.7 ± 0.1

[a]spiked with 0.7 ppm

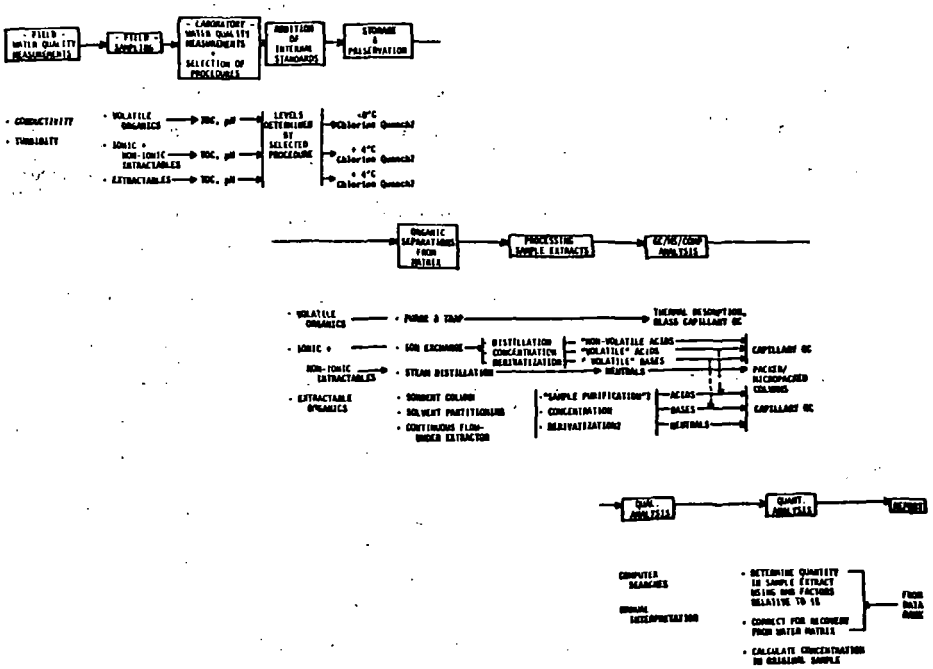

Figure 1. Flow diagram of sampling and analytical events for MAS

HIGH RESOLUTION MASS SPECTROMETRY OF tRNA HYDROLYSATES

H. Pang and James A. McCloskey
Department of Medicinal Chemistry
University of Utah
Salt Lake City, Utah 84112

Transfer RNA functions as an intermediary between the information-carrying mRNA and the functional macromolecule of the cell, the protein. One of the characteristics of tRNA is that it contains a high proportion of modified nucleosides besides the four common ones. At present, about 60 modified nucleosides have been identified in tRNA. In most cases, specific modified residues occur once per molecule of tRNA and a given isoaccepting tRNA will contain 5 - 15 modified nucleosides. Conventionally, two dimensional paper chromatography of enzymatic hydrolysates is used to detect the presence of modified nucleoside in the tRNA. Other methods based on post labeling with ^{32}P have been developed, but which ultimately rely only on chromatographic mobility for identification. Mass spectrometry has proven to be an invaluable tool to determine the structure of purified nucleosides. In the present report, high resolution mass spectrometry with photographic recording is used to detect the presence of modified nucleosides in tRNA hydrolysates without prior chromatographic separation.

Transfer RNA was enzymatically degraded by RNase T_2 and alkaline phosphatase, and trimethylsilylated by standard procedures. The mixture was then introduced into the mass spectrometer by temperature programmed direct inlet for a single photographic recording. A sudden burst of sample was found to cause defocusing, thus, the amount of samples versus the time required for evaporation into the source without defocusing was studied. It required about 150-180 seconds to vaporize 4 μg of the hydrolysate. The TMS of the four predominant nucleosides (adenosine, guanosine, cytidine, and uridine) vaporized from 100-150°C. As a result, slow heating in this range was required. The evaporation profiles of the four predominant nucleosides and one modified nucleoside pseudouridine in the hydrolysate mixture were established using electrical recording.

Mass Spectra were recorded photographically using Ionomet evaporated silver bromide photoplates. Exact mass values from background and internal standards were eliminated in the mass range 400 to 940. Ions with fractional mass values outside the normal range of those from all known natural nucleoside TMS-derivatives were also eliminated. The remaining mass values were compared with an extensive preselected list of exact mass

values in order to identify known nucleosides. The remaining unidentified masses suggested the presence of new modified nucleosides in the hydrolysate.

As an example of sensitivity, the molecular ion of the modified nucleoside N^6-isopentenyl-2-methylthioadenosine in E. coli $tRNA^{Phe}$ was readily detected in 1 μg of tRNA at 20,000 resolutions. This nucleoside constitutes one out of the 76 that are present in the molecule; hence, about 15 ng of this nucleoside was detected.

Increasing resolution will improve the separation of ions with the same nominal mass but different elemental compositions, and will therefore decrease the ambiguity in assigning elemental compositions to unknown ions. However, increasing the resolution will cause a substantial decrease in sensitivity, and so the intensity of PFK lines on the photoplate versus the resolution was studied. It appears that resolution between 15,000 to 25,000 is the useful range for these applications. Higher resolution will cause a large compromise in sensitivity. As an example of potential interferences, the second isotope peak of the major nucleoside uridine interferes with the detection of a modified nucleoside dihydrouridine in the hydrolysate. At resolution 20,000, the $M-CH_3$ ion of dihydrouridine TMS-derivative was separated from second isotope peak of the corresponding uridine ion ($\Delta \simeq 0.018u$).

In summary, high resolution mass spectrometry is a rapid, sensitive and selective technique which is complimentary to conventional chromatography-based methods for analysis of nucleic acid hydrolysates. This method is currently being used to study the contents of modified nucleosides of tRNA from tumor tissues, in particular - Morris hepatoma.

QUANTITATION OF CYTOKININS BY GC-MS USING SELECTED ION MONITORING

Takeshi Hashizume
Laboratory of Bioorganic Chemistry
Tokyo University of Agriculture and Technology
Fuchu, Tokyo 183, Japan

Brenda Basile and James A. McCloskey
Department of Medicinal Chemistry
University of Utah
Salt Lake City, Utah 84112

Cytokinins are arbitrarily defined as substances which promote cell division and growth of certain plant tissues in nutrient media. However, in conjunction with other growth hormones, cytokinins regulate flowering, germination, branching, fruiting and senescence. Levels of cytokinins are generally measured by bioassays such as the tobacco callus assay in which activity is measured by sample weight after a period of growth. The assays have excellent sensitivity, but have several disadvantages. The relative activities of compounds may vary in different assays or even in the same assay utilizing different plant tissues. Another disadvantage is that all compounds must be purified before testing since the interaction of other bioactive substances may inhibit or enhance activity. Third, long incubation periods of several weeks are required. In order to alleviate some of these problems and to provide sensitivities comparable to the bioassays, an assay based on selected ion monitoring using deuterated internal standards has been developed for the cytokinins, N^6-isopentenyladenosine (i^6A), 2-methylthio-N^6-isopentenyladenosine (ms^2i^6A), cis- and trans-zeatin riboside (Z), and cis- and trans-2-methylthiozeatin riboside (ms^2Z).

Background due to the d_0 components in the internal standards ranged from less than 1.5% for i^6A to 3.0% for trans-ms^2Z. After correction for background, the detection limit is 0.4ng/g of plant extract material. Calibration plots show that the assays for i^6A and ms^2i^6A are linear from the detection limit to 20ng, and that the assays for Z and ms^2Z are linear to 12ng. In order to reduce the level of unlabeled material in the standards, new internal standards were synthesized from adenosine-$^{13}C_{10}$ isolated from ^{13}C-labeled *E. coli* which was supplied by the Los Alamos N.I.H. Biotechnology Resource.

The assays utilize an LKB 9000S mass spectrometer equipped with a 2mm x 3 ft 1% OV-17 column which is temperature programmed from 200° to 270° at 6°/min. Under the conditions, the cis and trans isomers of the zeatin compounds are separated. For selected ion monitoring, the molecular ion of i^6A and i^6A-d_6 is chosen for measurement, while the M-CH_3 ions are monitored for the other compounds (1).

A Japanese species of bamboo shoot, which grows at the remarkable rate of 120 cm per day, was analyzed for the presence of cytokinins. Cis-Z was found to be present at a level of 0.5ng/g of material and trans-Z was present at a level of 0.6ng/g of sample. None of the other cytokinins were detected.

The culture media of the infective agent of crown gall tumors, *Agrobacterium tumefaciens*, was also analyzed. Cis-Z was present at a level of 1.1ng/ml of culture, while the trans isomer was present at a level of 0.3mg/ml of culture. It is possible that trans-ms^2Z was present at a level of 0.2ng/ml of culture; however, better internal standards are needed to confirm this finding. In contrast, the avirulent strain of *A. tumefaciens*, which does not induce tumors, did not contain detectable cytokinins. This provides support for the theory that cytokinins play an important role in this disease.

Cytokinin levels can vary within tissues from the same plant. Extracts of tobacco plant roots contained all four of the zeatin compounds, while the extracts of tobacco plant tops contained only cis- and trans-Z. The levels of cis-Z were seven times higher in the top than in the root indicating that cytokinin biosynthesis is not restricted to plant roots, at least for the tobacco plant.

J. A. McCloskey acknowledges support from the National Institutes of Health (GM 21584) and the National Science Foundation (INT78-07474). B. Basile was recipient of an N.I.H. postdoctoral fellowship (GM 07400). T. Hashizume received support from the Japan Society for the Promotion of Science. The authors gratefully acknowledge receipt of ^{13}C-labeled E. coli from the Los Alamos Stable Isotopes Resource, supported by N.I.H. grant RR 0092.

Reference

1. T. Hashizume, T. Sugiyama, M. Imura, H. T. Cory, M. F. Scott and J. A. McCloskey. Anal. Biochem., 92, 111 (1979).

FIELD DESORPTION MASS SPECTROMETRY OF OLIGOPEPTIDES*

Terry D. Lee, Elisabeth Barofsky, William R. Anderson, Jr., Douglas F. Barofsky and G. Doyle Daves, Jr.

Department of Chemistry and Biochemical Sciences
Oregon Graduate Center, Beaverton, Oregon 97006

Field desorption (FD) mass spectra of the oligopeptide sequence series Leu-Trp-MetOH, Leu-Trp-Met-ArgOH, Leu-Trp-Met-Arg-PheOH and Leu-Trp-Met-Arg-Phe-AlaOH were obtained using conventional carbon microneedle emitters.

The peptides were purchased from Chemical Dynamics Corporation and were used without further purification. For analysis, the peptides were dissolved in 10% aqueous acetic acid (1 μg/μl) and 1-2 μl of the resulting solution was placed onto a carbon microneedle emitter using a syringe. FD mass spectra were recorded by photoplate as the emitter heating current was increased manually from 0-20 mA. The peptides desorbed at emitter heating currents of 14-17 mA. The spectrometer used was a CEC (DuPont)21-110 high resolution mass spectrometer modified for use in the FD mode.**

The FD mass spectra of the four structurally related oligopeptides are summarized in the following table:

Peptide	$M^{+\cdot}$	MH^+	Other Ions
Leu-Trp-MetOH	448	449	412, 299, 149
Leu-Trp-Met-ArgOH	-	605	561, 492, 306, 288
Leu-Trp-Met-Arg-PheOH	-	752	708, 604, 457, 322, 307, 304, 288
Leu-Trp-Met-Arg-Phe-AlaOH	-	823	804, 524, 378, 358

Despite the common structural units shared by the oligopeptides in this sequence series, their FD mass spectra exhibit few ions in common. The FD mass spectrum of the tripeptide, Leu-Trp-MetOH, exhibits an abundant $M^{+\cdot}$ ion ($^m/z$ 448) whereas the larger peptides show only MH^+ ions. Surprisingly, no cationized molecular ions (e.g., MNa^+) are observed. In the spectra of the three larger oligopeptides the MH^+ ion is the only abundant ion present.

The FD mass spectrum of Leu-Trp-MetOH exhibits, in addition to the $M^{+\cdot}$ ion at $^m/z$ 448 and an ion at $^m/z$ 412 corresponding to $(M-2H_2O)^{+\cdot}$, two important fragment ions--an unusually abundant (base) ion at $^m/z$ 299 and a complementary ion of low abundance at $^m/z$ 149. As shown in Scheme 1, these fragment ions arise by diketopiperazine formation by attack of the N-terminal amino group of leucine on the amide carbonyl group of the tryptophanyl residue with release of C-terminal methionine.

Although the spectra of the larger peptides do not exhibit ions at $^m/z$ 299 corresponding to the N-terminal diketopiperazine, this reaction remains an important process. This is shown by the presence in the spectra of Leu-Trp-Met-ArgOH (Scheme 2) and Leu-Trp-Met-Arg-Phe-AlaOH (Scheme 4) of ions characteristic of this cleavage with protonation and ion formation of the resulting C-terminal residue. Thus, the FD mass spectra of these peptides, which incorporate the highly basic arginine residue disclose peptide backbone cleavage at the Trp-Met linkage despite the fact that the diketopiperazine, which is presumably formed, does not give rise to an observable ion.

In the spectra of tetra-, penta-, and hexapeptides (Schemes 2-4), evidence for various other peptide backbone cleavages is observed. Each of the processes observed involves hydrogen transfer with (nominal) formation of two neutral species; in each instance only one of these peptide backbone cleavage products--that incorporationg the basic arginine residue--gives rise to an ion in the FD mass spectrum. Rupture of peptide backbone at amide bonds other than that (Trp-Met) leading to diketopiperazine formation also occurs: Leu-Trp (Scheme 2) and Met-Arg (Schemes 3,4); no cleavages of the Arg-Phe or Phe-Ala amide linkages which are nearer the C-termini of the peptides are observed. Peptide backbone cleavage with amide elimination producing $LeuTrpNH_2$ (Scheme 2) and $Leu\text{-}TrpMetNH_2$ (Schemes 3,4) is also observed.

The spectra of these oligopeptides of this sequence series contain relatively few ions. The spectra are devoid of ions representative of losses from amino acid side chain moieties. Similarly, ions arising by more complex processes such as sequential loss of two or more small molecules are observed in only two instances (Scheme 1, loss of $2H_2O$; Scheme 4, pep-

*An expanded version of this paper has been submitted to Biomedical Mass Spectrometry (1980).
**Modification of the 21-110 was carried out jointly by OGC and Nuclide Corp., State College-Pa. A description is given in these proceedings (Paper No. TPMP 18).

tide backbone cleavage with loss of CO_2); no doubly charged ions are apparent. The ions which are observed are, with few exceptions, readily assigned to peptidic fragments which arise by thermal rearrangements involving hydrogen transfer, followed (usually) by protonation. The majority of ions observed are of structural significance (Schemes 1-4). Each of the spectra exhibited ions which are interpretable to provide partial amino acid sequence information; in none of the four cases does the spectrum permit a complete sequence to be assigned.

Acknowledgement

We express appreciation to the National Institutes of Health (AM 20937, AI 14699) and to the M. J. Murdock Charitable Trust for financial support.

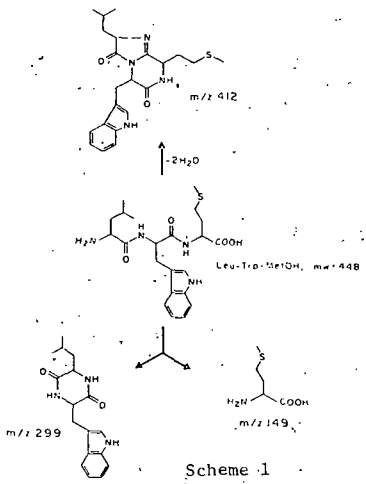

Scheme 1

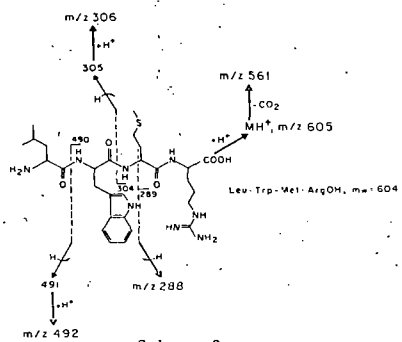

Scheme 2

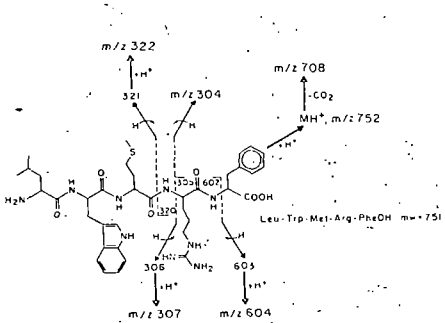

Scheme 3

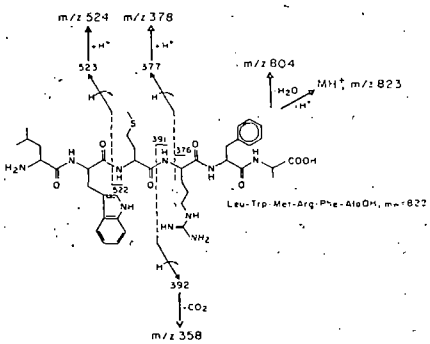

Scheme 4

Polypeptide Sequencing Using NICI and MS/MS

Donald F. Hunt, Mary Sisak, Alex Buko, John Ballard, Anne Giordani and Jeffrey Shabanowitz

Department of Chemistry
University of Virginia
Charlottesville, Virginia 22901

Methodology for the sequencing of large polypeptides is described. Methods applicable to the sequencing of neuropeptides which are presently only available in picomole quantities is also described.

Large polypeptides are enzymatically digested or hydrolyzed to a mixture of small more easily identified peptides. After derivatization which includes acetylation of all amine groups with a 1:1 mixture of d_0,d_6-acetic anhydride in methanol and substitution of all labile hydrogens with methyl groups by a strong base and methyl iodide, the peptide mixture is introduced into the chemical ionization source via a solids probe. The convential positive ion chemical ionization mass spectrum is extremely complex containing M+1, 29 and 41 ions of all the peptides as well as sequence ions resulting from the fragmentation of the M+1 ions. This makes anaylsis of the spectrum difficult. It can be simplified with the finnigan triple quadrupole (TSQ) which allows specific ions to be selected and analyzed.

The TSQ consists of a convential CI source and three consecutive sets of quadrupole rods. The analysis of peptides is done by a method of scanning which we have termed dual scanning. The first set of rods, q_1 is set at a slow scan rate of 1 amu/sec but are detuned to allow the passage of a window of masses such as 8 amu. These ions are directed into the collision chamber, q_2 which consists of an enclosed set of rods which only have a rf potential placed on them making them a high pass filter. The enclosure allows for the maintenance of a low nitrogen pressure. On entering the chamber, the ions undergo collisions with the N_2 which imparts sufficient energy to allow some of them to undergo further fragmentation to sequence ions generated by the cleavage of the amide bonds The third set of rods which analyzes the CAD fragments is set at a scan/sec. Thus for each 8 amu window that is allowed to pass through q_1 and undergo collisional decomposition, a complete spectrum of the fragments is obtained. An entire digest can be analyzed automatically after the parameters have been set.

Analysis of neuropeptides requires increased sensitivity due to the small sample sizes presently available. Analysis of these will be done with election capture chemical ionization mass spectrometry which has been shown to provide up to 300 times greater sensitivity. Derivatization of the amine groups is as previously described. The free carboxyl groups are esterified with pentafluorobenzyl bromide in acetonitrile and diisopropylethylamine. The introduction of the pentafluorobenzyl group increases the electron capture capability of the molecule which therefore increases the sensitivity. On electron capture the ester linkage is cleaved leaving the charge on the C terminal amino acid. The mass difference between the parent ion and fragment allows for the identification of the N terminal amino acid. This same derivative is being extended to single amino acids in an effort to develop a quick and sensitive amino acid analysis.

A possible approach to the analysis of neuropeptides that is being explored is to divide the peptide sample into two portions. The first is digested with dipeptidylaminopeptidase I and IV (DAP I & IV) to generate a mixture of dipeptides. The second portion is first subjected to a single Edman degradation to remove the N terminal amino acid followed by digestion with DAP I & IV to generate a second mixture of dipeptides. The series of overlapping dipeptides combined with the amino acid composition should allow the sequence of the peptide to be determined.

The amino acid analysis will be done by hydrolyzing the peptide to single amino acids which are then acetylated with d_0-acetic anhydride.

A standard mixture containing equal molar quantities of all amino acids acetylated with d_6-acetic anhydride will then be added and the entire mixture esterified as previously described. The resulting spectrum will contain anions indicative of all the amino acids acetylated with d_6-acetic anhydride as well as doublets at masses indicative of the peptide amino acids acetylated with d_0-acetic anhydride and standards derivatized with d_6-acetic anhydride. The ratio of the d_0 to d_6 should provide the empirical amino acid composition.

GAS CHROMATOGRAPHY/MASS SPECTROMETRY CHARACTERIZATION OF MANNANS DERIVED FROM MEDICALLY SIGNIFICANT YEASTS

L.W. Yert, E. Reiss, D.G. Patterson, B.K. Ibrahem, and J.S. Holler, Toxicology Branch, Center for Disease Control, Public Health Service, U.S. Department of Health and Human Services, Atlanta, Georgia 30333

Mannans are peptidopolysaccharide constituents of yeast cell walls. They are readily soluble homopolymers of mannose composed of a highly branched outer chain linked to a less branched inner core. The core is connected to a structural protein via a terminal chitobiosyl-aspartamido glycopeptide. The antigenically important outer chain of yeast mannans have a 'brushy' shape consisting of an $\alpha(1\text{—}6)$ linked backbone highly substituted with short oligomannoside side chains whose average degree of polymerization is 3 to 6. The internal linkages in the side chains are $\alpha(1\text{—}2)$ and $\alpha(1\text{—}3)$.

Mannans of medically important yeasts of the genus Candida are sloughed-off the cell walls during infection and are bound by immunoglobulins (Ig) and cleared from the circulation. Persons whose immune responses are compromised by cancer, autoimmune disease, or kidney transplants are at risk to develop systemic Candida infections. Such persons cannot mount an adequate Ig response and mannan antigenemia persists and can be exploited to form the basis of an unequivocal laboratory diagnosis. The serious nature of this disease in immunosuppressed patients and the discovery of mannan antigenemia has renewed interest in the structure of Candida mannans.

PURPOSE

The goals of GC/MS structural analysis of these mannans are: (1) To propose a repeating unit to account for the structural features of the antigenic (or heptemic) region of the outer chain. (2) To provide a criterion of purity for biological standards. (3) To compare the structures of mannans from various Candida species. (4) To understand the molecular basis of serotypes. (5) Ultimately, to discover a GLC method for the direct detection of mannans in body fluids which would remove the necessity for the use of immunoassay procedures.

RESULTS AND DISCUSSION

The use of standards generated from per-o-acelyladononitriles of D-mannose (1) permitted the structure of the various monosaccharides to be identified (see Figure 1 and Table I) by relative retention times and mass spectrometry. Determination of the relative amounts of the various monosaccharides suggests the types of linkages and the amount of branching, both in the side-chain and in the backbone of the polysaccharide. The length of the oligomannoside side chains and the extent of substitution on the backbone can contribute to serological activity.

The results shown in Table I for C. albicans (serotype B, see also Figure 3) are similar to those previously reported (2) using GLC. In our study, however, we do not find in any of the three yeasts (Table I) the 3,5-di-o-methyl derivative as previously reported to be present (3). Our results are also different for C. albicans (serotype A, see also Figure 2) since the data in Table I indicates that the oligosaccharides from serotype A may be longer than those in serotype B which is the opposite conclusion from data presented previously (2). There is a significant amount of (1—3—6) linked sugars (See Table I) in both serotypes A and B (three previous studies did not report this 2,4-di-o-methyl derivative). This (1—3—6) linkage has been detected previously in some other yeasts where it may represent up to 36 mole percent. This (1—3—6) linkage may be in the inner core as suggested by Ballou (3) in the case of Baker's yeast. The data (Table I) for Torulopsis Glabrata suggest that nearly all of the sugars in backbone are branched with very short sidechains and only a small amount of (1—3—6) branching.

---

(1) F. Seymour, R. Plattner, and M. Slodki, Carbohydrate Research, 44, 181 (1975).

(2) R. Yu, C. Bishop, F. Cooper, H. Hasenclever, and F. Blank, Can. J. Chemistry, 45, 2205 (1967).

(3) C. Ballou in A. Rose and D. Tempest (eds.), Advances in Microbiol. Physiology, 14, 93-153 (1976).

TABLE I. RELATIVE MOLE PERCENT OF PERACETYLATED NITRILES OF METHYL ETHERS OF MANNANS DERIVED FROM MEDICALLY SIGNIFICANT YEASTS

PEAK	METHYL ETHER	C. ALBICANS (SEROTYPE A)	C. ALBICANS (SEROTYPE B)	TORULOPSIS GLABRATA	TYPE SUGAR
B	2,3,4,6-TETRA-	23.0	28.6	36.6	TERMINAL NON-REDUCING SUGAR
C	-TETRA-	2.2	2.4	3.5	-
D	2,4,6-TRI-	4.7	3.5	2.4	(1-3) LINKED INTERNAL SIDE CHAIN SUGAR
E	3,4,6-TRI-	46.2	37.1	33.1	(1-2) LINKED INTERNAL SIDE CHAIN SUGAR
F	2,3,4-TRI-	7.6	7.9	1.3	(1-6) UNBRANCHED BACK-BONE
G	2,4-DI-	5.3	9.2	1.0	(1-3-6) BRANCHED
H	3,4-DI-	11.0	11.4	22.2	(1-2-6) BRANCHED BACK-BONE

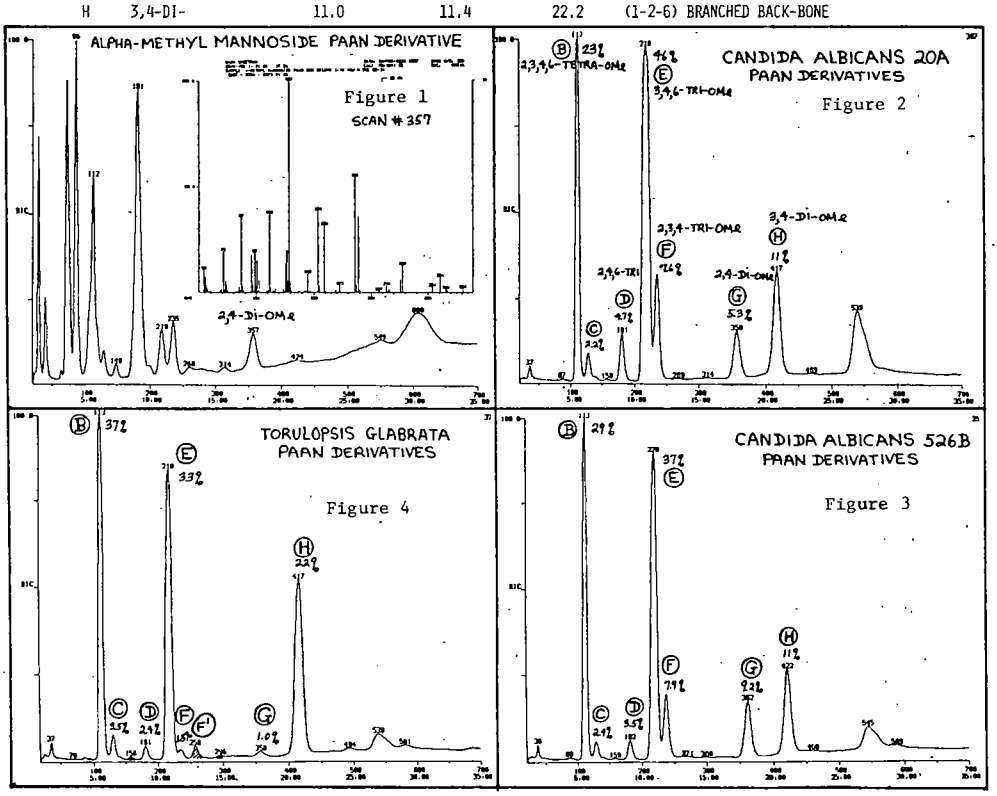

STRUCTURE ELUCIDATION OF SLOW REACTING SUBSTANCE AND SLOW REACTING SUBSTANCE OF ANAPHYLAXIS

H.R. Morris, G.W. Taylor, P.J. Piper*, J.R. Tippins*
& M.N. Samhoun*.
Dept. of Biochemistry, Imperial College, London, U.K.
*Dept. of Pharmacology, Institute of Basic Medical Sciences,
Royal College of Surgeons, London, U.K.

For many years, attempts have been made to elucidate the structures of Slow-Reacting Substances, the most interesting of which is probably the immunologically induced slow-reacting substance of anaphylaxis (SRS-A) from lung because of its putative bronchoconstrictor role in asthma. We have determined the complete structure of SRS-A by spectroscopic (mass spectrometry) and analytical protein chemical techniques as the novel peptidolipid 5-hydroxy-6 cysteinylglycinyl-7,9,11, 14 eicosatetraenoic acid. (1,2).

A milestone in the progress towards the goal of structure elucidation was the incorporation in 1978 of reverse phase HPLC in the purification of SRS-A and the demonstration that purified SRS-A possessed a characteristic U.V. spectrum ($\lambda_{max.}^{MeOH}$ 280 nm) (3) subsequently assigned to a conjugated triene (4). The HPLC purification procedure which we introduced allowed us to show the presence, in our preparations from lung, of a second less active SRS-A (cis→trans isomer, λ_{max}, 278 nm) and two other related compounds, the major one of which we identified by mass spectrometry as 5,12-dihydroxy-6,8,10,14-eicosatetraenoic acid (5).

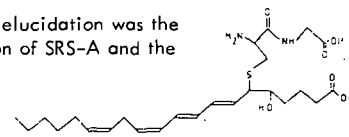

5-hydroxy-6-cysteinyl glycinyl-7,9,11,14-eicosatetraenoic acid

Early studies on the potentiation of release of SRS-A from lung indicated a precursor role for arachidonic acid (5); similar data has been reported for non-immunologically released SRS's (6). Initial structural investigations into SRS-A involved chemical and enzymic inactivation of biological activity by brief exposure to various reagents (without modifying the U.V. chromophore). We showed that SRS-A possessed α-amino (short acetylation), carboxyl (esterification) and thioether (CNBr) functions (5). The presence of a cis-cis 1-4 pentadiene moiety in SRS-A was suggested by our early work on lipoxygenase inactivation (7).

Our early attempts to produce a mass spectrum of SRS-A gave rise to a partial structure; at this point Samuelsson et al. announced the structure of a non-immunologically generated SRS as 5-hydroxy -6-cysteinyl 7,9,11,14 eicosatetraenoic acid (Leukotriene C). We reported that our data on SRS-A did not fit this structure (5), and it was subsequently withdrawn, the side chain being revised to show a 6-"R" substitution (8).

Because of the vanishingly small quantities of SRS-A released from lung making the structure elucidation extremely difficult, we investigated an SRS released non-immunologically from RBL-1 cells. We had previously shown that SRS-A and SRS had indistinguishable pharmacological, physico-chemical and chromatographic properties (4). SRS is released from cells in somewhat larger quantities, and with far fewer impurities, thus we used RBL-1 SRS as a model to optimise the conditions for our mass spectrometric studies on SRS-A.

Amino acid analysis of both SRS-A and the model RBL-1 SRS system at the 100 pmole level, showed the presence of only two amino acids, cysteine and glycine; N-terminal analysis by dansylation showed the presence of Dansyl-cysteine only, thus defining part of SRS-A as the dipeptide cysteinyl-glycine.

Structural data (above) had suggested the probability of certain functional groups in SRS and SRS-A (α-amino, carboxyl); short acetylation and esterification (MeOH : HCl or CH_2N_2) were chosen to block these functions. The 1 : 1 N-acetyl : d_3 acetyl derivative was prepared to facilitate identification of peptide derived ions in the mass spectrum (as 1 : 1 doublets, three mass units apart). The final derivatisation step was trimethylsilylation.

The mass spectrum of the derivative of RBL-1 SRS obtained (240°C fig. 1) defines the overall structure via (a) the molecular weight of a derivative (m/e 638: $M^{+\cdot}$) and thus of SRS itself (b) the peptide portion via ions at m/e 405/404 and m/e 315/314 (-TMSOH) (c) the existence and position of a hydroxyl group in the molecule (m/e 548 : $M^{+\cdot}$ -TMSOH, m/e 203: $TMS\overset{+}{O} = CH(CH_2)_3CO_2CH_3$). Analysis of the spectrum together with isotope labelling experiments (d_9TMS), accurate mass measurement, U.V. and inactivation data obtained earlier, allowed us to unequivocally define the first full

covalent structure of any SRS as the novel peptidolipid : 5-hydroxy-6-cysteinylglycinyl-7,9,11,14-eicosatetraenoic acid (1); concommitantly with this work, the structure of Leukotriene C was revised by comparison with a series of synthetic compounds, and shown to be the 6-glutathionyl derivative (9).

SRS-A from guinea-pig lung was derivatised (together with an equivalent quantity of RBL-1 SRS), as outlined above; 1 : 1 acetyl : d_3 acetyl labelling was used as a mass spectrometric marker. The spectra show unequivocally that SRS-A is identical to RBL-1 SRS (2). Due to the difficulties of determining structure on the extremely small quantity of SRS-A available ($\leqslant$ 4 µg) no molecular ion was observed in the mass spectrum. This in no way invalidates the interpretation as (a) no molecular ion was observed in the RBL-1 SRS control at this level (b) the complete structure may be found by combining the information from the fragment ions. The demonstration that a mass spectrum can be produced from undegraded SRS-A (1,2) using the readily formed derivatives suggested here, forms the basis for future qualitative and quantitative determinations of the slow-reacting substances. The complete stereochemistry of SRS(-A) has now been determined by extensive comparison with synthetic materials (10) and is shown to be 5(R) hydroxy 6(S) cysteinylglycinyl 7,9(trans) 11,14 (cis) eicosatetraenoic acid.

It is interesting to note that immunologically generated SRS-A from guinea-pig is identical to that produced non-immunologically from malignant basophils. High resolution chromatographic comparison of human and guinea-pig SRS-A (4) has shown co-elution, suggesting that human SRS-A also has the cysteinyl glycinyl structure. Further work is in progress on the rigorous spectroscopic identification of human SRS-A.

SRS-A is biosynthesised by an intriguing combination of lipoxygenase metabolism of arachidonic acid together with the glutathione detoxification pathway. Our studies on enzymes involved in these pathways (glutathione S-transferase, γ -glutamyl transferase) have shown a significant increase in these enzyme levels on SRS(-A) release (i.e. on antigen challenge or ionophore treatment) indicating their involvement in the genesis of SRS-A.

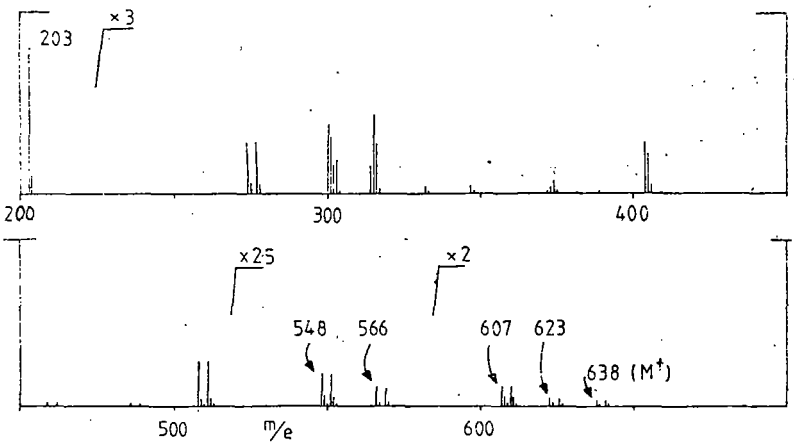

Fig. 1

RBL-1 SRS (1000 units) (5 µg) 240°C

TMS ether of the N-acetyl (1:1 CH_3CO/ CD_3CO) methyl ester

References:

1. Morris H.R., Taylor G.W., Piper P.J., Samhoun M.N. and Tippins J.R., Prostaglandins 19, 185-201 (1980).
2. Morris H.R., Taylor G.W., Piper P.J. and Tippins, JR., Nature 285, 104-106 (1980).
3. Morris H.R., Taylor G.W., Piper P.J., Sirois P. and Tippins J.R., FEBS lett. 87, 203-206, (1978).
4. Morris H.R., Piper P.J., Taylor G.W. and Tippins J.R., Br. J. Pharmac. 67, 179-184, (1979).
5. Morris H.R., Taylor G.W., Piper P.J. & Tippins J.R. in Prostaglandins and Inflammation, ed. K.D. Rainsford and A.W. Ford-Hutchinson, Agents and Actions Suppl. 6, 27-36, Birkhauser Verlag, Basel (1979a).
6. Parker C.W., J. Allergy and Clin. Immunology 63, 1-14 (1979).
7. Engineer D.M., Morris H.R., Piper P.J. and Sirois P., Br. J. Pharmac. 64, 211-218, (1978).
8. Murphy R.C., Hammarstrom S. & Samuelsson B., Proc. Natl. Acad. Sci. 76, No. 9, 4275-4279 (1979).
9. Hammarstrom S., Murphy R.C., Samuelsson B., Clark D.A., Miokowski C. & Corey, BBRC 91, 1266 (1979)
10. Rokach J., Girard Y. et al., Tetrahedron Letters 21, 1485-1488, (1980).

WAMOB7 USE OF CARBOXYL ^{18}O-LABELLED SPECIES IN EICOSANOID RESEARCH, R.C. MURPHY, R. MATHEWS, and W.C. PICKETT. Dept. of Pharmacol., Univ. of Colo. Med. Center, Denver, CO 80262

We have recently described the synthesis of amino acids labelled with two O-18 atoms at the carboxyl moiety and their utility as internal standards for quantitative mass spectrometry of plasma amino acids. We have extended the application of carboxyl O-18 species into the metabolites of arachidonic acid or eicosanoid family. Many metabolites in this family such as prostaglandins, thromboxanes, and leukotrienes are typically unstable to acid and elevated temperatures which prevents direct chemical exchange. However, we have found that O-18 can be incorporated by incubating a methyl ester derivative with porcine liver esterase in O-18 water. It was further observed that incubation of the free acid with the esterase in O-18 water resulted in the incorporation of two O-18 atoms into the carboxyl moiety. The half-life of this exchange reaction of the prostaglandin free acid is approximately 1 hour at 37°. The back exchange of these carboxyl labelled prostaglandins under physiological conditions as well as their utility as internal stnadards for quantitative mass spectrometry will be discussed.

O-18 labelled amino acids were used in the elucidation of the structure of leukotriene C (LT-C, slow reacting substance of anaphyaxis) which is another eicosaniod. The peptide portion of LT-C was investigated by hydrolysis in 6N HCl and the amino acids identified by GC-MS. Glycine and pyroglutamic acid in the LT-C hydrolysate were quantitated using the corresponding O-18 labelled amino acids and GC-MS techniques.

WAMOB8 CHEMICAL IONIZATION SELECTED-ION-MONITORING MASS SPECTROMETRIC ANALYSIS OF DEUTERIUM TRIPLE-LABELED BLOOD LIPIDS. WILLIAM K. ROHWEDDER. Northern Regional Research Center, AR,SEA,USDA,Peoria, Illinois 61604.

A new chemical ionization selected-ion-monitoring mass spectrometric technique has been developed to analyze triple-labeled blood lipids. In the triple-label experiments, human subjects are fed three isomers having different geometrical and positional configurations. These monounsaturated fatty acids are labeled with two, four and six deuterium atoms to determine if the human body differentiates between the isomers. Previous blood lipid work used electron impact selected-ion-monitoring mass spectrometry of the two fragments formed by loss of methanol and loss of methoxy from the methyl ester of the fatty acid. These two fragments together contain only 5% of the total ionization while the molecular ion contains only 1% of the total ionization. These low-intensity peaks limit the sensitivity of the analytical method. Chemical ionization of methyl esters using a mixture of methane and isobutane as the reagent gas produces a pseudo-molecular ion (M+1) that is the major ion in the spectrum. Selected-ion-monitoring of the pseudo-molecular ion peak gives a 10-fold improvement in the sensitivity over electron impact techniques.

Analysis of a blood phospholipid containing three different deuterium-labeled fatty acids will be utilized to demonstrate the capabilities of this methodology.

THE FIRST DEMONSTRATION OF AVENASTEROL IN HUMAN PLASMA

D.M. Desiderio[1], J.Z. Sabbatini[1], J. Ragland[2] and G. Whittington[2], Department of Neurology and [2]Stout Neuroscience Mass Spectrometry Laboratory and [2]Department Medicine, University of Tennessee Center for the Health Sciences, 800 Madison Avenue, Memphis, Tennessee 38163

A patient presented to GW with the following symptoms: At age three, tumor xanthomas were present and Type II familial hypercholesterolemia was manifested. At age ten, cholesterol increased to 600 mg% (normal = 200 mg%), tendonous xanthomas appeared and cholestyramine treatment tended to normalize cholesterol within one month with reduction of xanthomas. At age 18, 200 mg% of plasma sterols were found and, according to GC, 1/4 of these sterols were composed of major plant sterols plus minor sterols. In addition, small posterior cataracts and moderate hypertension were present. The patient was diagnosed to have cerebrotendonous xanthomatosis or CTX (1,2).

CTX is a rare, inherited disease marked by progressive cerebellar ataxia, dementia, cataracts and tendonous xanthomas. Cholesterol accumulates in white matter and xanthomas. Cholesterol is normal whereas cholestanol (3) is elevated several-fold. Tendon biopsy is generally required for diagnosis and, finally, there is a high incidence of atherosclerosis.

GC-MS data revealed high levels of plant sterols, a minor plant sterol, cholestanol and several phytostanols. Experimental conditions used a Hewlett-Packard (5950A) and Finnigan (9500) GC. Both employed a 6' column with SP 1000 coating on 100-120 mesh Supelcoport. Isothermal conditions: 230°. During GC-MS, temperature programming, at one degree per minute up to 250°, commenced after cholesterol elution. Mass spectra were recorded with Finnigan 3200 (EI) and Finnigan 1015 (CI, methane). Argentation thin layer chromatography (TLC) employed 10% silver nitrate sprayed on silica gel to separate Δ^5 and Δ^7 sterols from corresponding stanols.

Steroid structures were confirmed with low resolution MS data. Campesterol, stigmasterol, β-sitosterol and avenasterol were also present (4). The first three are the major plant sterols. The patient manifests indiscriminate gut sterol malabsorption - phytosterols increase and decrease according to the patient dietary intake (5).

The unknown, last eluting GC peak eluted much later than fucosterol and β-sitosterol and had the same molecular weight as fucosterol (412) but was not fucosterol because fucosterol eluted between sitosterol and the unknown peak. This peak corresponds to avenasterol, the Z-isomer of fucosterol (6). This is the first occurrence of avenasterol found in human plasma. The fucosterol mass spectrum (7,8,9) indicates (EI, CI, TMS, free) a McLafferty rearrangement peak at $(M-98)^{+\cdot}$. This ion occurs in both fucosterol and avenasterol spectra. MS and GC evidence support the presence of avenasterol in this patient's serum. This is the first finding of avenasterol in combination with phytosterols and cholestanol. These sterols and stanols are found in high concentration in this patient's serum.

Because reduced sterols were indicated in this patient's serum, argentation thin layer chromatography was employed to preferentially retain Δ^5 and Δ^7 sterols plus sterols with unsaturated side chains and to trace-enrich phytostanols and cholestanol.

A reconstructed GC from GC-MS data indicates some remaining cholesterol, campesterol and sitosterol in the serum extract and a relative increase of cholestanol, campestanol and "sitostanol".

However, four Δ^5 sterols and one Δ^7 sterol should yield the compound of molecular weight 416. This compound corresponds to avenastanol, spinastanol, stigmastanol, sitostanol and fucostanol. This one reduced compound could arise from all five sterols and its presence illustrates that the patient had indiscriminate phytostanol malabsorption problems in addition to the above-mentioned phytosterol problem.

It is interesting to note in passing that stigma-4-ene-3-one was found in one experiment. This product is an artifact and arises from oxidation of Δ^5 β-sitosterol by chromic acid-washed glassware.

In conclusion, an interesting combination of phytostanol and phytosterol absorption problems were found in a human patient. Cholestanol levels are elevated and major plant sterols (β-sitosterol, campesterol, stigmasterol and avenasterol) were present in addition to saturated plant sterols. Campestanol was found as well as the single compound corresponding to fucostanol-avenastanol-spinastanol-stigmastanol-sitostanol. Chronic sterol and phytostanol malabsorption problems occur. These findings represent the first occurrence of the above combinations for cholestanol (CTX), β-sitosterol (Xanthomas and β-sitosterolemia) phytosterolemia, and phytostanolemia.

REFERENCES

1. Hoshita, T., Yasuhara, M., Kihira, K. and Kuramoto, T., Steroids 5, 657-663 (1976).
2. Seyama, Y., Ichikawa, K. and Yamakawa, T., J. Biochem., 80, 223-228 (1976).
3. Tohma, M., Makata, Y. and Kurosawa, T., J. of Chromatog. 171, 469-472 (1979).
4. Rao, M.K. Govind, Perkins, E.G., Connor, William E., Bhattacharyya, Ashim K., Lipids 9, 921-927 (1975).
5. Dusza, J.P., J. Org. Chem. 25, 93 (1960).
6. Itoh, T., Tamura, T. and Matsumoto, T., JAOCS 50, 300 (1973).
7. Knights, B.A., Phytochem. Vol. 4, 857-862 (1965).
8. Brooks, C.J.W., Knights, B.A., Sucrow, W. and Raduchel, B., Steroids 20, 487-497 (1972).
9. Massey, Ian J. and Djerassi, C., J. Org. Chem., 44, 2448-2556 (1979).
10. Wegmann, A., Anal. Chem. 50, 830-832 (1978).

WAMOB10 RAPID SIMULTANEOUS ASSAY OF SERUM ESTRONE (E_1), ESTRADIOL (E_2), AND ESTRIOL (E_3) USING METHYL ETHER ACETATE (MEA) DERIVATIVES ON CAPILLARY GC-EI-MS.

Kou-Yi Tserng, Robert K. Danish, and Juliana S. Bendt. Dept. of Pediatrics, Case Western Reserve Univ. at Cleveland Metropolitan General Hospital, Cleveland, Ohio.

The measurement of E_1, E_2, and E_3 serum levels is usually done by radioimmunoassay (RIA), but requires three separate assays. A simple GC/MS method capable of measuring these estrogens simultaneously with a sensitivity close to that of RIA has been developed. This method also provides the opportunity to study estrogen metabolism in pregnant women with safe stable isotopic tracers.

The estrogens in serum are extracted with diethyl ether, and internal standards (3-O-C^2H_3-E_1,-E_2, and -E_3) are added. It is followed by converting to methyl ether compounds with an extractive alkylation procedure (methylene chloride,methyl iodide, and tetrabutylammonium hydroxide in alkaline solution). The methyl ethers are then acetylated in acetic anhydride and pyridine. Analysis is done using OV-17 capillary column gas chromatograph coupled with electron impact mass spectrometer.

Improved purification of the sample occurs with the extractive alkylation procedure and with the use of high resolution capillary column GC. In addition, the use of splitless mode capillary GC enhances the sensitivity. The estrogen-MEA derivatives are more stable chemically and give less fragmentation upon electron impact than the conventional trimethylsilyl derivatives. The use of selected ion monitoring of molecular ions and the corresponding internal standards (M+3) provides a sensitivity down to 10 pg for E_1. and E_2, and to 50 pg for E_3. The time for preparation of multiple samples is only hours as compared to days or weeks of the published GC/MS procedures.

The serum E_1, E_2, and E_3 basal levels of women in second and third trimester pregnancy, and their rises after administration of dehydroepiandrosterone sulfate have been measured with this technique for correlation with pregnancy outcome. E_2 levels measured by GC/MS and by RIA show good correlation.

COMPUTERIZED GAS CHROMATOGRAPHY MASS FRAGMENTOGRAPHIC ANALYSIS OF LITHOCHOLIC ACID IN LIVER TISSUE

Izumi Maruyama, Toshihiro Shinka, Tomiko Kuhara, °Ryukichi Kumashiro, °Kyuichi Tanikawa and Isamu Matsumoto

Research Institute of Medical Mass Spectrometry, Kurume University School of Medicine and °The 2nd Department of Internal Medicine, Kurume University School of Medicine, Kurume, Fukuoka 830, Japan

Lithocholic acid which induces experimental intrahepatic cholestasis is presumed to be one of the causal agents of human intrahepatic cholestasis (1,2). Most of the studies on biogenesis and enterohepatic metabolism of lithocholic acid, however, have been limited to bile, urine, blood and intestinal contents, and only a few papers have been concerned with the distribution of lithocholic acid in tissues (3,4,5). This is largely due to the lack of an adequate technique for isolation and quantitation of bile acids from cellular materials. As the most suitable method presently available, selected ion monitoring (SIM) was applied to the quantitation of the lithocholic acid in liver tissue.

Non-tumorous liver tissues (0.2g) from the resection of human hepatocellular carcinomas were obtained and immediately rinsed with a cold saline solution. They were homogenized with 95% ethanol cantaining 0.1% NH_4OH in a heated water bath at 80°C. Each 5 μg deuterium-labelled deoxycholic acid (D-DC) or 5β-cholanic acid per g wet weight tissue was added as an internal standard. Cholesterol was removed with hexane at pH 10.0. Then the remaining extracts were hydrolyzed with cholylglycine hydrolase for the enzymatic cleavage of bile acid conjugates (6). They were acidified to pH 1.0 and extracted with diethyl ether. The ether extracts were dried out and derivatized to trimethylsilyl (TMS) ether-methyl ester or trifluoroacethyl (TFA) ether-hexafluoroisopropyl (HFIP) ester (Fig.1) (7).

A JEOL JMS D-100 equipped with MID-unit was used for the analysis. For the analysis of TMS ether-methyl ester of bile acids, a 1.5% SE-30 column was used and column temperature was programmed at 8°C/min from 260°C to 290°C. The channel of MID-unit was focused on the ions at m/z 372 and 215 for lithocholic acid TMS ether-methyl ester and m/z 374 and 217 for 5β-cholanic acid methyl ester. The TFA ether-HFIP ester of bile acids was analysed with a 3% QF-1 column at a temperature of 220°C isothermally. The MID-unit was focused at m/z 622 for the lithocholic acid TFA ether-HFIP ester and m/z 623 for the D-DC TFA ether-HFIP ester (Fig. 2).

Through selected ion monitoring, the peak of lithocholic acid TMS ether-methyl ester on 1.5% SE-30 was hindered by unknown contaminants in the crude liver extracts but that of TFA ether-HFIP on 3% QF-1 was not (Fig.3). The distribution of the lithocholic acid determined by 3% QF-1 as TFA ether-HFIP ester was 1-8 μg/g liver. The values were lower than those reported by Nair et al. (3). This result may be firstly due to the lower recovery of lithocholic acid because protein-bound one was not isolated from the precipitates by the isolation method (Fig.1) and secondly due to no detection of lithocholic sulphates because solvolysis was not performed in this series. As a result of the first application to the detection of trace amounts of lithocholic acid from liver tissue, the SIM analytical method of lithocholic acid as TFA ether-HFIP ester on 3% QF-1 was found to give a sufficient sensitivity and specificity.

(1) Elias, E., Boyer, J. M., in "Progress in Liver Disease vol. VI" ed. by Popper, H., Shaffner, F., p. 457. Gurune & Stratton, New York (1979).
(2) Miyai, K., Mayr, W. W., Richardson, A., Lab. Invest. 32, 527 (1975).
(3) Nair, P. P., Solomon, R., Bankoski, J., Lipid 13, 966 (1978).
(4) Okishio, T., Nair, P. P., Gordon, M., Biochem, J. 102, 654 (1967).
(5) Mujitaba Naqri, S. H., Herndon, B. L., Kelley, M. T., Bleisch, V., Aexel, R. T., Nicholas, H. J., J. Lipid Res. 10, 115 (1969).
(6) Nair, P. P., in "Bile Salt Metabolism" ed. by Schiff, L., Carey, J. B., Deitschy, J. M., p. 172. Charles C. Thomas, Springfield (1969).
(7) Imai, K., Tamura, Z., Mashige, F., Osuga, T., J. Chromatogr. 120, 181 (1976).

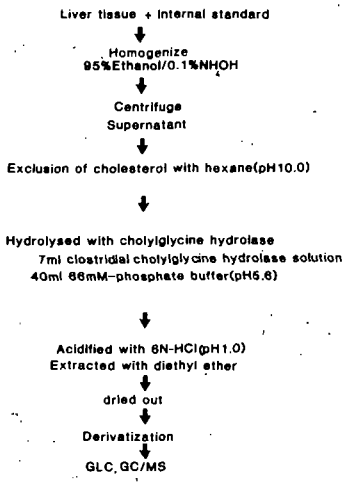

Fig.1. Isolation of bile acids from liver tissue.

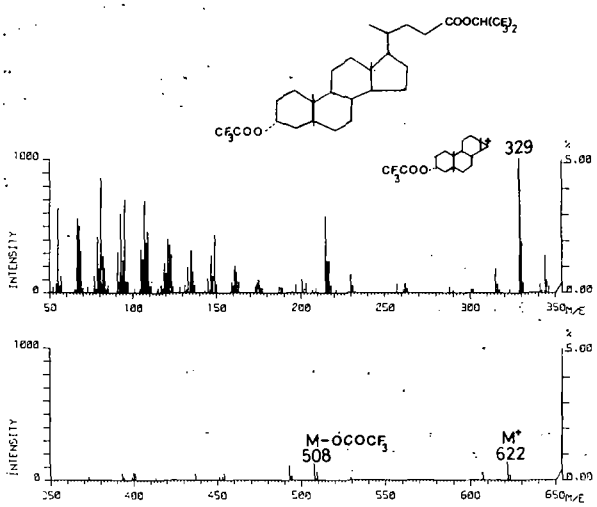

Fig.2. Mass spectrum of TFA ether-HFIP ester of lithocholic acid.

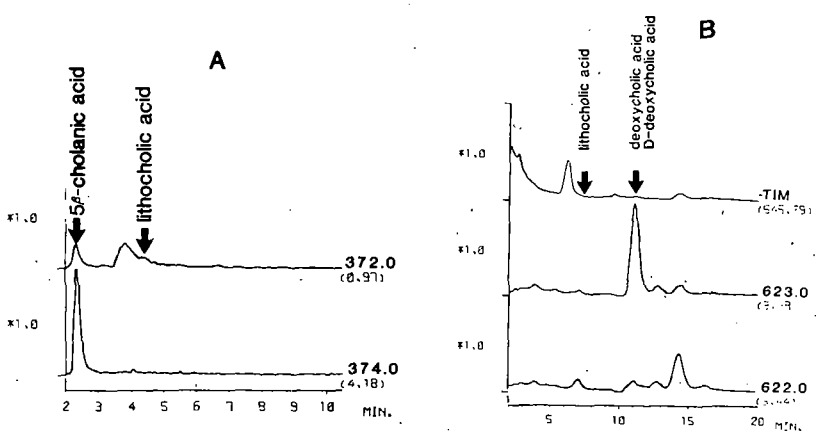

Fig.3. Mass fragmentograms of TMS ether-Methyl ester (A) and TFA ether-HFIP ester(B) of lithocholic acid from the extract of human liver tissue.

GC-MS IDENTIFICATION OF THE FECAL BILE ACIDS OF ALLIGATOR MISSISSIPPIENSIS, AN ANIMAL MODEL FOR HUMAN BILE ACID BIOSYNTHESIS.

G.S. TINT, B. DAYAL, A.K. BATTA, S. SHEFER and G. SALEN. VA Medical Center East Orange, NJ 07019, CMDNJ-New Jersey Medical School, Newark, NJ 07103, Cabrini Medical Center, New York City, NY 10013.

Bile acids are polyhydroxy steroidal acids which have a carboxyl group in the side chain. They are synthesized in the liver and secreted into the bile, and serve both as digestive detergents and as regulators of cholesterol metabolism. We have suggested the use of the American Alligator (A. Mississippiensis) as a model for the study of the oxidation and cleavage of the side chain of C_{27} cholesterol during its conversion to C_{24} bile acids in humans. This was prompted by our finding (1) that alligator bile contains C_{27} bile acids and bile alcohols which are suspected precursors of the human C_{24} bile acids, as well as the C_{24} bile acids themselves. However, in vivo metabolic studies require a knowledge of the fate of the biliary bile acids during their passage through the intestine.

Bile acids were extracted from alligator feces, methylated and separated by HPLC and TLC. The trimethylsilyl (TMSi) ether derivatives were formed and the C_{27} bile acid methyl esters were identified by comparing their EI GC-mass spectra with those of analogous C_{27} compounds.

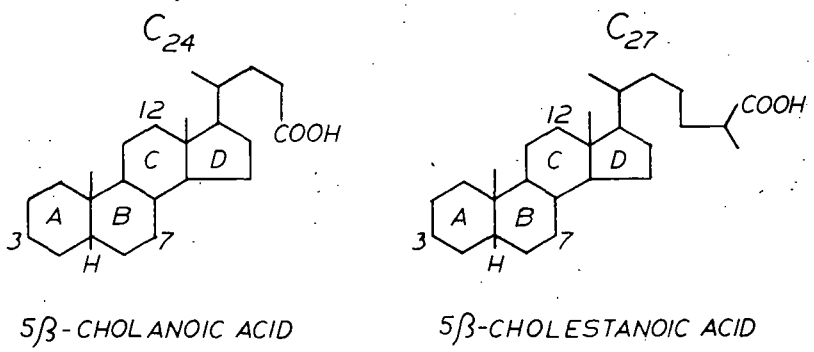

FIG. I: THE STRUCTURE OF THE C_{24} and C_{27} BILE ACIDS WITH CARBONS 3,7 and 12 MARKED.

The 3 carbon difference in the side chain did little more than shift portions of the C_{27} bile acid spectra by 42 amu with respect to their C_{24} analogues as illustrated in Table 1.

TABLE 1: DIAGNOSTIC PEAKS FROM TMSi ETHER METHYL ESTERS OF C_{27} (ALLIGATOR) AND C_{24} (MAMMALIAN) FECAL BILE ACIDS: * = FRAGMENTS WHICH CONTAIN THE SIDE CHAIN (SC)

	3α-Hydroxy		3α,12α-Dihydroxy	
	Alligator:C_{27} (Unknown)	Mammalian:C_{24} (Standard)	Alligator:C_{27} (Unknown)	Mammalian:C_{24} (Standard)
Fragment	m/z (%)	m/z (%)	m/z (%)	m/z (%)
M+	*504 (2)	*462 (1)	*592 (0.3)	*550 (0.4)
M-90	*414 (40)	*372 (42)	*502 (1)	*460 (1)
M-2x90	x	x	*412 (9)	*370 (13)
M-(90+SC)	257 (26)	257 (24)	345 (13)	345 (9)
M-(2x90+SC)	x	x	255 (100)	255 (100)
M-(A+B+C-11)	-	-	*250 (10)	*208 (22)
M-(C-16,17+SC)	230 (25)	230 (28)	-	-
M-(C-15,16,17+SC)	215 (100)	215 (100)	-	-

SC=Side Chain. C_{24}, 115 amu; C_{27}, 157 amu. 90 amu=TMSiOH. Instrument: Varian MAT-111

These structures were confirmed by means of "retention time ratios" as measured by GLC. We found that (1) if the TMSi ether bile acid methyl esters were chromatographed on 1%HIEFF-8BP (Applied Science) and if we define RT(Ni,Si)=retention time of compound with nucleus Ni and side chain Si then, RT(N1,S1)/RT(N2,S1)=RT(N1,S2)/RT(N2,S2).

We identified 9 mono-, di-, and trihydroxy C_{27} bile acids in alligator feces as shown in Table 2.

Table 2: C_{27} ALLIGATOR FECAL BILE ACIDS

Nuclear Hydroxyl Groups	% of Recovered Bile Acids
3α,7α	1
3α,7α,12α	4
3α,12α	36
*3α	26
*3β,7α,12α	1
*3β,7β	1
*3β	1
*3β,12β	0.4

*Not previously identified

Since the first two compounds listed were known to be primary bile acids synthesized by the alligator and none of the other 7 are detected in the bile, except perhaps in trace quanities, we can conclude that the alligator fecal bacteria are able to 7α-OH dehydroxylate C_{27} bile acids and to isomerize 3α,7α and 12α hydroxyl groups to their β configuration. These are exactly the same kinds of transformations that human intestinal bacteria carry out on C_{24} bile acids.

1. GS Tint, B Dayal, AK Batta, S Shefer, T Joanen, L McNease and G Salen. J. Lipid Res. 21,110 (1980).

WAMOB13 CHEMICAL IONIZATION MASS SPECTROSCOPIC APPROACH TO STRUCTURE DETERMINATION OF METABOLITES. AJAY K. BOSE AND BIRENDRA N. PARAMANIK*. Department of Chemistry and Chemical Engineering, Stevens Institute of Technology, Hoboken, NJ 07030.

In the course of a study of metabolic pathways to bile acids the conversion of a ^{14}C-labeled pentahydroxy steroid (I) to cholic acid (II) was examined. The biosynthetic intermediate (III) was separated as a radioactive TLC spot with chloroform-acetone-methanol (35:25:7.5, v/v/v). The intermediate III which appeared to be a ketone on the basis of a positive reaction with 2,4-dinitrophenylhydrazine, was eluted with ethyl acetate: methanol (85:15, v/v). Since this multifunctional compound of low volatility was found to be unsuitable for electron impact mass spectroscopy without derivatization, we decided to explore a chemical ionization mass spectral approach for structure determination.

Previous work[1] from our laboratory has shown that chemical ionization mass spectrometry using ammonia as the reagent gas, CIMS (NH_3), often leads to an intense pseudomolecular ion (PM) corresponding to $(M+NH_4)^+$ or $(M+18)^+$ for underivatized, polar compounds of very low volatility. For example, we have observed strong pseudomolecular ions at the expected m/z of 454 and 470 for tetrahydroxy and pentahydroxy derivatives of (5β-H)-cholestane, respectively.

Without further purification or derivatization, III was subjected to CIMS (NH_3) analysis and we observed a strong pseudomolecular ion $(M+NH_4)^+$ at m/z 468 compatible with a tetrahydroxycholestanone structure for III. For structure determination EI type fragmentation in CIMS (NH_3) of III would be useful; to induce such fragmentation a mixture of ammonia and argon was used as the reagent gas and the spectrum of III was re-recorded. A number of fragment ions were observed, one of which (m/z 366) corresponded to cleavage due to a McLafferty rearrangement of 24-keto-25-hydroxycholestane derivative. In view of the structure of the starting material I the structure III could now be represented as 3α, 7α, 12α, 25-tetrahydroxy-(5β-H)-cholestane-24-one.

To examine the validity of this structure assignment, a sequence of simple, high yielding chemical reactions was carried out on about 25 μg of III eluted from TLC plates but not purified further. The crude reaction products from each stage of this sequence was monitored by the CIMS (NH_3) technique.

The first reaction was periodic acid oxidation which would cleave an α-hydroxyketone to a carboxylic acid. The crude product from this oxidation of III displayed the PM ion at m/z 426 as would be expected for II. Diazomethane treatment of II gave IV the PM ion of which appeared at M/z 440 -consistent with II being a monocarboxylic acid. To confirm the presence of three secondary hydroxyl groups in IV, Jones oxidation (CrO_3/H_2SO_4) was carried out; as expected, the CIMS (NH_3) spectrum of the crude oxidation products showed the replacement of the m/z 440 peak by peaks at m/z 436 and 434 (see V).

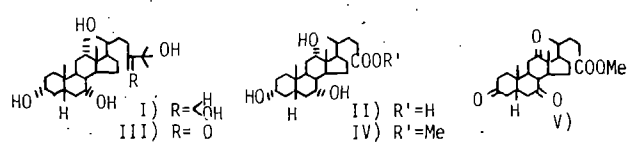

*Present address: Vick Divisions Research & Development, Richardson-Merrell Inc., One Bradford Road, Mount Vernon, NY 10553.

Since a synthetic sample of III was available, a mass spectral comparison with the metabolite under study became possible. A mixture of argon and ammonia was used as the reagent gas for CIMS to generate spectra with EIMS type of fragmentation - the two spectra agreed closely except for a few minor peaks which could be due to impurities in the samples.

On the basis of the above observations, the metabolite under study could be assigned with confidence the structure III.

1. A. K. Bose, H. Fujiwara, B. N. Paramanik, E. Lazaro and C. R. Spillert, Anal. Biochem., 89, 284 (1978).

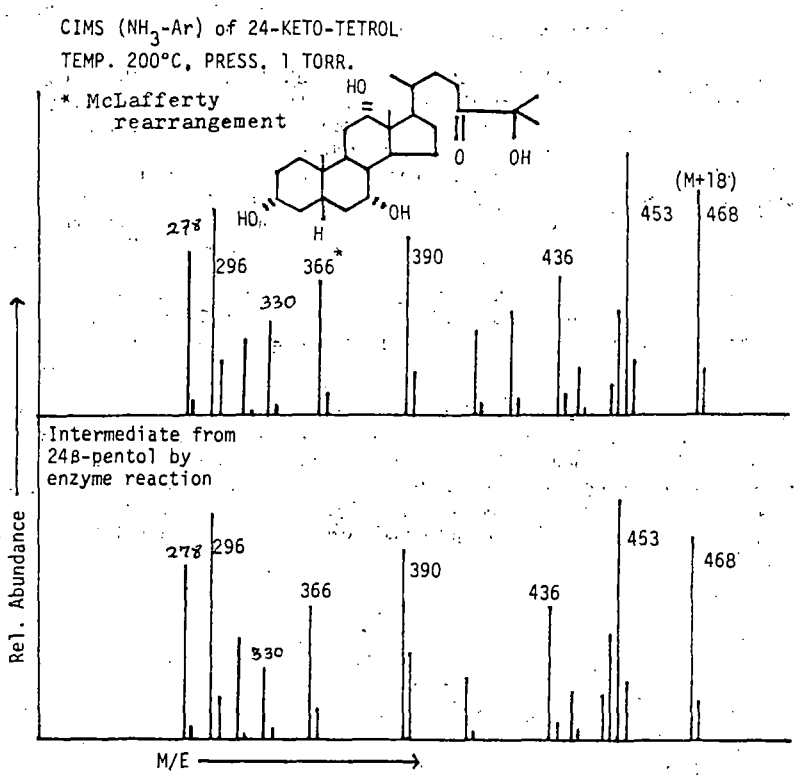

MASS SPECTRAL FRAGMENTATION OF STEROIDAL TRIENES GENERATED IN SITU, J.R. Dias, Dept. of Chem., Univ. of MO., Kansas City, MO 64110

The mass spectral fragmentation of the structures below will be delineated, and the genesis and identity of the diagnostic *m/z* 253 ion also found in bile acids will be examined. Loss of the 17-side-chain is activated in structure *4*, whereas loss of the 3β-OAc as HOAc is activated in structure *3a*. Cleavage of the D-ring is also enhanced in structure *4* relative to structure *3a*. The mass spectra of compounds *3b* and *5a* exhibit strong metastable peaks corresponding to simultaneous ejection of H_2O and CH_3• radical which is in harmony with the formation of the *m/z* 351 ion below; *5a* ejects the 7α-OH group as water to form *3b* in situ. This simultaneous loss is absent in the mass spectra *5b* to *5e* because ejection of the 3β-OAc group as acetic acid is faster than loss of the 7-OH group; the absence of stereochemically induced differences in the mass spectra of *5b* versus *5d* (and *5c* versus *5e*) is consistent with incipient charge ionization and localization at molecular locations other than at the 7-OH group.

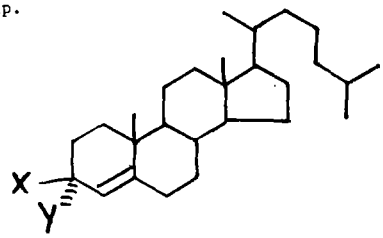

	X	*Y*
1a	OAc	H
1b	H	OAc
1c	OH	H

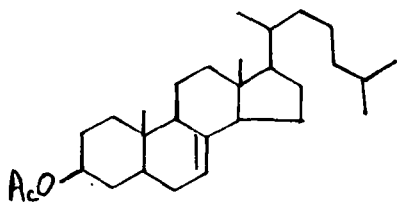

2

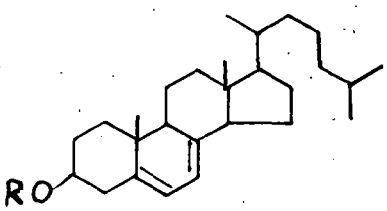

3a	R=Ac
3b	R=H

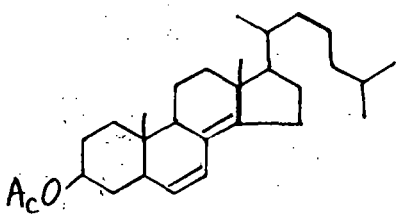

4

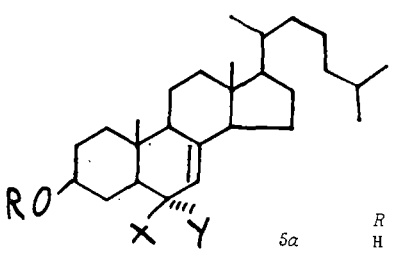

	R	*X*	*Y*
5a	H	H	OH
5b	Ac	H	OH
5c	Ac	D	OH
5d	Ac	OH	H
5e	Ac	OH	D
5f	Ac	H	OCH_3

The probable structures of other distinctive ions formed after electron impact of compounds *5a* to *5e* are also enumerated below.

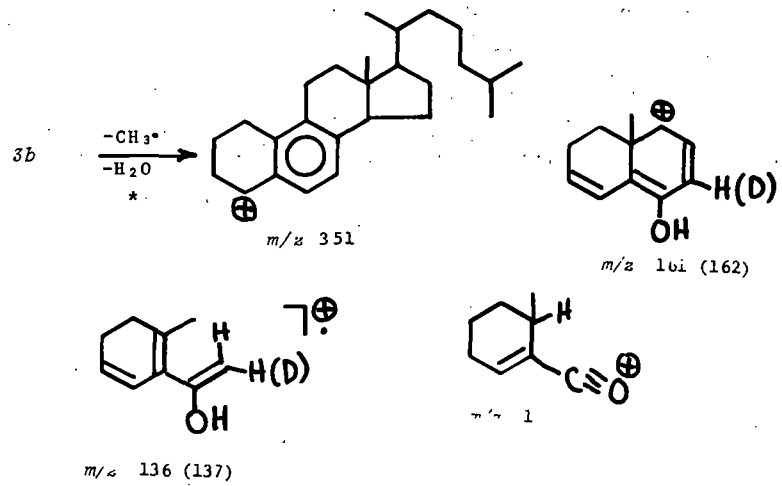

Our prior work demonstrated that electron impact induced loss of the 3-OAc group as HOAc was more facile than loss of the 3-OH group as H_2O. This is further illustrated by the mass spectra of *1a* versus *1c*. The base peak in the spectrum of *1a* corresponds to $[M-HOAc]^{+\cdot}$, whereas the relative intensity of the $[M-H_2O]^{+\cdot}$ peak in the spectrum of *1c* is no more than 15%; *m/z* 316 is a characteristic peak in the spectrum of *1c* and has no analog in the spectrum of *1a*. A characteristic ion of chenodeoxycholates and deoxycholates occurs at *m/z* 255 mass units and is present in the spectra of *1a*, *1b*, *1c*, and *2*; it results from 17-side-chain loss and is enhanced in the spectrum of deoxycholates relative to chenodeoxycholates. Consecutive loss of two HOAc molecules in ionized diacetate esters of chenodeoxycholates and deoxycholates occurs in the decreasing preferential order of 12α-OAc>7α-OAc>3α-OAc with loss of the second HOAc molecule being enhanced in the former. Since only moderate mass spectral loss of HOAc occurs in *2*, one must surmise that loss of the 7α-OAc group as HOAc in the spectrum of chenodeoxycholate diacetates must form the 6-double bond rather than the 7-double bond. The *m/z* 253 ion is a characteristic ion of cholates and is present in the mass spectra of *3a* to *5f*. The precise identity of the in situ generated ionized trienes (*m/z* 368 and *m/z* 253) in the mass of cholic acid ester derivatives remain undetermined. With this goal in mind, the mass spectra of *3a* to *5f* were investigated. The synchronous loss of H_2O and CH_3 was not observed in the mass spectra of methyl cholate and on this basis, we believe that the 5,7-diene system is not an electron impact induced intermediate.

THE GAS-PHASE HEATS OF FORMATION OF KETO AND ENOL IONS OF CARBONYL COMPOUNDS*,

JOHN L. HOLMES, Dept. of Chemistry, Univ. of Ottawa, Ottawa, Canada K1N 9B4, and F.P. LOSSING, Div. of Chemistry, Nat. Res. Council, Ottawa, Canada K1A 0R6.

Experimental values for the gas-phase heats of formation of thirteen enol positive ions of aliphatic aldehydes, ketones, acids, and esters have been measured and compared with those of the corresponding keto ions. The enolic ions were formed as daughter ions of appropriate precursors by loss of neutral C_2H_4 and C_3H_6 in McLafferty rearrangements. The energy thresholds for these dissociations were measured using impact of an energy-resolved electron beam. In earlier work[1] the enol ion of acetaldehyde, vinyl alcohol $CH_2=CHOH^{+\cdot}$, was shown to be 15 kcal mol^{-1} (63 kj mol^{-1}) more stable thermodynamically than the keto ion. In the present work the enol ion of acetone is found to be 14 kcal mol^{-1} (59 kj mol^{-1}) more stable than the keto ion, and the enol ion of acetic acid 22 kcal mol^{-1} (92 kj mol^{-1}) more stable than the acetic acid keto ion. For other species of formulae $C_3H_6O^{+\cdot}$, $C_4H_8O^{+\cdot}$, $C_3H_6O_2^{+\cdot}$ and $C_4H_8O_2^{+\cdot}$ the enol ions are generally 25-27 kcal mol^{-1} (105-113 kj mol^{-1}) more stable than the corresponding keto ions. A good correlation of the experimental heats of formation can be made using an empirical relationship between structure and ionic heat of formation to be presented in another paper in this Conference.

* To be published in J.A.C.S.

1 John L. Holmes, J.K. Terlouw, and F.P. Lossing, J. Phys. Chem. 80, 2860 (1976).

The Structure of the Gas Phase Ion $C_6H_5^+$

Chava Lifshitz and Dan Gibson

Department of Physical Chemistry, The Hebrew University of Jerusalem, Jerusalem, Israel

and

Karsten Levsen

Institut für Physikalische Chemie der Universität Bonn, W. Germany

The $C_6H_5^+$ ion is one of the major fragment ions of benzene and of linear isomers of benzene. Yet its structure remains an open question. Collision induced dissociation and charge stripping studies have indicated that the structure of the $C_6H_5^+$ ions formed from benzene and 1,5-hexadiyne radical cations is identical.

A question has been posed by Rosenstock, McCulloh and Lossing[1]: Does benzene form a linear $C_6H_5^+$ isomer or do the linear C_6H_6 isomers isomerize to form phenyl ions?

Time resolved breakdown curves for 1,5-hexadiyne have shown[2] that at 1 millisecond the only ion present at the lowest electron energies is $C_6H_5^+$. This is possible because the phenyl ion + hydrogen atom pair is more stable than $(HC{\equiv}C\text{-}CH_2\text{-}CH_2\text{-}C{\equiv}CH)^+$.

We have also found that $C_6H_5^+$ ions, formed by electron impact from 1,5-hexadiyne, undergo the same ion-molecule reactions as $C_6H_5^+$ ions formed by ion-assisted dehalogenation from halobenzenes[3]. These reactions were studied by us by Trapped Ion Mass Spectrometry and included,

$$C_6H_5^+ + C_2H_6 \rightarrow C_6H_7^+ + C_2H_4 \qquad (1)$$

$$C_6H_5^+ + CD_4 \rightarrow C_7H_5D_2^+,\ C_7H_4D_3^+,\ C_7H_3D_4^+,\ C_7H_5D_4^+ \qquad (2)$$

$$.38 \ : \ 1 \ : \ .48 \ : \ .14$$

Dehalogenation of halobenzenes by Brönsted acids is assumed to be a convenient source of phenyl cations[3,4].

Finally, the kinetic energy releases ($T_{0,5}$) by MIKES for $C_6H_5^+ \rightarrow C_4H_3^+ + C_2H_2$ are the same for benzene, 1,5-hexadiyne and several other precursor molecules; the metastable peak shapes are also identical.

Conclusion. Decomposing and non-decomposing $C_6H_5^+$ ions from various precursor molecules have the same structure independent of the precursor. This structure is that of the phenyl cation - as demonstrated by ion-molecule reactions of the stable non-decomposing ions. The phenyl ion structure is also formed from linear C_6H_6 isomers such as 1,5-hexadiyne.

[1]H.M. Rosenstock, K.E. McCulloh and F.P. Lossing, Int. J. of Mass Spectrom. and Ion Phys., 25 (1977) 327.

[2]C. Lifshitz and S. Gefen, Int. J. of Mass Spectrom. and Ion Phys., in press; C. Lifshitz, M. Weiss and S. Landau-Gefen, 25th ASMS Conference, Washington, D.C., 1977.

[3]M. Speranza, M.D. Sefcik, J.M.S. Henis and P.P. Gaspar, J. Am. Chem. Soc., 99 (1977) 5583.

[4]A.G. Harrison and P.-H. Lin, Can. J. Chem. 53 (1975) 1314; H.W. Leung and A.G. Harrison, ibid. 54 (1976) 3439.

WAMOC3 STRUCTURES OF SMALL POSITIVE IONS; $C_3H_5^+$ AND $C_2H_4N^+$, M. T. BOWERS, S. LIU, P. A. M. KEMPER, A. ILLIES, H. WEBB, R. STRADLING[a], D. H. AUE, J. R. GILBERT[b] and K. R. JENNINGS[a], Dept. of Chem., Univ. of Ca., Santa Barbara, CA 93106

Collision induced decompositions of ions are well known to yield quantitative structural information and in favorable cases allow isomeric distinction to be observed. Two such studies will be reported here. In the first study, $C_3H_5^+$ ions formed from a variety of sources are subjected to CID with two distinct patterns emerging; one is attributed to allyl cation, I, $[CH_2CHCH_2]^+$ and the second to 2-propenyl cation, II, $[CH_3\text{-}C{=}CH_2]^+$. The $C_3H_5^+$ ions exhibiting structure I are formed by electron impact on $ClCH_2CHCH_2$ and $BrCH_2CHCH_2$ and by the reaction of $C_2H_4^+$ with C_2H_4. Those exhibiting structure II are formed by electron impact on CH_3CBrCH_2 and by low energy protonation of allene and propyne. A variety of systems have been shown to yield part I and part II. The second system of interest is $C_2H_4N^+$. This ion is formed by a low pressure, bimoleuclar reaction, $CH_3^+ + HCN \rightarrow C_2H_4N^+$, whose rate constant is independent of pressure. The $C_2H_4N^+$ product ion has been shown to have a CID spectrum distinct from protonated CH_3NC and a number of $C_2H_4N^+$ ions formed by electron impact induced fragmentation. The results have implication for chemical synthesis in interstellar space.

a) Dept. of Chem. and Molecular Science, Univ. of Warwick Coventry, England.
b) Dept. of Chem., Univ. of Essex, Rochester, England.

ION STRUCTURES, REARRANGEMENTS AND ENERGY PARTITIONING IN $[ALKANE]^{+\cdot}$ FRAGMENTATIONS by

J.L. HOLMES, Y. MOLLAH, J.K. TERLOUW[1] and P.C. BURGERS[1]. Department of Chemistry, University of Ottawa, Ottawa, Ontario, K1N, 9B4, Canada.

Recent observations on butane (1) and methylpropane (2) molecular ions[2,3] have been interpreted as showing that the former does not isomerise to the latter prior to fragmentation. It was also concluded that the loss of internal C atoms from (1) as $CH_3^{\cdot}$ and CH_4 involves extrusions of $-CH_2-$ together with concerted H atom shifts. The appearance energy (AE) for $[C_3H_6]^{+\cdot}$ from (1) is sufficiently high for either $[cyclopropane]^{+\cdot}$ and/or $[propene]^{+\cdot}$ to be the daughter ions. Considerations related to the partitioning of this excess internal energy did not permit unequivocal identification of the $[C_3H_6]^{+\cdot}$ species but the problem has now been solved by charge stripping experiments,[4,5] which show $[propene]^{+\cdot}$ to be the predominent daughter ion. This work has been extended to $[pentane]^{+\cdot}$ (3) where, as with butane, loss of $CH_3^{\cdot}$ and CH_4 have the same AE, the former producing sec-$C_4H_9^+$ ions at the thermochemical threshold. The loss of ethane from (3) is however the fragmentation of lowest energy requirement and this reaction produces $[propene]^{+\cdot}$ at the thermochemical threshold. Charge stripping experiments confirm that the daughter ions predominently have this structure.

By analogy with the behavior of the $[C_4H_{10}]^{+\cdot}$ isomers it is concluded from the magnitude of the released kinetic energies in the methane loss from (3) and $[methylbutane]^{+\cdot}$, (4), that the most stable $[C_4H_8]^{+\cdot}$ species, $[CH_3CH{=}CHCH_3]^{+\cdot}$, is being generated by metastably fragmenting ions. Labelling experiments on (3) show that C-3 is lost with greater probability than either C-1 (or C-5) in the $CH_3^{\cdot}$ and CH_4 eliminations and that C-1 and C-2(C-4 and C-5) are predominently lost as C_2H_6. The question of isomerisation (3) → (4) prior to fragmentation, remains equivocal but further labelling experiments in progress should lead to a resolution of the problem.

1. Analytical Chem. Laboratory, University of Utrecht.

2. P. Wolkoff and J.L. Holmes, J.A. Chem. Soc., 100, 7346 (1978).

3. J.L. Holmes, P. Wolkoff and R.T.B. Rye, Chem. Commun. 544 (1979).

4. R.D. Bowen, M.P. Barbalas, F.P. Pagano, P.J. Todd and F.W. McLafferty, Org. Mass Spectrom. 15, 51 (1980).

5. J.L. Holmes, J.K. Terlouw, P.C. Burgers and R.T.B. Rye, Org. Mass Spectrom. 15, 149 (1980)

WAMOC5

Reactions of Transition Metal Containing Ions with Alkanes

D. P. Ridge, Department of Chemistry, University of Delaware, Newark, DE 19711

We wish to report the reactions in Table I of Mn_2^+ with CH_3OH and RBr. The reaction of Mn_2^+ with CH_3OH together with the reaction

$$Mn^+ + CH_3OH \longrightarrow MnOH^+ + CH_3$$

suggests the following intermediate for the Mn_2^+ reactions:

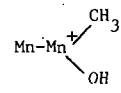

The reactions of Mn_2^+ with RBr can be interpreted in terms of a similar intermediate. A possible mechanism is

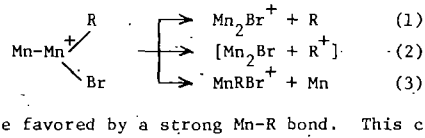

$$Mn_2Br^+ + R \quad (1)$$
$$[Mn_2Br + R^+] \quad (2)$$
$$MnRBr^+ + Mn \quad (3)$$

The third channel should be favored by a strong Mn-R bond. This channel is indeed least important where R = t-C_4H_9 which we might expect to be more weakly bound than propyl or ethyl radicals. The second channel is unobserved so we assume that further reaction of the kind

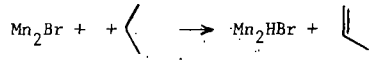

occurs before the ion-neutral complex separates. The importance of channel (2) should increase as the ionization potential of R decreases. This is what is observed.

We also wish to report the collision induced decomposition spectra of ions formed by the reaction

$$M(CO)^+ + C_4H_{10} \longrightarrow MC_4H_{10}^+ + CO.$$

Figure 1a is the collision induced decomposition spectrum of $FeC_4H_{10}^+$ formed from n-butane and 1 b is that of $FeC_4H_{10}^+$ formed from isobutane. Figure 2a is the CID spectrum of $CrC_4H_{10}^+$ formed from n-butane and Figure 2b is that of $CrC_4H_{10}^+$ formed from isobutane. The spectra show that the structure of $MC_4H_{10}^+$ depends on M and on the isomer of C_4H_{10}. If M=Fe and isobutane is C_4H_{10} the following structures are suggested by the CID spectra

1 2

If M=Fe and C_4H_{10} is n-butane, then the suggested structures are

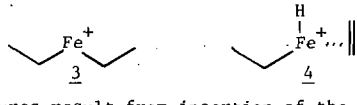

3 4

Other possible structures result from insertion of the metal into C-H bonds. Note especially the major fragment $FeC_2H_4^+$ in Fig. 1a which might be formed from 4. As expected no $FeC_2H_4^+$ fragment appears in Fig. 1b, only $FeC_3H_6^+$ formed from 2. Note that the major fragment in the $Cr(C_4H_{10})^+$ spectra is Cr^+ suggesting a loosely bound complex involving little, if any, metal insertion into bonds.

The $FeCH_3^+$ fragment in Fig. 1b presumably comes from structure 2. Since no $C_3H_7^+$ fragment is observed we conclude that I.P.($FeCH_3^+$)<I.P.(C_3H_7). If we take I.P.(C_3H_7) = 7.36[1] then we can conclude that D(Fe^+-CH_3)-D(Fe-CH_3) > 12 kcal/mole.

The CID spectra are consistent with the reactions of Fe^+ and Cr^+ with alkanes.[2] Fe^+, Co^+ and Ni^+ all eliminate methane from isobutane, ethane from n-butane and methane from

Table I.

$Mn_2^+ + CH_3OH \longrightarrow MnCH_3OH^+ + Mn$

$Mn_2^+ + C_2H_5Br \xrightarrow{65\%} Mn_2Br^+ + C_2H_5$

$\xrightarrow{13\%} Mn_2HBr^+ + C_2H_4$

$\xrightarrow{22\%} MnC_2H_5Br^+ + Mn$

$Mn_2^+ + C_3H_7Br \xrightarrow{63\%} Mn_2Br^+ + C_3H_7$

$\xrightarrow{20\%} Mn_2HBr^+ + C_3H_6$

$\xrightarrow{17\%} MnC_3H_7Br^+ + Mn$

$Mn_2^+ + i\text{-}C_3H_7Br \xrightarrow{50\%} Mn_2Br^+ + C_3H_7$

$\xrightarrow{35\%} Mn_2HBr^+ + C_3H_6$

$\xrightarrow{15\%} MnC_3H_7Br^+ + Mn$

$Mn_2^+ + t\text{-}C_4H_9Br \xrightarrow{34\%} Mn_2Br^+ + C_4H_9$

$\xrightarrow{62\%} Mn_2HBr^+ + C_4H_8$

$\xrightarrow{4\%} MnC_4H_9Br^+ + Mn$

propane. Cr^+ eliminates H_2 from a number of alkanes, but attacks a C-C bond only in n-butane to form $Cr(C_2H_4)^+$ as a minor product. Cr^+ reacts with isobutane only to eliminate H_2. This is probably because the CH_3-i-C_3H_7 bond is slightly stronger than the C_2H_5-C_2H_5 bond. This lower reactivity of Cr^+ towards C-C bonds is reflected in the CID results. We note that Mn^+, Co_2^+ and Mn_2^+ are unreactive with alkanes.

Metal ions were obtained by electron impact on metal carbonyls. Reactions were identified by ion cyclotron resonance. The CID spectra were obtained with the cooperation of Dr. Chuck McEwen and at the DuPont Experimental Station.

1. F. A. Houle and J. L. Beauchamp, J. Amer. Chem. Soc., 101, 4067 (1979).
2. J. Allison, R. B. Freas and D. P. Ridge, J. Amer. Chem. Soc., 101, 1332 (1979).

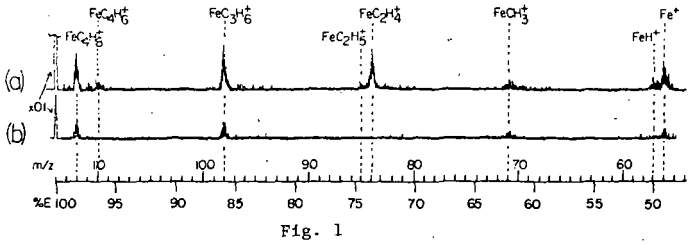

Fig. 1

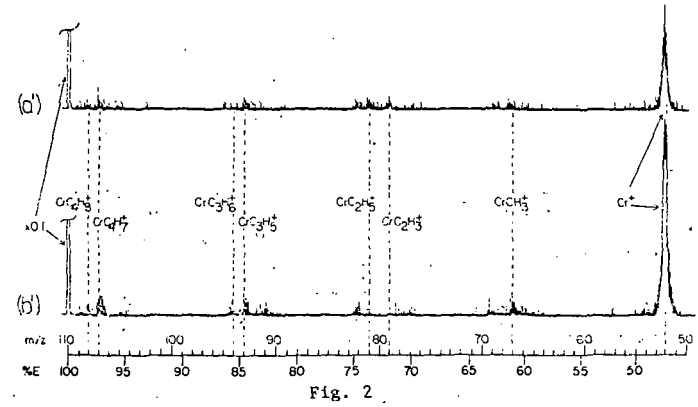

Fig. 2

THE THERMOCHEMISTRY AND DISSOCIATION DYNAMICS OF STATE SELECTED THIOPHENE IONS,

James J. Butler and Tomas Baer, Department of Chemistry, University of North Carolina at Chapel Hill, North Carolina 27514.

The threshold photoelectron spectrum (TPES) of thiophene and photoionization efficiency (PIE) curves for $C_4H_4S^+$, $C_4H_3S^+$, $C_2H_2S^+$, CHS^+, and $C_3H_3^+$ from thiophene were measured in the 8 to 14 eV photon energy range. The dissociation rates of internal energy selected thiophene ions in the 12 to 12.6 eV photon energy range and the average kinetic energy released in the dissociation to $C_2H_2S^+$ and C_2H_2 in the 13 to 14 eV photon energy range were measured by photoion-photoelectron coincidence (PIPECO).

The TPES and PIE scans were recorded on a spectrometer which has been described previously.[1] The spectrometer is comprised of an H_2 many-line resonance light source, a steradiancy analyzer for electrons and a quadrupole mass filter.

In the PIPECO experiments, threshold photoelectrons are recorded in delayed coincidence with their respective ions. The electron and ion signals are used as start and stop inputs to a time-to-pulse-height converter after which fragment ion TOF distributions, such as those shown in Fig. 1, are recorded on an MCA.

Fig. 2 illustrates the TPES and PIE curves for thiophene. From the TPES, we can determine the energies of the first three molecular ion states and the presence of resonance autoionization between 10 and 11.5 eV. From the TPES and the PIE curves, upper limits to the heats of formation in kcal/mole can be determined for several sulfur-containing ions and radicals to be the following: $C_4H_4S^+$ at 232.1 ± 0.2; $C_4H_3S^+$ at 274 ± 2.0; C_3HS^+ at 292 ± 3.0; CHS at 73 ± 2; and CHS^+ at 251 ± 2.

In the photon energy range between 12 and 12.7 eV only one fragment ion, $C_2H_2S^+$, is formed from thiophene ions with microsecond lifetimes. Asymmetric TOF distributions, as seen in Fig. 1, result in this energy region because of initial acceleration of the photoion as the parent and final acceleration as the daughter. Above 12.7 eV the TOF distributions are symmetric, Gaussian shaped peaks. The full width at half maximum (FWHM) was obtained for the symmetric curves by a nonlinear least squares fit of a Gaussian curve to the TOF distribution. The average kinetic energy released in dissociation was calculated from the FWHM using an equation reported by Stockbauer.[2] Fig. 3 is a plot of experimentally determined average kinetic energy released as a function of photon energy. The first two points of the plot were determined by a mass analyzed ion kinetic energy spectrometric (MIKES) experiment due to the asymmetric nature of the TOF distribution in the metastable region. Included in the plot are the results of a calculation using an empirical formula reported by Franklin[3] and the results of a QET calculation on a cyclic A and linear B structure for the $C_2H_2S^+$ fragment. Clearly, the calculation does not indicate which structure is the correct one. However, the appearance potential for the formation of $C_2H_2S^+$ can be determined to be 12.1 ± 0.1 eV from Fig. 3, corresponding to a heat of formation of $C_2H_2S^+$ of 253 ± 2 kcal/mole.

Decay rates of metastable thiophene ions can be determined by fitting a curve obtained by convoluting a parent TOF distribution with an exponential decay to the asymmetric TOF distribution for $C_2H_2S^+$. Fig. 4 is a plot of decay rate versus photon energy for the formation of $C_2H_2S^+$. Included in the plot are the results of an RRKM statistical calculation using a thiophene transition state and a thiovinylketene transition state and the results of a previous study by Andlauer and Ottinger.[4] In the calculation, the appearance

potential of 12.1 ± 0.1 eV as obtained from the kinetic energy release data was used. The "loose" thiovinylketene transition state reproduces the experimental data more effectively than a tight thiophene transition state. A thiovinylketene transition state would lead to a linear $C_2H_2S^+$ ion by undergoing a carbon-carbon bond break and a hydrogen migration. The linear structure for $C_2H_2S^+$ is further substantiated by Gaussian 70 *ab initio* calculations which indicate the linear structure is 1.1 eV more stable than its cyclic counterpart.

The possibility that the thiophene parent ion isomerizes to a more stable linear structure was considered. Several points argue against such an isomerization prior to dissociation. First, *ab initio* calculations indicate the thiophene ion is much more stable than the linear thiovinylketene ion. Secondly, a lower parent ion energy would have the effect of increasing the parent ion density of states which would decrease the RRKM calculated rate. Finally, the lower vibrational frequencies of the linear structure would predict calculated rates over 2 orders of magnitude less than the experimentally determined ones.

References

1. A. S. Werner and T. Baer, J. Chem. Phys. 62, 2900 (1975).
2. R. Stockbauer, Int. J. Mass Spectrom. Ion Phys. 25, 89 (1977).
3. M. A. Haney and J. L. Franklin, J. Chem. Phys. 48, 4903 (1968).
4. B. Andlauer and C. Ottinger, Z. Naturforschg. A27, 293 (1972).

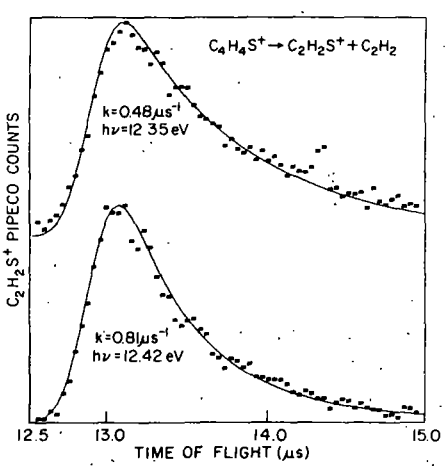

Fig. 1

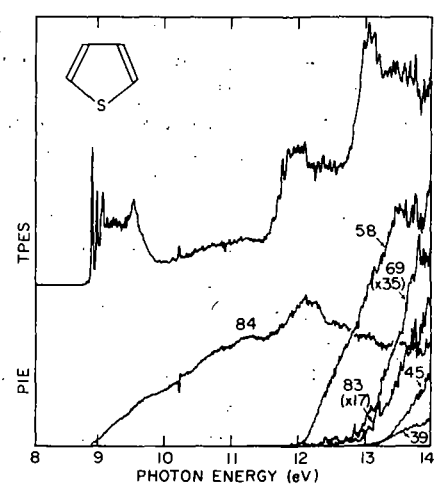

Fig. 2

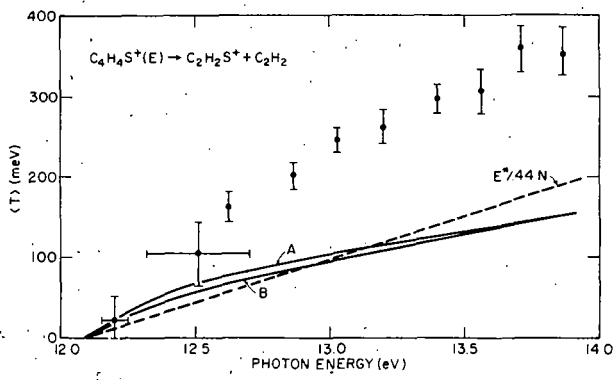
$C_4H_4S^+(E) \rightarrow C_2H_2S^+ + C_2H_2$
$E^*/44\,N$
A
B
⟨T⟩ (meV)
PHOTON ENERGY (eV)

Fig. 3

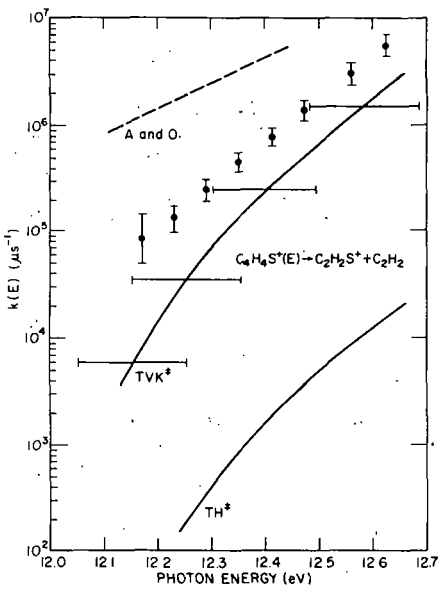
A and O.
$C_4H_4S^+(E) \rightarrow C_2H_2S^+ + C_2H_2$
$TVK^{\ddagger}$
$TH^{\ddagger}$
k(E) (μs^{-1})
PHOTON ENERGY (eV)

Fig. 4

INTERCONVERSION OF ION STRUCTURES: NITROMETHANE AND METHYLNITRITE IONS

T. Hsieh, J.P. Gilman, M.J. Weiss, and G.G. Meisels
Department of Chemistry, University of Nebraska

Threshold photoelectron-coincident photoion mass spectrometry provides a tool for the study of the chemical fates of ions produced in specific selected internal energy states (1,2). It amplifies other advantages of photoionization techniques, such as excellent energy resolution and threshold behavior which permits more accurate measurements of ionization onsets than electron impact. The structure from which fragmentation occurs is, however, not always clear.

Internal rearrangements lead to the loss of structure identity of isomeric species; sometimes molecular ions which can rearrange to the most stable structure before fragmentation have distinguishable mass spectra only because the total energies they possess above the most stable configuration are different. This is the case for the C_4H_8 isomers (3), but the generality of this concept has not been established. Here we report on the fragmentation processes of nitromethane and methylnitrite ions.

The threshold photoelectron-coincident photoion mass spectrometer has been described elsewhere (2,4). Either the hydrogen many line spectrum or the helium continum was used as a photon source, coupled to a 1 meter normal incidence grating monochromator. The overall energy resolution was 21meV at photon energy of 14eV (see MAMP 4). Relative error in the breakdown graph points is about 14%. Nitromethane was Aldrich gold label grade (99% pure) and was used without further purification. Methylnitrite was made by dripping diluted surfuric acid into a cold solution containing a stoichiometric mixture of methanol and sodium nitrite. The escaping gas was passed through a solution of sodium hydroxide to remove nitrogen oxides and through a drying tube containing calcium chloride. The purification procedures and trap to trap distillation were repeated several times before the product was stored in a dry ice-acetone cold bath. No impurities could be detected by IR or MS.

The breakdown graphs of methylnitrite (A) and nitromethane (B) are shown in figure 1. These graphs are plots of relative ion abundance as a function of excess internal energy (E*) above the most stable ionic isomer; in this system this is methylnitrite. This energy is calculated from the relationship $E^*(B) = h\nu + \Delta H(B^+-A) - IP(B)$, where the enthalpy term refers to the energy released when the ground state ion B^+ rearranges to A^+(methylnitrite ion). The dashed curves in figure 1 are breakdown graphs of nitromethane after correction for the non-zero energy electrons transmitted through the TPE detector. Above the 0.64 eV barrier to isomerization (1.03eV internal energy in figure 1) the breakdown graphs are similar only in a very narrow energy region. At higher internal energies of nitromethane, direct fragmentation competes with isomerization.

Ionization potentials and predominant ionic fragmentation processes for nitromethane and methylnitrite are summarized in Table I. In general, our results are in good agreement with those reported in the literature. The asymmetrically broadened TOF distributions for the ion of mass 31 from methylnitrite (figure 2) reflect a long lifetime of the precursor and fragmentation in the acceleration region. The peak becomes narrower as the rate constant increases with increasing internal energy. We believe that this ion has the CH_2OH^+ structure and that its formation is accompanied by translational energy release, in good agreement with the results obtained by Haney and Franklin (5). Extraction of the kinetic energy release distributions from TOF distributions is currently underway in our laboratory.

A hypothetical potential energy diagram is constructed and is shown in figure 3, based on the information in Table I and figure 1. We suggest that: (1) Isomerization of nitromethane ion to methylnitrite ion (which is 0.39 eV more stable), has a barrier of at least 0.64 eV. (2) Breakdown graphs of methylnitrite and nitromethane are the same only in a narrow energy range; at higher energies, direct cleavage and rearrangement compete as reaction channels for nitromethane fragmentation. (3) The mass 31 ion from methylnitrite, with some translational energy release at onset, has the CH_2OH^+ structure.

We are grateful for the support of the Department of Energy under contract EY-76-S-02-2567.

1. Tomas Baer in "Gas Phase Ion Chemistry" ed. by M.T. Bowers, Academic Press, New York (1979)
2. M.J. Weiss, T. Hsieh, and G.G. Meisels, J. Chem. Phys., 71, 567 (1979)
3. G.G. Meisels, M.J. Weiss, T. Hsieh, and G.M.L. Verboom presented at the 26th Annual Conference on Mass. Spec. and Allied Topics, St. Louis, MO. May 28 - June 2, 1978.
4. (a) C.F. Batten, J.A. Taylor, G.G. Meisels, J. Chem. Phys. 65, 3316 (1976) (b) C.F. Batten, J.A. Taylor, B.P. Tsai, and G.G. Meisels, J. Chem. Phys. 69, 2417 (1978)
5. M.A. Haney and J.L. Franklin, Trans. Faraday Soc., 65 1794 (1969)
6. Richard J. Kandel, J. Chem. Phys., 23, 84 (1955)
7. J. Collin, Bull. Soc. Roy. Sci. Liege, 194 (1954)
8. C.J.W. Rabalais, J. Chem. Phys., 57, 960 (1972)
9. K. Watanabe et. al. J. Quant. Spect. Radiat. Transfer. 2, 369 (1962)
10. A.J.C. Nicholson, J. Chem. Phys., 43, 1171 (1965)
11. L. D'Or and J. Collin, Bull. Soc. Roy. Sic. Liege, 285 (1953)
12. A.J.C. Nicholson, in "Recent Development in Mass Spectrometry", University of Tokyo Press, p. 745 (1970)

BREAKDOWN GRAPH OF CH_3ONO AND CH_3NO_2

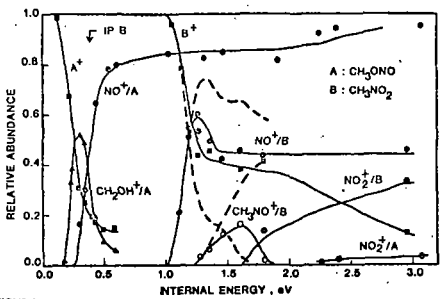

FIGURE 1

TPECPI - TOF SPECTRA OF CH_3ONO

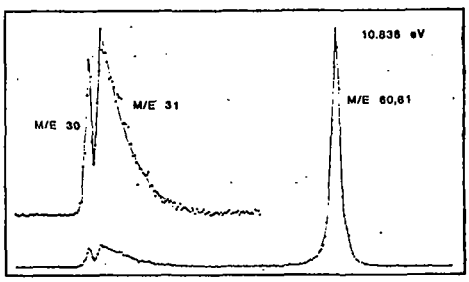

FIGURE 2

TABLE I

Process	Appearance Potential, eV literature	this work	Thermo. onset
1. $CH_3NO_2 \rightarrow CH_3NO_2^+$	11.34[a],12.0[b] 11.07[c],11.08[d] 11.13[e],11.04[h]	11.12	
2. $CH_3NO_2 \rightarrow NO^+ + CH_3O$	12.01[a],11.2[b],11.76[h]	11.76	10.96
3. $CH_3NO_2 \rightarrow CH_3N^+ + O_2$		11.85	
4. $CH_3ONO \rightarrow CH_3ONO^+$	10.7[f],10.47[h]	10.61	
5. $CH_3ONO \rightarrow CH_2OH^+ + NO$	11.9[f],10.98[g]	10.78	8.97
6. $CH_3ONO \rightarrow NO^+ + CH_3O$	10.7[f],11.11[e],10.92[h]	10.89	10.65

a.ref.6, b.ref.7, c.ref.8, d.ref.9, e.ref.10, f.ref.11, g.ref.5, h.ref.12.

THERMOCHEMICAL ASPECT OF CH_3ONO & CH_3NO_2

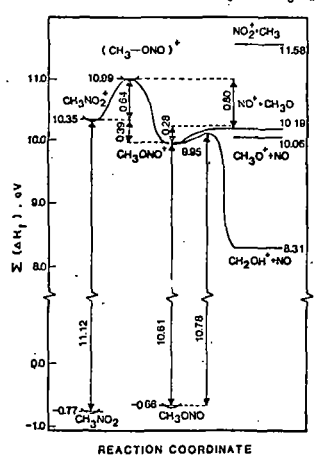

FIGURE 3 Hypothetical Potential Energy Diagram of Nitromethane and Methylnitrite

THE STRUCTURE AND STABILITY OF ALKALI HALIDE MOLECULES AND IONS

J. Berkowitz, G. L. Goodman and C. H. Batson

Physics Division
Argonne National Laboratory
Argonne, IL 60439

The vacuum ultraviolet photoelectron spectra of most of the diatomic halides of Na, K, Rb and Cs have been obtained in the past few years. The lithium halides have roughly equal abundances of dimer and monomer in their saturated vapor, and as a consequence yield a more complex spectrum. Recently, we have succeeded in unraveling this spectrum, utilizing a double-oven approach, and thereby have extended our knowledge of the monomer spectra to the lithium halides. In addition, we now have well-characterized photoelectron spectra of the "pure" dimer molecules of each of the lithium halides. In each instance, the first ionization potential of the dimer is larger than that of the corresponding monomer.

These results can be rationalized by ionic model calculations, and also agree with the limited ab initio Hartree-Fock calculations undertaken. We should like to extend our knowledge to still larger clusters, to see how the first ionization energies and the widths of the valence bands approach those of the corresponding microcrystals. We have made some progress toward this goal by studying the photoionization of lithium chloride using mass analysis.

The photoions detected were Li^+, $LiCl^+$, Li_2Cl^+ and $Li_3Cl_2^+$. The first two ions derive from neutral monomer, the third from dimer and the last from trimer. From the Boltzmann-determined thresholds for $LiCl^+$ and Li_2Cl^+, we deduce adiabatic ionization potentials for monomer and dimer which are in good agreement with our earlier values from photoelectron spectroscopy. The 0°K threshold for Li^+ (see Fig. 1) is ∿10.17 eV. Subtraction of the ionization energy of Li yields 4.77_8 eV for D_o (LiCl).

The $Li_3Cl_2^+$ intensity was only ca. 5% of the most abundant peak (Li_2Cl^+) and hence this experiment required optimum tuning, reduction of background to a few counts per minute and stability of the entire apparatus over a period of hours. The results are displayed in Fig. 2. The departure from linearity also occurs at ca. 10.17 eV. Within the statistical uncertainty, we conclude that Li_3Cl_3 has an adiabatic ionization potential very nearly that of Li_2Cl_2. Neither the ionic models nor the wave mechanical calculations are precise enough to demonstrate the experimental variation potential with cluster size

at the trimer level.

We have made detailed ionic model calculations of the geometric changes that occur to dimer and trimer molecules upon ionization, and also upon subsequent dissociation. The results of these calculations will be presented at the conference, if time permits.

This research was performed under the auspices of the Division of Basic Energy Sciences of the U. S. Department of Energy.

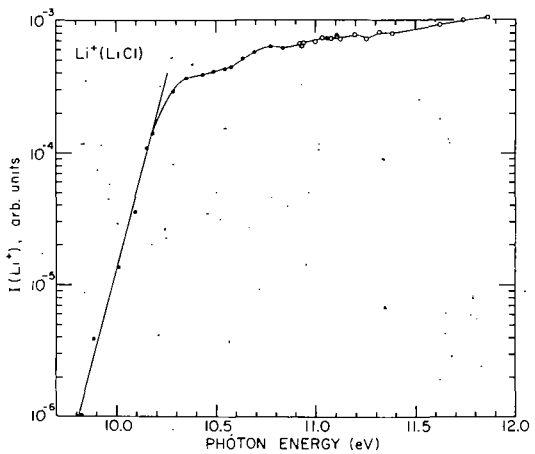

Fig. 1 Semilogarithmic plot of normalized Li^+ ion intensity vs. photon energy for the reaction $LiCl + h\nu \rightarrow Li^+ + Cl + \bar{e}$.

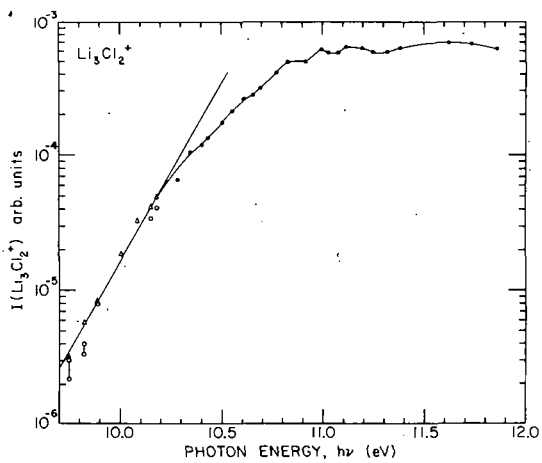

Fig. 2 Semilogarithmic plot of normalized $Li_3Cl_2^+$ ion intensity vs. photon energy for the reaction $Li_3Cl_3 + h\nu \rightarrow Li_3Cl_2^+ + Cl + \bar{e}$.

LASER INDUCED DISSOCIATION OF POSITIVE AROMATIC IONS, J.H. BEYNON, E.S. MUKHTAR, I.W. GRIFFITHS and F.M. HARRIS, Royal Society Research Unit, University College of Swansea, Swansea SA2 8PP, UK.

We have modified a large double-focusing mass spectrometer for studies of dissociation of molecular ions excited using radiation from an argon-ion laser. The radiation is introduced into the spectrometer via the source and, using externally mounted mirrors, is steered to pass through the source slit and along the length (706 mm) of the first field-free region. A beam locator is used to bring the ion and laser beams into coincidence. Maximum overlap of the beams is ensured by fine adjustment of the laser-beam position to maximize photofragment currents. An IKE photodissociation spectrum is obtained by scanning the voltage of an 800 mm radius electrostatic analyser positioned after the interaction region.

We have studied, so far, some thirty aromatic ions that photodissociate in the wavelength range of the laser (351 - 528.7 nm). The photo-absorption is wavelength dependent and examples are shown of photofragment yeilds increasing and decreasing with increasing wavelength. For many ions, unimolecular dissociation and photodissociation spectra are shown to be different, the differences being quite marked for the molecular ion of nitrobenzene and the three isomeric ions of nitrotoluene. For these ions, with the exception of o-nitrotoluene, unimolecular dissociation leads primarily to the loss of $NO^{\cdot}$ but photoexcitation with 2.41 eV photons, to the loss of $NO_2^{\cdot}$. These results can be readily explained qualitatively since the activation energies for $NO^{\cdot}$ loss are less than 1 eV for the three ions but, for $NO_2^{\cdot}$ loss, are just greater than 2 eV. A quantitative analysis to predict the magnitude of the currents observed is in progress.

We have also investigated the dependence on photoexcitation energy of the kinetic energy (T) released due to photodissociation. Reactions of the molecular ions of m-bromotoluene, ethyl benzene, n-propyl benzene and nitrobenzene were studied first. A linear increase of T with photon energy was observed with different gradients for the different ions. However, on investigating the molecular positive ion of anisole, and the photodissociations involving the loss of $CH_3^{\cdot}$ and CH_2O, T was found to decrease with increase in photon energy. These results will be discussed in terms of the partitioning of photoexcitation energy.

WAMOC10 REARRANGEMENTS OF DIENE RADICAL CATIONS USING PHOTODISSOCIATION SPECTROSCOPY, R. C. DUNBAR AND G. B. FITZGERALD, Chemistry Department, Case Western Reserve University, Cleveland, OH 44106

Photodissociation spectra were obtained via ion cyclotron resonance spectroscopy for a number of isomers of octadiene and pentadiene radical cations. Comparison of these spectra provides valuable structural information. Photodissociation spectra of conjugated diene radical cations typically contain two absorption peaks, one UV peak corresponding to a $\pi \rightarrow \pi^*$ transition, and one visible peak corresponding to a $\pi \rightarrow \pi$ transition. The photodissociation spectra of alkenes and non-conjugated dienes typically taper gradually from strong absorption in the UV to weak absorption in the visible region.
The spectra of the 1,3- and 2,4-octadiene radical cations display the two expected peaks. The former absorbs at 310 and 520 nm, and the latter absorbs at 330 and 500nm, indicating that the two radical cations are distinct from one another. The PDS of 1,4-octadiene is identical to that of the 2,4 isomer, indicating preferential rearrangement to the 2,4 conjugated form. The photodissociation spectrum of the 2,6-octadiene and 1,7-octadiene radical cations are distinct from one another, and the spectra are typical of non-conjugated dienes. Evidently, bond migration does not occur in radical cation dienes unless it is across only one bond to form a conjugated diene. This supports the general observation that the double bond in diene radical cations can only migrate by one position to come into conjugation. Cis-trans isomerization was investigated for 1,3-pentadiene radical cations and rearrangement of cis and trans isomers does not occur to any large extent.

CHLORIDE AFFINITIES AND HEATS OF FORMATION OF SUBSTITUTED BENZYL CATIONS OBTAINED FROM MEASUREMENTS OF CHLORIDE TRANSFER EQUILIBRIA.

D.K. Sen Sharma, K. Hiraoka and P. Kebarle, Chem. Dept., University of Alberta, Edmonton, Canada T6G 2G2

Studies of the kinetics and measurement of the ion molecule equilibria: $R^+ + R^1X = RX + R^{1+}$, where $X^- = Cl^-$ and H^- lead to chloride and hydride affinities of the carbonium ions R^+. The measurements were performed with a pulsed electron beam high ion source pressure mass spectrometer in the temperature range 300-600°K. An interconnecting staircase of equilibria was obtained containing $t\text{-}C_4H_9^+$ and the following substituted benzyl cations o, m, p F^-; o, m, p Cl^-; o, m, p CH_3^-; p-CH_3O^- α chloro, α,α dichloro, α phenyl, α methyl. The *ionization potentials of some of the corresponding meta, para substituted benzyl* free radicals were determined some 20 years ago by Harrison, Kebarle and Lossing (J. Am. Chem. Soc. 83, 777 (1961). A plot of the chloride affinities, versus the earlier measured ionization energies leads to a straight line plot with some small scatter. The slope obtained is ≈0.8. Since the chloride affinities depend on D(R-Cl) + I_p(R), the observation that the slope is 0.8 confirms the earlier supposition that the chloride affinities $D(R^+\text{-}Cl^-)$ are governed by the ionization potentials of the radicals. However since the slope is 0.8 and not 1, there seems to be a small increase of D(R-Cl) for substituents which decrease the ionization potential of R. This is a somewhat surprising result. The present results provide the first results for the effect of substituents in the ortho position. The stabilities of the F and Cl substituted benzyl cations increase in the order m, o, p, with a large gap between m and o and o and p. The significance of this result will be discussed.

THEORY FOR PREDICTING STRUCTURES OF INTERMEDIATE COMPLEXES OF CYCLOADDITIONS

J. O. Lay and M. L. Gross
Department of Chemistry
University of Nebraska
Lincoln, Nebraska 68588

The existence of cycloadduct intermediates in the ion-molecule reactions of various diene radical cations and neutral olefins or olefin radical ions and neutral dienes has been established.[1-4] However, an a priori means of predicting whether a cycloaddition will occur for a given set of reactants has not been developed. Given the constraints that such ion-molecule processes must occur with fairly high collision efficiency (at least 1%) and that there must be little or no activation barrier, it is proposed that cycloadditions will occur only when the reactants are drawn together by charge effects to produce maximum overlap of the relevant Frontier Molecular Orbitals (FMO's). The FMO's are the highest occupied molecular orbitals (HOMO) and lowest unoccupied molecular orbitals (LUMO) of the reacting ion and neutral. A facile reaction should involve maximum overlap which leads to large stabilization or lowering of the electronic energy in the incipient orbitals of the cycloadduct. This stabilization, ΔE, is given by

$$\Delta E \propto (H_{ij})^2/(\varepsilon_i-\varepsilon_j) \qquad (1)$$

where H_{ij} is a measure of the effective overlap of the HOMO of one reacting species and the LUMO of the other, while $(\varepsilon_i-\varepsilon_j)$ is the difference in energy between these orbitals.

It is proposed, then, that a necessary condition for an ion-molecule cycloaddition is sufficient stabilization, ΔE, of the newly forming molecular orbitals. As indicated in equation (1), this stabilization will be maximized with increased orbital overlap. This can be achieved with conservation of orbital symmetry. Such a requirement is well recognized for neutral-neutral cycloadditions.

Stabilization, ΔE, however, is not assured by orbital symmetry. In addition, the stabilization of incipient MO's increases with decreasing FMO energy differences. Thus the HOMO-LUMO energy difference between the reacting centers determines how strongly orbitals of appropriate symmetry may interact. While computational methods may be used to calculate orbital energy levels, ionization potentials and electron affinities for HOMO and LUMO energies can be used to assign appropriate relative energies for related systems.

A unique feature of radical ion reactions, not shown in equation 1, is the presence of the unpaired electron in the ion HOMO. It seems reasonable that for almost all likely HOMO-LUMO interactions, the stabilization of the intermediate from this one electron HOMO-LUMO interaction will be less than for a similar two electron interaction. This is because of the bond order of one half of the incipient molecular orbital in the one electron interaction. Thus, we postulate that the most important HOMO-LUMO interaction involves the neutral HOMO (IP) and cation LUMO (EA of the corresponding neutral).

An additional requirement, based on the fact that the cation is an electrophile, is that a major site of charge localization should be involved in bond formation. For charged butadienes, for example, bond formation in a cycloadduct should involve the terminal carbon atoms because they carry the majority of the charge.

In the following table, we present data for a number of systems which are capable of reacting by a cycloaddition pathway. For each system, we can show that the orbital symmetry and charge location are appropriate for cycloaddition. Furthermore, the IP-EA term is given as an assessment of the orbital stabilization in the complex. As can be seen, for reactants having an IP-EA difference of ∿11eV or less, the reaction proceeds as a cycloaddition. Of course, a pair of reactants having a larger difference would be expected to be unreactive or to react via another reaction channel.

CORRELATION OF EXPERIMENT AND THEORY

	RESULT	IP-EA(ev)
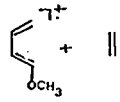	NO REACTION	13.0
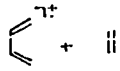	REACTION, NO CYCLOADDITION	11.1
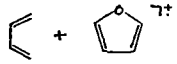	CYCLOADDITION	11.0
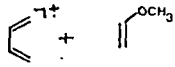	CYCLOADDITION	9.5
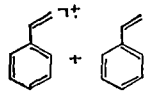	CYCLOADDITION	8.8
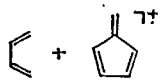	CYCLOADDITION	8.6

This work will be submitted to the J. Am. Chem. Soc. for publication.

1. C. L. Wilkins, M. L. Gross, J. Am. Chem. Soc., 93, 895 (1971).
2. M. L. Gross, D. H. Russell, R. Phongbetchara, and P. H. Lin, Advances in Mass Spectrometry, 7A, 129 (1978).
3. D. H. Russell and M. L. Gross, J. Am. Chem. Soc. (in press).
4. R. van Doorn, N. M. M. Nibbering, A. J. V. Ferrer-Correia, and K. R. Jennings, Org. Mass Spectrom., 13, 729 (1978).

PROTON-TRANSFER REACTIONS, HYDROGEN-EXCHANGE REACTIONS AND PROTON-TRANSFER/ HYDROGEN-EXCHANGE REACTIONS.

M.J. Henchman, Dept. of Chem., Brandeis Univ., Waltham, MA 02254,
D. Smith and N.G.Adams, Dept. of Space Research, Univ. of Birmingham, U.K.

We present a general model treating (I) proton-transfer reactions, (II) hydrogen-exchange reactions and (III) reactions involving proton transfer with concomitant hydrogen exchange. The conditions controlling these may be summarized: (I) $X >> 0$, (II) $X \leq 0$ and (III) $X > 0$. For reactants $DH^+ + A^-$, where A contains hydrogen sites, X is the proton affinity difference of A and D. Similarily for reactants $DH + A^-$, where A again contains hydrogen sites, X is the gas-phase acidity difference between AH and DH. Consideration of the Brauman reaction-coordinate diagram, with double minima and intervening barrier, sets a lower bound on X for the possibility of hydrogen exchange: for hydrogens to be exchanged, the system must be able to pass back and forth over the barrier, into the second basin. Thus hydrogen-exchange reactions, type (II), are only observed when respectively $0 < H < -D(D \cdot HA^+)$, the solvation energy for D to HA^+, and $0 < X < -D(D^- \cdot HA)$, the solvation energy for HA to D^-. This provides one criterion by which one can systemize the occurrence or non-occurrence of numerous hydrogen-exchange reactions reported in the literature.

Our experimental studies, using the Selected Ion Flow Tube technique, have focussed on Type (III) reactions. Thus, for $H_3O^+ + H_2O$, statistical product distributions, observed with isotopic labelling, reveal that the lifetime of the intermediate exceeds the relaxation time for hydrogen exchange within the intermediate. We report, in contrast, for $NH_4^+ + NH_3$, that these times are comparable, since the exchange, while extensive, is incomplete. The reaction coordinate diagram for the former exhibits a <u>single</u> minimum <u>without</u> intervening barrier while that for the latter shows the familiar double minimum and barrier.

PROTON AFFINITIES OF AROMATIC MOLECULES

D.A. Herold, T.A. Elwood, J.O. Johnson and J.H. Futrell
Department of Chemistry
University of Utah
Salt Lake City, Utah 84112

Despite considerable interest in the Proton Affinities (PA) of polycyclic aromatic systems only a few reports appear in the literature. This reflects, at least in part, experimental difficulties associated with the expected high proton affinities of these molecules along with their low volatilities.

Prediction of the PA's of these species with high accuracy by solution chemistry analogies or semi-empirical methods would be of enormous value in guiding practical experiments. The earliest attempts in this direction were done by Mackor et al.[1] who correlated Hückel ΔE vs. pK_B, followed by Franklin et al.[2] who demonstrated ordering of PA of xylenes according to pK_B values and most recently Hehre et al.[3] tabulated PA vs. STO-3G ΔE. From the preceding studies the use of pK_B to estimate PA of polynuclear arenes appeared to be a plausible method.

From a consideration of the reaction $B_1H^+ + B_2 \rightleftharpoons B_2H^+ + B$, where B_1H^+ is a reagent ion and B_1 is its conjugate base and B_2 is the arene base to be measured, then under near-equilibrium conditions $\Delta G = -RT\ln Keq = -RT\ln \frac{(B_2H^+)(B_1)}{(B_1H^+)(B_2)}$. Measurements are of ion intensity and of pressure of each species. Since $\Delta H - T\Delta S = \Delta G = -RT\ln Keq$, if the product $T\Delta S$ is small we may approximate the result $\Delta G \cong \Delta H$. However, for aromatics measured at 500°K, $T\Delta S$ can be a significant term.

Following, in part, the approach of Ausloos and Lias[4] we consider that the vibrational partition functions and electronic partition functions for the reactants and products are so similar that the ratio:

$$\phi^P_{elec}\ \phi^P_{vib}\ /\ \phi^R_{elec}\ \phi^R_{vib}$$

may be taken as unity. It is parenthetically noted that this would not be the case for charge-transfer reactions and for more complex kinds of ion-atom interchange reactions.

Other authors have considered the rotational partition function of reactant and products to be the same except for symmetry numbers and have suggested that the rotational symmetry number ratio is the major contribution to the entropy change for proton transfer equilibrium reactions. We have taken the alternative approach recommended by Bishop and Laidler[5] that "the correct procedure is to omit the symmetry members for the reactants and activated complexes and to multiply the rate expression by the statistical factor". It should be noted that both approaches give the same answer in many cases--but that exceptions do occur.

The most controversial aspect of the treatment by Lias[6] is the advocacy for the inclusion of an intermolecular entropy term in describing these reactions. The intermolecular entropy is given approximately by the equation $\Delta S_{int} = R\ln Z_f/Z_r$ where the Z terms refer to the collision rates of the reactions written for the forward and the reverse directions. These collision numbers are in turn evaluated from a consideration of the ion-induced dipole or ion-dipole interaction potential for the equilibrium reaction for the forward and reverse reactions, respectively. The AADO method of Su, Su and Bowers[7] may be used to evaluate this term.

The argument for inclusion of this term is the extreme departures of ion molecule reactions from the ideal gas postulated in the elementary formulation of statistical thermodynamics. In the limit of reactions occurring at every collision, which has been demonstrated for many exothermic ion molecule reactions, the collision rate is obviously the most important parameter for describing the reaction. In this limit the ratio of rate constants k_f/k_b may be replaced by Z_f/Z_b. In the present problem, however, the thermodynamic formulation of the non-ideality of the reactants and products requires that the ion-induced dipole or ion-dipole potentials be included in the partition function for the equilibrium constant. This formulation demonstrates that the non-ideality correction is negligible at reactant partial pressures below 1 Torr, the maximum pressure used in the present experiments.

The ΔS term is therefore taken as a sum of the ratio of reaction pathway degeneracy factors. The entropy contributions are then evaluated by taking the ℓn of each factor and multiplying by the gas constant, R.

The following table lists PA's relative to isobutene, determined using $\Delta G_{600°}$ published by Kebarle as bench marks. The PA's were computed by $PA = \Delta H = \Delta G + T\Delta S$. The plot of ΔH relative to isobutene vs. pK_B has a correlation coefficient of 0.997 demonstrating the predictive possibilities of pK_B to estimate PA of arenes.

References. 1) E.L. Mackor, A. Hofstra and J.H. van der Waals, Trans. Faraday Soc., 54, 66 (1958); 2) S.L. Chong and J.L. Franklin, J. Am. Chem. Soc., 94, 6630 (1972); 3) J.L. Devlin, III, J.F. Wolf, R.W. Taft and W.J. Hehre, J. Am. Chem. Soc., 98, 1990 (1976); 4) S.G. Lias and P. Ausloos, J. Am. Chem. Soc., 99, 4831 (1977); 5) D.M. Bishop and K.J. Laidler, J. Chem. Phys., 42, 1688 (1965); 6) S.G. Lias, "Thermodynamic Information from Ion-Molecule Equilibrium Constant Determinations", Lecture Notes in Chemistry, 7, Springer-Verlag, N.Y., 1978; 7) T. Su, E.C.F. Su and M.T. Bowers, J. Chem. Phys., 69, 2243 (1978);

THERMODYNAMIC LADDER (500°K)

Neutral	ΔG_R°	ΔH_R°	pK_B
$(CH_3)_2NH$	[-25.1]	[-23.7]	
	-24.1	-21.3	+6.1
	-18.6	-16.1	+3.5
$(CH_3)_2S=O$	[-17.5]	[-15.4]	-
	[-14.4]	[-13.0]	-
	-12.9	- 8.7	+0.6
	- 8.9	- 7.5	+0.1
NH_3	[- 7.6]	[- 6.8]	-
	- 6.1	- 3.5	-0.9
	- 3.5	- 1.5	-3.1
	- 2.1	+ 0.4	-3.6
	- 1.2	+ 1.7	-4.6
	[0.0]	[0.0]	-
	+ 0.5	+ 3.2	-5.8

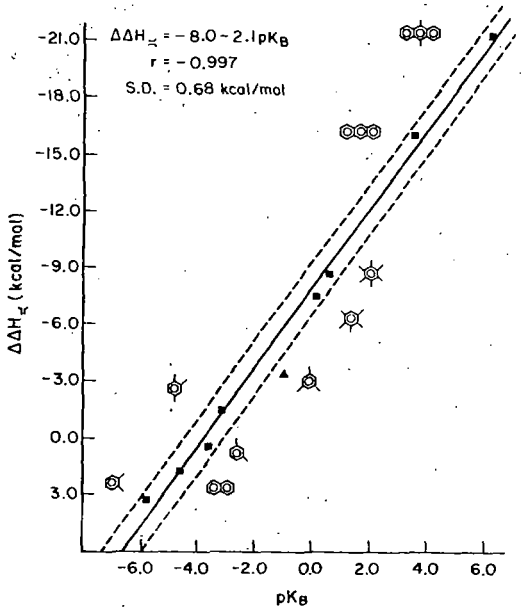

STUDIES OF ALKALI HALIDES BY THERMAL IONIZATION AND CHARGE-TRANSFER NEGATIVE IONIZATION IN A CHEMICAL IONIZATION SOURCE, J.R. Lloyd and F.H. Field, The Rockefeller University, New York, N Y 10021

Mass spectra of several alkali metal halides (MX) have been obtained by a technique which consists of placing the salt upon a rhenium ribbon, placing the ribbon inside the chemical ionization source of a quardupole mass spectrometer, and heating the ribbon with a dc current. Positive metal ions, M^+, are observed when the ribbon is heated with 5-8 amps. Introducing N_2 into the source with pressure in the range 0.5-2 torr increases the sensitivity by a factor of three. Sensitivity depends on the location of the ribbon, but not critically. Under optimum conditions 10-1000 pg. of Li can be detected, and quantitation can be effected using ^6Li as an internal standard with multiple ion monitoring (MIM).

Specifically, we are interested in quantitating ^6Li and ^7Li in the biological fluids of individuals undergoing treatment for manic-depressive psychosis[1]. The response for lithium in biological fluids can be dramatically increased if the proteins are removed by trichloroacetic acid precipitation. For example, no Li^+ response was observed for a 1 µl urine sample that was spiked to a concentration of 100 pg Li/µl. However, when the proteins were removed from the spiked sample, a good response for a 1 µl sample was obtained.

Urine samples (proteins precipitated) from three male workers in this laboratory showed no lithium in the 10 to 100 pg/µl range. This is not surprising when one considers that a possible major source of lithium in our diet, New York City tap water, contains less than 10 pg Li/µl. In contrast to NYC tap water, which is supplied from lakes, we were able to quantitate lithium at about the 200 pg/µl level in a bottled mineral water which is produced in W. Germany. Coincidentally, Schulten[2] has reported lithium levels of 10-100 pg/µl in the urine of his W. German laboratory workers. Thus, normal phsyiological levels of lithium can vary dramatically depending upon such factors as the source of the water supply for a particular area.

Thermal ionization of halide ions (X^-) vaporized from heated wires has not been much studied. We are able to produce copious quantities of X^- ions from MX under negative chemical ionization conditions. MX is loaded on the rhenium ribbon; approximately 2.5 torr of N_2O is introduced into the ion source; the N_2O bombarded with electrons emitted from the regular mass spectrometer filament external to the ion source; and the rhenium ribbon is heated by the dc current. X^- ions are detected at low dc current levels (0.5-2.5 amps.).

X^- ions are observed only if the reactant ions (O_2^-, N_2O^-, $N_2O_2^-$, etc.) are present. In fact, as the sample filament is monotonically heated, the increase in X^- intensity is equal to the decrease in intensity of the reactant ions. We believe that the X^- ions are produced by a charge-transfer mechanism from O_2^-, etc. to $X\cdot$ atoms emitted from the rhenium ribbon , and not by thermal ionization of MX to give M^+ and X^-. Charge transfer from the reactant ions to $X\cdot$ should be quite favorable since the electron affinities of the reactant ions are well below those of the halide ions.

Scheme 1 summarizes the postulated sequence of reactions that MX undergoes as the sample filament is heated monotonically from 0-8 amps. At low filament currents the MX bond is cleaved and a halogen atom is vaporized from the surface. Under N_2O NCI conditions $X\cdot$ is ionized to form X^-. The metal atom remains bound to the surface until the filament current reaches 5 amps at which temperature M^+ is produced by thermal ionization.

Scheme 1.

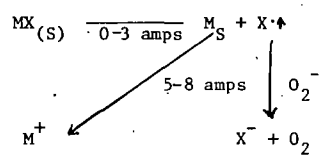

THERMAL IONIZATION N_2O NCI

Quantitation of Cl^- (from NCI of MCl) in the 20-200 ng Cl^-/µl range can be effected by using Br^- as an internal standard and MIM. Quantitation of I^- can be effected in a similar way. The detection limit for I^- from CsI is about 100 femtograms of I. A quantitative determination requires 20-30 minutes for either positive or negative ions, and the sensititivity and reproducibility (relative standard deviation of about 7%) of the method lead us to believe that it will be of practical utility.

1. K.W. Lieberman, G.J. Alexander and P. Stokes, Pharm. Biochem. and Behavior 1979,10,933
2. W.D. Lehamann, U. Bahr, and H.R. Schulten, Biomed. Mass Spectrom. 1978, 5, 536.

Kinetics of Thermal Desorption and Phase Transformation of Amorphous Carbon Films

Margaret A. Frisch
IBM Research Center
PO Box 218
Yorktown Heights, NY 10598
and
Joyce A. Thompson
Materials Science and Engineering
Massachusetts Institute of Technology
Cambridge, MA 02139

The thermal stability of amorphous carbon films, prepared by the plasma decomposition of propane-argon, was examined by high temperature mass spectrometry. These films are especially interesting because of their diamond-like properties. In addition to studies on the desorption of hydrogen and hydrocarbons from the films, the kinetics of phase transitions in the amorphous phase were determined via the release of argon incorporated in the film.

The thin carbon films, deposited on silicon, were heated in a Knudsen cell at a linear rate while monitoring the gaseous products after beam modulation with a quadrupole mass spectrometer. Because of the large conductance of the orifice with respect to the the cell volume, the ion signals are a direct measure of reaction rates. The cell and mass spectrometer are in separate differentially pumped UHV systems. The quadrupole electronics, signal measurement and temperature programming are all under the control of an IBM System 7 computer.

For reactions controlled by kinetics, the activation energy and reaction order were derived from the shape of the ion intensity-temperature data by comparison with theoretical curves, obtained by integrating the rate equation with respect to temperature. For diffusion controlled processes, the activation energy and D_0 were obtained by comparing the time dependence of the ion signals with theoretical curves calculated for both spherical and slab diffusion.

The main features of the thermal desorption spectra are as follows:

1) Below 720K, argon diffuses from the film with an activation energy of 200 kJ/mole.
2) Isothermal annealings in 10K increments from 680 to 720K show that a phase transition of the amorphous carbon occurs after a thermally activated incubation period, with an activation energy of 270 kJ/mole. However, no crystallinity could be detected by HEED studies on the heated films.
3) Following this transition, the argon diffusion rate is larger by an order of magnitude but with the same activation energy as the pretransition region.
4) Desorption of H_2, CH_4 and C_2H_x occurrs subsequent to the phase transition. Complete desorption of H_2 requires heating the films to at least 1200K while the desorption of CH_4 and C_2H_x is complete by 900K. The activation energy for the H_2 desorption is 240 kJ/mole but the reaction order cannot easily be established because of the several overlapping peaks.
5) The CH_4 desorbs in a single second order process which peaks at 845K. The activation energy derived from the peak shape is 300 kJ/mole. A small amount of unbonded CH_4 was also observed which diffuses from the film below 790K. The mechanism for the formation of H_2 and CH_4 is probably via the dissociation of hydrogen atoms from CH_x sites which then diffuse through the film until they react with other C-H and CH_3 groups. These products rapidly diffuse to the film surface and are free to desorb.

WAMP4 NEW SOFTWARE STRATEGIES FOR HIGH PRECISION SOLID SAMPLE ISOTOPE ANALYSIS.

THE MAT 261, K. HABFAST and H. RAVENS, Varian MAT GmbH, Bremen/West Germany

High precision and high accuracy Multiple Filament Thermionic Source (MFTIS) isotope measurements have, for years, been performed using varying amounts of automation. With the introduction of fully computer controlled mass spectrometer hardware, fully automatic measurement procedures are now available.
In high precision fully automatic measurements the prerequisite is the same as in manual or partly automatic measurements: A predictable sample behaviour, in other words, the knowledge that the sample in question can be analyzed according to the experimentally proven measuring procedure for that specific type of samples.
Some general measuring procedures, which can be modified by specific sets of parameters, will be presented together with some experimental results on geological Sr-samples.

The Determination of Beryllium in Ambient Air Particulate by Spark Source Mass Spectrometry,

E. Hunter Daughtrey, Jr. and J. Kent Bostick, Jr., Northrop Services, Inc., P.O. Box 12313, Research Triangle Park, North Carolina 27709.

INTRODUCTION

The presence of beryllium in ambient air particulate is of environmental concern, due to its known toxicity. One of the chief methods of collecting ambient air particulate is the hi-volume sampler, which employs glass fiber filter as the collecting medium. Air is pulled through the filter, and the particulate in the air is collected in/on the filter. The presently used method of analysis for beryllium (ICP emission spectrometry survey analysis) requires extraction of the sample from the filter by hot, mixed-acid ultrasonication. In order to verify the recovery from the extraction method, another independent method which does not require solubilization of the sample, was sought. Spark source mass spectrometry should meet this requirement due to its trace-level sensitivity and solids analysis capability.

MASS SPECTROMETRY

Problem

Positive, qualitative identification of beryllium is complicated by several factors:

- Beryllium is monoisotopic.
- The doubly-charged isotope line, $^{9}Be^{+2}$ at m/e 4½, is outside the normal mass range (6-240) of the instrument.
- Interferences at the nominal mass (9) of beryllium are numerous and of high intensity.

Solution

Positive identification of beryllium is possible by high resolution densitrometry and careful mass measurement.

The densitometer under computer control can measure a line position to within ±5 microns.

Species	Position, Micron	Measured Mass, amu	Accurate Mass, amu
$^{23}Na^{+3}$	3145	Reference	7.66325
$^{28}Si^{+3}$	8640	Reference	9.32564
$^{9}Be^{+1}$	7640 ± 5	9.0120 ± 0.0006	9.01219

The nearest interfering line is removed by at least 0.01 amu. Mass spectral resolution is sufficient to resolve the Be line from the interferences. The careful mass measurement offers confirmation that the response is due to beryllium.

SAMPLE PREPARATION

Problem

Removal of particulate sample from hi-vol filter while minimizing the amount of glass fiber substrate taken with the particulate.

Solution

Use of ultrasonic agitation to remove the particulate from the filter material, without dissolving the particulate sample. Cyclohexane was used as an inorganically inert ultrasonicating medium. Two experimental parameters, pre-soak time and ultrasonicating time, were optimized by use of modified simplex. The simplex converged fairly rapidly, using the weight found of Be, V, and Mn as indicators of extraction yield.

PROCEDURE

1. Cut two 3" sections from 1" x 8" filter strip.
2. Place each 1" x 3" strip into a centrifuge tube.
3. Add 20 ml cyclohexane, cap tube.
4. Let stand one hour.
5. Place tube in ultrasonic bath for 10 minutes.
6. Remove filter, then transfer residue with cyclohexane to evaporating dish.
7. Evaporate to dryness under IR lamp.
8. Spike residue with erbium internal standard and add graphite.
9. Mix, and evaporate slurry to dryness.
10. Homogenize in mixing mill.
11. Form electrodes via die and hydraulic press.
12. Spark electrodes.

ANALYSIS

Filters previously analyzed by ICP emission spectrometry were analyzed by SSMS with the following results:

CODE	AIR VOLUME, m^3	Be concentration, ng/m^3 SSMS	ICP-OES
BJDJ	1736	0.27	0.24
BNLK	1732	0.38	0.41
BLEE	1827	0.04	below L_D
Detection Limit		0.005	0.1

SUMMARY AND CONCLUSIONS

A method for extraction of particulate from hi-vol filters and subsequent SSMS determination of beryllium has been developed. The mass spectrometry requirements for analysis for beryllium were fairly easily met by high resolution densitometry and accurate mass computation. Analysis precision is affected by homogeneity problems due to sample size and low concentration of the sought-for element. Further refinement of the sample preparation method and its extension to other elements are planned.

This work was performed under Contract 68-02-2566 in support of the Environmental Monitoring Systems Laboratory, USEPA, Research Triangle Park, North Carolina.

SIMS SPECTRA OBTAINED FROM NBS 660 STEEL BOMBARDED BY CAESIUM$^+$ IONS

MARCEL BARIL

DEPARTEMENT DE PHYSIQUE, UNIVERSITE LAVAL

QUEBEC, CANADA G1K 7P4

FIVE DIFFERENT STEEL IDENTIFIED AS NBS 661 TO 665 HAVE BEEN ANALYSED BY SECONDARY ION MASS SPECTROMETRY USING 5KV CS^+ IONS AS THE PRIMARY BEAM. THE VERY LOW CONTENT OF ANY OTHER ELEMENTS APART FROM IRON HAS MODIFIED GREATLY THE SPECTRA COMPARED TO THOSE OBTAINED FROM STAINLESS STEEL SUCH AS 314 OR SPECIAL STEELS SUCH AS 5514 OR 5540 WHICH WE STUDIED PREVIOUSLY WITH VALLERAND (1). SOME PEAKS BETWEEN MASS 30 AND 50 ARE PARTICULARLY DIFFICULT TO INTERPRET.

RELATIVE INTENSITIES FOR VARIOUS ELEMENTS PRESENT AS TRACES IN THE SAMPLES DO NOT SEEM TO BE DIRECTLY AND LINEARLY RELATED TO THE KNOWN CONTENT OF THE RESPECTIVE ELEMENTS. IT APPEARS THAT THE ANALYSIS MUST BE DONE WITH A HIGH RESOLVING POWER MASS SPECTROMETER IF WE WANT TO BE ABLE TO PROVE THE PRESENCE OF AS MANY AS FOUR OR FIVE CONSTITUANTS IONS ON THE SAME MASS PEAK AND DEFINE CORRECTLY THEIR IDENTITIES.

A TENTATIVE INTERPRETATION OF A SPECTRUM OF 661 IS GIVEN AS EXAMPLE. THE METHOD USED, WHICH SEEMS RELIABLE WHEN APPLIED TO OTHER STEELS SUCH AS THOSE MENTIONED EARLIER, HAVE BEEN EXPOSED PREVIOUSLY (2).

(1) PROCEEDINGS 7TH INTL. VACUUM CONGRESS AND 3RD INTL. CONFERENCE SOLID SURFACES (VIENNA 1977) P. 2569-72.

(2) PROCEEDINGS 27TH ANNUAL CONFERENCE ON MASS SPECTROMETRY AND ALLIED TOPICS (SEATTLE 1979) P. 309-11.

MASS SPECTRUM OF NBS 661 STEEL

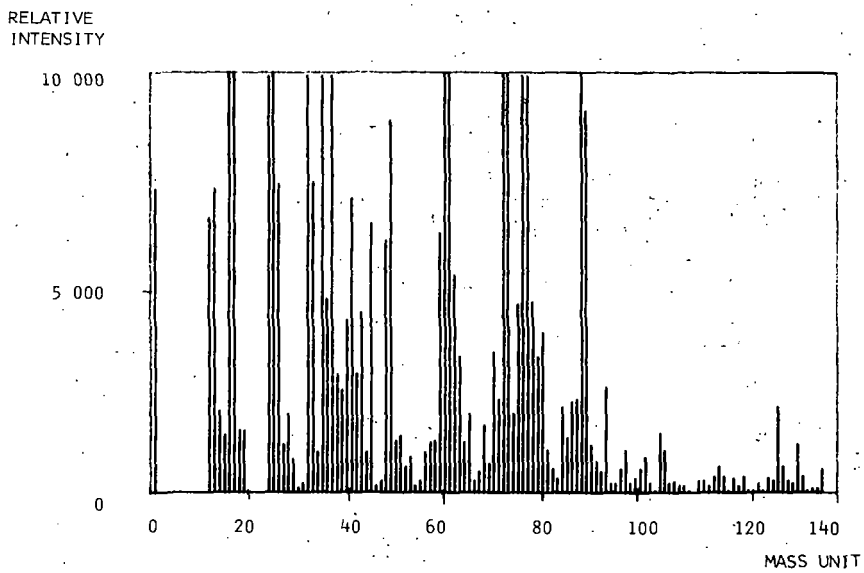

	Al	Si	P	Cl	Ti	V	Cr	Al_2	Mn	Fe	Ni	Co	Cu	Al_3	Nb	Mo	Al_4	Fe_2
Pure		2.03	0.21	13.19		1.34	0.76		0.19	1.07	1.82		3.33		2.05			0.33
H		0.77					0.94			1.29	9.17				0.13	1.05		
H_2		0.02																
O	4.23	1.06	0.20		1.32	0.49	1.93	2.65	1.60	10.95	2.44		2.12				0.20	2.46
OH		2.98			0.93		0.61			10.98	6.72							0.51
OH_2	3.65																	
O_2		10.37			5.02	0.29	2.39		1.49	10.93	1.38			0.28	0.06			
O_2H		7.73					1.31			9.69	1.11				0.08			
O_2H_2		4.63					1.63											
O_2H_3			0.17															
O_3		10.15			0.42		0.69	0.04		1.58								
O_3H		8.38			1.13		0.84			1.10								
O_3H_2		3.61																
O_3H_3		0.81	0.31															
O_4		0.18				0.39	0.70		0.31	0.19	0.07	0.06	0.33					
O_4H							0.40			0.44								
O_5						0.21	1.29		0.07	0.12								
O_5H							0.33			0.63								
Ni										0.22								
NiO										0.33								
TOTAL	7.88	52.72	0.89	13.19	8.82	2.72	13.82	2.69	3.66	49.22	22.71	0.06	5.78	0.28	2.32	1.05	0.20	3.30
POURC.	0.02	0.22	0.015	X	0.02	0.01	0.7	X	0.7	97.5	2.0	0.03	0.04	X	0.02	0.19	X	X

WAMP7 CHLOROETHYLNITROSOUREA QUANTITATION WITH GAS CHROMATOGRAPHY MASS SPECTROMETRY, R. J. WEINKAM and T.-Y. LIU, Dept. of Medicinal Chemistry, Purdue Univ., West Lafayette, IN 47907 and Brain Tumor Research Center, Univ. of California, San Francisco, CA 94143.

Chloroethylnitrosoureas are a class of cancer chemotherapeutic agents that has been in clinical use for several years. In spite of this, no general quantitative analytical method has been reported with the sensitivity required to monitor the biodistribution of parent drugs or the specificity to quantify biologically active metabolites in man or experimental animals. A glc-cims assay has been developed. This method circumvents the thermal lability an utilizes the chemical reactivity of the chloroethylnitrosourea function, $ClCH_2CH_2N(NO)CONHR$, by reacting the parent compound in basic anhydrous methanol. Under these conditions, the nitrosourea reacts to give a chloroethyldiazonium ion and a substituted isocyanate. The diazonium ion undergoes rearrangement and alkylation reactions while the isocyanate is efficiently trapped by solvent methanol as a methylcarbamate. The reagent-product mixture may be injected directly onto the glc column. Another chloroethylnitrosourea may be used as reference standard. The analyzed product, $CH_3OCONHR$, retains the characterizing R moiety and, therefore, different chloroethylnitrosoureas or active hydroxylated chloroethylnitrosourea metabolites may be separated and quantified. Assays have been developed for BCNU, CCNU, MeCCNU, PCNU, and ACNU; all of which are used clinically. Assay limits are approximately 100 ng/ml plasma. Plasma clearance of PCNU in individual rats has been determined from 100 ml plasma samples as an application of this proceedure.

SELECTED ION MONITORING CAPILLARY COLUMN GLC-MS ASSAY FOR TIMOLOL AND $^{13}C_3$-TIMOLOL IN HUMAN PLASMA.

J.R. Carlin*, R.W. Walker*, R.O. Davies**, R.F. Ferguson*** and W.J.A. Vandenheuvel*
Merck Sharp & Dohme Research Laboratories
*Rahway, N.J. 07065
**West Point, Pa. 19486
***Thomas Jefferson University Hospital, Philadelphia, PA 19107

An assay has been developed for the quantification of timolol (see below; a beta-adrenergic blocking agent) and its $^{13}C_3$- analog,

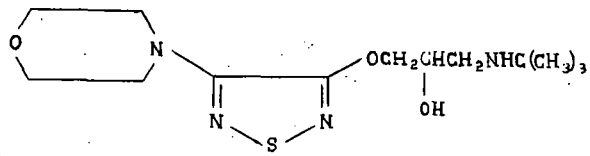

$RCH_2NHC(^{13}CH_3)_3$, in human plasma at the 0.5 ng/ml level. The method employs a C18 reversed phase Sep-Pak in the isolation from plasma of a drug-containing fraction, capillary column GLC of the TMSi derivatives of the compounds of interest and the internal standard [$RCH_2NHC(CD_3)_3$] and detection via selected ion monitoring. The ions monitored for quantification (m/e 86 from timolol and 89 and 95 from the $^{13}C_3$- and D_9 analogs, respectively) arise from the sidechains of the three compounds [e.g., $CH_2NHC(CH_3)_3$ for m/e 86]. Plasma levels of timolol and $^{13}C_3$-timolol in human subjects given 5 (or 10) mg of each of these compounds simultaneously were followed for 12 h post dose. Peak plasma levels for the individual compounds [∿12 ng/ml for 5 mg dose (average of two subjects); ∿34 ng/ml for 10 mg dose (average of two subjects)] occurred at 1-2 h post dose and fell to <3 ng/ml in each subject at 12 h. No evidence was found for a metabolic kinetic isotope effect as the ratios of the two species in the plasma samples were the same as the ratios in the administered drug.

GC-MS Quantitation of Impurities in Imipramine and Desipramine Standards and Pharmaceutical Formulations

J. Saady, N. Narasimhachari and R. O. Friedel
Department of Pathology, Medical College of Virginia
Richmond, Virginia 23298

Introduction

When setting up the tricyclic antidepressant (TCA) method in our laboratory using GC/MS/EI, we noticed that our "pure" imipramine working standard was contaminated with desipramine, as well as iminodibenzyl, the basic tricyclic nucleus. Upon further investigation we found that the same was true for imipramine tablets and USP-NF Reference Standards of imipramine. Similarly, in the same types of samples, we found that desipramine samples were contaminated with imipramine and iminodibenzyl. We systematically analyzed a series of imipramine and desipramine pharmaceutical formulations prescribed to patients as well as standards obtained from different sources.

Materials and Methods

Samples of imipramine and desipramine standards (as hydrochlorides) were obtained from the USP-NF and Pharmaceutical Companies. Pharmaceutical formulations were obtained from hospital Pharmacy from current lots and d_4-imipramine, d_4-desipramine and d_4-iminodibenzyl were prepared in our own laboratory by standard exchange procedures and were found to be over 99% isotopically pure. All solvents were pesticide grade. N-methyl-bistrifluoroacetamide was purchased from Regis Chemical Company, Chicago. The method of Narasimhachari et al. (1) was used for all determinations. It is rapid in that both the tertiary amine and its secondary amine metabolite are determined simultaneously, and it is less complicated than the CI modes in that the electron impact (EI) mode of GC/MS can be used.

GC-MS

GC-MS determinations were done on a Hewlett Packard 5985A or a Finnagan 4000 GC-MS data system. A 1 meter (2 mm I.D.) glass column, packed with 3% SP-2250 Supelcoport 80/100 mesh was used, with a helium flow of 35 ml/min. Column temperature was 200° programmed at 10° C/min. to 250° C. All contaminant compounds were identified by obtaining the total mass spectrum in the EI mode. Quantitative determinations were made by selected ion monitoring technique using both electron impact and methane chemical ionization methods.

Results

The EI mass spectra of iminodibenzyl and imipramine found as contaminants in the samples are shown in Figs. 1 - 2. These spectra are identical in all respects with the spectra of authentic standards. A selected ion recording for the desipramine contaminant is shown in Fig. 3. The results obtained with various samples are presented in Table I. It can be seen that all working standards including the sample obtained from the USP-National Formulary contained contaminants.

Discussion

We have shown by GC-MS methods that samples of imipramine and desipramine in pharmaceutical formulations and working standards contain the basic nucleus iminodibenzyl as a major contaminant. Further, formulations of imipramine contain desipramine and vice versa. While there are no specific limits on these impurities in the US Pharmacopeia, there are guidelines concerning the overall purity of the preparation itself. Indeed, the methodology used by the USP-NF (UV, IR, and spot tests) would not detect these impurities at the levels found. Our intention is not criticism but only to create an awareness of the presence of these impurities since these findings have an effect on the interpretation of results. For instance, the small concentrations of iminodibenzyl found in plasma samples of subjects receiving this drug may mostly be due to the presence of the compound in the drug itself and not due to drug metabolism as reported (2).

For a correct evaluation of plasma levels of the drug and its metabolites a strict quality control on the analytical method, the pharmaceutical preparation, and the working standard used in the analysis is a prerequisite.

References

[1] Narasimhachari, N., Friedel, R.O. and Saady, J.J., Res. Comm. in Psychol., Psy., and Beh., Vol. 4, #4, 471 (1979). [2] Bickel, M.H. and Weder, H.J., Archives Int. Pharmacodyn., Vol. 173, 433 (1968).

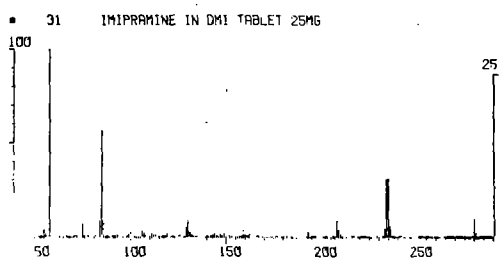

Fig. 1

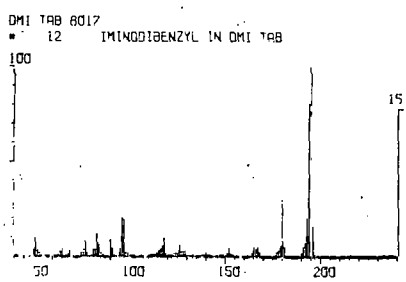

Fig. 2

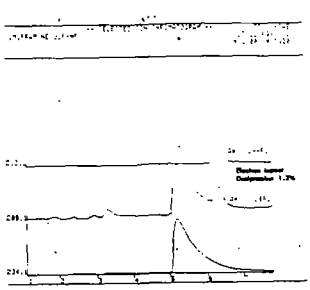

Fig. 3

PERCENT IMPURITY DETERMINED BY GC/MS

WORKING STANDARDS	IMINODIBENZYL	IMIPRAMINE	DESIPRAMINE
USP-MF IMIPRAMINE	0.5	x	1.7
USP-MF DESIPRAMINE	0.2	0.9	x
IMIPRAMINE FROM PHARMACEUTICAL COMPANY	3.3	x	3.3
DESIPRAMINE FROM PHARMACEUTICAL COMPANY	2.8	4.0	x
IMIPRAMINE AFTER ONE RECRYSTALLIZATION	0.7	x	0.5
IMIPRAMINE TABLET 25 mg. Lot #17397	0.4	x	0.9
IMIPRAMINE TABLET 25 mg. Lot #1818	0.6	x	2.3
DESIPRAMINE TABLET 25 mg. Lot #8017K8	2.7	2.0	x

Table 1

POTENTIAL GABA PRECURSORS: SYNTHESIS OF DEUTERIUM LABELED L-GLUTAMINE AND 4-AMINOBUTANAMIDE,

Martin Stogniew, Linda A. Geelhaar, and Patrick S. Callery, Dept. of Medicinal Chemistry/Pharmacognosy, University of Maryland, Baltimore, MD 21201

The amide bond in glutamine is much more labile toward hydrolysis than simple alkyl amides. Under physiologic conditions glutamine is readily converted to glutamic acid and 2-pyrrolidinone-5-carboxylic acid (pyroglutamic acid). The decarboxylation product of glutamine, 4-aminobutanamide (GABAMIDE) is potentially more labile toward hydrolysis than glutamine. Glutamine and GABAMIDE are being studied in a continuing effort to develop precursors or prodrugs of GABA and glutamic acid. SL 76002, a prodrug of GABA, has been developed.[1] This compound is converted in the central nervous system to GABAMIDE and GABA.

Isotopically labeled GABAMIDE and L-glutamine were required to evaluate these compounds as precursors in the presence of a large pool of unlabeled material in the central nervous system. In a single step, 6-carboxy-3(2H)-pyridazinone was reduced with deuterium gas to give racemic glutamine-2,3,4-$^2H_3$. L-Glutamine-2,3,4-$^2H_3$ was prepared by the stereospecific deacetylation of N^2-acetylglutamine-2,3,4-$^2H_3$ with acylase I. 4-Aminobutanamide-2,3,4-$^2H_3$ was synthesized from 3(2H)-pyridazinone in two steps. Reduction of 3(2H)-pyridazinone with deuterium gas gave the intermediate 1,4,5,6-tetrahydro-3(2H)-pyridazinone-4,5,6-$^2H_3$, which was further reduced with Raney nickel and hydrogen to yield 4-aminobutanamide-2,3,4-$^2H_3$.[2]

A GC-MS assay has been developed for GABAMIDE which is suitable for biological samples. GABAMIDE was purified by high voltage electrophoresis followed by derivatization with pentafluoropropionic anhydride to form N,N^1-dipentafluoropropionyl-4-aminobutanamide (1). On column decomposition of 1 to N-pentafluoropropionyl-4-aminobutyronitrile (2) was confirmed by IR, and GC-MS.

1) P. Krogsgaard-Larsen, J. Scheel-Krüger and H. Kofod (eds.), GABA-Neurotransmitters, Academic Press, New York (1979).

2) "Synthesis of Deuterium Enriched L-Glutamine and 4-Aminobutanamide from Pyridazinones," M. Stogniew, L.A. Geelhaar, and P.S. Callery, J. of Labelled Cmpds. Radiopharm., In press.

SIMULTANEOUS QUANTIFICATION OF PHENYTOIN, ITS PARA-HYDROXYLATED METABOLITE, AND THEIR STABLE ISOTOPE LABELLED ANALOGS BY GC-MS: DEVELOPMENT AND APPLICATIONS OF THE METHOD.

A. Van Langenhove, C.E. Costello, J.E. Biller, K. Biemann and T.R. Browne; Dept. of Chem. M.I.T., Cambridge, MA 02139 and V.A. Hospital, Boston, MA 02130.

A gas chromatographic-mass spectrometric (GC-MS) method was developed for the determination in biological fluids of 5,5-diphenylhydantoin (phenytoin) (I), its major metabolite in man, 5-(4-hydroxyphenyl)-5-phenylhydantoin (para-HPPH) (II), and simultaneously, their stable isotope labelled analogs [5,5-diphenyl-2-^{13}C-1,3-$^{15}N_2$-hydantoin (III) and 5-(4-hydroxyphenyl)-5-phenyl-2-^{13}C-1,3-$^{15}N_2$-hydantoin (IV)]. The stable isotope labelled phenytoin will be administered as a "pulse dose" to patients in order to study its specific pharmacokinetics.

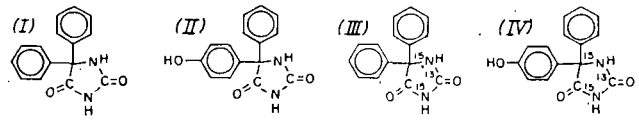

The method was evaluated for the analysis of I, II, and III in serum, and for III in urine (IV was not available as reference compound). Accuracy in quantification was achieved by isotopic dilution: 5,5-di(pentadeuterophenyl)hydantoin (V) and 5-(4-hydroxy-3, 5-dideuterophenyl)-5-phenyl-2-^{13}C-1,3-$^{15}N_2$-hydantoin (VI) were used as internal standards.

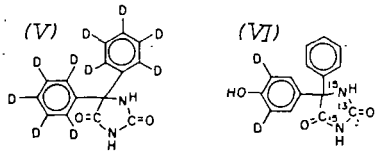

The chemical work-up procedure involves acid hydrolysis (cleavage of the para-HPPH-glucuronide bond), extraction at pH=7.4, and derivatization by an extractive methylation technique (1,2). The mass spectrometric measurement involves monitoring of two gas chromatographically resolved sets of compounds: I-III-V and II-IV-VI. Molecular ions of the permethylated derivatives, as they elute from the gas chromatograph, are measured by repetitive scanning over the appropriate m/z values. An already highly modified Hitachi RMU-6L and its computerized data acquisition system(3) was further adapted to allow linear scanning of the accelerating voltage. Data processing by the computer, and the ability to display both the total ionization plot and the monitored mass range on a CRT screen (Fig. 1) facilitate unambiguous measurement of ion abundances. In addition, interferences - if present - can be easily detected.

The precision of the GC-MS measurement was determined by replicate injections of the same sample extract; coefficients of variation (CV) were in the range of 0.3-1.0%, with the best precision obtained when equal amounts of analyte and internal standard were monitored. Precision of the overall procedure was measured at the extreme points of the calibration graphs. For N = 10, the CV remained below 5% in most cases. In addition, the between day precision of the analysis was verified over three consecutive days for selected serum and urine samples (CV = 0.3-5.9%). Linearity was demonstrated for the analysis of I and III in serum at levels of 0.1-30.0 µg/ml; for II at levels of 0.1-10.0 µg/ml; and for the analysis of II in urine at levels of 5.0-200.0 µg/ml.

"Pulse dosing" studies with stable isotope labelled tracers are only valid if the unlabelled and stable isotope labelled analogs are pharmacologically equivalent, i.e. if they have the same pharmacokinetics. The method was therefore applied to study the pharmacological equivalence of I and III in dogs and human volunteers.

A 1:1 mixture of I and III was administered intravenously and serial blood and urine collections were analyzed (dogs: 0-5 hours; man: 0-48 hours). For dogs, both meta-HPPH and para-HPPH were monitored because meta-HPPH is the major metabolite. A slight modification of the GC-MS procedure was therefore necessary. It was demonstrated that the ratio of unlabelled to stable isotope labelled drug and metabolite remained constant throughout the collection period. Pharmacokinetic analysis of the data also indicated no significant

differences in serum halflife, volume of distribution and renal clearance of the monitored analogs.

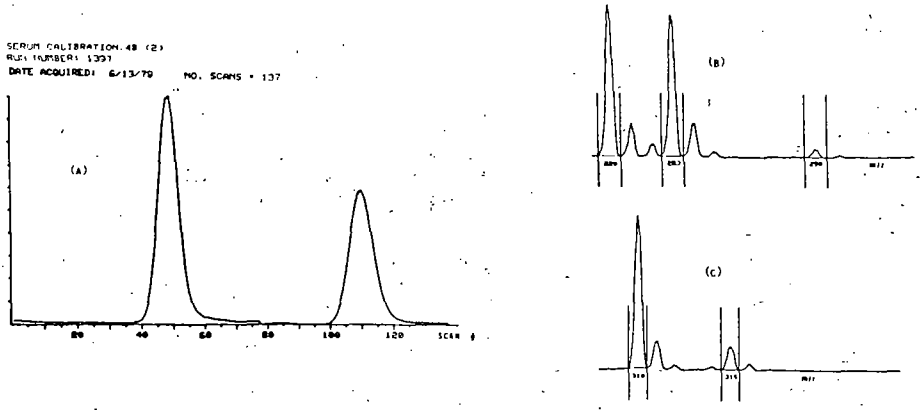

Fig. 1. COMPUTER TERMINAL DISPLAY OF (A) THE TOTAL IONIZATION PLOT CONSTRUCTED DURING ANALYSIS OF A SERUM SAMPLE (B) THE MASS RANGE SCANNED FOR THE DETERMINATION OF THE PHENYTOIN ANALOGS (C) THE MASS RANGE SCANNED FOR THE DETERMINATION OF THE PARA-HPPH ANALOGS. Shown here are data taken during analysis of a serum sample containing 10.0 µg/ml of I and III; 5.0 µg/ml of II, and 1.0 µg of the respective internal standards. Scan #52 and #113 are displayed in (B) and (C) respectively.

REFERENCES

(1) Hoppel, C., Garle, M., and Elander, M., J. Chromatog. 116, pp. 53-61 (1976).
(2) De Sagher, R., Pocius, J., and Thenot, J.-P., J. Chromatog. 156, pp. 43-53 (1978).
(3) Biemann, K., Biller, J.E., in Biochemical Applications of Mass Spectrometry, First Supplementary Volume, G.R. Waller and O.C. Dermer, Eds., Wiley Interscience, N.Y., 1980.

ACKNOWLEDGEMENTS

This study was supported in part by grants from the NIH Division of Research Resources (RR00317, to K. Biemann) and the Veterans Administration (to T.R. Browne).

REDUCTIVE METABOLISM OF FURAZOLIDONE IN THE RAT Joseph Cohen, Robert Abraham, Balwant Dixit, Joseph Knapp, Lan Wong and John Alvin: School of Pharmacy, University of Pittsburgh, Pittsburgh, PA 15261

The antimicrobial agent furazolidone (N-5-nitro-2-furfurylidene -3 amino-2-oxazolidinone)(FIG. 1) is extensively employed as a livestock feed additive for treating intestinal infections, promoting growth, and enhancing feed efficiency. In addition, it is used in humans as an antimicrobial in the treatment of enteric infections. However, chronic use of this agent is accompanied by a potent, long-lasting inhibition of the mitochondrial enzyme monoamine oxidase (MAO) in animals (Stern et al., J. Pharm. Exp. Therap. 156 (3), 492) and man (Pettinger et al., Clin. Pharm. Therap. 9 (4), 442). Significantly, furazolidone itself does not inhibit MAO in vitro as do classical MAO inhibitors. This implies that a metabolite of this compound mediates the toxicity. In the present study we report the reductive metabolism of furazolidone by S9 fraction of rat liver and aerobic cultures of rat gastrointestinal micro-organisms. This metabolite was isolated by HPLC and characterized by MS analysis.

The mass spectrum of the parent drug (FIG. 1) shows a molecular ion at m/e 225 and characteristic ions at m/e 87 and m/e 79, representing the oxazolidinone ring and the furan ring, respectively. Since direct probe analysis of the metabolite resulted in extensive decomposition, the methoxime derivative (FIG. 2) was prepared using methoxyamine. After purification by HPLC, this derivative was subjected to MS analysis by direct probe, and yielded a molecular ion at m/e 224. The base peak at m/e 87 indicates retention of the oxazolidinone moiety from the parent drug. Disappearance of the m/e 79 fragment indicates metabolic alteration of the furan ring. This information is compatible with the structure of 3-{[(3-cyano-1-oxopropyl) methylene] amino}-2-oxazolidinone. Appearance of peaks at m/e 138 and m/3 111 are consistent with fragmentation of the structure shown in FIG. 2. Metabolism of another 5-nitrofuran derivative, nitrofurantoin, by an analogous reaction provides a precedent for this metabolic pathway.

Our studies using ^{14}C-furazolidone have shown that extensive metabolism to more polar products occurs in vivo as well as in vitro. Indeed, after oral administration of ^{14}C-furazolidone to rats, virtually all of the radioactivity detected in extra-intestinal and extra-hepatic tissues was metabolically derived. Based on radiochromatographic data obtained from these experiments, we conclude that formation of the open chain nitrile described above constitutes a significant in vivo metabolic pathway for furazolidone.

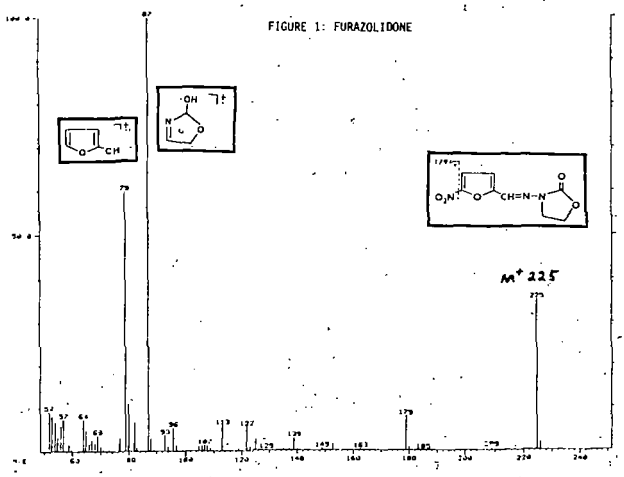

FIGURE 1: FURAZOLIDONE

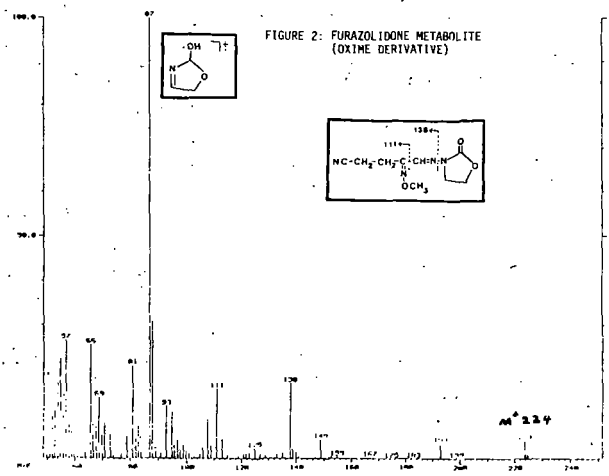

FIGURE 2: FURAZOLIDONE METABOLITE (OXIME DERIVATIVE)

SELECTED-ION-MONITORING EVIDENCE THAT ACETYLCHOLINE IS NOT A CORTICO-STRIATAL NEUROTRANSMITTER

PAT HAUG, NORBERT SCHRÖDER, JIN-SOO KIM, AND ROLF HASSLER

Neurobiologische Abteilung, Max-Planck-Institut für Hirnforschung, Deutschordenstraße 46, D-6000 Frankfurt/M - Niederrad, West Germany

The concentration of acetylcholine is known to be higher in the striatum than in any other brain area except the nucleus interpeduncularis (1). Direct cortico-striatal connections are well documented in the rat (2). An attempt was, therefore, made to determine whether acetylcholine is localized in these neurons by determining whether or not the concentration of acetylcholine decreases after cortical lesion.

The motor and premotor cortex of male Wistar albino rats was removed by suction from the left side. One week after operation, the animals were decapitated and both striata were removed. The striatum of the right side (contralateral to the lesion) served as control. Tissue samples weighing 6 - 11 mg were weighed with a digital Beckmann balance; an interface was constructed to automatically print out the time elapsed after death together with the sample weight.

The tissue was immediately homogenized for 20 min at 0°C in 1 ml of 4% perchloric acid to which had been added 10 nM acetylcholine D_9 perchlorate and 10 nM choline D_2 iodide as internal standards. After centrifugation, a 700 ul aliquot was added to 1.5 ml 0.5 M Na_2HPO_4. Ion pair formation was carried out with 1 ml of 2.4 mM dipicrylamine in dichloromethane (3) and derivatives suitable for GCMS formed by reaction with sodium benzenethiolate and propionyl chloride.

The slight increase in sensitivity did not balance the increased analysis time required for capillary columns so that the derivatives were separated using a 2 m x 2 mm packed glass column of 2.5% Poly A 135 and 2.5% OV 101 on Chromosorb WHP 100-120 mesh (silanized) at 110°C with a flow rate of 20 ml/min helium. The column was connected by means of a single stage jet separator to a Vacuum Generators Micromass 12 F mass spectrometer.

The Vacuum Generators solvent dump valve consisting of a thin tungsten blade fitting between the two capillaries of the jet separator was adjusted to slide back and forth on its steel rod with an electromagnet. A control unit was constructed to permit either manual selection of the solvent delay and run time in seconds or external control by a pulse from the computer. In order to avoid unnecessary solvent contamination of the source and to increase the precision of the measurement by establishing a reproducible baseline after a solvent impurity at m/z 58, the dump valve was opened 80 sec after injection of the sample.

The multiple-ion-monitoring unit (MS equipped with fast magnet) could be operated either with electric or magnetic alteration. Magnetic alteration has the advantage that the peak areas obtained are directly proportional to ion abundance whereas defocussing occurs with voltage alternation. However, magnetic alternation is less sensitive due to the time required for magnet stabilization. Preliminary measurements suggest that 200 milliseconds using voltage alternation successively cycling between m/z 58, 64, and 60 was optimal. Despite two reports (4,5) of increased sensitivity and selectivity using chemical ionization, electron impact (where over 50% of the ionization is contained in the dimethymethylenimmonium ions) was preferred for routine measurements. The areas were automatically calculated by the computer together with the absolute amounts obtained by comparison to an external standard (derivatives made from the internal standards). The source temperature was maintained at 200°C and the ionizing energy at 70 electron volts. A typical run is shown in Figure 1. Since significant hydrolysis or exchange of the labeled acetylcholine D_9 can be seen in the unexpected propionate peak, this contribution was corrected in the final calculation of the free choline.

No significant difference (Figure 2) was observed in the concentration of either acetylcholine or choline between the left (operated) and the right (unoperated) striatum (using the T-test for paired variables). The absence of any effect of frontal cortex ablation on the concentration of acetylcholine and choline suggests that these substances are not localized in the cortico-striatal fibers. This result correlates with the lack of effect of cortex lesion on choline acetyltransferase (7), the decrease in glutamic acid concentration (8) and uptake (9, 10) after cortex lesion, as well as the glutamic acid diethylester antagonization of cortical excitation of the striatum (11).

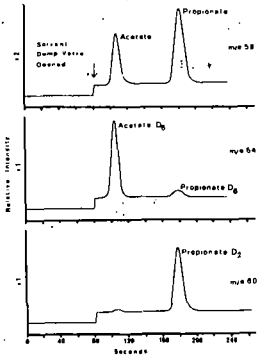

Figure 1: Multiple Ion Detection Chromatograms of ß-Dimethylaminoethyl Acetate and Propionate

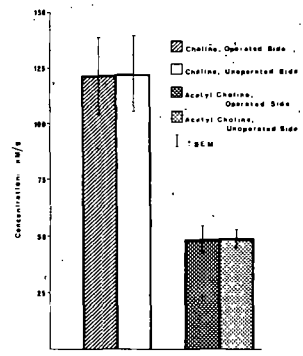

Figure 2: Concentration of Acetylcholine and Choline in Rat Striata after Frontal Cortex Lesion

1. K. Kataoka, Y. Nakamura, and R. Hassler, Brain Res. 62, 264 (1973)
2. K.E. Webster, J. Anat. (Lond.) 95, 532 (1961)
3. B. Karlen, I. Lundgren, I. Nordgren and B. Holmstedt, Choline and Acetylcholine, I. Hanin, ed., 163, Raven Press, New York (1974)
4. P. Haug, W. Wunn, M. Suzuki, C. Nitsch and B. Schmude, Proc. ASMS Meeting, New York, Abstract 300 (1980)
5. I. Hanin and R.F. Skinner, Anal. Biochem. 66, 568 (1975)
6. J.K. Khandelwal, P.I.A. Szilagyi and J.P. Green, Proc. ASMS Meeting, Seattle, WA. 216 (1979)
7. P. McGeer, E.G. McGeer, H.C. Fibinger and V. Wickson, Brain Res. 42, 308 (1971)
8. J. Kim, R. Hassler, P. Haug and K. Paik, Brain Res. 132, 370 (1977)
9. I. Divac, F. Fonnum, J. Storm-Mathisen, Nature, 266, 377 (1977)
10. P.L. McGeer, E.G. McGeer, U. Scherer and K. Singh, Brain Res. 128, 369
11. H.J. Spencer, Brain Res. 102, 91 (1976)

Acknowledgements: Thanks are given to J. Moritz, M. Kilb and W. Leber for technical assistance and to the Alexander von Humboldt Stiftung for a stipend (P. H.).

PLASMA DESORPTION MASS SPECTROMETRY OF UNDERIVATIZED METABOLITES OF CARBAMAZEPINE AND IMINOSTILBENE.

M. G. HORNING, K. LERTRATANANGKOON, AND J. NOWLIN. Institute for Lipid Research, Baylor College of Medicine, Houston, TX 77030.

Many metabolites of carbamazepine (CBZ) are thermally unstable and rearrange to iminostilbene derivatives during GC and GC-MS analysis. Iminostilbene (IMS) metabolites also rearrange under GC-MS conditions to acridine derivatives. For these reasons, plasma desorption mass spectrometry was used to confirm the structures of metabolites of CBZ and IMS isolated by HPLC. A Finnigan 1015 quadrupole mass spectrometer operated in the positive chemical ionization mode was used, with methane and isobutane as reagent gases, and with gold probe tips. In the spectra of CBZ metabolites, ions of high intensity were present at MH^+ in all instances. Loss of the carboxamide group was observed in some spectra. In contrast, molecular ions were either not present or were of low intensity in all EI spectra of CBZ metabolites obtained by GC-MS; the base peaks in EI spectra of CBZ derivatives indicated loss of the carboxamide group, and as a result appeared to be spectra of IMS rather than CBZ metabolites. For example, the base peak in the plasma desorption spectrum of underivatized carbamazepine-10,11-epoxide was the protonated molecular ion at m/z 253. When carbamazepine-10,11-epoxide (TMS derivative) was analyzed by a GC-MS system operated in the EI mode, loss of the carboxamide group was observed and a spectrum of iminostilbene-10,11-epoxide (M^+=209) was obtained. In addition, a second product was formed which indicated that carbamazepine-10,11-epoxide had also rearranged to acridine-9-carboxaldehyde (M^+=207). A similar rearrangement was observed for iminostilbene-10,11-epoxide. Under plasma desorption conditions, a protonated molecular ion (MH^+=210) was the base peak. When the analysis of iminostilbene-10,11-epoxide was carried out by GC-MS under EI conditions, a molecular ion was observed at m/z 207 indicating the epoxide had undergone rearrangement to acridine-9-carboxaldehyde. Thus plasma desorption mass spectrometry has proved useful in establishing the structures of CBZ and iminostilbene metabolites. Supported by NIH grant GM-24092.

IDENTIFICATION AND MASS SPECTRAL CHARACTERIZATION OF A DE-ETHYLATED PROCAINAMIDE METABOLITE

T.I. Ruo and J.P. Thenot
Clinical Pharmacology Center, Departments of Medicine and Anesthesia,
Northwestern University, Chicago, Illinois 60611

Procainamide (PA), used commonly to treat patients with cardiac arrhythmias, is metabolized by man mainly to N-acetylprocainamide (NAPA) [1] and other minor metabolites [2]. We recently measured plasma concentrations of one of these metabolites, p-acetamido-N-[2-(ethylamino)ethyl]benzamide (NAPADE) in patients receiving PA and NAPA, and found that both PA and NAPA are direct precursors of NAPADE. This led us to predict the formation of a hitherto unidentified PA metabolite, p-amino-N-[2-(ethylamino)ethyl]benzamide (PADE) [3].

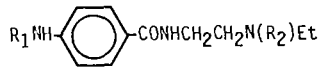

$R_1 = R_2 = H$	PADE
$R_1 = Ac$, $R_2 = H$	NAPADE
$R_1 = H$, $R_2 = Et$	PA
$R_1 = Ac$, $R_2 = Et$	NAPA

PADE was isolated from the urine of a patient treated with PA and identified by HPLC and mass spectrometry, using synthesized PADE as a reference. The quasi-molecular ion MH^+ was the base peak of the C.I. spectrum and confirmed the molecular weight of both isolated and synthesized PADE as shown in Figure 1. The E.I. fragmentation pattern of this new metabolite is similar to those of NAPADE, NAPA and PA. The base peak at 58 amu arises from cleavage of the carbon-carbon bond β to the secondary amine nitrogen atom and is analogous to the PA and NAPA base peaks at 86 amu. PADE collected under acidic conditions formed a possible cyclodehydrated imidazoline ring, as NAPADE·HCl did; that confounded mass spectral identification until basic conditions were used.

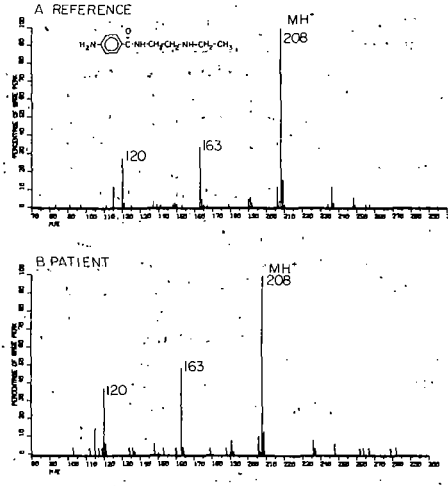

Figure 1: C.I. mass spectrum (methane) of PADE

[1] Dreyfuss J, Bigger JT Jr, Cohen AI, Schreiber EC, Clin Pharmacol Ther 13: 366-371, 1972.
[2] Taber DF, Jerningan JD, Watson JT, Carr K, Woosley RL, Drug Met Disp 7: 346, 1979.
[3] Ruo TI, Thenot J-P, Stec GP, Atkinson AJ Jr, Ther. Drug Monitoring (In Press).

MASS SPECTROMETRIC STUDIES ON IMPORTANT NEUROPEPTIDES

A. Dell, H.R. Morris & M. Judkins
Dept. of Biochemistry, Imperial College, London, U.K.

Mass spectrometry, with its mixture-handling capabilities and its potential for high sensitivity in the negative ion chemical ionisation (NCI) mode, offers unique advantages for the sequencing of biologically important peptides.[1] The power of low resolution electron impact mixture analysis procedures for the sequencing of small quantities of impure peptides has been clearly demonstrated by a number of important studies including the structure elucidation of the two enkephalins[2] and the sequencing of adipokinetic hormone, a neuropeptide isolated from locusts[3]. We now report the results of mass spectrometric studies of substances isolated from crude posterior pituitary extracts. These substances specifically stimulate rat adrenal zona glomerulosa cells or intact tissue to release steroids including aldosterone. No stimulation of fasciculata/reticularis cells was found indicating that the biological activity is not due to adrenocorticotrophic hormone. All structural work was carried out on materials isolated from commercial samples of pituitary extracts (Pitressin from Parke Davis). Similar biological activity was observed in extracts from bovine pituitaries.

Fractionation of Pitressin was achieved using reverse-phase high pressure liquid chromatography (HPLC) in a salt free system based upon acetic acid / propanol gradients. The conditions were identical to those which we have developed for other neuropeptide investigations[4]. Assay for glomerulosa cell stimulation yielded three peaks of biological activity, fractions 28, 29 and 31 (coded A, B and C respectively) of the preparative column gradient (see ref. 4 for details of conditions). Peaks of biological activity corresponded to peaks of U.V. absorbance measured at 280 nm. Peaks A and B have been further purified on HPLC and characterised using protein chemistry techniques and mass spectrometry. Treatment of both A and B with leucine aminopeptidase or carboxypeptidase Y had no effect on biological activity. However, elastase destroyed biological activity. These results indicated that the active materials were peptides blocked at both the N- and C-termini. Amino acid analyses of column fractions spanning the biological activity (fractions 26-31) were obtained. Although it was impossible to calculate accurate analyses of A and B due to contaminating peptides the data led us to the tentative conclusion that both A and B were about 15 residues long with 1 Lys and 1 Arg or multiples of this. Mass spectrometric studies were therefore carried out on the unpurified products of tryptic digestion. Good spectra were obtained for both A and B. Fig. 1 shows two representative spectra of A. The blocked N-terminus of the peptide is clearly established as acetyl-Ser-Tyr-Ser-Met via signals at m/e 158, 317, 432, 464, 577 and the blocked C-terminus is identified as Trp-Gly-Lys-Pro-Val-NH_2 via 'N-C cleavage' signals at m/e 184, 255, 456, 552, 553, 696, 750. Additional signals corresponding to an N-terminal Trp sequence were observed at other source temperatures suggesting that Trp is preceded by Lys or Arg (Arg if there is only one residue of each). Signals at m/e 98, 131, 134, 135 and 138 demonstrate the presence of Glx, Phe and His in the peptide and the lack of additional peptide signals in the spectra suggests that the peptide is approximately 15 rather than 30 residues in length. Overall the structural data may be summarised as: Acetyl-Ser-Tyr-Ser-Met-(Glx, Phe, His)-Arg-Trp-Gly-Lys-Pro-Val-NH_2. Comparison of these data with known structures of biologically active peptides suggests the probability that peak A in Pitressin is α-MSH which has the sequence Acetyl-Ser-Tyr-Ser-Met-Glu-His-Phe-Arg-Trp-Gly-Lys-Pro-Val NH_2. Accordingly synthetic α-MSH was chromatographed both separately and together with Pitressin and found to co-elute with peak A. Furthermore, it specifically stimulates zona glomerulosa cells in the same manner as Pitressin. This is a new biological activity for α-MSH whose function in animals other than amphibia remains to be established. Sample B exhibited very similar spectra to A and it is clearly a related peptide. The sequences AcSer-Tyr- and ...Trp-Gly-Lys-Pro-Val NH_2 could be assigned unambiguously. The remainder of the peptide is being characterised.

Many of our neuropeptide investigations are demanding the development of more sensitive methods of analysis. For example in our studies on the relationship of peptides to neurological disorders (e.g. schizophrenia) we need to be able to characterise and quantitate peptides at the 1-50 pmol level. For these reasons we have been examining the utility of NCI in the neuropeptide area. We are assessing a range of different derivatives and different ionisation methods to determine their potential for NCI studies of neuropeptides. Examples of derivatives applied to some of the important neuropeptides which we are studying include dansyl blocking of amino functions (including the imidazole ring of His), benzyl esters, fluoroacyl derivatives on amino functions and fluram derivatives.

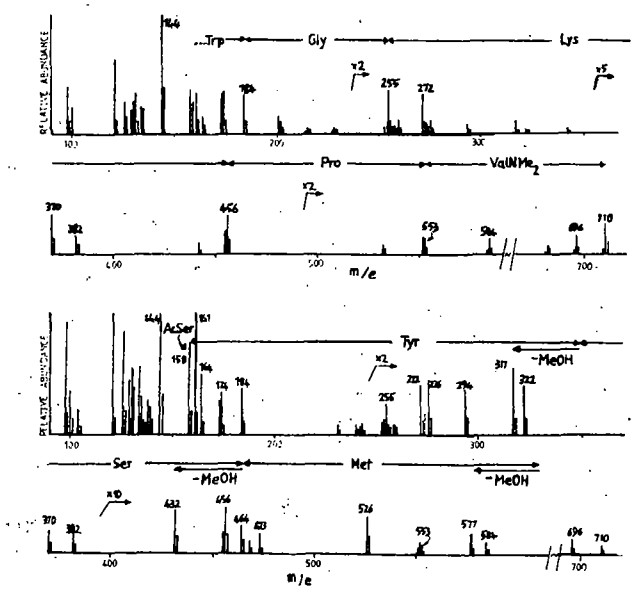

Fig. 1 : EIMS of deuteroacetyl permethyl derivative of tryptic digest of A at source temperatures of 300°C (upper) and 350°C (lower).

In addition we are examining methods of ionisation including chloride attachment and hydrogen abstraction with the aim of producing high intensity molecular or pseudo-molecular ions. Good data at the subnanomolar level has been obtained in Cl^- attachment ionisation of acetyl permethyl enkephalins. This is a significant result since the best derivative to date for sequencing peptides in the EI mode is the acetyl permethyl.

In previous work we have noted that the formation of N-fluoroacyl derivatives restricts the methylation of the acylated N. Coupled with other previously noted features of the permethylation reaction this behaviour can lead to spectra which would be extremely difficult to rationalise, if the phenomena were not recognised. For example pentafluoropropionyl permethyl enkephalin gives an intense signal at (M-5) rather than the molecular ion which would have been predicted from straightforward acylation and methylation.

Acknowledgements: We are grateful to Professor Don Hunt, University of Virginia, for the loan of a CI source.

References:

1. H.R. Morris, Phil. Trans. R. Soc. Lond. A 293, 39 (1979).
2. J. Hughes, T.W. Smith, H.W. Kosterlitz, L. Fothergill, B.A. Morgan, & H.R. Morris, Nature 258, 577 (1975).
3. J.V. Stone, W. Mordue, K.E. Batley & H.R. Morris, Nature 263, 207 (1976).
4. H.R. Morris, A.T. Etienne, A.Dell & R. Albuquerque, J.Neurochem., 34, 574 (1980).

GAS CHROMATOGRAPHIC MASS SPECTROMETRIC SEQUENCING OF PEPTIDES AND PROTEINS CONTAINING γ-CARBOXYGLUTAMIC ACID. S.A. Carr and K. Biemann, Dept. of Chem., M.I.T., Cambridge, MA 02139

γ-carboxyglutamic acid (Gla), has recently been identified as the vitamin K dependent post-translational modification in a number of plasma proteins including prothrombin.[1] Gla is generated by enzymatic carboxylation of specific glutamic acid residues in the polypeptide. This modification confers to the proteins their calcium and phospholipid membrane binding capacity, which is essential for the normal functioning of the blood coagulation cascade.

Gla containing proteins have also been found in high concentrations in bone (10-20% of the non-collagen protein), which has led to the implication of Gla in both normal and pathological tissue mineralization processes. Most of the Gla found in bone residues in a small acidic protein named osteocalcin which bears no apparent sequence homology to Gla containing plasma proteins.[2]

We have developed a generally applicable strategy for the primary sequence determination of peptides and proteins containing γ-carboxyglutamic acid.[3,4] Previously employed techniques (including the Edman degradation) were of limited value because Gla readily decarboxylates upon exposure to heat and/or acid rendering it indistinguishable from glutamic acid. In contrast, our method relies on the incorporation of a stable isotope label as the result of decarboxylation. The intact peptide or protein is either dissolved in, or allowed to come into vapor phase contact with, 0.05M DCl and then heated *in vacuo* at 110°C for several hours. Under these conditions Gla quantitatively decarboxylates and incorporates two atoms of deuterium per molecule, resulting in the formation of γ-dideutero-glutamyl residues (Scheme 1). Incorporation of deuterium occurs specifically and irreversibly at Gla residues; no other amino acid side chain is affected by the treatment with DCl.

The deuterium labelled decarboxylated protein is then chemically derivatized and analyzed by gas chromatographic mass spectrometry (GCMS).[3] The basic strategy is shown in Scheme 2.

The mixture is separated on a gas chromatographic column into individual or simple 2-3 component peak envelopes and mass spectra of the column effluent are continuously recorded. The mass spectra of these polyamino alcohols are quite simple; the peaks of highest intensity result from cleavage of the carbon-carbon bond of the ethylenediamine units. Fragmentation resulting in charge retention on the N-terminal portion of the molecule produces the "A" ion series; likewise, charge retention on the C-terminal fragment produces the "Z" ion series (Scheme 2).

Peptide fragments in which Gla was present show sequence ions in their mass spectra corresponding to those of glutamic acid, but shifted upwards by two mass units. The mass spectrum of the exchanged and decarboxylated polyamino alcohol derivative of Leu-Gla-Ala-Glu is shown in Figure 1. The (M-15), A4, A3, and A2 ions are shifted 2 a.m.u. upwards from where they would be found in the corresponding Glu containing peptide. Likewise, the Z3 sequence specific ion also exhibits this mass increment. In contrast the A1, Z1, and Z2 ions are, of course, not affected by the amino acid in position 2. Thus the presence of Gla and its position within the peptide fragment are clearly demonstrated.

This approach has been used to determine the complete amino acid sequence of the Gla containing bone protein osteocalcin (Figure 2). Following deuterium exchange and decarboxylation, chicken osteocalcin was subjected (in separate experiments) to partial acid hydrolysis and proteolytic cleavage by a series of enzymes. These complex mixtures of peptides were derivatized (according to Schemes 1 and 2) without isolation or purification of individual peptides. The mass spectrum of Leu-Gla-Ala-Glu (Fig. 1) was obtained by GCMS of a derivatized, partial acid hydrolyzate of osteocalcin. A total of 49 di- to hexapeptide derivatives were identified in this single experiment. Six different digests on a total of 15 mg of protein (~2.5 μmoles) were used to deduce the entire sequence.

REFERENCES

1. Magnusson, S., Sottrup-Jensen, L., Petersen, T.E., Morris, H.R., and Dell, A., FEBS Lett. 44, 189 (1976).
2. Hauschka, P.V. and Gallop, P.M. in Calcium Binding Proteins and Calcium Function, ed. by R.H. Wasserman, Elsevier North-Holland, Inc., Amsterdam (1977).
3. Biemann, K. in Biochemical Applications of Mass Spectrometry First Supplementary Volume, ed. by G.R. Waller and O.C. Dermer, Wiley Interscience, New York (1980).
4. Carr, S.A. and Biemann, K., Biomedical Mass Spectrometry, in press.

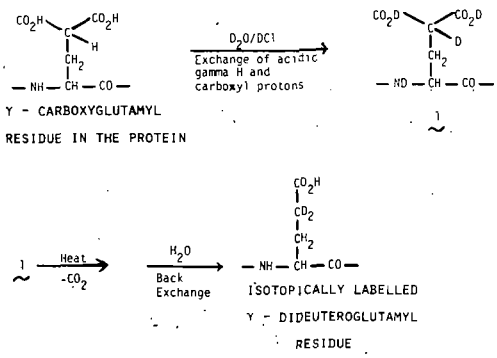

SCHEME 1

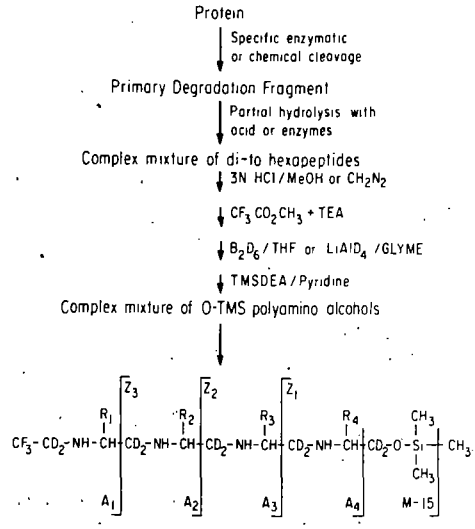

SCHEME 2

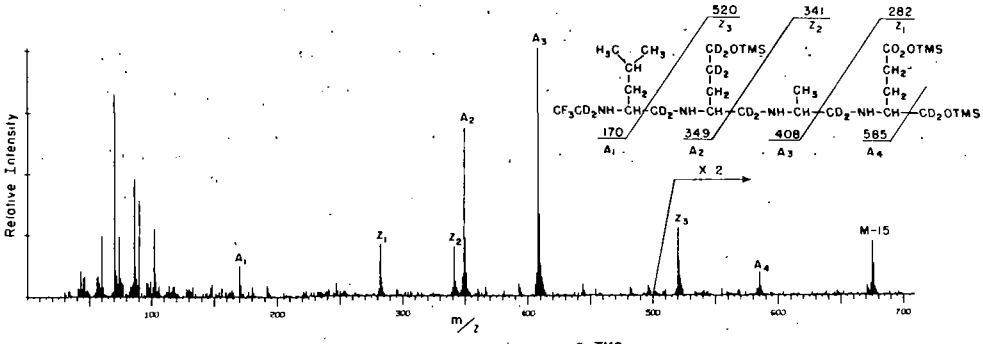

FIG. 1. MASS SPECTRUM CORRESPONDING TO THE O-TMS, POLYAMINO ALCOHOL DERIVATIVE OF LEU-GLA-ALA-GLU.

10 20

HIS TYR ALA GLN ASP SER GLY VAL ALA GLY ALA PRO PRO ASN PRO ILE GLA ALA GLX ARG

30 40

GLA VAL CYS GLA LEU SER PRO ASP CYS ASN GLX LEU ALA ASP GLU LEU GLY PHE GLN GLU

50

ALA TYR GLX ARG ARG PHE TYR GLY PRO VAL

Fig. 2. Amino acid sequence of chicken osteocalcin as determined by gas chromatographic mass spectrometry.

PYROLYSIS OF POLYESTER

F. Messier, McMaster University, Departement of Chemistry, 1280 Main S. W. Hamilton, Ontario, Canada L8S 4M1

D. C. DeJongh, Finnigan Institute, Atkinson Square, Bldg. 5, 11750 Chesterdale Road, Cincinnati, Ohio, USA 45246

We have develop a method for the pyrolysis of polyesters where it is possible to determine the yield of the crude mixture and the yield of each products in this crude mixture. The different products were identified by their mass and NMR spectra. The poly ε-caprolactone contained two hydrogens in the position gamma to the carboxyl group and in this case it was susceptible to the typical mechanism of the pyrolysys of an ester. It gave a mixture of carboxylic acid with an unsaturation at the end of the chain and a small amount of the ε-caprolactone (eq. 1).

The pyrolysis were performed in an oven and the products were collected in a series of traps. The mixture of the products was analysed by GC and by MS. The carboxylic acids were derivatized to facilitate the GC analysis. The underivatized acids were also separated by preparative TLC and analysed by probe MS.

With the GC it was possible to see the methyl ester of the 5-hexenoic acid through the methyl ester of the tetramer of this acid, and the ε-caprolactone. These 5 compounds formed about 98% of the crude mixture coming from the pyrolysis. When this crude mixture of the pyrolysis was analysed by the LC/MS it was possible to see the pentamer and the hexamer of the 5-hexenoic acid. This analysis was performed with a Finnigan LC/MS system in the chemical ionization mode with methane as the reagent gas. The acid mixture was spotted directly on the belt of the LC interface. We obtained the (MH)+ and the (M+29)+ ion for each acid. But when the methyl ester of the mixture of acids were separated and analysed by the LC/MS we lost the methyl ester of the hexamer du to its very low abundance in the mixture.

The yield of the crude mixture depends on the conditions that we used for the pyrolysis i.e. at the entrance or at the exit of the oven. But in all cases a mixture of acids formed the predominant products suggesting that the pyrolysis of the poly ε-caprolactone follow the typical mechanism of the pyrolysis of an ester. The utilization of the LC/MS interface can be very usefull for determining the presence of the unvolatile acids, compounds that we cannot see with the GC.

$$-\!\left[O\overset{O}{C}CH_2CH_2CH_2CH_2CH_2\right]\!- \xrightarrow{\Delta} CH_2{=}CHCH_2CH_2CH_2\overset{O}{C}OH$$

$$+\ \varepsilon\text{-caprolactone}$$

eq. 1

$$+\ CH_2{=}CH(CH_2)_3\!-\!\left[\overset{O}{C}O(CH_2)_5\right]\!-_{n}\overset{O}{C}OH$$

$n = 1, 2, 3, 4, 5$

WAMP20 PREPARATION OF DEUTERATED 4-HYDROXY-3-METHOXY-MANDELIC ACID. Kym F. Faull and Jack D. Barchas, Nancy Pritzker Laboratory of Behavioral Neurochemistry, Department of Psychiatry and Behavioral Sciences, Stanford University School of Medicine, Stanford, California 94305

Selected ion monitoring assays are now widely used for measuring the concentrations of monoamine neurotransmitters and their metabolites in urine, blood, cerebrospinal fluid and brain extracts. Although these assays have a high degree of sensitivity and particularly specificity, the successful application of them to routine work requires the availability of suitable internal standards. For precise and specific quantitative SIM assays isotopically labeled analogues are generally preferred as internal standards. Using the platimun catalysed reaction between aromatic ring protons and deuterium oxide, we have been able to prepare in good yield crystalline [$^2H_3$]-4-hydroxy-3-methoxy-mandelic acid which is suitable for use as an internal standard in SIM assays. Initial results suggest this approach is useful for preparing other deuterated aromatic compounds as exemplified by the successful preparation of deuterated alpha-(methylaminomethyl)vanillyl alcohol (metanephrine). This approach to the preparation of deuterated compounds is worthy of merit for the preparation of deuterated water soluble aromatic compounds on a small scale because it avoids complex synthetic chemistry, is simple, and affords the deuterated products in relatively high yield.

GC-MS QUANTITATION OF SEVERAL NITROGEN HETEROCYCLES IN SOLVENT REFINED COAL

K. L. Richie, L. R. Hilpert, J. M. Brown, F. R. Guenther, and H. S. Hertz

Organic Analytical Research Division
Center for Analytical Chemistry
National Bureau of Standards
Washington, DC 20234

Introduction

Recently, there has been a growing interest in the development of alternate fuel sources such as shale oil and solvent refined coal (SRC). Much of the research has been directed toward studying the toxic and/or carcinogenic components found in these fuel sources, with a large portion of this effort concentrating on polynuclear aromatic hydrocarbons. The nitrogen heterocycles, however, possibly represent a more serious threat to health and the environment. Thus as the interest in coal-derived materials increases, it becomes necessary to develop methods for the quantitation of individual toxic organic compounds in complex matrices such as solvent refined coal. Over the past year, our laboratory has developed methods for analyzing SRC by means of high performance liquid chromatography and gas chromatography-mass spectrometry with selected ion monitoring.

Experimental

The SRC samples used in these studies were a middle to heavy distillate from a fuel oil blend obtained from the Pittsburgh and Midway Coal Mining Co., Solvent Refined Coal Pilot Plant, Dupont, Washington. The SRC was ampouled in 5 mL amber ampoules for storage and analysis.

Quantitative data for acridine and carbazole in SRC were obtained using a standard addition technique. Approximately 1 g of the solvent refined coal oil was diluted 1:10 using methylene chloride as the solvent. The diluted samples were spiked with suitable amounts of acridine and carbazole and then fractionated by means of high performance liquid chromatography on a semi-preparative scale aminosilane column, with 40 percent methylene chloride in hexane as the mobile phase. Standards of acridine and carbazole were run prior to chromatography of the oil to determine elution volumes for fraction collection. The fractionated samples were concentrated to approximately 250 µL under a stream of dry nitrogen.

Gas chromatographic separations were carried out on a 20 m Pluronic (PL 64) wall-coated open tubular (WCOT) column. The gas chromatograph was interfaced to a quadrupole mass spectrometer through an open split fitting (1) constructed of deactivated nickel tubing (2).

Results and Discussion

The acridine and carbazole were detected with selected ion monitoring, using a standard addition technique for quantitation. The molecular ions for the acridine and carbazole were monitored in 0.1 amu increments to insure that the voltage was sampled at the top of the mass peak; a dwell time of 100 ms was used to give at least 20 data points across the chromatographic peak. An additional compound known to be natively present in the oil was also monitored as a volume correction standard (IS) to compensate for variable injection volumes into the GC.

Area ratios of the analyte peak to the IS peak were plotted against the spike concentration of the analyte added to the SRC. The concentrations of acridine and carbazole were determined from the intercept of the curve with the abcissa using a linear least squares analysis.

The results of these determinations were as follows: Acridine: 143.2 ± 21 ppm, Carbazole: 1956.5 ± 302 ppm. These results are compared in Table I with the concentrations obtained by participating laboratories in an inter-laboratory comparison of the SRC liquid analyses.

References: 1) G. Wells, K.J. Voorhees and J.H. Futrell, 27th Annual Conference on Mass Spectrometry and Allied Topics, Paper WAMP 7, 1979; 2) F. Farre-Ruis and G. Guiochon, Anal. Chem., 40, 998 (1968); 3) S.F. Urzendowski, Air Force Weapons Laboratory, Kirtland Air Force Base, New Mexico, 1969, AFWLTR-69-46; 4) J.H. Flynn and L.A. Wall, J. Res. Nat. Bur. Std., 70A, 487 (1966); 5) Samuel L. Madorsky, Thermal Degradation of Organic Polymers, John Wiley and Sons, New York (1974).

TABLE I

Kinetic Parameters for the Degradation of Polystyrene in a Helium Atmosphere

A (sec^{-1})	E (Kcal/mole)	Source
9.30×10^{19}	57	This Work
2.51×10^{19}	55.0	Farre-Ruis[2]
2.3×10^{19}	68.3	Urzendowski[3]
7.73×10^{16}	55	Wall and Flynn[4]
2.29×10^{19}	55	Madorsky[5]

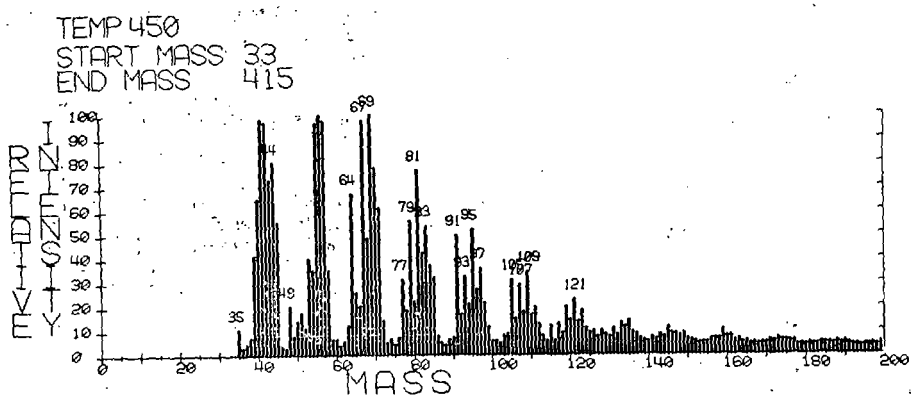

RAPID CHARACTERIZATION OF COAL SAMPLES BY PYROLYSIS MASS SPECTROMETRY.

Henk. L. C. Meuzelaar, Ralph E. Wood, Jean H. Futrell and L. H. Wojcik, Energy Research Center/Analytical Laboratory, University of Utah, Salt Lake City, UT. 84108.

Curie-point pyrolysis mass spectrometry, in combination with computerized pattern analysis (Cu Py-MS/COM), provides a powerful new tool for rapid characterization of coal samples. The technique requires minimal sample preparation, uses only microgram amounts of sample, is very fast and has already reached a high degree of automation as well as a promising level of standardization. In addition, the mass spectral patterns obtained are ideally suited to computerized data processing and, in view of the virtual absence of secondary reactions in Curie-point pyrolysis, provide readily interpretable information about the chemical nature of important building blocks of coal structure. Finally, because of the direct relationship between analytical and industrial pyrolysis processes, the patterns can provide valuable data on coal reactivity and conversion behavior.

Three Rocky Mountain coals previously analyzed by NMR (Zilm, *et al.*, *Fuel 58*,1978), are shown in Figure 1. The relative abundance of alifatic and aromatic constituents in the spectra closely agrees with the NMR findings. In addition, the pyrolysis mass spectra provide information on sulfur constituents, on alkyl substitutents in aromatic homologous series, and on relative abundance of benzenic and naphthalenic building blocks. Admittedly, the information obtained does not allow a detailed and precise interpretation of the structure of the coal samples analyzed. However, it is generally agreed that: *"It probably will not be possible in the foreseeable future actually to determine the "structure" of coal absolutely the way we can with, say, oragnic compounds. Coal is heterogeneous by nature and it varies in structure no less from millimeter to millimeter in the same seam than between coals from different rank formed from different species of plant matter in swamps hundreds or thousands of miles apart.* (NRC, Committee of Chem. Sci., Section I.1 Basic Res. in Coal Chem., 1979).

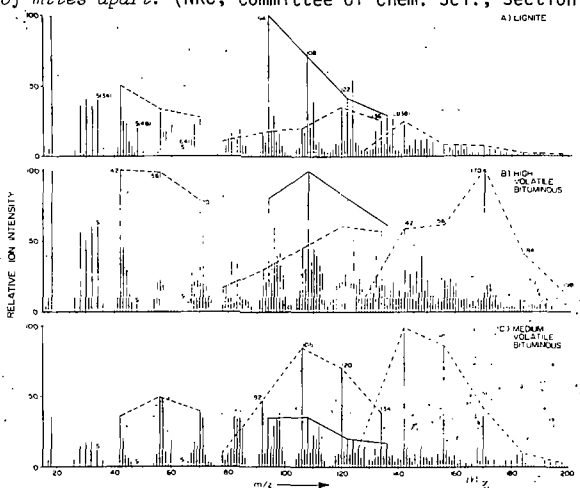

Figure 1. Pyrolysis mass spectra of three low rank coals from Rocky Mtn. coal fields, namely (A) Coalstrip, Montana, (B) Clear Creek Mine, Utah and (C) Coal Basin, Utah. The same coals were analyzed by ^{13}C NMR. Note the strong predominance of (alkyl) phenols at m/z 94, 108, 122 and 136 in lignite, the predominance of alkenes at m/z 42, 56 and 70, as well as naphthalenes at m/z 142, 156, 170, 184 and 198 in the high volatile bituminous coal sample and the strong relative increase in (alkyl) benzenes at m/z 92, 106, 120 and 134 in the medium volatile bituminous coal.

The Cu Py-MS/COM technique offers an attractive solution to the problem of coal heterogeneity. The ability to deal with large numbers of samples and to process the data by computerized techniques enables rapid classification of coal samples, thereby reducing the macroscopic heterogeneity to more manageable proportions. The high sensitivity of the technique allows analysis of minute quantities of coal macerals handpicked under the microscope (v. Graas *et al.*, Proc. IXth Int. Meeting on Org. Geo-chem., Newcastle upon Tyne, 1979), thereby reducing heterogeneity problems at the microscopic level. Finally, the fact that the technique directly interrogates key structural features affecting coal reactivity, enables correlation of pyrolysis mass spectral patterns with coal conversion behavior. This is demonstrated by the results of a preliminary study of 24 high volatile bituminous Utah coals (fully characterized by conventional, e.g petrographic techniques) all of which had previously been tested for their efficiency as feedstock in a laboratory scale Zn Cl_2 catalyzed coal liquefaction process (Garr, *et al.*, *Fuel Proc. Technol. 2*, 1979).

Finely ground aliquots of these coals were analyzed in quadruplicate with the automated Cu Py-MS/COM instrument at the FOM Institute for Atomic and Molecular Physics (Amsterdam, The Netherlands). Analytical conditions were as follows: sample size 20 µg (MeOH suspension),

AN INVESTIGATION OF THE PYROLYSIS OF A COMPOSITE GREEN RIVER OIL SHALE BY TGA-MS AND FAST-SCANNING PY-MS

L.H. Wojcik, D.L. Pope, L.R. Frank, C. Greenwalt, H.L.C. Meuzelaar, and J.H. Futrell
Departments of Chemistry and Materials Science and Engineering
University of Utah
Salt Lake City, Utah 84112

Several mass spectrometric techniques have been applied to the investigation of the pyrolysis kinetics of a composite sample (ASTM-T8) of oil shale taken from the Green River formation of Colorado and Utah. These include a thermal analysis apparatus interfaced to a Hewlett-Packard mass spectrometer via a jet separator, a Curie-point pyrolysis mass spectrometer (Extranuclear) and a modified, fast-scanning filament pyrolyzer mass spectrometer (Finnigan) described at the 1979 ASMS conference.[1]

Well-characterized specimens of polystyrene and laboratory-synthesized polyurethanes were investigated and shown to decompose with rates and mechanisms comparing favorably with literature reports. In combination with apparatus parameters, these data may be used to calculate ion profiles. The heating profile of the Chemical Data Systems Pyroprobe® may be approximated satisfactorily by a combination of straight line segments. The decomposition rates predicted by a non-isothermal kinetics treatment of these straight line segments, using the Arrhenius parameters deduced from TGA analysis, accurately predicts the mass spectral peak evolution profiles generated for polystyrene by the pyrolysis-mass spectrometer.

The equations used and the parameters used to fit the mass spectral peak evolution profiles are as follows:

Linear Ramp

$$\frac{dC}{dt} = \left[\frac{dC}{dT}\right]\left[\frac{dT}{dt}\right]$$

$$\frac{dC}{dT} = k[M]^n = Ae^{-E_a/RT}\,[M]^n$$

$$\frac{dT}{dt} = H_R$$

$$[A] = [A_o]\exp\left(-\frac{k_\infty}{\varepsilon}\,t^2\,e^{-\varepsilon/t}\right) \text{ where } \varepsilon = E/H_R{}^R$$

Isothermal Plateau

$$\frac{dC}{dt} = [M]^n\,Ae^{-E_a/RT}$$

Rate constant parameters deduced for polystyrene are, $n = 1$, $A = 9.30 \times 10^{19}$ (sec^{-1}), and E_a = 57 Kcal/mole. These may be compared with literature values in Table I.

The same techniques were then applied to the decomposition of ASTM-T8 oil shale. Three distinctive decomposition regimes were identified and overall Arrhenius rate constant parameters were measured. The low temperature mechanism is the distillation of benzene-soluble bitumen trapped in the shale matrix. The high temperature (650°C) decomposition is the breakdown of the inorganic matrix to generate CO_2 and SO_2. The main kerogen pyrolysis process occurs from 400-458°C and is adequately described by overall activation energy of 40 Kcal/mole and a frequency of 6.2×10^{10} sec^{-1}.

The extreme complexity of oil shale pyrolysis is exemplified by the mass spectrum of Figure 1 which is typical of the main kerogen decomposition region. Accordingly no attempt is being made to study the kinetics of generation of individual products. Rather rate constants will be sought in future work of alkanes, alkenes, and alkyl benzenes as classes of compounds generated by pyrolysis of oil shale kerogens.

Table I. Interlaboratory Comparison of SRC II Coal Liquid Analyses (parts per thousand)

	NBS	2	3	4	5	6	7
Acridine	0.14 ± 0.02	0.13 ± 0.02	0.43	0.118	0.145 ± 0.02	0.7	---
Carbazole	1.96 ± 0.30	---	2.23	2.44	1.87 ± 0.22	0.9	5.0
Benzo(a)pyrene	0.065 ± 0.002	0.18 ± 0.02	0.126	0.08 (1.145)	0.235 ± 0.02	0.031	0.07

References

(1) D. Henneberg, V. Henrichs, G. Schomburg, Chromatographia, 8, 449 (1975).

(2) D. C. Fenimore, J. H. Whitford, C. M. Davis, and A. Zlatkis, J. Chromatog., 140, 9 (1977).

Curie-point temp. 610°C, pyrolysis time 0.8 s, inlet temp. 175°C, electron impact energy 14eV, total scanning time 30 s (10 spectra/s).

Initial computer processing of the raw spectra revealed the presence of a series of highly characteristic mass peaks apparently belonging to a limited number of homologous compound series, as shown in Table 1. Multivariate statistical analysis of the spectra enabled visualization of the major differentiating tendencies in the data, e.g. by nonlinear mapping (see Figure 2) of a distance matrix obtained by applying a Chi square similarity coefficient to forty mass peaks with high outer/inner deviation ratio's (see Table 1). The major differentiation tendencies between the coal spectra proved to be due to sulfur containing ion signals at m/z 34, 48 and 76, to two series of assumedly alifatic fragment ion signals at m/z 83, 97, 111 and m/z 85, 99, 112 respectively and to ion signals at m/z 18 and 30 apparently representing some oxygen functional group. Interestingly, all three coals with poor conversion yields (less than 40%) showed unusually high sulfur containing ion signals at m/z 34, 48 and/or 76. This finding is all the more remarkable since no correlation was found between sulfur content as determined by elemental analysis and conversion behavior (Garr, *et al*, *Fuel Proc. Technol.* 2, 1979). Furthermore, all five high yield (more than 75%) coals are found within the central cluster in Figure 2, indicating the absence of specific chemical characteristics which distinguishes these coals from each other. Further studies involving chromatographic and spectrometric analyses of the coal liquids are underway to determine the presence of possible correlations between the pyrolysis patterns of parent coals and the detailed chemical composition of the corresponding coal liquids.

TABLE 1. FIFTEEN MASSES WITH HIGHEST CHARACTERISTICITY VALUES.

No.	m/z	Tentative Identity	Compound Class	Average Intensity*	Mean Inner Deviation*	Mean Outer Deviation	Characteristicity Value**
1	34	H_2S	(sulfide)	1.86	.18	1.42	7.85
2	76	CS_2	(disulfide)	.04	.01	.04	5.46
3	97	C_8H_{15}	(alkene)	1.90	.16	.81	5.21
4	48	CH_3SH	(thiol)	.23	.03	.17	5.10
5	30	CH_2O	(aldehyde)	1.91	.32	1.46	4.63
6	83	C_7H_{13}	(alkene)	2.48	.23	1.03	4.46
7	111	C_9H_{17}	(alkene)	1.10	.10	.45	4.34
8	61	?	?	.23	.06	.25	4.27
9	99	C_8H_{17}	(alkane)	.86	.06	.24	4.24
10	84	?	?	2.40	.13	.54	4.12
11	82	C_5H_6O	(furan)	2.79	.15	.62	4.11
12	113	C_9H_{19}	(alkane)	.73	.07	.29	3.97
13	68	C_4H_4O	(furan)	1.91	.10	.39	3.93
14	73	?	?	1.08	.20	.77	3.91
15	85	C_7H_{15}	(alkane)	1.97	.14	.52	3.62

* % of total ion intensity; ** mean outer deviation/mean inner deviation ratio.

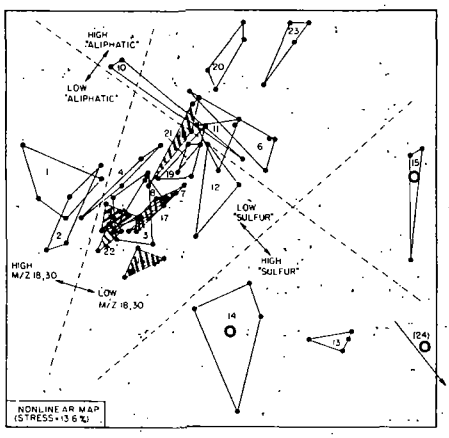

Figure 2. Nonsupervised "natural" clustering tendencies of pyrolysis mass spectra of HVB Utah coals visualized by nonlinear mapping (Kruskal method) of the distance matrix. Each dot represents a spectrum. Dots representing computer assisted interpretation of underlying chemical tendencies. Stress value of 13.6 % indicates reasonably good fit between original forty-dimensional matrix and present two-dimensional configuration in the map.
O= low yield (< 40%) coals;
///= high yield (> 75%) coals; all others intermediate yield (40-75%).
Sample numbering identical to numbering used by Garr *et al*, *Fuel Proc. Technol.* 2, 1979.

GAS PHASE ION STRUCTURES BY IN-SOURCE TRAPPING COLLISIONAL ACTIVATION MASS SPECTROMETRY

M. A. Rudat and C. N. McEwen
Central Research and Development Department
E. I. du Pont de Nemours and Co., Inc.
Wilmington, DE 19898

The extremely fast reaction between carbon-centered radicals and tetracyanoquinodimethane (TCNQ) in a chemical ionization source (1) can be utilized for the study of ion structures by taking advantage of the very efficient radical-producing mechanism of ion-electron recombination. Neutralized even-electron ions form radicals in which ion rearrangements are frozen out, permitting an instantaneous cross-section of ion structures present within the C.I. source to be captured by the TCNQ. Since collisional activation analysis of the radical anion in which the radical has replaced a CN group on TCNQ (I) produces a spectrum in which α-cleavage of the radical dominates the fragmentation pattern, a direct, interpretable link between the original, frozen ion structures and the CA spectrum is produced.

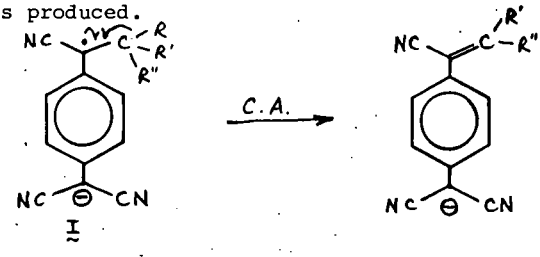

Isomerization of open-chain and cyclic alkyl ions produced in the C.I. source from alcohols have been studied using this technique, with the interpretation of the CA spectra being based on our experience with known radical structures.

Generally, our results parallel those from previous gas phase and superacid solution work when good previous studies are available, while adding additional details and, in some cases, filling in gaps or resolving controversies. For example, a study of the distribution of butyl ion structures produced from primary, secondary, and tertiary butyl alcohols confirmed that the primary ion mostly rearranged to a mixture of secondary and tertiary structures, the secondary ion mostly remains secondary, and

and the tertiary ion remains tertiary. However, we found that the amount of 2° and 3° ions from the 1° n-butyl ion rearrangement was dependent upon the pressure of the 1-butanol, and similarly, that the amount of 3° butyl produced from the 2° ions and the amount of 2° butyl produced from the isobutyl ion were dependent upon the pressure of butanol in the source. This is consistent with previous ICR results (2) and explains some of the experimental variation between researchers.

An example of a cyclic ion with which little previous gas-phase work has been done, but solution results are available, is the cyclopentyl ion. Superacid nmr results suggest that a cyclopentyl ion remains cyclic, and all of the hydrogens are equivalent (rapid equilibration of all ring positions). Our work suggests that many of the ions remain cyclic, but a significant portion ring-collapse to form the tertiary ethylcyclopropyl ion and some secondary ethylcyclopropyl (1-methylcyclopropyl carbinyl) ion.

Additional details and many more ion structure results will be published.

(1) C. N. McEwen and M. A. Rudat, JACS, 101, 6470 (1979)

(2) D. M. Shold and P. Auslous, JACS, 100, 7915 (1978).

RAMOA2 ISOMERIZATION REACTIONS IN METASTABLE $C_4H_6O^{7+}\cdot$ IONS, P.C. BURGERS, J.L. HOLMES (University of Ottawa, Ottawa, K1N6N5, Canada) and J.K. TERLOUW (Utrecht University, Utrecht, The Netherlands).

The ionic heat of formation of the molecular and principal product ions (mono-energetic electrons), the metastable ion characteristics and the CA spectra of fifteen isomeric $C_4H_6O^{7+}\cdot$ ions have been determined to study the occurrence of isomerization reactions (-CHO↔-CHOH, $CH_3C{\equiv}C$-↔$CH_2{=}C{=}CH$-↔$HC{\equiv}C$-CH_2-) in these unsaturated odd-electron ions. It is found that no (inter)conversion occurs between the enolic ions $CH_2{=}CH{-}CH{=}CH(OH)^{7+}\cdot$, $CH_2{=}CH{-}CH(OH){=}CH_2^{7+}\cdot$, $CH_2{=}CH{-}CH(OH){=}CH_2^{7+}\cdot$ and $CH_3(H)C{=}C{=}CHOH^{7+}\cdot$ with the corresponding keto forms $CH_2{=}CH{-}CH_2{-}CHO^{7+}\cdot$, $CH_3{-}CO{-}CH{=}CH_2^{7+}\cdot$ and $CH_3CH{=}CH{-}CHO^{7+}\cdot$ up to the threshold for the (common) losses of H·, $CH_3\cdot$ and CO, whereas $CH_2{=}C{=}CH{-}CH_2OH^{7+}\cdot$ undergoes a partial (prior to the loss of $CH_3\cdot$) isomerization via a 1,3-OH shift into $CH_2{=}CH{-}CH(OH){=}CH_2^{7+}\cdot$ to yield $C_3H_3O^+$ product ions of the type $CH_2{=}CH{-}C{=}O$, $CH_2{=}C{=}\overset{+}{C}{-}OH$ and $H{-}C{\equiv}C{-}\overset{+}{C}HOH$.
Fast isomerization reactions occur in the molecular ions of $HC{\equiv}C{-}CH_2{-}CH_2{-}OH$ and $HC{\equiv}C{-}CH_2{-}O{-}CH_3$ to yield the more stable allenylic molecular ions but this process is absent in $CH_3{-}C{\equiv}C{-}CH_2OH^{7+}\cdot$ and $CH_3{-}C{\equiv}C{-}O{-}CH_3^{7+}\cdot$ where fragmentation occurs from the intact molecular ions. The molecular ions of the latter compound lose $\cdot CH_3$ with a large kinetic energy release (~0,5 eV) to yield $CH_2{=}CH{-}\overset{+}{C}{=}O$ product ions. Large kinetic energy releases associated with the broad component of composite metastable peaks are also found for the loss of CO from several isomers. The energy partitioning quotient in some of these systems where the structure of the m/z 42 product ion(s) ($CH_3CH{=}CH_2^{7+}\cdot$, along with $C{-}C_3H_6^{7+}\cdot$ and/or ketene$^{7+}\cdot$) could unambiguously be established, will be discussed.

IDENTIFICATION OF THE STRUCTURAL ELEMENTS OF ORGANIC IONS BY TRIPLE QUADRUPOLE MASS SPECTROMETRY

RAM OA3

R. K. Latven, B. Newcome and C. G. Enke
Department of Chemistry
Michigan State University, East Lansing, Mich. 48824

The triple quadrupole mass analyzer at Michigan State University consists of two quadrupole mass filters bounded by a quadrupole collision chamber. Its operation for these experiments is shown in the top figure. In setting up the instrument for routine ion identification, it is important that all conditions which affect the relative abundances of the daughter ions be optimized and standardized.

Shown in the lower left figure is a plot of the effect collision cell pressure has on the collisionally activated decomposition (CAD) of propane molecular ion, $C_3H_8^+$. Two kinds of responses are seen: pressure dependent fragments which are shown by a majority of peaks, and products which appear metastable, i.e., only are a function of parent intensity, and are not attenuated at low pressures. Among the compounds studied so far, all losses of H and H_2 have been metastable, and no other. Acceptable response is seen in the 10^{-5} and low 10^{-4} torr range. Fragmentation efficiency at maximum daughter ion current here is 65%. Total daughter ion current with channeltron multiplier is in the tenths of microamps.

Axial energy is probably the single most important experimental parameter, and its behavior needs to be observed carefully. If parent ion intensity is plotted with increasing axial energy, we find an abrupt appearance of the ion as its axial energy overcomes the retarding bias impressed on the collision cell. The distribution of translational energies has a width at half height of about 2 volts. Decreasing the collision chamber voltage increases the axial energy of the positive ions, and, at about 3 volts negative of the voltage for 50% transmission, 99+% of the selected ion is transmitted.

The effect of the axial energy on the CAD process is marked. The set of three energy profiles demonstrates the way we record our collisional spectra. They are five-order logarithmic plots of the ion current versus axial energy of the parent ion, for each observable daughter. With increasing axial energy, the parent first appears, and its intensity increases over the whole range of detectability, until essentially all the parent ions are transmitted. Parent ion current then becomes independent of axial energy.

Shown in the center figure is a comparison of the C_2H_5 29^+ ion from three precursers: ethane, propane, and ethanol. $C_2H_5^+$ shows a M-2 metastable at 27, and fragments to form CH_2^+ and CH_3^+ at 14^+ and 15^+. The axial energy profile is then indicative of the composition of the parent ion, by both the ordering of the products and the energy of their appearance.

As an example of the usefulness of this technique, the fragmentation map of ethanol CAD can be determined unambiguously. It is shown in the lower right. Only those ions which are observed in the collisional spectrum of the parent, along with their respective CAD products are assumed to be part of the CAD fragmentation scheme. These are depicted in the lower half of the figure, below the $CH_3CH_2OH^+$ parent. EI ions not produced by CAD can still be determined and they are shown in the upper half of the figure. Fragmentation studies of the ions of ethanol show the parent produces 45^+, 31^+, 29^+ and 27^+. But CAD on 45^+ shows 29^+ and 27^+ in the same relative intensities as seen in the original 46^+. $C_2H_5^+$ loses H_2 to give 27^+, and each succeeding fragmentation loses a hydrogen until C_2^+ is reached. Parent 46^+ also loses methane by an α cleavage to produce characteristic 31^+, CH_3O^+. This ion can lose OH to give methylene at 14^+ and exhibits a M-2 metastable at 29^+. Similarly, 45^+ α-cleaves to give formyl ion, 30^+, which loses oxygen to again leave a CH_2^+ ion behind. Loss of CH_3 from 45^+ confirms that the hydrogen lost from the molecular ion is the acidic proton.

STRUCTURE ELUCIDATION

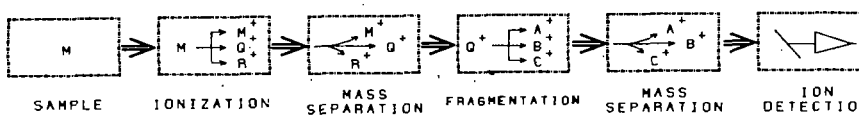

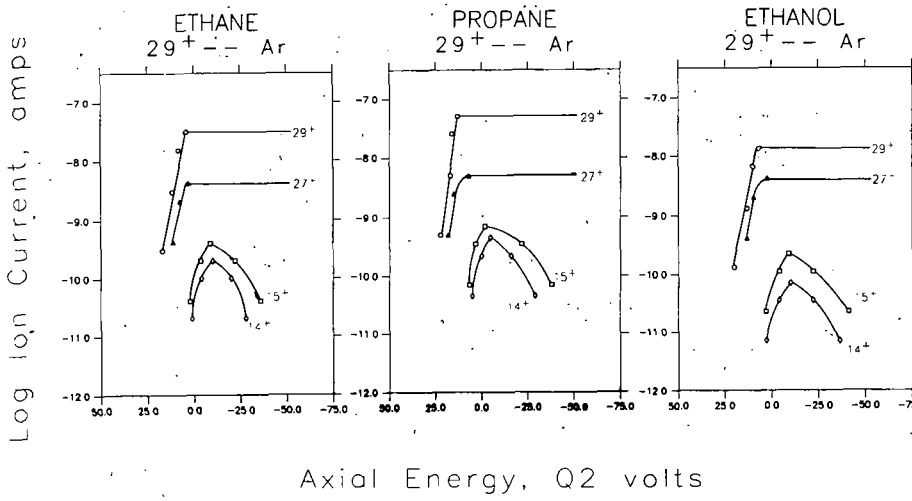

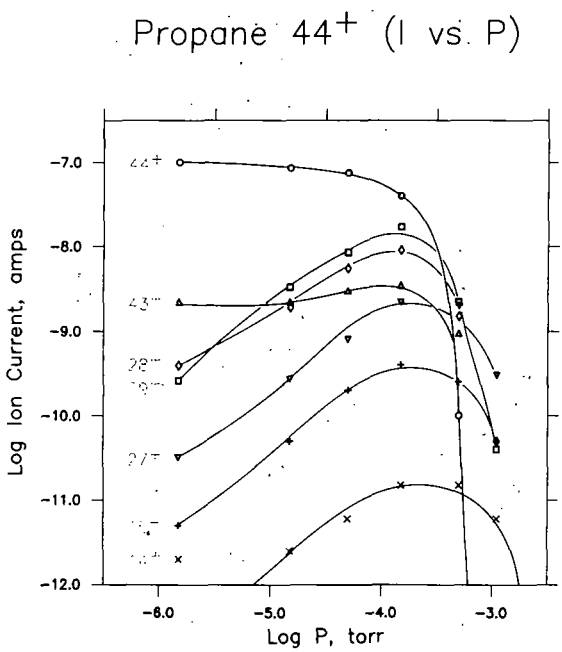

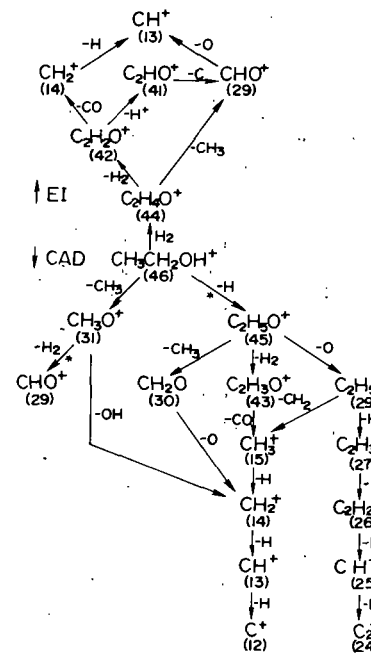

FIELD DESORPTION/COLLISION-INDUCED DISSOCIATION (FD/CID) MASS SPECTROMETRY OF DINUCLEOSIDE PHOSPHATES

M. Linscheid and A. L. Burlingame
Biomedical Mass Spectrometry Resource, Space Sciences Laboratory,
University of California, Berkeley, CA 94720

A FD/CID spectrum of an alkylated dinucleoside monophosphate was obtained in a recent study (1) and the loss of both nucleobases confirmed the proposed structure of the nucleotide.

To determine the scope and limitations of the method for analysis of isolated modified oligonucleotides and synthetic intermediates in oligonucleotide synthesis, it was necessary to study some dinucleoside phosphates on a systematic basis.

For this purpose we chose a set of four closely related dinucleoside phosphates: adenylyl(3'→5')cytidine and cytidylyl(3'→5')adenosine in the ribose series (ApC and CpA, respectively) and the same pair in the deoxyribose series (dApC and dCpA, respectively). The samples were purified and the cation changed by ion exchange chromatography on Whatman DE52 DEAE-Cellulose with 0.01 M trimethylammonium hydrogencarbonate buffer (TBK) as eluant; for FDMS, ca. 3-5 µg material in 0.2 M TBK buffer was applied to the emitter (2).

The mass spectrometer (Kratos MS-902) is equipped with a combined EI/FD source with the EI portion used as a collision chamber (3). The scan conditions were: mass range, 700-50 mu; scan rate, 8 sec/decade (in "normal" mode); scan time, 10.5 sec in "normal mode", 16.5 sec in B/E scan mode; rescan time, 7.5 sec. To minimize thermal fragmentation on the emitter surface, the current was very slowly increased during data acquisition (typically 11 ma, increasing to 13 ma in 10 min) and 20-30 scans were acquired. These data were added to yield a sum spectrum to improve the statistical basis.

The results are summarized in the Table. From these data it is possible to distinguish the different isomers on the basis of loss of cytidine from the MH^+ ion (most abundant in CpA and dCpA) and the occurrence of the signal for protonated cytidine (most abundant in ApC and dApC). The fragmentation with respect to adenine and adenosine does not seem to depend on the structural properties so the intensity of the signal of protonated adenine is generally high, whereas loss of adenosine and, particularly, loss of adenine are of minor importance.

The differences between FD spectra and B/E-CID spectra of the dinucleoside phosphates are that the B/E scan shows almost complete absence of nucleoside fragments in all samples and absence of the cyclophosphate ion in the ribonucleotides, while in the FD spectra they are present (4).

These findings and the observation that B/E scans of the MH^+ ions without collision gas contain no fragments at all suggest the following conclusions. All fragments in the FD spectra of dinucleoside phosophates are formed on the emitter surface. If protonations occurs at the phosphoric acid moiety, the cyclic phosphate can be formed. Judging from the B/E-CID data, protonation is most likely at the heterocyclic aromatic systems and here predominantly at adenine, the glycosidic bond of which is subsequently cleaved with high frequency. To cleave the glycosidic bond in cytidine, structural parameters seem to control the reaction, because the fragmentation becomes more likely when cytidine is in the 5'-position of the dinucleoside phosphate.

Acknowledgements: Financial support was provided by the National Institutes of Health, Division of Research Resources Grant RR00719. One of us (M.L.) acknowledges a grant from the Deutsche Forschungsgemeinschaft.

References

1. K.M. Straub and A.L. Burlingame, Advances in Mass Spectrometry, Vol. 8, Heyden and Son Ltd., London, 1980, in press.

2. M. Linscheid, G. Feistner and H. Budzikiewicz, Israel J. Chem. 17, 163 (1978).

3. A.L. Burlingame, H. Kambara and F.C. Walls, 26th Annual Conference on Mass Spectrometry and Allied Topics, St. Louis, MO, 1978, p. 184.

4. a) M. Linscheid, Ph.D. Thesis, University of Cologne, Germany, 1975.
b) H.R. Schulten and H. D. Schiebel, Nucleic Acid Res. 3, 2027 (1976).

DISTRIBUTIONS OF INTENSITIES OF FRAGMENTATIONS IN THE B/E CID SPECTRA OF DINUCLEOSIDE PHOSPHATES*

	MH^+ m/z 573 541	-CYTOSINE m/z 462 430	-ADENINE m/z 438 406	(DEOXY) -CYTIDINE m/z 348 332	(DEOXY) -ADENOSINE m/z 324 308	ADENINE m/z 136	CYTOSINE m/z 112
	26	1	-	8	3	34	28
ApC		1	-	11	4	47	38
	35	7	-	10	2	36	10
CpA		11	-	15	3	56	15
	40	2	1	5	2	18	32
d(ApC)		3	3	7	4	30	52
	62	5	-	13	1	15	5
d(CpA)		12	-	33	2	40	13

* THE NUMBERS ARE NORMALIZED ON THE SUM OF INTENSITIES INCLUDING THE MH^+ ION (UPPER LINE) OR EXCLUDING THE MH^+ ION (LOWER LINE).

APPLICATION OF MS/MS TECHNIQUES TO THE IDENTIFICATION OF POLYCYCLIC AROMATIC HYDROCARBON METABOLITES

Gary A. McClusky, Shing-Kwan S. Huang

Chemical Carcinogenesis Program
NCI Frederick Cancer Research Center
Frederick, MD 21701

Cynthia J. Moore, James K. Selkirk

Biology Division
Oak Ridge National Laboratory
Oak Ridge, TN 37830

The technique of mass spectrometry/mass spectrometry (MS/MS) has been shown in recent years to be a valuable methodology for the identification of components contained in a complex matrix[1,2]. The number of research groups involved in the innovation of new instrumentation[3], as well as the modification and further development of existing instruments designed primarily for MS/MS analysis, reflect the growing interest in this research tool. This type of mixture analysis is carried out entirely within a two-sector mass spectrometer. Our work is carried out on a reversed-geometry, double-focussing mass spectrometer, MM ZAB-2F, with a collision gas cell in the first and second field-free region. By allowing collision-induced dissociations in the second field-free region, the MS/MS methodology is specifically accomplished here by mass-analyzed ion kinetic energy spectrometry or MIKES. The magnetic analyzer (the first sector encountered by the ion beam) effects the separation of the component from the mixture by selection of an ion characteristic of the component (usually the molecular ion). The characterization and identification step is done by the electrostatic analyzer, which determines the kinetic energy and hence mass of the collision-induced fragments generated from the second field-free region collision cell.

The MS/MS method is a valuable tool in the identification of metabolites that can only be isolated in small quantities. The metabolism of the carcinogen benzo(a)pyrene by a number of *in vitro* systems, has been shown to result in the production of several oxygenated compounds, such as phenols, quinones, dihydrodiols, water soluble conjugates, and nucleoside adducts formed from the reaction of the dihydrodiolepoxides of benzo(a)pyrene (BP) and DNA. Of the 12 possible phenols of BP, only the two positional isomer (2-HO-BP) has a carcinogenic potential comparable to the parent hydrocarbon. It has now been found in this work that hamster embryonic cells incubated with 2-HO-BP produced one major metabolite, while mouse and human cells, which are the potential target tissues, produced an additional metabolite.

An inherent problem with in vitro metabolism studies by cell culturing techniques is the small quantities of metabolites produced. The electron impact mass spectrum of the first or common metabolite of all the cells of 2-HO-BP revealed the compound had not been completely purified by chromatographic techniques. However, subsequent exact mass measurements showed that only m/z 284 could be a polycyclic aromatic hydrocarbon, i.e., has a high carbon/hydrogen ratio. It is quite common for PAH compounds to have a mass spectrum where there is predominately just one or a few ions of substantial intensity. The MS/MS technique of CID/MIKES carried out on the ion of m/z 284 would therefore, separate the metabolite from the contamination and also structurally characterize the unknown compound. The salient fragmentations are the losses of 29 and 58, with much smaller losses of 17 and 34 for the high mass fragment ions. These fragmentations are most likely the sequential loss of CHO twice, and also HO twice. Thus, the metabolite was implied to be a hydroxylated derivative of 2-HO-BP. In confirmation, the isomers 1,6 and 3,6-dihydroxybenzo(a)pyrene produced a CID/MIKE spectrum indistinguishable from the 2-HO-BP metabolite.

This metabolite was further characterized mass spectrometrically by converting it to a trimethylsilyl derivative, obtaining a mass spectrum and CID/MIKE spectrum of m/z 428. Derivatization resulted in the disappearance of m/z 284 and the appearance of m/z 428. The shift in mass spectrum and fragment ions in the CID/MIKES demonstrated that the metabolite was a hydroxylated derivative of 2-HO-BP and not an epoxidated derivative. The second metabolite has not been characterized mass spectrometrically as yet.

Since collision cells have been built into both the first and second field-free regions, the techniques of CID/MIKES can be compared with that of linked scan (CID/B/E) on the same instrument as applied to mixture analysis. The most striking difference between the two techniques is that the resolution of the fragment ions for CID/B/E is much greater than for CID/MIKES of the same ion. This is, of course, due to the fact that the linked scan (B/E) removes the energy dispersion of the fragment ions. Counterbalancing this effect, is the poor primary mass resolution associated with CID/B/E, which has been noted previously. This would become an important consideration as a mixture becomes more complex in the mass region of interest.

References:

1. R.W. Kondrat, R.G. Cooks, Anal. Chem., 50, 81A (1978).
2. F.W. McLafferty, Acct. Chem. Res., 13, 33 (1980).
3. R.A. Yost, C.G. Enke, J. Am. Chem. Soc., 100, 2274 (1978).

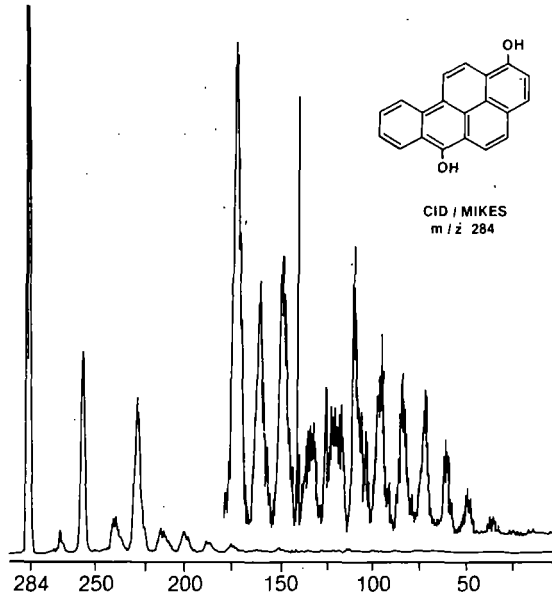
OH
OH
CID / MIKES
m / z 284
284
250
200
150
100
50

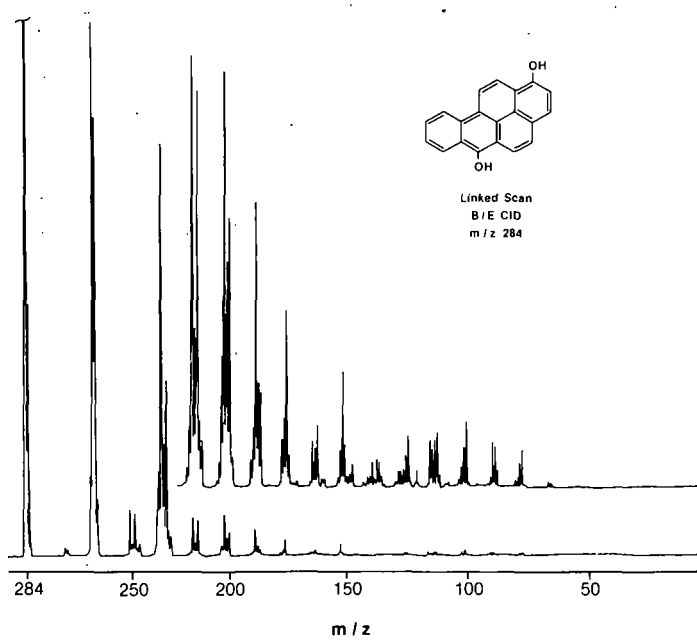
OH
OH
Linked Scan
B / E CID
m / z 284
284
250
200
150
100
50
m / z

DETERMINATION OF PYRROLIZIDINE ALKALOIDS IN RANGE PLANTS BY LINKED FIELD B^2/E SCANS.

WILLIAM F. HADDON AND RUSSELL J. MOLYNEUX, WESTERN REGIONAL RESEARCH CENTER, SEA, U. S. DEPARTMENT OF AGRICULTURE, BERKELEY, CA 94710.

A considerable increase in selectivity for mass spectral analysis may be obtained by employing chemical ionization (CI) and metastable ion (MI) analysis concurrently.[1] Linked field B-E scans provide the necessary defocused MI spectra on a conventional geometry magnetic mass spectrometer, in which the electric sector precedes the magnet. Daughter ions from the reaction $m_1^+ \rightarrow m_2^+ \rightarrow (m_1-m_2)$ occurring in the first field free region (f.f.r.[2]) may be recorded by one of three separate scans in the B-E plane: The B/E for constant m_1^+; the B^2/E scan for constant m_2^+; and the $B/E\sqrt{1-E}$ scan for constant neutral loss. Linked scans of 1st f.f.r. metastables yield MI spectra of high daughter ion resolution[2] in contrast to MIKE spectra, which have high precursor resolution. A method described previously allows us to record linked scan MI spectra rapidly and repetitively, and in addition provides the very accurate magnetic field measurement required by the B^2/E scans.[2]

The present study of pyrrolizidine alkaloid (PA) composition in the *Senecio* plant species is an example of a direct mixture analysis problem which exploits the high daughter ion resolution of linked MI scans. The PA's having the structures shown in Fig. 1 are of particular interest; they comprise the principle toxic alkaloids of the plants *S. longilobus* and *S. riddellii*, which are native to the semidesert regions of the southwestern U. S. and pose a health hazard to the cattle, horses and sheep which graze in these areas. Our interest in screening plant samples for PA content has prompted an investigation of MS/MS to complement methods based on NMR analysis and HPLC separation.[2]

The basis of our direct mixture analysis method is the MI reaction of the protonated molecular ion to yield the common daughter ion $C_8H_{10}N$ (m/e 120). This ion, and the protonated molecular ion, are the two major peaks in the isobutane CI spectra of these PA's as shown in Fig. 2 for riddelliine, and are prominent in the MI spectra, as shown in Fig. 3.

For qualitative analysis, whole plants may be analyzed directly with B^2/E scans as shown in Fig. 4 for *S. riddellii*, which contains only riddelliine. There is, however, a complication because a substantial percentage of PA's may be present as the N-oxides[3], which are not determined by the method. Fig. 4 shows the distribution of alkaloids in *S. longilobus*; A and B are the spectra obtained after 1 and 2 stages of extraction and purification and C is the total PA content after reduction of the N-oxides. Quantitative analysis requires that the reduction be carried out.

As an internal standard, we use the PA monocrotaline (MC), MW 326. Its molecular ion peak is not completely resolved from the SPH peak, as shown in Fig. 6B, but can be subtracted to yield the spectrum in C. Curve A is pure MC, and curve D is pure SPH. Fig. 7 shows a linear calibration between 100 and 2000 ng. of SPH, based on the ratio of 334 in SPH to 264 ($m-CO_2-H_2O$) of MC.

[1] McLafferty, F. W., Accounts of Chemical Res. (1980), 13, 33-39.

[2] W. F. Haddon, Anal. Chem. (1979), 51, 983-988.

[3] R. J. Molyneux, et al, J. Agric. and Food Chem. (1979), 27, 494-499.

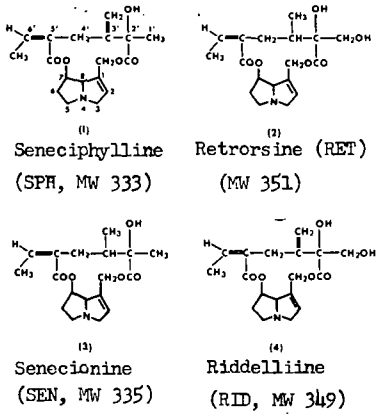

Figure 1.

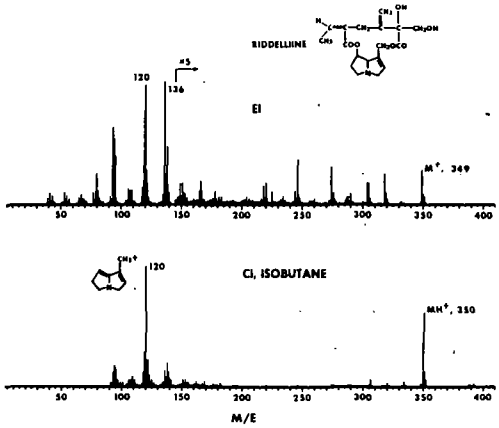

Figure 2. EI and Isobutane Spectra of Riddelliine

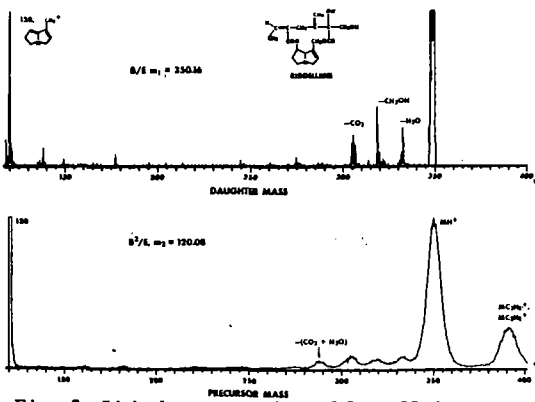

Fig. 3. Linked scan spectra of Riddelliine

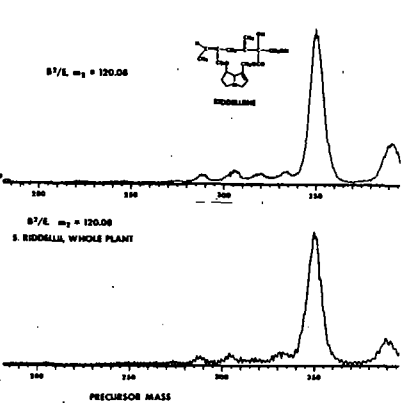

Fig. 4. Whole plant analysis.

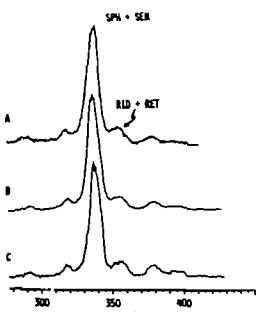

Fig. 5

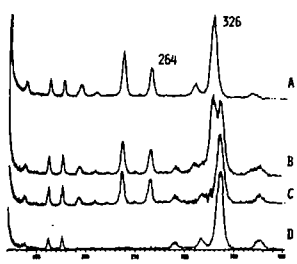

Fig. 6

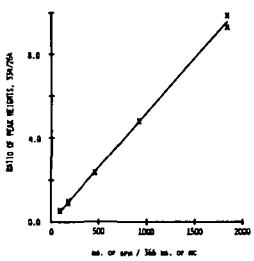

Fig. 7

DISTINGUISHING ISOMERIC FRAGMENT IONS FROM PENICILLINS BY COLLISIONAL ACTIVATION

J.L. Occolowitz, M.P. Barbalas and F.W. McLafferty
Eli Lilly and Co., Indianapolis, IN 46239
Department of Chemistry, Cornell University, Ithaca, New York 14853

Collisional activation mass spectra have been used to distinguish the $C_7H_{12}NO_2S^+$ ions derived from the fragmentation of penicillins, a dihydrocephalosporin, and tetramethylthiazolidine carboxylic acid.

The normal electron ionization mass spectra of the compounds contain an intense $C_7H_{12}NO_2S^+$ peak from the cleavage of the β-lactam ring for the first two types of compounds and the loss of methyl radical for the third.

The tandem double-focusing mass spectrometer used for the measurement of the CA spectra has sufficient sensitivity to distinguish the three structures with only single scans.

The collisional activation spectra of the ^{34}S-containing fragment peaks provide information on the origin of the peaks seen in the CA spectra. Peaks which contain sulfur are shifted up by two mass units while peaks that correspond to the loss of sulfur are unchanged in their position.

The fragment ions from the first two types of compounds are distinguishable by the loss of CH_3OH and $HCOOCH_3$ from the first while the second only loses $HCOOCH_3$. The fragment ions from the third compound lose HCOOH.

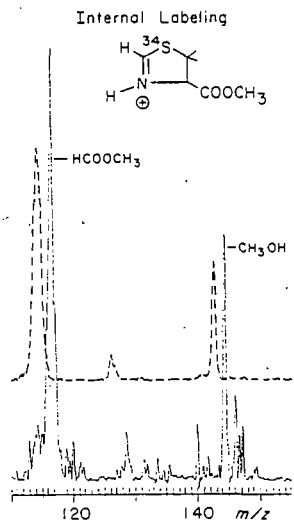

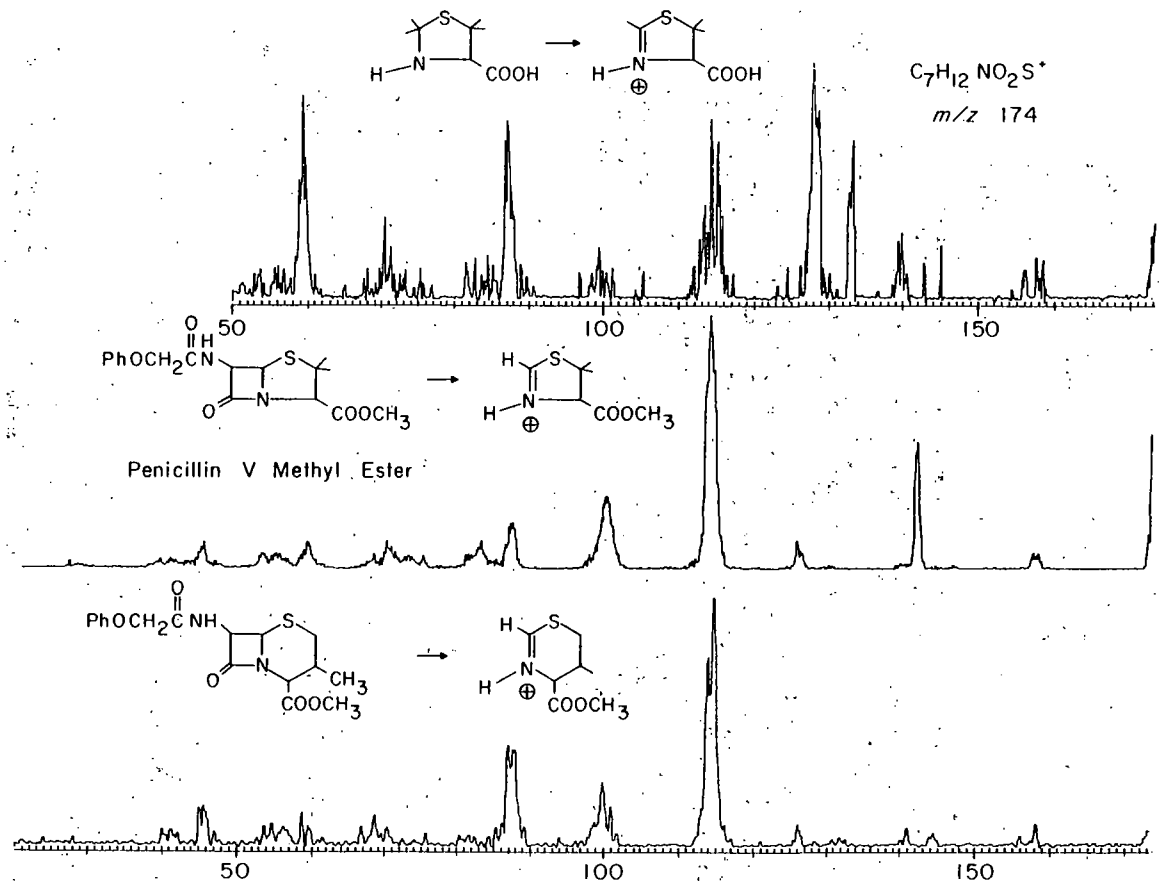
COOH
COOH
$C_7H_{12}NO_2S^+$
m/z 174
50
100
150
$PhOCH_2CNH$
$COOCH_3$
$COOCH_3$
Penicillin V Methyl Ester
$PhOCH_2CNH$
CH_3
$COOCH_3$
$COOCH_3$
50
100
150

ANALYTICAL APPLICATIONS OF TRIPLE STAGE QUADRUPOLE MASS SPECTROMETRY RAMOA8

Donald F. Hunt, Jeffrey Shabanowitz, and Anne B. Giordani

Department of Chemistry, University of Virginia, Charlottesville, Va. 22901

We report here further applications of an MS/MS technique, triple stage quadrupole (TSQ) mass spectrometry, for ion structure elucidation and mixture analysis.[1] Our Finnigan TSQ mass spectrometer, described in more detail elsewhere,[2] consists of a CI ion source, two quadrupole mass filters separated by a quadrupole collision chamber, and a conversion dynode/electron multiplier detector. The quadrupole collision chamber consists of a set of quadrupole rods housed in a stainless steel cylinder which can be filled with collision gas (typically N_2 at $\sim 2\text{-}6 \cdot 10^{-3}$ torr). Rather than the RF/DC voltages required for these rods to act as a mass filter, only an RF voltage is applied so that the rods function as an ion focusing device and transmit ions of all m/z.

Ion structure elucidation and mixture analysis is accomplished in the following steps. The compound or mixture in volatilized and ionized in the ion source, producing a mixture of ions of many different m/z. The first mass filter (Q1) is tuned to transmit the ion of intrest into the collision chamber (Q2). After collisionally activated decomposition (CAD), the resulting fragment ions are mass analyzed in Q3. The CAD fragment ions are used to deduce ion structure and/or quanitate the ion in the starting mixture. Clearly, mixture analysis by CAD is most efficient if each component affords a single ion characteristic of molecular weight. Thus our studies of $(M\text{-}1)^-$ ions—very little fragmentation accompanies their formation when a strong Bronsted base (such as MeO^- or OH^-) is used to abstract a proton from the sample molecule.

We have previously reported that the CAD spectrum of the $(M\text{-}1)^-$ ion from cyclohexanone consists of two losses: H_2 and C_2H_4.[2] The postulated mechanism for the loss of ethylene is a retro-Diels-Alder reaction of the enolate anion(1). Loss of hydrogen probably forms the conjugated diene of the enolate anion(2).

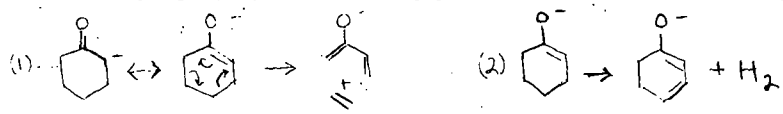

The CAD spectra of the $(M\text{-}1)^-$ ions of 2-methyl cyclohexanone and 4-t-butyl cyclohexanone show loss of ethylene and t-butyl ethylene respectively, thus confirming mechanism (1).

Deuterium exchange CIMS, combined with CAD analysis is an even more powerful tool for ion structure elucidation. With $MeOD/N_2O$ as the reagent gas, the $(M\text{-}1)^-$ ion of cyclohexanone has its three remaining α-hydrogens exchanged for deuteriums. The CAD spectra of this $d_3(M\text{-}1)^-$ ion and the $d_2(M\text{-}1)^-$ ion of 2-methyl cyclohexanone show loss of H_2 (no loss of HD or D_2) and loss of C_2H_4 (no loss of deutero-ethylene) thus confirming the predictions of equations (1) and (2) that the losses of C_2H_4 and H_2 in the CAD spectrum involve carbons 3 and 4 or carbons 4 and 5 with their attached hydrogens, only.

Similarly, the fragmentation observed in the CAD spectrum of the $d_3(M\text{-}1)^-$ ion of 4-decanone is consistant with a negative ion analog of the McLafferty rearrangement(3). The three α-deuteriums (again substituted into the $(M\text{-}1)^-$ by using $MeOD/N_2O$ reagent gas) remain in the ions, and only loss of nondeuterated ethylene and pentene is observed.

We have also examined CAD spectra of $(M\text{-}1)^-$ ions of carboxylic acids. The CAD spectrum of the $(M\text{-}1)^-$ ion of p-hydroxyphenylacetic acid shows an ion representing loss of 44 amu (CO_2) at a relative abundance less than that of the $(M\text{-}1)^-$ ion. The $(M\text{-}1)^-$ ions produced by using OH^- as the reagent ion could have either the phenolic anion structure or the carboxylic acid anion structure. Electron capture negative ion CIMS of the pentafluorobenzyl derivative of p-hydroxyphenylacetic acid generates the carboxylic acid anion structure only.

[1] R. A. Yost and C. G. Enke, Anal. Chem., 51, 1251A (1979).

[2] D. F. Hunt, J. Shabanowitz, and A. B. Giordani, Anal. Chem., 52, 386(1980).

The CAD spectrum of the $(M-1)^-$ ions produced in this fashion contains the ion representing the loss of 44 amu (CO_2) (4) at a relative abundance ~10 times greater than the $(M-1)^-$ ion. These experiments demonstrate that CAD spectra can be very sensitive to ion structure, and are thus an excellent probe of such.

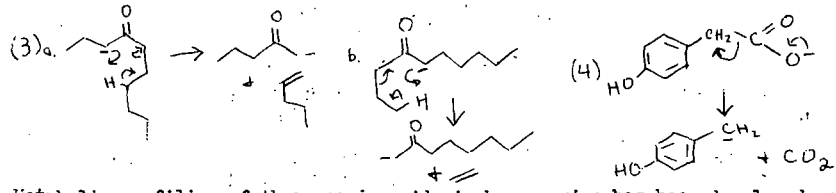

Metabolic profiling of the organic acids in human urine has been developed using capillary GC/MS by S. C. Gates et al.[3] The sample work up is time consuming, and the capillary GC/MS analysis lengthy. As an alternate method, we have examined TSQ MS for selectively profiling the carboxylic acids in urine. Gates lists 62 carboxylic acids identified in urine. We have run as standards CAD spectra of the $(M-1)^-$ ions of 38 of these acids. All but seven show loss of 44 or 62 (CO_2, H_2O) amu in their CAD spectra. We can selectively detect ions which loose 44 or 62 amu in the collision chamber by scanning Q1 and Q3 simultaneously, with Q3 scanning 44 or 62 amu lower in mass ("linked scanning"). The linked scan spectra of 5 µl of urine, acidified and then pumped to dryness under vacuum, show peaks corresponding to all of our acid standards. The sample preparation is carried out in a melting point capillary tube. The tip of the tube, containing the acidified urine residue, is put on the solids probe, inserted directly into the ion source, and then heated. Analysis time takes a maximum of ten minutes. Sensitivity is comparable to the capillary GC/MS methodology (nanogram range).

Linked scanning is thus a method of mixture analysis selective for compounds of a particular functional group. Another application of this methodology is the analysis of polyaromatic hydrocarbons (PAH). Ions of PAH are particularly resistant to collisionally activated decomposition. However, the nitro derivatives of PAH, prepared by bubbling N_2O_4 through an ether solution of same (5), are suitable for this type of analysis. The $(M+1)^+$ ions of the nitro derivatives show loss of 17 amu (•OH) in their CAD spectra (6). Thus a 17 amu linked scan analysis of the PICI (CH_4) spectrum of the nitro derivates of PAH can be used to selectively detect PAH in complex matrices such as sludge or oil.

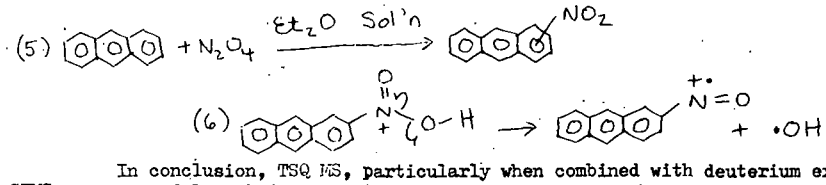

In conclusion, TSQ MS, particularly when combined with deuterium exchange CIMS is a powerful tool for ion structure elucidation. It has potentially even greater utility as a mixture analysis technique, particularly when the linked scan technique is used to incorporate selectivity to particular functional groups into the analysis.

[3] S. C. Gates, C. C. Sweeley, W. Krivit, D. DeWitt and B. E. Blaisdell, Clin. Chem., 24, 1689(1978).

SIMPLIFIED "TRIPLE QUADRUPOLE" FOR MS-MS

M. W. SIEGEL

Extranuclear Laboratories, Inc.
P.O. 11512 250 Alpha Dr.
Pittsburgh, PA 15238

In the rapidly developing field of MS-CID-MS, the unique properties of quadrupole-CID-quadrupole instruments have been recently recognized, e.g., the advantageous nature of low energy fragmentation processes in analytical applications, and the insensitivity of quadrupole analysers to the kinetic energy distribution of the fragments. Two quadrupoles separated by a simple collision cell have been known (in non-analytical applications) for many years, and have recently re-emerged for CID applications.[1] Equally recent has been the realization that the CID cell could be a quadrupole mass analyser excited with only an RF (confining) voltage, the normal DC (resolving) voltage being absent.[2] Since the RF-only quadrupole is a high mass pass filter, the amplitude of the RF voltage is made sufficiently large to produce the required confinement, but sufficiently small to avoid rejection of the light mass ions of interest.

This paper describes the concept, and some application tests, of a system combining the simplicity of the two quadrupole configuration with the advantages of the three quadrupole configuration. The method relies on the ability of resistive ("leaky dielectric") materials to shield their interiors from DC and low frequency field components, while transmitting, with some attenuation, high frequency field components. Thus these materials act as metals at DC and low frequencies, but as insulators at high frequencies. A cylindrical tube of an appropriately chosen resistive material joining two quadrupole mass analysers will thus contain the RF but not the DC fields, and will have the same effect as the middle quadrupole in triple-quadrupole systems.

By analogy with the case of a resistor-capacitor filter network, whose time constant is $T = RC$, the filtering characteristic of a resistive material is described by a time constant $T = \rho\varepsilon'$, where ρ is the resistivity of the material in ohm-m and ε' is its dielectric permittivity in farad/m. Since typical quadrupole operating frequencies are the order of 10^6 sec^{-1}, and the corresponding period is thus the order of 10^{-6} sec, minimal attentuation of the RF and excellent shielding of the DC will be obtained by choosing $\rho\varepsilon \approx 10^{-5}$ sec. Since dielectric permittivities will be in the range 10^{-11} to 10^{-10} farad/m (i.e., dielectric constants ε between 1 and 10), the corresponding appropriate resistivities will be in the range of 10^5 to 10^6 ohm-m (10^7 to 10^8 ohm-cm), the lower part of this range being most appropriate for the many common materials with dielectric constants approaching 10. The attenuation of the RF fields, required to transmit low mass fragment ions, is then determined by the inner and outer cylinder radii (a, b) and the dielectric constant via

$$\alpha = \frac{4\varepsilon}{(\varepsilon+1)^2 - (\varepsilon-1)^2 \left(\frac{a}{b}\right)^4} \qquad \text{(Eq. 1)}$$

α being the ratio of attentuated to unattenuated RF field strengths. Equation 1 is derived from simple electrostatic principles based on the continuity of the electric potential and displacement fields across the dielectric boundaries.[3] The minimum value of α is obtained for vanishingly small bores ($a \to 0$) and large values of ε ($\alpha \to 4/\varepsilon$), which in practice means that light fragment ions tend to be lost near the entrance end of the collision cell. This problem is easily corrected by locating the collision cell assymmetrically with respect to the quadrupoles, i.e., allowing it to penetrate only slightly into the first quadrupole and having most of its length in the second quadrupole. This configuration is depicted in Figure 1. With this geometry we can go to arbitrarily thin cylinder walls ($a \to b$), in which case $\alpha \to 1$, a condition for which the ions resolved by the second quadrupole must be on stable trajectories in the collision cell. Furthermore even very thick cylinder walls ($a \to 0$, $\alpha \to 4/\varepsilon$) result, for practical values of the dielectric constant, in a sufficiently strong RF confining field on the axis. The geometrical restriction of a small bore, resulting in loss of fragment ions because their trajectories intercept the walls, is balanced by the smaller gas load obtainable with small bores, and the dimensions actually used are an empirical compromise between these conflicting demands.

An interesting demonstrative application of this instrument and its capabilities is given by Figure 2, in which the ion source is loaded with D_2O vapor and the collision cell with H_2O vapor. The D_2O pressure is sufficient to result in the production of some D_3O^+, as well as the usual D_2O^+ and DO^+, and by ion-molecule reactions with residual H_2O in the ion source, D_2HO^+ at 21 amu, (probably) DH_2O^+ at 20 amu, H_3O^+ and/or DHO^+ at 19 amu, (probably) H_2O^+ at 18 amu, and OH^+ at 17 amu. The spectrum of primary ions at these masses is shown in the lowest trace of Figure 2, obtained by shutting off the collision gas and running one of the quadrupoles in an RF-only mode. The remaining traces show, from top to bottom, ion signals at 21, 20, 19, 18, and 17 amu parameterized along the horizontal scan by the primary ion mass. Thus, for example, by examining the uppermost horizontal trace (21: HD_2O^+), we see that the bulk of the signal at mass 21 originates from primary ions at mass 22 via the exchange reaction

$$D_3O^+ + H_2O \rightarrow HD_2O^+ + DHO$$

By looking vertically down the column of all ions originating from mass 21 we see that most of the HD_2O^+ present in the primary beam is ultimately observed at lower masses, especially 20 amu, via

$$HD_2O^+ + H_2O \rightarrow \left.\begin{array}{l} H_2DO^+ + DHO \\ D_2O^+ + H_2O + H \end{array}\right\} \text{at } 20$$

$$\rightarrow \left.\begin{array}{l} H_3O^+ + D_2O \\ HDO^+ + H_2O + D \end{array}\right\} \text{at } 19$$

By appropriate observation of the changes in the matrix of signals with source and collision cell pressure, all the relevant cross sections can in principle be measured.

An interesting final possibility, raised by the complexity of the data even under the simple conditions of this demonstration, is that of obtaining all the required information by MS/MS/MS, with the second collision cell containing perhaps helium or argon. While stacking up five quadrupole rod sets to do MS/MS/MS is probably unreasonably complicated, it is entirely conceivable that should the need arise, we could place this new kind of collision cell between each pair of quadrupoles in a "triple quadrupole".

Acknowledgement:

Data shown were collected by Ms. Z. F. Curry, assisted by Mr. M. Easterbrook.

References:

[1]D. Zakett, W. J. Fier, and R. G. Cooks, Anal. Chim. Acta., in press.
[2]R. A. Yost and C. G. Enke, Anal. Chem. (1979) 51, 1251A-74A.
[3]W. L. Fite, Rev. Sci. Instr. (1976) 47, 326-30.

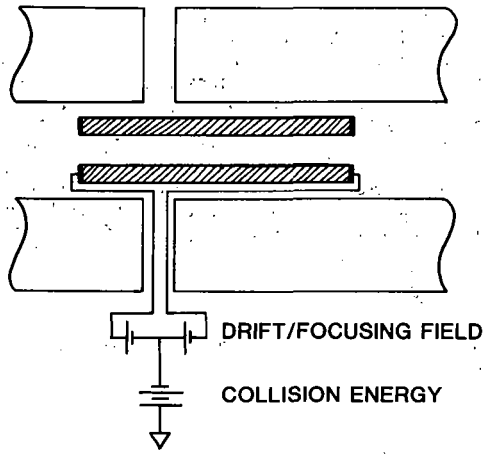

Figure 1

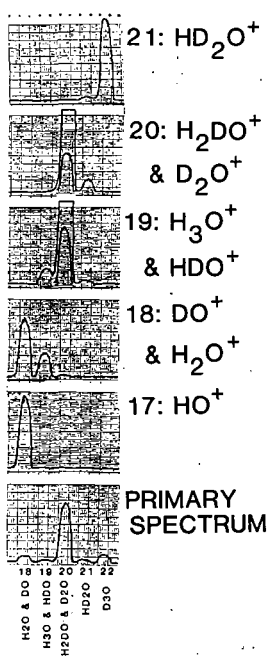

Figure 2

Figure 1. Ferrite ceramic collision cell between two quadrupole mass filters. Connections to both ends provides ability to control axial field as well as collision energy.

Figure 2. Primary spectrum and CID spectra of D_2O (and trace of H_2O) in ionizer and H_2O in collision cell. Horizontal scans always show the indicated product ion; peaks indicate intensity of product ion derived from parent ion in primary spectrum.

A TANDEM DOUBLE-FOCUSING MASS SPECTROMETER FOR GAS-PHASE ION STUDIES

P.J. Todd, D.C. McGilvery, M.A. Baldwin, and F.W. McLafferty

Department of Chemistry, Cornell University, Ithaca, New York 14853

An instrument has been constructed which appears to have unique capabilities for several types of ion studies. It consists of an Hitachi RMH-2 double-focusing mass spectrometer (MS-I) for precursor ion selection, interfaced by electrostatic lenses (A and B) to a collision chamber and a second double-focusing mass spectrometer (MS-II) for daughter ion mass analysis. The high resolution (~50,000) precursor ion beam is accelerated up to 30 KeV by lens A and focused onto a ribbon beam of helium orthogonal to the mean ion axis effusing from a 25 μm slit across the collision chamber. The daughter ions produced by the resulting collisions are focused onto the entrance slit of MS-II by lens B. Low resolution CA spectra are produced by scanning the electrostatic analyzer (ESA) of MS-II, and high resolution CA spectra by the linked scan of both the ESA and magnetic sectors. Instrument control and data acquisition are by a dedicated DEC PDP-11/45 computer. A recent publication gives a more complete description.[1]

CA spectra of isobaric $C_7H_7^+$ and $C_6H_5N^{+\cdot}$ ions show <2% interference despite a required resolving power of 7280. CA spectra of neutrals from metastable and CA decompositions are characteristic of their structures. Sensitivity is increased by more than an order of magnitude; 11% of 25 keV CH_4^+ ions are converted into collectable daughter ions. This sensitivity made possible the CA identification of two $C_3H_6^+$ isomers based on $[C_3H_6^{++}]$ representing 0.1% of the largest CA peak.

Improved resolution of the CA spectra using the double-focusing MS-II has been valuable. For the first time unit mass resolution or better can be achieved on both MS-I and MS-II of a high-collision-energy CA instrument. Despite the low stability of the magnet power supply temporarily used for MS-II, complete resolution can be achieved with a CA spectrum of benzoyl $C_7H_5O^+$ ions, and partial resolution for multiplets in the CA spectrum of the m/z 628 peak of hexabromobiphenyl, $C_{12}H_4{}^{79}Br_3{}^{81}Br_3$, whose abundance is 2% of that of the base peak in the EI spectrum.

Research using further capabilities of the instrument is planned. A magnet of 23 Kgauss field and 60 cm radius has been constructed to replace the present MS-I magnet; this will make possible high resolution (~100,000) separation of 4 keV ions of m/z 25,000; note that up to 20 kV can be added to these ions by lens A before collision. The molecular

beam collision region should make possible studies on CA decompositions taking place in picoseconds and at high angular-resolution.

---

[1] F.W. McLafferty, P.J. Todd, D.C. McGilvery, and M.A. Baldwin, J. Am. Chem. Soc., 102, 3360-3 (1980).

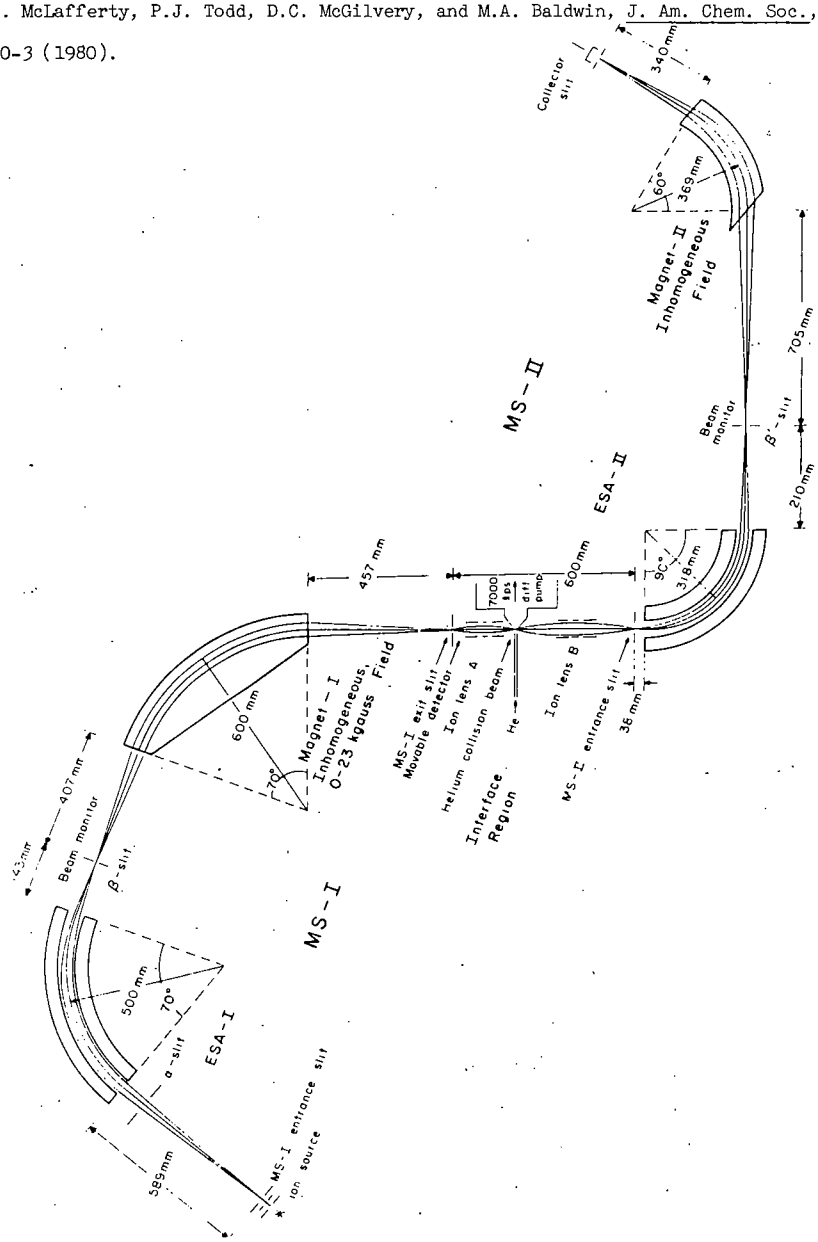

MASS SPECTRAL STUDY OF RAPIDLY HEATED POLYSTYRENE

H. R. Udseth and L. Friedman

Department of Chemistry
Brookhaven National Laboratory, Upton, NY 11973

A polystyrene standard of nominal molecular weight 2100 and weight distribution $M_w/M_n < 1.10$ was dissolved in benzene and nanogram quantities were placed directly on a ribbon filament. The ribbon was heated at a rate of 1000°C/sec. A rapidly scanned quadrupole was used to mass analyze the products and multiple runs were used to build up spectra from 300 to 3000 amu. The experiments were carried out under EI and CI conditions with both argon and methane used as the reagent gas. In addition to the mass measurements, Arrhenius plots of $\ln I$ vs $1/T$ were made for many of the peaks in each spectrum and activation energies were taken from these plots for the various processes. It was determined that the polymer sequence is accurately reproduced in the CI experiments and that the temperature region in which a specific polymer evaporates is primarily determined by the chain length and only slightly affected by the plasma whereas the qualitative nature of the evaporation process and the activation energies are highly dependent on both of these parameters. Mechanisms to explain the observed effects are proposed in terms of heterogeneous ion molecule reactions and transitions between one dominant process and another as the temperature increases.

Research carried out at Brookhaven National Laboratory under contract with the U.S. Department of Energy and supported by its Division of Basic Energy Sciences.

PHOSPHAZENE MIXTURES: REFERENCE COMPOUNDS FOR ELECTRON IMPACT, CHEMICAL IONIZATION AND FIELD DESORPTION MASS SPECTROMETRY, CHARLES R. SNELLING, JR., RICHARD M. MILBERG, J. CARTER COOK, JR., and KENNETH L. RINEHART, JR., School of Chemical Sciences, University of Illinois, Urbana, IL 61801

The increasing use of mass spectrometry in the structure elucidation of natural products, particularly those of high molecular weight, puts stringent demands on conventional reference materials. The usual standards, perfluoroalkane mixtures (PFA), tend to desensitize the emitter in the FI mode and have a useful mass range to only m/z 1000 in the EI mode. Moreover, the differences between the ionization processes in EI, CI and FD have led to a situation where no single reference standard exists for all three. Instead, each of the three ionization techniques has developed its own set of mass standards.[1-5]

Starting with the work of Olson,[6] we have investigated the multifluoroalkoxyphosphazenes as reference standards. The phosphazenes tend to give only molecular ions by FI and M + H ions by CI. The EI spectrum shows the molecular ion as the base peak with a few simple cleavages. Their peaks' negative mass defects rarely interfere with sample peaks at high or low resolution, while their volatility at low temperatures, even at mass 3300, provides a minimum of source memory effect.

The phosphazenes are produced by the reaction of hexachlorocyclotriphosphazene, 1, with the sodium salts of polyfluorinated alcohols.

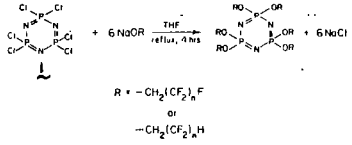

For example, from the alcohol 2,2,3,3-tetrafluoropropanol the resulting phosphazene is 1,1,3,3,5,5-hexakis(2,2,3,3-tetrafluoropropoxy)cyclotriphosphazene. The EI spectrum of this phosphazene has a molecular ion at m/z 921, the base peak, with large peaks at m/z 902, 870, and 790. These latter peaks correspond to the loss of F, CF_2H and $OCH_2CF_2CF_2H$, respectively, from the molecular ion. The CI and FI spectra contain only the M + H and M+ ions, respectively.

When alcohols of different molecular weight and concentrations are used in the phosphazene synthesis, the mixture produced follows multinomial statistics. After the initial failure of a complex mixture, hundreds of mixtures were analyzed through computer simulation. This study showed that no complex mixture would provide an adequate standard, and it was decided to use a series of binary mixtures rather than one complex mixture. Since some of these binary mixtures required alcohols not commercially available, some alcohols containing odd numbers of CF_2 units were prepared from alcohols with even numbers of CF_2 units by the following sequence of reactions:

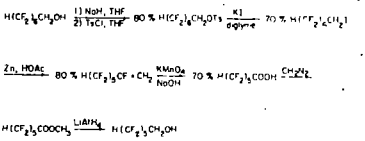

With these alcohols, binary mixtures have been synthesized that cover the mass range from m/z 729 to 3321. These mixtures have been used successfully for high resolution peak matching in EI, FI and FD modes. A binary mixture can cover a mass range as narrow as 200 mass units, while mixing of the binary mixtures can produce a standard that spans a range as broad as 2700 mass units. The entire mass range from m/z 700 to 1700 has been covered with high intensity ions (>10%) 50 mass units or less apart. The binary mixtures possess high volatility, negative mass defects and show minimal adverse effects to the source.

Spectra of several samples that would normally be obtained with an oscillographic recording device have been obtained with the computer. Figure 1 shows the EI spectrum of tris(perfluoroheptyl)triazene (both on and off scale) obtained using phosphazenes. The lower, off scale, spectrum shows the use of the computer in studying low intensity fragmentations. The binary mixtures have also facilitated the computer aquisition of high resolution measurements. Table 1 lists the high resolution data for tris(perfluoroheptyl)triazene.

As the table shows, all the major ions present in Fig. 1 were identified. The average mass accuracy from m/z 700 to 1200 was better than 4 ppm with the largest deviation being less than 8 ppm. The phosphazenes have also been used in the CI mode. The computer-acquired CI spectra of three important triglycerides are presented in Fig. 2. The triglycerides tristearin, triolein and tripalmitin (M = 890, 885, and 806, respectively) all give only quasi-molecular ions corresponding to M + NH_4 when ammonia is used as the reagent gas. Although the data system has been calibrated for high resolution CI, the design of our present CI source makes it virtually impossible to obtain high resolution measurements.

In conclusion, it can be seen that the phosphazenes provide a useful high molecular weight reference standard for both high and low resolution for EI, CI and FD spectra.

References

1. H. R. Schulten and H. D. Beckey, Org. Mass Spectrom., 6, 885 (1972).
2. D. V. Bowen and F. H. Field, Anal. Chem., 47, 2289 (1975).
3. I. Dzidic, D. M. Desiderio, M. S. Wilson, P. F. Crain, and J. A. McCloskey, Anal. Chem., 43, 1877 (1971).
4. Y. Hirata, K. Matsumoto, and T. Takeuchi, Org. Mass Spectrom., 2, 111 (1978).
5. W. V. Ligon, Anal. Chem., 50, 1228 (1978)
6. K. L. Olson, K. L. Rinehart, Jr., and J. Carter Cook, Jr., Biomed. Mass Spectrom., 4, 284 (1977).

Fig. 1: EI spectrum of the high mass region for tris(perfluoroheptyl)triazene.

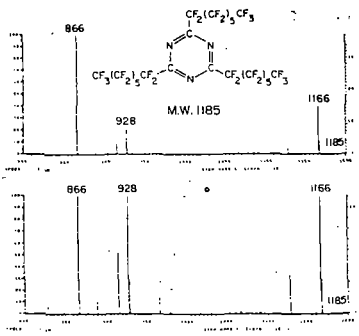

Table 1: HREI for tris-(perfluoroheptyl)triazene.

HREI of

Tris(perfluoroheptyl)triazine

m/z	%	COMPOSITION	Δ, mmu	ppm
866	100	$C_{18}F_{32}N_3$	3.5	4.0
1166	27	$C_{24}F_{44}N_3$	0.7	0.6
928	17	$C_{20}F_{34}N_3$	-1.1	-1.2
916	9	$C_{19}F_{34}N_3$	-5.0	-5.5
978	8	$C_{21}F_{36}N_3$	-5.6	-5.7
966	5	$C_{20}F_{36}N_3$	-6.8	-7.0
1128	3	$C_{24}F_{42}N_3$	3.0	2.6
1090	2	$C_{24}F_{40}N_3$	-8.4	-7.7
1185	2	$C_{24}F_{45}N_3$	2.1	1.7
			Avg. 4.0	3.7

Fig. 2: Low resolution CI spectra of a) tristearin, b) triolein and c) tripalmitin

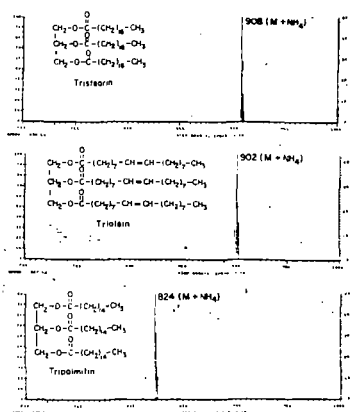

Characterization of Aniline-Acetone Condensation Products
by Liquid Chromatography and Mass Spectroscopy.

by

Robert P. Lattimer, E. Ray Hooser, and Paul M. Zakriski

The BFGoodrich Research & Development Center
9921 Brecksville Road
Brecksville, OH 44141

Liquid chromatography has proven to be an extremely valuable tool for many separations involving polymers and polymer chemicals, especially when used in conjunction with mass spectroscopy for chemical identification. The complex products of the condensation reaction of aniline with acetone have been characterized by liquid chromatography and mass spectroscopy. The LC separation procedure utilized a C_{18} Micro Bondapak (reverse phase) column with a water/tetrahydrofuran gradient system. Eluted peaks were trapped individually for field desorption mass spectral identification. Syringe deposition was used to transfer the isolated components to the field emitter. The major components found in the reaction mixture were oligomers of 2,2,4-trimethyl-1,2-dihydroquinoline (TMDQ), although several other monomeric and oligomeric side-products were observed and characterized. Forty-two components were identified in the product resin. These can be classified into eight major series of oligomers; all series have oligomers separated by the TMDQ monomer unit (173 amu). The liquid chromatogram is shown below, and the oligomeric series identified are on the opposite page.

Figure 1. Liquid Chromatogram of Aniline-Acetone Resin

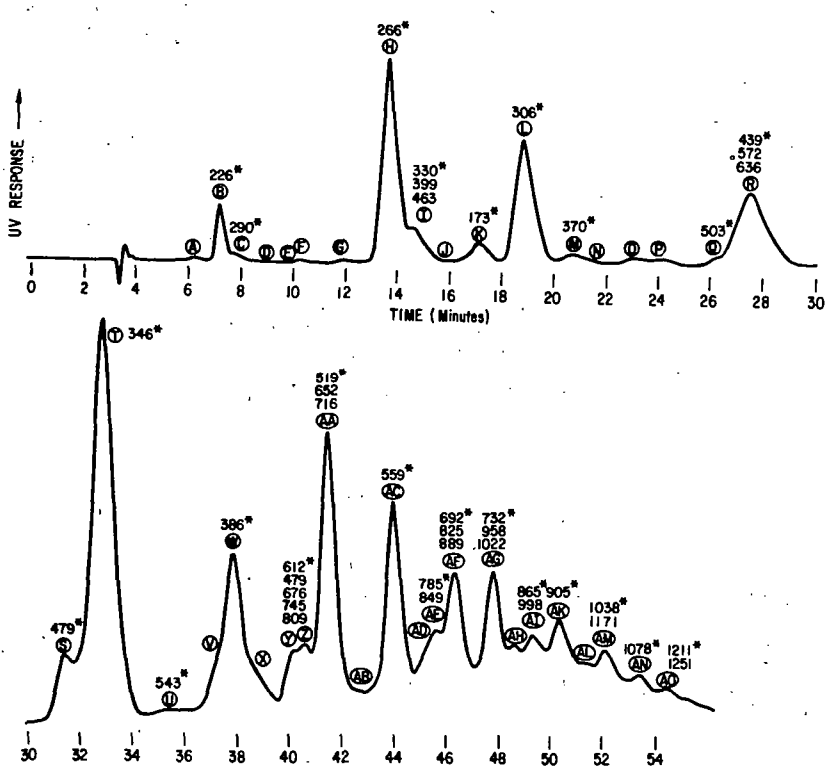

Table I. Components Identified in Aniline-Acetone Resin.

SERIES COMPOSITION	n	MOLECULAR WEIGHT[a]	LC PEAK[b]
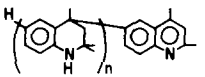 MW=157+(173)$_n$	1	330	I*
	2	503	Q*
	3	676	Y,Z
	4	849	AD,AE
	5	1022	AG
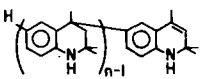 MW=(173)$_n$	1	173	K*
	2	346	T*
	3	519	AA*
	4	692	AF*
	5	865	AI*
	6	1038	AM*
	7	1211	AO*
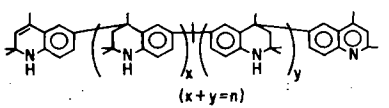 (x+y=n) MW=370+(173)$_n$	0	370	M*
	1	543	U*
	2	716	AA
	3	889	AF
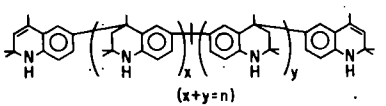 (x+y=n) MW=386+(173)$_n$	0	386	W*
	1	559	AC*
	2	732	AG*
	3	905	AK*
	4	1078	AN*
	5	1251	AO

SERIES COMPOSITION	n	MOLECULAR WEIGHT[a]	LC PEAK[b]
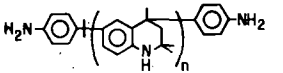 MW=226+(173)$_n$	0	226	B*
	1	399	I
	2	572	R
	3	745	Y,Z
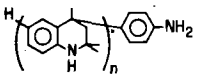 MW=93+(173)$_n$	1	266	H*
	2	439	R*
	3	612	Y,Z*
	4	785	AD, AE*
	5	958	AG
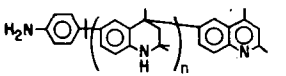 MW=290+(173)$_n$	0	290	C*
	1	463	I
	2	636	R
	3	809	Y,Z
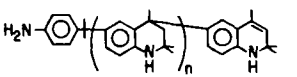 *OR* 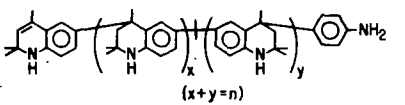 (x+y=n) MW=306+(173)$_n$	0	306	L*
	1	479	(S; Y,Z)[c]
	2	652	AA
	3	825	AF
	4	998	AI
	5	1171	AM

POLYMER CHARACTERIZATION BY ELECTROHYDRODYNAMIC IONIZATION MASS SPECTROMETRY,

S.-T. F. LAI,† K. W. CHAN, AND KELSEY D. COOK*, School of Chemical Sciences and Materials Research Lab, University of Illinois, Urbana, IL 61801

In studies to date employing electrohydrodynamic ionization mass spectrometry (EHMS)[1], there has been little evidence of any fragmentation, except for ion dissociation and solvolysis. Even these reactions are not a consequence of EH ionization, but take place (along with other typical solution chemistry) prior to EH sampling. In this regard, EH "ionization" is something of a misnomer; ionization actually takes place by dissociation or ion attachment in the liquid phase. Ions in solution are subsequently sampled via the action of a strong electric field resulting from a ∿ 4 - 9 kV potential applied between the capillary containing analyte solution and a surrounding extraction plate.

In order for EHMS to be a useful quantitative or semiquantitative tool, the relationship between detected ion intensities and related specie's concentrations must be known. It could be expected that the EH sampling process might discriminate in favor of light ions; i.e., it might be easier to pull light ions from solution than heavier ones. Additional complications arise from the chemistry of solvation and ion attachment or dissociation, which may vary substantially for different analytes.

To obtain some insight into the mass sampling range and the dependence on mass of EHMS sampling efficiency, we obtained spectra of a group of polyethylene glycols (PEG's) in glycerol solution. These samples do not ionize by dissociation in glycerol. It was found, however, that they do freely associate with sodium or lithium ions present as supporting electrolyte (NaI or LiCl). This is not surprising, because cyclic analogs of polyethylene glycols (crown ethers) are also known to strongly bind alkali cations.

The spectra obtained were dominated by ions attributable to attachment of one, two, or three sodium or lithium ions to intact PEG molecules. In general, multiple cationation was favored for heavier molecules (Figure 1), fortuitously lowering the mass-to-charge ratio at which heavy ions were detected. To test the possibility that singly charged heavy ions were not efficiently sampled, ion intensities attributable to each PEG n-mer were summed (weighted according to isotopic contributions; resolution was insufficient to resolve isotope peaks beyond ∿ m/z 600). The resulting total intensity plots (e.g., Figure 2) strongly resembled expected molecular weight distributions, and average molecular weights calculated from these distributions agreed well with averages determined by a standard ASTM end group titration method[2] (Table I). This suggests that, although prefered ionic form varies sensitively with exact analyte identity, total ionization (really, sampling) efficiency is roughly comparable for similar compounds of varying molecular weights. This in turn suggests that EHMS may provide a relatively simple and reliable means of obtaining molecular weight distributions for ionic (or ion attachable) polymers soluble in glycerol. Research directed at easing the vapor pressure limitations that impose the use of low volatility solvents is currently under way.

Two additional classes of ions were detected in the EHMS spectra of PEG's, besides the cationated PEG molecules. Ion series 2, 14, and 28 mass unit lower and 14 and 28 mass units higher than the main series were attributable to trace intra-chain impurities, whose abundances could be estimated from ion intensities (Table II). Finally, ion series of low intensity corresponding to protonated PEG molecules were detected only for samples of low molecular weight, in contrast to the tendency toward multiple cationation of large molecules (Figure 1). This suggests that the EHMS spectra may contain information concerning modes and mechanisms of ion attachment to large molecules. For example, large polyether molecules may spiral around alkali ions, surrounding more ions as chain length increases. Proton attachment may occur only at PEG hydroxyl end groups, which may become unavailable due to intramolecular hydrogen bonding in longer, more flexible chain molecules. Studies with homologous samples are presently under way testing whether this information can be used to test these models and develop others for similar interactions.

---

*Author to whom all correspondence should be addressed.
†Present address: Monsanto Plastics and Resins Co., Indian Orchard, MA 01151
ACKNOWLEDGEMENT:
This work was supported by NIH grant HEW PHS GM 19749

REFERENCES:

1. B. P. Stimpson and C. A. Evans, Jr., J. Electrostatics 5, 411 (1978).

2. American Soc. for Testing Materials, 1970 Annual Book of ASTM Methods, Part 26 (Method D 2849), p. 918 (Philadelphia, 1970).

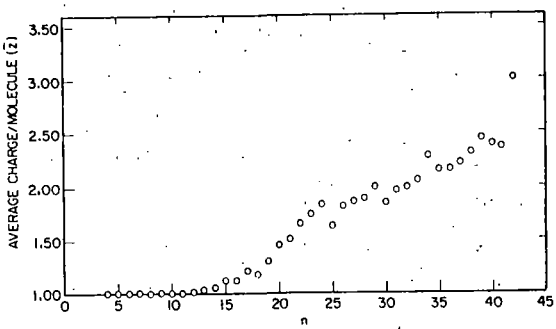

Figure 1: Average charge on a polyethylene gylcol n-mer in NaI-glycerol solution (6 mole % NaI, 3-9 weight % polymer). Data is composite from four samples (see Table 1 for sample specifications).

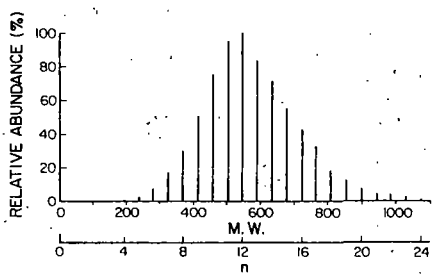

Figure 2: Molecular weight distribution determined by EHMS for polyethylene glycol sample of molecular weight 570-630.

Table 1: Various estimates of average molecular weight ($\bar{M}_n$) of four polyethylene glycol samples.

Manufacturer's Specifications	End Group Titration ($\bar{M}_n$)	EHMS Estimate ($\bar{M}_n$)
380-420	406	406
570-630	605	572
950-1050	1041	962
1300-1600	1396	1365

Table 2: Estimates of total vinyl, methylene, and propylene impurities within the polymer chains of polyethylene glycol sample of molecular weight 380-420 in NaI - glycerol solution.

Impurity	% of Total (Corrected) Intensity
One Vinyl	0.81
One Methylene	1.32
One Propylene	0.39
Two Methylenes	0.87
Two Propylenes	0.41

A GENERAL METHOD FOR ACQUISITION OF LOW INTENSITY MASS SPECTRA AT VERY HIGH MASS, WOODFIN V. LIGON, JR., General Electric Company, Corporate Research and Development, Schenectady, NY 12301

We have previously described the application of a Tracor-Northern Model 1700 pulse height analyzer operating in multichannel scaling (MCS) mode to the acquisition of field desorption mass spectra on the Varian-Mat-731 (ASMS, Seattle, June 1979, Paper WAMP-24). In the present paper we describe the application of this instrumentation to the specific problem of data acquisition above about mass 1500. Data acquisition in the higher mass ranges is hampered by a number of difficulties. Perhaps the most fundamental of these is the sensitivity reduction which arises solely from the need to use higher resolutions. Other contributing problems include frequently quite narrow optimum emitter temperatures and very short total desorption times. The MCS approach has proven particularly successful in overcoming these difficulties. System operation may be outlined as follows: A region of interest is defined by the selection of a particular magnet setting and a particular electric scan width. For example, with the magnet set at 2500 (6kV), it is possible to scan electrically from 2250 to 2750 AMU. A memory block width and channel dwell time are selected to give about 10 samples per nominal mass and a total acquisition time for a single sweep which equals the mass spectrometer electric scan time. For example, to monitor between 2250 and 2750 at 3000 resolution we would select 8192 channels with a dwell of 505μsec. giving a sweep time of 4 seconds and around 13-14 samples per peak. Acquisition would then be started by heating of the anode. The spectra are visible on the scope as acquired and repetitive spectra are automatically summed to give signal enhancement. Spectra are observed, therefore, to grow in. Required changes in tuning or anode temperature are immediately apparent to the operator and can be made without interfering with acquisition. After the FD spectrum is acquired, an EI spectrum of an appropriate Fomblin fluid[R] is acquired under exactly the same conditions and used for mass reference.

Figure 1 shows the result of the acquisition of a 135AMU wide scan from about 1880-2015. The upper trace shows the spectrum of an "unknown" with ions at 1971 and 1952. The lower trace shows the spectrum of Ultramark 2500F over the same range recorded in a second block of memory. Figure 2 shows an expansion of the "unknown" spectrum around mass 1971. Figure 3 shows the acquisition of data at very high mass and high resolution.

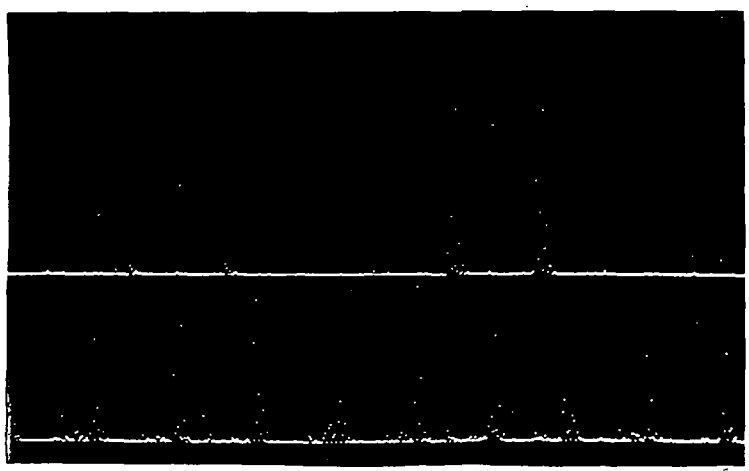

Figure 1

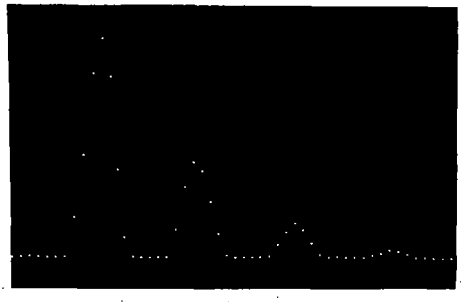

Figure 2

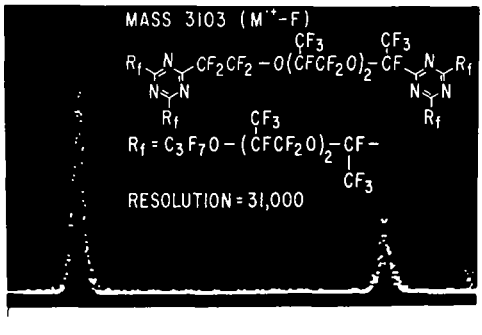

Figure 3

QUANTITATIVE ANALYSIS BY GC-MS OF VOLATILE ORGANIC COMPOUNDS IN WATER UTILIZING ISOTOPE DILUTION TECHNIQUES, HANS GRADE and WOODFIN V. LIGON, JR., General Electric Company, Corporate Research and Development, Schenectady, NY 12301

The purge and trap technique is a well established method for the quantitative analysis of volatile organics in water. This method is subject, however, to numerous efficiency factors which are unique to every compound studied. In this work the solvents, 1,1,1,-tri-chloroethane, methylene chloride, toluene and xylene were simultaneously analyzed by GC-MS using the purge and trap technique combined with isotopic dilution to largely eliminate efficiency considerations. The procedure used is outlined below. A standard consisting of the fully deuterated counterparts of the four solvents of interest was prepared in polyethylene glycol (average molecular weight 400). This non-purgeable, water miscible solvent allows the facile preparation by serial dilution of very dilute solutions of samples with very low water solubility. The use of this solvent eliminates the need to handle very small quantities without introducing a volatile organic diluent. Aliquots of the deuterated standards were added to the unknown samples and the solutions purged with nitrogen in the usual manner. The volatiles were trapped on various adsorbents, thermally desorbed and analyzed by GC/MS. Traps consisting of Tenax, Tenax-charcoal, Tenax-silica gel, and Porapak Q were evaluated, and it was found that Porapak Q is best suited for this analysis because Tenax alone trapped methylene chloride very poorly and the use of traps made of the combined materials resulted in dehydrochlorination of 1,1,1 trichloroethane. Data was acquired by rapid repetitive scans of the mass range of interest. The quantitative measurements were made by a comparison of the areas observed for the respective deuterated and undeuterated components using computer generated selected ion chromatograms. Potential differences in purge and trap and mass spectrometric behavior between the labeled and unlabeled material were evaluated. Using this procedure most errors due to instrumental variations and efficiency considerations are eliminated since the standards are carried through the entire analytical procedure. The limitations of this technique are largely confined to the availability of appropriate labeled standards.

HIGH MASS FIELD DESORPTION STUDIES OF BIOLOGICALLY IMPORTANT MOLECULES

A. Dell, R.A. McDowell and H.R. Morris
Department of Biochemistry, Imperial College, London, U.K.

Many of the important problems in modern-day biological chemistry are concerned with molecules of Mol. Wt. above m/e 1000 and which are therefore outside the mass range of conventional mass spectrometers operating at full accelerating voltage and hence maximum sensitivity. To facilitate the study of such high M.Wt. compounds a high-field (HF) magnet was built for the KRATOS MS50 mass spectrometer at Imperial College, London[1]. This magnet, which is now commercially available, extends the mass range of the MS 50 to m/e 3100 at full sensitivity. At slightly lower sensitivity (using accelerating voltages between 8 kV and 6 kV) polar compounds up to m/e 4000 can be examined successfully. For example we have obtained good spectra on two synthetic amino acid polymers. Signals up to m/e 3478 and 3830 were observed in the FD spectra of these two samples.

For a number of years we have been developing methods for carbohydrate and protein sequence analysis. In conjunction with EI sequencing of acetyl permethyl derivatives of both carbohydrates and glycopeptides, FD is proving to be an invaluable tool for defining the overall sizes of the molecules being examined. Fig. 1 shows the FD spectrum of the deuteroacetyl permethyl derivative of a mixture of neutral carbohydrates from human milk isolated after descending paper chromatography (30 days). The majority of the sample was used for EI studies from which partial sequences could be built up. The FD spectrum, obtained on less than 1 μg of derivatised carbohydrate can be rationalised as follows: m/e 1542 (M+H), 1528 (undermethylated (M+H)), 1564 (M+Na), 1550 (undermethylated (M+Na)), 1580 (M+K), 1566 (undermethylated (M+K)); a second component gives the signals above 1700 which are rationalised thus: m/e 1702, 1705 (M+H, parial exchange of the N-acetyl group has occurred), 1724, 1727 (M+Na), 1740, 1743 (M+K).

Fig. 1: FD of deuteroacetyl permethyl derivatives of milk oligosaccharides.

As part of a long term programme aimed at solving the difficult problem of glycoprotein structure determination, we are examining glycopeptides of unknown structure derived from the blood clotting factor prothrombin[2]. The glycodipeptide consisting of residues 76 and 77 of the prothrombin protein sequence together with the N-glycosidically linked oligosaccharide, has been isolated after extensive proteolytic digestion. A wide variety of techniques are being employed in the structure determination of the complex oligosaccharide and in these studies FD gives information complementary to the sequence data derived by EIMS. For example, after endoglycosidase treatment of the glycopeptide the acetyl permethyl derivative of the unpurified product yielded a good EI spectrum up to m/e 1800. FD on the remains of the permethylated material (<1 μg) gave a cluster of ions in the m/e 2200 region showing multiple undermethylation and losses of methanol. This data indicated that a further two sugar units are present in addition to those observed in the EI analysis.

We are extending our early work on vitamin B_{12} biosynthesis[3] to the study of other important porphyrin pathways. In order to confirm the postulated order of stepwise decarboxylation (rings D, A, B, C are assumed to decarboxylate in that order) of uroporphyrinogen III (uro III) to coproporphyrinogen, labelled uro III has been fed to a cell free enzyme system and the partially decarboxylated intermediates together with the fully decarboxylated coproporphyrinogen have been isolated as the methyl esters of the corresponding porphyrins. FD analysis of these materials isolated after feeding uro III containing $C^2H_2{}^{13}CO_2H$ in the C ring gave the data presented in Table 1. The results clearly show that the label is retained in all the intermediates and is only partially lost in the final step; hence ring C is the last to be decarboxylated.

Table 1

	M	M+1	M+2	M+3	M+4	M+5	M+6
uro	12.5	81	100	98	35	16	6
hepta ester	10	72	100	91	39	15	3
hexa ester	6	61	100	78	38	12	1
penta ester	12	65	100	88	48	15	3
copro	71	100	89	31	13	2	

Normalised intensities of signals in the molecular ion clusters of porphyrins (see text); the uro III contained 91 atom % ^{13}C in the C-ring acetate plus incomplete $^{2}H_2$ labelling.

The capability of our MS 50 for operation at maximum sensitivity between m/e 1000 and m/e 3000 has enabled the examination of very polar high mass compounds previously intractable to FD analysis. Vitamin B_{12} is a typical example of a complex biological compound which is difficult to handle by mass spectrometric methods and previous attempts to obtain FD spectra without laser assistance have been unsuccessful[4]. Using the HF MS 50 a good spectrum was obtained with direct heating of the emitter. The sample gave a molecular ion and an intense fragment at m/e 1350 corresponding to (M-HCN+Na), in addition to lower mass fragment ions.

Bleomycins and related compounds are an important family of complex glycopeptides which are clinically employed in cancer chemotherapy. These very polar molecules pose many problems for structural studies and molecular weight determinations are essential if errors in structure assignment are to be avoided. Despite the polarity and thermal instability of the bleomycins good FD spectra are obtainable using the HF magnet. We are characterising the components of mixtures of bleomycins isolated from Streptomyces and to facilitate this work we are examining purified bleomycins A_2 and B_2, phleomycins D_1 and E and tallysomycin A, all of which have given excellent spectra. Members of the bleomycin and phleomycin families which have terminal guanidino groups in the peptide chain may be readily recognised by a pair of ions due to (M+H) and (M+H-43) (see for example Fig. 2).

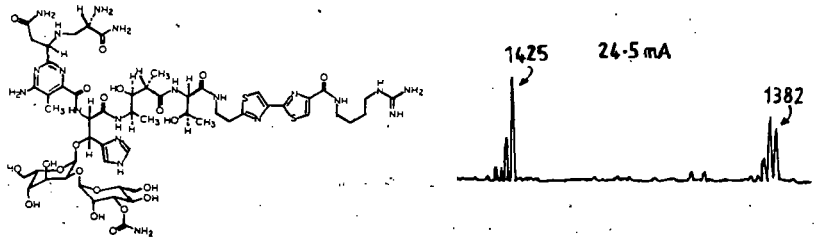

Fig. 2: Structure and FD spectrum of bleomycin B_2.

Bleomycin A_2 gives more complex spectra which we are rationalising by the use of labelled derivatives (e.g. acetyl). This work clearly demonstrates the value of the HF magnet for FD studies of complex antibiotics.

References:

1. H.R. Morris, A.Dell, A.E. Banner, S. Evans, R. McDowell & D. Hazelby, Annual Conf. on Mass Spectrometry and Allied Topics, Washington, 1977, p.73.
2. G.W. Taylor, H.R. Morris, T.E. Petersen & S. Magnusson, Advances in Mass Spectrometry, Vol.8, 1980.
3. H.R. Morris & R. McDowell, ref.1 p.488.
4. H.-R. Schulten & H.M. Schiebel, Naturwissenschaften 65, 223, 1978.

Acknowledgements We wish to thank Professor S. Hecht for samples of the bleomycins and phleomycins.

FIELD DESORPTION (FD) AND FIELD DESORPTION/COLLISION-INDUCED DISSOCIATION (FD/CID) MASS SPECTROMETRY OF MYCOBACTERIAL POLYSACCHARIDES

J. D'Angona[1], M. Linscheid[2], A.L. Burlingame[1,2], H. Yamada[3], C.E. Ballou[3] and A. Dell[4]

[1] Dept. Pharmaceutical Chemistry, University of California, San Francisco, CA 94143
[2] Space Sciences Laboratory, University of California, Berkeley, CA 94720
[3] Dept. of Biochemistry, University of California, Berkeley, CA 94720
[4] Dept. of Biochemistry, Imperial College of Science and Technology, London, England

Field desorption techniques have been shown to be invaluable in obtaining mass spectra on nonvolatile and thermally labile biological samples. We have applied the technique to several members of a family of oligosaccharides containing mannose (Man) and methylmannose (MeMan) having the general structure $Man_xMeMan_yOCH_3$ where x = 0-2 and y = 5-13. These compounds are isolated from growing cultures of Mycobacterium smegmatis (1) where they are thought to be involved in the regulation of fatty acid synthesis. These polymethyl polysaccharides are separated into two overlapping groups, one containing predominantly the smaller isomers and the other the larger ones, by column chromatography and final resolution to single isomers by HPLC and gel filtration.

Samples were dissolved in methanol and applied with a syringe to an FD emitter activated via the high temperature method described by Beckey (2). Emitter currents for these samples on 10 µm wire ranged from 10 to 25 milliamps. All samples were run on a Kratos/AEI MS-9 coupled to a Xerox Sigma 7 computer system operating LOGOS-II (3,4). Mass calibration was via a Hall probe used for controlling and measuring the magnetic field (5).

Each homolog gave a strong ion corresponding to the intact molecule plus sodium at the lower range of heating currents. With the higher heating currents (High Temp), pyrolysis and/or surface reactions predominate causing fragment formation which with these saccharides is fairly orderly and reproducible.

$MeMan_5$-OCH_3 (MM5) which has a molecular weight of 912.4 gives a strong molecular ion at m/z 935.4 $(M + Na)^+$ and fragment ions all of which contain Na at m/z 759, 583, 407 and 231. These ions result from sequential cleavage at the glycosidic bonds from the nonreducing end of the molecule. A further piece of information comes from an ion at m/z 479 which corresponds to the doubly charged molecular ion $(M + 2Na)^{++}$. The intensity of these doubly charged ions throughout the series is usually quite high and thus provides information on the mass of the parent ion(s) in a single or multicomponent mixture.

HPLC-4A, a molecule containing one more methylmannose unit than MM5, has a molecular ion at m/z 1111.5 $(M + Na)^+$. The fragmentation pattern of this molecule is very similar to that of MM5 except that fragmentation occurs starting one methylmannose unit higher and the doubly charged species occurs at m/z 567 as expected.

An oligosaccharide containing 7 methylmannose units terminating in a mannose, HPLC-7B, Man-$MeMan_7OCH_3$, gave a molecular ion at m/z 1450 $(M + Na)^+$. This ion had only 25% of the intensity of its doubly charged species and only about 75% of the intensity of its triply charged species. With these exceptions, its fragmentation occurred at glycosidic linkages and resulted in ions corresponding to the loss of each successive saccharide unit. At the upper temperature limits of this sample, the pyrolysis products of mannose appear at m/z 162 and 126, (Man - H_2O) and (Man - $3H_2O$) respectively.

HPLC 8B, Man_2MeMN_6, containing 2 mannose units on the nonreducing end again gave a molecular ion $(M + Na)^+$ at m/z 1436 and sequential loss of sugar units from the nonreducing end of the chain. Doubly and triply charged ions occurred at m/z 729 and 494 and were about 50% of the intensity of the molecular ion.

The largest oligosaccharide analysed in this series was MMPIV containing one mannose and nine methylmannose units giving a molecular weight of 1778.8 and a molecular ion at m/z 1802 $(M + Na)^+$ (see Fig. 1). Spectra for this molecule were recorded at 4 kV accelerating voltage. The base peak in this spectrum at m/z 912 was about 35% larger than the molecular ion and corresponded to the doubly charged species. Again at

elevated emitter currents, fragmentation at glycosidic linkages occurred; however, bond cleavage occurred from both ends of this molecule, giving two series of fragment ions. An ion at m/z 1087 corresponded to the doubly charged species of $ManMeMan_{11}$-OCH_3 with m/z 2154 $(M + Na)^+$. This was further supported by evidence of the fragmentation of this higher molecular weight saccharide resulting in ions at m/z 1992 and 1815, corresponding to the loss of one and two sugars from its nonreducing end. Final confirmation came from spectra of the sample obtained from an MS-50 with a high field magnet and scanning to 2350 showing ions at m/z 2154 and 1992.

FD-CID B/E linked scan spectra were obtained on MMPIV giving ions at m/z 1770 $(M + Na)^+$-CH_3OH and 180 Man^+, which were of very low intensity. The necessity for operation at 4 kV accelerating voltage is undoubtedly a drawback in producing useful CID spectra on these high molecular weight compounds because of reduced instrument sensitivity.

Clearly, because no derivatization was required, and fragmentation occurred primarily at glycosidic linkages, normal FD mass spectrometry provides a suitable method for sequencing these carbohydrate oligomers.

Acknowledgement: This work was supported by National Institutes of Health, Division of Research Resources Grant RR00719.

References

1. H. Yamada, R.E. Cohen and C.E. Ballou, J. Biol. Chem. 254, 1972-1979 (1978).

2. H.D. Beckey, Principles of Field Ionization and Field Desorption Mass Spectrometry, Pergamon Press, Oxford, 1977, pp. 68-72.

3. A.L. Burlingame, D.H. Smith, T.O. Merren and R.W. Olsen, in Computers in Analytical Chemistry, Vol. 4 in Progress in Analytical Chemistry Series, C.H. Orr and J.A. Norris, eds., Plenum Press, NY, 1970, pp. 17-38.

4. A.L. Burlingame, R.W. Olsen and R.V. McPherron, in Advances in Mass Spectrometry, Vol. 6, A.R. West, Ed., Applied Science Publishers, London, 1974, pp. 1053-1059.

5. H. Kambara, F.C. Walls, R.V. McPherron, K. Straub and A.L. Burlingame, 27th Annual Conference on Mass Spectrometry and Allied Topics, Seattle, WA, 1979, pp. 184-185.

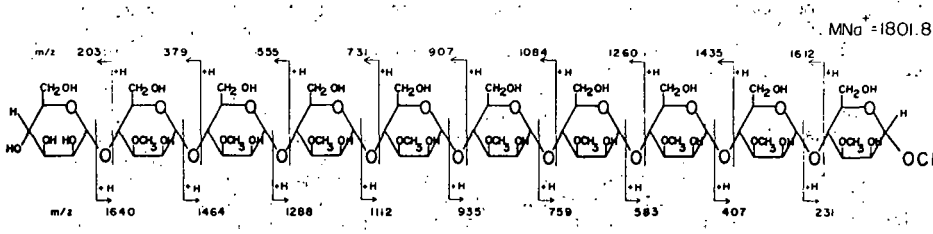

PRIMARY FRAGMENTATION PATHWAYS FOR FIELD DESORPTION MASS SPECTROMETRY OF MAN_3MEMAN_9-OCH_3

FORMATION OF COMPLEXES WITH MULTIVALENT IONS AS A MEANS OF EXTENDING THE MASS SCALE IN FDMS

Gordon W. Wood and Wing Fung Sun

Department of Chemistry, University of Windsor

Windsor, Ontario, CANADA N9B 3P4

For molecules which ionize with difficulty in FDMS, cationization is a useful alternative mode of ion formation. We now report the detection of doubly-charged ions formed by cationization of polar organic molecules with Ba^{2+} and Ca^{2+} ions.

Desorption of an equimolar mixture of sucrose (M = 342) and $Ba(NO_3)_2$ at 16 mA yielded four doubly-charged ions composed of Ba^{2+} with 1-4 molecules of sucrose. These underlined ions, which carry 70% of total current, are presented as monoisotopic ^{138}Ba species below.

m/z	240	411	542	582	753	(884?)
%	13	79	41	100	55	66

The raw data are considerably more complicated since at least the 5 major Ba isotopes (^{134}Ba - ^{138}Ba) are normally recorded, with half-integral mass separation for the doubly-charged ions.

Similar results from a trisaccharide, raffinose, and a tetrasaccharide, stachyose, are summarized in the Tables. For raffinose, M + Ba^{2+} is the base peak and the second most intense peak corresponds to fragmentation (loss of 162 = $C_6H_{10}O_5$) from a 2M + Ba^{2+} parent. With stachyose, fragmentation becomes more significant. Peaks corresponding to loss of mono-(C_6), di-(C_{12}), and tri-saccharide (C_{18}) units are seen.

Polyethylene glycols (PEG) have also been shown amenable to this form of cationization. Thus, PEG 1000, an oligomeric mixture of $H(OCH_2CH_2)_nOH$ with average n of 21-23 and M of 950-1050, is cationized by Ca^{2+} from the iodide. Results of an FDMS experiment on this mixture are shown in bar graph form opposite. The highest oligomer detected, corresponding to n = 30, M = 1338, has m/z 689 for the dominant isotope ^{40}Ca.

Extension of this method to oligomers and sugars of higher molecular weight is now underway. Reduced accelerating voltage promises to further extend the accessible mass range. Trivalent ions are also being evaluated.

FDMS of Raffinose + $Ba(NO_3)_2$

$C_{18}H_{32}O_{16}$, M = 504. 20mA.

m/z	%	
321	100	$M + Ba^{2+}$
492	79	$2M - 162 + Ba^{2+}$
527	6	$M + Na^{+}$
573	19	$2M + Ba^{2+}$
704	27	$M + Ba(NO_3)^{+}$
825	12	$3M + Ba^{2+}$

(Data recalculated to ^{138}Ba)

FDMS of Stachyose + $Ba(NO_3)_2$

$C_{24}H_{42}O_{21}$, M = 666. 18mA.

m/z	%	
163	17	$C_6H_{11}O_5$
402	40	$M + Ba^{2+}$
483	10	$2M - C_{18} + Ba^{2+}$
573	15	$2M - C_{12} + Ba^{2+}$
645	22	
654	15	$2M - C_6 + Ba^{2+}$
689	25	$M + Na^{+}$
735	100	$2M + Ba^{2+}$
749	31	
816	69	$3M - C_{18} + Ba^{2+}$
(906)	39	$3M - C_{12} + Ba^{2+}$

(Data recalculated to ^{138}Ba)

PEG 1000 + CaI_2 FDMS, 9-11mA

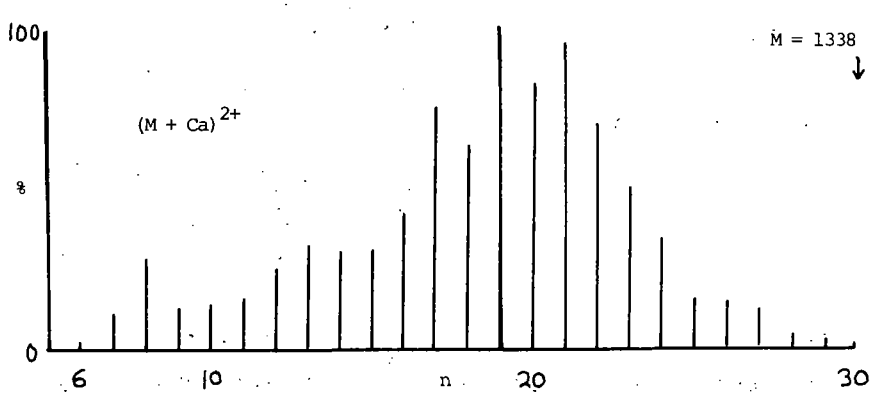

RAMOC1 KINETIC ENERGY RELEASE IN DISSOCIATIVE ELECTRON CAPTURE PROCESSES OF SULFURYL HALIDES, JIA-SHEN WANG and J. L. FRANKLIN, Dept. of Chem., Rice Univ., Houston, TX 77001

The sulfuryl halides, SO_2F_2, SO_2Cl_2, and SO_2ClF form several ions by dissociative electron capture. The ionization efficiency curves are determined for each process. Where the ion intensity was great enough the kinetic energy of the ion was measured over the greater part of the electron energy of the resonance. In most instances the kinetic energy of the ion increased linearly with electron energy over the range of the resonance. Extrapolation to zero kinetic energy release gives the electron energy corresponding to the heat of the dissociation reaction. The kinetic energy released in the formation of F_2^- and Cl_2^- was only slightly greater than that predicted by the quasi-equilibrium theory as would be expected from the fact that the molecule had to change its configuration during dissociation. Essentially all of the excess energy was released in translation when SO_2F^- was formed. F^- from SO_2F_2 and Cl^- from SO_2Cl_2 are formed in two separate resonances, and the kinetic energy lines extrapolate to thermal appearance potentials (ΔH_r) corresponding to the formation of SO_2 and the halogen atom. The ΔH_r for these reactions as well as that for Cl_2^- at their higher energy resonances appear to correspond to an electronic transition for SO_2 of 2.5 ev.

Time Resolved Appearance Potentials and Breakdown Curves by Trapped Ion Mass Spectrometry

Lifshitz, Chava, Dept. of Physical Chemistry,
The Hebrew University of Jerusalem, Israel.

We are employing in Jerusalem, since 1972, the method of Trapped Ion Mass Spectrometry (TIMS) for the measurement of time-resolved appearance potentials by the semilog method. In TIMS ions are trapped in an electron space charge for periods up to ∿2 msec.

Our attention has been devoted mainly to systems for which a large "kinetic shift" is predicted. We have studied, over the years, fragmentations in benzene[1], 1,5-hexadiyne[2,3], chlorobenzene[3] and - more recently - allene, pyridine and cyclo-octatetraene.

Following our early measurements on benzene[1], our method was adopted by Gordon and Reid[4] who re-measured benzene and also benzonitrile.

Since 1976 we have tried to treat kinetic shifts through analysis of time resolved breakdown graphs[3,5]. These are obtained from high-quality normalized second-derivative electron impact ionization efficiency curves, measured at different times following the ionization act.

The method of time-resolved breakdown graphs has been adopted by Stockbauer and Rosenstock for photoion-photoelectron coincidence (PIPECO) in their studies of kinetic shifts in allene[6], chlorobenzene[7], bromobenzene[8] and benzonitrile[8].

At this point it seems worthwhile to review the status of the TIMS method. A kinetic shift of 1.5 eV for $k(E) = 10^5 sec^{-1}$ was measured by us[1] for the reaction in benzene,

$$C_6H_6^+ \rightarrow C_6H_5^+ + H \qquad (1)$$

The currently accepted value for E_o based on the most recent value for ΔH_f (phenyl ion), is in excellent agreement with our earlier result, $E_o = 3.6 \pm 0.2$ eV.

More recently, we have observed[2,3] that the 1,5-hexadiyne ion is completely dissociated according to reaction (1) at times longer than a millisecond and at the threshold energy for ionization of the neutral. Isomerization of the 1,5-hexadiyne ion to the benzene ion structure prior to dissociation to form the phenyl ion has been invoked[2,3]. A similar conclusion was drawn recently[9], on the basis of measurements of absolute fragmentation rates in the microsecond range, by the photoion-photoelectron coincidence method.

The fragmentation reaction,

$$C_8H_8^+ \rightarrow C_6H_6^+ + C_2H_2 \qquad (2)$$

has the advantage that the product ion thermochemistry is accurately known. Several C_8H_8 isomers have previously been studied[10,11]. We have determined time resolved appearance potentials and breakdown graphs for this system, which will be discussed at the meeting, in greater detail.

An additional option is the determination of metastable peak shapes over a wide time range. This option has been employed for the reaction,

$$C_5H_5N^+ \rightarrow C_4H_4^+ + HCN \quad (3)$$

in pyridine.

Accurate measurements of ion-lifetimes are available now, for energy selected ions, by the PIPECO technique. Kinetic energy release measurements via IKES are also available. What seems to be needed, are accurate appearance potential measurements for very slow fragmentations. While TIMS does have the necessary time range, it employs electron impact and does not have therefore the necessary energy resolution. Appearance potential measurements for slow fragmentations are needed where the reactant ions are produced by photoionization. This can conceivably be achieved by pulsing the light-source and trapping the resultant photoions for several hundred microseconds prior to ejection from the ion-source for mass analysis.

REFERENCES

[1]C. Lifshitz, A.M. Peers, M. Weiss and M.J. Weiss, Advan. Mass Spectrom., 6 (1974) 871.
[2]C. Lifshitz and S. Gefen, Int. J. Mass Spectrom. & Ion Phys., in press.
[3]C. Lifshitz, M. Weiss and S. Landau-Gefen, Paper presented at the 25th Annual Conference on Mass Spectrometry, Washington, D.C., June 1977.
[4]S.M. Gordon and N.W. Reid, Int. J. Mass Spectrom. & Ion Phys., 18 (1975) 379.
[5]C. Lifshitz, 7th International Mass Spectrometry Conference, Florence, Italy (1976); Advan. Mass Spectrom. 7A (1978) 3.
[6]R. Stockbauer and H.M. Rosenstock, Int. J. Mass Spectrom. & Ion Phys. 27 (1978) 185.
[7]H.M. Rosenstock, R. Stockbauer and A.C. Parr, J. Chem. Phys. 71 (1979) 3708.
[8]H.M. Rosenstock, R. Stockbauer and A.C. Parr, J. Chem. Phys., submitted.
[9]T. Baer, G.D. Willett, D. Smith and J.S. Phillips, J. Chem. Phys. 70 (1979) 4076.
[10]J.L. Franklin and S.R. Carroll, J. Am. Chem. Soc. 91 (1969) 5940.
[11]D. Smith, T. Baer, G.D. Willett and R.C. Ormerod, Int. J. Mass. Spectrom. & Ion Phys. 30 (1979) 155.

SELF-SCAVENGING OF ELECTRONS IN METHYL IODIDE*

Cornelius E. Klots and R. N. Compton

Chemical Physics Section, Health and Safety Research Division, Oak Ridge National Laboratory, Oak Ridge, Tennessee 37830

As is well-known, the methyl iodide monomer attaches near-zero energy electrons, with a large cross-section, to yield I^-. We have found that this can be generalized. Van der Waals polymers of methyl iodide attach low-energy electrons in an analogous fashion:

$$e_o + (CH_3I)_n \rightarrow I^-(CH_3I)_{n-1} + CH_3 \quad . \tag{1}$$

At higher energies, near 4.8 and 6.2 eV, a distinctly different attachment mechanism sets in. The net reaction can be written:

$$e + (CH_3I)_n \rightarrow I^-(CH_3I)_{n-2} + (2CH_3 + I) \quad . \tag{2}$$

Figure 1 illustrates the $I^-(CH_3I)$ signal vs electron energy, originating from the trimer.

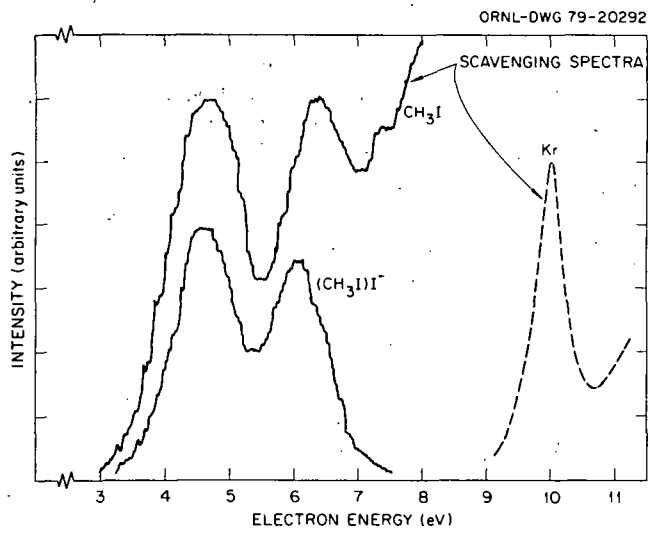

Fig. 1. Threshold excitation spectrum of methyl iodide, and the self-scavenging products from methyl iodide trimers, each as a function of electron energy.

The energies at which this mechanism occurs coincide with the first two peaks in the threshold excitation spectrum of methyl iodide, as obtained using the SF_6 scavenger technique. Evidently the threshold excitation of one member of a van der Waals cluster can be followed by attachment of the scattered electron to the rest of the cluster, as in reaction (1).

This mechanism can be thought of as attachment via a Feschbach resonance, but of a rather novel sort. The usual picture of such resonances involves excitation of an atom (or molecule) and simultaneous electron capture by the excited species. In the present instance, excitation and capture are thought to occur in separate regions of a van der Waals cluster.

Further details are given elsewhere.[1]

---

*Research sponsored by the Office of Health and Environmental Research, U.S. Department of Energy under contract W-7405-eng-26 with the Union Carbide Corporation.

[1] C. E. Klots and R. N. Compton, Chem. Phys. Lett. (in press).

Photoelectron-Photoion Coincidence Study of the Bromobenzene Ion

Roger Stockbauer
Surface Science Division
National Bureau of Standards
Washington, D.C. 20234

Henry Rosenstock
Radiation Physics Division
National Bureau of Standards
Washington, D.C. 20234

Albert C. Parr[†]
Dept. of Physics and Astronomy
University of Alabama
University, Alabama 35486

The technique of variable time photoelectron-photoion coincidence mass spectrometry has been applied to the fragmentation of bromobenzene ion producing a phenyl ion. A detailed analysis of the variation of the breakdown curve with parent ion residence time was performed. The results lead to ΔHf_0° (phenyl ion) = 270 ± 1 kcal/mol, in agreement with results recalculated from an earlier study on chlorobenzene. This, combined with other photoionization results leads to Hf_0° (phenyl radical) = 83 ± 3 kcal/mol, in agreement with the value obtained from neutral kinetics. The results will be compared with those of Baer, et al. (J. Chem. Phys. 64, 2460 (1976)).

The analysis leads to a rate-energy dependence for the fragmentation process and an equivalent 1000 K Arrhenius preexponential factor of $\sim 9.4 \times 10^{14}$ sec^{-1}, which may be compared to the value 2×10^{15} sec^{-1} for the analogous neutral process. The possible contribution of spin orbit splitting is discussed.

The complete results of this work has been accepted for publication in the Journal of Chemical Physics.

[†]Intergovernmental Personnel Act Appointee at the National Bureau of Standards, 1978-1980. Present address: National Bureau of Standards, Washington, D.C. 20234

RAMOC7 TWO-LASER MULTIPHOTON DISSOCIATION OF IODOBENZENE CATION, J. D. HAYS, J. P. HONOVICH, N. B. LEV and R. C. DUNBAR, Chemistry Department, Case Western Reserve University, Cleveland, OH 44106

The simultaneous irradiation of gas-phase iodobenzene ions with 610nm visible light and 10μ infrared light results in photodissociation of the ions at a rate strikingly faster than the photodissociation observed with either laser used separately. This simultaneous visible-infrared process has important implications for the nature of multiphoton events and relaxation processes in gas-phase species, and may represent the first observation of a combined visible-IR multiphoton dissociation. The IR wavelength dependence reflects a broad maximum around 10.2μ which is consistent with IR absorption by a vibrationally excited iodobenzene ion. At fixed itensity, the visible intensity dependence of photodissociation is somewhat stronger than linear, but much weaker than quadratic. The IR intensity dependence is weaker than linear. The pressure dependence is strong at low pressure, but becomes weaker at high pressure (the extent of dissociation decreasing with increasing pressure). Modelling indicates that a balance is rapidly established between IR excitation and relaxation such that the ion is maintained within a reasonably narrow energy range, from which single-photon photodissociation by the visible laser can proceed.

This experiment has useful implications for the study of properties of vibrationally excited species and vibrational relaxation processes.

TRANSMISSION CHARACTERISTICS OF COLLIMATED HOLE THRESHOLD PHOTOELECTRON DETECTORS

T. Hsieh, J. P. Gilman, M. J. Weiss, and G. G. Meisels, Chem. Dept.
University of Nebraska, Lincoln, NE 68588
and
P. M. Hierl, Chem. Dept., University of Kansas, Lawrence, KS 66045

Threshold photoelectron spectroscopy (TPES), a technique in which one detects only those photoelectrons which are produced with nominally zero kinetic energy (i.e., threshold electrons) by a photon beam whose energy can be varied over a range of ionization processes, is a form of ion spectroscopy which provides certain advantages over the traditional form of PES with its fixed photon energy. Moreover, detection of the photoion produced in coincidence with the threshold electron provides a method (TPECPI - threshold photoelectron coincidence photoionization) by which ions can be prepared in selected internal states and their subsequent reactions investigated.

In TPES and TPECPI experiments, the detection of threshold photoelectrons is usually accomplished by a steradiancy analyzer, the principle of which was proposed by Baer et al.,[1] and the transmission characteristics of which have been discussed by Spohr et al.[2] The major problem with a purely angular discriminator of this type is that the transmission function never goes completely to zero as the electron energy increases because those energetic electrons whose initial velocity vectors are parallel to the extraction field will be collected regardless of their energy. Knowledge of the analyzer transmission function is required to permit correction for the effect of energetic electrons.

Based upon geometric calculations for the cylindrical-channel angular discriminator, Spohr et al.[2] have derived an integral equation for the transmission function of steradiancy analyzers. In this work, we show that their equation can be solved in terms of complete elliptic integrals of the first and second kind which, in turn, can be expanded as power series to give the transmission function in analytic form. Convolution of the analyzer transmission function with the photon energy distribution gives the instrument function, which is then compared with experimental results.

If E_i is the initial kinetic energy of the photoelectron and E_g the kinetic energy it gains through acceleration, the fraction $T(E_i/E_g)$ of photoelectrons transmitted through a cylindrical-channel analyzer of diameter d and length ℓ can be shown to be given by the expressions

$$T(x) = 1 - c_1\left(\frac{x}{x+1}\right)^{\frac{1}{2}}\left[1 - \frac{c_1^2}{8}\left(\frac{x}{x+1}\right) - \frac{c_1^4}{64}\left(\frac{x}{x+1}\right)^2 - \frac{5c_1^6}{1024}\left(\frac{x}{x+1}\right)^3 - \ldots\right]$$

if $x \equiv E_i/E_g < (d/\ell)^2$, and

$$T(x) = c_2\left(\frac{x+1}{X}\right) + c_2^2\left(\frac{x+1}{x}\right)^2 + \frac{5}{2}c_2^3\left(\frac{x+1}{x}\right)^3 + \ldots$$

if $x > (d/\ell)^2$, where $c_1 = (1 + \ell^2/d^2)^{\frac{1}{2}}$ and $c_2 = 1/8c_1^2$. The functions given by these equations for T(x) are plotted vs. the energy ratio x for various values of the ratio ℓ/d in Figure 1.

Recent Photoelectron - Photoion Coincidence Studies on Benzonitrile and Pyridine Fragmentation

H. M. Rosenstock
Radiation Physics Division
National Bureau of Standards
Washington, D.C. 20234

Roger Stockbauer
Surface Science Division
National Bureau of Standards
Washington, D.C. 20234

Albert C. Parr†
Dept. of Physics and Astronomy
University of Alabama
University, Alabama 35486

The primary fragmentation processes of benzonitrile and pyridine ions have been studied by photoelectron-photoion coincidence techniques with variable ion residence time. The primary processes involve loss of HCN, resulting in the formation of $C_6H_4^+$ and $C_4H_4^+$ ions with a cyclic structure. Both processes show a significant kinetic shift. The fragmentation thresholds and activated complex parameters are deduced from the breakdown curves. The energy dependence of the fragmentation rates is established and critically compared with earlier studies by Schulte, Eland and Berkowitz. Some implications with respect to benzene fragmentation are discussed.

The results for benzonitrile will appear in the Journal de Chimie Physique special issue on molecular ion studies. The results for pyridine are being prepared for publication.

†Intergovernmental Personnel Act Appointee at the National Bureau of Standards, 1978-1980. Present address: National Bureau of Standards, Washington, D.C. 20234

Triply Differential Photoionization Studies of Small Molecules*

Albert C. Parr†
University of Alabama
University, Alabama 35486

Roger Stockbauer
Surface Science Division
National Bureau of Standards
Washington, D.C.

J. L. Dehmer
Argonne National Laboratory
Argonne, Illinois 60439

B. E. Cole and D. L. Ederer
Synchrotron Ultraviolet Radiation Facility
National Bureau of Standards
Washington, D.C. 20234

John B. West
Daresbury Laboratory
Science Research Council
United Kingdom

An angle resolved photoelectron spectrometer has been developed for triply differential photoionization studies. By triply differential we mean the measurement of the energy and angular distribution of photoelectrons as a function of incident photon energy. The instrument has been operating for the past year and has more than sufficient resolution to measure vibrational intensity and angular distributions in small molecules.

Several factors make this instrument unique. First, it uses the new high flux normal incidence monochromator at SURF II which provides $\sim 10^{11}$ photons sec^{-1} A^{-1} at 1000 A. Second, fast differential pumping, a light-pipe capillary at the exit slit and a nozzle-jet sample introduction system allows the instrument to operate windowless while maintaining a pressure differential of $\sim 10^5$ between the ionization region and the monochromator. Third, the electron spectrometer has constant focal length entrance optics and high electron throughout for high collection efficiency and low background count rates. Fourth, tne entire experiment is computer controlled through a CAMAC crate which allows efficient accumulation and analysis of a large amount of data with a minimum of effort. Recent results from the instrument include shape resonance affects on vibrational intensity and angular distributions in N_2[1] and CO.[2] Likewise effects of autoionization on intensity and angular distributions in N_2,[3] O_2,[3] CO,[3] and SF_6[3] have been observed. The instrument has been described fully in a recent publication.[4]

*Work supported in part by the Office of Naval Research.

†Intergovernmental Personnel Act Appointee at the National Bureau of Standards, 1979-1980. Present address: National Bureau of Standards, Washington, D.C. 20234

References

1) J. B. West, A. C. Parr, B. E. Cole, D. L. Ederer, R. Stockbauer, J. L. Dehmer, J. Phys. B 13, L105 (1980).
2) R. Stockbauer, B. E. Cole, D. L. Ederer, J. B. West, A. C. Parr, and J. L. Dehmer, Phys. Rev. Lett. 43, 757 (1979). B. E. Cole, D. L. Ederer, R. Stockbauer, K. Codling, A. C. Parr, J. B. West, E. D. Poliakoff, J. L. Dehmer, J. Chem. Phys., to be published.
3) Being prepared for publication.
4) A. C. Parr, R. Stockbauer, B. E. Cole, D. L. Ederer, J. L. Dehmer, and J. B. West, Nucl. Instrum. Meth. (in press).

Assuming that the photon energy distribution is triangular, we have convoluted the photon bandwidth with the equations for T(x) to obtain the overall instrument function for our threshold photoelectron spectrometer. Typical results are shown in Figure 2.

Calculated instrument functions for various sets of instrumental parameters clearly show that the most important factor affecting the overall energy resolution is the photon energy bandwidth. The value of the parameter ℓ/d is less important in determining the energy resolution, and the magnitude of the electrostatic field applied in the photoionization region has little effect on instrumental resolution (except when ℓ/d is very small).

A more complete account of this work is scheduled for publication in the International Journal of Mass Spectrometry and Ion Physics.

REFERENCES

1. T. Baer, W. B. Peatman, and E. W. Schlag, Chem. Phys. Lett. 4, 243 (1969).

2. R. Spohr, P. M. Guyon, W. A. Chupka, and J. Berkowitz, Rev. Sci. Instr. 42, 1872 (1971).

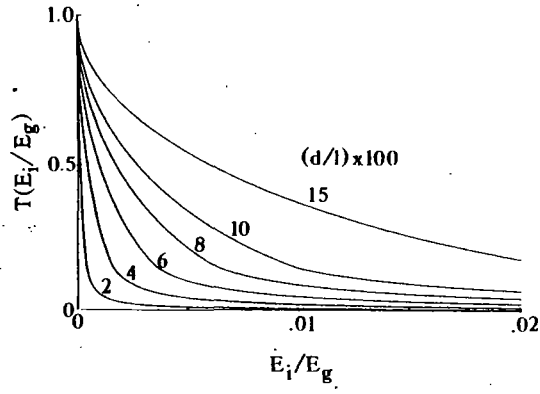

Figure 1: Transmission Function, ($T(E_i/E_g)$, vs. the ratio E_i/E_g, for the cylindrical-channel angular discriminator.

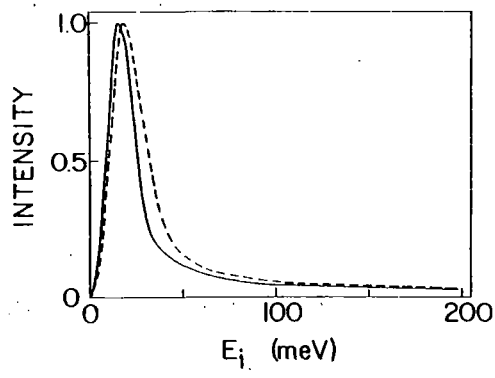

Figure 2: Experimental (dashed line) and calculated (solid line) electron transmissions at ℓ/d= 40, E_g=10 eV, 13 meV photon energy bandwidth, and 14 eV photon energy.

RAMOC9 MULTIPLE TRANSITION STATES IN ION-MOLECULE REACTIONS; A UNIFIED STATISTICAL THEORY APPROACH, WALTER J. CHESNAVICH, LEWIS BASS, and MICHAEL T. BOWERS, Dept. of Chem., Univ. of Ca., Santa Barbara, CA 93106

It has recently been recognized that rate constants of unimolecular ion-molecule reactions occurring on surfaces with little or no reverse activation energy are described by saddle point transition states (with properties resembling the reactant ion) while product kinetic energy distributions of these same reactions are described by orbiting transition states (with properties resembling the products).[1] These have been puzzling results and have brought into question whether or not microscopic reversibility is being properly accounted for in the theoretical treatments used to date. In this talk, the problem will be approached from the perspective of Unified Statistical Theory and it will be shown that, when properly formulated, statistical theory can account for processes occurring on surfaces with multiple transition states. In fact, in unimolecular reactions occurring on surfaces without significant reverse activation barriers, two transition states always naturally occur; one an orbiting TS and one a saddle point TS. The unified theory will be applied to reactions occurring on the $C_4H_8^+$ surface and compared with experimental rate constants, product distributions and product kinetic energy distributions measured by PIPECO, ICR, and Mass Spectrometry.

1. For examples and a discussion see W. J. Chesnavich and M. T. Bowers, J. Am. Chem. Soc. 99, 1705(1977).

RAMOC10 THE COINCIDENCE SPECTRUM FOR LOSS OF ACETIC ACID FROM 2-BUTYL ACETATE AND THE INLET TEMPERATURE DEPENDENCE OF THE STEREOSELECTIVITY FOR THAT LOSS, MARK M. GREEN, RICHARD McCLUSKEY, LOYD BUMM AND JÜRGEN VOGT, Departments of Chemistry, Clarkson College of Technology, Potsdam, NY 13676; Polytechnic Institute of New York, Brooklyn, NY 11201; Physikalisch-Chemisches Institut der Universität Basel, 4056 Basel, Switzerland.

We have carried out a normal mode analysis for 2-butyl acetate and thereby calculated the Boltzmann distribution for this molecule at various temperatures from 300°K to 1500°K. The coincidence energy band for the process 2-butyl acetate molecule ion loses acetic acid has also been determined and corresponds to the lowest energy band in the photoelectron spectrum. This coincidence band has been convoluted with the various Boltzmann distributions corresponding to varying temperatures of the ion source of the mass spectrometer in which the stereoselectivity for loss of the diastereotopic hydrogens (forming acetic acid) at C-3 of 2-butyl acetate was measured. The energy band products of these convolutions had average energies corresponding to thermal Boltzmann distributions approximately 500°K higher than the source temperatures. These were designated the quasi temperatures of the molecular ions undergoing the loss of acetic acid. The natural logorithm of the ratio of rates corresponding to the stereoselectivity was plotted against the inverses of the quasi temperatures to yield a good straight line with a slope and intercept quite reasonable for the conformational factors attendant to the rearrangement under observation.

FLUORESCENCE EXCITATION SPECTRA OF IONS AND NEUTRAL FRAGMENTS OF MOLECULES BY PHOTON IMPACT

A. Tabché-Fouhailé[+], K. Ito[+], H. Fröhlich[++], P. Morin[+], P. M. Guyon[++] and I. Nenner[+]
+ DPC/SPP - Centre d'Etudes Nucléaires de Saclay - BP n°2
91190 GIF sur Yvette.
++ LCAM - Bât. 351 - Université de Paris-sud - 91405 ORSAY cedex
and
LURE - Bât. 209 C - Université de Paris- sud - 91405 ORSAY cedex.

Photoionization processes in N_2, CO and N_2O are investigated in the 10 - 40 eV spectral range using synchrotron radiation from ACO Orsay's storage ring. Selected fluorescence is measured as a function of wavelength.

Experimental

Fluorescence is measured out of a differentially pumped cell filled with $\sim 5.10^{-3}$ torr of gas, as a function of exciting wavelength (1 Å and 0.4Å bandwidth). In order to select fluorescence, appropriate photomultipliers and optical filters are used. Two fluorescence signals are detected simultaneously, at right angles with respect to the incident photon beam. The incident light flux is monitored by a visible photomultiplier mounted behind a sodium salicylate coated window.

Results

1) N_2 and CO : the $A\,^2\Pi_u \rightarrow X\,^2\Sigma_g^+$ and $B\,^2\Sigma_u^+ - X\,^2\Sigma_g^+$ fluorescence spectra of N_2^+ are measured from threshold to 40 eV. Below the B onset, the A - X fluoresence cross section is largely dominated by autoionization of $(2\sigma_u)^{-1}$ nlλ Rydberg levels converging to B into the A $(1\pi_u)^{-1}$ ionization continuum. The signal shows a sharp steplike decrease, when one encompasses the B onset. This can be explained by the contribution of $(2\sigma_u)^{-1}$ nlλ Rydberg levels autoionization to the A cross section, which vanishes beyond the B limit, the nlλ electron being ejected in the B state continuum. Above the B onset, Rydberg series converging to the c $^2\Sigma_u^+$ state of N_2^+ are observed in both (B-X) and (A-X) cross sections ; the branching ratio B/A is estimated to be about 0.15. Lastly, broad structures are observed around 32 eV, in a region where a shape resonance has been observed in the X $^2\Sigma_g^+(3\sigma_g^{-1})$ partial photoionization cross section.

The B $^2\Sigma^+ \rightarrow X^2\Sigma$ and the A $^2\Pi \rightarrow X^2\Sigma$ fluorescence spectra of CO^+ have been measured in the same photon energy range. No autoionizing structure is observed above 19 eV as opposed to N_2. Agreement with "one electron model" theories is satisfactory. The existence of a broad shape resonance around 32 eV in the (B-X) $(4\sigma^{-1})$ partial cross section is confirmed.

These fluorescence excitation spectra are compared to partial photoionization cross section obtained by other techniques such as photoelectron spectroscopy (1-3).The similarities show that the final states of the ion do not interact in a first approximation and the emission distribution does not vary with photon energy. This agreement between both methods has been observed for N_2 and CO. However above 25 eV, there is a large discrepancy in N_2 unexplained at the present time.

2) N_2O : Figure 1 shows the fluorescence excitation spectrum in the 3000 - 6000 Å emission region, when N_2O is excited in the 16 - 21 eV range. The $\tilde{A}\,^2\Sigma^+ \rightarrow \tilde{X}\,^2\Pi$ fluorescence from N_2O^+ is observed below 756 Å, the $\tilde{A}$ (0,0,0) onset. A step is shown to occur at the $\tilde{A}$ (1,0,0) level. Beyond, only four autoionizing Rydberg series converging to N_2O^+, $\tilde{C}\,^2\Sigma_u^+$ are shown to decay in the $\tilde{A}\,^2\Sigma^+$ state of the ion, compared to the five series observed in photoionization mass spectrometry measurements (4). Figure 2 shows two fluorescence excitation spectra in the 3300 - 6000 Å and the 1850 - 3000 Å emission regions respectively, when N_2O is excited above its first ionization limit, in the 13.5 - 17 eV excitation range. At $\lambda > 756$ Å, structures superimposed on a broad

continuum are observed. They are associated to dissociation of excited N_2O (Rydberg states converging to $\tilde{A}$ and $\tilde{B}$) into excited fragments. This dissociation processes are in competition with autoionization into the $X^2\Pi$ state of N_2O^+.

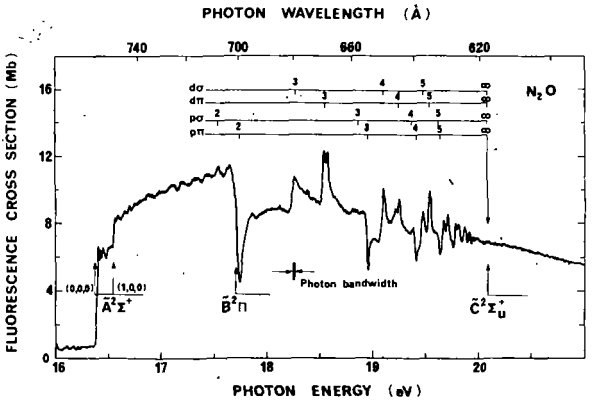

Figure 1 : Fluorescence excitation spectrum in the 3000 - 6000 Å emission range, from 16 to 21 eV photon energy.

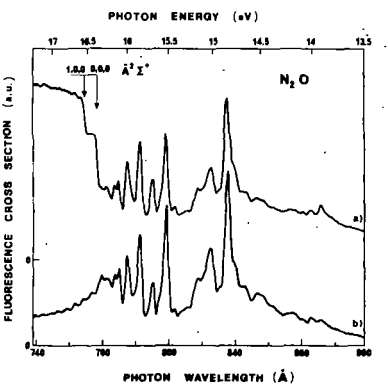

Figure 2 : a) (3300 - 6000 Å) fluorescence excitation spectrum and b) (1850 - 3000 Å) fluorescence excitation spectrum from 740 to 900 Å photon wavelength (13.5 to 17 eV)

References :

1. J. A. R. Samson, G. N. Haddad and J. L. Gardner, J. Phys B, 10, 1749 (1977)
   J. A. R. Samson and J. L. Gardner, J. Electron Spectrosc. 8, 35 (1976).
2. E. W. Plummer, T. Gustafsson, W. Gudat and D. E. Eastman, Phys. Rev. A, 15, 2339 (1977).
3. P. R. Woodruff and G. V. Marr, Proc. Roy. Soc. Lond., A 358, 87(1977).
4. J. Berkowitz and J. H. D. Eland, J. Chem. Phys. 67, 2740 (1977).

SYNTHESIS OF HIGH ISOTOPIC PURITY $^2H_3$-LABELED STANDARDS FOR THE MASS SPECTRAL QUANTITATION OF ESTRADIOL AND ESTRONE

IAN J. MASSEY AND LASZLO TÖKÉS

SYNTEX RESEARCH, 3401 HILLVIEW AVE, PALO ALTO, CA. 94304

Our need to validate radioimmunoassay quantitation of estradiol and estrone levels in edible cattle tissues by the GC-MS-MIS method required the use of suitable standards. We chose to use internal standards rather than external standards since it has been demonstrated that the use of the former significantly improves the accuracy and precision of the method[1]. We have selected deuterium labeled estradiol and estrone as the internal standards for quantitation. The use of isotopically labeled standards can help avoid many of the problems encountered in quantitation. Problems of incomplete extraction and loss during clean up of the compound to be quantitated can be overcome by addition of the standard to the tissue prior to extraction. Incomplete formation of GC-derivatives has no consequence and advantage can be taken of the carrier effect during GC-analysis when using these standards.

Our experience has shown that suitable standards for quantitation in the low picogram range (a) should contain at least three deuterium atoms which are located in positions such that exchange during derivatization and GC-analysis can not occur and (b) must be of very high chemical and isotopic purity. These requirements in conjunction with various synthetic considerations led us to select 16,16,17α-$^2H_3$-estradiol (1) and 14α,15,15-$^2H_3$-estrone (2) as the internal standards.

SYNTHESIS

Both compounds were synthesized starting from estrone. The $^2H_3$-estradiol (1) was obtained by alkaline H/^{2}H exchange of the C-16 protons and $LiAl^2H_4$ reduction of the C-17 keto function followed by back exchange of aromatic deuteriums.

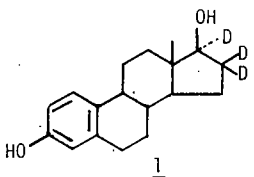

1

1%d_1, 3%d_2, 93%d_3, 3%d_4

The $^2H_3$-estrone (2) was synthesized by a fourteen step sequence which proceeded via the known protected estratetraenediol (3). Deuterioboration of 3 gave a mixture of alcohols 4 (86%) and 5 (13%). Oxidation of 4 and reduction of the resultant ketone with $LiAl^2H_4$ gave a mixture of 15α and 15β-alcohols 6 and 7. This mixture, under carefully controlled reaction conditions was converted to the corresponding mesylates 8. Reduction of the mesylates 8 with $LiEt_3B^2H_4$ gave a mixture of the trideuterio-estradiol derivative 9 and the tetraene 10 which were separated on silver nitrate impregnated silica gel. Removal of the protecting groups from 9 gave the trideuterio-estradiol 11 which was oxidized to the estrone 2. GC-MS analysis of the trimethylsilyl ether of 2 indicated the isotopic purity to be 3%d_2, 96%d_3, 1%d_4. The compound also contained 1% of an inseparable chemical impurity having the same molecular weight as unlabeled estrone. The impurity is probably an unsaturated dideuterio-estrone.

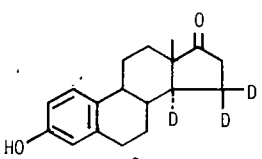

2

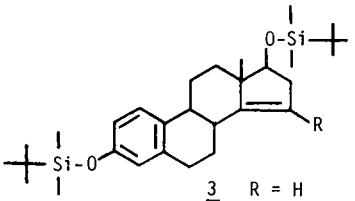

3 R = H

10 R = D

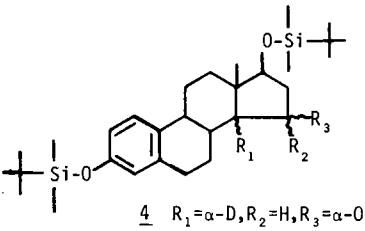

4 R_1=α-D,R_2=H,R_3=α-OH

5 R_1=β-D,R_2=H,R_3=β-OH

6 R_1=α-D,R_2=D,R_3=α-OH

7 R_1=α-D,R_2=D,R_3=β-OH

8 R_1=α-D,R_2=D,R_3=OSO_2CH_3

9 R_1=α-D,R_2=R_3=D

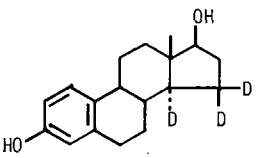

11

REFERENCE

1) B.J. Millard, "Quantitative Mass Spectrometry" Heyden and Sons Ltd., 1978, Chapters 3 and 4.

RAMP2 SYNTHESIS OF DEUTERATED OCTADECENOIC ACID POSITIONAL AND GEOMETRIC ISOMERS. E. A. Emken, R. O. Adlof, W. J. DeJarlais, H. Rakoff and W. K. Rohwedder. Northern Regional Research Center, AR,SEA,USDA, Peoria, IL 61604.

A general synthetic scheme has been developed for preparation of deuterium-labeled octadecenoic acid isomers for use in oral feeding studies with human volunteers. Deuterated cis and trans isomers of 8-, 9-, 10-, 11-, 12-, and 13-octadecenoic acids have been prepared by this procedure. These isomers were labeled with two, four, or six deuterium atoms in the alkenyl portion of the fatty acid chain. Introduction of deuterium was achieved by using tris-(triphenylphosphine) rhodium (I) chloride to catalytically deuterate an appropriate unsaturated aliphatic halide or tetrahydropyranyl ether. The deuterated alkyltriphenylphosphonium halide was prepared and coupled via the Wittig reaction with an appropriate aldehyde ester to form the desired positional cis-octadecenoic acid. Portions of these cis isomers were isomerized with nitrogen oxides to the corresponding trans isomers. Overall yields of deuterated octadecenoic acids were 55%. The isotopic purities based on the average number of deuterium atoms per molecule were 90-98% of theory. Deuterium scattering and exchange during catalytic deuteration resulted in fatty acids containing 70-93% of the desired d_2, d_4, or d_6 species. This scheme provides a practical method for synthesizing relatively large amounts (50-100 g) of chemically pure deuterated fatty acids.

SYNTHESIS OF PUTATIVE PRECURSORS OF SECONDARY NATURAL PRODUCTS LABELED WITH STABLE ISOTOPES [CARBON-13 AND NITROGEN-15],

Edward Leete, Jim McDonell, Joe Porwoll, and Ming-Li Yu, Department of Chemistry, University of Minnesota, Minneapolis, MN 55455

In recent years we have prepared several precursors of natural products which are labeled with two contiguous ^{13}C atoms or with contiguous ^{13}C and ^{15}N atoms. They have unique ^{13}C-NMR spectra due to spin-spin coupling of the contiguous ^{13}C atoms (satellites located on either side of the signals for the single labeled species). The syntheses of some of these compounds are outlined in the following schemes.

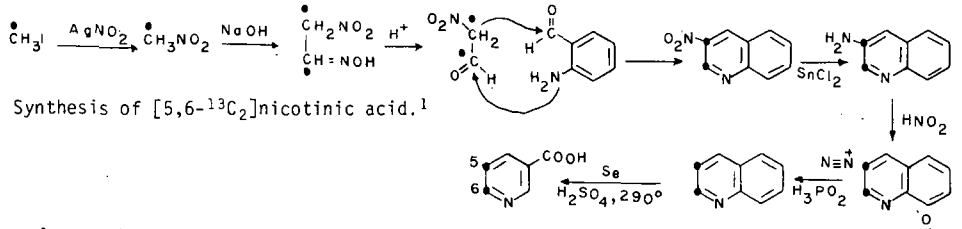

Synthesis of [5,6-$^{13}C_2$]nicotinic acid.[1]

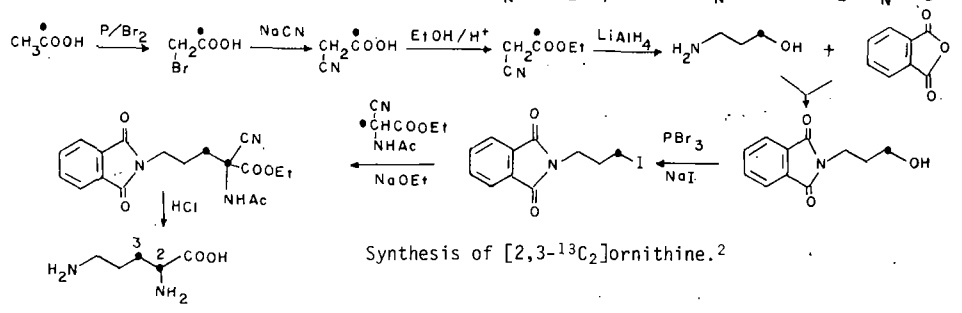

Synthesis of [2,3-$^{13}C_2$]ornithine.[2]

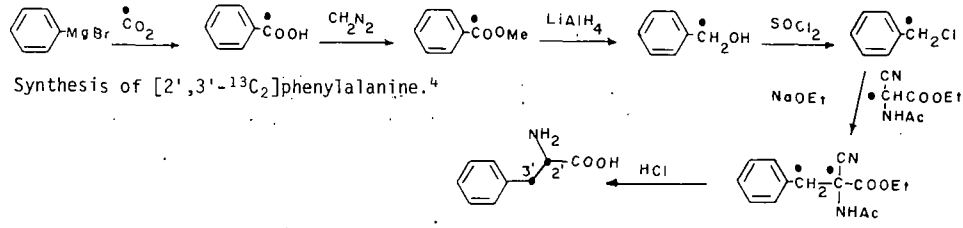

Synthesis of [2',3'-$^{13}C_2$]phenylalanine.[4]

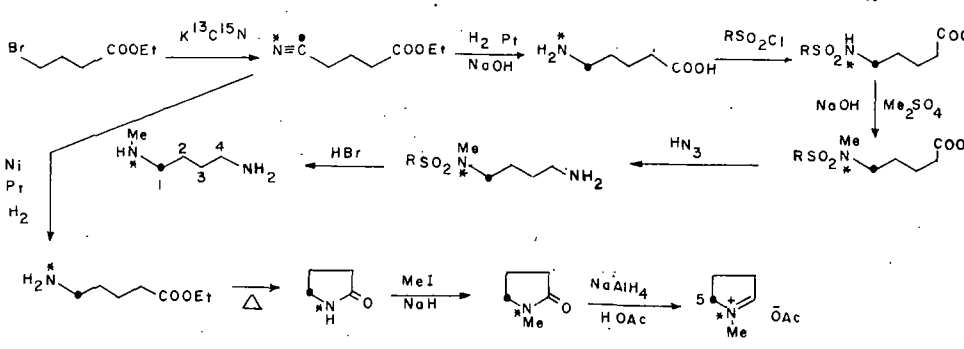

Synthesis of [1-^{13}C,*methylamino*-^{15}N]-N-methylputrescine and [5-^{13}C,^{15}N]-N-methyl-Δ^1-pyrrolinium acetate.[4]

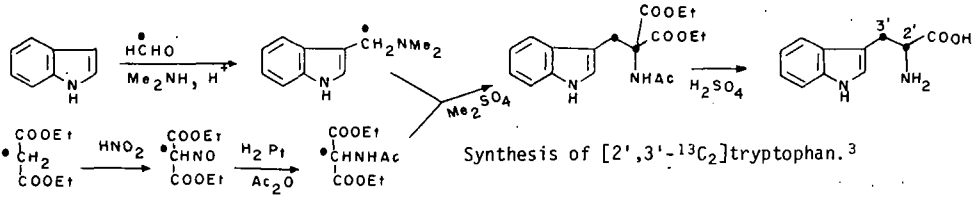

Synthesis of [2',3'-$^{13}C_2$]tryptophan.[3]

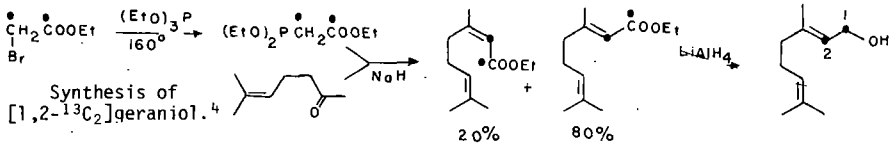

Synthesis of [1,2-$^{13}C_2$]geraniol.[4]

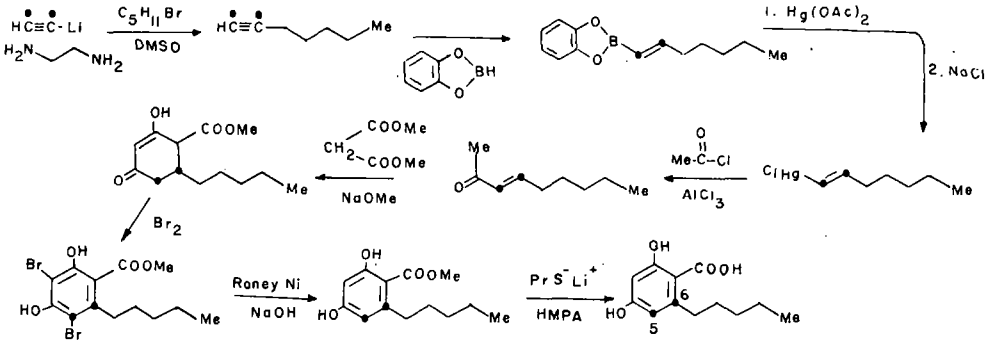

Synthesis of [5,6-$^{13}C_2$]olivetolic acid.[4]

These labeled compounds have been used to study the biosynthesis of a wide variety of natural products. The incorporation of [5,6-$^{13}C_2$]nicotinic acid into the tobacco alkaloids and dioscorine is illustrated below. This work was supported by a grant GM-13246 from the NIH.

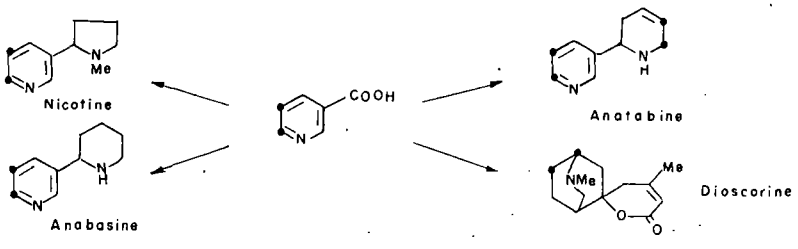

References

1. E. Leete, *Bioorganic Chem.*, 6, 273 (1977).
2. E. Leete and M.-Li Yu, *Phytochemistry*, in press (1980).
3. E. Leete, *J. Natural Products*, 43, 130 (1980).
4. E. Leete, J. Porwoll, and J. McDonell, unpublished work.

SYNTHESIS OF STABLE ISOTOPE ANALOGS OF BIOGENIC AMINES

S. P. Markey, W. J. W. Mayer (1), and J. Oliver

Laboratory of Clinical Science, NIMH
Bethesda, Maryland 20205

Introduction

Stable isotope analogs of biogenic amines are being used for human clinical research to determine the metabolism and kinetics of distribution and excretion of neurotransmitters. Common to many of the compounds of interest are catechol oxygens, generally enzymatically monomethylated during metabolism. We have studied general synthetic schemes useful for the preparation of highly enriched common intermediates for the synthesis of oxygen-18 catecholamines and their mono-deuteromethylated metabolites.

Oxygen-18 Labelled Catechols

Exchange Labelling: Acid catalyzed exchange of certain substituted catechols is a useful technique to produce small quantities of the more stable compounds (2). For example, dopamine-HCl (3,4 dihydroxy phenylethylamine, 0.3 g) was twice exchanged by heating a sealed tube at 180°C with 0.5 ml $H_2{}^{18}O$/HCl to produce .07 g (23%) of labelled (84.4% $^{18}O_2$, 14.7% $^{18}O_1$, 0.8% $^{18}O_0$) dopamine. Two disadvantages are inherent in exchange labelling. 1) Conditions required for exchange are sufficiently brutal to cause decomposition of many substituted catechols, resulting in very poor yields. 2) Exchange requires the use of highly enriched water as a solvent, most of which is not utilized, but is recovered with diluted ^{18}O content. We have explored alternate catalysts to promote exchange under milder conditions. Basic or neutral alumina effectively facilitates exchange of one catechol oxygen. Unfortunately, additional oxygen interchange occurs with alumina rather than with the catechol oxygen with consequent lack of efficient labelled compound recovery. It is evident that chemical synthesis would be preferred for many catechols.

Synthesis: Chromium tricarbonyl complexes (CTC) of mono-halogen substituted arenes (F, Cl) undergo nucleophilic replacement by alkoxide ions at considerably enhanced rates with respect to the free arenes (3,4). The chromium tricarbonyl moiety demonstrates approximately the same electron-withdrawing effect as the nitro group and enhances the rate of substitution of the arene to about the same degree as a p-nitro group. The activation of halobenzenes by means of their CTC provides a promising method for the introduction of an RO-group into the benzene ring. Therefore we investigated the possibility of converting o-dihalobenzenes (F, Cl) into catechols via their chromium tricarbonyl complexes.

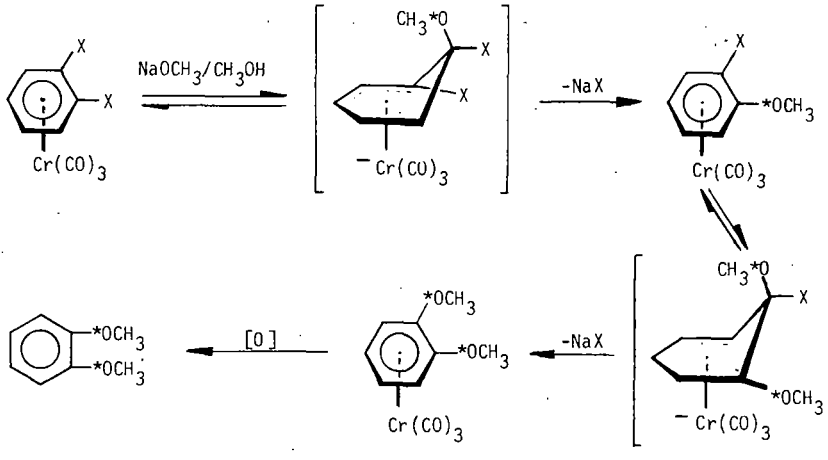

The complexes of o-difluoro- and o-dichlorobenzene were prepared as yellow sublimable solids in ca. 50% yield in a manner similar to the preparation of p-dihalobenzene complexes (5). o-Difluorobenzene-CTC reacted with $NaOCH_3$ in methanol (6) at r.t. in a fast reaction to yield exclusively o-dimethoxybenzene-CTC. For the labelling experiment methanol-^{18}O was synthesized from $^{18}O_2$ gas (≥ 90%) by oxidative decomposition of methyl magnesium bromide in ether (7). The $CH_3{}^{18}OH$ (6,8) was reacted with freshly cut sodium metal to provide $Na^{18}OCH_3$. To this o-difluorobenzene-CTC was added and the yellow mixture stirred at r.t. overnight. Removal of solvent under reduced pressure yielded a yellow solid which was decomposed with iodine in ether to liberate the labelled organic ligand. Workup and subsequent fractionation yielded labelled (92.6% $^{18}O_2$, 6.9% $^{18}O_1$, 0.36% $^{18}O_0$) veratrole in yields ≥ 90%. The same substitution reaction can be performed at r.t. with NaOH in $CH_3{}^{18}OH$ instead of $Na^{18}OCH_3$ in $CH_3{}^{18}OH$.

Reaction of o-dichlorobenzene-CTC with $NaOCH_3$ in CH_3OH and with NaOH in MeOH (r.t., ca. 15 hrs) led mostly to mono-substituted CTC together with unreacted starting material. Under reflux (65°C, ca. 15 hrs) mono-substitution predominated together with small amounts of disubstitution and unreacted starting material. At elevated temperatures considerable amounts of decomposition of the complexes occurred.

These results demonstrate that o-dihalobenzenes π-complexed with chromium tricarbonyl show an enhanced reaction rate towards nucleophiles such as alkoxide ion. There appears to be a distinct difference in reactivity of the CTC-derivatives of o-difluoro- and o-dichlorobenzene. Chromium tricarbonyl complexes of o-difluorobenzene are suitable substrates for the convenient and effective introduction of two labelled oxygen atoms into an aromatic ring. This appears to be the method of choice for the preparation of a di-^{18}O-labelled catechol building blocks for the synthesis of labelled catecholamines if direct labelling of catecholamines via exchange reaction is not applicable.

Deuteromethylated Catechols

In earlier reports (9), we described methods for the synthesis of methyl isotope labelled catecholamine metabolites through the labelled intermediate 2-deuteromethoxyphenol. Recently, we desired sufficient quantity (hundred mg) of optically pure D(-) 4-hydroxy-3-deuteromethoxyphenylethylene glycol to determine its metabolism and kinetics in humans. Synthesis of the precursor mandelic acid was achieved at the 15 g level, and the acid resolved by fractional crystallization of its brucine salt. The resolved deuterated mandelic acid was reduced to the desired phenylethylene glycol of 94.5% optical purity. This resolution and synthesis using earlier proven procedures demonstrates the utility of developing general chemical synthetic routes.

References and Comments

1. W.J.W.M. is a NIH Fogarty-Fellow and acknowledges support from the Deutsche Forschungsgemeinschaft, Bonn, West-Germany.
2. K.L. Clay and R.C. Murphy, Biomed. Mass Spectrom., in press, 1980.
3. B. Nichols and M.C. Whiting, J. Chem. Soc. 551 (1959).
4. D.A. Brown and J.R. Ragu, J. Chem. Soc. A, 40 (1966).
5. W. Strohmeier, Z. Naturforsch. 17b, 627 (1962).
6. All reactions were done under a nitrogen blanket in dry degassed solvents.
7. K.B. Wiberg, J. Amer. Chem. Soc. 75, 2665 (1953).
8. In ether (methanol-^{18}O:ether ca. 1:1).
9. S.P. Markey, K. Powers, D. Dubinsky, and I.J. Kopin, J. Labelled Compd. Radiopharm. 17, 103 (1980).

Biosynthesis with Fully Deuterated Microorganisms

Henry L. Crespi
Chemistry Division
Argonne National Laboratory
Argonne, IL 60439

A wide variety of plant microorganisms can be grown in fully deuterated form but higher plants and animals can withstand only partial deuteration. The effects of substituting heavy hydrogen (^2H, D) for ordinary hydrogen (^1H) in biological systems have been reviewed in detail (1, 2). In summary, the extent to which living systems will tolerate deuterium substitution in their tissue fluids is as follows: (1) Mammals can withstand up to 30 atom percent deuterium in their tissue water for extended periods. When the level reaches 30-35 atom percent deuterium, they die. Cells in tissue culture will grow at somewhat higher deuterium levels. (2) Higher plants can withstand up to 60 atom percent deuterium in their tissue fluids, and die at the 60-65 percent level. Seeds germinate at higher D_2O levels, some as high as 99.7 atom percent D. (3) Microorganisms can be cultured routinely in heavy water containing 99.8 atom percent deuterium and are a source of fully deuterated sugars, amino acids, lipids, plant pigments, proteins, nucleic acids, and other metabolites.

Many unicellular and filamentous algae have been cultured autotrophically in 99.8 atom percent D, both in flask and mass culture (1, 3-5). Such organisms as *Scenedesmus obliquus, Chlorella vulgaris, Synechococcus lividus, S. leopoliensis (Anacystis nidulans), Phormidium luridum, and Fremeylla diplosiphon* have been mass cultured in fully deuterated form for many years. These algae, and compounds obtained from them, have been particularly useful in magnetic resonance and mass spectrometric studies of photosynthesis and the components of the photosynthetic apparatus. Table 1 lists some of the properties of ^2H (vs. ^1H) that make deuteration such a useful tool in mass spectrometry, nuclear magnetic and electron spin resonance spectroscopy, neutron scattering, and infra-red and Raman spectroscopy.

Table 1. Some Properties of ^1H and ^2H

Property	^1H	^2H
Mass	1	2
Nuclear Spin	1/2	1
Magnetic Moment (Nuclear Magnetons)	2.79	0.86
Neutron Scattering Amplitude	$-3.74\ cm^{-13}$	$6.67\ cm^{-13}$

Algae are the basis for the culture of fully deuterated heterotrophic microorganisms. Sugars, amino acids, and complex substrates can be prepared from deuterated algae (6-8) and these materials can be used to grow a wide variety of bacteria, yeasts, and molds. A few chemically deuterated substrates, such as acetic acid-d_4 and succinic acid-d_6, are also useful for growing such organisms as Escherichia coli (9) and photosynthetic bacteria (10). Of particular utility are a D_2O extract of whole *S. obliquus* cells and an acid hydrolysate of algal cells (8). These materials enable one to culture organisms that require complex substrates, such as *Halobacterium halobium* and *Acetobacter xylinum* (10). The availability of fully deuterated microorganisms also gives one the opportunity to add ^1H compounds to the nutrient medium to form isotope hybrid compounds - compounds that are selectively protonated (11), e.g. ^2H-protein (^1H-amino acid).

Fully deuterated bacteriorhodopsin from *Halobacterium halobium* has been a particularly useful material. Neutron scattering (12) and resonance Raman (13) analyses of fully deuterated and isotope hybrid bacteriorhodopsin have contributed substantially to our understanding of the structure and function of this proton pump.

References

1. J. J. Katz and H. L. Crespi, Science **151**, 1187 (1966).
2. J. J. Katz and H. L. Crespi, in "Isotope Effects in Chemical Reactions", C. J. Collins and N. S. Bowman, Eds., van Nostrand Reinhold, New York, p. 286.
3. H. L. Crespi, S. M. Conrad, R. A. Uphaus, and J. J. Katz, Ann. N. Y. Acad. Sci. **84**, 648 (1960).
4. H. F. DaBoll, H. L. Crespi, and J. J. Katz, Biotechnol. Bioeng. **4**, 281 (1962).
5. R. G. Taecker, H. L. Crespi, H. F. DaBoll, and J. J. Katz, Biotechnol. Bioeng. **13**, 779 (1971).
6. M. I. Blake, H. L. Crespi, V. Mahan, and J. J. Katz, J. Pharm. Sci. **50**, 5 (1960).
7. H. L. Crespi, J. Marmer, J. J. Katz, J. Am. Chem. Soc. **84**, 3489 (1962).
8. H. L. Crespi and J. J. Katz, in "Methods in Enzymology", Vol. 26C, C. H. W. Hirs and S. N. Timasheff, Eds., Academic, New York, p. 627.
9. P. B. Moore and D. M. Engelman, in "Neutron Scattering for the Analysis of Biological Structures", Brookhaven Symposia in Biology, No. 27, p. V-12, Rep. BNL - 50453, National Technical Information Service, Springfield, Virginia, 22161 (June, 1975).
10. H. L. Crespi, in "Stable Isotopes in the Life Sciences", Panel Proceedings Series, International Atomic Energy Agency, STI/PUB/442, Vienna, 1977, p. 111.
11. J. J. Katz and H. L. Crespi, Pure Appl. Chem. **32**, 221 (1972).
12. G. I. King, W. Stoeckenius, H. L. Crespi, and B. P. Schoenborn, J. Mol. Biol. **130**, 395 (1979).
13. A. Lewis, M. A. Marcus, E. Ehrenberg, and H. L. Crespi, Proc. Nat. Acad. Sci, USA **75**, 4642 (1978).

ORGANIC SYNTHESIS WITH STABLE ISOTOPES: AMINO ACIDS, T. W. Whaley, Organic Chemistry Group, Los Alamos Scientific Laboratory, Los Alamos, NM 87545

Amino acids labeled with stable isotopes of carbon and nitrogen are useful compounds for studying chemical and biological processes. Experiments that employ amino acids with multiple isotopic labels are not uncommon. We have synthesized a number of labeled amino acids using synthetic schemes that allow the preparation of compounds with multiple labels as well as numerous isotope isomers.

GLYCINE AND L-ALANINE: The approach to the synthesis of these two amino acids involves the ammination of an α-bromocarboxylic acid, which is obtained from the parent carboxylic acid. The two carbon atoms in glycine are derived from acetic acid, which is prepared by the carbonylation of methanol [D. G. Ott and V. N. Kerr, J. Labelled Compds. Radiopharm., 12, 119 (1976)]. Nitrogen labeling of glycine is accomplished with potassium phthalimide. Glycine labeled with carbon-13 and/or nitrogen-15 can be used as a starting material for other amino acid synthesis. The alanine synthesis has been described for the 2,3-$^{13}C_2$ isomer [V. N. Kerr and D. G. Ott, J. Labelled Compds. Radiopharm., 15, 503 (1978)] and can be applied to other isotope isomers. Resolution of D,L-alanine is accomplished by enzymatic deacetylation of the N-acetylamides by Acylase I.

D,L-VALINE, D,L-ISOLEUCINE, AND D,L-ALLOISOLEUCINE: The synthesis of these amino acids is based on the Strecker synthesis, in which the amino acid is prepared from ammonia, cyanide ion, and an aldehyde containing the α-carbon of the desired amino acid and the carbons of the side chain. We have described a synthesis of D,L-valine in which the three carbons of the isopropyl group were labeled with carbon-13 [T. W. Whaley, G. H. Daub, V. N. Kerr, T. A. Lyle, and E. S. Olson, J. Labelled Compds. Radiopharm., 16, 809 (1979)]. An aldehyde synthesis using 2-methyl-2-thiazoline [A. I. Meyers and J. L. Durandetta, J. Org. Chem., 40, 2021 (1975)] was used to prepare labeled isobutyraldehyde from methyl iodide and sodium cyanide. The Strecker synthesis with isobutyraldehyde affords D,L-valine. Almost all isotope isomers of D,L-valine can be synthesized this way. Application of the Strecker synthesis to 2-methylbutanal, also available by the thiazoline method, affords a mixture of D,L-isoleucine and D,L-alloisoleucine. This mixture can be separated into the two racemic diastereomers by chromatography on a Dowex 50 (H+) column.

D,L-HISTIDINE: This synthesis of histidine involves the alkylation of a suitable derivative of glycine, ethyl acetamidocyanoacetate in this case, with 4-chloromethylimidazole [C. SooHoo, J. A. Lawson, and J. I. DeGraw, J. Labelled Compds. Radiopharm., 13, 97 (1977)]. Construction of the imidazole ring is accomplished by cyclization of C-formyl-N-formylglycine ethyl ester with sodium thiocyanate [R. G. Jones, J. Am. Chem. Soc., 71, 644 (1949)]. The carbon and nitrogen atoms of the imidazole ring are derived from glycine, ethyl formate, and sodium thiocyanate. A variety of labeling patterns are available by this method. We have applied the synthesis to labeling of the ring nitrogens using sodium thiocyanate-^{15}N and/or glycine-^{15}N.

L-ORNITHINE AND L-ARGININE: This synthesis of ornithine is based on the alkylation of a derivative of glycine, the benzophenone Schiff's base of glycine ethyl ester [M. J. O'Donnell, J. M. Boniece, and S. E. Earp, Tetrahedron Lett., 2641 (1978)]. In this case, the alkylation reaction involves a Michael addition using acrylonitrile. The carbon and nitrogen atoms in ornithine are derived from glycine and acrylonitrile. The resolution of D,L-ornithine is accomplished by enzymatic hydrolysis of the ester group in diacetylornithine ethyl ester with chymotrypsin. We have synthesized L-ornithine-2-^{13}C by this method. The synthesis of L-arginine is accomplished by the reaction of L-ornithine (complexed with Cu) with O-methylisourea tosylate, which is prepared from urea [T. W. Whaley and D. G. Ott, J. Labelled Compds., 11, 167 (1975)]. We have used this approach for labeling of the guanidino group in arginine and are currently synthesizing L-arginine-1-^{13}C by this method.

L-TRYPTOPHAN: The approach employed in this synthesis of tryptophan is the hydrogenation of an α,β-unsaturated carboxylic acid derivative, in this case the alkylidinehydantoin obtained from indole-3-carboxaldehyde and hydantoin [H. W. Bond, J. Biol. Chem. 175, 531 (1948)]. The synthesis affords racemic tryptophan. Chiral hydrogenations using chiral bisphosphine ligands complexed to rhodium catalysts have been reported by a number of workers. One such ligand is 1,2-bis(o-anisylphenylphosphino)ethane] W. S. Knowles, M. J. Sabacky, B. D. Vineyard, and D. J. Weinkauff, J. Am. Chem. Soc., 97, 2567 (1975)] which we have synthesized by the reaction scheme shown below. This catalyst is being used in a synthesis of L-tryptophan-1-^{13}C based on the hydrogenation of α,β-unsaturated carboxylic acid derivatives.

(This work was performed under the auspices of the U. S. Department of Energy, and was funded partially by National Institutes of Health Research Grant RR00962.)

BIOSYNTHESIS WITH STABLE ISOTOPES: ALGAL SYSTEMS

Victor H. Kollman, Organic Chemistry Group
Los Alamos Scientific Laboratory
Los Alamos, New Mexico 87545

INTRODUCTION

The green algae, *Chlorella pyrenoidosa* and *Chlamydomonous reinhardii*, and the blue-green algae, *Anacystis nidulans* and *Agmenellum quadruplicatum*, have been used to photosynthetically prepare amino acids, carbohydrates, lipids, and nucleotides and nucleosides. The algae were uniformly labeled with highly enriched carbon-13 and nitrogen-15 in single or double combinations. Carbon-13 was incorporated as carbon dioxide and nitrogen-15 was supplied to the organisms as ammonia or nitrate. The choice of algae used in a particular synthesis depends on the compound(s) desired since an organism can generally be found that will favor synthesis of the desired material. Further, organism selection is determined by availability of the precursor-labeling molecule(s). For example, an algae such as *C. reinhardii*, which lacks nitrate reductase and thus cannot utilize nitrate, must be supplied with nitrogen-15 ammonia in order to label the nitrogen-containing compounds.

Apparatus: The growth apparatus consists of three 40-ℓ polycarbonate chambers joined together on a common oscillating mechanism. The temperature of the algal cultures was maintained at 39°C during the growth period. Illumination of the growth chambers was from above and below the plane of oscillation (28 cpm) with very high-intensity, natural-outdoor fluorescent lamps. The pH of the cultures was maintained at the desired level by the automatic addition of pure-sterile $^{13}CO_2$. A positive pressure (10 cm H_2O) was maintained inside each chamber by venting the contained gases through two gas-washing bottles filled with CO_2-free 5 M sodium hydroxide. The terminal gas-washing bottles were fitted with ascarite-filled glass tubes to prevent atmospheric contamination of the sodium hydroxide solution. Cooling fans were mounted below the fluorescent lamps. Temperature control baths were located at the rear of the algae culture apparatus.

Cell Culture: Algal cultures were transferred aseptically from agar slants to 500-mℓ Bellco spinner flasks and grown in liquid medium for three days. When the culture density reached 0.5 g/ℓ (dry weight), the culture was transferred to a 2.4-ℓ flask and diluted with fresh medium. After three days of growth, the algal suspension was transferred to 18 ℓ of fresh growth medium. This solution was used to inoculate the growth chambers. Each of the three growth chambers was filled with 6 ℓ of algal suspension and 14 ℓ of fresh growth medium. The chambers were then sealed and the growth period was begun. After the appropriate growth period, the mature cells were removed from the chambers and rapidly cooled to 4°C in cold physiological saline. The cells were removed from solution by centrifugation using a Sharples Model 16 open-type, continuous-flow centrifuge. The cells were removed from the centrifuge bowl, lyophilized, and stored at -20°C.

PREPARATION AND ISOLATION OF CARBOHYDRATES FROM *AGMENELLUM QUADRUPLICATUM*

The blue-green algae, *Agmenellum quadruplicatum* (strain PR6), were grown in liquid culture as described. Growth was terminated after 120 h of incubation. The carbon-13 labeled simple carbohydrates (glucosylglycerol, glucosylglycerate, and sucrose) were extracted from the dry algae with 2:1 methanol-chloroform solution and isolated. The cell residue was lyophilized and hydrolyzed in a 2.5% cell suspension of 0.25 M trifluoroacetic acid (TFA). The glucose was isolated from solution and crystallized from ethanol. The isolated carbohydrates were identified by their n.m.r. spectra and by enzymic assay.

Nuclear Magnetic Resonance Spectroscopy: The ^{13}C-enriched cells of *A. quadruplicatum* that were to be used for n.m.r. spectroscopy were taken aseptically from the growth chambers and rapidly cooled to 4°C. They were removed from the growth medium by centrifugation at 10 000 x g for 10 min. The cells were washed twice with 40-mℓ volumes of cold, normal saline solution. After each wash, the cells were removed from the solution by centrifugation; they were resuspended in 2.5 mℓ of cold, normal saline and placed in a 12-mm n.m.r. tube. A few drops of D_2O were added to the cell sample to provide a lock. The cell concentration in the n.m.r. sample was 0.25 g (dry weight) per mℓ of solution. The ^{13}C n.m.r. spectra were obtained with a Varian Model XL-100-15 spectrometer (25 MHz) interfaced to a Nova Model 1210 computer.

Results: The cell mass produced during the 120-h growth period was 260 g (4.4 $g\ell^{-2}$). The nitrate-nitrogen provided during growth was 0.2 mol for each growth chamber; the nitrogen concentration was 1 μM after 48 h of growth. The cell concentration and cellular carbohydrates did not change significantly with increased culture times from 120 h to 220 h.

The carbon-13 labeled carbohydrates produced during each growth period were compared for *A. quadruplicatum* (strain PR6) and *N. tobacum L.* (Coker 319). Forty-one percent of the carbon incorporated by the algae was isolated as glucose-$^{13}C_6$, glucosylglycerol-$^{13}C_9$, glucosylglycerate-$^{13}C_9$, and sucrose-$^{13}C_{12}$, with glucose comprising 99% of the isolated carbohydrates. Sixty percent of the carbon incorporated by the tobacco was isolated as starch-$^{13}C_x$, glucose-$^{13}C_6$, fructose-$^{13}C_6$, and sucrose-$^{13}C_{12}$. In tobacco, the endogenous material typically averaged 10% of the isolated products. In contrast, the algae were enriched to the level of the administered ^{13}C, and thus the isolated carbohydrates contained no endogenous material.

PREPARATION AND ISOLATION OF AMINO ACIDS FROM *CHLORELLA PYRENOIDOSA*

The green algae, *Chlorella pyrenoidosa* (Sorokin strain), were grown in liquid culture as described in the cell culture section. They were harvested by centrifugation, washed with distilled water, and lyophilized. The cells were disrupted by extracting 100 g of lyophilized algae with trichloroacetic acid (TCA). Chlorophyll and other pigments and lipids were removed from the cell debris by repeated extraction with an ethanol-ethyl ether mixture and pure ethyl ether.

Hydrolysis of 39 g of the residue was accomplished by heating 20 h at 100°C with 6 M HCl in a sealed glass vessel. The insoluble residue (4 g) was washed with distilled water. Hydrochloric acid was removed from the acid-soluble fraction by repeated concentration to a syrup which weighed 50 g.

The amino-acid-containing syrup was diluted with water and placed on a column of Dowex 50 resin (5 cm x 100 cm; X2, H^+ form). After washing with water, elution was carried out with 6 M ammonium hydroxide. That portion of the eluant containing amino acids was concentrated and lyophilized. The lyophilized product weighed 30 g.

Separation of the amino acids was accomplished using modified methods of Jack S. Cohen and I. Putter (Biochimica et Biophysica ACTA 222, 515 (1970), and James K. Winters (Ph.D. Dissertation, The University of Texas at Austin, 1971). The best resolution of amino acids was obtained by us using the two-column ion exchange techniques of Winters. The method employs two ion exchange resins, Dowex 1 X8 and Dowex 50 X8. The sample is first placed on a column of Dowex 1 X8 (acetate form) for the separation of tyrosine, glutamic, and aspartic acids from neutral and basic amino acids. The remaining amino acids are separated on a column of Dowex 50 X8 (hydrogen form). The amino acid yield was about 50% of the theoretical yield based on the protein content.

PREPARATION AND ISOLATION OF NUCLEOTIDES AND NUCLEOSIDES FROM *ANACYSTIS NIDULANS*

Deoxy- and ribonucleic acids were extracted from the blue-green algae, *Anacystis nidulans*. The extraction procedure is a modification of that described by J. Marmur in J. Mol. Biol. (1961) 3, 208. The cell mass extracted was increased by a factor of 10 for our use. Elution of the nucleotides from the column of Dowex 50 (X4, -400 mesh, 9 mm x 75 cm) was accomplished with 0.05 M ammonium formate, pH 3.2. The order of elution was TMP, GMP, CMP, and AMP.

Approximately 1.3% of the dry weight of blue-green algae was extracted as DNA, while 0.33% was extracted as RNA. These values compare with estimates of the total amount of DNA and RNA present in blue-green algae as described by C. P. Wolk in Bacteriol. Rev. (1973) 37, 32 (0.43 to 1.7% of the dry weight as DNA; 0.37 to 0.50% of the dry weight as RNA).

"A Regiospecific Synthesis of the Pyrimidine Ring"[1]

John L. Roberts, C. Dale Poulter and Richard H. Griffey

Uracil and Uridine are commonly used intermediates in chemical and biological syntheses. Although short routes[2] to these compounds are available, there are no general regiospecific approaches suitable for introducing isotopic labels into the pyrimidine ring. For example, the one-step synthesis of uracil via the acid-catalyzed condensation of malic acid and urea gives good yield,[3] but does not allow differential labelling of the ring nitrogens. Longer regiospecific routes[4] suffer from steps with low yields. We decided that the pyrimidine ring could best be constructed via a condensation of potassium cyanate and β-alanine, since each of the ring atoms in the base can be introduced unambiguously. As shown in Scheme 1, C(4) and C(5) of uracil are derived from C(1) and C(2) in acetic acid C(6) and N(1) from potassium cyanide and C(2) and N(3) from potassium cyanate. The three building blocks are simple compounds and are available commercially with ^{13}C and ^{15}N at any position.

Scheme 1. Synthesis of 2',3',5'-Tri-O-benzoyluridine

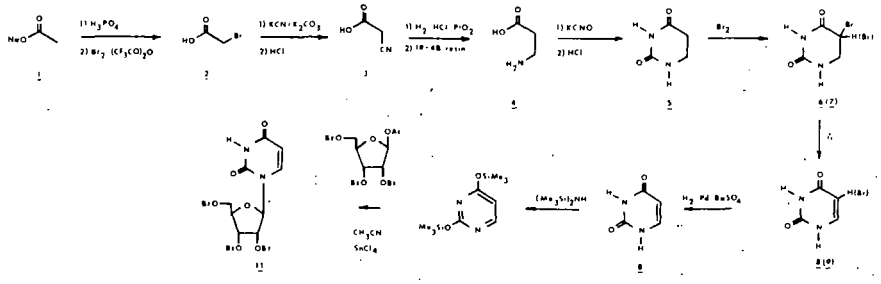

In synthesizing (1-^{15}N)uracil, bromoacetic acid was reacted with potassium (^{15}N)cyanide to give (^{15}N)cyanoacetic acid. The nitrile was cleanly reduced to the desired amino acid in 24 h at 50 psi with Adam's catalyst. By carrying out the reduction in the presence of hydrochloric acid, it was possible to supress the side reactions which are common during the reduction of cyanides to amines. The β-alanine hydrochloride could be converted to the free amino acid and condensed with potassium cyanate giving dihydrouracil according to the procedure developed by Lengfield and Stieglitz.[5]

The bromination-dehydrobromination sequence of Gabriel[6] was used to introduce the C(4)-C(5) double bond. In order to assure complete conversion, the dihydrouracil was deliberately overbrominated to give 6 and 7. After carrying out the thermal elimination of hydrogen bromide, the resulting mixture was then treated with hydrogen in the presence of palladium on barium sulfate. Under these conditions, 5-bromouracil was smoothly converted

Table 1

Compound	Assignment	Chemical Shifts, ppm[d] δ^1H	$\delta^{15}N$	Coupling Constants, Hz[e] J_{HH}	J_{NH}	$^2J_{NH}$
(^{15}N)Cyanoacetic acid[a]	CH_2	3.80				3.0
	NC^2		136.7			
(^{15}N)Aminopropionic acid[c]	C(2)	3.21(Br t)		6.6		
	C(3)	2.59(d of t)		6.6		2.5
	NH_3	6.78(d)	344.7		77	
(1-^{15}N)-5,6-dihydrouracil[c]	C(5)	2.87(Br t)		6.9		
	C(6)	3.67(d of t)		6.9		3.0
	N(1)	7.54(Br d)	254.4		98	
	N(3)	9.63(Br s)				
(3-^{15}N)-5,6-dihydrouracil[c]	C(5)	2.93(Br t)		7.0		
	C(6)	3.73(Br t)		7.0		
	N(1)	7.48(s)				
	N(3)	9.67(Br d)	236.8		96	
(1-^{15}N)Uracil[b]	C(5)	5.50(Br d)		7.8		
	C(6)	7.43(d of d)		7.8		4.5
	N(1)	10.80(Br d)	248.3		91	
	N(3)	11.10(s)				
(3-^{15}N)Uracil[b]	C(5)	5.48(d of d)		7.8		
	C(6)	7.45(d)		7.8		
	N(1)	10.85(Br s)				
	N(3)	11.02(Br d)	221.1		90	

[a] D_2O. [b] Me_2SO-d_6. [c] Trifluoroacetic acid. [d] ^1H shifts downfield from Me_4Si, ^{15}N shifts upfield from 75% CH_3NO_2. [e] Absolute value.

to uracil, which was resistant to hydrogenation. The (^{15}N)uracil could be purified via hydrolysis of the bistrimethylsilyl derivative,[7] or converted to the nucleoside via stannic chloride fusion[8] with 1-O-acetyl-2,3,5,-tri-O-benzoyl-β-D-ribofuranoside.

Condensation of β-alanine with potassium (^{15}N)cyanate gives (3-^{15}N)dihydrouracil. This material was converted to (3-^{15}N)uracil via the method described above. Nuclear magnetic resonance data for all compounds is listed in Table 1.

The 2',3',5'-tri-O-benzoyluridine is a precursor for the synthesis of a large number of biologically important pyrimidine nucleosides such as 4-thiouridine,[9] 2-thiouridine,[10] cytidine[11] and 2-thiocytidine[11a]. In addition, uracil has been converted into pseudouridine.[12] Hence, this approach serves as a regiospecific method of labelling uracil, cytidine and the uracil-derived bases.

We wish to thank Dr. N. Matwiyoff of Los Alamos for generously providing potassium (^{15}N)cyanide.

1. Taken in part from Roberts, J.L. and Poulter, C. Dale, J. Org. Chem., 43, 1547 (1978).
2. Perry, C.W., Burger, W., Bader, G.J., and Liebman, A.A., J. Labelled Compd., 11, 583 (1975). Zee Cheng, K.Y., Robins, R.K., and Cheng, C.C., J. Org. Chem., 26, 1877 (1961).
3. Davidson, D. and Baudisch, O., J. Am. Chem. Soc., 48, 2379 (1926).
4. Shaw, G., Warrener, R.N., Macquire, M.H. and Ralph, R.K., J. Chem. Soc., 2294 (1958). Cusack, N.J. and Shaw, G., Chem. Commun., 1114 (1970).
5. Lengfeld, F. and Stieglitz, J., Am. Chem. J., 15, 504 (1893).
6. Gabriel, S., Ber., 38, 1689 (1905).
7. Wittenberg, E., Chem. Ber., 101, 2132 (1968). Niedballa, U. and Vorbruggen, H., J. Org. Chem., 39, 3654 (1974).
8. Niedballa, U. and Vorbruggen, H., J. Org. Chem., 39, 3660, 3664, 3668, 3672 (1974).
9. Saneyoshi, M., Chem. Pharm. Bull., 23, 1146 (1975).
10. Vorbruggen, H., Strehlke, P. and Schulz, G., Angew. Chem., 81, 997 (1969).
11. Saneyoshi, M., Chem. Pharm. Bull., 19, 493 (1971).
12. Brown, D.M., Bridges, S.D. and Conrad, R.P.L., Nucl. Acid Res., S.P. 4, s121 (1980).

RAMP9 SURVEY OF STABLE ISOTOPE LABELED MATERIALS AVAILABLE FOR USE IN CONNECTION WITH MASS SPECTROMETRY, J.C. BRADLEY, A.M. AJAMI, AND S.S. YUAN, KOR ISOTOPES, 56 ROGERS ST., CAMBRIDGE, MA 02142

The recent increase in research utilizing stable isotopes as standards and tracers is closely related to the availability of the labeled compounds. KOR ISOTOPES has made available a wide variety of new labeled compounds for use in the fields of environmental chemistry, pharmacology, biochemical and biomedical research. A selection of compounds from several different classes will be presented which illustrate these applications. Areas covered will include:

-Low level detection and quantification of environmental contaminants through the use of heavy isotope labeled internal standards,

-Drug level monitoring through the use of labeled drugs and metabolites,

-Compounds which can be used in clinical areas to give patient diagnostic information, and

-Materials useful in medical research for the study of deviations and changes in basic metabolic functions.

ISOTOPICALLY-ENRICHED CARBOHYDRATES: SYNTHESIS AND USE IN CHEMICAL AND BIOCHEMICAL STUDIES.

A. S. SERIANNI, H. A. NUNEZ, J. PIERCE, P. R. ROSEVEAR, E. L. CLARK AND R. BARKER. DEPARTMENT OF BIOCHEMISTRY, MICHIGAN STATE UNIVERSITY, EAST LANSING, MI 48824, AND SECTION OF BIOCHEMISTRY, MOLECULAR AND CELL BIOLOGY, CORNELL UNIVERSITY, ITHACA, NY 14853.

Aldoses, aldose phosphates and deoxyaldoses labeled with isotopes of carbon, hydrogen and/or oxygen can be prepared by catalytic hydrogenolysis of aldononitriles, aldononitrile phosphates and deoxyaldononitriles using 5% palladium on barium-sulfate. Parent aldoses, aldose phosphates and deoxyaldoses were condensed with isotopically-labeled potassium cyanide ($K^{13}CN$, $K^{14}CN$) at controlled pH (7.5-8.0) to yield the respective enriched aldononitriles. The aldononitriles were hydrogenolyzed under various conditions (pH 1.7-4.3; 1 atm. to 60 lb. in.^{2} H_2) to aldoses in 70 to 90 percent yield. Isotopes of hydrogen were introduced by hydrogenolysis with $^{2}H_2$ gas. Oxygen isotopes were introduced by exchange of O-1 of the parent aldose with labeled water before the addition of cyanide. The method permits the insertion of isotopes of carbon and hydrogen at C-1 and H-1, respectively, and of oxygen at O-2 for each cycle of cyanide condensation and hydrogenolysis.

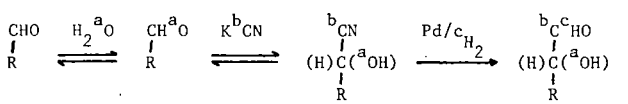

Using this procedure, C_2 to C_6 aldoses, C_2 to C_5 aldose phosphates, and several deoxyaldoses (6-deoxyhexoses, 5-deoxypentoses, 3- and 4-deoxytetroses) were prepared with ^{13}C-, ^{2}H- and/or ^{17}O-enrichment at various sites.

Carbon-13 enriched carbohydrates were used to study NMR properties and solution chemistry. The ^{13}C NMR spectra of the (1-^{13}C)tetroses show the presence of four conformers in aqueous solution, namely, α-furanose, β-furanose, linear hydrate and linear aldehydo. At 30°C, the aldehydo form composes about 1 percent of the mixture. The amounts of each form in solution can be conveniently determined as a function of temperature and solvent. In addition, $^{1}J_{C1,H1}$ can be measured for each enriched carbon. These values range from 163 Hz for the linear hydrate (in H_2O) to 179 Hz for the aldehydo form (in 80% dioxane). T_1 Relaxation times at 28°C for C-1 of the linear hydrates (2-3 s) appear shorter than those of either cyclic furanose (4-5 s).

(^{13}C,^{2}H)-Enriched compounds permit an evaluation of $^{1}J_{C,2H}$ (22-27 Hz) and isotope shifts. Deuterated compounds facilitate the interpretation of complex ^{1}H spectra. The 180 MHz ^{1}H NMR spectrum of DL-(3-^{2}H)threose permitted the determination of homonuclear ^{1}H-^{1}H coupling and ^{1}H chemical shifts for the three major forms in $^{2}H_2O$.

Enzymatic conversions were also monitored by ^{13}C NMR using (^{13}C)-enriched substrates. D-(2-^{13}C)Glucose was converted to D-(2-^{13}C)fructose 1,6-bisphosphate by hexokinase, myokinase, phosphoglucoisomerase, phosphofructokinase and Mg^{2+}-ATP. D-(2-^{13}C)Ribulose 1,5-bisphosphate (RUDP) was prepared by incubation of D-(2-^{13}C) ribose 5-phosphate with phosphoriboisomerase, ribulose 5-phosphate kinase and Mg^{2+}-ATP. The ^{13}C NMR spectrum of purified D-(2-^{13}C)RUDP shows the presence of two forms in aqueous solution, keto (88%) and keto hydrate (12%).

Chemical reactions can be monitored by ^{13}C NMR by using (^{13}C)-enriched reactants. The cyanohydrin reaction was examined at several pH values (7.0-12.7) using $K^{13}CN$ and/or (^{13}C)-enriched erythrose. Intermediates were observed as a function of time to obtain reaction profiles. All intermediates were identified. The imido-1,4-lactone intermediate was characterized at pH 10.5 through the use of double carbon-13 enrichment (^{13}C-1,3 and ^{13}C-1,4) which permitted simultaneous evaluation of chemical shifts of the enriched nuclei and $J_{C,C}$ during the reaction.

Rates of anomerization of furanose sugars were examined by ^{13}C NMR and saturation-transfer ^{1}H NMR. D-Threose in $^{2}H_2O$ was studied by ^{1}H NMR (80 MHz) at 56°C by irradiation of H-1 aldehydo ($\delta \approx 10$ ppm). The extent of transfer of saturation to H-1 nuclei of the cyclic and hydrate forms was monitored as a function of decoupling time, and ring-opening rates and relaxation times were estimated. Using equilibrium constants determined from ^{13}C NMR spectra of D-(1-^{13}C)threose at 56°C, ring-closing rates were evaluated.

RAMP11 THE PREPARATION OF SOME C-DEUTERATED CARBOHYDRATES BY CATALYTIC EXCHANGE, H. J. KOCH, Merck Frosst Laboratories, Pointe Claire-Dorval, Quebec, H9R 4P8

Suitably derivatized carbohydrate derivatives are readily C-deuterated by deuterium oxide in the presence of "deuterated" Raney nickel catalyst. The preparation of several specifically C-deuterated carbohydrates by this method is described. For example, methyl α-D-glucopyranoside is converted to methyl α-D-glucopyranoside-2,3,4,6,6-$^2H_6$, and D-mannitol to per-C-deuterated D-mannitol.

MASS SPECTROMETRY IN FORENSIC TOXICOLOGY AND DRUG ANALYSIS

M.J. WHITEHOUSE AND L.V. JONES
Metropolitan Police Forensic Science Laboratory
109 Lambeth Road London SE1 7LP U.K.

INTRODUCTION

The majority (90%) of the mass spectrometry caseload (c.750 cases) at this laboratory involves the identification of drugs and metabolites from a variety of sources and is used in approximately 15% of cases dealt with by the drugs and toxicology section. The most demanding involve the identification of drugs, metabolites, pesticides etc. in body fluids and organs or food and drinks. The examination by MS of drugs in pharmaceutical or illicit preparations is restricted to those where the sample is limited in quantity or other techniques do not provide complete identification. Only two aspects of the work will be considered in detail i.e. the detection of drugs in motorists and some features of negative ion chemical ionisation (NICI) mass spectrometry.

EXPERIMENTAL

Intrumentation. Two low resolution GC/MS instruments have been used: a V.G. M.M. 12F magnetic sector and a V.G. M.M. 12-12 quadrupole both of which employ a dual EI/CI source and have multiple ion detection (MID) facilities. In addition the V.G. M.M. 12F has negative ion capabilities achieved by operating with an accelerating voltage of -4KV and multiplier voltage of -2.5KV and by reversing the magnet current. The reagent gas employed was isobutane at a source housing pressure of 5×10^{-5} Torr and 5×10^{-6} Torr for positive ion chemical ionisation (PICI) and NICI respectively. The source temperatures were 200-230°C for EI and 140-160°C for CI with emission currents of 200μA and 2mA for PICI and NICI respectively. Except where otherwise stated the GC columns employed were 6' x ⅛" glass, packed with 3% OV-17 on Chromosorb G. A temperature programme of 160-260°C at 10°C per minute was employed for screening purposes and the columns were operated isothermally at temperatures between 240 and 260°C for MID. Both instruments have full data processing facilities; the V.G. M.M. 12F having a V.G. Data systems 2000 data sytem and the V.G. M.M. 12-12 a 2050 foreground/background data system. The latter combination is employed on the routine case work instrument in order to ensure maximum utilisation of mass spectrometer time by being able to simultaneously acquire and interpret data with one or two operators.

The extraction procedures are too numerous to mention and follow classical patterns involving simple one or two step procedures to yield fractions containing acid plus neutral drugs and basic drugs. These extracts are submitted to TLC and GC screens and potentially positive cases are then submitted for MS confirmation.

RESULTS AND DISCUSSION

Drug Screening of motorists. This field has received little attention except for the work of Bonnichsen et al [1] and that carried out in this laboratory [2] In 1979 c.25,000 alcohol cases were dealt with of which 218 were also examined for drugs. Of the latter 150 were examined by mass spectrometry and 100 found to be positive. These cases are particularly demanding due to the low levels of drugs and the limited amount of blood (1-4 ml) and/or urine (c.30 ml). In the ideal situation urine may be used to screen for nearly all drugs likely to cause impairment and the blood sample used to estimate the concentration of the drug present. Table 1 shows the range of drugs encountered while Table 2 indicates the frequency as determined by MS. It can be seen that the large dose sedatives (barbiturates and methaqualone) and the benzodiazepine tranquillisers are met most frequently.

It is impossible in this paper to mention in detail the mass spectral properties of all these drugs. Certain drugs particularly basic ones have poorly characteristic mass spectra with no molecular ion and only weak ions at higher masses. Other compounds have poor GC properties or yield artifacts due to on-column decomposition [3]. These problems can be resolved by the use of PICI, GC retention data and suitable derivatives or the fact that the metabolites exhibit characteristc spectra. In this way it is possible to maintain a high through-put of 95% of the casework by GC/MS under EI conditions.

TABLE 1

DRUGS/METABOLITES DETECTED IN DRIVERS BY M.S.

AMPHETAMINE	DIHYDROCHODEINE	PEMOLINE
BARBITURATES	DIPHENHYDRAMINE	PHENMETRAZINE
BENZODIAZEPINES	DIPIPANONE	PHENYTOIN
CHLORMETHIAZOLE	GLUTETHIMIDE	PRIMIDONE
COCAINE	MEPROBAMATE	PROCAINE
CODEINE	METHADONE	SALICYLATE
CYCLIZINE	METHAQUALONE	TOLUENE
DEXTROPOXYPHENE	MORPHINE	TRICHLORETHANOL
DIETHYLPROPION	PARACETAMOL	

TABLE 2

INCIDENCE OF VARIOUS DRUGS BY M.S.

DRUG	NO.CASES(B + U)
BARBITURATES	67
BENZODIAZEPINES	13
METHAQUALONE	13
PARACETAMOL	7
PEMOLINE	6
AMPHETAMINE	5
METHADONE	5
DIPHENHYDRAMINE	5
CHLORMETHIAZOLE	3
DIETHYLPROPION	3
PROPOXYPHENE	3
MORPHINE	3
OTHERS (14)	20

Multiple Ion Detection is employed in a small but growing proportion of drugs/driving cases for the confirmation of drugs initially detected by radioimmunoassay methods. Morphine (as the bis-trimethylisilyl derivative), diazepam and nitrazepam are confirmed by this technique. Other drugs e.g. cocaine and tetrahydrocannabinol are only encountered from time to time. Work is currently in progress to develop a suitable assay by this technique for the metabolites of tetrahydrocannabinol.

GC/MS of Barbiturates. Of the thirty or so barbiturates available pharmaceutically only five are commonly encountered in toxicology work i.e. buto-, amylo-, pento-, quinal-and pheno-barbitone. The latter has a highly characteristic spectrum whereas the 5 ethyl substituted barbiturates buto-, amylo and pento-barbitone exhibit very similar spectra[4] dominated by intense fragment ions at m/z 169 and 184 (when dimethylated). Quinalbarbitone has a spectrum typical of 5-allyl substituted barbiturates with intense fragment ions at m/z of 195 and 196. The metabolites arising from these barbiturates also have spectra with the same intense ions. Therefore, mass chromatograms utilising these ions are particularly useful for evaluating GC/MS data from extracts of blood and urine when barbiturates are encountered at low levels and/or partially obscured by unresolved co-extractives. The barbiturates do not show ions of significant intensity in the molecular ion region and due to the large number of cases dealt with, final identification rests on GC retention data rather than the use of PICI.

Negative Ion Chemical Ionisation

The Characterisation of barbiturates has been investigated by NICI with a view to overcoming the limitations of EI and PICI. The work was stimulated by proposed new legislation to place some or all of the barbiturates under restriction. Thirty barbiturates were examined using the direct insertion probe and with quantities of the order of 1μg. The simple spectra obtained can be rationalised in terms of the following scheme proposed by Hunt et al[2].

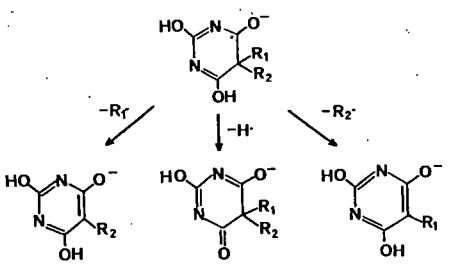

The ions corresponding to $(M-H)^-$, $(M-R_1)^-$ and $(M-R_2)^-$ unambiguously identify the majority, whilst the relative intensities serve to differentiate the isomeric ones as shown in the spectra below

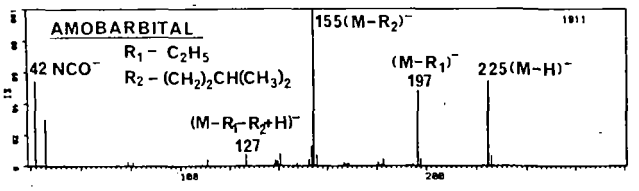

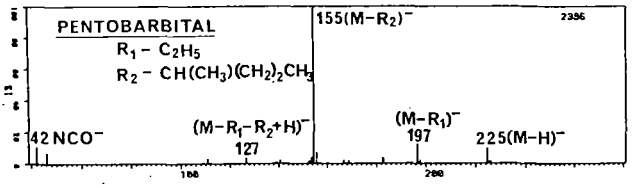

In the case of the allyl barbiturates a base peak corresponding to the loss of the allyl substituent from the M- ion is the base peak. Although the $(M-H)^-$ ion is weak it can be assigned with confidence due to the low background interference. Furthermore the ion corresponding to $(M-R_1-R_2+H)^-$ provides additional confirmation of the structures. All the barbiturates could be distinguished except butalbital and idobutal neither of which is branched at the carbon atom in the substituent immediately adjacent to the ring. It appears that branching at this position is a prerequisite for differentiating the isomeric barbiturates.

The Detection of Benzodiazepines by NICI would appear to be favourable since these compounds have good electron capturing properties. This has been partially borne out and strong M^- ions are seen with some fragmentation although the majority of the ion current is carried by the halide ion. NICI does allow the more ready detection of benzodiazepines in dirty extracts and when used with MID partially overcomes the non-specific responses due to co-extractives. The NICI spectra of the benzophenones derived by hyrolysis of the benzodiazepines are characterised by M^- ions except for compounds like lorazepam (see spectrum below) for which the highest mass ion corresponds to $(M-CL)^-$

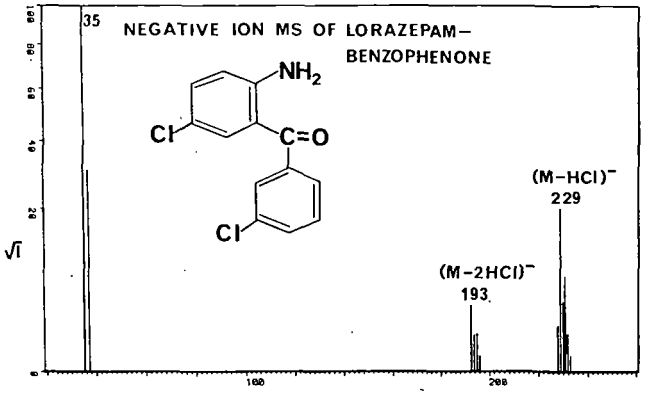

The detection limits for pure standards of lorazepam using MID was about the same (100 pg) for NICI and EI but five times better than PICI (500 pg). For bloods 'spiked' with lorazepam, the detection limit using EI was 10 ng/ml whereas using NICI 1 ng/ml was readily detected.

CONCLUSIONS

It has only been possible to highlight two areas where mass spectrometry is used in this laboratory for toxicology and drugs analysis. However, there is no doubt that during the past ten years this has been the most significant new technique introduced in this field. As instruments become more widespread and hopefully relatively cheaper, it is to be expected that a greater proportion of forensic toxicology and drugs cases will be dealt with by MS since it has the advantage of speed, specificity and sensitivity. That is not to say that MS is the answer to all problems in this field and research and development is still required to extend the capabilities of routine mass spectrometers at a reasonable cost.

Referenes

1. R. Bonnichsen, A.C. Maehly, Y. Marde, R. Ryhage and B. Schubert, Z. Rechtsmedizin 67 19 (1970)

2. M.J. Whitehouse and L.V. Jones in Recent Developments in Mass Spectrometry in Biochemistry and Medicine 6. A. Figerio and M. McCamish (Eds) Elsevier in press.

3. A.J. Clatworthy, L.V. Jones and M.J. Whitehouse, Biomed Mass Spectrom 4 248 (1977).

4. R.F. Skinner, E.G. Gallaher and D.B. Predmore Anal.Chem., 45 574 (1973).

5. D.F. Hunt, G.C. Stafford, F.W. Crow and J.W. Russell, Anal.Chem., 48 2098 (1976).

RPMOA2 GAS CHROMATOGRAPHY-MASS SPECTROMETRY, AN ESSENTIAL TECHNIQUE IN MEDICO-LEGAL INVESTIGATION. B. S. FINKLE, PH.D. Center For Human Toxicology, Univ. of Utah, Salt Lake City, Utah 84112.

The determination of cause and manner of death in sudden, unexplained fatalities is the responsibility of Medical Examiners and Coroners. Their decisions can have profound public health consequences, involve the financial and social welfare of the bereaved, influence industrial and public safety regulations, and often effect criminal trials. There are three elements to the medico-legal investigation of these cases; the circumstances surrounding the death, the forensic autopsy, and laboratory studies. The last of these assumes prime importance in cases of suspected poisoning and, therefore, analytical toxicology techniques used to detect, identify and quantitate poisons, drugs and their pharmacologically active metabolites are critical. Chronic exposure to very small concentrations of these agents which modern industrial and medicinal chemists can synthesize in extremely potent forms, may be undetectable by conventional analytical chemistry. Gas chromatography-mass spectrometry in all its various guises has provided the required separation, qualitative specificity and sensitive quantitation, and has thus become the one essential technique in forensic toxicology. Some typical, multi-drug and metabolite fatalities will be described in which quantitative GC-chemical ionization-MS was used. These cases will include cocaine, phencyclidine and some narcotic analgesics as abused drugs, but the determination of the role of widely available therapeutic agents such as the benzodiazepines will also be discussed. GC-CIMS-computer techniques have proven to be one of the few indispensable approaches to the resolution of forensic toxicology cases. This assertion and its limitations will be discussed and illustrated.

RPMOA3 "APPLICATION OF GAS CHROMATOGRAPHY/MASS SPECTROMETRY TO PROBLEMS IN FORENSIC DRUG ANALYSIS", JEFFREY M. WEBER AND GEORGE F. YAMNITZKY, Drug Enforcement Administration, 555 West 57th Street, New York, NY 10019

Gas Chromatography/Mass Spectrometry (GC/MS) Analysis assisted by a computer is used in our laboratory for the analysis of licit and illicit drug samples. GC/MS capabilities have been available to this laboratory for approximately eight years, but only recently has its versatility been fully utilized as an aide in analysis since the addition of a data system two years ago. The small quantity of material needed coupled with the computer capability has allowed for the identification of trace quantities of adulterants in complex mixtures. Several examples will be presented illustrating the use of "Limited Mass Plots" in conjunction with the library search system to identify these adulterants.

DISCRIMINATING BETWEEN METHAMPHETAMINE AND PHENTERMINE BY CHEMICAL IONIZATION-MASS SPECTROMETRY, STEVEN K. LORCH and JOHN D. SNYDER, Narcotics and Dangerous Drug Unit, Madison Heights Laboratory, Forensic Science Division, Michigan State Police, 30303 Stephenson Highway, Madison Heights, Michigan 48071

Methamphetamine and phentermine both have a molecular weight of 149. Due to close structural similarity, they are not easily distinguishable by Electron Impact Ionization-Mass Spectrometry. Chemical Ionization-Mass Spectrometry (Finnigan Model 3100F) using methane as the reactant gas yields easily distinguishable spectra. Both compounds form a protonated molecular ion $(M{\cdot}H)^+$, M/e 150, $(M+1)^+$. Methamphetamine, a secondary amine, then loses NH_2CH_3, yielding a large fragment of M/e 119, whereas phentermine, a primary amine, loses NH_3, yielding its base peak, M/e 133. Furthermore the base peak of methamphetamine is its $(M+1)^+$, M/e 150, while the $(M+1)^+$ of phentermine is approximately 23% of its base peak. An $(M-1)^+$, M/e 148, which is indicative of an aliphatic amine, is present in the spectra of both compounds. However M/e 148 in methamphetamine is larger than in phentermine. Common to the spectra of both compounds is the tropylium ion C_7H_7, M/e 91. The adduct ions $(M+C_2H_5)^+$, M/e 178, and $(M+C_3H_5)^+$, M/e 190, as well as the ions $(M+C_2H_5)^+ - NH_2CH_3$, M/e 147, and $(M+C_3H_5)^+ - NH_2CH_3$, M/e 159, are observed in the spectrum of methamphetamine, while ions $(M+C_2H_5)^+ - NH_3$, M/e 161, and $(M+C_3H_5)^+ - NH_3$, M/e 173, are observed in the spectrum of phentermine.

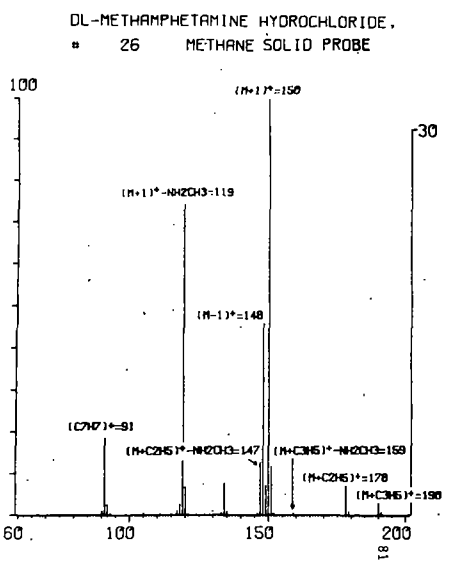

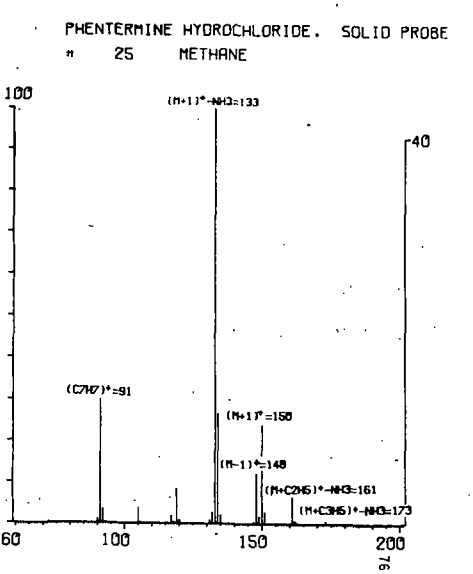

MASS SPECTRAL COMPARISON OF DIPHENETHYLAMINES OF FORENSIC INTEREST,

T. C. KRAM, 8 Feather Rock Pl., Rockville, MD 20850

A number of forensic laboratories in this country and abroad have been concerned with the characterization of impurities found in drugs of illicit manufacture. The identification of these compounds has often been instrumental in determining the source of manufacture. Generally, these impurities fall into three groups: reactants, intermediates, and by-products.

A good deal has been written concerning the identification of impurities in illicit amphetamine and methamphetamine, in recent years. In most instances, structural determination has required the combined application of spectrometric techniques. However, a recognizable pattern of mass spectral fragmentation has emerged which characterizes diphenylalkylamines of structural type I.

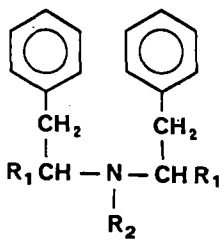

I

			m/e of the ion produced			
MW	R_1	R_2	a	b	c	d
239	H	CH_3	148	105	44	91
253	CH_3	H	162	119	44	"
267	CH_3	CH_3	176	119	58	"
281	CH_3	CHO	190	119	72	"

TABLE I

The pattern is featured by the presence of four intense ions which permit the prediction of strucure on the basis of mechanisms already well documented:

(a) cleavage β to N (1)

(b) fragmentation of the ion from (a) alpha to N with charge transfer to the phenylalkyl moiety (2)

(c) α, β cleavage to N with H rearrangement (1) and

(d) formation of a tropylium ion at m/e 91 from benzyl with additional fragmentation at m/e 77, 65, 51, and 39 (3)

Fragments accounted for by these processes may be observed in the data obtained by Weibel and Hesse (2) in their comprehensive work on N-methyldiphenethylamine (R_1 = H, R_2 = CH_3) and its β ring substituted analogs. They supported mechanism (b) from the examination of metastables. Similar compounds have been observed in methamphetamine (table 1,

second and third compounds) and amphetamine (second and fourth compounds)(4-7). Although they differ from the Weibel- Hesse compounds in that they possess an α-methyl group, their fragmentation follows the same pattern. Analysis of the second compound by a magnetic sector instrument also indicated a metastable for the transition of ion (b) to ion (c).

The last of these compounds is especially interesting in that it is an amide and that it appears in the GLC of illicit amphetamine as a doublet (OV-1 or alkaline Apiezon), both peaks of which produce identical mass spectra. Support for the amide structure is provided by production of a fragment predictable from a mechanism proposed by Gilpin (8) which is a variation of (c) in which the α-cleavage is at the amide C-N linkage. This would result in the formation of a m/e 162 fragment which is observed in the spectrum although it is not of great intensity.

Isolation of the doublet components was achieved by reverse phase HPLC (65% methanol; Waters μ-Bondapak C_{18}) which permitted further examination by IR, confirming the amide group, and by PMR, which, although it supported the two-dimensional representation predicted from the mass spectral data, clearly showed differences attributable to diastereoisomerism.

It is not unlikely that other compounds of structural type I will be found in the future, particularly in the examination of other phenthylamine drugs that have not yet received the attention accorded to amphetamine and methamphetamine.

(1) Gohlke, R. S. and McLafferty, F. W., Analytical Chemistry, 34 (10), 1281 (1962)

(2) Weibel, P. A. and Hesse, M., Helvetica Chimica Acta, 56 (7), 2460 (1973)

(3) Grubb, H. M. and Meyerson, S., in "Mass Spectrometry of Organic Ions," F. W. McLafferty, Ed., Academic Press, New York, 1963, p. 505.

(4) Bailey, K., Boulanger, J. G., Legault, P., and Taillefer, S. L., Journal of Pharmaceutical Sciences, 63 (10), 1575 (1974)

(5) Barron, R. P., Kruegel, A. V., Moore, J. M., and Kram, T. C., Journal of AOAC, 57 (5), 1147 (1974).

(6) Kram, T. C. and Kruegel, A. V., Journal of Forensic Sciences, 22 (1), 40 (1977)

(7) Kram, T. C., ibid., 24 (3), 596 (1979)

(8) Gilpin, J. A., Analytical Chemistry, 31 (5), 935 (1959)

PYROLYSIS MASS SPECTROMETRY IN FORENSIC SCIENCE

IAN JANE
Metropolitan Police Forensic Science Laboratory, 109 Lambeth Road, London SE1 7LP.

Pyrolysis Mass Spectrometry (PyMS) has been in use in this laboratory for a number of years and a number of instrumental arrangements have been investigated (1,2). This paper illustrates the advantages and disadvantages of the various methods for the analysis of forensic samples. The computer analysis of results in an attempt to maximise their evidential value is discussed.

EXPERIMENTAL

We have the choice of two low resolution mass spectrometers: a quadrupole instrument (VG Micromass 12-12) and a magnetic sector instrument (VG Micromass 12F). Both instruments are equiped with dual Electron Impact (EI) / Chemical Ionisation (CI) sources. The fast scan rates possible with a quadrupole mass spectrometer offers the possibility of detection of transient pyrolysis species. In addition sufficient scans can be obtained from a rapidly changing pyrolysis flux to enable a representative pyrogram to be obtained. Since magnetic sector instruments can not compare in scan speeds the pyrolysis flux must be introduced more slowly into the mass spectrometer, the spectra produced are inherently more stable leading to more reproducible pyrograms. Although CI mass pyrograms are more readily interpretable, EI has the advantages of higher sensitivity, better reproducibility and low molecular weight pyrolysis products are not excluded by the background from the CI reagent gas.

The pyrolysis systems were either Curie-Point (Pye Unicam Curie-Point pyrolyser, VG Micromass Pyrolysis Probe), or filament (Chemical Data Systems pyroprobe) type pyrolysers. The Curie-Point pyrolysers, in which the sample is crimped into a Curie-Point wire, have the advantages of very rapid sample heating and accuracy of pyrolysis temperature the absolute value being determined by the composition of the wire. The filament pyrolyser, in which the sample is loaded into a quartz tube inside the filament, has a slower heating rate since the sample tube must be heated before the sample but the heating is still reproducible. In this case sample loading is easier and sequential pyrolysis at successively higher temperatures may be performed on a single sample thus providing an additional dimension to the analysis. The pyrolysers can be coupled to the mass spectrometer via a standard jet separator with the pyrolysate being swept by a flow of helium into the instrument. Alternatively, as in the case

of the VG pyrolysis probe, the pyrolysate is drawn into the mass spectrometer under vacuum via a lenght of microbore glass lined tube.

RESULTS AND DISCUSSION

For forensic applications there are two requirements of a PyMS system, i.e. identification of a sample and comparison of control and suspect materials. The former is relatively simple, since the mass pyrogram can be compared in a 'fingerprint' sense with those obtained from standard samples or individual components of the pyrogram can be identified from their mass spectra. Any of the possible arrangements of instrumentation will provide good characterisation of most organic polymer systems. The evaluation of data from control and suspect comparison is more challenging and requires good reproducibility in both short and long term.

Reproducibility was evaluated using the three pyrolysis systems coupled to the magnetic sector mass spectrometer (3). The mass spectrometer was tuned to give a standard spectrum for toluene introduced through a vapour inlet. Samples of an acrylic paint, known to pyrolyse reproducibly, and an alkyd paint, which pyrolyses irreproducibly, were analysed over a six week period. A number of significant ions from each sample were monitored for relative intensity variation. Good results were obtained on all systems for the acrylic paint (long term inter compound reproducibility 3 - 8% R.S.D.). Intra compound variation as measured by m/z 103/104 ratio from styrene, a component in the acrylic paint pyrolysate, showed good reproducibility (better than 3% R.S.D. for all systems). For the alkyd paint the results were considerably worse (long term inter compound reproducibility 6 - 60% R.S.D.), indicating that the problem lay in the pyrolysis and interface and not the mass spectrometer. The same samples examined by the quadrupole mass spectrometer gave results which were qualitatively the same but the intra compound variation was considerably worse (6 - 9% R.S.D.). Some problems were also encountered in tuning the quadrupole instrument to give standard spectra for the toluene.

In order to improve the results for the alkyd paints attention was concentrated on the filament pyrolyser in combination with the magnetic sector mass spectrometer. By close control of pyrolysis and interface parameters, especially pyrolysis temperature and rise time together with interface temperatures and activity, we have been able to obtain similar reproducibility for alkyd paints as for the acrylics. It is possible to obtain good identification of the chemical type of a paint with as little as 0.5ug. of sample, but at least 5ug. samples are required before the most reproducible ion intensities are obtained.

COMPUTER ASSESSMENT OF RESULTS

One of the major advantages of PyMS as a forensic analytical technique is the suitability of the mass pyrograms for data processing methods. The library software on **our** mass spectrometer computer (VG Data System model 2000) was used to store and compare pyrolysis results. This provides for storage of the mass - intensity data from the pyrograms together with associated sample information. In addition it is possible to control the depth of search by the use of software filters which were originally intended by the manufacturer to reduce searching times. They can however be used to ensure that only a certain type of sample is compared with the suspect. The filters that we use correspond to: type of sample; date of analysis; imput parameters (e.g. pyrolysis temperature); car manufacturer and make; date of manufacture; and colour. Thus for a control and suspect comparison of for example a red vehicle paint the use of filter values allows us to give a fit factor value and state that the control and suspect were more similar with each other than with a certain number of previously analysed red vehicle paints. The search is measured on the basis of a fit factor value as defined by:

$$\text{Fit factor} = 1000 \left(1 - \frac{\Sigma(Ix - Iy)^2}{\Sigma(Ix^2 + Iy^2)}\right)$$

were Ix and Iy are the normalised intensities of a given ion in the two pyrograms. A perfect fit would be 1000 and from identical samples analysed on the same day we would expect a fit value better than 995.

This system is perfectly adequate for the majority of cases where there are significant chemical differences between the samples, however in cases where there is very similar chemical composition it is limited.

FIGURE 1

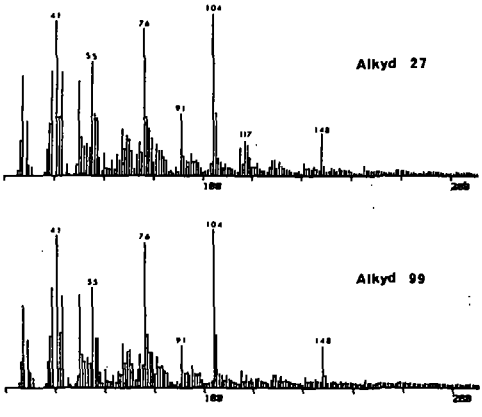

Household Gloss Paint - Alkyd 27

HD19V		D	17	FITS
FIT	S.REF		BASE	CN
999	R	4	104	ALKYD 27
993	R	15	41	ALKYD C1
992	R	10	104	ALKYD 81
991	R	5	41	ALKYD 36
991	R	12	104	ALKYD 99
990	R	14	41	ALKYD C2
989	R	11	41	ALKYD 90
987	R	14	41	ALKYD 117
985	R	17	41	ALKYD C3
983	R	9	41	ALKYD 72
978	R	8	41	ALKYD 63
977	R	7	41	ALKYD 54
974	R	3	41	ALKYD 18
948	R	13	104	ALKYD 108
821	R	18	41	ALKYD C4
454	R	6	118	ALKYD 45
575	R	19	118	ALKYD C5

Alkyd paints produce a complex pyrogram with numerous ions at significant intensities all arising from the basic alkyd. If a small amount of a chemical modifier is included, as is common in alkyd paints, then small but significant ions can be seen in the pyrogram. However because they are only present at low intensity they can not provide much change in the fit factor value and a false positive match can be obtained. Figure 1 shows an example of two alkyd paint pyrograms with very significant differences at m/z 117 and 118 for which the fit value is quite high (991) as can be seen from the library search result. Multivariate analysis of a range of alkyd paint pyrograms on an off-line computer has shown that there are a limited number of significant ions (m/z 50, 55, 57, 60, 77, 91, 104, 105, 147) from which discrimination can be achieved. Use of these in addition to the fit factor makes PyMS a good dicriminatory technique for alkyd paints (4).

CONCLUSIONS

PyMS is a good technique for the identification of organic polymers, it can be easily operated in conjunction with a GC-MS sytem. If control suspect comparisons are required for forensic purposes much greater control must be exercised over the variables in the sytem but it is possible to obtain results reproducible enough to allow good discrimination of the materials commonly encountered in forensic analysis.

REFERENCES

1. Hughes J.C., Wheals B.B., Whitehouse M.J. Forensic Sci. 1977, 10 217.
2. Hughes J.C., Wheals B.B., Whitehouse M.J. Analyst 1978, 103 482.
3. Hickman D.A., Jame I. Analyst 1979, 104 334.
4. To be published (information from author on request).

GUNPOWDER ANALYSIS BY GAS CHROMATOGRAPHY/CHEMICAL IONIZATION MASS SPECTROMETRY

D. R. Hardy, FBI Laboratory, Research Unit, Washington, D. C. 20535

Several practical objectives involving the chemical analysis of gunpowders in forensic laboratories were outlined as follows: (1) the ability to differentiate between single base and double base gunpowders; (2) the ability to differentiate various canister and commercially loaded gunpowders; (3) the ability to match or associate one or two powder flakes from a fired weapon (cartridge case or shell) with a flake of powder on a victim's clothing.

A rapid, simple and highly specific method of sampling the headspace vapors of smokeless powders under vacuum has provided a very accurate means of achieving the first objective. Eighteen canister powders chosen at random were successfully identified as single or double base in a blind test based upon the presence or absence of nitroglycerine.[1]

The second objective was achieved by utilizing a gas chromatograph/chemical ionization quadrupole mass spectrometer system. The column was 3% OV-101 on HP-AW Chromasorb W 100/120 mesh. The temperatures for analysis were somewhat critical. The gas Chromatograph injector and gas chromatograph/mass spectrometer interface temperatures were held at $155^{o} \pm 5^{o}$ C. The mass spectrometer source temperature was $175^{o} \pm 5^{o}$ C. Three randomly chosen commercial gunpowders were chosen for this part and the third part of the feasibility test. Powder samples were extracted with acetone and aliquots were directly injected into the gas chromatograph. The qualitative and relative quantitative results indicate that this method does have the ability to differentiate various gunpowders.

Finally, acetone extracts were taken from fired cartridge cases and from particles recovered from a cotten cloth target at close range and compared with the original total reconstructed mass chromatograms of the unfired powders. For all three samples examined the reconstructed mass chromatograms of the powder, fired cartridge and cloth target were similar and at least one unique component's chemical ionization mass spectrum from each sample was comparable. Hence, this technique could be used in some cases as a necessary but not sufficient examination in linking a fired weapon to the victim and/or the scene of a crime.

There appeared to be no interferences from blood, sweat, or dyes utilizing this sample extraction method and no measurable loss of materials is experienced when samples are analyzed up to four weeks after test firing.

Several additional questions were then addressed: (1) can volatile organic components (VOC) from gunshot residues taken from handswabs be detected by gas chromatography/mass spectrometry; (2) are there more efficient or more selective solvent extraction systems for the VOC; (3) what is the range limitation based upon minimum detectable levels of VOC extracted from cloth targets?

The results of extensive work in this laboratory showed that no detectable amount of VOC were present in acetone handswabs using the methods outlined above. It was also found that most moderately polar organic solvents were suitable for the extractions from cloth or cartridge cases.

The firing range limitation question was expanded at this point in order to attempt to answer the more difficult question: is there a statistically valid correlation between the relative amounts of VOC and firing distance?

Based upon signal/noise ratios, ease of sample preparation, relative signal heights and relative deviations, a twelve cm diameter (centered on the bullet hole) sample was chosen as optimal. Forty shots were then fired into cotten cloth targets, five each at one to eight foot range in one foot intervals. A log plot of the signal heights for two of the VOC (diphenylamine and dibutyl phthlate) vs firing range distance showed that a correlation does exist, but standard deviations were so great in most cases that no conclusions could be drawn at distances greater than two feet.

Krishnan[2] has attempted much more successfully to correlate firing distance with amounts of antimony deposited on cloth targets using neutron activation analysis. His relative deviation was about 25% in all cases and in some cases he was able to tell firing distances accurately up to ten feet. He discarded all data from samples which contained the bullet hole itself as those samples gave much higher relative deviations and precluded drawing any conclusions of firing distance from calibration curves. He feld that there may have been a wipe-off effect in the bullet hole area causing the widely varying results. At the present time the firing range experiment is being repeated in the light of this work on inorganic constituents of gunpowders.

(1) D. R. Hardy and J. J. Chera, J. Foren. Sci. 24(3), 618 (1979).

(2) S. S. Krishnan, J. Foren. Sci. 12(1), 112 (1967).

THE TOXICOLOGICAL ANALYSIS OF DRUGS IN RACEHORSE URINE USING TLC-GC/MS

G.A. Maylin and J.D. Henion
New York State College of Veterinary Medicine
Cornell University, Ithaca, NY 14853

Introduction

The detection, isolation and confirmation of drugs and their metabolites in the blood and urine of racehorses is a challenging analytical problem. A wide variety of drugs including stimulants, depressants, narcotics, anesthetics and analgesics are used in very small doses to alter the performance of race horses illegally. Consequently, an effective testing program must be capable of detecting and properly identifying several thousand drugs and metabolites at concentrations less than a microgram per ml of blood or urine. Sensitivity as low as several nanograms per ml or lower are often required.

Microtechnique thin layer chromatography (MTLC)[1] complimented by gas chromatography/mass spectrometry provides an affordable, efficient method for screening a large number of samples and confirming the identity of drugs with the specificity afforded by GC/MS. The ability to optimize the techniques of MTLC and GC/MS applied to drug testing can provide the maximum sensitivity and specificity possible today. Other analytical techniques including UV spectra, RIA and LC and GC data are often not required.

MICROTECHNIQUE THIN LAYER CHROMATOGRAPHY (MTLC)

MTLC is the application of conventional TLC on a miniature scale. It differs from HPTLC in that conventional TLC plates are used so that larger amounts of biological extract can be applied to the plate. All procedures including extraction, concentration of extract, sample application, development solvents and visualization by chromogenic spray reagents are optimized for sensitivity. In addition to being used as a screening method, it also serves as a clean-up for GC/MS when used in the preparative role.

Sample clean-up or partial purification of a complex mixture by means of selective extraction is an important preliminary step for any chromatographic method. The extraction method should remove the desired compound or class of compounds from the interfering matrix in a selective manner. The best extraction is one that provides a "clean extract" as compared to an extract that contains slightly more compound of interest but significantly more background. Although the class of compound to be analyzed is important, the matrix or "background" material often dictates the amount of sample, the pH of the aqueous phase and the polarity of the solvent used in the extraction. Optimized extraction can only be achieved experimentally by trial and error with urine or blood from horses administered realistic drug doses.

MTLC uses as standard protocol separate, 10 ml urine volumes which are extracted at pH 3 with hexane/dichloromethane/diethyl ether: 1/1/1 and at pH 8 and at pH 12 with dichloromethane/isopropanol: 3/1. Because extraction of small urine volumes is readily automated and consumes small volumes of solvent, additional extractions with a variety of solvents such as petroleum ether may be conducted as special tests. In addition, routine acid and enzyme hydrolysis of glucuronide and ethereal sulfate conjugates are facilitated by use of small urine volumes. Silica gel 60 microcolumns with a bed volume of 0.5 cm x 3 cm are used for preparative clean-up of extracts when required. Contrary to popular belief, use of large volumes in extraction procedures does not necessarily improve sensitivity limits.

Concentration of biological extracts is the most commonly used method to improve sensitivity. Concentration of solvents under vacuum or concentration by means of a gentle stream of nitrogen at 60°C in subdued light is imperative in order to optimize recovery. If care is taken to prevent exposure to large surfaces of glass, many reactive compounds will not absorb providing that trace amounts of alcohol are present.

Through the judicious use of selective extraction and sample concentration, an extract can be suitably prepared for application to the TLC plate. Conventional, 0.25 mm precoated silica gel 60, F254, TLC plates (EM Laboratories, Darmstadt, Germany) are used in the microtechnique mode. HPTLC plates are not used because they are readily overloaded by most biological extracts, they are expensive and are not readily available. By spotting 5 to 10 microliters of extract redissolved in 25 to 50 microliters of ethyl acetate, relative sensitivities comparable to HPTLC are attainable. It is imperative to limit spot size to less than 2 mm in diameter since diffusion is a major factor in limiting sensitivity. Glass capillaries, one mm i.d., hand-drawn to approximately 10 micron i.d. tips, are used to facilitate applying small spots. Care must be taken to prevent overspotting.

Selection of development solvents to achieve the desired separation of components is best accomplished by trial and error. Separation of drugs and metabolites from interfering background material is often more difficult than separating drugs from each other. Ideally, background is left at the origin or moved to the solvent front so that drugs can be detected in the middle part of the chromatoplate. In linear TLC, the upward solvent velocity decreases with the distance that the solvent has migrated and the more diffuse the spots become. Thus, short development times or distances enhance sensitivity and still provide the desired separations. In MTLC standard development distances are 4 cm in unsaturated tanks.

Standard development solvents used in MTLC are as follows: acid extractable drugs are developed in chloroform/cyclohexane/acetic acid: 4/4/2 and chloroform/ethanol: 9/1; neutral and base extractable drugs are developed in ethyl acetate/methanol/ammonium hydroxide: 85/10/5 and methanol/ammonium hydroxide: 100/1.5; following acid or enzyme hydrolysis base extractable drugs are developed in chloroform/methanol/propionic acid: 72/18/10.

An important aspect of MTLC is the visualization of separated components. A combination of fluorigenic and chromogenic reagents are used to provide selectivity for classes or groups of compounds. Standard visualization reagents for use in MTLC are as follows: acid extractable drugs are detected by quenching, acid-induced fluorescence and reaction with sodium metavanadate (Mandelin's reagent); neutral and base extractable drugs are detected by a combination of fluorescamine, Mandelin's reagent and Dragendorff's reagent, copper chloride and sodium nitrite spray sequences. Phenothiazine tranquilizers are detected with FES reagent (ferric chloride 500 mgs, sulfuric acid 50 ml, ethanol 250 ml). A number of additional reagents including Fearon's, acidified iodoplatinate, Ehrlich's and diphenylcarbazone-silver nitrate-mercuric sulfate are routinely used to supplement standard protocol.

GC/MS

For GC/MS analyses, samples are extracted and concentrated as described above for MTLC. If the drug or metabolite are present in sufficient quantity, analysis by GC/MS using conventional packed columns may be possible. However, in many instances, the concentration of drugs are sufficiently low so that background or components eluting from the GC at any given time provides "mixed" mass spectra. These data can cause difficulty in interpretation and identification due to discrepancies in the spectra. There are several ways of avoiding mixed mass spectra during GC/MS analyses. Capillary columns have significantly enhanced our ability to separate similarly eluting components and chemical ionization GC/MS can facilitate detecting coeluting components. However, careful control of packed column GC conditions coupled with preparatory thin layer chromatography can provide the necessary pruification step prior to mass spectral analysis. If necessary, mass spectra data can be obtained from the direct insertion probe following preparative MTLC in two different solvent systems.

The Hewlett-Packard 5992A GC/MS equipped with packed columns has proven to be a dependable, sensitive mass spectrometer when used in conjunction with MTLC. Because of its relative low cost, it can be used to replace conventional gas chromatographs and UV spectrophotometers normally used in many drug testing laboratories. Through the judicious use of derivatizing agents, most drugs and metabolites can be converted to volatile, thermally stable compounds suitable for GC/MS analyses. Mass spectrometers equipped with capillary columns, positive and negative CI, LC interfaces and direct insertion probes are required only in special circumstances.

Drug library search systems greatly facilitate the identification of unknowns. In addition to the limited library of the 5992A, commercially available mass spectral search systems are available. The Probability Based matching System (PBM) and Self Training Interpretival Retrieval System (STIRS) developed by McLafferty's group[2] is used extensively.

The utility of MTLC and GC/MS in drug analysis is shown in Table 1. Following the administration of 0.1 mg of fentanyl to a 1000 pound horse, the major metabolite, fentanyl beta-ketoacid is hydrolyzed to despropionyl fentanyl which can be screened by MTLC and confirmed by GC/MS. The minimum detectable level for the major metabolite is five nanograms per ml urine.

References

1. Maylin, G.A. Thin Layer Chromatography: Quantitative Clinical and Environmental Applications. (ed., J.C. Touchstone and D. Rogers) Wiley-Interscience, N.Y. 1980.

2. Dayringer, H.E., McLafferty, F.W. Venkataraghavan, R. Org. Mass Spectrom. 11, 895 (1976).

ANALYSIS OF FENTANYL METABOLITES IN URINE

FLOW DIAGRAM

10ml URINE (fentanyl beta-ketoacid, despropionyl fentanyl)

↓ 1ml 9N HCl
15 psi for 20 minutes

HYDROLYZED URINE

↓ 1ml 10N NaOH

BASE URINE (despropionyl fentanyl)

↓ 5 ml petroleum ether

EXTRACT

↓ N_2

RESIDUE

a ↙ ↓ b ↘ c

TLC	GC/MS	COLUMN CHROMATOGRAPHY
GC		TLC
		GC/MS

GC/MS of Alkylated Acids in Toxicology

Acid Drugs

Many drugs used in veterinary practice and human therapeutics are acid extractable compounds. These drugs cover a very broad range of therapeutic action such as analgesia, anti-inflammation, diuresis, hypnosis and sedation. They are from many families of compounds, such as barbiturates, fenamic acids, and ibufenacs, and characteristically contain acidic N-protons, carboxylic acid groups, and phenols. From a toxicological and forensic standpoint, there has arisen a need to analyze and screen for these compounds via GC/MS.

Current Procedures and Problems

Gas Chromatography and Mass Spectrometry

Gas chromatography of these drugs with a versatile stationary phase (e.g. OV-101) and with most conventional detection means is not a substantial problem; trimethylsilyl (TMS) derivatives lend a sufficient polarity change to these compounds for elution (1). However, these derivatives, when subjected to mass spectrometry, yield substantially altered spectra relative to those of the underivatized (parent) compounds (2).

Mass spectral analysis of TMS derivatives of these drugs (see Table) results in three readily observed phenomena. 1. All of the compounds fragment the TMS group, resulting in a substantial 73 m/e peak. This lowers the uniqueness of the spectrum of any one compound relative to the spectra of other similarly derivitized compounds. 2. The majority of the compounds yielded the 73 m/e peak as the base peak of the spectrum. In the case of fenoprofen, an ibufenac, the TMS fragment comprised 30% of the total ion current. This factor leads to normalization problems and makes lower abundance mass peaks harder to rationalize. 3. The addition of 72 amu to the parent compound makes a widened mass scan mandatory. This decreases the S/N and makes for a longer scan time.

Solution

An alternative to the TMS derivative which has proven to be much less of an interpretive problem is the methyl derivative. It may be obtained easily through the method of extractive alkylation. This procedure is simple, clean and not overly time consuming. Extractive alkylation is slightly more selective than silylation and can be used as a general screen for a large number of acid extractable drugs (see Figure).

drug	MW	methylate base peak CI	methylate base peak EI	methylate Ret Ind	location fig.
amobarbital	226	255	169	1.12	4
barbital	184	213	169	1.00	1
butabarbital	212	241	169	1.07	2
clonixin	262	277	263	1.62	9
fenoprofen	242	257	197	1.63	12
flunixin	296	311	295	1.66	7
meclofenamic acid	295	310	242	1.64	10
mefenamic acid	241	256	223	1.57	8
mephobarbital	246	261	232	1.27	6
motrin	206	221	161	1.27	11
naproxen	230	245	185	1.72	13
oxyphenbutazone	324	353	352	2.07	16
pentobarbital	226	255	169	1.10	3
phenylbutazone	308	323	183	1.73	14
secobarbital	238	267	196	1.15	5
tolmetin	257	272	212	1.74	15

Table

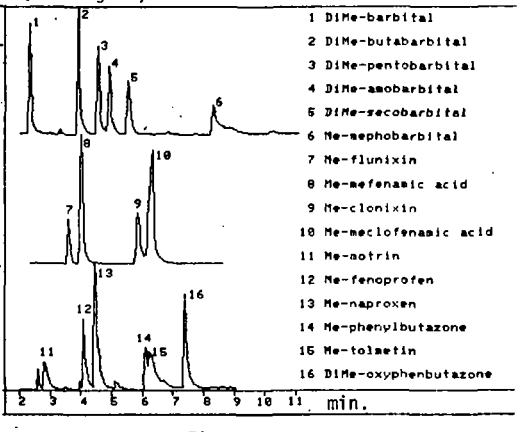

Figure

Experimental

Derivatization

Methyl derivatives were formed by a modification of the method of Lindström, et al (3,4,5). 1-ml volumes of aqueous 1-mg/ml solutions of the drugs (see Table) were acidified with 0.5-ml of 2N HCl. The mixtures were then extracted with 5-ml of dichloromethane, centrifuged, and the organic phase recovered. Additions of 2-ml of 0.2N sodium hydroxide, 0.1-ml of tetrahexylammonium hydrogen sulfate, and 0.1-ml of methyl iodide were made atop the dichloromethane organic phase. The mixtures were then shaken at room temperature for 15 min. After centrifugation and recovery, the organic phases were taken to dryness under a stream of dry air at 55°C. After 2-ml of aqueous saturated sodium borate solution and 4-ml of hexane were added to the residues, the mixtures were shaken vigorously for 5 min.

at room temperature and centrifuged. A 1-ml portion of the hexane layer was removed and diluted with 5-ml of clean hexane. Four microliters of this dilution were injected into the GC/MS.

Instrumental

The samples were chromatographed on a Hewlett-Packard 5840 GC containing a 10 meter 3% OV-101 WCOT column. Splitless injection mode was used with helium carrier gas. The temperature was programmed from 80°-260° C at 30°/min. with a one minute initial delay. Chromatographic detection and mass spectral acquisition were carried out on a Hewlett-Packard 5985B quadrupole MS system in both 70 eV E.I. and 180 eV methane C.I. modes.

Results and Discussion

Alkylation

On examination of the mass spectra acquired, it appears that methylation occurs fairly predictably at three sites of acidity. N-methylation occurs at secondary nitrogens adjacent to strongly electron withdrawing groups. Methyl esters and methyl ethers form at carboxylic acid groups and phenols, respectively. Another site of methylation has been observed and confirmed by the NMR spectrum of phenylbutazone. This compound methylates at the tertiary carbon atom adjacent to two electron withdrawing carbonyls.

Gas Chromatography

On examination of the capillary GC results, all alkylates chromatographed with sufficient resolution on the OV-101 stationary phase at temperatures which posed no threat of column damage. The highest elution temperature of the samples analyzed was that of dimethyloxyphenbutazone, which eluted at 225° C. It was also noted that most retention characteristics of the alkylates were very comparable to those of their TMS analogs. In many cases the alkylates showed less tailing than their TMS analogs.

Mass Spectrometry

Mass spectral analysis of the alkylates in the methane C.I. mode contributed data illustrating the degree of methylation of each sample.

Electron impact spectra of the alkylates supplied more detailed information as to the nature of the derivatives. From all appearances, loss of a charged methyl group (15 m/e) does not have nearly the frequency as a loss of a charged TMS from a silyl analog. Spectra of methyl derivatives prove to be quite predictable and fine spectral detail varies minimally from that of the parent compound.

From the data compiled, three general observations have been made which may prove helpful to the analysis of unknown samples and forensic work. 1. Mono-methyl derivatives, for the most part, retained the same base peak as their parent compound. Thus, data search by base peak will yield evidence for the parent compound. 2. Mono-methyl derivatives did not appear to alter the low end fingerprint of the parent compound's spectrum appreciably. This again favors the data searching process. 3. Shifted mass locations increase as multiples of 14 and most predominantly above the parent compound's base peak. Should all of these observations prove to be consistent phenomena, fairly accurate spectrum reconstruction for parent compounds from their methyl derivatives can be simple and systematic, something not afforded through TMS derivatives.

D. E. Gallis, J. A. Rudy, and C. B. Woodward
Equine Toxicology Center
PA State Harness Racing Commission
West Chester State College
West Chester, PA 19380

References

1. B.J. Gudzinowicz, M.J. Gudzinowicz, and H.F. Martin, Fundamentals of Integrated GC-MS, 1976, Marcel Dekker
2. M. Klein, A.V. Kruegel, Stanley P. Sobol, Ed., Instrumental Applications in Forensic Drug Chemistry, U.S.D.E.A., 1978
3. B. Lindström and M. Molander, J. Chrom., 101, 219 (1974)
4. B. Lindström, M. Molander, and M. Groschinsky, J. Chrom., 114, 459 (1975)
5. C. Fagerlund, P. Hartvig, and B. Lindström, J. Chrom., 168, 107 (1979)

THE DEVELOPMENT OF AN ANALYSIS FOR Δ9-THC IN BLOOD, MICHAEL P. MCGEE, JAMES C. VALENTOUR, PH. D., AND RANDALL P. EDWARDS, DEPARTMENT OF GENERAL SERVICES, DIVISION OF CONSOLIDATED LABORATORY SERVICES, BUREAU OF FORENSIC SCIENCE, RICHMOND, VA. 23219.

Approximately 10% of the drivers arrested for driving under the influence of alcohol in Virginia have blood alcohol concentrations less than the statuatory limit of 0.10% weight/volume. It was decided to analyze those samples less than 0.10% alcohol for the presence of drugs other than alcohol. One drug of particular interest was Δ9-tetrahydrocannabinol(THC), an active component of marijuana.

As the method would require a minimum detectable level of 5 anaograms per ml or less, it was decided to investigate the formation of electron-capturing derivatives of THC, with the idea of screening by electron-capture gas chromatography, and confirming positives by gas chromatography-mass spectroscopy. The pentafluorobenzyl derivative of THC(THC-PFB) was chosen. The derivatization was phase-transfer catalyzed by tetrahexylammonium chloride (THA) with pentafluorobenzyl bromide(PFBB).

One ml of blood and one ml of pH 9.2 saturated sodium borate are extracted with two 5 ml aliquots of hexane. The combined hexane layers are washed with 0.1N NaOH and then with 0.1N sulfuric acid. To the hexane layer is added 1 ml of water, 0.5 ml of saturated sodium bicarbonate, 25 microliters of 4000 mg/L THA in methanol, and 10 microliters of PFBB. The tube is rotated for at least 30 minutes. The hexane layer is then evaporated to dryness. At this point, the residue is too dirty to analyze directly by GC, so the residue is cleaned up by liquid chromatography. The residue is reconstituted with 60 microliters of mobile phase(3% water in acetonitrile), and 50 microliters are injected on the LC. The LC column is RP-18, 10 micron, and the flow is 1.2 ml/minute. The retention volume of THC-PFB is about 20 ml. Three ml of the eluate, centered on the retention volume of THC-PFB is collected and diluted to 10 ml with water. Then 100 microliters of toluene is added, the tube is shaken and centrifuged, and 4 microliters of the toluene layer is injected into the GC. The GC is equipped with a Nickel-63 linearized electron-captur detector, a 4-foot glass column, packed with 3% OV-17 on Gas-Chrom Q. The carrier gas is 10% methane in argon, with a flow of 30 ml/minute. The column oven is operated at 230°C isothermally. THC-PFB has a retention time of about 400 seconds. Positive samples are confirmed by evaporating the remaining toluene in a reactivial, reconstituting with 10 microliters of methanol, and injecting into the mass spectrometer. The mass spectrum of THC is shown in figure 1. The mass spectrometer(Hewlett-Packard 5993) is operated in the selected-ion mode, monitoring m/e 494.2 and 313.2. The appearance of both ions at the retention time of THC-PFB is confirmatory. The selected-ion plots from two cases found to contain THC are shown in figure 2.

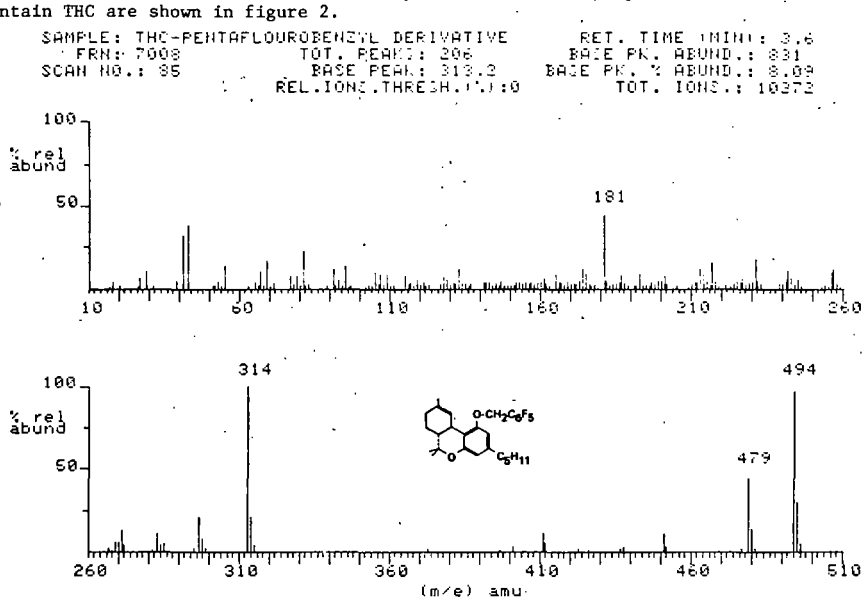

Figure 1

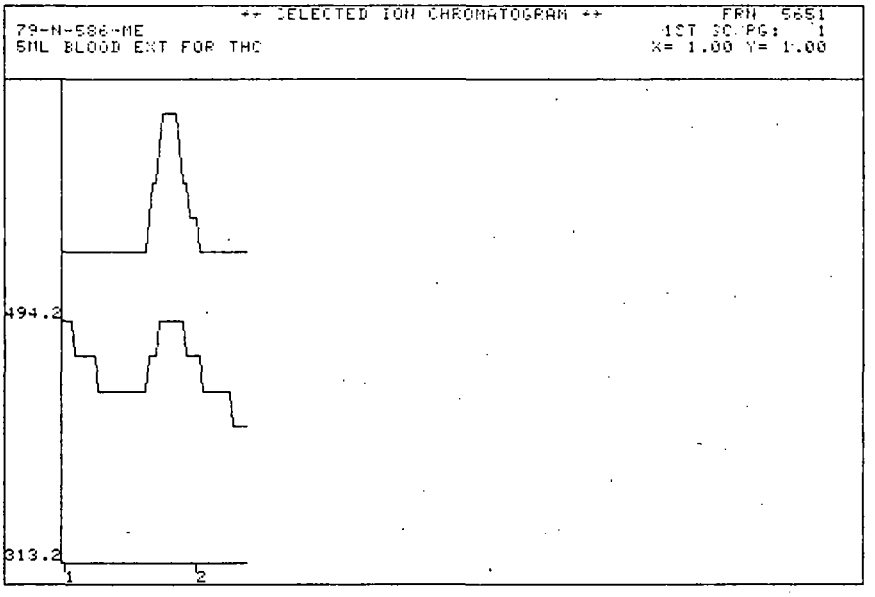
** SELECTED ION CHROMATOGRAM **
FRN 5651
79-N-586-ME
1ST SC/PG: 1
5ML BLOOD EXT FOR THC
X= 1.00 Y= 1.00
494.2
313.2
1
2

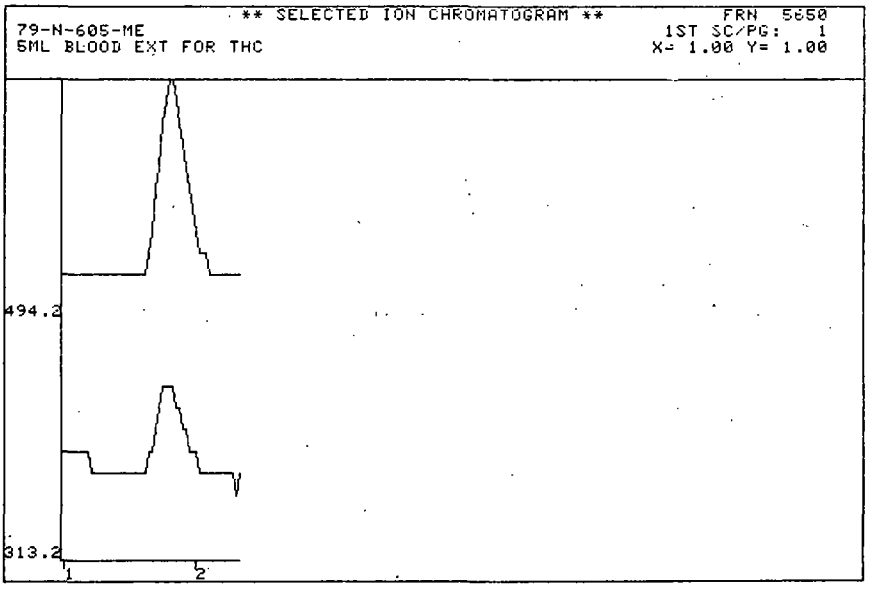
** SELECTED ION CHROMATOGRAM **
FRN 5650
79-N-605-ME
1ST SC/PG: 1
5ML BLOOD EXT FOR THC
X= 1.00 Y= 1.00
494.2
313.2
1
2

Figure 2

STEROID PROFILES OF HEALTHY INDIVIDUALS

SPITELLER, G., PFEIFER, P. and REINER, J., Lehrstuhl für Organische Chemie I der Universität Bayreuth, Postfach 3008, D-8580 Bayreuth West Germany

We mainly investigate profiles of urinary steroids, since urine is easily available and the information obtained from blood and urine steroid profiles is often similar. Our aim is to see whether there are differences between healthy and sick individuals.

First of all we had to clarify the question of how a normal profile[1] changes with time. For this purpose we investigated steroid excretion during different periods in a day, a week, or even a month. We took samples about every four hours.

A profile of urinary steroids must be divided into two parts: androgens show much lower retention times than the heavier cortico steroids. We prefer to react the latter into TMS enol-ethers instead of TMS-MO derivatives[2], since the corticosteroids thus come off much earlier. Main androgenes usually are androsterone and etiocholanolone. The main corticoid is tetrahydrocortison[1].

Usually the excretion of all these steroids increases from morning till noon and drops in the afternoon. The variation in steroid excretion during a day is high. It is usually tried to compensate for this known phenomen by analysis of 24 hour specimens.

In comparing the excretion over several days we often observed variations of 100 % and even more (Fig. 1). These changes can not be avoided by taking 24 hour specimens.

The profiles reveal that the ratio of excreted steroids remains rather constant. An exceptional behaviour is only observed for one steroid - dehydroepiandrosterone (DHEA). This steroid is excreted at very different rates depending on the individual and the time of day. This excretion rate is not in correlation with the excretion rates of the other steroids[3]. Most individuals (80 %) show a very low level of DHEA excretion. But if the individual suffers from psychic stress it increases to rates as high as the excretion rates of androsterone and etiocholanolone. For instance in students just before a final examination the DHEA levels is increased by a 40-50 fold amount over normal values[4]. After the stress situation and during a rest period (sleep) the values drop to normal ones. Interestingly 9 out of 10 people react to psychic stress in the same manner, but no change is observed in the profile of one individual out of ten, although this individual is equally stressed. Thus varying response to stimulation must be assumed: A small group of individuals - one out of ten - shows a different behaviour: beginning after waking the DHEA excretion rises rapidly to a high level and remains at this level till night (Fig. 1).

Obviously the varying DHEA excretion indicates that the steroid metabolism in some individuals (20 %) differs strongly from the usual one.

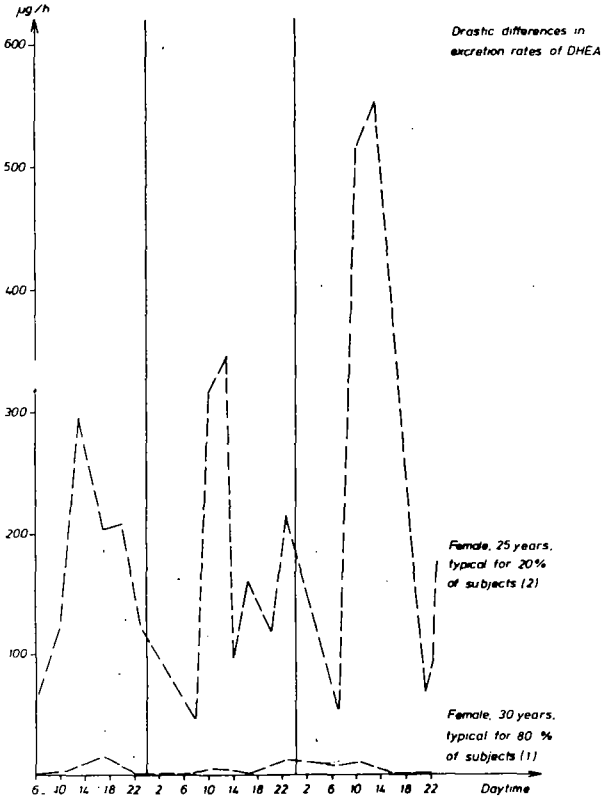

REFERENCES

1) E.C. Horning, C.J.W. Brooks, L. Johnson and W.L. Gardiner, Sep. Sci., 1, 555 (1966)
2) J.-P. Thenot and E.C. Horning, Anal. Lett., 5, 955 (1972)
3) M.G. Metcalf, Clin. Biochem. 11, 65 (1978)
4) H. Ludwig, M. Spiteller, H.-J. Egger and G. Spiteller, Israel J. of Chem. 16, 7 (1977)

STEROID PROFILES IN CHRONIC DISEASES

SPITELLER, G., PFEIFER, P., REINER, J. EGGER, H.-J., Lehrstuhl für Organische Chemie der Universität Bayreuth, Postfach 3008, 8580 Bayreuth

LUDWIG-KÖHN, H., MATTHAEI, H., Universität Göttingen, 3400 Göttingen (W.-Germ.)

HOLZMANN, H., BENES, P., Universität Mainz, 6500 Mainz (West Germany)

It is well known from other investigations that in chronic liver diseases the excretion of steroids changes. An increase of 3-keto-Δ^4-steroids in urine is especially observed[1]. Our investigation confirmed these results. In addition we observed intense peaks in the gas chromatograms far beyond the region of corticoids.

Fig. 1: Urinary steroid profile of a patient suffering from a severe liver desease

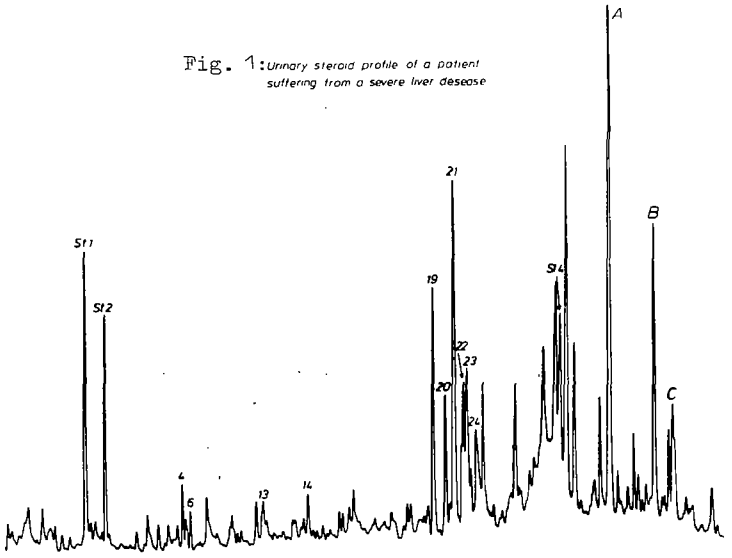

The peaks marked with A, B, and C are only observed if very efficient columns are used, otherwise these compounds are lost. The mass spectra of these compounds (Fig. 2) revealed that they correspond to highly oxygenated compounds carrying 4 and 5 OH-groups recognizable by a subsequent loss of trimethylsilanol.

The similarity of the published mass spectrum of 3α, 7α, 12α, 24-tetrahydroxycholestan[2] and compound A (Fig. 2) suggested the presence of a 3,7,12 and 24-hydroxylated saturated steroid.

The C.I. spectrum revealed a molecular weight of 798, confirmed by a peak of mass 708 (loss of trimethylsilanol) in the E.I. spectrum. The main peak in the high mass region corresponded to the loss of a fragment with 117 MU. A complementary peak at mass 117 indicated the structure of the missing residue to probably be:

$$CH_3\text{-}\overset{+}{C}H\text{-}OTMS$$

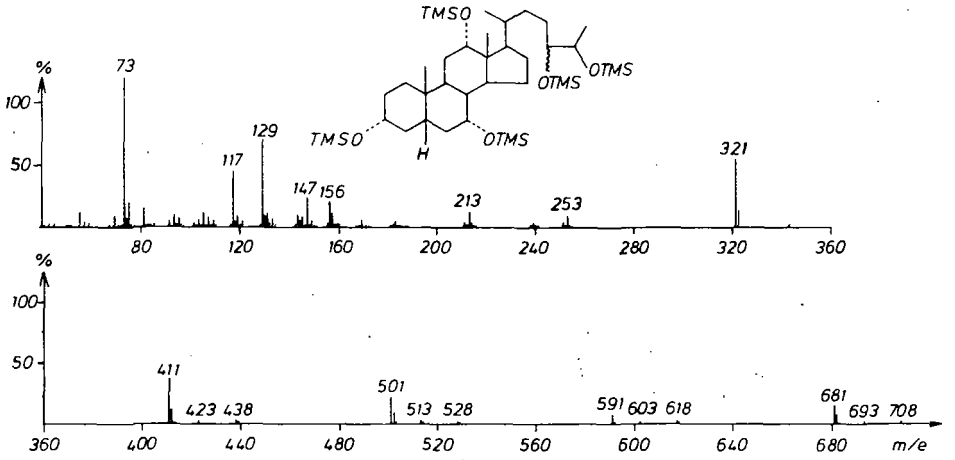

Fig. 2: Mass spectrum of compound A

Thus we were able to define the structure as a 3,7,17,24,25 pentahydroxy nor-cholestane. If this assumption - so far not proven by synthesis - is correct, one of the main metabolites in chronic liver diseases is a previously unknown alcohol, obviously an accumulation product on the way from cholesterol to cholic acid.

The other compounds are pentahydroxy cholestanes, all with 27 carbon atoms. All these alcohols are also found in healthy subjects, but in much lower amounts.

Steroid metabolism seems to be affected not only in kidney[3] and liver diseases. The blood steroid profiles of psoriatic patients are rather similar to those of uremic patients. They also show a decrease in DHEA excretion[4].

Since the investigation of blood profiles is very cumbersome and time consuming, we also tried to find differences in the urine steroid pattern. At first glance the urine profiles were rather similar to normal ones.

A careful quantitative measurement revealed that at least in the case of a heavy attack of psoriasis the corticoid excretion was lowered to 1/4 or less of its normal value. The rate of androgen excretion was also diminished.

A disease rather similar to psoriasis is the "endogenous eczema". The urine steroid patterns of such patients again show a much lower excretion of corticoidsteroids.

We only investigated profiles of a few types of patients suffering from chronic diseases. It must be anticipated that analogous effects will be detected in other diseases, too. This would possibly not only be true of the steroid pattern but also of other groups of compounds, e.g. amino acids, peptides, etc. Thus profiling combined with MS may provide us with a better understanding of metabolic diseases.

REFERENCES

1) D.H.P. Streeten, Gastroenology, 37, 643 (1959)
2) T. Cronholm and G. Johansson, Eur. J. Biochem. 16, 373 (1970)
3) H. Ludwig-Köhn, G. Spiteller, D. Mattaei and F. Scheeler, J. Chromatogr. 146, 381 (1978)
4) H. Ludwig-Köhn, F. Messing and G. Spiteller, J. Chromatogr. 162, 573 (1979)

RPMOB3 PLASMA LEVELS OF FENTANYL IN DOGS BY GAS CHROMATOGRAPHY-MASS SPECTROMETRY, SHEN-NAN LIN, Tseng-Pu F. Wang, and Richard M. Caprioli, Analytical Chemistry Center, and Benjamin P.O. Mo, Department of Anesthesiology, The University of Texas Medical School, Houston, Texas 77025

Gas Chromatograph-Mass Spectrometry (GC/MS) methods have been developed to measure the extremely low levels of fentanyl, N-phenyl-N-[1-(2-phenylethyl)-4-piperidinyl] propanamide, a potent narcotic analgesic which is widely used as a clinical anesthetic. Deuterated fentanyl is synthesized for use as an internal standard. Two chemical reactions are involved in the synthesis. First, fentanyl is hydrolyzed in 20% DCl solution to form the deuterated despropionyl fentanyl. The latter component is re-esterified by propionyl chloride. Fentanyl-D_3 produced in this way is free from the intact drug and can be readily used as internal standard, provided two extraction procedures are performed during the synthesis. The drug in the biological fluid is extracted into ethyl acetate followed by analysis with gas chromatography-selective ion chemical ionization mass spectrometry. The detection limit is 200 picograms. The method is highly selective and is suitable for monitoring the time course of the plasma levels of fentanyl. By conventional graphic methods, the evaluation of the pharmacokinetic data reveals three linear regions of first order kinetics. The observation is in agreement with the literature. Two of the speculated major metabolites, despropionyl fentanyl and norfentanyl are also examined. In 28 plasma samples, no measurable amount of these two compounds are detected. Further investigations on the metabolism of fentanyl will be discussed.

FORMYLATION OF SECONDARY AMINES WITH DIMETHYLFORMAMIDE DIMETHYLACETAL

J.P. Thenot, T I. Ruo, and O.J. Bouwsma*
Clinical Pharmacology Center and Anesthesia Department, Northwestern University, Chicago, Ill. 60611;* Dow Chemical Texas Division, Freeport, Texas 77541

Dimethylformamide dialkylacetal (DMF-DMA) is a useful reagent for the derivatization of various functionnal groups, particularly carboxylic acids and amines. This reagent methylates acidic groups and reacts with primary amines to yield dimethylaminomethylene derivatives. This allows the one step derivatization of GABA. However, by-products are sometimes observed. For example after reaction of lysine hydrochloride with DMF-DMA, a small amount of N-methoxymethylene derivative may be formed by elimination of dimethylamine and not methanol from the following intermediate.

$$-NH_2 \longrightarrow -NH-CH(OR)N(CH_3)_2 \begin{cases} \nearrow -N{=}CHN(CH_3)_2 + ROH \\ \searrow -N{=}CH(OR) + NH(CH_3)_2 \end{cases}$$

With secondary amines there is no hydrogen to allow the elimination of dimethylamine or methanol and a rearrangement usuallly occurs to give the formyl derivative (1,2). We have confirmed this by identifying N-formylpiperidine as the product of the reaction of piperidine with DMF-DMA and N-formyl desipramine as the product of reaction of desipramine with this reagent.

$$=NH \longrightarrow =N-CH(OR)N(CH_3)_2 \longrightarrow =N-CHO$$

This finding contradicts a report that N-ethyldesipramine was formed under these conditions. The reaction is not limited to the dimethylacetal but is expected whenever alkylacetal used. In accordance with its polarity, N-ethyl desipramine is eluted before the N-formyl derivative on non polar phases such as SE-30 or OV-1. The CI spectra (methane) of these two derivatives are quite similar but the different basicity of the side chain nitrogen induces a different fragmentation pattern.

Deuterated imipramine and related antidepressants can be prepared by reducing the formyl derivative of the appropriate desalkyl compound with lithium aluminum deuteride, figure 1.

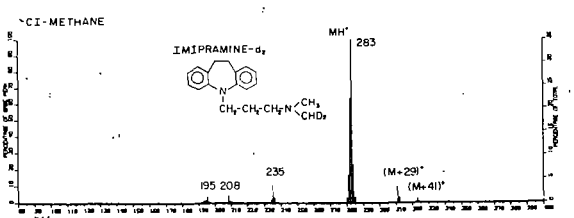

Figure 1: CI mass spectrum (methane) of Imipramine-d_2

1. J.P. Thenot, T.I. Ruo, and O.J. Bouwsma, Anal. Letters (in press).
2. The same conclusion was reached by M.S.B. Nayar and P.S. Callery (personnal communication)

ANALYSIS OF THE ANTICANCER DRUG METHYL-G BY GAS CHROMATOGRAPHY AND MASS SPECTROMETRY

Carl Johann Nielsen, Sylvia K. Daley, and Jon N. Peace
Cancer Pharmacology and Drug Chemistry Section
Biological Markers Program, NCI-Frederick Cancer Research Center
Frederick, Maryland 21701

Methyl-G (methylglyoxal-bis-guanylhydrazone, structure below) is an antitumor drug that has shown activity against experimental animal tumors in addition to a number of human cancers including endometrial, renal cell, and colorectal carcinoma. While the exact mechanism of action of this drug is as yet unknown, a growing body of evidence has demonstrated that it inhibits S-adenosylmethionine decarboxylase activity giving rise to decreased levels of spermidine.

METHYL-G (NSC 32946)

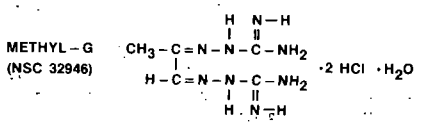

Methyl-G often produces marked toxicity when administered to cancer patients in effective doses on a daily basis. This problem can be alleviated by less frequent administration suggesting that the drug is cleared very slowly from the human system. Current studies from this laboratory are directed at determining if this is actually the case. While methyl-G has received considerable attention over the last several years, no definitive means of analyzing it chemically in biological samples has been presented. The purpose of this report is to describe some of the initial studies being conducted in this laboratory in an effort to solve these and related problems.

Methyl-G can be conveniently analyzed by gas chromatography after trimethylsilyl derivatization. This reaction readily proceeds to completion in approximately one and a half hours at 40°C using the trimethylsilylating agent MSTFA (N-methyl-N-trimethylsilyl-trifluoroacetamide). Under the same conditions, methylethyl-G, the analog being used in this laboratory as an internal standard, also reacts to completion. Increasing the temperature to 70°C causes an increase in reaction rate but speeds the process of degradation of the desired product. Lowering the temperature markedly protracts the reaction time. The product of this reaction starting with either methyl-G or methylethyl-G is the corresponding tetratrimethylsilyl derivative in which four of the guanyl protons are substituted as shown in the following diagram.

Both of these derivatives may be gas chromatographed using a column (4 ft x 2 mm) packed with 1% SP 2100 on 100-120 mesh Supelcoport. The retention indices are 2555 and

2600 for methyl-G-TMS_4 and methylethyl-G-TMS_4, respectively.

Mass spectral analysis of these two derivatives with a quadrupole system showed rather similar fragmentation patterns as interpreted in the diagram and table below. In the diagram, the drug and the internal standard are distinguished by the R notation on the left. The dotted lines describe the bond cleavages that give rise to the fragments noted by the small letters. This fragment notation is tabulated in the left column of the table along with the m/z values of the corresponding peaks from the mass spectra of the two derivatives. The Δm/z values are shifts in m/z seen in the spectrum of the derivative containing perdeuterated trimethylsilyl groups. The values of M^+ for both compounds correspond to the molecular ion of the tetra-substituted derivative. The Δm/z values of 36 in both cases confirm this. The base peak in both spectra corresponds to fragment a with m/z = 187.

The utility of methylethyl-G as an internal standard is exemplified by its similar mass spectrum as well as its similar derivatization reaction kinetics. A standard plot based on flame ionization detector peak area ratios of these two derivatives shows a linear relationship over the range 1 mg to 10 μg using 0.25 mg of the standard. The correlation coefficient of the resultant regression line determined by least squares fit is 0.9997. Maximum sensitivity achieved to date is 125 ng injected on column.

These methods are presently being applied to biological samples after partial prepurification. This can be achieved for concentrated samples with C-18 reversed phase mini-columns from which the drug can be eluted with acetone. Samples with concentrations in the micromolar range or less require ion exchange chromatography.

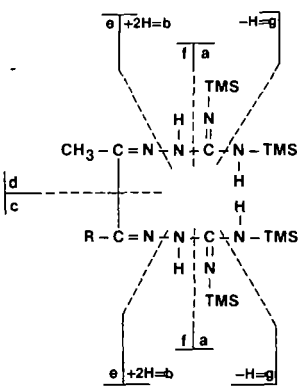

Fragment	Methyl-G (drug) (R = H) m/z	Δ m/z from d_9-TMS	Methylethyl-G (standard) ($R = CH_3CH_2$) m/z	Δ m/z from d_9-TMS
a	187	18	187	18
b	204	18	204	18
c	229	18	257	18
d	243	18	243	18
e	270	18	298	18
f	285	18	313	18
g – 15	368	24	396	24
g	383	27	411	27
M^+ – 29	–	–	471	36
M^+ – 15	457	33	485	33
M^+	472	36	500	36

Research supported by the National Cancer Institute under Contract No. N01-CO-75380 with Litton Bionetics, Inc.

GC-MS STUDIES OF PHENELZINE AND ITS ACYL DERIVATIVES

N. Narasimhachari and R. O. Friedel
Department of Psychiatry
Medical College of Virginia/Virginia Commonwealth University
Richmond, Virginia 23298

Phenelzine, β-phenethylhydrazine is one of the hydrazine type monoamine oxidase inhibitors used as an antidepressant in the treatment of some types of depression which do not respond to tricyclic antidepressants. Though there was a report on the mass spectral characteristics of various types of hydrazine derivatives by direct solid probe mass spectrometry, there is as yet no method available for the quantitation of phenelzine in human plasma or urine by gas chromatographic-mass spectrometry. Several gc methods for the assay of phenelzine in plasma and urine are described[1,2]. In recent clinical trials on human subjects with phenelzine, we used successfully a radioenzymatic method to monitor plasma levels. To evaluate the results obtained by this method we needed a reliable and specific method for its quantitation and therefore investigated the gcms-sim method for the quantitation of phenelzine in biological samples.

Phenelzine sulfate in ethylacetate suspension was heated in separate experiments with trifluoroacetic anhydride, acetic anhydride, and deuteroacetic anhydride at 80° for 15 monutes. Samples were evaporated and redissolved in ethyl acetate to contain 1 mg/ml. Similarly ethylacetate extracts of phenelzine from solutions in water, plasma and urine at pH 7 and 10 were derivatized with trifluoroacetic anhydride or acetic anhydride. A 3% OV-17 on Chromosorb WHP or 3% OV-101 on Chromosorb WHP were used for gc and Finnigan 4000 GC-MS Data system was used for mass spectral analysis.

Phenelzine forms multiple derivatives with trifluoroacetic anhydride, the mono and di-TFA derivatives were identified by methane chemical ionization mass spectrometry. Direct trifluoroacetylation of solid sample as well as organic estracts at pH 7 and 10 yield mixture of products (Fig. 1). Mild acetylation of phenelzine gives a monoacetate (Fig. 2) and prolonged acetylation with acetic anhydride or with pyridine and acetyl chloride gives the diacetyl derivative (Fig. 3).

Using 1-phenyln-propyl hydrazine as an internal standard and acetyl derivative for gc-ms we were not able to detect any phenelzine in plasma samples of patients on 60 mg/day of phenelzine dose. To test if phenelzine was metabolized by acetylation we also determined N-acetylphenelzine in plasma and urine samples using deuteroacetyl phenelzine as an internal standard. We monitored fragment ions m/z 87 and 90 for EI and mz 179 and 182 for methane CI. The levels of N-acetyl phenelzine were very low both in plasma and urine and there were no differences in the levels of acetylphenelzine between responders and nonresponders to the drug.

References:

1. B. Caddy, W. J. Tilstone and E. C. Johnstone Br. J. Clin. Pharmac. 3,633 (1976).

2. B. Caddy and A. H. Stead Analyst, 102, 42 (1977).

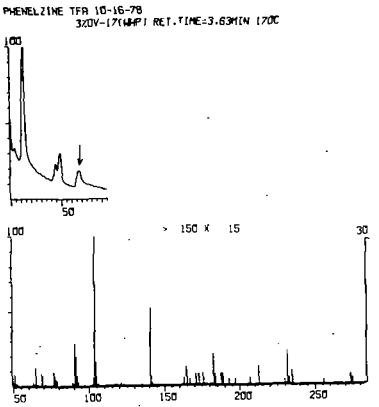

fig. 1

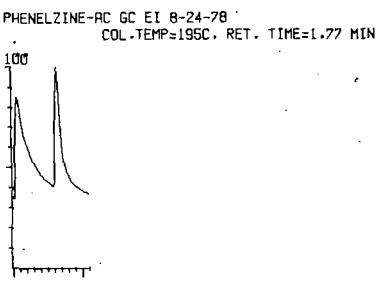

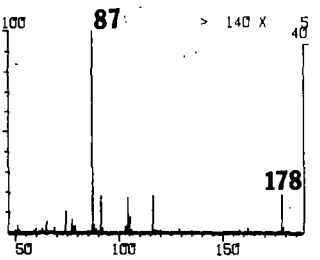

fig. 2

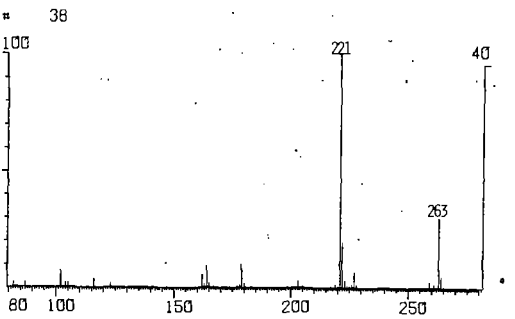

fig.3
CH_4-CI spectrum of N_1N_2-diacetyl phenelzine

A SELECTED ION RECORDING GCMS-TECHNIQUE USED IN BIOAVAILABILITY STUDIES OF ETILEFRINE.

H.-J. Förster and K.L. Rominger, Division of Research,
C.H. Boehringer Sohn, 6507 Ingelheim am Rhein, Germany.

Etilefrine, 2-ethylamino-1-(3-hydroxyphenyl)-ethanol, I, is a sympathomimetic amine used for many years in treatment of orthostatic disorders. The drug experiences a pronounced first pass effect, so that small concentrations of I, 1 - 10 ng ml^{-1}, together with 10 - 20 times larger concentrations of its sulfate conjugate, II, are present in plasma very shortly after administration [1]. Consequently an assay intended for use in bioavailability studies must not only be rather sensitive but in addition provide for a clear distinction of free and conjugated I.

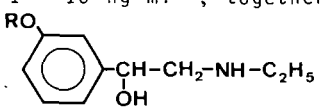

I (R=H), II (R=SO_3H)

The required sensitivity was achieved by an electron impact selected ion recording GCMS procedure with etilefrine-D_5 as internal standard and measuring of the N-acyl ions (m/z 254 and 259) of the N,O-heptafluorobutyryl derivatives. 0.5 ng ml^{-1} of I could still be assayed with a signal/background ratio of 3 : 1 (Finnigan-Incos 4023). Calibration curves obtained from plasma supplemented with varying amounts of I-HCl and 20 ng ml^{-1} of the internal standard were linear over the range of 0.5 - 15 ng ml^{-1}. The precision was $\pm$ 7 % (n = 32) at the 1 ng ml^{-1} - and $\pm$ 4 % (n = 32) at the 5 ng ml^{-1} -level. Mean concentrations of I in plasma determined by the described assay deviated from gravimetrically given "true" concentrations by -2 % (n = 8) at 0.5 ng ml^{-1} and by -1% (n = 4) at 5 ng ml^{-1}.

The results of analysis of variance (Table 1) performed separately for each concentration indicate that at low concentrations the GCMS-method (σ^2_{GCMS}) contributes more to the total variance ($\sum_1^3 \sigma^2$) than the sample work-up, whereas at high concentrations variance due to extraction ($\sigma^2_{Extr.}$) is larger. The largest contribution to the total variance, however, comes from a day to day variability (σ^2_{Days}). The quality of the chromatographic column as well as the ion source conditions are difficult to keep constant over prolonged periods of time. This together with the daily prepared final dilutions of I-HCl and the internal standard are probable sources of the observed day to day variability. As in bioavailability studies drug concentrations are compared which have been measured several weeks apart, this source of variation should not be overlooked. The coefficient of variability $K_V = \frac{100}{\bar{Y}}\sqrt{\sum_3^1 \sigma^2}$ can serve as an estimate of error for a single ratio measurement during a 10 week study ($\bar{Y}$, mean of peak height ratios; N, number of measurements). Ion pair formation with tetraphenylborate anion was employed in order to extract free I from plasma into organic solvents [2]. The selectivity of

different separation methods for free and conjugated etilefrine was investigated (Table 2) in experiments with plasma containing only the internal standard and 100 ng ml^{-1} synthetic II. Any II which finds its way into the free amine fraction will be converted to N,O-acyl-I during derivatization. Ion pair extraction as well as separation by weak cation exchange resins gave free amine fractions which only contained etilefrine-D_5. In contrast, the strong cation exchange resin Dowex 50 W x 2 retained a considerable amount of II in protonated form which was subsequently detected as derivatized I. Use of a strong cation exchange resin in bioavailability studies of etilefrine [3] would appear to result in erroneously high concentrations of I in plasma. Thus the effectiveness of different separation methods has immediate bearings on the plasma level time curves and the bioavailability data derived from them.

Table 1: Results of analysis of variance of peak height ratios over a period of ten weeks.

ng ml^{-1}	N	$10^7\sigma^2_{GCMS}$	$10^7\sigma^2_{Extr.}$	$10^7\sigma^2_{Days}$	$10^7\sum_1^3\sigma^2$	$10^3\bar{Y}$	K_V(%)
0.5	45	←45→		105	150	26.25	14.8
1	66	61	41	186	288	50.41	10.6
2	52	188	116	560	864	100.46	9.2
5	68	498	241	623	1362	241.97	4.8
10	40	282	1327	2695	4304	481.05	4.3
15	16	←1042→		2883	3925	752.50	2.6

Table 2: Selectivity of different separation methods for free and conjugated etilefrine. ng I-HCl found in free amine fraction of plasma containing 1 µg II and 20 ng ml^{-1} of etilefrine-D_5-HCl.

Ion Pair Extraction		Amberlite CG 50-II		Dowex 50 W x 2	
a	b	a	b	a	b
0	0	0	0	8	78

a: before and b: after sulfatase treatment

Acknowledgement: We are indebted to Mrs. E. Ecker, Mr. E. v. d. Oever and Mr. A. Wittrock for excellent technical assistance, to Dr. J. O'svath for the statistical treatment of the calibration data.

References:

1. K.L. Rominger and G. Hitzenberger, Int. clin. Pharmacol. 18, 150 (1980).
2. L.E. Martin, J. Rees and R.J.N. Tanner, Biomed. Mass. Spectrom., 3, 184 (1976).
3. J.H. Hengstmann, U. Weygand and H.J. Dengler, Europ. J. Clin. Pharmacol. 9, 179 (1975).

RPMOB8 AN IMPROVED GC-MS METHOD TO MEASURE TELE-METHYLHISTAMINE IN RAT BRAIN.

J.K. Khandelwal, Lindsay B. Hough & Jack Peter Green.
Dept. Pharmacology, Mt. Sinai Sch. Med., of the City Univ. of New York, New York, N.Y. 10029

The presence of tele-methylhistamine (1-methyl-4-(β-aminoethyl)-imidazole; t-MH), the metabolite of histamine in rat brain, and its relationship to putative histaminergic transmission have been the subjects of recent work. We modified the GC-MS method of Hough et al. (Anal. Biochem., 96:56-63, 1979) to enhance both sensitivity and reproducibility. The substitution of KOH for NaOH in extraction of t-MH considerably improved the recovery. Evaporation of the extract in 0.2N HCl, as used in the earlier method, reduced the formation of the heptafluorobutyryl derivative; substitution with 0.01N HCl more than doubled the recovery of the derivative. The derivatization procedure itself was changed. To the residue remaining after evaporation of HCl, 25 μl of toluene is added before adding the derivatizing reagents. This modification significantly improved reproducibility. T-MH standard curves obtained at different times after derivatization were indistinguishable. The modified method is capable of measuring less than 1 pmole of t-MH. The t-MH content found in nine rat brain regions agree with the values found by Hough et al. (loc. cit.).
Supported by a grant (MH-31805) from the National Institute of Mental Health).

DEVELOPMENT OF PRECISE QUANTITATIVE METHODS FOR USE IN CLINICAL CHEMISTRY

J.S. Holler, D.G. Patterson, and L.W. Yert, Toxicology Branch, Center for Disease Control, Public Health Service, Department of Health and Human Services, Atlanta, Georgia 30333

Since the early 1970's, a system for insuring accuracy in clinical chemistry has evolved, based upon a hierarchy of methods (1). Currently isotope dilution-mass spectrometry (ID-MS) is the best approach for the definitive method (i.e., most accurate and precise) for organic constituents.

A number of trials have been conducted to determine the precision of the ratio measurement of bromine isotopes in bromobenzene in evaluating instruments for these analyses. The magnetic sector instrument is a LKB9000 with a System Industries 150 data system. The quadrupole instrument is a Finnigan 4000 interfaced to an INCOS 2300 data system. Sample amounts from 500 pg to 1 ug bromobenzene injected on-column are analyzed monitoring molecular ions at m/z = 156 and 158 under optimum scan conditions. Precision of the ratio measurement approaches 0.2 to 0.15 in both instrument systems for the largest samples. Loss of precision is observed for the smaller samples, and generally a standard deviation greater than 1.0 is observed for samples in the range 1-5 ng.

Optimum instrument parameters developed in these tests have been used in developing a quantitative method for serum cortisol. Clinically, cortisol measurement is used to ascertain adrenal activity. The sample preparation used is adapted from that of Bjorkhem (2). The internal standard used is the commercially available D-4 compound (actually >75% D-3 in composition). Peaks are monitored at m/z = 605 for the dimethoxytrisilyl cortisol and m/z = 608 for the internal standard. During a series of analyses, high and low standards at concentrations approximately 1.2 and 0.8 times that of the standard are made using cortisol SRM. Samples are quantitated by linear interpolation between the two standards after correcting for contributions of the labelled compound to the 605 peak and unlabelled compound to the 608 peak.

This method has been applied to the determination of cortisol in a series of samples used recently in a proficiency testing program. The comparison with the routine, clinical methods is presented below. The results obtained using the magnetic sector instrument (Instrument 1) are confirmed by those obtained using the quadrupole instrument (Instrument 2). The coefficients of variation (1.7 and 1.3) for the ID-MS methods are better than those previously reported for serum cortisol (2,3), and continued development should meet the 1% accuracy requirement suggested by the American Association for Clinical Chemistry Cortisol Study Group.

CORTISOL REFERENCE MATERIAL

Method	# Lab	Mean (ug/dl)	SD
Analysis by RIA			
Beckman	14	40.09	3.23
Clinical Assays	124	29.19	3.24
Corning	40	24.54	2.98
Diagnostic Products	23	31.43	4.61
Micromedic Diagnostics	11	26.69	5.31
New England Nuclear	16	31.76	1.73
Other	45	28.98	5.65
Analysis by ID-MS (4 Vials)			
1st Instrument	16 Det.	31.74	0.53
2nd Instrument	14 Det.	32.32	0.41

1. N.W. Tietz, Clin. Chem., 25, 833 (1979).

2. I. Bjorkhem et al, Clin. Chim. Acta, 56 241 (1974).

3. L. Sickmann, J. Steroid Biochem., 11, 117 (1979).

Use of trade names is for identification only and does not constitute endorsement by the Public Health Service or by the U. S. Department of Health and Human Services.

Negative Ion Chemical Ionization Mass Spectrometry As A Structural Tool in the Determination of the Major Metabolites of Probucol In The Monkey

John Coutant, Ester Madrid Bargar, and Robert Barbuch
Dow Chemical U.S.A., Indianapolis, IN 46268

Probucol [4,4'-(isopropylidenedithio)bis-(2,6-di-tert-butyl phenol)] is a currently marketed hypocholesterolenic agent. In order to support chronic toxicity studies, including an eight year long-term study in the monkey which elicited no adverse effects, a study was undertaken to define the major biotransformation products of probucol in selected tissues of the monkey.

The positive ion spectra of probucol and its metabolites (both electron impact and chemical ionization) contain only a few, low intensity, high mass fragment ions and the spectra are often not unique. The use of negative ion chemical ionization (methane) produced unique spectra as well as intense high mass ions characteristic of the molecular weight. In addition many of the fragment ions in the negative chemical ionization spectra reveal important structural information absent in the positive ion spectra.

Metabolites in liver and adipose tissue from monkeys administered probucol were isolated and prepared by HPLC. In i.v. study, probucol labelled with 14_C and 13_C was used to assist in the identification of metabolites. Prepared samples were run by GC/MS or direct probe.

The unique structural information from negative ion chemical ionization mass spectra as well as complimentary information from positive ion chemical ionization mass spectra and electron impact mass spectra were combined to give an overall description of the biotransformation of probucol in the monkey.

This work to be published in Drug Metabolism and Disposition.

RPMOB11 MASS SPECTROMETRY AND CHEMISTRY OF REDUCED PYRIMIDINE NUCLEOSIDES AND RELATED ANALOGUES, J.A. KELLEY, V.E. Marquez, P.S. Liu and J.S. Driscoll, Drug Design and Chemistry Section, LMCB, NCI, NIH, Bethesda, MD 20205

Reduced pyrimidine and pyrimidine-like nucleosides are of considerable interest because of their broad spectrum of biological activity. Tetrahydrouridine is a potent inhibitor of bacterial and mammalian cytidine deaminase, while dihydro-5-azacytidine and its arabinosyl analogue show significant antitumor activity. A program undertaken to produce an improved transition-state inhibitor of cytidine deaminase resulted in the synthesis of a series of 1,3-diazepin-2-one nucleosides that were up to ten times more active than tetrahydrouridine. Mass spectrometry proved to be a highly useful means of characterizing these and similar synthetic nucleosides and, in conjunction with gas and liquid chromatography, for studying certain aspects of the chemistry of these biologically active compounds. A series of reduced pyrimidine, s-triazine and 1,3-diazepin-2-one nucleosides in which both the base and sugar varied were examined in both a free and derivatized form. Isotopically labelled derivatives were employed to correlate mass spectral structure information. An unusual acid-catalyzed isomerization of certain perhydropyrimidine and 1,3-diazepin-2-one nucleosides was observed and elucidated using GC/MS. The pentose sugars of reduced nucleosides that did not possess extended conjugation in the base could be easily isomerized from a furanose to a pyranose configuration with a concomitant reduction in biological activity. Control of this isomerization was crucial for successful synthesis of fully active inhibitors.

A RAPID METHOD FOR DETECTION OF VITAMIN B_{12} AND FOLIC ACID DEFICIENCY BY GCMS

EJ NORMAN, HK BERRY, OJ MARTELO, MD DENTON
DEPT. OF MED., UNIV. OF CINTI, CINTI, OH
45267

We have developed a rapid method for detection of both vitamin B_{12} and folic acid deficiency. The procedure consists of assaying 50 µl of urine for elevated methylmalonic acid (MMA) and formiminoglutamic acid (FIGLU).

Megaloblastic anemia results from either vitamin B_{12} or folic acid deficiency. Present clinical methods for determining levels of these vitamins rely on a radioassay. For proper evaluation of megaloblastic anemia determination of red cell folate, serum B_{12}, and serum folate is recommended.[1] This procedure is further complicated since measurement of serum B_{12} by radioassay can give both false high and low values.

Our mass spectrometric procedure has several advantages. It is rapid and noninvasive. In addition, it gives a more accurate picture of vitamin function and tissue stores since acid levels correlate with enzymatic activity. MMA requires B_{12} to be converted to succinic acid and FIGLU requires folate for transformation to glutamic acid. Consequently, an elevated amount of MMA or FIGLU indicates a vitamin B_{12} or folic acid deficiency, respectively.

The method consists of pipetting 50 µl of urine in a small bottle. After cyclohexyl esters are made,[2] 200 µl of ethyl acetate and 100 µl of trifluoroacetic anhydride are added and left at 80°C for 30 minutes. The mixture is evaporated with nitrogen at r.t. and 200 µl of methanol are added. GCMS analysis is accomplished using a 3% OV-17 column programmed from 125° to 275° C, 15° C/min., with selected ion monitoring of m/z 119 (MMA), m/z 199 (FIGLU), and m/z 133 (ethylmalonic acid).

The past two years we have assayed 341 patients for urinary MMA. Of these 302 were less than 5 µg MMA/ml, 23 between 5 and 10 µg MMA/ml and 16 between 10 and 3,000 µg MMA/ml. All 16 above 10 µg MMA/ml were diagnosed as having pernicious anemia, terminal ileum resection or methylmalonic aciduria. However, two of the proven pernicious anemia patients gave false normal levels of serum B12 using the radioassay method. Since radioassay of serum B_{12} has given false values an additional method of determining B_{12} deficiency is advantageous.

Measurements of urinary FIGLU gave 162± 72 µg FIGLU/mg creatinine (C) for 15 normals. Folate deficient patients revealed 1206 µg FIGLU/mg C, 659 µg FIGLU/mg C, and 809 µg FIGLU/mg C. This corresponded to serum folate levels of 1.8, 0.5, and 1.7 ng/ml respectively, with normal being >3.0. Two infants gave 916 and 6987 µg FIGLU/mg C indicating children with long illness resulting in poor caloric intake, vomiting or diarrhea should be monitored for folate deficiency. One folate deficient patient gave a normal FIGLU value indicating a histidine loading test should be administered for positive diagnosis.[3]

Since mass spectrometric analysis allows multiple assays on the same specimen other vitamin deficiencies or disease states could be similarly detected through monitoring urinary chemical markers.

1. Proc. of 22nd Ann. Mtg. of Am. Soc. of Hem., 1979, p. 91.

2. EJ Norman, HK Berry, MD Denton: Biomedical Mass Spectrometry 6: 12, 1979.

3. AL Luhby, JM Cooperman, DN Teller: American Journal of Clinical Nutrition 7:397,1959.

RPMOB13 THE STUDY OF THEOPHYLLINE METABOLISM IN PREMATURE INFANTS USING GC/MS. K.-Y. Tserng, K. C. King, F. N. Takieddine, and P. Adam. Dept. of Pediatric Case Western Reserve University at Cleveland Metro. General Hospital, Cleveland, Ohio.

In premature infants, theophylline (TP) is converted to caffeine; also, the biological half life is prolonged. To assess the metabolic alterations of TP during development of premature infants, a sensitive and simple GC/MS method was developed which quantifies the relevant metabolites of TP in plasma, blood cells, and urine.

Theophylline and its metabolites in the sample are converted to N-propyl derivative using n-propyl iodide in dimethylformamide with K_2CO_3 catalyst, and are analyzed under isothermal conditions on a GC/MS with a 3% OV-17 column. Deuterated caffeine (DC) is used as inter-nal standard. The ion current ratios between DC ($^m/e$ 197) and caffeine (C, $^m/e$ 194), TP($^m/e$ 222), theobromine (TB, $^m/e$ 222), 3-methylxanthine (3-MX, $^m/e$ 250), 1,3-dimethyluric acid (1,3-DU, $^m/e$ 280), and 1-methyluric acid (1-MU, $^m/e$ 308) are monitored. The total analysis time is 12 minutes with a detection limit down to pg.

No large variance in the composition of metabolites was observed among premature infants. A typical pattern is shown below:

	C	TP	TB	3-MX	1,3-DU	1-MU
Urine	8.7%	51.5%	7.2%	1.8%	21.8%	9.0%
Plasma	25.4%	64.8%	4.6%	1.0%	3.1%	1.1%
Red Cells	28.7%	57.4%	5.7%	5.0%	2.6%	0.6%

The change in metabolite patterns during infant development will be presented.

REACTIONS OF ORGANIC ANIONS WITH ORGANOMETALLIC COMPOUNDS, S. A. Sullivan and C. H. DePuy, Dept. of Chem., Univ. of Colo., Boulder, CO. 80309

We have initiated flowing afterglow investigations[1] of the reactions of organometallic compounds, in particular cyclopentadienyl nickel nitrosyl (CpNiNO), with a variety of negative ions including NH_2^-, OH^-, O_2^-, F^- and several carbanions (i.e. allyl and c-hexadienyl anions). Among the reactions observed are addition (1,2), proton abstraction from the c-C_5H_5 ligand (3) and displacement (4,5).

$$OH^- + CpNiNO \longrightarrow (CpNiNO)OH^- \quad (1)$$

$$F^- + CpNiNO \longrightarrow (CpNiNO)F^- \quad (2)$$

$$NH_2^- \ (OH^-) + CpNiNO \longrightarrow C_5H_4NiNO^- + NH_3 \ (H_2O) \quad (3)$$

$$O_2^- + CpNiNO \longrightarrow CpNiO_2^- + NO \quad (4)$$

$$NH_2^- + CpNiNO \longrightarrow C_5H_5^- + NH_2NiNO \quad (5)$$

Carbanions, as for example, allyl (6) and c-hexadienyl anion (7) react primarily by addition. With c-$C_6H_7^-$, a second reaction, hydride transfer (8) competes with addition.

$$C_3H_5^- + CpNiNO \longrightarrow (CpNiNO)C_3H_5^- \quad (6)$$

$$c\text{-}C_6H_7^- + CpNiNO \longrightarrow (CpNiNO)C_6H_7^- \quad (7)$$

$$c\text{-}C_6H_7^- + CpNiNO \longrightarrow (CpNiNO)H^- + C_6H_6 \quad (8)$$

The nickel hydride ion also results from direct addition of H^-(9). The source of H^- is electron impact on NH_3[2].

$$NH_3 + e^- \longrightarrow H^- + NH_2 + CpNiNO \longrightarrow (CpNiNO)H^- \quad (9)$$

In an attempt to measure the hydride affinity (HA) of CpNiNO, the reactions of $(CpNiNO)H^-$ with compounds of known hydride affinity were examined. In the series[3]: NO, CO_2, O_2, CH_3CHO, $C_6H_5CHCH_2$ and $CH_2CHCOCH_3$, definitive hydride transfer was observed only to $CH_2CHCOCH_3$, methyl vinyl ketone (10), which has a hydride affinity of 50±2 kcal/mole[3]. We roughly bracket the HA(CpNiNO) as 55±5 kcal/mole. The nickel hydride ion also reacts rapidly and quantitatively with $Fe(CO)_5$ forming $HFe(CO)_5^-$ (11), however, it did not transfer hydride to $Fe(CO)_3$.

$$(CpNiNO)H^- + CH_2{=}CHCOCH_3 \longrightarrow CH_3CHCOCH_3^- + CpNiNO \quad (10)$$

$$(CpNiNO)H^- + Fe(CO)_5 \longrightarrow HFe(CO)_5^- + CpNiNO \quad (11)$$

The proton transfer product, $C_5H_4NiNO^-$, reacts rapidly with CpNiNO by addition (12) and displacement of NO (13) forming nickel dimers. Similarly, $C_5H_4NiNO^-$ adds to many organic neutrals including dienes, olefins, alcohols,

$$C_5H_4NiNO^- + CpNiNO \longrightarrow (CpNiNO)C_5H_4NiNO^- \quad (12)$$

$$C_5H_4NiNO^- + CpNiNO \longrightarrow (CpNi)C_5H_4NiNO^- + NO \quad (13)$$

ketones and aldehydes. As shown in equation (14), for acetaldehyde, this reaction may proceed via initial proton transfer to the C_5H_4-moiety.

$$C_5H_4NiNO^- + CH_3CHO \longrightarrow [(C_5H_4NiNO)CH_3CHO]^- \text{ or } [(CpNiNO)CH_2CHO]^- \quad (14)$$

We can not say if a Ni-C bond is formed in reaction (14) or in carbanion addition to CpNiNO (6,7). All such addition products have proven to be unreactive with a wide range of organic and inorganic species. In particular, no reactions equivalent to ligand exchange have been detected.

Hydrogen-deuterium exchange of anions with deuterated reagents is a useful probe of ion structure.[4] Attempts to elucidate the structure of $C_5H_4NiNO^-$ have been unsuccessful, since no exchange is observed on addition of D_2O, CH_3OD, C_2H_5OD or CF_3CH_2OD. Interestingly, in each case, a peak appears at m/e 66, possible $C_5H_4D^-$. When NH_2^- is used to generate $C_5H_4NiNO^-$, a substantial amount of $C_5H_5^-$, m/e 65, is present. When the stable anion $C_5H_5^-$ is produced by base attack on c-pentadiene, it does not undergo exchange with any of the reagents noted above[5]. A possible mechanism for formation of m/e 66 involves deuterium abstraction from the RO-D bond (15).

$$C_5H_4NiNO^- + RO\text{-}D \longrightarrow C_5H_4D^- + (RONiNO)\ ? \quad (15)$$

In summary, we have examined the gas phase reactions of strong bases and carbanions with CpNiNO. These reactions produce interesting organonickel anions whose structure and reactivity we have just begun to probe. We have bracketed the HA(CpNiNO) at 55±5 kcal and observed hydride transfer reactions which suggest that it will be possible to determine relative hydride affinities for a range of organometallic compounds.

References:

1. E.E. Ferguson, F.C. Fehsenfeld and A.L. Schmeltekopf, Adv. At. Mol. Phys., 5, 1-56 (1969) and V.M. Bierbaum, C.H. DePuy, R.H. Shapiro and J.H. Stewart, J. Am. Chem. Soc., 98, 5229 (1976).

2. C.E. Melton, J. Chem. Phys., 45, 4414 (1966).

3. Hydride Affinities can be calculated from ΔHf_{298} of appropriate anions, which are available from gas phase acidity measurements. See J.E. Bartmess and R.T. McIver, Jr. in "Gas Phase Ion Chemistry" Vol.2, Academic Press, New York, 1979.

4. J.H. Stewart, R.H. Shapiro, C.H. DePuy and V.M. Bierbaum, J. Am. Chem. Soc., 99, 7650 (1977).

5. V.M. Bierbaum, C.H. DePuy, G.K.King and R.H. Shapiro,presented at the Twenty-Sixth Annual Conference on Mass Spectrometry and Allied Topics, held in St.Louis, Missouri, May 28 - June 2, 1978.

ON THE FORMATION OF ANIONIC CLUSTER IONS FROM DIETHYL ETHER AND ETHYL VINYL ETHER UNDER ICR CONDITIONS

R. van Doorn and K. R. Jennings

Department of Chemistry and Molecular Sciences,
University of Warwick, Coventry, CV4 7AL, U.K.

Although solvated ions are readily formed by three-body reactions in a chemical ionisation source or flowing afterglow apparatus, they are formed at low pressures under ICR conditions in two-body reactions of the type

$$B^- + AHM \rightarrow (AHB)^- + M \qquad (1)$$

providing that a suitable neutral species can be eliminated and that the energetics of the reaction are correct. Such ions have been observed in reactions of alkoxide ions with alkyl formates[1] and in base-induced elimination reactions of haloethanes with bases of appropriate base strength[2].

Earlier work in this laboratory[3] has demonstrated that the reaction

$$OH^- + (C_2H_5)_2O \rightarrow (C_2H_5O...H_2O)^- + C_2H_4 \qquad (2)$$

occurs by β-H atom transfer and the solvated ethoxide ions form the major product in this system. The present work describes a study of the energy requirements of this type of reaction under low pressure conditions in a number of related systems. We have investigated reactions of the three bases NH_2^-, OH^- and F^- with the three substrates diethyl ether, ethyl vinyl ether and vinyl acetate. In these systems, the competition between reaction (1), in which a solvated ion is formed, and the reaction

$$B^- + AHM \rightarrow BH + M + A^- \qquad (3)$$

is of interest ($B^- = NH_2^-$, OH^- or F^-, AHM is the neutral reactant and M is the neutral molecule eliminated from the reaction complex in forming the solvated ion AHB^-). The observed product ions together with the calculated enthalpies of reactions in which the unsolvated ion A^- is formed are summarised in the Table.

It can be seen that when NH_2^- is the reactant ion, A^- is by far the major ionic product and reaction (3), which is exothermic in all three cases, predominates over reaction (1). In the reactions of OH^- ions with diethyl ether and vinyl acetate, reaction (1) competes effectively with reaction (3) which, in each system, is close to thermoneutral. In the OH^-/ethyl vinyl ether system, reaction (3) is much more exothermic and as in the reactions of NH_2^-, it is much faster than reaction (1). The weaker base F^- does not react with diethyl ether, presumably because reaction (3) is appreciably endothermic, whereas in the F^-/ethyl vinyl ether system, it is approximately thermoneutral and reaction (1) once again competes effectively with reaction (3). In the F^-/vinyl acetate system, a somewhat different type of behaviour is observed in that although reaction (3) is appreciably endothermic, product ions are observed and reaction (1) predominates over reaction (3). In discussing these results, it is convenient to distinguish the ester from the two ethers.

The carbonyl group in vinyl acetate leads to the α-H atoms being rather acidic so that proton abstraction even by F^- ions is likely to be thermoneutral or exothermic. If one regards this as the first step of a concerted reaction in which ketene is

TABLE

	Diethyl Ether Relative Intensities			Ethyl Vinyl Ether Relative Intensities			Vinyl Acetate Relative Intensities		
B^-	A^-	AHB^-	ΔH_3[a]	A^-	AHB^-	ΔH_3[a]	A^-	AHB^-	ΔH_3[a]
NH_2^-	97	3	-29.7	99	1	-112.1	95	3	-50.2
OH^-	44	56	+ 7.1	99	1	- 75.3	82	18	-13.4
F^-	-	-	+86.6	79	21	+ 4.2	17	83	+66.1

a kJ mol^{-1}

eliminated yielding the $(CH_2CHO...HF)^-$ ion, the overall exothermicity will be increased by 120-200 kJ mol^{-1}. Since reaction (3) is estimated to be ∿ 66 kJ mol^{-1} endothermic, reaction (1) is estimated to be at least 60 kJ mol^{-1} exothermic. In the corresponding reaction with methyl acetate, no products are observed, presumably because in this system reaction (1) is estimated to be at least 20 kJ mol^{-1} endothermic.

Proton abstraction from the ethers will be more endothermic in the absence of acidic hydrogen atoms so that it is likely to occur only as part of a concerted reaction in which the C-O bond breaks, leading to a reaction complex consisting of loosely-bound entities $C_2H_5O^-$, HB and C_2H_4 being formed. If these separate as products, the energy of activation ≥ ΔH_3 and if this is large and positive, no reaction occurs. If ΔH_3 is close to zero, reaction (3) will occur but the reaction complex will be long-lived, allowing the solvated anion to be formed before the neutral entity is lost, i.e. reaction (1) will occur. However, if ΔH_3 is appreciably negative, the reaction complex will have a much shorter lifetime so that little solvation can occur, and the products will be essentially those of reaction (3), as has been suggested for similar reactions of fluoroethanols[4].

References

1. J. F. J. Faigle, P. C. Isolani and J. M. Riveros, *J. Amer. Chem. Soc.*, 98, 2049 (1976)
2. S. A. Sullivan and J. L. Beauchamp, *J. Amer. Chem. Soc.*, 96, 3559 (1974)
3. B. J. Stapleton, A. J. V. Ferrer-Correia and K. R. Jennings (unpublished work)
4. R. L. Clair and T. B. McMahon, *Int. J. Mass Spectrom. Ion Phys.*, 33, 21 (1980)

BIMOLECULAR CLUSTERING OF ALCOHOLS WITH ALKOXIDES. J.E. Bartmess and G.W. Caldwell, Department of Chemistry, Indiana University, Bloomington, IN 47405

We have observed the exothermic addition of alcohols to alkoxide ions in the icr in the 10^{-7} Torr pressure range for trifluoroethanol and for aliphatic alcohols of C_4 and greater. The observed rate constants are pressure independent and increase with increasing carbon number. This is in spite of the fact that the well depth for the hydrogen-bonded species does not change appreciably in this series. For the symmetric species used, any increase in hydrogen bond donation by the alcohol is offset by an equal decrease in alkoxide basicity. We believe such reactions occur by scheme 1.

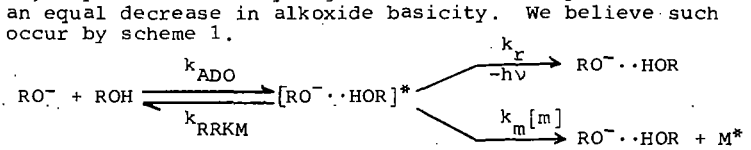

Model calculations based on this scheme agree with the observed rates: for C_3 and less, the overall rate is less than the loss rate from the icr cell. For larger alcohols, k_r is nearly constant; it is the decrease in the RRKM rate with increasing size that controls the overall rate. The uncertainty of the calculations (principally due to the estimation of frequencies and intensities for the hydrogen bonding coordinates) does not allow a clear decision as to whether collision or radiative emission is the principle stabilizing mode for the aliphatic alcohols at 10^{-6} Torr; k_r and $k_m[m]$ are comparable. For trifluoro ethanol, however, the dimer appearance is controlled by k_r, which increases by more than an order of magnitude over aliphatic alcohols with comparable k_{RRKM}. This is due to the C-F bond having both a large dipole and a stretch of ca. 1000 cm^{-1} which is ideal for radiative emission.

REACTIONS OF ANIONS WITH ALKYL NITRITES IN THE GAS PHASE.

Gary K. King, M. Matti Maricq and Charles H. DePuy, Dept. of Chem., University of Colorado, Boulder, CO. 80309

The investigation of the reactions of a variety of carbanions with alkyl nitrites in the gas phase has provided new insight into the complexity of ion-molecule reactions. A number of new and interesting ions containing carbon, nitrogen and oxygen have been observed as products of these reactions. The reactions are exemplified in Scheme 1 in which ionic products can be explained in terms of further reactions within an activated long-lived intermediate complex, such as (I) for the reaction of acetone enolate with neopentyl nitrite.

Scheme 1

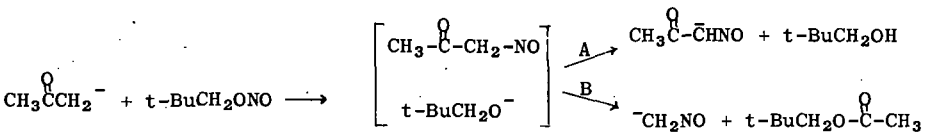

(I)

The initial step in this reaction is presumed to be nucleophilic attack by the carbanion on the nitrogen, generating alkoxide ion. Since no alkoxide is observed in the product spectrum, it must be reacting further, while still a part of the intermediate (I). The most common reaction is proton abstraction (Path A). We have observed this reaction with ions derived from ketones, aldehydes, nitriles, alkenes, dienes and alkynes. In some cases, the alkoxide may act as a nucleophile (Path B) leading to the interesting ion, $^{-}CH_2NO$. When proton abstraction in the intermediate complex is not possible, for example in reactions of $(CH_3)_2\bar{C}CHO$, only $(CH_3)_2\bar{C}NO$ is observed. Larger ketones may undergo a third reaction (C) involving a rearrangement of the intermediate to give a carboxylate anion.

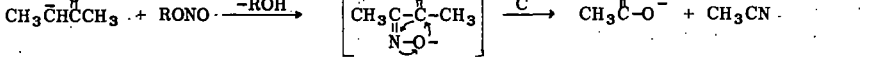

Unsymmetrical methyl ketones show very little of the higher mass carboxylate presumably since the less sterically hindered configuration (II) of the intermediate is less favorable for cleavage.

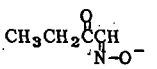

(II)

Reaction of the nitrites with propargyl anion, $^{-}CH_2C{\equiv}CH$, is another example of the complexity of the chemistry of these systems (Scheme 2).

Scheme 2

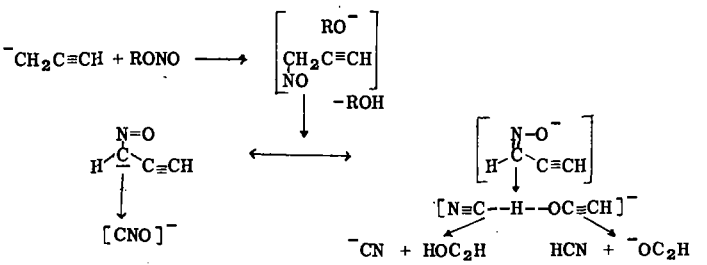

The mechanism of CNO^- formation is not well understood. Further study of this structurally and chemically interesting species is planned.

When an unsaturated ion such as $CH_2{=}\bar{C}{-}CN$ or $CH_2{=}\bar{C}{-}\overset{O}{\overset{\|}{C}}{-}H$ is reacted with the nitrites, hydride transfer from the transient alkoxide is observed.

$$CH_2{=}\bar{C}CN + t\text{-}BuCH_2ONO \longrightarrow \left[\begin{array}{c} CH_2{=}\overset{NO}{\overset{|}{C}}{-}C{\equiv}N \\ t\text{-}BuCH_2O^- \end{array}\right] \longrightarrow CH_3{-}\overset{NO}{\overset{|}{\underline{C}}}{-}C{\equiv}N + t\text{-}BuCHO$$

In addition to the study of the reactions of carbanions with alkyl nitrites, we have discovered several other interesting reactions with non-carbon containing nucleophiles. Amide ion reacts with alkyl nitrites primarily to produce NO_2^-, which may come from either displacement or elimination.

$$NH_2^- + CH_3ONO \longrightarrow NH_2CH_3 + NO_2^-$$

$$NH_2^- + CH_3CH_2ONO \longrightarrow NH_3 + CH_2{=}CH_2 + NO_2^-$$

If amide is reacted with neopentyl nitrite, in which both of these pathways are effectively blocked, it produces the interesting ion HN_2O^- via a reaction similar to Path A.

We would also like to report here the first reaction in which we have used our new Selected Ion Flow Tube (SIFT) to study the reaction of a neutral with an extremely pure injected ion. We have produced fluoride ion in a low pressure ion source, mass selected only this ion, injected it into our flow tube and reacted it with a series of alkyl nitrites. Generally the major pathway is production of NO_2^- in a manner similar to that observed for amide. However, in cases where these reactions are hindered or slow, a third reaction corresponding to the $E_{co}2$ mechanism is observed.

$$F^- + (CH_3)_3CCH_2ONO \xrightarrow{85\%} HF + NO^- + (CH_3)_3CCHO$$

$$\xrightarrow{15\%} FHNO^- + (CH_3)_3CCHO$$

In this case we have observed some of the ionic product of the reaction clusters with one of the neutral products of the reaction. In this way we have observed, from the reaction of fluoride with $(CH_3)_3CCD_2ONO$, that hydrogen (deuterium) is abstracted from the methylene position.

EXCESS ENERGY AND FRAGMENTATION IN 1,3-DITHIANES AND 1,3-DITHIOLANES.

J.E. Bartmess, R.L. Hays and S.R. Wilson, Dept. of Chemistry, Indiana University, Bloomington IN 47405

We have investigated the negative ion-molecule chemistry of 1,3-dithanes and 1,3-dithiolanes by ICR, and find that their gas phase chemistry differs from that in solution on several important points. The 1,3-dithiane forms a stable 2-lithio derivative in solution, but treatment by a variety of bases in the gas phase yields successive elimination products as well, as shown in Scheme 1 and Table 1. The deprotonation leading to 3 ceases when base strength is less than that of neopentoxide. This has been confirmed by blocking the elimination reaction: 5,5-dimethyl-1,3-dithiane is 0.4 kcal/mole less acidic than neopent yl alcohol, or comparable inacidity to acetonitrile and DMSO. The second elimination of 2 → 3 occurs only when the first elimination is highly exothermic (ca. ≈59 kcal/mole for NH_2^-, -27 kcal/mole for $neoC_5H_{11}O^-$).

The reactions of 1,3-dithiolane are similar save that 4 is not observed; deprotonation at the 2-carbon does not give a stable anion but a further retro (2+4) reaction to 5, as in solution[1].

(1). Wilson, S.R.; Georgiadis, G.M.; Khatri, H.N.; and Bartmess, J.E., J.Am.Chem.Soc. (1980) 102, 3577-3582.

Table 1. Products of Base Treatment of 1,3-Dithiane

Base	1	2	3
NH_2^-	0.36	0.34	0.18
MeO^-	0.30	0.52	0.11
$nPrO^-$	0.11	0.82	0.05
$neoC_5H_{11}O^-$	0.0	1.0	0.0
MeS^-	0.0	0.0	0.

Table 2. Products of Base Treatment of 1,3-Dithiolane

Base	4	5	6	7
NH_2^-	0.0	0.5	0.0	0.5
MeO^-	0.0	0.25	0.0	0.75
$nPrO^-$	0.0	0.25	0.25	0.5
$neoC_5H_{11}O^-$	0.0	0.10	0.80	0.1
MeS^-	0.0	0.0	0.0	0.0

Scheme 1

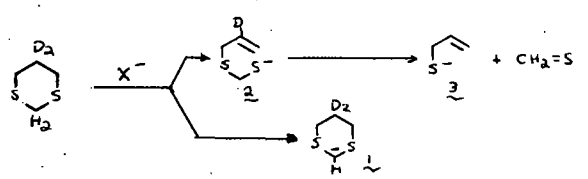

Scheme 2

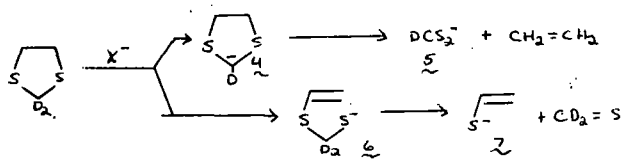

REACTIONS OF $Fe(CO)_5$ NEGATIVE IONS WITH ACTIVATED OLEFINS

G.H.Weddle, Dept. of Chemistry, Fairfield University, Fairfield, Conn. 06430
D.P.Ridge, Dept. of Chemistry, University of Delaware, Newark, Delaware 19711

The examination of the negative ion behavior of $Fe(CO)_5$, prompted by recent condensed phase results of ESR studies which suggested the existence of $Fe(CO)_4^-$ radical anion as an important intermediate[1], proved to be a fruitful exercise. Earlier gas phase ICR studies[2] yielded only two primary negative ions $Fe(CO)_3^-$ and $Fe(CO)_4^-$ and one secondary ion $Fe_2(CO)_6^-$, the product of $Fe(CO)_3^-$ reacting with $Fe(CO)_5$.

Introduction of various organic molecules to $Fe(CO)_5$ yields the expected ligand substitution reactions illustrated by (1) and (2).

$$Fe(CO)_3^- + L \rightarrow Fe(CO)_2L^- + CO \qquad (1)$$
$$\rightarrow Fe(CO)L^- + 2CO$$

$$Fe(CO)_4^- + L \rightarrow Fe(CO)_3L^- + CO$$
$$\rightarrow Fe(CO)_2L^- + 2CO \qquad (2)$$
$$\rightarrow Fe(CO)L^- + 3CO$$

The number of carbonyls displaced by each organic ligand, L, from $Fe(CO)_3^-$ and $Fe(CO)_4^-$ is indicated in Table I.

Using the number of carbonyls displaced an an indication of the metal-ligand bond strength, the relative order of strengths pertaining to this study is

This ordering points toward the importance of conjugation of polar and non-polar unsaturation in determining the degree of metal-ligand interaction.

It seems possible only to speculate upon how the metal attaches to the organic molecule. The observation that alcohols do not displace carbon monoxide while ketones do suggests structure (I), representing nucleophillic attack by the metal.

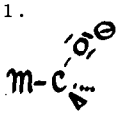

(I)

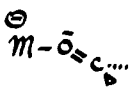

(II)

This is in contrast to structure (II) which represents electrophillic attack by the metal. The question arises as to the role of the metal in these interactions. $Fe(CO)_3^-$ is a $15e^-$ species and normally behaves as a Lewis acid. The presence, however, of the negative charge on the ion would tend to lend Lewis basicity to the complex. The extent to which these two effects contribute is not entirely clear, however, it appears that in order to explain all of the results the Lewis base approach is necessary.

One unique reaction observed was the decarbonylation of maleic anhydride

$$Fe(CO)(C_4H_2O_3)^- + C_4H_2O_3 \rightarrow Fe(C_7H_4O_5)^- + 2CO \qquad (3)$$

This type of reaction can be rationalized on the basis of charge delocalization in the intermediate. The reaction sequence may be as follows:

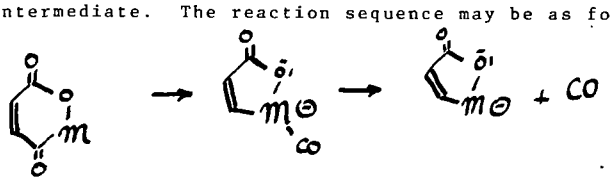

This sequence supports metal attachment at the carbonyl carbon as opposed to attachment as in (III)

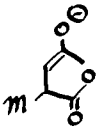

(III)

which is typical for α,β-unsaturation. It is interesting to note that extensive delocalization of charge is not possible with the other organic α,β-unsaturated molecules in this study as well as with succinic anhydride.

TABLE I

NEGATIVE ION RESULTS FOR $Fe(CO)_5$ WITH ACTIVATED OLEFINS

$Fe(CO)_5$ with	# of CO displaced $Fe(CO)_3^-$	$Fe(CO)_4^-$
	1	0
	1	0
	1	0
	1	0
	1	0
	0	0
	0	0
	0	0
HI	0	0
	2	1
	2	1
	2	3
	1	0

REFERENCES

1) P. J. Krusic & J. San Filippo, private communication.

2) R. C. Dunbar, J. F. Ennever and J. P. Fackler, Jr., Inorg. Chem., 12, 2734 (1973).

RPMOC7 A LOW PRESSURE STUDY OF THE REACTION $CH_3^+ + HCN \rightarrow CH_3 \cdot HCN^+$; A CASE FOR RADIATIVE ASSOCIATION,

V. G. ANICICH and W. T. HUNTRESS, JR., Jet Propulsion Laboratory, 4800 Oak Grove Dr., Pasadena, CA 91103, M. J. McEWAN, Dept. of Chem., University of Canterbury, Christchurch 1, New Zealand, P. R. KEMPER and M. T. BOWERS, Dept. of Chem., University of California, Santa Barbara, CA 93106.

Results are presented of an ion-cyclotron-resonance investigation of the association reaction between CH_3^+ and HCN in the pressure range 1×10^{-6} to 2×10^{-2} Torr. The results are interpreted in terms of an unstable excited intermediate $(CH_3 \cdot HCN^+)^*$ for which there are two channels open for stabilization. At pressures below 4×10^{-3} Torr, stabilization by radiation is the important mechanism. At higher pressure, stabilization by collision dominates. Rate coefficients at 300K for low pressure (radiative) and high pressure (collisional) association rates are 2×10^{-10} cm^3 $molecule^{-1}$ s^{-1} and $\sim 5 \times 10^{-25}$ cm^6 $molecule^{-2}$ s^{-1}, respectively.

Ion-molecule reactions are an important mechanism for the production of molecules in interstellar clouds. Although successful for explaining the production of most of the smaller polyatomic species in interstellar clouds, until now the gas phase ion-molecule reaction theory has failed to produce sufficient abundances for the largest of interstellar molecules. In searching for missing sources, theoreticians have invoked a special type of ion-molecule reaction, radiative association, which has never before been observed in the laboratory. Our observation provides evidence that radiative association is an important process for the synthesis of interstellar molecules.

EFFECTS OF SOLVATION ON INTRAMOLECULAR HYDROGEN BONDING

M. MEOT-NER (MAUTNER), E. P. HUNTER, P. HAMLET and F. H. FIELD, The Rockefeller University, New York, NY 10024.

The thermochemistry of association of protonated diamines and amino alcohols with up to 4 H_2O molecules was measured. The enthalpy ΔH_{cyc} and entropy ΔS of cyclization of the hydrated ion, i.e. of reaction IV, is then determined from the thermochemical cycle

$$\begin{array}{ccccc} X(CH_2)n\ NH_3^+ & + & nH_2O & \xrightarrow{III} & X(CH_2)n\ NH_3^+ \cdot nH_2O \\ \downarrow I & & & & \downarrow IV \\ X(CH_2)n\ NH_3^+ & + & nH_2O & \xrightarrow{II} & X(CH_2)n\ NH_3^+ \cdot nH_2O \end{array}$$

where the thermochemistry for solvation of the open form (reaction III) is obtained from a model monoamine, and cyclization of the naked ion (reaction I) is obtained from proton transfer equilibria. In general, the first two hydration steps destabilize the internal bond by decreasing $-\Delta H_{cyc}$, and the higher hydration steps destabilize the internal bond by making ΔS_{cyc} more negative. As a consequence the temperature required for thermal opening of the cyclic form, $T_{op} = \Delta H_{cyc}/\Delta S_{cyc}$, decreases with increasing solvation. For example, for $NH_2(CH_2)_3\ NH_3^+ \cdot nH_2O$ the following applies:

n	$-\Delta H_{cyc}$(kcal)	$-\Delta S_{cyc}$(e.u.)	T_{op}(°K)
0	14.2	14.7	966
1	10.5	13.0	808
2	8.8	11.9	739
3	8.9	16.9	527
4	8.4	20.0	420

ION CHEMISTRY OF METHYLFLUOROPHOSPHINES AND PHOSPHORANES.

J. Radtke, K.-P. Wanczek, and H. Hartmann
Institute of Physical Chemistry, University of Frankfurt,
Robert-Mayer-Str. 11, 6000 Frankfurt/M. 1, FRG

The ion chemistries of $MePF_2$, Me_2PF, Me_2PF_3, and Me_4P_2 (Me = CH_3), and of some of their mixtures were studied by ICR spectrometry in the mass range m/e = 1 - 200. A trapped ion cell and a pulsed marginal oscillator were utilized. Fluoride transfer reactions of PR_2^+ and PR_4^+ ions with phosphines and phosphoranes, respectively, are the main ion-molecule reactions. The rate constants of fluoride transfer reactions of phosphonium ions are smaller than those of PR_2^+ ions, following the general trend in reactivity. The ion chemistry of dimethylfluorophosphine at trapping times of approximately 200 ms resembles more closely to the reactions in the liquid phase[1] than indicated by previous results[2] obtained with the drift cell. The ion chemical reaction corresponding to the decomposition

(1) $2\ Me_2PF \rightarrow Me_2PPF_2Me_2$

(2) $Me_2PPF_2Me_2 \overset{M}{\rightarrow} Me_2PPMe_2 + Me_2PF_3$

was detected and studied in pure Me_2PF and mixtures of Me_2PF_3 and Me_4P_2. The product ion $Me_2PPFMe_2^+$ can be interpreted as ionic analogue of the neutral $Me_2PPF_2Me_2$, which is formed as an intermediate in reaction (1). The reaction of m/e 141

$$Me_2PPFMe_2^+ + Me_2PF \rightarrow Me_6P_3^+ + (F_2) \quad (3)$$

$$Me_2PPFMe_2^+ + Me_2PF \rightarrow Me_5P_3F^+ + (MeF) \quad (4)$$

yields again stable condensation products, which do not further dissociate. Product ions with and without fluorine appear from dimethylfluorophosphine. The ions without fluorine are well-known from the ion chemistry of the methylphosphines MePRR' (R = H, Me, PMe_2; R' = H, Me). The product ions without fluorine and masses higher than the molecular ion do not appear in drift ICR measurements. This fact and specific reaction pathways in the formation of secondary and tertiary ions led to the conclusion that

fluorine containing product ions should have bridged diphosphinofluoronium structures different from the diphosphonium structures of the ions formed in the reactions of methylphosphines. In the light of the measurements with the trapped ion cell, the question whether the ions containing no fluorine are diphosphonium ions and those containing fluorine are fluorine bridged diphosphinofluoronium ions may be discussed in more detail, now. The differences between the ion chemistry of Me_2PF in the drift cell and that in the trapped ion cell are discussed in relation to the number of collisions and the residence time.

Literature:

1) F. Seel et al. : Z. anorg. allgem. Chem. 363, 233 (1968)

2) K.-P. Wanczek, G. V. Roeschenthaler : Dynamic Mass Spectrometry 4, 163 (1976)

STUDIES IN NEUTRALIZED ION BEAM SPECTROSCOPY (ENERGETICS OF HIGHLY UNSTABLE NEUTRALS) Brian Wesley Williams, Paul M. Curtis*, and Richard F. Porter, Dept. of Chem., Cornell University, Ithaca, N.Y. 14853.

In recent years, the question of the existence of the radicals H_3O and NH_4 has led to numerous experimental and theoretical investigations. Bernstein (1) from thermodynamic considerations, originally suggested that such radicals might be stable with respect to dissociation to hydrogen and a stable molecule. Although less effort has been expended on the isoelectronic radical CH_5, this radical is also of interest because of the role it plays in the reaction of CH_4 and H. Despite past investigations, however, experimental data on the stabilities of these radicals is scarce. The associative reaction $RH + H \rightarrow RH_2$ is energetically unfavorable in a number of cases. In the present report we describe an experimental technique for the production of H_3O, NH_4 and CH_5 by an electron capture process of the type $RH_2^+ + M \rightarrow RH_2 + M^+$ where the target metal atom has an ionization potential nearly equal to the electron affinity of the cation. Since the precursor ions H_3O^+, NH_4^+, and CH_5^+ can easily be produced by ion-molecule reactions, the electron capture process creating neutral radicals provides an opportunity to measure the energetics of fragmentation. Based on estimated electron affinities for these ions, we have chosen Na and K as appropriate target atoms.

Three kinds of information were obtained. First, total electron capture cross sections for 5keV H_3O^+, NH_4^+, and CH_5^+ ions with Na and K have been measured from spatial beam profiles. Second, fragmentation energies for the neutral radicals and vertical electron affinities (Table 1) for the ions can be determined with the assumption that the fragmentation process $RH_2 \rightarrow RH + H$ is the correct mode of decomposition. Finally, a determination of the dissociative lifetime of ND_4 was made, as this radical did not undergo complete fragmentation prior to detection. The development of a low temperature ion source, presently under way, should allow measurement of the dissociative lifetimes of a number of metastable radicals. With further development, we believe neutralized ion beam spectroscopy should offer a valuable tool for the study of radicals which can be produced through electron capture.

(1) H. J. Bernstein, J. Am. Chem. Soc. 85, 484 (1963).

FRAGMENTATION ENERGIES (FE) OF RH_2 RADICALS

FORMED BY ELECTRON CAPTURE FROM Na

RH_2	FE ($RH_2 \rightarrow RH + H$) (eV)	PA (RH) (eV)	EA (RH_2^+) (eV)
CH_5	-2.65 ± .14	5.55	5.40
CD_5	-2.81 ± .08	-	-
NH_4	-.22 ± .03	8.83	4.55
ND_4	-.28 ± .02	-	-
H_3O	-1.12 ± .07	7.18	5.30
D_3O	-1.01 ± .05	-	-

$EA(RH_2^+) = IP(H) + FE(RH_2) - PA(RH)$

ION-MOLECULE REACTIONS OF THIIRANE AND ITS MIXTURE WITH AMMONIA. ION STRUCTURE DETERMINATION WITH ICR.

G. Baykut, K.-P. Wanczek and H. Hartmann
Institute of Physical Chemistry, University of Frankfurt,
Robert-Mayer-Str. 11, 6000 Frankfurt/M. 1, FRG

Ion-molecule reactions of thiirane (thiacyclopropane) have been studied by pulsed ICR spectrometry. Typical reactions in the ion chemistry are sulfur transfer reactions. In the ion chemistry of the molecular ion, there are consecutive reactions to form the product ions $C_2H_4S_2^+$, $C_2H_4S_3^+$, and finally $C_2H_4S_4^+$. In the pressure range up to $5 \cdot 10^{-4}$ no further sulfur transfer product ion is detected, even with trapping times up to one second.

$$C_2H_4S^+ + \triangleright S \longrightarrow C_2H_4S_2^+ + C_2H_4 \qquad (1)$$

$$C_2H_4S_2^+ + \triangleright S \longrightarrow C_2H_4S_3^+ + C_2H_4 \qquad (2)$$

$$C_2H_4S_3^+ + \triangleright S \longrightarrow C_2H_4S_4^+ + C_2H_4 \qquad (3)$$

The main reactions of the protonated molecule, which is formed by HCS^+, are also sulfur transfers, which yield the product ions $C_2H_5S_2^+$ and $C_2H_5S_3^+$:

$$HCS^+ + \triangleright S \longrightarrow C_2H_5S^+ + CS \qquad (4)$$

$$C_2H_5S^+ + \triangleright S \longrightarrow C_2H_5S_2^+ + C_2H_4 \qquad (5)$$

$$C_2H_5S_2^+ + \triangleright S \longrightarrow C_2H_5S_3^+ + C_2H_4 \qquad (5)$$

The ion $C_2H_4^+$ is formed by a "pseudo reverse" reaction of the molecular ion with the neutral molecule, $C_2H_4S_2$ is assumed to be formed as neutral molecule.

$$C_2H_5S^+ + \triangleright S \longrightarrow C_2H_4^+ + C_2H_4S_2 \qquad (7)$$

The product $C_4H_9S_2^+$ is generated by a reaction of the protonated molecule. $C_4H_9S_2^+$ may have the structure of a proton-bridged dimer of thiacyclopropane or a protonated 1,4-dithian.

$$C_2H_5S^+ + \triangleright S \longrightarrow C_4H_9S_2^+ \qquad (8)$$

Finally the product ion m/e 85 formed by a reation of $C_2H_2S^+$ with the neutral molecule should be mentioned. This ion has the formula $C_4H_5S^+$ and ring structure.

$$C_2H_2S^+ + \triangleright S \longrightarrow C_4H_5S^+ + HS \qquad (9)$$

Gross and McLafferty[1)] investigated the reactions of cyclopropane and of propene with ammonia. The molecular ion of cyclopropane forms $CH_2NH_2^+$ and $CH_2NH_3^+$. With propene no such reaction occurs. The molecular ion of phosphirane[2)] reacts in the same way and transfers a PH^+ ion to ammonia.

The thiirane molecular ion transfers several parts of the ring to ammonia, which indicates a cyclic structure of this ion, as has been shown for cyclopropane and phosphirane

$$C_2H_4S^+ + NH_3 \longrightarrow CH_2NH_2^+ + SCH_3 \qquad (10)$$

$$C_2H_4S^+ + NH_3 \longrightarrow SNH_2^+ + C_2H_5 \qquad (11)$$

The reactions with ND_3 yield $CH_2ND_2^+$ and ND_2S^+.

Oxirane also forms the ion $CH_2NH_2^+$ in a mixture with ammonia. The molecular ion of acetaldehyde, the open-chain isomer does not react. However its fragment ion CH_3^+ shows a CH_2^+ transfer reaction.

$$CH_3^+ + NH_3 \longrightarrow CH_2NH_2^+ + H_2 \qquad (12)$$

Dimethylsulfide may be compared with thiirane because it is a similar open-chain molecule. The ion $CH_2NH_2^+$ is formed by a reaction of the molecular ion with ammonia. However the signal is very weak and appears only at high pressures.

$$(CH_3)_2S^+ + NH_3 \longrightarrow CH_2NH_2^+ + (CH_4S + H_2) \qquad (13)$$

A further reaction of the thiirane molecular ion with NH_3 and ND_3 yields $C_2H_4NH_3^+$ and $C_2H_4ND_3^+$, respectively.

$$C_2H_4S^+ + NH_3 \longrightarrow C_2H_4NH_3^+ + S \qquad (14)$$

The first sulfur transfer product of thiirane, $C_2H_4S_2^+$ also reacts with ammonia and forms $NH_3S_2^+$:

$$C_2H_4S_2^+ + NH_3 \longrightarrow NH_3S_2^+ + C_2H_4 \qquad (15)$$

with ND_3, $ND_3S_2^+$ is obtained.

In a mixture of thiothionylfluoride, SSF_2, with ammonia, the following transfer reactions of S^+ and S_2^+ are observed.

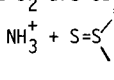

$$NH_3^+ + S{=}S{<}^{F}_{F} \longrightarrow NH_3S^+ + SF_2 \qquad (16)$$

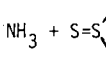

$$NH_3 + S{=}S{<}^{F^+}_{F} \longrightarrow NH_3S^+ + SF_2 \qquad (17)$$

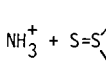

$$NH_3^+ + S{=}S{<}^{F}_{F} \longrightarrow NHS_2^+ + 2HF \qquad (18)$$

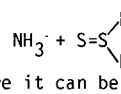

$$NH_3 + S{=}S{<}^{F^+}_{F} \longrightarrow NHS_2^+ + 2HF \qquad (19)$$

Therefore it can be concluded that the ion $C_2H_4S_2^+$ may have the three-ring structure with an exocyclic sulfur (20a) and that the four-ring structure (20b) is unreactive

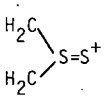

(a)

(b) (20)

if also present.

Literature:

1. M.L Gross and F.W. Mc Lafferty, J. Am. Chem. Soc. 93, 1267 (1971)
2. Z.-C. Profous, K.-P. Wanczek and H. Hartmann, Z. Naturforsch. 30a, 1470 (1975)

RPMOC12. THE REACTIONS OF ELECTRONICALLY EXCITED O^+ IONS,

B. Rowe, D. W. Fahey, F. C. Fehsenfeld, and D. L. Albritton, Aeronomy Laboratory, NOAA/ERL, Boulder CO 80302

The reactions of excited O^+ ions play an important role in thermospheric ion chemistry.[1] Two of the most important reactions of the excited O^+ ions are those with N_2 and O_2;

$$O^{+*} + N_2 \rightarrow \text{products} \quad (1)$$

$$O^{+*} + O_2 \rightarrow \text{products} \quad (2)$$

We have measured the rate constant for reactions 1 and 2 as a function of kinetic energy in a selected-ion flow-drift system. We find $k_1 = 8.5 \pm 3.4 \times 10^{-10}$ cm^3 s^{-1} and $k_2 = 8.5 \pm 3.4 \times 10^{-10}$ cm^3 s^{-1}. The rate constants for these reactions are essentially independent of energy from thermal to 0.3 eV. In addition we find the mobility of O^{+*} in helium to be $\mu_o(O^{+*})$. 20.4 (cm^2 V^{-1} s^{-1}) at E/N = 6.1 Td and 300 K, which is approximately 10% less than that of the ground state atomic oxygen ion under these conditions. The implication of these results for thermospheric ion chemistry will be discussed.

[1] D. G. Torr, K. Donahue, D. W. Rusch, M. R. Torr, A. O. Nier, D. Kayser, W. B. Hanson, and J. H. Hoffman, J. Geophys. Res. 84, 3479, 1979.

KINEMATICS OF $Ar^+ + H_2O$ COLLISIONS: CHARGE TRANSFER (H_2O^+) AND CHEMICAL REACTION (ArH^+)

Z. Herman[a*] and J. Glosík[b]

[a]J. Heyrovský Institute of Physical Chemistry and Electrochemistry, Prague, and Joint Institute for Laboratory Astrophysics, Univ. of Colo. and NBS, Boulder, Colorado
[b]School of Mathematics and Physics, Charles University, Prague

Kinematics of the reactions

$$Ar^+ + H_2O \rightarrow Ar + H_2O^+ \qquad -\Delta H_R = 3.1 \text{ eV} \qquad (1)$$

$$Ar^+ + H_2O \rightarrow ArH^+ + OH \qquad -\Delta H_R = 1.0 \text{ eV} \qquad (2)$$

was investigated over the collision energy range 0.7-3 eV (c.m.) in crossed beam experiments using the beam machine EVA II. Complete scattering diagrams obtained (e.g., Fig. 1) show that reaction (1) proceeds over this energy range mostly by the simple electron jump mechanism, in which the oncoming water molecule suffers no or small angular deflection. Intimate collisions, giving rise to large-angle scattering of H_2O^+, account for no more than about 20% of the total scattering. The scattering diagrams indicate no long-lived intermediate formation in this collision energy range.

Results on the energy deposition in the strongly exoergic reaction (1) were obtained from translational energy analysis of the scattering diagrams and are shown in Fig. 2, where the product relative translation energy is plotted against the change in relative translational energy before and after the reaction, $T'-T = \Delta T'$. The distributions peak closely to $\Delta T' = 0$ ("resonant" charge exchange), within 0.1 eV for the simple electron-jump mechanism and within 0.3 eV for intimate collisions, both regions being analyzed separately. The distribution is somewhat broader for the intimate collision part of the scattering and at T = 1.85 eV it shows clearly the formation of the B^2B_2 excited state of the water ion in inelastic charge transfer collisions at the expense of the reactant translational energy.

The excess energy in reaction (1) is thus deposited as the internal excitation of the product H_2O^+ ion formed in either the ground electronic state X^2B_1 or, possibly, in the first excited state A^2A_1.

Results on ArH^+ formation in parallel reaction (2) show that the product ion is sharply peaked forward and that the reaction proceeds via the impulsive, spectator stripping mechanism in the collision energy range 0.7-2 eV (c.m.).

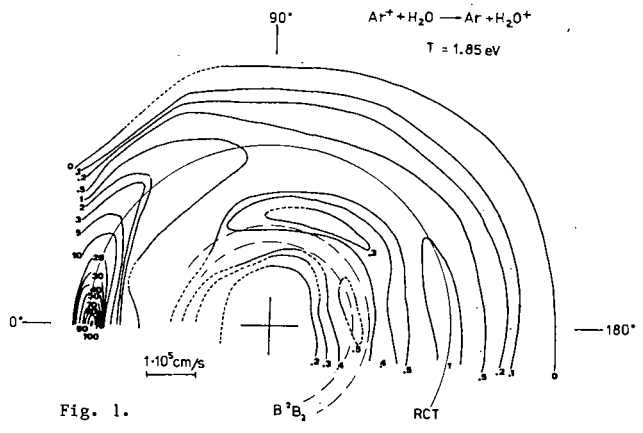

Fig. 1.

*JILA Visiting Fellow, 1979-80.

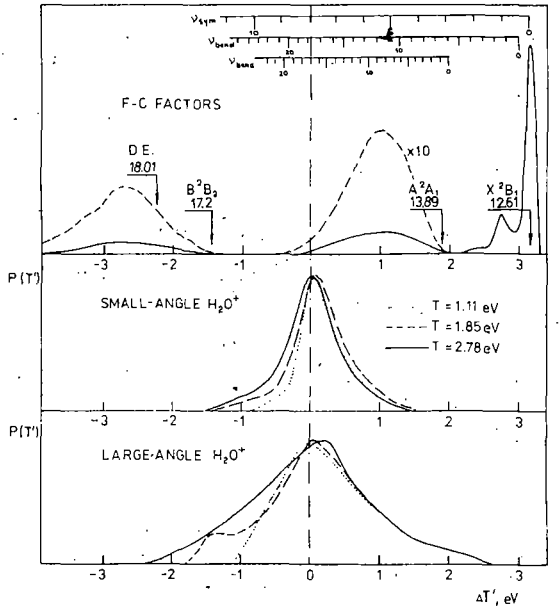
F-C FACTORS
D.E.
18.01
B²B₂
17.2
x10
A²A₁
13.89
X²B₁
12.61
P(T')
SMALL-ANGLE H₂O⁺
T = 1.11 eV
T = 1.85 eV
T = 2.78 eV
P(T')
LARGE-ANGLE H₂O⁺
ΔT', eV

Fig. 2

MASS SPECTROMETRY CONFIRMATION AND QUANTIFICATION OF
2,3,7,8-TETRACHLORODIBENZO-P-DIOXIN IN FRESH WATER FISH #59

R. L. HARLESS and R. G. Lewis U.S. Environmental Protection Agency, Health Effects Research Laboratory, ETD, ACB (MD-69), Research Triangle Park, North Carolina 27711

High resolution glass capillary column gas chromatography (GC) directly coupled[1] with high resolution mass spectrometry (HRMS) is one of the most powerful tools in analytical chemistry. Low concentrations, nanogram- and picogram-per-gram (ng/g and pg/g) levels, of toxic organic compounds in complex sample media can be unambiguously identified and quantified utilizing this technique. A capillary column GC-HRMS method of analysis was developed for the quantitative measurement of 2,3,7,8-tetrachlorodibenzo-p-dioxin (TCDD) in various sample types in 1976. The comprehensive sample preparation procedures and capillary column GC-HRMS methods of analysis for TCDD are described elsewhere[2]. The minimum limit of detection ranged from 2 to 20 ppt for fish tissues. Sample weight varied from 2 to 10 g. The minimum limit of detection was defined as the amount of TCDD that would provide clearly defined peak shapes for the masses m/z 320 and m/z 322 in the proper isotopic ratio and with a signal-to-noise ratio greater than 2.5:1. The sample weight and sample size used in analysis, sample preparation efficiency, sample matrix effects and the electronic noise present in the time frame of measurement affect the minimum detection limit.

Fish samples were collected in the state of Michigan (Tittabawassee, Grand and Saginaw rivers and Saginaw Bay) under the direction of EPA Region V. The species of fish were channel catfish, carp, yellow perch, small mouth bass, and sucker. A chain-of-custody procedure was maintained from time of collection through completion of analyses.

The quality assurance (QA) program was initiated prior to sample preparation and consisted of: (1) fortification of real and QA samples with 2.5 to 10 ng of $^{37}Cl_4$-TCDD; (2) fortification of QA samples with 0 to 1250 pg (0-125 ppt) TCDD; and (3) submission of real samples with QA sample extracts (60 µl) to the GC/MS laboratories in a blind fashion (i.e., there was no way to distinguish between QA and actual samples). The efficiency, accuracy, precision and validity of TCDD analyses were dependent upon the incorporated QA program.

The edible portions (2.5 to 10 g) of the respective fish samples were fortified with 2.5 to 10 ng of ^{37}Cl-TCDD and subjected to acid/base extraction and the normal clean-up procedure[2]. A typical GC-HRMS multiple ion selection (MIS) analysis of an extract of ocean perch and the extract fortified with ^{37}Cl-TCDD and TCDD is shown in Figure 1. Unusual and high concentrations of chlorinated organic contaminants and TCDD were encountered in samples of fish collected from polluted water (Figure 2). These masses differed from the exact mass of TCDD and were not found in the analysis of fish taken from other locations.

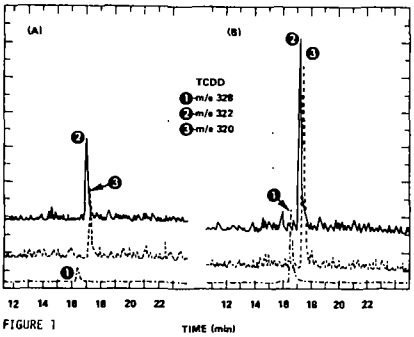

FIGURE 1
QA fish sample fortified with 5 ng ^{37}Cl-TCDD and 37 ppt TCDD: (a) sample, (B) sample fortified with quantification standard. Experimental results: 50% recovery of ^{37}Cl-TCDD; 34 ppt TCDD detected; 4 ppt detection limit.

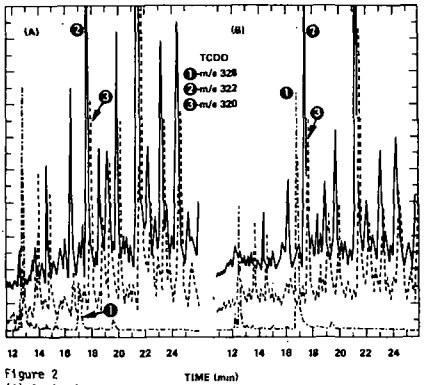

Figure 2
(A) 1 µl of catfish extract (B) 0.5 µl of extract fortified with quantification standard. Experimental results: 80% recovery of ^{37}Cl-TCDD; 93 ppt TCDD detected; 6 ppt TCDD detection limit.

The high concentrations of coextractable chlorinated components caused problems, such as overload of sample preparation procedures, capillary column overload, coelution of components and decreased MS sensitivity. To minimize or cancel these effects, a very high MS sensitivity and small sample size were necessary. Peak height measurement for the m/z 328 (^{37}Cl-TCDD) and the m/z 320 and m/z 322 (TCDD) of sample and the sample fortified with a quantification standard were used to determine: (1) The percent recovery of ^{37}Cl-TCDD (sample preparation efficiency); (2) the residue level of TCDD; and (3) the limit of detection for TCDD. Typical concentrations of quantification standards were 50 to 300 pg/µl ^{37}Cl-TCDD and 1 to 5 pg/µl TCDD.

The capillary column GC/HRMS MIS analysis for 2,3,7,8-TCDD residues had to satisfy the following criteria to be considered a confirmed positive sample: Correct capillary column GC/ HRMS retention time of 2,3,7,8-TCDD; correct responses for the co-injection of samples fortified with ^{37}Cl-TCDD and TCDD standard; correct chlorine isotope ratio of the molecular ion (m/z 320 and m/z 322); correct capillary column GC/HRMS multiple ion monitoring response for TCDD masses and ^{37}Cl-TCDD mass (simultaneous response for elemental composition of m/z 320, m/z 322, and m/z 328); and response of m/z 320 and m/z 322 must be greater than 2.5 times noise level. Supplemental criteria were also applied to a representative number of these samples: MIS simultaneous response of m/z 320, m/z 322, and m/z 324 to confirm the tetra-chloro isotope ratio; MIS simultaneous responses of m/z 320, m/z 322, m/z 257, and m/z 259 to confirm the M-COCl loss, which is indicative of TCDD structure; and capillary column GC-HRMS peak-matching analyses at 10,000 mass resolution in real time were used to confirm the TCDD masses m/z 319.8965 and m/z 321.8936. Exact masses corresponding to three TCDD isomers were also confirmed in these analyses. High concentrations of contaminant masses differing from the exact mass of TCDD were observed and were measured to determine the elemental compositions. Tentative identifications were assigned to 10 of the components, PCBs, chlorinated benyzlphenyl ethers, etc. Four highly contaminated samples were also subjected to a neutral extraction and cleanup procedure for confirmation of TCDD residues.

A summary of analytical results for the quantitative measurement of 2,3,7,8-TCDD in fish showed that: 26 of 35 samples contained detectable quantities of TCDD; 11 samples contained concentrations greater than 40 ppt; concentrations ranged from 4 ppt to 690 ppt; the highest concentrations were detected in catfish and carp (bottom feeders); the lowest concentrations were detected in perch and sucker from the Saginaw Bay (commercial fishing waters); a river dilution effect was evident from results obtained for fish samples collected at specific points on the Tittabawassee River, which flows into the Saginaw Bay; three compounds which satisfied the analytical criteria for TCDD isomers were detected in several fish samples at very low concentrations. Two other laboratories[3,4] have also reported the presence of TCDD in fish from the Tittabawassee River.

Evaluation of QA results indicated that reasonably accurate TCDD values were obtained in the presence of high concentrations of chlorinated contamination. The number of QA samples with zero fortification levels of TCDD were very important in these analyses because of the large number of positive fish extracts and the unusual and high concentrations of chlorinated contaminants. Accurate results were obtained for a positive fish sample fortified with a known amount of TCDD. False positive results were not detected in the QA program.

References:

(1) Harless, R. L. and Oswald, E. O., (Paper No. RP-7), 26th Annual Conf. on Mass Spectrometry and Allied Topics, St. Louis, Mo., June 1978.

(2) Harless, R. L., Oswald, E. O., Wilkinson, M. K., Dupuy, A. E., Jr., McDaniel, D. D., and Tai, Han, Anal. Chem., In Press, June 1980.

(3) The Chlorinated Dioxin Task Force, The Michigan Division, Dow Chemical USA. The Trace Chemistries of Fire - A Source of and Routes for the Entry of Chlorinated Dioxins Into the Environment, 1978.

(4) Kuehl, D. W., Dougherty, R. C., Tondeur, Y., Stalling, D. L., Smith, L. M. and Rappe, C., Negative Chemical Ionization Studies of Polychlorinated Dibenzo-p-Dioxins, Dibenzofurans and Naphthalenes in Environmental Samples, Unpublished report, 1979.

EVALUATION OF COMMERCIALLY AVAILABLE CAPILLARY COLUMNS AND CHROMATOGRAPHIC CONDITIONS FOR THE ANALYSIS OF SPECIFIC TETRACHLORODIBENZO-P-DIOXIN ISOMERS

by
B. M. Hughes, J. R. Troost, J. F. Ryan
Gulf South Research Institute
New Orleans, Louisiana 70126
and
A. E. Dupuy, Jr.
EPA/OPTS, Survey and Analysis Division
Field Studies Branch, Toxicant Analysis Center
Bay St. Louis, Mississippi 39529

INTRODUCTION. A series of capillary gas chromatographic/mass spectrometric [$(GC)^2$/MS] analyses was performed to define and optimize parameters important for analysis of polychlorinated-dibenzo-p-dioxin (PCDD) isomers using commercially available columns. The object of this study was to determine what parameters are important for the separation of specific TCDD isomers and to identify the parameters that allow a wide range of dioxins to be quantified with a minimum analysis time. For trace-level dioxin analyses; qualitative and quantitative accuracy is highly dependent upon chromatographic performance. Maximum chromatographic resolution is necessary to distinguish between isomers, and chromatographic activity must be kept to a minimum to maintain high levels of sensitivity and quantificative accuracy. In addition, since qualitative determinations at low levels are based upon mass spectral response of a small number of ions, separation from the typical environmental or biological matrix is very important. From a cost standpoint, analysis time must be kept to a minimum in cases where quantification requires multiple GC/MS determinations (such as in the standards addition method). This decreased analysis time also reduces the probability of mass spectrometer sensitivity changes during a series of injections. An ideal column for these purposes would have no activity and would provide adequate resolution with minimum analysis time.

Several commercially available capillary columns were obtained to compare chromatography differences for various dioxin isomers. Operating parameters were varied to determine their effects on separation and analysis time. These results should not be used to predict column performance for applications other than dioxin chromatography. In our laboratory, we have observed that a particular column may be well suited for one type of analysis and poor for another. Since activity may take many forms, different classes of chemical compounds must be evaluated separately.

EXPERIMENTAL. Seven WCOT capillary columns were obtained commercially. Dexsil 300 and Carbowax 20M coated columns with 0.25 mm i.d. were purchased from Applied Science (State College, Pennsylvania). OV-101 columns with 0.1 and 0.2 mm i.d. were obtained from Scientific Glass and Engineering (Austin, Texas). An SP-2250 column with 0.24 mm i.d. was supplied by Supelco, Inc. (Bellfonte, Pennsylvania), a fused-silica SP-2100 column with 0.21 mm i.d. was obtained from Hewlett-Packard (Avondale, Pennsylvania), and a fused-silica Carbowax 20M column of 0.23 mm i.d. was furnished by Quadrex Corporation (New Haven, Connecticut). All columns used in this study were advertized "high performance" grade with the exception of the 0.1 and 0.2 mm OV-101 columns from Scientific Glass and Engineering. Column lengths varied from 15 to 100 m, and column temperatures ranged from 200°C to 260°C. Head pressures for helium and hydrogen carrier gases ranged from 6 to 50 psi.

For evaluation, columns were installed in a HP 5985A GC/MS system equipped with a capillary split/splitless injection system, backflush and septum flush, quartz injection liner, and a low-volume injector. The injection-port temperature was maintained at 275°C. All chromatographic runs were performed in the splitless mode using tetradecane as the solvent. Injection volume was 2 µl, and backflush actuation time was 30 sec throughout the series of experiments.

The capillary columns were coupled directly to the ion source of the mass spectrometer via 1/16 inch glass-lined metal tubing. The interface valve remained open throughout the run, and an automated solvent-diversion system was employed. The interface temperature zones were 275°C, and the dual CI/EI source was operated in EI mode at an electron energy setting of 75 eV. The source temperature was maintained at 200°C. A specific EI tune was created to enhance sensitivity for the molecular ion region of TCDD. Data were acquired by using Hewlett-Packard's SIM (selected ion monitoring) program. For tetra-CDD analysis, the ions (m/z) 320 and 322 (for native-TCDDs) and 328 (for ^{37}Cl-labeled TCDD) were monitored simultaneously. Masses 286 and 288 were monitored for tri-CDDs, 390 and 392 for hexa-CDDs, 424 and 426 for hepta-CDDs and 458, and 460 for octa-CDD.

LIQUID PHASE COMPARISON. A tetra-CDD isomer standard with up to six isomers was evaluated for resolving capability and peak shape using four different liquid phases of differing polarity. Temperatures and head pressures were manipulated to retain a narrow retention range for the tetra-CDD isomers (6 to 14 min). In spite of differing column lengths, optimum flow and temperature considerations were ignored in favor of minimum retention times. All parameters were maintained constant with the exception of head pressure, carrier gas, and column temperature. The columns were removed and installed meticulously so that no other part of the system was altered. The elution order of the six isomers on the nonpolar OV-101 liquid phase is identical to that on the Carbowax 20M phase, yet the 2,3,7,8- and 1,2,3,4-TCDDs are reversed on the polymethylphenylsiloxane (SP-2250) phase. To insure that noted differences were the result of a change of column (only) and not of the injection system or interface to the mass spectrometer, the installation and order of installation of these columns was repeated and reversed. Identical results were obtained. The Carbowax column exhibited far superior inertness and separation efficiency. A 50 m fused-silica Carbowax 20M column, similarly evaluated, produced results similar to the glass Carbowax column.

HELIUM VERSUS HYDROGEN CARRIER GAS COMPARISON. The advantages of using hydrogen as a carrier gas were studied by using the Dexsil 300 and Carbowax 20M columns described above. The velocity characteristic of hydrogen (product of viscosity and square root of molecular weight) is five times that of helium. Theoretically, a separation problem requiring a specific number of plates could be resolved five times as fast by using hydrogen rather than helium. The elution of the tetra-CDD isomers on two different columns, maintaining all other parameters constant except carrier gas, shows that at a given pressure, the use of hydrogen decreases analysis time by approximately one-half. However, as expected, no significant improvement in resolution was observed.

HEAD PRESSURE COMPARISON. The head pressures and consequently carrier gas velocities used in analyses with the 0.2 mm i.d. OV-101 and 0.25 mm i.d. Dexsil 300 columns were widely varied to examine effects on separation and elution of the six-component TCDD standard. It is evident that little separation efficiency is gained by varying carrier flow using either hydrogen or helium carrier gas. Very slight differences were observed in resolution when linear gas velocities were varied. Since TCDD is highly retained by these liquid phases (k values are on the order of 10-20), changes in carrier gas linear flow velocities do not drastically affect chromatographic resolution.

COLUMN LENGTH COMPARISON. To study the effect of column length on chromatography of TCDD isomers, the 30-m Carbowax 20M column used in the earlier studies was split in half, and the chromatographic conditions were otherwise unchanged. As expected, analysis time was reduced by two-thirds, and the resolution between the 1,2,3,4- and the 2,3,7,8-TCDD isomers decreased by approximately 1.64.

EFFECT OF CHROMATOGRAPHIC TEMPERATURE. The 100-m Dexsil 300 column was used to demonstrate the effect of chromatographic temperature upon resolution and peak width. Lower column temperature produced longer retention times and larger peak widths. No significant change in chromatographic resolution was observed from changing column temperature.

COMPARISON OF THE CHROMATOGRAPHY OF A PERFORMANCE STANDARD. The elution of a multicomponent performance standard was studied on the Carbowax 20M glass column supplied by Quadrex and the SP-2100 (fused-silica) column supplied by Hewlett-Packard to examine the differences in the column performances. Visual comparison of the chromatograms reveals that both capillary columns show little chromatographic distortion of the compounds in the performance standard. Conventional performance mixtures do not readily depict TCDD chromatographic behavior.

CONCLUSIONS. From the above studies, it is apparent that the most important parameter in selecting columns and conditions for the chromatographic separation of specific TCDD isomers is the nature of the liquid phase. The results obtained indicate that the construction material of the column may be of secondary importance. This is very likely a false conclusion however. The construction material of the column is probably the site of chromatographic activity affecting the dioxins. Carbowax 20M is known to coat glass and fused silica with exceptional efficiency. It is, in fact, used by several manufacturers as a preliminary (deactivating) coating for the other phases. This could explain the almost complete absence of tailing obtained from the Carbowax columns. The enhanced separating power of this column is an added feature. Although fused silica is more inert than glass, a small percentage of contamination exists, enough, apparently, to distort the chromatography for TCDD at trace levels, using liquid phases other than Carbowax 20M.

ACKNOWLEDGMENT. The authors would like to thank the Environmental Protection Agency for support of this study (EPA Contract No. 68-01-4887).

ANALYSIS OF TCDD USING METASTABLE AND COLLISIONAL ACTIVATION METHODS

E. K. Chess, F. W. Crow, P. A. Lyon, and M. L. Gross
Department of Chemistry
University of Nebraska
Lincoln, Nebraska 68588

A method of analysis of tetrachlorodibenzo-p-dioxin (TCDD) has been developed in which the loss of COCl from the molecular ion in the first field-free region of a double focusing mass spectrometer is monitored. Because this reaction is anticipated to be highly specific for TCDD's, the sample can be introduced into the mass spectrometer using the direct insertion probe. From the analysis of standard solutions, the method has been evaluated in terms of precision, quality of calibration, and minimum detection limit. Fifty picogram quantitites of 2,3,7,8-TCDD have been detected with a signal-to-noise ratio of 8:1. The accuracy and specificity of the procedure have been tested using soil samples taken in the vicinity of a chemical industry landfill. These had been previously analyzed using gas chromatography/high resolution mass spectrometry. The accuracy of the method is acceptable but not as good as the GC/HRMS. The specificity, using the soil samples and others contaminated with polychlorinated biphenyls, is comparable to the GC/HRMS method. We conclude analysis is appropriate for rapid screening of sample extracts and for validating other methods of analysis.

Experimental

A 1 gram sample of soil was extracted with 1:1 hexane/acetone two times. The combined organic solution was washed with 1F KOH, distilled water, and five times with concentrated sulfuric acid. After drying with sodium carbonate, the solvent was evaporated and the residue chromatographed on a 5cm column of alumina. The column was first eluted with 6ml of CCl_4, and the TCDD's were pulled off using CH_2Cl_2.

All mass spectrometric data was acquired using a Kratos MS-50 high resolution mass spectrometer operated under the following conditions: source temperature, 250° C; accelerating voltage, 8kV; electron energy, 70eV. For the direct probe metastable analyses, the instrument was tuned to 2,000 resolution and the collector slit opened as wide as possible so as to still maintain a Gaussian peak shape. The magnet was set at about m/z 207, which allowed the mass range m/z 206-208.5 to be seen on the oscilloscope when the instrument was scanned over 20 parts-per-thousand using the repetitive scanning

circuitry. This allows us to oberve the various losses of COCl from the molecular ions of TCDD (m/z 320 and 322). The voltage, E_0, which defocuses the main ion beam and allows only those ions containing 80.3% of the energy of the main beam to pass the ESA. This instrumental setup is equivalent to manually selecting one point from a B/E linked scan surface. The daughter ions formed in the first field-free region metastable decompositions of $320^{+\cdot} \rightarrow 257^{+} + CO^{35}Cl\cdot$ and $322^{+\cdot} \rightarrow 259^{+} + CO^{35}Cl\cdot$ fit both the magnet and ESA criteria established, and will be collected over a narrow scan of the accelerating voltage.

The capillary tubes containing the sample residues were inserted into the source and heated at 70°C. The metastable peak profiles were acquired by scanning the accelerating voltage over a mass range of 20 parts-per-thousand at a repetition frequency of 2Hz. The output was acquired with a Nicolet Model 1170 signal averager, and the stored signals smoothed 20 times using a 3-point smoothing routine. The concentration of TCDD was calculated from a calibration curve using the maximum peak heights of the accumulated metastable signals corresponding to m/z $320^{+\cdot} \rightarrow 257^{+}$ and $322^{+\cdot} \rightarrow 259^{+}$ as the response parameters.

An account of this work will be submitted to Analytical Chemistry.

DEVELOPMENT OF METHODOLOGY AND INSTRUMENTATION FOR THE DETERMINATION OF CHLORODIOXINS IN ENVIRONMENTAL SAMPLES BY CAPILLARY-LOW RESOLUTION MASS SPECTROSCOPY

G.F. VanNess, J.G. Solch, M.L. Taylor, and T.O. Tiernan

The Brehm Laboratory and Departments of Chemistry and Pharmacology/Toxicology
Wright State University
Dayton, Ohio 45435

Assaying large numbers of environmental samples and chemical sludge specimens (such as those which were obtained at Love Canal, New York, Jacksonville, Arkansas, and Verona, Missouri) for tetrachlorodibenzo-p-dioxins (TCDDs) has necessitated the development of new analytical procedures in our laboratory. Previously published procedures (1,2) for TCDD analysis entail an initial wet-chemical procedure which affects a separation of TCDD from constituents of the sample matrix and from other trace environmental pollutants. This sample preparation procedure yields an extract containing TCDD, the concentration of which is enriched relative to the original constituents of the matrix. Such extracts have reportedly been analyzed by several different analytical techniques, but most frequently by gas chromatography-mass spectrometry. The specificity of the overall method depends upon the enrichment factor achieved during sample preparation and the specificity of the analytical technique employed to quantitate the TCDD in the extract obtained. Currently the most unequivocal and sensitive analytical methods for quantitating TCDD entail the use of gas chromatography-high resolution mass spectrometry. However, such instrumentation is very intricate and not well suited for analysis of hundreds of samples. In our laboratory we have also developed both electron capture gas chromatographic and gas chromatographic-low resolution mass spectrometric procedures which are used to screen samples prior to analysis using the more complicated instrumentation described above. The extraction methodology and the analytical techniques are described below.

For preparation of the samples, 1) a known quantity of $^{37}Cl_4$-TCDD internal standard is added and the sample is extracted with petroleum ether (Burdick and Jackson); solid samples such as tissues are digested (using ethanolic KOH) at room temperature for 16 hours prior to extraction; 2) the organic layer is washed with concentrated sulfuric acid, then water; 3) the organic layer is dried over sodium sulfate; 4) the extract is concentrated and purified by elution chromatography, further purification by high pressure liquid chromatography may be necessary; 5) the purified extract is further concentrated and the TCDD content is determined by high resolution gas chromatography-low resolution mass spectrometry as described below.

The analytical instrumentation employed to determine TCDDs in the extract comprises a Varian 3740 Capillary Gas Chromatograph which is directly coupled to an Extranuclear Quadrupole Mass Spectrometer. The gas chromatograph is interfaced to the mass spectrometer via a 0.5 mm I.D. glass-lined, heated, stainless steel capillary tube which in turn is directly coupled to the WCOT column by means of a zero dead volume fitting. The pumping system and other features of the mass spectrometer have been previously described (2). The instrumental parameters employed for the determination of TCDDs are 1) Gas chromatographic parameters: 60 M glass WCOT column (Supelco AA Grade), carrier gas hydrogen at a flow rate of 40 cm/sec (linear velocity); injection mode: splitless (tridecane solvent), injector temperature 230°, column temperature 190° for 2 minutes then programmed to 230° at 1°/minute; 2) transfer line temperature 320°; 3) mass spectrometer parameters: ionizing voltage, 23.5 eV; multiplier voltage, 3200 V; resolution, 1:350; source temperature, 150°; analyzer temperature 120°.

Theoretically 22 TCDD isomers are possible. The system above is calibrated using 12 of of the 22 TCDD isomers available in our laboratory. The result of injection of 1 Ng quantities of these isomers is shown in Figure 1 where a dual ion trace obtained for m/z 320 and m/z 322 are shown (intensities of the two traces are not directly comparable).

This methodology has been found to yield very reliable (< 10% false positives) when applied to the determination of TCDD isomers in a wide variety of samples such as fireplace soot (Figure 2), cottonmouth water moccasin liver (Figure 3) soil and chemical sludge (Figure 4).

References:

1. H. R. Buser, J. Chromatogr. 107, 295 (1975).

2. S. D. Erk, M. L. Taylor and T. O. Tiernan, Chemosphere 8, 7 (1979).

Fig.1 Capillary GC-Low Resolution Mass Chromatogram (m/e 320 and 322) For A TCDD Isomer Mixture

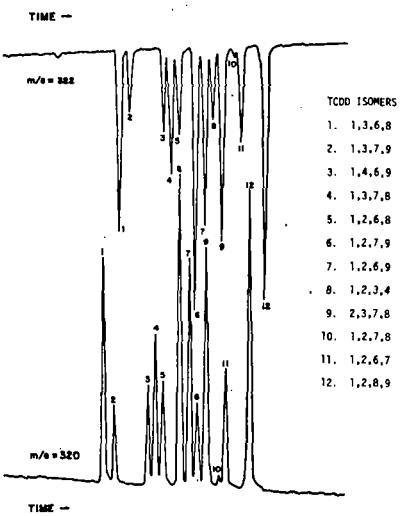

Fig. 2 Capillary Column GC - Mass Chromatogram (m/e 322) for TCDD Isomers Mixture (A) and Home Fireplace Extract (B)

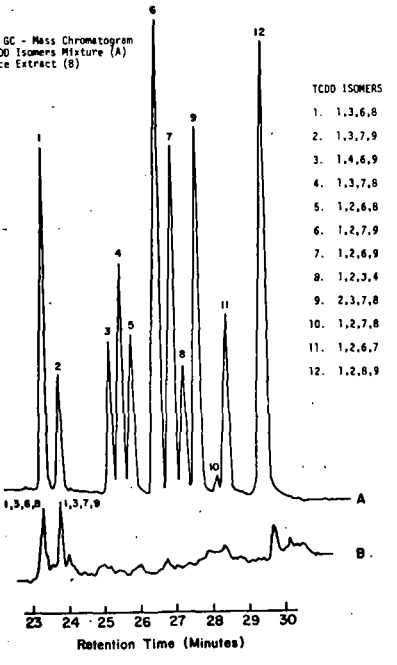

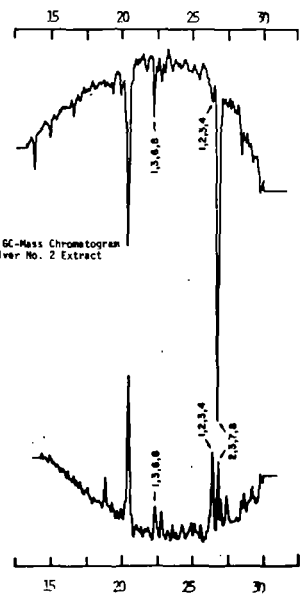

Fig.3 Capillary Column GC-Mass Chromatogram of Cottonmouth Liver No. 2 Extract for TCDD Isomers

Fig.4 Capillary Column GC-Mass Chromatograms (m/e 322) for a TCDD Isomer Mixture and for Two Sample Extracts

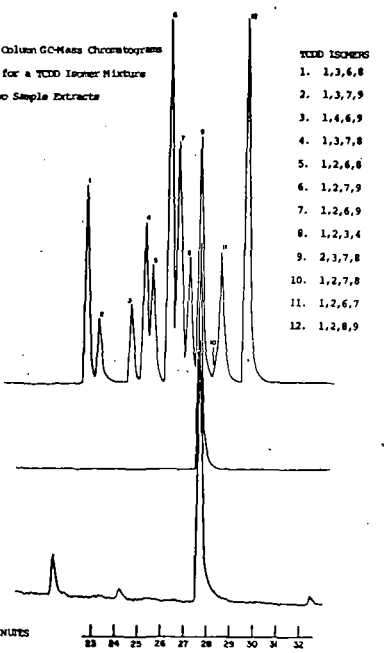

2

AN IMPROVED SIGNAL AVERAGED HIGH RESOLUTION SELECTED ION MONITORING SYSTEM FOR THE ANALYSIS OF TETRACHLORODIBENZO-p-DIOXINS (TCDD'S)

F.L. DEROOS, L.E. SLIVON, Battelle Columbus Laboratories, Columbus, Ohio

Introduction

2,3,7,8-tetrachlorodibenzo-p-dioxin (2,3,7,8-TCDD) is an extremely toxic material often found as a trace environmental contaminant. Signal averaged high resolution selected ion monitoring (HRSIM) is a technique that provides a high degree of selectivity, as well as the sensitivity required to perform analyses at the low parts per trillion level. Several laboratories are utilizing signal averaging of high resolution selected ion monitoring data for 2,3,7,8-TCDD analyses, however, a number of limitations exist. In the following sections we briefly describe some of these limitations along with our improvements to this technique.

Limitations of Most Signal Averaged HRMID Systems

Three major limitations are evident in most signal averaged HRMID systems. These are:

(1) Usually mass profile data can be acquired for only two mass ranges.
(2) Mass drift is not automatically corrected.
(3) The signal averager has a limited ability with respect to data handling.

Most signal averaged HRMID data acquisition systems utilize the peak matching facilities of the mass spectrometer to obtain repetitive profile data across the mass ranges of interest. Consequently only a limited number of mass ranges (usually two) can be sequentially scanned. For TCDD analyses it is desirable to scan the two most abundant peaks in the molecular ion cluster of native TCDD's (m/e 320 and m/e 322) as well as at least one peak from an internal standard (m/e 328 or m/e 334). Although one can acquire this data by performing two separate analyses monitoring two ions each time, a higher degree of confidence is obtained if all of the ions are monitored during one analysis.

Another limitation present with many signal averaged HRMID systems is the lack of correction for mass drift during the analyses. If the mass drift is minor, the mass profiles will be broadened resulting in an apparent loss of resolution, however, if the drift is large, the peaks of interest can be totally missed.

A third limitation concerns the relatively inflexible data handling provided by the signal averager. Usually the smoothing routine utilizes a small number of points (e.g., 3 point-smoothing), the data output format is fixed, and little provision is made for mass storage of the raw data. The ability to store the raw data is a major requirement for quality assurance.

Technical Approach

A VG MM-7070H high resolution mass spectrometer including the "Digital MID" and "Peak Matching" units was used. The combination of these two units provides the ability to scan over up to eight mass ranges at high resolution ($\frac{M}{\Delta M} \simeq 10{,}000$). One of the mass ranges was used to scan over the C_6F_{13} peak (m/e 318.9792) from PFK to provide a "lock mass" while three other channels were used to scan over m/e 321.8936, m/e 319.8965, and m/e 333.9338 (internal standard). Since the lock mass was continuously displayed, it provided an indication of the mass spectrometer tuning as well as the correct magnet setting. The "Digital MID" provided automatic correction for mass drift.

A Finnigan INCOS data system was used for post-acquisition processing using software specifically designed for this task. The real-time analog intensity signal provided by the digitally controlled MID was initially processed with a 4K word Nicolet 1170 signal averager. No modifications were made to the Nicolet hardware. The Nicolet/INCOS interface consists of an inexpensive standard Data General 4066 digital I/O module added to the Nova chassis. The Nicolet/INCOS link consists of a twisted-pair parallel 8-bit path with additional control lines. A special software driver was designed for INCOS to perform floating point formatting coincident with reading of the binary Nicolet data while providing a transfer rate of approximately 30,000 bytes/second.

Data reduction software developed provided flexible display formatting, quantitation, smoothing and hardcopy. Additionally, quantitative data may be written to or appended to a conventional quantitation list for further processing by conventional INCOS software.

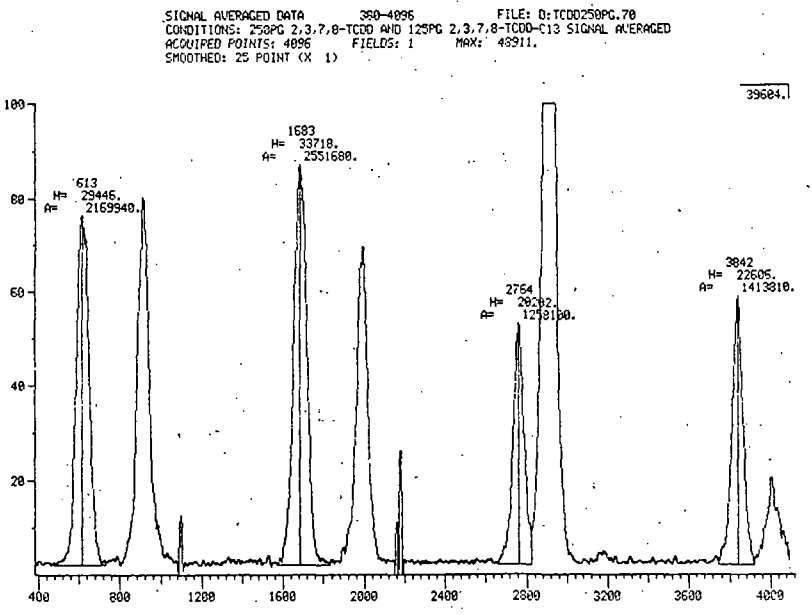

QUANTITATION OF TCDD'S IN ENVIRONMENTAL SAMPLES USING HIGH RESOLUTION MULTIPLE ION DETECTION

Mark Weiss, Finnigan Corporation, 575 Maude, Sunnyvale, California, 94086
Don J. Harvan and J. Ron Hass, NIEHS, Box 12233, Research Triangle Park, N.C., 27514

The determination of 2,3,7,8-tetrachlorodibenzodioxin in environmental samples has stimulated considerable interest in the past few years. The positive identification of TCDD is particularly difficult because the typical sample usually contains compounds with similar properties, which are present in concentrations orders of magnitude greater than TCDD. Thus it is necessary for the detection system to offer the greatest possible discrimination between TCDD and interferences, and offer the most information about the properties unique to TCDD.

For quantitation of TCDD by electron impact mass spectrometry, we believe this requires the measurement of exact masses of the molecular ion and the characteristic fragment ion (m/z 322 and 257), the intensity ratio of these ions, and a GC retention time the same as authentic TCDD.

We have thus modified our GC/MS/DS so that accurate mass measurements and intensity ratios could be made without loss of GC retention time information. Multiple Ion Detection (MID) using very narrow mass windows was employed to increase detection sensitivity. To evaluate the system, we examined a set of orthochlorophenol samples reputed to contain TCDD.

Experimental: We wished to scan our mass spectrometer (a ZAB-2F) in MID mode at resolution 10,000, with a scan window of just one mass peak width (100ppm). We used the VG-Micromass "lockmass" MID hardware to insure that the MID windows would not drift. The lockmass was set to scan accurately centered windows near m/z 254 (I_2 ion of C_2I_4), 257, and 322. The lockmass was scanned for 50 ms, and the other windows for 200 ms, with a total scan cycle time of 500 ms. The scan cycle was triggered by our INCOS data system, whch also collected the mass profile data.

The acquired MID data was assigned a mass by the data sytem. However, the hardware lockmass adjustment continually changed the calibration of mass, and mass assignment was made relative to the window, whose accurate mass position was kept constant by the lockmass hardware. Even at 10,000 resolution, interfering ions can sneak into a 100 ppm window, but the shifted centroids gave them away.

The orthochlorophenol samples were extracted by first partitioning them with basic ethanol/cyclohexane, batch separating on QAE-Sephadex, and finally chromatographing them on A-540 alumina with hexane/methylene chloride. The 20% methylene chloride fraction contained the TCDD's.

An SE-30 30 meter capillary column, directly connected to the EI source, had samples applied directly on column.

Results: For a series of authentic 2,3,7,8 TCDD standards, masses could be assigned correctly, with a standard deviation of 9 ppm in the range 10-1000 picograms. Mass intensity ratios were 2.3 ± 0.3 (m/z 322/257). Quantitation curves based on both the masses were linear in the same concentration range.

A typical orthochlorophenol sample contained only 4 GC peaks with both m/z 322 and 257 centered in the MID window. Other GC peaks could be eliminated by the absence of either 257 or 322, or by an incorrect (uncentered) mass profile.

In the case of the 4 components which had both m/z 322 and 257, we found the mass peaks to be centered in the windows and thus have the correct exact mass for TCDD (standard deviation of the masses - 19 ppm). The coinjection of authentic 2,3,7,8 TCDD did not cause either GC peak or mass peak broadening, but only increased peak intensities. However, the intensity ratio 322/257 was 4.8, higher than authentic TCDD by a factor of 2. Therefore we concluded that there was another component besides the 2,3,7,8 TCDD present in the major peak. Without measurement of the intensity ratio, positive interference (in this case pehaps due to another isomer coeluting) would have gone undetected.

The combination of accurate mass information, intensity ratio, and GC retention time together give positive identification of 2,3,7,8 TCDD. Quantitation is possible at the picogram level.

RPMP7 TG-MS Study of the Vacuum Thermal Degradation of the PBT and PBO Rigid Rod Polymer Systems.[1]

E. Grant Jones, James M. Pickard and Donald L. Pedrick, Research Applications Division, Systems Research Laboratories, Inc., Dayton, Ohio 45440 and Ivan J. Goldfarb, AFWAL/MLBP, Wright-Patterson Air Force Base, Ohio 45433.

The rigid rod system poly(paraphenylenebenzobisthiazole) and poly(paraphenylenebenzobisoxazole) referred to as PBT and PBO, respectively, possess desirable properties for future structural applications. The vacuum thermal behavior of PBT, PBO and several of their phenyl-substituted analogues is reported based on the TG-MS technique. Temperature profiles of the intensity of the major volatile products including H_2S,HCN,$CS_2$$CO_2$ and C_6H_6 evolved during a programmed heating rate of 4 deg min^{-1} are reported. Weight loss, temperature onset of product detection, shape and location of the maximum in the rate of product evolution are correlated to assess the relative thermal stability and to propose mechanisms for describing the vacuum thermal degradation in the PBT and PBO systems.

[1]Supported in part under United States Air Force Contract No. F33615-77-C-5175 to SRL, Inc.

PYROLYSIS MASS SPECTROMETRY OF MACROMOLECULAR BIOMATERIALS

J. Haverkamp[a], W. Eshuis[a] and P.M.M. van Haard[b]

[a]FOM Institute for Atomic and Molecular Physics, Kruislaan 407, Amsterdam, The Netherlands
[b]Dept. of Biochemistry, University of Nijmegen, The Netherlands

Complex, non-volatile organic materials can readily be characterized by pyrolysis mass spectrometry [1]. This method offers the possibility to apply mass spectrometric analysis in the field of macromolecular compounds without the necessity of any pretreatment such as chemical derivatization or degradation.

Pyrolysis mass spectra obtained from chemically complex materials are rather complicated and are in the first instance used as "fingerprints". Close comparison of series of such fingerprint-spectra obtained from related materials is carried out by computer-multivariate analysis [2]. This process involves:

a) Normalization procedures.
b) Selection of the most informative mass values on the basis of peak intensity reproducibility and peak intensity difference between the various samples.
c) Calculation of dissimilarity values for each pair of spectra within the series, based on the selected peaks. These values express numerically the observed chemical differences between the analyzed materials.
d) Graphical representation of these calculated numerical differences for the set of spectra in nonlinear maps.

Such a comparative analysis can give qualitative and quantitative information about the sample compositions.

During the past few years pyrolysis-m.s. has been used for various purposes ranging from classification and identification (comparison with spectra of reference materials) towards quality control and chemical analysis of complex biomaterials e.g. biochemical fractions, tissues, cells, body fluids, micro-organisms, soils, sludges and fossil matter. Some recent applications are the following:

1) Detection of the virulence factor K1 (the capsular antigen colominic acid, a sialic acid polymer with $\alpha(2\rightarrow8)$ linkages) in hospital *Escherichia coli* strains [3]. The pyrolysis mass spectra of the complete bacterial cells show differences, related to the presence of this acidic polysaccharide, as is shown in the nonlinear map given in Fig. 1. This map is a graphical representation of the numerical differences between the spectra on the basis of the 10 most informative peaks. The two highest ranked mass peaks are m/z 67 and 109, and are characteristic peaks in the Py-mass spectrum of pure K1, isolated from *E.coli* bacterial cells.

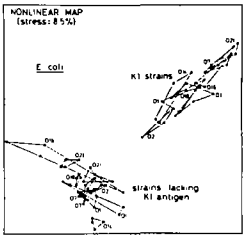

Fig. 1 - Nonlinear map of the Py-mass spectra of a series of 8 *E.coli* K1 strains and 10 *E. coli* non-K1 strains of different O-serotypes (obtained from Dr. P.A.M. Guinée, Natl. Inst. Publ. Health, Bilthoven, The Netherlands). Samples were taken directly from the culture plates. Each point represents a spectrum; quadruplicate analyses are connected.

The %-intensities of these two peaks are sufficient for classification of the bacterial strain as K1 or non-K1

2) Quantitative determination of DEAE-Dextran impurities in polio-virus preparations. Small amounts of this toxic, technical polymer could be introduced during the virus isolation procedure. The pyrolysis mass spectrum of DEAE-Dextran is dominated by the fragment at m/z 86, which is tentatively assigned to $Et_2NCH_2]^+$ originating from the diethylaminoethyl substituents. The relative intensity at m/z 86 in the spectra of the virus concentrates can be used as a quantitative measure for the DEAE-Dextran content with a detection limit of ~ 20 ppm.

3) Biochemical changes in human eye lens nuclei (protein matrix) on development of nuclear cataract [4]. Progressive coloration of the eye lens turns out to be correlated with the oxidation of sulfur-containing amino acid moieties and is expressed in the pyrolysis mass spectra of the lens nucleus homogenate mainly by increased intensities at m/z 64 (SO_2) and m/z 80 (see Fig. 2)

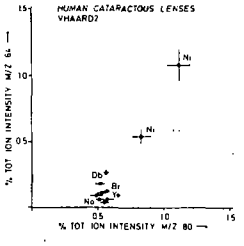

Fig. 2 - Plot of peak intensities in the Py-mass spectra of human eye-lens nuclei in different stages of cataract. No = normal; Ye(llow), Br(own), D(ark) b(rown), and Ni(gra) are different stages of cataract with increasing coloration. Average values of 4 spectra are given; bars indicate SD-values.

Probably, the generation of methionine sulfoxide, methionine sulfone and/or cysteic acid plays a part on cataract development.

Literature

[1] H.L.C. Meuzelaar et al. Adv. Mass Spectrom. 7 (1978) 1452
[2] W. Eshuis et al. in Analytical Pyrolysis (C.E.R. Jones and C.A. Cramers, eds.) Elsevier, Amsterdam (1977) p.151
[3] J. Haverkamp et al., Adv. Mass Spectrom. 8 (1980) in press
[4] P.M.M. van Haard et al., Biochim. Biophys. Acta (1980). in press

DETERMINATION OF VOLATILE CONSTITUENTS OF INSTALLED POWER CABLE BY GC/MS

M. S. Miller, R. W. Morrow, E. T. Creech
T. R. Oldham, and C. C. Wright

Union Carbide Corporation, Nuclear Division
P. O. Box P, Oak Ridge, TN 37830

During site updating, large amounts of 15 kV power cables were installed. The 15 kV cable is approximately 4 in. in diameter with three triplexed copper or aluminum conductor elements. Each conductor is insulated with an inner coat of ethylene propylene rubber, an outer coat of polyvinyl chloride, and wrapped with a bare copper corona discharge shielding tape. Cable interstices are filled with paper and polyvinyl chloride or sulfur vulcanized rubber rods. A fabric wrap is used to contain the filler rods and conductors within a galvanized steel armor that is jacketed in a PVC covering.

During installation, corrosion was observed on the copper shielding in the cable. Laboratory tests indicated that the corrosion resulted from the presence of the sulfur vulcanized rubber filler rods. Examination of the black corrosion deposits by X-ray diffraction and scanning electron microscopy/X-ray analysis identified the material as CuS. Further studies indicated the corrosion to be proceeding at a rate as to render the cable useless after 3 to 5 years of energization.

Installation of the cable required runs of 150 to 1,500 ft in length. Many cables containing sulfur rubber filler were found by visual inspection of the exposed cable ends. The remaining installed cables presented a very challenging problem. The manufacturer's records were not sufficient to exclude intermittent use of sulfur rubber fillers in long cable runs in cases where inspection of the ends indicated only PVC fillers to be used.

Our development laboratory was asked to establish a nondestructive method to identify the presence of sulfur rubber fillers in installed power cables. Thermalgravimetric quadrupole mass spectrometric (TGA/MS) analysis of sulfur rubber fillers identified carbonyl sulfide (COS) and hydrogen sulfide (H_2S) as characteristic gases given off during the heating of rubber. Due to the presence of volatile sulfur-containing gases, it was decided to monitor the volatile organics found inside the cable. Several methods of trapping were evaluated including adsorbant, bubbling through zinc acetate, and cryogenic. Comparison studies showed cryogenic trapping the most feasible method.

The analytical methodology involves purging the interstitial cable with helium, collecting the volatiles in a series of four cryogenic traps, and subsequent analysis of trapped material by gas chromatography/mass spectrometry. The first two glass traps are refrigerant 113/dry ice cooled (-80°C). These act as pre-traps to remove water and organics of low volatility. The next two Monel traps are liquid nitrogen cooled (-210°C) and remove carbonyl sulfide and any breakthrough organics from the first traps. The liquid nitrogen traps are then analyzed by either GC/MS or gas inlet mass spectrometry for carbonyl sulfide which is characteristic of rubber filled cable.

GC/MS analysis indicated COS to be present in rubber filled cable and not in PVC filled cable (Figure 1). Analysis of the same samples by gas inlet mass spectrometry produced peaks at 60 m/e for the rubber filled cable and none for the PVC filled cables.

To prove that these results were reproducible, two spools of as-received rubber filled cable and two spools of PVC filled cable (lengths 150 to 250 ft) were analyzed. Carbonyl sulfide was detected in the rubber filled cables and not in the PVC filled cables. The method was again tested on rubber filled and PVC filled cables (lengths to 500 ft) installed in K-31 building. Again COS was detected in the rubber filled cable and not in the PVC filled cable. The test proved that in situ sampling procedures are successful.

The analysis was repeated on previously sampled cables. Carbonyl sulfide was present in the rubber filled cable and not in the PVC filled cable. Therefore, repetitive sampling of the same cable could be performed and valid results obtained.

Testing of 44 installed cables was completed. Both of the liquid nitrogen traps from the same cable were analyzed separately. No discrepancy of results was observed between traps from the same sample. Three cables were found to contain sulfur rubber.

Cables containing rubber filler were successfully found at two UCC-ND plants using this method. As a result of evidence obtained in this matter, the supplying company has agreed to replace the cable containing the rubber filler.

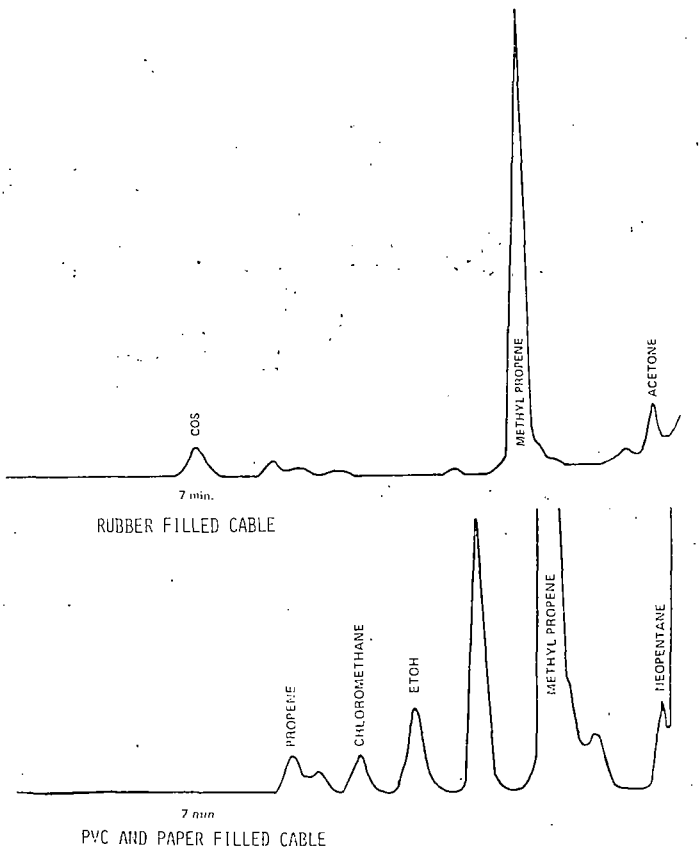

Figure 1

CABLE SAMPLING RESULTS

APPLICATIONS OF THE BALDWIN-MCLAFFERTY LC/MS INTERFACE TO THE ANALYSIS OF MOLECULES OF BIOCHEMICAL IMPORTANCE

Christine N. Kenyon, Hewlett-Packard Co., 1601 California Avenue, Palo Alto, CA 94304

A number of techniques have been utilized for sequencing oligo- and poly- saccharides, among them a partial hydrolysis method described by Valent et al[1]. This method involves partial acid hydrolysis, reduction and ethylation of a permethylated polysaccharide, the products of hydrolysis being subsequently separated by reverse phase high pressure liquid chromatography (HPLC). Oligosaccharides present in the various HPLC fractions are collected and their composition is determined by gas-liquid chromatography/mass spectrometry of the acetylated alditols obtained following total hydrolysis of each fraction. Since the oligosaccharides which are separated overlap with respect to the polysaccharide from which they were derived, the glycosyl sequence of the original polysaccharide can be determined.

Since oligosaccharides do not show ultraviolet absorption, it is necessary to detect them using a refractive index (RI) detector as they elute from an HPLC column. There are two disadvantages of using this type of detection: a gradient elution cannot be employed and the RI detector is not very sensitive.

This paper describes the utilization of the mass spectrometer as a detector for the analysis of partially hydrolysed polysaccharides. The separation was carried out with a Hewlett-Packard Model 1084-B HPLC, coupled to an HP 5985B GC/MS System with LC/MS Interface Option 004. The HPLC column was a DuPont Zorbax ODS column (25 cm long x 4.6 mm ID). A guard column (7 cm long x 2 mm ID) packed with reverse-phase pellicular packing (Whatman CO:Pell ODS) was also employed. The eluting solvent was a mixture of water (J.T. Baker Chemical Co., analyzed HPLC reagent) and acetonitrile (Burdick and Jackson Laboratories Inc., distilled in glass acetonitrile (UV)). The illustrations show the total ion chromatogram, selected extracted ion profiles and selected spectra from the analysis of oligosaccharides resulting from the partial acid hydrolysis of lichenan (isocratic and gradient elution from the HPLC column), and from the partial acid hydrolysis of starch (gradient elution from the HPLC column).

In Figure 1 are shown the total ionization chromatogram and mass chromatograms for the mono-, di-, and trisaccharide fragments obtained following LC/MS analysis of $NaBD_4$ reduced, permethylated and partially hydrolyzed starch. The spectrum of the trisaccharide is shown in Figure 2.

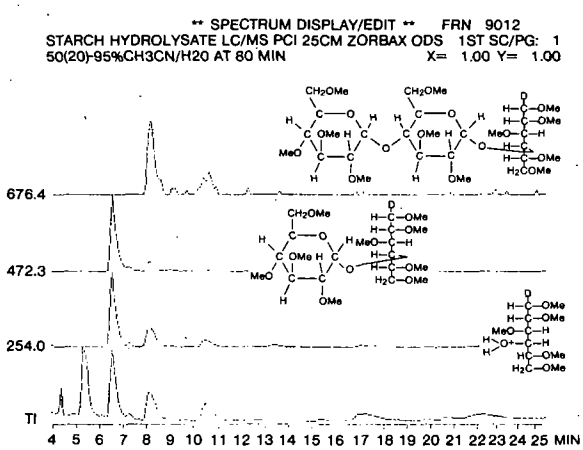

Figure 1. Extracted ion profiles for the LC/MS Analysis of $NaBD_4$ reduced, permethylated and partially hydrolyzed starch.

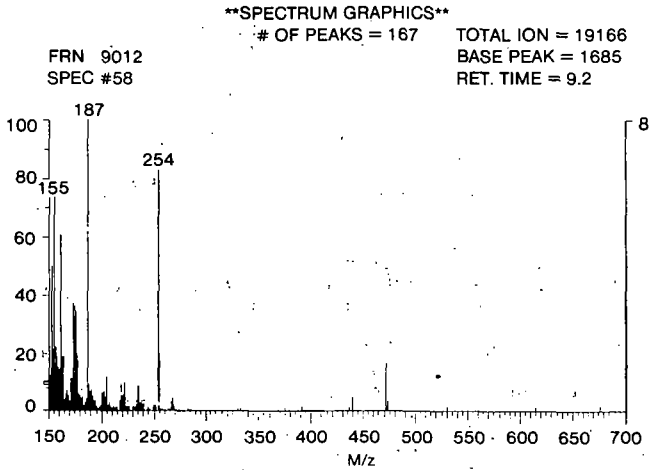

Figure 2. Mass spectrum for the trisaccharide seen in the run shown in Figure 1.

The positive and negative chemical ionization mass spectra of Ergotamine obtained using the same LC/MS interface show significantly different and complementary patterns. A molecular ion is obtained in the negative ion mode in addition to fragments. In the postive ion mode, the only significant peak obtained is lysergic acid (Figure 3).

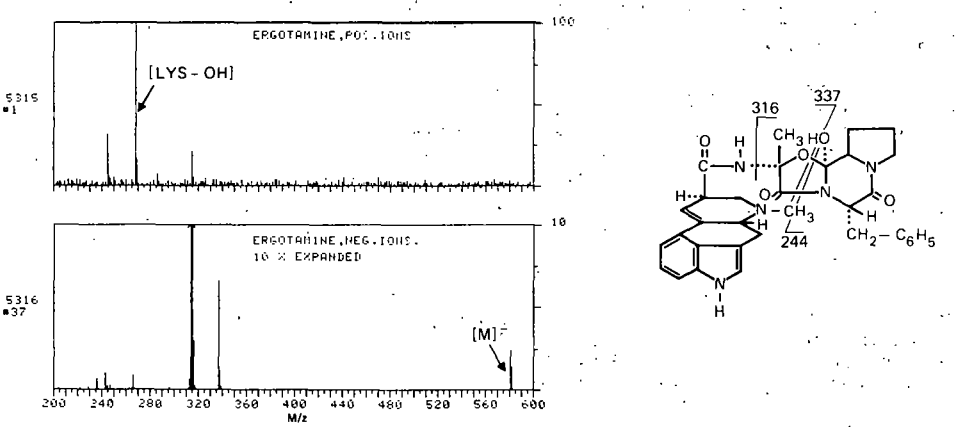

Figure 3. Positive and negative ionization analysis of Ergotamine.

It is possible to inject compounds directly into the LC/MS probe when using a pressurized container as source of solvent instead of the HPLC itself. An example of this mild direct insertion technique is the analysis of Erythromycin in the positive chemical ionization mode. The total ionization chromatogram and the spectrum obtained are illustrated. The Erythromycin spectrum clearly shows fragments corresponding to the losses of the sugar moieties of the molecule in addition to a strong quasimolecular ion at M/Z 734.6.

[1]Valent, B.S., A.G. Darvill, M. McNeil, B.K. Robertsen, and P. Albersheim, Carbohydrate Research, in press.

SIMPLE INTERFACE PROBE FOR LC/MS, P. C. Price, R. A. McDonie, and S. L. Wellons, Union Carbide Technical Center, South Charleston, WV 25303

In 1974, an interface probe for direct coupling of LC to a mass spectrometer ion source was first reported (1). The LC eluent was utilized as the chemical ionization reagent gas. Since that time, those researchers and others (Henion, Melera) have continued to work on direct LC/MS methods.

We have developed a new probe design for directly coupled LC/MS that remedies several problems with earlier devices. Our probe design is easily fabricated, and can be simply modified to fit any chemical ionization source with a solids probe inlet. The new interface probe consists of a steel body with Teflon insulating tip. The probe tip contains a "molecular leak" that is inside the ion source volume during operation. Teflon tubing (1/16 inch OD, 0.005 inch ID) passes from the LC, through a 1/16 inch Swagelok at the rear of the probe, inside the probe body, and out the Teflon tip. The tip also aligns the tubing with the ion source. Molecular leaks are fabricated in our laboratory by plating chromium over the end of a short section of stainless steel micro tubing. This tubing (0.25 inches long, 0.008 inches OD, approx. 0.0001 inches ID at tip) is inserted into the end of the Teflon tubing where it enters the ion source. Gas leaks of any desire conductance can be made by varying the plating time (usually 15 to 20 hours). A plating current of 6 ma is supplied by a variable 6 volt power supply. The plating solution is 300 g of CrO_3, 2 g H_2SO_4, 2 g sucrose, and 40 g NaOH, all diluted with water to make one liter. The counter electrode is a one inch diameter by 0.01 inch stainless steel disk placed in the bottom of a 50 ml plating bath.

Directly coupled LC/MS necessitates solvent flow rates of less than 20 microliters/min to the ion source. Splitting the effluent from a "standard" LC results in degraded performance. There is one commercial manufacturer of micro LC equipment that uses flows of 4-8 microliters/min. We have taken this equipment and replaced the injection system, columns, and interconnections, and have added low volume 2 micron filters. Samples are injected with a Valco valve, and sample size is 1 microliter. Total LC system void volume from injector to ion source is less than 50 microliters.

The data shown is from a one microliter injection containing 300 nanograms each of diethyl fumarate and glycidyl methacrylate. The eluent was 4% methanol in hexane, with a flow rate of 4 microliters per minute. The mass spectrometer, an AEI MS3074, was scanned from m/z 650 to 30 at 3 seconds per decade. The major reagent gas ions, m/z 33 and 85 both act as proton donors. We estimate that the source pressure during this run was between 0.20 and 0.35 Torr; the source temperature was 150 degrees.

This new LC/MS interface probe and modified micro LC have been used in our labs for almost one year. The current system has a "full scan" detection limit of about 50 nanograms on column, and a chromatographic efficiency of better than 1500 theoretical plates for an 8 cm silica column. Some thermally labile compounds give intense parent ions with little fragmentation. The entire system - chromatograph, interface, chromatography, and chemical ionization is still being developed and optimized.

1. P. Arpino, M. A. Baldwin and F. W. McLafferty, Biomedical Mass Spectrometry 1, 80(1974).

SUMMATION OF ALL IONS BETWEEN M/Z 142 AND 650

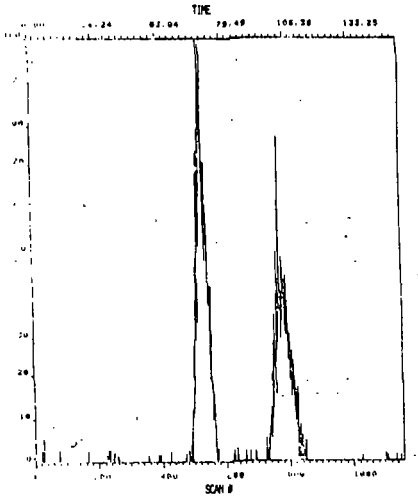

SINGLE ION TRACES

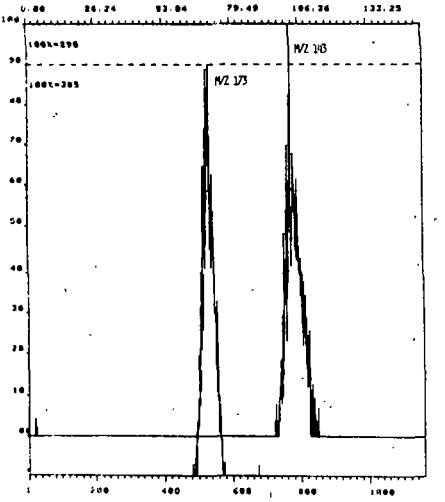

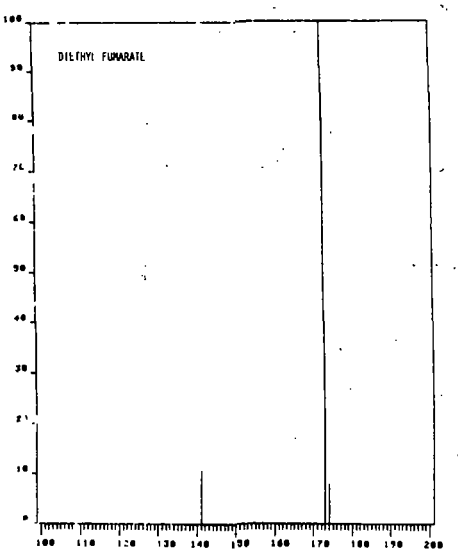

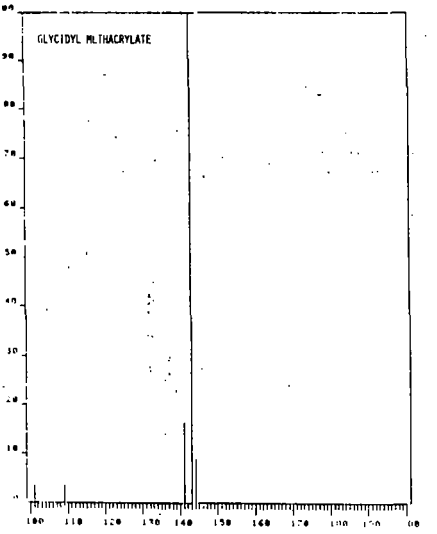

CHEMICAL DERIVATIZATION FOR COMBINED HIGH PERFORMANCE LIQUID CHROMATOGRAPHY - MASS SPECTROMETRY

M.A. QUILLIAM and E.Y. OSEI-TWUM

Dept. of Chemistry, McMaster University,
Hamilton, Ontario, Canada, L8S 4M1.

High performance liquid chromatography/mass spectrometry (HPLC/MS) is envisioned by many as the panacea that should afford high sensitivity detection and structural information for compounds that cannot be analyzed by GC/MS. Unfortunately, HPLC/MS with the band transport type of interface and electron-impact ionization (which is most valuable for structural work and library searches) is still limited to species with a volatility suitable for solid probe MS.

Early in the development of GC and MS, chemical derivatization was recognized as an essential consideration for much of the analytical work. It seems reasonable that it should be possible to use derivatization to extend the range of compounds that can be analyzed by HPLC/MS. Derivatization of polar compounds should lead to an improved compatibility of HPLC and MS by allowing the use of non-polar, volatile chromatographic solvents and by enhancing their volatility for the mass spectrometer. In addition, derivatization can often lead to improved separations and better mass spectral behavior that includes abundant molecular ions and structurally significant fragmentations.

The principal derivatization technique that we have examined thus far is the formation of O-tert-butyldimethylsilyl (TBDMSi) derivatives of hydroxyl and carboxyl containing compounds. This paper presents results of our investigation into the TBDMSi derivatization and HPLC of polar compounds such as nucleosides and bile acids and some preliminary analyses with the new VG HPLC/MS interface attached to a VG 7070 mass spectrometer.

Figure 1 illustrates the HPLC/MS analysis of a set of dimeric nucleosides as O-TBDMSi derivatives. The silylation was performed by reacting the compounds with 1 M tert-butyldimethylchlorosilane and 2 M imidazole in pyridine for one hour at 80 . The reaction mixture was cleaned up on a micro Sephadex LH-20 column (hexane:ethyl acetate, 3:1). HPLC was performed on a reverse phase column (RP-8, 25 cm x 0.4 mm ID) with 0.9 ml/min acetonitrile as mobile phase. Mass spectra were acquired by scanning from 1250 to 60 amu at 2 seconds/decade with 1500 resolution. The mass spectra of these compounds contain abundant $(M-tBu)^+$ ions and a number of fragment ions valuable for structural work. The underivatized compounds require the use of an aqueous buffer as mobile phase and pyrolyze during electron impact probe MS analysis. Derivatization after HPLC was very difficult due to the buffer in the eluent.

Figure 2 gives the combined HPLC of some bile acids and cholesterol. The conditions were the same as for figure 1 except that spectra were scanned from 650 to 60 at 1 second/decade. Sterically hindered hydroxyls on the bile acids were not derivatized under the conditions used. The abundant $(M-57)^+$ ions in the spectra of these compounds should be useful for selected ion monitoring.

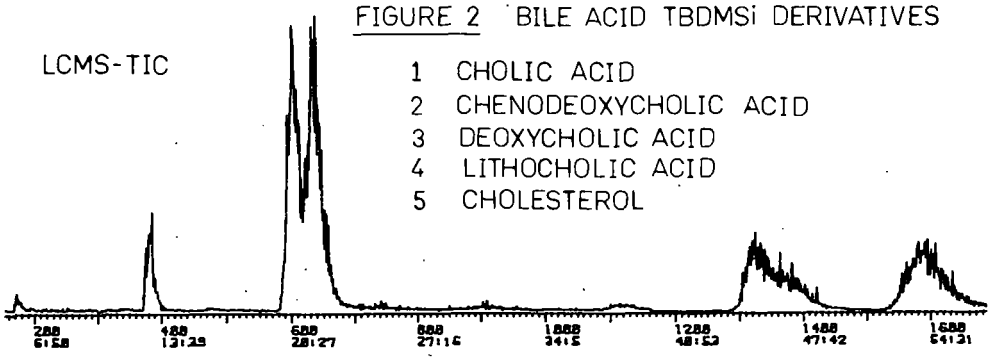

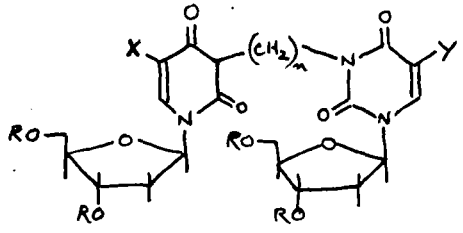

Compound #	X	Y	m
1	H	H	1
2	H	CH_3	1
3	CH_3	CH_3	1
4	CH_3	CH_3	2
5	CH_3	CH_3	6

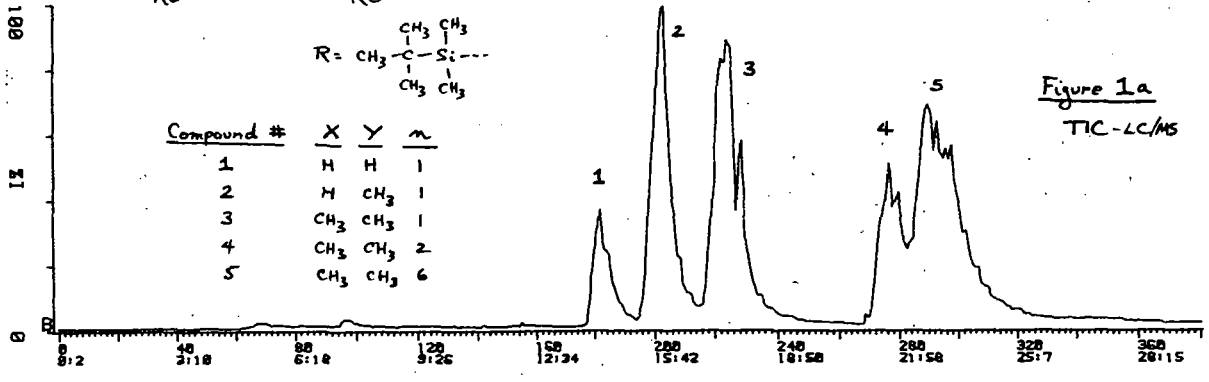

Figure 1a
TIC-LC/MS

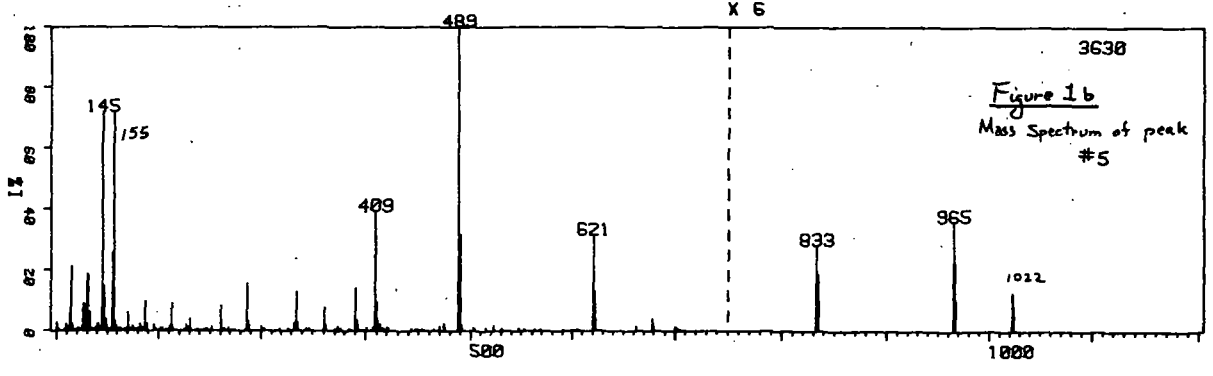

Figure 1b
Mass Spectrum of peak #5

LC/MS APPLICATION TO TANNERY EFFLUENT ANALYSIS

Alfred D. Thruston, Jr. and John M. McGuire
U.S. Environmental Protection Agency
Environmental Research Laboratory
Athens, Georgia 30613

Combined LC/MS using a moving belt interface was used to study five tannery and leather finishing industry discharge extracts. LC separation was performed with a Zorbax CN column using a normal phase solvent system of hexane/methylene chloride/methanol. Parameters for examining environmental samples using a moving belt LC/MS interface were developed.

LC/MS chromatograms of tannery effluent extracts were produced based on the total ion currents in both the EI and methane CI modes.

Compounds found by LC/MS were phenol, binaphthyl sulfone, cholesterol, nitroaniline, p-cresol, o-cresol, caffeine, o-phenyl phenol, trichlorophenol, pentachlorophenol, methylene biphenol (3 isomers), naphthol, chlorocresol, nitrophenol, phenyl formamide, trihydroxycoumarin, n-propylthiophene, dihydroxyphenylpropanol, and long-chain alkyl alcohols.

Binaphthyl sulfone, which is not gas chromatographable, was one of the major components in all five tannery extracts. It was tentatively identified by mass spectral cracking patterns. The mass spectrum was absent from available literature or data bases, so the compound was synthesized; the LC retention time, UV response, and mass spectrum matched those of the sample extract.

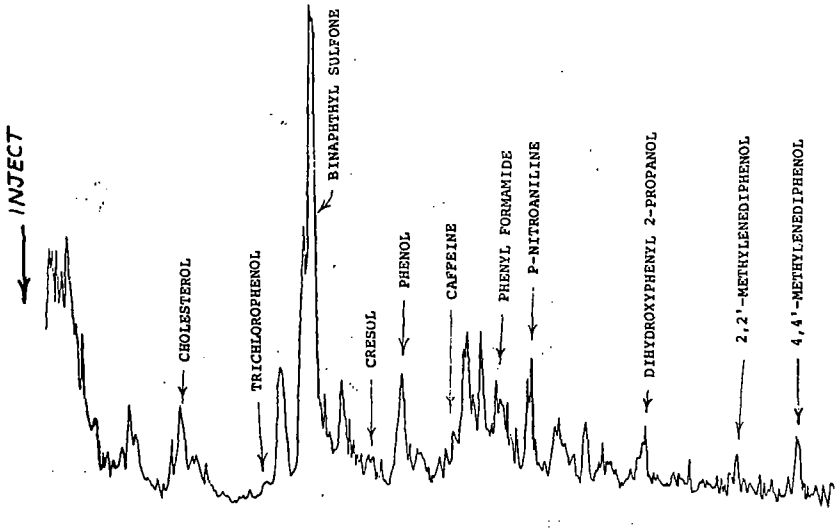

TIC trace obtained by EI LC/MS of a tannery extract.

APPLICATION OF COMBINED LC/MS TO THE ANALYSES OF SELECTED CEPHALOSPORINS AND PENICILLINS

Roy, T. A., DeRoos, F. L., Hidy, B. J., and Howard, C. C.

BATTELLE
Columbus Laboratories
505 King Avenue
Columbus, Ohio 43201

The feasibility of characterizing formulated penicillins and cephalosporins antibiotics by combined LC/MS has been investigated. HPLC methods have been previously developed for these compounds; however, LC/MS analysis requires modification of the commonly used mobile phases which contain high aqueous concentrations and involatile inorganic buffers. More importantly, LC/MS analysis requires that these compounds, often formulated as the acid salts, be properly volatilized so as to allow characterization and differentiation of the individual members of the group.

To investigate this latter point, belt-spectra were obtained for 15 commercially available penicillins and cephalosporins using a Finnigan moving-belt interface coupled to a Finnigan 4000 GC/MS/DS. The compounds formulated as free acids, Zwitterions and inner salts are volatilized intact and their isobutane chemical ionization and mass spectra display intense M + 1 and/or ions resulting from loss of CO_2 from an M + 1. The mass spectra of those compounds formulated as sodium or potassium salts show no significant ionization in the molecular weight region. However, they do display intense ions which characterize the substituents on the acid nuclei as well as the acid nuclei themselves. The most characteristic ion found throughout this series appears to be of the general form:

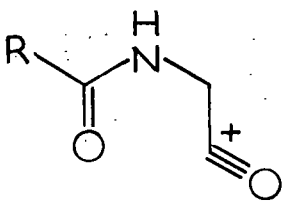

This ion defines the major side-chain substituent and, together with other ions which characterize the acid nuclei, differentiation is possible for all compounds investigated.

LC conditions compatible with the mass spectrometer necessitate minimizing the aqueous content of the mobile phase. MeOH/aqueous HOAc (0.2%) binary mixtures ranging from 90:10 to 60:40 (v/v) on a 1/4" x 25 cm Partisil 5 ODS column were used. The penicillins can be successfully chromatographed and analyzed using these parameters. The quality of their LC/MS spectra is comparable to the belt-spectra and the summed ion chromatograms of ions unique to individual compounds permit unambiguous identification of mixture components. The cephalosporins appear to be chemically degraded by the chromatographic process; a change of LC conditions (column) can be expected to resolve this difficulty.

LASER DESORPTION MASS SPECTROMETRY OF INVOLATILE SAMPLES

E. D. Hardin and M. L. Vestal

Department of Chemistry
University of Houston
Houston, TX 77004

Laser Desorption Mass Spectrometry has recently been shown to be useful for the analysis of involatile bimolecules.(1) This technique uses a submicrosecond laser pulse delivering ~10^6 w/cm^2 to the sample resulting in desorption of quasimolecular ions. Ionization is mainly by alkali attachment but proton transfer also occurs for some classes of biomolecules. There is little fragmentation due to the low internal energy of the ions formed.

In our work we have developed a scanning LDMS which uses a quadrupole mass filter and a rotating stainless steel belt onto which the sample is electrosprayed for continuous sample introduction. Surface coverages are typically 1 μg/cm^2. Ionization is with a N_2 pumped dye laser delivering approximately 400 μJ over a 10 nsec pulse width at 20 pps. Scan times allowing for ~5 pulses/amu are used. Ion detection is with an EM tube and a current amplifier gated through a boxcar integrator for S/N enhancement. A Finnigan INCOS Data System is used to acquire and display the data.

Preliminary results from this instrument show that it is applicable to sugars, peptides, and nucleosides. The spectra of sucrose, Figure 1, shows intense alkali attached molecular ions and no fragmentation. The same occurs for amino acids and dipeptides, Figure 2. Nucleosides show alkali attached molecular ions and alkali attached base fragment ions as shown in Figure 3. Intense quasimolecular ions have also been obtained from Na_2GMP (not shown) and Na_2ATP as shown in Figure 4.

The spectra obtained on the same sample but from different portions of the belt are qualitatively reproducable; however, the intensities vary somewhat from scan to scan. This probably results from variations in the homogeniety of the surface layer as shown by the reconstructed ion chromatograms. There are also as yet uninterpretable fragment peaks in some spectra such as raffinose, Na_2GMP, and Na_2ATP as well as the absence of expected fragment peaks. Some of these uninterpretable fragment peaks may be due to impurities or solvents adsorbed on the belt.

In the future we plan to use the capabilities of this instrument to produce a steady ion current at any selected mass to study the KE of desorbed ions for a more fundamental understanding of the LD process. We will also continue to study the analytical potential of LDMS and eventually interface an LC to this instrument to study the possibility of LC-LDMS.

Acknowledgement

This work was supported by the NIGMS under grant GM24031 and by the Robert A. Welch Foundation.

Reference

1. M. A. Posthumus, P. G. Kistemaker, H. L. C. Meuzelaar, and M. C. Ten Noever de Brauw, Anal. Chem., 50, 985 (1978).

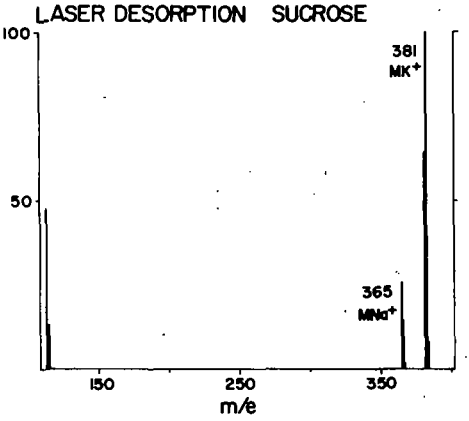

Figure 1. LD spectrum of sucrose showing alkali attached molecular ions and no fragmentation. Peaks at 113 and 115 are from $KCl \cdot K^+$.

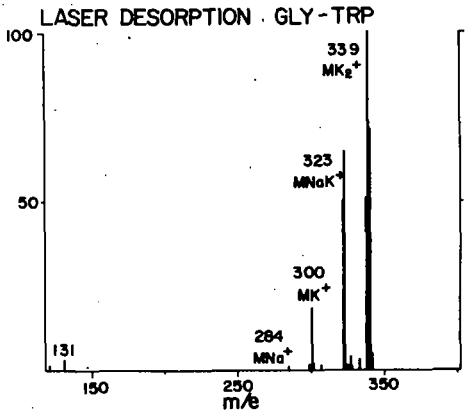

Figure 2. LD spectrum of the dipeptide, glycyl tryptophan, showing alkali attached molecular ions and dimers.

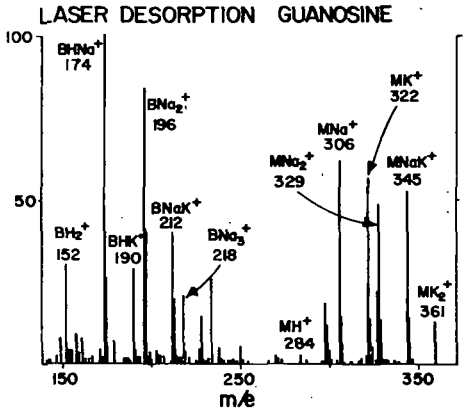

Figure 3. LD spectrum of the nucleoside, guanosine, showing alkali attached molecular ions and alkali attached base fragment ions and dimers. $(B+2H)^+$ and $(M+H)^+$ are also present.

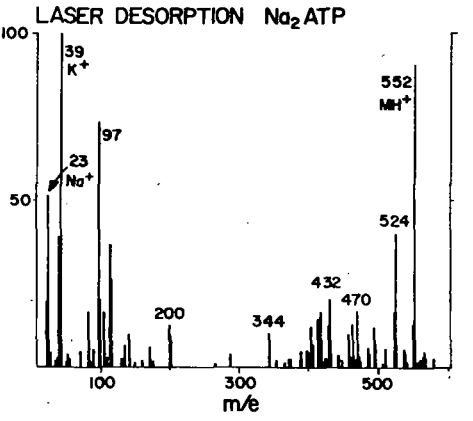

Figure 4. LD spectrum obtained from $1 \mu g/cm^2$ of Na_2ATP showing intense MH^+.

LASER DESORPTION CHEMICAL IONIZATION

ROBERT J. COTTER and CATHERINE FENSELAU, Dept. of Pharmacology and Experimental Therapeutics, The Johns Hopkins University, Baltimore, MD. 21205.

Preliminary work has been carried out to test the feasibility and practicality of using laser desorption in combination with a high pressure chemical ionization source for production of molecular ions from compounds which are non-volatile and/or thermally labile. The significant feature of this instrument is the mating of a short pulsed (40nS) low duty cycle (1 Hz) CO_2 laser with a scanning magnetic instrument. Minimum sample destruction is achieved by the short, infrequent laser pulses (in a cold ion source); sensitivity is enhanced by the chemical ionization of the more abundant desorbed neutral molecules; and scanning is made possible by the increase in ion production and ion residence times during which ions are emitted from the high pressure source. This paper describes the instrumentation and some early results for several steroid glucuronides and bile acid conjugates.

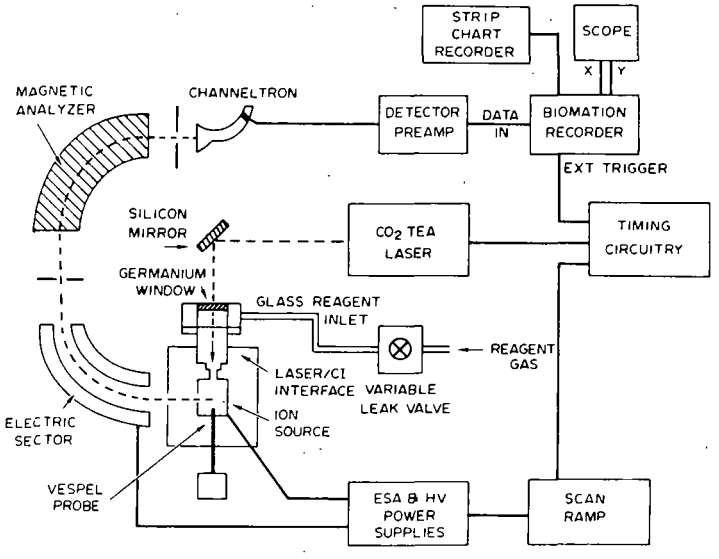

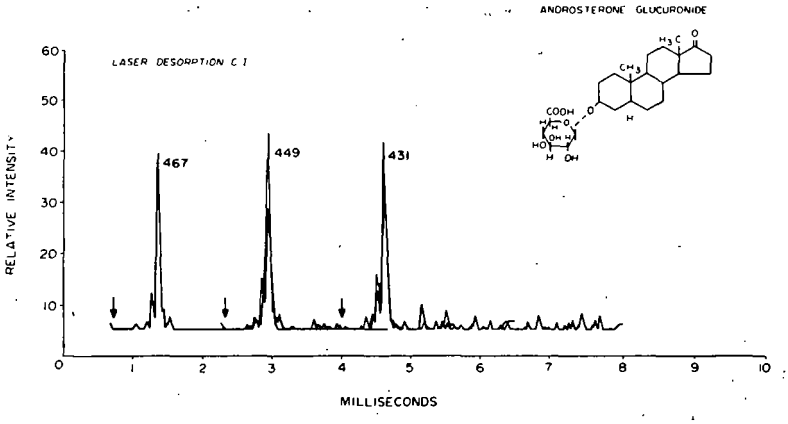
ANDROSTERONE GLUCURONIDE
LASER DESORPTION C I
RELATIVE INTENSITY
467
449
431
MILLISECONDS

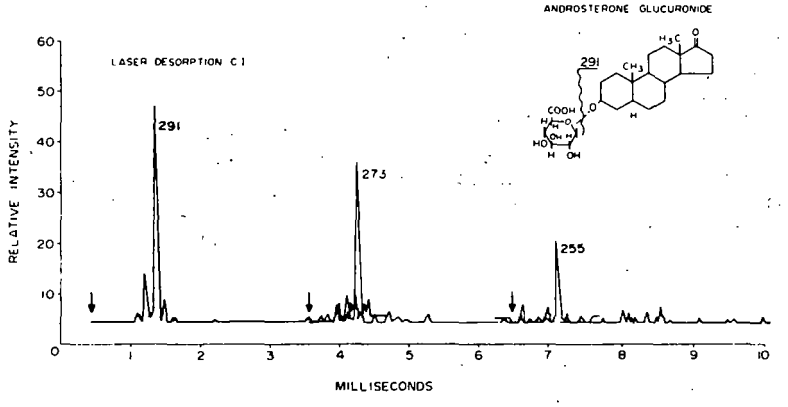
ANDROSTERONE GLUCURONIDE
LASER DESORPTION C I
RELATIVE INTENSITY
291
273
255
MILLISECONDS

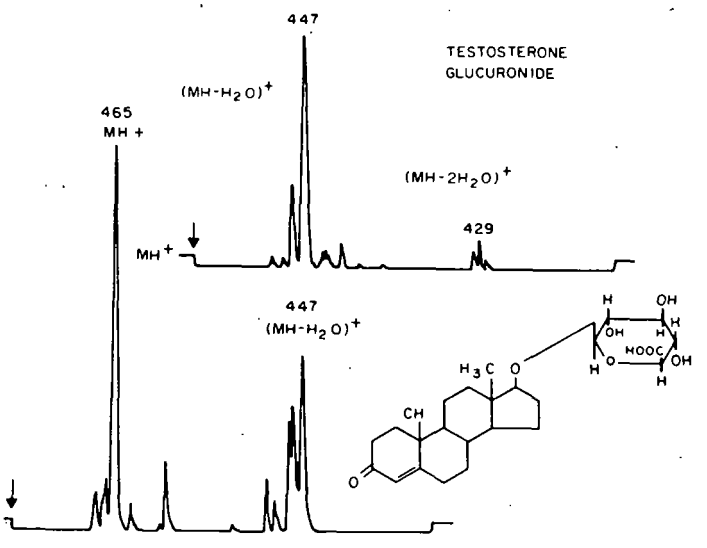
TESTOSTERONE
GLUCURONIDE
465
MH +
447
(MH-H2O)+
(MH-2H2O)+
429
MH+
447
(MH-H2O)+

Laser Desorption CI Mass Spectrometry

Donald F. Hunt, William M. Bone and Jeffrey Shabanowitz

Department of Chemistry
University of Virginia
Charlottesville, Virginia 22901

A Gen-Tec pulsed CO_2 laser capable of 1 megawatt peak pulse power and 200 pulses/sec has been interfaced to a Finnigan 4000 quadrupole mass spectrometer. The laser beam is focused onto a $1mm^2$ spot inside the CI source. The pulse duration is about 200 nsec although it can be varied from 150 nsec to 500 nsec depending on the gas mixture inside the laser cavity.

Initial experiments were performed using a solids probe with a copper tip to introduce samples. When the laser is focused onto the copper probe in the CI source with Ar at 0.5 torr the Cu^+ signal intensity exceeds that of Ar^+. When the Townsend discharge, located on the bottom of the ion source, is turned on the Cu^+ ion intensity increases by a factor of ten. As the laser power is decreased metal ions from the probe cease to be generated although sample ions are still seen. The laser is normally operated at a power just below the threshold for metal ion formation.

A Finnigan LC interface was modified to pass through the ion source so that nonvolatile samples could be continuously introduced and analyzed. A Townsend discharge was also constructed which could be inserted through the solids probe inlet. This allows laser desorbed neutrals to be ionized under CI conditions usually with an Ar discharge.

The CI source with the moving belt (SS) maintains its integrity in that 50 ng of either strychnine or coronene are easily detected off the belt. Samples are generally from $2ng/cm^2$ to $20\ ng/cm^2$ although larger samples are sometimes needed.

Raffinose (MW 504), a thermally labile trisaccharide, yields an excellent LDCI mass spectrum. When doped with alkali metal salts, ions corresponding to $M+Na^+$, $M+K^+$, and $M+Cs^+$ dominate the high mass end of the spectrum obtained from this molecule.

Leu-Enkephalin (MW555), a pentapeptide (Tyr-Gly-Gly-Phe-Leu) affords an intense molecular ion in addition to fragmentation data corresponding the amino acid sequence of the molecule using 100 nmoles of the underivatized sample.

ELECTRON IONIZATION-FLASH DESORPTION MASS SPECTROMETRY:

A DEVICE TO CONTROL SAMPLE PROBE HEATING AND BEAM SWITCHING

Terry D. Lee, William R. Anderson, Jr., and G. Doyle Daves, Jr.

Department of Chemistry and Biochemical Sciences
Oregon Graduate Center
Beaverton, Oregon 97006

EI-flash desorption mass spectrometry is a technique which has been used to analyze a large variety of involatile and thermally labile compounds. Under typical conditions, a sample on a metal grid is heated rapidly (1,000 - 50,000° c/sec) to a final temperature of 700 - 2,000° C with photoplate detection of the ions formed.

A control device has been constructed which facilitates production of EI-flash desorption spectra and has led to a better understanding of the desorption process. The rate at which the sample is heated can be controlled either by varying the amplitude of the voltage pulse to the grid, or by varying the length of the pulse (5 msec → 1 sec). Convenient monitoring of single ion desorption profiles is made possible by a circuit which triggers a storage oscilloscope connected to the output of the photomultiplier detector of the mass spectrometer. There is also a circuit which can be used to vary the length of time ions are collected on a photoplate.

At faster heating rates (150° - ∿ 1400°C in 50 msec) there is little variation among classes of compounds in the position and shape of desorption profiles of ions containing molecular weight information. Consequently, a large variety of compounds can be run under a standard set of conditions. Desorption initiates 8 - 15 msec from the start of the flash with a duration of 25 - 35 msec. Intensity varies in accordance with the expected thermal stability of the compounds.

Thermally labile compounds require rapid heating rates in order to observe MH^+ ions. When sucrose is heated to ∿ 900°C in 250 msec, the MH^+ ion (m/z 343) is observed. If the time is extended to 500 msec, the MH^+ ion is not detected.

Although desorption of MH^+ ions is complete in most instances before the end of the heating flash, the ion beam monitor of the mass spectrometer indicates ion production several seconds after the flash. These lower mass ions appear to originate from pyrolysis of the sample. Considerable improvement of the EI-flash desorption spectra can be obtained by using the device to terminate ion collection shortly after MH^+ ion desorption is complete.

APPLICATIONS OF A NEW DIRECT INTRODUCTION PROBE FOR DESORPTION CHEMICAL IONIZATION

J.R. Chapman, S. Evans, C.J. Wakefield, K.R. Compson, D. Hazelby
Kratos Ltd. Barton Dock Road, Urmston, Manchester M31 2LD, England.

The design of a new direct introduction probe for solid samples encompasses a number of desirable features. The probe tip itself takes the form of a metal coil of low thermal mass that can be heated extremely rapidly (up to $100^{o}C\ sec^{-1}$) whilst also acting as a temperature sensor for feedback control. The probe tip is detachable from the main shaft and may be replaced by other types as required.

The probe is designed to fit a standard Kratos vacuum lock so that the only modification required for existing instruments is the provision of a single contact for the heater supply mounted off the source. When introduced fully, the probe body provides a good source seal for chemical ionization and the tip itself extends almost to the centre of the source. This positioning, combined with the facility for rapid heating, allows the probe to be used to provide desorption chemical ionization (DCI) spectra. The probe tip is robust enough to allow it to be cleaned by flaming. Insulation on the shaft allows the probe to be used at source potentials up to 8000 volts.

Three examples of DCI spectra produced under fast heating conditions and using ammonia as the chemical ionization reagent gas are shown in Figures 1-3. These are the spectra of glucose, riboflavin and cortisone acetate respectively. In each case, the spectrum is characterised by an intense quasi-molecular ion together with some fragment ions. In addition to providing very rapid heating for DCI spectra, the probe also provides controlled heating for the smooth evaporation of less labile samples. Figure 4 shows some data obtained with this probe on samples of homologous choline esters, again run with ammonia as the chemical ionization reagent gas, although at a lower source pressure than the preceding examples.

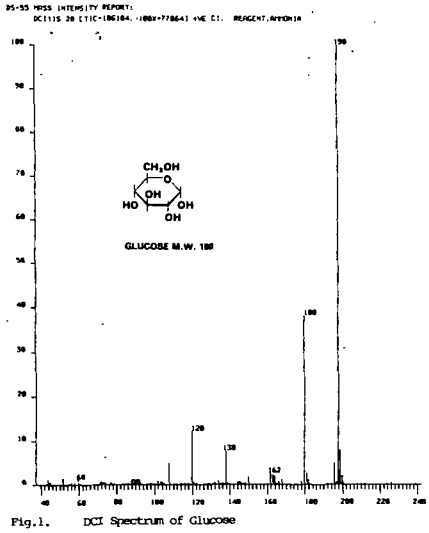

Fig.1. DCI Spectrum of Glucose

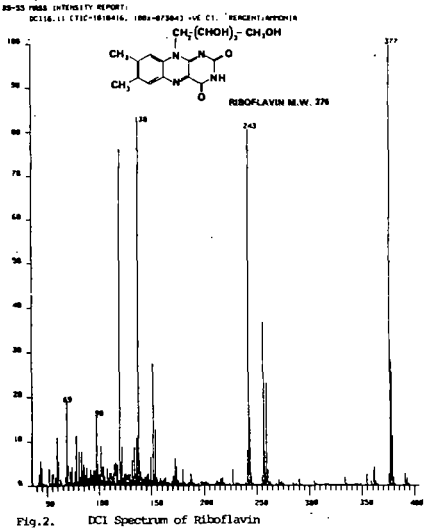

Fig.2. DCI Spectrum of Riboflavin

The three pairs of spectra in Figure 4 were obtained by alternate CI-EI scanning (ACE) analysis of acetyl, propionyl and butyryl choline chlorides (R = CH_3, C_2H_5, C_3H_7 respectively). Linked B/E scanning of the major ion in each of these CI spectra provided metastable spectra again corresponding to acetyl, propionyl and butyryl choline respectively. The losses shown were 45 a.m.u. (probably $(CH_3)_2NH$) in each case and a loss corresponding to a molecule of the esterifying acid. These metastable transitions provide a means by which the presence of choline esters in complex extracts may be monitored.

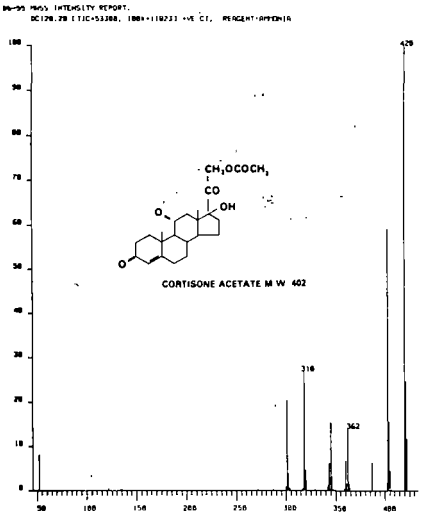

Fig.3. DCI Spectrum of Cortisone Acetate

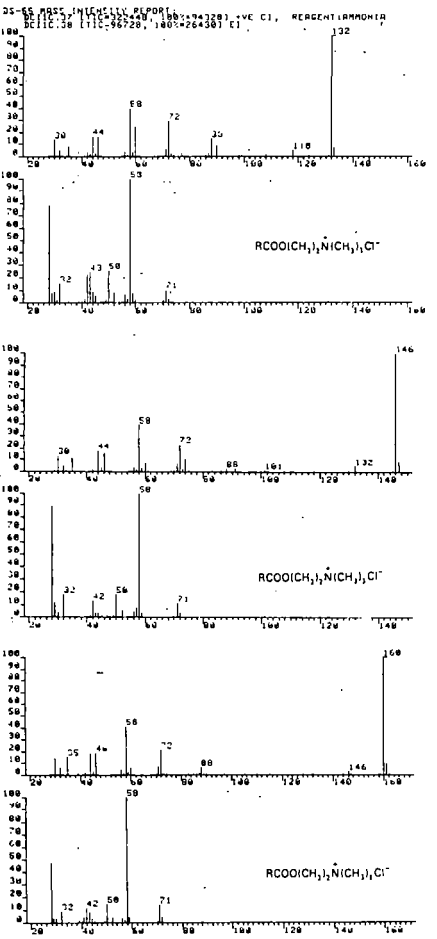

Fig.4. ACE Spectra Choline Esters

The First Viable EI/CI LC/MS Interface

Paul P. Dymerski
Toxicology Center, Div. of Laboratories and Research
New York State Dept. of Health, Albany, New York, 12201

An LC/MS interface should meet the following requirements:

1. Permit electron impact and chemical ionization mass spectrometry.
2. Accomodate at least 50% water for reverse phase liquid chromatography.
3. Accomodate flow rates of at least 0.5 cc/min but preferably 1-2 cc/min.
4. Maintain sensitivity to 50-100 ng full scan injected (regardless of splitting ratios).

An LC/MS system has been developed which exceeds any available interface in meeting these requirements. It is a Finnigan moving belt interface, modified to correct for deficiencies in solvent handling characteristics.

The following modifications were made:

	REASON	MODIFICATION
1.	REDUCE AIR CONDUCTANCE	"TUNNEL" ISOLATION PORTS
2.	COMPENSATE FOR ΔH (VAPORIZATION)	AUXILIARY BELT HEATERS
3.	IMPROVE BELT SOLVENT CAPACITY	INCREASE BELT SPEED
4.	INCREASE SOURCE PUMPING CAPACITY	TURBOMOLECULAR PUMP (optional)

The above modifications improve the flow characteristics over those presented previously[1,2], using a Kaptan belt.

MODIFIED INTERFACE FLOW CHARACTERISTICS (cc/min)

% Water/	Acetonitrile[a]	Methanol
Ø	1.8 - 1.9	1.8
1Ø	- 1.6	1.0
3Ø	1.3 - 1.3	0.6
5Ø	0.4 - 0.7	0.4

(a) Variance is a function of the particular belt.

This modified interface has been applied in several areas. Polynuclear aromatics (PNA) in extracts from Niagara river fish and PNA derivatives from diesel exhaust have been detected both by full scanning and MID. The isomers (22 in the standard) ranged from napthalene to coronene with no loss in chromatographic resolution. Vitamin K_1 and vitamin K_1-oxide were examined in rat liver extracts under chemical ionization conditions with methane as the reagent gas of choice. Dichlorobiphenyls (DCB) and their metabolites from in vitro incubations with P-450 were examined. The postulated metabolites, DCB-OH, DCB-$(OH)_2$, and DCBdihydrodiol were detected. A DCB-quinone detected by solid probe methods was not seen by LC/MS.

CAPABILITIES

- Electron impact and CI mass spectrometry
- Gradient elution for water (acetonitrile) from 30% at 1.33 cc/min and 50% at 0.4 cc/min without splitting.
- Organic solvents to 1.9 cc/min, direct.
- Self aligning slits for rapid belt replacement.
- Can be added to standard interface.

LIMITATIONS

- At present only Kaptan belts can be used.
- Background still limits scanning to greater than m/e 100.

---

1. P. Champlin and Paul P. Dymerski, 27th Annual Conf. of Mass Spec. and Allied Topics, Seattle, Wash., June, 1979, pps 446-447.

2. W.H. McFadden, et al., American Laboratory, October, 1977, pps. 55, 74.

EFFECT OF REACTION EXOTHERMICITY ON PROTON TRANSFER CI MASS SPECTRA

J. A. Herman and A. G. Harrison

University of Toronto
Toronto, Canada

By using a variety of protonating agents, XH^+, in which the proton affinity of X varies, the effect of reaction exothermicity on proton transfer chemical ionization mass spectra may be examined. The present study reports the use of the following protonating agents (proton affinity of X, kcal $mole^{-1}$, in brackets): H_3^+ (101), N_2H^+ (114), CO_2H^+ (127), N_2OH^+ (135), and HCO^+ (139) in a study of the CI mass spectra of some representative alkanols and acetate esters. The N_2H^+, CO_2H^+, N_2OH^+, and HCO^+ reactant ions were produced by electron impact ionization of mixtures of the appropriate X (∿10%) in H_2 at source pressures of ∿0.2 Torr. Under these conditions the XH^+ was the only significant reactant ion except for the N_2O/H_2 mixture where appreciable NO^+ was observed.

The CI mass spectra of eight isomeric C_5 alkanols were determined. The major fragmentation pathway involves H_2O elimination from the protonated alcohol with further fragmentation of the resultant $C_5H_{11}^+$ ions by loss of H_2, CH_4, and C_2H_4, the last process being most important. The extent of fragmentation of $C_5H_{11}^+$ decreases as the exothermicity of the initial protonation reaction decreases and is greatest for $C_5H_{11}^+$ ions derived from primary alcohols, less for those derived from secondary alcohols, and is very small for $C_5H_{11}^+$ derived from t-amyl alcohol. These results indicate that isomerization to more stable alkyl ionic structures does not occur to any significant extent before or during H_2O elimination from the protonated alcohol.

Similar results were obtained in the study of isomeric C_6 alkanols, including the dependence of the further fragmentation on the nature of the original alcohol (primary > secondary > tertiary). The major fragmentation reactions observed for $C_6H_{13}^+$ were

$$[1] \quad C_6H_{13}^+ \rightarrow C_3H_7^+ + C_3H_6$$

$$[2] \quad \rightarrow C_4H_9^+ + C_2H_4$$

Bowen and Williams (1) have proposed that the reacting structure for [1] is the 3-methyl-2-pentyl ion and that the reacting structure for [2] is the 3,3-dimethyl-1-butyl ion. We observe that $C_6H_{13}^+$ ions derived from 3,3-dimethyl-1-butanol show a pronounced preference for loss of C_2H_4 in agreement with this proposal. However, the $C_6H_{13}^+$ ion derived from 3-methyl-2-pentanol does not show the expected preference for loss of C_3H_6, suggesting that this may not be the reacting configuration for propylene elimination.

The CI mass spectra of alkyl acetates show two major fragmentation reactions of the protonated molecule, [3] and [4].

$$[3] \quad CH_3CO_2R.H^+ \rightarrow CH_3CO_2H_2^+ + R-H$$

$$[4] \quad \rightarrow CH_3CO_2H + R^{+\cdot}$$

In most cases [3] is thermochemically favoured over [4]; however, significant fragmentation by [4] is observed, presumably because [3], being a rearrangement reaction, has less favourable frequency factor than the simple bond cleavage [4] and cannot compete effectively for ions of high internal energy. In agreement with this suggestion, reaction [3] increases in importance relative to [4] as the exothermicity of the protonation reaction decreases, thus decreasing the average internal energy of the fragmenting ions. The competition between [3] and [4] depends strongly on the structure and, thus, the stability of the R^+ ion with the result that [4] becomes the dominant fragmentation channel when stable tertiary alkyl ions may be formed.

Full details of this work will be published.

(1) R. D. Bowen and D. H. Williams, J. Chem. Soc., Perkin II, 1976, 1479.

TEMPERATURE DEPENDENT IONIC FRAGMENTATION IN THE CHEMICAL IONIZATION MASS SPECTRA OF SEMICARBAZONES

D.A. Herold
Department of Pathology
University of Virginia Medical Center
Charlottesville, Virginia 22901

and

T.A. Elwood and J.H. Futrell
Department of Chemistry
University of Utah
Salt Lake City, Utah 84112

It is generally observed that chemical ionization mass spectrometry generates an abundant quasi molecular ion; the intensity of $(M+1)^+$ or the adduct ions $(M+Ad)^+$ is commonly greater than the corresponding molecular ion, M^+, generated by electron impact ionization. However, this is clearly not the case for semicarbazones, as demonstrated in our laboratory by an investigation of medium molecular weight ketones and their semicarbazone derivatives.

A study of 3-methyl-2-hexanone (I) and of semicarbazone (II) serves to illustrate this general characteristic of these compounds.

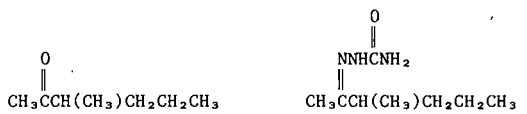

(I) (II)

Electron impact analysis of (I) provided high intensities of the molecular ion while the methane CI spectrum of (I) consists almost entirely of the protonated molecular ion, consistent with the general observations of electron impact and chemical ionization mass spectra. Under electron impact conditions, (II) generated a weak molecular ion. Although we anticipated that the chemical ionization spectrum of (II) would include an intense $(M+1)^+$ ion at 230°C, its CI spectrum gave a base peak at m/z 97 with the second largest peak at m/z 115 and almost no protonated molecular ions. Smaller intensities were observed at m/z 114. These results suggested the rearrangement mechanism indicated in Figure 1.

To characterize this rearrangement we investigated the intensities of the ions in the chemical ionization mass spectra over the temperature range of 156°C to 235°C. The relative intensities of the protonated molecular ion and the fragment ions exhibited a strong temperature dependence. The observed temperature effect could be explained in terms of the thermal stability of the semicarbazone or in terms of a temperature dependent rearrangement and fragmentation mechanism of the type illustrated in Figure 1.

The temperature stability of this and other semicarbazones was investigated by thermogravimetric and differential thermal analyses. These data indicated that (II) melts at 70°C and vaporizes at 180°C without decomposition. A comparison of mass spectral data with TGA data resulted in no correlation between the endothermic processes indicated by the DTA data and features of the mass spectra. We therefore conclude that the major temperature effects observed in the chemical ionization mass spectra result from the temperature dependent fragmentation of the protonated molecular ion.

Further kinetic analysis of the data provides evidence for two temperature dependent mechanisms. A plot of the fraction of total ionization present as the molecular ion as a function of reciprocal absolute temperature is shown in Figure 2. Intersection of the two straight line portions of this semi-log plot at a temperature of 210°C suggests a transition from a mechanism dominated by an "activation energy" of 9 Kcal/mole in the low temperature regime to a higher activation energy process of about 35 Kcal/mole. Alternatively, we

identify the lower activation energy process as the overall activation energy for the fragmentation mechanism of Figure 1. It is plausible that the higher temperature decomposition process dominated by the generation of m/z 115 represents the thermal decomposition of the semicarbazone to regenerate (I). We therefore suggest that the low intensity of the quasi molecular ion of semicarbazones and chemical ionization mass spectra results from both a temperature dependent fragmentation process of the quasi molecular ion and thermal decomposition of the neutral, depending upon the temperature range in which the experiments are carried out.

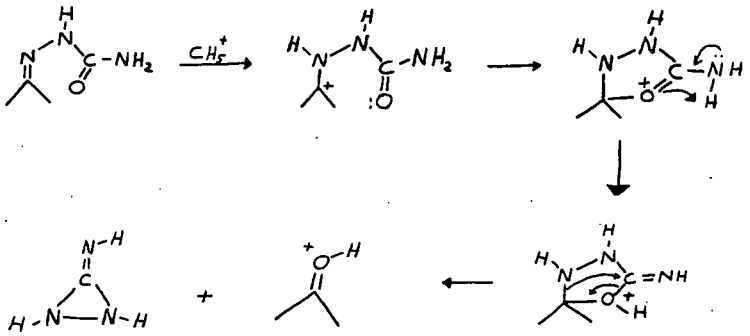

Figure 1. Postulated CI rearrangement mechanism for semicarbazone.

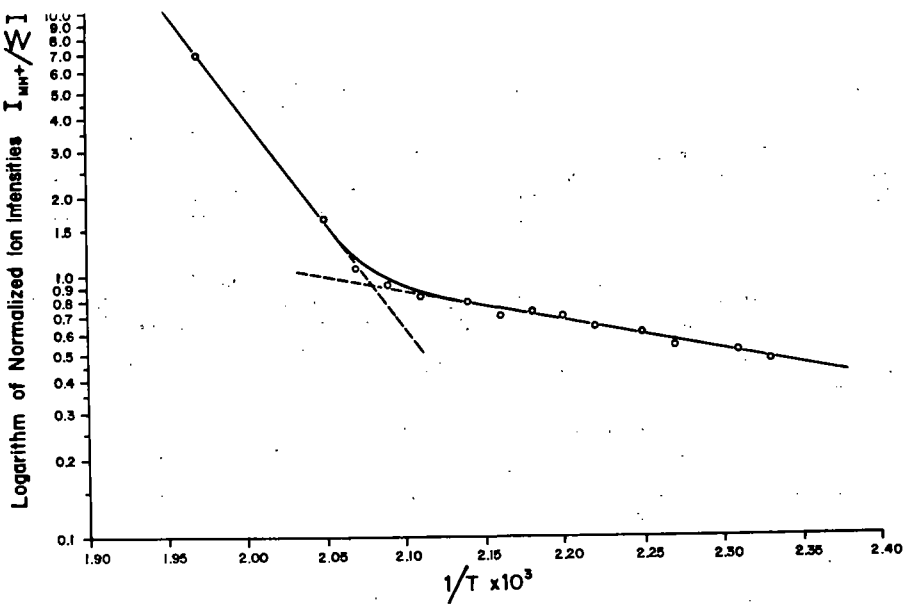

Figure 2. Semilogarithmic plot of normalized ion intensities. Activation energies of 9 and 35 Kcal/mole may be deduced for low and high temperature regions, respectively.

FAMOA3 T JUMP TYPE EXPERIMENTS WITH A CI SOURCE,

T.F. MAGNERA, J. SUNNER and P. KEBARLE, Dept. of Chemistry, University of Alberta, Edmonton, Canada T6G 2G2

T-jump type relaxation experiments have been performed with a mass spectrometer fitted with a CI source. The normal field free condition of the source is interrupted by a short pulse of high frequency voltage applied to the source repeller. If the source pressure is sufficiently high (a few torr), the oscillating field increases the translational energy of the ions without causing a significant increase of ion wall current i.e. loss of ion detection sensitivity. Ion molecule reactions which have reached equilibrium are generally sensitive to changes of the translational ion temperature. Therefore they become displaced from equilibrium by the application of the field. The maximum displacement depends on the field strength, the frequency and the relaxation time (ν forward + ν reverse, where ν = rate constant). Displacements greater than several % were observed and the relaxation time was determined for the association equilibrium: Cl^- +DMSO= Cl^-(DMSO). Total pressure ~3 torr (CH_4), field grequency 750 k Hz field strength ~60 Volt/cm. The oscillating field can be useful in tracing the origin of unidentified ions. For example unidentified ions resulting from an association reaction of an ion with trace amounts of an unknown impurity, will have long relaxation times because of the low concentration of the impurity. The determined relaxation times can be also used for the evaluation of equilibrium constants.

AN INVESTIGATION OF STANDARD COMPOUNDS FOR EVALUATING INSTRUMENT PERFORMANCE IN POSITIVE ION AND NEGATIVE ION CHEMICAL IONIZATION MASS SPECTROMETRY

Steven J. Stout, M. O. Poeppel, S. J. Cardaciotto, W. G. Millen

American Cyanamid Company, Agricultural Research Division, P. O. Box 400, Princeton, New Jersey 08540

Decafluorotriphenylphosphine has been shown to be a useful compound for checking the overall performance of GC-MS systems in the electron impact (EI) mode of operation [1]. This paper reports the results obtained on several compounds evaluated for their utility in checking mass spectrometric performance in the chemical ionization (CI) mode of operation. The ideal compound should be capable of being admitted to the ion source from both the solid probe inlet and the gas chromatographic inlet, should respond in both positive ion (PI) and negative ion (NI) modes, should have as high a molecular weight as possible (preferably >400), should generate an abundant ion indicative of the molecular weight and several significant fragment ions covering a wide mass range in PICI(CH_4), and should generate less fragmentation in PICI with less exothermic reagent gases.

Following an evaluation which included such compounds as benzophenone, decafluorotriphenylphosphine, octacosane (n-$C_{28}H_{58}$), triacontane (n-$C_{30}H_{62}$), and methyl stearate, lauryl laurate (MW = 368) was found to satisfy best the criteria for the ideal compound. This compound also offered the best compromise between a compound of low enough molecular weight to go through the GC and of high enough molecular weight to evaluate mass spectrometric performance to about m/z 400.

As shown in Figure 1, PICI (CH_4) of lauryl laurate generates $(M+H)^+$ and $(M-H)^+$ ions of about 20% relative intensity in the molecular weight region. There are also alkyl adduct ions at $(M+29)^+$ and $(M+41)^+$. The base peak is the protonated carboxylic acid at m/z 201^+. There are also significant fragment ions at m/z 183^+ ($C_{11}H_{23}CO^+$) and m/z 167^+ ($C_{12}H_{23}^+$). The alkyl fragment ions in the low mass region (m/z 60-120) facilitate evaluation of the low mass end. However, there are, unfortunately, more alkyl fragment ions in this region than would be necessary for the evaluation.

Figure 2 shows the mass spectrum of lauryl laurate generated by GC-NICI (CH_4). The predominant ion in the spectrum is the $(M-H)^-$ ion at m/z 367^-. The fragment ion of about 10% relative intensity at m/z 199^- corresponds to the carboxylate anion of the ester. Since the intensity of the m/z 367^- ion has been found to be about equal in intensity to the m/z 201^+ ion, the PICI and NICI modes of operation can be checked simultaneously and their performances compared.

As expected on going to the less exothermic reagent gas, isobutane, the fragmentation in PICI is markedly reduced. The $(M+H)^+$ ion is the base peak. The m/z 201^+ ion is reduced to about 30% relative intensity. The $(M-H)^+$ ion and the low mass alkyl fragment ions are essentially eliminated. There are also fragment ions at m/z 185^+, 183^+ and 169^+. The NICI (isobutane) spectrum is unchanged from that of NICI (CH_4), and the intensity of the m/z 367^- ion is about equal to that of the m/z 369^+ ion.

Lauryl laurate shows no fragmentation in PICI (NH_3). Only the $(M+H)^+$ and $(M+NH_4)^+$ ions are generated.

Lauryl laurate volatilizes from the solid probe at 100° - 120°C and has been found to elute satisfactorily from silicon polymer liquid phases containing some combination of the more commonly used functional groups. In fact, the retention behavior of lauryl laurate appears to be almost independent of the polarity of the liquid phase as might be expected on the basis of its extensive hydrocarbon character.

In conclusion, while perhaps not the ideal compound, lauryl laurate has proven to be a useful compound for checking mass spectrometric performance in both the PICI and NICI modes from either the solid probe or the gas chromatograph.

(1) J. W. Eichelberger, L. E. Harris, W. L. Budde, Anal. Chem., 47, 995 (1975).

FIGURE 1

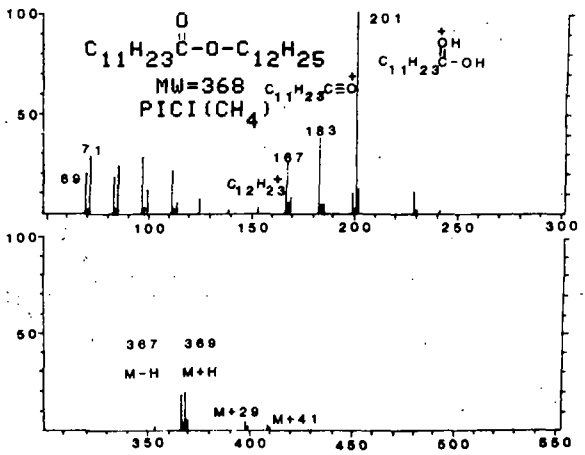

FIGURE 2

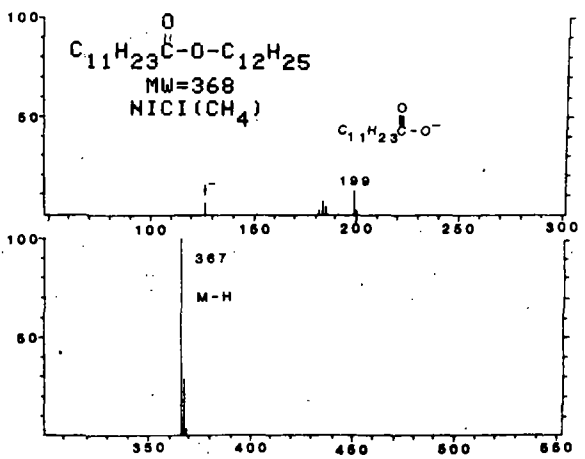

REAL-TIME TRACE ANALYSIS BY ATMOSPHERIC PRESSURE CHEMICAL IONIZATION: TRACE COMPOUND IDENTIFICATION BY HIGHLY SELECTIVE CHEMICAL IONIZATION, W.R. DAVIDSON AND S. NACSON, SCIEX INC., 55 Glencameron Road, Unit 202, Thornhill, Ontario, Canada, L3T-1P2

Atmospheric pressure chemical ionization mass spectrometry (APCI/MS) is a versatile analytical tool which allows the instantaneous or real-time detection of trace compounds in a complex chemical matrix. To unambiguously identify molecular or pseudo-molecular ions in real-time requires the addition of various techniques which can provide supplementary information about these ions. Such techniques are:

a) Class separation by selective chemical ionization.
b) Controlled molecular ion fragmentation.
c) Isotope ratio information.
d) Positive ion/negative ion response comparisons.
e) Context (useful in targeted compound analysis).

This paper describes some recent developments in the first of these techniques, i.e. selective chemical ionization, studied on the TAGA™ 3000 APCI/MS system.

In the positive ion mode of operation, the major reactant ions in APCI are the proton hydrates, $H_3O^+(H_2O)_n$. These ions react with trace neutrals, T, mainly through proton transfer reactions in which a proton or a proton and some water molecules are transferred:

$$H_3O^+(H_2O)_n + T \longrightarrow TH^+ + (n+1)H_2O \quad (1)$$
$$H_3O^+(H_2O)_n + T \longrightarrow TH^+(H_2O)_m + (1+n-m)H_2O \quad (2)$$

This type of reaction can be quite unselective in that any neutral with an "effective" proton affinity greater than water will be ionized. For example, both diethyl ether and dimethylnitrosamine form MH^+ ions at mass 75 under normal atmospheric pressure chemical ionization conditions. However, the addition of ammonia to the ambient air carrier gas stream preferentially ionizes the nitrosamine rather than the ether since the proton affinity of diethyl ether is lower than ammonia (Figure 1).

A charge transfer reagent, such as benzene, may be added to the carrier gas to create reactant ions which will undergo charge transfer reactions with specific trace neutrals.

$$C_6H_6^+ + T \longrightarrow T^+ + C_6H_6 \quad (3)$$

It should be noted that under APCI conditions benzene does not protonate, i.e. reaction (2) is endothermic, even though its proton affinity is greater than water. This methodology has been applied to polycyclic aromatic hydrocarbons (PAH's) to uniquely identify them from other compounds of the same molecular weights. Addition of a charge transfer reagent can also enhance detection of trace compounds which normally are not detected since they are not protonated by the water clusters; for example, polychlorinated biphenyls (PCBs).

In the negative ion mode of operation, O_2^- and its water clusters are the main reactant ions. These ions react with traces through proton transfer, reaction (4); charge transfer, reaction (5); and dissociative charge transfer, reaction (6).

$$O_2^- + T \longrightarrow (T-H)^- + HO_2 \quad (4)$$

$$O_2^- + T \longrightarrow T^- + HO_2 \quad (5)$$

$$O_2^- + T \longrightarrow X^- + Y + O_2 \quad (6)$$

Reactions (4) and (5) are much more specific than their counterparts in the positive mode since only a few classes of compounds have acidities greater than HO_2 or electron affinities greater than O_2. However, a chemical ionization reagent may be added which creates an ion of lower basicity than O_2^- or an ion corresponding to a neutral of lower electron affinity than O_2. A good example is the chloride anion formed from chloroform, which abstracts protons from only very acidic compounds, such as some substituted carboxylic acids and phenols, and inorganic acids such as nitric and sulfuric acid.

When a corona discharge is used to initialize ionization in an APCI source, a series of odd oxygen containing ions are formed as additional reactant ions (O_3^-, NO_3^-, CO_3^-, HCO_3^- and their water clusters). The ozone anion undergoes a highly

specific addition reaction with aldehydes as opposed to other compounds with the molecular formula $C_nH_{2n}O$ (Figure 2). Thus, even though ethylene oxide and acetaldehyde produce positive ions at mass 45, only acetaldehyde produces the ozone adduct in the negative mode.

The chloride anion may be used as a reactant ion, again with the addition of chloroform to the carrier gas stream, to form highly selective chloride adducts with acids of comparable strength to HCl. Adducts of Cl^- with compounds of much lower or much higher acidities tend to fall apart in the inert gas membrane, which separates the source region from the high vacuum region in the TAGA™ system. Chloride attachment is of particular importance when monitoring for an acid such as HONO which normally forms NO_2^-, an anion also formed from NO_2^-. The Cl^-(HONO) adduct is a highly specific indicator of nitrous acid, whereas NO_2^- is not. Other anions behave in similar ways and may be used individually to cover the complete acidity scale, for example F^-, Br^-, NO_3^- and so on. Chloride attachment can also be used to enhance sensitivity for compounds such as nitroglycerine which forms an extremely stable complex with Cl^- due to its five acidic protons.

1) D.A. Lane, T. Sakuma and E.S.K. Quan, "Real-Time Analysis of Gas Phase Polycyclic Aromatic Hydrocarbons Using a Mobile Atmospheric Pressure Chemical Ionization Mass Spectrometer System", 4th International Symposium on Polynuclear Aromatic Hydrocarbons. Columbus, Ohio, October, 1979.

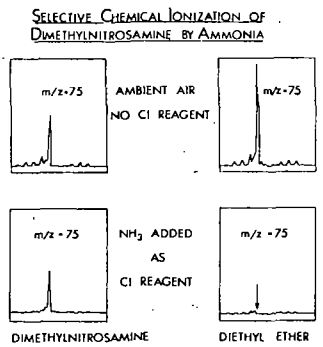

Figure 1

SELECTIVE IONIZATION of ALDEHYDES by "OZONE" ADDITION REACTIONS

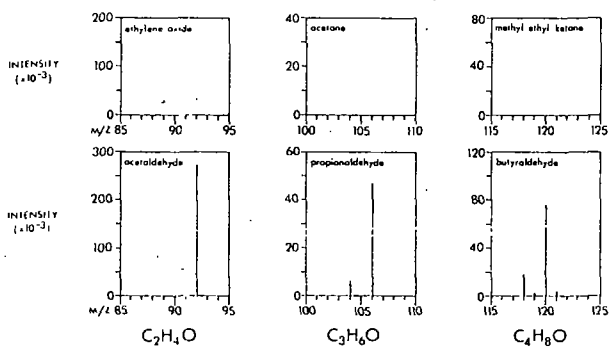

Figure 2

THE LOCATION OF OLEFINIC BONDS IN MONO- AND DI-UNSATURATED COMPOUNDS

Roger J. Greathead and Keith R. Jennings

Department of Chemistry and Molecular Sciences,
University of Warwick, Coventry, CV4 7AL, U.K.

Despite the success of electron impact mass spectrometry in yielding structural information on many classes of compounds, it rarely allows one to differentiate between isomeric compounds such as mono-olefins or di-olefins. The molecular ions of such compounds isomerise to a common structure or mixture of structures, thereby giving rise to very similar fragmentation patterns. A more promising approach is provided by chemical ionisation in which vinyl methyl ether (VME) is used as a reagent gas to yield molecular ions which react specifically with an olefinic molecule to yield products which vary with the position of the double bond[1,2]. A VME molecular ion is considered to add across the olefinic bond to yield a substituted methoxycyclobutane ion as a reaction complex which dissociates by one of several competing reaction pathways (loss of $CH_3\cdot$, CH_3OH or an olefin), the last of which gives ionic products indicative of the position of the olefinic bond in the original molecule.

The early work suffered from the fact that VME molecular ions react with VME molecules to yield numerous product ions which both reduce the sensitivity of the method and mask peaks of possible interest at the lower end of the mass spectrum. A slight improvement was obtained[1] by using a 9:1 mixture of CO_2 and VME but more recently[3], much improved results have been obtained using a 75:20:5 mixture of N_2, CS_2 and VME, in which VME molecular ions are produced primarily by charge-transfer from $CS_2^{+\cdot}$ ions. This mixture has been used in an MS1073 (Kratos Scientific Instruments Ltd.) instrument equipped with a dual purpose electron-impact/chemical ionisation source to investigate reactions between VME molecular ions and octenes and octadienes introduced by means of a reservoir probe fitted with a manual leak valve.

The VME molecular ion reacts with octenes to give a reaction complex of m/z = 170 but this is not observed; in each case, however, peaks are observed at m/z = 155 and 138 due to the loss of $CH_3\cdot$ and CH_3OH respectively from the reaction complex. The main products given by the octenes were those in which an olefin was eliminated from the reaction complex yielding ions containing the methoxy group. Thus 1-octene eliminates C_2H_4 to give the m/z = 142 ion only; the alternative elimination of 1-octene cannot be detected since it would lead to products indistinguishable from the starting materials. However, both 2-octene and 3-octene give two products of this type at m/z = 72 and 128 and m/z = 86 and 114, respectively, arising from the elimination of an olefin from each of the two possible reaction complexes given by the octene. For each octene, the peak given by the higher mass ion is the more intense, indicating the preferential loss of the smaller olefin. In the case of 4-octene, the two possible reaction complexes are identical and the elimination of 1-pentene from the reaction complex yields a product of m/z = 100. Hence the four linear mono-octenes can readily be distinguished by these reactions.

In its reaction with the conjugated species, 1,3-octadiene, the peak at m/z = 138, arising from the loss of CH_3OH from the reaction complex, was the sole product, consistent with an earlier study of its reaction with 1,3-butadiene[4]. The reaction with the unconjugated 1,7-octadiene gives peaks at m/z = 153 and 136 due to the loss of $CH_3\cdot$ and CH_3OH by the reaction complex, together with a single peak at m/z = 140 due to the elimination of C_2H_4 from a reaction complex formed by reaction at either of the olefinic bonds. The absence of any other peaks of this type is sufficient to locate the positions of both olefinic bonds.

The symmetrical, unconjugated 2,6-octadiene gives peaks at m/z = 72 and 126 arising from the loss of 1,5-heptadiene and propene respectively from the two possible collision complexes. These peaks, together with the absence of other peaks arising from olefin elimination, are sufficient to determine the positions of both double bonds. The unsymmetrical, unconjugated 1,4-octadiene gives a more complicated spectrum owing to its lack of symmetry. A peak at m/z = 140 arises from the loss of C_2H_4 from the reaction complex formed by reaction at the terminal olefinic bond and peaks at m/z = 98 and 100 arise from the losses of 1-pentene and 1,5-pentadiene respectively from the reaction complex formed by reaction at the olefinic bond in the 4-position. Again, these observations are sufficient to indicate unequivocally the positions of the two double-bonds in 1,4-octadiene.

REFERENCES

1. A. J. V. Ferrer-Correia, K. R. Jennings and D. K. Sen Sharma, *Org. Mass Spectrom.*, 11, 867 (1976)

2. A. J. V. Ferrer-Correia, K. R. Jennings, and D. K. Sen Sharma, *Advan. Mass Spectrom.*, 7 (Ed. Daly), 287 (1977)

3. A. G. Harrison (private communication)

4. R. van Doorn, N. M. M. Nibbering, A. J. V. Ferrer-Correia and K. R. Jennings, *Org. Mass Spectrom.*, 13, 729 (1978)

FAMOA7 SIMPLIFIED TECHNIQUE FOR POSITIVE AND NEGATIVE ION ADDUCT CHEMICAL IONIZATION MASS SPECTRA OF MULTIFUNCTIONAL COMPOUNDS OF LOW VOLATILITY

A. K. BOSE, B. PRAMANIK, K. TABEI AND A. D. BATES, Dept. of Chemistry, Stevens Institute of Technology, Hoboken, New Jersey 07030.

Soft ionization techniques with high potential for producing intense pseudomolecular ions in the mass spectra of complex molecules are of great value to biomedical and biosynthetic studies. We describe here a simple technique that permits the recording of both positive and negative ion CI mass spectra of the same sample using a quadrupole mass spectrometer with a single particle multiplier. This multiplier has been modified to detect both positive and negative ions (Smirt et al., 1976).

Our method involves the direct probe insertion of a mixture of the sample with ammonium chloride while using methane or ammonia under about 1 torr pressure as the reagent gas. When the ion source temperature is in the 150-280° range, most multifunctional compounds including polar compounds of negligible volatility produce $(M+NH_4)^+$ and $(M+Cl)^-$ ions which can be recorded in succession by reversing the source and multiplier potential.

Other ammonium salts such as NH_4Br and NH_4SCN generate $(M+Br)^-$ and $(M+SCN)^-$ ions. Such salts when labeled with stable isotopes (^{15}N, ^{2}H, ^{13}C) produce characteristic changes in the mass of ions observed.

The fragment ions observed in some cases are different from the major ions found in EI spectra. This difference in the case of penicillin is due to chemical reactivity of a substituted ketene, a known penicillin fragment, toward ammonia. One major advantage of the method described here is that salts (such as the potassium salt of penicillin G) can be used directly: the spectra correspond to the free acid (or the free base in the case of alkaloid hydrochlorides and similar salts).

Positive and negative ion adduct chemical ionization mass spectra of various steroids, alkaloids, antibiotics, and other biologically interesting compounds have been obtained by this technique.

The most striking results were obtained with curamycins which are oligosaccharide antibiotics of molecular weight of about 1400. Using the technique described here NCIMS of curamycin A was recorded - a number of chloride ion adduct negative ions were detected up to the mass limit of the quadrupole mass filter (approx. 1000 daltons) in our Biospect spectrometer. Since these fragments corresponded to both ends of the molecule, it was possible to deduce the molecular weight of the intact antibiotic. The sequence of sugars was determined from the fragmentation pattern.

The most significant aspect of this NCIMS process is the limited but unique fragmentation pattern produced: only fragments corresponding to cleavage of glycosidic bonds of oligosaccharides are observed. Furthermore, often cleavage of the glycosidic bond by the NCI process parallels the behavior of those bonds toward chemical hydrolysis - thus providing valuable information for planning classical type chemical degradation studies of these multifunctional, complex, molecules. Inspection of this NCI fragmentation allows sequence determination of the oligosaccharides without the extensive chemical work necessary for structure determination by classical methods.

NCI ($NH_4Cl + NH_3$) MS OF CURAMYCIN A

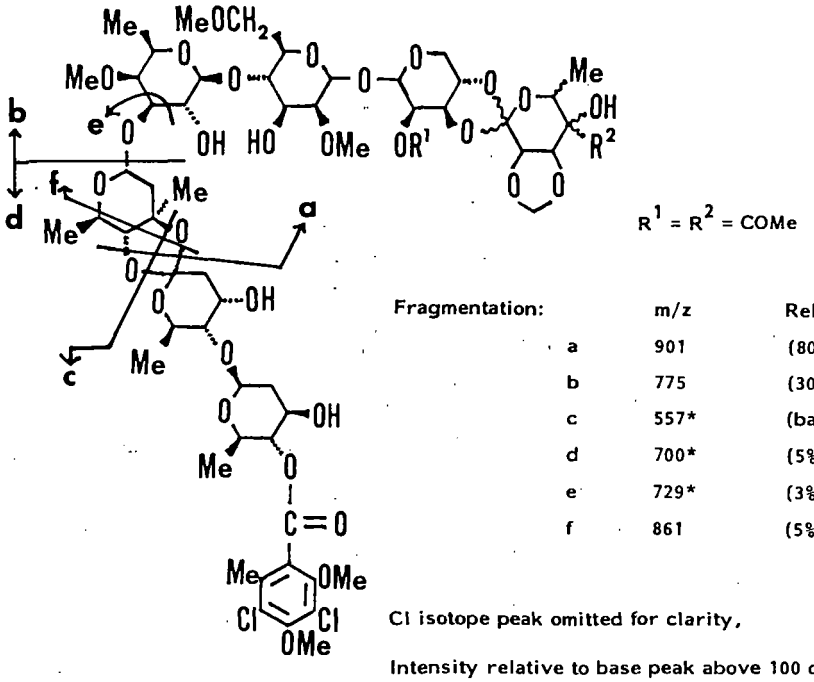

Fragmentation:	m/z	Rel. Int.
a	901	(80%)
b	775	(30%)
c	557*	(base)
d	700*	(5%)
e	729*	(3%)
f	861	(5%)

Cl isotope peak omitted for clarity,

Intensity relative to base peak above 100 dalton.

*Broad Peak (contains the dichlorophenyl moiety).

FAMOA8 NEW CHEMICAL IONIZATION REAGENT IONS: REACTIONS OF Cu^+ WITH ESTERS AND KETONES IN THE GAS PHASE, R. C. BURNIER, G. D. BYRD, and B. S. FREISER, Department of Chemistry, Purdue University, W. Lafayette, IN 47907

The gas-phase ion chemistry of Cu^+, generated by laser ionization from the pure metal plate, with a series of esters and ketones is reported. Dissociative attachment by Cu^+ is observed as a primary pathway for both classes of compounds. Esters are observed to cleave to either carboxylic acids and alkenes or alcohols and ketenes. Ketones are split into either H_2O and dienes or alkenes and smaller ketones. These products undergo secondary reactions in which the parent compound displaces the neutral fragment at the Cu^+ center. Competing reactions observed include CH_3^- abstraction by Cu^+ from ketones and carboxylate abstraction from esters. Mechanisms are proposed which explain the products observed and their distribution. Comparisons are made to the results from a number of related studies. Several limits on bond strengths are obtained from the reactions observed.

Acetal Formation in Polyols and Detection by Mass Spectrometry, R. A. Sanders and R. P. D'Alonzo, Winton Hill Technical Center, The Procter & Gamble Company, 6071 Center Hill Road, Cincinnati, Ohio 45224

Introduction

The reaction of aldehydes with alcohols in the presence of anhydrous acid to form acetals is well known. If the alcohol is a polyol, the resulting acetal may be cyclic. The synthesis of polyglycerol may be accompanied by the formation of 2-propenal (acrolein) in unusual circumstances. Thus, there is potential for producing "bound" acrolein species -- acrolein-polyglycerol acetals such as I. The formation

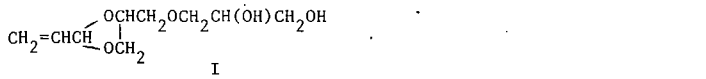

I

of molecules such as I is important, since they prevent accurate determination of total acrolein by methods such as GC headspace. In order to assure the complete removal of any acrolein which might form under unusually harsh conditions, the presence of such acetals must be determined. In this study, direct mixture analysis methods were used to conclusively identify I in a sample of diglycerol which had been spiked with acrolein. In order to avoid possible chemical alterations of the system caused by derivatization required for gas chromatography of these components, samples were introduced to the ion source by direct probe, and accurate mass chemical ionization was used in conjunction with metastable ion scanning to produce definitive spectra. Experiments were also performed to show that acid hydrolysis of the acrolein-spiked diglycerol causes I to decompose, freeing acrolein to be measured in the headspace.

Experimental

Linear diglycerol (G_2) was prepared by molecular distillation of a polyglycerol mixture, and its purity was determined by gas chromatography to be 83%. Most of the impurity was determined (by GC and mass spectrometry) to be linear triglycerol (G_3). The acrolein-spiked G_2 sample was prepared by adding acrolein to produce a 0.5% solution. A portion of the acrolein-spiked G_2 was hydrolyzed with dilute (0.75%) phosphoric acid for 30 minutes at 30°C. Approximately 1 µl of each sample was placed in a glass sample holder for insertion into the ion source. To insure that the water present in the hydrolyzed sample would not effect the sensitivity for the acetal component, a portion of the acrolein-spiked G_2 was diluted with water and analyzed immediately after dilution. The result was similar to that observed in the undiluted, acrolein-spiked sample. All mass spectra were obtained on a Kratos MS-30 with a CI source operated in the dual beam mode at 3000 resolution and 3 s/decade. The reference beam was perfluorokerosene and its electron impact spectrum allowed accurate (to approximately 15 ppm) determination of the masses produced in the chemical ionization source. The protonated G_2 molecular ion (m/z=167.092) was used to assess the mass accuracy and to correct the measured masses of unknown ions. Metastable ion spectra of m/z 167 (protonated G_2) and m/z 205 in the isobutane spectrum were obtained by scanning the magnetic and electric sector fields such that their ratio was constant (B/E constant scan).

Results and Discussion

The isobutane chemical ionization spectra of G_2 and acrolein-spiked G_2 are compared in Figure 1. Note the large increase in intensity of the m/z 205 ion in the acrolein-spiked sample. When ammonia was used, an analogous effect was observed at m/z 222. In Figure 2, ion chromatograms are shown for the m/z 205 ions resulting from isobutane chemical ionization of G_2, acrolein-spiked G_2, and hydrolyzed, acrolein-spiked G_2. These results indicate that a compound of molecular weight 204 amu is formed when G_2 is spiked with acrolein, and that this compound is effectively decomposed by acid hydrolysis. The accurate mass measurement, averaged over four scans across the peak and corrected as described in the previous section, is 205.1085 amu which indicates the molecular formula $C_9H_{17}O_5$ (205.1076) for the protonated molecular ion. This is consistent with structure I. The m/z 205 metastable ion spectrum is shown in Figure 3. Ions at $(M-17)^+$ and $(M-73)^+$ were observed in the protonated G_2 metastable ion spectrum and, thus, are not attributable to the acetal part of the molecule. The most intense metastable ion, $(M-55)^+$, is probably due to elimination of acrolein from the protonated molecular ion. That this ion is characteristic of acrolein acetals was confirmed by obtaining the "normal" isobutane chemical ionization spectrum of pure propylene glycol-acrolein acetal. $(M-55)^+$ was the most intense fragment ion by far.

Conclusions

The simple mixing of acrolein with diglycerol results in the formation of acrolein-diglycerol acetal. The acetal was identified utilizing accurate mass chemical ionization and linked B/E scanning to generate detailed data on a minor component of the mixture. Acid hydrolysis effectively decomposes the acetal freeing acrolein to be measured in the headspace.

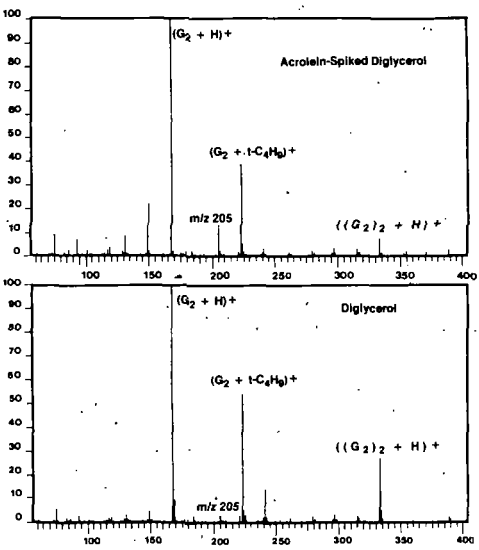

ISOBUTANE CI SPECTRA

Figure 1

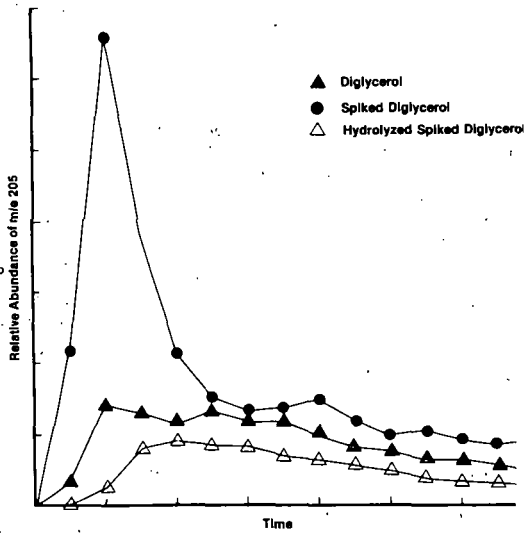

Probe Isobutane CI/MS of Diglycerols Following the m/e 205 (Acrolein Diglycerol Acetal)

Figure 2

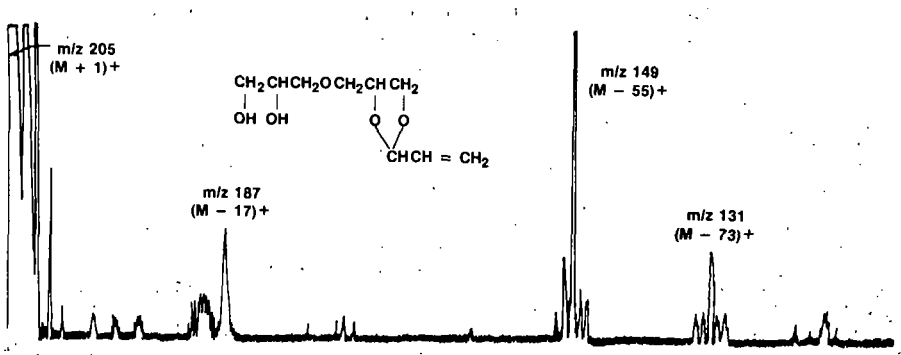

B/E Constant Scan of m/z 205 (Isobutane CI)

Figure 3

FAMOA10 DETECTION OF NEUTRAL PRODUCTS FROM CHEMICAL IONIZATION REACTIONS, CHARLES R. HAUER, JEFFREY M. McGUIRE, and BURNABY MUNSON, Department of Chemistry, University of Delaware, Newark, DE 19711.

The dominant ion in the methane chemical ionization mass spectrum of t-butylbenzene is the t-butyl ion at m/z = 57. This ion is produced in part by dissociative proton transfer from CH_5^+:

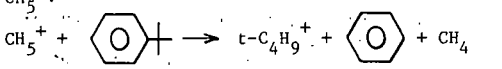

(1)

A very minor ion that is also observed in the CH_4 CI mass spectrum of t-butylbenzene is presumably protonated benzene at m/z = 79. This ion is also produced by dissociative proton transfer from CH_5^+:

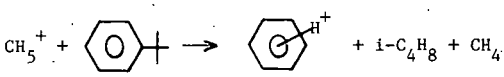

(2)

Efforts were made to detect the neutral benzene molecules that were formed in reaction (1). Modification of our CI source by enlarging the electron entrance allowed the detection of radical products at high electron currents.[1] Experiments with t-butyl benzene indicated a marked increase in the ratio, I_{79}/I_{57}, with increasing electron current: I_{79}/I_{57} = 0.004 with an emission current of 50 μamp and I_{79}/I_{57} = 0.04 with an emission current of 500 μamp. This variation with electron current suggests that the neutral benzene produced in reaction (1) is subsequently reacting with CH_5^+.

[1] C. N. McEwen and M. A. Rudat, J. Am. Chem. Soc., 101, 6470 (1979).

Field-induced ion evaporation mass spectroscopy. B. A. Thomson, J. V. Iribarne and P. Dziedzic, McLennan Physical Laboratories, University of Toronto.

Ions do not normally evaporate from aqueous solutions for energetic reasons. However, when an electrically charged droplet evaporates and its content of nonvolatile solute is low enough, it may reach a stage at which the field at the surface (inversely proportional to the square of the radius) becomes sufficient to produce ion emission. This phenomenon is competitive with that of liquid disruption by Rayleigh instability. In the first case, when ions separate individually from the liquid they do so clustered with water molecules and sometimes with other neutral molecules present in the solution. This process has been developed into a new technique that can be applied to analytical purposes.

The ion source uses a sprayer producing a fine mist. The droplets' electrical charges are enhanced by an induction electrode close to the nozzle. The mist, carried by unsaturated air, passes in front of an orifice (about 25 μm in diameter) leading to the enclosure of a quadrupole mass filter. The ions produced in front of the orifice by evaporation are deflected towards the orifice by a transversal field. The whole ion source is at atmospheric pressure. The ions passing through the mass filter arrive to a detector followed by a pulse counting system. The pulses are sent to a multichannel signal averager swept synchronically with the mass spectrometer, in order to obtain the mass spectrum The ion source is weak; signals at a fixed mass peak are usually in the order of hundreds of counts per second. A spectrum is usually taken in 10-15 minutes.

Monovalent ions present in the solution, both positive and negative, can in most cases be detected by this technique. The total nonvolatile solute must not exceed about 0.1 g/liter. It is essentially a nondestructive technique. Ions evaporate as clusters, and if stable in gas phase, reach an equilibrium distribution over cluster hydrates with different numbers of water molecules and are detected as such. Polyvalent ions do not evaporate. These basic characteristics of the process are in agreement with a previously developed theory. An example of stable ion giving a "clean" spectrum is shown in Fig.1. If the ions are not so stable, they may transfer charge to other molecules in gas phase (such as impurities) or react with them. They may also attach them onto the cluster. See Fig. 2. Certain neutral molecules also evaporate, clustered with ions: see Fig. 3.

The method has been tested with a variety of ionic substances. The following is an enumeration where it is understood that the results were positive (i.e. the tested ions, hydrated or not, could be clearly identified in the spectrum), unless otherwise stated.

POSITIVE IONS. Inorganic: H^+, NH_4^+, alkaline ions, $CaOH^+$. Transition elements (Ag^+, Cu^+, Tl^+) do not evaporate, but $Ag(NH_3)_2^+$ does; except this ion, complex ions were not observed. Tetrasubstituted ammonium: tested with n-alkyls with chains of 1 to 6 carbons and giving strong signals. Aminoacids in acid solution: 3 tested. Alkaloids: 16 tested. Miscellaneous: urea. $HgCH_3^+$ gave no signal.

NEGATIVE IONS. Inorganic: OH^-, halides, HCO_3^-, HSO_3^-, HSO_4^-, NO_3^-, MnO_4^-, $HCrO_4^-$, ClO_3^-, ClO_4^-, CNS^-. Complex ions were not observed. Carboxylic acids gave in general complex spectra, only some with direct identifying signals; this suggests high reactivity in gas phase. Sulfonic acids: 3 tested. Phenols: in a series of nitrophenols with 0, 1, 2, 3 nitro groups, only the last two gave positive result, with strong signals. Sulfonamides: benzenesulfonamide and two sulfanilamides were tested.

NEUTRAL MOLECULES. Glycerol, glucose, methanol, urea, acetanilide, benzophenone and several alkaloids were observed to evaporate clustered with various ions.

Quantitative application is possible by calibrating the ions signal against that of a well known ion added to the solution (two examples are given in Fig. 4), or else following a technique in which unknown and reference solutions are tested in rapid succession while the mass spectrograph is fixed on a significant mass peak. With the latter technique, curves of relative signal intensity as a function of concentration can be obtained; an example is given in Fig. 5.

The relative evaporability of different ions depends of different factors: molecular structure, molecular weight, surface activity and other less obvious specific properties; all of which appear to contribute to evaporability in a complex way. In some cases, inferences about the structure of the evaporated ions can be obtained from the spectra. If two ions are present in concentrations c_1, c_2 in the sprayed solution, the ratio of their signals (as given, for instance, by the sum of their peak heights) follows a relation of the type

$$\Sigma_1 / \Sigma_2 = \alpha \, (c_1^{\gamma_1} / c_2^{\gamma_2})$$

where Σ_1, Σ_2 are the signals and $\alpha, \gamma_1, \gamma_2$ constants depending on the pair of ions. The

constants γ_1 and γ_2 vary within the range 0.5-1.0. When $c_1 = c_2 = c$, Σ_1/Σ_2 may be taken as a measure of the relative evaporability, which is seen to depend in general on c .

The sensitivity of the method with the present instrumentation lies mostly in the range of 0.1-1 μmol/liter. In special cases (strong signals from tetrasubstituted ammonium) it can be as low as 0.001 μmol/liter.

References J.V. Iribarne and B.A. Thomson, J. Chem. Phys. 64, 2287-2294, 1976.
B.A. Thomson and J.V. Iribarne, J. Chem Phys. 71, 4451-4463, 1979.

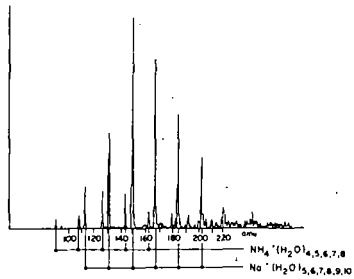

Fig. 1 - Spectrum of positive ions from 10^{-3} M NaCl solution.

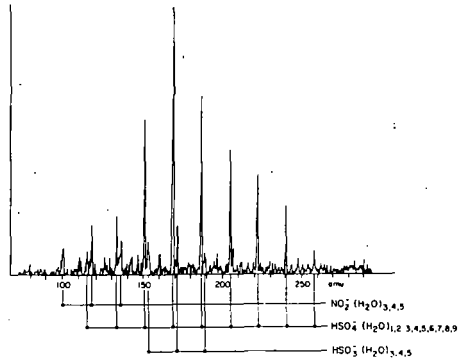

Fig. 2 - Spectrum of negative ions from 10^{-3} M $NaHSO_4$ solution.

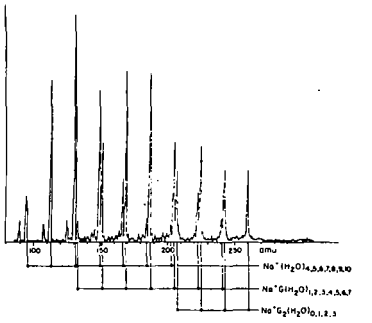

Fig. 3 - Spectrum of positive ions from 10^{-3} M NaBr + 10^{-2} M glycerol (G) .

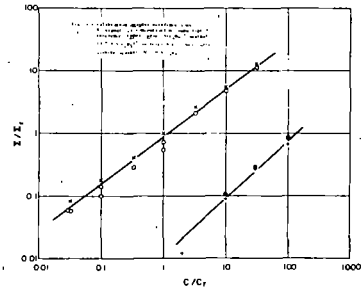

Fig. 4 - Calibration against reference ions. N: signal; c: concentration; subscript r: reference. Upper curve :$N(C_4H_9)^+$ against 10^{-4} M $N(C_2H_5)^+$ as reference. Lower curve: quinine against 10^{-5} M $N(C_4H_9)^+$.

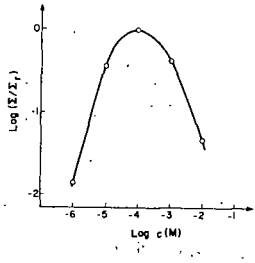

Fig. 5 - Signal vs. concentration. Cocaine. Σ_r = 500 counts/s, at $c_r = 10^{-4}$ M. Σ: counts/s at concentration c.

IONIZATION OF INVOLATILE COMPOUNDS BY FLASH VAPORIZATION OF SOLUTION DROPLETS

E.R. Lory and F.W. McLafferty

Department of Chemistry, Cornell University, Ithaca, New York 14853

A key step in the ionization of solids to obtain mass spectral data is the separation of the molecules from each other prior to or during ionization. For the variety of methods in which such molecular separation is effected thermally, pyrolytic degradation is a major limitation for non-volatile molecules. In the electrospray method of Dole,[1] the sample molecules are first separated by dissolving them in solution. By making the droplets sufficiently small (~100 nm) and the solution sufficiently dilute (~10^{-6} M), most charged droplets contain only one molecule, so their evaporation yields a charged molecular ion. Friedman[2] has recently obtained polystyrene ions of 80,000 daltons with this technique.

For several years we have been trying a similar approach using much more concentrated solutions and larger droplets. If these can be vaporized in a sufficiently short time (<1 μsec), the macromolecules should not reagglomerate, and will be ionized in a CI source using the solvent as the ionizing reagent gas. Sample introduction into a CI source using an LC/MS interface[4] produces a liquid jet of small (10 μm diam.) droplets. We have previously demonstrated that rapid vaporization of these droplets can be accomplished using short (100 nsec) pulses of CO_2 laser radiation,[3] but the low duty cycle and positioning requirements of the available apparatus severely limited this approach.

Here we report tests on systems incorporating two alternative sources of fast energy deposition for solution droplet vaporization. A 45 KV pulsed DC discharge of 5 μsec duration, under CI conditions (1 torr background pressure) vaporizes approximately 100 droplet/pulse. However, tests of this technique on a Finnigan 1015 quadrupole CI mass spectrometer show that the method has major disadvantages. Extensive shielding of the MS electronics was necessary because of the large RF noise pulse accompanying each discharge, seriously reducing sensitivity. Further, the discharge characteristics were very sensitive to pressure and surface charge effects so that it was very difficult to operate under reproducible conditions.

A second flash vaporization system tested employed ion bombardment of the droplets utilizing a 4 KV discharge hollow-cathode ion gun producing a ~2 mA ion beam focused

in a ~1 mm spot in the ion source. Despite cyrogenic auxiliary pumping, the added gas load of the high pressure gun made quadrupole operation marginal. In addition, RF noise was again a problem, and extended ion bombardment seriously degraded ion source parts.

Thus it would appear that the laser approach has very distinct advantages in producing no additional gas load to the pumping system and minimum electrical noise. CO_2 lasers are now available which will produce <1 μsec pulses of 200 mJ energy at a 200 hz rate; this should be sufficient to vaporize ~0.05 ml/min of solution droplets of 50 μm diameter with a laser focal spot large enough to minimize difficulties of positioning the droplet stream.

---

[1] M. Dole, H.L. Cox, Jr. and J. Gieniec, Adv. Chem. Ser., 125, 73 (1971)

[2] L. Friedman, Brookhaven National Laboratory, private communication, September 1979.

[3] E.R. Lory and F.W. McLafferty, Adv. Mass Spectrom., 8, in press.

[4] F.W. McLafferty, R. Knutti, R. Venkataraghavan, P.J. Arpino and B.G. Dawkins, Anal. Chem., 47, 1503-5 (1975).

ELECTRON IONIZATION MASS SPECTRA OF TETRA-ALKYL AMMONIUM HALIDE SALTS OBTAINED BY THE ELECTRON IONIZATION FLASH DESORPTION TECHNIQUE

Terry D. Lee, William R. Anderson, Jr. and G. Doyle Daves, Jr.

Department of Chemistry and Biochemical Sciences
Oregon Graduate Center
Beaverton, Oregon 97006

Electron ionization (EI) mass spectra of tetra-alkyl ammonium halide salts have been recorded using the new technique of EI-flash desorption. These spectra exhibit R_4N^+ ions and fragment ions which characterize the structure of the quaternary ammonium cation and are qualitatively very similar to spectra of these ionic compounds obtained by field desorption mass spectrometry (with collision activation) and other new techniques for mass spectrometry of involatile and thermally unstable molecules.

The mechanism of formation of R_4N^+ ions and/or their separation from neutralizing anions in the mass spectrometer has not been established. Some results of the current study appear pertinent. First, no ionization occurs in the absence of an ionizing electron beam or in the absence of the rapid heating involved in the flash desorption process. Second, R_4N^+ ions are formed in the gas phase by electron ionization of volatile precursors. Third, gas phase formation of quaternary ammonium ions from trialkyl amines and alkyl halides is unimportant; dealkylation to produce alkyl halide and trialkylamine occurs rapidly ($R_3N^{+\cdot}$ ions appear within 10 msec of initiation of sample heating) probably in a condensed phase and the resulting products are quickly separated by volatilization and ionization precluding back reaction to reform quaternary ammonium ions.

These results are consistent with a mechanism for ion formation which involves formation of quaternary ammonium ions from volatile precursors other than trialkyl amine and alkyl halide. The available data do not permit this volatile precursor to be identified with certainty. Two possibilities are considered:

$$R_4N_n^+X_n^- \text{ (s)} \xrightarrow{\Delta} R_4N_n^+X_n^- \text{ (g)} \xrightarrow[\text{electrons}]{70\text{ eV}} R_4N^+ \text{ (g)} \qquad (1)$$

$$R_4N_n^+X_n^- \text{ (s)} \xrightarrow{\Delta} R_4N^{\cdot} \text{ (volatile)} \xrightarrow[\text{electrons}]{70\text{ eV}} R_4N^+ \text{ (g)} \qquad (2)$$

One possibility (eq. 1) is that gaseous R_4N^+ ions arise by fragmentation of gaseous R_4NX molecules i.e., quaternary ammonium halide salts (and/or neutral clusters, $R_4N_n^+X_n^-$) may possess a finite volatility.

Alternatively, formation of gaseous R_4N^+ ions (eq. 2) may involve thermal reduction of solid (or molten) salt to yield neutral R_4N followed by its volatilization and electron impact ionization. This general mechanism appears well established in the case of EI mass spectrometry of aryl ammonium salts where the readily reduced aryl moiety is available to accept an electron (or two). Aryl ammonium salts, e.g., alkylpyridinium salts, yield EI mass spectra which exhibit ions corresponding to the masses of the respective ammonium cations. Such ions are known to arise by a complex process which involves initial thermal reduction (one or two electron) of the arylammonium cation to produce volatile free radical and/or dihydro derivatives which, upon electron ionization (free radical) or electron ionization and subsequent fragmentation (dihydro derivative) yield ions characteristic of the mass of the original aryl ammonium cation.

DIRECT EXPOSURE CHEMICAL IONIZATION MASS SPECTROMETRY OF EXPLOSIVES

JEHUDA YINON

Department of Isotope Research, The Weizmann Institute of Science, Rehovot, Israel.

The analysis of explosives presents severe difficulties because of the thermal instability of most of these compounds and the low volatility of some of them. Much effort has been invested in finding a mass spectrometric method in which explosives could be analysed at the lowest possible temperature and in which mass spectra with highly abundant molecular ions could be obtained.

Chemical ionization (CI) has made mass spectrometry an important and widely used tool for the analysis of explosives (1). CI mass spectra having an MH^+ ion base peak are obtained mainly for nitroaromatic compounds, while the CI mass spectra of nitric esters and nitroamines contain abundant fragment ions and usually a low abundant MH^+ ion or none at all. Almost all the CI mass spectra were obtained at source temperatures above 100°C causing in many cases thermal decomposition prior to ionization.

In an effort to find a method for obtaining CI mass spectra at source temperatures below 100°C, direct exposure chemical ionization mass spectrometry has been investigated for the analysis of explosives.

The essence of the direct CI technique (2-4) is to bring the sample, by an extension of the probe tip, into the ion plasma of the CI source.

Direct exposure CI mass spectra, with isobutane as reagent, were obtained with a Varian MAT CH7 mass spectrometer modified for CI operation. The probe tip made of Vespel, makes an angle of 90° with the electron beam and is about 1 mm from its center. The sample was deposited on the tip by dipping the tip in a solution containing the sample and allowing the solvent to evaporate.

The sample, after introduction into the source, is heated by the reagent gas, which is heated by the source. The source is heated only by the filament. As our ion source is not a cooled source, in order to study mass spectra of explosives below 100°C, samples were analysed during heat-up of the source by the filament. Analysed explosives included TNT, Tetryl, Nitroglycerin, PETN, RDX and HMX. Mass spectra were recorded at source temperatures of 50°-100°C.

Figures 1, 2, 3 and 4 show the direct exposure CI mass spectra of Nitroglycerin (NG), PETN, RDX and Tetryl.

An MH^+ of NG appeared already at 35°C.

Variations in the CI mass spectra were found to occur at different temperatures and reagent gas pressures. This is a problem for quantitative work, which can be overcome by working at predetermined conditions. A cooled ion source would facilitate the analysis of explosives by working at a fixed temperature.

Feferences

1. J. Yinon, Critical Rev. Anal. Chem. 7, 1 (1977).
2. M.A. Baldwin and F.W. McLafferty, Org. Mass Specct. 7, 1353 (1973).
3. G. Hansen and B. Munsen, Anal. Chem. 50, 1130 (1978).
4. R.J. Cotter, Anal. Chem. 51, 317 (1979).

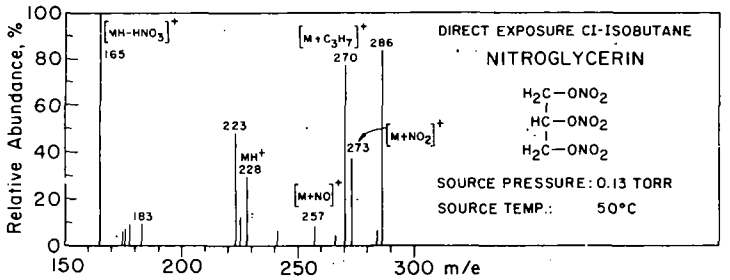

Figure 1.

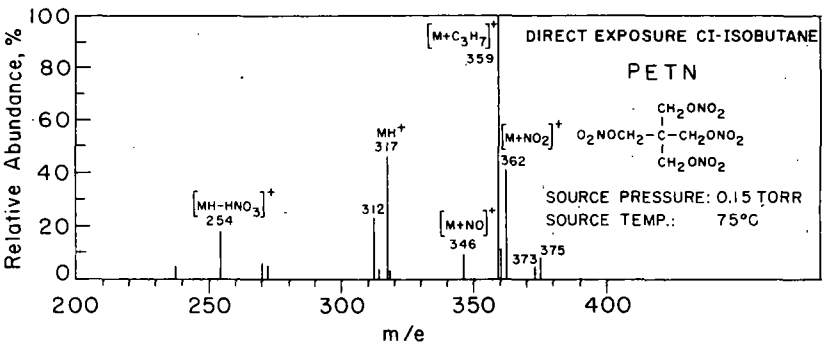

Figure 2.

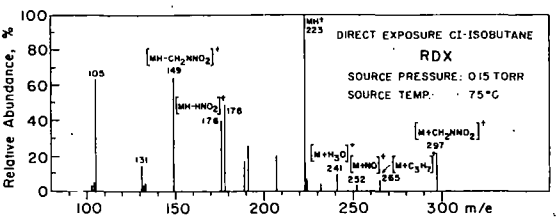

Figure 3.

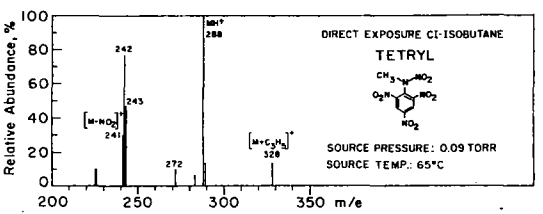

Figure 4.

MASS SPECTRA OF LESS VOLATILE COMPOUNDS BY LIQUID SURFACE IONIZATION AT ATMOSPHERIC PRESSURE

M.TSUCHIYA, K.SEITA and T.TAIRA
Faculty of Engineering, The University of Tokyo
Hongo, Bunkyo-ku, Tokyo, Japan 113

We have developed a new method for the ionization of organic compounds as liquids or in solution under atmospheric pressure. Mass spectra of less and non volatile compounds such as amino acids and synthetic compounds were measured by this method using a modified quadrupole mass spectrometer with the new ion source described in previous papers[1,2].

Amino acids As these compounds do not give any ions at room temperature, it is necessary to heat the sample for obtaining their mass spectrum. Figure 1 shows the effect of temperature, that is the relation between the abundance of the MH^+ ions of leucine and the heating current of a sample holder (Fig.2) in which a nichromewire is installed. The temperature of a sample estimated from the measurement using a thermocouple is about 100°C and 130°C at the heating current of 0.6 A and 0.9 A, respectively. No ion was observed at 0.5 A. Most of amino acids gave the MH^+ ion (the base peak), the M_2H^+ ions and some fragment ions at 0.8 - 0.9 A. An aliquot (1 - 5 µl) of about 1 % aqueous solution deposited on the sample holder was used for amino acids and peptides.

As an example, mass spectra of glutamic acid measured by this method (LI) are shown in Fig.s 3a and 3b compared with those of EI and in beam CI (Fig.3c and 3d). The M^+ ions can not be observed by EI and only a small MH^+ peak at m/z 148 is observed even by CI. The m/z 84 peak is sometimes larger than that shown in Fig.3d. The FD spectrum shows the MH^+ ions with no fragment ion. In contrast, this method (LI) gives the MH^+ ions as the base peak when the potential of the pinhole is kept at 20 V (Fig.3a), and the main fragment ions observed at the pinhole potential of 100 V are similar to those of EI, such as m/z 84 ($MH^+ - H_2O - HCOOH$), m/z 56 ($CH_2{=}CH{-}CH{=}NH_2^+$), m/z 41 ($C_3H_5^+$) and m/z 28 ($CH{\equiv}NH^+$). M_2H^+ ions were also observed for most of amino acids and di-peptides measured at 20 V. Thus it is easy to determine the molecular weight of the compound. The reason of resemblance in LI and EI is probably because of the stability of mass 84 ions. In the case of EI, the mass 84 ions must be produced by the elimination of H_2O and COOH from the M^+ ions.

Oligomer An unknown compound synthesized by the reaction between acetophenone and benzaldehyde with catalyst was measured by this method. The compound is white crystal, decomposed at about 260°C. An aliquot of 1 % solution in acetone was used and heated up to about 100°C. The mass spectrum shown in Fig.4a suggested that the mass 537 ions, mass 519 ions and mass 105 ions might correspond to MH^+, $MH^+ - H_2O$ and $C_6H_5CO^+$, respectively. From such information with its ^{1}H-NMR spectrum, the structure shown in the top of Fig.4 was predicted and the LI mass spectrum measured at the pinhole potential of 40 V (Fig.4b), namely the peaks at m/z 417, 329 and 209, corresponds very well to the structure of the compound. At 100 V the m/z 105 peak becomes to be the base peak. The FD spectrum (Fig.4d) also indicates that the molecular weight may be 536 and the peak at m/z 518 may correspond to the $M^+ - H_2O$ ions. The estimated structure agreed with the result of its X-ray diffraction analysis. The mass 745 ions which has been the largest ions ever measured by this instrument, may be the fragment ions ($MH^+ + 208$) of the M_2H^+ ions. Because many compounds gave their M_2H^+ ions which sometimes are more abundant than MH^+ ions (e.g., glycilglycine).

Ionization mechanism Ionization reaction mechanism is now clearer than before. That is; the reaction (1) to (4) may occur in the carrier gas, resulting cluster ions of water. The value k ranges from 2 to 5 and the most abundant ion is $(H_2O)_4H^+$ in the gas phase. Therefore $(H_2O)_kH^+$ ions are the reactant ions for chemical ionization in this method. At the liquid surface, reactions (5) and (6) may occur to produce MH^+ and M_mH^+ ions. If solvent (S)

was not used, $(H_2O)_kH^+$ ions act as SH^+ in the reaction (6).

$$Ar \xrightarrow{\text{Corona discharge}} Ar^+ + e \quad -- (1), \quad Ar^+ + H_2O \longrightarrow H_2O^+ + Ar \quad --(2)$$

$$H_2O^+ + H_2O \longrightarrow H_3O^+ + OH \quad ---(3); \quad (H_2O)_{k-1}H^+ + H_2O + Ar \longrightarrow (H_2O)_kH^+ + Ar \quad ---(4),$$

$$(H_2O)_kH^+ + S \longrightarrow SH^+ + k\,H_2O \quad --- (5)$$

$$SH^+ + n\,M \longrightarrow M_mH^+ + (n-m)M + S \quad --- (6) \qquad (m = 1, 2, --- n)$$

M_mH^+ ions are observed at low pinhole potential (5 - 20 V). At a little high pinhole potential, LI mass spectrum is similar to that of CI, especially that of drift tube CI spectrum[3]. Therefore the fragment ions are produced by a kind of collision induced dissociation. At high pinhole potential (60 - 100 V or higher), LI spectrum become similar to EI spectrum. Therefore LI mass spectrum gives as useful information as all of EI, CI and FD mass spectra do. This method is also useful for LC-MS combination.

1) M.Tsuchiya and T.Taira, Int. J. Mass Spectrom. Ion Phys., 34, 351 (1980)
2) M.Tsuchiya and T.Taira, 27th Ann. Conf. on Mass Spectrometry and Allied Topics, Seattle (1979) pp.94 and pp.320
3) P.C.Price, H.S.Swofford,Jr. and S.E.Buttrill,Jr., Anal. Chem.,50,1127 (1978)

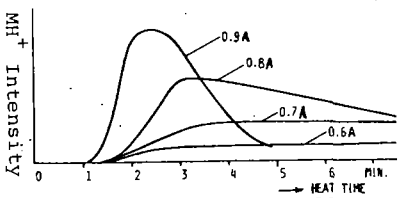

Fig.1 Temperature effect

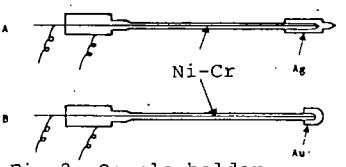

Fig.2 Sample holder

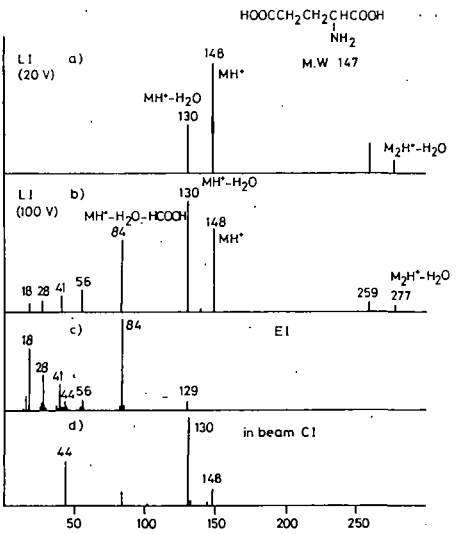

Fig.3 Mass spectra of glutamic acid

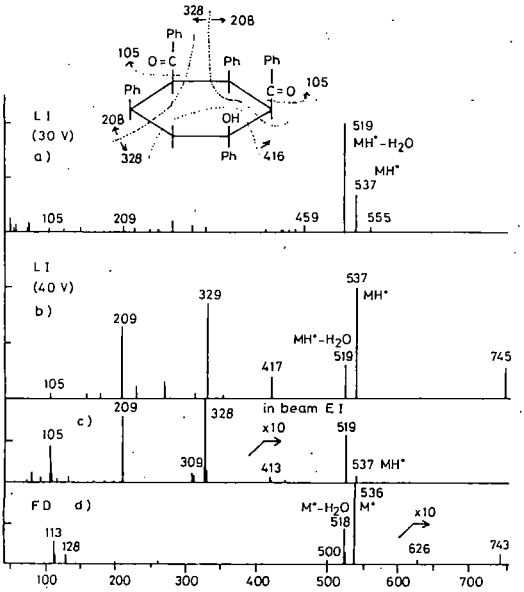

Fig.4 Mass spectra of oligomer

FAMOB6 Field Assisted Charge Transfer Mechanisms in Thermally Generated Reaction Zones on Field Emitters.

R. Olinger, J. Dye, and J. Holland, Biochemistry and Chemistry Depts., Michigan State University, East Lansing, Mi. 48824

The role of field in field ionization techniques has been shown to be essentially twofold: ion collection and ion generation. One of the major ion generation mechanisns involves field assisted charge transfer (FACT) between neutral species as they desorb from the emitter surface. The effects of the dielectic constant, the concentration of the sample, the presence of electron acceptors or doners, and the general influence of the matrix environment on the emitter have been calculated and are the subject of experimental confirmation. Known amounts of a series of compounds producing ions of the type M^+ and MH^+ have been analyzed with sample matrices of varying composition. Correlations between predicted FACT behavior and experimental results confirm the validity of this mechanism in ion formation.

LASER DESORPTION MASS SPECTROMETRY OF ORGANIC MOLECULES

P.G. Kistemaker, G.J.Q. van der Peyl, A.J.H. Boerboom and J. Haverkamp
FOM-Institute for Atomic and Molecular Physics,
Kruislaan 407, 1098 SJ Amsterdam, The Netherlands

Despite the violent perturbations induced in organic sample layers by laser irradiation, quasi-molecular ions of type $M+H^+$, $M+Na^+$, $M+K^+$ and $M-H^-$ are formed and can escape from the irradiated region with a relatively low degree of fragmentation. After the first observation of this phenomenon, various articles have been published, wherein exciting experimental results have been reported on the analysis of model compounds for oligosaccharides, nucleotides and oligopeptides. Moreover, phorphyrins, vitamins, antibiotics and quaternary ammonium salts have been analyzed [1-9]. Lasers of different wavelength, pulse time and energy output have been used with more or less success. From the experimental data, however, it is hard to select the optimal system for laser desorption mass spectrometry. Furthermore, the understanding of the fundamental chemical and physical mechanisms underlying the desorption and ionization processes is quite limited. Consequently, a systematic study concerning the experimental parameters in laser desorption is required.

In this report some qualitative results and interpretations concerning the influence of laser wavelength, laser intensity, laser pulse time and the substrate material will be given. It has to be noted that these results cannot be generalized for the following reasons:

- Independent variation of one laser parameter is hard to achieve and most results are obtained by a simultaneous change of various parameters. The individual contributions of the variables involved cannot be resolved uniquely.
- Most of the results are obtained with one sample compound. Although it has been shown that the data are representative for biochemically related samples, different results have been obtained for non-related compounds.

Next, we summarize some results obtained for the disaccharide sucrose, chosen as a oligosaccharide model compound.

Laser wavelength: A wavelength dependent response of the desorption and fragmentation processes can be expected at strong absorption lines of the sample and substrate material. However, the data available are obtained at single wavelengths and accurately scanning of the laser wavelength over the absorption bands has not been performed. For thick sample layers (>100 µm) direct absorption by the sample dominates [9], whereas for thin sample layers ($<10^{-1}$ µm) it has been found that absorption by the substrate material is an important process [8].

Laser intensity: Desorption of quasi-molecular ions has been observed with lasers radiating at quite different intensity levels. For oligosaccharides desorption of alkali-ion cationized molecules has been observed with CO_2 lasers radiating with intensities as low as 30 W/cm^2 and also with intensities up to 10^8 W/cm^2. From these experiments it can be concluded that, at least for oligosaccharides, the laser intensity is not a crucial parameter in the desorption process. Thus, multiphoton processes and field induced desorption processes can be neglected. It is more likely, that the temperatures of the sample and substrate are

the relevant parameters. This is supported by the observation of "induction times" for desorption at low laser intensities ($< 10^3$ W/cm^2) and furthermore by the observed dependence of the quasi-molecular ion currents on the laser intensity at relatively high intensities ($> 10^7$ W/cm^2)[10].

Laser pulse time: Laser pulse time is a parameter of secondary importance in laser desorption of oligosaccharides and has to be considered in connection with the laser intensity. For a particular laser intensity, the pulse time has to be sufficiently long to initiate the desorption process at the relevant temperatures. For other samples, e.g. oligopeptides and nucleotides, quasi-molecular ions are generated only by high intensity lasers emitting in short pulses, and a comparison of spectra obtained with different intensity-pulse length combinations has not been made.

Substrates: Quasi-molecular ion generation is not limited to samples deposited on metallic substrates. Spectra have been recorded with semiconductor (Si) and non-conducting (quartz) materials as well. For sucrose the afforded laser intensities can be correlated with the absorption coefficients of the substrate material.

References:

1) F.J. Vastola and A.J. Pirone, Adv.Mass Spectrom., 4 107 (1968).
2) F.J. Vastola, R.O. Mumma and A.J. Pirone, Org.Mass Spectrom., 3 101 (1970).
3) R.O. Mumma and F.J. Vastola, Org.Mass Spectrom., 6 1373 (1972).
4) M.A. Posthumus, P.G. Kistemaker, H.L.C. Meuzelaar and M.C. ten Noever de Brauw, Anal. Chem., 50 985 (1978).
5) H.J. Heinen, R. Wechsung, H. Vogt, F. Hillenkamp and F. Kaufman, Biotechn.Umschau 2 346 (1978).
6) E. Unsöld, G. Renner, F. Hillenkamp and R. Nitsche, Adv.Mass Spectrom., 7 1425 (1978).
7) H.J. Heinen, St. Meier, H. Vogt and R. Wechsung, Adv.Mass Spectrom., 8, in press.
8) P.G. Kistemaker, M.M.J. Lens, G.J.Q. van der Peyl and A.J.H. Boerboom, Adv.Mass Spectrom. 8, in press.
9) R. Stoll and F.W. Röllgen, Org.Mass Spectrom. 14 642 (1979).
10) G.J.Q. van der Peyl, private communication.

FAMOB8 MASS SPECTROMETRY OF INORGANIC AND ORGANIC SUBSTANCES USING LASER INDUCED DESORPTION AND IONIZATION.

L. V. PHILLIPS, Inficon-Leybold-Heraeus, Inc., East Syracuse, NY 13057, H. J. HEINEN, S. MEIER, H. HENNING, H. VOGT, and R. WECHSUNG, Leybold-Heraeus, GmbH, Cologne, West Germany.

The LAMMA (Laser Microprobe Mass Analyzer) is based on time-of-flight (TOF) mass spectrometry of ions generated by the volatilization and ionization of solid samples by a focused laser beam. The use of laser ionization is of growing interest in mass spectrometry due to the unique characteristics the laser imparts to the analysis. Since the diameter of the laser beam at the sample can be less than 1 micrometer, microanalysis is an inherent capability of the LAMMA method. The laser intensity is adjustable over four orders of magnitude offering analyses ranging from full atomization to completely parent compound. Nearly all types of solids independent of their chemical or physical properties can be directly analyzed. Negative ion production is almost equal to that of positive ions offering new information from solids. Sample preparation is minimal and typical analyses are completed in less than 10 minutes by even inexperienced operators. The applications of the LAMMA range from recording elemental distributions of ppm constituents in biomedical tissues to the analyses of single micron refractory particles such as atmospheric particulates or crystals of synthetic products. Spectra will be shown of pure inorganic and organic salts, as well as a few larger organic molecules (sugars, basic and acidic drugs). For compounds of molecular weight above 300, alkali ion attachment is an adequate method of generating relatively intense quasimolecular ions. Na and free base will be demonstrated. Lastly, spectra of single particles of NBS Standard Urban Dust will demonstrate the inhomogeneity of the sample on a particulate basis.

REPETITIVE PULSING - A VERSATILE, SCANNING-INSTRUMENT-COMPATIBLE TECHNIQUE FOR LASER DESORPTION MASS SPECTROMETRY OF NONVOLATILE ORGANIC COMPOUNDS

F. Heresch, E.R. Schmid and J.F.K. Huber
Inst. of Analytical Chem., Univ. Vienna, A-1o9o Vienna, Austria

INTRODUCTION

Compared to other methods used for the mass spectrometric analysis of nonvolatile and thermo-labile compounds, laser pulse induced desorption (LD) offers a variety of well controllable parameters, as shown in Fig. 1.

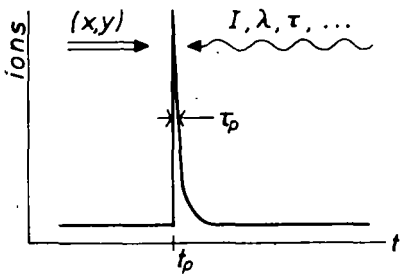

I, λ, τ ... laser irradiance, wavelength, pulse width

(x,y) ... position of irradiated spot

t_p, τ_p ... timing, duration (at half maximum) of ion pulse

Fig. 1 Parameters and Characteristics of Laser Desorption

From the methodological point of view, the duration of the ion pulse, τ_p, which typically lies in the sub-millisecond range, plays a fundamental role. On one hand it reduces the consumption of sample and thus renders the method very sensitive, in comparison to techniques where the ion production is maintained for a relatively long period. On the other hand, however, any experimental change during an ion pulse, e.g. the performance of a mass scan, is excluded.

As another characteristic of LD, the timing of the ion pulse, t_p, and also pulse repetition can be controlled. This possibility becomes particularly important whenever a continuous ion signal is required. For such cases, the continuum can be replaced by a controlled sequence of discrete, i.e. pulsed, signals by means of laser pulse repetition. We call this concept repetitive laser desorption (RLD). Its main features are:

i) Experimental performance is independent on pulse duration and can therefore be adjusted to mass spectrometric requirements.
ii) Sensitivity of pulsed operation is maintained. The number of pulses and, consequently, the consumption of sample, can be kept at the necessary minimum.

Experimental

Based on these considerations, a scanning-type magnetic instrument (MS-9o2, Kratos-AEI, Manchester, U.K.) was equipped with a pulsed Nd-YAG Laser (QSY1/3000, JK Lasers, Rugby, U.K.) and adapted for LD-operation as reported recently[1]. Laser conditions were: wavelength 1060 nm, pulse width 80 µs, power density 0.1 to 1.0 MW/cm^2, pulse repetition rate $\leq$ 10/s. For further experimental details see ref. 1.

RESULTS AND DISCUSSION

Our experiments show that ion pulse series, i.e. series of ion signals each resulting from a laser pulse, can be produced by repetitive laser irradiation of a single sample spot. With sucrose as a test compound, it was found that extended (> 1000 pulses per spot) and reproducible (relative standard deviation of intensity < 25%) ion pulse series are obtained with

relatively thick (> 1 $\mu g/mm^2$) sample layers after appropriate surface pretreatment. This pretreatment which was described recently[1], has proved to be crucial for the generation of such ion pulse series, however, its effect is not yet fully understood.

On the basis of the performance achieved at present, the applicability of RLD has been tested. We have already reported[1] our investigations concerning the optimization of instrumental parameters for LD-operation. In addition, the generation of LD-mass spectra with scanning-type instruments was studied. For this purpose the sequence of repetitive laser pulses was mass-scan-synchronized as shown in Fig. 2.

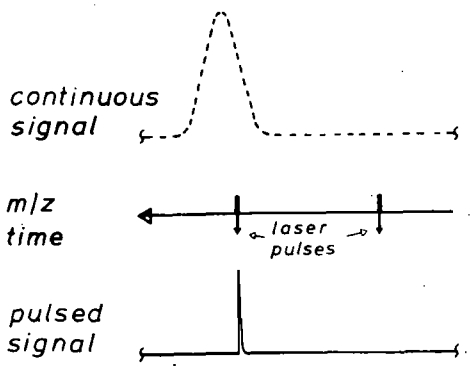

Fig. 2

Schematic Graph of the Scan-Synchronization of Laser Pulsing

With this technique low resolution RLD-mass spectra of various interesting compounds, such as oligosaccharides, steroid glycosides, amino acids, oligopeptides, nucleotides etc., were recorded. Although obtained under different excitation conditions (laser wavelength, pulse width), our spectra exhibit good agreement with data so far reported on LD[2].

These results already demonstrate the potential of the RLD-technique. Based on the above mentioned independence on pulse duration, it was possible to work under the optimum conditions of our mass spectrometer, i.e. at rather slow scanning speeds (19 and 38 min/decade). Under the laser conditions described, no effects of repetitive irradiation, such as pyrolysis etc., have been observed with the compounds investigated so far. The reproducibility of spectra which were measured successively by irradiation of the same sample spot, i.e. within the same ion pulse series, was the same as that found for ion pulse series themselves.

No details are available, at present, on the sensitivity of RLD-operation, due to the difficulty to estimate the sample consumption per laser shot within an extended ion pulse series. It should be pointed out, however, that the required quantity of sample is rather determined by the minimum amount of sample neccesary to allow appropriate preparation. At present state, this limit is the μg-range.

In conclusion, repetitive pulsing can be considered readily as a useful alternative technique for LD. As a major advantage, RLD permits to optimize ion analysis independently of the ionization process, which, for instance, enables to record RLD-mass spectra on conventional scanning-type instruments.

REFERENCES

1 F. Heresch, E.R. Schmid and J.F.K. Huber, Anal. Chem., in press.
2 M.A. Posthumus, P.G. Kistemaker, H.L.C. Meuzelaar and M.C. Ten Noever de Brauw, Anal. Chem. 50, 985 (1978).

POSITIVE AND NEGATIVE FISSION FRAGMENT (^{252}Cf) MASS SPECTRA OF EIGHT COMPOUNDS. B.T.Chait, F.H. Field and W.C. Agosta, The Rockefeller University, New York, N.Y. 10021

Complete mass spectra for both positive and negative ions for a variety of involatile compounds of biological interest have been obtained on the ^{252}Cf fission fragment time-of-flight mass spectrometer constructed at the Rockefeller University. Fig. 1 shows a portion of a typical time-of-flight mass spectrum illustrating satisfactory behavior of the device. Shown in the upper half of fig. 2 is the (M+1) and (M+Na) positive quasi-molecular ion peaks for the tripeptide ala-ala-ala. As is frequently observed for the quasi-molecular ions (1), the (M+1) peak is broad and exhibits prominent wings. By inserting a grid with a positive (decelerating) potential directly in front of the ion detector, the peak shapes shown in the lower half of fig. 2 are obtained. It thus appears that considerable metastable decomposition occurs in flight for this (and perhaps other) molecular ions and that the peak shapes may be effectively sharpened by suppressing the metastable decomposition products.

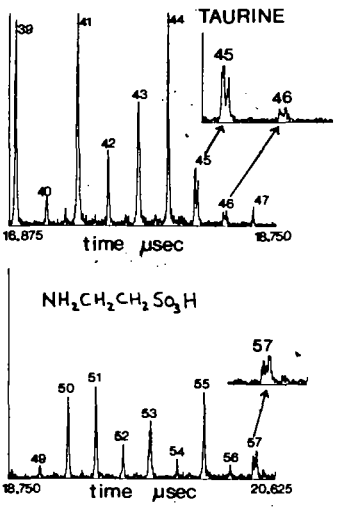

FIG. 1

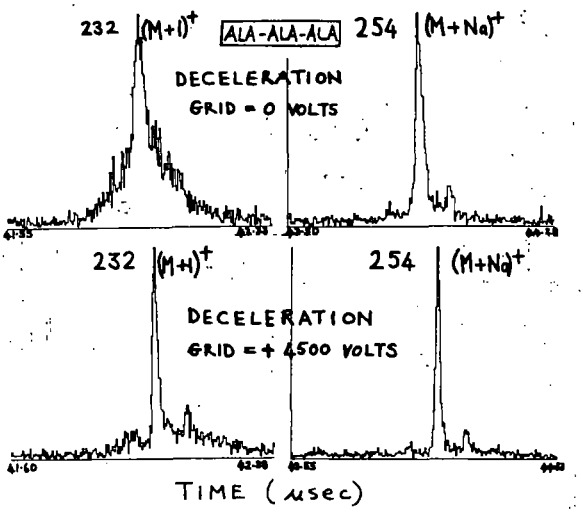

FIG. 2

Fig. 3 shows the background substracted histogram bar mass spectrum for the positive and negative ions from sucrose. The H^+, Na^+ and H^- ion are ommitted from these spectra since these ions are always present in copious amounts, even from a clean bare sample foil, and thus their origin is uncertain. For several of the compounds studied, we have observed the same overall pattern of the quasi-molecular ion peak, a large gap with little small molecule loss from the parent ion apparent, the major component ions (e.g., the m= 163 sugar ring in the positive sucrose spectrum) and an extensive low mass fragmentation. Although quasi-molecular ion peaks were observed in both the positive and negative ion spectra for all the compounds studied they often take a relatively small fraction of the total ionization as shown below. The numbers shown are percentages of the total ionization.

SUCROSE $(M+Na)^+$ 2.1, $(M-1)^-$ 1.6
ALANINE $(M+1)^+$ 10.2, $(M-1)^-$ 15.7
ARGININE $(M+1)^+$ 3.7, $(M+Na)^+$, 0.2, $(M-1)^-$ 3.3
GUANOSINE $(M+Na)^+$ 4.2, $(M-1+2Na)^+$ 1.9, $(M-1)^-$ 0.4
5'AMP $(M+1)^+$ 0.8, $(M-1)^-$ 0.5
ALA-ALA-ALA $(M+1)^+$, 3.7, $(M+Na)^+$, 5.4, $(M-1+2Na)^+$ 0.9, $(M-1)^-$ 8.5
LYS-TYR-THR $(M+1)^+$ 0.2, $(M+Na)^+$ 0.4, $(M-1+2Na)^+$, 0.2, $(M-1)^-$ 0.1

A complex pattern of quasi-molecular ion peaks was also obtained for the amino acid salt cystine dihydrochloride

Attempts were made to rationalize the observed fragmentation pattern of several of these molecules using known reactions of ionic organic chemistry. We illustrate this by giving a couple of proposed reaction mechanisms for the positive ions from sucrose.

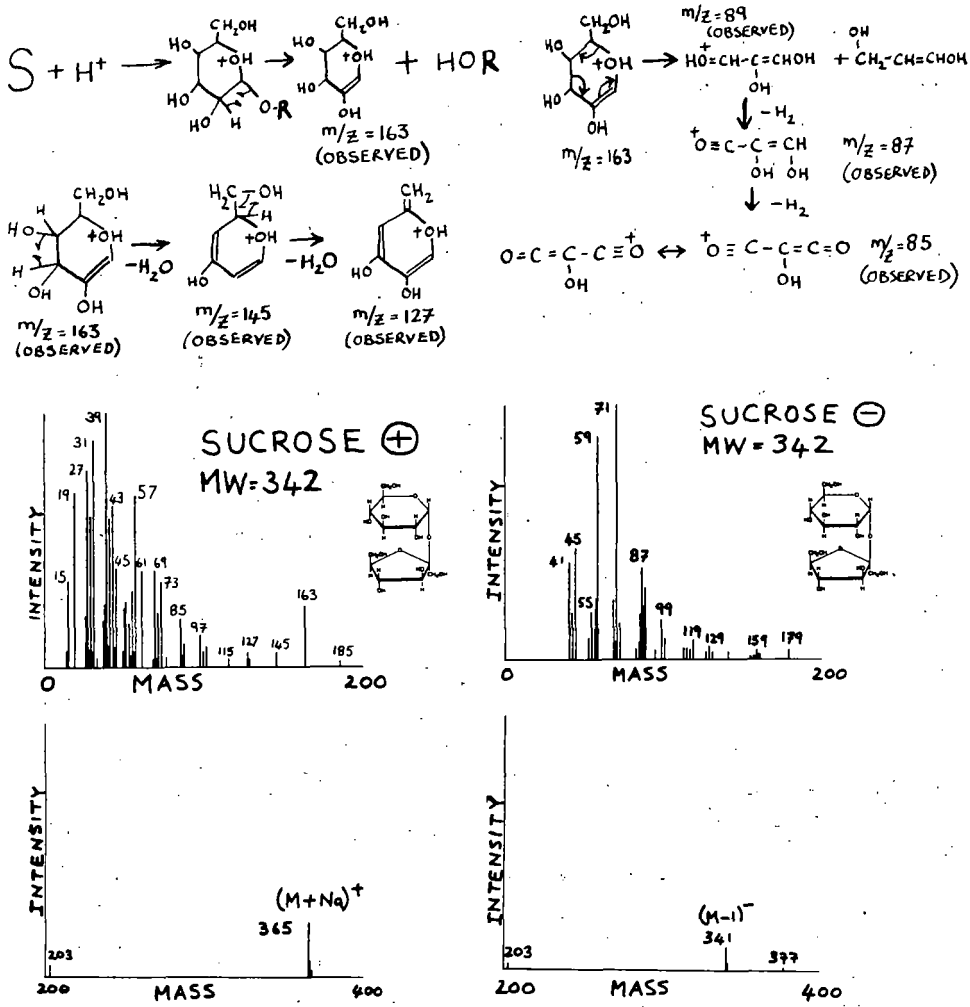

FIG. 3

In this way we have been able to rationalize reaction mechaisms for most of the major ions in both the positive and negative ion spectra of sucrose and several of the other compounds studied. In all the nitrogen containing compounds cyanide ion formation is a dominant feature of the negative ion spectra.

In summary it seems to us that the observed fragment ions indicate that rather high energy processes are at work. On the other hand, we have observed quasi-molecular ions in both positive and negative spectra for all the compounds studied thus far, indicating that at least some component of the desorption and ionization process is remarkably gentle. We feel that this feature of observing at least some quasi-molecular ion confirms the analytical utility of the method that has been reported by Macfarlane (1). We think that while in some cases somewhat familiar chemistry appears to be at play, that the fragmentation patterns are oftentimes rather perculiar and that further work is required to determine to what extent they will be of use in structure determination.

1. Macfarlane, R.D. & Torgerson, D.F. (1976) Science 191, 920-925.

CHLOROPHYLL: A PROBE INTO THE MECHANISMS OF ^{252}Cf-PDMS

Jerry E. Hunt and R.D. Macfarlane
Department of Chemistry
Texas A&M University
College Station, Texas 77843

Continuing developments in the description of a mechanism for fast heavy ion induced desorption of thermally labile molecules have made possible insights into the formation of ions in ^{252}Cf-plasma desorption mass spectrometry. The mechanistic process that is generally agreed upon is based on the occurrence of electron density fluctuations produced by the passage of fast fission fragments through the solid sample. However, the effect that the electronic density fluctuations have on ion production and desorption is under considerable debate. Recently, Sundqvist and coworkers, by observing the yield of molecular ions as a function of projectile velocity, concluded that desorption is induced by electron density fluctuations analyogous to an electronic shockwave. They also suggest that perhaps the most sensitive test of this phenomenon is the desorption of ions from the heavy ion track. The effect of these processes, the production and desorption of chlorophyll ions, is discussed along with the most promising new theory of ion desorption, that of Sieberling and coworkers.

Chlorophyll a (Chl a) is a reduced porphyrin found in all living photosynthetic green plants. The ^{252}Cf-PDMS spectrum of Chl a, ($\bar{M}$=893.5 u), exhibits ions formed by electron transfer, therefore in both negative and positive ion mass spectra an ion occurs at 893 u. Krueger and Wien have shown that the process $M(s) \quad M^+(g) + e^-$ has a low probability for occurrence in ^{252}Cf-PDMS. To be sure, the electron transfer is a function of the electron affinity of the molecule. Chl b, known to have a higher electron affinity than Chl a, exhibits a much more intense negative molecular ion relative to the positive molecular ion than does Chl a.

The effects of electron transfer reactions in ^{252}Cf-PDMS are dramatically demonstrated by binary mixtures of Chls a and b. In the positive ion spectrum of an equimolar mixture, ions are observed as expected at 893 u and 907 u. The relative intensity of the ions is not 1:1, but rather 2.5:1, Chl a:Chl b. However, in the negative ion spectrum, the relative ratio is reversed, exhibiting a 1 to 2 ratio. In a 2:1 molar mixture of Chl a: Chl b the trend continues, forming very little Chl b ion in the positive ion spectrum, and much more Chl b ion intensity in the negative ion spectrum. The observation of electron transfer products presumes that a Chl a · Chl b dimer exists. The ^{252}Cf-PDMS spectrum of the dimer region shows indeed two peaks, corresponding to $(\text{Chl a})_2^{+\cdot}$ and $(\text{Chl a}\cdot\text{Chl b})^{+\cdot}$. These results suggest a very efficient energy coupling mechanism between the electron oscillations caused by the passage of the fission fragment and the chlorophyll molecules. A mixture of Chl a and Pheo a does not show the expected results of electron transfer between the two molecules. The Chl a · Pheo a dimer ion is very weak, reflecting little Chl a · Pheo a interaction.

On ionization molecular ions are produced having a range of excitational energies distributed among their electronic, vibrational, and rotational degrees of freedom. The molecular ion decomposes only when intramolecular relaxation is concentrated in appropriate vibrational degrees of freedom. In the ^{252}Cf-PDMS of Chl, 95% of the ion intensity is devoted to fragmentation of the molecule. The production of very highly excited states apparently occurs in ^{252}Cf-PDMS. Fragment ions are formed which correspond to the loss of all of the side chain groups on the chlorin ring.

Fragmentation is not the only process mediated by the electron density fluctuations. The desorption of massive ions of chlorophyll oligomer chains up to 7148 u, the octamer of a Chl chain, are observed from chlorophyll samples.

The most recent description of the complex mechanism associated with ^{252}Cf-PDMS ion desorption is that of Sieberling and coworkers. The occurrence of enhanced sputtering yields during bombardment by high energy (MeV) charged particles is explained not in terms of an ion explosion or thermal spike alone, but rather as a model that is thermal in nature incorporating the concept of an ion explosion. Measurements of the energy spectra as well as yield data were used to form the model. The velocity spectrum of uranium sputtered from UF_4 by 4.72 MeV $^{19}F^{+2}$ fits the thermal equilibrium model well. This model presents

for the first time a convincing method for the transfer of heat to the sample molecules. In effect, energy is transferred into motion by collisions of the target ions (thereby thermalizing) before heat can be conducted away. Thus the desorption process can be explained by a combination of thermal and ion explosion processes. This model predicts that materials with a high thermal conductivity would not show such effects.

FAMOB12 A DIRECT EXPERIMENTAL COMPARISON OF MASS SPECTRA OBTAINED WITH LOW ENERGY ION AND HIGH ENERGY ^{252}Cf FISSION FRAGMENT BAMBARDMENT, K. G. Standing and W. Ens, Physics Dept., Univ. of Manitoba, Winnipeg, Canada R3T 2N2, and B. T. Chait and F. H. Field, The Rockefeller Univ., New York, NY 10021

Recently two new techniques have been developed for obtaining mass spectra of involatile organic compounds. These involve simultaneous desorption directly from the solid state and ionization of the molecules either by energetic heavy ions (~100 Mev) from a spontaneously fissioning ^{252}Cf source (1) or by low energy (a few Kev) argon (2) or potassium (3) ions. It is of considerable theoretical and practical interest to make a comparison of these techniques. Since sample preparation and surface conditions appear to play an important role in the spectra obtained, it is desirable to remove this variable. We report a direct comparison of mass spectra obtained on the University of Manitoba pulsed ion time-of-flight mass spectrometer (3) and the Rockefeller University fission fragment ionization time-of-flight mass spectrometer. The same samples on the same sample foils were used in both studies. Comparisions are made for both positive and negative ion mass spectra. In the case of alanine, for example, certain characteristics of the mass spectra are similar in that $(M+1)^+$ and $(M-1)^-$ quasi-molecular ions and the major fragment ions are common to both. However, significant differences are observed. In particular while alkali metal cation attachment is observed in the californium spectra they appear to be absent from the low energy ion spectra.

(1) R. D. Macfarlane and D. F. Torgerson, Science 191(1976) 920; (2) A. Benninghoven and W. Sichtermann, Anal. Chem. 50 (1978)1180; (3) B. T. Chait and K. G. Standing, 27th ASMS Conf. 1979, p. 699.

GAS CHROMATOGRAPHIC FOURIER TRANSFORM MASS SPECTROMETRY

Edward B. Ledford, Jr., Robert L. White, Sahba Ghaderi,
Charles L. Wilkins and Michael L. Gross

Department of Chemistry
University of Nebraska
Lincoln, Nebraska 68588

An important step in the development of Fourier transform mass spectrometry (FTMS) into an analytically useful technique is coupling the FT mass spectrometer to a gas chromatograph. We report here preliminary studies of a GC-FTMS system constructed in our laboratory.

The basic strategy of GC-FTMS must be to capitalize upon the ultra high resolution capabilities of the Fourier transform mass spectrometer. High resolution GCMS can be performed with magnetic sector instruments. However, high resolution data is available only over a narrow mass range during a given GC run owing to the fact that the field strength of the magnetic sector must be held constant. "Peak switching" or multiple ion detection (MID) in FTMS involves switching the frequency of an rf sine wave, as opposed to the accelerating/electrostatic analyzer voltages or the strength of a magnetic field. With commercially available computer programmable frequency synthesizers, peak switching can be accomplished in microseconds across arbitrarily wide regions of the mass scale. The ultimate goal of our work, then, is a mass spectrometer capable of extracting high resolution data from several regions of the mass scale within the characteristic elution time of a high resolution capillary column GC peak. Such an experiment would provide ultra specific analysis and, in general, allow for positive identification of GC eluents.

Our initial studies have concerned the problems unique to GC-FTMS, particularly the issue of mass resolution as it relates to carrier gas flow rates and sample enrichment schemes. Two configurations have been tested to date. In the first configuration, a SCOT column was coupled directly to a fast pumped vacuum system housing the FTMS analyzer cell. In the second scheme, effluent was passed through a jet separator prior to introduction into the high vacuum system.

In the direct couple mode, an operating pressure of 5×10^{-6} torr was achieved with a pumping speed at the analyzer cell of 360 ℓ/s. In FTMS, attainable mass resolution is critically dependent upon pressure. The resolution obtained was 8000 (FWHH) at m/e 78, a figure consistent with the operating pressure observed. Simple separations of benzene, toluene, and xylene proved straightforward and reliable giving good reproducibility (Figure 1).

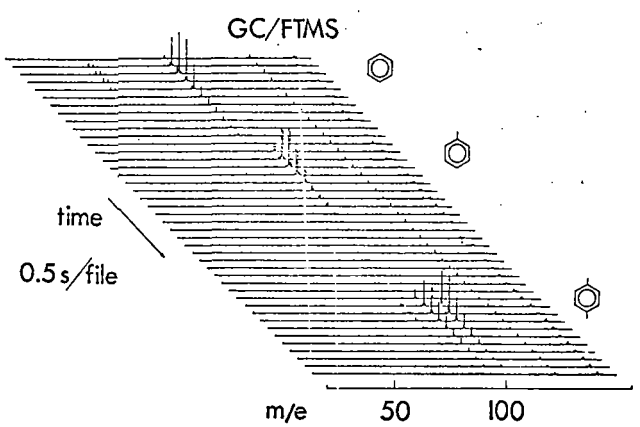

Figure 1. Separation of benzene, toluene, and xylene in GC-Fourier transform mass spectrometer

A sample size determination was undertaken in the direct coupled mode. Sample was vaporized into the nineteen liter volume of the vacuum housing, of which the analyzer cell occupied one cubic inch. Taking into account this inefficient method of sample delivery, and a 30:1 split ratio at the GC injector, we calculate that about 25ng of each material in Figure 1 entered the FTMS analyzer cell. An isobaric doublet at m/e 106 derived from xylene and benzaldehyde (the latter introduced via an inlet system) was successfully resolved in a direct coupled GC run.

With a jet separator driven by the capillary column and helium makeup gas, an operating pressure of 5×10^{-7} torr was achieved. Mass resolution of 23,000 at m/e 78 was attainable, and the aforementioned doublet at m/e 106 readily resolved.

FTMS offers the possibility of performing low pressure chemical ionization, a potentially useful analytical technique. For example, isobutane reagent gas was introduced via an inlet system, and methyl formate injected into the GC. When methyl formate eluted, the background reagent ionization (predominantly m/e 43) shifted to the $(m + H)^+$ of methyl formate (m/e 61), then recovered in intensity as the methyl formate GC peak disappeared (Figure 2).

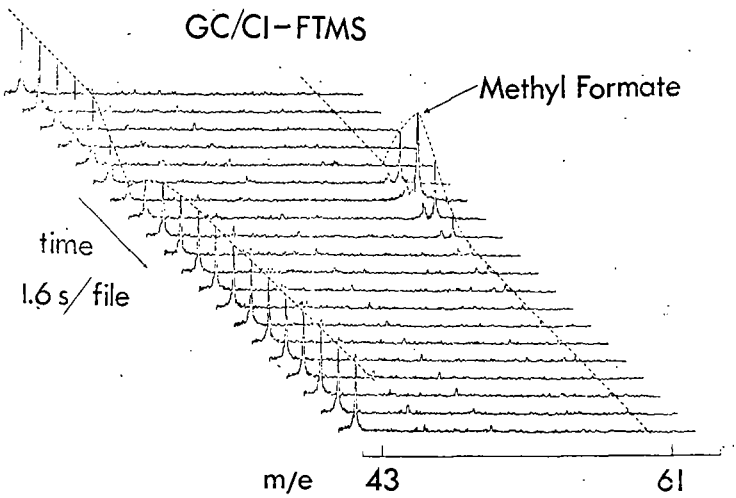

Figure 2. Low pressure chemical ionization (isobutane reagent gas) by GC-Fourier tranform mass spectrometry

The present results indicate that high resolution GC-FTMS is feasible, and that low pressure CI can be used in this mode.

An important problem is efficient sample handling. Ideally, effluent sample should be transported directly to a "gas tight" analyzer cell to avoid rapid loss to the pumps. However, to maintain low pressure, hence high mass resolution, in such a cell, carrier gas should be removed. The requirement for GC separator enrichment is 1000 to 10,000 times greater than for conventional GCMS systems, and demands some innovation. A cryogenically cooled moving belt delivery system seems a likely approach to the problem. Such a system is under construction in our laboratory.

FAMOC2 A SECOND-GENERATION RAPID SCAN ION CYCLOTRON RESONANCE MASS SPECTROMETER, RICHARD L. HUNTER and ROBERT T. McIVER, JR., Dept. of Chem., Univ. of Calif., Irvine, CA 92717.

Rapid Scan ion cyclotron resonance spectroscopy (Rapid Scan ICR) has proven to be a useful technique for analysis of low vapor pressure compounds using low pressure chemical ionization. However, hardware constraints have limited the scan rate and mass resolution severely. A 200 amu scan range effectively limited the mass resolution at mass 100 to approximately 5000 at a scan rate of 200 kHz/second.

This talk describes a second generation Rapid Scan ICR instrument developed in our laboratory which allows increased scan rates and mass resolution on the order of 100,000. Our studies have defined practical conditions required for obtaining high resolution signals. In addition to the well characterized effect of sample pressure on resolution, we have characterized the effects of irradiation RF level, trapping potentials, electron beam energy and density, and scan rate. The mass resolution is also limited by the hardware used to digitize and store the transient ion signals. There is not only a trade-off between mass resolution and scan range (which has been described before) but also a trade-off between scan rate and mass resolution. As the scan rate is increased, the speed of the A/D converter must be increased to maintain high resolution signals.

The parameters which limit and contribute to high resolution Rapid Scan ICR signals will be discussed and compared with the Fourier Transform ICR technique.

ICR Spectroscopy : Three Basic Experiments.

G. Parisod and T. Gäumann
Institute of Physical Chemistry
Federal School of Technology
CH-1015 Lausanne, Switzerland

The design and capability of our spectrometer are similar to those already described by Comisarow and coworkers {1}. A special effort has been made to improve its versatility. Using different pulsing sequences, three experiments can be run with the same instrument:

1. FT-ICR spectroscopy : a limited amount of processing leads to magnitude-mode spectra.
2. Convolution FT-ICR spectroscopy: a method based on the properties of linear systems has been suggested by Marshall; it allows to get absorption and dispersion-mode spectra {2}.
3. Correlation FT-ICR spectroscopy or rapid scan ICR {3,4}.

A minor modification of the pulsing sequence corresponding to experiment 1 is needed to get phased spectra by convolution FT-ICR. One has just to make sure of the exact coincidence of the beginning of the detection period with the start of the excitation chirp pulse. Then correlation and convolution spectroscopy are so closely related that a FT-ICR spectrometer can be run indifferently in the two modes using the same equipment and software. This simplified way of doing rapid scan ICR without a dedicated electronics has a drawback. The processing can't be limited to the cross-correlation of the crude spectrum with a reference line. A first-order phase correction or the calculation of a magnitude-mode spectrum have to be applied to correct for a continuous phase shift {4}.

It is possible to commute rapidly between convolution and correlation FT-ICR allowing the operator to work efficiently with his spectrometer. Both methods have interesting features and we would like to point out two of them:

- In the rapid scan mode, the acquisition frequency can be kept in the range corresponding to the access time of mass storage devices.
- With convolution FT-ICR, the duration of the excitation chirp pulse can be fairly short in comparison to the usual experimental time scale. This advantage is essential if one has to study the kinetics of processes involving ions trapped in the ICR cell.

Results obtained by each technique are shown on Fig. 1 and 2 to illustrate the ability of our spectrometer to produce phased spectra over a broad mass range.

{1} M.B. Comisarov, G. Parisod and V. Grassi, 26th Annual Conference on Mass Spectrometry, St Louis, MO, May 28-June 2, 1978, Paper W12.

{2} A.G. Marshall, Chem. Phys. Letters 63 (1979) 515

{3} R.L. Hunter and R.T. McIver, American Laboratory 9 (1977) 13

{4} G. Parisod and T. Gäumann, Chimia (in press)

Figure 1

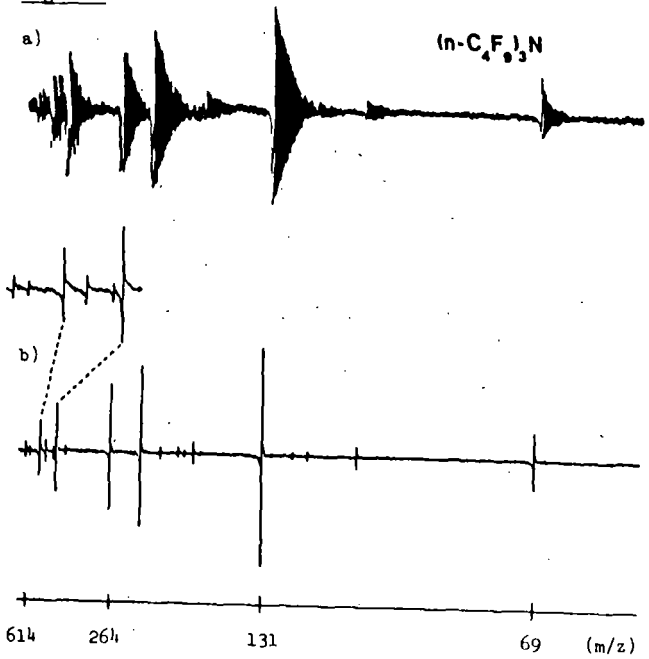

a) Rapid scan response observed at 7 10^{-7} torr.

b) Result obtained after cross-correlation of a) with an experimental reference line followed by a first-order phase correction.

Figure 2

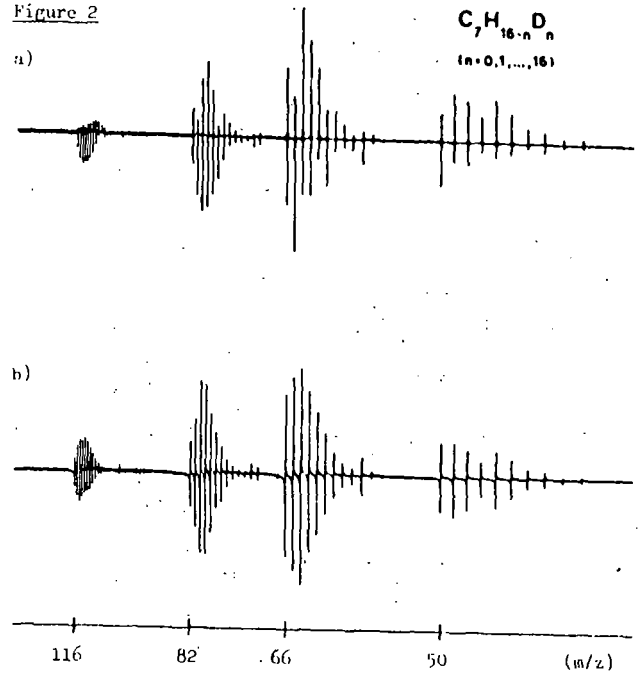

a) Fourier transform of a transient measured by convolution FT-ICR

b) Dispersion-mode spectrum given by the division in the frequency domain of the ICR signal by the excitation signal and after a zero-order phase correction.

RESOLUTION AND SIGNAL-TO-NOISE IN FOURIER TRANSFORM MASS SPECTROMETRY*

Sahba Ghaderi, Robert L. White, Edward B. Ledford, Jr.
Charles L. Wilkins, and Michael L. Gross

Department of Chemistry
University of Nebraska
Lincoln, Nebraska 68588

The ability to make high resolution measurements is important for application of mass spectrometry to structure proofs, trace analysis by single ion monitoring, and GC/MS. Using an instrument constructed in our laboratory we have obtained resolution in excess of 750,000 (FWHH definition) for the molecular ion of benzene at a magnetic field strength of 1.2 Tesla (Figure 1). In a related experiment, the m/z 84 doublet from a mixture of d_6-benzene and cyclohexane (Figure 2) at a total pressure of 2×10^{-8} torr was resolved.

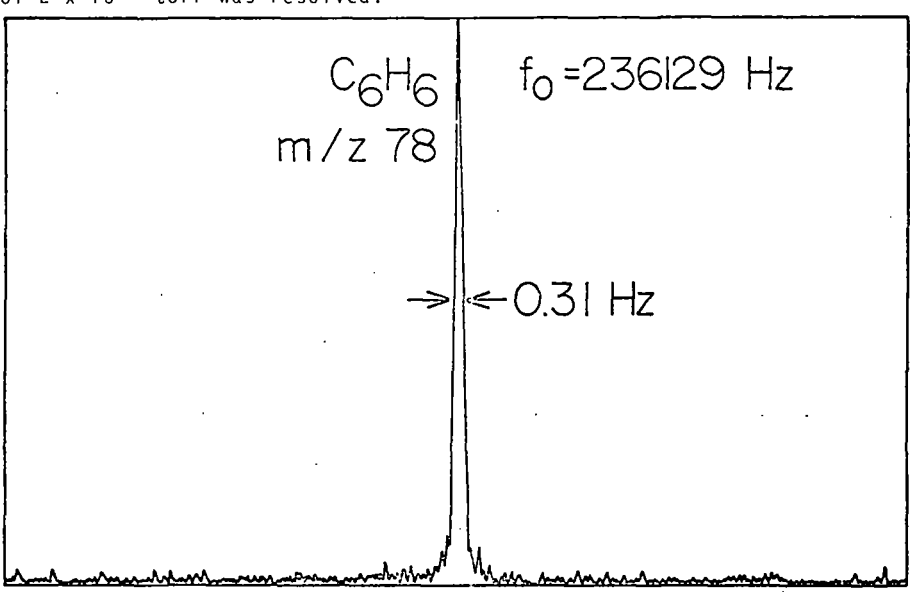

Figure 1--Ultra-high resolution absorption (not magnitude mode) spectrum of benzene at m/z 78, obtained from a signal with τ of 1.0 second at a magnet field strength of 1.2 Tesla. Resolution is 760,000 (FWHH definition).

These high resolution capabilities have stimulated interest in the relationship between mass resolution and signal-to-noise ratio (S/N) in the FT/MS experiment. A simple model of FT/MS lineshape has revealed that it is possible to simultaneously increase mass resolution and S/N.

The detailed experimental validation of this concept, as well as the demonstration that the essential trade off in FT/MS is resolution versus mass range rather than resolution versus signal-to-noise will be discussed. We believe these experimental data have important implications regarding the expected analytical applications of FT/MS, particularly with respect to gas chromatographic FT/MS experiments similar to those reported in another of our papers at this Conference.

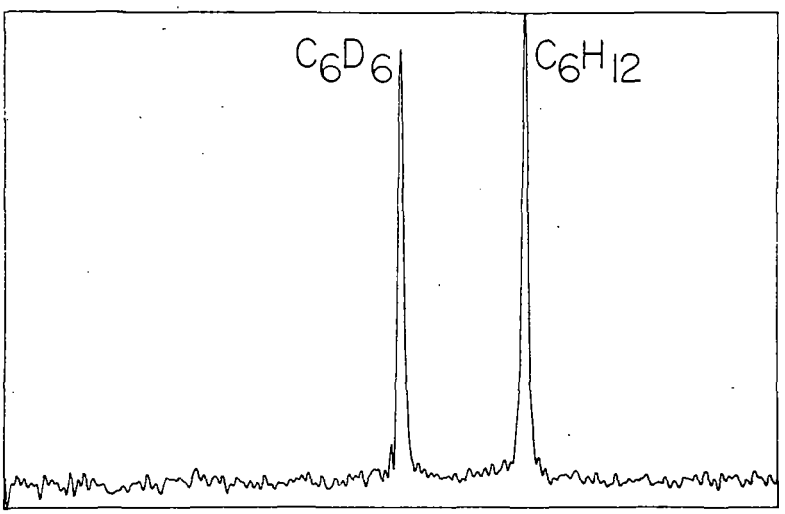

Figure 2--Resolved d_6-benzene/cyclohexane m/z 84 doublet, absorption mode at 1.2 Tesla. Resolution is 220,000 (FWHH definition).

* This research was supported by National Science Foundation Grant CHE-77-03964 and a grant from the Gulf Oil Foundation.

PHASE CORRECTION IN FOURIER TRANSFORM MASS SPECTROMETRY

Robert B. Spencer and William J. Horsley
Nicolet Instruments Corp.,
5225 Verona Road
Madison, WI 53711

In Fourier Transform Mass Spectrometry (FTMS), the mass spectrum is obtained as the Fourier transform of time-domain signal resultins from the coherent motion excited in the ions. The spectrum is most easily obtained as a magnitude (absolute value) mode transform, even though this yields a spectrum of lower resolution, with distortion of the shapes of closely-neighboring peaks, and non-linear noise characteristics. Because of the simplicity of the magnitude calculation, and its insensitivity to phase effects, it is the normal mode of choice for the transformation.

When magnitude mode calculation is not acceptable, in particular when the highest possible resolution is desired, a means for obtaining absorption mode spectra is needed. This necessitates phase correction. Marshall has described an experimental method of phase correction[1], which has been demonstrated by Ledford et al[2]. The method described here is a simple theoretical derivation for the frequency sweep phase function, and an experimental determination of the electronic phase function.

The largest phase effects are created by the linear frequency ramp used to excite ion motion, and may be up to several thousand radians. By comparison, the combined phase shifts due to the electronic components of the spectrometer are only a few radians. Clearly, if the phase effects of the excitation may be removed, the resulting (complex) spectrum will be more amenable to manual phase correction.

Consider first a linear (continuously varing frequency) sweep:

$$F = F_0 + F't. \qquad (1)$$

The frequency is the rate of change of phase with respect to time (actually, d (phase) / dt = 2 π F), so that it may be integrated to yield the phase as a function of time:

$$\text{phase} = F_0 t + 1/2\ F'\ t^2. \qquad (2)$$

The phase of a signal of constant frequency F is:

$$\text{phase} = Ft \qquad (3)$$

so that the phase difference is given by:

$$\text{phase difference} = Ft - (F_0 t + 1/2\ F'\ t^2) \qquad (4)$$

Solving (1) for t and substituting:

$$\textit{phase difference} = (F - F_0)^2 / 2F' \qquad (5)$$

Thus, the phase of a linear frequency sweep is a quadratic function of frequency, and is inversely proportional to the sweep rate.

For a stepwise sweep, the above substitution for time is not possible. The difference between the phase function for the continuous sweep and a stepwise sweep is, however, a linear function of frequency, proportional to the time interval between frequency updates. This is most easily obtained by applying the above quadratic phase correction to the spectrum of a stepwise sweep, and then manually correcting the remaining phase shift. Only the linear and constant terms need be changed. Once the combined (calculated quadratic plus manually obtained linear) corrections are known, they can be applied to

an experimental mass spectrum. The remaining phase effects in the spectrum may then be manually compensated. Figure 1 illustrates phase compensation for a calculated stepwise ramp from 0 to 1 Mhz. The top trace is a magnitude calculation of the ramp spectrum, the bottom trace is a phase-compensated Fourier transform spectrum, and the middle trace the difference between the two.

If desired, the phase function of the electronics may be determined as the difference between the (known) phase function of the sweep and the phase function of the signal obtained by passing the sweep through the electronics.

To facilitate this process, a quadratic phase-correction program has been written, which allows both numeric entry of the quadratic coefficients and adjustment of the coefficients via knobs. The procedure described above has been applied to several spectra, including a group of 1,1,1,2-tetrachloroethane spectra obtained from the University of Nebraska. These latter were taken using several different sweep rates, with data acquisition after excitation. In addition to the above phase compensation, an additional, linear, phase correction was applied, to correct for the time between the start of the excitation and the start of acquisition. (The time-reference point for the phase of the sweep is the beginning of the sweep; that for the spectrum is the beginning of acquisition.) Figure 2 shows a portion of one such spectrum, obtained in an experiment using a piecewise frequency sweep from 0 to 200 khz, swept at a rate of 1141.714 hz/microsecond.

1. Marshall, A. G., Chem. Phys. Lett. 63, 515 (1979)
2. Ledford, E. B., White, R. L., Ghaderi, S., Gross, M. L. and Wilkins, C. L., Anal. Chem. (in press).

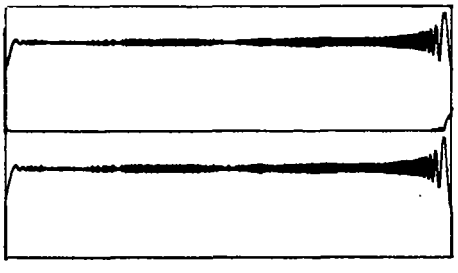

Figure 1. Spectra of Calculated Linear Frequency Sweeps. Top: MC Bottom: FT Phase-Compensated. Middle: difference between the two.

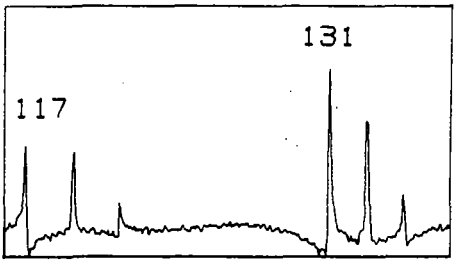

Figure 2. Phase-Compensated Partial Mass Spectrum of $C_2H_2Cl_4$.

ELECTRON IMPACT IONIZATION OF ISOTOPICALLY-ENRICHED OXYGEN AND NITROGEN. GEORGE M. WOOD, NASA Langley Research Center, Hampton, VA, 23665; BILLY T. UPCHURCH, Old Dominion University, Norfolk, VA, 23508; PATRICIA A. PAULIN, NASA Langley Research Center, Hampton, VA, 23665; RONALD F. HOYT, NASA Langley Research Center, Hampton, VA, 23665; EDWIN L. WILDNER, Newport News, VA, 23606; and DAVID B. HUGHES, E. I. DuPont de Nemours, Wilmington, DE, 19898.

The use of reduced ionizing electron energy in trace gas analysis, exemplified by the determination of methane in air, was discussed by some of us at a prior ASMS meeting.[1] This technique, along with isotopic labeling to form odd numbered isotope masses has been used in several studies to unambiguously identify the production of doubly-charged molecular oxygen and nitrogen species by electron impact; to monitor the reaction of oxygen with elemental carbon in stainless steel; and to study copper (II) oxide (CuO) for oxygen exchange with free oxygen up to 300° C. The purpose of this paper is, by examining these results, to demonstrate the efficacy of the technique through the unambiguous identification of species, which allows one to uniquely determine chemical and ionization processes.

The isotopic composition of the oxygen (O_2*) used was 7.9, 2.2, 16.4, 40.7, and 32.8% m/e 32, 33, 34, 35, and 36, respectively, and the nitrogen 34.9, 64.8, and 0.4% m/e 28, 29, and 30. Normal krypton was introduced along with each sample to provide a measure of ion source effects. The mass spectrometer was a 180° magnetic deflection Dempster type, modified to provide for continuous variation and measurement of the ionizing electron energy.

The identification of doubly-charged species through the use of odd-numbered isotopes has been described by Dorman and Morrison for nitrogen [2,3] and oxygen.[3] The large ion currents obtained from our heavily-enriched isotopes easily substantiated their results and the second order dependence of the double ionization. Ionization efficiency curves were obtained for an approximately one-to-one mixture of oxygen and krypton (Fig. 1), and the square root and first derivative of ionization efficiency plotted in figure 2. The threshold of approximately 37 volts is in good agreement with theory and previous measurements, and the linearity of the first derivative demonstrates the square law process.

To determine if the reaction $CuO + O_2^* \rightarrow CuO^* + OO^*$ would proceed at temperatures up to 300° C, 5.1 grams of CuO were placed in a 347 stainless-steel tube 15-cm long and 0.44 cm in diameter, sealed at both ends with stainless-steel frits (5-micron porosity) and valves. Prior to each measurement, the tube was evacuated, and then backfilled with O_2* to 350 torr, and placed in an oven. Following 10 minutes at the desired temperature, 750 torr of krypton was added to the tube, and the gas mixture introduced into the mass spectrometer at ambient temperature. Two spectra are shown in figures 3 and 4. These data show that at the higher temperatures the labeled oxygen reacts with the elemental carbon in the stainless steel to form CO_2*. Further, since the isotopic ratios of the $^{35}O_2/^{36}O_2$ and $^{47}CO_2^*/^{48}CO_2^*$ are maintained equal, the process is shown to involve a molecular oxygen reaction, e.g., $C + O_2^* \rightarrow CO_2^*$ without producing CO as an intermediate. Further, since exchange of the O_2* with the $Cu^{16}O$ or the $^{32}O_2$ would alter these ratios, it follows that neither of these reactions occur in the temperature interval studied.

REFERENCES

1. G. M. Wood, B. T. Upchurch, and D. B. Hughes, Paper FA6, 26th Ann. Conf. Mass. Spec. and Allied Topics, St. Louis, MO, May 1978.

2. F. H. Dorman and J. D. Morrison, J. Chem. Phys., 35, 575 (1961).

3. F. H. Dorman and J. D. Morrison, J. Chem. Phys., 39, 1906 (1963).

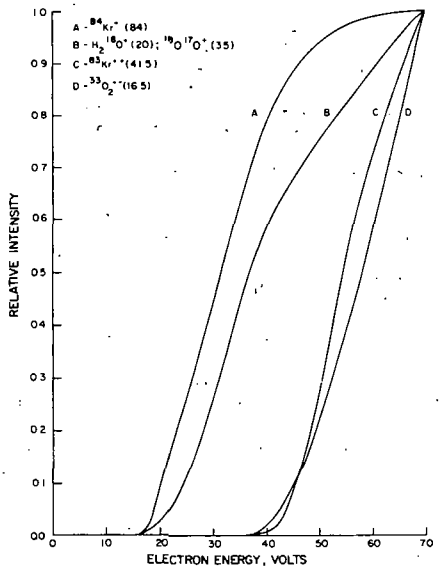

FIGURE 1

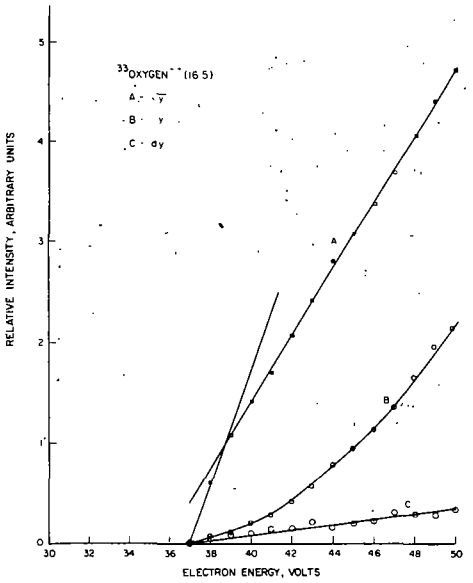

FIGURE 2

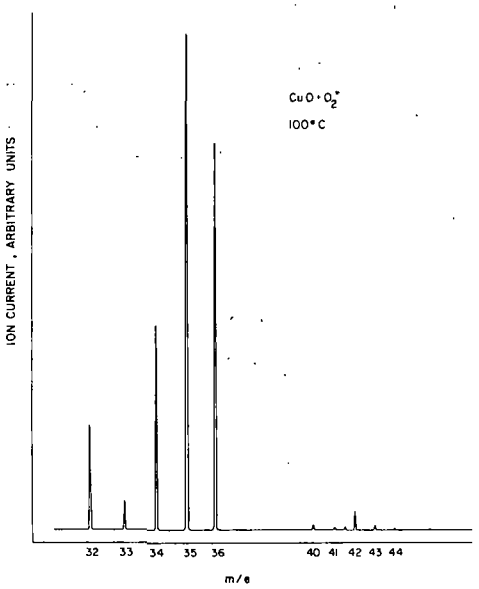

FIGURE 3

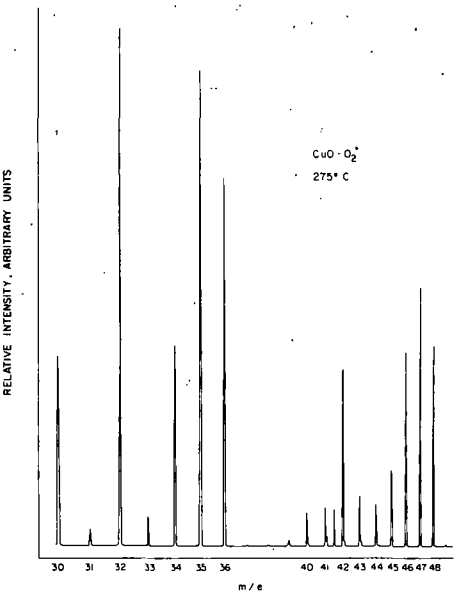

FIGURE 4

TOWNSEND DISCHARGE IONIZATION PROBE FOR A FINNIGAN 4000 MASS SPECTROMETER

R. C. Scheibel, O. P. Tanner and K. V. Wood
Monsanto Company, 800 North Lindbergh Blvd., St. Louis, MO. 63166

Townsend discharge ionization is an important complementary analytical tool in mass spectrometry, particularly with the growth of negative ion chemical ionization. The Townsend discharge replaces the conventional hot filament as a source of ionizing electrons, thereby providing a distinct advantage when using oxidizing reagent gases. These gases (N_2O, NO, O_2, etc.) are important in both positive and negative ion chemical ionization mass spectrometry where proton or hydride abstraction by the reagent ion is the desired reaction. For this reason a Townsend discharge ionization probe was developed for a Finnigan 4000 mass spectrometer.

This probe was constructed from a blank solids probe and was designed to have a variable discharge gap distance. The probe consists of three components, a) the exterior probe housing b) the electrode and c) the probe tip. The total length of this assembly is approximately 40 centimeters.

N_2O, a good reagent gas for discharge formation, was used to characterize and optimize the Townsend discharge ionization probe. The variables studied were discharge voltage, source gas pressure, discharge gap distance and probe tip configuration. The reagent ion intensity, as well as the sample ion intensity, maximized at two different gap distances. The difference in the two positions was related to the positioning of the electrode with respect to the ceramic insulator - probe tip junction and was very small. Using the Townsend discharge ionization probe, the intensity of the (M-H) ion in both the positive and negative ion modes was considerably increased over the filament mode positive ion isobutane CI $(M+H)^+$ ion.

The successful development and characterization of a Townsend discharge ionization probe for a Finnigan 4000 mass spectrometer will enable a variety of novel reagent gases for both positive and negative ion chemical ionization applications to be investigated.

COMPUTER MODELLING FOR ION SOURCE DESIGN.

R. N. Stillwell and D. I. Carroll, Institute for Lipid Research, Baylor College of Medicine, Houston, Texas 77030

While the principles of electromagnetic field calculation and ion optics are well understood and applied to the design of mass analyzers, ion source and lens design remains an empirical science. That this is so is shown by the fact, for example, that currently produced chemical ionization sources and lenses differ little in geometry from those of the original design. Calculations show that at least 90% of the ions formed in such a source are lost in the source pump. For the analysis of substances such as petroleum fractions, which are available in virtually unlimited supply, this is of little moment, but for biomedical research sensitivity of detection is all-important.

Computer programs are being developed for the modelling and optimization of mass spectrometer ion sources and lenses. These programs are intended to permit the development of sources and lenses of substantially higher transmission than are now available, for the construction of a mass spectrometer of very high sensitivity for biomedical applications. The programs, which are written primarily in Flecs-Fortran for a PDP-11/45, will model gas dynamics in the source as well as geometric and electrostatic parameters.

Programs developed to date calculate the electrostatic field in an ion lens, calculate the ion paths, and plot the field contours and ion paths. Efficient virtual memory routines have been developed to handle the large arrays required. Calculation of the electrostatic field is performed by a successive overrelaxation method; about 20 passes per minute can be performed on 10,000 points. Convergence requires 250-300 passes. Ion paths are calculated by Runge-Kutta-England integration of the relevant differential equations, using the GASP simulation package(1). This approach makes alteration of the model or parameters easy. A contour-following algorithm is used for plotting. Interpolation of field values between grid points is performed by a modification of the Akima bicubic interpolation algorithm(2) which provides the partial derivatives of the potential as well as the value.

This work was supported by NIGMS grant GM-13901.

(1) A. A. B. Pritsker, The GASP IV Simulation Language, Wiley-Interscience, New York, 1974.
(2) H. Akima, Bivariate Interpoation and Smooth Surface Fitting based on Local Procedures, Coll. Alg. ACM, No. 474.

A TOTALLY AUTOMATED DATA ACQUISITION/REDUCTION SYSTEM FOR ROUTINE TREATMENT OF MASS SPECTROSCOPIC DATA BY FACTOR ANALYSIS

P. C. Tway and L. J. Cline-Love

Department of Chemistry
Seton Hall University
South Orange, N. J. 07079

Hugh B. Woodruff

Merck Sharp & Dohme Research Laboratories
P. O. Box 2000
Rahway, N. J. 07065

Although chromatographic methods, especially those using capillary columns, offer high selectivity and resolution, it is often difficult to separate completely two or more components in a complex mixture or to determine conclusively if a peak is due to a single component. Information about such possible multi-component peaks may be obtained from the mass spectra recorded at intervals across the peak. The technique of mass chromatography is frequently used in an effort to determine the integrity of a peak in a GC/MS analysis. Factor analysis, a multi-parameter curve fitting method which enables the spectroscopist to explain trends within a multi-dimensional data set, has been used to determine the number of compounds present in the mass spectra of mixtures.(1,2) In the present work principal component factor analysis has been successfully applied to typical GC/MS and solid probe mass spectrometry data to rapidly determine the number of components in unresolved or partially resolved peaks.

In order to determine the practicality of factor analysis for routine sample handling, it was necessary to interface the data system from a GC/MS with a larger computer capable of doing factor analysis, to apply factor analysis to typical samples to check its value on real world problems, and to determine the limit of detection of a minor impurity under a chromatographic peak as a function of resolution. This work was done on a Finnigan Incos Data System consisting of a Nova minicomputer and peripherals interfaced to a mainframe CDC Cyber 172 computer. All data manipulations and formatting were done on the Nova, and the data were transmitted via a phone modem to the Cyber where subsequent treatment by factor analysis was performed. The results were returned to the Nova and printed in the mass spectrometry laboratory. This system completely eliminates all intermediate batch processing so that samples of questionable purity can be studied by factor analysis quickly and easily.

The limit of detection of an impurity under a chromatographic peak was determined from simulation studies on compounds with similar mass spectra. For two-component mixtures with resolutions between 0.05 and 1, the limit of detection is less than 1% using error-free data and about 4% for data containing random noise.

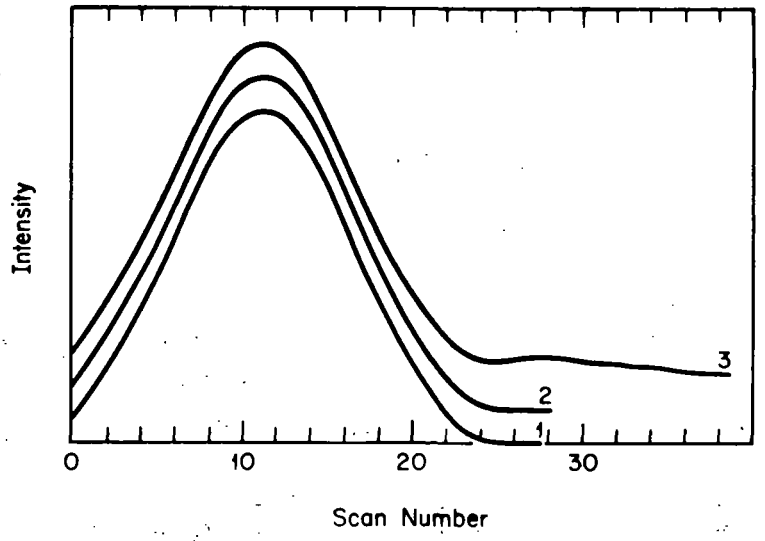

To gain a fuller appreciation of the effects such low levels of impurity have on a reconstructed ion chromatogram, compare the three curves in the figure shown above. The difference between curve 1, a pure compound, and curve 2, the same compound with the addition of a 4% impurity and a resolution of 0.048, is virtually impossible to discern visually. Factor analysis, however, easily predicted two components for curve 2. Curve 3 shows the same level of impurity with a resolution of 0.809.

1. E. R. Malinowski and D. G. Howery, "Factor Analysis in Chemistry," John Wiley, New York (1980).

2. J. McK. Halket, J. Chromatogr., 175, 229 (1979).

AN INTERFACE AND DATA ACQUISITION SYSTEM FOR TWO SPECTROMETERS[1]

T. R. Mueller, H. S. McKown, R. J. Warmack, and D. H. Smith

Analytical Chemistry Division
Oak Ridge National Laboratory
Oak Ridge, Tennessee 37830

ORNL has two high abundance sensitivity mass spectrometers. They are designed with thermal ionization sources. Because we must often deal with samples in the range of 1-10 ng, which may also be radioactive, we use pulse counting for detection of the ion beam. Both instruments have two 12-in. radius, 90° magnetic sectors; one has an additional 90° electrostatic sector. In order to obtain data that represent nearly simultaneous information about all analytically significant masses in a sample, a rapid scan of the accelerating potential is employed. In order to maximize the fraction of time spent collecting data from significant masses, a peak-hopping scan is used. Statistical improvements are realized by spending a greater amount of time collecting data at the less abundant mass positions. The analytical protocol is to move rapidly to a position just slightly to one side of the centroid of a mass position, to scan across the "peak" the desired number of times while collecting data, to repeat this process for each mass, to average the data collected from several sweeps across all masses of interest, and then to calculate sample composition. The implementation of this technique requires a controller that is electronically switched.

Our system has provision for including up to 16 mass positions in a sweep. Potentiometers on the controller/interface (CI) panel are positioned by the operator so that their potentials (offsets) represent the starting mass positions for a scan. The scan is actually a series of 32 equal steps, the magnitude of the sum of which is the same for all masses. The scan is produced by a digital-to-analog converter whose input is driven by the computer and whose output is summed with the offsets. The desired dwell time at each step is selected on the CI panel and read by the computer during a pre-analysis setup routine.

We use a DEC[2] PDP[2]-11/34 as a program development and data processing computer. As new operating programs are developed on this computer, they can be transferred to DEC MINC[2] computers where they are stored on floppy discs. There is a MINC with each spectrometer. The MINC has a keyboard, video display, dual floppy disc controllers, and four serial input/output (I/O) ports. Parallel I/O is via ADAC, Inc., 1632TTL boards which plug into the bus. Analytical programs are written in FORTRAN. These programs call machine language routines which provide, in conjunction with the CI, the control and data acquisition functions. The system operates under DEC's RT-11. Since RT-11 does not support inter-computer communication, we have written programs to accomplish file and program transfers.

One of the MINC's discs is used for system and operating programs. The second disc is used for data. When all of the data for a sample has been acquired, the operator can call a FORTRAN program which locates the data to be transmitted to the PDP-11/34 and calls a machine language routine that effects the actual transfer. The operator at the PDP-11/34 console then selects the desired calculation programs from a library stored on RK05 discs. The formatted report is printed on an LS120 Decwriter[2] III.

Our present system evolved from an initial effort using a PDP-11/10 computer on a single spectrometer. That system has been operating for nearly four years in the IAEA, Vienna, Austria. Although we are still finding ways to improve our operations, the system described meets our needs for high precision analytical mass spectrometry.

---

[1]Research sponsored by the U. S. Department of Energy, Division of Basic Energy Sciences, under Contract W7405-eng-26 with the Union Carbide Corporation.

[2]DEC, PDP, MINC, DECWRITER are copyrighted trademarks of the Digital Equipment Corporation.

By acceptance of this article, the publisher or recipient acknowledges the U.S. Government's right to retain a non-exclusive, royalty-free license in and to any copyright covering the article.

A SSMS NEAR SURFACE ANALYSIS OF B IN IRRADIATED ZIRCALOY-2: ION IMPLANTATION STANDARDS AS A CALIBRATION TECHNIQUE*

W. H. Christie, J. A. Carter, R. E. Eby, L. Landau
and W. R. Musick
Analytical Chemistry Division
Oak Ridge National Laboratory
Oak Ridge, Tennessee 37830

Ion implantation standards were used to calibrate a spark source mass spectrometer (SSMS) near surface region analytical method. Standards were prepared by ion implanting $^{11}B^+$ at 100 keV into zircaloy-2 at doses in the 3×10^{15} to 3×10^{16} ^{11}B atoms cm^{-2} range. The analytical method was predicated on the idea that both standards and samples could be sparked in a SSMS under essentially identical and reproducible conditions. Calibration plots gave linear log-log results for plots of $^{11}B^+/^{122}Sn^+$ versus B concentration in the standards. Calibration plots were determined on the basis of 5 to 6 replicate determinations for 3 different implant standard concentration levels. A series of irradiated Zircaloy-2 cladding samples were analyzed and shown to contain not more than 0.06 μg cm^{-2} total B in the near surface region.

The point in question in this study was to determine whether or not significant ^{10}B had become permanently associated with the surface of Zircaloy-2 clad irradiated fuel elements that had been stored in an aqueous solution containing 5000 wt. ppm of B, isotopically enriched in ^{10}B. Consideration of the possible physical and chemical consequences of the type of exposure to B that the samples had undergone led to the belief that B penetration was probably limited to 10 μm or less depth in the Zircaloy-2 surface.

SSMS was the method of choice for this analysis because of its demonstrated sensitivity and because our laboratory possessed a SSMS that was specifically modified to handle radioactive samples. A technique that has been shown to produce good surface and analytical standards is the ion implantation method. The method is completely general in that any element can be implanted into a properly prepared surface of almost any solid material in a precisely known dose with a known concentration profile. Consequently, we prepared implantation standards at three different concentration levels using this approach. The pertinent data for these three standards are reported in Table 1.

Table 1. ^{11}B Implant Standards

Std. No.	Implant Dose Atoms/cm^2	ug/cm^2	Peak Conc. Atom %
1	3×10^{16}	0.55	2.6
11	9×10^{15}	0.165	0.78
111	3×10^{15}	0.055	0.26

Secondary ion mass spectrometry (SIMS) was used to verify the $^{11}B^+$ implant relative dose levels in the three standards. SIMS data were taken from a number of locations on the surface of each standard to verify the lateral dose homogeneity. These data are reported in Table 2. The integral count values were used to calculate the ratios shown under the heading SIMS. The ratios under the heading Theory were calculated from the measured ^{11}B dose delivered to each standard during ion implantation. The agreement is within the spread typically observed in SIMS depth profiling studies.

Because the Zircaloy-2 samples were radioactive, small specimens for SSMS analysis were obtained by sawing with an Al_2O_3 cut-off wheel in a hot cell. Blanks were prepared from unirradiated samples at the same time. The specimens, blanks, and implantation standards were then subjected to SSMS analysis. The group integrity was maintained so that the SSMS data for each group of specimens, its blank, and implantation standard were contained on a single photoplate.

The sparking technique used for analysis of the standards and sample specimens consisted of making a 0.03 nC exposure using a 25 μsec pulse length at a 30 Hz repetition

*Research sponsored by the U. S. Department of Energy, Division of Basic Energy Sciences, under contract W7405-eng-26 with the Union Carbide Corporation.

Table 2. ^{11}B in Zircaloy-2 Implantation Standards

	^{11}B Integral Counts X 1000			Ratios		
	Std I	Std II	Std III	Stds	SIMS	Theory
	1441	398.6	138.7	(I/III)	10.9	10.0
	1344	388.4	105.8			
	1180	322.3	125.1	(II/III)	3.0	3.0
	1493	384.7	124.9			
	1281	399.8		(I/II)	3.5	3.3
	1463	390.0				
	1200					
Avg.	1343	380.6	123.6			

rate at 30 kV peak-to-peak spark voltage. This was repeated at five locations on a specimen surface while integrating all transmitted ions at a single photoplate rack position to give a total exposure of 0.15 nC. A single 0.03 nC exposure created a crater on the Zircaloy surface that was generally 0.5 to 0.7 mm in diameter. The depth of this crater was visually estimated to be about 10% of the crater diameter using an optical microscope.

The ratio of the intensities $^{11}B^+/^{122}Sn^+$ was used as a calculation indexing technique for these samples. The isotope ^{122}Sn (a component of Zircaloy-2) produced photoplate line intensities suitable for ratioing to the ^{11}B line from the implant standards. Replicate values of this ratio for the three implant standards are listed in Table 3.

Table 3. SSMS Observed $^{11}B^+/^{122}Sn^+$ Ratios from ^{11}B Ion Implantation Standards

	Std I 0.55 ug/cm $^{11}B^+/^{122}Sn^+$	Std II 0.165 ug/cm $^{11}B^+/^{122}Sn^+$	Std III 0.055 ug/cm $^{11}B^+/^{122}Sn^+$
	6.48	1.50	1.11
	5.21	1.41	1.06
	3.05	1.28	0.88
	3.40	3.23	0.97
	4.06	2.37	1.20
	5.96	2.85	0.93
Avg.	4.69 ±1.4*	2.11 ± .83	1.02 ± .11

*Standard Deviation (1σ).

The average values of the ratio were used to construct a linear log-log standard response curve (plotting the average ratio versus the ^{11}B concentration in the standard). This working curve technique was used to determine the boron concentration present in the near surface region of the irradiated Zircaloy-2 unknowns. The results indicated that none of the samples were contaminated with ^{10}B at levels greater than 0.06 μg cm^{-2}. A detailed account of this work has been published (1).

By acceptance of this article, the publisher or recipient acknowledges the U.S. Government's right to retain a non-exclusive, royalty-free license in and to any copyright covering the article.

(1) Anal. Lett. 12(A10), 1123 (1979).

FAMOC 11 DECONVOLUTION OF PEAK SEQUENCES BASED ON ISOTOPE DISTRIBUTION

J. van Katwijk, Koninklijke/Shell-Laboratorium, Amsterdam (Shell Research B.V.)
Badhuisweg 3, 1031 CM Amsterdam, THE NETHERLANDS

1. INTRODUCTION

The mass spectrometric analysis of complex mixtures, e.g. petroleum fractions, poses a special problem as one has to account for every peak in order to obtain a quantitative breakdown of the sample. With the currently attainable resolving power and the available fractionating techniques, optimization of the interpretation procedures is imperative. This paper deals with the use of a combination of two sources of information: the known intensity distribution in isotope clusters and the shapes of the peaks. Each of these separately had already received attention at an earlier stage[1,2,3].

Particularly in cases where the peak due to an ion species is influenced by isotope contributions from other compounds present in larger quantities, one is bound to introduce errors when treating a high-resolution mass spectrum as a series of unrelated precision mass measurements, as is done in the conventional centroid technique. Figure 1 demonstrates that even at a resolving power of 30 000 the peak of the hydrocarbon $C_{41}H_{56}$ will be overlooked due to influences of species with their major contribution at lower masses.

2. PRINCIPLE OF THE NEW METHOD

In order to correct for the (predictable) influences of isotope contributions we developed an evaluation method which uses the data collected over three nominal mass values in one calculation step. This method will be elucidated with special reference to Figure 2 and can be summarized as follows:

(1) Collect from a high-resolution mass spectrum the intensities of all data samples which belong to relevant peaks over three nominal mass values.

(2) Search out the formulae of candidate ion species whose mass values are within the mass ranges of the peak bases (combinations of main isotopes only). Measured trace and candidate ion species are in part A of Figure 2.

(3) Determine of each of the possibilities the relative contributions of main and isotope peaks to the data set, assuming Gaussian peak shapes (Figure 2B).

(4) Calculate the intensities of the candidate ion species which show the best agreement between measured and calculated trace.

In actual practice all information is available in digital form. For each data sample we can write the following equation:

$$y_n = a_{n,1}x_1 + a_{n,2}x_2 + \dots\dots\dots + a_{n,m}x_m$$

where y = the measured ion intensity at data sample n,

$a_{n,m}$ = the relative contribution of ion species m to data sample n, and

x_m = the relative concentration of ion species m.

As the number of data samples n is far greater than the number of possible compounds m we can apply a least squares calculation in order to obtain the best values for the relative intensities.

3. APPLICATION

This procedure was applied to a concentrate of polycyclic aromatics with a high sulphur content. The sample was run on the Varian MAT 731 mass spectrometer with data collection as described by Markwardt[4]. All subsequent calculations were carried out with a Sigma 7 computer. The scan time was 2356s for a mass decade with an amplifier bandwidth of 1000 Hz. Figure 3 shows an example of the measured and calculated traces of one of the peaks in this sample.

4. CONCLUSIONS

Application of this procedure to several samples has shown that there is every

reason to consider the peak shapes, which if carefully recorded, contain essential information. Actually it is our experience that in cases where we find large mass deviations, using the centroid technique, it is usually this technique rather than the mass spectrometer recording that is to blame. An additional feature of this technique is a built-in-check on the quality of the results. Faulty instrument performance or incorrect calculation parameters are readily detected.

5. REFERENCES

1. A.L. Burlingame, "Recent Developments in Mass Spectroscopy", Koreicichi Ogata and Teruo Hayakawa, ed., University of Tokyo Press, 1970.
2. Renchagari Vendataraghavan, F.W. McLafferty and J.W. Amy, Anal. Chem. 39 (1967) 178.
3. D.D. Tunnicliff and P.A. Wadsworth, Anal. Chem. 40 (1968) 1826.
4. U. Markwardt, Messtechnik, 78 (1970) 13.

PUBL. 80.039

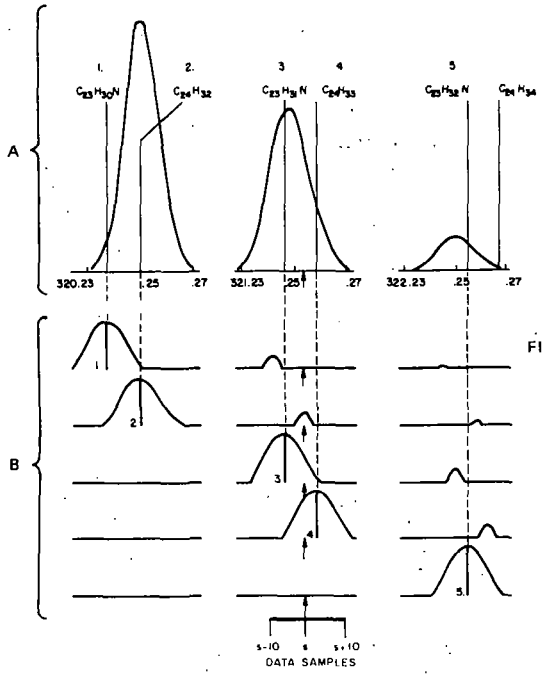

A MEASURED MASS SPECTRAL TRACE

B CALCULATED TRACES FOR FIVE CANDIDATE ION SPECIES

FIG. 2: EXAMPLE OF EVALUATION OF PART OF A HIGH RESOLUTION MASS SPECTRUM WITH INVESTIGATION OF PEAK SHAPES AND ISOTOPE CONTRIBUTIONS

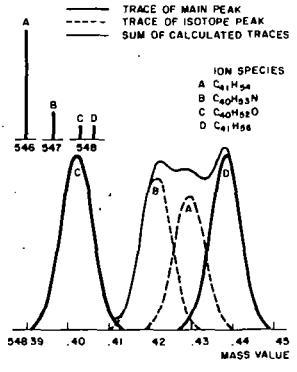

FIG. 1: SIMULATED MASS SPECTRAL TRACE

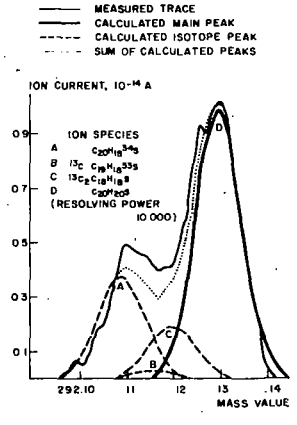

FIG. 3: MEASURED AND CALCULATED MASS SPECTRAL TRACES

DRAWN Dr
DWG 80.05.2000

DECONVOLUTION OF MASS SPECTROMETER DATA, JULIETTE W. IOUP,* Physics/Pre-Engineering Department, Xavier University, New Orleans, LA, 70125; GEORGE M. WOOD, JR., NASA Langley Research Center, Hampton, VA, 23665; BILLY T. UPCHURCH, Dept. of Chemistry, Old Dominion Univ., Norfolk, VA, 23508; GEORGE E. IOUP,** Dept. of Physics, Univ. of New Orleans, New Orleans, LA 70122; and GRAYSON H. RAYBORN, JR., Dept. of Physics, Univ. of Southern Mississippi, Hattiesburg, MS, 39401

Mass spectrometer data in the form of percent transmission of ions versus mass number may include overlapping mass peaks. For such data, the identification of masses and their relative abundances can be difficult. Peak locations and areas are necessary, and the overlap often prevents accurate evaluation. Effective increase of the resolution of the data by numerical deconvolution can increase the separation of overlapping peaks and lead to improved analysis.[1-3]

In this work two approaches to deconvolution have been used: a function domain iterative technique[1,2,4-8] and a Fourier transform method which uses transform domain function continuation.[9,10] The iterative technique is based on Morrison's noise removal[1,5,6] and van Cittert's deconvolution.[1,2,4,6,7,11] A major difficulty of the iterations is that they do not converge for many instrument response functions.[1,2,4,12] The iterative approach has been modified so that convergence is achieved.[8] The Fourier method uses transform domain inverse filtering and the transform of an artificial function to replace the high frequency part of the inverse solution.[9,10] A transition region is defined so that the two may be smoothly joined. Computer algorithms and codes have been developed for both these approaches.

To test the deconvolution procedures, data were obtained from a magnetic mass spectrometer operated in both high and low resolution modes. Low resolution data with overlapping peaks have been deconvolved and compared with the data taken at high resolution (better than 1 part in 2500).

Fig. 1 shows narrow slit data (Curve A) and wide slit data (Curve B) for an O and CH_4 mixture. An isolated mass peak for argon was used to deduce the response function for the wide slit case. Both the Fourier method (Curve C) and the iterative technique (Curve D) show two mass peaks after deconvolution of the low resolution data and are in good agreement with the high resolution result. (Exact alignment was not simply attainable because the data sampling interval was not fine enough. The skewed shapes of the narrow slit data are effects of instrument operating conditions.) It would not be possible to anticipate this result solely from visual inspection of the wide slit data.

Fig. 2 is the same case, with Curves A and B as in Fig. 1. Curve C shows straightforward Fourier deconvolution (inverse filtering) combined with ideal low pass filtering. Curve D is the same as Curve C of Fig. 1. It is the result of fitting an artificial function to Curve C of Fig. 2 and then using the artificial function transform to continue the low pass filtered Fourier deconvolution to higher frequencies.

For the data of Fig. 3 a different mixture of O and CH_4 was used. Again Curve A is the narrow slit data while Curve B gives that taken with a wide slit. Curve C is an iterative deconvolution of the narrow slit data while Curve D is an iterative deconvolution of the wide slit data. Although the narrow slit deconvolution is further resolved, the two results are in good agreement. (Again, exact alignment is not achieved because of the coarse sampling.) Not even the high resolution data gives as much information on the smaller peak as the deconvolved low resolution data.

Fig. 4 illustrates a run with five masses present: $O, C^{12}H_4$, $C^{13}H_3$, $N^{14}H_2$, and $N^{15}H$ (Curve A). Both the iterative deconvolution (Curve B) and the Fourier result (Curve C) show all five peaks and are in fairly close agreement, whereas the original data had only two peaks resolved. (None of the Fourier results have been normalized to the original curve areas.)

Although further development is necessary before the use of the methods will be routine, both show significant promise for applications in mass spectrometry.

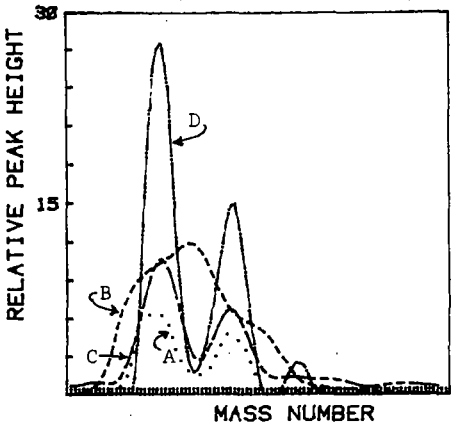

Fig. 1

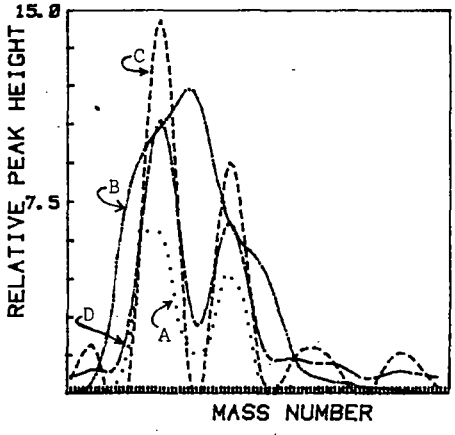

Fig. 2

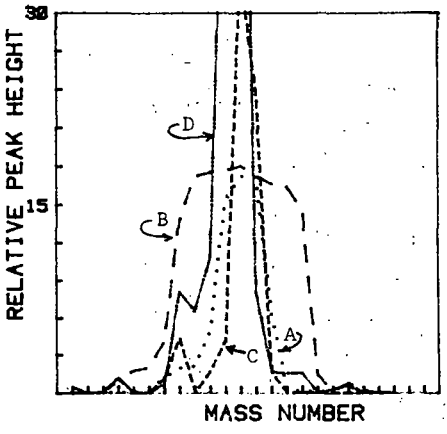

Fig. 3

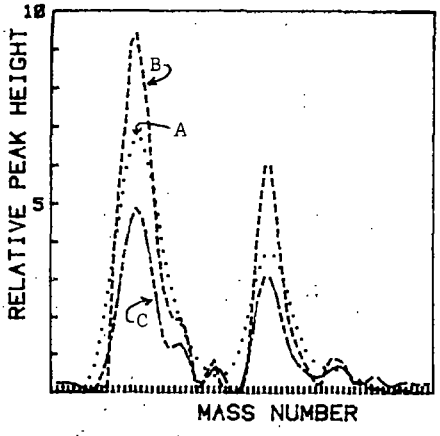

Fig. 4

*Supported in part by NASA Research Grants NSG-1361 and NAG 1-16.
**Supported in part by NASA Research Grant NSG 1460.

[1]G.E.Ioup, Analysis of Low Energy Atomic and Molecular Collisions: Semi-classical Elastic Scattering Calculations and Deconvolution of Data, Ph.D. Dissertation, Univ. of Fla., 1968
[2]B.R.Frieden, Image Enhancement and Restoration, in T.S.Huang, ed., Picture Processing and Digital Filtering, Vol. 6, Topics in Applied Physics, Springer-Verlag, Berlin, 1975
[3]S.G.Rautian, Sov. Phys.-Usp. 66, 245 (1958)
[4]R.N.Bracewell and J.A.Roberts, Australian J. Phys. 7, 615 (1954)
[5]J.D.Morrison, J. Chem. Phys. 39, 200 (1963)
[6]G.E.Ioup and B.S.Thomas, J. Chem. Phys. 46, 3959 (1967)
[7]P.A.Janssen, J. Op. Soc. Am. 60, 184 (1970)
[8]G.E.Ioup (in preparation)
[9]S.J.Howard, New Techniques in Fourier Deconvolution of Gas Chromatographic Data, Master's Thesis, Univ. of Southern Miss., 1978
[10]S. Howard and G.H.Rayborn, NASA Contractor Report 3229, 1980
[11]P.H. van Cittert, Z. Physik 69, 298 (1931)
[12]N.R.Hill and G.E.Ioup, J. Opt. Soc. Am. 66, 487 (1976)

FAMP1 MEASUREMENT OF OXYGEN ISOTOPE EXCHANGE IN VIVO AS AN INDEX OF BIOLOGICAL ACTIVITY.

K.L. CLAY and R.C. MURPHY. University of Colorado Medical Center, Denver, Colo 80262

Amino acids labelled in the carboxyl moiety with oxygen-18 can be readily prepared by acid catalyzed exchange in ^{18}O-H_2O and are well-suited as internal standards in GC-MS quantitation procedures. In vivo, however, a rapid exchange of carboxyl oxygen atoms with the aqueous milieu has been observed. At pH 1-2 and at room temperature, $^{18}O_2$-leucine back exchange has a half life of about 13 days. In a suspension of rat erthrocytes, the back exchange has a half life of approximately 4 hours. At 4° C, $^{18}O_2$-tyrosine in an erythrocyte suspension showed no evidence for back exchange, but back exchange was quite rapid at 37°. The back exchange in vivo is stereospecific in contrast to the chemical exchange. D-stereoisomers of many amino acids have been labelled with ^{18}O and then incubated with cell suspensions, but none has exhibited any back exchange. The corresponding L-isomers, however, have all undergone back exchange in the presence of cells, with the exception of $^{18}O_4$-L-aspartic acid. The reaction is not limited to blood cells, but has been observed to occur in many tissues and cell types, including mastocytoma cells and hepatoma cells maintained in monolayer tissue culture. The back exchange in vivo can be effectively inhibited by other amino acids and appears to exhibit saturation kinetics. Taken as a whole, the data is consistent with the hypothesis that the back exchange is occurring during, or as a consequence of, amino acid transport. The implication of these observations for a molecular mechanism of amino acid transport will be discussed.

FAMP2 DEUTERIUM ISOTOPE EFFECTS IN THE DEAMINATION OF PUTRESCINE WITH DIAMINE OXIDASE, E.M. Jakubowski and P.S. Callery, Dept. of Medicinal Chem./Pharmacognosy, University of Maryland, Baltimore, Md. 21201

The biosynthesis and catabolism of putrescine (1,4-diaminobutane) is thought to be closely related to regulation of the growth and proliferation of mammalian cells. Diamine oxidase catalyzes the oxidative deamination of putrescine to yield 4-aminobutyraldehyde which spontaneously cyclizes to Δ^1-pyrroline. The purpose of the current studies is to provide information on the mechanism of action of diamine oxidase through the analysis of isotope effects. 1,1,4,4-$^2H_4$-putrescine was synthesized by the catalytic reduction (PtO) of succinonitrile with deuterium gas. Putrescine and $^2H_4$-putrescine in varying concentrations were incubated with commercial purified hog kidney diamine oxidase in pH 6.8 phosphate buffer for 60 minutes at 38°C in the presence of 2-aminobenzaldehyde as derivatizing reagent. Formation of Δ^1-pyrroline was monitored spectrophotometrically as the derivative 2,3-trimethylene-1,2-dihyroquinazolinium hydroxide. The calculated isotope effect for $^2H_4$-putrescine expressed as a k_H/k_D ratio was 1.4. In order to differentiate between the influence of the deuterium atoms at C-1 and C-4, 1,1-$^2H_2$-putrescine was prepared. Condensation of potassium phthalimide with 4-chlorobutyronitrile gave 4-phthalimidobutyronitrile. Reduction with deuterium gas followed by hydrolysis in acid yielded 1,1-$^2H_2$-putrescine as the dihydrochloride salt.

LOCATION OF DEUTERIUM LABEL IN BIOSYNTHESIZED BIOTINE : I. USE OF LINKED SCAN AND MIKES TECHNIQUES TO STUDY THE ORIGIN AND STRUCTURE OF THE ION m/z 166.

D. FRAISSE, F. FRAPPIER, M. JOUANY, A. MARQUET AND J.C. TABET

CENTRE DE SPECTROMÉTRIE DE MASSE - SERVICE CENTRAL D'ANALYSE
B.P. 22 - VERNAISON - FRANCE

EI MASS SPECTROMETRY HAS BEEN USED TO DETERMINE THE LOCATION OF DEUTERIUM ATOM IN POSITION AND TO THE SULFUR ATOM IN BIOTINE BIOSYNTHESIZED FROM DEUTERATED DITHIOBIOTINE. THE ION AT M/Z 184 (A) GIVES INFORMATION ABOUT DEUTERIUM POSITION ON THE SULFUR CONTAINING RING, WHILE THE ION AT M/Z 185 DUE TO THE LOSS OF THE RADICAL .CH2COOR FROM $M^{+\cdot}$ INTERFERED WITH BY ISOTOPE ION A, DOES NOT ALLOW ACCURATE MEASUREMENTS. THEREFORE FRAGMENTATION PATTERN OF BIOTINE METHYL ESTER HAS BEEN INVESTIGATED. IN THIS CASE THE ION AT M/Z 184 SHIFTS TO M/Z 198 AND NO LONGER INTERFERES WITH ION AT M/Z 185 (B). THE EI MASS SPECTRA OF MONO AND DI-DEUTERATED BIOTINE METHYL ESTER SHOW THAT THE ION ET M/Z 185 SHIFTS TO M/Z 186 AND M/Z 187. BUT THE PERCENTAGE OF THE ION AT M/Z 198 SHIFTING TO M/Z 200 IS ONLY 40 % IN THE BIOTINE -1,1D2 METHYL ESTER MASS SPECTRUM ; THIS OBSERVATION SUGGESTS THE PRESENCE OF TWO ISOBAR IONS AT M/Z 198. ELEMENTAL COMPOSITIONS OF THESE IONS HAVE BEEN DETERMINED. IN ANY CASE THE PRESENCE OF TWO IONS AT M/Z 198 PRECLUDES THE USE OF THIS ION IN THE ACCURATE DETERMINATION OF DEUTERIUM. THE ONLY ION INTENSE ENOUGH TO BE USED FOR THE DETERMINATION OF DEUTERIUM POSITION OCCURS AT M/Z 166. THE ORIGIN AND STRUCTURE OF M/Z 166 HAVE BEEN INVESTIGATED USING LINKED SCAN AND MIKES TECHNIQUES. THE MASS SPECTRA OF DEUTERIUM LABELLED COMPOUNDS CONFIRM THE UNIQUE ORIGIN OF ION M/Z 166 THAT ALLOWS SPECIFIC DETERMINATION OF DEUTERIUM IN BIOSYNTHESIZED BIOTINE.

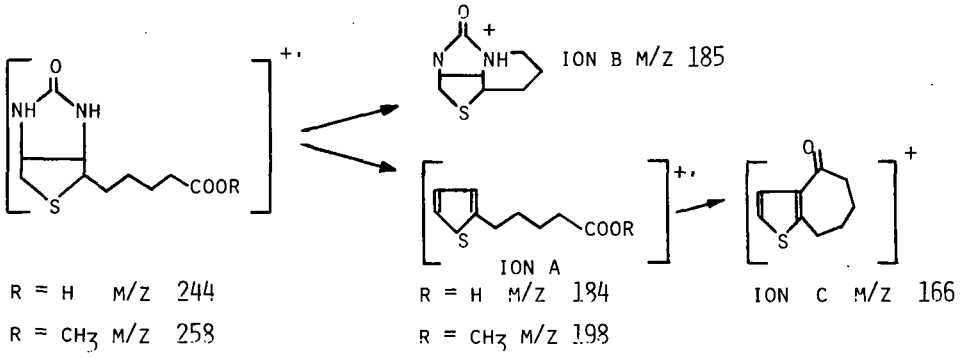

FAMP4 MASS SPECTRAL APPROACHES TO GLYCOCONJUGATE ANALYSIS; SENSITIVITY STUDIES,

V. N. REINHOLD, Dept. of Biological Chemistry, Harvard University Medical School, Boston, MA

An understanding of carbohydrate involvement in the biological processess of adhesion and cell sociability requires better analytical methodology. Demands of sensitivity as well as specificity in the analysis of carbohydrate components as regards to composition and sequence arrangement have initiated studies comparing alternative derivatization methods and ionization techniques. Glycolipids, glycoproteins and bacterial oligosaccharides are under investigation in this laboratory. Samples prepared as methyl glycosides for composition analysis or as methylated alditols and alditol nitriles, as products of linkage studies, have been derivatized with selected fluoronated reagents to enhance volatility and detectability. Methylated alditol nitriles prepared from the corresponding oximes by trifluoracetylation are suitable derivatives for linkage studies when analyzed by gas chromatography and fragmented by electron impact ionization. The nitrile group at position one avoids the possibility of molecular symmetry with certain of the methylated derivatives and the position of methylation (non-linked hydroxyl in the original polymer) is easy to interpretate from the fragmentation pattern. Negative ion production from these derivatives is markedly diminished but appears to be enhanced by chemical ionization and negative ion analysis. We have applied this latter approach to maximize our sensitivity in these glycoconjugate studies.

NEGATIVE CHEMICAL IONIZATION SPECTRA OF SOME GLUCURONIDES, INTRODUCED BY THERMAL DESORPTION FROM A PLATINUM WIRE INSIDE THE CI SOURCE, ANDRIES P. BRUINS, Dept. of Pharmacy, State University, A. Deusinglaan 2, 9713 AW Groningen, The Netherlands.

Field desorption is a widely used method for taking mass spectra of nonvolatile substances. The availability of this technique is however limited to users of larger magnetic sector instruments. As a consequence, the development of improved sample handling techniques that can also be used in small routine GC-MS systems with EI/CI sources, evolves rapidly[1]. Varian MAT and Ribermag (France)[2] offer the desorption CI method as an optional extra for their instruments. A sample is deposited on a bare rhenium or tungsten wire and is desorbed inside the CI source by passing a current through the wire. Excellent spectra of difficult molecules have been presented.

A similar probe of simple construction, of which a platinum wire is the essential part, has been made in our laboratory[3]. The combination of this probe with OH^- negative CI[5] has successfully been applied to polyhydroxylated substances (sucrose, glycosides from digitalis[4]). It was a logical step to explore the potential of OH^- CI further and glucuronides were chosen because of the interest in drug metabolism in our department.

Molecular weight information is expected from the $[M-H]^-$ ion produced by proton abstraction, while structural information is expected from the cleavage of the C-O bond between glucuronic acid and, for example a steroid, by nucleophilic substitution, by base induced elimination, or by unimolecular decomposition of the $[M-H]^-$ ion.

The spectrum of o-aminophenyl-β-D-glucuronide shows the $[M-H]^-$ ion as the base peak, while the o-aminophenolate anion (m/z 108) has a relative abundance of 25 %.

The $[M-H]^-$ ion of 4-methylumbelliferyl-β-D-glucuronide has a relative abundance of only 20 %, and m/z 175 (4-methylumbelliferone - H) is the base peak.

The spectrum of p-nitrophenyl-β-D-glucuronide differs markedly from the two examples above: electron capture is more efficient than proton abstraction, the most abundant peaks (>5 %) are:

$M^{-\cdot}$	m/z	315	85 %
$[M-H]^-$		314	25
$[M-OH]^-$		298	100
p-nitrophenol$^{-\cdot}$		139	30
p-nitrophenolate		138	50

The spectra of five steroid glucuronides (purchased from Sigma) all showed the $[M-H]^-$ ion as the base peak, loss of water from this ion amounted to a maximum of 20 % and the fragment ion corresponding with the hydroxysteroid - H was observed with

a relative abundance varying from 25 to 90 %.

The appearance of the spectra is greatly dependent on the current passed through the Pt wire. At high currents fragmentation becomes excessive, and the 'best' spectrum is generally obtained before the maximum of the total ion current has been reached.

Desorption chemical ionization with OH^- as the reactant ion provides a viable alternative for field desorption of underivatized glucuronides. The same is true for desorption CI with isobutane as the reactant gas or protonated pyridine as the reactant ion[6,7]. In practice the presence of interfering compounds in biological extracts will probably determine which method will give the best spectra.

1. G.D. Daves, Acc. Chem. Res. 1979, 12, 359-365.
2. P.J. Arpino and G. Devant, Analusis 1979, 7, 348-354.
3. A.P. Bruins, Anal. Chem. 1980, 52, 605-607.
4. A.P. Bruins, paper presented at the 8th International Mass Spectrometry Conference, Oslo, Norway, 1979, Adv. Mass Spectrom. in press.
5. A.L.C. Smit and F.H. Field, J. Am. Chem. Soc. 1977, 99, 6471.
6. R.J. Cotter, Anal. Chem. 1979, 51, 317.
7. C. Fenselau, R.J. Cotter and L. Johnson, paper presented at the 8th International Mass Spectrometry Conference, Oslo 1979.

OPENING OF THE BAY-REGION DIOL-EPOXIDE IN POLYCYCLIC AROMATIC HYDROCARBONS

Lan K. Wong and Jinn Wu
Department of Pharmaceutics, University of Pittsburgh, Pittsburgh, PA 15261 and
Department of Pharmacology, Ohio State University, Columbus, OH 43210

The carcinogenicity of many polycyclic aromatic hydrocarbons (PAH) has been attributed to the bay-region diol-epoxide metabolites of these compounds. A bay-region diol-epoxide is an epoxide situated at the angular ring of a PAH which has undergone prior diol formation. It is uniquely different from other epoxides of PAH in that it is an aliphatic epoxide as supposed to an arene oxide. Theoretical calculations predict that it has a notably higher tendency to form a bay-region carbonium which then interacts with cellular macromolecules in the carcinogenic or mutagenic process. In this study, we have employed 3,4-dihydroxy-1,2-epoxy-1,2,3,4-tetrahydrobenz[a]anthracene (i.e., the bay-region diol-epoxy of benz[a] anthracene) as the model compound. We studied the solvolysis of this bay-region diol-epoxide in methanol by GC-MS analysis.

The mass spectrum (fig. a) of the trimethylsilyl ether derivative of the 1,2,3,4-tetrahydrotetraol shows a molecular ion at m/z 584. The base peak is at m/z 380, indicative of a facile retro-Diels-Alder (RDA) fragmentation ion. The prominent ion at m/z 191 is a di-(trimethylsilyloxyl) ion reminiscent of a vicinial dihydrodiol moiety present at a non K-region location of the polycyclic skeleton (Wong et al, Biomed. Mass Spec. 6, 305). Since the RDA fragment retains the substituents at C_1, it is useful for determining the orientation of the oxirane ring opening process for the bay-region epoxide. If a nucleophile should attack the bay-region epoxide at C_1 as predicted by the bay-region hypothesis of carcinogenesis, the RDA fragment should reflect the formation of such an adduct at that particular site of the molecule.

The product from the methanolysis of the benz[a]anthracene bay-region diol-epoxide (I) was consonant with the bay-region hypothesis. As shown in its mass spectrum (fig. b), this compound has the expected molecular ion at m/z 526 signifying the introduction of a methoxyl group. The RDA fragment was found at m/z 322 which clearly indicated that the attack of methanol occurred at the C_1 position. The base peak at m/z 133 is attributed to a methoxy-trimethylsilyloxy ion similar to the m/z 191 ion for the di-(trimethylsilyloxyl) fragment.

We have also investigated the methanolysis of the 1,2-dihydrodiol-3,4-epoxide of benz[a]anthracene, a non bay-region diol-epoxide analogue. The mass spectrum (fig. c) of the methanolysed product revealed that the methoxyl group was introduced to C_4 of the epoxide. This is again consistent with the theoretical prediction that the benzylic position at C_4 would be more reactive than C_3. Theoretical calculations also indicated that the bay-region diol-epoxide (I) should be more reactive than the non bay-region 1,2-dihydrodiol-3,4-epoxide. This is in parallel with the observed mutagenicity of these ring A epoxides. In our experiments, we observed that after 2 hrs., the bay-region diol-epoxide underwent about 40% conversion to its methanolate while the non bay-region analogue underwent less than 0.1% conversion. These experimental data clearly show that the C_1 position of the benz[a]anthracene bay-region diol-epoxide is particularly reactive. The RDA fragment noted in this report is particularly suited for the characterization of diol-epoxide biomolecular adducts postulated in the carcinogenic process of these compounds. (This work was supported by a NCI grant CA27928.)

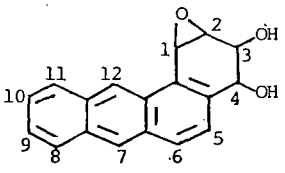

I

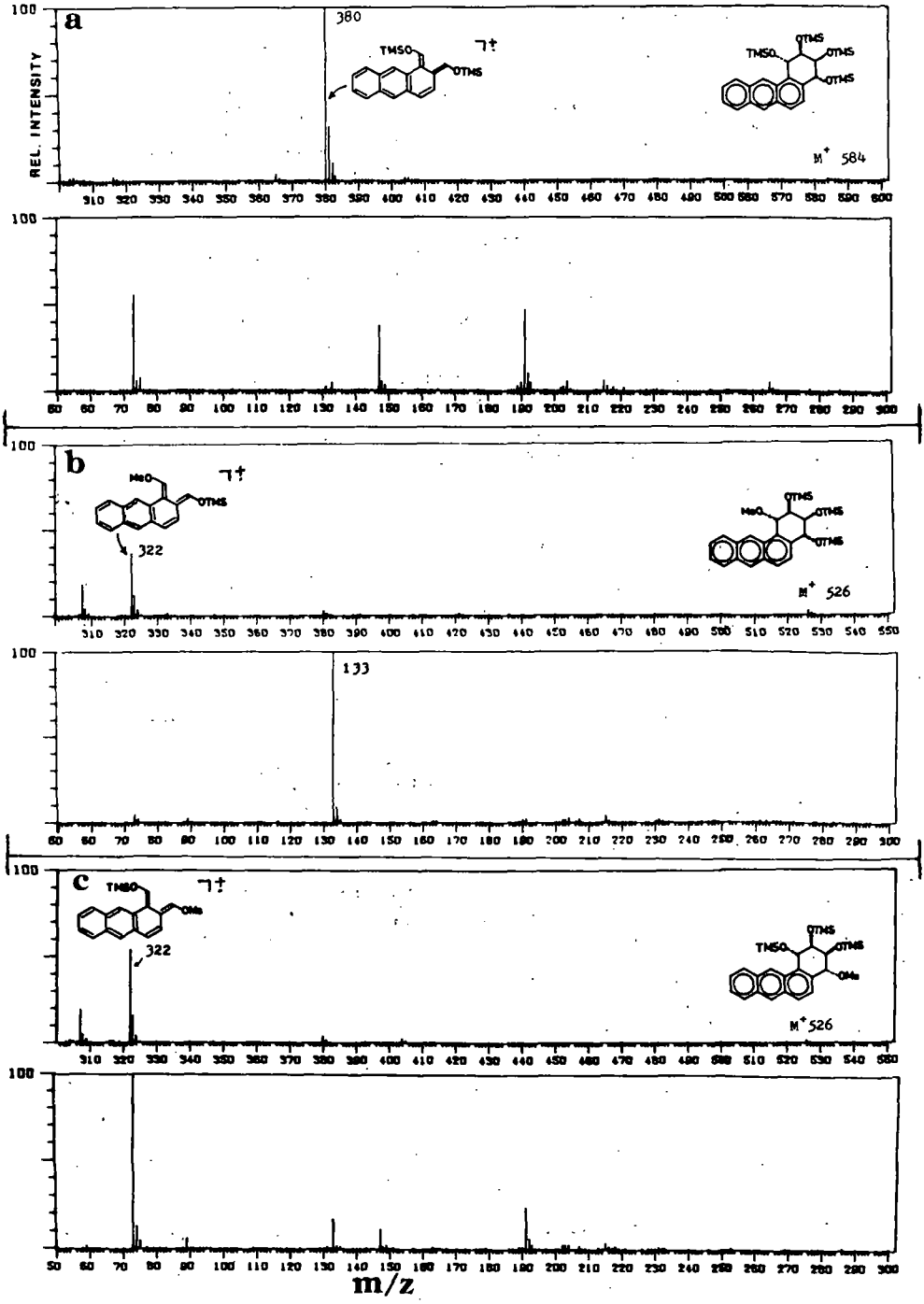
a
380
TMSO
OTMS
M+ 584
REL. INTENSITY
b
MeO
OTMS
322
M+ 526
133
c
TMSO
OMe
322
M+ 526
m/z

THE MASS SPECTRAL CHARACTERIZATION OF DITHIASUCCINOYL (DTS) AMINES AND AMINO ACIDS (1)

GEORGE BARANY (2), D.V. BOWEN (3), R.B. MERRIFIELD, and F.H. FIELD
The Rockefeller University, New York, N.Y. 10021

As part of our program to develop the dithiasuccinoyl (Dts) protecting group for amines and α-amino acids (4,5), we relied extensively on electron-impact and chemical ionization mass spectrometry for proving the structures of these novel sulfur-containing heterocycles. Ion compositions were verified by high resolution mass measurements and isotope clustering patterns.

In EIMS, molecular ions were obtained for essentially all Dts compounds tested. Samples were introduced by direct probe insertion, with source temperatures as low as possible (usually 100° - 130° C). Higher temperatures or different handling procedures generally led to greatly reduced amounts of molecular ions, and extensive decomposition and fragmentation. The base ion was usually $S_2^{+\cdot}$, at m/e 64, and the principal neutral losses characteristic of the Dts ring were (a) elimination of carbon monoxide (M - 28); (b) elimination of a second equivalent of carbon monoxide (M - 56); (c) loss of carbonyl sulfide and sulfur (M - 92) giving rise to an isocyanate ion; and (d) loss of two carbonyl sulfide molecules (M - 120) to produce an imine fragment (observed in one case). Fragmentation (b) was somewhat surprising, but has been established experimentally beyond a doubt. Since controls showed that N^{α}-protected amino acids and their esters did not themselves lose carbon monoxide, it was concluded that both carbon monoxide equivalents were derived from the heterocycle. The fragmentation was best reconciled with the proposed Dts structure by assuming a rearrangement involving sulfur migration.

As already mentioned, the Dts ring was sufficiently stable upon electron impact in the gaseous phase to permit formation of molecular ions. The ring also remained intact in two additional fragmentations that have been described (6) as characteristic for N^{α}-protected amino acids and their esters: (e) loss of an alkoxy radical to form an acylium ion; and (f) α-cleavage to produce a Dts-imine fragment [these are, respectively, $M^{+\cdot} - {}^{\cdot}OR'$ and $M^{+\cdot} - {}^{\cdot}CO_2R'$ in Figure of the CIMS shown below on this page]. Finally, a major process in the EIMS of all phenylalanine derivatives, which was not found in any other cases, was (g) cleavage at the N^{α}-C^{α} bond, with removal of the entire dithiazolidine ring (M - 134, M - 135). This particular fragmentation is most likely side-chain dependent.

Upon isobutane CIMS, quasi-molecular $(M + 1)^+$ ions were generally the base peak, and fragmentations were observed giving the (a) protonated isocyanate; (b) protonated imine ester; and (c) acylium ions (Figure). At higher temperatures, the isocyanate and imine ester ions became the base peaks, and the fragmentation ions of elemental sulfur ($S_n^{+\cdot}$, n = 2-8) became prominent.

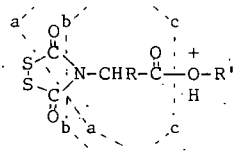

(a) $O{=}C{=}\overset{+}{N}(H)\text{-}CHR\text{-}CO_2R'$

(b) $H_2\overset{+}{N}{=}CR\text{-}CO_2R'$

(c) $Dts\text{-}N\text{-}CHR\text{-}C{\equiv}O^+$

In CIMS, the fragmentation ions of Dts-amino acid derivatives were the same as some of those we described earlier (6) as arising from N^{α}-urethane amino acid derivatives. In contradistinction to the case noted above in the EIMS, loss of carbon monoxide from the Dts heterocycle did not appear to be an important process in the CIMS.

Mass spectrometry was also of great utility in a systematic investigation of the course of synthetic reactions used to prepare Dts-amines and amino acids. The reaction (7,8) of alkoxythiocarbonyl-amines (I) with chlorocarbonylsulfenyl chloride (II) yielded not only Dts-amines (III), but also a variety of low-level impurities as originally evidenced by NMR and GC of crude product mixtures.

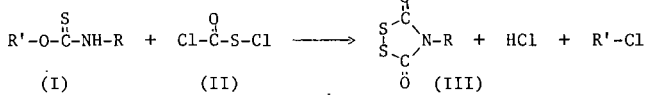

Structural formulas for by-products of this reaction were proposed on the basis of GC/MS experiments. All of these structures (IV, V, and VI; see following page) were proven by alternative syntheses of the authentic compounds by unambiguous routes, followed by comparisons of NMR and mass spectra, and by GC-cochromatography (4). Also, once the by-product structures had been elucidated, e.g. the 1,2,4-thiadiazolidine-3,5-dione (IV),

their appropriate molecular ions were occasionally revealed in a retrospective examination of the high resolution EIMS of the crude product mixtures from syntheses of (III).

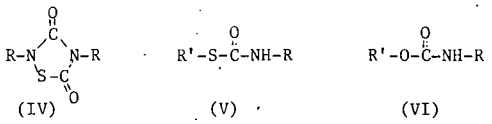

(IV) (V) (VI)

As an instructive prototype example, the identification of (V), which is the thermodynamically more stable isomer of the starting material (I) of the synthetic reaction diagrammed on the previous page, is shown for R = CH_3, R' = C_2H_5.

Ion	m/e	Relative Intensity (%)		
		$CH_3NHC(=S)OC_2H_5$ [a]	$CH_3NHC(=O)SC_2H_5$ [a]	GC-component [b]
$M^{+\cdot}$	119	87	34	71
$CH_3NHCS^+ = M^{+\cdot} - C_2H_5O^\cdot$	74	42	-	-
$C_2H_5SH^{+\cdot}$	62	11	41	56
$CH_3NHCO^+ = M^{+\cdot} - C_2H_5S^\cdot$	58	100	100	100

[a] Introduced by gas handling system; source temperature 140° C. Electron ionization results were relatively temperature insensitive.

[b] GC-EIMS: 3% OV-17 (5 ft. column), He flow rate 25 ml/min. Column temperature raised from 50° to 130° C at 8° per min. Elution time of unknown component was 5.7 min. It cochromatographed with the thiourethane (V), and appeared as a separate peak just before starting thionourethane (I) when these were coinjected. Source temperature for EIMS was 180° C.

Urethanes are characteristically cleaved (6) at the carbamyl-heteroatom bond to yield a protonated isocyanate or isothiocyanate ion (see Equation). Alkoxythiocarbonyl-amines (I)

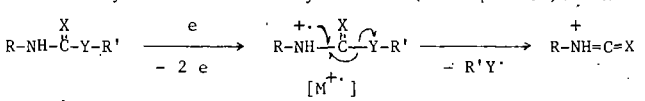

X,Y = O,S

undergo an unusual fragmentation insofar as the observed losses include not only the predicted loss of an alkoxy radical, but also, most strikingly, the loss of an alkylthio radical as well. In contrast, the isomeric (alkylthio)carbonyl-amines (V) fragment specifically with only the loss of an alkylthio radical, as predicted. These patterns are clearly seen in the above Table.

The knowledge of the structures of the impurities IV, V, and VI that contaminate preparations of desired Dts derivatives III has suggested some modified synthetic procedures which should circumvent the formation or isolation of the by-products altogether.

Our investigations, highlighted in this and a previous report (6), have demonstrated the value of mass spectrometry for addressing complex issues of product analysis and quality control in amino acid and peptide chemistry.

REFERENCES AND NOTES:

(1) Supported by the Division of Research Resources, N.I.H., RR 841 to F.H. Field.
(2) Present address: Department of Chemistry, University of Minnesota, Minneapolis, MN 55455.
(3) Present address: Union Carbide Corporation, Tarrytown, New York 10591.
(4) George Barany, Ph.D. thesis, The Rockefeller University, New York, 1977. Dissertation Abstr. 38, 5893-B. Consult this work for experimental conditions, and complete tabulations of low and high resolution mass spectral data.
(5) George Barany and R.B. Merrifield. J. Am. Chem. Soc. 99, 7363-7365 (1977).
(6) George Barany, A.L.C. Smit, D.V. Bowen, R.B. Merrifield, and F.H. Field. In "Proceedings of Twenty-Fourth Annual Conference on Mass Spectrometry and Allied Topics, San Diego, California", pp. 178-180 (1976).
(7) G. Zumach, W. Weiss, and E. Kühle. Belgian Pat. 682,991 (June 23, 1966); British Pat. 1,136,737 (June 21, 1966); Chem. Abstr. 70, 77951p (1969).
(8) G. Zumach and E. Kühle. Angew. Chem. Int. Ed. Engl. 9, 54-63 (1970). [REVIEW]

CHARACTERIZATION OF COMPLEX FATTY ACIDS BY POSITIVE/NEGATIVE ION AMMONIA CIMS,

Roger A. Upham, Gary R. Gray, M. Y. H. Wong, and S. J. Danielson, Department of Chemistry, University of Minnesota, Minneapolis, Minnesota 55455.

Mycolic acids are complex, high molecular weight fatty acids produced by all mycobacteria. They were first isolated from a human strain of *M. tuberculosis* (1,2), but they have since been found in a wide variety of pathogenic and non-pathogenic *Mycobacteria* (3). Our interest in these fatty acids arises because they are constituents of preparations that are being evaluated in an experimental animal model (4-7), as well as clinically (8,9), as immunotherapeutic agents in the treatment of cancer.

All of the known mycolic acids possess the basic structure 1, wherein R^1 is either a C_{22} or C_{24} linear alkane and R^2 is a more complex structure comprised of 30-60 carbon atoms and containing a variety of functional groups. Within a given *Mycobacterium* species, 2-4 types of mycolates are present which contain different but discrete sets of functional groups in R^2. The isolation and subsequent structural characterization

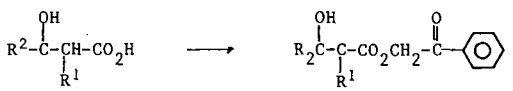

1 2

of these fatty acids is complicated by the fact that each mycolate type is present as a mixture of homologs differing by two methylene units. Recent advances in chromatographic methodologies have enabled us to fractionate these complex fatty acids, as their phenacyl ester (2), into pure components whose structures can be determined (10). In the course of this work, new procedures based on positive and negative ion ammonia CIMS have been developed for the characterization of these fatty acids. The procedures were illustrated for the mycolic acids derived from *M. smegmatis* (11,12).

Normal phase HPLC of the phenacyl esters on μ porasil yielded two major components - mono-alkene series and a di-alkene series. Reverse phase HPLC of the mono-alkene mycolic acid esters separated them into four components. The dialkene-mycolic acid esters were resolved into ten components by reverse phase HPLC. Five of these components were found to have an additional C-methyl group by biosynthetic labeling with tritiated methionine.

The size of the R^1 and R^2 groups and subsequently the whole molecule were determined by probe pyrolysis at 275°-330°C of the individual phenacyl esters under (+/-)ammonia CIMS conditions. The β-hydroxy ester pyrolizes to give an ester characteristic of R^1 and an aldehyde characteristic of R^2.

Location of the double bond in the mono-alkene series was accomplished by reductive ozonolysis with zinc and acetic acid. GC-MS of the resulting mixture showed a mono-aldehyde and a fragment containing an aldehyde and the β-hydroxy ester linkage which on pyrolysis yielded a dialdehyde moiety.

The dialkene series was characterized by oxidative ozonolysis as shown below:

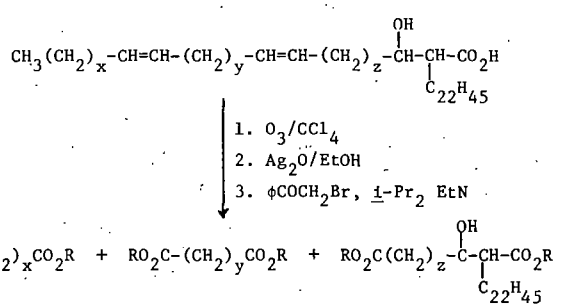

Using a very powerful reverse phase HPLC system of CH_3CN: 95% EtOH (7:3) in water, the resulting mixtures were separable down to components differing by a single methylene

group. Ammonia CIMS (+/-) of the collected fractions permitted unequivocal identification of the double bond locations. It is interesting to note that for a given chain length in R_2 the double bond or double bonds were consistently located within 1-2 methylenes from one member of the series to another.

References

(1) Anderson, R. J. (1929) *J. Biol. Chem.* 85, 351-354

(2) Stodola, F. H., Lesuk, A., and Anderson, R. J. (1938) *J. Biol. Chem.* 126, 505-513

(3) Asselineau, J. (1966) *The Bacterial Lipids*, pp 122-143, Holden-Day, Inc., San Francisco

(4) Ribi, E. E., Meyer, T. J., Azuma, I., and Zhar, B. (1973) *National Cancer Inst. Monogr.* 39, 115-119

(5) Meyer, T. J., Ribi, E., Azuma, I., and Zhar, B. (1974) *J. Natl. Cancer Inst.* 52, 103-111

(6) Gray, G. R., Ribi, E., Granger, D., Parker, R., Azuma, I., and Yamamoto, K. (1975) *J. Natl. Cancer Inst.* 55, 727-730

(7) Ribi, E., Takayama, J., Milner, K., Gray, G. R., Goren, M., Parker, R., McLaughlin, C., and Kelley, M. (1976) *Cancer Immunol. Immunother.* 1, 265-270

(8) Vosika, G., Schmidtke, J., Goldman, A., Parker, R., Ribi, E., and Gray, G. R. (1979) *Cancer Immunol. Immunother.* 6, 135-142

(9) Vosika, G. J., Schmidtke, J. R., Goldman, A., Ribi, E., Parker, R., and Gray, G. R. (1978) *J. Biol. Chem.* 44, 495-503

(10) Steck, P. A., Schwartz, B. A., Rosendahl, M. S., and Gray, G. R. (1978) *J. Biol. Chem.* 253, 5625-5629

(11) Wong, M. Y. H., Steck, P. A., and Gray, G. R. (1979) *J. Biol. Chem.* 254, 5734-5740

(12) Wong, M. Y. H. and Gray, G. R. (1979) *J. Biol. Chem.* 254, 5741-5744

STRUCTURAL DETERMINATION OF ALKENES AND ESTERS OF MONO-UNSATURATED FATTY ACIDS BY GCMS.

D.A. Kidwell and K. Biemann, Dept. of Chem., M.I.T., Cambridge, MA 02139

Most isomeric alkenes have similar if not identical mass spectra. Derivatization of the double bond is therefore necessary to determine its position and geometry. Oxidation by osmium tetraoxide and trimethylsylation of the resultant vicinal diol has been widely used. However, the mass spectra of these derivatives do not allow one to determine the geometry of the original double bond.

We have developed a new, less laborious procedure for the determination of both the position and the geometry of a double bond. It involves the Diels-Alder addition of a chlorinated cyclopentadiene 1 or 2 to the olefin (Scheme I). The adduct fragments by loss of either substituent (Scheme II) but this loss is much more pronounced in the product derived from the *cis*-olefin.

The advantages of this technique are:

1) One step, high yield reaction
2) Only one product obtained
3) Clear distinction between *cis* and *trans* isomers
4) Clear indication of molecular weight (from $M^{+\cdot}$ - Cl·)
5) Clear recognition of important ions from the chlorine isotope patterns

The disadvantage is:

1) Significant decrease in volatility of the adducts compared to the olefin, which therefore complicates the use for polyenes.

SCHEME I

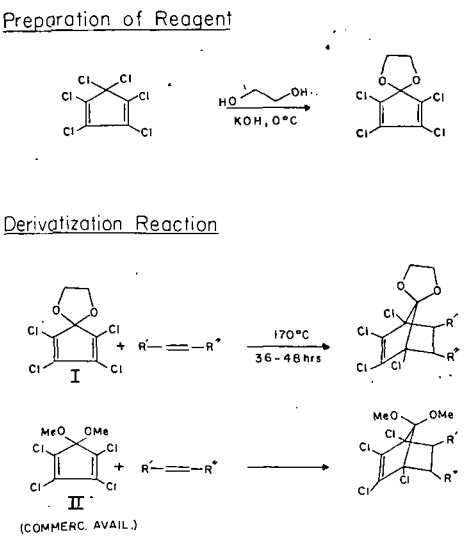

SCHEME II

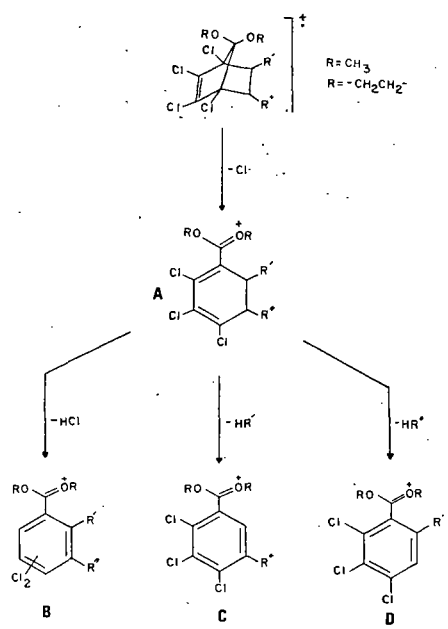

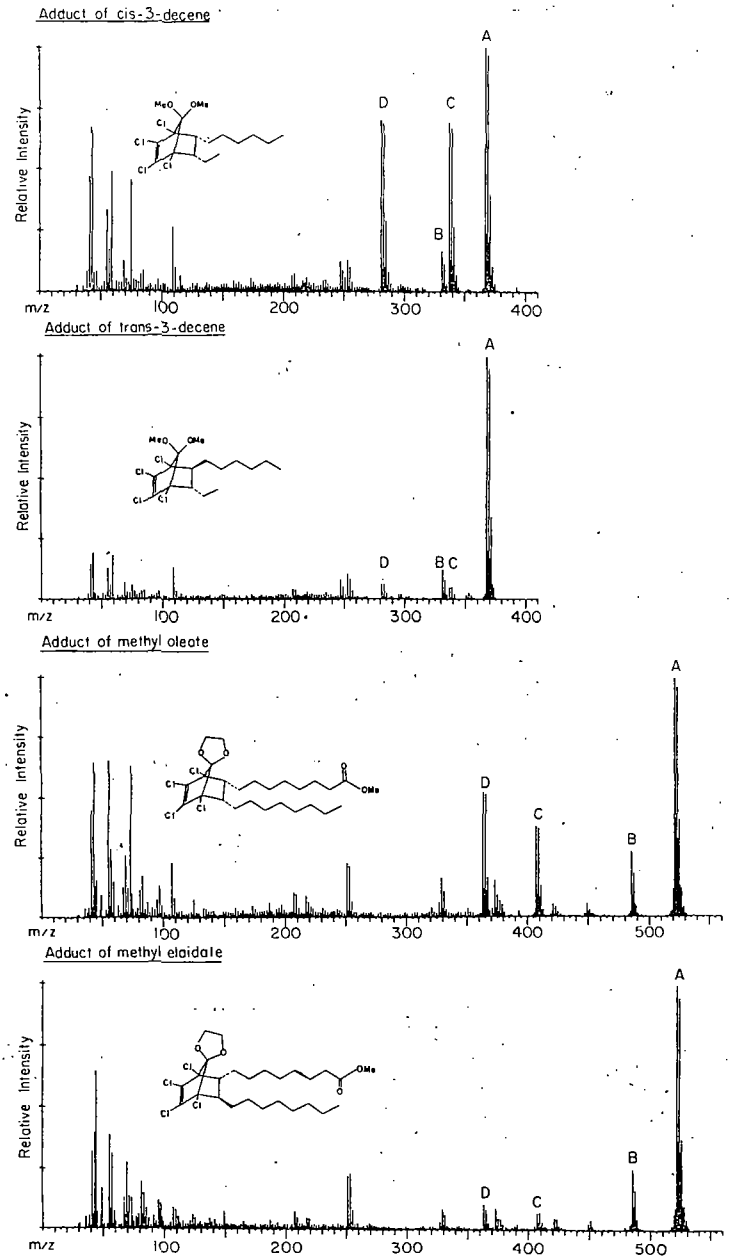

REPRESENTATIVE SPECTRA OF ADDUCTS OF 1 AND 2

THE MECHANISM OF THE MAIN FRAGMENTATION REACTION IN VITAMIN D_3.

ZE'EV V.I. ZARETSKII, Isotope Department, The Weizmann Institute of Science, Rehovot, Israel.

The main fragmentation process characteristic of vitamin D_3 formally requires the cleavage of 7,8-double bond[1], which is known to be an energetically unfavorable reaction, and up to now the mechanism of this fragmentation remained unclear. The use of various deuterium derivatives of vitamin D_3 and its analogues (1-5), as well as metastable defocusing and appearance potentials measurements, shed a new light on the $M^{\cdot+} \rightarrow$ a reaction.

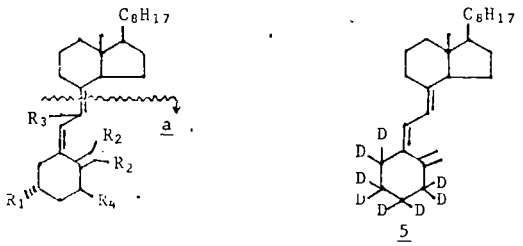

1 R_1 = OH, R_2 = D, R_3 = R_4 = H

2 R_1 = OD, R_2 = R_3 = R_4 = H

3 R_1 = R_4 = OH, R_2 = H, R_3 = D

4 R_1 = R_3 = R_4 = H, R_2 = D

The determination of I(M) of isomers of vitamin D_3 series showed the I(M) to be affected by the location of the double bonds and makes it possible to suggest that vitamin D_3 molecular ion retains the $\Delta^{5,7}$-conjugated double bond system characteristic to its molecule. This fact as well as the finding that, according to the labelling results, the 19-methylen group remains intact in vitamin D_3 molecular ion, are hardly correlated with the intermediate formation of the suprasterol-like form of the molecular ion, preceding the formation of the ion a[2]. The labelling compounds (1-4) study showed ion a to contain ring A together with C-6 and C-7; the formation of this ion is not accompanied by any substantial H-migration toward the rings C and D, or reciprocal H-exchange between ring A, together with C-6 and C-7, and rings C and D. Based on the results of the study, the following mechanism of the formation of the ion a, is proposed:

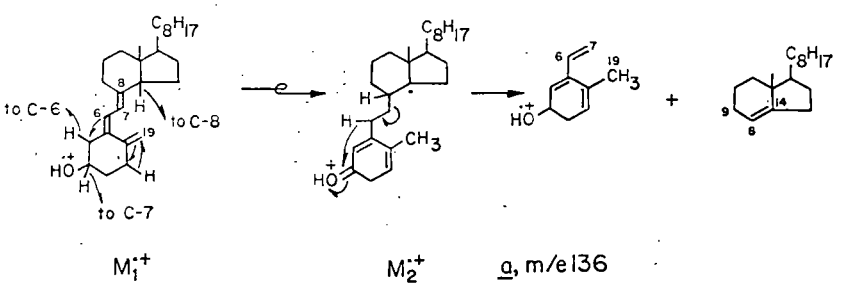

References

[1](a) J.W. Blunt, H.F. DeLuca and H.K. Schnoes, Biochem. 7, 3317 (1968);
(b) Z.V.I. Zaretskii, Steroids 33, 595 (1979).

[2]W.H. Okamura, M.L. Hammond, H.J.C. Jacobs and J. van Thuijl, Tetrahedron Lett. 4807 (1976).

ANALYSIS OF LEUCINE METABOLITES IN THE URINE OF A PATIENT ACCOMPANYING A DEFECT OF TYROSINE METABOLISM

Toshihiro Shinka, Tomiko Kuhara, Isamu Matsumoto and °Masahiko Kawamura

Research Institute of Medical Mass Spectrometry, Kurume University School of Medicine, Kurume, Fukuoka 830 and °Meijo Hospital, Nagoya, Aichi 460, Japan

We have developed a rapid diagnosis screening system of inborn errors of metabolism using GC/MS/COM. Usually a relatively large amount of abnormal metabolites are contained in the body fluids of patients with inborn errors of metabolism and can be easily detected by our screening system. Here we report the case of a 2.5-year-old girl who has both mental and physical retardation and hepato-renal dysfunction. The clinical abnormality found was significantly and constantly elevated excretion of 4-hydroxyphenyllactate, 4-hydroxyphenylpyruvate and 4-hydroxyphenylacetate, which are the intermediates of tyrosine catabolism. Hence, tyrosinosis was suspected. After one year tyrosine restriction, tyrosine metabolites were extremely reduced, whereas 3-methylglutarate and 3-methylglutaconate which are the intermediates of leucine catabolism were found in her urine in large amounts. Our interest, therefore, was focused on the relationship between tyrosine and leucine metabolism. For this purpose, we examined the metabolic profiles after loading tests.

Urine was frozen to -20°C immediately after collection and stored at this temperature until analysis. On the loading tests, a dose of 100 mg/kg body weight of each test compound was given orally with ordinary milk, and the amount of urine produced in 12 hrs was collected. Organic acids were separated by gas chromatography on column packed with 3% OV-17 on Gas Chrom Q. Oven temperature was maintained at 80°C for 2 min, then programmed from 80°C to 290°C at 6°C/min. A JEOL JMS-D 100 gas chromatography-mass spectrometer on lined with a JMA-2000 data acquisition and processing system was used. Ionizing and accelerating potentials were 75 eV and 3 kV respectively, and ion source temperature was 200°C.

The excretion of the abnormal metabolites were markedly reduced by tyrosine restriction, but not by galactose restriction. When the patient was given ordinary milk, two intermediates of leucine catabolism, 3-methylglutarate and 3-methylglutaconate, which are not excreted in the urine of healthy subjects, were detected in relatively large peaks. The excretion of these metabolites was enhanced when either tyrosine or leucine was loaded, although the excretion of tyrosine metabolites was less affected by tyrosine load. 3-Hydroxy-3-methylglutarate was found in the urine only in the case of leucine loading concomitant with heavy ketoacidosis.

Hepato-renal dysfunction in this patient did not result from galactosemia because the patient failed to respond to galactose restriction. 3-Methylglutaconate is known to be cleaved to acetyl-CoA and acetoacetate via 3-hydroxy-3-methylglutaryl-CoA, and had been found in the urine of a patient with 3-hydroxy-3-methylglutaric aciduria, a disease of HMG-CoA lyase deficiency (1-4). 3-Methylglutarate is probably formed from 3-methylglutaconate by reduction. It is evident from the above experiment that both tyrosine and leucine catabolism are closely connected with each other. Viewed from this standpoint, a potential candidate of the end-product of leucine metabolism can be presumed to be acetoacetate, a catabolic intermediate of tyrosine. However, those abnormal metabolites of tyrosine and leucine could not be detected in the patient with ketoacidosis who also accumulated acetoacetate in large amounts. These results suggest that the utilization of acetoacetate is impaired in this patient, and probably our patient might have a deficiency of HMG-CoA synthetase. As far as we know, it is the first time that the complicated abnormal tyrosine and leucine metabolites have been found in a patients urine simultaneously.

(1) Wysocki, S. J., Wilkinson, S. P., Hahnel, R., Wong, C. Y. B. and Panegyres, P. K. Clin. Chim. Acta., 70, 399 (1976).
(2) Wysocki, S. J. and Hahnel, R., Clin. Chim. Acta, 73, 373 (1976).
(3) Faull, K. F., Bolton, P. D., Halpern, B., Hammond, J. and Danks, D. M., Clin. Chim. Acta. 73, 553 (1976).
(4) Greter, J., Hagberg, B., Steen, G. and Soderhjelm, U., Eur. J. Pediatr., 129, 231 (1978).

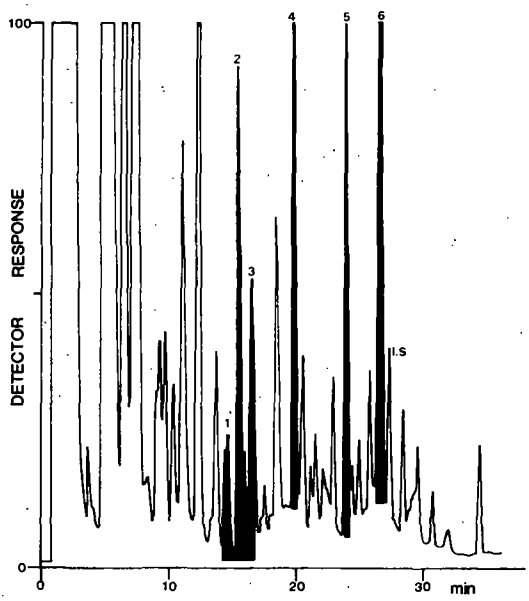

1: 3-Methylglutarate 2,3: 3-Methylglutaconate

4: 4-Hydroxyphenylacetate 5: 4-Hydroxyphenyllactate

6: 4-Hydroxyphenylpyruvate

Fig. 1 Gas chromatogram of organic acids extracted from the patient's urine.

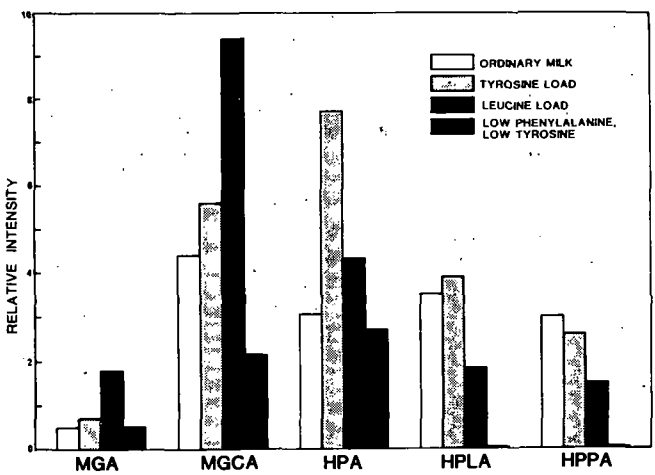

MGA: 3-Methylglutarate, MGCA: 3-Methylglutaconate, HPA: 4-Hydroxyphenylacetate
HPLA: 4-Hydroxyphenyllactate HPPA: 4-Hydroxyphenylpyruvate

Fig. 2 Quantitative variations of organic acids in the urine after loading tests. The value plotted in the vartical axis indicates the relative peak area ratio against internal standard.

KETONE BODY FORMATION AND BRANCHED CHAIN AMINO ACID CATABOLISM IN STARVATION AND IN DIABETES MELLITUS

Isamu Matsumoto, Tomiko Kuhara, Izumi Maruyama, °Ryukichi Kumashiro and °Kyuichi Tanikawa
Research Institute of Medical Mass Spectrometry and The 2nd Department of Internal Medicine, Kurume University School of Medicine, Kurume, Fukuoka 830, Japan

Serum and urinary organic acid profiles, which are obtainable most effectively using a GC/MS/COM system, reflect the metabolism of carbohydrate, lipids and amino acids in the body, because the levels of lactate, free fatty acids, 3-hydroxybutyrate, acetoacetate and catabolites of amino acids, especially of branched chain amino acids, are shown on a single profile. Experiments were undertaken to investigate the metabolic changes and their time course under starved and diabetic conditions both characterized by ketoacidosis.

A forty-eight-hour fasting experiment was carried out by a healthy subject. Unexpectedly diabetes mellitus was detected in the subject four months after the feeding experiments. Sera and urine samples were stored at -20°C until analyses. To the urine equivalent to 1 mg of creatinine or 0.5 ml of serum was added 40 μg of n-heptadecanoic acid as an internal standard. The serum was deproteinized with ethanol, the extraction of the organic acids was carried out with ethyl ether and ethyl acetate, and the extracts were trimethylsilylated. Gas chromatographic separation was carried out on a 2m-long glass column packed with 3% OV-17 by temperature programming from 80°C to 290°C at a rate of 6°C/min. Quantitation was achieved from the relative peak area ratios to the internal standard computed from the areas integrated by the data system. For GC/MS analysis a JEOL JMS-D 100 and a JMA-2000 data acquisition and processing system were used. Two minutes after sample injection, repetitive scanning was started from m/z 40 to m/z 600 in a 5 second cycle.

Table 1 shows the relative amounts of several organic acids at various durations of fasting and the effects of insulin on the metabolism in diabetes. The urinary level of 3-hydroxybutyrate increased from 0.15 to 73 during 48 hr-fasting and that of acetoacetate from 0.02 to 19.31 (not shown). The serum level of 3-hydroxybutyrate also increased from 0.32 to 3.98 in parallel with the level of serum fatty acids. The level of serum lactate gradually increased, plateaued after 12 hr-starvation, and decreased thereafter. When the subject was suffering from diabetes, the levels of serum fatty acids and 3-hydroxybutyrate increased; however, the level of lactate was low. Two hour after a single 12 units insulin injection, the serum level of lactate slightly increased (1.79), that of fatty acids greatly decreased (2.46), and that of 3-hydroxybutyrate to one-half of the original value. At that time, 2-hydroxyisovalerate (2HIV) was detected in the serum and the amount increased during hypoglycemia. The elevated levels of 2HIV without a concomitant increase of α-keto acids and α-hydroxy acids derived from branched chain amino acids had been reported in the urine of patients with lactic acidosis and ketoacidosis (1). No obvious correlation, however, existed between the urinary excretion of 2HIV and of lactate or 3-hydroxybutyrate. As shown in Table 1, the appearance of 2HIV in the blood of our subject depended on neither a high serum level of lactate nor that of 3-hydroxybutyrate at that time. It is known that the branched chain amino acids transaminate with α-keto acids mainly with extrahepatic tissues (2) (Fig. 1) and that the muscles of both diabetic and fasted rats have an increased capacity to burn these fuels instead of glucose, providing energy for muscles.

Recent findings suggest that oxidative degradation of valine is enhanced by addition of fatty acids (3) and that glucose inhibites oxidation of leucine and isoleucine (4). Leucine is potently ketogenic, isoleucine ketogenic as well as glycogenic, and valin glycogenic. Therefore, it is considered that 2HIV accumulates in the blood of diabetic patient after insulin treatment because the formation of 2-ketoisovalerate from valine via transamination with pyruvate is enhanced firstly by the high level of the amino acid and secondly by the rapid increase in the production of pyruvate from glucose due to the ability for muscle to take up glucose and because the rate of oxidative degradation of 2-ketoisovalerate is decreased by a rapid drop in the levels of serum free fatty acids.

(1) Landaas, S. and Jakobs, C., Clin. Chim. Acta, 78, 489 (1977).
(2) Odessey, R., Khairallah, E. A. and Goldberg, A. L., J. Biol. Chem., 249, 7623 (1974).
(3) Spydevold, Ø, Eur. J. Biochem., 97, 389 (1979).
(4) Chang, T. W. and Goldberg, A. L., J. Biol. Chem., 253, 3696 (1978).

TABLE 1

Changes in levels of several metabolites in human serum after starvation and before and after insulin-tretment during diabetes mellitus and at hypoglycemia

	2HIV [a]	Lactate	3HB [b]	Fayyt acid [c]	Glucose [d]
A) Fasting experiment					
0 hr		2.47	0.32	2.09	
12		3.05	0.49	5.07	
24		2.47	1.17	5.69	
36		2.22	2.90	6.66	
48		1.82	3.98	6.10	
B) Diabetes					
no insulin		1.33	1.15	4.44	292
no insulin		1.24	1.10	6.11	179
plus insulin	++	1.79	0.53	2.46	328
plus insulin [e]	++	3.20	0.09	3.56	66
plus insulin	+	8.86	0.13	2.92	172

Values are expressed as the peak ratios relative to the internal standard, computed from areas integrated by the data system. a) 2-hydroxyisovalerate, b) 3-hydroxybutyrate, c) sum of palmitate, palmitoleate, stearate, oleate and linoleate, d) not determined by our profiling method, mg/dl., e) severe hypoglycemia

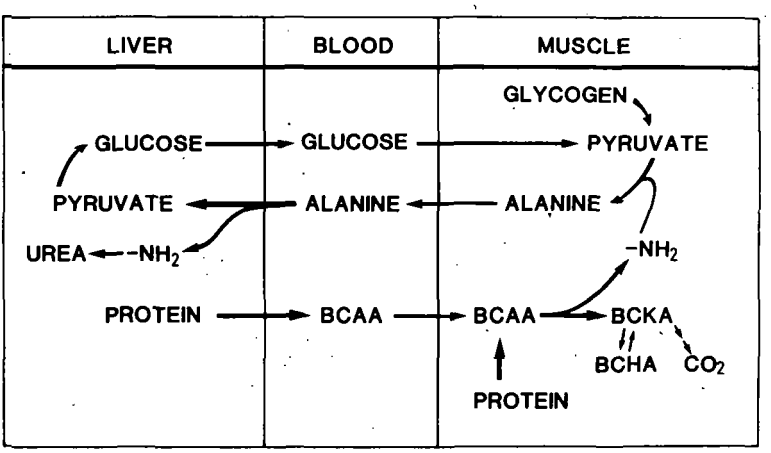

Fig.1. Branched chain amino acid-alanine cycle [2]
BCAA : branched chain amino acid, BCKA : branched chain keto acid, BCHA : branched chain hydroxy acid.

COMPARISON OF THE QUANTITATION OF MURAMIC ACID SELECTED ION MONITORING AND SINGLE REACTION MONITORING

T.W. Cochran[1], A. Fox[2], J.H. Schwab[2], D.J. Harvan[1], C.E. Parker[1], and J.R. Hass[1]

[1]NIEHS, P.O. Box 12233, Research Triangle Park, North Carolina 27709

[2]Department of Bacteriology, University of North Carolina, Chapel Hill, North Carolina 27514

Muramic acid is a compound characteristic of bacterial cell walls. By monitoring the muramic acid levels in various animal tissues, the presence of both viable and non-viable bacterial material can be ascertained. There seems to be a correlation between the presence of muramic acid in joints of laboratory rats which have been injected intraperitoneally with a purified preparation of cell walls and the development of arthritic joints in these animals. There is an absence of detectable muramic acid and the symptoms of arthritis in animals not injected.

Tissues to be studied were homogenized, dialyzed against water, and then acid hydrolyzed. Neutralized hydrolysate was then applied to a TLC plate; the muramic acid containing band was drawn from the plate using a fritted pipette and vacuum. After separation from the solid materials, the muramic acid fraction was derivatized to alditol acetates and was ready for analysis. More extensive clean-up procedures resulted in intolerable losses of the analyte and excessive sample preparation times and handling.

Quantitation of pentaacetyl muramicitol has been performed by using both electron impact and chemical ionization methods on a VG Micromass 70/70F mass spectrometer equipped with a Hewlett-Packard 5710A gas chromatograph and a VG 2050 data system with selected ion monitoring (SIRS) software. A packed 3% SP-2330 phase, 2 meter glass column or a 25 meter OV-1 capillary column was used for the analysis.

Two methods have been used for the quantitation of the derivatized muramic acid: selected ion monitoring and single reaction monitoring. For selected ion monitoring, m/z 126, 168, 210, and 228 from the 70 eV electron impact spectrum of the compound were monitored. Results were reproducible and compared favorably with radioimmunoassays already employed. Tissue samples from joints, however, contained only trace quantities of muramic acid and interferences from other materials made quantitation unreliable, even at higher resolution. A chemical ionization method was explored but showed signs of interferences as well. In a B/E scan of the m/z 446 ion of the CI spectrum, two major daughter ions were found: m/z 386 and m/z 404. One of these ions, m/z 386, was found to be reliable for single reaction monitoring of the muramic acid levels in tissues.

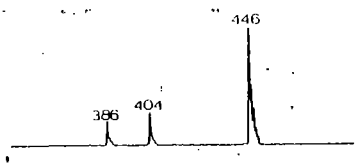

CID - B/E SCAN OF M/Z 446 (CI)

A comparative study has shown that the single reaction monitoring method is superior to selected ion monitoring for trace analysis if the sample is introduced into the system through a gas chromatograph for additional separation from interfering materials. When the direct probe inlet is used, severe matrix effects from these materials were observed, making quantitation unreliable for trace levels, as was the case for the selected ion monitoring method. Response in the single reaction monitoring mode appears to be linear in the range tested, from 100 pg to 40 ng.

ROUTINE HIGH RESOLUTION GAS CHROMATOGRAPHY/MASS SPECTROMETRY OF COMPLEX BILE ACID MIXTURES FROM BIOLOGICAL SAMPLES. J.O. Whitney, E. Roitman, M.M. Thaler, and A.L. Burlingame, Department of Pediatrics and Department of Pharmaceutical Chemistry, Univ. of California, San Francisco, CA. 94143, Space Sciences Laboratory, Univ. of California, Berkeley, Ca. 94720.

The quantitative and qualitative pattern of bile salts present in human tissues and fluids may be characteristic of various hepatobiliary disorders. Bile acid analysis is technically difficult and time consuming, however, due to lengthy conventional methodology including extraction (solvent partioning or solid extraction on a resin such as Amberlite XAD-2) in addition to prolonged solvolysis and hydrolysis. We have developed simple and rapid procedures for extraction, concentration, partial purification and preparation of bile salts from plasma, urine, bile, amniotic fluid and tissue homogenates which when combined with the high sensitivity and resolution of HRGC/MS should allow routine screening of clinical samples for diagnostic and research applications.

Aliquots of biological samples (22,23 bisnor-5-cholenoic acid added as internal standard) and analytical mixtures were quantitatively extracted on commerically available 1 x 1 cm cartridges (Sep-Pak C^{18}) packed with an octadecylsilyl reversed phase material following the protocol described in Figure 1. The void volume of the cartridge was approximately 0.44 ml and flow rates up to 20 ml/min could be used without significant loss. A 50 ml sample, therefore, could be processed in less than 10 min. Table I demonstrates that recovery (monitored by addition of ^{3}H-taurocholate) generally was greater than 95%. Similar quantitative extraction was obtained with the more polar bile acid ^{35}S-lithocholate-3-sulfate and the less polar compound ^{3}H-lithocholate. Considerable purification was accomplished since organic hydrophobic impurities including protein and inorganic salts were removed with the sample effluent and water wash. The total capacity of the cartridge determined by extracting increasing concentrations of bile salt dissolved in saline was in excess of 50 mg of organic substance, allowing for the concentration of appreciable quantities of material for analysis.

After extraction, samples were solvolyzed for ½ hr in ether acidified with HCl and hydrolyzed enzymatically with cholylglycine hydrolase (½ hr). The hydrolysate was clarified with water and freed bile acids extracted by Sep-Pak procedure (Table I). Repetitive gas chromatographic analysis of bile acids from duplicate samples of rat liver prepared in the manner were reproducible (94±5% for cholate and chenodeoxycholic acid; >90% for minor components) and were statistically comparable to samples prepared by conventional methods requiring up to 3 days preparation time per sample. For HRGC/MS methyl ester/trimethylsilyl ethers of bile acids were prepared and analyzed on an Hitachi M-52 mass spectrometer equipped with a 25 m, 0.325 mm I.D. glass capillary column, wall coated with carbowax 20 M. After splitless injection at room temperature, the column was rapidly heated to 200° and then programmed to 250° at 5°/min. The bile acid regions of total ion chromatograms of samples prepared by these procedures are illustrated in Figures 2-4. Peaks were resolved and quantifiable for such diverse samples as normal human amniotic fluid, serum from a patient with familial intrahepatic cholestasis and duodenal aspirate from a patient with cystic fibrosis. No additional chromatographic purification, such as HPLC or thin layer chromatography was needed. Spectra taken from peaks in this area were uncontaminated and are being used to confirm the presence of both common and uncommon bile acids in clinical situations. These improved work-up procedures should make HRGC/MS a useful and practical adjunct in the diagnosis and understanding of abnormalities of bile salt metabolism in liver disease.

This work was supported by USPHS grants HD03148 and HD11645 to Dr. M. M. Thaler and the NIH Division of Research Resources grant RR00719.

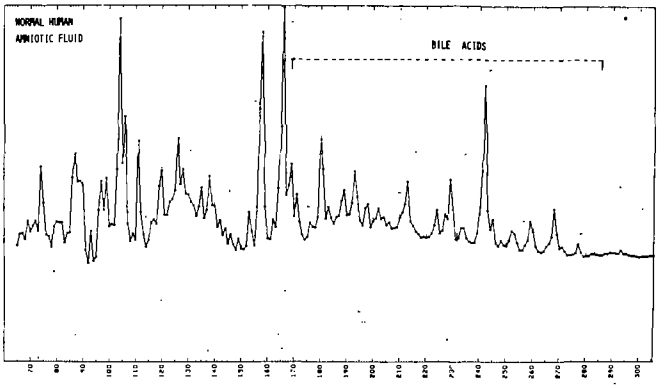

FIGURE 2

1) CONNECT CARTRIDGE TO A SYRINGE.

2) PRE-WET CARTRIDGE WITH 2 ML OF WATER MISCIBLE SOLVENT (MeOH, ACETONITRILE, ETC) AND FLUSH WITH ABOUT 5 ML OF CLEAN H_2O.

3) POUR SAMPLE SOLUTION INTO SYRINGE BARREL.

4) PUSH SAMPLE THROUGH CARTRIDGE AT A FLOW RATE NOT EXCEEDING 20 ML/MIN.

5) WASH CARTRIDGE WITH 5-10 ML H_2O.

6) EXTRACT BILE SALTS WITH 3-5 ML MeOH.

FIGURE 1

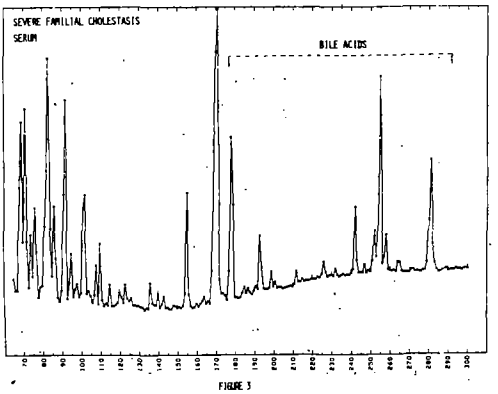

FIGURE 3

TABLE 1
RECOVERY OF ^{3}H-TAUROCHOLATE USING SEP-PAK C^{18} CARTRIDGES FOR EXTRACTION

SAMPLE	BIOLOGICAL FLUIDS VOLUME (ML)	RECOVERY (% ± S.D.)
URINE	20 (4)*	99 ± 4
	50 (6)	96 ± 4
	500 (1)	95
	750 (1)	92
SERUM	5 (6)	99 ± 3
AMNIOTIC FLUID	30 (5)	94 ± 2
BILE	0.2 (6)	95 ± 5
RAT LIVER HOMOGENATE	1 6 (6)	94 ± 3
	ANALYTICAL PROCEDURES VOLUME (ML)	RECOVERY (% ± S.D.)
ALKALINE HYDROLYSIS	80	94 ± 5
HELIX POMATIA JUICE (SULFATASE)	25	94 ± 3
CHOLYLGLYCINE HYDROLASE	20	94 ± 5

* ( ) = NO. OF INDIVIDUAL DETERMINATIONS

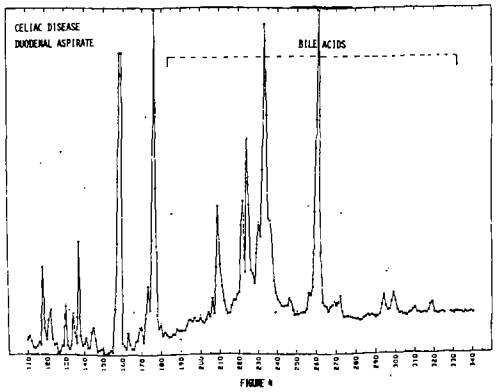

FIGURE 4

EVALUATION OF FLUOROMETRIC ASSAY METHODS FOR SEROTONIN IN PLATELETS, PLASMA AND WHOLE BLOOD SAMPLES BY GCMS

Mumtaz,M.M., Narasimhachari,N. and Friedel, R.O.
Psychiatry department, Medical College of Virginia
P.O.Box 710, Richmond, Va 23298

Different methods have been used for the determination of serotonin (5HT) in human blood platelets, whole blood and plasma samples, but there have been very few reports on inter-method correlations. We now report the evaluation of fluorometric method using o-phthalaldehyde (OPT), with ^{3}H-5HT as internal standard and gcms method using deuterated (d_4) 5HT as internal standard. Basic extracts (pH 9.5) of sonicated platelet samples, hemolyzed blood or plasma samples were converted to trifluoroacetyl (TFA) or pentafluoropropionyl (PFP) derivatives. An aliquot of the basic extract (10%) was used for ^{3}H count to determine the percent recovery. From 20 µl of the derivatized sample 2 µl was used for gcms and the rest for quantitation by OPT fluorescence (E_{max} 360 µm and F_{max} 460 µm)[1]. In another series, duplicate samples were extracted, one for fluorometry with ^{3}H-serotonin as internal standard and the second for gcms with d_4-serotonin as internal standard. Ions m/e 351 and 354 were monitored for the TFA and m/e 451 and 454 for PFP derivatives.

Platelets samples were obtained from volunteers routinely for monoamine oxidase determinations. Part of this, 0.5 ml of sonicated platelet preparation containing 1 to 2 mg of protein/ml was used for serotonin determination. To determine serotonin levels in plasma or whole blood (hemolyzed) 2 ml volume samples were used.

Serotonin-TFA shows the same fluorescence characteristics as other 5-OH indole derivatives and has an added advantage that the fluorescence produced by the TFA derivative with OPT reagent is at least 3 times higher than produced by serotonin itself. The recovery data of serotonin from platelet samples with added ^{3}H-serotonin are shown in table 1. There is good reproducibility in these recovery studies. However, since each sample is spiked with this internal standard high reproducibility is not a prerequisite with this assay, except that it is a control on the extraction procedure. The data on replicate analysis of a pooled sample of platelets is also shown in table 1. For gcms quantitation the ions m/e 351 and 354 were monitored for the sample and the internal standard respectively. The SIM recordings of TFA derivatives of standard and some samples are shown in figure 1. The comparison of serotonin in platelet samples, plasma and whole blood samples by OPT fluorescence and gcms methods is shown in table 2. Using the above procedures, platelet samples of normal controls and different diagnostic groups of mental disorders were analyzed and the results are shown in table 3.

We have compared the OPT fluorescence method for serotonin assay with a more specific method viz. gcms SIM method. While the fluorescence method provides enough sensitivity for the assay, in tissue samples it has not been validated by a more specific method and this cross validation provides reliability to the less expensive and more commonly used fluorometric method. Since serotonin in circulating blood is commonly believed to be mainly stored platelets, whole blood and plasma samples were analyzed for serotonin by some investigators to compare the serotonin levels of normal controls and patients with psychiatric disorders. The present studies show that while there is a good correlation (Corr. coeff. 0.93) for platelet serotonin by fluorescence and gcms methods, the correlation was poor for blood and plasma samples, where the fluorometric values were consistently higher than the gcms values.

ACKNOWLEDGEMENT : our thanks are due to Dr.G.W.Milne, NIH for a generous gift of d_4-serotonin used in this study.

1. MAICKEL,R.P. and MILLER,F.P. (1966) Anal.Chem. 38, 1937-38

FIGURE 1

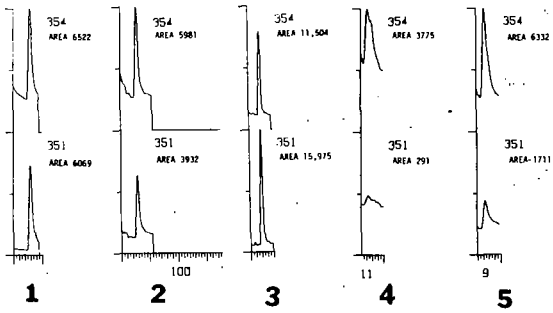

1.Standard mixture of 5HT and d_4-5HT 2.Platelet sample from normal control 3. Platelet sample from patient on Lithium 4.Plasma from depressed patient 5. Plasma from patient on Lithium.

Table 1

RECOVERY STUDIES ON 5HT FROM PLASMA AND PLATELET SAMPLES

	Expt. 1	Expt. 2
Plasma	38.76 ± 2.2%	38.25 ± 2%
n =	4	6
Platelets	36.3 ± 1.2%	35.0 ± 1.5%
n =	2	2
Pooled platelets*	186.0 ± 43ng	226.0 ± 58ng

*Duplicate analysis of 0.5 ml aliquots from pooled platelet samples

Table 2

CORRELATION BETWEEN GC-MS-SIM AND FLUOROMETRIC ASSAY

Sample	N	Correlation Coefficient
Platelets	10	0.93
Plasma	5	0.63
Blood	5	0.60

Table 3

PLATELET SEROTONIN LEVELS OF DRUG FREE PATIENTS AND CONTROLS

Diagnostic group	N	Serotonin ng/mg protein
Major depressive disorder	9	737.8 ± 701.7
Manic	4	869.0 ± 899.3
Schizophrenics	12	1342.0 ±2011.0
Normal controls	19	547.6 ± 311.2

COMPARISON OF PATTERN RECOGNITION METHODS FOR THE ANALYSIS OF METABOLIC PROFILES.

R. Abbott, M. Anbar, J. McReynolds, M. Scanlon, and L. Verkh.
Dept. of Biophysical Sciences, SUNYAB, Buffalo, New York 14214.

Alternative computerized statistical techniques have been compared to establish their diagnostic power and limitations for the classification of biochemical profiles obtained by mass spectroscometric techniques.

A set of 11 urine samples representing primarily alcoholic hepatitis were compared to a control group of 12 samples obtained from healthy volunteers. Urine samples were collected and frozen until analysis. Salt saturated urine (1 ml, pH 7.2) was absorbed onto a column of chromosorb P which was then eluted with 5 ml of CH_2Cl_2.

FIMS molecular weight profiles were obtained for each sample in duplicate. Each spectra was normalized to the unit total area, with individual peak areas greater than 5 percent of the total area excluded from the normalization sum.

A molecular weight range of m/e 60-360 was used to compare Wilcoson-WNI (weighted noncorrelation index) and Discriminant Analysis Programs P7M and P3D on a BMDP package were used for discriminant analysis and comparison of two groups with t-test, respectively.

The Wilcoxon test is used to calculate probabilities (p values) for the observed distributions in the rank sums of intensities of each m/e value (variable) between control and pathological spectra.

For this data set 20 variables with $p \leq .001$ used in computing "WNI" with a weighting factor of $(1/p)^{1/2}$ gave a correct classification of 22 out of 23 samples.

"Unknown" samples deleted one at a time from their respective group averages in WNI calculation were all classified correctly.

Discriminant analysis (P7M) is used to find a classification function (linear combination of variables) that maximize ratio of the average-group sum of squares to the within-group sum of squares. Correlation analysis of variables in the classification function is used so that each new variable brings only that amount of information which is unique to it and not already carried by the earlier ones.

This program requires large computer capacity and can analyze a maximum of 50 variables. For this reason we use the program P3D for an initial selection of variables to be used by the discriminant analysis program. For two sample sets 90 percent of the variables selected by the t-test and Wilcoxon method are identical. The discriminant analysis program correctly classified all samples in this data set including "unknowns" which were not used to derive the classification function.

Both the Wilcoxon-WNI and Discriminant analysis methods were tested for their sensitivity to five fold changes in the intensities of up to five diagnostic peaks. This type of test simulates errors that might occur with actual unknown samples due to drug metabolites or major nutritional changes. Neither increases or decreases in diagnostic variables changed the classification obtained by either method.

The Wilcoxon-WNI method has the advantage of simplicity and the ability to use small sample sets. Discriminant analysis provides a more powerful separating method with further capabilities for multiple group classification and the rejection of co-variates. Core space requirement and the necessity for initial variable selection, however, does not allow the utilization of the entire spectra with this program.

A full description of this study has been submitted to Clinical Chemistry.

This study was sponsored in part by the U.S. Army Medical Research and Development Command under Contract No. DAMD17808035 and a grant from the Whitaker Foundation. The BMDP programs were developed at the Health Sciences Computing Facility, UCLA, under NIH Special Research Resources Grant RR-3.

DIAGNOSIS OF VIRAL INFECTIONS BY MULTICOMPONENT MASS SPECTROMETRIC ANALYSIS. R. Abbott, M. Anbar, H. Faden, J. McReynolds, W. Rieth, M. Scanlon, L. Verkh & B. Wolff. Dept. of Biophysical Sciences, SUNYAB, Buffalo, New York, 14214.

Metabolic profiles of urine extracts of humans with viral infections and media of virus infected tissue cultures have been obtained by FIMS and CIMS. Spectra obtained were analyzed by a number of statistical procedures to detect diagnostic pattern changes.

In a longitudinal study, fully informed consenting volunteers received sandfly fever virus vaccine or a placebo injection. Morning urine samples were collected and frozen 4 days before, on the day of injection and 8 successive days thereafter, and finally after 28 days. Salt saturated urine (1ml, pH 7.2) was adsorbed onto a column of chromosorb P which was then eluted with 5 ml of CH_2Cl_2.

The eluate, evaporated to dryness on a strip of glass fiber filter paper was placed in the solid probe for FIMS analysis. Spectra were acquired using a graphite fiber field ionization source, with repetitive scans acquired during probe temperature programming from 25 to 200°C. Duplicate samples from each day of the study for three individuals were analyzed and the molecular weight profiles obtained after summing the individual scans were normalized and processed by programs in the BMDP statistical package. Using program P7D a t-test was performed on spectra from days -4 and 0 versus days 3 through 5 to select masses showing changes ($p \leq 0.001$) in intensity during the period of observed symptoms and mild fever. Cluster analysis (P2M) using 40 m/e's selected separated the control and response periods of 2 individuals receiving the virus injection.

Day 2 of one individual was placed in the response period cluster. Stepwise discriminant analysis (P7M) was used to derive a classification function for control and response period patterns that was used to classify all other days as unknowns. Complete separation of the control and response patterns was obtained and the classification of the other days showed the appearance of the response pattern by day 2 for one person, the persistence of the pattern for days 7, 8 in another subject, and a return to the control pattern for both subjects on day 28. A third individual who received a placebo injection was classified as healthy for all days.

The molecular weight profiles of seven other subjects were obtained by isobutane CIMS on a 1 μl aliquot of urease treated urine. In this case the major constituents observed by direct sampling did not reveal a strong diagnostic pattern. A similar classification procedure gave 8% false positives and 27% false negatives with only 12 m/e's selected by the t-test ($p \leq 0.001$).

In an <u>in vitro</u> study we also analyzed the cell free media of human embryonic lung tissue cultures infected with polio virus. Infected and non-infected cultures were analyzed at 0,6 and 24 hours. FIMS was performed using 75 μ l of the cell free media adjusted to pH 2. Variables selected using the t-test to compare 0 and 24 hour infected cultures showed changes due to both cell growth and virus infection. Discriminant analysis gave a classification function that separated spectra into five groups as shown in Table 2.

A full description of this study has been submitted to <u>Clinical Chemistry</u>.

This study was sponsored in part by the U.S. Army Medical Research and Development Command under Contract #DAMD177808035 and a grant from the Whitaker Foundation. The BMDP programs were developed at the Health Sciences Computing Facility, UCLA, under NIH Special Research Resources Grant RR-3.

TABLE 1

MAHALANOBIS D SQUARE FROM AND POSTERIOR PROBABILITY FOR GROUP

GROUP B				CONTROL		FEVER	
Case	Day	Ind.	Class.				
9	2	J	F	******	0.000	******	1.000
10	2	J	F	******	0.000	******	1.000
11	2	L	C	******	1.000	******	0.000
12	2	L	C	******	1.000	******	0.000
GROUP D							
Case	Day	Ind.					
23	7	J	C	******	1.000	******	0.000
26	7	J	F	******	0.000	******	1.000
24	8	J	C	******	1.000	******	0.000
27	8	J	C	******	1.000	******	0.000
25	28	J	C	******	1.000	******	0.000
28	28	J	C	******	1.000	******	0.000
29	7	L	F	******	0.000	******	1.000
32	7	L	F	******	0.000	******	1.000
30	8	L	F	******	0.000	******	1.000
33	8	L	F	******	0.000	******	1.000
31	28	L	C	******	0.000	******	0.000
34	28	L	C	******	1.000	******	0.000

Table 1 Stepwise discriminant analysis of longitudinal samples from two individuals receiving sandfly fever vaccine using 40 m/e values (variables). Classification function based on days -4, 0 (C) and 3, 4, 5 (F) used to classify samples from all other days.

TABLE 2

AVG MAHALONOBIS D SQUARE (+ SD) FROM AND AVERAGE POSTERIOR PROBABILITY FOR GROUPS

Group	Cases	A all 0hr	B Virus 6hr	C Virus 24hr	Y Control 6hr	Z Control 24hr
A	12	13(4) 1.00	173 (26) 0.00	177 (30) 0.00	222 (27) 0.00	244 (31) 0.00
B	6	171 (32) 0.00	11 (2) .998	35 (10) 0.00	32 (7) 0.00	45 (11) 0.00
C	4	171 (17) 0.00	34 (13) 0.00	7 (2) 1.00	73 (20) 0.00	36 (10) 0.00
Y	6	223 (43) 0.00	34 (14) 0.03	80 (22) 0.00	14 (3) .97	60 (13) 0.00
Z	4	242 (17) 0.00	44 (8) 0.00	39 (11) 0.00	57 (12) 0.00	11 (5) 1.00

Table 2 Stepwise discriminant analysis of tissue culture samples, analyzed at pH 2 using 25 m/e values (variables). Infected and non-infected samples from zero, six and 24 hours classified into five groups.

Selected Ion Monitoring Validation of Chromatographic and Spectrophotometric Methods of Quantitation for Biological Systems

Susan E. Hattox and Frank Hatch*

Departments of Psychiatry, Pharmacology and Chemistry, Yale University School of Medicine, New Haven, CT 06510

A wide variety of analytical techniques are employed for the quantitation of compounds in biological tissues and fluids, including chromatographic, spectrophotometric and receptor binding methods. These techniques are readily accessible and can provide high sensitivity for relatively low cost; however, they suffer from lack of specificity. The combined specificity and sensitivity of selected ion monitoring make it useful for the validation of less specific techniques. Although time consuming, validation of other methodologies will have the long term advantage of freeing mass spectrometers to solve those problems which cannot be solved by alternative techniques. We present here the results of a comparison of three methods for measuring trace components in cerebrospinal fluid (CSF) and an on-going project requiring development of a method to validate HPLC analysis of the drug haloperidol in plasma. All experiments have been carried out employing Finnigan Corp. Model 3200 mass spectrometers equipped with programmable multiple ion monitors (PROMIM) and light beam oscillograph recorders.

Comparison of Methods for Measuring CSF HVA and 5-HIAA

Homovanillic acid (HVA) and 5-hydroxyindoleacetic acid (5-HIAA) are major metabolites of the central nervous system (CNS) neurotransmitters dopamine and 5-hydroxytryptamine, respectively. CSF levels of these metabolites may reflect CNS activity since the fluid is contiguous with many structures within the brain. Selected ion monitoring has been used to explore the accuracy of two other methods for measuring HVA and 5-HIAA: (a) high performance liquid chromatography (HPLC) of unprocessed CSF followed by fluorometric detection as described by Anderson et al. (1) and (b) a standard fluorometric procedure employing organic extraction of acidic CSF as described by Gerbode and Bowers (2). The selected ion monitoring procedure involves addition of 0.5 ml 1 N HCl, 0.5 mg sodium metabisulfite and 500 ng each deuterated HVA and 5-HIAA to 500 ul CSF. The ethyl acetate extract is evaporated with dry nitrogen and the residue derivatized with pentafluoropropanol and pentafluoropropionic anhydride. Samples are introduced into the electron impact mass spectrometer via a 5 ft. glass U tube packed with 3% OV-17 liquid phase coated on inert support. M/z 438 and 440, derived from loss of $COOCH_2CF_2CF_3$ from M^+ of 5-HIAA and 5-HIAA-d_2 and m/z 460 and 462, M^+ of HVA and HVA-d_2 are monitored. CSF was obtained by lumbar puncture from 20 psychiatric patients who had received 80 mg/kg probenecid over the previous 24 hours.

Fig. 1 shows the correlations found among the three methods for 5-HIAA in CSF. The dashed line indicates slope = 1.0, while the solid line indicates the best fit for the data. Neither the HPLC nor the standard fluorometric method shows good correlation with GC/MS results. Closer analysis of the data suggests that, while the majority of the samples correlate well, a small number give low results by both methods using fluorometric detection as compared to GC/MS analysis. Apparently interfering substances are present in these few samples, emphasizing the necessity of monitoring more than one set of ions to preserve the specificity inherent in selected ion monitoring. Fig. 2 shows the correlations found among the three methods for HVA in CSF. HPLC and GC/MS analysis give comparable results; the fluorometric procedure, however, did not correlate well with either of the other methods and gave consistently lower results.

Fig. 1

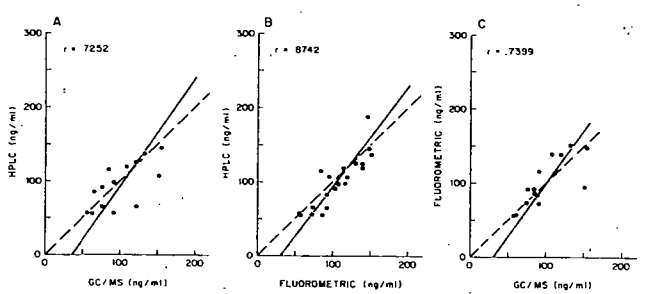

Fig. 2

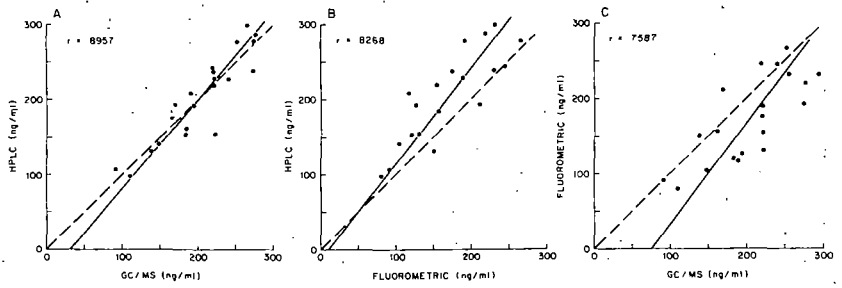

Direct Insertion Probe Haloperidol Analysis

Haloperidol is a neuroleptic butyrophenone administered in dosage regimens providing plasma levels of free drug of 10 ng/ml and lower. Sensitive and selective techniques are required for the quantitation of this compound in plasma. Several GC methods utilizing electron capture (3) and nitrogen specific (4) detection have appeared providing quantitation down to the 1 ng/ml level. Hornbeck et al. (5) employed GC/methane CIMS with selected ion monitoring to increase the specificity of the analysis at 1-2 ng/ml. The GC procedures, which employ high temperatures and 1% liquid phase loading on packed columns, suffer from poor peak shape and potential thermal degradation of labile haloperidol at low nanogram levels. The compound is also resistive to suitable derivative formation. An HPLC method is currently under development for the routine determination of haloperidol in plasma (6). The present work deals with the potential of direct insertion probe CIMS for quantitating haloperidol and validating the HPLC procedure.

The 70 eV mass spectrum exhibits extensive fragmentation and is unsuitable for selected ion monitoring quantitation. Both isobutane and 10% NH_3/isobutane reagent gas systems provide good CIMS spectra with $(M+H)^+$ as the base peak. Isobutane provies a strong $(M-OH)^+$ m/z 358 with haloperidol and $(M+H)^+$ m/z 392 for the internal standard, suitable for direct probe quantitation. The NH_3/isobutane gas mixture would be more suitable for GC/MS analysis as suggested by Hornbeck et al. (5).

The direct insertion probe technique has some advantages for the quantitation of low volatility or thermally labile compounds if the problems of sample clean-up can be overcome. Direct sample vaporization from glass probe tips deactivated with SE-30 coating allow detection of 1 nanogram quantities. With ballistic heating (60° → 205°C in 30 seconds) a linear calibration curve was obtained based on peak heights covering a 1 to 25 nanogram range.

Preliminary results for haloperidol quantitation in plasma, employing the usual acid/base clean-up extractions and a combination acid/base/Sep-Pak (Waters Associates) procedure, have been unsuccessful to date. Major problems are attributed to the different elution characteristics of haloperidol and its dichloro analog from C-18 Sep. Pak cartridges. These and other problems may be overcome by the future use of a deuterated haloperidol internal standard. However, more complicated and time consuming clean-up procedures are not attractive for routine quantitative methods. Plasma may be too complicated a matrix for the direct probe technique of quantitation. Analysis of haloperidol by more sophisticated techniques, e.g., capillary column GC/MS, LC/MS and direct probe MS/MS is reasonable if instrumentation is available. The direct probe technique for quantitation is potentially very useful for low volatility and thermally labile compounds not amenable to GC/MS if sample clean-up is not prohibitive.

(1) Anderson, G. M., Young, J. G. and Cohen, D. J., J. Chromatogr., 164, 501-505 (1979).
(2) Grabode, F. A. and Bowers, M. B., J. Neurochem., 15, 1053-1055 (1968).
(3) Forsman, A., Martensson, E., Nyberg, G. and Ohman, R., Naunyn-Schmiedeberg's Arch. Pharmacol., 286, 113-124 (1974).
(4) Bianchetti, G. and Morselli, P. L., J. Chromatogr., 153, 203 (1978).
(5) Hornbeck, C. L., Griffiths, J. C., Neborsky, R. J. and Faulkner, M. A., Biomed. Mass Spectrom., 6, 427-430 (1979).
(6) Jatlow, P., Yale University School of Medicine, in preparation.

*Present Address: Boehringer Ingelheim, Ltd., Ridgefield, CT 06877.

EFFECT OF LARGE INGESTIONS OF VITAMIN C ON URINARY METABOLIC PROFILES

B.Edwin Blaisdell,J.C.Engels,Constance S.Tsao,Alan Sheets,William Aberth
Linus Pauling Institute of Science and Medicine, Menlo Park, CA 94025

The interest of the Linus Pauling Institute of Science and Medicine in the possible improvement in health attendant upon ingestion of large amounts of vitamin C is well known (1,2). At present, little is known about how vitamin C affects the human body (3). This research is a global phenomenalistic investigation of the extent of the modification of human metabolism by vitamin C.

A volunteer ingested 10 g of supplementary vitamin C (ascorbic acid) per day (2.5g at breakfast, lunch, supper, and bedtime) for a period of one week; no supplementary C for a second week; 10 g/day for a third week; none for the fourth and fifth weeks. Diet was otherwise uncontrolled. 24-hour urine samples were collected (ending with the first morning voiding) on days 1C, 3C, 5C, 7C, 8, 10, 12, 14, 15C, 17C, 19C, 21C, 22, 24, 26, 28, 29, 31, 33, 35 in bottles stored at -40 deg C. (appended C designates a day on which supplementary C was ingested.) For each sample its volume, pH, C content, and dehydroascorbic acid (DHA) content were determined (by wet methods). For each sample, a volcano field ionization mass spectrum, VFIMS, (metabolic profile) was determined from mass 84 to 371. For each sample (some in replicate) a high pressure liquid chromatogram, HPLC, of primary amines (ninhydrin positive substances) was determined for 52 peaks.

The data from the wet analyses and the metabolic profiles were subjected to analysis of variance and covariance using program P2V of the BMDP package (4). The results for the wet analyses and a small selection of the metabolic profiles (3 out of 288 for VFIMS, 3 out of 52 for HPLC) are summarized in Tables I and II. In these tables PSET is the probability that the distance between the estimted centers of gravity of the measured values for the C weeks (1,3) and the non-C weeks (2,4,5) is zero. PC is the probability that the least squares straight line for the measured values as a function of urine collection date during the C weeks has slope zero (t test). BC is the least squares estimate of this slope. PNC and BNC are the same for the non-C weeks. PSEQ is the probability that the least squares straight line for the measured values for the total of 5 weeks as a function of the run number on the analytical instrument has slope zero. BSEQ is the least squares estimate of this slope.

Table I. Centers of Gravity
(Corrected for Linear Trends with Urine Collection Data and Run Number)

Wet Analyses			VFIMS			HPLC		
	C	NOC		C	NOC		C	NOC
c/day	198	032	mass232	165	185	peak32	279	284
sd	027	014		009	018		014	014
dha/day	166	084	mass233	149	168	peak33	632	632
sd	010	021		010	014		035	036
pH	595	622	mass234	163	187	peak34	223	197
sd	019	021		009	017		030	017

Table II Analyses of Variance and Covariance

	PSET	PC	PNC	PSEQ	BC	BNC	BSEQ
	Wet Analyses						
C/DAY	000	172	434		083	-024	
DHA/DAY	004	306	043		005	-005	
pH	165	081	101		-105	055	
			VFIMS				
mass232	975	296	223	001	167	-089	151
mass233	975	062	018	000	187	-055	073
mass234	398	051	037	000	118	-058	103
			HPLC				
peak32	751	012	018	977	100	-051	000
peak33	996	076	110	763	176	-087	-004
peak34	261	227	043	000	068	-064	039

The values in the tables are derived from pooled measurements on non-contiguous week sets (1,3) and (2,4,5). The run numbers are purposely sequenced to be independent of the urine collection dates so that estimates of time trends in metabolic profile and of instrumental drift can each be

determined unaffected by the other. Note that even when the slopes are not significnt at the conventional 5% level they are all positive for the C weeks and negative for the non-C weeks (except for pH where the reversal in sign means an increase in acidity during the C weeks and a decrease during the non-C weeks). Note also that the C, DHA and pH results contrast with the results on the substances measured by VFIMS or HPLC. The wet results show a significant difference between the centers of gravity of the measurements for the C and non-C weeks but generally no significant trend with time during the weeks on a given regimen. The pattern of the VFIMS and HPLC results is just the converse.

The results in Tables I and II are from a very small sample (<2%) of the peaks measured by VFIMS and HPLC. Some comprehension of the probabilities (significances) of the estimated slopes for all peaks can be obtained from the cumulative histograms of the probabilities, Fig. 1.

If the data show no effect of the kind being estimated, the cumulative histogram will approximate the uniform distribution, the diagonal straight line. The significance of the departure from the uniform (no effect) distribution can be assessed by the Kolmogorov-Smirnov statistic as given in Table III, where A = the value of the KS statistic and B = the probability for large samples (>50) that this value be exceeded if there be no effect.

Table III Significance of the KS statistic (for samples >50)

A	1.07	1.14	1.22	1.36	1.63	1.73	1.95
B	0.20	0.15	0.10	0.05	0.01	0.005	0.001

The estimated values of the KS statistic from the VFIMS and HPLS metabolic profiles are given in Table IV. The table shows that the differences between the estimated centers of gravity of the measured intensities for the C and non-C weeks are of little significance but that the estimates of the slopes of the trends are generally highly significant. The significant trends with urine collection date for the C and non-C weeks have been found in the presence of a much more significant instrumental drift.

Table IV Values of the KS Statistic

	PSET	PC	PNC	PSEQ
VFIMS	1.44	3.09	5.40	12.35
HPLC	0.61	1.31	2.19	2.29

REFERENCES

(1) L.Pauling, Vitamin C and the Common Cold. Freeman, San Francisco (1970)
(2) E.Cameron and L.Pauling. Cancer and Vitamin C, Linus Pauling Institute, Menlo Park, CA (1979)
(3) A.L.Lehninger, Biochemistry, Worth, New York (1975) p.351
(4) BMDP, Health Sciences Computing Facility, UCLA, NIH Grant RR-3 (1977)

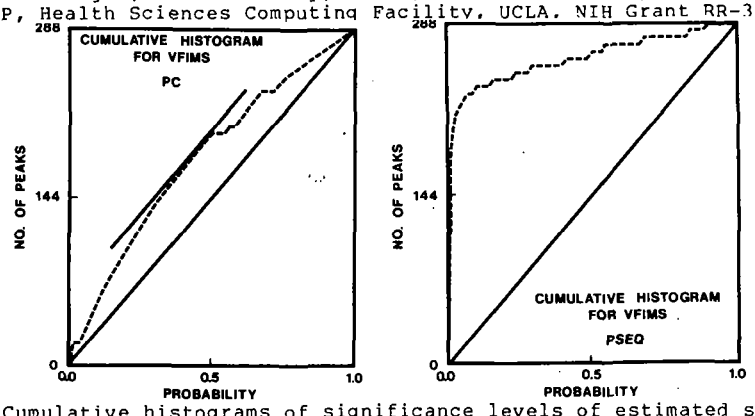

Fig.1. Cumulative histograms of significance levels of estimated slopes for VFIMS. Left: PC, Right PSEQ. Abscissa: probability. Ordinate: number of peaks.

ANALYSIS OF FOOD, DRUG AND COSMETIC DYES BY FIELD DESORPTION AND DESORPTION CHEMICAL IONIZATION MASS SPECTROMETRY, PETER A. DREIFUSS, JOHN A.G. ROACH, SANDRA J. BELL, DENIS ANDRZEJEWSKI, WILLIAM C. BRUMLEY, JAMES A. POPPITI AND JAMES A. SPHON, U.S. Food and Drug Administration, Washington, D.C. 20204

Each batch of dye certified by the Food and Drug Administration for use in foods, drugs, or cosmetics must meet specifications set for the presence of intermediates and by-products. Since many of these food, drug & cosmetic (FD&C) dyes (sulfonates) and their impurities are not amenable to analysis by electron-impact or chemical ionization mass spectrometry (MS), other techniques must be used. In this investigation, field desorption (FD) and desorption chemical ionization (DCI) were both employed to evaluate and compare their usefulness for the analysis of dye materials.

DCI was first described by Hunt [1]; in this technique, compounds of low volatility are ionized from an activated field emitter in a chemical ionization source. Here, we describe the use of DCI with simultaneous pulsed positive ion/negative ion [2] data acquisition with methane as the reagent gas. The mass spectrometer used was a Finnigan 3300 fitted with a direct insertion DCI probe and programmable emitter heating current controller [3]. FD spectra were obtained on a Varian MAT CH-5DF and a VG Micromass ZAB-2F mass spectrometer.

Meaningful FD and DCI spectra of the sodium salts of the dyes could be obtained after conversion to the corresponding sulfonic acid by rapidly passing the aqueous dye solution through a bed of Biorad AG 50W X12 ion exchange resin.

The DCI and FD spectra of FD&C Yellow #6 are typical of those obtained for many dye sulfonic acids. The DCI spectrum is shown in the figure below. Only the negative ion response (lower trace) is informative. The negative ions produced correspond to $M^{-\cdot}$ (m/z 408), $[M-SO_3]^{-\cdot}$ (m/z 328), and a likely pyrolysis product representing the right hand side of the structure as shown (m/z 239). The FD spectrum has ions corresponding to $M^{+\cdot}$ AND $[M+H]^+$ (m/z 408 and 409, respectively) with $M^{+\cdot}$ somewhat more intense, $[M-SO_3]^{+\cdot}$ (m/z 328), and a likely pyrolysis product corresponding to the left hand side of the structure (sulfanilic acid, m/z 173).

The two techniques were found to be complementary. In general, the DCI spectra provided structural information with ions corresponding to the principal subunits from which the dyes were synthesized. Negative ion DCI spectra were more informative than positive ion DCI. DCI, however, did not always produce molecular ions. FD, on the other hand, did not always provide structural information, but did give unambiguous molecular weight data.

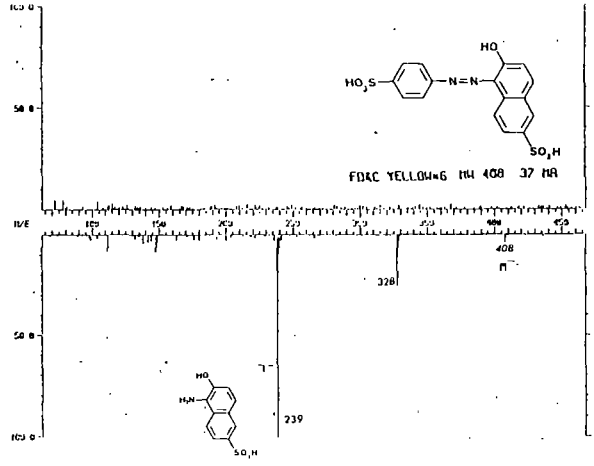

References

1. D.F. Hunt, J. Shabanowitz, F.K. Botz, D.A. Brent, Anal. Chem. 1977, 49, 1160

2. D.F. Hunt, G.C. Stafford, Jr., F.W. Crow, J.W. Russell, Anal. Chem. 1976, 48, 2098

3. J.A. Sphon, D. Andrzejewski, W. Brumley, P. Dreifuss, and J. Roach, paper presented at the Eight International Mass Spectrometry Conference, Aug. 12-18, 1979, Oslo, Norway; Adv. Mass Spectrum. Vol. 8

FIELD DESORPTION CONSTANT TEMPERATURE REGULATOR

David F. Fraley, W. Stephen Woodward, and Maurice M. Bursey

Department of Chemistry
Univ. of North Carolina
Chapel Hill, NC 27514

A novel electronic power supply called a Constant Temperature Regulator (CTR) has been developed to provide a constant reproducible temperature for Field Desorption emitters. The device is configured to regulate the emitter heating current in either the new constant temperature mode or the traditional constant current mode. The power supply employs a feedback system that utilizes the physical property that the resistance of a tungsten wire varies as a known function of temperature. Thus by maintaining a constant resistance, a constant temperature is likewise maintained. Since different manufactures produce FD instruments utilizing different emitter geometries (typically either 4, 5, or 6 mm between posts), different lengths of tungsten wire will produce different temperatures for a given constant current (the problem with constant current power supplies). This device produces a constant temperature in any emitter but with varying heating currents.

Operation of the CTR is as follows: (1.) with S1 in the Balance position and R2 = 0, balance the Wheatstone Bridge at room temp. with the LED such that this ratio holds: R-Balance : (R1 + R2) = 5 ohms : R-Emitter. (2.) with S1 in the Heat position, by increasing the temp. control R2, the total current through the bridge is greater and the emitter heats up. (3.) since the emitter is now hotter, it's resistance is greater thus the bridge is back in balance but at a new temperature level. The CTR depends on ratios of resistivities to control the emitter temperature, never on the absolute resistance of the wire.

Additionally, a computer program has been developed to theoretically compare the differences in temperature distribution along a bare, pure tungsten wire of any length with any heating current. The program solves the nonlinear second-order boundary-value differential equation problem that describes the heat flow for a rod electrically heated in vacuo. The program includes accurate temperature variations for the following physical parameters: thermal conductivity, resistivity, specific heat, Thomson effect, linear thermal expansion, and total emissivity of tungsten. The accuracy of the determined temperature distribution matched within 3% of earlier experimental work on tungsten filaments.

The results indicate that (1.) a large temperature gradient exists along the wire (see the Temp. vs. Distance plot). Thus Best Anode Temperature values are truly a spread of temperatures, not one precise temperature value. (2.) The maximum center temperature is a function of the length of the tungsten wire. For example, 30 mA corresponds to approximately a 340 degree C hotter temperature in the center of a 5 mm vs. a 4 mm bare wire. (3.) Since the process of growing carbon dendrites changes only part of the tungsten wire to tungsten carbide, only rough temperature approximations may be made for actual carbon emitters but still a 4 mm emitter is cooler than a 5 mm one at a given heating current.

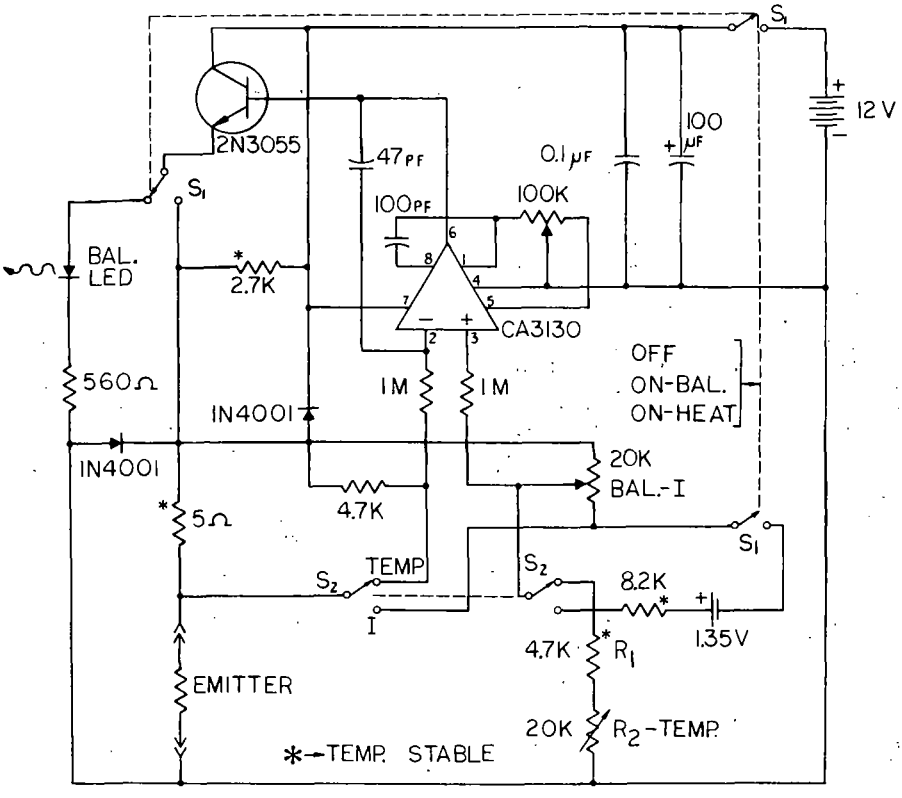

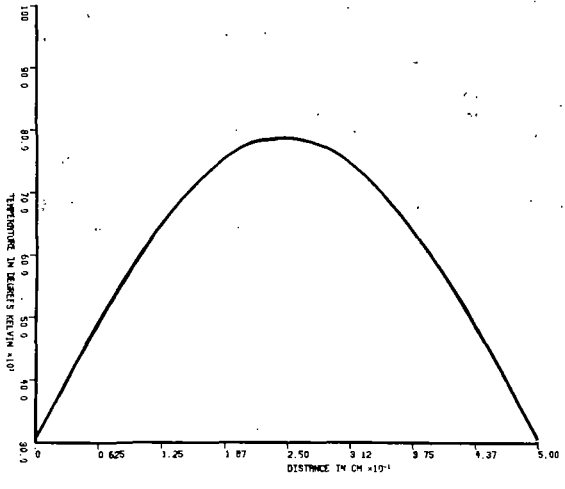

Above: Schematic for the FD Constant Temperature Regulator

Left: Temperature distribution along a bare, pure tungsten wire which is 10 microns in diameter, 5 mm long (Varian style), and is heated by 30 mA. The center temperature is 795 degrees Kelvin.

FURTHER SURFACE MODIFICATION STUDIES ON FIELD DESORPTION EMITTERS

Tim L. Youngless, Neil B. H. Henis, and Maurice M. Bursey

Department of Chemistry
Univ. of North Carolina
Chapel Hill, NC 27514

Although Field Ionization and Field Desorption Mass Spectrometry offer the advantage of molecular ion formation and FD is extremely useful for obtaining spectra of nonvolatile and thermally labile compounds, both FI and FD offer less sensitivity and less structural information than conventional EI. For this reason, emitter surface modifications have been studied to enhance sensitivity and gain structural information through selective ionization.

To study organic surface modifications it is necessary that the organic compound on the emitter does not desorb under the FI or FD conditions employed. For this reason, chemically bonded surfaces were studies. These studies were done on cobalt emitters. Both ESCA and Transmission Electron Microscopy indicate that the cobalt dendrite surface is composed mainly of cobalt oxide.

Commercially available silanes are known to react with surface hydroxyl groups as shown:

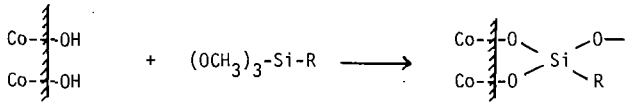

We do not necessarily imply two points of attachment for each silyl group. R can be any one of several various functional groups commercially available. Polymer formation through reaction with surface water is also possible. A carboxylic acid emitter surface was prepared with R = $CH_2CH_2CH_2COCl$ and then hydrolyzed by soaking in water for 5 minutes.

Field ionization spectra of a variety of compounds were then obtained and the following conclusions may be made: (1.) Compounds with functional groups form M+1 ions, while saturated hydrocarbons form M-1 ions. (2.) Protonation is from the carboxyl proton. This is confirmed by deuterium labeling. (3.) Protonation occurs at a threshold heating current of approximately 20 mA. However, this will vary from emitter to emitter. (4.) Emitters have given stable spectra for as long as 6 hours. This does not represent an upper limit to emitter lifetimes, but corresponds to the time the emitter was used before it was destroyed by a spark.

In addition the EI and FD mass Spectra of some metal crown ether salts are presented. The EI spectra show no trace of any metal containing ions; only peaks due to the crown ethers and fragmentations of the crown ethers are present. Field Desorption, on the other hand, leads to intense peaks characteristic of the compound of interest. The effects of different emitter surfaces on the appearance of the FD spectra was also studied. On Co surfaces, there are many ions corresponding to exchange between the metal in the crown complexes and advantitious free metal ions found in the dendritic matrix. On Ni surfaces, these exchange reactions are markedly reduced.

THE VOLCANO FIELD IONIZATION SOURCE*

C. A. Spindt
Physical Electronics Group, Advanced Development Division
SRI International, Menlo Park, California 94025

Investigations have continued to characterize and improve the volcano field ion source, and support the field ion mass spectrometry studies reported in these proceedings by Aberth and by Buttrill et al.

The volcano source consists of a tiny, hollow, volcano-like cone between 5 and 20 μm in diameter. Sample gas to be ionized is passed through the cone. When a voltage of 1 to 3 kV is applied between the volcano and a nearby counterelectrode screen, the sample gas is field ionized in the region of the sharp rim at the end of the hollow cone. In the original device, the volcano was mounted 25 to 50 μm from a screen with square openings.

A significant improvement has been development of techniques for mounting the 20-μm diameter volcano in the plane of the counterelectrode screen and centered on a 60-μm diameter circular screen opening. This geometry improves the ion optics, prevents sample gas and ions from hitting the counterelectrode, reduces the typical operating voltage to the 1.5-kV range, and eliminates contamination of the counterelectrode by polymerizable samples. Figure 1 is a scanning electron micrograph of a volcano and round screen. A second heater has been added to the source to improve temperature control and eliminate contamination and memory effects resulting from sample buildup. Figure 2 is a schematic of the ionizer structure, showing the location of the heaters.

With most organic samples tested (e.g., fuel oil, toluene, urine), about 200°C at the volcano is sufficient to prevent sample buildup and contamination of the source. In addition, we find that "activation" or whisker growth, normally associated with field ionization sources, does not occur on the anode (volcano rim) at this temperature with these samples, and that many volcanos work very well without this whisker growth. This is important, because the whiskers tend to be unstable and can produce a beam with a large energy spread when the whiskers have high resistivity.

Ionizer performance tests with toluene and a simple focus lens have shown the volcano to produce a 10^{-4} to 10^{-3} μA ion beam about 1 mm or less in diameter with 1 to 2 kV applied to the ionizer. Total ionization efficiency with toluene as the sample gas is usually of the order of 10^{-5} ions/molecule, and has been as high as 10^{-3} ions/molecule with a heavily activated 5-μm diameter volcano. Net efficiency (viz., at the detector of a mass spectrometer) has been measured at 5×10^{-6} ions/molecule. Figure 3 is typical of the performance of the volcano structure using toluene as a sample gas.

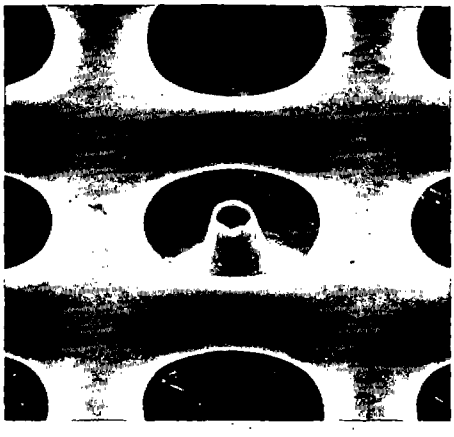

|-25μm-|

FIGURE 1 SCANNING ELECTRON MICROGRAPH OF A VOLCANO FIELD ION SOURCE

*Supported by NIH, Bethesda, Maryland

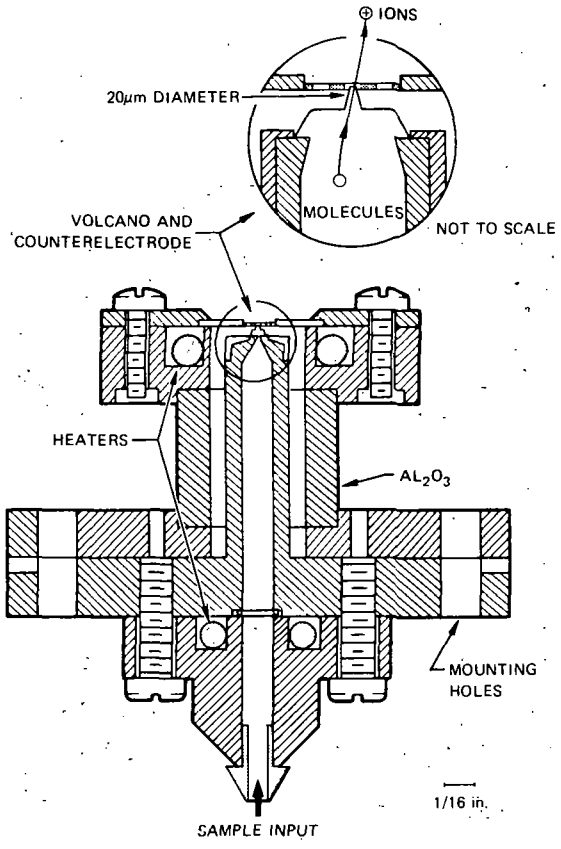

FIGURE 2 CROSS SECTION OF VALCANO-TYPE FIELD-ION SOURCE

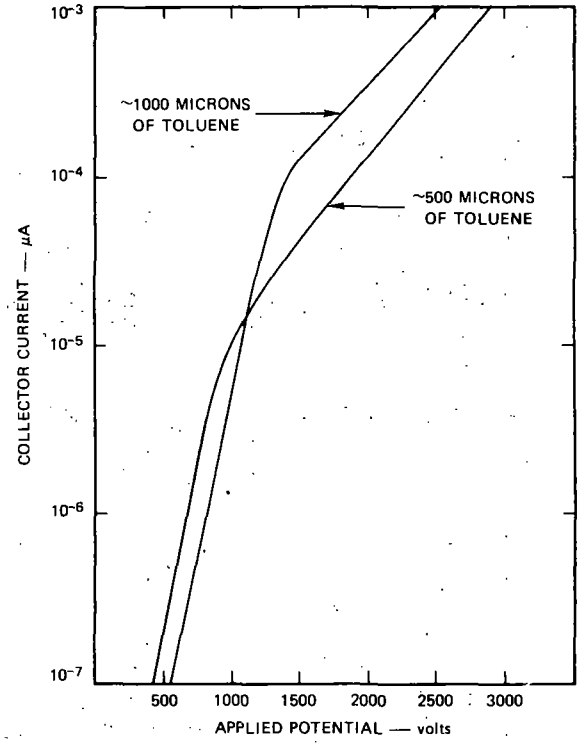

FIGURE 3 ION EMISSION vs APPLIED VOLTAGE FOR TWO 20-μm DIAMETER VOLCANOS

AUTHOR INDEX

FAMP16 Abbott, R.....709
FAMP17 Abbott, R.....710
TPMOB8 Abe, H.....288
MAMOC7 Abernathy, R.N..... 61
MAMOC8 Abernathy, R.N..... 63
FAMP19 Aberth, W.....714
TPMOB9 Aberth, W.....290
WAMP13 Abraham, Robert.....444

TPMP3 Ackman, R.G.....324
TPMOB3 Adam, Peter.....278
RPMOB13 Adam, Peter.....571
WAMOC13 Adams, N.G.....427
RAMP2 Adlof, R.O.....516
FAMOB10 Agosta, W.C.....657
RAMP9 Ajami, A.M.....528
RPMOC12 Albritton, D.L.....589
TAMP16 Albritton, D.L.....256
TAMP20 Albro, P.W.....262
WAMP13 Alvin, John.....444
FAMP16 Anbar, M.....709
FAMP17 Anbar, M.....710
RPMP19 Anderson, William R.,Jr.....621
FAMOB3 Anderson, William R.,Jr.....646
WAMOB3 Anderson, William R.,Jr.....388
TPMP17 Anderson, William R.,Jr.....347
FAMP20 Andrzejewski, Denis.....716
RPMOC7 Anicich, V.G.....582
MAMP19 Aplin, R.T.....100
MAMOA2 Ashe, T.R..... 16
MPMP19 Atwater, B.L.....186
WAMOC3 Aue, D.H.....411
MPMOC9 Ausloos, Pierre.....151
TAMP3 Ausloos, P.....233
WAMOC6 Baer, T.....415
MAMP8 Baer, T..... 83
MAMOC9 Baird, M.C..... 65
RAMOA10 Baldwin, M.A.....481
WAMOB4 Ballard, John M.....390
RAMOB7 Ballous, C.E.....495
RAMP7 Barany, George.....692
RAMOA7 Barbalas, M.P.....474
TPMP19 Barbalas, M.P.....351
RPMOB10 Barbuch, Robert.....568
WAMP20 Barchas, Jack D.....455
RPMOB10 Bargar, Ester Madrid.....568
WAMP6 Baril, Marcel.....435
RAMP10 Barker, R.....529
TPMOC1 Barlak, T.....298
WAMOA7 Barnes, Michael L.....372
WAMOA5 Barofsky, Douglas F.....368
WAMOB3 Barofsky, Douglas F.....388
TPMP17 Barofsky, Douglas F.....347
WAMOB3 Barofsky, Elisabeth.....388
WAMOA1 Barquet, Ana.....360
RPMOC5 Bartmess, John E.....579
MAMP20 Bartmess, John E.....102
RPMOC3 Bartmess, John E.....576
MAMOA2 Baset, Z..... 16
WAMOB2 Basile, Brenda.....386
RAMOC9 Bass, Lewis.....510
FAMOA7 Bates, A.D.....636
WAMOC8 Batson, C.H.....420
WAMOB12 Batta, A.K.....403
TAMOC8 Baumgartner, Erwin.....229
RPMOC11 Baykut, G.....587
WAMOA8 Bel, P.....374
FAMP20 Bell, Sandra J.....716
WAMOB10 Bendt, Juliana S.....400
TAMP21 Benoit, Frank M.....264
TPMOC7 Bentz, B.L.....308
WAMOC8 Berkowitz, Joseph.....420
RPMOB12 Berry, H.K.....570
MAMOA1 Best, H.T..... 14
MPMP7 Betowski, D.....169
WAMOC9 Beynon, J.H.....422
TPMP1 Beynon, J.H.....322
MPMOC6 Beynon, J.H.....147
MAMP16 Beynon, J.H..... 95
TPMP23 Beynon, J.H.....358
WAMP12 Biemann, K.....442
WAMP18 Biemann, K.....452
FAMP9 Biemann, K.....696
MPMOC11 Bierbaum, Veronica M.....153
MPMP23 Bill, J.C.....193
TPMP7 Bill, J.C.....331
WAMP12 Biller, J.E.....442
TAMP9 Bjorseth, Alf.....245
FAMP19 Blaisdell, B.E.....714
TPMOB9 Blaisdell, B.E.....290
TPMOC9 Blakley, C.R.....312
TPMOC13 Blakley, C.R.....320
TAMOB4 Blum, M.S.....213
MAMP18 Bobenrieth, M.-J..... 98
WAMOA11 Boettger, H.....380
FAMOB7 Boerboom, A.J.H.....652
MPMOA1 Boerboom, A.J.H.....103
MPMOA2 Boitnott, Charles A.....105
RPMP18 Bone, William.....620
TAMP2 Borer, P.N.....232
FAMOA7 Bose, A.K.....636
WAMOB13 Bose, A.K.....405
WAMP5 Bostick, J. Kent, Jr.....433
MAMP10 Botter, R..... 87
RPMOB4 Bouwsma, O.J.....559
FAMP7 Bowen, D.V.....692
RPMOC7 Bowers, M.T.....582
RAMOC9 Bowers, M.T.....510
TPMP21 Bowers, M.T.....355
MPMOC8 Bowers, M.T.....150
WAMOC3 Bowers, M.T.....411
MPMOC6 Bowie, J.H.....147
TAMP10 Boyd, Robert K.....246
TAMOC7 Boyer, Joseph H.....227

RAMP9 Bradley, J.C. 528
TAMP11 Brancaleoni, E. 247
MAMP16 Brenton, Gareth A. 95
WAMOA4 Briggle, Thomas V. 366
WAMOA1 Briggle, Thomas V. 360
MAMP5 Brill, Fred W. 80
TPMP4 Britten, R.A. 326
TAMOA5 Brletic, K.A. 201
MAMOA5 Brown, J.M. 20
WAMP21 Brown, J.M. 456
WAMP12 Brown, T.R. 442
FAMP5 Bruins, Andries P. 688
MAMP17 Bruins, Andries P. 96
FAMP20 Brumley, William C. 716
TAMP11 Bruner, F. 247
MAMOB8 Brunnee, C. 41
TPMP11 Buckley, T.J. 337
MPMP21 Budde, William L. 190

WAMOB4 Buko, Alexander M. 390
RAMOC10 Bumm, Loyd 511
TPMOC8 Burger, James E. 310
RAMOA2 Burgers, P.C. 464
WAMOC4 Burgers, P.C. 412
RAMOA4 Burlingame, A.L. 467
FAMP14 Burlingame, A.L. 705
RAMOB7 Burlingame, A.L. 495
TPMP8 Burlingame, A.L. 333
FAMOA8 Burnier, R.C. 638
TPMP16 Burns, P. 345
MPMP4 Bursey, J. 162
MPMP5 Bursey, J. 165
MPMP6 Bursey, J. 167
WAMOA13 Bursey, J. 382
FAMP22 Bursey, Maurice M. 719
FAMP21 Bursey, Maurice M. 717
MPMP13 Bursey, Maurice M. 175
TPMP22 Bursey, Maurice M. 356
TPMOC2 Busch, K. 299
WAMOC6 Butler, James J. 415
MAMOA8 Buttrill, S.E., Jr. 24
TPMP9 Buttrill, S.E., Jr. 334
FAMOA8 Byrd, G.D. 638
MAMP20 Caldwell, G. 102
RPMOC3 Caldwell, G. 576
TPMOB11 Callery, P.S. 294
WAMP11 Callery, P.S. 441
FAMP2 Callery, P.S. 685
TAMOA6 Callis, E.L. 202
MAMOC9 Camicioli, R. 65
TPMP15 Campana, J.E. 343
MPMOA4 Campana, J.E. 109
TPMOC1 Campana, J. 298
TPMP14 Cantor, D.D.M. 341
TAMOA2 Capellen, J. 196
RPMOB3 Caprioli, Richard M. 558
FAMOA4 Cardaciotto, S.J. 630
WAMP8 Carlin, Josephine R. 438
TPMOC9 Carmody, J.C. 312
TPMOC13 Carmody, J.C. 320
WAMP18 Carr, S.A. 452
MPMOB5 Carrick, A. 127
MPMP20 Carrick, A. 188
MAMOB1 Carrick, A. 30
FAMOC8 Carroll, D.I. 674
MAMP14 Carroll, D.I. 92
MAMP13 Carroll, D.I. 91
TPMOC5 Carter, J.A. 305
MAMOC10 Castleman, A.W., Jr. 68
TAMP13 Castleman, A.W., Jr. 251
FAMOB10 Chait, B.T. 657
FAMOB12 Chait, B.T. 661
MPMOC2 Chakel, John 142
RAMOB4 Chan, K.W. 488
MAMOB3 Chang, C. 34
MPMP20 Chapman, J.R. 188
RPMP20 Chapman, J.R. 622
MAMOB1 Chapman, J.R. 30
RAMOC9 Chesnavich, Walter J. 510
MPMOC8 Chesnavich, Walter J. 150
RPMP3 Chess, E.K. 596
MPMOC13 Chowdhury, A.K. 156
MAMOA5 Christensen, R.G. 20
TPMOC5 Christie, W.H. 305
TAMOA3 Christophorou, L.G. 197
TAMP11 Ciccioli, P. 247
TAMP8 Clark, Charles R. 243
RAMP10 Clark, E.L. 529
FAMP1 Clay, K.L. 684
FAMOC9 Cline-love, L.J. 675
FAMP13 Cochran, T.W. 704
TAMP20 Cochran, T. 262
MAMP7 Coggiola, G. 82
MAMOB9 Cohen, A. 42
WAMP13 Cohen, J. 444
TPMP5 Colby, B.N. 328
MPMOB8 Colby, B.N. 132
RAMOC5 Cole, B.E. 505
TPMOC1 Colton, R.J. 298
MPMOB5 Compson, K.R. 127
MPMP20 Compson, K.R. 188
RPMP20 Compson, K.R. 622
MAMOB1 Compson, K.R. 30
RAMOC3 Compton, R.N. 503
TAMOA2 Conzemius, R.J. 196
RAMOB2 Cook, J. Carter, Jr. 484
RAMOB4 Cook, Kelsey D. 488
TPMOC2 Cooks, R.G. 299
TPMP10 Cooks, R.G. 335
MAMOA3 Cooks, R.G. 18
TPMOA3 Cooks, R.G. 265
WAMOA3 Cooper, Aaron D. 364
MAMP7 Cosby, P.C. 82
WAMP12 Costello, C.E. 442
MAMP19 Cottam, G.P. 100
RPMP17 Cotter, Robert J. 618
RPMOB10 Coutant, John 568
MPMOB3 Cramers, C.A. 123
RPMP10 Creech, E.T. 606
TAMP11 Crescentini, G. 247
RAMP5 Crespi, Henry L. 521
MPMOA3 Crow, F.W. 107
TAMP9 Crow, F.W. 245
RPMP3 Crow, F.W. 596
TAMP2 Cruz, P. 232
RPMOC10 Curtis, Paul M. 586

FAMOA9 D'analozo, R.P.....639
RAMOB7 D'angona, J.....495
TPMP8 D'angona, J.....333
TPMP7 D'arcy, P.H.....331
RPMOB5 Caley, Sylvia K.....560
FAMP8 Danielson, S.J.....694
WAMOB10 Danish, Robert K.....400
MAMOA1 Danner, D.A..... 14
WAMP5 Daughtrey, E. Hunter, Jr.....433
RPMP19 Daves, G. Doyle, Jr.....621
FAMOB3 Daves, G. Doyle, Jr.....646
WAMOB3 Daves, G. Doyle, Jr.....388
FAMOA5 Davidson, W.R.....632
MPMP18 Davidson, Walter C.....184
WAMP8 Davies, R.O.....438
MPMOB10 Dawe, R.....135
TPMOC2 Day, R.J.....299
WAMOB12 Dayal, B.....403
TPMOC1 Decorpo, J.J.....298
RAMOC5 Dehmer, J.L.....505
RAMP2 Dejarlais, W.J.....516
WAM19 DeJonge, D.C.....454
RAMOB6 Dell, A.....493
WAMP17 Dell, A.....450
RAMOB7 Dell, A.....495
RPMOB12 Denton, M.D.....570
RPMOC1 Depuy, C.H.....572
RPMOC4 Depuy, C.H.....577
RPMP15 Deroos, F.L.....615
RPMP5 Deroos, F.L.....600
WAMOB9 Desiderio, D.M.....398
MAMOC6 Destefano, A.J..... 59
WAMOB14 Dias, J.R.....407
TAMOC5 Dias, J.R.....223
MAMP1 Dielmann, G..... 73
WAMOA12 Dielmann, G.....381
MAMOC5 Diem, Hugh E..... 57
MAMP10 Dimicoli, I..... 87
WAMP13 Dixit, Balwant.....444
MPMOA8 Douglas, D. 117
TPMP11 Doyle, R.J., Jr.....337
FAMP20 Dreifuss, Peter A.....716
RPMOB11 Driscoll, J.S.....569
WAMOA9 Dubay, G.R.....376
MPMOB7 Dudding, Gerald F.....130
MAMOB2 Dufour, H.R..... 32
TAMP12 Dugger, Donald L.....249
TPMP20 Duholke, Wayne K.....353
WAMCO10 Dunbar, Robert C.....423
RAMOC7 Dunbar, Robert C.....507
MAMP7 Dunbar, Robert C..... 82
MAMP6 Dunbar, Robert C..... 81
TAMOA5 Dunstan, L.P.....201
RPMP2 Dupuy, Aubry E.....594
MAMP8 Dutuit, O..... 83
FAMOB6 Dye, J.....651
MPMP9 Dymerski, Paul P.....170
RPMP21 Dymerski, Paul P.....624
MAMP14 Dzidic, Ismet..... 92
FAMOB1 Dziedzic, P.....642
TPMOC5 Eby, R.E.....305
TPMOC12 Eckers, Christine.....318
RAMOC5 Ederer, D.L..... 505
RPMOA10 Edwards, Randall P..... 552
RPMOB2 Egger, H.-J..... 556
TAMOA3 Ellis, H.W..... 197
MPMOC11 Ellison, G. Barney..... 153
FAMOA2 Elwood, T.A..... 627
WAMOC14 Elwood, T.A..... 428
RAMP2 Emken, E.A..... 516
FAMP19 Engels, J.C..... 714
TPMOB9 Engels, J.C..... 290
MPMOC2 Enke, Chris..... 142
RAMOA3 Enke, Chris..... 465
FAMOB12 Ens, W..... 661
RPMP9 Eshuis, W..... 604
TPMP17 Eskew, T.J..... 347
MPMOA9 Eskew, T.J..... 119
TAMOA6 Essling, A.E..... 202
RPMP20 Evans, S..... 622
MPMOA3 Evans, S..... 107
TPMP11 Eyler, John R..... 337
MAMP5 Eyler, John R..... 80
RAMP17 Fadden, H..... 710
RPMOC12 Fahey, D.W..... 589
TAMOC1 Falick, Arnold M..... 215
MAMOB12 Fassett, J.D..... 47
WAMP20 Faull, Kym F..... 455
RPMOC12 Fehsenfeld, F.C..... 589
TAMP16 Fehsenfeld, F.C..... 256
RPMP17 Fenselau, Catherine..... 618
WAMP8 Ferguson, R.F..... 438
FAMP7 Field, F.H..... 692
RPMOC8 Field, F.H..... 583
TAMP3 Field, F.H..... 233
FAMOB10 Field, F.H..... 657
WAMP2 Field, F.H..... 430
FAMOB12 Field, F.H..... 661
TPMP13 Fies, William J..... 340
TPMOA1 Fingas, M..... 263
RPMOA2 Finkle, Bryan S..... 535
MPMOB9 Finlay, Elizabeth M.H..... 133
TPMOB13 Fischer, J..... 297
WAMOC10 Fitzgerald, G.B..... 423
WAMOA10 Flinn, C.G..... 378
TAMOB3 Flynn, D.L..... 209
RPMOB7 Forster, H.-J..... 564
TAMOC6 Foster, Norman G..... 225
FAMP13 Fox, A..... 704
TPMP20 Fox, Lloyd E..... 353
TAMOC4 Fraiman, Ana..... 221
FAMP3 Fraisse, D..... 686
FAMP21 Fraley, David F..... 717
MAMOB11 Frank, D.J..... 46
WAMP22 Frank, L.R..... 458
RAMOC1 Franklin, J.L..... 499
FAMP3 Frappier, F..... 686
TAMOA3 Frees, L.C..... 197
TAMP18 Freiser, Ben S..... 258
FAMOA8 Freiser, Ben S..... 638
MPMP1 French, J.B..... 158
MPMOA8 French, J.B..... 117
RPMOB6 Friedel, R.O..... 562
WAMP9 Friedel, R.O..... 439

FAMP15 Friedel, R.O. 707
TAMOA9 Friedlander, S.K. 204
RAMOB1 Friedman, L. 483
TPMP15 Friedman, M.H. 343
MPMOA4 Friedman, M.H. 109
WAMP3 Frisch, Margaret A. 431
RAMOC11 Frolish, H. 512
MPMOC12 Fukuda, Elaine K. 155
MPMP1 Fulford, J. 158
FAMOA2 Futrell, J.H. 627
WAMOC14 Futrell, J.H. 428
WAMP22 Futrell, J.H. 458
WAMP23 Futrell, J.H. 460
MAMOA9 Gallegos, E.J. 26
RPMOA9 Gallis, D.E. 550
TPMOC12 Games, David E. 318
TPMOC11 Games, David E. 316
TPMOC12 Games, M.L. 318
MPMOB10 Gara, M. 135
TAMOA5 Garner, E.L. 201
WAMOA13 Garrison, A.W. 382
MPMOB9 Gaskell, Simon J. 133
FAMOC3 Gaumann, T. 665
TAMOC1 Gaumann, T. 215
MPMP4 Gebhart, J. 162
WAMOA13 Gebhart, J. 382
TPMOB11 Geelhaar, L.A. 294
WAMP11 Geelhaar, L.A. 441
WAMOA8 Gefen, L. 374
TPMOA5 Gemmell, D.S. 270
MAMP20 Georgiadis, R. 102
TPMOB1 Gershfeld, N.L. 275
FAMOC4 Ghaderi, Sahba 667
FAMOC1 Ghaderi, Sahba 662
WAMOC2 Gibson, D. 410
MPMOA7 Giffin, C.E. 115
MPMP23 Gilbert, A.J. 193
WAMOC3 Gilbert, J.R. 411
MAMP4 Gilman, J.P. 78
RAMOC8 Gilman, J.P. 508
WAMOC7 Gilman, J.P. 418
TAMOA4 Gingerich, K.A. 199
RAMOA8 Giordani, Anne B. 476
WAMOB4 Giordani, Anne B. 390
TAMP17 Gleitman, Y. 257
TPMP10 Glish, G.L. 335
RPMOC13 Glosik, J. 590
MAMP2 Goldberg, N.D. 74
RPMP7 Goldfarb, Ivan J. 603
TAMOC5 Gomiscek, S. 223
WAMOC8 Goodman, G.L. 420
MAMP8 Govers, T. 83
MPMP11 Grade, Hans 172
MAMP2 Graff, G. 74
FAMP8 Gray, Gary R. 694
MAMOB5 Grayson, Michael A. 38
FAMOA6 Greathead, R.J. 634
MPMOB12 Green, B.N. 139
TPMP16 Green, B.N. 345
RPMOB8 Green, Jack Peter 566
RAMOC10 Green, Mark 511
TAMOA10 Greene, Frank T. 206
WAMP22 Greenwalt, C. 458
TPMP14 Greenwood, G.J. 341
RAMP8 Griffey, Richard H. 526
TAMOA9 Griffin, C. 204
TPMP4 Griffin, C.E. 326
TAMOC9 Griffin, G.W. 231
WAMOC9 Griffiths, I.W. 422
MPMOA3 Gross, M.L. 107
RPMP3 Gross, M.L. 596
WAMOC12 Gross, M.L. 425
FAMOC4 Gross, M.L. 667
FAMOC1 Gross, M.L. 662
MAMP19 Grossel, M.C. 100
WAMP21 Guenther, F.R. 456
MAMOC11 Gupta, Chakra 70
TAMOA4 Gupta, S.K. 199
RAMOC11 Guyon, P.M. 512
MAMP8 Guyon, P.M. 83
MAMOB7 Habfast, K. 40
WAMP4 Habfast, K. 432
RAMOA6 Haddon, William F. 472
MAMOC11 Hall, David G. 70
MAMOB10 Hall, E.F. 44
MPMOB12 Hall, K. 139
RPMOC8 Hamlet, P. 583
TAMP3 Hamlet, P. 233
TAMP8 Hanson, Ray L. 243
TAMOA4 Haque, R. 199
TPMOB4 Haraguchi, Shin-Ichi 282
MPMP19 Haraki, K.S. 186
RPMP16 Hardin, E.D. 616
RPMOA7 Hardy, D.R. 544
MPMOB4 Hargrove, William F. 125
RPMP1 Harless, R.L. 592
WAMOC9 Harris, F.M. 422
TAMOC2 Harrison, A.G. 217
FAMOA1 Harrison, A.G. 625
TPMOC7 Harrison, W.W. 308
TPMOC6 Harrison, W.W. 306
RPMOC9 Hartmann, H. 584
RPMOC11 Hartmann, H. 587
MPMP14 Harvan, D.J. 177
RPMP6 Harvan, D.J. 602
FAMP13 Harvan, D.J. 704
WAMOB2 Hashizume, Takeshi 386
MPMP14 Hass, J.R. 177
TPMP22 Hass, J.R. 356
RPMP6 Hass, J.R. 602
FAMP13 Hass, J.R. 704
MAMP18 Hass, J.R. 98
MPMP13 Hass, J.R. 175
WAMP14 Hassler, Rolf 446
TPMOB12 Hassler, Rolf 295
TPMOB10 Hassler, Rolf 292
FAMP18 Hatch, Frank 712
FAMP18 Hattox, Susan E. 712
FAMOA10 Hauer, Charles R. 641
WAMP14 Haug, Pat 446
TPMOB12 Haug, Pat 295
TPMOB10 Haug, Pat 292
MAMOC2 Haverkamp, Johan 51

MAMOC1 Haverkamp, J. 49
RPMP9 Haverkamp, J. 604
FAMOB7 Haverkamp, J. 652
MPMOA1 Haverkamp, J. 103
RAMOC7 Hays, J.D. 507
RPMOC5 Hays, R.L. 579
MPMP20 Hazelby, D. 188
RPMP20 Hazelby, D. 622
TAMP4 Headley, J.V. 235
TAMOC2 Hegedus-vajda, J. 217
WAMOA2 Heikes, David L. 362
FAMOB8 Heinen, H.J. 654
MPMP21 Heller, R.S. 190
MPMP21 Heller, S.R. 190
TAMP13 Helm, H. 251
TPMP10 Hemberger, P.H. 335
TPMOA3 Hemberger, P.H. 265
WAMOC13 Henchman, Michael J. 427
MPMOC3 Henchman, Michael J. 144
TAMP8 Henderson, Thomas R. 243
MAMP9 Hendricks, Lloyd J. 85
RPMOA8 Henion, Jack D. 546
FAMP22 Henis, Neil B.H. 719
FAMOB8 Henning, M. 654
FAMOB9 Heresch, F. 655
FAMOA1 Herman, J.A. 625
RPMOC13 Herman, Z. 590
FAMOA2 Herold, D.A. 627
WAMOC14 Herold, D.A. 428
MAMOA5 Hertz, H.S. 20
MAMOB9 Hertz, H.S. 42
WAMP21 Hertz, H.S. 456
TPMP17 Herzog, L.F. 347
TPMP18 Herzog, L.F. 349
MPMOA9 Herzog, L.F. 119
MPMP7 Hiatt, M. 169
TPMOC10 Hidy, B. 314
RPMP15 Hidy, B. 615
RAMOC8 Hierl, Peter M. 508
MAMP3 Hiller, J.E. 76
MAMOA5 Hilpert, L.R. 20
WAMP21 Hilpert, L.R. 456
WAMOC11 Hiraoka, K. 424
TAMP14 Hirst, D.M. 253
MPMP14 Hoffmann, M.K. 177
MAMP15 Hohn, M. 94
FAMOB6 Holland, Jack F. 651
MPMP22 Holland, Jack F. 192
TPMOB2 Holland, James 277
MAMOC10 Holland, P.M. 68
TAMP19 Holler, J.S. 260
RPMOB9 Holler, J.S. 567
WAMOB% Holler, J.S. 392
WAMOC1 Holmes, John L. 409
RAMOA2 Holmes, John L. 464
WAMOC4 Holmes, John L. 412
TPMOA1 Holmes, John L. 263
RAMOC7 Honovich, J.P. 507
RAMOB3 Hooser, E. Ray 486
MAMOC5 Hooser, E. Ray 57
TPMP7 Hopkinson, J. 331
MAMP14 Horning, E. 92
MAMP13 Horning, E. 91
TAMOC9 Horning, M.G. 231
WAMP15 Horning, M.G. 448
FAMOC5 Horsley, William J. 669
RPMOB8 Hough, Lindsay B. 566
RPMP15 Howard, C.C. 615
MPMOC6 Howe, I. 147
TPMP23 Howe, I. 358
MPMOB5 Hoyle, M.J. 127
WAMOC7 Hsieh, Ta-Cheng 418
MAMP4 Hsieh, Ta-Cheng 78
RAMOC8 Hsieh, Ta-Cheng 508
MAMOA7 Hsu, C.S. 23
RAMOA5 Huang, Shing-Kwan 469
FAMOB9 Huber, J.F.K. 655
TPMOA3 Hubik, A. 265
RPMP2 Hughes, B. Mason 594
RAMOA8 Hunt, Donald F. 476
RPMP18 Hunt, Donald F. 620
WAMOB4 Hunt, Donald F. 390
FAMOB11 Hunt, J.E. 659
RPMOC8 Hunter, E.P. 390
TAMP3 Hunter, E.P. 233
TAMP2 Hunter, R.L. 232
FAMOC2 Hunter, R.L. 664
RPMOC7 Huntress, W.T. 582
WAMOB5 Ibrahim, B.K. 392
TPMP21 Illies, Andreas J. 355
WAMOC3 Illies, Andreas J. 411
MPMP9 Insalaco, Samuel 170
FAMOC12 Ioup, George E. 682
MPMOA5 Ioup, Juliette W. 111
FAMOC12 Ioup, Juliette W. 682
FAMOB1 Iribarne, J.V. 642
WAMOA5 Isabelle, Lorne M. 368
RAMOC11 Ito, K. 512
MAMP8 Ito, K. 83
MAMOC2 Jacobsen, Marcus 51
FAMP2 Jakubowski, E.M. 685
WAMOA10 Jamieson, W.D. 378
TPMP3 Jamieson, W.D. 324
RPMOA6 Jane, Ian 540
MAMOB4 Jarrell, J.A. 36
TAMP14 Jarrold, M.F. 253
RPMOC2 Jennings, K.R. 574
TAMP4 Jennings, K.R. 235
FAMOA6 Jennings, K.R. 634
TAMP14 Jennings, K.R. 253
WAMOC3 Jennings, K.R. 411
TPMP4 Johansen, R. 326
MPMOA7 Johansen, R. 115
WAMOC14 Johnson, J.O. 428
MPMP22 Johnson, S. 192
MAMP11 Jones, E. Grant 89
RPMP7 Jones, E. Grant 603
RPMOA1 Jones. L.V. 531
TAMP5 Jones, Roger W. 237
RAMP3 Jouany, M. 686
WAMP17 Judkins, M. 450
TPMOB8 Kabashima, K. 288
TPMOB3 Kalhan, Satish 278

TAMP6 Kappes, Manfred M.....239
TPMOC10 Karger, B.L.....314
TAMOC3 Karni, Miriam.....219
TPMOB3 Kato, T.....288
FAMP11 Kawamura, M.....700
TAMP15 Kebarle, P.....255
FAMOA3 Kebarle, P.....629
WAMOC11 Kebarle, P.....424
MAMOC10 Keesee, R.G..... 68
RPMOB11 Kelley, J.A.....569
MAMOA7 Kelliher, J.M..... 23
TPMP6 Kelner, Leonid.....329
TPMP15 Kelner, Leonid.....343
MPMOA4 Kelner, Lenoid.....109
WAMOC3 Kemper, P.A.M.....411
RPMOC7 Kemper, P.R.....582
RPMP11 Kenyon, Christine N.....608
MAMOC6 Keough, T..... 59
RPMOB8 Khandelwal, J.K.....566
FAMP9 Kidwell, D.A.....696
WAMP14 Kim, Jin-Soo.....446
RPMOC4 King, Gary K.....577
MAMOB4 King, J.G..... 36
RPMOB13 King, K.C.....571
TPMOC10 Kirby, D.P.....314
MAMOC1 Kistemaker, P.G..... 49
FAMOB7 Kistemaker, P.G.....652
RAMOC3 Klots, Cornelius S.....502
WAMP13 Knapp, Joseph.....444
TPMOB7 Kobayashi, K.....286
TPMOB6 Kobayashi, K.....284
RAMP11 Koch, H.J.....530
TPMOB1 Kody, M.H.....275
RAMP7 Kollman, Victor H.....524
TPMP1 Kralj, B.....322
RPMOA5 Kram, T.C.....538
MAMP2 Krick, Thomas P..... 74
WAMOB11 Kuhara, T.....401
TPMOB8 Kuhara, T.....288
FAMP11 Kuhara, T.....700
FAMP12 Kuhara, T.....702
TPMOB4 Kuhara, T.....279
TPMOC12 Kuhnz, Wilhelm.....318
WAMOB11 Kumashiro, R.....401
FAMP12 Kumashiro, R.....702
TAMOA1 Lagergren, C.R.....195
MPMOA6 Lagergren, C.R.....113
RAMOB4 Lai, S.-T.F.....488
MAMOC7 Lampe, F.W..... 61
MAMOC8 Lampe, F.W..... 63
TPMOC5 Landau, L.....305
MPMP2 Lao, R.C.....160
TPMOA3 Laramee, J.L.....265
TPMP23 Larka, Edmund A.....358
RAMOB3 Lattimer, Robert P.....486
MAMOC5 Lattimer, Robert P..... 57
MAMOC3 Lattimer, Robert P..... 52
RAMOA3 Latven, R.K.....465
MPMOC10 Laudenslager, James B.....152
WAMOC12 Lay, J.O.....425
MAMOC5 Layer, Robert W..... 57
MPMOB3 Leclercq, P.A.....123
FAMOC4 Ledford, Edward B., Jr.....667
FAMOC1 Ledford, Edward B., Jr.....662
MAMOC10 Lee, N..... 68
MPMP2 Lee, S.W.....160
RPMP19 Lee, Terry D.....621
FAMOB3 Lee, Terry D.....646
WAMOB3 Lee, Terry D.....388
RAMP3 Leete, Edwards.....517
TPMP22 Lehman, Thomas A.....356
MPMOC11 Leone, Stephen R.....153
WAMP15 Lertratanangkoon, K.....448
RAMOC7 Lev, N.B.....507
WAMOC2 Levsen, K.....410
MAMP18 Levy, L.A..... 98
MPMOB11 Lewis, D. Scott.....136
TPMOC12 Lewis, Emyr.....318
RPMP1 Lewis, R.G.....592
MPMOC9 Lias, Sharon G.....151
MAMP16 Liehr, Joachim G..... 95
RAMOC2 Lifshitz, Chava.....500
WAMOC2 Lifshitz, Chava.....410
TAMP17 Lifshitz, Chava.....257
MPMP11 Ligon, Woodfin V., Jr.....172
RAMOB5 Ligon, Woodfin V., Jr.....490
MPMOB1 Ligon, Woodfin V., Jr.....121
RPMOB3 Lin, Shen-Nan.....558
RAMOA4 Linscheid, M.....467
RAMOB7 Linscheid, M.....495
TPMOC2 Liu, L.....299
RPMOB11 Liu, P.S.....569
TPMP21 Liu, Shuying.....355
WAMOC3 Liu, Shuying.....411
WAMP7 Liu, T.Y.....437
WAMP2 Lloyd, J.R.....430
TAMP2 Locke, M.J.....232
RPMOA4 Lorch, Steven, K.....537
RAMOB2 Lory, E.R.....644
WAMOC1 Lossing, F.P.....409
TPMOA1 Lossing, F.P.....263
MPMOA1 Louter, G.J.....103
TPMOC6 Loving, T.J.....306
MPMOA3 Lyon, P.A.....107
RPMP3 Lyon, P.A.....596
FAMOB11 Macfarlane, R.D.....659
TPMOB7 Maeda, K.....286
TPMOB6 Maeda, K.....284
FAMOA3 Magnera, T.F.....629
TPMOA6 Maier, John P.....274
TAMOC3 Mandelbaum, Asher.....219
TAMOC4 Mandelbaum, Asher.....221
MPMP15 Manuel, A.J.....179
MPMOB10 Marconi, Marcia.....135
RPMOC4 Maricq, M. Matti.....577
MPMOC11 Marilq, M.....153
MAMOC10 Mark, T.D..... 68
TAMP13 Mark, T.D.....251
TPMOB5 Markey, S.P.....282
RAMP4 Markey, S.P.....519
FAMP3 Marquet, A.....686
RPMOB11 Marquez, V.E.....569

TPMOC6 Marquis, R.W.....306
TPMP1 Marsel, J.....322
TPMP18 Marshall, D.J.....349
RPMOB12 Martelo, O.J.....570
MPMP22 Martin, F.....192
MPMP21 Martinsen, D.P.....190
WAMOB11 Maruyama, Izumi.....401
FAMP12 Maruyama, Izumi.....702
TAMP4 Mason, R.S.....235
RAMP1 Massey, Ian J.....514
WAMOB7 Mathews, R.....396
WAMOB11 Matsumoto, I.....401
TPMOB8 Matsumoto, I.....288
FAMP11 Matsumoto, I.....700
FAMP12 Matsumoto, I.....702
TPMOB4 Matsumoto, I.....279
RPMOC8 Mautner, M.....583
TAMP3 Mautner, M.....233
MPMOB1 May, Ralph J.....121
MAMOA5 May, W.E..... 20
RAMP4 Mayer, W.J.W.....519
RPMOA8 Maylin, G.A.....546
TPMP2 Mcbay, E.H.....323
MAMP16 Mccloskey, James A..... 95
WAMOB2 Mccloskey, James A.....386
WAMOB1 Mccloskey, James A.....384
RAMOC10 Mccluskey, Richard.....511
RAMOA5 Mcclusky, Gary.....469
MPMOC13 Mcdonald, Richard N.....156
RAMP3 Mcdonell, Jim.....517
RPMP12 Mcdonie, R.A.....610
RAMB6 Mcdowell, R.A.....493
RPMOC7 Mcewan, M.J.....582
RAMOA1 Mcewan, C.N.....462
RPMOA10 Mcgee, Michael P.....552
RAMOA10 Mcgilvery, D.C.....481
FAMOA10 Mcguire, Jeffery M.....641
RPMP14 Mcguire, John M.....614
TAMP2 Mciver, Robert T., Jr.....232
FAMOC2 Mciver, Robert T., Jr.....664
MPMOC12 Mciver, Robert T., Jr.....155
FAMOC10 Mcdown, H.S.....677
FAMOB2 Mclafferty, Fred W.....644
RAMOA7 Mclafferty, Fred W.....474
MPMP19 Mclafferty, Fred W.....188
TPMP19 Mclafferty, Fred W.....351
RAMOA10 Mclafferty, Fred W.....481
TPMP8 Mcpherron, R.....333
MPMP22 Mcpherson, M.....192
FAMP16 Mcreynolds, James H.....709
FAMP17 Mcreynolds, James H.....710
MPMP7 Meier, E.P.....169
FAMOB8 Meier, S.....654
MPMOC7 Meisels, G.G.....148
WAMOC7 Meisels, G.G.....418
MAMP4 Meisels, G.G..... 78
RAMOC8 Meisels, G.G.....508
MAMOB10 Merren, T.O..... 44
FAMP7 Merrifield, R.B.....692
WAMP19 Messier, F.....454
MPMOC8 Metiu, Horia.....150
MAMOC2 Meuzelaar, Henk L.C..... 51
WAMP22 Meuzelaar, Henk L.C.....458
WAMP23 Meuzelaar, Henk L.C.....460
TAMOA6 Meyer, R.J.....202
WAMOA13 Michael, L.C.....382
TAMOC2 Middlemiss, N.E.....217
RAMOB2 Milbert, Richard M.....484
FAMOA4 Millen, W.G.....630
MAMOB2 Miller, C.D..... 32
RPMP10 Miller, M.S.....606
MPMOB12 Millington, D.S.....139
TPMP16 Millington, D.S.....345
MPMP21 Milne, G.W.A.....190
TPMP12 Mintz, Donald M.....338
TAMOB3 Mitscher, L.A.....209
TPMOB8 Mitsutake, K.....288
RPMOB3 Mo, Benjamin P.O.....558
WAMOC4 Mollah, Y.....412
RAMOA6 Molyneux, Russel J.....472
MAMP14 Montgomery, F..... 92
WAMOA1 Morgade, Carmen.....360
MPMOC1 Morgenthaler, L.N.....140
RAMOC11 Morin, P.....512
MAMP8 Morin, P..... 83
TPMOB10 Moritz, Jutta.....292
RAMOB6 Morris, H.R.....493
WAMOB6 Morris, H.R.....394
WAMP17 Morris, H.R.....450
RPMP10 Morrow, R.W.....606
MAMOC11 Morton, Thomas Hellman..... 70
MPMOA5 Mosharrafa, Mostofa.....111
TPMP2 Mueller, T.R.....323
FAMOC10 Mueller, T.R.....677
WAMOC9 Mukhtar, E.S.....422
MPMP12 Mulcahy, M.F.R.....173
FAMP15 Mumtaz, M.....707
MPMP19 Mun, I.K.....286
FAMOA10 Munson, Burnaby.....641
FAMP1 Murphy, R.C.....684
WAMOB7 Murphy, R.C.....396
TAMOB2 Murphy, R.C.....208
TPMOC5 Musick, W.R.....305
WAMOA2 Myers, Donald L.....362
FAMOA5 Nacson, S.....632
TAMOA4 Nappi, B.M.....199
RPMOB6 Narasimhachari, N.....562
FAMP15 Narasimhachari, N.....707
WAMP9 Narasimhachari, N.....439
WAMOA6 Natusch, D.F.S.....370
TPMOB11 Nayar, M.S.B.....294
MPMOB10 Nelson, D.....135
RAMOC11 Nenner, I.....512
MAMP8 Nenner, I..... 83
TPMOC4 Newbury, D.E.....303
RAMOA3 Newcome, B.....465
TAMOC2 Nibbering, N.M.M.....217
RPMOB5 Nielsen, Carl Johann.....560
MAMOB8 Nielsen, H..... 41
MAMOC4 Nikora, J.A..... 54
TAMP15 Nishizawa, K.....255
TPMOB12 Nitsch, Cordula.....295
TPMOB10 Nitsch, Cordula.....292
TPMOB7 Niwa, T.....286

TPMOB6 Niwa, T.....284
RPMOB12 Norman, Eric J.....570
TAMOA9 Norris, D.....204
WAMP15 Nowlin, J.....448
MAMP13 Nowlin, J..... 91
RAMP10 Nunez, H.A.....529
MPMP13 Nystrom, J.A.....175
RAMOA7 Occolowitz, J.L.....474
MPMOB11 Ogle, Larry D.....136
TPMOB7 Ohki, T.....286
TPMOB6 Ohki, T.....284
RPMP10 Oldham, T.R.....606
FAMOB6 Olinger, R.....651
RAMP4 Oliver, J.....519
TAMP19 Orti, D.L.....260
RPMP13 Oseitwum, E.Y.....612
MPMOB6 Ouchi, Glenn I.....129
TPMP19 Pagano, F.P.....351
MAMOA2 Pancirov, R.J..... 16
WAMOB1 Pang, H.....384
WAMOA5 Pankow, James.....368
FAMOC3 Parisod, G.....665
MPMOB5 Park, C.D.....127
TAMOB3 Park, Y.H.....209
TAMP20 Parker, C.E.....262
FAMP13 Parker, C.E.....704
WAMOA7 Parks, Sandy P.....372
RAMOC5 Parr, Albert C.....505
RAMOC4 Parr, Albert C.....504
RAMOC6 Parr, Albert C.....506
MPMOB12 Parr, V.....139
TAMOC7 Patel, Jayanti R.....227
TAMP19 Patterson, D.G.....260
RPMOB9 Patterosn, D.G.....567
WAMOB5 Patterson, D.G.....392
MPMOC3 Paulson, J.F.....144
MPMOC1 Paulson, J.F.....140
RPMOB5 Peace, Jon N.....560
RPMP7 Pedrick, Donald L.....603
TPMP19 Pegues, R.F.....351
TAMOA4 Pelino, M.....199
MPMP4 Pellizzari, E.....162
MPMP5 Pellizzari, E.....165
MPMP6 Pellizzari, E.....167
WAMOA13 Pellizzari, E.....382
MAMOA6 Pelroy, R.A..... 22
WAMOA4 Peoples, Anita J.....366
MPMP4 Perry, D.....162
MPMP5 Perry, D.....165
MPMP6 Perry, D.....167
TPMOC10 Petersen, B.....314
MAMOA6 Petersen, M.R..... 22
MAMP7 Peterson, J.R..... 82
MAMOC10 Peterson, K.I..... 68
TAMP13 Peterson, K.I.....251
WAMOA9 Petty, J.D.....376
WAMOA4 Pfaffenberger, Carl D.....366
WAMOA1 Pfaffenberger, Carl D.....360
RPMOB1 Pfeifer, Peter.....554
RPMOB2 Pfeifer, Peter.....556
FAMOB8 Phillips, L.V.....654
RPMP7 Pickard, James M.....603
WAMOB7 Pickett, W.C.....396
RAMP10 Pierce, J.....529
MPMOB9 Pike, Adrian W.....133
WAMOB6 Piper, P.J.....394
MPMP12 Plumb, I.C.....173
FAMOA4 Poeppel, M.O.....630
MPMP15 Poeppel, M.O.....179
MAMOC2 Pope, David L..... 51
WAMP22 Pope, David L.....458
TAMOC8 Popitsch, A.....229
FAMP20 Poppiti, James A.....716
RPMOC10 Porter, Richard F.....586
RAMP3 Porwoll, Joe.....517
RAMP8 Poulter, C. Dale.....526
MPMP23 Powers, P.....193
TPMP7 Powers, P.....331
FAMOA7 Pramanik, B.....636
WAMOB13 Pramanik, B.....405
WAMOA3 Pramanik, Birendra N.....364
TPMOB13 Preiss, J.....297
RPMP12 Price, Philip C.....610
TPMP1 Proctor, C.J.....322
MAMP18 Priutt, L..... 98
TPMOB13 Przybylski, M.....297
RPMP13 Quilliam, M.A.....612
RPMOC9 Radtke, J.....584
WAMOB9 Ragland, J.....398
RAMP2 Rakoff, H.....516
TPMP3 Ramaley, Louis.....324
MPMP4 Rando, L.....162
MPMP5 Rando, L.....165
MPMP6 Rando, L.....167
WAMOA13 Rnado L.....382
MAMP1 Rapp, Uwe..... 73
MAMP15 Rapp, Uwe..... 94
WAMOA12 Rapp, Uwe.....381
WAMOA9 Rappe, C.....376
WAMP4 Ravens, H.....432
FAMOC12 Rayborn, Grayson H., Jr.....682
TAMOA6 Reedy, G.....202
TAMP18 Reents, William D.....258
MPMP1 Reid, N.M.....158
RPMOB1 Reiner, Josef.....554
RPMOB2 Reiner, Josef.....556
FAMP4 Reinhold, V.N.....687
MPMP23 Reinsch, R.....193
WAMOB5 Reiss, E.....392
MAMOC5 Rhee, C.K..... 57
WAMOA9 Ribick, M.A.....376
MAMOA5 Richie, K.L..... 20
WAMP21 Richie, K.L.....456
MAMP16 Richter, Wilhelm J..... 95
RPMOC6 Ridge, Douglas P.....580
WAMOC5 Ridge, Douglas P.....413
FAMP17 Rieth, W.....710
RAMOB2 Rinehart, Kenneth L., Jr.....484
TAMOB1 Rinehart, Kenneth L., Jr.....207
FAMP20 Roach, John A.G.....716
RAMP8 Roberts, John L.....526
TAMP20 Robinson, J.....262
TPMOB2 Roboz, John.....277
WAMOB8 Rohwedder, William K.....397

RAMP2 Rohwedder, William K.....516
FAMP14 Roitman, E.....705
RPMOB7 Rominger, K.L.....564
TPMP5 Rosecrance, A.R.....328
MPMOB8 Rosecrance, A.R.....132
RAMOC4 Rosenstock, Henry.....504
RAMOC6 Rosenstock, Henry.....506
MPMOB4 Rosenthal, David.....125
TPMP6 Rosenthal, David.....329
RAMP10 Rosevear, P.R.....529
RPMOC12 Rowe, B.....589
TAMP16 Rowe, B.....256
RPMP15 Roy, T.A.....615
TAMP8 Royer, Robert E.....243
RAMOA1 Rudat, M.A.....462
RPMOA9 Rudy, J.A.....550
WAMP16 Ruo, T.I.....449
RPMOB4 Ruo, T.I.....559
TPMP2 Russell, D.H.....323
RPMP2 Ryan, J.F.....594
MPMP4 Ryan, J.F.....162
MPMP5 Ryan, J.F.....165
MPMP6 Ryan, J.F.....167
WAMOA13 Ryan, J.F.....382
MPMP12 Ryan, K.R.....173
MPMOB5 Ryan, P.A.....127
MAMOB1 Ryan, P.A..... 30
WAMOA6 Ryan, P.W.....370
TPMOC2 Ryan, T.M.....299
WAMP9 Saady, J.....439
WAMOB9 Sabbatini, J.Z.....398
TPMOB7 Saito, A.....286
TPMOB6 Saito, A.....284
MPMP1 Sakuma, T.....158
WAMOB12 Salen, g.....403
WAMOB6 Samhoun, M.N.....394
FAMOA9 Sanders, R.A.....639
TAMOA3 Sauers, I.....197
MPMP7 Sauter, A.D.....169
TPMOC6 Savickas, P.J.....306
FAMP16 Scanlon, M.....709
FAMP17 Scanlon, M.....710
MAMOB9 Schaffer, R..... 42
FAMOC7 Scheibel, R.C.....673

MPMOB3 Scherpenzeel, G.J.....123
FAMOB9 Schmid, E.R.....655
TPMOB12 Schmude, B.....295
TAMP7 Schoengold, D.M.....241
MAMOA6 Schoengold, D.M..... 22
WAMP14 Schroder, Norbert.....446

TAMOA8 Schubert, Rudolf.....203
TPMOB2 Schulman, Gail.....277
WAMOA12 Schulte, E.....381
WAMOA6 Schure, M.R.....370
FAMP13 Schwab, J.H.....704
TPMP15 Seeliger, E.H.....343

FAMOB5 Seita, K.....649
RAMOA5 Selkirk, James K.....469

WAMOC11 Sen Seharma, D.K.....424
MAMOC8 Senzer, S.N..... 63
RAMP10 Serianni, A.S.....529
MPMOC13 Setser, D.W.....156
RAMOA8 Shabanowitz, Jeffery.....476
RPMP18 Shabanowitz, Jeffery.....620
WAMOB4 Shabanowitz, Jeffery.....390
TPMOB9 Sheets, A.....290
FAMP19 Sheets, A.....714
WAMOB12 Shefer, S.....403
WAMOA13 Sheldon, L.S.....382
MAMOA10 Shen, Jacob..... 28

WAMOB11 Shinka, T.....401
TPMOB8 Shinka, T.....288
FAMP11 Shinka, T.....700
TPMOB4 Shinka, T.....279
TAMP10 Shushan, Bori.....246
RAMOA9 Siegel, M.W.....478
TAMP3 Sieck, L.....233
MPMOC11 Simon, C.....153
TPMOC4 Simons, D.S.....303
WAMOA6 Sine, M.R.....370
TAMOCA9 Sinha, Mahadeva P.....204
WAMOB4 Sisak, Mary.....390
RPMP5 Slivon, L.E.....600
WAMOC13 Smith, D.....427
FAMOC10 Smith, D.H.....677
MAMOC4 Smith, G.F..... 54
TPMOC8 Smith, Richard D.....310
RAMOB2 Snelling, Charles R., Jr.....484
MAMOB9 Sniegoski, L..... 42
RPMOA4 Snyder, John D.....537
MPMP17 Sokolow, Steve.....183
RPMP4 Solch, J.G.....598
MAMOB2 Solch, J.G..... 32
MPMOB7 Sorensen, Gerald T.....130
FAMOC5 Spencer, Robert B.....669
FAMP20 Sphon, James A.....716
FAMP23 Spindt, C.A.....720
RPMOB1 Spiteller, Gerhard.....554
RPMOB2 Spiteller, Gerhard.....556
MAMOC9 Splinter, D..... 65
MAMOA8 St. John, G.A..... 24
TAMP5 Staley, Ralph H.....237
TAMP6 Staley, Ralph H.....239
WAMOA9 Stalling, D.L.....376
FAMOB12 Standing, K.G.....661
MPMOA2 Steiner, Urs.....105
MPMP15 Steller, W.A.....179
TAMP13 Stephan, K.....251
MPMP12 Steven, J.R.....173
TPMP14 Stewart, J.F.....341
FAMOC8 Stillwell, R.N.....674
MAMP13 Stillwell, R.N..... 91
TAMOC9 Stillwell, Wanda G.....231
RAMOC5 Stockbauer, Roger.....505
RAMOC4 Stockbauer, Roger.....504
RAMOC6 Stockabuer, Roger.....506
TAMOA1 Stoffels, J.J.....195
TPMOB11 Stogniew, M.....294

WAMP11 Stogniew, M. 441
MAMOC9 Stone, J.A. 65
MPMOA2 Story, Michael S. 105
FAMOA4 Stout, Steven J. 630
MPMP15 Stout, Steven J. 179
WAMOC3 Stradling, R. 411
MPMP20 Street, F.J. 188
RPMOC1 Sullivan, S.A. 572
MPMP16 Sun, Tung. 181
RAMOB8 Sun, Wing Fung. 497
TAMP15 Sunner, J. 255
FAMOA3 Sunner, J. 629
TPMOB12 Suzuki, Manabu. 295
TPMOB10 Suzuki, Manabu. 292
TPMOB2 Suzuki, Robert. 277
TAMOA2 Svec, H.J. 196
MAMOA1 Swansiger, John T. 14
TAMOB3 Swayze, J.K. 209
MPMOC6 Szulejko, J.E. 147
RAMOC11 Tabche-fouhaile, A. 512
MAMP8 Tabche-fouhaile, A. 83
FAMOA7 Tabei, K. 636
FAMP3 Tabet, J.C. 686
FAMOB5 Taira, T. 649
RPMOB13 Takieddine, F.N. 571
WAMOB11 Tanikawa, K. 401
FAMP12 Tanikawa, K. 702
FAMOC7 Tanner, O.P. 673
WAMOB6 Taylor, G.W. 394
RPMP4 Taylor, M.L. 598
MAMOB2 Taylor, M.L. 32
TAMOC1 Tecon, P. 215
RAMOA2 Terlouw, J.K. 464
WAMOC4 Terlouw, J.K. 412
MPMP18 Terwilliger, D. Thomas. 184
TPMOB5 Tetsuo, M. 282
FAMP14 Thaler, M.M. 705

WAMP16 Thenot, J.P. 449
RPMOB4 Thenot, J.P. 559
MPMP2 Thomas, R.S. 160
WAMP3 Thompson, Joyce A. 431
MPMP1 Thomson, B.A. 158
FAMOB1 Thomson, B.A. 642
RPMP14 Thruston, Alfred D., Jr. 614
RPMP4 Tiernan, T.O. 598
MAMOB2 Tiernan, T.O. 32
MPMOC5 Tiernan, T.O. 145
WAMOB12 Tint, G.S. 403
WAMOB6 Tippins, J.R. 394
TPMP19 Todd, P.J. 351
RAMOA10 Todd, P.J. 481
RAMP1 Tokes, L. 514
MPMP4 Tomer, K. 162
MPMP5 Tomer, K. 165
MPMP6 Tomer, K. 167
WAMOA13 Tomer, K. 382
MPMP13 Tondeur, Y. 175
TPMOB4 Toshima, H. 279
RPMP2 Troost, J.R. 594
TAMOC9 Tsang, W.-S. 231
FAMP19 Tsao, C.S. 714
WAMOB10 Tserng, Kou-Yi. 400
TPMOB3 Tserng, Kou-Yi. 278
RPMOB13 Tserng, Kou-Yi. 571
FAMOB5 Tsuchiya, M. 649
MAMP6 Turner, D.W. 81
MAMOB10 Turner, P.J. 44
MAMOB7 Tuttas, D. 40
FAMOC9 Tway, Patricia C. 675
RAMOB1 Udseth, H.R. 483
TPMOC2 Unger, S.E. 299
FAMOC12 Upchurch, Billy T. 682
FAMP8 Upham, Roger A. 694
TAMP6 Uppal, Jack S. 239
RPMOA10 Valentour, C. 552
MAMOC1 Valerio, D. 49
FAMOB7 Van De Peyl, G.J.Q. 652
RPMOC2 Van Doorn, R. 574
RPMP9 Van Haard, P.M.M. 604
FAMOC11 Van Katwijk, J. 680
WAMP12 Van Langenhove, Agnes. 442
WAMP8 Vandenheuvel, W.J.A. 438
RPMP4 Vanness, G.F. 598
MAMOB2 Vanness, G.F. 32
TPMOC3 Vasile, M.J. 301
MPMP19 Venkataraghavan, R. 186
FAMP16 Verkh, L. 709
FAMP17 Verkh, L. 710
MAMP3 Vestal, Marvin L. 76
RPMP16 Vestal, Marvin L. 616
TPMOC9 Vestal, Marvin L. 312
TPMOC13 Vestal, Marvin L. 320
TAMOB3 Veysoglu, T. 209
TAMP16 Viggiano, A.A. 256
WAMOA8 Vincze, A. 374
FAMOB8 Vogt, H. 654
FAMOC10 Vogt, Jurgen. 511
MAMOC3 Voorhees, Kent J. 52
TPMOC10 Vouros, Paul. 314
TPMOB10 Wagner, Alan. 292
RPMP20 Wakefield, C.J. 622
MPMOB5 Wakefield, C.J. 127
MPMP20 Wakefield, C.J. 188
WAMP8 Walker, R.W. 438
MPMP23 Wallington, M.J. 193
TPMP7 Wallington, M.J. 331
TPMP8 Walls, F.C. 333
RPMOC9 Wanczek, K.-P. 584
RPMOC11 Wanczek, K.-P. 587
RAMOC1 Wang, Jia-Shen. 499
RPMOB3 Wang, Tseng-Pu F. 558
MPMP20 Warburton, G.A. 188
MAMOB1 Warburton, G.A. 30
FAMOC10 Warmack, R.J. 677
WAMOC3 Webb, H. 411
RPMOA3 Weber, Jeffrey M. 536
FAMOB8 Wechsung, R. 654
RPMOC6 Weddle, Gary H. 580
TPMOC11 Weerasinghe, Nakandalage, C.A. 316
WAMP7 Weinkam, R.J. 437
RPMP6 Weiss, Mark. 602

MPMP17 Weiss, Mark.....183
WAMOC7 Weiss, Morris J.....418
RAMOC8 Weiss, Morris J.....508
MAMOB9 Welch, Michael J..... 42
RPMP12 Wellons, S.L.....610
RAMOC5 West, John B.....505
TPMOC11 Westwood, Steven A.....316
RAMP6 Whaley, T.W.....523
MAMOA5 White, E..... 20
MAMOB9 White, E..... 42
FAMOC4 White, Robert L.....667
FAMOC1 White, Robert L.....662
RPMOA1 Whitehouse, Michael J.....531
FAMP14 Whitney, Joanne O.....705
WAMOB9 Whittington, G.....398
FAMOC4 Wilkins, C.L.....667
FAMOC1 Wilkins, C.L.....662
RPMOC10 Williams, Brian Wesley.....586
MPMOB11 Williams, C. Herndon, Jr.....136
TAMP21 Williams, David T.....264
MAMOA6 Wilson, B.W.....22
RPMOC5 Wilson, S.R.....579
MAMOC1 Windig, W..... 49
WAMOA7 Windsor, John G., Jr.....372
WAMOA13 Wiseman, R.W.....382
WAMP22 Wojcik, L.H.....458
WAMP23 Wojcik, L.H.....460
MAMOB5 Wolf, Clarence J..... 38
FAMP17 Wolff, B.....710
MAMP15 Wolstenholme, W.A..... 94
FAMP6 Wong, Lan K.....690
WAMP13 Wong, Lan K.....444
FAMP8 Wong, M.Y.H.....694
MPMOA5 Wood, George M., Jr.....111
FAMOC12 Wood, George M., Jr.....682
FAMOC6 Wood, George M., Jr.....671
RAMOB8 Wood, Gordon W.....497
FAMOC7 Wood, K.V.....673
WAMP23 Wood, Ralph E.....460
FAMOC9 Woodruff, Hugh B.....675
TPMOA4 Woods, R. Claude.....269
RPMOA9 Woodward, C.B.....550
FAMP21 Woodward, W. Stephen.....717
RPMP10 Wright, C.C.....606
FAMP6 Wu, Jinn.....690
MPMOC5 Wu, Richard L.C.....145
TAMOB3 Wu, T.Z.....209
TPMOB10 Wunn, W.....292
TPMOB12 Wunn, Wolfgang.....295
TPMOC1 Wyatt, J.R.....298
RAMOB7 Yamada, H.....495
RPMOA3 Yamnitzky, George F.....536
TPMOB1 Yergey, A.L.....275
TPMP15 Yergey, A.L.....343
MPMOA4 Yergey, A.L.....109
TAMP19 Yert, L.W.....260
RPMOB9 Yert, L.W.....567
WAMOB5 Yert, L.W.....392
FAMOB4 Yinon, Jehuda.....647
TPMP9 Young, Steve.....334
FAMP22 Youngless, Tim L.....719
RAMP3 Yu, Ming-Li.....517
RAMP9 Yuan, S.S.....528
WAMOA13 Yung, S.L.....382
TPMP10 Zakett, D.....335
MAMOA3 Zakett, D..... 18
RAMOB3 Zakriski, Paul M.....486
FAMP10 Zaretskii, Ze'ev V.I.....698
TPMP23 Zaretskii, Ze'ev V.I.....358
TAMOC5 Zigon, M.....223
TPMP5 Zinnecker, M.E.....328
WAMOA10 Zitko, V.....378
MPMOC11 Zwier, Timothy S.....153
TAMOC2 Zwinselman, J.J.....217

Minutes of the Business Meeting of the American Society for Mass Spectrometry, Wednesday, 28 May 1980, at the Waldorf Astoria Hotel, New York City

President James A. McCloskey opened the meeting at 6:00 PM and asked for officers' reports. Secretary H. M. Fales presented the election results as follows:

Vice President for Programs	C. C. Fenselau	387
	F. L. Saalfeld	312
Treasurer	M. A. Frisch	681
Board member at Large	J. T. Watson	401
	W. L. Harrington	208

The President introduced the winning candidates.

The Secretary then presented the current categorical membership status of the Society and stated that the total (1653) indicates about the same rate of growth of the Society as in past years.

Treasurer Frisch then reviewed the budget, commenting that the Society is in a healthy financial state with total assets of $82,014.80 (May 16, 1980). The Conference registration figures as of Wednesday were sufficient to insure against significant loss at this Conference.

Vice President for Programs Munson then showed several slides, the first correllating submitted paper arrival time with the announced deadline, and noted the tendency of the membership to engage in brinksmanship - 206 papers arrived on the deadline. Another slide demonstrated that little change had occurred since last year in the distribution of topics. Regarding geographical distribution of contributed papers, California is still highest although an unusually large number was received from overseas. About 60% of those attending the Conference were members and about 45% of the attendees presented papers. Finally, Munson thanked all for being flexible in accepting either oral or poster assignments.

Vice President for Arrangements A. Wolstenholme stated that about 485 rooms at the Hotel had been occupied, about as expected; the ASMS check in had been aggravated by slow check out of the leaving group. He mentioned that rates in Minneapolis will be much lower (about $35 single, about $42 double) and that San Antonio is being considered as a site for 1984 Conference where two hotels having different rates are under consideration. He showed several slides of San Antonio and McCloskey discussed the location and logistics at some length based on his recent visit there. McCloskey pointed out that a group as large as ASMS will inevitably have trouble locating space in a single hotel while multiple hotels introduce a new set of problems. In response to a favorable comment about San Diego where several motels were used, McCloskey agreed, but stated that transportation had not been ideal at that location. McCloskey then identified the meeting Parliamentarian (M. Levenberg) and the Nominating Committee and its Chairman, Tom Aczel, urging the membership to provide input to the latter since it is becoming more difficult to identify suitable individuals willing to undertake the responsibilities of ASMS office.

McCloskey then read the names of the recipients of the travel fellowships and they were applauded by the assembly.

McCloskey and the Society also expressed its thanks to Past President Jean Futrell on completing his term on the Board of Directors.

McCloskey and the Society also applauded Vice President for Arrangements B. Munson for providing a fine technical program at the Conference.

McCloskey then recognized F. Vane who reviewed the events surrounding her efforts to have the Society lend its name in support of the Equal Rights Amendment. She suggested that the recent ballot results against her proposal reflected, not an anti-ERA attitude among Society members, but their desire not to become embroiled in such issues. She urged the membership of ASMS, as well as other scientific societies, to try to overcome this "ivory tower" attitude. Finally she expressed her appreciation to the Board of Directors for providing her with the opportunity for expressing her views.

S. Markey then read a letter to be mailed to selected members urging them to assist in the identification of less expensive Conference sites, particularly in universities. He stressed that the atmosphere of the Conference was also very important and that location at a university site would be beneficial. This stimulated a discussion on all of the requisites of an effective site, including availability of lecture halls, housing quantity and quality, proximity to major airports, liquor laws, etc. Former Vice President for Arrangements W. Brubaker recalled a previous attempt to meet at the Univ. of California at Santa Barbara and the myriad problems it had presented. Markey agreed, but continued to urge the membership precisely for this reason to seek out viable alternatives. T. Aczel pointed out that there exist many peripheral ways to save money in connection with the Conference, special air rates, food outside the hotel, etc., arguing that most members of ASMS are outside the student category. On a straw vote, 57 were in favor of seeking alternatives to current Conference locations and 44 against.

T. Aczel then asked that some form of recognition (mention in the Proceedings, etc.) be provided for retiring members. There was no discussion on the point.

One member requested that larger print size be provided on the program.

The meeting was adjourned at 7:08. No motions were made.

Submitted,

Henry M Fales

H. M. Fales, Secretary

ASMS COMMITTEES

Fundamentals	Dr. Gerhard G. Meisels, Department of Chemistry University of Nebraska, Lincoln, Nebraska 68588
Computer Applications	Dr. David V. Bowen, Union Carbide, Tarrytown, New York 10591
Isotope Ratio Measurements	Mr. Ernest L. Garner, Analytical Chemistry Division National Bureau of Standards, Washington, D.C. 20234
	Mr. D.J. Rokop, Los Alamos Scientific Laboratory P.O. Box 1663, Mail Stop 514, Los Alamos, New Mexico 87544
Quantitative Organic Analysis	Dr. Sanford P. Markey, Building 10, Room N321 National Institutes of Mental Health, Bethesda, Maryland 20014
Biomedical Applications	Dr. Klaus Biemann, Department of Chemistry Massachusetts Institute of Technology, Cambridge, Massachusetts 02139
Solids & Surface Analysis	Dr. William Harrington, RCA Laboratories Princeton, New Jersey 08540
Qualitative Organic Techniques	Dr. Michael L. Gross, Department of Chemistry University of Nebraska, Lincoln, Nebraska 68588
Education	Dr. Larry Bone, Dow Chemical Company B-1226, Freeport, Texas 77541
Environmental Applications	Dr. Joan T. Bursey, Chemistry and Life Science Division Research Triangle Institute, Research Triangle Park, North Carolina 27709
Forensic Applications	Dr. Richard Saferstein, New Jersey State Police Laboratory, P.O. Box 7068, West Trenton, New Jersey 08625
High Temperature And Inorganic	Dr. Donald L. Hildenbrand, SRI International 333 Ravenswood Avenue, Menlo Park, California 94023
Nomenclature	Dr. John Beynon, Royal Society Research Unit University College of Swansea, Singleton Park, Swansea SA2 8PP Great Britian
Nominating	Dr. Thomas Aczel, Exxon Research and Engineering Company Box 9255, Baytown, Texas 77520

ASMS COMMITTEE ON FUNDAMENTALS

Technical Activities

The Committee on Fundamental Aspects sponsored two major events at the 28th Annual meeting on Mass Spectrometry and Allied Topics, held at the Waldorf Astoria Hotel in New York City, May 25-30, 1980. The first of these was a symposium, arranged by Professor Robert C. Dunbar of Case Western Reserve University, on the topic "Structures and Energetics of Gaseous Ions in honor of Dr. Fred P. Lossing". In his introductory remarks, Professor Dunbar paid tribute to the many contributions Dr. Lossing had made to our understanding in this field, and to insights he even now is providing on these subjects. The symposium consisted of five invited papers on Tuesday afternoon and a session of contributed papers on Wednesday morning. A sixth invited paper could not be presented because of a death in the speaker's family. Both sessions were very well attended with a great deal of constructive and lively discussion following a number of papers.

The second major event was a workshop on "The Measurement of Thermodynamic Properties of Gaseous Ions" which was chaired by Professor Robert T. McIver (University of California at Irvine). The workshop was attended by approximately 40 individuals and consisted of a number of short presentations by Dr. Sharon Lias (National Bureau of Standards), Professor McIver, Professor Paul Kebarle (University of Alberta), and Professor Gerry Meisels (University of Nebraska). The major portion of the workshop, which lasted approximately an hour and fifteen minutes, was dedicated to open discussion and, in the words of one participant, it was much appreciated that all participants really "let down their hair" and discussed so openly the problems of the various techniques.

Business Meeting

The business meeting of the committee preceeded the workshop, and was attended by approximately 35 individuals. After extensive discussion, those present requested the committee chairman to seek approval from the program committee for the following:

1. A plenary speaker. First choice was Professor Richard Zare on "Multiphoton Ionization". Second was a speaker on "Extraterrestial Molecules and Their Formation and Reactions". No specific speaker was recommended, but among the names mentioned prominently were Professor Klemperer and Professor Dalgarno. It is to be understood that extraterrestial molecules may cover a variety of topics such as interstellar molecules, the planetary atmospheres, upper atmosphere molecules, etc.
2. Two symposia. The first should be entitled "Theory of Structures and Dynamics of Gaseous Ions", with the understanding that the symposium should include one or two introductory papers of a very general and basic nature so that the topics would be understandable to those not expert in these fields. Even such items as basic collision dynamics, capture processes, and the Langevin formalism should be covered. Possible organizers of this symposium would be Professor Michael Bowers (University of California at Santa Barbara) and Dr. Henry Rosenstock (National Bureau of Standards) with strong consideration to be given to having joint chairmen because of the diversity of the topics to be covered. The second subject recommended for a symposium is "Metallic Ions and Ionospheric Chemistry", a field currently particularly active and worthy of consideration. Suggested chairpersons for the symposium are either Professor Jack Beauchamp (California Institute of Technology) or Professor Douglas Ridge (University of Delaware).

Among other topics discussed, it was felt that a symposium on MS-MS, or the general topic described by this and other names, be held in the near future, but that 1981 would probably be premature. The possibility of such a symposium in 1982 is recommended for consideration to the Committee when it meets in Minneapolis in 1981. Similarly, a symposium on laser induced processes covering both ionic and neutral processes was thought to be worthy of consideration for 1982.

Minutes respectfully submitted by,

Gary Meisels

G. G. Meisels, Chairman
ASMS Committee on Fundamentals
Department of Chemistry
University of Nebraska

COMMITTEE ON COMPUTER APPLICATIONS

Report for 1979/80.

David V. Bowen
Chairman

Workshop: Use of GC Retention Times to Identify Compounds.

An audience of about 30 heard Drs. Klaus Biemann, John Holland and Dennis Lin describe different ways of calculating and utilizing gas chromatographic retention data. Kovats retention index, based on the times at which the normal alkanes elute, can be calculated if some n-alkanes are included in each GC/MS run. For biomedical work between 3 and 10 n-alkanes are added to each sample. In environmental studies the n-alkanes are sometimes present in samples. Therefore hexaethylbenzene is used and relative retention times are computed.

The retention data obtained are stored in libraries. Each of the panelists maintains a library of retention data, and each is willing to provide these data to others. For further details write directly to the group whose data interest you.

Several different applications of the retention data were described. They can be used as a prefilter to speed library searching. In this case the data need only be accurate (for example) to ± 5%. More precise retention data (±0.1%) can be used as an aid to library searching or as a method of determining the isomeric forms of compounds identified. Retention data can sometimes be predicted (e.g. for peptides or for some drug metabolites), and the predicted retention times can be used alone to identify isomers or to identify a peptide residue.

Gas chromatographic stationary phases were discussed by the panel and the meeting at large. There was general agreement that most chromatography could be performed with an OV-1 type phase (SP2100, SE-30, OV-101), or with a Carbowax phase (Carbowax 20M, SP-1000) or with a polar silicone phase like OV-17. However, many of those present have observed significant variations of retention among closely related phases, or even from batch to batch of the same phase (OV-17 seems prone to batch variability).

There was discussion as to whether ASMS should collect retention data, and also as to whether ASMS should recommend that the NIH-EPA data base include retention data. No decision was reached on either question.

Business Meeting.

The Committee on Computer Applications business meeting was attended by about 25 ASMS members. All of those present agreed that the Committee was useful and should be continued; the Chairman agreed to recommend this to the ASMS Board. Some specific ideas were discussed, and the Chairman, David Bowen, agreed to recommend these to the new Chairman when that person had been appointed.

There was interest in the subject of communication between computers. The group agreed that a sub-committee should compile a list of the present data formats and work with manufacturers to achieve an industry-wide standard so that labs with more than one data system could interface them.

There was also general agreement that an inventory of data system users should be compiled by the Committee. This inventory should include details of hardware and software. It should also identify those ASMS members who might be willing to donate software to others, and to identify ASMS members who would be willing to consult with others on hardware or software problems.

It was felt that the inventory of data system users, by flagging those members with software to share, would replace the present ASMS software exchanges. Since these are very little used, it was unanimously agreed to recommend that the ASMS exchanges

of high level and of low level software be discontinued. Future exchanges can be more effectively made by person-to-person contact without using ASMS as an intermediary.

Everyone present agreed that it would be good for ASMS to encourage donations of reference mass spectra to major data bases. At present both the NBS-NIH-EPA Chemical Information System and the Cornell University PBM/STIRS search maintain libraries that are available to the public for searches (after payment of suitable fees). There was no agreement as to how ASMS could help to encourage the donation of additional spectra to these libraries. The group therefore asks their colleagues to send spectra to one or both of these libraries.

In this connection a poll showed that of the 25 people present at that point, 12 do time-sharing library searches, and of those 12, 4 have been troubled by poor quality spectra in the library and 5 have been troubled by finding certain types of chemical not well represented in the library.

Finally, the group asked that the ASMS Board continue to hold a session on Computer Applications as part of each ASMS meeting. It was felt that poster sessions were very suitable for this. D.V. Bowen agreed to carry this recommendation to the Board and to transmit this report and the list of those present to the new Chairman of the Committee once Dr. Munson had chosen one.

ASMS Committee IV. Isotope Ratio Measurements

At the New York meeting of the ASMS, the Committee on Isotope Ratio Measurements presented three workshops: (1) Automated Mass Spectrometry, Fact or Fiction; (2) Sample Mounting Techniques; and (3) Vacuum Techniques. Limitation of the number of speakers per workshop to a maximum of three, combined with the choice of general interest topics, resulted in lively discussions, free exchange of ideas and an overall learning process for all participants. Thus, after three years of searching for a format to promote audience participation, we have finally met success in our final year as chairmen.

This year there was a decrease in attendance among the members of the isotope ratio core group, however, new participants did attend and contribute heavily to the most successful program of our tenure. A major oversight in planning the workshops was in not providing sufficient advance information about the sessions. An advance mailing outlining the specific topics and general content in the form of a brief abstract would have helped attendance.

At the time the Committee on Isotope Ratio Measurements was formed, the charge included the latitude to form an interest group of both organic and inorganic analysis. Based upon input from members of the Society and from observation of many different sessions, we believe that this format will not work. The interest group in inorganic isotope ratio measurements is small and shares few major areas of mutual concern with the organic group. Furthermore, this committee provides the only focal point of its kind in a scientific society for regular and meaningful group discussion of inorganic isotope ratio measurements. To sponsor joint activities in areas of mutual concern is feasible and needed, but to adopt topics of a strictly organic nature will cause a loss of interest and a reduced level of participation.

Our tenure co-chairmen of the Committee on Isotope Ratio Measurements has been a unique experience during its formative years. As such, we express our appreciation to the many speakers and participants who have made our efforts rewarding. On behalf of our small interest group, we express our thanks to the Society for its support and for providing a format for the free exchange of ideas. Being together with our colleagues at one location annually has benefited us all.

In conclusion, congratulations to the next chairman, Dr. Lura Powell Dunstan of the National Bureau of Standards. We solicit your support, suggestions and cooperation for a continuation of the work of this vital committee.

Respectfully submitted,

D. J. Rokop
E. L. Garner
Co-chairmen, Committee IV

Quantitative Organic Analysis Committee Report

* Activities

Two workshops and a poster symposium were organized and sponsored or co-sponsored by this committee. The jointly sponsored workshop on "Quantitative Analysis of Drugs of Abuse" (with Forensic Applications Committee) was a well organized but very poorly attended session, perhaps due to program conflicts. The workshop "Quantitation by Positive or Negative Chemical Ionization - Special Problems" was well attended with good audience participation as summarized below. A poster symposium "Synthesis of Stable Isotope Labelled Compounds for Mass Spectrometry" was organized by Nick Matwiyoff and had eleven participants who represented a wide variety of synthetic interests.

* Workshop: "Quantitation by Positive or Negative Chemical Ionization"

Summarized by Fred Abramson

The workshop was held using a panel of experienced c.i. users to answer questions posed by attendees. Sandy Markey of NIH was the Chairman and the panelists were Al Yergey of NIH, Bill Garland of Hoffman-LaRoche, Dave Hachey of Argonne, Dwight Matthews of Washington University, Fred Falkner of Pfizer and Rodger Foltz of the University of Utah. All panelists described their applications which centered upon quantitation of compounds of biochemical or pharmaceutical interest. Most used GC/MS although several applications did utilize direct probe sample introduction. Following these introductory remarks, questions of quantitation by c.i. came from the floor.

A question was asked about the linearity and precision of c.i. compared to e.i. methods. Dwight Matthews said that they were similar, but that the c.i. assays were cleaner. This seemed to be agreed on, but later a series of questions about factors leading to variability were discussed. It was agreed that source temperature is a very critical parameter, perhaps moreso in negative c.i. assays. In most assays the source temperature should be carefully stabilized, if not actually controlled. There were no special problems noted with the use of a fragment ion rather than a pseudomolecular ion in c.i. quantitative analysis.

There was agreement about the procedure for optimizing and reproducing the c.i. conditions. The source pressure should be adjusted to maximize the signal from the analyte, and then the characteristics of the reagent gas (intensity, ratio of primary, secondary, tertiary, etc. ions) noted. Subsequent analyses would begin by reestablishing that set of reagent gas parameters. Favorite tune-up compounds for n.c.i. were given as Fomblin with nitrogen or methane as described by Adries Bruins in a poster session. Other compounds such as perfluorotributylamine give spectra useful in only a very limited mass range (400-600).

There was a discussion of how much improvement in sensitivity could be expected with n.c.i. as compared to e.i. It was noted that such a comparison must be properly made; that is, the best e.i. conditions versus the best c.i. conditions. It is unlikely that both these would result from the same source conditions. Sandy Markey said his n.c.i. biogenic amine assays were approximately 30-fold more sensitive than the best e.i. he could do. In addition to the possible increase in absolute sensitivity which the cascade of low energy electrons in the source produce for n.c.i., the selectivity of the ionization process generally resulted in cleaner backgrounds, thus giving an increase in abundance sensitivity. Asked whether saturation in n.c.i. was a problem, the panelists felt that at the low levels normally used, less than 100 ng, this was not a problem, especially when using natively capturing compounds. When derivatization is used, relatively large amounts of endogenous materials may capture the bulk of electrons and reduce sensitivity, as well as give rise to very large interfering background ions, similar to those encountered in e.i. or positive c.i. of derivatized extracts.

There were several questions about reagent gases. Why is methane the best moderator in electron capture n.c.i.? It does work better than nitrogen, helium or argon, presumably because its vibrational energy states moderate the mean electron energy to lower values than the other simpler gases. Isobutane was said to work equally well. Both are good third-body stabilizers. Ammonia was suggested for p.c.i. assay of saturated hydrocarbons, while water was suggested for olefins. Although not as widely applicable, ammonia produces the cleanest p.c.i. spectra. Otherwise, isobutane is recommended.

It was noted by a member of the audience that all the panelists have quadrupole instruments of one design or another. Did that mean that they were inherently better for c.i.? The answer was no, but their low-voltage operation meant that the electrical discharge problems were reduced compared to magnetic machines. It was also noted that quadrupoles appear to tolerate elevated analyzer pressures better than magnetic instruments. On the other hand, quadrupoles seemed much more susceptible to contamination in the souce and multiplier regions. There was no consensus on whether isobutane caused more contamination than either methane or ammonia.

* Business Meeting

A meeting to discuss next year's program was held following the workshop on c.i. quantitation. Topics suggested included a workshop on calculations used in quantitative analysis (comparison and illustration of alternate methods); a workshop on useful compromises or shortcuts in the selection of assay parameters; a symposium with invited speakers to address the mathematics of quantitative analysis (didactic session), a comparison of alternate methodologies to GC/MS and their limitations (RIA, hplc-electrochemical detection), and bioavailability studies by GC/MS.

*Announcement

Two technical manuals of interest to biomedical mass spectroscopists are to be released shortly by the National Institute of Drug Abuse, and are available without charge.

Abused Drug Assays by GC-MS. Rodger L. Foltz (Editor)
GC-MS assays were developed in several laboratories under NIDA contracts and have been compiled in a very useful, practical format. Assays are presented for cocaine, THC, diazepam, methadone, methaqualone, morphine, phencyclidine, and phenylalkylamines.

The Analysis of Cannabinoids in Biological Fluids. R.L. Hawks (Editor)
Chapters describe methodologies for quantification of THC and its metabolites in this multi-authored volume.

For copies of either of these volumes, mail a request to:

NIDA Research Monograph Series
Division of Research
National Institute on Drug Abuse, Room 9-46
5600 Fishers Lane
Rockville, Maryland 20857

ASMS Committee on Biomedical Applications.

The Committee organized two events during the 28th Annual Conference: A symposium on Structure Elucidation of Natural Products and a Workshop on Ion Decomposition Spectra and their use in Identification and Structure Determination.

The symposium consisted of four presentations (TAMOB 1-4) covering various areas of natural products chemistry, stressing the whole picture rather than concentrating on the mass spectrometric aspects, to give an audience a broad view of each of the subjects discussed. The symposium was well attended and the speakers captured the interest of the audience.

The workshop was intended to dwell on the use, advantage and shortcomings of the various techniques which allow the characterization of an ion from the spectrum generated by its decomposition (either spontaneous or through collisional activation). R.G. Cooks, D.F. Hunt and W.F. Haddon discussed the use of these data for the identification of specific compounds, as well as possible sources of error.

J.R. Hass and M.L. Gross described their approaches to the use of the technique for quantitative analysis and its application to the measurement of tetrachlorodibenzo-dioxin, where high specificity in the presence of large amounts of other chlorinated compounds is of great importance.

During the discussion of both topics the question of inter-laboratory reproducibility of such data was brought up and M.P. Barbalas described briefly an effort that is underway at F.W. McLafferty's laboratory at Cornell University to compile MIKES or collisional activation spectra of ions which have been published in the literature or determined in their own laboratory. Presently the collection comprises about 600 spectra. The speaker expressed the hope that other laboratories would contribute their data to the collection and offered to make the existing collection available to others.

The workshop was attended by about 100 people, too large a group to lead to the intimate exchange possible in a much smaller forum but the interest in the subject was high and time ran out (1½ hours) before all aspects of the subjects could be fully discussed.

Klaus Biemann
Chairman

ASMS COMMITTEE ON SOLIDS AND SURFACE ANALYSIS

Summary of Activities at 28th Annual Conference

A combined business meeting and workshop was held on Monday evening, May 26 from 8:00-9:30 p.m. Average attendance throughout the session was 20-25.

At the business meeting, the following items were discussed:

(1) Recommendation of a new committee chairman for the following years. A letter concerning this recommendation was given to B. Munson at the Committee-Board Luncheon on Thursday, May 29.

(2) Topics for future workshops.
   A. Secondary ion mass spectrometry of organic solids.
   B. Laser excitation for inorganic solids analysis.
   C. Training course, symposium, or workshop on the interpretation of secondary ion mass spectrometry combined with other surface analytical techniques, i.e., Auger electron spectroscopy, X-ray photoelectron spectroscopy, Rutherford backscattering, etc.

At the workshop entitled "Add-on SIMS: A Round-Robin Performance Evaluation", results were discussed for a sample of boron-implanted silicon which had been distributed to seven laboratories. Due to a number of complications, only two sets of results were presented. These presentations established, however, that large differences can exist between instruments and that the distributed sample was very informative as a performance standard. Points discussed were sputter rate (determined from a known mean projected range of the implant), depth resolution and crater edge rejection (determined from a calculation of straggle of the implant as well as the background reached on the back side of the implant), and the useful yield for the instrument and analytical conditions used for the analysis.

The topic and the two sets of results created sufficient interest to warrant expansion of this effort to include additional laboratories and to allow more time to those who did not respond. It was decided that the round-robin evaluation will be continued with results to be distributed in a committee mailing.

Respectfully submitted,

William L. Harrington
Chairman

ASMS COMMITTEE REPORT

Qualitative Organic Techniques

"Workshop on High Mass Measurements"

This is a report on a workshop entitled "High Mass Measurements in Mass Spectrometry" held at the 1980 American Society for Mass Spectrometry meeting in New York City. The workshop was sponsored by the committee on Qualitative Organic Analysis.

Various methods of mass analysis were presented for consideration: (1) high field magnets---adapted to commercial mass spectrometer systems, (2) new high field or large radius magnet systems, (3) low frequency quadrupole mass analyzers, and (4) time-of-flight analyzers (such as used with Cf-252 desorption). Other methods were proposed by attendees. For example, William Aberth suggested a Wien filter which has a demonstrated resolution of 3000 and an upper mass limit which is yet to be determined. Robert McIver pointed out that an Ion Cyclotron Resonance spectrometer equipped with a superconducting magnet at 120 kilogauss may produce unit resolution at m/z 10,000. Upper mass limits of at least m/z 1000 have been demonstrated at about 20kG using Fourier Transform techniques.

Commercial magnet systems were described by Roy McDowell of Imperial College--London. He pointed out that electromagnets equipped with carbon-steel pole faces can be used to study masses up to about m/z 1000 at 8kV of acceleration (as on a Kratos MS-50, for example). "Extended field" magnets have been introduced. They are equipped with silicon-steel pole faces and can be used up to m/z 1750 at 8kV. Finally, cobalt-steel pole faces have been used on "high field" magnets (up to m/z 3000 at 8kV). The "extended" and "high field" magnets cannot be scanned such that equal time is spent on each m/z-signal. In fact, more time is spent on the higher mass peaks, and this may be an advantage.

Fred McLafferty reported on a tandem mass spectrometer that he and his coworkers have constructed at Cornell University. Ultimately the instrument will be equipped with two 60cm high field magnets which should permit mass selection, activation, and mass analysis of ions of mass greater than 3000. This instrument may be useful for analysis of mixtures containing high molecular weight components (such as complex oligopeptides).

A low frequency quadrupole was described by Lewis Friedman. He pointed out that an upper mass of 100,000 can be obtained by reducing the frequency applied to the rods by a factor of 10. This increase of a factor of 100 in mass limit is because the mass is inversely proportional to square of the frequency. In fact masses in the range of 80,000 have been investigated using a system located at Brookhaven National Laboratory. Dr. Friedman pointed out that correctly designed rods and power supplies may give a resolving power of 20,000.

Peter Derrick was expected to participate in the workshop, but he was unable to attend. His high mass instrument at La Trobe University has been constructed using a 78cm magnetic sector and a 100cm electrostatic analyzer. Using this instrument, polypropylene glycols with nominal mass-average relative molecular masses of 1000, 2000, 3000, and 4000 have been studied using field desorption. The highest mass ion observed to date is m/z 7400.

Methods of vaporization and ionization were also considered. Various techniques were proposed: (1) field desorption, (2) rapid heating, (3) fission fragment desorption and (4) electrospray techniques. He has studied various polyethylene glycol oligomers. Conventional mass analysis was accomplished using multi-charged ions formed by attachment of one or more Ba^{+2} or Na^{+} ions to the polymer component molecules.

The results of a detailed analysis of various polystyrene fractions was discussed by Robert Lattimer of B.F. Goodrich. His work was conducted on the "high field" MS-50 at the Johns-Hopkins NSF Regional Instrumentation facility. Average molecular weights were determined using field desorption and integrating scans. The results were in good agreement with those determined using vapor phase osmometry.

Although field desorption appears to be a useful vaporization/ionization method for molecular weights in the 1000 to 3000 range (and higher for synthetic polymers), the technique does not appear applicable to higher molecular weight materials, particularly biopolymers. This was demonstrated in a 1976 study of Glucagon, a peptide containing 29 amino acids, by Winkler, Beuhler, and Friedman. They employed a single sector magnetic instrument with a 152cm radius and field desorption ionization. The highest mass signal observed was m/z = 2110 which has 18 amino acids. Dr. Friedman pointed out the rapid heating procedures will have a similar upper mass limit. Both techniques suffer from the relatively large desorption energy of biomolecules which, for a molecule containing many

polar groups, will exceed bond energies.

A method that appears promising for high molecular weight materials is the electrospray technique developed by Malcolm Dole. Both Professor McLafferty and Dr. Friedman discussed aspects of this technique which involves rapid evaporation of tiny droplets which are formed by electrospraying solutions into the source. Each droplet contains ideally one molecule of analyte. Professor McLafferty has proposed to couple an HPLC and his tandem MS/MS instrument for studies of high molecular weight substances. He speculated that collisional activation may be important for removing the last few molecules of solvent.

Jerry Hunt, a coworker of Professor R. D. McFarlane at Texas A and M University, reported on recent experiments using an alternative method of ionization; i.e. Cf-252 fission fragments. Synthetic nucleotides up to mass 12,000 have been studied; only $(M + H)^+$ ions were observed in the positive ion mode whereas extensive fragmentation yielding sequence information was found for negative ions. Furthermore, chlorophyll clusters have been seen up to m/z 8000, and these may be useful as mass standards. A sample size of about 100 micrograms is required, and 5 to 6 hours are required to complete the experiment. A discussion ensued on whether postacceleration is necessary for triggering an electron multiplier with high mass particles.

Another issue was considered briefly and that is mass calibration. This may not be a serious problem; fomblin can be used in the 1000-3000 amu range. Dr. Friedman suggested that calibration will be no problem at higher masses either. One needs only to expand into the source rather common solvents using a jet to grow clusters which have an established repeating unit.

An interesting discussion occurred on whether mass spectroscopists should tackle the problem of high molecular weight materials or defer to more classical technologies such as ultracentrifugation or light scattering. There are compelling reasons to pursue high mass measurements in addition to the scientists' quest to constantly improve his methodology. For example, classical techniques can never yield exact molecular masses. Furthermore, mass spectrometers produce information on molecular weight distributions for mixtures and on the general purity of the sample provided fragmentation can be minimized in the vaporization and ionization steps. Finally, as pointed out by Dr. Friedman, the development of controlled nuclear fusion may depend entirely on our capability for high mass measurements. Space charge effects currently limit current density in fusion plasmas, and this can be minimized with ion clusters. Of course, the study of large ion clusters will require high mass measurements.

Approximately 150 persons attended the workshop.

Michael L. Gross
University of Nebraska
Committee Chairman

Acknowledgement: The author is grateful to Drs. P.G. Kistemaker and R. J. Cotter for assistance in preparing this report.

EDUCATION COMMITTEE

The Education Committee sponsored two short courses on the weekend preceding the 28th Annual Conference in New York City. A short course entitled "Interpretation of Mass Spectra" had an enrollement of 21. The instructional staff consisted of Martha Vestling, Ed White, David Bowen, and Larry Bone. The other course entitled "Quantitative Mass Spectrometry" had an enrollement of 23. The staff members were Bill Garland, Claudia Elkins, Jim Smith, and Gene Heath.

The registration fee for the courses was $200 for regular participants and $100 for graduate or undergraduate students. This fee included lunch both days, coffee breaks, and a textbook. The income was sufficient to cover expenses and yield an excess which was placed in a scholarship fund.

Respectfully submitted,

Larry Bone

Larry I. Bone
Education Chairman

ASMS Committee on Environmental Applications

(XI)

Business Meeting and Workshop

Chairman: Joan T. Bursey
Analytical Sciences Division
Chemistry and Life Sciences Group
Research Triangle Institute
Research Triangle Park, NC 27709

The meeting was opened by Dr. Joan Bursey, who called for suggestions for ongoing activities for the Environmental Committee, as well as suggestions for plenary lecturers, symposium topics, and workshop topics for the following year's ASMS meeting. Members of the committee were to contact Dr. Bursey at the address given above if there were any suggestions.

The workshop format was a panel discussion, with three panel members who made brief presentations: Dr. T. Michael Harvey (Newbel Industries), Dr. Lewis Shadoff (Dow Chemical Co.), and Dr. Mason Hughes (Gulf South Research Institute). Dr. Harvey discussed the care required in placing internal standards into the analytical system, and discussed an example from his laboratory where deuterated benz(a)pyrene to be used as an internal standard was spiked on one type of filter prior to exposure and 0% recovery of the compound was observed. When the compound was spiked onto another type of filter, approximately 65% recovery was observed. The amount of air pulled through the filter was immaterial, but if no air were passed through the first type of filter, no degradation of standard was observed. It is always crucial, therefore, to be certain that a compound used as a standard will survive the sampling/analysis process intact in order to be valid for use as a standard.

Dr. Lewis Shadoff discussed the utility of an isotopically labeled standard for quantitative analysis. He cited several advantages in their use: they have chemical identity to the compound of interest, and can be used to advantage for their carrier effect in minimizing sample losses. They provide an internal check on recovery of the compound of interest, can be used as quantitation standards, retention time standards, and to minimize the matrix effects in chemical ionization. Dr. Shadoff described some examples of the use of isotopically labeled compounds in the quantitation of TCDD in his laboratory and discussed some suppliers of these compounds.

Dr. Hughes described the utility of deuterated compounds as analytical standards for a complex mixture (e.g., pulp/paper mill effluent). In this example, d_{10}-anthracene was

used to check for good chromatography and system sensitivity and as a standard for quantitation. Completely deuterated stearic acid was used as an internal standard to assess recovery.

Discussion and interchange from the floor centered on the topics of the chemical and chromatographic properties of isotopically labeled standards, with differences in some chemical properties being observed as a function of extent of deuteration. The effect these changes might have on the use of a deuterated compound as a standard for recovery was mentioned. The use of non-labeled homologs as an alternative to the use of relatively expensive isotopic labeling to give equally good results in several cases was also discussed. Problems associated with various standards (such as d_{10}-anthracene and d_{22}-decane) were mentioned. The problem of making a relevant spike of relatively water-insoluble compounds into an aqueous matrix was discussed. Dr. Harry Hertz (National Bureau of Standards) discussed some micro-capsules containing deuterated standards which can be put into aqueous samples and crushed to release standards which are being prepared in his laboratory and will be tested by the Research Triangle Institute. Dr. Hertz also mentioned some generator columns which are being prepared by NBS and will be released for the preparation of standard solutions of PNAs in water. There is also a possibility that these generator columns will have some utility in the preparation of standard air mixtures of PNAs, and they are being tested for this purpose.

ASMS COMMITTEE ON FORENSIC APPLICATIONS

The Forensic Applications Committee was involved in two activities at the New York City meeting. A workshop on Quantitative Analysis of Drugs of Abuse was co-sponsored with the Quantitative Organic Analyses Committee. The workshop was organized and chaired by Dr. Richard Hawks of NIDA. Poor attendance (20 people) was attributed to an unfortunate conflict in scheduling. Apparently, a workshop of similar subject content was held at the same time in another area of the hotel. The second event was a half day symposium on Forensic Applications of Mass Spectrometry. The symposium consisted of 10 papers encompassing a variety of forensic topics including equine toxicology. Many favorable remarks were heard concerning the content of the symposium. Attendance was estimated to vary between 75 to 125 people.

A major topic of discussion at the business meeting was steps that could be taken to increase participation of the forensic science community in ASMS meetings and related functions. Based on comments at this years symposium, as well as successfully conducted past forensic symposiums, there is apparently a high level of interest among ASMS members in the forensic sciences. However, the fate of the Forensic Science Committee in ASMS will depend, in part, on our ability to generate and sustain the interests and participation of practicing forensic scientists in ASMS activities. To the end, it was agreed upon to form a committee of regional representatives. Members will initiate contact with forensic mass spectroscopists in their respective regions and endeavor to stimulate interest in ASMS activities. It is hoped that with this type of support, future chairpersons will be in a better position to organize forensic symposiums and workshops.

The following individuals volunteered to be regional representatives for the Forensic Applications Committee:

Dan Pearce - Western Region

Mike McGee - Southern Region

Steven Lorch - Mid-Western Region

Richard Saferstein - Eastern Region

Respectfully submitted,

Richard Saferstein

Richard Saferstein, Ph.D.

ASMS COMMITTEE ON HIGH TEMPERATURE MASS SPECTROMETRY

The Committee was formed in early 1980 following an expression of interest from active workers in this field seeking restoration of ties with ASMS, hopefully leading to renewed participation in Society meetings and to the use of ASMS as a forum for their scientific activities. Seven persons attended a brief organizational business meeting on May 29, called on relatively short notice, and discussed primarily the possibility of sponsoring a symposium on High Temperature Mass Spectrometry at a future ASMS meeting. Program topics, the mix of invited/contributed papers, and the selection of a keynote speaker to deliver a general overview paper were explored. It was agreed that such a symposium was desirable, based on comments from those present as well as written input from others in the field, and specific recommendations in this regard for the 1981 ASMS meeting in Minneapolis will be forwarded to the Vice President for Programs. There was also a consensus that a workshop session should be organized for the 1981 meeting; topics and format were discussed, with specifics to be arranged after further consultation with other scientists. We earnestly solicit input on these and other topics related to High Temperature Mass Spectrometry. It is hoped that ASMS will once again become the focal point for activities in the field.

Donald L. Hildenbrand
Chairman

REPORT ON MEETING OF COMMITTEE III ON NOMENCLATURE - New York, May 26, 1980

32 members attended.

The Chairman reminded the meeting that, following the reactivation of the Committee, a Workshop was held at the Seattle meeting in 1979. Several recommendations were made to the Directors and they decided as follows :

1. That every assistance be given to the International Union of Pure and Applied Chemistry in formulating nomenclature, especially when this has interdisciplinary implications.

2. That ASMS should give a lead in recommending terms that are of use mainly or exclusively in mass spectroscopy and that a start should be made as soon as possible in cataloguing terms (and any recommended abbreviations).

3. That lists of such terms should be issued on a regular basis by ASMS.

4. That a preliminary list of terms for selected areas should be generated by the appointed Chairman and circulated to ASMS members, before the New York meeting, for their comments.

5. After the New York meeting, the Nomenclature Committee will make recommendations for acceptance to the ASMS Board of Directors. If the Board agrees, the recommended term or definition can be issued; if not, the term will need to be reconsidered (or dropped).

6. That all recommendations should be in the English language. Terms accepted by the Board of Directors should be circulated for information to all other National Mass Spectroscopy Groups.

A preliminary list of terms covering suggested nomenclature for the fields of (i) ionization (ii) ion/molecule processes and (iii) types of ions, had been prepared by the Chairman and circulated to all members. A variety of comments had been received which were read to the members present at the meeting. In some cases, alternative terms to those on the list had been suggested; some additional terms had also been put forward.

A helpful letter had been received from the Chairman of ASTM Committee E-14 enclosing a draft of their 'Standard Recommended Practice for combined Gas Chromatography and Mass Spectrometer Terms' for comments.

After a full discussion, it was decided unanimously that no term should be on the recommended list unless it was defined. For many of the terms the definition could be very short. There was no lack of volunteers to write the definitions.

It was reported to the meeting that an independent group had met recently and had decided upon the nomenclature (and abbreviations) that they would use in future in the area of instrumentation. The Chairman suggested that he should write to the convener of this meeting to see how many of these terms could be recommended.

The Committee then decided on the following actions :

1. Lists of terms should be generated, and definitions written, to cover the various areas as follows :

a)	Ionization nomenclature. Probe methods.	Harry J. Svec
b)	Ion/molecule processes. Scanning methods.	Robert K. Boyd and Ray E. March
c)	Types of ions.	Norman Foster
d)	Mass analysis	Herman Curtis
e)	Detection of ions. Instrumentation. Sample introduction.	John Roboz
f)	Vacuum system.	Mike Story
g)	Data systems. Data manipulation.	Alan Carrick

The Chairman will send copies of his preliminary list of terms to the people concerned with a), b) and c) and copies of all comments received to each volunteer. Definitions will be sent to the Chairman by September 1, 1980 so that he can edit them to a uniform style.

The edited definitions and terms will be circulated to all members before the meeting in Minneapolis in 1981 so that they may send any comments they may have to the Chairman. Depending upon the comments received, the Chairman will prepare three lists of terms for consideration by Committee III on Nomenclature at the Minneapolis meeting.

1. Terms recommended for approval.
2. Terms <u>not</u> recommended.
3. Terms <u>for</u> which further discussion is necessary.

It is hoped that, following our Committee's meeting at Minneapolis, a final list of recommended terms can be prepared for submission for approval to the ASMS Directors.

2. The Chairman will write to the independent group who have decided on the nomenclature they are intending to adopt, asking for a copy of their decisions. He will send this, as appropriate, to the volunteers who are writing our definitions. It is hoped that, in future, groups wishing to make progress in nomenclature will be persuaded that it is in the best interests of all if they work through Committee III.

3. When the list of definitions is circulated to ASMS members, they will be asked to suggest additional terms that need definition and other areas of mass spectroscopy to be covered.

It was emphasised that it is not the purpose of the Committee to legislate against the use of any expression couched in generally accepted English. Thus it might be expected that, in many cases, alternative expressions would be acceptable. For example, both 'collisional activation' and 'collision induced dissociation' might appear as recommended terms.

On the other hand, the increasing use of invented jargon and the unnecessary use of abbreviations was deplored. The primary purpose should always be clarity rather than brevity and to make mass spectrometric papers understandable to the widest possible audience. Members were reminded of the recommendation made at last year's Workshop that no abbreviation should ever be used in a paper unless it needs to be employed at least five times.

Meeting of ASTM Committee D-2 Research Division IV, Section M

The meeting of Research Division IV, Section M on Mass Spectrometry, of ASTM D-2 was held on May 26, 1980, 2 p.m., at the Waldorf Astoria Hotel, New York City, New York. Thirteen members were in attendance. Thomas Aczel, Chairman, presided. He also acted as Chairman of the Task Group on Shale Oil Analysis, and of the Task Group on Analysis of Coal Derived Liquids, as the chairmen of these groups, respectively, F. Duffy of DOE, LETC, Laramie, and C. E. Schmidt, DOE, PETC, Pittsburgh, could not attend the meeting because of government restrictions on travel.

The meeting was called to order by the Chairman, who expostulated at some length on the need for reliable analytical methods for the MS analysis of shale oils and coal liquids, either in an "as is" state or as separated fractions. There was a unanimous concensus on these ideas. The section then decided on the following actions:

1) Continue and complete the high and/or low resolution MS analysis of the basic and non-basic polar fractions of a coal liquid that were distributed in 1979.

2) Determine the statistical precision of ASTM D2786, Saturates Analysis by retesting petroleum derived saturates fraction as a cooperative sample, to be furnished by Exxon Research and Engineering Company, Baytown Research and Development Division.

3) Start to standardize high resolution MS analysis of an aromatic fraction of a petroleum crude, also to be furnished by Exxon as above. Details of the conditions to be used for this cooperative experiment will be worked out by an "ad hoc" committee, headed by T. Ashe.

4) Procure shale oil middle distillate fractions and analyze it with ASTM D2425 or D2424 methods. We will request DOE, LETC to furnish suitable fractions for this purpose.

This action plan was approved unanimously. Laboratories willing to participate in the various cooperative programs indicated so by signing the attendance sheet that is reproduced in Table I.

The meeting was adjourned by the Chairman at 2:55 p.m.

Respectfully submitted,

Thomas Aczel

Thomas Aczel, Chairman

Table I

Participants to D-2 Meeting

Monday, May 26, 1980

Name	Affiliation	Desires to receive samples		
		A	B	C
Thomas Jackson	Mobil Res & Dev	X		
S. Meyerson	Standard Oil Co. (Ind.)			
Raoul Schafranek	Pullman Kellogg	X		
Roy Pancirov	Exxon Research & Eng.	X	X	X
Arthur Moore	Marathon Oil Company			
J. M. Kelliher	Exxon Research & Eng.	X	X	X
I. P. Fisher	Gulf Canada R&D	X	X	
Rod Page	ARCO	X	X	
Gil Greenwood	Phillips Petroleum Co.	X	X	
Roy W. Vander Haar	Standard Oil Co. (Ind.)	X	X	X
R. T. Moir	Imperial Oil Limited	X		X
T. R. Ashe	Exxon Research and Eng.			

A - Saturates test (2)

B - Aromatics test (3)

C - Shale oil test (4)

ASTM E-14 QUANTITATIVE GC/MS WORKSHOP

A workshop was held by ASTM Committee E-14 on the subject of quantitative GC/MS methods and techniques. A panel of four speakers with different areas of expertise was present. Bruce Colby made some introductory remarks and indicated that the workshop would be informal to the extent that questions and/or comments could be raised during the presentations. Fred Faulkner presented a discussion of common aspects of quantitative mass spectrometry and made available a handout on the subject. Mike Carter described the approach EPA is currently using to identify and quantitate priority pollutants in industrial effluents and Drew Sauter discussed the quality assurance aspects of quantitation.

Initially, there seemed to be two fundamentally different approaches to quantitation being discussed. One of these utilized selected ion monitoring for data acquisition and was employed primarily for activities involving samples and molecules of pharmacological significance; the second utilized full spectrum data acquisition and was generally associated with materials of environmental concern. As discussions continued, it became evident that both approaches to quantitation involved a similar series of considerations in setting up an analysis, carrying it out, and assuring that acceptable results are produced. Topics which were discussed in detail included:

- Selection of m/z's for quantitation,
- Ways to handle problems associated with component coelution,
- Appropriate ways to create and evaluate calibration curves,
- Frequency with which method evaluation standards and quantitative calibration standards should be analyzed, and
- The use of marker or surrogate compounds to monitor analytical quality.

No specific recommendations concerning quantitative GC/MS were anticipated as a result of this workshop.

Bruce N. Colby
Co-Chairman

Fred C. Faulkner
Co-Chairman

MINUTES OF THE 1980 ASTM E-14 BUSINESS MEETING

The Business Meeting of ASTM Committee E-14 on Mass Spectrometry was held on May 27, 1980, in New York, New York. Representatives of industrial, academic and government organizations were in attendance.

The meeting was opened by the Chairman, M. C. Hamming, who introduced the officers for the current term. They are:

Chairman:	M. C. Hamming, CONCO, Inc., Res. & Dev. Department, Box 1267, Ponca City, OK 74601
Vice-Chairman:	Thomas Aczel, Exxon Research & Engineering Co., Box 4255, Baytown, TX 77520
Secretary-Treasurer:	E. M. Chait, duPont Instruments, Quillen Building, Concord Plaza, Wilmington, DE 19898

Also introduced was our Staff Manager, Ms. Janet Schroeder. It was explained that E. M. Chait would be resigning as Secretary-Treasurer owing to a redirection of his professional activities.

The minutes of the previous business meeting were presented by E. M. Chait, who also gave a brief fiscal status report.

The members of ASTM Committee E-14 wish to thank Ed Chait for his enthusiastic efforts in behalf of the comiittee.

Terry Ashe moved to have Bruce N. Colby (Systems, Science and Software, Box 1620, La Jolla, CA 92038) installed as the new Secretary-Treasurer. The motion was passed.

Janet Schroeder described E-14 as an expanding committee, with a current membership of 63 persons. She also mentioned the decision by the Office of Management and Budget to utilize accepted standards and methods, such as those generated by ASTM (Federal Register, January 21, 1980) in lieu of the government creating additional ones.

Phil Pierce, Chairman of Subcommittee E14.14 on General Practices, gave a report on the two existing E-14 recommended practices. The first, "Use and Evaluation of Mass Spectrometers for Mass Spectrochemical Analysis of Solids," E304-68, was recommended for a title change to be decided upon by the subcommittee. The second, "Evaluation of Mass Spectrometers for Use in Chemical Analysis" was also recommended for a title change to more accurately describe its intended application.

Terry Ashe, Chairman of Subcommittee E14.13 on GC/MS, gave a status update on the GC/MS practice which is in preparation; a fourth draft is anticipated in the following year.

Jacob Shen, Chairman of Task Force E14.13.02 on GC/MS Terminology, now has a draft available for comment.

Bruce Colby, Chairman of Subcommittee E14.92 on Long Range Planning, discussed plans for the "Quantitative GC/MS Workshop" which will take place on June 28, 1980.

A subcommittee on Good Laboratory Practices was established with Tony Delefano as Chairman.

A discussion of a possible E-14 award to a deserving mass spectroscopist took place. A motion was passed to establish an Awards Subcommittee which will decide on appropriate award and a mechanism for making the award. The Executive Committee will establish the Awards Subcommittee who will act by February 1981. Possible awards of cash, a book, or a plaque were discussed.

A motion was passed to establish a committee to nominate next year's officers. Interested parties should contact M. C. Hamming.

An informal executive meeting was held by the officers after the Business Meeting. They discussed the above topics with ASMS representatives.

Respectively submitted,

Bruce N. Colby

Bruce N. Colby
Secretary-Treasurer

Workshop Report on

GC-MS Quantitation of Drugs of Abuse

A workshop was held to discuss several applications of quantitative GC-MS in the forensic and drug abuse area. Four panel members gave brief presentations and this was followed by a discussion period with the audience.

Panel members included:

Dr. Richard Hawks, National Institute on Drug Abuse
Dr. David Hachey, Argonne National Laboratories
Dr. Bryan Finkle and Dr. Roger Foltz, Center for Human Toxicology, University of Utah

The meeting was opened with a short review of the activities of the National Institute on Drug Abuse (NIDA), involving support of GC-MS quantitative development. NIDA has been active in the development of deuterated standards for a variety of drugs; for the development and field testing of GC-MS quantitative methods; and for the use of these methods in contract service laboratories which aid researchers by providing a source of quantitative assays. The question of standards availability was discussed. NIDA supplies material free of charge to bona fide research programs, but forensic needs must generally be met by commercial organizations.

Dr. Hachey presented data from a pharmacokinetic research project on chronic methadone treatment. Pharmacokinetic parameters are under investigation by use of a sophisticated procedure involving three deuterated methadone species. A single dose of 50:50 d- and l-methadone (separately labeled) is given during the course of chronic methadone clinical treatment and the individual optical isomers are then quantitated by a third deuterated species. Influences on the kinetic parameters of the d- and l- forms of methadone due to chronic administration, alcohol abuse and liver dysfunction are being investigated.

Dr. Foltz discussed a general development approach of a quantitative GC-MS-CI method for new drugs. The general scheme emphasizes simplicity of work-up by taking advantage of the selectivity of the MS and the relative spectral simplicity of CI-NH_3 systems. Discussion was stimulated on the questions of equilibrium time for addition of internal standards and on the need to simplify assay systems as much as possible to provide the flexibility and efficiency essential to a forensic laboratory.

Dr. Bryan Finkle next presented an intriguing case of mysterious accidental poisoning and its resolution by GC-MS quantitation. The case history illustrated the practical problems presented by forensic cases and how the complexity of some of these cases is only resolvable by use of quantitative GC-MS, a technique common to members of this Society but still in limited use in the forensic community.

The workshop concluded after some 40 minutes of questions, answers and general audience participation.

Respectfully submitted,

Richard L. Hawks, Ph.D.
Research Division
National Institute on Drug Abuse
5600 Fishers Lane
Rockville, Maryland 20857

Report on Workshop 13

USE OF GC RETENTION TIMES TO IDENTIFY ORGANIC COMPOUNDS

The workshop was held on Thursday, May 29, 1980. About 40 persons attended the workshop. The panelists were: Drs. Klaus Biemann, MIT, Dennis Lin, Battelle Memorial Institute, and John Holland, Michigan State University.

Each of the panelists gave a short presentation describing the way in which they made use of GC retention times to augment spectral data from GC/MS systems.

Dr. Biemann uses Kovatz indices for drug analysis. Normal saturated hydrocarbons in the range of C_{10} to C_{40} are used to calibrate the retention time scale. Retention times are not used for precise compound identification, but rather to provide a search window to limit the range of library compounds which need to be considered for searching purposes. His system operates in an interactive mode, in which the operator can recognize well-defined components in the mixture and use the retention indices so derived for the identification of other known or unknown drugs and their metabolites. The system thus is able to aid the human interpreter throughout the course of his search in the identification of compounds of interest.

Another technique is used by Dr. Biemann for peptide identification. In this case, the computer makes use of the fact that the retention time of polypeptides can be computed roughly by the summation of a series of numbers which have been determined independently for each amino acid residue. As a result, given the known amino acid composition of an unknown peptide, sequencing can be materially simplified by the elimination of possible sequences whose calculated retention index is incompatible with the observed values. Thus, by combining the retention time information with the possibilities derived from the mass spectral fragmentation patterns, the structure of an individual polypeptide can usually be uniquely established.

Dr. Lin discusssed his work in the analysis of environmental samples. In his laboratory, initial identification of unknowns is carried out by direct forward search, and afterwards, confirmation of identity is made by comparison of retention indices with those stored in the reference library. Dr. Lin uses a single standard, hexaethylbenzene, elution time: 63-65 min, as a reference compound for the determination of retention indices. At present, he has a working library containing 1200 reference retention indices.

Relative retention times depend on a great number of variables, including column efficiency, column polarity, film thickness, mode of injection, solvent volume, and reproducibility of GC temperature programming, particularly at low temperatures. Dr. Lin felt that although multiple internal standards can be used, satisfactory results were achieved with the use of a single standard.

Dr. Holland's system was designed primarily for urinary metabolites, and he has found that retention indices are highly reproducible (ca. 0.2%) and serve as a very accurate analytical parameter for the identification of compounds important for metabolic profiling. His procedure is to coinject hydrocarbons as standards. Since these are rarely compounds sought, they do not interfere with the analytical procedure. After the components have eluted, narrow windows are used to define their retention indices and the compounds are identified by reverse search procedures. Identification of specific unknowns is made by the comparison of precise retention indices and key individual ions present in common between the library file and the unknown. His program is used both for qualitative and quantitative identification of specific metabolites.

In the discussion that ensued, the participants concluded that it might be possible to develop sets of retenion indices which could be used by broad segments of the mass spectrometry community. The data bases which have been generated by the three contributing laboratories will be made available to interested scientists on request. Strong interest was expressed in the possibility of including retention indices as an integral part of mass spectral data bases and it was hoped that efforts would be made in the future to provide such information in the widely distributed national and international collections of mass spectral data.

Respectfully submitted,

David Rosenthal,
Chairman

Workshop 1 - Good Laboratory Practices

The workshop on Good Laboratory Practices (GLP) was held on Monday, May 26, 1980 at 8:00 p.m. Approximately 40 people were in attendance.

The meeting began with a brief review of the GLP regulations which were published in the Federal Register in 1979. A set of GLP guidelines for mass spectrometry laboratories was written by us using input from a previous meeting and published in the 1978 ASMS bound volume and in the first supplementary volume of George Waller's book "Biochemical Applications of Mass Spectrometry". The guidelines deal primarily with the documentation needed by a laboratory to show that GLP regulations were met at the time the analysis was performed.

Henry Sacco from KRATOS Scientific Instruments gave a short presentation dealing with the GLP regulations from the point of view of an instrument manufacturer's service manager. He again stressed the importance of proper documentation and volunteered to send a rough copy of an instrument checklist he has prepared to those in attendance. Any other interested person may obtain copies of the checklist by writing to Henry Sacco, KRATOS Inc., 160 Tillman St., Westwood, N.J. 07675. Comments on ways to improve the relevance of the checklist are welcome.

A suggestion was made by Dr. R. King, University of Florida, to continue having meetings dealing with government regulations at future ASMS conferences. Accordingly, a motion was unanimously passed asking the chairman to petition ASMS for permanent committee status. In addition, Dr. T. R. Ashe, Exxon Research and Engineering, suggested establishing a GLP subcommittee for ASTM Committee E-14. Thus, on May 27, committee E-14 officially establilshed a GLP subcommittee with A. J. DeStefano as chairman. It was agreed that we would try to rewrite the GLP guidelines in a form suitable for issuance as an ASTM standard.

Several workshop attendees volunteered to help organize next year's meeting. These include

Barbara L. Jelus - Tyror, Avon Products Inc.
Philip Price, Union Carbide
H. Sacco, KRATOS Scientific Instruments
Ed Silveira, Shell Development

The chairman will welcome any other assistance offered.

Respectfully submitted,

Anthony DeStefano

Anthony DeStefano
Chairman

ASTM COMMITTEE E-14 AND
THE AMERICAN SOCIETY FOR MASS SPECTROMETRY

Year	President	Vice President Programs	Vice President Arrangements	Vice President Data & Stds.
1961-2	V. H. Dibeler	R. E. Fox	R. A. Brown	-
1963-4	R. E. Fox	N. D. Coggeshall	A. G. Sharkey	-
1965-6	N. D. Coggeshall	H. M. Rosenstock	M. K. Testerman	-
1967-8	H. M. Rosenstock	J. L. Franklin	D. B. Harrington	-
1968-9	J. L. Franklin	R. E. Honig	C. E. Johannsen	-
		ASMS		
1970	J. L. Franklin	R. E. Honig	C. E. Johannsen	H. R. Harless
1971-2	R. E. Honig	F. H. Field	G. L. Kearns	H. R. Harless
1972-4	F. H. Field	H. J. Svec	A. H. Struck	E. Lumpkin
1974-6	H. J. Svec	J. H. Futtrell	W. H. Brubaker	*Position was deleted in 1973-4
1976-8	J. H. Futtrell	J. A. McCloskey	E. J. Bonelli	-
1978-9	J. A. McCloskey	B. Munson	E. J. Bonelli	
1979-80	J. A. McCloskey	B. Munson	W. A. Wolstenholme	

Year	Secretary	Treasurer	Directors at Large	
		ASTM E-14		
1961	C. F. Crable	-	J. H. Beynon	C. F. Robinson
1963-4	H. E. Lumpkin	-	S. Meyerson	A. L. Wahrhaftig
1965-6	G. L. Cook	-	H. I. Schiff	W. M. Hickam
1967-8	A. B. King	-	E. E. Muschlitz	R. M. Teeter
1969	J. M. McCrea	-	R. F. Porter	J. T. Herron
		ASMS		
1970	J. M. McCrea	H. D. Cook	R. F. Porter	J. T. Herron
1971-2	F. E. Saalfeld	H. D. Cook	A. G. Sharkey	A. L. Wahrhaftig
1972-4	F. E. Saalfeld	M. T. Laug	J. Berkowitz	E. B. Owens
1974-6	J. A. McCloskey	M. T. Laug	P. Kebarle E. M. Emery+	J. L. Margrave
1976-7	K. E. McCulloh	M. T. Laug	H. M. Fales	A. G. Harrison
1977-8	H. M. Fales	M. A. Frisch	H. M. Fales E. G. Carlson +	A. G. Harrison
1978-9	H. M. Fales	M. A. Frisch	C. C. Fenselau M. C. Hamming +	A. G. Harrison
1979-80	H. M. Fales	M. A. Frisch	C. C. Fenselau M. C. Hamming +	W. L. Fite

*ASTM E-14 Chairman was dropped as a Vice President and made a Director at Large in 1974.
+ASTM E-14 Chairman

THE AMERICAN SOCIETY FOR MASS SPECTROMETRY

CONSTITUTION AND BYLAWS

ARTICLE I. NAME

The name of this Society shall be "The American Society for Mass Spectrometry".

ARTICLE II. PURPOSE

It is the purpose of this Society to promote and disseminate knowledge of mass spectrometry and allied subjects.

ARTICLE III. MEMBERSHIP

Membership in the American Society for Mass Spectrometry shall be open to any individual, or with approval of the Board of Directors, to any corporate entity with a bona-fide interest in mass spectrometry.

ARTICLE IV. MANAGEMENT

The management of the Society shall be vested in the Board of Directors which shall consist of the following members: the officers of the society hereafter listed, two elected members-at-large, the immediate Past-President, the Chairman of ASTM Committee E-14 on Mass Spectrometry.

The Officers of the Society shall be:

President
Vice President for Programs, who shall be President-Elect of the Society
Vice President for Arrangements
Secretary
Treasurer

ARTICLE V. DUTIES OF OFFICERS

Section 1. The President shall be the chief executive officer of this Society; he shall preside at all meetings of the members and directors; he shall have general and active management of the business of this Society; he shall see that all orders and resolutions of the Board of Directors are carried out; he shall execute all bonds, mortgages, and all contracts of this Society and cause or direct the affixing of the corporate seal thereto; he shall have general superintendence and direction of all other officers of this Society and see that their duties are properly performed; he shall submit a report of the operations of the Society for the fiscal year to the Board of Directors and members at their annual meeting, and from time to time shall report to the Board of Directors all matters within his knowledge that may affect this Society; he shall be ex-officio a member of all committees except the Nominating and Audit Committees and shall have the power and duties and management

usually vested in the office of President in a corporation; he shall appoint all committees, except as may be otherwise provided; and he shall send, or cause to be sent by the Secretary, notices of any meetings of the Board of Directors.

Section 2. The Vice President for Programs shall be vested with all the powers and shall perform all the duties of the President during the absence of the latter and shall have such other duties as may, from time to time, be determined by the Board of Directors. The same shall be true of the Vice President for Arrangements who shall be next in the line of succession. In the event that the President shall be absent at any meeting, the Vice President for Programs shall preside, and if neither is present at a meeting, then the Vice-President for Arrangements shall preside.

Section 3. The Secretary or a deputy appointed by the President shall attend all meetings of the Board of Directors and all general meetings of the society and act as a clerk thereof; he shall record all votes and minutes of all proceedings; he shall perform such other duties as may be prescribed by the Board of Directors or the President; and he shall be the custodian of the corporate seal and all of the books and records of the Society except as may be otherwise provided.

Section 4. The Treasurer shall have charge of the funds of the Society and shall deposit them in the name of the Society in depositories designated by the Board of Directors; he shall arrange for the payment of all valid Society bills and debts from Society unds, and shall make a complete and accurate report of the finances of the Society at each annual meeting of the members, or at any other time upon request, to the Board of Directors.

ARTICLE VI. DUTIES AND POWERS OF THE BOARD OF DIRECTORS

Section 1. The property and business of the Society shall be managed by the Board of Directors.

Section 2. In addition to the general powers of the Board of Directors by virtue of their office, the powers and authority expressly given by law, by terms of the Charter of this Society, and elsewhere in these bylaws, the following specific powers are expressly conferred on the Board of Directors: To purchase or otherwise acquire for the Society any property, right or privilege which it is authorized to acquire at such price or consideration and upon such terms as they deem expedient; To appoint, to remove or suspend subordinate agents or servants, to determine their duties and affix their salaries; To remove or suspend any subordinate officer or servants; To determine who shall be authorized on behalf of the Society to sign bills, notices, receipts, acceptances, endorsements, checks, releases, contracts and any other instruments; To delegate any of the powers of the Board to any standing committee, special committee, or to any officer or agent of the Society, with such powers as the Board may deem fit and proper to grant; Generally to do all such lawful acts and things as are not by law, or by charter, or by these bylaws directed or required to be done by members of the Board of Directors.

Section 3. Any action which may be taken at a meeting of the Board of Directors, may be taken without a meeting by a letter ballot sent by and filed with the Secretary of the Society and provided all the members of the Board of Directors file ballots.

Section 4. In the event that the office of any elected officer or member of the Board of Directors shall become vacant, the Board of Directors shall immediately fill the vacancy for the remainder of the unexpired term; however, no member who thus fills a vacancy in the office of Vice President for Programs shall automatically succeed to the presidency, but the Society shall in such event elect its next President. A President who vacates office before the conclusion of his term shall not retain membership on the Board of Directors as Past-President as described in Article IV.

Section 5. The ballot of the election to membership on the Board of Directors of the Society shall be by closed, written ballot.

Section 6. Any member shall be eligible to hold office in the Society.

ARTICLE VII. FIDELITY BONDS

The Board of Directors may require such officers or agents to be bonded as it shall deem necessary; for any amount or amounts as it may deem requisite, at the expense of the Society.

ARTICLE VIII. LOCATION

The principal office of this Society shall be located in the City of Pittsburgh, Commonwealth of Pennsylvania.

ARTICLE IX. DISSOLUTION

In the event of either voluntary or involuntary dissolution of the Society, the funds or assets of the Society, remaining after discharging all just debts of the Society or its officers in the name of the Society, shall be distributed without encumbrances to a non-profit group, organization or institution of learning engaged in the field of mass spectrometry within the contemplation of Section 170 (c) (2) of the Internal Revenue Code (1954). The selection of the recipient or recipients shall be made by the majority vote of the Board of Directors in office at the time of dissolution but in no event shall the assets be distributed to any member or members of the Society.

ARTICLE X. SOCIETY SEAL

The Society shall have a seal, upon which shall be inscribed the name of the Society, the year of its creation, and the word "Pennsylvania", the state of the Society's incorporation.

Article XI. AMENDMENTS

Section 1. A proposed amendment to the Constitution and the Bylaws of the Society, signed by at least three members of the Board of Directors or by fifty members of the Society must be submitted to the Secretary at least fifteen weeks before the regular annual business meeting at the Annual Conference of the Society. The Secretary shall send or cause to be sent the proposed amendment to each member within a reasonable time and at least prior to thirty days before the Annual Conference. After the amendment has been discussed at that meeting, the Secretary will send a letter ballot on the proposed amendment as amended at the meeting to all Society members; if two-thirds of the votes obtained by letter ballot within six weeks are in favor of the proposed amendment, it shall be adopted.

Section 2. The Board of Directors shall also have the power to amend the Bylaws by a two-thirds vote of its membership.

Section 3. The Board of Directors is authorized to re-number articles and sections of the Constitution and Bylaws to correspond with any changes that may be made.

Section 4. Proceedings for removal of members of the Board of Directors shall be conducted as outlined above for amendments to the Constitution (Article XI, Section 1). If the request for removal is supported by two-thirds of the letter ballots received within six weeks, the Board member or members in question shall be removed from office and a replacement selected by the Board of Directors in accordance with Article VI, Section 4.

Article XII. ARCHIVIST

The Board of Directors shall appoint a Society Archivist whose duties shall be the collation and preservation of all documents deemed to be of historical interest. All records will be reproduced on microfilm from time to time and all of the original documents will be reviewed by the Archivist before they are disposed of. The Archivist shall report his activities to the Board of Directors annually and will report them to the general membership whenever appropriate.

The Archivist shall be nominated by the President and appointed to the office by a two-thirds vote of the Board of Directors. The incumbent shall be reviewed annually and may be reappointed at the pleasure of the Board.

Expenses incurred by the Archivist on Society business shall be reimbursed.

BYLAWS

1. Membership

1.1 Application for membership shall be made in writing, on a form to be specified by the Board of Directors. The membership year shall commence January 1 and end December 30.

1.2 Membership becomes effective upon receipt by the Treasurer of dues and a properly executed application.

1.3 Failure to pay dues by February 1 shall automatically terminate membership. Payment of current dues shall suffice for reinstatement; however, dues received after May 1 will reinstate membership effective July 1 of the same year.

1.4 Membership may be terminated without prejudice by written notice to the Secretary.

1.5 Every member of record as of February 1 shall have the right to vote and to hold office.

1.6 The books, accounts and records of the Society shall be open for inspection to any member of the Board of Directors at any time. Members of the Society may upon written request to the Board of Directors, inspect such books, accounts and records of the Society at such reasonable times as the Board of Directors may designate.

1.7 The Secretary will prepare or cause to be prepared at least one annual membership report to the Board of Directors.

2. Collections and Disbursements

2.1 Membership classes and dues within such classes shall be determined by the Board of Directors.

2.2 The Board of Directors is authorized to determine separately a registration fee for each general meeting to cover the expenses of holding the meeting. Payment of this fee is a requirement for attendance.

2.3 Disbursements shall be made by approval of a majority of the Board of Directors. Disbursement in excess of $500.00 shall be made by check signed by two members of the Board.

2.4 The fiscal year of the Society shall be from January 1 to December 31.

2.5 The Treasurer will prepare or cause to be prepared an annual financial report to the Board of Directors.

3. *Terms of Office and Election*

3.1 The elected officers and directors-at-large shall hold office for a term of two years, except as otherwise provided in Article VI of the Constitution, with their term year commencing on July 1 and ending on June 30.

3.2 Upon assuming office, the President shall appoint a nominating committee consisting of five members representing diverse areas of mass spectrometry. He shall not be a member of this committee. This selection shall be approved by the Board of Directors by a two-thirds vote. The committee shall serve for two years concurrent with the tenure of the President. It shall nominate a slate of at least one candidate for each of three offices to be filled in alternate years according to the following rotation:

Even Years - Vice President for Programs
- Treasurer
- Member-at-large

Odd Years - Vice President for Arrangements
- Secretary
- Member-at-large, who shall serve in the capacity of Editor of the Conference Proceedings.

The committee will report in writing to the Board of Directors before June 30 each year. These reports will include a statement of each candidate's consent to serve and a professional resume for each candidate. Each slate of candidates and the resumes will be distributed to the members by the Secretary before September 15.

3.3 Any Society member can nominate another member for any office except President by submitting to the Secretary before January 15 of the election year:

a. signatures of at least 50 Society members endorsing the nomination;

b. signed statement of the nominee indicating his agreement to hold office if elected;

c. professional resume of the nominee.

3.4 The Secretary shall prepare, or cause to be prepared, a ballot to be mailed on or before March 1 to members of record on February 1 of the same year. Marked ballots are to be returned by April 15.

3.5 The election results shall be made known at the next annual business meeting and the new officers shall assume office as specified in paragraph 3.1 of the Bylaws.

4. Committees

4.1 The President shall appoint such committees as are necessary to accomplish the purposes of the Society. The terms of these appointments shall not exceed the term of office of the President. He may terminate a committee at any time. Members and chairmen may be reappointed by the incoming President.

5. Meetings

5.1 The Society shall meet at least once a year in order to present scientific papers and conduct business. Fifty members shall constitute a quorum for the transaction of business.

5.2 The time and place of the general meeting shall be determined by the Board of Directors.

5.3 Meetings of the Board of Directors may be called by the President or, in his absence, by the Vice President for Programs. Alternatively, two-thirds of the Board of Directors may call a meeting by written request to the President. Five directors shall constitute a quorum of the Board of Directors.

5.4 A simple majority of those present shall be required to pass any motion at any meeting of the members or Board of Directors, unless otherwise provided (see Article XI, Section 3).

5.5 Each Director shall be entitled to two weeks notice of any meeting of the Board of Directors.

5.6 Notice of the annual general meeting shall be sent to each member at least thirty days before the meeting.

5.7 The President shall, in response to a petition bearing the signatures of not fewer than twenty members and requesting that the Board of Directors consider a specified question, place this item on the agenda of the first meeting of the Board of Directors which is scheduled to convene on a date not preceding the thirtieth day following receipt of the petition. The member whose signature appears first on the petition shall be entitled to two weeks notice of such meeting, and the same member or a member designated by him shall be entitled to attend such meeting and discuss the specified question with the Board of Directors.

5.8 Whenever any notice is required to be given by the provisions of the Bylaws, a waiver thereof in writing, signed by the person or persons entitled to such notices whether before or after the time stated therein, shall be equivalent to the required notice.

5.9 The Ppresident may appoint any member of the Society, not a member of the Board of Directors, to be parliamentarian for the duration of a given business meeting.

6. Compensation

6.1 No member of the Board of Directors of the Society shall receive salaries or fees for his services.

6.2 Members of the Board of Directors of the Society shall be reimbursed for all reasonable expenses incurred in connection with their official duties.

7. Miscellaneous

7.1 The incoming President shall cause the financial records of the Society to be audited within the first six months of his term of office.

7.2 The business of the Society shall be conducted in accordance with the latest edition of Roberts' Rules of Order unless otherwise specified herein.

VLADIMÍR ČERMÁK (1920-1980)

RnDr. Vladimír Čermák, Dr. Sc., Senior Scientist of the J. Heyrovský Institute of Physical Chemistry and Electrochemistry, Czechoslovak Academy of Sciences, Prague, died suddenly in Prague on January 4, 1980.

He was born in Budejovice, Czechoslovakia, in 1920 and received his education in Prague. At the conclusion of World War II in 1945 he entered the Charles University in Prague. He studied under Professors Brdička and Heyrovský in the School of Natural Sciences and obtained his degree in 1949 for work in polarography. He then joined the laboratory of the recently organized Czechoslovak Academy of Sciences which became shortly afterwards the Institute of Physical Chemistry--the place to which he devoted his entire scientific career. There he and his colleagues initiated work in mass spectrometry--an entirely new branch of science in Czechoslovakia (in 1954 he was a recipient of the Czechoslovak State Prize for the construction of the first mass spectrometer in the country). In the late fifties his interest turned to the collisions of ions investigated by the mass spectrometric method, a field to which he made several important contributions (reactions of electronically excited ions, break-up of polyatomic molecular ions upon charge-transfer, highly excited Rydberg states of noble gas atoms). In 1963 work in his laboratory on ionization in collisions of metastable noble gas atoms with molecules led to the electron spectroscopy of these processes--Penning ionization electron spectroscopy --which was to be his main interest for the rest of his life. Several stays abroad (Visiting Fellow of the Joint Institute for Laboratory Astrophysics of the University of Colorado, Boulder, Colorado, 1964-1965 and 1969, and Visiting Professor, Université de Paris-Sud, Orsay, 1969-1970) helped him in developing the method.

He was for many years in charge of the Department of Mass Spectrometry of the Prague Institute and organized most of the mass spectrometric activity in Czechoslovakia. Also, for several years he acted as a member of the General Committee of the International Conference on the Physics of Electron and Atomic Collisions and served on the Editorial Board of the Journal of Electron Spectroscopy. In 1977 he was awarded the Marcus Marci Medal for advancing spectroscopy in Czechoslovakia.

His contributions in mass spectrometry and electron spectroscopy have been given worldwide recognition. He was a well-known and respected personality at international meetings in these fields. Whenever he had an opportunity, he participated in the ASMS conferences, the last time in 1976 when he was an invited plenary speaker for the San Diego meeting of the ASMS.

G P	ARSENAULT	PO BOX 2210, R R 1			KINGSTON, ONTARIO	K7L	4V1	CANA
M	BARIL	UNIVERSITE LAVAL	PHYSICS DEPT		QUEBEC, QUEBEC	G1K	7P4	CANA
G	BAUER	HEWLETT-PACKARD LTD	275 HYMUS BOUL		PIE CLAIRE, QUEBEC	H9R	1G7	CANA
F M	BENOIT	HEALTH-WELFARE DEPT	ENVIRONMENTAL HEALTH	TUNNEYS PASTURE	OTTAWA, ONTARIO	K1A	0L2	CANA
M	BERTRAND	UNIV OF QUEBEC	INRS	7401 HOCHELAGA	MONTREAL, QUEBEC	H1N	3M5	CANA
R F	BONNER	MINISTRY ENVIRONMENT	PO BOX 213		REXDALE, ONTARIO	M9W	5L1	CANA
R K	BOYD	UNIV OF GUELPH	CHEMISTRY DEPT		GUELPH, ONTARIO	N1G	2W1	CANA
J A	BUCKLEY	SCIEX INC	55 GLENCAMERON RD	SUITE 202	THORNHILL, ONTARIO	L3T	1P2	CANA
P	BURGERS	UNIV OF OTTAWA	CHEMISTRY DEPT		ONTARIO	K1N	9B4	CANA
J	COBURN	CAN CNTR INLAND WTRS	WATER QUALITY LAB	867 LAKESHORE ROAD	BURLINGTON, ONTARIO	L7R	4A6	CANA
M B	COMISAROW	UNIV BRIT COLUMBIA	CHEMISTRY DEPT	2036 MAIN MALL	VANCOUVER, BC	V6T	1Y6	CANA
P L	COULOMBE	DATACOMP ELECTRONICS	1610-85 ALBERT ST		OTTAWA, ONTARIO			CANA
W R	DAVIDSON	SCIEX INC	55 GLENCAMERON RD	SUITE 202	THORNHILL, ONTARIO	L3T	1P2	CANA
D J	DOUGLAS	SCIEX INC	55 GLENCAMERON RD	SUITE 202	THORNHILL, ONTARIO	L3T	1P2	CANA
G K	EIGENDORF	UNIV BRIT COLUMBIA	CHEMISTRY DEPT		VANCOUVER, BC	V6T	1Y6	CANA
I P	FISHER	GULF CANADA LTD	RESEARCH & DEVELOP	2489 N SHERIDAN WAY	SHERIDAN PARK, ONT	L5K	1A8	CANA
M G	FOSTER	MINISTRY ENVIRONMENT	OTC	PO BOX 213	REXDALE, ONTARIO	M9W	5L1	CANA
J B	FRENCH	UNIV OF TORONTO	AEROSPACE STUDIES	4925 DUFFERIN ST	DOWNSVIEW, ONTARIO	M3H	5T6	CANA
J E	FULFORD	SCIEX INC	55 GLENCAMERON RD	SUITE 202	THORNHILL, ONTARIO	L3T	1P2	CANA
D D	GODSE	CLARKE INST PSYCHIAT	250 COLLEGE STREET		TORONTO, ONTARIO	M5T	1R8	CANA
M	GORDON	MERCK-ISOTOPES	612-1209 RICHMOND ST		LONDON, ONTARIO	N6A	3L7	CANA
A G	HARRISON	UNIV OF TORONTO	CHEMISTRY DEPT		TORONTO, ONTARIO	M5S	1A1	CANA
J A	HERMAN	UNIVERSITE LAVAL	CHEMISTRY DEPT		QUEBEC, QUEBEC	G1K	7P4	CANA
K	HERMAN	UNIVERSITE LAVAL	CHEMISTRY DEPT		QUEBEC, QUEBEC	G1K	7P4	CANA
A M	HOGG	UNIV OF ALBERTA	CHEMISTRY DEPT		EDMONTON, ALBERTA	T6G	2G2	CANA
L	HOGGE	PRARIE REGIONAL LAB			SASKATOON, SASK	S7N	0W8	CANA
J L	HOLMES	UNIV OF OTTAWA	CHEMISTRY DEPT		OTTAWA, ONTARIO	K1N	9B4	CANA
J V	IRIBARNE	29 BANSTOCK DR			WILLOWDALE, ONTARIO	M2K	2H5	CANA
W D	JAMIESON	NRC	1411 OXFORD ST		HALIFAX, NOVA SCOTIA	B3H	3Z1	CANA
M	KALLOO	MERCK SHARP & DOHME	PO BOX 899		POINTE CLAIRE QUEBEC	H9R	4P7	CANA
P	KEBARLE	UNIV OF ALBERTA	CHEMISTRY DEPT		EDMONTON, ALBERTA	T6G	2G2	CANA
H J	KOCH	MERCK-FROSST LABS	PO BOX 1005		POINTE CLAIRE, QUEBEC	H9R	4R7	CANA
R C	LAO	ENVIRONMENT CANADA	CHEMISTRY DIV	APCD	OTTAWA, ONTARIO	K1A	1C8	CANA
P Y	LAU	HEALTH PROTECTION BR	FOOD RESEARCH	TUNNEYS PASTURE	OTTAWA, ONTARIO	K1A	0L2	CANA
F P	LOSSING	NAT RESEARCH COUNCIL	CHEMISTRY DIV		OTTAWA, ONTARIO	K1A	0R6	CANA
A M	LOVETT	SCIEX INC	55 GLENCAMERON RD	SUITE 202	THORNHILL, ONTARIO	L3T	1P2	CANA
R E	MARCH	TRENT UNIVERSITY			PETERBOROUGH, ONT	K9J	7B8	CANA
A	MARTINEAU	UNIV OF MONTREAL	CHEMISTRY DEPT	CP6210 SUCC A	MONTREAL, QUEBEC	H3C	3V1	CANA
F Y	MESSIER	MCMASTER UNIVERSITY	CHEMISTRY DEPT	1280 MAIN ST WEST	HAMILTON, ONTARIO	L8S	4M1	CANA
W F	MILES	PLANT PRODUCTS	LAB SERVICES DIV	BLDG #22, C.E.F.	OTTAWA, ONTARIO	K1A	0C6	CANA
R T	MOIR	IMPERIAL OIL LTD	RESEARCH DEPT	PO BOX 3022	SARNIA, ONTARIO	N7T	7M1	CANA
J B	OLTHUIJEN	2710 BRABANT MARINEAU			MONTREAL, QUEBEC	H4S	1L1	CANA
F I	ONUSKA	CCIW-AMRS	PO BOX 5050		BURLINGTON, ONTARIO	L7R	4A6	CANA
O	PELLETIER	HEALTH PROTECTION BR	ROOM 277, HPB BLDG	TUNNEYS PASTURE	OTTAWA, ONTARIO	K1A	0L2	CANA
M A	QUILLIAM	MCMASTER UNIVERSITY	CHEMISTRY DEPT		HAMILTON, ONTARIO	L8S	4M1	CANA
L	RAMALEY	DALHOUSIE UNIVERSITY	CHEMISTRY DEPT		HALIFAX, NOVA SCOTIA	B3H	4J3	CANA
N M	REID	SCIEX INC	55 GLENCAMERON RD	SUITE 202	THORNHILL, ONTARIO	L3T	1P2	CANA
R W	SADLIER	10 WOODMAN DR, #02			HAMILTON, ONTARIO	L8K	4E1	CANA
J P	SCHMIT	SHERBROOKE UNIV	CHEMISTRY DEPT		SHERBROOKE,	J1K	2R1	CANA
D K	SENSHARMA	UNIV OF ALBERTA	CHEMISTRY DEPT		EDMONTON, ALBERTA	T6G	2G2	CANA
B I	SHUSHAN	UNIV OF GUELPH	CHEMISTRY DEPT		GUELPH, ONTARIO	N1G	2W1	CANA
K	STANDING	UNIV OF MANITOBA	PHYSICS DEPT		WINNIPEG, MANITOBA	R3T	2N2	CANA
J A	STONE	QUEEN'S UNIVERSITY	CHEMISTRY DEPT		KINGSTON, ONTARIO	K7L	3N6	CANA
W F	SUN	UNIV OF WINDSOR	CHEMISTRY DEPT		WINDSOR, ONTARIO	N9B	3P4	CANA
J A	SUNNER	UNIV OF ALBERTA	CHEMISTRY DEPT		EDMONTON, ALBERTA	T6G	2G2	CANA
W C	TAM	PHOTOVAC INC	134 DONCASTER AVE #2		THORNHILL, ONTARIO	L3T	1L3	CANA
B	THOMSON	SCIEX INC	55 GLENCAMERON RD	SUITE 202	THORNHILL, ONTARIO	L3T	1P2	CANA
H M	TOSINE	MINISTRY ENVIRONMENT	PESTICIDES SECTION	PO BOX 213	REXDALE, ONTARIO	M9W	5L1	CANA
B C	TRUDELL	ESSO CHEMICAL CANADA	INSPECTION LAB	PO BOX 3004	SARNIA, ONTARIO	N7T	7M5	CANA
A	WILLIAMS	GULF CANADA LTD	RESEARCH & DEVELOP	2489 N SHERIDAN WAY	SHERIDAN PK, ONTARIO	L5K	1A8	CANA
G W	WOOD	UNIV OF WINDSOR	CHEMISTRY DEPT		WINDSOR, ONTARIO	N9B	3P4	CANA

M P ALLEMANN	HAUS NR 602	OBERKEMPTEAL		8311 OTTIKON	SWITZERLAND
R T APLIN	DYSON PERRINS LAB	SOUTH PKS RD		OXFORD	ENGLAND
E W BAUMGARTNER	UNIVERSITY OF GRAZ	INST F INORG CHEM		A-8010 GRAZ	AUSTRIA
J H BEYNON	UNIVERSITY COLLEGE	CHEMISTRY DEPT		SWANSEA, SA2 8PP	WALES
M BIHART	RES INST CHEMISTRY	HUNGARY ACAD SCIEN	PF 17, 1525	BUDAPEST	HUNGARY
J C BILL	VG DATA SYSTEMS LTD	4 TAMERE CLOSE	SANDBACH	CHESHIRE	ENGLAND
A J BOERBOOM	FOM INSTITUTE	KRUISLAAN 407		AMSTERDAM	HOLLAND
C BOURDONNAIS	V G INSTRUMENTS	3 MAL DE LATTRE	TASSIGNY	78,150 LE CHESNAY	FRANCE
A P BRUINS	STATE UNIVERSITY	PHARMACY DEPT	A DEUSINGLN 2	9713-AW GRONINGEN	NETHERLANDS
F BRUNER	INST SCIENC CHIMICHE	UNIVERSITA URBINO	P RINDSCIMENTO, 6	61023 URBINO	ITALY
C BRUNNEE	VARIAN MAT GMBH	BARKHAUSENSTR 2	POSTFACH 14 4062	D-2800 BREMEN 10	WEST GERMANY
A P BUCHS	UNIV DE GENEVE	MASS SPECTROMETRY	16 BD D'YVOY, SCI 1	CH-1211 GENEVE 4	SWITZERLAND
A CARRICK	KRATOS SCIEN APP LTD	BARTON DOCK ROAD	URMSTON	MANCHESTER, M31 2LD	ENGLAND
J R CESARIO	CEA B3 RCP	BP 561	CEDEX	92542 MONTROUGE	FRANCE
C CHRISTIAN	NERMAG	49 QUAI DU HALAGI		92500 RUEIL MALMAISO	FRANCE
D COVENCY	KRATOS SCIEN APP LTD	BARTON DOCK ROAD	URMSTON	MANCHESTER, M31 2LD	ENGLAND
A DELL	IMPERIAL COLLEGE	BIOCHEMISTRY DEPT		LONDON, SW7	ENGLAND
D R DENNE	KRATOS SCIEN APP LTD	BARTON DOCK ROAD	URMSTON	MANCHESTER, M31 2LD	ENGLAND
G DEVANT	NERMAG S A, RIBERMAG	49 QUAI DU HALAGE		92502RUEIL MALMAISON	FRANCE
O DUTUIT	UNIV ORSAY	LREI CENTRE	BAT 350	91405 ORSAY	FRANCE
S EVANS	KRATOS SCIEN APP LTD	BARTON DOCK ROAD	URMSTON	MANCHESTER, M31 2LD	ENGLAND
S M FACCHETTI	CCR-EURATOM			21020 ISPRA-VARESE	ITALY
H W FEHLHABER	HOECHST AG			6230 FRANKFURT 80	WEST GERMANY
M A FERREIRA	FACULTY OF SCIENCES	CHEMISTRY DEPT		1294 LISBON CODEX	PORTUGAL
H J FOERSTER	C H BOEHRINGER SOHN			D-6507 INGELHEIM	WEST GERMANY
D J FRAISSE	MICROANALYSE	43 BLVD 11 NOV 1918	CEDEX	69621 VILLEURBANNE	FRANCE
M D FRIESEN	IARC/CIRC	150 COURS A THOMAS		69372 LYON	FRANCE
D E GAMES	UNIVERSITY COLLEGE	CHEMISTRY DEPT	PO BOX 78	CARDIFF, CF1 1XL	WALES
S J GASKELL	TENOVUS INSTITUTE	FOR CANCER RESEARCH	WELSH NAT'L SCH MED	CARDIFF, CF4 4XX	UNITED KINGD
G R GOTTHARDT	VARIAN MAT	BARKHAUSENSTR 2		D2800 BREMEN	WEST GERMANY
J GOWER	BECCHAM PHARMACEUTIC	BROCKHAM PARK		BEIGHWORTH, SURREY	ENGLAND
B N GREEN	VG ORGANIC LTD	TUDOR RD		ALTRINCHAM, CHESHIRE	ENGLAND
K E HABFAST	VARIAN MAT GMBH	BARKHAUSENSTR 2	POSTFACH 14 4062	D-2800 BREMEN 10	WEST GERMANY
K D HAEGELE	MERRELL INTL	RESEARCH CENTER		67084 STRASBOURG	FRANCE
J H HAHN	MAX PLANCK INST CHEM	SAARSTR 23		D-6500 MAINZ	WEST GERMANY
S I HARAGUCHI	KURUME UNIVERSITY	RESEARCH INST GC-MS	SCHOOL OF MEDICINE	FUKUOKA, 830	JAPAN
P A HAUG	FELDBERG STR 24			D-6095 GINSHEIM	WEST GERMANY
J HAVERKAMP	FOM INSTITUTE	KRUISLAAN 407		AMSTERDAM	THE NETHERLA
F HERESCH	UNIVERSITAT WIEN	INST F ANAL CHEMIE	WAHRINGERSTRASSE 38	A-1090 VIENNA	AUSTRIA
S ISHII	JEOL LTD	AKISHIMA	NAKAGAMI CHO 1418	TOKYO, 196	JAPAN
Y ITAGAKI	JEOL LTD	AKISHIMA	NAKAGAMI CHO 1418	TOKYO, 196	JAPAN
K R JENNINGS	UNIV OF WARWICK	CHEMISTRY & MOLECULAR	SCIENCES DEPT	COVENTRY, CV4 7AL	ENGLAND
F JOELLE	LERS	31 AVE PV COUTURIER		92220 BAGNEUX	FRANCE
J A JONCKHEERE	BRANDSTRAAT 49 G			B-9131 BEERVELDE	BELGIUM
T R KEMP	VG ORGANIC	3 TUDOR ROAD		ALTRINCHAM, CHESHIRE	UNITED KINGD
P G KISTEMAKER	FOM INSTITUTE	KRUISLAAN 407		AMSTERDAM	NETHERLANDS
H KNOLL	HEINKE KNOLL	FUTSENTAL 28		2800 BREMEN	WEST GERMANY
I KUBODERA	SHIMADZU SEISAKUSHO	NISHINOKYO NAKAGYO		KYOTO, 604	JAPAN
E A LARKA	ROYAL SOC RES UNIT	UNIV COLL OF SWANSEA	NSINGLETON PARK	SWANSEA	GREAT BRITAI
L W LAUWERS	JANSSEN PHARMACEUTIC	TURNHOUTSE BAAN		B-2340 BEERSE	BELGIUM
P A LECLERCQ	EINDHOVEN UNIV TECH	PO BOX 513		5600-MB EINDHOVEN	NETHERLANDS
C LIFSHITZ	HEBREW UNIVERSITY	PHYSICAL CHEM DEPT		JERUSALEM	ISRAEL
V LUIG	VARIAN MAT	BARKHAUSENSTR 2		D-2800 BREMEN	WEST GERMANY
A MACCOLL	UNIVERSITY COLLEGE	CHEMISTRY DEPT	20 GORDON ST	LONDON, WC1H 0AJ	ENGLAND
K MAEDA, KENJI	NAGOYA UNIVERSITY	BRANCH HOSPITAL	1-1-4 DAIKO-CHO	HIGASHI, NAGOYA	JAPAN
J P MAIER	UNIVERSITAT BASEL	PHYSIKAL-CHEM INST	KLINGELBERGSTR 80	4056 BASEL	SWITZERLAND
A MANDELBAUM	TECHNION	CHEMISTRY DEPT		HAIFA, 32000	ISRAEL
T D MARK	INST F EXPERIMENTAL	PHYSIK	KARL SCHORHERRSTR 3	A-6020 INNSBRUCK	AUSTRIA
K M MARNELA	TAMPERE UNIV	PO BOX 607		33101 TAMPERE 10	FINLAND
I M MARUYAMA	KURUME UNIVERISTY	RES INST OF GC/MS		FUKUOKA, 830	JAPAN

I M	MATSUMOTO	KURUME UNIVERSITY	RESEARCH INST GC-MS	SCHOOL OF MEDICINE	FUKUOKA, 830	JAPAN
R A	MCDOWELL	IMPERIAL COLLEGE	BIOCHEMISTRY DEPT		LONDON, SW7 2AZ	ENGLAND
D S	MILLINGTON	VG ORGANIC LTD	TUDOR ROAD	ALTRINCHAM	CHESHIRE, WA14 5RZ	ENGLAND
K M	MITSUTAKE	KURUME UNIVERSITY	RES INST OF GC/MS		FUKUOKA, 830	JAPAN
M	MONTAGNA	INST OF LEGAL MED	VIA FORLANINI 12		27100 PAVIA	ITALY
H R	MORRIS	IMPERIAL COLLEGE	BIOCHEMISTRY DEPT		LONDON	ENGLAND
I J	NENNER	CEN SACLAY	DPC/SPP	BP 2	91190 GIF SUR YVETTE	FRANCE
T	NIWA	NAGOYA UNIV HOSPITAL	INTERNAL MEDICINE	1-1-4, DAIKO-CHO	HIGASHI-KU, NAGOYA	JAPAN
T	OHKI	BIODYNAMICS RES INST	1-3-2 TAMAMIS CHO		MIZUHOKU, NAGOYASHI	JAPAN
G	PARISOD	EPFL-ECUBLENS	INST DE CHIMIE PHYS		CH- 015 LAUSANNE	SWITZERLAND
J H	PLUMP	MOECKERNSTR 42-44			D-2800 BREMEN	WEST GERMANY
P	POWERS	296 BRAMHALL LANE	SO BRAMHALL		CHESHIRE, SK7 3DJ	ENGLAND
M P	PRZYBYLSKI	UNIV MAINZ	INST ORG CHEMIE		D-6500 MAINZ	WEST GERMANY
J A	RACE	VG ORGANIC LTD	TUDOR ROAD	ALTRINCHAM	CHESHIRE	ENGLAND
H	RADDATZ	VARIAN MAT-GMBH	BARKHAUSENSTR 2		D-2800 BREMEN	WEST GERMANY
J H	RADTKE	DORTELWEILERSTR 4			D-6000 FRANKFURT 60	WEST GERMANY
U	RAPP	VARIAN GMBH	BARKHAUSENSTR 2		D-2800 BREMEN	WEST GERMANY
J D	ROBINSON	VG DATA SYSTEMS	TRIBUNE ROAD		ALTRINCHAM, CHESHIRE	ENGLAND
B	ROWE	LAB D'AIROTHERM CNRS	4 TER ROUTE DES GARD		92190 MEUDON	FRANCE
K R	RYAN	CSIRO	N.M.L.	PO BOX 218	LINDFIELD, NSW 2070	AUSTRALIA
P A	RYAN	KRATOS SCIEN APP LTD	BARTON DOCK ROAD	URMSTON	MANCHESTER, M31 2LD	ENGLAND
U P	SCHLUNEGGER	UNIVERSITAT BERN	INSTIT ORGAN CHEMIE	FREIESTRASSE 3	CH-3012 BERN	SWITZERLAND
E R	SCHMID	UNIVERSITAT WIEN	INST F ANAL CHEMIE	WAHRINGERSTRASSE 38	A-1090 VIENNA	AUSTRIA
D	SCHUCH	LEGIENSTRASSE 33A			D-6230 FRANKFURT 80	WEST GERMANY
T S	SHINKA	KURUME UNIVERSITY	RES INST OF MED MS		FUKUOKA, 830	JAPAN
G	SPITELLER	UNIV BAYREUTH	BODENSEERING 71		D-858 BAYREUTH	WEST GERMANY
G T	STEEL	ICI LTD	CENTRAL TOXICOLOGY	ALDERLEY PARK	CHESHIRE, SK10 4TG	ENGLAND
W	STEK	TECHMATION	BUILDING 106		SCHIPHOL EAST	HOLLAND
I	SZABO	UNIVERSITY OF LUND	CHEMICAL CENTER	PO BOX 740	S-22007 LUND 7	SWEDEN
R F	TABACCHI	UNIV DE NEUCHATEL	INST DE CHIMIE	AV DE BELLEVAUX 51	CH-2000 NEUCHATEL	SWITZERLAND
J C	TABET	ECOLE POLYTECHNIQUE	LAB SYNTHESE ORGAN	91 120 PLATEAU	DE PALAISEAU	FRANCE
E	TAJIMA	871-1 TSUDA	KATSTA-SHI		IBARAKI-KEN	JAPAN
M	TSUCHIYA	4 37 27 KUGAYAMA	SUGINIMI KU		TOKYO, 168	JAPAN
P J	TURNER	VG MICROMASS LTD	ION PATH	ROAD THREE	WINSFORD, CHESHIRE	ENGLAND
J	VAN KATWIJK	KON SHELL LABORATORI	POSTBUS 3003		1003-AA AMSTERDAM	NETHERLANDS
W C	VAN NIERERK	PRIVATE BAG X 256			PRETORIA 0001	SOUTH AFRICA
A	VINCZE	ISRAEL INST BIOL RESP	PO BOX 19		NESS ZIONA, 70400	ISRAEL
J D	WALDRON	KRATOS SCIEN APP LTD	BARTON DOCK RD	URMSTON	MANCHESTER, M31 2LD	ENGLAND
K P	WANCZEK	PARKALLEE 197			D-2800 BREMEN	WEST GERMANY
M	WANCZEK	PARKALLEE 197			D-2800 BREMEN	WEST GERMANY
M	WEISS	NRC NEGEV	PO BOX 9001		BEER-SHEVA	ISRAEL
M	WHITEHOUSE	METROPOLITAN POLICE	FORENSIC SCIENCE LAB	109 LAMBETH RD	LONDON SE1	ENGLAND
J L	WIEBERS	UNIVERSITY COLLEGE	CHEMISTRY DEPT		SWANSEA, SA2 8PP	WALES
R E	WOLFF	INST DE CHIMIE	1 RUE BLAISE PASCAL	BP 296 R/8	67008 STRASBOURG	FRANCE
M	YAMATA	JEOL LTD	AKISHIMA	NAKAGAMI CHO 1418	TOKYO	JAPAN
J	YINON	WEIZMANN INS SCIENCE			REHOVOT	ISRAEL
Z V	ZARETSKII	WEIZMANN INS SCIENCE	PO BOX 26		REHOVOT	ISRAEL

H B ARAJIAN	HOFFMANN-LAROCHE, INC	BLDG 71, RM 108	340 KINGSLAND RD	NUTLEY	NJ	07110 USA
L E ABBEY	GEORGIA TECH	CHEMISTRY DEPT		ATLANTA	GA	30332 USA
R N ABERNATHY	PENN STATE UNIV	152 DAVEY LAB		UNIVERSITY PARK	PA	16802 USA
W ABERTH	LINUS PAULING INST	2700 SAND HILL RD		MENLO PARK	CA	94025 USA
R T ABRAHAM	UNIV OF PITTSBURGH	SCHOOL OF PHARMACY	1015 SALK HALL	PITTSBURGH	PA	15216 USA
F P ABRAMSON	GEORGE WASHINGTON UN	PHARMACOLOGY DEPT		WASHINGTON	DC	20037 USA
T ACZEL	EXXON R/E	PO BOX 4255		BAYTOWN	TX	77520 USA
R A ADAMS	3480 TANBARK CT NE			ATLANTA	GA	30319 USA
W W AKSAMIT	SEARLE LABORATORIES			P O BOX 5110	CHICAGO,	USA
R T ALESSANDRO	12 FULLER AVE			FLORAL PK	NY	11001 USA
A ALLEGRINO	STAUFFER CHEMICAL CO			DOBBS FERRY	NY	10522 USA
J ALLISON	MICHIGAN STATE UNIV	CHEMISTRY DEPT		EAST LANSING	MI	48824 USA
M ALTERAS	SCHERING CORP	60 ORANGE STREET		BLOOMFIELD	NJ	07003 USA
J ALVIN	UNIV OF PITTSBURGH	SCHOOL OF PHARMACY	1004 SALK HALL	PITTSBURGH	PA	15216 USA
R J ANDEREGG	UNIV OF MAINE	473 AUBERT HALL		ORONO	ME	04469 USA
F W ANDERSON	IBM CORP	Z41 C		HOPEWELL JUNCTION	NY	12533 USA
W R ANDERSON, JR	OREGON GRAD CENTER	19600 NW WALKER RD		BEAVERTON	OR	97005 USA
B D ANDRESEN	OHIO STATE UNIV	PHARMACOLOGY DEPT	333 W 10TH AVE	COLUMBUS	OH	43210 USA
D A ANDRZEJEWSKI	4114 DAVIS PLACE NW	APT 303		WASHINGTON	DC	20007 USA
V G ANICICH	8036 GRAYSTONE			SUNLAND	CA	91040 USA
P ARMENTROUT	BELL LABORATORIES	600 MOUNTAIN AVENUE		MURRAY HILL	NJ	07974 USA
T R ASHE	EXXON R/E	PO BOX 121		LINDEN	NJ	07036 USA
P J AUSLOOS	700 NEW HAMPSHIRE AV			WASHINGTON	DC	20037 USA
R J AYERS	1560 E JEFFERSON			DETROIT	MI	48207 USA
L BACZYNSKYJ	THE UPJOHN CO	301 HENRIETTA		KALAMAZOO	MI	49001 USA
D A BAFUS	4114 CLOVERNOOK LANE			SEABROOK	TX	77586 USA
T S BAKER	GIIT	BOX 12137	RES TRIANGLE PARK	DURHAM	NC	27709 USA
J M BALLARD	UNIV OF VIRGINIA	CHEMISTRY DEPT		CHARLOTTESVILLE	VA	22901 USA
J BANAR	1936 CAMINO MANZANA			LOS ALAMOS	NM	87544 USA
M P BARBALAS	CORNELL UNIV	BAKER LAB		ITHACA	NY	14853 USA
T M BARLAK	NAVAL RESEARCH LAB	CODE 6112	4555 OVERLOOK DR	WASHINGTON	DC	20375 USA
D J BARNARD	BOX 235C LOTE 13	FERNLANE	TURF MOBILE COURT	CLIFTON PARK	NY	12065 USA
D F BAROFSKY	OREGON GRAD CENTER	19600 NW WALKER RD		BEAVERTON	OR	97005 USA
T L BARRY	FDA	850 3RD AVE		BROOKLYN	NY	11232 USA
D R BARTHOLOMEW	CORNELL UNIVERSITY	G-24 URIS HALL		ITHACA	NY	14853 USA
J E BARTMESS	INDIANA UNIV	CHEMISTRY DEPT		BLOOMINGTON	IN	47405 USA
P J BARTNER	SCHERING CORP	60 ORANGE		BLOOMFIELD	NJ	07003 USA
B P BASILE	UNIV OF UTAH	MEDICINAL CHEMISTRY	SKAGGS HALL	SALT LAKE CITY	UT	84112 USA
M L BAZINET	43 CYPRESS RD			NATICK	MA	01760 USA
A J BEATTIE	E I DUPONT	EXPERIMENTAL STATION	BLDG 256	WILMINGTON	DE	19898 USA
G F BECKNER	UNIV OF TEXAS HSC	ANALYTICAL CHEMISTRY	PO BOX 20708	HOUSTON	TX	77030 USA
D P BEGGS	HP SCIENTIFIC INSTR	1601 CALIFORNIA AVE		PALO ALTO	CA	94304 USA
B F BEIER	EXXON RES & ENG	PO BOX 4255		BAYTOWN	TX	77565 USA
V E BELL	HOFFMANN-LAROCHE, INC			NUTLEY	NJ	07110 USA
F A BENCSATH	430 E 63RD ST	APT 39		NEW YORK	NY	10021 USA
J G BENDORAITIS	MOBIL RESEARCH & DEV			PAULSBORO	NJ	08066 USA
S D BENJAMIN	GTE SYLVANIA			TOWANDA	PA	18848 USA
C H BENNEY	1 STRAWBERRY HILL AV			STAMFORD	CT	06902 USA
W BENZ	HOFFMANN-LAROCHE, INC			NUTLEY	NJ	07110 USA
P S BERGER	TERNIVENT CORP	9261 OLD BONHOMME RD		ST LOUIS	MO	63132 USA
J BERKOWITZ	ARGONNE NATIONAL LAB	PHYSICS DIV	9700 S CASS AVE	ARGONNE	IL	60439 USA
R J BEUHLER	BROOKHAVEN NATL LAB	CHEMISTRY DEPT		UPTON	NY	11973 USA
K BIEMANN	MIT	CHEMISTRY, 56-010		CAMBRIDGE	MA	02139 USA
J E BILLER	MIT	CHEMISTRY, 56-025	77 MASS AVE	CAMBRIDGE	MA	02139 USA
R C BINIAKEWITZ	25 WARDWELL ST			STAMFORD	CT	06902 USA
G M BIRD	SUN CHEMICAL CO	631 CENTRAL AVE		CARLSTADT	NJ	07072 USA
B E BLAISDELL	LINUS PAULING INST	2700 SAND HILL RD		MENLO PARK	CA	94025 USA
M S BLUM	UNIV OF GEORGIA	ENTOMOLOGY DEPT		ATHENS	GA	30602 USA
R D BOARD	HP SCIENTIFIC INSTR	1601 CALIFORNIA AVE		PALO ALTO	CA	94304 USA
M J BOBENRIETH	NIEHS	PO BOX 12233,		RESEARCH TRIANGLE PKRC		27709 USA

F M BOCKHOFF	JET PROPULSION LAB	183-901		4800 OAK GROVE DR	PASADENA	CA 91103 USA
H G BOETTGER	5346 N STARDUST RD				LA CANADA	CA 91011 USA
L I BONE	DOW CHEMICAL	B-1226			FREEPORT	TX 77541 USA
W M BONE	UNIV OF VIRGINIA	CHEMISTRY DEPT			CHARLOTTESVILLE	VA 22901 USA
B J BOONE	FDA	HFO-620		5600 FISHERS LANE	ROCKVILLE	MD 28517 USA
A K BOSE	STEVENS INST OF TECH				HOBOKEN	NJ 07030 USA
O J BOUWSMA	DOW CHEMICAL				FREEPORT	TX 77541 USA
D V BOWEN	UNION CARBIDE	CENTRAL SCIENCE LAB			TARRYTOWN	NY 10591 USA
M T BOWERS	UNIV OF CALIFORNIA	CHEMISTRY DEPT			SANTA BARBARA	CA 93106 USA
D E BRACKEN	GENERAL ELECTRIC CO	BLDG EP3, ROOM 23		PO BOX 4840	SYRACUSE	NY 13221 USA
J C BRADLEY	KOR ISOTOPES	56 ROGERS			CAMBRIDGE	MA 02142 USA
D A BRENT	BURROUGHS WELLCOME	3030 CORNWALLS			RESEARCH TRIANGLE PKNC	27709 USA
K BRIZINSKY	PRINCETON UNIVERSITY	MAE DEPT			PRINCETON	NJ 08540 USA
T V BRIGGLE	6321 SW 25TH ST				MIAMI	FL 33155 USA
G M BRILLIS	256 E HARMON AVE	APT A-2			LAS VEGAS	NV 89109 USA
F W BRILL	UNIV OF FLORIDA	CHEMISTRY DEPT		BOX 61 LEIGH HALL	GAINESVILLE	FL 32611 USA
R A BRITTEN	84 WEST MARIPOSA ST				ALTADENA	CA 91001 USA
H O BROTHERTON	1100 SW 8TH AVE #106				GAINESVILLE	FL 32601 USA
S A BROTHERTON	MICHIGAN TECH UNIV	CHEMISTRY & CHEM ENG			HOUGHTON	MI 49931 USA
H L BROWN, JR	UTI	325 N MATHILDA AVE			SUNNYVALE	CA 94086 USA
W M BRUBAKER	1954 HIGHLAND OAKS				ARCADIA	CA 91006 USA
L E BRUGGEMAN	ARCO CHEMICAL CO	PO BOX 85			GLENOLDEN	PA 19036 USA
T J BUCKLEY	1911 NW 55TH TERRACE				GAINESVILLE	FL 32608 USA
J BUONO	GILETTE CO	GILLETTE PARK 2T2			BOSTON	MA 02106 USA
J D BURDEN	UTI	325 N MATHILDA AVE			SUNNYVALE	CA 94086 USA
D J BURINSKY	PURDUE UNIVERSITY	CHEMISTRY DEPT		BOX 321	WEST LAFAYETTE	IN 47907 USA
A L BURLINGAME	UNIV OF CALIFORNIA	PHARMCEUTICAL CHEM			SAN FRANCISCO	CA 94143 USA
R C BURNIER	PURDUE UNIVERSITY	CHEMISTRY DEPT		PO BOX 341	WEST LAFAYETTE	IN 47907 USA
P H BURR	286 S ROOSEVELT AVE				PASADENA	CA 91107 USA
J T BURSEY	RES TRIANGLE INST	PO BOX 12194		CLSD	RESEARCH TRIANGLE PKNC	27709 USA
M M BURSEY	UNIV NORTH CAROLINA	CHEMISTRY DEPT 045A			CHAPEL HILL	NC 27514 USA
K L BUSCH	WOODFIELD ACRES #6				WEST LAFAYETTE	IN 47906 USA
J J BUTLER	UNIV NORTH CAROLINA	VENABLE LABS 045A			CHAPEL HILL	NC 27514 USA
S C BUTTRILL, JR	SRI INTERNATIONAL	333 RAVENSWOOD AVE		RM 204A	MENLO PARK	CA 94025 USA
W H BUTTRILL	1616 MEETING HOUSE				ANNAPOLIS	MD 21401 USA
P S CALLERY	UNIV OF MARYLAND	636 W LOMBARD ST			BALTIMORE	MD 21201 USA
E L CALLIS	ARGONNE NATIONAL LAB	BLDG 200		9700 S CASS AVE	ARGONNE	IL 60439 USA
D CAMERON	UNION OIL CO OF CA	SCI & TECH DIV			BREA	CA 92621 USA
J E CAMPANA	NAVAL RESEARCH LAB	CHEMISTRY DIVISION		CODE 6170	WASHINGTON	DC 20375 USA
R M CAPRIOLI	UNIV OF TEXAS HSC	PO BOX 20708			HOUSTON	TX 77030 USA
S CARBONE	4 MARK VINCENT DR				POUGHKEEPSIE	NY 12603 USA
J R CARLIN	MERCK SHARP & DOHME	RESEARCH LABORATORY		PO BOX 2000	RAHWAY	NJ 07065 USA
S A CARR	MIT	CHEMISTRY, 56-012			CAMBRIDGE	MA 02139 USA
D I CARROLL, DAVID	BAYLOR COLL MEDICINE	INST LIPID RESEARCH		TEXAS MEDICAL CENTER	HOUSTON	TX 77030 USA
G T CARTER	CIBA-GEIGY CORP	OLD MILL RD			SUFFERN	NY 10901 USA
A W CASTLEMAN, JR	UNIV OF COLORADO	CHEMISTRY DEPT		BOX 215	BOULDER	CO 80309 USA
L C CATTRAN	HEWLETT PACKARD	1601 CALIFORNIA AVE			PALO ALTO	CA 94304 USA
B CHAIT	500 EAST 63ST #20D				NEW YORK	NY 10021 USA
J A CHAKEL	MICHIGAN STATE UNIV	CHEMISTRY DEPT			EAST LANSING	MI 48824 USA
W S CHAMBERLIN	2183 B, 36TH ST				LOS ALAMOS	NM 87544 USA
C CHANG	WRIGHT STATE UNIV	BREHM LAB			DAYTON	OH 45431 USA
E S CHANG	UNIV OF HOUSTON	BIOPHYSICAL SCIENCES			HOUSTON	TX 77004 USA
S CHANG	MCNEIL LABORATORIES	CAMP HILL RD			FORT WASHINGTON	PA 19034 USA
T L CHANG	AMERICAN CYANAMID	1937 W MAIN ST			STAMFORD	CT 06904 USA
R W CHAPMAN	FINNIGAN INSTRUMENTS	1383 PICCARD DR #100			ROCKVILLE	MD 20850 USA
D A CHATFIELD	SAN DIEGO STATE UNIV	CHEMISTRY DEPT			SAN DIEGO	CA 92182 USA
E K CHESS	UNIV OF NEBRASKA	CHEMISTRY DEPT		BOX 715	LINCOLN	NE 68588 USA
G B CHIEDA	ROSWELL PRK INSTITUT	666 ELM STREET			BUFFALO	NY 14263 USA
T C CHIANG	JOHNSON & JOHNSON	RESEARCH CENTER		RT 1	NORTH BRUNSWICK	NJ 08903 USA
D M CHINN	UNIV OF UTAH	CTR HUMAN TOXICOLOGY		SKAGGS HALL 38	SALT LAKE CITY	UT 84112 USA

R L CHOI	USV PHARMACEUTICAL	1 SCARSDALE RD		TUCKAHOE	NY	10707 USA
W H CHRISTIE	ORNL, UNION CARBIDE	PO BOX Y, BLDG 9735		OAK RIDGE	TN	37830 USA
M D CHU	254 W 261			BRONX	NY	10471 USA
L B CHURCHILL	UOP INC	TEN UOP PLAZA	ALGONQUIN/MI PRSPECT	DES PLAINES	IL	60016 USA
D J CLANCY	6415 MC CAHILL DR			LAUREL	MD	20810 USA
K L CLAY	UNIV OF COLORADO	MEDICAL CENTER	4200 E 9TH AVE	DENVER	CO	80262 USA
M L COATES	824-D CABELL AVE			CHARLOTTESVILLE	VA	22903 USA
T W COCHRAN	NIEHS	PO BOX 12233		RESEARCH TRIANGLE	PKNC	27709 USA
A I COHEN	SQUIBB INST MED RES	PO BOX 4000		PRINCETON	NJ	08540 USA
R B COHEN	AEROSPACE CORP	PO BOX 92957		LOS ANGELES	CA	90009 USA
B N COLBY	SCIENCE AND SOFTWARE	SYSTEMS	PO BOX 1260	LA JOLLA	CA	92037 USA
G J COLLINS	STAUFFER CHEM CO	LIVINGSTONE AVE		DOBBS FERRY	NY	10522 USA
C CONE	IFF R&D	1515 HIGHWAY 36		UNION BEACH	NJ	07735 USA
R J CONZEMIUS	1211 GARFIELD AVE			AMES	IA	50010 USA
J C COOK, JR	UNIV OF ILLINOIS	CHEMICAL SCIENCES		URBANA	IL	61801 USA
K D COOK	UNIV OF ILLINOIS	CHEMICAL SCIENCES	44 ROGER ADAMS LAB	URBANA	IL	61801 USA
R G COOKS	PURDUE UNIVERSITY	CHEMISTRY DEPT		WEST LAFAYEITE	IN	47907 USA
R A COOMBS	106 COLEMAN AVE			CHATHAM	NJ	07928 USA
R R CORDERMAN	BROOKHAVEN NATL LAB	DEE - BLDG 480		UPTON	NY	11973 USA
C E COSTELLO	MIT	CHEMISTRY, 56-029	77 MASS AVE	CAMBRIDGE	MA	02139 USA
D B COSULICH	LEDERLE LABORATORIES			PEARL RIVER	NY	10965 USA
E COTLIER	75 MAPLEVALE DRIVE			WOODBRIDGE	CT	USA
R J COTTER	JOHNS HOPKINS UNIV	MID ATLANTIC MS LAB	725 N WOLFE ST	BALTIMORE	MD	21205 USA
J E COUTANT	DOW CHEMICAL	PO BOX 68511		INDIANAPOLIS	IN	46268 USA
J W COWENS	54 IRVING PLACE			BUFFALO	NY	14201 USA
P F CRAIN	UNIV OF UTAH	PHARMACY DEPT		SALT LAKE CITY	UT	84112 USA
D W CRAWFORD	7725 S WOODWARD AVE	#3-B		WOODRIDGE	IL	60515 USA
R W CRAWFORD	LLL	PO BOX 808, L-325		LIVERMORE	CA	94550 USA
H L CRESPI	ARGONNE NATIONAL LAB	BLDG 200		ARGONNE	IL	60439 USA
F W CROW	UNIV OF NEBRASKA	CHEMISTRY DEPT	MCMS	LINCOLN	NE	68588 USA
P CRUZ	UNIV OF CALIFORNIA	CHEMISTRY DEPT		IRVINE	CA	92714 USA
T A CULLUM	7524 ROBINSON			ALLEN PARK	MI	48101 USA
Z F CURRY	51 OAKHURST CIRCLE			PITTSBURGH	PA	15238 USA
H M CURTIS, JR	HALLIBURTON SERVICES	CHEMISTRY DEPT		DUNCAN	OK	73533 USA
P M CURTIS	PRINCETON UNIV	MAE DEPT		PRINCETON	NJ	08544 USA
J R DAHLGRAN	O H MATERIALS	14 TRIANGLE PARK DR	SUITE 14	CINCINNATI	OH	45246 USA
S K DALEY	4890 BATTERY LANE			BETHESDA	MD	20014 USA
H S DANACEAU	7 BROOKES AVE			GAITHERSBURG	MD	20760 USA
J L D'ANGONA	430 CORDOVA ST			SAN FRANCISCO	CA	94112 USA
E H DAUGHREY, JR	NORTHRUP SERVICES	PO BOX 12313		RESEARCH TRIANGLE	PKNC	27709 USA
G D DAVES	OREGON GRAD CENTER	19600 NW WALKER ROAD		BEAVERTON	OR	97005 USA
W C DAVIDSON	213 STARVIEW CT			MAHWAH	NJ	07430 USA
B A DEBARBIERI	37 WARREN ST	APT 3A		NUTLEY	NJ	07110 USA
J A DEFEVER	14469 ELLEN DR			LIVONIA	MI	48154 USA
D C DEJONGH	FINNIGAN INSTITUTE	ATKINSON SQ, BLDG 5	11750 CHESTERDALE	CINCINNATI	OH	45246 USA
J E DELMORE	ACC	ANALYTICAL DIV	550 2ND ST	IDAHO FALLS	ID	83401 USA
T L DEROOS	BATTELLE LABS	505 KING AVE		COLUMBUS	OH	43201 USA
D M DESIDERIO	UNIV OF TENNESSEE	STOUT NEUROSCIENCE	800 MADISON AVE	MEMPHIS	TN	38163 USA
A J DE STEFANO	PROCTER & GAMBLE	MIAMI VALLY LAB	PO BOX 39175	CINCINNATI	OH	45239 USA
J R DIAS	UNIV OF MISSOURI	CHEMISTRY DEPT		KANSAS CITY	MO	64110 USA
R DIMARTINI	LONG ISLAND UNIV	CHEMISTRY DEPT	UNIVERSITY PLAZA	BROOKLYN	NY	11201 USA
J J DINO, JR	NEW YORK UNIVERSITY	INST OF ENV MEDICINE	LONGMEADOW RD	TUXEDO	NY	10987 USA
D P DIZIO	ICI AMERICAS INC	BIOMEDICAL RESEARCH		WILMINGTON	DE	19897 USA
R J DOUCET	VACUMETRICS INC	2261-#1 PALMA DR		VENTURA	CA	93003 USA
P A DREIFUSS	FDA	HFF-459	200 C ST SW	WASHINGTON	DC	20204 USA
G R DUBAY	COLUMBIA NATIONAL	FISHERIES RESEARCH	ROUTE 1	COLUMBIA	MO	65201 USA
G F DUDDING	GENERAL ELECTRIC CO	SILICONE PRODUCTS	BLDG 12-7	WATERFORD	NY	12188 USA
D L DUGGER	114 LEOLETS DR			MARLBORO	MA	01752 USA
W K DUHOLKE	THE UPJOHN CO	7171 PORTAGE RD		KALAMAZOO	MI	49001 USA
R C DUNBAR	CASE WESTERN RESERVE	CHEMISTRY DEPT		CLEVELAND	OH	44106 USA

L P DUNSTAN	NBS	BLDG 221, RM A21		WASHINGTON	DC 20234 USA
P P DYMERSKI	OH MATERIALS	PO BOX 1022		FINDLAY	OH 45840 USA
I DZIDIC	BAYLOR COLL MEDICINE	INST LIPID RESEARCH	TEXAS MEDICAL CENTER	HOUSTON	TX 77030 USA
D R EATON	MONSANTO	800 N LINDBERG	T2B	ST LOUIS	MO 63166 USA
M W ECHO	EXXON NUCLEAR	PO BOX 536		IDAHO FALLS	ID 83401 USA
C G EDMONDS	UNIV OF UTAH	COLLEGE OF PHARMACY	MEDICINAL CHEM DEPT	SALT LAKE CITY	UT 84112 USA
R S EGAN	MCNEIL LABORATORIES			FORT WASHINGTON	PA 19034 USA
W N EINOLF	PHILIP MORRIS USA	RESEARCH CENTER	PO BOX 26583	RICHMOND	VA 23261 USA
J F ELDER, JR	R J REYNOLDS TOBACCO	RESEARCH DEPT		WINSTON-SALEM	NC 27102 USA
C H ELKINS	STAUFFER CHEMICAL	EAST RESEARCH CENTER		DOBBS FERRY	NY 10522 USA
R E ELLEFSON	MRC	MOUND LAB R171		MIAMISBURG	OH 45342 USA
B ELLIS	HEWLETT PACKARD	ROUTE 41 & STARR RD		AVONDALE	PA 19311 USA
J F ENG	PRINCETON UNIV	CHEMISTRY DEPT		PRINCETON	NJ 08544 USA
C G ENKE	MICHIGAN STATE UNIV	CHEMISTRY DEPT		EAST LANSING	MI 48824 USA
P EPSTEIN	ENVIRONMENTAL RESRCH	117 NORTH FIRST		ANN ARBOR	MI 48104 USA
T J ESKEW	NUCLIDE CORP	642 E COLLEGE AVE		STATE COLLEGE	PA 16801 USA
D G ETTINGER	ARGONNE NATIONAL LAB	BLDG 211	9700 S CASS AVE	ARGONNE	IL 60439 USA
J E EVANS	E KENNEDY SHRIVER	CTR MENTAL RETARDATN	200 TRAPELO ROAD	WALTHAM	MA 02154 USA
J R EYLER	UNIV OF FLORIDA	CHEMISTRY DEPT		GAINESVILLE	FL 32611 USA
D W FAHEY	US DEPT OF COMMERCE	NOAA AERONOMY LAB		BOULDER	CO 80303 USA
H M FALES	6502 STONEHAM RD			BETHESDA	MD 20034 USA
A M FALICK	UNIV OF CALIFORNIA	CHEMISTRY DEPT		BERKELEY	CA 94720 USA
F C FALKNER	PFIZER INC	METAB		GROTON	CT 06340 USA
J D FASSETT	NBS	BLDG 221, RM A21		WASHINGTON	DC 20234 USA
K F FAULL	STANFORD UNIVERSITY	PSYCHIATRY DEPT	MEDICAL SCHOOL	STANFORD	CA 94305 USA
J FELSHER	KRATOS INC	24 BOOKER ST		WESTWOOD	NJ 07675 USA
P FENG	4806 HAMILTON AVE	APT C4		BALTIMORE	MD 21206 USA
C C FENSELAU	JOHNS HOPKINS UNIV	PHARMACOLOGY DEPT	725 N WOLFE ST	BALTIMORE	MD 21205 USA
G J FERGUSSON	PERKIN-ELMER CORP	AEROSPACE DIVISION	PO BOX 2801	POMONA	CA 91766 USA
D D FETTEROLF	UNIV OF FLORIDA	124 LEIGH HALL		GAINESVILLE	FL 32611 USA
F H FIELD	ROCKEFELLER UNIV	1230 YORK AVE		NEW YORK	NY 10021 USA
W J FIES, JR	155 CHEROKEE WAY			PORTOLA VALLEY	CA 94025 USA
P M FIGURA	260 CHURCH ST	APT 5B-4		WHITE PLAINS	NY 10603 USA
H FINEGOLD	5218 WOOD STOVE LN			COLUMBIA	MD 21045 USA
W L FITE	EXTRANUCLEAR LAB	250 ALPHA DRIVE	PO BOX 11512	PITTSBURGH	PA 15238 USA
G B FITZGERALD	12804 BUCKEYE RD #2			CLEVELAND	OH 44120 USA
R H FLEMING	SRI INTERNATIONAL	333 RAVENSWOOD		MENLO PARK	CA 94025 USA
R L FOLTZ	UNIV OF UTAH	CTR HUMAN TOXICOLOGY		SALT LAKE CITY	UT 84112 USA
N G FOSTER	2719 ROBINWOOD LANE			DENTON	TX 76201 USA
D F FRALEY	BOX 350			APPALACHIA	VA 24216 USA
R J FRANCEL	1937 WEST MAIN ST			STAMFORD	CT 06904 USA
T J FRANCEL	UNIV OF CALIFORNIA	CHEMISTRY DEPT		IRVINE	CA 92717 USA
D J FRANK	LOS ALAMOS SCIEN LAB	PO BOX 1663, CNC-11	103 CARLSBAD	LOS ALAMOS	NM 87544 USA
J W FRANK	DOW-CORNING	MS#27	PO BOX 1592	MIDLAND	MI 48640 USA
J L FRANKLIN	RICE UNIVERSITY	CHEMISTRY DEPT	PO BOX 1892	HOUSTON	TX 77005 USA
R B FREAS, III	11-2 THORN LANE			NEWARK	DE 19711 USA
L C FREES	ORNL, UNION CARBIDE	4500S, H151 BOX X		OAK RIDGE	TN 37830 USA
B S FREISER	PURDUE UNIVERSITY	CHEMISTRY DEPT		WEST LAFAYETTE	IN 47907 USA
N M FREW	387 TURTLEBACK RD			MARSTONS MILLS	MA 02648 USA
L FRIEDMAN	BROOKHAVEN NATL LAB	CHEMISTRY DEPT		UPTON	NY 11973 USA
M H FRIEDMAN	MERADCOM	DRDME-ND		FT BELVOIR	VA 22060 USA
M A FRISCH	IBM RESEARCH CENTER	PO BOX 218		YORKTOWN HEIGHTS	NY 10598 USA
M E FRITSCH	IBM CORP	D339/B300-41C		HOPEWELL JUNCTION	NY 12533 USA
E W FU	SANDOZ INC	BLDG 404/3	ROUTE 10	EAST HANOVER	NJ 07936 USA
J D FUHRMAN	MONSANTO	800 N LINDBERGH BLVD		ST LOUIS	MO 63166 USA
H FUJIWARA	MONSANTO	800 N LINDBERGH		ST LOUIS	MO 63141 USA
E K FUKUDA	UNIV OF CALIFORNIA	CHEMISTRY DEPT		IRVINE	CA 92717 USA
P T FUNKE	E R SQUIBB	PO BOX 4000		PRINCETON	NJ 08540 USA
J H FUTRELL	UNIV OF UTAH	CHEMISTRY DEPT		SALT LAKE CITY	UT 84112 USA
P J GALE	SARNOFF RES CENTER	RCA LABS		PRINCETON	NJ 08540 USA

K L GALLAHER	SOHIO	4440 WARRENSVILLE RD		CLEVELAND	OH 44128 USA
E J GALLEGOS	CHEVRON	PO BOX 1627		RICHMOND	CA 94804 USA
D E GALLIS	WESTCHESTER STATE	CHEMISTRY DEPT		WEST CHESTER	PA 19380 USA
W A GARLAND	HOFFMAN-LAROCHE, INC	BIOCHEMISTRY DEPT		NUTLEY	NJ 07110 USA
E L GARNER	NBS	BLDG 222, RM A219		WASHINGTON	DC 20234 USA
D A GARTEIZ	8797 STURBRIDGE			CINCINNATI	OH 45236 USA
J GEIGERT	CETUS CORP	600 BANCROFT WAY		BERKELLY	CA 94710 USA
G GELLENE	CORNELL UNIV	BAKER LAB, BOX 168		ITHACA	NY 14853 USA
D S GEMMELL	ARGONNE NATIONAL LAB	PHYSICS DIV D203		ARGONNE	IL 60439 USA
J N GERBER	HEWLETT PACKARD	1021 EIGHTH AVE		KING OF PRUSSIA	PA 19406 USA
T E GESELLE	158 BEACHFIELD DR			BATTLE CREEK	MI 49015 USA
S GHADERI	UNIV OF NEBRASKA	HAMILTON HALL	BOX 721	LINCOLN	NE 68588 USA
B GIBSON	MIT	CHEMISTRY DEPT		CAMBRIDGE	MA 02138 USA
C E GIFFIN	JET PROPULSION LAB	11-116	4800 OAK GROVE DR	PASADENA	CA 91103 USA
L GILBERT	CVC PRODUCTS	525 LEE RD		ROCHESTER	NY 14603 USA
J P GILMAN	UNIV OF NEBRASKA	CHEMISTRY DEPT		LINCOLN	NE 68588 USA
K A GINGERICH	TEXAS A&M UNIVERSITY	CHEMISTRY DEPT		COLLEGE STATION	TX 77843 USA
A B GIORDANI	240 MONTE VISTA AVE			CHARLOTTESVILLE	VA 22903 USA
G G GIRDAUKAS	UNIV OF WISCONSIN	PHARMACY DEPT		MADISON	WI 53706 USA
H F GLAVISH	ANAC INC	3067 OLCOTT ST		SANTA CLARA	CA 95051 USA
G L GLISH	216-5 NIMITZ DR			WEST LAFAYETTE	IN 47906 USA
H GOLDSTEIN	15645 HEATHER HILL	DRIVE		BROOKFIELD	WI 53005 USA
P C GOODLEY	MURRAY STATE UNIV	MASS SPECTOMETRY CTR		MURRAY	KY 42071 USA
G W GOODLOE	UNIV OF DELAWARE	034 BROWN LAB		NEWARK	DE 19711 USA
S M GORDON	IITRI	CHEMISTRY DIVISION	10 W 35 ST	CHICAGO	IL 60616 USA
L A GORMAN	VARIAN	134 JUNEDALE DR		CINCINNATI	OH 45218 USA
H GRADE	GENERAL ELECTRIC CO	R&D CENTER	BLDG K-1, PO BOX 8	SCHENECTADY	NY 12301 USA
M M GRADE	GENERAL ELECTRIC	R&D CENTER	BLDG K-1, PO BOX 8	SCHENECTADY	NY 12301 USA
W L GRADY	36 BERKSHIRE MANOR			CARRBORO	NC 27510 USA
J W GRAMLICH	NBS	A21 PHYSICS		WASHINGTON	DC 20234 USA
K GRANLUND	HEWLETT-PACKARD	1601 CALIFORNIA AVE		PALO ALTO	CA 94022 USA
P W GRAVES	LAKE RD			BROOKFIELD	MA 01506 USA
M A GRAYSON	427 GLENMEADOW DR			BALLWIN	MO 63011 USA
J GREAVES	MT SINAI HOSPITAL	11 E 100 ST		NEW YORK	NY 10029 USA
L A GREEN	MOBIL RESEARCH & DEV			PAULSBORO	NJ 08066 USA
M M GREEN	CHEMISTRY DEPT	POLYTECHNIC INST	OF NEW YORK	BROOKLYN	NY 11201 USA
F T GREENE	MIDWEST RESRCH INST	425 VOLKER BLVD		KANSAS CITY	MO 64110 USA
S H GREENHOUSE	21 OAK TERRACE	APT 1A		SOMERVILLE	NJ 08876 USA
R C GREENOUGH	UNIROYAL INC	OXFORD MGMT & RES	R-G-20	MIDDLEBURY	CT 06749 USA
G J GREENWOOD	PHILLIPS PETROLEUM	224 RESEARCH, BLDG 1		BARTLESVILLE	OK 74003 USA
H R GREGG	MICHIGAN STATE UNIV	CHEMISTRY DEPT		EAST LANSING	MI 48824 USA
R H GRIFFEY	UNIV OF UTAH	CHEMISTRY DEPT		SALT LAKE CITY	UT 84112 USA
R J GRITTER	IBM RESEARCH LAB	DEPT K13/282		SAN JOSE	CA 95193 USA
G S GROENEWOLD	UNIV OF NEBRASKA	720 HAMILTON HALL		LINCOLN	NE 68588 USA
M L GROSS	UNIV OF NEBRASKA	CHEMISTRY DEPT		LINCOLN	NE 68588 USA
S L GROTCH	LLL	PO BOX 808, L-325		LIVERMORE	CA 94550 USA
W M GULICK, JR	607 W SOUTH AVE			HOUGHTON	MI 49931 USA
N HAARBYE	PURDUE UNIV	CHEMISTRY DEPT		WEST LAFAYETTE	IN 47907 USA
D L HACHLY	ARGONNE NATIONAL LAB	9700 S CASS AVE		ARGONNE	IL 60439 USA
W F HADDON	USDA	WESTERN REG LAB		ALBANY	CA 94710 USA
J E HALVERSON	1901 WHITEBARK AVE			NORTH AUGUSTA	SC 29841 USA
M C HAMMING	CONTINENTAL OIL CO			PONCA CITY	OK 74601 USA
G E HANSEN	JOHNS HOPKINS UNIV	PHARMACOLOGY DEPT	725 N WOLFE ST	BALTIMORE	MD 21205 USA
E D HARDIN	DEPT OF CHEMISTRY	UNIV OF HOUSTON		HOUSTON	TX 77004 USA
E A HARDWIDGE	UPJOHN CO	UNIT 7830-233-1	7171 S PORTAGE RD	KALAMAZOO	MI 49001 USA
D R HARDY	FBI LAB	ROOM 3254, JEH	9TH & PENNA AVE NW	WASHINGTON	DC 20535 USA
R L HARLESS	701 WHITE OAK DR			CARY	NC 27511 USA
W D HARMAN	UNION CARBIDE	Y12-PLANT		OAK RIDGE	TN 37830 USA
D N HARPOLD	GODDARD SPC FLT CTR	CODE 962		GREENBELT	MD 20771 USA
W L HARRINGTON	RCA LABORATORIES			PRINCETON	NJ 08540 USA

W W HARRISON	UNIV OF VIRGINIA	CHEMISTRY DEPT		CHARLOTTESVILLE	VA	22901 USA
D J HARVAN	NIEHS	PO BOX 12233		RESEARCH TRIANGLE	PKNC	27709 USA
J R HASS	NIEHS	PO BOX 12233		RESEARCH TRIANGLE	PKNC	27709 USA
T W HATCH	BOEHRINGER INGELHEIM	90 EAST RIDGE	PO BOX 368	RIDGEFIELD	CT	06877 USA
S E HATTOX	YALE UNIVERSITY	PHARMACOLOGY DEPT	MEDICAL SCHOOL	NEW HAVEN	CT	06510 USA
R L HAWKS	2032 BELMONT RD	APT 507		WASHINGTON	DC	20009 USA
J D HAYS	CASE WESTERN RESERVE	CHEMISTRY DEPT		CLEVELAND	OH	44106 USA
D L HEIKES	FDA	1009 CHERRY		KANSAS CITY	MO	64106 USA
R E HEIN	NICOLET INSTRUMENTS	5225 VERONA RD		MADISON	WI	53711 USA
D N HELLER	JOHN HOPKINS UNIV	B-6 BIOHPYSICS DEPT	725 N WOLFE ST	BALTIMORE	MD	21205 USA
S R HELLER	2413 LILLIAN DRIVE			SILVER SPRING	MD	20902 USA
J C HELMER	VARIAN ASSOC	611 HANSEN WAY		PALO ALTO	CA	94303 USA
M J HENCHMAN	BRANDEIS UNIV	CHEMISTRY DEPT		WALTHAM	MA	02254 USA
T R HENDERSON	5609 DON FELIPE CT S			ALBUQUERQUE	NM	87105 USA
L J HENDRICKS	125 S 34TH STREET			BOULDER	CO	80303 USA
J D HENION	CORNELL UNIVERSITY	NYS COL VET MEDICINE	132 DIAGNOSTIC LAB	ITHACA	NY	14853 USA
P R HENKEL	GALILEO	ELECTRO-OPTICS	GALILEO PK	STURBRIDGE	MA	01566 USA
W C HERLIHY	MIT	CHEMISTRY, 56-016		CAMBRIDGE	MA	02139 USA
Z HERMAN	UNIV OF COLORADO	JILA	CAMPUS BOX 440	BOULDER	CO	80309 USA
D A HEROLD	UNIV OF VIRGINIA	PATHOLOGY DEPT	MEDICAL CENTER	CHARLOTTESVILLE	VA	22901 USA
E J HERON	HP SCIENTIFIC INSTR	1601 CALIFORNIA AVE		PALO ALTO	CA	94304 USA
H S HERTZ	NBS	A113 CHEMISTRY		WASHINGTON	DC	20234 USA
L F HERZOG	NUCLIDE CORP	642 E COLLEGE AVE		STATE COLLEGE	PA	16801 USA
E A HETT	4010 OLD CHAPEL HILL			DURHAM	NC	27707 USA
B J HIDY	BATTELLE LABS	505 KING AVE		COLUMBUS	OH	43201 USA
P M HIERL	UNIV OF KANSAS	CHEMISTRY DEPT		LAWRENCE	KS	66044 USA
D L HILDENBRAND	SRI INTERNATIONAL			MENLO PARK	CA	94025 USA
D R HILKER	HIGHLAND HILLS	APT 2601		EAST GREENBUSH	NY	12061 USA
J F HILLER	UNIV OF HOUSTON	FLEMING BLDG		HOUSTON	TX	77004 USA
J HILLS	MCNEIL LABORATORIES	BIOCHEMISTRY		FORT WASHINGTON	PA	19034 USA
L R HILPERT	NBS	BLDG 222, RM B124		WASHINGTON	DC	20234 USA
D M HINDENLANG	ALLIED CHEMICAL CORP	PO BOX 1021R		MORRISTOWN	NJ	07960 USA
R A HITES	INDIANA UNIV	400 E SEVENTH ST		BLOOMINGTON	IN	47405 USA
A G HLAVAC	STERLING WINTHROP CO			RENSSELAER	NY	12144 USA
B J HODSHON	HOFFMANN-LAROCHE, INC			NUTLEY	NJ	07110 USA
H T HOFFMAN, JR	AMERICAN CAN CO	PO BOX 50		PRINCETON	NJ	08540 USA
M K HOFFMAN	USDA-FSQS			BELTSVILLE	MD	20705 USA
D H HOLKEBOER	231 WINDCREST DR			CAMILLUS	NY	13031 USA
J F HOLLAND	MICHIGAN STATE UNIV	BIOCHEMISTRY DEPT		EAST LANSING	MI	48824 USA
J S HOLLER	CENTER DISEASE CNTRL	TOXICOLOGY BRANCH		ATLANTA	GA	30333 USA
W F HOLMES	WASHINGTON UNIV	BIOCHEMISTRY DEPT	660 S EUCLID	ST LOUIS	MO	63110 USA
J P HONOVICH	CASE WESTERN RESERVE	CHEMISTRY DEPT	MILLIS SCIENCE CENTR	CLEVELAND	OH	44106 USA
E C HORNING	11610 STARWOOD DR			HOUSTON	TX	77024 USA
M G HORNING	BAYLOR COLL MEDICINE	INST LIPID RESEARCH	TEXAS MEDICAL CENTER	HOUSTON	TX	77030 USA
O H HOWARD	146 W BEVERLY CIRCLE			OAK RIDGE	TN	37830 USA
T HSIEH	UNIV OF NEBRASKA	HAMILTON HALL	BOX 532	LINCOLN	NE	68588 USA
C S HSU	EXXON R/E	P O BOX 121		LINDEN	NJ	07036 USA
W Y HUANG	SUNMARK EXPLORATION	600 N CENTRAL EXPWAY		RICHARDSON	TX	75080 USA
J E HUDSON	UNIV OF TEXAS	CHEMISTRY DEPT	103W WELCH HALL	AUSTIN	TX	78712 USA
B M HUGHES	1101 RUE LIMOGES PTON			SLIDELL	LA	70458 USA
S V HUMMEL	UNIV OF FLORIDA	CHEMISTRY DEPT	311 LEIGH HALL	GAINESVILLE	FL	32605 USA
H L HUNG	CHEMISTRY DEPT	NORTHWESTERN UNIV	2145 SHERIDAN RD	EVANSTON	IL	60201 USA
D F HUNT	UNIV OF VIRGINIA	CHEMISTRY DEPT		CHARLOTTESVILLE	VA	22901 USA
J E HUNT	TEXAS A&M UNIVERSITY	CHEMISTRY DEPT		COLLEGE STATION	TX	77843 USA
R L HUNTER	UNIV OF CALIFORNIA	CHEMISTRY DEPT		IRVINE	CA	92717 USA
W T HUNTRESS, JR	JET PROPULSION LAB	SSD		PASADENA	CA	91103 USA
W G HYDE	IOWA STATE UNIV	VET DIAG LAB		AMES	IA	50011 USA
C R IDEN	SUNY	CHEMISTRY DEPT		STONY BROOK	NY	11794 USA
A J ILLIES	3889 CINCO AMIGOS			SANTA BARBARA	CA	93105 USA
R N INFANTE	CATHOLIC UNIV	CHEMISTRY DEPT		PONCE	PR	00731 USA

S E INSALACO	OH MATERIALS CO	PO BOX 1022		FINDLAY	OH 45840	USA
G E IOUP	UNIV OF NEW ORLEANS	PHYSICS DEPT		NEW ORLEANS	LA 70122	USA
J W IOUP	XAVIER UNIV	PHYSICS/PRE-ENGINEER		NEW ORLEANS	LA 70125	USA
A P IRSA	BROOKHAVEN NATL LAB	CHEMISTRY DEPT		UPTON	NY 11973	USA
P IRVING	BALZERS HIGH VACUUM	8 SAGAMORE PARK RD		HUDSON	NH 03051	USA
S C ISRAEL	UNIV OF LOWELL	CHEMISTRY DEPT		LOWELL	MA 01854	USA
D ISSACHAR	MICHIGAN STATE UNIV	BIOCHEMISTRY DEPT		EAST LANSING	MI 48824	USA
T J JACKSON	1614 RICHFOREST			RICHARDSON	TX 75081	USA
M L JACOBS	COMMERICAL TESTING	AND ENGINEERING	490 ORCHARD ST	GOLDEN	CO 80401	USA
W M JAKUBOWSKI	626 WASHINGTON BLVD			BALTIMORE	MD 21230	USA
J JANZER	PITMAN-MOORE, INC	PO BOX 344		WASHINGTON CROSSING	NJ 08560	USA
I JARDINE	MAYO CLINIC	PHARMACOLOGY DEPT		ROCHESTER	MN 55901	USA
J A JARRELL	MIT	RM 26-457		CAMBRIDGE	MA 02139	USA
B L JELUS-TYROR	AVON PRODUCTS			SUFFERN	NY 10901	USA
E E JENKINS	1617 MAPLE AVE			SALT LAKE CITY	UT 84106	USA
D JEROLAMON	ALLIED CHEMICAL CORP	PO BOX 1021-R		MORRISTOWN	NJ 07960	USA
B M JOHNSON	PFIZER INC	CENTRAL RESEARCH		GROTON	CT 06340	USA
E G JONES	WRIGHT STATE UNIV	CHEMISTRY DEPT		DAYTON	OH 45431	USA
G G JONES	STANDARD OIL INDIANA	PO BOX 400		NAPERVILLE	IL 60540	USA
R JONES	CORNELL UNIVERSITY	CHEMISTRY DEPT		ITHACA	NY 14850	USA
C M JUDSON	562 E MENDOCINO ST			ALTADENA	CA 91001	USA
J D JUSTICE	HP SCIENTIFIC INSTR	1601 CALIFORNIA AVE		PALO ALTO	CA 94304	USA
R J KAIER	E I DUPONT	EXPERIMENTAL STATION	BLDG 336/6	WILMINGTON	DE 19898	USA
G J KALLOS	DOW CHEMICAL CO	BUILDING 574		MIDLAND	MI 48640	USA
K A KALMBACH	260 ELKTON RD G-2			NEWARK	DE 19711	USA
A I KALTENBACK	MARATHON OIL CO	PO BOX 269		LITTLETON	CO 80160	USA
N M KAN	FINNIGAN INSTRUMENTS	1383 PICCARD DR #100		ROCKVILLE	MD 20850	USA
G E KANANEN	HEWLETT PACKARD CO	ROUTE 41		AVONDALE	PA 19311	USA
M M KAPPES	MIT	CHEMISTRY 6-029		CAMBRIDGE	MA 02165	USA
B KATZ	EXXON RES &DEV	PO BOX 2226		BATON ROUGE	LA 70821	USA
P KAUFMANN	12903 MEMORIAL DRIVE			HOUSTON	TX 77079	USA
G L KEARNS	58 BUCKINGHAM DR			STAMFORD	CT 06902	USA
R KEEFE	UNIV OF VIRGINIA	CHEMISTRY DEPT	MCCORMICK RD	CHARLOTTESVILLE	VA 22901	USA
G W KEEN	CONTINENTAL OIL CO	1000 SOUTH PINE		PONCA CITY	OK 74601	USA
J A KELLEY	NIH	NCI, DRUG DESIGN	BLDG 37, RM 6023	BETHESDA	MD 20205	USA
P E KELLEY	FINNIGAN CORP	2334 WALSH AVE		SANTA CLARA	CA 95050	USA
J M KELLEHER	EXXON RESEARCH	BOX 121		LINDEN	NJ 07036	USA
L KELNER	14600 KING LEAR CT			SILVER SPRING	MD 20906	USA
D L KEMP	1813 RIDGE ROAD			MARTINSVILLE	NJ 08836	USA
E J KEMPSTER	INFICON LH CORP	6500 FLY ROAD		EAST SYRACUSE	NY 13057	USA
C N KENYON	HP SCIENTIFIC INSTR	1601 CALIFORNIA AVE		PALO ALTO	CA 94304	USA
T W KEOUGH	8557 CAVALIER DR			CINCINNATI	OH 45231	USA
J K KHANDELWAL	MT SINAI MED SCHOOL	PHARMACOLOGY DEPT	100 ST AND 5TH AVE	NEW YORK	NY 10029	USA
P H KIANG	WEST COMPANY	TECHNICAL CENTER	ROUTE 113	PHOENIXVILLE	PA 19460	USA
D A KIDWELL	MIT	CHEMISTRY 56-042		CAMBRIDGE	MA 02139	USA
W E KILLINGER	W R GRACE & CO	RESEARCH DIV	7379 ROUTE 32	COLUMBIA	MD 21044	USA
L B KILLMER,JR	325 N EDGEMONT ST			MEDIA	PA 19063	USA
B J KIMBLE	UNIV OF CALIFORNIA	LEHR		DAVIS	CA 95616	USA
G K KING	956 MARINE ST	API 6		BOULDER	CO 80302	USA
J W KING	231 ACALANES #2			SUNNYVALE	CA 94086	USA
R W KING	UNIV OF FLORIDA	CHEMISTRY DEPT		GAINESVILLE	FL 32611	USA
R D KINSER	PHILIP MORRIS USA	RESEARCH CENTER	PO BOX 26583	RICHMOND	VA 23261	USA
D P KIRBY	IBM CORP	D/339 B/300-41C	ROUTE 52	HOPEWELL JUNCTION	NY 12533	USA
T G KITSON	3 HARTFORD PLACE			NEWARK	DE 19711	USA
C E KLOTS	ORNL, UNION CARBIDE			OAK RIDGE	TN 37830	USA
D R KNAPP	MED UNIV SO CAROLINA	PHARMACOLOGY DEPT		CHARLESTON	SC 29403	USA
C Y KO	MCNEIL LABS	500 OFFICE CENTER DR		FORT WASHINGTON	PA 19034	USA
V H KOELMAN	LOS ALAMOS SCIEN LABS	-5, MS 890		LOS ALAMOS	NM 87545	USA
M G KOLOR	GENERAL FOODS CORP	555 SO BROADWAY		TARRYTOWN	NY 10591	USA
K W KONDRAT	SHELL DEVELOPMENT CO	WESTHOLLOW RESEARCH	PO BOX 1380	HOUSTON	TX 77001	USA

T E	KOPROWSKI	106 OGDEN CIRCLE			OAK RIDGE	TN 37830 USA
R A	KORNFELD	PHILLIP MORRIS USA	RESEARCH CENTER	PO BOX 26583	RICHMOND	VA 23261 USA
T C	KRAM	8 FEATHER ROCK PL			ROCKVILLE	MD 20850 USA
J M	KRECISZ	3424 S STATE ST			CHICAGO	IL 60616 USA
T	KRICK	UNIV OF MINNESOTA	BIOCHEMISTRY DEPT		ST PAUL	MN 55108 USA
T	KRISHNAMURTHY	JIC ENVIRONMENTAL	CONSULTANTS, INC	7979 OLD GEORGETOWN	BETHESDA	MD 20014 USA
Y	KURODA	UNIV OF ROCHESTER	CHEMISTRY DEPT		ROCHESTER	NY 14627 USA
L	KURZWEG	4 N COLLINGWOOD DR			PITTSBURGH	PA 15215 USA
C R	LAGERGREN	2110 HOWELL AVE			RICHLAND	WA 99352 USA
S T	LAI	419 MONTCALM ST	APT 424M		CHICOPEE	MA 01020 USA
F W	LAMPE	PENN STATE UNIV	150 DAVEY LAB		UNIVERSITY PARK	PA 16802 USA
P W	LANGVARDT	DOW CHEMICAL CO	574 BLDG		MIDLAND	MI 48640 USA
R P	LATTIMER	B F GOODRICH R & D	9921 BRECKSVILLE RD		BRECKSVILLE	OH 44141 USA
R K	LATVEN	MICHIGAN STATE UNIV	CHEMISTRY DEPT		EAST LANSING	MI 48824 USA
J B	LAUDENSLAGER	JET PROPULSION LAB	MS 183-601	4800 OAK GROVE DR	PASADENA	CA 91103 USA
M T	LAUG	ARGONNE NATIONAL LAB	PO BOX 2528		IDAHO FALLS	ID 83401 USA
J L	LAWRENCE,JR	ANALOG TECHNOLOGY	15859 E EDNA PLACE		IRWINDALE	CA 91706 USA
J W	LAWRENCE	SHELL DEVELOPMENT CO	PO BOX 1380		HOUSTON	TX 77478 USA
J O	LAY,JR	UNIV OF NEBRASKA	CHEMISTRY DEPT		LINCOLN	NE 68502 USA
J A	LEARY	MIT	CHEMISTRY 56-035		CAMBRIDGE	MA 02139 USA
T D	LEE	OREGON GRADUATE CENT	19600 NW WALKER RD		BEAVERTON	OR 97006 USA
E	LEETE	UNIV OF MINNESOTA	CHEMISTRY DEPT		MINNEAPOLIS	MN 55455 USA
J P	LEHMAN	3645 ELMLEY AVE			BALTIMORE	MD 21213 USA
T A	LEHMAN	PO BOX 435			NORTH NEWTON	KS 67117 USA
S W	LESLIE	1465 LAKE SHORE DR S			BARRINGTON	IL 60010 USA
N B	LEV	CASE WESTERN RESERVE	CHEMISTRY DEPT		CLEVELAND	OH 44106 USA
M I	LEVENBERG	ABBOTT LABS	DEPT 417		NORTH CHICAGO	IL 60064 USA
W T	LEWIS	MOBIL CHEMICAL CO	PO BOX 240		EDISON	NJ 08817 USA
S G	LIAS	NBS			WASHINGTON	DC 20234 USA
J G	LIEHR	UNIV OF TEXAS HSC	ANALYTICAL CHEMISTRY	PO BOX 20708	HOUSTON	TX 77030 USA
W V	LIGON	GENERAL ELECTRIC CO	DR&D CENTER	BLDG K1, PO BOX 8	SCHENECTADY	NY 12301 USA
D C	LIN	BATTELLE LABS	505 KING AVE		COLUMBUS	OH 43201 USA
K C	LIN	UTI	325 N MATHILDA AVE		SUNNYVALE	CA 94086 USA
S N	LIN	UNIV OF TEXAS HSC	ANALYTICAL CHEMISTRY	PO BOX 20708	HOUSTON	TX 77030 USA
M W	LINSCHEID	551 COLUSA AVE			BERKELEY	CA 94707 USA
D M	LITTLE	PRINCETON UNIV	FRICK CHEMISTRY LAB		PRINCETON	NJ 08540 USA
J F	LITTON	OCC RESEARCH	PO BOX 19601		IRVINE	CA 92713 USA
D C	LITWIN	ICI AMERICAS INC	CRDL-RM 125		WILMINGTON	DE 19897 USA
J R	LLOYD	1230 YORK AVE	BOX 253		NEW YORK	NY 10021 USA
M J	LOCKE	UNIV OF CALIFORNIA	CHEMISTRY DEPT		IRVINE	CA 92717 USA
S K	LORCH	MICHIGAN ST POLICE	30303 STEPHENSON HWY		MADISON HEIGHTS	MI 48075 USA
E R	LORY	CORNELL UNIVERSITY	CHEMISTRY DEPT		ITHACA	NY 14853 USA
T J	LOVING	UNIV OF VIRGINIA	CHEMISTRY DEPT		CHARLOTTESVILLE	VA 22901 USA
W R	LUSBY	8028 NEW RIGGS RD			ADELPHI	MD 20783 USA
P A	LYON	UNIV OF NEBRASKA	28 HAMILTON HALL	MCMS	LINCOLN	NE 68588 USA
L T	LYTLE	412 MELODY LANE			CARY	NC 27511 USA
J L	MACDONALD	RALSTON PURINA CO	3RS CHECKERBOARD SQ		ST LOUIS	MO 63188 USA
B A	MACKINNON	ANAC INC	3067 OLCOTT ST		SANTA CLARA	CA 95051 USA
H R	MACQUEEN	28 WILDWOOD DR			WAPPINGERS FALLS	NY 12590 USA
N H	MAHLE	DOW CHEMICAL CO	574 BLDG		MIDLAND	MI 48640 USA
J J	MANURA	SCIENTIFIC INSTR SVC	363-D RD 1		PENNINGTON	NJ 08534 USA
M A	MARCONI	3219 W 54TH ST			CHICAGO	IL 60632 USA
S P	MARKEY	NIH	NIMH	BLDG 10, RM 2D46	BETHESDA	MD 20005 USA
R W	MARQUIS	UNIV OF VIRGINIA	CHEMISTRY DEPT	MCCORMICK RD	CHARLOTTESVILLE	VA 22901 USA
T D	MARRIOTT	RICE UNIVERSITY	CHEMISTRY DEPT		HOUSTON	TX 77005 USA
P C	MARSH	UNIV OF COLORADO	MEDICAL CENTER, C233	4200 E 9TH AVE	DENVER	CO 80262 USA
D J	MARSHALL	PO BOX 315			ACTON	MA 01720 USA
F E	MARTIN	MICHIGAN STATE UNIV	BIOCHEMISTRY DEPT		EAST LANSING	MI 48824 USA
D P	MARTINSEN	5 SUGARLOAF CT	APT T-1		BALTIMORE	MD 21209 USA
T J	MASSEY	SYNTEX RESEARCH	3401 HILLVIEW AVE		PALO ALTO	CA 94304 USA

W R MATHEWS	1433 ST PAUL			DENVER	CO	80206 USA
D E MATTHEWS	WASHINGTON UNIV	METABOLIC DIV	SCHOOL OF MEDICINE	ST LOUIS	MO	63110 USA
N A MATWIYOFF	LOS ALAMOS SCIEN LAB	CNC-DO		LOS ALAMOS	NM	87544 USA
M MAUTNER	NBS			WASHINGTON	DC	20234 USA
R J MAY	615 BEDFORD RD			SCHENECTADY	NY	12308 USA
W J MAYER	5803 SONOMA ROAD			BETHESDA	MD	20034 USA
D R MCADAMS	EXXON R/D	PO BOX 2226		BATON ROUGE	LA	70821 USA
T A MCCARRICK	313 WILLOW AVE			ITHACA	NY	14850 USA
E R MCCARTHY	ALLIED CHEMICAL CORP	PO BOX 1021-R		MORRISTOWN	NJ	07950 USA
J A MCCLOSKEY	UNIV OF UTAH	COLLEGE OF PHARMACY	MEDICINAL CHEM DEPT	SALT LAKE CITY	UT	84112 USA
G A MCCLUSKY	FREDERICK CANCER	RES CTR, BLDG 538	PO BOX B	FREDERICK	MD	21701 USA
R N MCDONALD	KANSAS STATE UNIV	CHEMISTRY DEPT		MANHATTAN	KS	66506 USA
R A MCDONIE	PO BOX 8361			SOUTH CHARLESTON	WV	25303 USA
W H MCFADDEN	FINNIGAN CORP	845 W MAUDE AVE		SUNNYVALE	CA	94086 USA
M P MCGEE	BUR FORENSIC SCIENCE	PO BOX 999		RICHMOND	VA	23208 USA
J H MCGLOTTEN	SCHERING CORP	60 ORANGE		BLOOMFIELD	NJ	07003 USA
J M MCGUIRE	93 AMSTEL AVE	APT E20		NEWARK	DE	19711 USA
R T MCIVER	UNIV OF CALIFORNIA	CHEMISTRY DEPT		IRVINE	CA	92717 USA
L W MCKEEN	E I DUPONT	3500 GRAYS FERRY AVE		PHILADELPHIA	PA	19146 USA
M C MCKEOWN	EXTRANUCLEAR LAB	250 ALPHA DRIVE	PO BOX 11512	PITTSBURGH	PA	15238 USA
F W MCLAFFERTY	CORNELL UNIVERSITY	CHEMISTRY DEPT	BAKER LABORATORY	ITHACA	NY	14853 USA
S A MCLUCKEY	PURDUE UNIVERSITY	CHEMISTRY DEPT	PO BOX 600	WEST LAFAYETTE	IN	47907 USA
J H MCREYNOLDS	SUNY MEDICAL SCHOOL	BIOPHYSICAL SCIENCE	118 CARY HALL	BUFFALO	NY	14214 USA
J R MEEKS	MOBILE OIL CORP	TOXICOLOGY DIVISION	PO BOX 1026	PRINCETON	NJ	08540 USA
S MEISELMAN	NBS	CHEMISTRY 4113		WASHINGTON	DC	20234 USA
G G MEISELS	UNIV OF NEBRASKA	CHEMISTRY DEPT	HAMILTON HALL	LINCOLN	NE	68588 USA
C MERRITT, JR	FOOD SCIENCE LAB	CHEMISTRY	US ARMY NATICK LABS	NATICK	MA	01760 USA
J A MESCHER	UNIV OF DAYTON	RESEARCH INSTITUTE		DAYTON	OH	45469 USA
H L MEUZELAAR	BIOMAT PROFILING CTR	391 S CHIPETA WAY		SALT LAKE CITY	UT	84108 USA
S MEYERSON	STANDARD OIL INDIANA	RESEARCH DEPT	PO BOX 400	NAPERVILLE	IL	60540 USA
M A MICKE	UNIV OF WISCONSIN	BIOCHEMISTRY DEPT	420 HENRY MALL	MADISON	WI	53706 USA
B S MIDDLEDITCH	UNIV OF HOUSTON	BIOPHYSICAL SCIENCES		HOUSTON	TX	77004 USA
C H MIDGETT	US TOBACCO CO	905 HARRISON ST		NASHVILLE	TN	37203 USA
M S MILLER	107 EDINBORO LN	C21		OAK RIDGE	TN	37830 USA
G W MILNE	NIH	LC-NIHLBI	BLDG 10, RM 7N318	BETHESDA	MD	20005 USA
B H MIN	HOFFMANN-LAROCHE, INC			NUTLEY	NJ	07110 USA
R D MINARD	PENN STATE UNIV	152 DAVEY LAB		UNIVERSITY PARK	PA	16802 USA
D M MINTZ	FINNIGAN CORP	845 W MAUDE AVE		SUNNYVALE	CA	94086 USA
J MITCHELL	CALIFORNIA INST TECH	CHEMISTRY 127-72	1201 E CALIFORNIA	PASADENA	CA	91125 USA
L A MITSCHER	UNIV OF KANSAS	MEDICINAL CHEMISTRY		LAWRENCE	KS	66045 USA
R MOLCSAN	VARIAN MAT	25 HANOVER ROAD		FLORHAM PARK	NJ	07932 USA
K R MONSON	ICI AMERICAS INC	BIOMEDICAL RES LAB		WILMINGTON	DE	19897 USA
F E MONTGOMERY, JR	BAYLOR COLL MEDICINE	INST LIPID RESEARCH	TEXAS MEDICAL CENTER	HOUSTON	TX	77030 USA
A MOORE	MARATHON OIL CO	PO BOX 269		LITTLETON	CO	80210 USA
L N MORGENTHALER	AFGL/LKB			HANSCOM AFB	MA	01731 USA
K MORRILL	TENNESSEE EASTMAN	B-150		KINGSPORT	TN	37662 USA
T H MORTON	BROWN UNIVERSITY	CHEMISTRY DEPT	PO BOX H	PROVIDENCE	RI	02912 USA
T R MUELLER	ORNL, UNION CARBIDE	PO BOX Y BLDG 9735		OAK RIDGE	TN	37830 USA
S MUIR	CALIFORNIA INST TECH	CHEMISTRY 127-72	1201 E CALIFORNIA BL	PASADENA	CA	91125 USA
M M MUMTAZ	MEDICAL COL VIRGINIA	PSYCHIATRY DEPT	PO BOX 710	RICHMOND	VA	23298 USA
I K MUN	CORNELL UNIVERSITY	BAKER LABORATORY	PO BOX 231	ITHACA	NY	14853 USA
B MUNSON	UNIV OF DELAWARE	CHEMISTRY DEPT		NEWARK	DE	19711 USA
E MURAD	AFGL-LKD			HANSCOM AFB	MA	01731 USA
R C MURPHY	UNIV OF COLORADO	MEDICAL CENTER	PHARMCOLOGY DEPT	DENVER	CO	80262 USA
B D MUSSELMAN	BEST FOODS	1120 COMMERCE AVE		UNION	NJ	07083 USA
Y NAITO	JEOL CORP	235 BIRCHWOOD AVE		CRANFORD	NJ	07016 USA
N NARASIMHACHARI	MEDICAL COL VIRGINIA	PSYCHIATRY DEPT		RICHMOND	VA	23298 USA
B NAYAR	UNIV OF MARYLAND	MEDICINAL CHEMISTRY	& PHARMACOGNOSY DEPT	BALTIMORE	MD	21201 USA
T NESTRICK	DOW CHEMICAL COMPANY	ANALYTICAL LABS	BLDG 574	MIDLAND	MI	48640 USA
M L NGUYEN	SUNTECH INC	PO BOX 1135		MARCUS HOOK	PA	19061 USA

J A NIKORA	B F GOODRICH CENTER	CHEMISTRY DIVISION	PO BOX 122	AVON LAKE	OH 44012	USA
M G NISHIOKA	97 GROTON DRIVE			WESTERVILLE	OH 43081	USA
H, NJUGUNA	ALLIED CHEMICAL CO	PO BOX 1271R		MORRISTOWN	NJ 07960	USA
D L NOEL	INTERNATIONAL PAPER	CORPORATE RESEARCH	PO BOX 797	TUXEDO PARK	NY 10987	USA
D R NORDLUND	PRINCETON UNIV	FRICK CHEMISTRY LAB	MAGIE 7S	PRINCETON	NJ 08544	USA
E J NORMAN	1044 SUNWOOD CT			CINCINNATI	OH 45231	USA
J G NOWLIN	BAYLOR COLL MEDICINE			HOUSTON	TX 77030	USA
C P NULTON	SOUTHWEST RES INST	6220 CULEBRA RD		SAN ANTONIO	TX 78238	USA
J A NYSTROM	UNIV NORTH CAROLINA	CHEMISTRY DEPT		CHAPEL HILL	NC 27514	USA
J L OCCOLOWITZ	ELI LILLY RES LABS			INDIANAPOLIS	IN 46285	USA
V O'CONNELL	TEKNIVENT CORP	10774 TRENTON AVE		ST LOUIS	MO 63132	USA
R W ODOM	4331 PEMBROKE DR			CONCORD	CA 94521	USA
M J OHARE	USV PHARMACEUTICAL	1 SCARSDALE RD		TUCKAHOE	NY 10707	USA
R G OLDHAM	RADIAN CORP	PO BOX 9948		AUSTIN	TX 78766	USA
I A OLEARY	USV PHARMACEUTICAL	1 SCARSDALE RD		TUCKAHOE	NY 10707	USA
R OLINGER	MICHIGAN ST UNIV	BIOCHEMISTRY DEPT	ROOM 219	EAST LANSING	MI 48824	USA
D D OLM	EASTMAN KODAK CO	BLDG 34	KODAK PARK	ROCHESTER	NY 14650	USA
R O'MALLEY	UNIV SOUTH FLORIDA	CHEMISTRY DEPT	4202 E FOWLER AVE	TEMPA	FL 33620	USA
J D ONSTOT	MIDWEST RES INST	425 VOKLER BLVD		KANSAS CITY	MO 64110	USA
C F PACHUCKI	GENERAL ELECTRIC CO	KNOLLS ATOM POW LAB	PO BOX 1072	SCHENECTADY	NY 12301	USA
R P PAGE	A/R CO	400 E SIBLEY BLVD		HARVLY	IL 60426	USA
S L PALLANTE	JOHNS HOPKINS UNIV	PHARMACOLOGY DEPT	725 N WOLFE ST	BALTIMORE	MD 21205	USA
R J PANGIROV	EXON RES & ENG CO			LINDEN	NJ 07036	USA
R C PANDEY	FREDERICK CANCER	RESEARCH CENTER	PO BOX B	FREDERICK	MD 21701	USA
H Y PANG	978 E 600 SO ST	APT 2		SALT LAKE CITY	UT 84102	USA
J PAO	HOFFMANN-LAROCHE, INC	BLDG 86		NUTLEY	NJ 07110	USA
D M PARCES	AIR PRODUCTS & CHEM	PO BOX 538		ALLENTOWN	PA 18105	USA
C E PARKER	PO BOX 232	ROUTE 3		APEX	NC 27502	USA
G A PARKER	UNIV OF VIRGINIA	CHEMISTRY DEPT		CHARLOTTESVILLE	VA 22901	USA
V PARMAKOVICH	COLUMBIA UNIV	CHEMISTRY DEPT	PO BOX 555	NEW YORK	NY 10027	USA
A C PARR	NBS	BLDG 221, RM A251		WASHINGTON	DC 20234	USA
L G PARTRIDGE	STAUFFER RESEARCH	1200 SO 47TH ST		RICHMOND	CA 94804	USA
J R PATEL	SANDOZ INC	CROP PROTECTION	ROUTE 10, BLDG 407	EAST HANOVER	NJ 07936	USA
S M PATEL	1339 VENTURA DRIVE			LAKEWOOD	NJ 08701	USA
D S PEARCE	HEWLETT-PACKARD	1601 CALIFORNIA AVE		PALO ALTO	CA 94304	USA
G L PEELE	VACUMETRICS INC	2261-#1 PALMA DR		VENTURA	CA 93003	USA
D R PELSTER	8104 DEVENS DR			BRENTWOOD	TN 37027	USA
G D PERKINS	PERKIN-ELMER CORP	2771 N GAREY AVE		POMONA	CA 91767	USA
D L PERRY	GULF SOUTH RES INST	6409H FITZHENRY CT		NEW ORLEANS	LA 70126	USA
B A PETERSEN	BATTELLE LABS	505 KING AVE		COLUMBUS	OH 43201	USA
H A PETERSEN	13106 ADVANCE			HOUSTON	TX 77065	USA
G A PETZINGER	9 LAMBERT STREET			WOODBRIDGE	NJ 07095	USA
C D PFAFFENBERGER	3301 N E 5TH AVE	#1107		MIAMI	FL 33137	USA
L V PHILLIPS	INFICON L-H INC	6500 FLY ROAD		EAST SYRACUSE	NY 13057	USA
W C PICKETT	U COLORADO MED SCH	PHARMACOLOGY DEPT	4200 E 9TH STREET	DENVER	CO 80262	USA
R C PIERCE	COLGATE-PALMOLIVE	909 RIVER RD		PISCATAWAY	NJ 08854	USA
A J PIRONE	10 KENLEIGH CT			WILMINGTON	DE 19808	USA
R PLATTNER	NORTHERN REGIONAL LA	1815 N UNIVERSITY ST		PEORIA	IL 61604	USA
M O POEPPEL	3 HOLLYHOCK WAY			MERCERVILLE	NJ 08619	USA
C W POLLEY, JR	OXIRANE INTL	201 COLLEGE RD EAST		PRINCETON	NJ 08540	USA
R F PORTER	CORNELL UNIVERSITY	CHEMISTRY DEPT		ITHACA	NY 14853	USA
M L POWELL	HOFFMANN-LAROCHE, INC	BLDG 86, BIOCHEMISTRY& DRUG METABOLISM		NUTLEY	NJ 07110	USA
S E POWERS	4017 HIRST DRIVE			ANNANDALE	VA 22003	USA
B N PRAMANIK	ONE BRADFORD RD			MT VERNON	NY 10553	USA
P C PRICE	UNION CARBIDE	TECHNICAL CENTER	PO BOX 8361	SOUTH CHARLESTON	WV 25303	USA
L C RAMIREZ	160 CLAREMONT AVENUE			NEW YORK	NY 10027	USA
H G RAMJIT	MERCK INSTITUTE OF	THERAPEUTIC RESEARCH	DEPT 805	WEST POINT	PA 19486	USA
G H RAYBORN	UNIV SO MISSISSIPPI	S.S: PO BOX 8123		HATTIESBURG	MS 39401	USA
C E REGNSTEINER, JR	2906 STEARNS HILL RD			WALTHAM	MA 02154	USA
W D REENTS, JR	103-16 MARRIED	STUDENT COURTS		WEST LAFAYETTE	IN 47906	USA

V N REINHOLD	HARVARD MEDICAL SCH	THRRB	45 SHATTUCK ST	BOSTON	MA	02115 USA
R W REISER	E I DUPONT	EXPERIMENTAL STATIONBIOCHEM, BLDG 324		WILMINGTON	DE	19898 USA
M E RENNEKAMP	ASHLAND OIL INC	MS LAB	PO BOX 2058	COLUMBUS	OH	43216 USA
T P REYNOLDS	PO BOX 314			BETHEL	CT	06801 USA
K L RICHIE	NBS			WASHINGTON	DC	20234 USA
B H RICHTER	JOHN HOPKINS UNIV	PHARMACOLOGY DEPT	725 N WOLFE ST	BALTIMORE	MD	21205 USA
D P RIDGE	UNIV OF DELAWARE	CHEMISTRY DEPT		NEWARK	DE	19711 USA
K L RINEHART	UNIV OF ILLINOIS	454 ROGER ADAMS LAB		URBANA	IL	61801 USA
D J RIZZO	GENERAL FOODS CORP	555 SO BROADWAY		TARRYTOWN	NY	10591 USA
G D ROBERTS	691 CRESSMAN RD			HARLEYVILLE	PA	19438 USA
D H ROBERTSON	FOOD SCIENCE LAB	ANALYTICAL CHEM GRP	US ARMY NATICK LABS	NATICK	MA	01760 USA
D W ROBINSON	PENNWALT	900 FIRST AVE		KING OF PRUSSIA	PA	19406 USA
R J ROBINSON	DOW CORNING CORP	MAIL 23		MIDLAND	MI	48640 USA
J ROBOZ	123 PHELPS AVE			CRESSKILL	NJ	07626 USA
D K ROHRBAUGH	125 ST PAUL ST			BROOKLINE	MA	02146 USA
W K ROHWEDDER	205 CHATEAU TOURAINE	3900 N STABLE COURT		PEORIA	IL	61614 USA
D J ROKOP	208 DOS BRAZOS			LOS ALAMOS	NM	87544 USA
L J ROMANCZYK	MCCORMICK & COMP INC	204 WIGHT AVE		HUNT VALLEY	MD	21031 USA
A E ROSECRANCE	SYSTEMS, SCIENCE AND	SOFTWARE	PO BOX 1620	LA JOLLA	CA	92037 USA
H ROSELIUS	35 BROOKLYN MT RD			HOPATCONG	NJ	07843 USA
R T ROSEN	FMC CORP	PO BOX 8		PRINCETON	NJ	08540 USA
H M ROSENSTOCK	NBS	RADIATION PHYSICS DVN	ATL BUR STANDARDS	WASHINGTON	DC	20234 USA
D ROSENTHAL	RES TRIANGLE INST	PO BOX 12194		RESEARCH TRIANGLE PK	NC	27709 USA
R ROTHCHILD	605 EAST 14TH ST			NEW YORK	NY	10009 USA
S M ROTHSTEIN	CVC PRODUCTS	525 LEE RD		ROCHESTER	NY	14603 USA
S ROTTSCHAEFER	1195 HART LANE			HARTSVILLE	PA	18974 USA
K L ROWLAND	NATIONAL CENTER FOR	TOXICOLOGICAL RESRCH		JEFFERSON	AR	72079 USA
T A ROY	BATTELLE LABS	505 KING AVE		COLUMBUS	OH	43201 USA
H RUBINSTEIN	15 FAIRBANKS RD			CHELMSFORD	MA	01824 USA
T RUBIO	HOFFMANN LA ROCHE	BIOCHEMISTRY & DRUG		NUTLEY	NJ	07110 USA
M A RUDAT	E I DUPONT	EXPERIMENTAL STATION	CENTRAL RES, -228/101	WILMINGTON	DE	19898 USA
M I RUEPPEL	954 WHITECLIFF DR			KIRKWOOD	MO	63122 USA
T I RUO	NORTHWESTERN UNIV	CLINICAL PHARMACOLOG	303 E SUPERIOR	CHICAGO	IL	60611 USA
D H RUSSELL	ORNL, UNION CARBIDE	PO BOX X		OAK RIDGE	TN	37830 USA
J W RUSSELL	MEAD TECH LABS	PO BOX 12652		RESEARCH TRIANGLE PK	NC	27709 USA
P W RYAN	COLORADO STATE UNIV	CHEMISTRY DEPT		FORT COLLINS	CO	80523 USA
J SABBATINI	UNIV OF TENNESSEE	STOUT NEUROSCIENCE	L2A07 COLEMAN BLDG	MEMPHIS	TN	38163 USA
R SAFERSTEIN	277 ST DAVID CT			MT LAUREL	NJ	08054 USA
V G SALTAMACH	COLUMBIA UNIVERSITY	HAVEMEYER BLDG	119TH ST & B'WAY	NEW YORK	NY	10027 USA
P C SAMSON	112 E BARRETT LANE			SCHAUMBURG	IL	60193 USA
R A SANDERS	1900 WILTSHIRE BLVD			FAIRFIELD	OH	45014 USA
J SANTROCK	INDIANA UNIVERSITY	CHEMISTRY DEPT		BLOOMINGTON	IN	47401 USA
A D SAUER	EMSL-USLAP	944 E HARMON AVE		LAS VEGAS	NV	89109 USA
J SAVGERMAN	MEAD JOHNSON & CO	2404 PENNSYLVANIA AV		EVANSVILLE	IN	47721 USA
P J SAVICKAS	UNIV OF VIRGINIA	CHEMISTRY DEPT		CHARLOTTESVILLE	VA	22901 USA
M D SCAMUFFA	HEWLETT-PACKARD	5201 TOLLVIEW DR		ROLLING MEADOWS	IL	60008 USA
M D SCANLON	SUNY	BIOPHYSICS DEPT		BUFFALO	NY	14214 USA
R SCHAERANEK	16200 PARK ROW			HOUSTON	TX	77084 USA
R J SCHMITT	SRI INTERNATIONAL	333 RAVENSWOOD AVE	F249	MENLO PARK	CA	94025 USA
W C SCHNUTE	FINNIGAN CORP	845 W MAUDE AVE		SUNNYVALE	CA	94086 USA
A E SCHOEN	PURDUE UNIVERSITY	CHEMISTRY DEPT	PO BOX 737	WEST LAFAYETTE	IN	47907 USA
D M SCHOENGOLD	2305 EASTON			RICHLAND	WA	99352 USA
K H SCHRAM	UNIV OF ARIZONA	COLLEGE OF PHARMACY		TUCSON	AZ	85721 USA
R SCHUBERT	BELL LABORATORIES	6200 E BROAD ST		COLUMBUS	OH	43068 USA
M R SCHURE	COLORADO STATE UNIV	CHEMISTRY DEPT		FORT COLLINS	CO	80521 USA
S SENZER	PENN STATE UNIV	BOX 81	152 DAVEX LAB	UNIVERSITY PARK	PA	16802 USA
R L SETTINE	UNIV OF ALABAMA	GCMS CENTER		BIRMINGHAM	AL	35294 USA
B SEUGER	UNIV OF DELAWARE	CHEMISTRY DEPT		NEWARK	DE	19711 USA
J SHABANOWITZ	UNIV OF VIRGINIA	CHEMISTRY DEPT		CHARLOTTESVILLE	VA	22901 USA
L A SHADOFF	DOW CHEMICAL CO	574 BLDG		MIDLAND	MI	48640 USA

T E SHARP	LOCKHEED RES LAB	3251 HANOVER	D52-35 B204	PALO ALTO	CA	94304 USA
C J SHAW	12 RUTGERS DRIVE			DELRAN	NJ	08075 USA
K B SHLAKER	THOMPSON-HAYWARD	CHEMICAL CO		KANSAS CITY	KANSAS	6 USA
P W SHCARER	HERCULES INC	RESEARCH CENTER		WILMINGTON	DE	19899 USA
J SHEN	SOHIO RESEARCH	4440 WARRENSVILLE	CENTER ROAD	CLEVELAND	OH	44128 USA
D C SHEW	EPA	PO BOX 1198		ADA	OK	74820 USA
S R SHRADER	SHRADER ANAL LAB	3450 LOVETT		DETROIT	MI	48210 USA
Y Y SHUM	WARNER LAMBERT	/PARKE DAVIS	2000 PLYMOUTH RD	ANN ARBOR	MI	48105 USA
G D SIDES	1732 TAHITI LANE			ALABASTER	AL	35007 USA
M M SIEGEL	319 NORTH 8TH AVE			EDISON	NJ	08817 USA
M W SIEGEL	EXTRANUCLEAR LAB	250 ALPHA DRIVE	PO BOX 11512	PITTSBURGH	PA	15238 USA
A D SILL	MERRELL-NATIONAL LABANALYTICAL CHEM DEPT		2110 E GALBRAITH RD	CINCINNATI	OH	45215 USA
E J SILVEIRA,JR	SHELL BSRC	PO BOX 4248		MODESTO	CA	95352 USA
D S SIMONS	NBS	BLDG 222, RM A121		WASHINGTON	DC	20234 USA
M P SINHA	JET PROPULSION LAB	MS 11-111	4800 OAK GROVE ST	PASADENA	CA	91103 USA
M E SISAK	UNIV OF VIRGINIA	CHEMISTRY DEPT		CHARLOTTESVILLE	VA	22901 USA
P A SKOTNICKI	HOOKER CHEMICALS	PO BOX 344		NIAGARA FALLS	NY	14302 USA
L E SLIVON	BATTELLE LABS	505 KING AVE		COLUMBUS	OH	43201 USA
D E SMITH,DANNE	44 CENTER GROVE RD	APT T 12		DOVER	NJ	07801 USA
D L SMITH	UNIV OF UTAH	311 SKAGGS HALL		SALT LAKE CITY	UT	84112 USA
J L SMITH	380 SEMINARY AVE			RAHWAY	NJ	07065 USA
J S SMITH	ALLIED CHEMICAL CORP	PO BOX 1021-R		MORRISTOWN	NJ	07960 USA
R A SMITH	MONSANTO	800 N LINDBERGH	Q3D	ST LOUIS	MO	63166 USA
R D SMITH	BATTELLE-NW	BLDG 329, AREA 300		RICHLAND	WA	99352 USA
C R SNELLING,JR	UNIV OF ILLINOIS	PO BOX 101	RAL	URBANA	IL	61801 USA
R G SNOOK	6 CHENANGO ST			CAZENOVIA	NY	13035 USA
J G SOLCH	4967 TANNER DRIVE			DAYTON	OH	45424 USA
B H SOLKA	7813 W ROSEDALE			CHICAGO	IL	60631 USA
J J SOLOMON	NEW YORK UNIV	ENVIRON MEDICINE	MEDICAL CENTER	TUXEDO PARK	NY	10987 USA
B D SOLTMANN	406 THORNWOOD DR			CHAPEL HILL	NC	27514 USA
E A SORBAN	STAUFFER CHEMICAL CO	400 FARMINGTON AVE		FARMINGTON	CT	06032 USA
O D SPARKMAN	1657 LUTKA PLACE			CAMPBELL	CA	95008 USA
R B SPENCER	5121 FLAMBEAU RD			MADISON	WI	53705 USA
J A SPHON	FDA	HFF-459	200 C ST SW	WASHINGTON	DC	20204 USA
C A SPINDL	SRI INTERNATIONAL	333 RAVENSWOOD AVE		MENLO PARK	CA	94025 USA
A W SPRATLEY,JR	UNION CARBIDE	PO BOX 50		HAHNVILLE	LA	70057 USA
R G SPRLIN	UNIV OF DELAWARE	BROWN LABORATORY		NEWARK	DE	19711 USA
S R SRINIVAS	J MANHEIMER INC	47-22 PEARSON PLACE		LONG ISLAND CITY	NY	11101 USA
B STACKLER	BOX 572			DAVIS	CA	95616 USA
R H STALEY	MIT	CHEMISTRY, 6-128A		CAMBRIDGE	MA	02139 USA
D B STAUFFER	114 SUMMIT ST			ITHACA	NY	14850 USA
J. L STAUFFER	ARTHUR D LITTLE INC	ACORN PARK		CAMBRIDGE	MA	02140 USA
J D STEIN	GENERAL ELECTRIC	1334 KATHY CT		LIVERMORE	CA	94550 USA
F A STEVIE	BELL LABORATORIES	RM 1A-341	600 MOUNTAIN AVE	MURRAY HILL	NJ	07974 USA
R N STILLWELL	BAYLOR COLL MEDICINE	INST LIPID RESEARCH	TEXAS MEDICAL CENTER	HOUSTON	TX	77030 USA
W G STILLWELL	BAYLOR COLL MEDICINE	INST LIPID RESEARCH	TEXAS MEDICAL CENTER	HOUSTON	TX	77030 USA
R L STOCKBAUER	NBS	BLDG 222, RM B248		WASHINGTON	DC	20234 USA
J J STOFFELS	BATTELLE-NW	BLDG 320, AREA 300		RICHLAND	WA	99352 USA
M STOGNIEW	UNIV OF MARYLAND	MEDICINAL CHEM &	PHARMACOGNOSY	BALTIMORE	MD	21201 USA
M S STORY	15745 WOODACRES RD			LOS GATOS	CA	95030 USA
S J STOUT	AMERICAN CYANIMID	AGRICULTURAL DIV	PO BOX 400	PRINCETON	NJ	08540 USA
C L SULLIVAN	AVILA CO	11901 WORNALL ROAD		KANSAS CITY	MO	64145 USA
S A SULLIVAN	UNIV OF COLORADO	CHEMISTRY DEPT		BOULDER	CO	80309 USA
I SUN	USDA-FSQS	PO BOX 6085		ATHENS	GA	30604 USA
R K SUZUKI	1829 PALMER AVE			LARCHMONT	NY	10538 USA
H J SVEC	IOWA STATE UNIV	CHEMISTRY DEPT		AMES	IA	50011 USA
J T SWANSIGER	GULF CORP	RESEARCH & DEVELOP	PO DRAWER 2038	PITTSBURGH	PA	15230 USA
B J SWETMAN	VANDERBILT UNIV	PHARMACOLOGY DEPT		NASHVILLE	TN	37232 USA
C R TALLEY	E I DUPONT	EXPERIMENTAL STATION	PETRO CHEM, BLDG 336	WILMINGTON	DE	19898 USA
Y L TAN	DOE	ENVIRON MEAS LAB	376 HUDSON ST	NEW YORK	NY	10014 USA

O P TANNER	12664 MARKAIRE			ST LOUIS	MO	63141 USA
A R TAYLOR	CONOCO INC	1000 SOUTH PINE		PONCA CITY	OK	74601 USA
R T TEISS	PRINCETON UNIV	CHEMISTRY DEPT		PRINCETON	NJ	08544 USA
D I TERWILLIGER	29 CHEIWYND RD			PAOLI	PA	19301 USA
M TETSUO	NIH	NIMH, CLINICAL SCIEN		BETHESDA	MD	20205 USA
J P THENOT	NORTHWEST MEM HOSP	CLIN PHARMACOLOGY	303 E SUPERIOR ST	CHICAGO	IL	60611 USA
D W THOMAS	SRI INTERNATIONAL	333 RAVENSWOOD AVE	B-011	MENLO PARK	CA	94025 USA
F THOMAS	NIH	BLDG 10, RM 7N115		BETHESDA	MD	20005 USA
Q V THOMAS	1383 PARK WAY COURT			FAIRFIELD	OH	45014 USA
J R THORP	3111 WINDMILL			SUGAR LAND	TX	77478 USA
A D THRUSTON, JR	ENVIRON PROTECTION	AGENCY	ENVIRON RES LAB	ATHENS	GA	30613 USA
R G THURMAN	UNION CAMP CORP	PO BOX 412		PRINCETON	NJ	08540 USA
T O TIERNAN	WRIGHT STATE UNIV	BREHM LAB		DAYTON	OH	45431 USA
G W TINDALL	TENNESSEE EASTMAN COB	LDG 54		KINGSPORT	TN	37662 USA
G S TINT	EAST ORANGE VA HOSP			EAST ORANGE	NJ	07019 USA
P J TODD	CORNELL UNIVERSITY	BAKER LABORATORY	PO BOX 380	ITHACA	NY	14853 USA
A D TOMASSIAN	JET PROPULSION LAB	4800 OAK GROVE AVE		PASADENA	CA	91103 USA
K B TOMER	RES TRIANGLE INST	PO BOX 12194	CLSD	RESEARCH TRIANGLE	PKNC	27709 USA
Y TONDEUR	NIEHS	PO BOX 12233		RESEARCH TRIANGLE	PKNC	27709 USA
S C TONG	CORNING GLASS WORKS	RESEARCH & DEVELOP		CORNING	NY	14830 USA
J C TOU	DOW CHEMICAL CO	ANALYTICAL LAB	B-574	MIDLAND	MI	48640 USA
V T TRAN	UNIV OF DELAWARE	CHEMISTRY DEPT		NEWARK	DE	19711 USA
R S TSAI	UNIV PUERTO RICO	COLLEGE STATION	PO BOX 5767	MAYAGUEZ	PR	00708 USA
K Y TSERNG	17006 BEAVER CIRCLE			STRONGSVILLE	OH	44136 USA
J R TURBETT	JAMESTOWN STAR ROUTE			BOULDER	CO	80302 USA
P C TWAY	MERCK-SHARP & DOHME	RESEARCH LABORATORY	PO BOX 2000	RAHWAY	NJ	07065 USA
H R UDSETH	UNIV OF OF UTAH	CHEMISTRY DEPT	PO BOX 43	SALT LAKE CITY	UT	84112 USA
S E UNGER	150 ARNOLD DR	APT #4		WEST LAFAYETTE	IN	47906 USA
B T UPCHURCH	OLD DOMINION UNIV	CHEMISTRY DEPT		NORFOLK	VA	23508 USA
R A UPHAM	UNIV OF MINNESOTA	CHEMISTRY DEPT		MINNEAPOLIS	MN	55455 USA
A K VADEN	217 FOREST AVE			RICHMOND	VA	23223 USA
K VALENTIN	AMERICAN CYNAMID CO	BLDG 4C, ROOM 71		BOUND BROOK	NJ	0880 USA
W J VANDEN HEUVEL	MERCK SHARP & DOHME	RESEARCH LABORATORY	PO BOX 2000	RAHWAY	NJ	07065 USA
R W VANDER HAAR	STANDARD OIL INDIANA	PO BOX 400		NAPERVILLE	IL	60540 USA
F M VANE	HOFFMANN-LAROCHE, INC			NUTLEY	NJ	07110 USA
A M VAN LANGENHOVE	MIT	CHEMISTRY, 56-016		CAMBRIDGE	MA	02139 USA
G F VAN NESS	WRIGHT STATE UNIV	BREHM LAB	COL GLENN HWY	DAYTON	OH	45435 USA
M J VASILE	BELL LABORATORIES	RM 1A-259	600 MOUNTAIN AVE	MURRAY HILL	NJ	07974 USA
G W VAUGHN	MIDWEST RESRCH INST	425 VOLKER BVD		KANSAS CITY	MO	64110 USA
D M VEA	1712 SADLERS WELLS D			HERNDON	VA	22070 USA
L VERKH	307 WENDEL			BUFFALO	NY	14223 USA
M L VESTAL	UNIV OF HOUSTON	CHEMISTRY DEPT	4800 CALHOUN	HOUSTON	TX	77004 USA
M M VESTLING	SUNY	CHEMISTRY DEPT		BROCKPORT	NY	14420 USA
S VICKERS	SLOTTER RD	R R 2	BOX 243	PERKASIE	PA	18944 USA
K J VOORHEES	COLORADO SCH MINES	CHEMISTRY DEPT		GOLDEN	CO	80401 USA
R A VORDENBERG	1275 SECTION RD			CINCINNATI	OH	45237 USA
P VOUROS	NORTHEASTERN UNIV	INST CHEMICAL ANAL		BOSTON	MA	02115 USA
R D VOYKSNER	203-A BRANSON ST			CHAPEL HILL	NC	27514 USA
V T VU	JOHNS HOPKINS UNIV	PHARMACOLOGY DEPT	725 N WOLFE ST	BALTIMORE	MD	21205 USA
T WACHS	CORNELL UNIVERSITY	CHEMISTRY DEPT		ITHACA	NY	14853 USA
R W WALKER	MERCK SHARP & DOHME	RESEARCH LABORATORY	PO BOX 2000	RAHWAY	NJ	07065 USA
G R WALLER	OKLAHOMA STATE UNIV	BIOCHEMISTRY DEPT		STILLWATER	OK	74074 USA
F C WALLS	UNIV OF CALIFORNIA	SPACE SCIENCES LAB		BERKELEY	CA	94720 USA
D C WALTERS	1236 KEVIN DR			FAIRBORN	OH	45324 USA
J R WALTON	ORNL, UNION CARBIDE	PO BOX Y, BLDG 9735		OAK RIDGE	TN	37830 USA
B P WANG	7614 QUAILMEADOW DR			HOUSTON	TX	77071 USA
J S WANG	93 SHADOW RIDGE RD			STAMFORD	CT	06905 USA
S I WANG	ABBOTT LABS	DEPT 417		NORTH CHICAGO	IL	60064 USA
P L WARREN	FINNIGAN CORP	845 W MAUDE AVE		SUNNYVALE	CA	94086 USA
J T WATSON	DEPT BIOCHEMISTRY	MICHIGAN STATE UNIV		EAST LANSING	MI	48824 USA

G H WEDDLE	FAIRFIELD UNIV	CHEMISTRY DEPT		FAIRFIELD	CT	06430 USA
L A WEIBEL	RALTECH SCIENTIFIC	SERVICES	PO BOX 7545	MADISON	WI	53707 USA
R J WEINKAM	PURDUE UNIVERSITY	MEDICINAL CHEMISTRY		WEST LAFAYETTE	IN	47907 USA
M WEISS	124 FOXWOOD			PORTOLA VALLEY	CA	94025 USA
M J WEISS	PERKIN-ELMER CORP	AEROSPACE DIVISION	2771 NO GAREY AVE	POMONA	CA	91767 USA
K J WEIGH	SC JOHNSON & SON, INC	ANAL R&D STA #56	1525 HOWE ST	RACINE	WI	53403 USA
M J WEIGH	1774 STONEHAVEN			FREDERICK	MD	21701 USA
C W WESDEMIOTIS	709 TRIPHAMMER ROAD			ITHACA	NY	14850 USA
R B WESTERBERG	1704 FOREST CREEK LN			WEST DEPTFORD	NJ	08066 USA
D G WESTMORELAND	ROHM & HAAS CO			SPRING HOUSE	PA	19477 USA
A F WESTON	HOOKER CHEMICALS	GRAND ISLAND COMPLEX	LONG ROAD	GRAND ISLAND	NY	14072 USA
T W WHALEY	LOS ALAMOS SCIEN LAB	GROUP LS-5 MS 890		LOS ALAMOS	NM	87501 USA
E WHITE	NBS	A113 CHEMISTRY		WASHINGTON	DC	20234 USA
J O WHITNEY	UNIV OF CALIFORNIA	1434 HSW		SAN FRANCISCO	CA	94143 USA
J T WILDER	UNIV OF CALIFORNIA	1474 FIELDCREST CIR		PLEASANT HILL	CA	94523 USA
B E WILKES	UNION CARBIDE	PO BOX 8361	BLDG 770-318	SOUTH CHARLESTON	WV	25303 USA
C L WILKINS	UNIV OF NEBRASKA	CHEMISTRY DEPT		LINCOLN	NE	68588 USA
B W WILLIAMS	CORNELL UNIVERSITY	BAKER LAB	BOX 433	ITHACA	NY	14853 USA
C H WILLIAMS, JR	RADIAN CORP	PO BOX 9948		AUSTIN	TX	78766 USA
P WILLIAMS	UNIV OF ILLINOIS	MATERIALS RES LAB		URBANA	IL	61801 USA
R M WILLIAMS	RESEARCH CORP	405 LEXINGTON AVE		NEW YORK	NY	10174 USA
B W WILSON	BATTELLE-NW	BLDG 329, AREA 300		RICHLAND	WA	99352 USA
R R WILSON	NATIONAL LEAD	PO BOX 39158		CINCINNATI	OH	45239 USA
J G WINDSOR, JR	NORTHROP SERVICES	PO BOX 12313		RESEARCH TRIANGLE PKNC		27709 USA
D L WINMILL	HERCULES INC	RESEARCH CENTER		WILMINGTON	DE	19899 USA
D WOBSCHALL	SUNY	4232 RIDGE LEA		AMHERST	NY	14226 USA
L H WOJCIK, JR	U OF U ENERGY CENTER	391 S CHIPETA WAY		SALT LAKE CITY	UT	84108 USA
B H WOLFF	238 PARKRIDGE AVE			BUFFALO	NY	14215 USA
M S WOLFF	MT SINAI MEDICAL SCIEN	VIRONMEN SCIEN LAB	10 E 102ND ST	NEW YORK	NY	10029 USA
W A WOLSTENHOLME	KEARNS GROUP	58 BUCKINGHAM DR		STAMFORD	CT	06902 USA
T L WONGT	UNIROYAL CHEM CO	BLDG #81	ELM ST	NAUGATUCK	CT	06457 USA
C M WONG	LLL	PO BOX 808, L-325		LIVERMORE	CA	94550 USA
L K WONG	UNIV OF PITTSBURGH	SCHOOL OF PHARMACY	721 SALK HALL	PITTSBURGH	PA	15261 USA
D WOOD	19 HILLCREST AVE			DARIEN	CT	06820 USA
G M WOOD, JR	2 LITTLE BLUFF RD			NEWPORT NEWS	VA	23606 USA
K V WOOD	MONSANTO	800 N LINDBERGH	S3C	ST LOUIS	MO	63141 USA
R L WOODIN	EXXON R/E	PO BOX 45		LINDEN	NJ	07036 USA
D R WOODS	ASHLAND PETROLEUM CO	PO BOX 391		ASHLAND	KY	41101 USA
J W WOODS	8 RICHARDS RD			LYNNFIELD	MA	01940 USA
R C WOODS	UNIV OF WISCONSIN	CHEMISTRY DEPT	1101 UNIVERSITY AVE	MADISON	WI	53706 USA
J WRONKA	5011 GARFIELD AVE			PENNSAUKEN	NJ	08109 USA
P C WSZOLEK	CORNELL UNIV	TOXIC CHEMICALS LAB		ITHACA	NY	14853 USA
A T WU	FDA	HFF-458	200 C ST SW	WASHINGTON	DC	20204 USA
R L WU	WRIGHT STATE UNIV	BIOMM LABORATORY		DAYTON	OH	45431 USA
W N WU	MCNEIL LABORATORIES	BIOCHEMISTRY DEPT		FORT WASHINGTON	PA	19034 USA
J R WYATT	NRL	CODE 6110		WASHINGTON	DC	20375 USA
S YAMADA	UNIV OF TENN	NEUROLOGY DEPT	800 MADISON AVE	MEMPHIS	TN	38163 USA
G F YAMNITZKY	DRUG ENFORCEMENT ADM	555 WEST 57TH ST	ROOM 1886	NEW YORK	NY	10019 USA
R O YELTON	116 WALDEN FARM CIR			UNION	OH	45322 USA
A L YERGEY	NIH	BLDG 6, RM 408		BETHESDA	MD	20005 USA
R A YOST	UNIV OF FLORIDA	CHEMISTRY DEPT		GAINESVILLE	FL	32611 USA
S E YOUNG	2455 THADDEUS			MOUNTAIN VIEW	CA	94043 USA
T L YOUNGLESS	UNIV NORTH CAROLINA	CHEMISTRY DEPT		CHAPEL HILL	NC	27514 USA
M YOUSSEFF	UNION CARBIDE	ONE RIVER RD		BOUND BROOK	NJ	08854 USA
A G ZACCHEI	MERCK SHARP & DOHME	RESEARCH LABORATORY		WEST POINT	PA	19486 USA
D ZAKETT	PURDUE UNIVERSITY	CHEMISTRY DEPT	POX 835	WEST LAFAYETTE	IN	47907 USA
J A ZIRROLLI	AFESC/RDVC			TYNDALL AFB	FL	32403 USA
T S ZWIER	UNIV OF COLORADO	JILA		BOULDER	CO	80309 USA